RECENT AND EMERGING INNOVATIONS IN DEEP-SEA TAXONOMY TO ENHANCE BIODIVERSITY ASSESSMENT AND CONSERVATION

EDITED BY: Stefanie Kaiser, Magdalena Błażewicz, Kevin M. Kocot, Torben Riehl, Daniel Leduc and Greg W. Rouse

PUBLISHED IN: Frontiers in Marine Science

frontiers Research Topics

Frontiers eBook Copyright Statement

The copyright in the text of individual articles in this eBook is the property of their respective authors or their respective institutions or funders. The copyright in graphics and images within each article may be subject to copyright of other parties. In both cases this is subject to a license granted to Frontiers.

The compilation of articles constituting this eBook is the property of Frontiers.

Each article within this eBook, and the eBook itself, are published under the most recent version of the Creative Commons CC-BY licence. The version current at the date of publication of this eBook is CC-BY 4.0. If the CC-BY licence is updated, the licence granted by Frontiers is automatically updated to the new version.

When exercising any right under the CC-BY licence, Frontiers must be attributed as the original publisher of the article or eBook, as applicable.

Authors have the responsibility of ensuring that any graphics or other materials which are the property of others may be included in the CC-BY licence, but this should be checked before relying on the CC-BY licence to reproduce those materials. Any copyright notices relating to those materials must be complied with.

Copyright and source acknowledgement notices may not be removed and must be displayed in any copy, derivative work or partial copy which includes the elements in question.

All copyright, and all rights therein, are protected by national and international copyright laws. The above represents a summary only. For further information please read Frontiers' Conditions for Website Use and Copyright Statement, and the applicable CC-BY licence.

ISSN 1664-8714
ISBN 978-2-83250-329-4
DOI 10.3389/978-2-83250-329-4

About Frontiers

Frontiers is more than just an open-access publisher of scholarly articles: it is a pioneering approach to the world of academia, radically improving the way scholarly research is managed. The grand vision of Frontiers is a world where all people have an equal opportunity to seek, share and generate knowledge. Frontiers provides immediate and permanent online open access to all its publications, but this alone is not enough to realize our grand goals.

Frontiers Journal Series

The Frontiers Journal Series is a multi-tier and interdisciplinary set of open-access, online journals, promising a paradigm shift from the current review, selection and dissemination processes in academic publishing. All Frontiers journals are driven by researchers for researchers; therefore, they constitute a service to the scholarly community. At the same time, the Frontiers Journal Series operates on a revolutionary invention, the tiered publishing system, initially addressing specific communities of scholars, and gradually climbing up to broader public understanding, thus serving the interests of the lay society, too.

Dedication to Quality

Each Frontiers article is a landmark of the highest quality, thanks to genuinely collaborative interactions between authors and review editors, who include some of the world's best academicians. Research must be certified by peers before entering a stream of knowledge that may eventually reach the public - and shape society; therefore, Frontiers only applies the most rigorous and unbiased reviews.
Frontiers revolutionizes research publishing by freely delivering the most outstanding research, evaluated with no bias from both the academic and social point of view. By applying the most advanced information technologies, Frontiers is catapulting scholarly publishing into a new generation.

What are Frontiers Research Topics?

Frontiers Research Topics are very popular trademarks of the Frontiers Journals Series: they are collections of at least ten articles, all centered on a particular subject. With their unique mix of varied contributions from Original Research to Review Articles, Frontiers Research Topics unify the most influential researchers, the latest key findings and historical advances in a hot research area! Find out more on how to host your own Frontiers Research Topic or contribute to one as an author by contacting the Frontiers Editorial Office: frontiersin.org/about/contact

RECENT AND EMERGING INNOVATIONS IN DEEP-SEA TAXONOMY TO ENHANCE BIODIVERSITY ASSESSMENT AND CONSERVATION

Topic Editors:
Stefanie Kaiser, Senckenberg Research Institute and Natural History Museum Frankfurt, Germany
Magdalena Błażewicz, University of Łódź, Poland
Kevin M. Kocot, University of Alabama, United States
Torben Riehl, Senckenberg Museum, Germany
Daniel Leduc, National Institute of Water and Atmospheric Research (NIWA), New Zealand
Greg W. Rouse, University of California, San Diego, United States

Citation: Kaiser, S., Błażewicz, M., Kocot, K. M., Riehl, T., Leduc, D., Rouse, G. W., eds. (2022). Recent and Emerging Innovations in Deep-Sea Taxonomy to Enhance Biodiversity Assessment and Conservation. Lausanne: Frontiers Media SA. doi: 10.3389/978-2-83250-329-4

Table of Contents

05 ***Editorial: Recent and Emerging Innovations in Deep-Sea Taxonomy to Enhance Biodiversity Assessment and Conservation***
Stefanie Kaiser, Magdalena Błażewicz, Kevin M. Kocot, Daniel Leduc, Torben Riehl and Greg W. Rouse

10 ***Recommendations for the Standardisation of Open Taxonomic Nomenclature for Image-Based Identifications***
Tammy Horton, Leigh Marsh, Brian J. Bett, Andrew R. Gates, Daniel O. B. Jones, Noëlie M. A. Benoist, Simone Pfeifer, Erik Simon-Lledó, Jennifer M. Durden, Leen Vandepitte and Ward Appeltans

23 ***Hadal Mud Dragons: First Insight Into the Diversity of Kinorhyncha From the Atacama Trench***
Katarzyna Grzelak, Daniela Zeppilli, Mauricio Shimabukuro and Martin V. Sørensen

45 ***High Species Richness and Extremely Low Abundance of Cumacean Communities Along the Shelf and Slope of the Gulf of Guinea (West Africa)***
Anna Stępień, Krzysztof Pabis, Robert Sobczyk and Bjorn Serigstad

66 ***Better Alone Than in Bad Company: New Species of Caudofoveate Limifossorid (Mollusca, Aplacophora) Unravels Patterns of Distribution Hidden in the Deep Atlantic***
Flávio Dias Passos, Paulo Vinicius Ferraz Corrêa and Marcel Sabino Miranda

84 **Pseudotanais** ***Sars, 1882 (Crustacea: Tanaidacea) From the SE Australian Slope: A Gap in Our Knowledge***
Magdalena Błażewicz, Aleksandra Jakiel and Graham J. Bird

108 ***Pandora's Box in the Deep Sea –Intraspecific Diversity Patterns and Distribution of Two Congeneric Scavenging Amphipods***
Anna M. Jażdżewska, Tammy Horton, Ed Hendrycks, Tomasz Mamos, Amy C. Driskell, Saskia Brix and Pedro Martínez Arbizu

130 ***A Global Red List for Hydrothermal Vent Molluscs***
Elin A. Thomas, Aoife Molloy, Nova B. Hanson, Monika Böhm, Mary Seddon and Julia D. Sigwart

140 ***DNA Barcoding of Scavenging Amphipod Communities at Active and Inactive Hydrothermal Vents in the Indian Ocean***
Katharina Kniesz, Anna Maria Jażdżewska, Pedro Martínez Arbizu and Terue Cristina Kihara

160 ***Computed Microtomography (Micro-CT) in the Anatomical Study and Identification of Solenogastres (Mollusca)***
Jesús Martínez-Sanjuán, Kevin Kocot, Óscar García-Álvarez, María Candás and Guillermo Díaz-Agras

181 ***Framing Cutting-Edge Integrative Deep-Sea Biodiversity Monitoring via Environmental DNA and Optoacoustic Augmented Infrastructures***
Sergio Stefanni, Luca Mirimin, David Stanković, Damianos Chatzievangelou, Lucia Bongiorni, Simone Marini, Maria Vittoria Modica, Elisabetta Manea, Federico Bonofiglio, Joaquin del Rio Fernandez, Neven Cukrov, Ana Gavrilović, Fabio C. De Leo and Jacopo Aguzzi

198 ***Correct Species Identification and Its Implications for Conservation Using Haploniscidae (Crustacea, Isopoda) in Icelandic Waters as a Proxy***
Karlotta Kürzel, Stefanie Kaiser, Anne-Nina Lörz, Sven Rossel, Eva Paulus, Janna Peters, Martin Schwentner, Pedro Martinez Arbizu, Charles Oliver Coleman, Jörundur Svavarsson and Saskia Brix

219 ***A Paradise for Rare Species: Tanaidacean Fauna of the West African Continental Margin***
Piotr Jóźwiak, Krzysztof Pabis, Robert Sobczyk and Bjorn Serigstad

235 ***Diversity of Pacific* Agathotanais *(Peracarida: Tanaidacea)***
Anna Stępień, Piotr Jóźwiak, Aleksandra Jakiel, Alicja Pełczyńska and Magdalena Błażewicz

260 ***Challenges and Advances in the Taxonomy of Deep-Sea Peracarida: From Traditional to Modern Methods***
Inmaculada Frutos, Stefanie Kaiser, Łukasz Pułaski, Maciej Studzian and Magdalena Błażewicz

frontiers | Frontiers in Marine Science

TYPE Editorial
PUBLISHED 12 September 2022
DOI 10.3389/fmars.2022.989245

Check for updates

OPEN ACCESS

EDITED AND REVIEWED BY
Clara F. Rodrigues,
University of Aveiro, Portugal

*CORRESPONDENCE
Stefanie Kaiser
ssm.kaiser@gmail.com

SPECIALTY SECTION
This article was submitted to Deep-Sea Environments and Ecology, a section of the journal Frontiers in Marine Science

RECEIVED 08 July 2022
ACCEPTED 24 August 2022
PUBLISHED 12 September 2022

CITATION
Kaiser S, Błażewicz M, Kocot KM, Leduc D, Riehl T and Rouse GW (2022) Editorial: Recent and emerging innovations in deep-sea taxonomy to enhance biodiversity assessment and conservation.
Front. Mar. Sci. 9:989245.
doi: 10.3389/fmars.2022.989245

COPYRIGHT
© 2022 Kaiser, Błażewicz, Kocot, Leduc, Riehl and Rouse. This is an open-access article distributed under the terms of the Creative Commons Attribution License (CC BY). The use, distribution or reproduction in other forums is permitted, provided the original author(s) and the copyright owner(s) are credited and that the original publication in this journal is cited, in accordance with accepted academic practice. No use, distribution or reproduction is permitted which does not comply with these terms.

Editorial: Recent and emerging innovations in deep-sea taxonomy to enhance biodiversity assessment and conservation

Stefanie Kaiser[1,2,3]*, Magdalena Błażewicz[1], Kevin M. Kocot[4], Daniel Leduc[5], Torben Riehl[3] and Greg W. Rouse[6]

[1]Department of Invertebrate Zoology and Hydrobiology, Laboratory of Polar Biology and Oceanobiology, University of Lodz, Łódź, Poland, [2]INES – Integrated Environmental Solutions UG, Wilhelmshaven, Germany, [3]Department Marine Zoology, Senckenberg Research Institute and Natural History Museum Frankfurt, Frankfurt, Germany, [4]Department of Biological Sciences and Alabama Museum of Natural History, University of Alabama, Tuscaloosa, AL, United States, [5]Oceans Centre, National Institute of Water & Atmospheric Research, Wellington, New Zealand, [6]Scripps Institution of Oceanography, University of California, San Diego, La Jolla, CA, United States

KEYWORDS

taxonomy, deep sea, biodiversity assessment, monitoring, conservation, new species

Editorial on the Research Topic

Recent and emerging innovations in deep-sea taxonomy to enhance biodiversity assessment and conservation

Deep-sea areas that extend from the shelf break down into hadal trenches are vast and cover more than half of the Earth's surface. In the early days of deep-sea exploration, the deep sea was seen as an enormous, dark, and hostile environment barren of life (Tyler, 2003; Danovaro et al., 2014), but it has since become clear that the deep ocean is in fact an environment rich in biodiversity, which provides essential ecosystem services (Cochonat et al., 2007; Armstrong et al., 2012; Thurber et al., 2014). Deep-sea ecosystems are of immense importance for biogeochemical processes and cycles at a global scale (Armstrong et al., 2012), and the latter are inevitably linked to biodiversity (Danovaro et al., 2008). Increasing anthropogenic pressures on deep-sea ecosystems, stemming from resource exploitation, pollution and climate change (Clark and Dunn, 2012; Pham et al., 2014; Sweetman et al., 2017; Smith et al., 2020) will lead to a loss of biodiversity in deep-sea ecosystems, thus affecting their structure and function (e.g., Danovaro et al., 2008; Niner et al., 2018). Therefore, protecting deep-sea biodiversity should be a global concern, and now is the time to grow our knowledge in this area.

Species are a basic unit of biodiversity. Taxonomy, the classification and naming of taxa, is the fundamental science for exploring biodiversity and its drivers, thus underpinning conservation management initiatives. However, with its high undescribed diversity, taxonomy in the deep sea is facing major challenges. Most of the species collected

from greater depths are new to science (Glover et al., 2002; Brandt et al., 2007; Poore et al., 2015). Furthermore, with more sampling and expeditions, also using advanced equipment such as Remotely Operated Vehicles (ROV), help to more (new) species being discovered (Bribiesca-Contreras et al., 2022). This large unknown biodiversity not only impairs adequate estimation of global deep-sea biodiversity, but also poses a great risk that species will be lost before they are even discovered, let alone named. A declining number of taxonomists (a rapidly growing issue known as the taxonomic impediment) further exacerbates the situation (Convention on Biological Diversity [CBD], 2010; Mora et al., 2011; Engel et al., 2021). Deep-sea taxonomy is thus caught between the need to robustly describe species and the implicit requirement to do so as quickly as possible to keep up with ongoing environmental changes.

Our aim for this Research Topic in Frontiers in Marine Science was to bring together studies that advance the taxonomic analysis of deep-sea metazoan species with focus on the application of new methods and approaches. In particular, we sought to highlight the role of taxonomy as a key discipline for understanding and ultimately conserving deep-sea biodiversity. This Research Topic comprises 14 scientific papers that shed light on deep-sea taxonomy from very different perspectives, involving different taxonomic groups and different organizational levels of biodiversity – from genes to ecosystems.

To discriminate species and identify them as known or new to science is the first step in taxonomy. However, even this can often prove very difficult. Traditionally, deep-sea species have been delineated and identified by their morphological appearance. The presence of morphologically identical or similar but genetically distinct species, polymorphisms, ontogenetic plasticity or severe sexual dimorphism have led to incorrect species assignments (e.g., Vrijenhoek, 2009; Brasier et al., 2016; Christodoulou et al., 2020). A number of studies in this Research Topic highlight these issues and provide novel approaches to solving them. Several studies advocate an integrative taxonomic approach as the most robust method for accurately delimiting species. For example, using species' biogeographical or bathymetric distributions, ecological requirements, or phylogenetic origins, can help distinguish between different species. Kürzel et al., for example, combined evidence from morphological and molecular (DNA barcoding and proteomics) analyses of a family of Icelandic isopods with species distribution models to elucidate species boundaries. In particular, they found proteomic fingerprinting to be a promising tool for rapid and inexpensive species differentiation. In addition, the authors recommend the use of interactive keys, so-called multiple-access keys, especially for the identification of deep-sea species, since they are very flexible and can be modified to include newly described species. Frutos et al. present a comprehensive overview of traditional and new methods for peracarid crustacean taxonomy, with a focus on morphological tools, but providing an overarching presentation of molecular genetic methods as part of an integrative practice. Fixation and imaging procedures are presented in great detail. Great importance has been attached to some microscopic techniques, some of which have only rarely been applied to deep-sea species, on the one hand to improve the morphological analysis and on the other hand as a bridge to other biological disciplines. Martínez-Sanjuán et al., used computed microtomography (Micro-CT) for taxonomic research on species in the molluscan class Solenogastres. While it was not possible to obtain a sufficient resolution of some body parts, micro-CT seems to be particularly valuable as a non-destructive technique for morphological analysis in this taxon, and other rare deep-sea animals. Micro-CT thus joins a number of other microscopy techniques, including Confocal Laser Scanning Microscopy (CLSM) or Environmental Scanning Electron Microscopy (ESEM, Frutos et al.), in which the individual specimen is not destroyed but remains available, for example as invaluable collection material for future analyses including, under certain conditions, also for molecular applications. As deep-sea organisms are often only collected in limited numbers, these methods enable high-quality imaging of this precious material, while keeping a voucher as a reference.

In a deep-sea context, one is often confronted with the inability to identify species unequivocally, whether due to damaged specimens, cryptic species or if the species is new to science. Open Nomenclature (ON) procedures are therefore used to make these identifications consistent and thus available for biodiversity data sets (e.g., Sigovini et al., 2016). Prerequisite for this is that a physical specimen is present. However, assessment of the biodiversity of deep-sea megafauna is often based on analysis of still or video images. In their study, Horton et al. provide guidelines for using ON for image-based identifications and its implementation into repositories for biodiversity data. The standardized use of ON is likely to significantly improve the quality and comparability of biodiversity datasets, thereby aiding monitoring of deep-sea biodiversity changes.

Estimates of how many species occur in the deep sea are greatly divergent (Grassle and Maciolek, 1992; May, 1992; Poore and Wilson, 1993) because our view of deep-sea biodiversity is strongly biased – both geographically and taxonomically. Some areas are better sampled than others, e.g. sampling effort in many areas of the North Atlantic is greater than knowledge of the Southern hemisphere (e.g., Howell et al., 2020 and citations therein). Furthermore, species with larger body sizes and wide-ranging distributions tend to be discovered and described earlier, while knowledge about small-bodied, less conspicuous groups and those with restricted ranges is much more limited (Mora et al., 2011; Higgs & Attrill, 2015). As different taxa have been shown to exhibit different biodiversity patterns in the deep sea (e.g., Brandt et al., 2007; Washburn et al., 2021), and small-bodied taxa in particular contribute significantly to overall biodiversity (Hessler and Sanders, 1967;

Rex et al., 2006), a fundamental improvement in our knowledge here is crucial. In this Research Topic, a number of papers focused on understudied geographic regions or taxonomic groups where much more research is required. Kniesz et al. studied scavenging amphipod communities associated with active and inactive hydrothermal vents in the Central and South East Indian Ocean. Since the first vent fields in the Indian Ocean were only discovered at the beginning of this century, they are among the least explored habitats in the deep sea. The authors discovered a rich assemblage of amphipods. Yet, although the region was poorly explored, several species were already known. A vent-endemic fauna could not be inferred with certainty; however, some species appear to be well adapted to the extreme conditions, particularly high temperatures and hypoxia, that prevail at vents. Jażdżewska et al. investigated the distribution of two widespread scavenging amphipod species by means of integrative taxonomy. The authors were able to provide evidence of cosmopolitanism in a species spanning the Atlantic, Pacific and Indian Oceans, while the other species likely represents a complex of six previously undescribed species.

Australia has a very extensive continental slope, but sampling at this depth in the region has been remarkably limited (McCallum et al., 2015; Poore et al., 2015; O'Hara et al., 2020). Very few samples have been taken especially within the Australian Exclusive Economic Zone (EEZ), which has been shown to have a highly diverse fauna (Poore et al., 2015; O'Hara et al., 2020). The focus of the study by Błażewicz et al. were tanaidacean crustaceans of the genus *Pseudotanais* collected from the southern Australian slope. Prior to this, only one species was known from Australian waters, with the authors' new descriptions increasing the number to six. Similar to Australia, national waters of many countries include deep-sea habitats. Yet, although the deep sea is here practically on the doorstep, it is often only little explored (cf. Woodall et al., 2021; Amon et al., 2022). The studies by Stępień et al. and Jóźwiak et al. examining the biodiversity of cumaceans and tanaidaceans along a bathymetric gradient along the Ghanaian slope (West Africa, central Atlantic) help to fill one of these major biogeographic gaps. A high level of diversity was found in both taxa, with most species previously undescribed. In fact, Stępień et al. label the region as a biodiversity hotspot for cumaceans. The region is exposed to hydrocarbon pollution from the oil industry, which poses significant risks to biodiversity.

The discipline of biogeography relies on formally described species (Glover et al., 2018). Grzelak et al. presents a description of a new kinorhynch species collected from hadal depth of the Atacama Trench (SE Pacific), thus contributing to expanding the understanding of biogeographical patterns of isolation and connectivity of the trench fauna. Similarly, the study by Passos et al. focuses on a group that has only been little examined in the deep sea by describing a new species of caudofoveate mollusc from the Brazilian slope. Using species distribution models, their distribution was evaluated in comparison to other congenerics, with strong differences in the ecological requirements and thus in the distribution of the species in this group being identified. Finally, the study by Stępień et al. examined the tandaidacean genus *Agathotanais* from across the Pacific. The authors provided a synopsis of the genus and a description of five new species, bringing the total to 17 species known worldwide, although it is likely that many more exist.

All studies of this Research Topic contributed to the goal of expanding knowledge of deep-sea biodiversity through taxonomy and thus offering tools and/or solutions for deep-sea conservation. To be highlighted here are the studies by Stefanni et al. and Thomas et al. Assessing the impact of human activities on the deep-sea floor requires accurate data on the distribution of biodiversity and its components - populations, species and communities. Due to the spatial and temporal dynamics of deep-sea ecosystems, the collection of long-term data is of crucial importance. Cabled observatories play a key role here, as they can record biodiversity data and relevant environmental parameters continuously and over the long term. Stefanni et al. present an overview of environmental DNA (eDNA) metabarcoding in conjunction with cabled observatories to support deep-sea biodiversity assessment. Due to the high biodiversity in the deep sea, coupled with low specimen numbers and the taxonomic issues of species identification and delineation mentioned above, eDNA metabarcoding is emerging as a very valuable tool for the study and monitoring of deep-sea biodiversity. In particular, the integration of optoacoustic technologies and eDNA seems to very much complement each other to more fully capture deep-sea biodiversity and its changes.

The risk of extinction of deep-sea species due to human activities is very real (Barbier et al., 2014). In addition to mapping and describing deep-sea biodiversity, conservation strategies need to be evaluated. The International Union for Conservation of Nature (IUCN) Red List of Threatened Species is one such tool to increase the visibility of threatened biodiversity and provide objective guidelines for conservation actions by listing species that are endangered or at the brink of becoming extinct. However, Red List criteria have rarely been applied to deep-sea species, although it has proven to be an ideal tool for identifying threats to species and protecting them (Sigwart et al., 2019). Thomas et al. evaluated the Red List status of more than 180 species of hydrothermal molluscs, particularly in light of forthcoming mining activities to exploit deep-sea minerals from these habitats and the associated risks to fauna. Given that only one deep-sea species has previously been Red listed (Sigwart et al., 2019), the study by Thomas et al. is unparalleled by classifying more than 62% of the assessed species as threatened. At the same time, the authors call for genuine conservation measures to protect deep-sea fauna, such as the designation of marine protected areas (MPAs), and, in the absence of sufficient knowledge of the deep-sea biota, advocate a precautionary approach to managing resource exploitation of deep-sea ecosystems and thus safeguarding their high biodiversity.

The destruction of habitats and the depletion of their resources will have unpredictable consequences on the largely undescribed deep-sea biodiversity, with further potential cascading effects on ecosystem functions and services. The articles summarized in this Research Topic each contributed a piece of the puzzle by using taxonomic information to advance our understanding of deep-sea biodiversity. Obviously, many gaps remain, but we think it has been convincingly demonstrated that taxonomic research will continue to play an important role in deep-sea exploration and conservation. Future directions in this discipline include encouraging the development of tools and techniques to describe biodiversity as quickly and accurately as possible, but also identifying ways to ensure stable taxonomy and taxonomic expertise over the long term. The latter concerns enabling the training of future taxonomists, but above all increased funding initiatives as well as employment opportunities for taxonomists. Taxonomy cannot be viewed in isolation, but is a highly integrative field and must remain open to interlinking with other biological disciplines. Similarly, the description of a species is greater than the sum of its parts; "*Every species is a masterpiece, exquisitely adapted to the particular environment in which it has survived. Who are we to destroy or even diminish biodiversity?*" (E.O. Wilson). Taxonomists are passionate about their research and it is also up to them to spread the spark and convey the value and appreciation of the variety of life in the deep sea.

Author contributions

All authors listed have made a substantial, direct and intellectual contribution to the work, and approved it for publication.

Funding

SK acknowledges a grant by the Polish National Agency for Academic Exchange (NAWA) under the ULAM program (PPN/ULM/2019/1/00169).

Acknowledgments

We thank the authors for their contributions on this research topic, the journal for agreeing to its compilation, and the reviewers for their time and effort in improving manuscripts related to deep-sea taxonomic research. This is contribution #6 of the Senckenberg Ocean Species Alliance (SOSA).

Conflict of interest

The authors declare that the research was conducted in the absence of any commercial or financial relationships that could be construed as a potential conflict of interest.

Publisher's note

All claims expressed in this article are solely those of the authors and do not necessarily represent those of their affiliated organizations, or those of the publisher, the editors and the reviewers. Any product that may be evaluated in this article, or claim that may be made by its manufacturer, is not guaranteed or endorsed by the publisher.

References

Amon, D. J., Rotjan, R. D., Kennedy, B. R., Alleng, G., Anta, R., Aram, E., et al. (2022). My deep Sea, my backyard: a pilot study to build capacity for global deep-ocean exploration and research. *Philos. Trans. R. Soc. B* 377 (1854), 20210121. doi: 10.1098/rstb.2021.0121

Armstrong, C. W., Foley, N. S., Tinch, R., and van den Hove, S. (2012). Services from the deep: Steps towards valuation of deep sea goods and services. *Ecosyst. Serv.* 2, 2–13. doi: 10.1016/j.ecoser.2012.07.001

Barbier, E. B., Moreno-Mateos, D., Rogers, A. D., Aronson, J., Pendleton, L., Danovaro, R., et al. (2014). Protect the deep sea. *Nature* 505, 475–477. doi: 10.1038/505475a

Brandt, A., Gooday, A. J., Brandao, S. N., Brix, S., Brökeland, W., Cedhagen, T., et al. (2007). First insights into the biodiversity and biogeography of the southern ocean deep sea. *Nature* 447 (7142), 307–311. doi: 10.1038/nature05827

Brasier, M. J., Wiklund, H., Neal, L., Jeffreys, R., Linse, K., Ruhl, H., et al. (2016). DNA Barcoding uncovers cryptic diversity in 50% of deep-sea Antarctic polychaetes. *R. Soc. Open Sci.* 3 (11), 160432. doi: 10.1098/rsos.160432

Bribiesca-Contreras, G., Dahlgren, T. G., Amon, D. J., Cairns, S., Drennan, R., Durden, J. M., et al. (2022). benthic megafauna of the western clarion-clipperton zone, pacific ocean. *ZooKeys* 1113, 1–110. doi: 10.3897/zookeys.1113.82172

CBD, Secretariat of the Convention on Biological Diversity (2010). Guide to the global taxonomy initiative. *CBD Tech. Ser.* 30 (1–195), i–viii.

Christodoulou, M., O'Hara, T., Hugall, A. F., Khodami, S., Rodrigues, C. F., Hilario, A., et al. (2020). Unexpected high abyssal ophiuroid diversity in polymetallic nodule fields of the northeast pacific ocean and implications for conservation. *Biogeosciences* 17 (7), 1845–1876. doi: 10.5194/bg-17-1845-2020

Clark, M. R., and Dunn, M. R. (2012). Spatial management of deep-sea seamount fisheries: balancing sustainable exploitation and habitat conservation. *Environ. Conserv.* 39 (3), 204–214. doi: 10.1017/S0376892912000021

Cochonat, C., Durr, S., Gunn, K., Herzig, P., Mevel, C., Mienert, J., et al. (2007). *The deep-sea frontier: Science challenges for a sustainable future* (Luxembourg: European Commission. Office CDMA), 53 p. 03/156 B-1049.

Danovaro, R., Gambi, C., Dell'Anno, A., Corinaldesi, C., Fraschetti, S., Vanreusel, A., et al. (2008). Exponential decline of deep seabed ecosystem functioning linked to benthic biodiversity loss. *Curr. Biol.* 18 (1), 1–8. doi: 10.1016/j.cub.2007.11.056

Danovaro, R., Snelgrove, P. V., and Tyler, P. (2014). Challenging the paradigms of deep-sea ecology. *Trends Ecol. Evol.* 29, 465–475. doi: 10.1016/j.tree.2014.06.002

Engel, M. S., Ceríaco, L. M. P., Daniel, G. M., Dellapeí, P. M., Löbl, I., Marinov, M., et al. (2021). The taxonomic impediment: A shortage of taxonomists, not the lack of technical approaches. *Zool. J. Linn. Soc.* 193, 381–387. doi: 10.1093/zoolinnean/zlab072

Glover, A. G., Smith, C. R., Paterson, G. L. J., Wilson, G. D. F., Hawkins, L., and Sheader, M. (2002). Polychaete species diversity in the central pacific abyss: local and regional patterns, and relationships with productivity. *Mar. Ecol. Prog. Ser.* 240, 157–170. doi: 10.3354/meps240157

Glover, A. G., Wiklund, H., Chen, C., and Dahlgren, T. G. (2018). Point of view: managing a sustainable deep-sea 'blue economy' requires knowledge of what actually lives there. *Elife* 7, e41319. doi: 10.7554/eLife.41319.005

Grassle, J. F., and Maciolek, N. J. (1992). Deep-sea species richness: regional and local diversity estimates from quantitative bottom samples. *Am. Nat.* 139 (2), 313–341. doi: 10.1086/285329

Hessler, R. R., and Sanders, H. L. (1967). Faunal diversity in the deep sea. *Deep-Sea Res.* 14, 65–78. doi: 10.1016/0011-7471(67)90029-0

Higgs, N. D., and Attrill, M. J. (2015). Biases in biodiversity: wide-ranging species are discovered first in the deep sea. *Front. Mar. Sci.* 2, 61. doi: 10.3389/fmars.2015.00061

Howell, K. L., Hilário, A., Allcock, A. L., Bailey, D. M., Baker, M., Clark, M. R., et al. (2020). A blueprint for an inclusive, global deep-sea ocean decade field program. *Front. Mar. Sci.* 999. doi: 10.3389/fmars.2020.584861

May, R. (1992). Bottoms up for the oceans. *Nature* 357, 278–279. doi: 10.1038/357278a0

McCallum, A. W., Woolley, S., Błażewicz-Paszkowycz, M., Browne, J., Gerken, S., Kloser, R., et al. (2015). Productivity enhances benthic species richness along an oligotrophic Indian ocean continental margin. *Global Ecol. Biogeo.* 24, 462–471. doi: 10.1111/geb.12255

Mora, C., Tittensor, D. P., Adl, S., Simpson, A. G., and Worm, B. (2011). How many species are there on earth and in the ocean? *PloS Biol.* 9 (8), e1001127. doi: 10.1371/journal.pbio.1001127

Niner, H. J., Ardron, J. A., Escobar, E. G., Gianni, M., Jaeckel, A., Jones, D. O. B., et al. (2018). Deep-sea mining with no net loss of biodiversity–an impossible aim. *Front. Mar. Sci.* 53. doi: 10.3389/fmars.2018.00053

O'Hara, T. D., Williams, A., Ahyong, S. T., Alderslade, P., Alvestad, T., Bray, D., et al. (2020). The lower bathyal and abyssal seafloor fauna of eastern Australia. *Mar. Biodiver. Records* 13 (1), 1–27. doi: 10.1186/s41200-020-00194-1

Pham, C. K., Ramirez-Llodra, E., Alt, C. H., Amaro, T., Bergmann, M., Canals, M., et al. (2014). Marine litter distribution and density in European seas, from the shelves to deep basins. *PloS One* 9 (4), e95839. doi: 10.1371/journal.pone.0095839

Poore, G. C., Avery, L., Błażewicz-Paszkowycz, M., Browne, J., Bruce, N. L., Gerken, S., et al. (2015). Invertebrate diversity of the unexplored marine western margin of Australia: taxonomy and implications for global biodiversity. *Mar. Biodiver.* 45 (2), 271–286. doi: 10.1007/s12526-014-0255-y

Poore, G. C. B., and Wilson, G. D. (1993). Marine species richness. *Nature* 361 (6413), 597–598.

Rex, M. A., Etter, R. J., Morris, J. S., Crouse, J., McClain, C. R., Johnson, N. A., et al. (2006). Global bathymetric patterns of standing stock and body size in the deep-sea benthos. *Mar. Ecol. Prog. Ser.* 317, 1–8.

Sigovini, M., Keppel, E., and Tagliapietra, D. (2016). Open nomenclature in the biodiversity era. *Methods Ecol. Evol.* 7 (10), 1217–1225. doi: 10.1111/2041-210X.12594

Sigwart, J. D., Chen, C., Thomas, E. A., Allcock, A. L., Böhm, M., and Seddon, M. (2019). Red listing can protect deep-sea biodiversity. *Nat. Ecol. Evol.* 3 (8), 1134–1134. doi: 10.1038/s41559-019-0930-2

Smith, C. R., Tunnicliffe, V., Colaço, A., Drazen, J. C., Gollner, S., Levin, L. A., et al. (2020). Deep-sea misconceptions cause underestimation of seabed-mining impacts. *Trends Ecol. Evol.* 35 (10), 853–857. doi: 10.1016/j.tree.2020.07.002

Sweetman, A. K., Thurber, A. R., Smith, C. R., Levin, L. A., Mora, C., Wei, C. L., et al. (2017). Major impacts of climate change on deep-sea benthic ecosystems. *Elementa: Sci. Anthropoc.* 5, 4. doi: 10.1525/elementa.203

Thurber, A. R., Sweetman, A. K., Narayanaswamy, B. E., Jones, D. O., Ingels, J., and Hansman, R. L. (2014). Ecosystem function and services provided by the deep sea. *Biogeosciences* 11 (14), 3941–3963. doi: 10.5194/bg-11-3941-2014

Tyler, P. A. (2003). *Ecosystems of the deep oceans* (Amsterdam: Elsevier Science).

Vrijenhoek, R. C. (2009). Cryptic species, phenotypic plasticity, and complex life histories: assessing deep-sea faunal diversity with molecular markers. *Deep Sea Res. Part II: Topical Stud. Oceanogr.* 56 (19-20), 1713–1723. doi: 10.1016/j.dsr2.2009.05.016

Washburn, T. W., Menot, L., Bonifácio, P., Pape, E., Błażewicz, M., Bribiesca-Contreras, G., et al. (2021). Patterns of macrofaunal biodiversity across the clarion-clipperton zone: An area targeted for seabed mining. *Front. Mar. Sci.* 8. doi: 10.3389/fmars.2021.626571

Woodall, L. C., Talma, S., Steeds, O., Stefanoudis, P., Jeremie-Muzungaile, M. M., and de Comarmond, A. (2021). Co-Development, co-production and co-dissemination of scientific research: a case study to demonstrate mutual benefits. *Biol. Lett.* 17 (4), 20200699. doi: 10.1098/rsbl.2020.0699

frontiers in Marine Science

ORIGINAL RESEARCH
published: 08 February 2021
doi: 10.3389/fmars.2021.620702

Recommendations for the Standardisation of Open Taxonomic Nomenclature for Image-Based Identifications

Tammy Horton[1], Leigh Marsh[2,3,4], Brian J. Bett[1], Andrew R. Gates[1], Daniel O. B. Jones[1], Noëlie M. A. Benoist[1,2], Simone Pfeifer[1,2], Erik Simon-Lledó[1], Jennifer M. Durden[1], Leen Vandepitte[5] and Ward Appeltans[6]*

[1] National Oceanography Centre, Southampton, United Kingdom, [2] Ocean and Earth Science, University of Southampton, Southampton, United Kingdom, [3] Charles Darwin Research Station, Charles Darwin Foundation, Puerto Ayora, Ecuador, [4] Exploration Technology Lab, National Geographic Society, Washington, DC, United States, [5] Flanders Marine Institute (VLIZ), Oostende, Belgium, [6] Ocean Biodiversity Information System (OBIS), IOC Project Office for IODE, Intergovernmental Oceanographic Commission (IOC) of UNESCO, Oostende, Belgium

OPEN ACCESS

Edited by:
Greg W. Rouse, University of California, San Diego, United States

Reviewed by:
Michael Vecchione, National Oceanic and Atmospheric Administration (NOAA), United States
Pedro A. Ribeiro, University of Bergen, Norway

***Correspondence:**
Tammy Horton
tammy.horton@noc.ac.uk
orcid.org/0000-0003-4250-1068

Specialty section:
This article was submitted to Deep-Sea Environments and Ecology, a section of the journal Frontiers in Marine Science

Received: *23 October 2020*
Accepted: *14 January 2021*
Published: *08 February 2021*

Citation:
Horton T, Marsh L, Bett BJ, Gates AR, Jones DOB, Benoist NMA, Pfeifer S, Simon-Lledó E, Durden JM, Vandepitte L and Appeltans W (2021) Recommendations for the Standardisation of Open Taxonomic Nomenclature for Image-Based Identifications. Front. Mar. Sci. 8:620702. doi: 10.3389/fmars.2021.620702

This paper recommends best practice for the use of open nomenclature (ON) signs applicable to image-based faunal analyses. It is one of numerous initiatives to improve biodiversity data input to improve the reliability of biological datasets and their utility in informing policy and management. Image-based faunal analyses are increasingly common but have limitations in the level of taxonomic precision that can be achieved, which varies among groups and imaging methods. This is particularly critical for deep-sea studies owing to the difficulties in reaching confident species-level identifications of unknown taxa. ON signs indicate a standard level of identification and improve clarity, precision and comparability of biodiversity data. Here we provide examples of recommended usage of these terms for input to online databases and preparation of morphospecies catalogues. Because the processes of identification differ when working with physical specimens and with images of the taxa, we build upon previously provided recommendations for specific use with image-based identifications.

Keywords: image-based analysis, taxonomy, identification, nomenclature, standardisation, biodiversity informatics, taxonomic databases

INTRODUCTION

Improved technology and approaches for surveying the marine environment have led to a rapid increase in the number of *in situ* images of both shallow water and deep-sea taxa, that are now being used for biodiversity studies (Durden et al., 2016). The appropriate identification of organisms in these images is critical to scientific, environmental management, and conservation assessments (Durden et al., 2016; Thomson et al., 2018). Increasingly, these image-based methods are being used to supplement or replace traditional approaches, in scientific research, in baseline surveys of an ecosystem, and in repeat monitoring programmes. Such assessments are used to support applications for the industrial extraction of marine resources, e.g., for oil and gas (Gates et al., 2017); seabed mining (Amon et al., 2016; Durden et al., 2018; Simon-Lledó et al., 2020); and

fisheries (Clarke et al., 2009; Murphy and Jenkins, 2010). This approach is also used in conservation assessment (Bean et al., 2017), and in the monitoring of Marine Protected Areas (MPAs; Benoist et al., 2019). In all cases, these efforts require the accurate and repeatable monitoring of biodiversity data (Huvenne et al., 2016).

One major challenge for the identification of organisms in images is a lack of knowledge of the local fauna. Image-based surveys are often used to study remote locations, such as the deep sea, where extensive knowledge of the fauna is often limited (e.g., Jones et al., 2014). In deep-sea regions globally, high proportions of species are new to science, with estimates varying from 35 to 95% (Poore et al., 2015). Consequently, this has led to the development of local or regional field guides (and catalogues) describing the fauna recorded on images or videos, including example images with textual descriptions of the characteristics that helped identify the organisms, frequently without access to corresponding physical specimens (Tilot, 2006; Gowlett-Holmes, 2008; Jones and Gates, 2010; Gervais et al., 2012; HURL, 2013; Jacobsen Stout et al., 2015; National Oceanic and Atmospheric Administration, 2020).

Such catalogues aim to improve consistency between operators and surveys, and provide a morphological taxonomy of the putative taxa encountered (Amon et al., 2017). However, these catalogues lack consistency, are difficult to combine, have missing details, are often only housed locally, and are rarely machine readable without significant additional effort. This greatly reduces the utility of the information from these surveys, and therefore limits their scientific value. There are coordinated international efforts to develop databases and reference guides for the identification of marine species from images within a region. For example, the Standardised Marine Taxon Reference Image Database (SMarTaR-ID) that takes the North Atlantic deep sea as a case study (Howell et al., 2019).

In situ images provide contextual advantages over *ex situ* photographs and preserved specimens, including information about natural habitat, colour in life, behaviour, interspecific associations, and other ecological data (particularly useful for relation of a species to habitat). Additional features from images, such as shadows, may also be useful in detection of taxa and for identification. In some cases, published works contain taxonomic identifications from physical specimens together with corresponding *in situ* photographs, though such works are comparatively rare (Rogacheva et al., 2013).

There are numerous inherent challenges to the identification of taxa from images without a corresponding specimen (Howell et al., 2014, 2019; Durden et al., 2016). For example, image orientation may mean that features normally used for identification with a physical specimen are not visible. Organisms may appear rotated, overturned, and may be retracted or in unusual positions, while sessile animals may have only a single plane of view (e.g., dorsal rather than lateral or ventral), so diagnostic features may be hidden. Particular difficulties arise when diagnostic features are internal or on the ventral or lateral view. Similarly, the quality of the image may impact the identification, and is determined by a number of factors including the environmental conditions (e.g., turbidity and backscatter), distance from the camera to the subject, illumination, camera and/or video settings and platform (e.g., towed-platform, autonomous underwater vehicles, remotely operated vehicles, and baited remote underwater video systems) (Durden et al., 2016). Improvements in platform stability, camera and/or lighting technology may result in different taxonomic resolution between datasets over time (Macreadie et al., 2018). Some image annotation software, commonly used for marine studies, such as the Video Annotation and Reference System (Schlining and Stout, 2006), SQUIDLE+ (Williams and Friedman, 2015) and BIIGLE (Langenkämper et al., 2017), provide tools for recording levels of certainty of identification, such as classifying identifications as 'certain,' 'provisional,' or 'unconfirmed' (Durden et al., 2016), although explanations of these terms and how and when to apply them is lacking.

Given these limitations, it is common practice in the interpretation of image data to identify taxa to a taxonomic level higher than species (e.g., genus, family or higher rank), with individual taxa referred to as 'morphospecies,' 'morphotypes,' or given operational taxonomic unit (OTU) reference codes, rather than conventional taxonomic names. These OTU reference codes are often used instead of binomial Linnaean names to refer to organisms in publications, databases, and morphospecies image catalogues (Althaus et al., 2015; Howell et al., 2019).

Minelli (2019) refers to a 'Galaxy of non-Linnaean names,' outlining the variety of non-Linnaean names currently in use, and the problems arising in biodiversity informatics as a result of the lack of standardisation of their usage. Conventional Linnaean names are governed by codes of nomenclature (the International Code of Zoological Nomenclature (International Commission on Zoological Nomenclature [ICZN], 1999); the International Code of Nomenclature for algae, fungi, and plants (Shenzhen Code), (ICN, Turland et al., 2018); the International Code of Nomenclature of Prokaryotes (ICNP, Parker et al., 2019) and the International Committee on the Taxonomy of Viruses [ICTV, Lefkowitz et al., 2018)]. Minelli (2019) divided non-code compliant names into three groups: (1) open nomenclature; (2) temporary names for undescribed species; and (3) 'mixed lists' where formal Linnaean names are mixed with informal names [e.g., in databases such as the Barcode of Life Data System, BOLD, 2020[1] (Ratnasingham and Hebert, 2007); and GenBank, 2020[2] (Benson et al., 2008)]. Informal names are not currently governed by any code, resulting in a wide array of usage, and greatly complicating attempts to make comparisons between datasets. There are also several issues with the data available in genetic databases, a key one being the increasing number of sequences deposited without reference to formal scientific names, which has resulted in an explosion of 'dark taxa' (Page, 2016). This is a substantial problem that results in the generation of additional 'taxonomic entities' with limited scientific meaning.

Open Nomenclature signs, hereafter ON signs, are commonly used in taxonomic, ecological, and biodiversity studies, and

[1]http://www.boldsystems.org/

[2]https://www.ncbi.nlm.nih.gov/genbank/

are extensively used in the designation of morphospecies and OTUs. They provide a means to explain the uncertainty of an identification. For example, '*Brisinga* sp.' where the addition of the ON sign 'sp.' after the genus name indicates that this entity is identified as a species within the genus *Brisinga*, but that the species is not known (which may be for a variety of reasons). Sigovini et al. (2016) provided a review of the history, a thorough discussion, and an updated list of recommended open nomenclature signs, as well as some preliminary suggestions for the standardisation of their use when a physical specimen is available.

Despite the very useful recommendations by Sigovini et al. (2016) in providing clear definitions of the ON signs in current usage, it has become apparent that the implementation of these terms in practice is not well known or understood by many who use them, particularly those working on image-based identifications. There remains a need for clearer recommendations for the use of ON signs for this purpose. This need for improved guidance in ON use is happening alongside moves toward improved biodiversity data standards to facilitate access to and comparability among datasets online through a variety of openly accessible global databases and is an essential step to ensure that biodiversity data generated from marine images can meet FAIR data principles (Findable, Accessible, Interoperable, and Reuseable; Wilkinson et al., 2016). There are many such efforts underway with guidance on the standardisation of names being discussed and implemented by a variety of global databases and working groups (Welter-Schultes, 2012; Vandepitte et al., 2015, 2018; Horton et al., 2017; TDWG, 2020[3]).

There are several online data repositories holding primary biodiversity data, with differing applications, focussing separately on sequence data or species occurrences (Table 1 in Rabone et al., 2019 provides a comprehensive list and links). These include GenBank and BOLD, Catalogue of Life (CoL[4]; Roskov et al., 2020), the World Register of Marine Species (WoRMS[5]; WoRMS Editorial Board, 2020), the Global Biodiversity Information Facility (GBIF[6]; GBIF, 2020), and the Ocean Biodiversity Information System (OBIS[7]; OBIS, 2020). One of the most commonly used standards for sharing information about biodiversity online is Darwin Core[8] (Wieczorek et al., 2012), which is maintained by the organisation Biodiversity Information Standards (TDWG). The DarwinCore Archives data package (DwC-A) is used for most datasets that are input to biodiversity databases, with most data providers using GBIF's Integrated Publishing Toolkit[9].

In this article we primarily draw on our experiences in dealing with images from the deep-sea environment, where the problems are particularly acute. Nevertheless, the same issues arise throughout the marine, and indeed terrestrial, environment. There are numerous reasons why an image-based identification may not be able to provide any given specimen with a full binomial Linnaean name, our recommendations for ON usage may, therefore, be applicable in numerous applications, from microscopic imagery of the plankton (Culverhouse et al., 2014) to baited stereo-video surveys of fish assemblages (Langlois et al., 2020) to aerial photographs of marine mammals (Schweder et al., 2010).

We present recommendations for the best practice of ON usage for taxon identification from images, including a discussion of usages of ON signs and those to avoid, and suggestions for integration with the Darwin Core. We present a flowchart for decision-making of ON signs to use, and provide clear examples for illustration from marine image datasets.

DIFFERENT USAGES OF ON SIGNS

A Flowchart to Aid ON Sign Selection

In considering the means to standardise the application of ON signs to an identification, it is important to recognise that ON signs are used for a variety of applications (Minelli, 2019). There are currently three main types of ON sign usage employed in association with image-based identification; (1) nomenclature applied to an individual taxon in a single image to be used in a publication and/or for entry to a database in a standardised format (e.g., Darwin Core); (2) nomenclature applied to one or more specimen images in a catalogue or morphospecies guide, with explanations provided in the text (e.g., figure legends, titles of sections on each morphospecies) and; (3) nomenclature applied to a group of specimens for the purposes of data reporting or formation of a data matrix for statistical analysis. In the latter case, this could involve the amalgamation and refinement of the nomenclature applied to associated individual specimens and may include taxonomic roll-up to higher taxonomic ranks (more confident identifications) and/or morphotype complexes. The decision of which ON sign to use may vary depending on the final application.

Sigovini et al. (2016) provided a flow chart to indicate which ON sign should be used for a particular level of certainty in identification. That flow chart can be applied at lower taxonomic ranks of identification (higher resolution/more detail), both when a specimen is available, and for an image-based identification. However, image-based identifications pose their own challenges and are more often made at higher taxonomic ranks (lower resolution/less detail) than identifications of physical specimens. In our assessments of a broad range of deep-sea images and taxa, attempts to employ ON signs to images (using Sigovini et al., 2016) frequently resulted in uncertainties in usage rather than improved clarification and consistency in the datasets. Consequently, we have developed a similar method that has been specifically adjusted to use for image-based identification. The simple flowchart we provide, **Figure 1**, has been trialled and refined by both taxonomic experts and variously experienced image annotators. Following these trials, it is important to note that we now recommend that the usage of certain ON signs should be limited to physical specimens only.

[3]https://www.tdwg.org/
[4]https://www.catalogueoflife.org/
[5]http://www.marinespecies.org/
[6]https://www.gbif.org/
[7]https://obis.org/
[8]https://dwc.tdwg.org/
[9]https://www.gbif.org/ipt

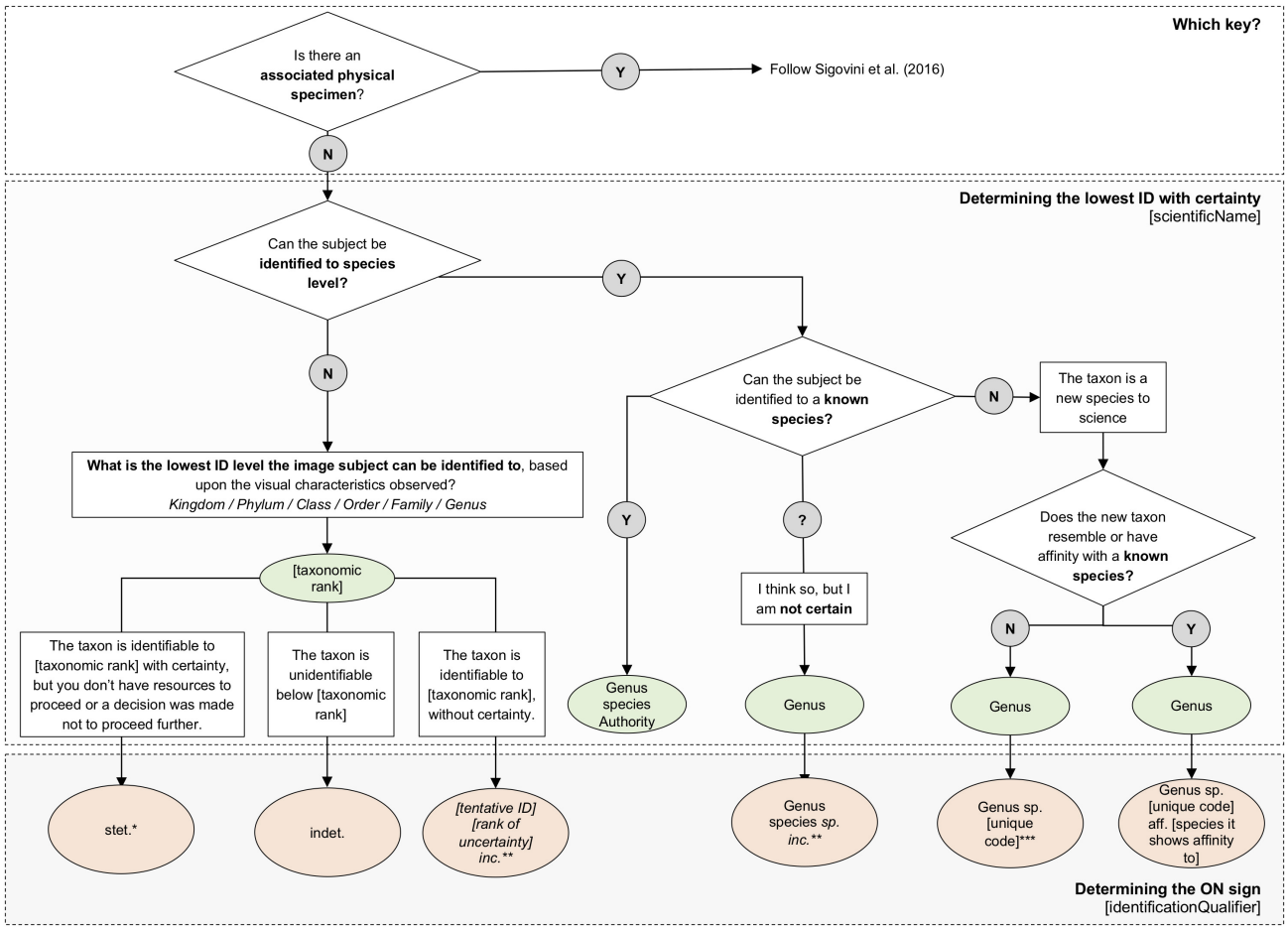

FIGURE 1 | Key steps to identification of taxa in images. The flowchart provides a means to determine the lowest rank of identification with certainty, and provides an example of the ON sign to use in each case. For each ON sign the identifier can check (**Figures 2**, **3**, **5**, **6**) for examples formatted for output in Darwin Core terms. *There are various reasons for using *stet*., which will depend on the operator applying the ON sign. The reason for stopping should be given in the identificationRemarks field, e.g., no experience of ID of this taxon (indicating it may be possible for another identifier with more experience of the group to take the identification further). ***incerta* can be used at any level of the identification (phylum inc., class inc., order inc., fam. inc., gen. inc., sp. inc.). It indicates the identification is not absolutely certain and should be added after the rank of uncertainty (e.g., *Brisinga* gen. inc.; *Brisinga costata* sp. inc.) If uploading the occurrence data to GBIF/OBIS, the lowest taxonomic rank should be entered in the scientificName field and the ON sign in the identificationQualifier field. ***The use of 'sp. nov.' should be avoided for input to the field identificationQualifier as it is required by nomenclatural codes to explicitly indicate a new species, and may also result in non-unique identifiers. The use of a unique sequential, alphanumeric code for new taxa is recommended for entry to the identificationQualifier field (see text and examples in **Figures 2**, **3**, **6**) with further information about the new taxon held in the identificationRemarks field.

Open Nomenclature Signs in Darwin Core Format

Examples of the usage of each ON sign are provided here for input in the Darwin Core format for entry to online databases and for peer-reviewed publications. The Ocean Biodiversity Information System (OBIS) provides a manual for the entry of taxonomic and identification data to Darwin Core in the database fields 'scientificName' and 'identificationQualifier' as follows:

> *"…'scientificName' (required term)… The name should be at the lowest possible taxonomic rank, preferably at species level or lower, but higher ranks, such as genus, family, order, class etc. are also acceptable…The scientificName term should only contain the name and not identification qualifications (such as ?, confer or affinity), which should instead be supplied in the identificationQualifier term…"*[10].

Darwin Core format therefore allows for the incorporation of ON signs in the field identificationQualifier, and also for the inclusion of remarks about an identification in the identificationRemarks field[11]. Darwin Core also includes a taxonConceptID field, defined as "An identifier for the taxonomic concept to which the record refers – not for the nomenclatural details of a taxon", that can be used to form a namestring that combines scientificName and identificationQualifier. In the case of non-code compliant names, the use of a namestring

[10] http://obis.org/manual/darwincore/

[11] dwc.tdwg.org/terms/

or coding that is a combination of the scientificName and the identificationQualifier similarly becomes the taxonConceptID and therefore we recommend this field for these entries. It is most important that these fields are used in a standardised way in biodiversity informatics, in publications, and in field guides or morphospecies catalogues.

We have assessed the number of unique values of these three Darwin Core terms. Currently there are 1,048,576 records from 499 datasets that use at least one of these three DwC terms in OBIS. There are 4315 unique values of identificationQualifier, 411 unique values of identificationRemarks, and 3623 unique values of taxonConceptID.

While we would expect numerous unique values to appear in the identificationRemarks field, it is clear that this field is not very well used. There are very large numbers of unique values in the other two fields suggesting that to date, there has been little attempt to standardise these data.

DISCUSSION OF ON SIGNS TO USE/AVOID FOR IMAGE-BASED IDENTIFICATION

We have provided in **Figures 2**, **3** some clear examples of the recommended usage of open nomenclature and how it should be applied in Darwin Core format. Importantly, the usage in different formats (biodiversity informatics, publications, field guides, and morphospecies catalogues) may drive the decision on which ON sign to use.

Species (Singular), sp.

Species rank is the basic, gold-standard, taxonomic level to which ecological studies generally aspire. However, in many image-based identifications it is not possible to know, with certainty, the species-level identity of an organism. In such cases, the taxon is usually given the ON sign 'sp.' i.e., *Genus* sp. The use of this ON sign alone is discouraged, as it does not indicate the reason that the identification was not determined to the species level. As indicated by Sigovini et al. (2016), we recommend that the term be supplemented with an additional qualifier, either *stet.* (*stetit*) or *indet*. (*indeterminabilis*) [see sections "*Stetit (stet)*" and "*Indeterminabilis (indet.)*]. Where neither of these terms apply, for example in the case of confirmed, but undescribed new species, a unique taxon identifier code (e.g., *Eurythenes* sp. DISCOLL.PAP.JC165.674) should be used. Simple alphanumeric codes are commonly encountered in both publications and databases (i.e., *Eurythenes* sp. 1 or *Eurythenes* sp. A) and should be avoided. Such simple codes are unlikely to remain unique identifiers beyond the dataset in question. By providing a more complex coding system relating to a collection or sample number (for physical specimens), or expedition/dive number/time stamp (for image-based taxa) when combined with the higher taxon, the namestring used becomes a unique identifier for that OTU. Chapman (2005) referred to this issue as 'Domain Schizophrenia' and emphasised the importance of establishing a formula to produce 'unpublished names' that remain unique once databases begin to be combined. For example, the unique species code could take the form adopted by the Australian Botanical community: <*Genus*> sp. <colloquial name or description> (<voucher>): (see Chapman, 2005); or could be formulated as is currently being recommended in the OBIS manual for creating a unique code for the Darwin Core field occurrenceID:

> *"There are no guidelines yet on designing the persistence of this ID, the level of uniqueness (from dataset to global) and the precise algorithm and format for generating the ID, but in the absence of a persistent globally unique identifier, one could be constructed by combining the institutionCode, the collectionCode and the catalogNumber (or autonumber in the absence of a catalogNumber)"* (**Figure 4**).

We therefore recommend that for taxa confirmed as new to science, temporary names be constructed for input to the 'identificationQualifier' field, and where physical specimens are available, the same temporary name should be used on specimen labels, input to museum databases and genetic sequence databases etc. thus facilitating links between these important datasets. The name construction can be managed by using a combination of the institution, museum or collection code (e.g., as found on the Global Registry of Scientific Collections[12]), and the sample number or museum accession number, or a combination of the expedition/dive number/time stamp (for image-based taxa).

Species (Plural) spp.

The ON sign 'spp.' is used to indicate the presence of more than one species of the same genus, whose identification was not achieved (Sigovini et al., 2016). The usage of 'spp.' applied to image-based identifications depends much on the planned output (see section "Different Usages of ON Signs"). In single image identifications for upload to online databases in Darwin Core, usage of 'spp.' is discouraged as clearly a single specimen cannot be identified to multiple species. In these cases, we recommend that, sp. *indet.* [see section "*Indeterminabilis (indet.)*] is used.

For use in morphospecies catalogues or in analyses, Durden et al. (2016) advocate for the use of *spp*. to indicate a species complex, noting that "of forty rockfish species (*Sebastes* spp.), five are visually very similar unless an extreme close-up view of the gill cover and erect dorsal fin are obtained. All five species can be listed as separate terms, along with an additional term '*Sebastes* complex,' for use when species-level identification is not appropriate, but where species-level identification can also contribute to '*Sebastes* complex' quantification."

However, for reporting or analysis purposes, taxa may need to be merged where consistent identification or discrimination of those taxa was not possible across all the images annotated, or to enable comparison with other datasets. For example, two morphotypes can be identified as belonging to the same taxonomic group (e.g., genus or family) based on visible characteristics, but the identifier is unable to distinguish these two morphotypes consistently in the entire set of images, because the distinguishing features are not always visible (e.g., owing

[12]https://www.gbif.org/grscicoll

	Darwin Core Term		Image
Example 1:	**100% confidence**		
Family	scientificName	Pandalidae	
Genus		*Plesionika*	
Species		*trispinus*	
Preferred ON	identificationQualifier	N/A	
Full Temporary name	taxonConceptID	N/A	
Comments on identification	identificationRemarks	Key identifying features including rostrum and colour pattern are clear.	
Example 2:	**Incerta**		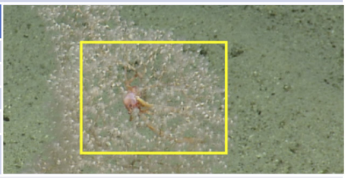
Family	scientificName	Chirostylidae	
Genus		*Uroptychus*	
Species		*compressus*	
Preferred ON	identificationQualifier	sp. inc.	
Full Temporary name	taxonConceptID	*Uroptychus compressus* sp. inc.	
Comments on identification	identificationRemarks	Species of *Uroptychus* are characteristic inhabitants of the soft coral *Chrysogorgia*. *Uroptychus compressus* has been reported in the area of study.	
Example 3:	**Indeterminabilis**		
Family	scientificName	Nematocarcinidae	
Genus		*Nematocarcinus*	
Species		unknown	
Preferred ON	identificationQualifier	sp. indet.	
Full Temporary name	taxonConceptID	*Nematocarcinus* sp. indet.	
Comments on identification	identificationRemarks	The elongate, thread-like legs of this shrimp are easy to see in this photograph. However, the image is were taken too far away to see features of the teeth on the rostrum or the relative length of the rostrum to the carapace and so cannot be identified beyond *Nematocarcinus*.	
Example 4:	**Higher taxon indet.**		
Family	scientificName	Mathildellidae	
Genus		unknown	
Species		unknown	
Preferred ON	identificationQualifier	gen. indet.	
Full Temporary name	taxonConceptID	Mathildellidae gen. indet.	
Comments on identification	identificationRemarks	Appears to be a goneplacoid crab. The overall habitus, aspects of the shape and colouration of the claws and shape of the carapace all fit well with Mathildellidae, based on the author's extensive examination of many species of this group.	
Example 5:	**Higher taxon (two possible families)**		
Superfamily	scientificName	Penaeoidea	
Genus		unknown	
Species		unknown	
Preferred ON	identificationQualifier	fam. indet.	
Full Temporary name	taxonConceptID	Penaeoidea fam. indet.	
Comments on identification	identificationRemarks	Could belong to Aristeidae or Benthesicymidae. It has a short rostrum with teeth and elongate pleopods. The image shows possible white corneas, seen previously amongst the Benthesicymidae. It is not possible to tell if the shrimp in the photograph has true white eyes or the white colour is a reflection from the strobe light.	
Example 6:	**Taxon new to science**		
Family	scientificName	Galatheidae	
Genus		*Janetogalathea*	
Species		unknown	
Preferred ON	identificationQualifier	sp. [unique code] aff. *californiensis*	
Full Temporary name	taxonConceptID	*Janetogalethea* sp. [unique code] aff. *californiensis*	
Comments on identification	identificationRemarks	This crustacean looks much like *J. californiensis* (Baba and Wicksten 1997). If so, it constitutes a major range extension, because previous records of the species are no further south than the Gulf of California, Mexico. To date, there is only one species known of *Janetogalathea*, but the animal in the photograph differs from those previously described, because of the slender fingers of the chelae, without spines. This might be a variant of *J. californiensis* or something undescribed.	

FIGURE 2 | Example usage of the recommended ON signs for image-based identifications and how to format the identification for input to online databases such as OBIS/GBIF in Darwin Core format. Examples images and identifications are provided from Arnés-Urgellés et al. (2020).

	Darwin Core Term	Image 1	=, ≠, or unknown	Image 2
Scenario 1				
Family	scientificName	Freyellidae	=	Freyellidae
Genus		unknown	unknown	unknown
Species		sp.458	≠	sp.460
Preferred ON	identificationQualifier	gen.indet.sp.458	≠	gen.indet.sp.460
Full temporary name	taxonConceptID	Freyellidae gen.indet.sp.458		Freyellidae gen.indet.sp.460
Comments on identification	identificationRemarks	Provide information about how the taxa differ.		Provide information about how the taxa differ.
		e.g. Two clearly different species but unknown genera of Freyellidae are present, 458 and 460.		
Scenario 2				
Family		Munidopsidae	=	Munidopsidae
Genus	scientificName	*Munidopsis*	=	*Munidopsis*
Species		unknown sp.319	≠	unknown sp.328
Preferred ON	identificationQualifier	sp.indet.319		sp.indet.328
Full temporary name	taxonConceptID	*Munidopsis* sp.indet.319		*Munidopsis* sp.indet.328
Comments on identification	identificationRemarks	Provide information about how the taxon differs from *Munidopsis* sp.indet.328		Provide information about how the taxon differs from *Munidopsis* sp.indet.319
		e.g. These images were taken at too great a distance to see fine details of the antennae, spines of the anterior carapace or other distinguishing features. However, they can be determined to belong to different species by the shape of the chelae, the colour and the length of the pereopods.		
Scenario 3		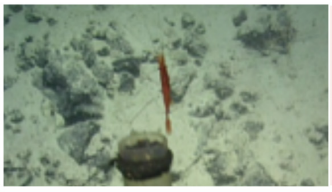		
Family		Nematocarcinidae	=	Nematocarcinidae
Genus	scientificName	*Nematocarcinus*	=	*Nematocarcinus*
Species			unknown	
Preferred ON	identificationQualifier	sp. indet.		sp. indet.
Full temporary name	taxonConceptID	*Nematocarcinus* sp.indet.		*Nematocarcinus* sp.indet.
Comments on identification	identificationRemarks	*Nematocarcinus* have elongate, thread-like legs, barely visible in this image.		The elongate, thread-like legs of this shrimp are easy to see in this photograph.
		e.g. The images were taken too far away to see features of the teeth on the rostrum or the relative length of the rostrum to the carapace cannot be identified beyond *Nematocarcinus.* Furthermore, it cannot be determined whether they are the same species or not		

FIGURE 3 | Examples of more diffcult scenarios encountered in deciding on an image-based identification, and how to format the identification for input to online databases in Darwin Core format. Example scenarios are for two taxa indicating where identification at the taxonomic levels of family, genus, and species, are the same '=,' different '≠' or if this information is unknown. Scenario 1 taxa are reproduced from Buglass et al. (2019). Scenario 2 and 3 images are from Arnés-Urgellés et al. (2020).

to variation in image quality and altitude of the camera). In such cases it is reasonable to merge the taxa to the next higher taxonomic rank (also called taxonomic roll-up) and to label this new merged group, which obviously contains more than one taxon, Family spp. or *Genus* spp. An example of this usage is provided in **Figure 5**.

institutionCode	collectionCode	catalogNumber	occurrenceID
UGhent	NSBS	123	UGhent_NSB_123
UGhent	NSBS	456	UGhent_NSB_456

FIGURE 4 | The recommended method used to construct unique occurrenceID terms for OBIS, from the OBIS Manual (http://obis.org/manual/darwincore/).

	Image 1	Image 2	Image 3	Image 4
[Darwin Core Term]				
Order	Decapoda	Decapoda	Decapoda	Decapoda
Superfamily		Penaeoidea	Penaeoidea	Penaeoidea
Family			Aristeidae	Aristeidae
Genus				*Cerataspis*
Species				*monstrosus*
Preferred ON [identificationQualifier]	indet.	fam. indet.	stet.	-
[scientificName]	Decapoda	Penaeoidea	Aristeidae	*Cerataspis monstrosus*
Full temporary name [taxonConceptID]		Penaeoidea fam. indet.	Aristeidae stet.	-
Comments on identification [identificationRemarks]	Image too blurred/poor quality to allow further identification.	Could belong to Aristeidae or Benthesicymidae. It has a short rostrum with teeth and elongate pleopods. The image shows possible white corneas, seen previously amongst the Benthesicymidae. It is not possible to tell if the shrimp in the photograph has true white eyes or the white colour is a reflection from the strobe light.	I do not have the time or resources to identify further, but I think this could be a species of *Cerataspis*.	
Suggested taxonomic roll-up	Decapoda natant sp. indet.	Penaeoidea sp. indet	Aristeidae spp. indet.	
	-	Penaeoidea spp. indet		
	Decapoda natant spp. indet.			

FIGURE 5 | An example of the different levels of certainty of an identification as applied to different images of the same possible taxon, along with recommended ON signs for each. Image 1 and 2 are from Arnés-Urgellés et al. (2020), Image 3 is reproduced with permission from the National Geographic Society's Exploration Technology Lab, and Image 4 is from NOAA Offce of Ocean Exploration and Research Benthic Deepwater Animal Identification Guide (https://www.ncei.noaa.gov/waf/okeanos-animal-guide/Dendrobranchiata006.html).

Similarly, in the case of an image catalogue, where a series of photographed specimens of two or more taxa that cannot be discriminated confidently are provided, the use of spp. is reasonable. In these cases, the series of photographed specimens is provided with an identification qualifier, such as *Colus* spp., to indicate that there are two (or more) known species in the region and these taxa cannot be separated with confidence, and is usually accompanied by some notes indicating the difficulties

of image-based identification, along with further information about the known species in the region (Jones and Gates, 2010; Fourt et al., 2017; Stefanoudis et al., 2018).

Higher Taxa

Sigovini et al. (2016) indicate the use of fam. sp. and fam. gen. sp. (which can also be abbreviated to e.g., Zoarcidae sp. and Nematoda sp.), which has the same ON sign meaning as 'sp.' alone, and indicates that the taxon has not been identified beyond that higher taxonomic rank. For greater consistency of datasets, since *Genus* sp. without an explanatory ON sign is discouraged, so are Zoarcidae gen. sp. or Nematoda fam. gen. sp. as there is no indication as to why the identification stopped at that level, and therefore, should not be input to the identificationQualifier field. This may be particularly important for image-based identification, as confident taxonomic identification is often limited to higher taxonomic ranks than are possible if we have a specimen at hand, better image resolution, or different planes of view. In such cases, we recommend that *stet., inc.,* or *indet*. are incorporated into the identificationQualifier [see sections "*Stetit (stet),*" "*Indeterminabilis (indet.)*, and "*Incerta (inc.)*"].

Stetit (stet.)

This ON sign means it stood/stays or remained here, indicating the identification stopped at this taxonomic rank. *Stetit* can be employed for a variety of reasons, which require clarification. It may be used in the sense of Sigovini et al. (2016), indicating that it is a *choice* to go no further, i.e., "I called this taxon 'Ostracoda *stet*.' because I did not attempt to identify the ostracods any further; I simply noted they were ostracods and stopped there."

Alternatively, the identifier may have been unable to take the identification further, so the identification stayed at that rank, i.e., "I called this taxon 'Ostracoda *stet*.' because although I made every attempt to identify the ostracods to a lower taxonomic rank, I did not have the expertise/time/identification resources available, so Ostracoda was the lowest rank to which I could identify the taxon."

In many cases, image annotators will be providing identifications for images across a range of phyla, and by using '*stet.*' in a dataset, image-based identifications with this ON sign can then be easily collated, and sent to a taxonomic expert who may be able to provide a more precise identification to a lower taxonomic rank. It is therefore important that the reason for stopping is recorded, this can be via the identificationRemarks field, or in the text of a morphospecies catalogue, e.g., 'no experience in identifying this taxon' (indicating it is possible to take the identification further). In cases where the identifier wishes to indicate that the same (or another) image annotator or indeed an expert taxonomist would be unable to identify the same image-based taxon further, then the ON sign should be '*indet.*' [see section "*Indeterminabilis (indet.)*"].

Indeterminabilis (indet.)

We follow the recommendation of Sigovini et al. (2016) that the ON sign *indet*. is taken to mean that the taxon is indeterminable beyond a certain taxonomic level. For the cases considered by Sigovini et al. (2016), this inability to identify a specimen further was considered to result from to the deterioration or lack of diagnostic characters, particularly in the case of damaged material or partial specimens. This is also equally relevant to image-based identifications, where diagnostic characters are often not visible or resolvable in the image, which could be owing to the resolution of the image, or the orientation of the taxon in the field of view. This ON sign can be applied at any taxonomic rank.

Incerta (inc.)

Sigovini et al. (2016) recommended the ON sign '*inc*.' to indicate 'uncertain identification' and to replace the use of the question mark symbol '?' which is considered as a variable character (wildcard) by most computing software. In image-based identifications, this ON sign can be used at all taxonomic levels (e.g., Aristidae fam. *inc.*), while it is less likely to be used at higher taxonomic ranks when a physical specimen is available. *Incerta* differs from *indeterminabilis* [see section "*Indeterminabilis (indet.)*"] which is used where the identifier cannot identify further as the characters are not visible/present, whereas *incerta* is to be used where characters are visible, but the identification remains uncertain. Even if the taxon in an image is clearly identifiable, absolute certainty may not always be possible. *Incerta* can be used at any level of the identification and since it indicates the identification is not absolutely certain, it should be added after the rank of uncertainty (e.g., *Chimaera* gen. inc.; *Hydrolagus trolli* sp. inc.). The choice of which taxonomic rank to enter into the scientificName field will depend on the level of certainty of the identifier. We have provided 2 examples of the possible different entries that may be needed for an 'image annotator' versus a 'taxonomic expert' in **Figure 6**. Such distinctions will allow these tentative identifications to be easily collated for later identification by an expert, as for the '*stet*.' example.

Species affinis (sp. aff.)

Imaged specimens are commonly identifiable to an entity close to, or with an affinity to, a known taxon (family, genus or species), but with clear distinction from it. This ON sign is often used in the taxonomic literature to signify that the identifier believes the taxon to be a new species, such as '*Eurythenes* sp. nov. aff. *sigmiferus*'. We recommend that the term 'sp. nov.' is not used in the identificationQualifier field, which, as indicated in Sigovini et al. (2016), is a nomenclatural act. Although use of this ON sign in online datasets and catalogues does not make a name available with respect to the current codes of nomenclature (International Commission on Zoological Nomenclature [ICZN], 1999; ICN, Turland et al., 2018; ICNP, Parker et al., 2019), we recommend that the terms 'sp. nov.' and 'sp. nov. aff.' be avoided to prevent confusion. Information about the potential new-to-science taxon may be included in the identificationRemarks field. The terms may be used in published papers and morphospecies catalogues, where a taxon is believed to be new but is not described, as this commonly occurs with image-based identifications, particularly in deep-sea studies (Pawson et al., 2015). The examples in Pawson et al. (2015) are written as *Paroriza* ? new species, which could cause problems if input in this format to global biodiversity databases. Therefore, we recommend that confirmed new taxa

	Darwin Core Term	Image 1	=, ≠, or unknown	Image 2
Scenario 1a **Image annotator**				
Family	scientificName	Goniasteridae	=	Goniasteridae
Genus		uncertain	≠	uncertain
Species		sp.572	≠	sp.533
Preferred ON	identificationQualifier	gen.inc.sp.572		gen.inc.sp.533
Full temporary name	taxonConceptID	Goniasteridae gen.inc.sp.572		Goniasteridae gen.inc.sp.533
Comments on identification	identificationRemarks	**Image annotator** – this could possibly be *Hippasteria* genus, but I am not confident.		**Image annotator** – this could possibly be *Evoplosoma* gen. inc. but I am not confident.
Scenario 1b **Taxonomic expert**				
Family	scientificName	Hippasteria	=	Evoplosoma
Genus		uncertain	≠	uncertain
Species		sp.572	≠	sp.533
Preferred ON	identificationQualifier	gen.inc.sp.572		gen.inc.sp.533
Full temporary name	taxonConceptID	*Hippasteria* gen.inc.sp.572		*Evoplosoma* gen.inc.sp.533
Comments on identification	identificationRemarks	**Taxonomic expert** – this is most likely *Hippasteria* genus, but since I do not have a specimen to confirm, I have used gen.inc.		**Taxonomic expert** – this is most likely *Evoplosoma* genus, but since I do not have a specimen to confirm, I have used gen.inc.

FIGURE 6 | Examples of how to format the identification for input to online databases in Darwin Core format for an image annotator vs. taxonomic expert identification. Example scenarios are for two taxa indicating where identification at the taxonomic levels of family, genus, and species are the same '=,' different '≠,' or if this information is unknown. Image 1 and 2 are reproduced from Buglass et al. (2019).

should be amended to the format *Paroriza* sp. [unique123] aff. *pallens*, including a description of why the taxon differs from *P. pallens* (Koehler, 1895) and is considered new to science, in the identificationRemarks field or in the text, as in Pawson et al. (2015). Duffy et al. (2016) referred to '*Paracallisoma* sp. 6' and there is a discussion in the text indicating that it is likely to be a new taxon. The simple alphanumeric code used by the authors is not recommended [see section "Species (Singular), sp."]; a better option would have been '*Paracallisoma* sp. DISCOLL.56761'. Using a unique namestring for probable new taxa when referring to them in publications and databases, allows a consistent means of referring to them and allows them to be clearly referenced in later papers, including in the synonymy of a new species description, and to provide links between datasets.

Confer (cf.)

As indicated in Sigovini et al. (2016), *cf.* is from the Latin *confer*, meaning to be compared with. The use of this ON indicates that the identifier cannot be certain of the identity of the species (or higher taxonomic rank) until a more detailed comparison can be made, for example with some type or reference material, or to consult a taxonomic expert.

This ON sign is very widely used in image-based identifications to indicate that the identifier believes the species to be similar, or most likely equates to a certain species (or higher taxonomic rank) but they cannot say for certain without further study of more images or a physical specimen. Since the terms *cf.* and *aff.* are often confused and their current usage is inconsistent, the term *cf.* is discouraged in application to image-based identifications, and in particular for use in online datasets. Where diagnostic features are unclear, the lowest level of identification should be moved up a rank to, e.g., *Calamocrinus* sp. indet. (or *Calamocrinus diomedae* sp. inc.) instead of *Calamocrinus* cf. *diomedae*, and the information regarding the likely identity of the species should be included in the identificationRemarks field and/or in the corresponding text section of an image catalogue.

There are cases where *confer* is used for image-based identifications in the true sense. In Simon-Lledó et al. (2019) the image of *Bathystylodactylus* is referred to as *Bathystylodactylus* cf. *echinus*, and this is because a specimen was available and even after study of the specimen, and consultation with a taxonomic expert, the authors determination remained that comparison with more material was indeed necessary (pers. comm. Sammy De Grave, Oxford University Natural History Museum).

DISCUSSION

When identifying taxa from images, there are numerous challenges (Durden et al., 2016), but the decisions on how to indicate a standard level of identification, enabling comparisons between datasets have not been explored in detail to date. There will always be a degree of uncertainty with taxon identifications solely from images (i.e., without a corresponding specimen), and while this cannot be eliminated from image-based biodiversity datasets, the provision of a robust decision mechanism to standardise and clarify the uncertainty will improve the subsequent use and comparability of datasets.

In this article, we recommend the use of consistent open nomenclature, as commonly applied with physical specimens, and recently updated and clarified by Sigovini et al. (2016) to provide a robust set of standard terms for use in image-based identifications.

Today numerous published datasets and papers make use of ON signs. Yet, there is currently much confusion and little evidence of standardisation in the usage of these ON signs, or even explanations as to what is meant by them. The current lack of standardisation presents a clear risk for the future use of many datasets.

There are some good examples of consistent use of ON signs, or at least, clear explanations of the usage in particular cases. For example, Glover et al. (2016) in their paper on the Echinodermata from the Clarion-Clipperton Zone, indicate that for a species "similar to a morphologically well-defined species name where we lack comparable genetic data from type material or from the type locality, or when genetic data previously published in Genbank is incompatible with ours, we use the open nomenclature expression "cf."." In their dataset, the morphological identifications are provided with a clear coding, e.g., Asteroidea sp. (NHM_054) or *Freyastera* cf. *benthophila*, the meaning of which is clearly defined in the text of their paper.

The decision on which ON to use in image-based identifications can be difficult, particularly so when working with taxonomic experts, accustomed to making species-level determinations and to using ON signs for physical specimens. In cases where the expert taxonomic opinion is 'I cannot be certain, as I cannot see the necessary morphological characters, but it looks most like the species *Xus yus*.' then that taxon must be regarded as *indeterminabilis*, it cannot be determined further, and should be recorded as *Xus* indet. However, the use of *Xus* cf. *yus* is regularly seen being used for such cases with image-based identifications, and this ON usage should be discouraged.

As we have detailed in this article (see section "Discussion of ON Signs to Use/Avoid for Image-Based Identification"), appropriate and consistent use of open nomenclature and Darwin Core terms enables both: (a) secure biodiversity data consistent with the FAIR principles (Wilkinson et al., 2016) – Findable, Accessible, Interoperable, and Reuseable; and (b) the ability to capture and record additional information on potential identifications and putative new taxa without compromising the immediate reusability of initial standardised identifications.

In the case of the image-based identifications of deep-sea taxa from which we have developed our ideas, we recommend the uniform banking of such data with the Ocean Biodiversity Information System. It is clear from our brief analysis of the current usage of the relevant Darwin Core terms in OBIS, that there is already a critical need to provide guidance on the unambiguous and standardised entry of ON signs into the right data fields. Annotation software could incorporate these ON signs to facilitate outputs with suitable references to the certainty of identifications in images. Our recommendations are equally applicable in comparable shallow-water operations, and indeed in non-marine settings. We hope that this article will help both taxonomic experts and image analysts to make informed choices in applying ON signs in the future, and thus improve the quality, comparability, and longevity of biodiversity datasets.

DATA AVAILABILITY STATEMENT

The datasets generated for this study can be found in online repositories. The names of the repository/repositories and accession number(s) can be found in the article/ supplementary material.

AUTHOR CONTRIBUTIONS

TH and LM jointly conceived the ideas for manuscript. All authors defined the scope of manuscript. TH and LM wrote the initial outline. LM and WA undertook data analysis and contributed figures. All authors contributed to the writing and editing process.

FUNDING

TH, BB, DJ, NB, JD, and AG were funded by Climate Linked Atlantic Section Science (CLASS) programme (NE/R015953/1) supported by United Kingdom Natural Environment Research Council (NERC) National Capability funding to the National Oceanography Centre. JD and AG were supported by NERC grant NE/S009426/1 "Sustained autonomous environmental monitoring of offshore oil fields" and the EU Horizon 2020 Project "EMSO-Link" grant ID 731036. LV was supported by the Flemish Contribution to LifeWatch Belgium, funded through the Research Foundation Flanders (FWO). DJ received funding through the One Ocean Hub, a collaborative research for sustainable development programme funded by United Kingdom Research and Innovation through the United Kingdom Global Challenges Research Fund under NERC grant NE/S008950/1. SP was supported by the United Kingdom Natural Environmental Research Council (grant number NE/L002531/1), and a CASE studentship 'Collaborative Awards in Science and Engineering.'

ACKNOWLEDGMENTS

The authors would like to thank the attendees of the Deep-Sea Taxonomy Workshop held in May 2019 in Frankfurt, and attendees of the International Seabed Authority Taxonomic

Workshop, September 2020, for their contribution to discussions on this topic. The authors are also grateful to the scientific team, taxonomic experts and volunteers working on the Seamounts Research Project at the Charles Darwin Foundation and members of the Deep-sea Research Project at the National Geographic Society's Exploration Technology Lab for their valuable contributions to discussions on the use of the suggested ON signs for image-based analysis in newly explored regions of the deep ocean. Images from the Galapagos and have been reproduced with permission and were obtained from the Ocean Exploration Trusts expedition NA064 under research permits PC-26–15 and PC-45-15 granted by the Galapagos National Park. This publication is contribution number (2382) of the Charles Darwin Foundation for the Galapagos Islands.

REFERENCES

Althaus, F., Hill, N., Ferrari, R., Edwards, L., Przeslawski, R., Schonberg, C. H. L., et al. (2015). A standardised vocabulary for identifying benthic biota and substrata from underwater imagery: the CATAMI classification scheme. *PLoS One* 10:e0141039.

Amon, D., Ziegler, A., Dahlgren, T., Glover, A. G., Goineau, A., and Gooday, A. J. (2016). Insights into the abundance and diversity of abyssal megafauna in a polymetallic-nodule region in the eastern Clarion-Clipperton Zone. *Sci. Rep.* 6:30492. doi: 10.1038/srep30492

Amon, D., Ziegler, A., Kremenetskaia, A., Mah, C., Mooi, R., O'Hara, T., et al. (2017). Megafauna of the UKSRL exploration contract area and eastern Clarion-Clipperton Zone in the Pacific Ocean: echinodermata. *Biodiv. Data J.* 5:e11794. doi: 10.3897/bdj.5.e11794

Arnés-Urgellés, C., Buglass, S., Ahyong, S., Salinas-de-León, P., Wicksten, M., and Marsh, L. (2020). Arthropoda; crustacea; decapoda of deep-sea volcanic habitats of the galapagos marine reserve, tropical eastern pacific. *Biodiv. Data J.* 8:e54482. doi: 10.3897/BDJ.8.e54482

Bean, T. P., Greenwood, N., Beckett, R., Biermann, L., Bignell, J. P., Brant, J. L., et al. (2017). A review of the tools used for marine monitoring in the UK: combining historic and contemporary methods with modeling and socioeconomics to fulfill legislative needs and scientific ambitions. *Front. Mar. Sci.* 4:263. doi: 10.3389/fmars.2017.00263

Benoist, N. M. A., Morris, K. J., Bett, B. J., Durden, J. M., Huvenne, V. A. I., Le Bas, T. P., et al. (2019). Monitoring multiple biotopes in a marine conservation zone by autonomous underwater vehicle. *Conserv. Biol.* 33, 1174–1186. doi: 10.1111/cobi.13312

Benson, D. A., Karsch-Mizrachi, I., Lipman, D. J., Ostell, J., and Wheeler, D. L. (2008). GenBank. *Nucleic Acids Res.* 36, D25–D30. doi: 10.1093/nar/gkm929

BOLD (2020). *The Barcode of Life Data System*. Available at https://www.boldsystems.org/ (accessed September 23, 2020).

Buglass, S., Arnés-Urgellés, C., Marsh, L., and Nagy, S. (2019). *Macroinvertebrate Groups Found on Deep-Sea Volcanic Habitats in the Galapagos Marine Reserve in the Eastern Tropical Pacific Ocean: Echinoderms. Version 1.9*, Puerto Ayora: Charles Darwin Research Station, doi: 10.15468/zigswe Occurrence dataset.

Chapman, A. D. (2005). *Principles and Methods of Data Cleaning – Primary Species and Species-Occurrence Data, Version 1.0*. Copenhagen: Report for the Global Biodiversity Information Facility.

Clarke, M. E., Tolimieri, N., and Singh, H. (2009). "Using the seabed AUV to assess populations of groundfish in untrawlable areas," in *The Future of Fisheries Science in North America*, Vol. 31, eds R. J. Beamish and B. J. Rothschild (Netherlands: Springer), 357–372. doi: 10.1007/978-1-4020-9210-7_20

Culverhouse, P. F., Macleod, N., Williams, R., Benfield, M. C., Lopes, R. M., and Picheral, M. (2014). An empirical assessment of the consistency of taxonomic identifications. *Mar. Biol. Res.* 10, 73–84. doi: 10.1080/17451000.2013.810762

Duffy, G., Lawler, S., and Horton, T. (2016). Scavenging amphipods of the Angolan deep-sea habitat, with a focus on *Abyssorchomene distinctus* Birstein & Vinogradov, 1955. *J. Crust. Biol.* 36, 417–426. doi: 10.1163/1937240X-00002448

Durden, J. M., Lallier, L. E., Murphy, K., Jaeckel, A., Gjerde, K., and Jones, D. O. B. (2018). Environmental impact assessment process for deep-sea mining in 'the Area'. *Mar. Policy* 87, 194–202. doi: 10.1016/j.marpol.2017.10.013

Durden, J. M., Schoening, T., Althaus, F., Friedman, A., Garcia, R., Glover, A. G., et al. (2016). Perspectives in visual imaging for marine biology and ecology: from acquisition to understanding. *Oceanogr. Mar. Biol. Annu. Rev.* 54, 1–72. doi: 10.5281/zenodo.202685

Fourt, M., Goujard, A., Pérez, T., and Chevaldonné, P. (2017). *Guide de la Faune Profonde de la mer Méditerranée : Explorations des Roches et Canyons Sous-Marins des côtes FRANÇAISES*. Paris: Muséum National d'Histoire Naturelle, 184.

Gates, A. R., Benfield, M. C., Booth, D. J., Fowler, A. M., Skropeta, D., and Jones, D. O. B. (2017). Deep-sea observations at hydrocarbon drilling locations: contributions from the SERPENT Project after 120 field visits. *Deep Sea Res. II* 137, 463–479. doi: 10.1016/j.dsr2.2016.07.011

GBIF (2020). *The Global Biodiversity Information Facility (2020) What is GBIF?*. Available online at: https://www.gbif.org/what-is-gbif (accessed September 23, 2020).

GenBank (2020). *GenBank*. Available online at: https://www.ncbi.nlm.nih.gov/genbank/ (accessed September 23, 2020).

Gervais, F., Lemieux, N., Juniper, K., and Matabos, M. (2012). *Marine Life Field Guide*. Victoria: NEPTUNE Canada.

Glover, A., Wiklund, H., Rabone, M., Amon, D., Smith, C., O'Hara, T., et al. (2016). Abyssal fauna of the UK-1 polymetallic nodule exploration claim, Clarion-Clipperton Zone, central Pacific Ocean: echinodermata. *Biodivers. Data J.* 4:e7251. doi: 10.3897/BDJ.4.e7251

Gowlett-Holmes, K. (2008). *A Field Guide to the Marine Invertebrates of South Australia*. Tasmania: Notomares, 333.

Horton, T., Gofas, S., Kroh, A., Poore, G. C. B., Read, G., Rosenberg, G., et al. (2017). Improving nomenclatural consistency: a decade of experience in the World Register of Marine Species. *Eur. J. Taxon.* 389, 1–24. doi: 10.5852/ejt.2017.389

Howell, K. L., Bullimore, R. D., and Foster, N. L. (2014). Quality assurance in the identification of deep-sea taxa from video and image analysis: response to Henry and Roberts. *ICES J. Mar. Sci.* 71, 899–906. doi: 10.1093/icesjms/fsu052

Howell, K. L., Davies, J. S., Allcock, A. L., Braga Henriques, A., Buhl-Mortensen, P., Carreiro-Silva, M., et al. (2019). A framework for the development of a global standardised marine taxon reference image database (SMarTaR-ID) to support image-based analyses. *PLoS One* 14:e0218904. doi: 10.1371/journal.pone.0218904

HURL (2013). University of Hawai'i Undersea Research Laboratory, Deep-sea Animal Identification Guide. Available at http://www.soest.hawaii.edu/HURL/HURLarchive/guide.php (accessed September 23, 2020).

Huvenne, V. A. I., Bett, B. J., Masson, D. G., Le Bas, T. P., and Wheeler, A. J. (2016). Effectiveness of a deep-sea cold-water coral Marine Protected Area, following eight years of fisheries closure. *Biol. Conserv.* 200, 60–69. doi: 10.1016/j.biocon.2016.05.030

International Commission on Zoological Nomenclature [ICZN] (1999). *International Code of Zoological Nomenclature. Fourth Edition*. London: The International Trust for Zoological Nomenclature.

Jacobsen Stout, N., Kuhnz, L., Lundsten, L., Schlining, B., Schlining, K., and von Thun, S. (2015). *The Deep-Sea Guide (DSG)*. Moss Landing, CA: Monterey Bay Aquarium Research Institute (MBARI).

Jones, D. O. B., and Gates, A. R. (2010). *Deep-sea life of Scotland and Norway*. Ophiura: Southampton.

Jones, D. O. B., Walls, A., Clare, M., Fiske, M. S., Weiland, R. J., O'Brien, R., et al. (2014). Asphalt mounds and associated biota on the Angolan margin. *Deep Sea Res. Part I Oceanogr. Res. Pap.* 94, 124–136. doi: 10.1016/j.dsr.2014.08.010

Koehler, R. (1895). Dragages profonds exécutés à bord du *Caudan* dans le golfe de Gascogne (Août-Septembre 1895). Ů Rapport préliminaire sur les Échinodermes. *Revue Biologique du Nord de la France* 7, 439–496.

Langenkämper, D., Zurowietz, M., Schoening, T., and Nattkemper, T. W. (2017). BIIGLE 2.0 - browsing and annotating large marine image collections. *Front. Mar. Sci.* 4:83. doi: 10.3389/fmars.2017.00083

Langlois, T., Goetze, J., Bond, T., Monk, J., Abesamis, R. A., Asher, J., et al. (2020). A field and video annotation guide for baited remote underwater stereo-video

surveys of demersal fish assemblages. *Methods Ecol. Evol.* 11, 1401–1409. doi: 10.1111/2041-210X.13470

Lefkowitz, E. J., Dempsey, D. M., Hendrickson, R. C., Orton, R. J., Siddell, S. G., and Smith, D. B. (2018). Virus taxonomy: the database of the international committee on taxonomy of viruses (ICTV). *Nucleic Acids Res.* 46, D708–D717. doi: 10.1093/nar/gkx932

Macreadie, P. I., McLean, D. L., Thomson, P. G., Partridge, J. C., Jones, D. O. B., Gates, A. R., et al. (2018). Eyes in the sea: unlocking the mysteries of the ocean using industrial, remotely operated vehicles (ROVs). *Sci. Total Environ.* 634, 1077–1091. doi: 10.1016/j.scitotenv.2018.04.049

Minelli, A. (2019). The galaxy of the non-Linnaean nomenclature. *History Philos. Life Sci.* 41:31. doi: 10.1007/s40656-019-0271-0

Murphy, H. M., and Jenkins, G. P. (2010). Observational methods used in marine spatial monitoring of fishes and associated habitats: a review. *Mar. Freshw. Res.* 61, 236–252. doi: 10.1071/MF09068

National Oceanic and Atmospheric Administration (2020). Office of Ocean Exploration and Research Benthic Deepwater Animal Identification Guide V3. Available online at: http://oceanexplorer.noaa.gov/okeanos/animal_guide/animal_guide.html (accessed September 23, 2020).

OBIS (2020). *Ocean Biodiversity Information System*. Paris: Intergovernmental Oceanographic Commission.

Page, R. D. M. (2016). DNA barcoding and taxonomy: dark taxa and dark texts. *Philos. Trans. R. Soc. B* 371:20150334. doi: 10.1098/rstb.2015.0334

Parker, C. T., Tindall, B. J., and Garrity, G. M. (eds) (2019). International code of nomenclature of prokaryotes, prokaryotic Code (2008 Revision). *Int. J. Syst. Evol. Microbiol.* 69, S1–S111. doi: 10.1099/ijsem.0.000778

Pawson, D. L., Nizinski, M. S., Ames, C. L., and Pawson, D. J. (2015). Deep-sea echinoids and holothurians (Echinodermata) near cold seeps and coral communities in the northern Gulf of Mexico. *Bull. Mar. Sci.* 91, 167–204. doi: 10.5343/bms.2014.1064

Poore, G. C. B., Avery, L., Błazewicz-Paszkowycz, M., Browne, J., Bruce, N. L., Gerken, S., et al. (2015). Invertebrate diversity of the unexplored marine western margin of Australia: taxonomy and implications for global biodiversity. *Mar. Biodivers.* 45, 271–286. doi: 10.1007/s12526-014-0255-y

Rabone, M., Harden-Davies, H., Collins, J. E., Zajderman, S., Appeltans, W., Droege, G., et al. (2019). Access to marine genetic resources (MGR): raising awareness of best-practice through a new agreement for biodiversity beyond national jurisdiction (BBNJ). *Front. Mar. Sci.* 6:520. doi: 10.3389/fmars.2019.00520

Ratnasingham, S., and Hebert, P. D. N. (2007). BOLD: the barcode of life data system (www.barcodinglife.org). *Mol. Ecol. Notes* 7, 355–364. doi: 10.1111/j.1471-8286.2006.01678.x

Rogacheva, A., Gebruk, A., and Alt, C. H. S. (2013). Holothuroidea of the charlie gibbs fracture zone area, northern mid-atlantic ridge. *Mar. Biol. Res.* 9, 587–623. doi: 10.1080/17451000.2012.750428

Roskov, Y., Ower, G., Orrell, T., Nicolson, D., Bailly, N., Kirk, P. M., et al. (2020). *Species 2000 & ITIS Catalogue of Life, 2020-09-01 Beta*. Leiden: Naturalis.

Schlining, B. M., and Stout, N. J. (2006). *MBARI's Video Annotation and Reference System. OCEANS 2006*. Boston, USA: IEEE, 1–5.

Schweder, T., Sadykova, D., Rugh, D., and Koski, W. (2010). Population estimates from aerial photographic surveys of naturally and variably marked bowhead whales. *J. Agric. Biol. Environ. Stat.* 15, 1–19. doi: 10.1007/s13253-009-0002-1

Sigovini, M., Keppel, E., and Tagliapietra, D. (2016). Open nomenclature in the biodiversity era. *Methods Ecol. Evol.* 7, 1217–1225. doi: 10.1111/2041-210X.12594

Simon-Lledó, E., Bett, B. J., Huvenne, V. A. I., Schoening, T., Benoist, N. M. A., Jeffreys, R. M., et al. (2019). Megafaunal variation in the abyssal landscape of the Clarion-Clipperton Zone. *Prog. Oceanogr.* 170, 119–133. doi: 10.1016/j.pocean.2018.11.003

Simon-Lledó, E., Pomee, C., Ahokava, A., Drazen, J. C., Leitner, A. B., Flynn, A., et al. (2020). Multi-scale variations in invertebrate and fish megafauna in the mid-eastern Clarion Clipperton Zone. *Prog. Oceanogr.* 187:102405. doi: 10.1016/j.pocean.2020.102405

Stefanoudis, P. V., Smith, S. R., Schneider, C., Wagner, D., Goodbody-Gringley, G., Xavier, J., et al. (2018). *Deep Reef Benthos of Bermuda: Field Identification Guide*. Oxford: Nekton, 168. doi: 10.6084/m9.figshare.7333838

TDWG (2020). *Biodiversity Information Standards (TDWG)*. Available at https://www.tdwg.org/ (accessed September 23, 2020).

Thomson, S. A., Pyle, R. L., Ahyong, S. T., Alonso-Zarazaga, M., Ammirati, J., Araya, J. F., et al. (2018). Taxonomy based on science is necessary for global conservation. *PLoS Biol.* 16:e2005075. doi: 10.1371/journal.pbio.2005075

Tilot, V. (2006). *Biodiversity and Distribution of Megafauna. Vol. 1: The Polymetallic Nodule Ecosystem of the Eastern Equatorial Pacific Ocean; Vol. 2: Annotated Photographic Atlas of the Echinoderms of the Clarion-Clipperton Fracture Zone*. Paris: UNESCO/IOC. (IOC Technical Series, 69).

Turland, N. J., Wiersema, J. H., Barrie, F. R., Greuter, W., Hawksworth, D. L., Herendeen, P. S., et al. (eds) (2018). *International Code of Nomenclature for Algae, Fungi, and Plants (Shenzhen Code) Adopted by the Nineteenth International Botanical Congress Shenzhen, China, July 2017*. Glashütten: Koeltz Botanical Books, doi: 10.12705/Code.2018 Regnum Vegetabile 159.

Vandepitte, L., Vanhoorne, B., Decock, W., Dekeyzer, S., Trias Verbeeck, A., Bovit, L., et al. (2015). How Aphia—the platform behind several online and taxonomically oriented databases—can serve both the taxonomic community and the field of biodiversity informatics. *J. Mar. Sci. Eng.* 3, 1448–1473. doi: 10.3390/jmse3041448

Vandepitte, L., Vanhoorne, B., Decock, W., Vranken, S., Lanssens, T., Dekeyzer, S., et al. (2018). A decade of the world register of marine species - general insights and experiences from the data management team: where are we, what have we learned and how can we continue? *PLoS One* 13:e0194599. doi: 10.1371/journal.pone.0194599

Welter-Schultes, F. W. (2012). *Guidelines for the Capture and Management of Digital Zoological Names Information. Version 1.1, Released on March 2013*. Copenhagen: Global Biodiversity Information Facility, 126.

Wieczorek, J., Bloom, D., Guralnick, R., Blum, S., Döring, M., Giovanni, R., et al. (2012). Darwin core: an evolving community-developed biodiversity data standard. *PLoS One* 7:e29715. doi: 10.1371/journal.pone.0029715

Wilkinson, M., Dumontier, M., Aalbersberg, I., Appleton, G., Axton, M., Baak, A., et al. (2016). The FAIR Guiding Principles for scientific data management and stewardship. *Sci. Data* 3:160018. doi: 10.1038/sdata.2016.18

Williams, S., and Friedman, A. (2015). *SQUIDLE. Sydney*. Sydney, NSW: University of Sydney.

WoRMS Editorial Board (2020). *World Register of Marine Species*. Available at http://www.marinespecies.org at VLIZ (accessed September 22, 2020).

Conflict of Interest: The authors declare that the research was conducted in the absence of any commercial or financial relationships that could be construed as a potential conflict of interest.

Copyright © 2021 Horton, Marsh, Bett, Gates, Jones, Benoist, Pfeifer, Simon-Lledó, Durden, Vandepitte and Appeltans. This is an open-access article distributed under the terms of the Creative Commons Attribution License (CC BY). The use, distribution or reproduction in other forums is permitted, provided the original author(s) and the copyright owner(s) are credited and that the original publication in this journal is cited, in accordance with accepted academic practice. No use, distribution or reproduction is permitted which does not comply with these terms.

frontiers in Marine Science

ORIGINAL RESEARCH
published: 04 June 2021
doi: 10.3389/fmars.2021.670735

Hadal Mud Dragons: First Insight Into the Diversity of Kinorhyncha From the Atacama Trench

Katarzyna Grzelak[1,2], Daniela Zeppilli[3], Mauricio Shimabukuro[3,4] and Martin V. Sørensen[2]*

[1] Marine Ecology Department, Institute of Oceanology, Polish Academy of Sciences, Sopot, Poland, [2] Natural History Museum of Denmark, University of Copenhagen, Copenhagen, Denmark, [3] Laboratoire Environnement Profond, Institut Français de Recherche pour l'Exploitation de la Mer (IFREMER), Plouzané, France, [4] Nordcee and HADAL, Department of Biology, University of Southern Denmark, Odense, Denmark

Deep-sea trenches are one of the last frontiers for deep-sea exploration and represent a large reservoir of undiscovered biodiversity. This applies in particular to organisms belonging to smaller-size classes, such as meiofauna. Among different meiofauna taxa, kinorhynchs represent a large gap in our knowledge about global marine biodiversity in general, but primarily in extreme deep-sea environments. Out of the more than 300 known mud dragon species, only a single species has ever been described from hadal depths (> 6000 m), i.e., *Echinoderes ultraabyssalis* from the Kuril-Kamchatka Trench. The results presented in this paper are based on material collected during a research expedition in 2018 investigating the Atacama Trench environment. We provide a first overview and comparison of the diversity and abundance of mud dragons in the Atacama Trench, the adjacent abyssal plain and continental slope off Chile. The study revealed six species of *Echinoderes*. Of these, *Echinoderes mamaqucha* sp. nov. is described as a new species and morphological data of three undescribed species are given. Because of the low number of available specimens, we provide only a brief description of these three species and comparison with their morphologically closest congeners, but formal descriptions are not given. Moreover, *Echinoderes juliae* and *Echinoderes pterus* were also recovered. *Echinoderes juliae* was described from the abyssal plain off Oregon and along the continental rise off California, at 2702 to 3679 m depth. *Echinoderes pterus* is known from the high Arctic, the North Atlantic, and the Mediterranean Sea, and has also been reported to show a wide bathymetric distribution, from 675 to 4403 m. Interestingly, *E. mamaqucha* sp. nov. dominated at the trench stations and it reached its highest abundance at the deepest station, at 8085 m water depth. The only other single individual that was found in the Atacama Trench was *Echinoderes* sp.1. The remaining four species were all found at the abyssal and slope stations. The obtained results seem to confirm previous hypotheses about geographic isolation of deep-sea trenches and relatively low connectivity with other habitats, reflected by limited diversity of sediment dwelling fauna, particularly in the deepest parts of trenches.

Keywords: deep-sea, meiofauna, *Echinoderes mamaqucha*, new species, taxonomy

OPEN ACCESS

Edited by:
Torben Riehl,
Senckenberg Museum, Germany

Reviewed by:
Birger Neuhaus,
Museum of Natural History Berlin (MfN), Germany
Christoph Plum,
University of Oldenburg, Germany

****Correspondence:***
Katarzyna Grzelak
kgrzelak@iopan.gda.pl

Specialty section:
This article was submitted to Deep-Sea Environments and Ecology, a section of the journal Frontiers in Marine Science

Received: *22 February 2021*
Accepted: *07 May 2021*
Published: *04 June 2021*

Citation:
Grzelak K, Zeppilli D, Shimabukuro M and Sørensen MV (2021) Hadal Mud Dragons: First Insight Into the Diversity of Kinorhyncha From the Atacama Trench. Front. Mar. Sci. 8:670735. doi: 10.3389/fmars.2021.670735

INTRODUCTION

Kinorhynchs, small meiobenthic organisms with retractable, scalid-covered head and segmented trunk, also known as mud dragons, are exclusively marine invertebrates that occur mostly in muddy or fine-grained sandy sediments, from the shallow waters to the hadal depths (Neuhaus, 2013). A clearer picture of kinorhynch fauna, diversity and community structure at shallower depths is emerging (Sørensen et al., 2012; Yamasaki et al., 2012; Dal Zotto and Todaro, 2016; Landers et al., 2018, 2020; Cepeda et al., 2019a,b; Grzelak and Sørensen, 2019a,b), but knowledge about mud dragons at abyssal (3000–6000 m) and hadal depths (>6000 m) [for definition of depth zone see Harris et al. (2014) and Jamieson et al. (2010)] is still extremely limited. This is mostly due to the remoteness of the deep-sea ecosystem, technical difficulties in obtaining reliable samples and scarcity of taxonomic expertise.

Deep-sea trenches can reach depths of 11000 m and their geomorphological features (funnel-like topography, very steep walls, and high hydrostatic pressure) constitute a challenge for logistics and equipment, and thus a serious constrain for biodiversity studies of these habitats (Jamieson et al., 2010). However, information from trenches is essential not only to understand bathymetric patterns in diversity and their regulatory mechanisms in deep-sea environments, but also overall of marine biodiversity and biogeography. These habitats may provide new insights into the factors shaping distribution patterns at the deep-sea floor and modify existing ecological paradigms. Trenches are separated from each other by remoteness spaces at abyssal depths, what might support high level of species endemism (Belyaev, 1989). In terms of meiofauna taxa, this statement still needs to be verified.

Hadal trenches remain the least studied and their kinorhynch fauna is almost completely unexplored, as we so far only know about a single identified hadal species, *Echinoderes ultraabyssalis* Adrianov and Maiorova (2019), described from 9411–9540 m water depth in the Kuril-Kamchatka Trench (Adrianov and Maiorova, 2019). The only other known records of kinorhynchs from hadal depths are the finding of an unidentified specimen of *Echinoderes* from 9000 m in the Kermadec Trench (unpublished finding by D. Leduc, see Zeppilli et al., 2018) and unidentified kinorhynchs from 7200 m in the Atacama Trench, reported by Danovaro et al. (2002).

The first kinorhynch identified from abyssal depth was *Fissuroderes rangi* Neuhaus and Blasche (2006) described from the Hikurangi Plateau east of New Zealand at 3202 m water depth by Neuhaus and Blasche (2006). A few years later Neuhaus and Sørensen (2013) reported *Campyloderes* cf. *vanhoeffeni* Zelinka (1913) in the Guinea Basin at 5064 m and in the southeastern deep-sea region of Canary Island at depths between 5055 m and 5118 m. Sánchez et al. (2014a,b) described three additional species, *i.e.*, *Mixtophyes abyssalis* Sánchez et al. (2014a,b), *Cristaphyes nubilis* (Sánchez et al., 2014a,b), and *Krakenella farinelli* (Sánchez et al., 2014a,b), from the Guinea Basin, at depths between 5100–5175 m. The remaining and more recent reports of identified abyssal kinorhynchs are restricted to five areas: (1) abyssal plains, 3100–3300 m, around North Atlantic seamounts, from where Yamasaki et al. (2019) describe *Echinoderes kaempfae* Yamasaki et al., 2019; (2) the East Mediterranean, 675–4403 m, from where Yamasaki et al. (2018a) describe *Echinoderes pterus* Yamasaki et al., 2018a,b; (3) abyssal plains, 3351–5766, in the vicinity of the Kuril-Kamchatka Trench, from where Adrianov and Maiorova (2015, 2016, 2018a,b) describe *Cristaphyes abyssorum* (Adrianov and Maiorova, 2015), *Condyloderes kurilensis* Adrianov and Maiorova (2016), *Meristoderes okhotensis* Adrianov and Maiorova (2018a), and *Parasemnoderes intermedius* Adrianov and Maiorova (2018b); (4) the abyssal plains, 3250–3853 m, off the Northwest American continental slope, from where Sørensen et al. (2018) describe *E. anniae, E. dubiosus, E. hamiltonorum, E. juliae, E. lupherorum, E. hviidarum, E. yamasakii*, and Sørensen et al. (2018, 2019) report three additional known kinorhynch species, *E.* cf. *unispinosus* Yamasaki et al. (2018a,b), *Fissuroderes higginsi* Neuhaus and Blasche (2006), and *C. kurilensis*; (5) the Clarion-Clipperton Fracture Zone, 4319–5012 m, in the tropical East Pacific, from where Sánchez et al. (2019) describe *Cephalorhyncha polunga, Echinoderes shenlong,* and *Meristoderes taro*.

The present contribution is the result of studies of kinorhynchs found in samples collected during Cruise SO261, which took place in 2018, in the Atacama Trench region, as part of the multidisciplinary HADES European Research Council (HADES-ERC) study of deep trench systems. Previous studies conducted in the Atacama Trench established the presence of abundant metazoan meiofauna community (Danovaro et al., 2002, 2003) and protozoan Foraminifera (Sabbatini et al., 2002). Despite the fact, that meiobenthos is a key component of benthic fauna inhabiting the Atacama Trench, biodiversity studies have been conducted only for nematodes (Gambi et al., 2003). The main purpose of this study is to provide the first assessment of the species richness and distribution of Kinorhyncha in the Atacama Trench and the adjacent abyssal plain. Here, we contribute with the description of a new species of *Echinoderes*, the second deepest kinorhynch species described so far. Furthermore, we provide detailed morphological data of three additional undescribed species and report two known species.

MATERIALS AND METHODS

Study Area

The study area is located in the Atacama Trench, part of the Peru-Chile Trench system, which is the longest trench of the Pacific Ocean, stretching for almost 6000 km along the coast of Peru and Chile (**Figure 1**). The Atacama Trench is narrower than other Pacific trenches (64 km in width), and with a maximum depth of 8065 m it is the deepest trench of the East Pacific and tenth deepest trench in the world (Jamieson et al., 2010). The Atacama Trench was formed by the subduction of the Nazca and Antarctic plates beneath the continental South American Plate. It is a seismically active area, resulting in occasional gravity-driven sediment slides

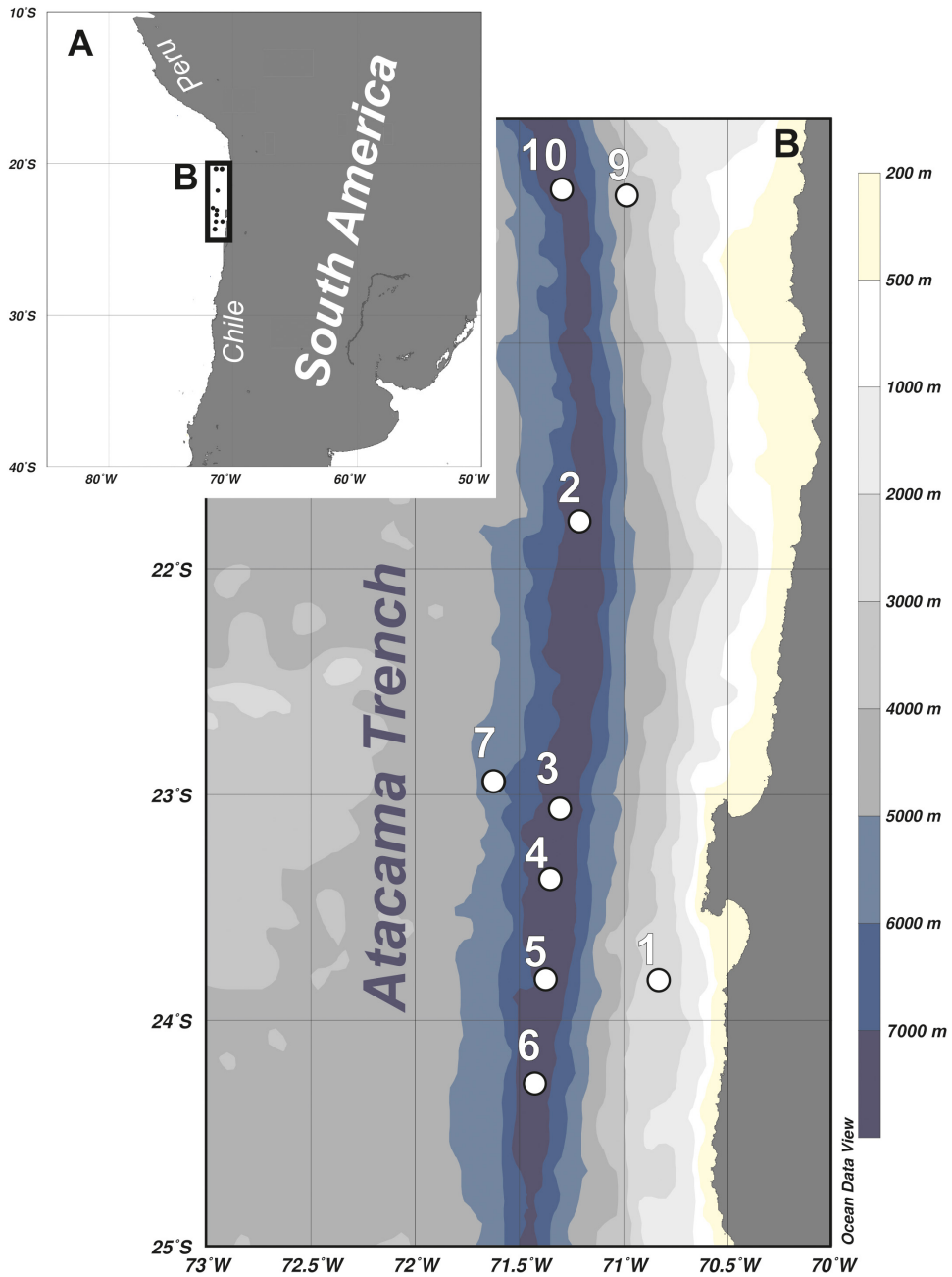

FIGURE 1 | Maps showing location of the Atacama Trench area **(A)** and detailed overview of the sampling stations **(B)**.

(Lemenkova, 2019). The Atacama Trench is located in an area with significant upwelling events that lead to high primary production (Fossing et al., 1995).

Sample Collection and Preparation

The sampling was undertaken in March 2018, during the cruise (SO261) with German research vessel RV '*Sonne*,' within a framework of the multidisciplinary HADES European Research Council (HADES-ERC) study of deep trench systems. A multi-corer with tubes of 9 cm internal diameter was used to retrieve bottom sediment from six stations arranged along the 450-km transect in the Atacama Trench (stations 2 to 6, and 10) and three stations located at the abyssal plain (7) and continental slope (1 and 9) off the Atacama Trench (**Table 1** and **Figure 1**). From each deployment, three cores were taken from the MUC and subsampled for meiofauna analysis (5 cm in length and 2.9 cm in diameter). The samples were fixed with 4% buffered formaldehyde. In the laboratory samples were washed with freshwater in a 20 μm sieve and meiofauna organisms were extracted using centrifugation

TABLE 1 | Coordinates and basic data of sampling stations and *Echinoderes* species identities; total no of kino.- total number of processed kinorhynchs (adults and juveniles), species- species identity, together with number of recorded *Echinoderes* adult specimens, LM-light microscopy, SEM-scanning electron microscopy, NHMD-no – Natural History Museum of Denmark catalog number.

Station	Location	Date	Latitude (S)	Longitude (W)	Depth (m)	Total no of kino.	Species	Mounting	NHMD-no
1	continental slope	06.03.2018	23° 48.72′	70° 50.04′	2560	4	*E. juliae* (1),	LM	NHMD-872652
							Echinoderes sp. 3 (1)	LM	NHMD-872651
2	trench	23.03.2018	21° 46.86′	71° 12.48′	7994	12	*E. mamaqucha* sp. nov. (3)	LM + SEM	NHMD-872645-46
3	trench	17.03.2018	23° 02.94′	71° 18.12′	7915	11	*E. mamaqucha* sp. nov. (2)	LM + SEM	NHMD-872647
4	trench	14.03.2018	23° 21.78′	71° 20.60′	8085	26	*E. mamaqucha* sp. nov. (10)	LM + SEM	NHMD-872636-43
5	trench	11.03.2018	23° 49.02′	71° 22.32′	7770	14	*E. mamaqucha* sp. nov. (2)	LM	NHMD-872648-49
6	trench	08.03.2018	24° 15.96′	71° 25.38′	7720	12	*E. mamaqucha* sp. nov. (2)	LM + SEM	NHMD-872635
							Echinoderes sp.1 (1)	LM	NHMD-872653
7	abyssal plain	20.03.2018	22° 56.22′	71° 37.08′	5500	5	*E. mamaqucha* sp. nov. (1)	LM	NHMD-872650
							Echinoderes sp. 2 (1)	LM	NHMD-872654
9	continental slope	28.03.2018	20° 19.97′	70° 58.70′	4050	5	*E. pterus* (1)	SEM	
10	trench	26.03.2018	20° 19.14′	71° 17.46′	7770	7	*E. mamaqucha* sp. nov. (1)	LM	NHMD-872644

with LUDOX solution, following the standard protocol (Vincx, 1996). Kinorhynchs were picked up and stored in a 4% formaldehyde solution. For preparation of light microscopy (LM) slides, specimens were dehydrated through a graded series of glycerine and mounted in Fluoromount-G. The specimens were examined with an Olympus BX51 microscope with differential interference contrast, and photographed with an Olympus DP27 camera. Measurements were made with Cell^D software. Line art figures were made with Adobe Illustrator CS6. Specimens for scanning electron microscopy (SEM) were dehydrated through a graded alcohol-acetone series and critical point dried. Dried specimens were mounted on aluminum stubs, sputter coated with a platinum/palladium mix and examined with a JEOL JSM-6335F Field Emission scanning electron microscope.

All specimens were identified to species level, except for the juveniles. Identification of kinorhynchs to species level was based on the relevant taxonomic literature (Herranz et al., 2018; Sørensen et al., 2018; Yamasaki et al., 2018b, 2020; Adrianov and Maiorova, 2019).

RESULTS

Systematics

Class Cyclorhagida Zelinka (1896) *sensu* Sørensen et al. (2015)

Order Echinorhagata Sørensen et al. (2015)

Family Echinoderidae Carus (1885)

Genus *Echinoderes* Claparède (1863)

Echinoderes mamaqucha sp. nov.

ZooBank.org lsid: zoobank.org:pub:1A9867FF-1C58-4F17-A869-F7534B262518.

Material Examined

Holotype

Adult female, collected on March 8, 2018 at station 6 (**Figure 1** and **Table 1**), from 7720 m depth, in the Atacama Trench (24°15.96′S 71°25.38′W), mounted in Fluoromount-G, deposited at the Natural History Museum of Denmark, under catalog number NHMD-872635.

Paratypes

Eleven females and four males collected at stations (station 2, 3, 4, 5, 7, 10) located along the Atacama Trench axis (**Figure 1** and **Table 1**), mounted in Fluoromount-G, deposited at the Natural History Museum of Denmark (NHMD-872636 to NHMD-872650).

Additional Material

Four females and one male mounted for SEM and stored in the personal collection of MVS.

Etymology

The species name refers to Mama Qucha, sea- and fish goddess in Inca Mythology, protectress of sailors, and Sea Mother.

Diagnosis

Echinoderes with middorsal acicular spines on segments 4 to 8, and in lateroventral positions on segments 6 to 9. Tubes present in subdorsal and ventrolateral positions on segment 2, lateroventral positions on segment 5, lateral accessory positions on segment 8 and laterodorsal positions on segment 10; tubes on segment 2 very short and truncate.

Description

Adults with head, neck and eleven trunk segments (**Figures 2A,B**, **3A**, **4A**). Overview of measures and dimensions are given in **Table 2**. Distribution of cuticular structures, i.e., sensory spots, glandular cell outlets, spines and tubes, is summarized in **Table 3**.

The head consists of a retractable mouth cone and an introvert (**Figure 4B**). The external mouth cone armature consists of nine outer oral styles, each composed of two joined units, arranged as one style anterior to each introvert sector, except the middorsal sector 6; each outer oral style with basal fringe consisting of six spinous tips. The introvert was partly retracted in one specimen, and otherwise fully retracted in remaining ones; hence information was only available for the anteriormost scalid

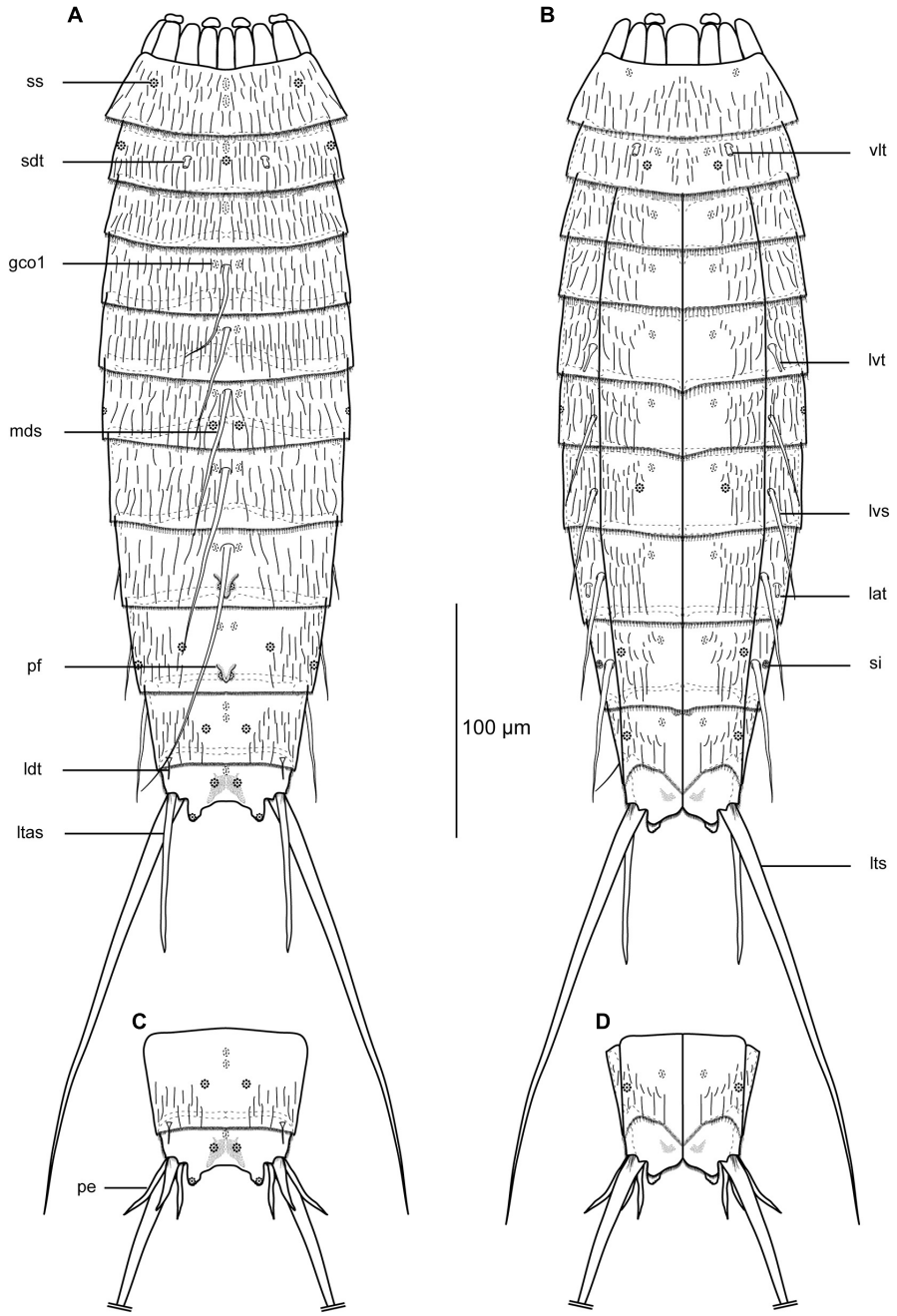

FIGURE 2 | Line art illustrations of *Echinoderes mamaqucha* sp. nov. **(A)** female, dorsal view; **(B)** female ventral view; **(C)** male, segments 10–11, dorsal view; **(D)** male, segments 10–11, ventral view. *gco1*, glandular cell outlet type 1; *lat*, lateral accessory tube; *ldt*, laterodorsal tube; *ltas*, lateral terminal accessory spine; *lts*, lateral terminal spine; *lvs*, lateroventral spine; *lvt*, lateroventral tube; *mds*, middorsal spine; *pe*, penile spines; *pf*, papillary flap; *sdt*, subdorsal tube; *si*, sieve plate; *ss*, sensory spot; vlt, ventrolateral tube.

rings. Ten primary spinoscalids present, each consisting of a basal sheath and a distal end piece with a blunt tip. The sheaths have two distinctively differentiated transverse fringes: a most basal fringe with fringe tips attaching to the surface of the scalid, and a slightly more distal fringe where the fringe tips emerge from a transverse furrow; distal to this second fringe, the sheath has a dense hair cover. End pieces are smooth and flexible. Ring 02 has 10 spinoscalids, and Ring 03 has 20. All spinoscalids in these rings are well-developed, and consist of a basal sheath and a pointed end piece; the basal sheaths of spinoscalids in both rings terminate into fine, fringed margins, whereas those of Ring 03 have in addition a strong, basal median spike (**Figure 4B**). The number of spinoscalids and their exact morphology could not be determined posterior to Ring 3.

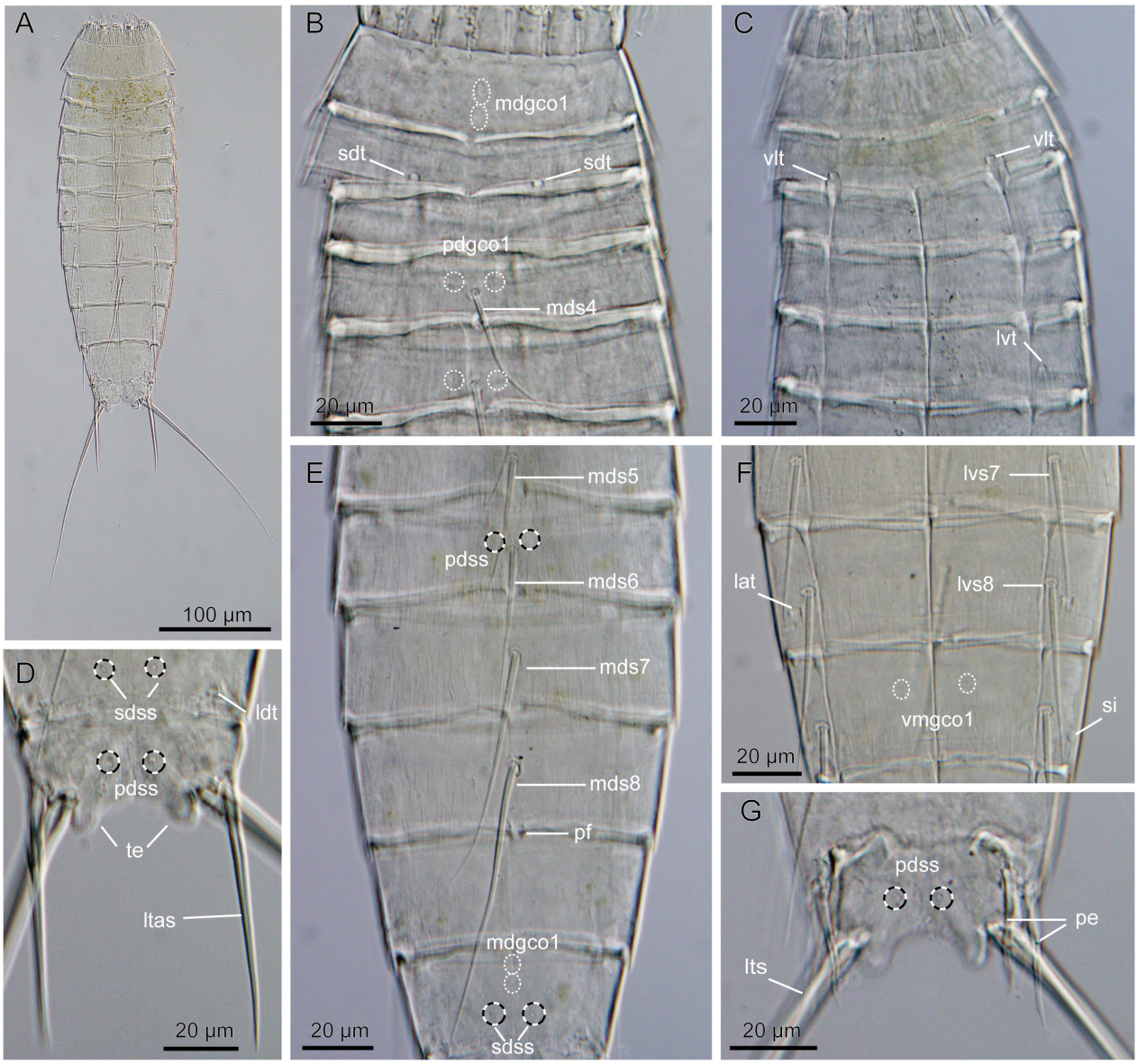

FIGURE 3 | Light micrographs showing overview and details of *Echinoderes mamaqucha* sp. nov. **(A,D–F)** Female holotype (NHMD-872635). **(B,G)** Male paratype (NHMD-872636). **(C)** Female paratype (NHMD-872641). **(A)** Ventral overview. **(B)** Segments 1 to 5, dorsal view. **(C)** Segments 1 to 5, ventral view. **(D)** Segments 10 to 11, dorsal view. **(E)** Segments 5 to 10, dorsal view. **(F)** Segments 7 to 9, ventral view. **(G)** Segments 10–11, dorsal view. *lat*, lateral accessory tube; *ldt*, laterodorsal tube; *lts*, lateral terminal spine; *ltas*, lateral terminal accessory spine; *lvs*, lateroventral spine, followed by segment number; *lvt*, lateroventral tube; *mdgco1*, middorsal glandular cell outlet type 1; *mds*, middorsal spine, followed by segment number; *pdgco1*, paradorsal glandular cell outlet type 1; *pdss*, paradorsal sensory spot; *pe*, penile spine; *pf*, papillary flap; *sdss*, subdorsal sensory spot; *sdt*, subdorsal tube; *si*, sieve plate; *te*, tergal extension; *vlt*, ventrolateral tube; *vmgco1*, ventromedial glandular cell outlet type 1.

Neck with 16 placids. Midventral placid broadest, 12 µm in width and 18 µm in length. Remaining placids narrower, 9 µm in width and 17 µm in length, similar in size. Four dorsal and two ventral trichoscalid plates are present, each carrying a thick and bushy trichoscalid.

Segment 1 consists of a complete cuticular ring (**Figures 2A,B**, **3B,C**, **4A,C,D**). One pair of sensory spots is located in laterodorsal positions, anterior on the segment, but not at anterior margin. Sensory spots on this and following segments small and rounded, with numerous micropapillae surrounding a central pore (**Figures 4C,D,F–H**). Two longitudinally arranged glandular cell outlets type 1 present in middorsal position, and one additional pair present in lateroventral positions (**Figures 4C,D**). Cuticular hairs relatively well-spaced, distributed evenly around the segment, except in hairless ventromedial areas on anterior segment half (**Figures 4C,D**). Posterior segment margin almost straight, forming a pectinate fringe; pectinate fringe tips

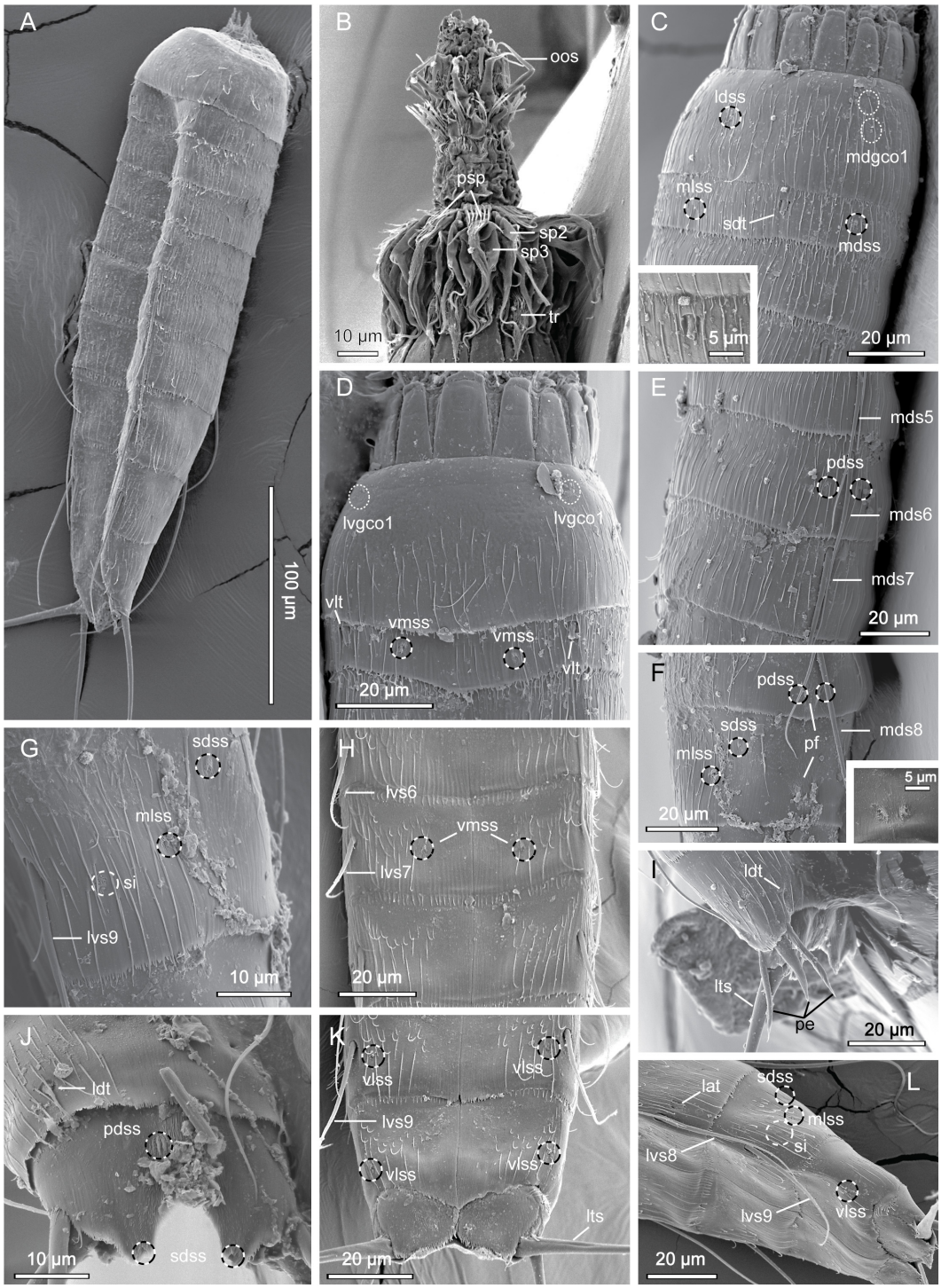

FIGURE 4 | Scanning electron micrographs showing overviews and details of *Echinoderes mamaqucha* sp. nov. **(A)** Lateroventral overview. **(B)** Mouth cone and introvert sectors 8 to 7. **(C)** Segments 1 to 3, dorsolateral view, with close-up showing subdorsal tube on segment 2. **(D)** Segments 1 to 2, ventral view. **(E)** Segments 5 to 7, dorsolateral view. **(F)** Segments 8 to 9, dorsolateral view, with close-up showing papillary flap on segment 9. **(G)** Segment 9, lateral view. **(H)** Segments 6 to 8, ventral view. **(I)** Segments 10 to 11 of male, lateral view. **(J)** Segments 10 to 11 of female, dorsal view. **(K)** Segments 9 to 11 of female, ventral view. **(L)** Segments 8 to 11, lateroventral view. *lat*, lateral accessory tube; *ldss*, laterodorsal sensory spot; *ldt*, laterodorsal tube; *lts*, lateral terminal spine; *lvgco1*, lateroventral glandular cell outlet type 1; *lvs*, lateroventral spine, followed by segment number; *mdgco1*, middorsal glandular cell outlet type 1; *mds*, middorsal spine, followed by segment number; *mdss*, middorsal sensory spot; *mlss*, midlateral sensory spot; *oos*, outer oral style; *pdss*, paradorsal sensory spot; *pe*, penile spine; *pf*, papillary flap; *psp*, primary spinoscalid; *sdss*, subdorsal sensory spot; *sdt*, subdorsal tube; *si*, sieve plate; *sp*, spinoscalid followed by introvert ring number; *tr*, trichoscalid; *vlss*, ventrolateral sensory spot; *vlt*, ventrolateral tube; *vmss*, ventromedial sensory spot.

TABLE 2 | Measurements from light microscopy of *Echinoderes mamaqucha* sp. nov. (in μm) from the Atacama Trench, including number of measured specimens (*n*) and standard deviation (SD).

Character	*n*	Range	Mean	SD
TL	16	252–325	296	20.8
MSW-6	16	63–69	67	1.7
MSW-6/TL	16	20.8–26.7%	22.9%	1.8%
SW-10	16	53–56	54	0.9
SW-10/TL	16	16.8–21.6%	18.4%	1.4%
S1	16	28–35	31	1.8
S2	16	24–30	26	1.6
S3	16	24–31	27	1.7
S4	16	28–35	30	1.9
S5	16	29–36	32	1.8
S6	16	34–40	36	1.9
S7	16	34–42	38	1.8
S8	16	39–45	42	1.6
S9	16	39–44	41	1.7
S10	16	33–43	36	3.2
S11	16	25–32	28	2.0
MD4 (ac)	16	35–43	40	2.4
MD5 (ac)	15	43–53	47	3.1
MD6 (ac)	15	47–57	52	3.5
MD7 (ac)	16	63–80	72	4.6
MD8 (ac)	16	96–120	109	7.5
LV6 (ac)	16	34–42	38	2.4
LV7 (ac)	16	40–49	45	2.9
LV8 (ac)	16	49–57	54	2.1
LV9 (ac)	16	58–69	64	3.3
LTS	16	170–206	187	9.7
LTS/TL	16	54.4–75.8%	63.5%	6.7%
LTAS	12	58–72	68	3.9

(ac), acicular spine; LTAS, lateral terminal accessory spine; LTS, lateral terminal spine; LV, lateroventral; MD, middorsal; MSW-6, maximum sternal width, measured on segment 6 in this species; S, segment lengths; SW-10, standard width, always measured on segment 10; TL, trunk length.

thin, weakly developed, well-spaced with even shorter and finer tips in between.

Segment 2 consists of a complete cuticular ring, with minute (<5 μm) tubes located in subdorsal and ventrolateral positions (**Figures 3B,C**, **4C,D**); tubes are not differentiated into thick proximal part and thinner distal tubular part with lateral wings, but are merely short tubular, truncate tips. Sensory spots present in middorsal, midlateral and ventromedial positions. Glandular cell outlets type 1 present in middorsal and ventromedial positions. Pachycyclus of anterior segment margin interrupted in middorsal position. Secondary pectinate fringe present near anterior segment margin of this and following segments, but usually covered by the preceding segment. Cuticular bracteate hairs lightly scattered on ventral side and more densely in dorsal and lateral areas. Pectinate fringe tips slightly longer than on preceding segment, but still very flexible; margin between tips very finely serrated.

Segment 3, and remaining segments, consists of one tergal and two sternal plates; pachycycli of anterior segment margins with interruption in middorsal positions and around tergosternal and midsternal junctions. Segment with glandular cell outlets type 1, located in middorsal and ventromedial positions. On this and following seven segments, cuticular hairs arranged in two to three rows across the tergal plate, except for hairless midlateral areas, and on the lateral halves of the sternal plates; paraventral and ventromedial areas devoid of hairs. Pectinate fringe as on preceding segment.

Segment 4 with flexible acicular spine in middorsal position and pairs of glandular cell outlets type 1 located in paradorsal and ventromedial positions (**Figures 2A,B**, **3B**). Cuticular hairs, and pectinate fringe of posterior margin as on preceding segment.

Segment 5 with acicular spine in middorsal position and relatively short (10 μm) tubes in lateroventral positions (**Figures 2A,B**, **3C,E**); tubes are longer and more slender than those on segment 2, but without the common differentiation into thick bases and end piece with lateral wings. Pectinate fringe tips of posterior margin slightly longer; glandular cell outlets type 1, and cuticular hairs otherwise as on preceding segments.

Segment 6 with acicular spines in middorsal and lateroventral positions (**Figures 2A,B**, **3E**, **4E,H**). Sensory spots present in paradorsal and midlateral positions. Glandular cell outlets type 1, and pectinate fringe of posterior margin as on preceding segment.

Segment 7 with acicular spines in middorsal and lateroventral positions (**Figures 2A,B**, **3E,F**, **4E,H**). One pair of sensory spots located ventromedially. One specimen (out of five examined under SEM) lacked this character and one showed only one sensory spot on the right sternal plate; for some specimens examined under LM presence/absence of ventromedial sensory spots could not be confirmed. Other structures as on preceding segment.

Segment 8 with acicular spines in middorsal and lateroventral positions (**Figures 2A,B**, **3E,F**, **4L**). Middorsal spine long, reaching posterior part of segment 11, but never exceeding its margin (**Figure 3G**). Short tubes (<10 μm) present in lateral accessory positions (**Figures 3F**, **4L**); tubes resemble those on segment 2. Sensory spots located in paradorsal positions only, hardly visible due to the presence of a papillary flap - a V-shaped structure present middorsally at the posterior part of the segment (**Figures 2A**, **3E**, **4F**). Glandular cell outlets type 1 present in paradorsal and ventromedial positions. Cuticular hairs on sternal plates as on preceding segment; hairs on tergal plate scarcer with hairless middorsal and paradorsal patches (**Figure 4H**). Pectinate fringe of posterior margin with shorter tips, on dorsal side much less developed in comparison to preceding segment.

Segment 9 with a pair of lateroventral spines. Rounded and very small sieve plates present in sublateral positions (**Figures 2B**, **3F**, **4G**). Sensory spots present in paradorsal, subdorsal, midlateral and ventrolateral positions (**Figures 2A,B**, **4F,G,K,L**). Paradorsal pair difficult to detect due to the presence of a papillary middorsal flap, which however is smaller than on preceding segment (**Figure 4F**). Cuticular hair covering less dense than on preceding segment; central part of the tergal plate devoid of hairs. Pectinate fringe tips slightly shorter on lateral

TABLE 3 | Summary of nature and location of sensory spots, glandular cell outlets, tubes and spines arranged by series in *Echinoderes mamaqucha* sp. nov.

Position Segment	MD	PD	SD	LD	ML	SL	LA	LV	VL	VM
1	gco1,gco1			ss				gco1		
2	gco1,ss		tu		ss				tu	gco1,ss
3	gco1									gco1
4	ac	gco1								gco1
5	ac	gco1						tu		gco1
6	ac	gco1,ss			ss			ac		gco1
7	ac	gco1						ac		gco1,ss*
8	ac	gco1,ss					tu	ac		gco1
9		gco1,ss	ss		ss	si		ac	ss	gco1
10	gco1,gco1		ss	tu					ss	gco1
11	gco1	ss	ss		pe x3 (♂)		ltas(♀)	lts		

*LA, lateral accessory; LD, laterodorsal; LV, lateroventral; MD, middorsal; ML, midlateral; PD, paradorsal; SD, subdorsal; SL, sublateral; VL, ventrolateral; VM, ventromedial; ac, acicular spine; gco1, glandular cell outlet type 1; ltas, lateral terminal accessory spine; lts, lateral terminal spine; si, sieve plate; ss, sensory spot (*not present in all specimens); tu, tube; (♀), female condition of sexually dimorphic characters; (♂), male condition of sexually dimorphic characters.*

sides, otherwise as on preceding segment. Glandular cell outlets type 1 as on preceding segments.

Segment 10 with minute, very slender laterodorsal tubes near posterior segment margin (**Figures 2A,C**, **3D**, **4I,J**); appearance of the tubes similar in both sexes. Sensory spots present in subdorsal and ventrolateral positions. Subdorsal pair located in the middle of the segment, but in a few cases, one sensory spot is shifted posteriorly to a position very close to posterior segment margin. Glandular cell outlets type 1 present as two middorsal ones and one pair in ventromedial position. Cuticular hairs scarcer than on preceding segment. Anterior part of the tergal plate devoid of hairs; hairs on the sternal plates short and present mostly on the lateral halves and near posterior segment margin. Margins of the sternal plates extend midventrally (**Figure 4K**). Pectinate fringe with very short tips.

Segment 11 with a pair of long lateral terminal spines (**Figures 2A,B**, **3A**). Females with strong, stout lateral terminal accessory spines (**Figures 2A,B**, **3A,D**). Males with three pairs of penile spines; median penile spine stouter than dorsal and ventral ones, but all three pairs generally stout and rigid, gradually tapering in distal 1/4 (**Figures 2C,D**, **3G**, **4I**). Sensory spots present in paradorsal and subdorsal positions. The latter ones located at the posterior margin of the tergal extensions (**Figure 4J**). One middorsal glandular cell outlet type 1 present. Tergal extensions short and rounded (**Figures 2**, **3D,G**). The posterior margin of the sternal plates also rounded, not exceeding beyond, but nearly as long as tergal extensions. Pectinate fringe of posterior margin with short tips, except in lateral positions where longer and more flexible fringe tips are present. The segment completely devoid of cuticular hairs, but has a relatively dense covering of hair-like extensions in the mid- and paradorsal positions, as well as small patches present in paraventral and ventromedial areas.

Differential Diagnosis

The spine and tube distribution in the middorsal and lateroventral series of *E. mamaqucha* sp. nov., with middorsal spines on segments 4 to 8, and tubes/spines in lateroventral positions of segments 5 to 9 is the most common pattern observed among species of *Echinoderes* and is shared by 44 congeners (Yamasaki et al., 2020). However, when we combine these characters with the presence of subdorsal and ventrolateral tubes on segment 2 we shorten the list to only 3 species, i.e., *E. adrianovi* Herranz et al. (2014), *E. levanderi* Karling (1954), *E. kanni* Thormar and Sørensen (2010) (Karling, 1954; Thormar and Sørensen, 2010; Herranz et al., 2014; Sørensen, 2018). Despite the coincidence of spine/tube formula *E. mamaqucha* sp. nov. can still be easily distinguished from the abovementioned species based on other traits, e.g., very short tubules, dimensions of acicular spines, shape of tergal extension, and general appearance of primary pectinate fringe. *Echinoderes levanderi* cannot in any way be confused with *E. mamaqucha* sp. nov. since the morphometrics of both species differ significantly. *Echinoderes levanderi* is conspicuously larger, has markedly longer lateral terminal spines, and consequently, shows a larger proportion of lateral terminal spine to trunk length (90.5%) than *E. mamaqucha* sp. nov. (63.5%). Most importantly, however, *E. levanderi* possesses sublateral tubes on segments 5 and 8, very characteristic large sieve plates, pointed tergal extension and extremely well-developed pectinate fringes with very long tips throughout the body (Sørensen, 2018). *Echinoderes mamaqucha* sp. nov. is more similar to *E. kanni* and *E. adrianovi*, and shares the presence of lateral accessory tubes on segment 8, dorsal tubes on segment 10 and the absence of glandular cell outlet types 2 (Thormar and Sørensen, 2010; Herranz et al., 2014). Nevertheless, both species can be distinguished from *E. mamaqucha* sp. nov. by their markedly longer (up to 2–4 times) tubes, much shorter and thinner lateral accessory terminal spines, and pointed tergal extensions (Thormar and Sørensen, 2010; Herranz et al., 2014; Yamasaki et al., 2019). Both species also have very prominent cuticular perforation sites which are missing in *E. mamaqucha* sp. nov.

Interestingly, *E. mamaqucha* sp. nov. shows a much closer general resemblance with *E. bathyalis* Yamasaki et al. (2018a,b) and *E. dubiosus* Sørensen et al. (2018). Both are deep-water

species, described from East Atlantic (> 2500 m water depth) and North-Eastern Pacific (> 3500 m water depth), respectively (Sørensen et al., 2018; Yamasaki et al., 2018b). *Echinoderes mamaqucha* sp. nov. and these two species share identical spine patterns and are characterized by having a long middorsal spine on segment 8 and long lateroventral spines on segment 9. The spines easily reach and even extend beyond the posterior margin of segment 10. However, in *E. mamaqucha* sp. nov. none of them extends beyond the posterior margin of segment 11, whereas in the two latter species the middorsal spine on segment 8 and lateroventral spines on segment 9 always extent beyond the terminal segment (Sørensen et al., 2018; Yamasaki et al., 2018a,b). *Echinoderes mamaqucha* sp. nov. also resemble the two species in terms of trunk shape and length, and in possessing short tergal extension. Nevertheless, the posterior edge of the tergal plate is more pointed in E. *bathyalis* and *E. dubiosus*. In addition, *E. mamaqucha* sp. nov. has uncommon middorsal structures on segments 8 and 9 that resemble those reported for the first time from *E. dubiosus* and described as papillary flap (Sørensen et al., 2018). This trait is present on segment 9 only in *E. dubiosus*, but its similarity with the structures found on segments 8 and 9 in *E. mamaqucha* sp. nov. is striking. Sørensen et al. (2018) described the structure as "papillary flap or tuft of papillae, flanked by a pair of paradorsal sensory spots," which is exactly what can be observed for *E. mamaqucha* sp. nov. Furthermore, similar to *E. dubiosus*, *E. mamaqucha* has laterodorsal tubes on segment 10 and lateral tubes on segment 8. In the latter species, tubes are located in lateral accessory position, whereas they are sublateral in *E. dubiosus*. The most striking difference between *E. mamaqucha* sp. nov and two other species is, however, the tube arrangement on segment 2. While *E. mamaqucha* sp. nov. is characterized by the presence of subdorsal and ventrolateral tubes on this segment, both *E. dubiosus* and *E. bathyalis* lack this character, and have instead one pair of glandular cell outlet type 2 in midlateral position. Even though the tubes in the new species are extremely short and sometimes difficult to visualize in LM, and that the attachments of tubes might sometimes resemble glandular cell outlets type 2, the structures still appear in different positions. Therefore, presence of tubes on segment 2 makes *E. mamaqucha* sp. nov. easily distinguishable from its two other deep-sea, and potentially closely related, congeners.

Other Species of *Echinoderes*

Besides *E. mamaqucha* sp. nov. five additional species of *Echinoderes*, represented by one specimen each, were identified in the investigated material. One specimen was identified as *Echinoderes juliae* Sørensen et al. (2018) and one as *Echinoderes pterus* Yamasaki et al. (2018a,b), whereas the three remaining ones could not be identified with certainty. All three unidentified species share several characters with already described species, but they also showed character traits that made exact identification uncertain. Although they might represent undescribed species, formal descriptions will not be provided since all specimens occurred only as singletons.

Echinoderes juliae Sørensen et al. (2018) (Figure 5 and Table 4)

Material examined: adult female, collected on March 6, 2018, at station 1, at 2560 m depth, on abyssal plain, east of the Atacama Trench (23°49′S 70°50′W) (**Figure 1** and **Table 1**), mounted in Fluoromount-G, deposited at the Natural History Museum of Denmark, under catalog number NHMD-872652.

Brief Description

Echinoderes with middorsal spines on segments 4 to 8 and spines in lateroventral positions on segments 6 to 9. Tubes present in lateroventral position on segment 5 only. Glandular cell outlets type 2 present in subdorsal, laterodorsal, sublateral and ventrolateral positions on segment 2, in sublateral positions on segments 3, 4 and 8, and in midlateral positions on segment 5 (**Figures 5B–D**). Tergal extensions conspicuous long and slender, with long, flexible tips (**Figure 5E**).

Remarks

Echinoderes juliae belongs to one of the deep-sea species originally found on the abyssal plain off Oregon and along the continental rise off California, the Northeast Pacific at 2702 to 3679 m depth (Sørensen et al., 2018). Despite significant geographical distance (*ca.* 7000 km) between the type locality and the Atacama Trench region, the morphology and morphometrics of the examined specimen are completely in line with the original description of *E. juliae* in Sørensen et al. (2018) (**Figure 5** and **Table 4**). Differences were detected neither in sensory spots positions nor in glandular cell outlets types 1 and 2.

Echinoderes pterus Yamasaki et al. (2018a,b) (Figure 6)

Material examined: adult female, collected on March 28, 2018, at station 9, at 4050 m depth, on abyssal plain, east of the Atacama Trench (20°20′S 70°59′W) (**Figure 1** and **Table 1**), mounted in aluminum stub for SEM and stored in the personal collection of MVS.

Brief Description

Echinoderes with middorsal spines on segments 4 to 8 and spines in lateroventral positions on segments 6 to 9. Tubes present in lateroventral position on segment 5 and in laterodorsal position on segment 10. Characteristic tufts of long hairs present in laterodorsal positions on segment 9. Glandular cell outlets type 2 absent.

Remarks

Echinoderes pterus is a species with a wide geographic distribution, ranging from the high Arctic, the North Atlantic, and into the Mediterranean Sea (Yamasaki et al., 2018a), and it has also been reported to show a wide bathymetric distribution, from 675 to 4403 m. Besides having this unusually wide range, *E. pterus* possesses a set of traits that easily distinguishes it from other congeners. The most characteristic is the presence of tufts of hairs on segment 9 - a structure unique for *E. pterus*. The second feature is the conspicuously thick and long lateroventral

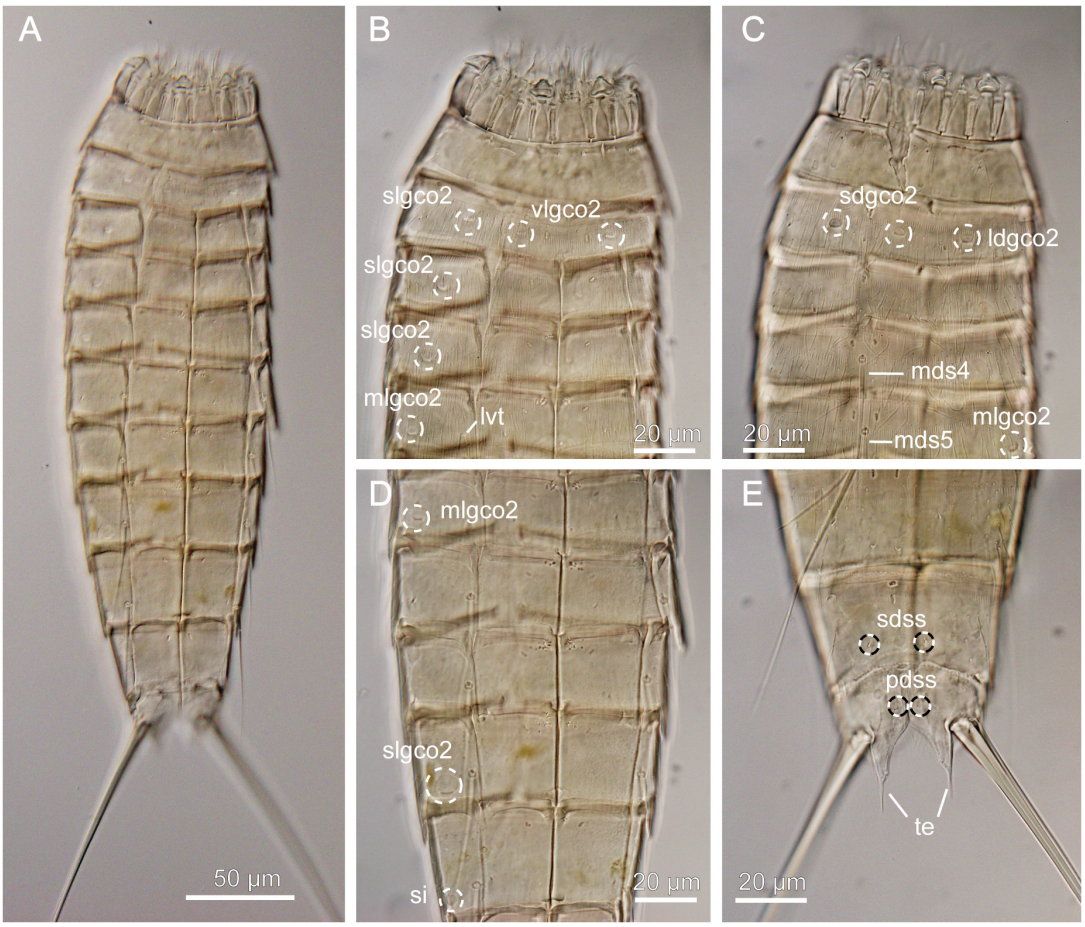

FIGURE 5 | Light micrographs showing overview and details of female *Echinoderes juliae* (NHMD-872652) collected at station 1. **(A)** Ventral overview. **(B)** Segments 1 to 5, ventral view. **(C)** Segments 1 to 5, dorsal view. **(D)** Segments 5 to 9, ventral view. **(E)** Segments 9 to 11, dorsal view. *ldgco2*, glandular cell outlet type 2; *lvt*, lateroventral tube; *mds*, middorsal spine, followed by segment number; *mlgco2*, glandular cell outlet type 2; *pdss*, paradorsal sensory spot; *sdgco2*, subdorsal glandular cell outlet type 2; *sdss*, subdorsal sensory spot; *si*, sieve plate; *slgco2*, sublateral glandular cell outlet type 2; *te*, tergal extension; *vlgco2*, ventrolateral glandular cell outlet type 2.

spines on segment 9, however this character is observed only in the male representatives of the Arctic and North Atlantic populations (Yamasaki et al., 2018a). In the examined material we found only one female specimen, thus lateroventral spines on segment 9 could not be used as a diagnostic character. Exact morphometric details of our specimen are also unavailable because it was mounted for SEM. Nevertheless, the examined specimen possesses the diagnostic key features of *E. pterus,* i.e., the spine and tube pattern and the presence of the tufts of hairs on segment 9 (**Figures 6D,G**). Moreover, we were able to confirm the presence of almost all sensory spots, according to the original description provided by Yamasaki et al. (2018a); the only exception were sensory spots in paraventral positions on segment 8 and in subdorsal positions on segment 10 that could not be observed due to the mounting position of the examined specimen. In addition to this, our specimen, similar to *E. pterus*, has long, rather thin cuticular hairs distributed along the body (except segment 1), and a primary pectinate fringe with long, thin tips, characteristically curved in the paraventral sectors of segment 1 and 2 (**Figure 6**, see also Figure 6C in Yamasaki et al., 2018a). Segment 1 is completely hairless, except for hairs associated with the relatively large sensory spots present in subdorsal and laterodorsal positions (**Figures 6A,B,E,F**), which is also characteristic for the type specimens of *E. pterus*. Therefore, the identity of the examined specimens seems to be unquestionable.

Echinoderes sp. 1 (Figure 7 and Table 4)

Material examined: one female, collected on March 8, 2018, at station 6, at 7720 m depth in the Atacama Trench (24°16′S 71°25′W) (**Figure 1** and **Table 1**), mounted in Fluoromount-G, deposited at the Natural History Museum of Denmark, under catalog number NHMD-872653.

Brief Description

Echinoderes with middorsal spines on segments 6 and 8, and spines in lateroventral positions on segments 6 to 9. Tubes present in ventrolateral positions on segment 2, lateroventral

TABLE 4 | Measurements from light microscopy of *Echinoderes* species from the Atacama Trench with comparison of measurements for the closely related species.

Character	*E. juliae* present study	*E. juliae* Sørensen et al., 2018	*Echinoderes* sp. 1	*E. ultraabyssalis* Adrianov and Maiorova, 2019	*Echinoderes* sp. 2	*E. dubiosus* Sørensen et al., 2018	*Echinoderes* sp. 3	*E. hakaiensis* Herranz et al., 2018
TL	300	285–327	257	255–340	278	238–281	211	266–382
MSW	56	51–54	59	53–60	60	60–70	47	62
MSW/TL	18.7%	15.6–18.6%	23.0%	16–22%	21.7%	22–25%	22.3%	16–23%
SW-10	44	41–47	46	42–49	51	51–57	39	46–47
SW-10/TL	14.7%	12.8–15.4%	17.9%	13–17%	18.6%	19–22%	18.5%	12–17%
MD4 (ac)	48	31–44			51	30–52	55	40
MD5 (ac)	55	42–56			56	41–78		
MD6 (ac)	broken	59–70	59	42–51	69	64–87	85	60
MD7 (ac)	80	67–78			113	68–93		
MD8 (ac)	97	71–98	70	65–76	193	96–136	81	75–80
LV6 (ac)	47	33–43	35	31–40	45	28–56	26	30–31
LV7 (ac)	50	41–48	39	38–42	58	32–68	30	30–34
LV8 (ac)	55	44–61	45	39–49	74	39–91	30	25–34
LV9 (ac)	62	40–60	46	47–60	94	79–120	30	27–33
LTS	222	205–248	234	181–205	337	186–323	145	128
LTS/TL	74.0%	68.8–78.8%	91.1%	59–73%	121%	75–118%	69%	48–33%
LTAS	126	128–133	50	42–47	70	61–78	49	35–38

(ac), acicular spine; LTAS, lateral terminal accessory spine; LTS, lateral terminal spine; LV, lateroventral; MD, middorsal; MSW, maximum sternal width; S, segment lengths; SW-10, standard width, always measured on segment 10; TL, trunk length.

positions on segment 5, lateral accessory positions on segment 8 and laterodorsal positions on segments 9 and 10.

Adults with head, neck and eleven trunk segments (**Figures 7A,D**). Overview of measures and dimensions are given in **Table 4**.

Segments 1 and 2 composed of complete cuticular rings. Segment 1 with glandular cell outlet type 1 in middorsal position and sensory spots in subdorsal and ventrolateral positions (**Figure 7C**). Posterior margin of this and following nine segments with primary pectinate fringe. Segment 2 with ventrolateral tubes and pair of ventromedial glandular cell outlets type 1 (**Figure 7B**). No structures observed on the tergal plate. Cuticular hairs on both segments relatively long, distributed around the segments, but covering only the posterior parts. Segments 3 to 11 consist of one tergal and two sternal plates. Pachycycli of anterior segments margins with clear interruptions in middorsal positions and around tergosternal and midsternal junctions (**Figures 7A,D**). Segments 3 and 4 with ventromedial glandular cell outlet type 1 only; no sensory spots or other traits observed. Segment 5 with lateroventral tube, a pair of sensory spots located midlaterally, and ventromedial glandular cell outlets type 1; similar outlets present at following four segments as well (**Figure 7E**). Segment 6 with middorsal acicular spine, lateroventral spines, paradorsal, midlateral and ventromedial sensory spots and glandular cell outlets type 1 in paradorsal position (**Figures 7D,E**). Segment 7 with lateroventral spines, pair of paradorsal and midlateral sensory spots and paradorsal glandular cell outlets type 1 present. Segment 8 with spines in middorsal and lateroventral positions, lateral accessory tubes, paradorsal sensory spots and paradorsal glandular cell outlets type 1 (**Figures 7D,E**). Segment 9 with lateroventral spines, distinct, long laterodorsal tubes and three pairs of sensory spots, located in paradorsal, subdorsal and ventrolateral positions; small sieve plate located in lateral accessory positions (**Figure 7F**). Segment 10 with laterodorsal tubes, sensory spot and two glandular cell outlets type 1 located middorsally, and a pair of sensory spots in ventrolateral position. Segment 11 with a pair of very long lateral terminal spines (**Figure 7A**), nearly reaching trunk length (**Table 4**). Female with relatively strong and long lateral terminal accessory spines. Sensory spots present in paradorsal positions. A protuberance-like structure emerges between segments 10 and 11 in middorsal position (**Figure 7F**).

Remarks

The spine pattern with middorsal acicular spines on segment 6 and 8 is extremely rare among *Echinoderes* species. This trait is shared only with three species, i.e., *E. daenerysae* Grzelak and Sørensen (2018) in Grzelak and Sørensen (2018), *E. hviidarum* Sørensen et al. (2018) and *E. ultraabyssalis* Adrianov and Maiorova (2019) (Grzelak and Sørensen, 2018; Sørensen et al., 2018; Adrianov and Maiorova, 2019). The latter two are typical deep-water species, described from the Northeast Pacific (*ca.* 2700 m water depth) and Northwest Pacific (< 9000 m water depth), respectively, while *E. daenerysae* is known from shallower waters of the Arctic Ocean (100–250 m water depth).

A second very rare feature of *Echinoderes* sp. 1 is the presence of laterodorsal tubes on segment 9. Interestingly, all three abovementioned species have laterodorsal tubes on this segment, which suggests that these four species might be closely related. The only other species with tubes in this position on the tergal plate is *Echinoderes belenae* Pardos et al. (2016), but this species cannot in any way be confused with *Echinoderes* sp. 1 due to the presence of 3 middorsal spines, on segment 4, 6 and 8,

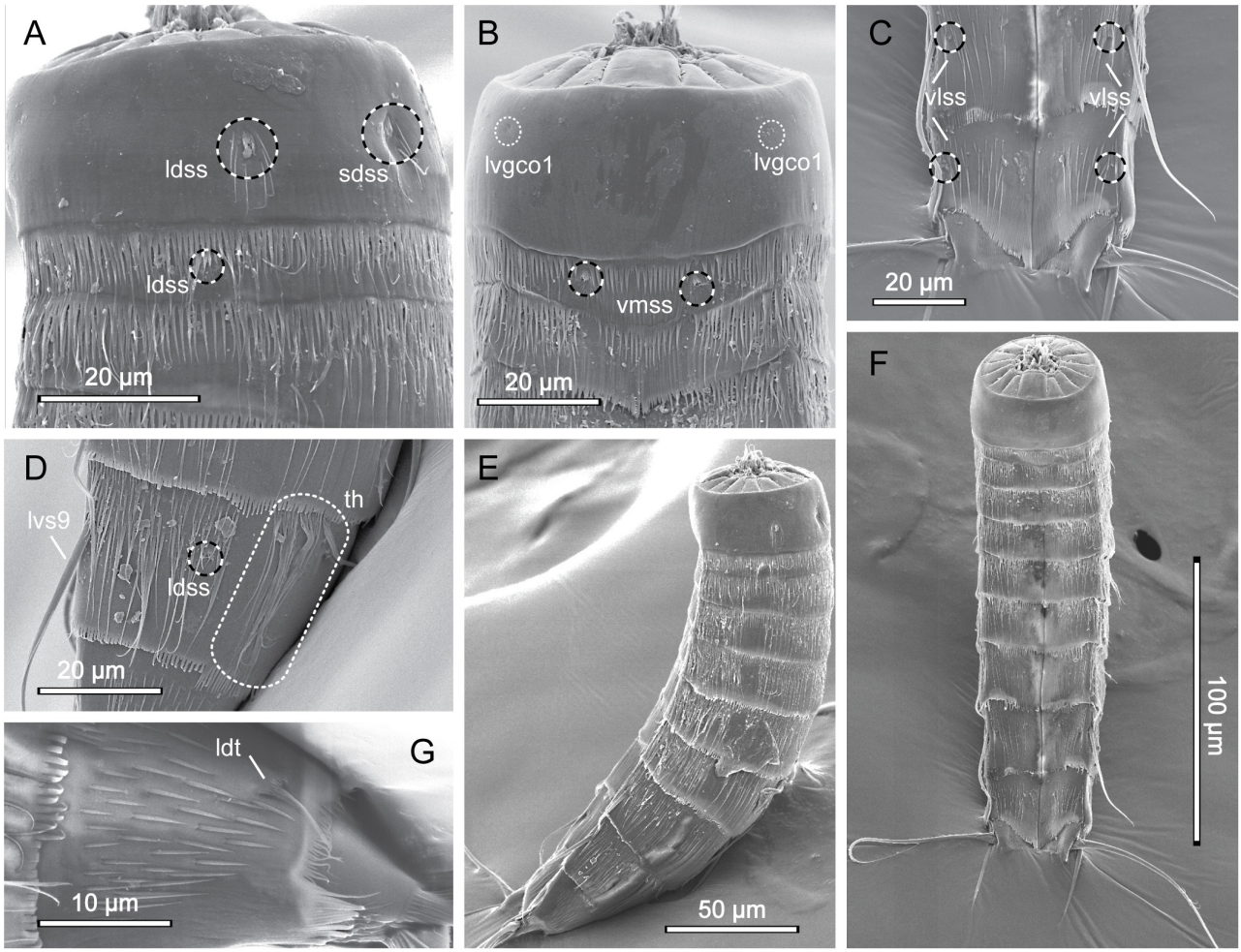

FIGURE 6 | Scanning electron micrographs showing overview and details of female *Echinoderes pterus* collected at station 9. **(A)** Segments 1 to 3, lateral view. **(B)** Segments 1 to 3, ventral view. **(C)** Segments 9 to 11, ventral view. **(D)** Segment 9, lateral view. **(E)** Lateral overview. **(F)** Ventral overview. **(G)** Segment 10, lateral view. *ldss*, laterodorsal sensory spot; *ldt*, laterodorsal tube; *lvgco1*, lateroventral glandular cell outlet type 1; *lvs*, lateroventral spine, followed by segment number; *sdss*, subdorsal sensory spot; *th*, tuft of hairs; *vlss*, ventrolateral sensory spot; *vmss*, ventromedial sensory spot.

numerous tubes in various positions and short lateral terminal spines (Pardos et al., 2016).

Echinoderes sp. 1 shares different features with *E. daenerysae, E. hviidarum* and *E. ultraabyssalis*. These include the relatively small body size (<300 µm), presence of tubes in lateroventral positions on segment 5 and in lateral accessory positions on segment 8, as well as long lateral terminal spines and absence of glandular cell outlet type 2. *Echinoderes* sp. 1 furthermore shares the presence of a middorsal protuberance between segments 10 and 11 with the latter two species. Nevertheless, *E. hviidarum* is easily distinguished from *Echinoderes* sp. 1 by the absence of tubes on segment 2. In contrast, *E. daenerysae* and *Echinoderes* sp. 1 share the presence of ventrolateral tubes on segment 2, whereas only *E. daenerysae* has tubes in laterodorsal positions also. Among the three species, *E. ultraabyssalis* appears to be morphologically closest to *Echinoderes* sp. 1. This is the deepest kinorhynchs species described so far, and similar to *Echinoderes* sp. 1, it possesses one pair of tubes, located ventrolaterally on segment 2. Morphometrics of both species also show great resemblance (**Table 4**), with the exception of the proportions of the lateral terminal spines vs. trunk length. *Echinoderes* sp. 1 has longer lateral terminal spines, nearly as long as the trunk length (LTS/TL = 91%), while the lateral terminal spines in *E. ultraabyssalis* are no longer than 2/3 of the trunk length (mean LTS/TL = 59%). It appears that also the arrangement and number of sensory spots show some differences between these two species. Although only one specimen was available for examination and we cannot exclude the possibility that some sensory spots were missed, we can at least confirm their presence in subdorsal positions on segment 11 and in midlateral positions on segments 5 and 6. None of these were described for *E. ultraabyssalis*. However, the key character to distinguish *Echinoderes* sp. 1 from *E. ultraabyssalis* is the presence of laterodorsal tubes on segment 10. Although the presence of such tubes can be difficult to visualize with LM, the tubes are well visible in *Echinoderes* sp. 1, while their absence in *E. ultraabyssalis* was confirmed

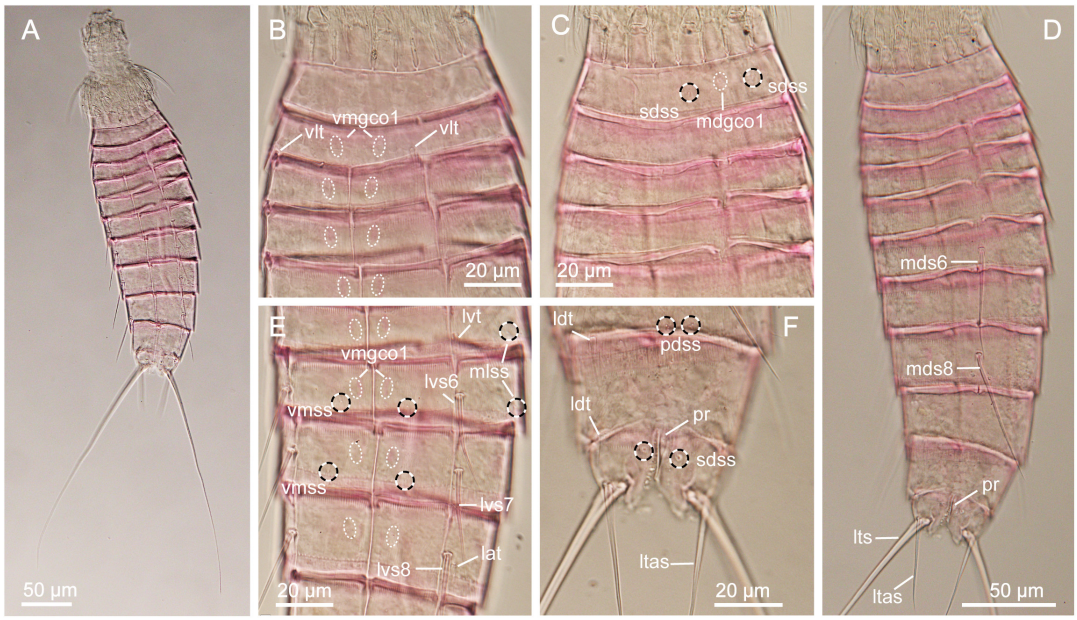

FIGURE 7 | Light micrographs showing overview and details of female *Echinoderes* sp. 1 (NHMD-872653) collected at station 6. **(A)** Ventral overview. **(B)** Segments 1 to 5, ventral view. **(C)** Segments 1 to 5, dorsal view. **(D)** Dorsal overview. **(E)** Segments 5 to 8, ventral view. **(F)** Segments 9 to 11, dorsal view. *lat*, lateral accessory tube; *ldt*, laterodorsal tube; *ltas*, lateral terminal accessory spine; *lts*, lateral terminal spine; *lvs*, lateroventral spine, followed by segment number; *lvt*, lateroventral tube; *mdgco1*, middorsal glandular cell outlet type 1; *mds*, middorsal spine, followed by segment number; *mlss*, midlateral sensory spot; *pdss*, paradorsal sensory spot; *pr*, protuberance; *sdss*, subdorsal sensory spot; *vlt*, ventrolateral tube; *vmgco1*, ventromedial glandular cell outlet type 1; *vmss*, ventromedial sensory spot.

with SEM (Adrianov and Maiorova, 2019). Therefore, we believe that, even though the differences between *Echinoderes* sp. 1 and *E. ultraabyssalis* are subtle, we should consider them as diagnostic until more material becomes available for comparison. It seems clear that the two species are closely related hadal/deep-sea trench species.

Echinoderes sp. 2 (Figure 8 and Table 4)

Material examined: one female, collected on March 20, 2018, at station 7, at 5500 m depth in the Atacama Trench (22°56′S 71°37′W) (**Figure 8** and **Table 1**), mounted in Fluoromount-G, deposited at the Natural History Museum of Denmark, under catalog number NHMD-872654.

Brief Description

Echinoderes with middorsal spines on segments 4 to 8, and spines in lateroventral positions on segments 6 to 9. Tubes present in lateroventral positions on segment 5, lateral accessory positions on segment 8 and laterodorsal position on 10.

Adults with head, neck and eleven trunk segments (**Figures 8A,D**). Overview of measures and dimensions are given in **Table 4**.

Segments 1 and 2 composed of complete cuticular rings. Segment 1 with sensory spots in subdorsal and laterodorsal positions, two glandular cell outlets type 1 in middorsal position and pair in ventrolateral positions (**Figure 8C**). Posterior edge of this and following nine segments with primary pectinate fringe. Segments 2 and 3 without any conspicuous cuticular structures, except for one middorsal glandular cell outlet type 1 (**Figure 8B**). Segment 4 with acicular middorsal spine; paradorsal and ventromedial glandular cell outlets types 1, present on this and following five segments (**Figures 8C,F**). Segment 5 with acicular spine in middorsal position and tubes in lateroventral positions (**Figures 8A,C**). Segment 6 with acicular spines in middorsal and lateroventral positions; sensory spots present in midlateral position. Segment 7 with acicular spines in middorsal and lateroventral positions; sensory spots present in ventromedial positions. Segment 8 with acicular spines in middorsal and lateroventral positions; middorsal spine very long, exceeding posterior part of segment 11 (**Figure 8A**). Tubes present in lateral accessory positions (**Figure 8F**). Sensory spots located in paradorsal positions only, but hardly visible due to the presence of a middorsal papillary flap on the posterior part of the segment (**Figure 8E**). Segment 9 with long lateroventral spines, which exceed way beyond the terminal segment (**Figure 8G**). Sensory spots present in paradorsal and ventrolateral positions. Papillary flap, smaller than on preceding segment, present middorsally on the posterior part of the segment (**Figure 8E**). Rounded, small sieve plates present in lateral accessory positions (**Figure 8F**). Segment 10 with well visible, relatively long laterodorsal tubes, paradorsal sensory spots and glandular cell outlets type 1 present in middorsal and ventromedial positions. Segment 11 with long lateral terminal spines. Specimen with thick lateral terminal accessory spines. Sensory spots present in subdorsal position. Two glandular cell outlets type 1 located middorsally. Tergal extensions short and pointed/triangular (**Figure 8G**). The posterior margins of the sternal plates rounded, much shorter than tergal extensions (**Figure 8G**).

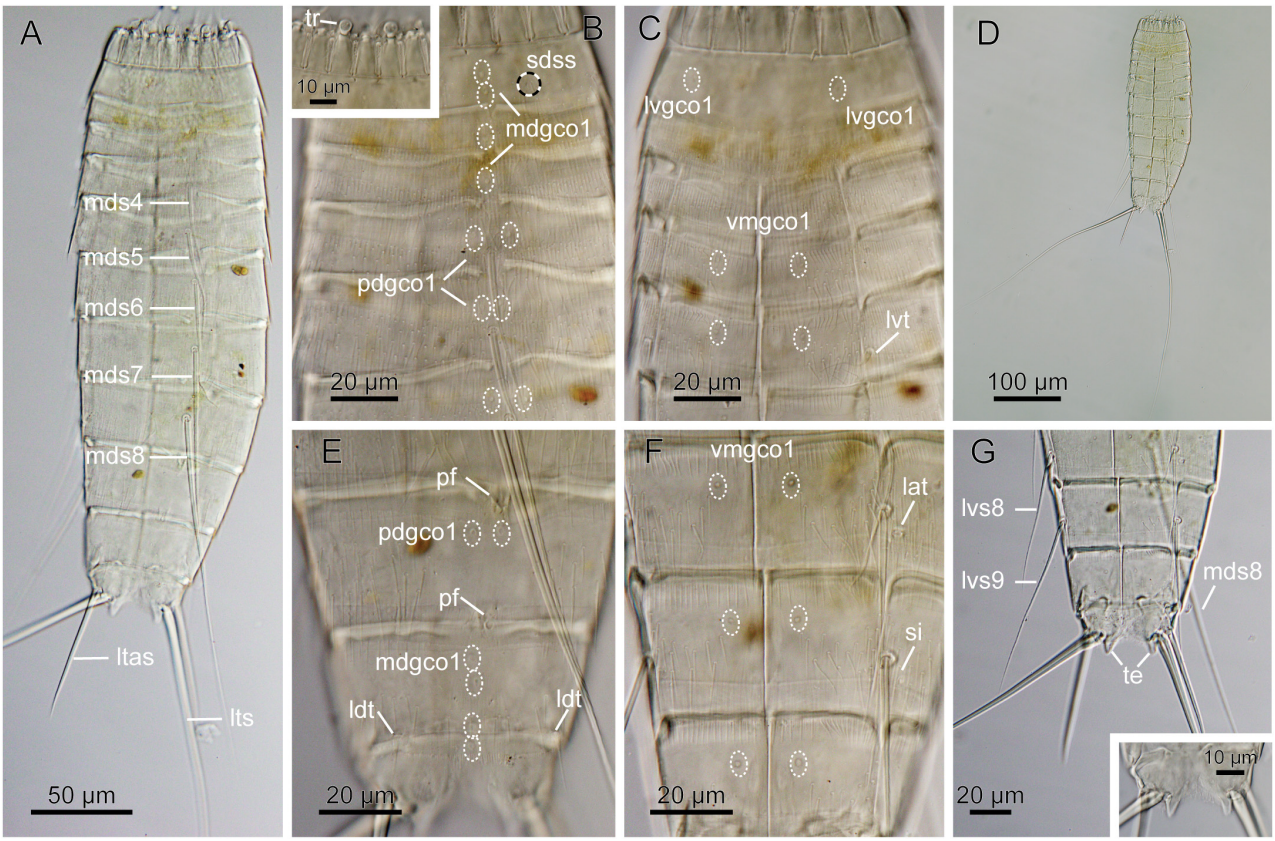

FIGURE 8 | Light micrographs showing overview and details of female *Echinoderes* sp. 2 (NHMD-872654) collected at station 7. **(A)** Dorsal overview. **(B)** Segments 1 to 6, dorsal view, with close-up showing trichoscalids. **(C)** Segments 1 to 5, ventral view. **(D)** Dorsal overview, showing full length of lateral terminal spines. **(E)** Segments 8 to 11, dorsal view. **(F)** Segments 8 to 10, ventral view. **(G)** Segments 8 to 11, ventral view, with close-up on segment 11 showing tergal extension. *lat*, lateral accessory tube; *ldt*, laterodorsal tube; *ltas*, lateral terminal accessory spine; *lts*, lateral terminal spine; *lvgco1*, lateroventral glandular cell outlet type 1; *lvs*, lateroventral spine, followed by segment number; *lvt*, lateroventral tube; *mdgco1*, glandular cell outlet type 1; *mds*, middorsal spine, followed by segment number; *pdgco1*, paradorsal glandular cell outlet type 1; *pf*, papillary flap; *sdss*, subdorsal sensory spot; *si*, sieve plate; *te*, tergal extension; *tr*, trichoscalid; *vmgco1*, ventromedial glandular cell outlet type 1.

Remarks

The spine and tube pattern of *Echinoderes* sp. 2, with presence of middorsal spines on segments 4 to 8, tubes/spines in lateroventral positions of segments 5 to 9, tubes in lateral accessory position on segment 8 and in laterodorsal position on segment 10, is shared with 7 species (Yamasaki et al., 2020), i.e., *E. adrianovi*, *Echinoderes barbadensis* Cepeda et al. (2019a), *Echinoderes dujardini* Claparède (1863), *Echinoderes gerardi* Higgins (1978), *Echinoderes muricatus* Pardos et al. (2016), *Echinoderes parrai* G^{a}Ordóñez et al. (2008), *Echinoderes* sp. 2 in Yamasaki et al. (2018b) (Higgins, 1978; G^{a}Ordóñez et al., 2008; Herranz et al., 2014; Pardos et al., 2016; Yamasaki et al., 2018b; Cepeda et al., 2019a; Sørensen et al., 2020). Nevertheless, *Echinoderes* sp. 2 is unique among the congeners by its absence of tubes or glandular cell outlets type 2 on segment 2. If we do not consider the presence of tubes on segment 8 in the comparison, which sometimes might be difficult to see with LM, *Echinoderes* sp. 2 may resemble three other species, i.e., *Echinoderes kaempfae*, *E. pterus* and *Echinoderes stockmani* Adrianov (1999) in Adrianov and Malakhov (1999) (Adrianov and Malakhov, 1999; Yamasaki et al., 2018a, 2019). Nevertheless, all species can easily be discriminated from *Echinoderes* sp. 2. *Echinoderes pterus* can be distinguished by the presence of the tufts of hairs on segment 9 - a structure unique for this species (see discussion above). *Echinoderes stockmani* possesses additional pairs of tubes on segments 7 and 9, in laterodorsal and subdorsal positions, respectively. Among the abovementioned species, *E. kaempfae* appears to be most similar to *Echinoderes* sp. 2. *Echinoderes kaempfae* is a deep-sea species, described from 3110 m depth at the foot of Senghor Seamount in the Northeast Atlantic (Yamasaki et al., 2019). Next to the spines and tubes pattern (with exception of presence/absence of lateral accessory tube on segment 8), *Echinoderes* sp. 2 and *E. kaempfae* share the presence of long and thin terminal spines and general appearance/shape of the trunk. However, the two species are conspicuously different in tergal extension shape, which appears significantly longer and more pointed in *E. kaempfae*. The latter species also

have shorter spines than *Echinoderes* sp. 2, both on dorsal and ventral sides.

Echinoderes sp. 2 shows the closest resemblance to the deep-sea species *E. dubiosus*. Although the latter possess glandular cell outlets type 2 on segment 2 that are missing in *Echinoderes* sp. 2, the two species are conspicuously similar. Both share the same spines patterns on the dorsal and ventral side, the presence of laterodorsal tubes on segment 10, presence of papillary flaps - middorsal structures previously described for only *E. dubiosus* and *E. mamaqucha* sp. nov. - and very similar sensory spot distribution patterns. Moreover, both species show great similarity in terms of morphometrics (**Table 4**). Very long spines, especially lateral terminal spines that are equal or sometimes longer than trunk length, characterize both species (**Table 4**). However, the middorsal spines on segments 7 and 8 are even longer in *Echinoderes* sp. 2 compared to those in *E. dubiosus*. Especially the middorsal spine of segment 8 extends well beyond the terminal segment in *Echinoderes* sp. 2, opposite to *E. dubiosus* where it only reaches segment 11 (Sørensen et al., 2018). *Echinoderes* sp. 2 also has tubes in lateral accessory positions on segment 8, which differs from *E. dubiosus* that very clearly has its tubes in sublateral positions, leaving a conspicuously larger gap between the tubes and the lateroventral spines. Therefore, based on all abovementioned differences we assume the examined specimen represents an undescribed species. However, since only a single specimen is available, it is too premature to provide a formal description.

Echinoderes sp. 3 (Figure 9 and Table 4)

Material examined: one female, collected on March 6, 2018, at station 1, at 2560 m depth on abyssal plain, east of the Atacama Trench (23°49′S 70°50′W) (**Figure 1** and **Table 1**), mounted in Fluoromount-G, deposited at the Natural History Museum of Denmark, under catalog number NHMD-872651.

Brief Description

Echinoderes with middorsal spines on segments 4, 6, and 8, and spines in lateroventral positions on segments 6 to 9. Tubes present in subdorsal, laterodorsal, sublateral and ventrolateral positions on segment 2, lateroventral position on segment 5, sublateral position on segment 8 and laterodorsal position on segment 10.

Adults with head, neck and eleven trunk segments (**Figure 9A**). Overview of measures and dimensions are given in **Table 4**.

Segments 1 and 2 composed of complete cuticular rings. Segment 1 with sensory spots in subdorsal and lateroventral positions, glandular cell outlet type 1 in middorsal position and pair located ventrolaterally (**Figures 9B,C**). Posterior margin of this and following nine segments with primary pectinate fringe, with well-developed, thin and long fringe tips (**Figures 9D–F**). Segment 2 with subdorsal, laterodorsal, sublateral and ventrolateral tubes, single sensory spot and glandular cell outlet type 1 present middorsally and paired glandular cell outlets type 1 located ventromedially (**Figures 9B,C**). Cuticular hairs on this and following eight segments generally abundant, long, distributed continuously around the segments, except the ventromedial sectors of the segments. Segments 3 to 11 consist of one tergal and two sternal plates. Pachycycli of anterior segments margins with clear interruptions in middorsal positions and around tergosternal and midsternal junctions (**Figures 9B–H**). Segment 3 with subdorsal sensory spots, single glandular cell outlet type 1 in middorsal position and paired ones in ventromedial positions; ventromedial outlets present at following seven segments as well (**Figures 9C,K**). Segment 4 with middorsal acicular spine. Glandular cell outlet type 1 observed in paradorsal positions; no sensory spots present. Segment 5 with lateroventral tubes and single middorsal glandular cell outlet type 1. Segment 6 with middorsal acicular spine, lateroventral spines, paradorsal and ventromedial sensory spots and glandular cell outlets type 1 in paradorsal position (**Figures 9D,K**). Segment 7 with lateroventral spines, pair of ventromedial sensory spots and single middorsal glandular cell outlet type 1. Segment 8 with spines in middorsal and lateroventral positions, sublateral tubes, paradorsal sensory spots and paradorsal glandular cell outlets type 1 (**Figures 9G,H,K**). Segment 9 with lateroventral spines, two pairs of sensory spots, located in paradorsal and ventrolateral positions and paradorsal glandular cell outlets type 1; small sieve plate located in lateral accessory positions. Segment 10 with laterodorsal tubes, sensory spot and glandular cell outlet type 1 located middorsally, and pair of sensory spots in subdorsal and ventrolateral positions. Segment 11 with pair of long lateral terminal spines (**Figure 9A**). Female with relatively strong and long lateral terminal accessory spines (**Figure 9A** and **Table 4**). Sensory spots present in subdorsal position; two glandular cell outlets type 1 located middorsally. Tergal extensions short and pointed, with two small serrations at the posterior inner margin (**Figure 9J**).

Remarks

Echinoderes sp. 3 resembles *Echinoderes hakaiensis* described by Herranz et al. (2018) from 88–140 m depth at Calvert Island, British Columbia, and subsequently found at markedly greater depth, 2719 m, off the United States west coast (Herranz et al., 2018; Sørensen et al., 2018). There is no other species with acicular spines in middorsal position on segments 4, 6 and 8 and four pairs of tubes on segment 2. In addition, both species share the presence of tubes on segment 8 in sublateral position, the positions of several glandular cell outlets type 1 and sensory spots, as well as shape of tergal extensions. Nevertheless, we did not assign *Echinoderes* sp. 3 to *E. hakaiensis* because of some morphological differences between two species. Considering the wide bathymetrical and geographical distance between British Columbia and the Atacama Trench region and the fact that only a single specimen was available for investigation, we cannot be sure whether observed morphological discrepancies result solely from inter-population variations or indicate two, closely related species. The major difference between *Echinoderes* sp. 3 and *E. hakaiensis* are morphometric details. *Echinoderes* sp. 3 is markedly smaller in trunk length than *E. hakaiensis* (TL: 211 μm vs. 324 μm, respectively), but has significantly longer middorsal spines on segments 4 and 6 (MDS4: 55 μm and MDS6: 85 μm in *Echinoderes* sp. 3, whereas MDS: 40 μm and MDS: 60 μm in *E. hakaiensis*) and longer lateral terminal spines (LTS: 145 μm

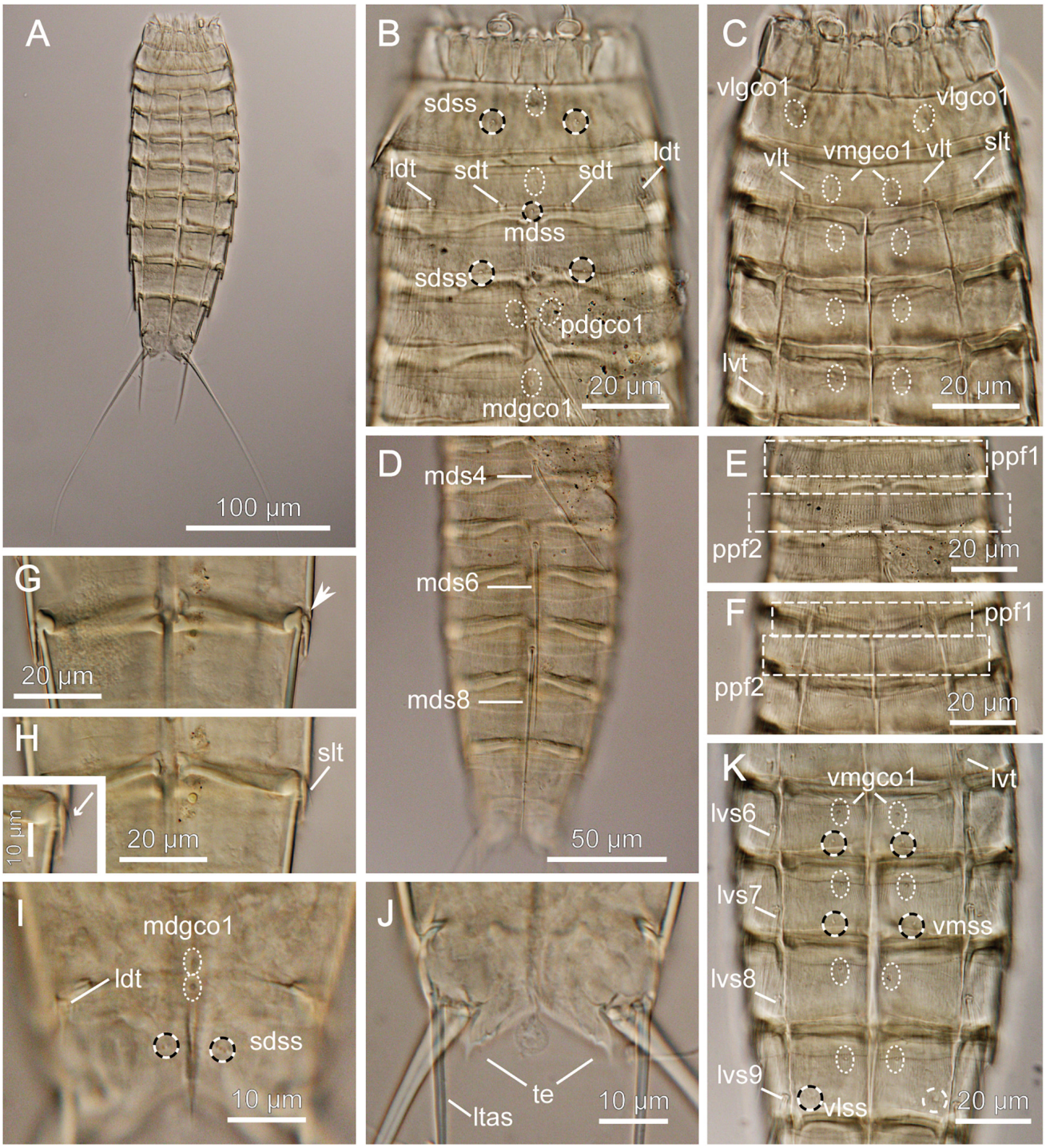

FIGURE 9 | Light micrographs showing overview and details of female *Echinoderes* sp. 3 (NHMD-872651) collected at station 1. **(A)** Ventral overview. **(B)** Segments 1 to 5, dorsal view. **(C)** Segments 1 to 5, ventral view. **(D)** Segments 4 to 11, dorsal view. **(E)** Segments 2 to 4, dorsal view. **(F)** Segments 2 to 4, ventral view. **(G)** Segments 8 to 9, ventral view. **(H)** Segments 8 to 9, ventral view with close-up showing sublateral tube. **(I)** Segments 10 to 11, dorsal view. **(J)** Segment 11, ventral view. **(K)** Segments 5 to 9, ventral view. *ldt*, laterodorsal tube; *ltas*, lateral terminal accessory spine; *lvs*, lateroventral spine, followed by segment number; *lvt*, lateroventral tube; *mdgco1*, middorsal glandular cell outlets type 1; *mds*, middorsal spine, followed by segment number; *pdgco1*, paradorsal glandular cell outlets type 1; *ppf*, primary pectinate fringe, followed by segment number; *sdss*, subdorsal sensory spot; *sdt*, subdorsal tube; *slt*, sublateral tube; *te*, tergal extension; *vlgco1*, ventrolateral glandular cell outlets type 1; *vlss*, ventrolateral sensory spot; *vlt*, ventrolateral tube; *vmgco1*, ventromedial glandular cell outlets type 1. Arrow in G shows sublateral interruption.

vs. 128 μm) (**Table 4**). Differences in trunk and lateral terminal spine lengths result in higher TL/LTS ratio in *Echinoderes* sp. 3 in comparison to *E. hakaiensis* (TL/LTS: 69 vs. 40%, respectively). In *Echinoderes* sp. 3 the pectinate fringe tips of the primary pectinate fringe on segments 1 and 2 are long and thin, both on the dorsal and ventral side (**Figures 9E,F**), whereas the pectinate fringe tips in *E. hakaiensis* are much shorter and less-developed, almost absent in the ventral sector of segment 2 (see Figure 12C in Herranz et al., 2018). Another character that makes *Echinoderes* sp. 3 differ from *E. hakaiensis* is the presence of laterodorsal tubes on segment 10 in the female. Although tubes in this position were observed in male representatives of *E. hakaiensis*, their absence in female was confirmed with SEM (Herranz et al., 2018). In the investigated specimen, the tubes are difficult to visualize, but they are certainly present (**Figure 9I**). Abovementioned differences leave it uncertain whether the examined specimen is identical with *E. hakaiensis*, but since only a single specimen is available, we hesitate to describe the species as a new species.

DISCUSSION

Nearly 75% of the seafloor is at abyssal and hadal depths (> 3000 m) making it the largest benthic habitat globally (Harris et al., 2014). However, our understanding of the lower-abyssal and particularly the hadal zones (> 6000 m) is still very much in its initial stage. Trench biology represents a major frontier in deep-sea studies and the fauna inhabiting these regions probably represents the least understood communities in our ocean (Blankenship-Williams and Levin, 2009). The present study provides the first overview of mud dragon species inhabiting the Atacama Trench and adjacent abyssal and bathyal depths. Our material revealed six species of *Echinoderes*. Of these, *Echinoderes mamaqucha* sp. nov. is described as a new species and morphological data of three undescribed species are given. Moreover, two already known species, i.e., *Echinoderes juliae* and *Echinoderes pterus* were recovered.

Abundance and Species Richness in Hadal Zone

It seems to be a general trend that benthic abundance decreases with increasing water depth (Rex et al., 2006; Wei et al., 2010). Nonetheless, studies conducted in hadal trenches have revealed relatively abundant benthic communities, particularly meiofauna (Danovaro et al., 2002; Schmidt and Martínez Arbizu, 2015; Leduc et al., 2016). Many hadal trenches are close to land and receive organic inputs from terrestrial and coastal sources, increasing microbial activity (Wenzhöfer et al., 2016; Glud et al., 2021) and supporting higher benthic densities than expected for greater depths (Danovaro et al., 2002; Jamieson et al., 2010). In addition, the persistent rain of particulate organic matter (POM) from the surface layers is deposited along the trench axis (von Huene and Scholl, 1991; Turnewitsch et al., 2014). Among others, the Atacama Trench underlies one of the most productive surface waters, which results in high total trench POC flux (Steward and Jamieson, 2018; Glud et al., 2021), reduced sediment grain size and exceptionally high meiofaunal abundance at hadal depths (7800 m) (Danovaro et al., 2002). As reported by Danovaro et al. (2002), abundance of all meiofauna taxa were notably higher at hadal station in comparison with bathyal depths, and this trend also includes the kinorhynchs (0.2 ± 0.3 and 46 ± 40 ind./10 cm^2, at 1050 and 7800 m, respectively). In our study, the abundance of kinorhynchs recorded at trench stations was not as high as reported in the previous study by Danovaro et al. (2002) (5.7 ± 2.7 ind./10 cm^2), but a clear increase in mud dragons abundance with water depth was observed (**Figure 10**). The highest number of individuals in the deepest station (**Figure 10**), is in accordance with observations for other trenches (Schmidt and Martínez Arbizu, 2015; Leduc et al., 2016). The steep slopes of the trenches create a gravity-driven downward transport and therefore elevated deposition of organic matter and intensified microbial metabolism, which support high faunal standing stocks at the greatest depth of hadal trenches (Danovaro et al., 2003; Glud et al., 2013).

Even though they are rich in terms of abundance and/or biomass, hadal benthic communities are rather poor in number of species. Moreover, a high degree of endemism is attributed to the hadal fauna as a whole and also within each trench (Wolff, 1960; Belyaev, 1989; Eustace et al., 2016), although, the selective pressures driving such picture remains unclear. Physical/geographical isolation, sufficiently different environmental conditions experienced by each trench and/or geological age of the trench habitats are considered to be major contributing factors to low species diversity and high endemism of trench bottom fauna (Jamieson et al., 2010). Interestingly, the kinorhynch community at the Atacama Trench hadal stations was dominated by a single species, namely. *E. mamaqucha* sp. nov. that occurred at all six sites along the trench axis and was present almost exclusively at hadal depths (**Figure 10** and **Table 1**). The only exception was the abyssal station at 5550 m, where a single specimen of *E. mamaqucha* sp. nov. was found. Stations at the trench floor extend across > 400 km, but the north–south alignment of the trench axis probably acts as dispersal corridor and thereby facilitates similarity among the kinorhynch fauna along a longitudinal gradient. A similar picture was obtained from an amphipod study at hadal depths in the Atacama Trench (Perrone et al., 2002), where only one undescribed species was documented. A single dominating amphipod species at hadal depths was also found in northwest Pacific trenches (Kuril-Kamchatka, Japan, Izu-Bonin, Mariana, and Philippine trenches; Kamenskaya, 1981; France, 1993) and southwest Pacific trenches (Kermadec and Tonga trenches; Blankenship et al., 2006). This could suggest that *E. mamaqucha* sp. nov. likewise represents an endemic hadal mud dragon form for the Atacama Trench. This assumption should be taken with caution though, since our knowledge of the distribution of microscopic marine animals suffers from lack of data and sampling bias (Boakes et al., 2010) and assessing true biogeographical ranges or distribution patterns is very challenging, especially for a group such as kinorhynchs.

Hadal vs. Abyssal and Bathyal Depths

It is noteworthy that the mud dragon species observed at the trench floor differed from those collected at the surrounding

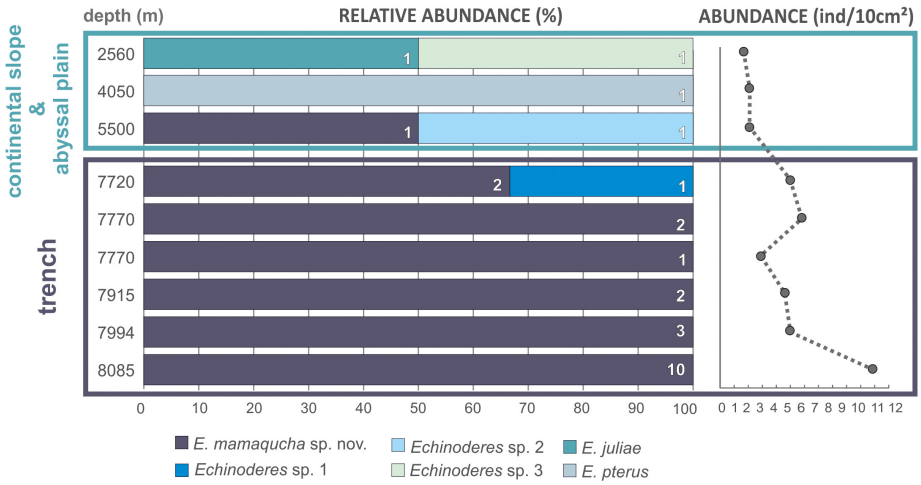

FIGURE 10 | Bathymetric distribution of *Echinoderes* spp. (left side of the plot) and total abundance of kinorhynchs (right side of the plot) collected along the Atacama Trench hadal zone, adjacent abyssal plain and continental slope.

abyssal plain and continental slope (**Figure 10** and **Table 1**). Even though, abundance of kinorhynchs was very low and small sample size might have important implication on the assessment of kinorhynchs diversity, our results are in line with other hadal studies. It has already been documented that trenches and their adjacent abyssal plain can differ significantly in their macrobenthic (Jamieson et al., 2011; Fujii et al., 2013; Gallo et al., 2015) and meiobenthic communities (Kitahashi et al., 2013; Leduc et al., 2016; Schmidt et al., 2019), due to the combination of environmental conditions at trenches floor that are not found in any other deep-sea environment. However, these geographical and depth gradients do not act as sharp boundaries but rather as transitional zones (Jamieson et al., 2011), thus still the hadal zone can share few fauna species with abyssal communities, but less likely with bathyal ones (Eustace et al., 2016; Brandt et al., 2019). The precise depth at which this transition occurs is expected to be trench-specific (Fujii et al., 2013; Schmidt and Martínez Arbizu, 2015), and may vary within trenches. Our results seem to fit well with these previous observations, as species turnover between hadal, abyssal and bathyal depths can be clearly noted (**Figure 10**). Individuals of *E. mamaqucha* sp. nov. dominated at the hadal zone, sediments of abyssal stations were inhabited by *E. pterus*, *Echinoderes* sp. 2 and *E. mamaqucha* sp. nov., while *E. juliae* and *Echinoderes* sp. 3 were found at the shallower station located at the continental slope. Nevertheless, it should also be noted, that all mud dragon species of the Atacama Trench region belong to one genus *Echinoderes*. *Echinoderes* is the most common, widely distributed and species-rich mud dragon genus. However, from the currently 24 known abyssal mud dragon species, only 11 belong to *Echinoderes*, which indicates that the generic diversity of deep-sea kinorhynchs is higher than it would seem to be, given our results. On the other hand, a very extensive study performed on the northeastern Pacific clearly showed that the deep-sea kinorhynch fauna in this region is dominated by echinoderids (Sørensen et al., 2018). It is therefore difficult to predict whether the observed diversity pattern, with representatives of only one mud dragon genus, reflects limitation in the data or low diversified kinorhynch community, distinctive for the Atacama Trench region. A lack of characterization of Kinorhyncha communities across the Pacific abyssal plain makes it difficult to assess the geographic distribution of deep-sea forms.

Community Composition and Comparison With Other Deep-Sea Species

What should be highlighted though, is that the newly described species (*E. mamaqucha* sp. nov.) as well as the other three potentially new species (*Echinoderes* sp. 1, *Echinoderes* sp. 2, and *Echinoderes* sp. 3) show a very close resemblance to other deep-water species of *Echinoderes*. *Echinoderes mamaqucha* sp. nov. and *Echinoderes* sp. 2 show a close similarity to *E. dubiosus* that was described from the North-Eastern Pacific (> 3500 m water depth) (Sørensen et al., 2018) and *E. bathyalis* described from the East Atlantic (> 2500 m water depth) (Yamasaki et al., 2018b). The second striking morphological similarity can be noted between the specimen of *Echinoderes* sp. 1 found at 7720 m and *E. ultraabyssalis* described from the deepest depression of the Kuril-Kamchatka Trench (> 9000 m; Adrianov and Maiorova, 2019). In other words, even though each trench and surrounding abyssal plains seem to host a unique fauna at the species level, there is still a close phylogenetic relationship between the species at these extreme depths. This either suggests a certain gene flow between these deep habitats, or that they originally were invaded by a few species that subsequently speciated further. The potential of gene flow of pan-oceanic scale has been already documented for some benthic deep-sea taxa (Eustace et al., 2016; LaBella et al., 2017), including meiofaunal organisms (Pawlowski et al., 2007; Bik et al., 2010;

Fontaneto, 2019 and references therein). Hence, similarities between geographically distinct species is highly possible, as a result of incomplete lineage sorting following the historicaltectonic movements (e.g., formation of the Isthmus of Panama) or dispersal over large distance, e.g., through thermohaline circulation (Pawlowski et al., 2007; Ptatscheck and Traunspurger, 2020). The latter may seem even more likely, as in the material from abyssal station at 4050 m we found *E. pterus*. This species was already noted at several locations in the Arctic Ocean, in the North Atlantic and the Mediterranean, from the continental shelf to the deep-sea floor and on seamounts (Yamasaki et al., 2018a, 2019). A similar example is the presence of *E. juliae* and *Echinoderes* sp. 3 in the sediments collected from continental slope station at 2560 m. *Echinoderes juliae* is known from the abyssal plain and continental rise off California (Sørensen et al., 2018) and despite significant geographical distance (ca. 7000 km) we found considerable consistency of morphological characters between *E. juliae* at its type locality and the individual from the Atacama Trench region. In contrast, *Echinoderes* sp. 3 shows close morphological resemblance to *E. hakaiensis* – a species described from British Columbia (Herranz et al., 2018) and later found in the deep-water off California (Sørensen et al., 2018). These findings support the previous suggestions about the capability of deep-sea kinorhynchs species to disperse over great distances (Neuhaus and Sørensen, 2013; Sørensen et al., 2018; Yamasaki et al., 2018a, 2019). Yet, the distribution process, the ongoing dispersal directions and migration routes are unknown.

Hadal trenches remain among the least sampled deep-sea habitats, although their unusual isolation and distribution offer exceptional opportunities to test many ecological and evolutionary theories (Blankenship-Williams and Levin, 2009). Therefore, we hope that this first evaluation of mud dragon diversity in the Atacama Trench add to other hadal studies providing new information about species diversity, which at last will enhance our understanding of biodiversity patterns in the deep-sea.

DATA AVAILABILITY STATEMENT

The original contributions presented in the study are included in the article/supplementary materials, further inquiries can be directed to the corresponding author/s.

AUTHOR CONTRIBUTIONS

KG acquired the funding for taxonomic studies, performed morphological examinations and taxonomic work, and prepared the original draft and figures. DZ conceived the general idea of the study and acquired the funding for the deep-sea cruise. MSh processed meiofauna samples. MSø conceived the general idea of the taxonomic study, supervised morphological and taxonomic studies, and manuscript writing. All authors proof-read the manuscript prior to submission, contributed to the final version and approved the submitted version.

FUNDING

This study was funded by the project "Prokaryote-nematode Interaction in marine extreme envirONments: a uniquE source for ExploRation of innovative biomedical applications" (PIONEER) funded by the Total Foundation and IFREMER (2016–2019). Financial support was also provided through the European Research Council (HADES-ERC Project Grant No. 669947) and by the Danish National Research Foundation (Grant No: DNRF145, Danish Center for Hadal Research, HADAL). The first author was supported by the Polish National Agency for Academic Exchange NAWA, the Bekker Programme Fellowship (PPN/BEK/2019/1/00160/00001) at Natural History Museum of Denmark and partly by the statutory funds from the Institute of Oceanology, Polish Academy of Sciences (IO PAN).

ACKNOWLEDGMENTS

We are indebted to Ronnie Glud (SDU) for the invitation to work on Atacama meiofauna. Special thanks go to the chief scientists (Ronnie Glud/SDU, Frank Wenzhöfer/AWI, and Matthias Zabel/MARUM), captain, and crews of the cruise SO261 (R/V SONNE, 02/03-02/04/18). We thank Sophie Arnaud and Miriam Brandt for support during sampling activities. We would also like to thank Nuria Sánchez (Ifremer/UCM) for help in preparation of animals, Nicolas Gayet (Ifremer) for help in the SEM preparation, Eve Julie Pernet (Ifremer) for support in the laboratory, and Emilia Trudnowska (IOPAN) for help with map preparation. This article is registered at www.zoobank.org under urn:lsid:zoobank.org:pub:1A9867FF-1C58-F17-A869-F7534B262518.

REFERENCES

Adrianov, A. V., and Maiorova, A. S. (2015). *Pycnophyes abyssorum* sp. n. (Kinorhyncha: Homalorhagida), the deepest kinorhynch species described so far. *Deep Sea Res. II Top. Stud. Oceanogr.* 111, 49–59. doi: 10.1016/j.dsr2.2014.08.009

Adrianov, A. V., and Maiorova, A. S. (2016). *Condyloderes kurilensis* sp. nov. (Kinorhyncha: Cyclorhagida) - a new deep water species from the abyssal plain near the Kuril-Kamchatka Trench. *Russ. J. Mar. Biol.* 42, 11–19. doi: 10.1134/s1063074016010028

Adrianov, A. V., and Maiorova, A. S. (2018a). *Meristoderes okhotensis* sp. nov. – the first deep-water representative of kinorhynchs in the Sea of Okhotsk (Kinorhyncha: Cyclorhagida). *Deep Sea Res. II Top. Stud. Oceanogr.* 154, 99–105. doi: 10.1016/j.dsr2.2017.10.011

Adrianov, A. V., and Maiorova, A. S. (2018b). *Parasemnoderes intermedius* gen. n., sp. n. - the first abyssal representative of the family Semnoderidae (Kinorhyncha: Cyclorhagida). *Russ. J. Mar. Biol.* 44, 355–362. doi: 10.1134/s1063074018050024

Adrianov, A. V., and Maiorova, A. S. (2019). *Echinoderes ultraabyssalis* sp. nov. from the Kuril-Kamchatka Trench – the first hadal representative of the Kinorhyncha (Kinorhyncha: Cyclorhagida). *Prog. Oceanogr.* 178:102142. doi: 10.1016/j.pocean.2019.102142

Adrianov, A. V., and Malakhov, V. V. (1999). *Cephalorhyncha of the World Ocean*. Moscow: KMK Scientific Press. (in Russian with English translation).

Belyaev, G. M. (1989). *Deep-sea Ocean Trenches and Their Fauna*. Moscow: Nauka Publishing House.

Bik, H. M., Thomas, W. K., Lunt, D. H., and Lambshead, P. J. D. (2010). Low endemism, continued deep-shallow interchanges, and evidence for cosmopolitan distributions in free-living marine nematodes (order Enoplida). *Evol. Biol.* 10:1e10.

Blankenship, L. E., Yayanos, A. A., Cadien, D. B., and Levin, L. A. (2006). Vertical zonation patterns of scavenging amphipods from the hadal zone of the Tonga and Kermadec Trenches. *Deep-Sea Res. I* 53, 48–61. doi: 10.1016/j.dsr.2005.09.006

Blankenship-Williams, L. E., and Levin, L. A. (2009). Living deep: a synopsis of hadal trench ecology. *Mar. Technol. Soc. J.* 43, 137–143. doi: 10.4031/mtsj.43.5.23

Boakes, E. H., McGowan, P. J. K., Fuller, R. A., Chang-qing, D., Clark, N. E., O'Connor, K., et al. (2010). Distorted views of biodiversity: spatial and temporal bias in species occurrence data. *PLoS Biol.* 8:e1000385. doi: 10.1371/journal.pbio.1000385

Brandt, A., Alalykina, I., Brix, S., Brenke, N., Błażewicz, M., Golovan, O. A., et al. (2019). Depth zonation of Northwest Pacific deep- sea macrofauna. *Prog. Oceanogr.* 176:102131. doi: 10.1016/j.pocean.2019.102131

Carus, J. V. (1885). *Prodromus Faunae Mediterraneae sive Descriptio Animalium maris Mediterranei incolarum Quam Comparata Silva Rerum Quatenus Innotiut Adiectis et Nominibus Vulgaribus Eorumque Auctoribus in Commodum Zoologorum*, Vol. I, *Coelenterata, Echinodermata, Vermes, Arthropoda*. Germany: E. Schweizerbarfsche Verlagshandlung.

Cepeda, D., Pardos, F., and Sánchez, N. (2019a). Kinorhyncha from the Caribbean, with the description of two new species from Puerto Rico and Barbados. *Zool. Anz.* 282, 127–139. doi: 10.1016/j.jcz.2019.05.014

Cepeda, D., Sánchez, N., and Pardos, F. (2019b). First extensive account of the phylum Kinorhyncha from Haiti and the Dominican republic (Caribbean Sea), with the description of four new species. *Mar. Biodivers.* 49, 2281–2309. doi: 10.1007/s12526-019-00963-x

Claparède, A. R. E. (1863). *Zur Kenntnis Der Gattung Echinoderes Duj. Beobachtungen über Anatomie und Entwicklungsgeschichte Wirbelloser Thiere an der Küste von Normandie Angestellt*. Leipzig: Engelmann

Dal Zotto, M., and Todaro, M. A. (2016). Kinorhyncha from Italy, a revision of the current checklist and an account of the recent investigations. *Zool. Anz.* 265, 90–107. doi: 10.1016/j.jcz.2016.01.004

Danovaro, R., Gambi, C., and Della Croce, N. (2002). Meiofauna hotspot in the Atacama Trench, eastern south Pacific Ocean. *Deep Sea Res. I* 49, 843–857. doi: 10.1016/s0967-0637(01)00084-x

Danovaro, R., Della Croce, N., Dell'Anno, A., and Pusceddu, A. (2003). A depocenter of organic matter at 7800m depth in the SE Pacific Ocean. *Deep Sea Res. I* 50, 1411–1420. doi: 10.1016/j.dsr.2003.07.001

Eustace, R. M., Kilgallen, N. M., Ritchie, H., Piertney, S. B., and Jamieson, A. J. (2016). Morphological and ontogenetic stratification of abyssal and hadal Eurythenes gryllus (Amphipoda: Lysianassidae) from the Peru-Chile Trench. *Deep Sea Res. Part I* 109, 91–98. doi: 10.1016/j.dsr.2015.11.005

Fontaneto, D. (2019). Long-distance passive dispersal on microscopic aquatic animals. *Movement Ecol.* 7:10.

Fujii, T., Kilgallen, N. M., Rowden, A. A., and Jamieson, A. J. (2013). Deep sea amphipod community structure across abyssal to hadal depths in the Peru–Chile and Kermadec trenches. *Mar. Ecol. Prog. Ser.* 492, 125–138. doi: 10.3354/meps10489

Fossing, H., Gallardo, V. A., Jørgensen, B. B., Hüttel, M., Nielsen, L. P., and Schulz, H. (1995). Concentration and transport of nitrate by mat-forming sulphur bacterium Thioploca. *Nature* 374, 713–715. doi: 10.1038/374713a0

France, S. C. (1993). Geographic variation among three isolated populations of the hadal amphipod *Hirondellea gigas* (Crustacea: Amphipoda: Lysianassoidea). *Mar. Ecol. Prog. Ser.* 92, 277–287. doi: 10.3354/meps092277

Gallo, N. D., Cameron, J., Hardy, K., Fryer, P., Bartlett, D. H., and Levin, L. A. (2015). Submersible- and lander-based community patterns in the Mariana and New Britain trenches: influence of productivity and depth on epibenthic and scavenging communities. *Deep Sea Res. I* 99, 119–133. doi: 10.1016/j.dsr.2014.12.012

Gambi, C., Vanreusel, A., and Danovaro, R. (2003). Biodiversity of nematode assemblages from deep-sea sediments of the Atacama Slope and Trench (South Pacific Ocean). *Deep Sea Res. I* 50, 103–117. doi: 10.1016/s0967-0637(02)00143-7

G[a]Ordóñez, D., Pardos, F., and Benito, J. (2008). Three new *Echinoderes* (Kinorhyncha, Cyclorhagida) from north Spain, with new evolutionary aspects in the genus. *Zool. Anz.* 247, 95–111. doi: 10.1016/j.jcz.2007.07.001

Glud, R. N., Wenzhöfer, F., Middelboe, M., Oguri, K., Turnewitsch, R., Canfield, D. E., et al. (2013). High rates of microbial carbon turnover in sediments in the deepest oceanic trench on Earth. *Nat. Geosci.* 6, 284–288. doi: 10.1038/ngeo1773

Glud, R. N., Berg, P., Thamdrup, B., Larsen, M., Stewart, H. A., Jamieson, J., et al. (2021). Hadal trenches are dynamic hotspots for early diagenesis in the deep sea. *Commun. Earth Environ.* 2:21.

Grzelak, K., and Sørensen, M. V. (2018). New species of *Echinoderes* (Kinorhyncha: Cyclorhagida) from Spitsbergen, with additional information about known Arctic species. *Mar. Biol. Res.* 14, 113–147. doi: 10.1080/17451000.2017.1367096

Grzelak, K., and Sørensen, M. V. (2019a). Diversity and community structure of kinorhynchs around Svalbard: first insights into spatial patterns and environmental drivers. *Zool. Anz.* 282, 31–43. doi: 10.1016/j.jcz.2019.05.009

Grzelak, K., and Sørensen, M. V. (2019b). Diversity and distribution of Arctic *Echinoderes* species (Kinorhyncha: Cyclorhagida), with description of one new species and redescription of *E. arlis* Higgins, 1966. *Mar. Biodivers.* 49, 1131–1150. doi: 10.1007/s12526-018-0889-2

Harris, P. T., Macmillan-Lawler, M., Rupp, J., and Baker, E. K. (2014). Geomorphology of the oceans. *Mar. Geol.* 352, 4–24. doi: 10.1016/j.margeo.2014.01.011

Herranz, M., Sánchez, N., Pardos, F., and Higgins, R. P. (2014). New Kinorhyncha from Florida coastal waters. *Helgol. Mar. Res.* 68, 59–87. doi: 10.1007/s10152-013-0369-9

Herranz, M., Yangel, E., and Leander, B. (2018). *Echinoderes hakaiensis* sp. nov.: a new mud dragon (Kinorhyncha, Echinoderidae) from the northeastern Pacific Ocean with the redescription of *Echinoderes pennaki* Higgins, 1960. *Mar. Biodivers.* 48, 303–325. doi: 10.1007/s12526-017-0726-z

Higgins, R. P. (1978). *Echinoderes gerardi* n. sp. and *E. riedli* (Kinorhyncha) with descriptions of closely related species. *Trans. Am. Microsc. Soc.* 97, 171–180. doi: 10.2307/3225589

Jamieson, A. J., Fujii, T., Mayor, D. J., Solan, M., and Priede, I. G. (2010). Hadal trenches: the ecology of the deepest places on Earth. *Trends Ecol. Evol.* 25, 190–197. doi: 10.1016/j.tree.2009.09.009

Jamieson, A. J., Kilgallen, N. M., Rowden, A. A., Fujii, T., Horton, T., Lörz, A. N., et al. (2011). Bait-attending fauna of the Kermadec Trench, SW Pacific Ocean: evidence for an ecotone across the abysal-hadal transition zone. *Deep Sea Res. I* 58, 49–62. doi: 10.1016/j.dsr.2010.11.003

Kamenskaya, O. E. (1981). The amphipods (Crustacea) from deep-sea trenches in the western part of the Pacific Ocean. *Trudy Instituta Okeanologii* 115, 94–107. (in Russian with English summary).

Karling, T. G. (1954). *Echinoderes levanderi* n. sp. (Kinorhyncha) aus der Ostsee. *Arkiv för Zoologi* 7, 189–192.

Kitahashi, T., Kawamura, K., Kojima, S., and Shimanaga, M. (2013). Assemblages gradually change from bathyal to hadal depth: a case study on harpacticoid copepods around the Kuril Trench (north-west Pacific Ocean). *Deep Sea Res. I* 74, 39–47. doi: 10.1016/j.dsr.2012.12.010

LaBella, A. L., Van Dover, C. L., Jollivet, D., and Cunningham, C. W. (2017). Gene flow between Atlantic and Pacific Ocean basins in three lineages of deep-sea clams (Bivalvia: Vesicomyidae: Pliocardiinae) and subsequent limited gene flow within the Atlantic. *Deep Sea Res. II* 137, 307–317. doi: 10.1016/j.dsr2.2016.08.013

Landers, S. C., Sørensen, M. V., Beaton, K. R., Jones, C. M., Miller, J. M., and Stewart, P. M. (2018). Kinorhynch assemblages in the Gulf of Mexico continental shelf collected during a two-year survey. *J. Exp. Mar. Biol. Ecol.* 02, 81–90. doi: 10.1016/j.jembe.2017.05.013

Landers, S. C., Basshman, R. D., Miller, J. A., Ingels, J., Sánchez, N., and Sørensen, M. V. (2020). Kinorhynch communities from Alabama coastal waters. *Mar. Biol. Res.* 16, 494–504. doi: 10.1080/17451000.2020.1789660

Leduc, D., Rowden, A. A., Glud, R. N., Wenzhöfer, F., Kitazato, H., and Clark, M. R. (2016). Comparison between infaunal communities of the deep floor and edge

of the Tonga Trench: possible effect of differences in organic matter supply. *Deep Sea Res. I* 116, 264–275. doi: 10.1016/j.dsr.2015.11.003

Lemenkova, P. (2019). Geomorphological modelling and mapping of the Peru-Chile Trench by GMT. *Polish Cartographic Rev.* 51, 181–194. doi: 10.2478/pcr-2019-0015

Neuhaus, B., and Blasche, T. (2006). *Fissuroderes*, a new genus of Kinorhyncha (Cyclorhagida) from the deep sea and continental shelf of New Zealand and from the continental shelf of Costa Rica. *Zool. Anz.* 245, 19–52. doi: 10.1016/j.jcz.2006.03.003

Neuhaus, B. (2013). "Kinorhyncha (=Echinodera)," in *Handbook of Zoology. Gastrotricha, Cycloneuralia and Gnathifera*, Vol 1, *Nematomorpha, Priapulida, Kinorhyncha, Loricifera*, ed. A. Schmidt-Rhaesa (Berlin: De Gruyter).

Neuhaus, B., and Sørensen, M. V. (2013). Populations of *Campyloderes* sp. (Kinorhyncha, Cyclorhagida): one global species with significant morphological variation? *Zool. Anz.* 252, 48–75. doi: 10.1016/j.jcz.2012.03.002

Pardos, F., Herranz, M., and Sánchez, N. (2016). Two sides of a coin: the phylum Kinorhyncha in Panama. II) Pacific Panama. *Zool. Anz.* 265, 26–47. doi: 10.1016/j.jcz.2016.06.006

Pawlowski, J., Fahrni, J., Lecroq, B., Cornelius, N., Excoffier, L., Cedhagen, T., et al. (2007). Bipolar gene flow in deep-sea benthic foraminifera. *Mol. Ecol.* 16, 4089–4096. doi: 10.1111/j.1365-294x.2007.03465.x

Perrone, F. M., Dell'Anno, A., Danovaro, R., Della Croce, N., and Thurston, M. H. (2002). Population biology of *Hirondellea* sp. nov. (Amphipoda: Gammaridea: Lysianassoidea) from the Atacama Trench (south-east Pacific Ocean). *J. Mar. Biol. Assoc.* 82, 419–425. doi: 10.1017/s0025315402005672

Ptatscheck, C., and Traunspurger, W. (2020). The ability to get everywhere: dispersal modes of free-living aquatic nematodes. *Hydrobiologia* 847, 3519–3547. doi: 10.1007/s10750-020-04373-0

Rex, M. A., Etter, R. J., Morris, J. S., Crouse, J., McClain, C. R., Johnson, N. A., et al. (2006). Global bathymetric patterns of standing stock and body size in the deep-sea benthos. *Mar. Ecol. Prog. Ser.* 317, 1–8. doi: 10.3354/meps317001

Sabbatini, A., Morigi, C., Negri, A., and Gooday, A. J. (2002). Soft-shelled benthic foraminifera from a hadal site (7800 m water depth) in the Atacama Trench (SE Pacific): preliminary observations. *J. Micropalaeontol.* 21, 131–135. doi: 10.1144/jm.21.2.131

Sánchez, N., Pardos, F., and Sørensen, M. V. (2014a). A new kinorhynch genus, *Mixtophyes* (Kinorhyncha: Homalorhagida), from the Guinea Basin deep-sea, with new data on the family Neocentrophyidae. *Helgol. Mar. Res.* 68, 221–239. doi: 10.1007/s10152-014-0383-6

Sánchez, N., Pardos, F., and Sørensen, M. V. (2014b). Deep-sea Kinorhyncha: two new species from the Guinea Basin, with evaluation of an unusual male feature. *Org. Divers. Evol.* 14, 349–361. doi: 10.1007/s13127-014-0182-6

Sánchez, N., Pardos, F., and Martínez Arbizu, P. (2019). Deep-sea Kinorhyncha diversity from the polymetallic nodule fields at the clarion-clipperton fracture zone (CCZ). *Zool. Anz.* 282, 88–105. doi: 10.1016/j.jcz.2019.05.007

Schmidt, C., and Martínez Arbizu, P. (2015). Unexpectedly higher metazoan meiofauna abundance in the Kuril-Kamchatka trench compared to the adjacent abyssal plains. *Deep Sea Res. II: Top. Stud. Oceanogr.* 111, 60–75. doi: 10.1016/j.dsr2.2014.08.019

Schmidt, C., Sattarova, V. V., Katrynski, L., and Martìnez Arbizu, P. (2019). New insights from the deep: meiofauna in the Kuril-Kamchatka Trench and adjacent abyssal plain. *Prog. Oceanogr.* 173, 192–207. doi: 10.1016/j.pocean.2019.02.010

Sørensen, M. V. (2018). Redescription of *Echinoderes levanderi* Karling, 1954 (Kinorhyncha: Cyclorhagida) - a kinorhynch tolerant to very low salinities. *Eur. J. Taxon.* 436, 1–17.

Sørensen, M. V., Rho, H. S., Min, W.-G., Kim, D., and Chang, C. Y. (2012). An exploration of *Echinoderes* (Kinorhyncha: Cyclorhagida) in Korean and neighboring waters, with the description of four new species and a redescription of *E. tchefouensis* Lou, 1934. *Zootaxa* 3368, 161–196. doi: 10.11646/zootaxa.3368.1.8

Sørensen, M. V., Dal Zotto, M., Rho, H. S., Herranz, M., Sánchez, N., Pardos, F., et al. (2015). Phylogeny of Kinorhyncha based on morphology and two molecular loci. *PLoS One* 10:e0133440. doi: 10.1371/journal.pone.0133440

Sørensen, M. V., Rohal, M., and Thistle, D. (2018). Deep-sea Echinoderidae (Kinorhyncha: Cyclorhagida) from the Northwest Pacific. *Eur. J. Taxon.* 456, 1–75.

Sørensen, M. V., Thistle, D., and Landers, S. C. (2019). North American *Condyloderes* (Kinorhyncha: Cyclorhagida: Kentrorhagata): female dimorphism suggests moulting among adult Condyloderes. *Zool. Anz.* 282, 232–251. doi: 10.1016/j.jcz.2019.05.015

Sørensen, M. V., Goetz, F. E., Herranz, M., Chang, C. Y., Chatterjee, T., Durucan, F., et al. (2020). Description, redescription and revision of sixteen putatively closely related species of *Echinoderes* (Kinorhyncha: Cyclorhagida), with the proposition of a new species group – the *Echinoderes dujardinii* group. *Eur. J. Taxon.* 730, 1–101. doi: 10.5479/si.00810282.248

Steward, H. A., and Jamieson, A. J. (2018). Habitat heterogeneity of hadal trenches: considerations and implications for future studies. *Prog. Oceanogr.* 161, 47–65. doi: 10.1016/j.pocean.2018.01.007

Thormar, J., and Sørensen, M. V. (2010). Two new species of *Echinoderes* (Kinorhyncha: Cyclorhagida) from the Solomon Islands. *Meiofauna Mar.* 594, 67–96.

Turnewitsch, R., Falahat, S., Stehlikova, J., Oguri, K., Glud, R. N., Middleboe, M., et al. (2014). Recent sediment dynamics in hadal trenches: evidence for the influence of higher-frequency (tidal, near-inertial) fluid dynamics. *Deep Sea Res. I* 90, 125–138. doi: 10.1016/j.dsr.2014.05.005

Vincx, M. (1996). "Meiofauna in marine and fresh water sediments," in *Methods for the Examination of Organismal Diversity in Soils and Sediments*, ed. G. S. Hall (Cambridge: CAB International, University Press), 214–248.

von Huene, R., and Scholl, D. W. (1991). Observations at convergent margins concerning sediment subduction, subduction erosion, and the growth of continental crust. *Rev. Geophys.* 29, 279–316. doi: 10.1029/91rg00969

Wei, C.-L., Rowe, G. T., Escobar-Briones, E., Boetius, A., Soltwedel, T., Caley, M. J., et al. (2010). Global patterns and predictions of seafloor biomass using random forests. *PLoS one* 5:e15323. doi: 10.1371/journal.pone.0015323

Wenzhöfer, F., Oguri, K., Middelboe, M., Turnewitsch, R., Toyofuku, T., Kitazato, H., et al. (2016). Benthic carbon mineralization in hadal trenches: assessment by in situ O2 microprofile measurements. *Deep Sea Res. I* 116, 276–286. doi: 10.1016/j.dsr.2016.08.013

Wolff, T. (1960). The hadal community, an introduction. *Deep Sea Res.* 6, 95–124. doi: 10.1016/0146-6313(59)90063-2

Yamasaki, H., Kajihara, H., and Mawatari, S. F. (2012). First report of kinorhynchs from Hokkaido, Japan, including a new species of *Pycnophyes* (Pycnophyidae: Homalorhagida). *Zootaxa* 3425, 23–41. doi: 10.11646/zootaxa.3425.1.2

Yamasaki, H., Grzelak, K., Sørensen, M. V., Neuhaus, B., and George, K. H. (2018a). *Echinoderes pterus* sp. n. showing a geographically and bathymetrically wide distribution pattern on seamounts and on the deep-sea floor in the Arctic ocean, Atlantic ocean, and the Mediterranean sea (Kinorhyncha, Cyclorhagida). *ZooKeys* 771, 15–40. doi: 10.3897/zookeys.771.25534

Yamasaki, H., Neuhaus, B., and George, K. H. (2018b). Three new species of Echinoderidae (Kinorhyncha: Cyclorhagida) from two seamounts and the adjacent deep-sea floor in the Northeast Atlantic Ocean. *Cah. Biol. Mar.* 59, 79–106.

Yamasaki, H., Neuhaus, B., and George, K. H. (2019). Echinoderid mud dragons (Cyclorhagida: Kinorhyncha) from senghor seamount (NE Atlantic Ocean) including general discussion of faunistic characters and distribution patterns of seamount kinorhynchs. *Zool. Anz.* 282, 64–87. doi: 10.1016/j.jcz.2019.05.018

Yamasaki, H., Herranz, M., and Sørensen, M. V. (2020). An interactive key to species of Echinoderidae (Kinorhyncha). *Zool. Anz.* 287, 14–16. doi: 10.1016/j.jcz.2020.05.002

Zelinka, C. (1896). Demonstration der Tafeln der *Echinoderes*-monographie. *Verh. Dtsch. Zool. Ges.* 6, 197–199.

Zelinka, C. (1913). *Der Echinoderen der Deutschen Südpolar-Expedition, 1901-1903. Band 14*. Berlin: Walter de Gruyter.

Zeppilli, D., Leduc, D., Fontanier, C., Fontaneto, D., Fuchs, S., Gooday, A. J., et al. (2018). Characteristics of meiofauna in extreme marine ecosystems: a review. *Mar. Biodivers.* 48, 35–71. doi: 10.1007/s12526-017-0815-z

Conflict of Interest: The authors declare that the research was conducted in the absence of any commercial or financial relationships that could be construed as a potential conflict of interest.

Copyright © 2021 Grzelak, Zeppilli, Shimabukuro and Sørensen. This is an open-access article distributed under the terms of the Creative Commons Attribution License (CC BY). The use, distribution or reproduction in other forums is permitted, provided the original author(s) and the copyright owner(s) are credited and that the original publication in this journal is cited, in accordance with accepted academic practice. No use, distribution or reproduction is permitted which does not comply with these terms.

frontiers in Marine Science

ORIGINAL RESEARCH
published: 04 August 2021
doi: 10.3389/fmars.2021.703547

High Species Richness and Extremely Low Abundance of Cumacean Communities Along the Shelf and Slope of the Gulf of Guinea (West Africa)

Anna Stępień[1], Krzysztof Pabis[1], Robert Sobczyk[1] and Bjorn Serigstad[2]*

[1] Department of Invertebrate Zoology and Hydrobiology, University of Łódz, Łódz, Poland, [2] Center for Development Cooperation in Fisheries, Institute of Marine Research, Bergen, Norway

The Gulf of Guinea belongs to the most scarcely sampled marine basins in the oceans of the world. We have analyzed diversity and distribution patterns of cumacean communities on the shelf and slope, along the coast of Ghana. The material was collected in October and November of 2012 using a van Veen grab (0.1 m^2) on nine transects. Six stations were located at each transect (25, 50, 100, 250, 500, and 1,000 m). Sixty-three species of Cumacea were recorded with *Leucon* and *Eocuma* as the most speciose genera, with 12 and eight species, respectively. Comparisons of species richness with literature data pointed that the Ghanaian coast hosts very diverse communities. About 95% of species were new to science, and the number of cumacean species known from the West Africa increased by over 100%. Nevertheless, most of the species had extremely low abundance, 13 singletons and 15 doubletons were found. Mean density of cumaceans was estimated at only 1.5 ind./0.1 m^2. Species accumulation curve did not reach the asymptotic level, suggesting undersampling, despite the fact that sampling effort was high (250 samples). The highest species richness was recorded in the inner shelf (25–50 m) and on the slope (1,000 m). Cluster analysis separated shallow water communities from deeper regions on the shelf and upper slope. The most unique species composition was found at 1,000 m. Principal component analysis showed the importance of oxygen, sediments, and human-related disturbance for distribution of cumacean communities. In the shallows, oxygen content and presence of gravel were the most important factors structuring communities. In the deeper bottom areas (250–1,000 m), cumacean fauna was affected by local pollution, mainly by higher concentration of barium, other heavy metals, and THC.

Keywords: Cumacea, depth gradient, diversity, pollution, Gulf of Guinea

OPEN ACCESS

Edited by:
Torben Riehl, Senckenberg Museum, Germany

Reviewed by:
Mauricio Shimabukuro, University of Southern Denmark, Denmark
Gustavo Fonseca, Federal University of São Paulo, Brazil

***Correspondence:**
Anna Stępień
anna.stepien@biol.uni.lodz.pl

Specialty section:
This article was submitted to Deep-Sea Environments and Ecology, a section of the journal Frontiers in Marine Science

Received: *30 April 2021*
Accepted: *29 June 2021*
Published: *04 August 2021*

Citation:
Stępień A, Pabis K, Sobczyk R and Serigstad B (2021) High Species Richness and Extremely Low Abundance of Cumacean Communities Along the Shelf and Slope of the Gulf of Guinea (West Africa). Front. Mar. Sci. 8:703547. doi: 10.3389/fmars.2021.703547

INTRODUCTION

Continental margins constitute about 11% of the oceans of the world and are shaped by a complex set of environmental factors that are dynamically changing along a depth gradient (Levin and Sibuet, 2012). They are characterized by high habitat heterogeneity and belong to the most important marine biodiversity hot spots (Danovaro et al., 2009; Menot et al., 2010; Levin and Sibuet, 2012). At the same time, continental margins belong to areas of special economic interests,

such as fishery and oil industry (Menot et al., 2010). This makes them one of the most interesting natural laboratories for studies of biodiversity, ecosystem services, and environmental gradients as well as influence of human activities and climate change on marine biota (Levin and Sibuet, 2012; Birchenough et al., 2015). On the other hand, recent analysis based on over 10 million records obtained mostly from the Ocean Biogeographic Information System (OBIS), revealed a strong sampling bias in the marine biodiversity assessment. There is a large gap in the knowledge about marine fauna associated with tropical areas, and it is visible not only in the deep sea (bathyal and abyssal) but also on the shelf, with average number of sampling events an order of magnitude lower than in northern and southern mid latitudes (Menegotto and Rangel, 2018). The authors of this research pointed out a lack of scientific infrastructure and funding for marine research in developing tropical countries as the main reason of this situation. It is highly visible in the case of African marine fauna.

The West African continental margin belongs to the most scarcely sampled regions. Most of the available studies were focused on the shallows and based on low sampling effort (Buchanan, 1957; Longhurst, 1958, 1959; Bassindale, 1961; Le Loeuff and Intés, 1999; Bamikole et al., 2009). There is a particular lack of ecological research based on quantitative sampling and lack of detailed biodiversity inventories based on species level identification. The deep sea communities of the Gulf of Guinea are almost completely neglected in earlier research, with the exception of the areas affected by organic discharge from the Congo River (e.g., Gaever et al., 2009; Galéron et al., 2009; Menot et al., 2009) and most recent studies from Gabon (Friedlander et al., 2014) and Ghana (Pabis et al., 2020; Sobczyk et al., 2021). At the same time, the Gulf of Guinea is facing serious problems associated with various types of anthropogenic impacts, such as pollution events associated with the oil industry (Scheren et al., 2002; Ayamdoo, 2016), but those problems are only scarcely studied and need further research based on the analysis of various taxonomic groups (Pabis et al., 2020; Sobczyk et al., 2021). Influence of heavy metals, hydrocarbons, and other pollutants might have a substantial influence on the composition, diversity, and abundance of benthic communities (Olsgard and Gray, 1995; Gomez-Gesteira et al., 2003; Stark et al., 2020). However, there are no studies demonstrating the influence of anthropogenic disturbance on Cumacea.

Based on literature data, Le Loeuff and Cosel (1998) listed only 1,440 benthic species from the large part of the West African coast, starting from the Mauretania and ending in the Namibia (up to 200 m depth), although the study was focused mostly on megafauna (corals, echinoderms, and decapod crustaceans) as well as polychaetes and bivalves. Analysis of the same set of samples as in the cumacean study of the authors revealed 253 species of Polychaeta (Sobczyk et al., 2021), only from the small fragment of the Ghanaian coast, placing this area amongst the important biodiversity hot spots for those marine annelids. We can expect that similar hidden biodiversity can be encountered for many other taxonomic groups, especially so important like small peracarid crustaceans.

Cumacea are classified as one of the orders of Peracarida. With about 1,400 recognized species (Gerken, 2018), this order is on the third place in terms of species richness within Peracarida, after Ampipoda (9,500 species) and Isopoda (about 6,000 species), and together with Tanaidacea (about 1,400 species). Their true diversity is vastly underestimated, mostly because of taxonomic expertise bias (Appeltans et al., 2012). As all peracarids Cumacea are small brooders with no planktonic larvae, they borrow in the surface layer of the sediment (Pilar-Cornejol et al., 2004). They are often found in the first few centimeters of sediments and occur from the intertidal, down to abyssal depths (Watling and Gerken, 2021). Cumacea are significant element of benthic communities, that in particular regions or depth zones (e.g., deep sea and tropical areas) might be one of the most diverse groups of crustaceans (Jones and Sanders, 1972; Cartes et al., 2003; Doti et al., 2020). For example, at the upper slope off Portugal, Cumacea together with Isopoda reached the highest number of the species (Cunha et al., 1997); while in the Angola Basin off Namibia, they were the third most abundant group of Peracarida, after Isopoda and Tanaidacea (Brandt, 2005). Moreover, some species might reach locally high abundance, even up to 500 individuals per square meter, both on the shelf, and in the deep sea (Bishop, 1982; Swaileh and Adelung, 1995). Cumacea also play an important role in the trophic webs, especially as food source for fish and some macroinvertebrates, such as decapods (Cartes, 1993; Watling and Gerken, 2021). For example, *Diastylis rathkei* might constitute even 35% of the diet of flounder (Swaileh and Adelung, 1995).

Available studies demonstrated that cumaceans display preferences to particular grain size, which makes them a good indicator of sediment type (Dixon, 1944; Wieser, 1956; Jones, 1976). Some species are known to be sensitive to environmental stress. Two dominant species in Algeciras Bay (*Cumella limicola* and *Nannastacus unguiculatus*) were strongly influenced by hydrodynamism, sedimentation, and water turbidity (Alfonso et al., 1998). Some species of Cumacea are also good indicators of eutrophication, and have been proposed as organisms appropriate for biomonitoring (Corbera and Cardell, 1995; Ateş et al., 2014). Nevertheless, studies on biology and ecology of particular species or distribution patterns and structure of cumacean communities are still scarce, especially in the deep sea (e.g., Gage et al., 2004; Pabis and Błazewicz-Paszkowycz, 2011; Corbera and Sorbe, 2020 and references therein).

The knowledge about cumacean fauna of the Ghanian coast is highly scattered and based mostly on taxonomic publications (e.g., Băcescu, 1961, 1972; Day, 1975, 1978, 1980; Mühlenhardt-Siegel, 1996, 2000; Petrescu, 1998). So far, only 154 species of Cumacea are known from the whole African coast (Watling and Gerken, 2021), which makes 11% of the world fauna (Gerken, 2018). From West Africa, 59 species have been recorded, mostly from the continental shelf (Watling and Gerken, 2021), and only three were found on the Ghanaian coast (Jones, 1956; Petrescu, 2018). There are no quantitative studies on cumacean communities conducted on the African coast. Most earlier studies were focused on taxonomy.

Biodiversity assessments of the tropical continental margins are among the most important priorities of the current

marine science (Menegotto and Rangel, 2018). Therefore, the main aim of this study was to assess cumacean diversity on the continental shelf and slope of the Gulf of Guinea (25–1,000 m depth, Ghanaian coast) and compare it with literature data. We hypothesize that the Ghanaian continental margin hosts speciose cumacean communities with many species new to science. We wanted also to analyse the influence of various natural (e.g., oxygen, sediment type, salinity, and temperature) and anthropogenic (heavy metals and hydrocarbons) factors on the diversity and distribution patterns of those crustaceans. We hypothesize that local pollution might lower the abundance and diversity of those small crustaceans with limited dispersal abilities.

MATERIALS AND METHODS

Study Area

The Gulf of Guinea is a large open basin located in West Africa, influenced by a complex set of currents (Guinea Current, Benguela Current, South Equatorial Counter Current; Ukwe et al., 2003, 2006) and upwelling events (Nieto and Mélin, 2017). The north part of the Gulf of Guinea is influenced by seasonal upwelling, bringing nutrient-rich mid-depth waters to the surface and increasing the primary production (Binet and Marchal, 1993). The southern part depends rather on nutrient input from land drainage and river flood, mostly the Volta River, which is the only larger river system located along the almost 600-km long Ghanaian coast (Buchanan, 1957; Ukwe et al., 2003). The Gulf of Guinea is classified as a province in the Tropical Atlantic Realm, with rich fishery resources as well as large oil and gas reserves, and its sectors (e.g., north, central, and south) are considered a separate ecoregion (Spalding et al., 2007). The heterogeneity of habitats on continental margins has influence on high diversity of habitats for benthic fauna. At the same time, industrialization and the oil industry create numerous sources of disturbance that can potentially affect marine communities (Germain and Armengol, 1999; Owusu-Boadi and Kuitunen, 2002).

Sampling

The material was collected in October and November of 2012 from the board of RV Fridtjof Nansen. Nine transects were distributed along the whole coast of Ghana (**Figure 1**). Six stations were designated at each transect (25, 50, 100, 250, 500, and 1,000 m). Five replicate samples were collected at each station using a van Veen grab (0.1 m^2) supported with the Video Assisted Multi Sampler (VAMS), allowing for appropriate sediment penetration. The samples were washed using 0.3 mm mesh size and preserved in 4% formaldehyde solution. The material was collected in the framework of the Oil for Development (OfD) program, and supported by the Food and Agriculture Organization of the United Nations (FAO).

Environmental Factors

Physical and chemical properties of the sediment and water were also analyzed at each station. Temperature, conductivity, and oxygen level were measured using a Seabird 911 CTD Plus and SBE 21 Seacat thermosalinograph. Sediment structure (percentage content of gravel, sand, and silt) was also analyzed. Diameter of particles was calculated using the equations of Buchanan (1984), and Folk and Ward (1957). Level of total hydrocarbons (THC), toxic metals: arsenic (As), barium (Ba), cadmium (Cd), chromium (Cr), copper (Cu), nickel (Ni), lead (Pb), zinc (Zn), and content of total organic matter (TOM) were also measured. Total hydrocarbon content was analyzed using a gas chromatograph with a flame ionization detector (GC/FID), as outlined in the Intergovernmental Oceanographic Commission, Manuals and Guides No. 11, UNESCO Intergovernmental Oceanographic Commission (1982) while toxic metals contents were analyzed *via* inductively coupled plasma-atomic emission spectrometry (ICP-AES) (Jarvis and Jarvis, 1992; Elezz et al., 2018). Total organic matter was determined as the weight loss in a 2–3-g dried sample (dried at 105°C for 20 h) after 2 h of combustion at 480°C.

Analysis of Diversity and Abundance

Specimens were identified at the morphospecies level (Wägele, 2005). We have calculated species richness (S—number of species per sample), diversity (Shannon Index) and evenness (Pielou Index) (Magurran, 2012) as well as abundance [ind./0.1 m^2] for each sample. Mean values with standard deviations (SD) of those indices were calculated for each depth zone and for the whole material. Statistical differences between the depth zones were assessed by non-parametric Kruskal–Wallis test. *Post-hoc* testing was done by Dunn's test. This part of the analysis was performed using a STATISTICA 13 package (StatSoft, 2006).

Species accumulation curves averaging over 999 permutations were created using the PRIMER package. The curve plotted the cumulative number of different species observed as each new sample was added (Clarke and Warwick, 2001).

We have also assessed the number of rare species recorded in the material. The number of singletons (species represented by only one individual in the whole material, in all collected samples) and doubletons (represented by two individuals), and the number of unique species (species found in one sample only) and duplicates (species found in two samples only) were also calculated. Additionally, we have calculated the number of species recorded only in a given depth zone or given transect as well as the number of species common to given depth zones and transects. Frequency of occurrence (F—percentage of samples where a species was found in total number of samples) was calculated for each species.

Multivariate Analysis

Hierarchical agglomerative clustering analysis, based on the Bray–Curtis formula, was performed to check for faunistic similarity among the stations. For the analysis, mean values of abundance of each species calculated for each station were used. Data were square root-transformed, and the group average method was used. A SIMPROF test with 1% significance level was performed to check the multivariate structure within groups. This part of the analysis was performed using a Primer package (Clarke and Warwick, 2001).

The R software was used for all analyses of environmental factors influence on cumacean communities (R Core Team,

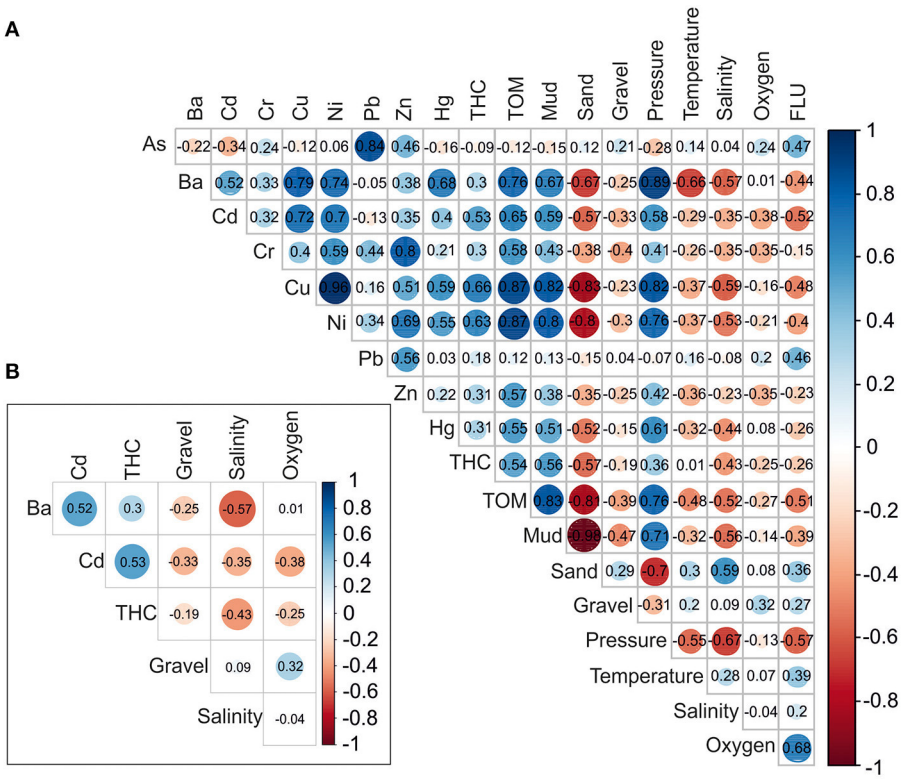

FIGURE 1 | Correlation matrices with Pearson's r correlation coefficients calculated for: **(A)** all predictors and **(B)** the least correlated predictors. For full list of environmental variables please see **Supplementary Table 1**.

2020). We used the Pearson correlation matrix (*corrplot::corrplot*; Wei and Simko, 2017) to assess pair-wise cross-correlation between each environmental variable. Based on strong correlation ($r > 0.6$), we included six variables from the initial set of 19 variables into further analysis, assuming they have an ecologically important role in explaining the richness of cumaceans.

Finally, six variables: Ba, Cd, THC, oxygen, gravel, and salinity were added into further analysis (**Figure 2**). For full list of environmental variables, please see **Supplementary Table 1**. Salinity was used in principal component analysis (PCA) only. Yeo-Johnson power transformation [*caret::preProcess()*; Kuhn, 2020] was used for reducing deviations linked with unequal ranges off selected factors (e.g., Ba). Next, PCA was performed to show dissimilarities in species composition among transects and stations [*vegan::rda*(); Oksanen et al., 2019]. Additionally, ranges of salinity were added to the PCA [*vegan::ordisurf*(); Oksanen et al., 2019] to demonstrate salt content relations in arrangement of stations in ordination space.

Species richness and PCA axis were used to fit generalized linear models (glm; for species richness) or linear models (lm; for PCA axis 1 and axis 2) with five environmental variables (Ba, Cd, THC, oxygen, and gravel) as fixed effects using the stats4 package [*stats4::lm()*, *stats4::glm()*; R Core Team, 2020]. Poisson distribution was used for species richness. To choose the best fitted models based on corrected Akaike Information Criterion (AICc), the dredge function was used (*MuMIn::dredge*; Bartoń, 2018). To calculate estimates of function slopes for the models with ΔAICc < 2, model averaging was employed [*MuMIn* package *model.avg()*, *confset95p()*, and *avgmod.95p()*]. The RSquareAdj function (*vegan::RSquareAdj*; Oksanen et al., 2019) was computed to reveal how much variance was explained by averaged models for PCA axes 1 and 2.

Hierarchical partitioning function (*hier.part::hier.part()*; Walsh and Mac Nally, 2013) for species richness as well as PCA axes 1 and axis 2 was used for checking the independent effect (%) of each environmental variable and its joint contribution to all other predictors. To compute it, goodness-of-fit measures for all model combinations with all predictors, with Gaussian (for PCA axes 1 and 2) or Poisson distribution (for species richness) were used. Statistical significance of the relative contribution of each predictor were determined by randomization test [*hier.part::rand.hp()*] with implementing *P*-values and *z*-scores (confidence limit < 0.95).

RESULTS

Diversity and Abundance

Altogether, 63 species (391 individuals) of Cumacea were identified. They represented 13 genera and six families (**Table 1**). It is assumed that 95% of species (60 species) are new to science. The most speciose genera were: *Leucon* (12 species), *Eocuma* (8), *Iphinoe*, and *Diastaylis* (both genera with seven species). The most abundant genera were: *Eocuma*

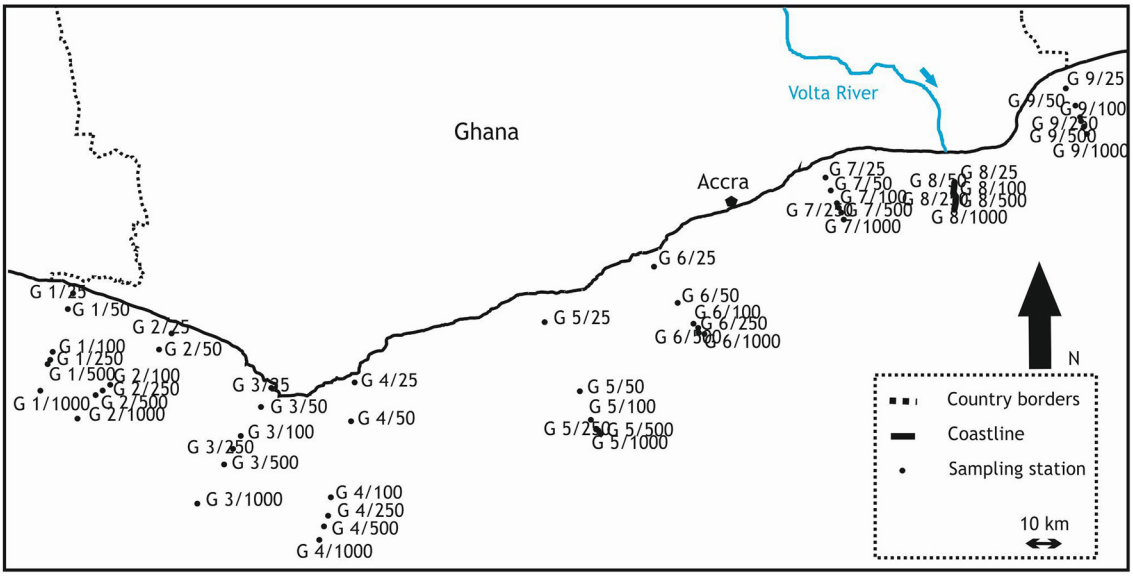

FIGURE 2 | Distribution of sampling stations in the Gulf of Guinea.

(95 individuals), *Bodotria* (60 individuals), and *Leucon* (50 individuals). Together, they constituted over half of the material. The most speciose and abundant families were: *Bodotridae* (23 species, 235 individuals), *Leuconidae* (15 species, 66 individuals), *Nannastacidea* (10 species, 67 individuals), and *Diastylidae* (10 species, 20 individuals). A large number of rare species were also recorded. In the whole material, 13 singletons and 15 doubletons were found. Seventeen species were found only in one sample, and 14 in two samples only. Frequency of occurrence of species in the whole material was extremely low. Only five species had frequency higher than 4%. The species with the highest frequency of occurrence in the whole material was *Eocuma* sp. 7 that was found only in 7% of the samples (**Table 1**). The species accumulation curve did not reach the asymptotic level, suggesting undersampling of the studied area (**Figure 3**).

The mean density of cumaceans calculated for all collected samples equalled to only 1.5 ind./0.1 m^2. General species richness and abundance decreased along a depth gradient. The highest number of species was found at 25 and 50 m with 17 and 28 species recorded, respectively (**Table 2**). Moreover, 15 species were common in those two depth zones (**Table 3**). On the outer shelf and upper slope, the number of species was lower and increased again to 19 species at 1,000 m stations (**Table 2**). It is also the depth zone with the most unique fauna, as 14 out of 19 species were recorded only here (**Table 2**). The general number of species was similar in most of the transects (**Table 2**). The highest number of species was found in a transect G6 (29 species), while the lowest species richness was recorded in transects G8 and G9 with seven and 10 species, respectively (**Table 2**). The highest number of species common with other transects was recorded in transect G6, but generally there was no clear pattern observed (**Table 4**).

Mean species richness and diversity per sample were the highest on the shallows (25 m – number of species per sample 1.04 ± 1; Shannon Index 0.2 ± 0.3, 50 m – number of species per sample 1.4 ± 1.2, Shannon Index 0.4 ± 0.4) and at 250 m (number of species per sample 1.1 ± 1, Shannon Index 0.3 ± 0.3) (**Figure 4**). Evenness was the highest at 1,000 m [0.9 ± 0.03 (**Figure 4**)]. Mean abundance changed along the depth gradient, and the highest values were observed at 50 (2.2 ± 2.2 ind./0.1 m^2) and 250 m (1.8 ± 1.8 ind./0.1 m^2). Below 250 m, it decreases with increasing depth (**Figure 4**).

Cluster Analysis

Four groups were distinguished in the cluster analysis although at low similarity level (20% or less), but all were significantly differentiated by the SIMPROF (**Figure 5**). Inner shelf areas were clearly separated from the outer shelf and slope showing strong depth zonation of cumacean communities. Two clusters (B and C) of grouped samples were collected at depth 25–50 m. The next two clusters consist of samples collected at depth 100−500 (cluster A) and 500–1,000 m (cluster D). The clusters differ in family and genera composition, number of species, and frequency of the species.

In the samples grouped in cluster A, 22 species were found, and eight of them belong to family Bodotridae, and six to family Diastylidae. Genus *Diastylis* was represented by six species and genus *Iphione* and *Eocuma* by three species each. The highest frequency of occurrence (56%) was observed for *Campylapsis* sp 2 and *Eocuma* sp 7.

Eleven species were found in samples forming cluster B, and nine of them represent family Bodotridae. The most speciose genera were *Bodotria* with five species and *Iphinoe* with two species. *Vaunthampsonia* sp 1 was present in 80% of the samples, and *Bodotria* sp 2 and *Eudorellopsis* sp 1 were present in 60% of the samples.

TABLE 1 | List of species with total abundance, frequency of occurrence in samples, and depth range.

Family	Genus	Number of specimens	Frequency [%]	Depth range [m]
Bodotriidae	*Eocuma* sp. 1	10	2.0	25–50
Bodotriidae	*Eocuma* sp. 2	14	2.8	50
Bodotriidae	*Eocuma* sp. 3	13	2.8	25–50
Bodotriidae	*Eocuma* sp. 4	5	1.6	25–50
Bodotriidae	*Eocuma* sp. 5	4	1.6	25–150
Bodotriidae	*Eocuma* sp. 6	8	2.4	25–50
Bodotriidae	*Eocuma* sp. 7	37	7.2	100
Bodotriidae	*Eocuma* sp. 8	4	1.2	250
Bodotriidae	*Bodotria* sp. 1	16	2.8	25–50
Bodotriidae	*Bodotria* sp. 2	9	3.2	25–50
Bodotriidae	*Bodotria* sp. 3	17	4.0	25–250
Bodotriidae	*Bodotria* sp. 4	14	2.4	25–50
Bodotriidae	*Bodotria* sp. 5	3	0.8	25–50
Bodotriidae	*Bodotria* sp. 6	1	0.4	50
Bodotriidae	*Cyclaspis* sp. 1	1	0.4	1,000
Bodotriidae	*Iphinoe* sp. 1	4	1.6	50–100
Bodotriidae	*Iphinoe* sp. 2	31	4.8	25–100
Bodotriidae	*Iphinoe* sp. 3	2	0.8	25
Bodotriidae	*Iphinoe* sp. 4	1	0.4	50
Bodotriidae	*Iphinoe* sp. 5	2	0.8	50
Bodotriidae	*Iphinoe* sp. 6	1	0.4	50
Bodotriidae	*Iphinoe* sp. 7	2	0.8	250
Bodotriidae	*Vaunthompsonia* sp. 1	14	3.2	25–100
Diastyliade	*Diastylis* sp. 1	1	0.4	250
Diastylidae	*Diastylis* sp. 2	3	0.8	50–100
Diastylidae	*Diastylis* sp. 3	4	1.6	50–250
Diastylidae	*Diastylis* sp. 4	1	0.4	50
Diastylidae	*Diastylis* sp. 5	2	0.8	100
Diastylidae	*Diastylis* sp. 6	1	0.4	250
Diastylidae	*Diastylis* sp. 7	3	1.2	50–1,000
Diastylidae	*Makrokylindrus* sp. 1	1	0.4	1,000
Diastylidae	*Makrokylindrus* sp. 2	2	0.8	1,000
Diastylidae	*Makrokylindrus* sp. 3	2	0.4	1,000
Lampropidae	*Lampropidae* sp. 1	14	2.4	250
Lampropidae	*Lampropidae* sp. 2	7	1.2	250
Leuconidae	*Eudorella* sp. 1	2	0.8	50–100
Leuconidae	*Eudorella* sp. 2	2	0.4	1,000
Leuconidae	*Eudorellopsis* sp. 1	4	1.6	25–50
Leuconidae	*Leucon (Epileucon)* sp. 1	18	2.8	500–1,000
Leuconidae	*Leucon (Epileucon)* sp. 2	1	0.4	1,000-
Leuconidae	*Leucon (Macrauloleucon)* sp. 3	6	2.4	100–500
Leuconidae	*Leucon (Macrauloleucon)* sp. 4	5	1.2	500
Leuconidae	*Leucon (Macrauloleucon)* sp. 5	1	0.4	1,000
Leuconidea	*Leucon (Crymoleucon)* sp. 6	3	0.8	1,000
Leuconidea	*Leucon (Leucon)* sp. 7	2	0.8	500
Leuconidea	*Leucon (Leucon)* sp. 8	7	1.2	500
Leuconidea	*Leucon (Leucon)* sp. 9	2	0.8	1,000
Leuconidea	*Leucon (Leucon)* sp. 10	3	1.2	500–1,000
Nannastacidae	*Campylaspis* sp. 1	7	2.0	25–1,000
Nannastacidae	*Campylaspis* sp. 2	20	5.6	50–250
Nannastacidae	*Campylaspis* sp. 3	15	4.4	25–500

(Continued)

TABLE 1 | Continued

Family	Genus	Number of specimens	Frequency [%]	Depth range [m]
Nannastacidae	*Campylaspis* sp. 4	4	1.2	25
Nannastacidae	*Campylaspis* sp. 5	1	0.4	1,000
Nannastacidae	*Cumella* sp. 1	2	0.4	250
Nannastacidae	*Cumella* sp. 2	2	0.4	1,000
Nannastacidae	*Cumella* sp. 3	2	0.8	500
Nannastacidae	*Cumella* sp. 4	5	1.6	1,000
Nannastacidae	*Nannastacidae* sp. 1	9	2.8	500–1,000
Pseudocumatidae	*Pseudocumatidae* sp. 1	2	0.8	1,000
	indet sp. 1	2	0.8	500
	indet sp. 1	1	0.4	1,000

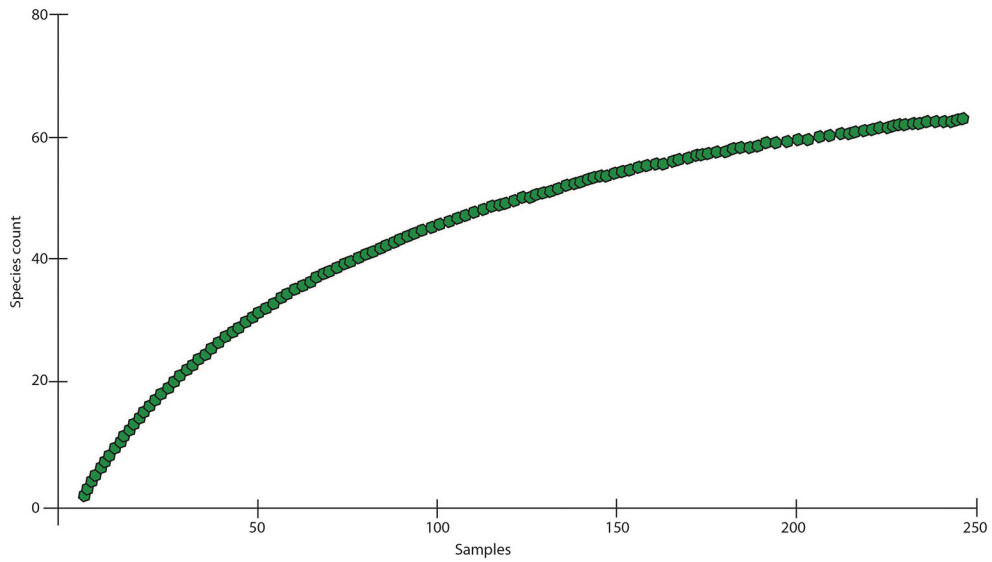

FIGURE 3 | Species accumulation curve for cumacean fauna sampled at the Gulf of Guinea.

Within cluster C, 28 species in total were observed, and 16 species belong to family Bodotridae. The most speciose genera were *Eocuma* with six species and *Bodotria* with five species. *Iphinoe* sp 2 and *Eocuma* sp 2 were characterized by the highest frequency of occurrence, which was 73 and 56%, respectively.

In the samples from cluster D, 25 species were recorded, and 10 belong to family Leuconidae and seven to Nannastacidae. *Leucon* was the most speciose genus (10 species), followed by *Cumella* (three species) and *Campylapsis* (three species). Nannastacidae sp. 1 had the highest frequency of occurrence, and it was present in 40% of the samples.

Influence of Physical and Chemical Factors on Cumacean Communities

PCA1 and PCA2 axes explained about 20% of variance. The first axis (10.7% variance explained) showed high dissimilarity between stations located at 100 m, and all other sites followed dissolved oxygen and salinity gradient. Three groups were established in the PCA mostly along the PCA2 axis (9% variance explained) (**Figure 6**). The first one (lower part of gradient) contained shallow water samples (25–50 m), characterized by higher concentration of oxygen and gravel. Here, a sandy type of substratum with relatively high contribution of gravel (depth zone 25–50 m) was noticed. Content of Ba, Cd, as well as THCs was significantly lower. The second group (higher part of gradient) contained samples from 250–1,000 m deep; and here, the samples were characterized by higher concentration of Ba, Cd, and THC. Lower concentration of oxygen and lower content of gravel and sand were noted here. Bottom deposits constituted mostly of silt. Salinity reached low to average values with high range (34.8–35.6‰). The third group contained samples from 100 m depth. The samples were distinguished from the other groups by high salinity content with low values range (35.7–35.8‰), and bottom substrate was dominated by sand and silt.

A set of two most parsimonious (with ΔAICc $<$ 2) linear models for PCA axis 1 revealed that high content of gravel

TABLE 2 | Total number of species in each depth zone/transect and number of species recorded only in a given depth zone/transect.

Depth zone	Number of unique species	Total number of species	Percentage of unique species
25 m	2	17	11.7
50 m	7	28	25.0
100 m	2	11	18.1
250 m	7	15	46.6
500 m	5	10	50.0
1,000 m	14	19	73.6
Transect			
G1	1	22	4.5
G2	1	19	5.2
G3	2	19	10.5
G4	8	24	33.3
G5	2	19	10.5
G6	1	29	3.4
G7	4	17	23.5
G8	2	7	28.5
G9	0	10	0

TABLE 3 | Species common between the depth zones.

Depth zone	25	50	100	250	500
25					
50	15				
100	2	7			
250	3	6	4		
500	1	1	1	2	
1,000	1	2	0	1	3

TABLE 4 | Species common between the transects.

Transect	G1	G2	G3	G4	G5	G6	G7	G8
G1								
G2	8							
G3	7	8						
G4	8	10	7					
G5	7	10	8	8				
G6	15	12	12	11	13			
G7	8	2	5	4	4	8		
G8	2	4	0	3	2	3	2	
G9	4	5	4	3	5	9	3	1

(estimate slope: -0.30, $p = 0.05$) as well as oxygen (estimate slope: 0.25, $p < 0.001$) shaped species composition along the axis. The influence of gravel was negatively correlated with species composition along axis 1. However, higher concentration of oxygen dissolved in water had a positive influence on it (**Table 5**, **Figure 7A**, **Supplementary Table 2**). The model explained about 31% of total variance. Hierarchical partitioning revealed that only the influence of oxygen (relative contribution: 64.3%) was significant for PCA axis 1 (**Figure 8**).

Form the three models best describing species composition along PCA axis 2 (containing Ba, THCs, oxygen, and gravel) we noted statistical significance of oxygen, gravel, and Ba. The higher content of oxygen (estimate slope: -0.16, $p < 0.001$) and gravel (estimate slope: -0.39, $p = 0.002$) had a negative influence on species composition along axis 2, while Ba (estimate slope: 0.21, $p = 0.01$) enhanced it (**Table 5**, **Figure 7B**, **Supplementary Table 2**). The model explained about 62% of total variance of cumaceans. The relative contribution of each factor supports the previous results. The influence of barium, gravel, and oxygen (independent effect: 29.3, 29.7, and 19%, respectively) was statistically significant (**Figure 8**).

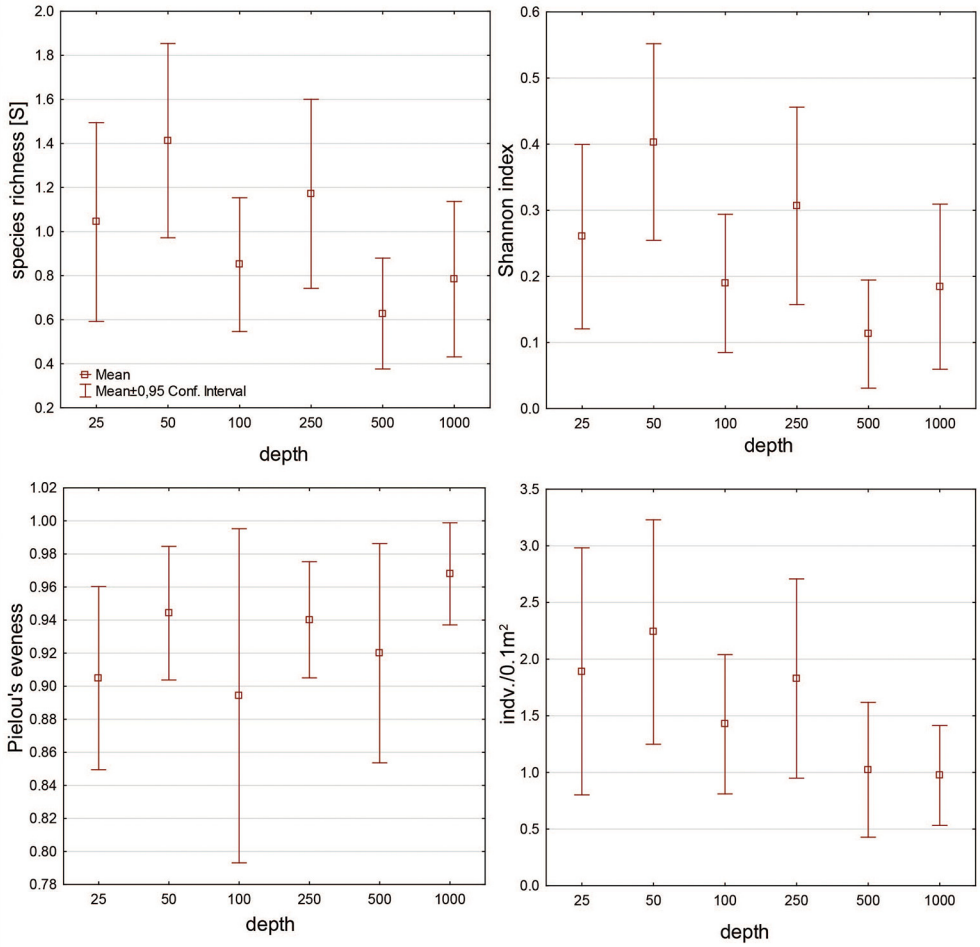

FIGURE 4 | Mean value of species richness, diversity, evenness, and abundance calculated for cumacean fauna in each depth zone.

A set of four most parsimonious models with ΔAICc < 2 best explained richness of cumaceans species. Ba, gravel, and oxygen were included into best averaged model; however, only the adverse effect of Ba (estimate slope: -0.37, $p = 0.04$) was statistically significant and caused decrease in species richness (**Table 5**, **Figure 9**, **Supplementary Table 2**). Based on the results of hierarchical partitioning, we found that the influence of Ba and oxygen (relative contribution: 24 and 32.1%, respectively) was significantly correlated with species richness (**Figure 8**).

DISCUSSION

Species Richness

Despite very low total abundance, the cumacean species richness on the Ghanaian coast was very high, and the species accumulation curves still showed substantial undersampling (**Figure 3**). Taking into account generally high sampling effort (much larger than in most of other cumacean studies, see **Table 6**) and large number of sampled stations, it can be assumed that great species rarity was the main reason behind this result. Large number of singletons and doubletons as well as large number of species recorded in a very low number of samples was typical feature of cumacean communities along the Ghanaian coast (**Table 1**). Moreover, the primary analysis indicates that 95% of collected species are new to the science. The results demonstrated the highly underestimated diversity of those crustaceans in the Gulf of Guinea, even compared with the global diversity of Cumacea, which was estimated at about 1,400 species (Gerken, 2018). After this study, the list of known cumacea from the coast of Guinea increased from 3 to 66 species (Watling and Gerken, 2021), which is a significant result for about 500-km long part of the coastline.

Comparisons with other studies of cumacean species richness are difficult because of large discrepancies in type of gear used, scale of the sampling area, sampling effort, and studied depth range, not to mention the differences in local environmental conditions or geological history of various regions (**Table 6**). Nevertheless, the number of 63 species is comparable even with much larger areas that were sampled extensively for a very long time. For example, in the whole Antarctic waters, 86 species of cumacea were recorded (De Broyer and Danis, 2011). Extensive

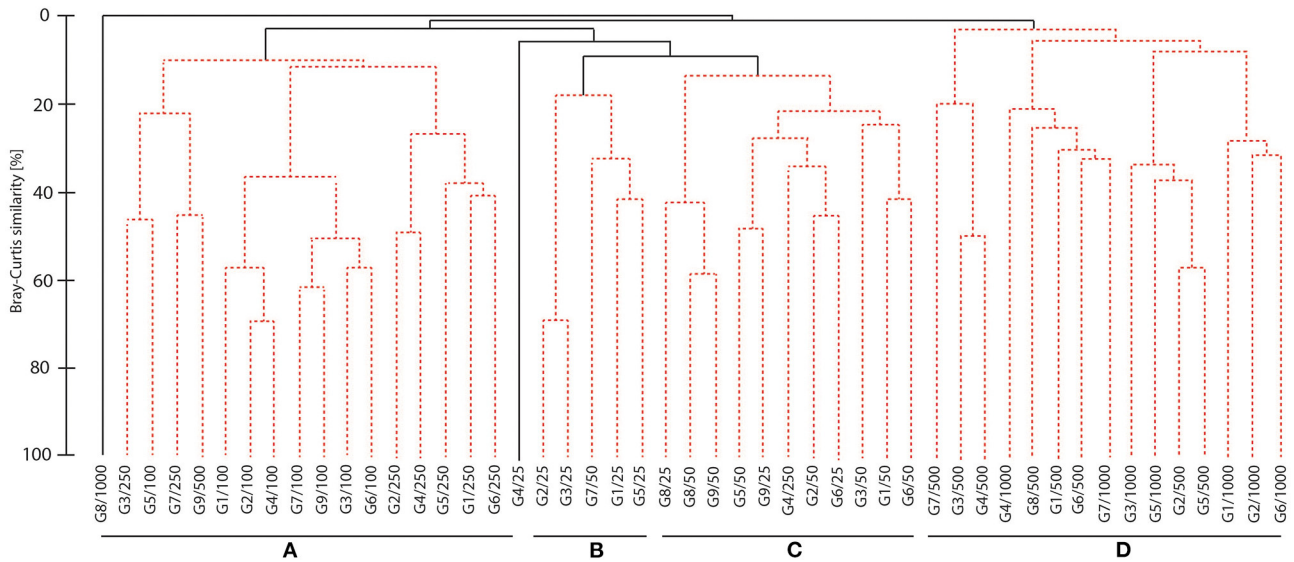

FIGURE 5 | Dendrogram of samples, for Bray Curtis similarity, square root transformed data, and group average grouping method. (Spotted lines indicate the samples that cannot be significantly differentiated by SIMPROF).

analysis of literature data resulted in the list of 172 species recorded from Iberian waters (Atlantic and Mediterranean) including 142 species found in bathyal (200–3,000 m) (Corbera, 1995). The current list of all Mediterranean cumaceans (such as Tyrrhenian, Adriatic, Aegena, and Levantine Seas) includes 99 species (Coll et al., 2010). Analysis of large set of 122 epibenthic sledge samples collected in the deep Atlantic (500–4,000 m depth) revealed the presence of 225 species, although from a large number of almost 56,000 individuals (Gage et al., 2004). On the other hand, only 29 species were recorded from a whole region of tropical Eastern Pacific (Jarquin-Gonzalez and Garcia-Madrigal Mdel, 2013) and only 34 species from the whole Chilean coast (Thiel et al., 2003). Even in the intensively sampled, large open system of the Bay of Biscay, the number of recorded cumacean species was lower than in this study. In the subtidal zone (up 63 m depth) 18 species were recorded in over 100 samples collected using the van Veen grab (Cacabelos et al., 2010; Corbera et al., 2013; Corbera and Galil, 2016). At the deeper areas of the bay in Kostarrenkala area, 42 species in total were collected (13 species were found at 170 m, six species at 300 m, nine species at 400 m, 18 species at 724 m, and 24 species at 1,000 m) (Frutos and Sorbe, 2014). We have analyzed sampling effort and cumacean species richness from 39 different sampling campaigns (**Table 6**). In majority of the studies, the number of species was lower than 35, even if the sampling effort was high, and even if an epibenthic sledge or other gears collecting large number of individuals and species were used. Nevertheless, it is worth mentioning that this study was conducted in a relatively wide depth range. Cumaceans have low dispersal potential (Jones and Sanders, 1972; Pilar-Cornejol et al., 2004), therefore, large depth range sample (25–1,000 m), together with large diversity of microhabitats and differences in environmental conditions, could result in recognition of a larger number of species. It is clearly visible in the analysis of species common in different depth zones (**Table 3**) and in the results of the cluster analysis (**Figure 5**).

Based on current data, we cannot postulate that the Gulf of Guinea is a hot spot of cumacean diversity, although that kind of assumptions is likely possible. There were previous suggestions that this region might be an important center of cumacean diversity. In the deeper parts of the Angola Bay (5,125–5,415 m), 45 species were recorded in just seven epibenthic sledge samples (Brandt, 2005; Mühlenhardt-Siegel, 2005), while Bochert and Zettler (2011) described 16 additional species from the shelf of the Angolan and Namibian waters. High diversity of Cumacea on the equator was already mentioned by Jones and Sanders (1972) and later supported by large scale latitudinal analysis of the deep Atlantic cumacean richness, although authors declare that it is difficult to say if this pattern is related to geological and evolutionary history (e.g., glaciation in the northern hemisphere) or differences in more recent changes in local ecological conditions (e.g., high productivity in tropical areas; Gage et al., 2004). Confrontation of those observed patterns with the knowledge about large sampling bias in the tropical marine waters (Menegotto and Rangel, 2018) demonstrates that many important questions regarding the distribution patterns and diversity are still open and need further comprehensive studies. Based on the current data, it is impossible to discuss about the dependencies between local (e.g., Ghanaian coast) and regional (e.g., whole Atlantic African coast, West Africa, and Gulf of Guinea) species pools (Witman et al., 2004) or provide any generalizations about factors influencing diversity on a larger scale. At the same time, we did not observe large differences in species composition on intermediate scale (between investigated transects). There were some transects with very low (G8 – 7 species) or very high (G6 – 29 species) total number of species, but at the same time the number of species unique to a given transect was very low (**Table 2**),

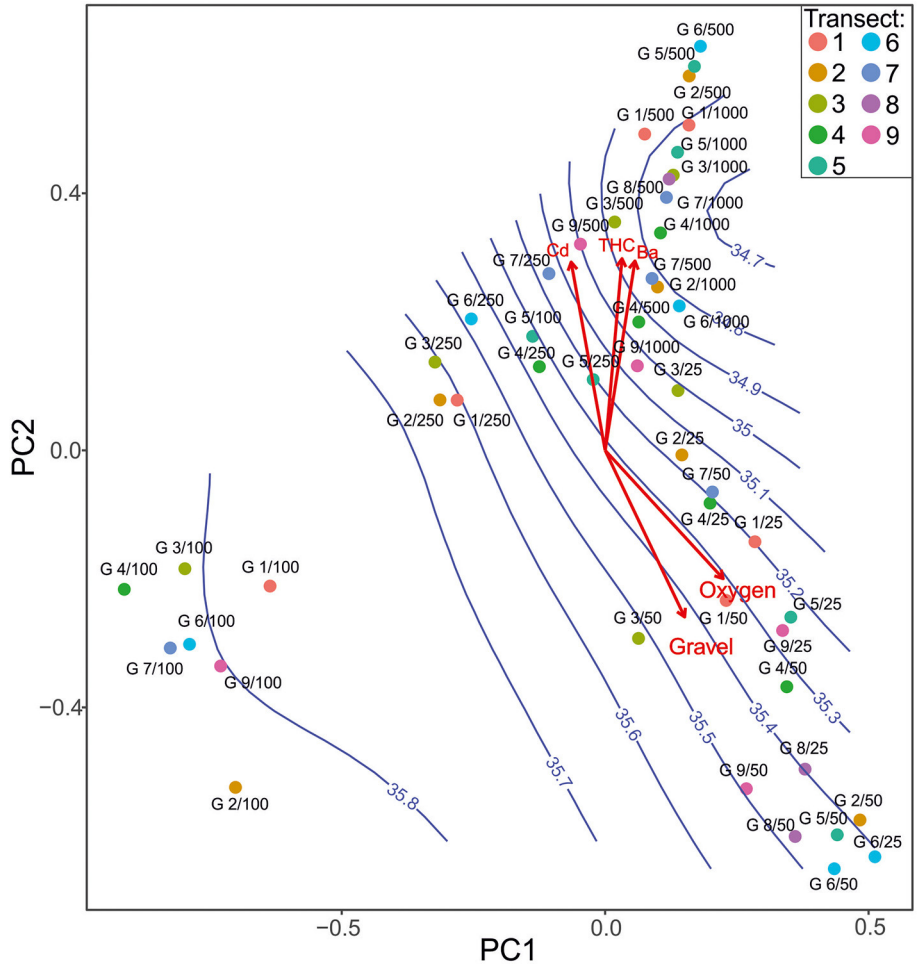

FIGURE 6 | Principal component analysis showing species composition differences in each sampling site according to environmental factors with sampling sites (points) and ranges of salinity (blue isolines).

and there was no clear spatial pattern in species common to different transects, even from opposite parts of the Ghanaian coast (**Table 4**). Those differences are rather not related to distance between the transects but are most probably due to the influence of local environmental conditions as shown in the PCA analysis.

Distribution Patterns and Diversity on a Background of Environmental Conditions

Oxygen content and sediment type (especially content of gravel) drive species composition and diversity especially in the 25–50 m stations. Well-oxygenated water and elevated primary production may increase species richness (Levin and Sibuet, 2012; McCallum et al., 2015). On the other hand, in previous studies, Pabis et al. (2020) reported low oxygen concentration at 250–500 m depth on the coast of Ghana, and those factors might also cause decrease in cumacean abundance and species richness in this depth zone, although the pattern is not clear, and visible only at 500 m. Lower oxygen concentrations might be caused by sinking organic matters resulting from seasonal upwelling at the Ghanaian coast (Nieto and Mélin, 2017).

There is no evidence that increased salinity may reduce the abundance and species richness of cumacea. We suspect that higher salinity values at 100 m were a result of seasonal and oceanographic factors such as upwelling events, bottom currents, temperature, or rainy seasons (Ukwe et al., 2003; Djagoua et al., 2011; Nieto and Mélin, 2017). Martin et al. (2010) showed that decrease in salinity may increase the activity of cumaceans in water column, although we have observed only slight differences in salinity along the coast of Ghana. Therefore, based on available data, we cannot speculate about its influence on cumacean communities.

Earlier studies support our result, pointing substrate grain size and organic matter content as the most important drivers of cumacean assemblages (Corbera and Cardell, 1995; Dos Santos and Pires-Vanin, 1999; Cristales and Pires-Vanin, 2014; Corbera and Sorbe, 2020). In the study of the shallow water communities of the Persian Gulf, the presence of gravel also had a positive

TABLE 5 | Most supported (ΔAIC < 2) models testing for impacts of environmental factors on species composition (site scores along PCA ordination axes 1 and 2, linear regression) and richness of cumaceans (generalized linear model with Poisson distribution).

Response variable	Model	df	logLik	AICc	ΔAICc	Weight
Site scores along PCA ordination axis 1	Gravel + Oxygen	4	−10.68	30.3	0.00	0.310
	Ba + Gravel + Oxygen	5	−10.30	32.0	1.73	0.131
Site scores along PCA ordination axis 2	Ba + Gravel + Oxygen	5	4.87	1.7	0.00	0.409
	Ba + Gravel + Oxygen + THC	6	5.66	2.7	1.02	0.245
	Ba + Cd + Gravel + Oxygen	6	5.34	3.3	1.66	0.178
Richness of cumaceans	Ba + Oxygen	3	−90.00	186.6	0.00	0.155
	Ba + Gravel + Oxygen	4	−88.87	186.8	0.16	0.143
	Ba	2	−91.76	187.8	1.20	0.085
	Ba + Gravel	3	−90.84	188.3	1.67	0.067

influence on cumacean fauna (Martin et al., 2010). The positive effect of gravel on the shallow water communities was also confirmed in the study of polychaete functional diversity in the Ghanaian waters (Sobczyk et al., 2021). The presence of coarser sediment fractions might increase habitat complexity and heterogeneity for small infaunal invertebrates such as cumaceans or various groups of polychaetes, resulting in higher number of microhabitats and/or ecological niches and increased diversity (Sebens, 1991; Carvalho et al., 2017). We also have to take into account interactions with other benthic organisms occurring in the shallows. Generally, the abundance and diversity of benthic fauna of the Ghanaian coast were highest in the 25–50 m depth range (Pabis et al., 2020). This fact might increase the diversity of mutual interactions between various organisms, for example, because of higher level of sediment bioturbation, which could influence oxygenation of the sediment and food availability (Aller and Cochran, 2019). Such conclusions are supported by high abundance and diversity of burrowing polychaetes recorded in this depth zone along the Ghanaian coast (Sobczyk et al., 2021).

Sediment character might be crucial for cumacean survival, as it can be strictly related to the feeding strategy and respiratory mechanism (Dixon, 1944 in Dos Santos and Pires-Vanin, 1999). Cumacea feed on microorganism (especially diatoms) and/or detritus (Błazewicz-Paszkowycz and Ligowski, 2002). It is assumed that mud-dwellers filter small particles of suspension, while sand dwellers scrub food from sand grains. However, studies on *Cumella vaulgaris* demonstrated that the attractiveness of a particular substratum depends on the amount and type of food (Wieser, 1956). The type of substrate is also suggested to have some impact on filter apparatus appearance in some cumaceans. Species that live in muddy sediment have the filter apparatus equipped with finely feathered bristles that allow easier water flow. For example, members of the *Diastylis* are known to have filter apparatus adapted to catching small particles of food from water (Dixon, 1944). Nevertheless, the knowledge on diet, habitat preferences, and other aspects of the cumacean biology is extremely scarce. We know nothing about the ecology and biology of majority of genera, and it is impossible to link the results with any data about the biology of particular species recorded in West Africa.

Slope communities were also affected by disturbance associated with the influence of barium, other heavy metals, and hydrocarbons that are associated mainly with increasing activities of petroleum companies. The oil industry (e.g., Jubilee Oil Field) combined with pollution from other sources such as the dyeing industry, leaks from crude oil storage, and inputs of polluted fresh water have an important influence on the Gulf of Guinea (Acquah, 1995; Owusu-Boadi and Kuitunen, 2002; Scheren et al., 2002; Ayamdoo, 2016; Hanson and Kwarteng, 2019). For example, between 2009 and 2011, there was a spill of oil-based mud in Ghanaian waters, and the control of pollution in this region remains poor and not well-documented, although it is considered to continuously increase (Ayamdoo, 2016). Moreover, Ghana is importing barite for the dyeing industry (Sobczyk et al., 2021). Larger concentration of Ba on the slope is also not surprising because of the influence of pressure on the solubility of barite (Neff, 2002). At the same time, elevated levels of barium were not visible in all slope stations, but only on part of the transects (Pabis et al., 2020), confirming that pollution has local anthropogenic origin. Despite the fact that cumacean abundance and species richness per sample were generally low along the whole depth range, we have noticed decreased values in the slope samples, where muddy sediments are characterized by higher content of barium, other toxic metals, and hydrocarbons (Pabis et al., 2020). Those factors might influence benthic communities (e.g., Olsgard and Gray, 1995; Gomez-Gesteira et al., 2003; Stark et al., 2020), and it is known that heavy metals might accumulate in cumacean bodies (Swaileh and Adelung, 1995). Ba and other heavy metals may affect development and cause decrease in abundance of benthic invertebrates (Lira et al., 2011), or influence embryos of crustaceans and bivalves (Macdonald et al., 1988). Similar effects were described for hydrocarbons (Main et al., 2015; Honda and Suzuki, 2020). Nevertheless, there are only scarce data about exact doses of various pollutants that could influence particular species or taxonomic groups of benthic organisms (Lira et al., 2011). We already noticed in the earlier study (Pabis et al., 2020) that levels of Ba and other toxic metals in the Gulf of Guinea were close to background levels according to OSPAR and KLIF (Norwegian Pollution Authority) guidelines (OSPAR, 2017), although literature data from other regions demonstrated that even low concentrations of Ba and other pollutants might influence benthic communities (Olsgard and Gray, 1995). The influence of local pollution associated with oil exploration in Ghanaian waters and dying industry was also visible in the study on polychaete functional diversity that was based on the same set

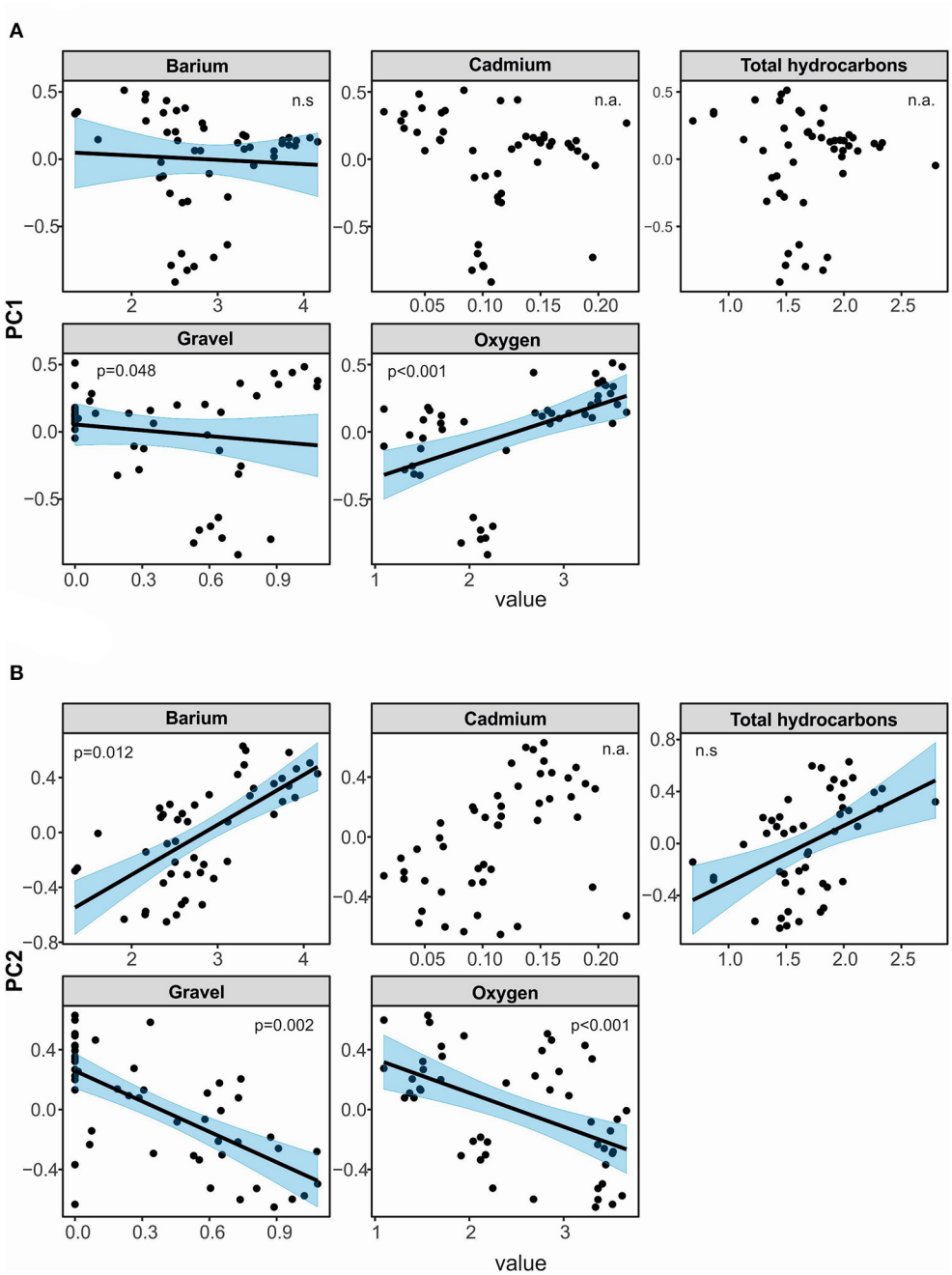

FIGURE 7 | Visualization of linear models testing for effects of selected environmental factors on species composition of cumaceans, expressed as site scores along PCA ordination axis 1 **(A)** and axis 2 **(B)**. Phrase "n.a." means that environmental factor was not included in a set of the most parsimonious models. Phrase "n.s." means its explanatory power was not significant despite the fact that means environmental factor was included in a set of the most parsimonious models.

of samples (Sobczyk et al., 2021). Patterns observed in cumacean study are very similar, although not that obvious and strong as in the case of polychaetes, which is most probably caused by generally very low abundance of those crustaceans. Moreover, polychaetes are considered perfect model organisms for various studies on ecosystem response to natural or anthropogenic changes and disturbances (Olsgard et al., 2003; Giangrande et al., 2005), and it is not surprising that they are good indicators of disturbance.

Cumaceans are small benthic brooders with limited dispersal potential. Therefore, they are considered to be sensitive to changes in environmental factors (Corbera and Cardell, 1995; Alfonso et al., 1998), although there are no data on influence of pollution on their communities, except those of one study

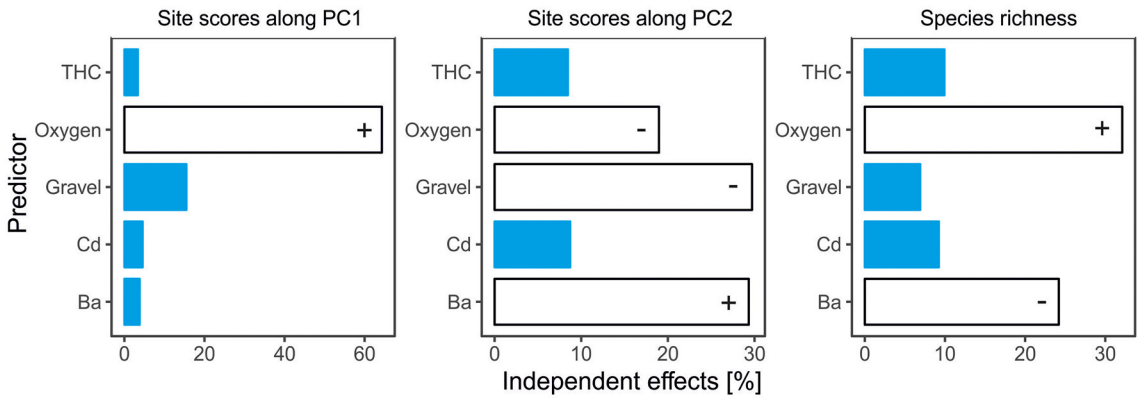

FIGURE 8 | Relative contribution of each environmental factor to shared variability of full models testing for effects of environmental factors on species composition (expressed as site scores along PCA ordination axes (1 and 2) and richness of cumaceans. Predictors that had significant effect on response variables are given in white. Plus (+) signs express positive impact of predictors on response variables, and minus (-) signs express negative influences. For full predictor names, see **Supplementary Table 1**.

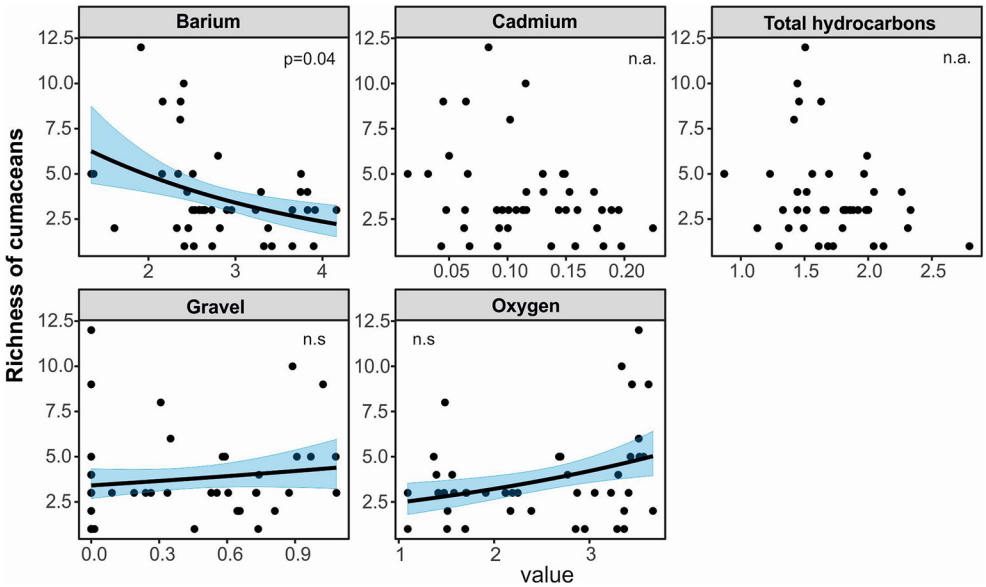

FIGURE 9 | Visualization of generalized linear model testing for effects of environmental factors on species richness of cumaceans. Phrase "n.a." means that environmental factor was not included in a set of the most parsimonious models. Phrase "n.s." means its explanatory power was not significant despite the fact that means environmental factor was included in a set of the most parsimonious models.

showing decrease in abundance in the polluted site (de-la-Ossa-Carretero et al., 2012). However, studies on similar small peracarid crustaceans such as Tanaidacea demonstrated that they might be good indicators of disturbance processes (Guerra-García and García-Gómez, 2004). The influence of local pollution on the Ghanaian coast was visible even in the case of higher taxa, although the taxonomic level of phyla and orders is normally not sufficient for meaningful assessments of ecosystem health (Pabis et al., 2020). Moreover, we have to remember that despite the fact that Ba was a significant factor in the analysis, other variables such as hydrocarbons and other heavy metals such as Cd, Cu, and Ni could also be responsible for combined influence on cumacean communities (Sobczyk et al., 2021). In such cases, it is difficult to unequivocally assess the influence of one out of multiple stressors on benthic communities (Borja et al., 2011; Lenihan et al., 2018), even by advanced multivariate analysis and especially when we analyse communities of less abundant taxa-like cumaceans. The results of the PCA are not strong, since first PC axis explained only 10% of variance, which is due to very low abundance, large number of singletons, and highly patchy distribution of majority of species. Nevertheless, the results are supported by analysis based on the abundance of macrozoobenthic higher taxa and polychaete communities (Pabis et al., 2020; Sobczyk et al., 2021). Moreover, similar results of the PCA are sometimes sufficient for

TABLE 6 | Sampling effort, species richness, and total abundance of Cumacea from various studies.

Area	Gear	Total number of samples	Depth [m]	Number of individuals	Number of species	Abundance	References
off Santos, SE Brazil	Box corer (0.1 m^2)	21	10–100	919	24	nd	Cristales and Pires-Vanin, 2014
E Mediterranean Sea	Box corer, epibentic sledge, beam trawl	161	45–4,398	nd	29	nd	Mühlenhardt-Siegel, 2009
W Mediterranean Sea,coast of Barcelona	Dredge (0.1 m^2)	40	5–70	nd	22	0–613 indv/m^2	Corbera and Cardell, 1995
Ross Sea	Dredge	19	84–515	5,287	28	nd	Rehm et al., 2007
Tropical Eastern Pacific	Grabbing	13	Max 10	378	29	nd	Jarquin-Gonzalez and Garcia-Madrigal Mdel, 2013
Algeciras Bay, Giblartar Strait	Scuba diving	25	Shallow	2,058	3	nd	Alfonso et al., 1998
Bermuda	Scuba diving	23	1–6	825	7	nd	Petrescu and Sterrer, 2001
California coast (Dillon Beach)	Scuba diving	20	1–21.5	952	12	1–209 indv/0.04 m^2	Gladfelter, 1975
Puerto Morelos Reef National Park Mexico	Scuba diving	nd	3–12	177	30	nd	Monroy-Velázquez et al., 2017
W Mediterranean Sea, Creixell beach	Sledge	1,800	0.5–3	Nd	6	nd	San Vicente and Sorbe, 1999
Bay of Seine, English Channel	Sledge	38	8–13	Nd	5	352.6–15.5 indv/ 100 m^3	Wang and Dauvin, 1994
Hendaya and Creixell beaches, Bay of Biskay	Sledge	132	Up to 10	Nd	5	0.1–96.9 indv/ 5 m^2	San Vicente and Sorbe, 2001
Portuguese coast	Sledge	5	21–299	24	nd	14–61 indv/100 m^2	Cunha et al., 1997
Beagle Channel, Argentinian coast	Sledge, dredge	18	25–665	15,662	25	nd	Mühlenhardt-Siegel, 1999
South Shetland Island, Trinity Islands	Sledge	24	45–649	1,236	25	1–289	Corbera, 2000
Bellingshausen Sea, Antarctic Peninsula	Sledge	26	85–1,870	557	35	4.2–652.2 indv/1,000 m^2	Corbera et al., 2008; San Vicente et al., 2009
Mediterranaean Sea	Sledge	27	100–4,000	1,505	33	nd	Reyss, 1973
Falcland Island	Sledge	3	103–202	8,074	13		Doti et al., 2020
Kostarrenkala area, Bay of Biscay	Sledge	10	175–1,000	1,476	37	nd	Frutos and Sorbe, 2014
NE Greenland	Sledge	8	197–2,681	7,868	24	nd	Brandt, 1997
E Meditteranean Sea, SW Balearic Island, Algerian Basin,	Sledge and bottom trawl	6 sledges, 12 trawls	249–1,620	Nd	24	nd	Cartes et al., 2003
Cap Ferret Canyon, Bay of Biscay	Sledge	13	346–1,099	1,885	42	2.8–55.8 indv/100 m^2	Corbera and Sorbe, 2020
Cap Ferret Canyon, Bay of Biscay	Sledge	12	386–420	472	9	2.1–32.2 indv/100 m^2	Sorbe and Elizalde, 2014
E Meditteranean Sea, Catalan Sea	Sledge	21	389–1,859	2,747	32	nd	Cartes and Sorbe, 1997
Capbreton area, Bay of Biscay	Sledge	nd	500–797	Nd	03.gru	nd	Frutos and Sorbe, 2017
Capbreton canyon (site A and B), Bay of Biscay	Sledge and box corer	17 box corer and 17 slegdes	A: 923–1,002, B: 971–1,027	Nd	A: sledges: 8 species, box corer - 2 species B: sledges: 18 species, box: 4 species	nd	Marquiegui and Sorbe, 1999

(Continued)

TABLE 6 | Continued

Area	Gear	Total number of samples logic	Depth [m]	Number of individuals	Number of species	Abundance	References
Angola Basin	Sledge	7	5,125–5,415	479	45	nd	Brandt, 2005
E MediterraneanSea, Catalan Sea	Trawl with net and sledge	35	398–1,808	3,159	Upper slope - 5 the most abundant species; middle slope−6 most abundant, lower slope−7	nd	Cartes and Sorbe, 1997
W MediterraneanSea, coast of Israel	Trawl	nd	1,241–1,557	575	12	nd	Corbera and Galil, 2016
Ría de Pontevedra, Galicia coast	van Veen grab (0.056 m^2)	135	Subtidial	473 (2.7% of collected peracarids)	14	nd	Lourido et al., 2008
Ria de Vigo, Galicia coast	van Veen grab (0.056 m^2)	145	0–28.2	Nd	4	nd	Cacabelos et al., 2010
W MediterraneanSea, coast of Israel	van Veen grab (0.08m^2)	443	1.9–63	31,508	18	nd	Corbera and Galil, 2016
SE Brazilian continental shelf	van Veen grab (0.1 m^2), dredge and beam-trawl	108 samples	10–124	1,587	19	nd	Dos Santos and Pires-Vanin, 1999
Mexico, Bay of All Saints	van Veen grab (0.1 m^2)	60	<15	Nd	12	1–124 indv/0.1m^2	Donath-Hernández, 1987
E MediterraneanSea,Bay of Blanes	van Veen grab (600 cm^2 = 0.06 m^2)	nd	15	Nd	10	Max 333 indv/m^2	Corbera et al., 2013
Persian Gulf, Iranian coast	van Veen grab (0.1 m^2)	15	up to 30	232	8	nd	Martin et al., 2010
Admiralty Bay, Antarctic	van-Veen grab (0.1 m^2)	105	20–500	685	11	nd	Pabis and Błazewicz-Paszkowycz, 2011
Mobile Bay, Alabama, Gulf of Mexico	nd	3,150	2.5–6	nd	5	Up to: 69 indv/m^2 for Oxvurostylissmithi, 11 indv/m^2 for Leucon americanus, 6 indv/m^2 for Cyclaspisvarians and for Eudorella monodon	Modlin and Dardeau, 1987

description of ecological patterns (Sarthou et al., 2010), although they have to be treated cautiously.

Nevertheless, it is, to some point, surprising that we have noticed two peaks in the general number of species, one in the shallows and one in the 1,000 m (**Table 2**), where the influence of Ba and hydrocarbons was the highest. Moreover, the cumacean fauna recorded at 1,000 m stations was also the most unique. Those facts might be associated with the general pattern showing that bathyal is the main biodiversity hot spot for benthic fauna due to higher habitat diversity (Danovaro et al., 2009; Rex and Etter, 2010). High diversity of bathyal cumacean communities was already demonstrated in many previous studies (e.g., Corbera, 1995; Gage et al., 2004; Corbera and Sorbe, 2020 and citations therein).

Distribution of genera and/or families along a depth gradient might also be at least partially explained by earlier studies on cumacean evolution and phylogeny, although we also know very little about those important problems (Gerken, 2018 and references therein). There are only scarce data about the possible origin of various families or genera and their affinities to given depth zones or regions. For example, Bodotriidae are classified as typical shallow water crustaceans (Day, 1978; Mühlenhardt-Siegel, 1996; Petrescu, 1998), while members of Leuconidae are more often recorded in the deep sea (Mühlenhardt-Siegel, 2005, 2011; Gerken, 2016). *Diastylis*, on the other hand, is considered to have relatively wide bathymetric distribution, from shallows to bathyal depths (Băcescu and Petrescu, 1991; Mühlenhardt-Siegel, 2005). On the other hand, those general patterns might be affected by some local conditions. For example, the presence of

preferred sediment type might extend the bathymetric range of cumaceans, recognized as shallow water, even to upper bathyal depths (Corbera and Sorbe, 2020), demonstrating that similar generalizations are still far from being conclusive. Brandt et al. (2012) summarized the information about widely distributed peracarid crustaceans. According to this analysis, there are at least 48 eurybathic cumacean species in the deep sea, and at that least 25 have a very wide geographic distribution (two or more oceans), although we have to remember that those numbers could substantially change after detailed molecular studies.

The results suggest high level of undescribed cumacean diversity in West African waters. Future biodiversity studies should be focused on bathyal communities, especially in areas not affected by human related disturbance processes, and explore a wider depth range. The use of dredges or epibenthic sledge could also allow to collect a larger number of individuals than point scale samplers such as the van Veen grab. Probably, the most appropriate sampling strategy should include the use of both quantitative and semiquantitative methods, as it was already demonstrated in case of tanaidaceans (Józwiak et al., 2020). The hypothesis of the high diversity of cumacean fauna in tropical African waters still cannot be verified because of strong sampling bias. The great rarity, small population densities, and high level of patchiness in the distribution of particular species suggest the necessity of sampling at larger number of stations, allowing for more comprehensive biodiversity inventory of those small crustaceans. The high diversity of Cumacea observed in this study showed that small peracarids should be included in future research, especially since the pressure of human activities in large marine ecosystems such as the Gulf of Guinea could lead to substantial loss in marine diversity yet unknown. There is also a great need for further taxonomic studies on the region. They could help to accelerate the further analysis of ecological interactions occurring in West African seabed ecosystems, because they constitute an important base of any ecological research and biodiversity inventories.

DATA AVAILABILITY STATEMENT

The original contributions presented in the study are included in the article/**Supplementary Material**, further inquiries can be directed to the corresponding author/s.

AUTHOR CONTRIBUTIONS

AS: concept of the paper, taxonomic identification, statistical analysis, and manuscript writing. KP: concept of the paper, statistical analysis, writing of the manuscript, sampling design, and coordination of benthic ecology in the project. RS: statistical analysis. BS: sampling design, proofreading, and head of the FAO project. All authors contributed to the article and approved the submitted version.

FUNDING

The sampling cruise and the environmental data analysis within this program were funded by the Norwegian Agency for Development Cooperation (NORAD) (Oil for Development Program—OfD) and by the Food and Agriculture Organization of the United Nations (FAO). AS and KP were also supported by University of Lodz.

ACKNOWLEDGMENTS

The authors want to thank Dr. Ute Mühlenhardt-Siegel for helping with identifying species.

SUPPLEMENTARY MATERIAL

The Supplementary Material for this article can be found online at: https://www.frontiersin.org/articles/10.3389/fmars.2021.703547/full#supplementary-material

REFERENCES

Acquah, P. (1995). *Natural Resources Management and Sustainable Development: The Case of the Gold Sector in Ghana*. Geneva: United Nations Conference on Trade and Development (UNCTAD).

Alfonso, M. I., Bandera, M. E., López-González, P. J., and García-Gómez, J. C. (1998). The cumacean community associated with a seaweed as a bioindicator of environmental conditions in the Algeciras Bay (Strait of Gibraltar). *Cah. Biol. Mar*. 39, 197–205.

Aller, R. C., and Cochran, J. K. (2019). The critical role of bioturbation for particle dynamics, priming potential, and organic C remineralization in marine sediments: local and basin scales. *Front. Earth Sci*. 7:157. doi: 10.3389/feart.2019.00157

Appeltans, W., Ahyong, S. T., Anderson, G., Angel, M. V., Artois, T., Bailly, N., et al. (2012). The magnitude of global marine species diversity. *Cur. Biol*. 22, 2189–2202. doi: 10.1016/j.cub.2012.09.036

Ateş, A. S., Katagan, T., Sezgin, M., Özdilek, H. G., Berber, S., and Bulut, M. (2014). The effects of some domestic pollutants on the cumacean (Crustacea) community structure at the coastal waters of the Dardanelles, Turkey. *Arthropods* 3, 27–42. Available online at: http://www.iaees.org/publications/journals/arthropods/onlineversion.asp

Ayamdoo, N. A. (2016). Protecting the Gulf of Guinea in an oil boom: regulating offshore 618petroleum pollution in a divided world. *J. World Energy Law Bus*. 619, 219–232. doi: 10.1093/jwelb/jww007

Băcescu, M. (1961). Contribution à la connaissance du genere Makrokylindrus Stebbing (Crustacea: Cumacea). *Rev. Biol*. 6, 325–333.

Băcescu, M. (1972). Archaeocuma and Schizocuma, new genera of Cumacea from the American tropical waters. *Rev. Roum. Biol. Academia RepubliciiSocialiste Romania* 17, 241–250.

Băcescu, M., and Petrescu, I. (1991). New Cumacea (Crustacea, Peracarida) from the littoral waters of Brazil. *Trav. Mus. Natl. Hist. Nat*. 31, 327–340.

Bamikole, W., Ndubuisi, A., Ochuko, A. P., and Olamide-Olaronke, O. P. (2009). Macrobenthic faun aof Snake Island area of Lagos lagoon, Nigeria. *Res. J. Biol. Sci*. 4, 272–276. Available online at: https://medwelljournals.com/abstract/?doi=rjbsci.2009.272.276

Bartoń, K. (2018). *MuMIn: Multi-model inference. R package version 1.42.1*. Available online at: https://CRAN.R-project.org/package=MuMIn (accessed January 15, 2021).

Bassindale, R. (1961). On the marine fauna of Ghana. *Proc. Zool. Soc. Lond*. 137, 481–510. doi: 10.1111/j.1469-7998.1961.tb06086.x

Binet, D., and Marchal, E. (1993). "The large marine ecosystem of shelf areas in the Gulf of Guinea: long-term variability induced by climatic changes," in *Large*

Marine Ecosystems. Stress, Mitigation, and Sustainability, eds K. Sherman, L. D. Alexander and B. D. Gold (Washington, DC: AAAS Press), 104–118.

Birchenough, G. M. H., Johansson, M. E., Gustafsson, J. K., Bergström, J. H., and Hansson, G. C. (2015). New developments in goblet cell mucus secretion and function. *Mucosal Immunol*. 8, 712–719. doi: 10.1038/mi.2015.32

Bishop, J. D. D. (1982). Three new species of the genus Leucon Kröyer, 1846 (Crustacea: Cumacea) from the continental slope off Surinam. *Zool. J. Linnean Soc*. 74, 345–357. doi: 10.1111/j.1096-3642.1982.tb01157.x

Błazewicz-Paszkowycz, M., and Ligowski, R. (2002). Diatoms as food source indicator for some Antarctic Cumacea and Tanaidacea (Crustacea). *Antarct. Sci*. 14, 11–15. doi: 10.1017/S0954102002000524

Bochert, R., and Zettler, M. L. (2011). Cumacea from the continental shelf of Angola and Namibia with descriptions of new species. *Zootaxa* 2978, 1–33. doi: 10.11646/zootaxa.2978.1.1

Borja, A., Belzunce, M. J., Garmendia, J., Rodríguez, J. G., Solaun, O., and Zorita, I. (2011). "Impact of pollutants on coastal and benthic marine communities," in *Ecological Impacts of Toxic Chemicals*, eds F. Sánchez-Bayo, P. J. van den Brink and R. M. Mann (Sharjah: Bentham Science Publishers), 165–186. doi: 10.2174/978160805121210165

Brandt, A. (1997). Abundance, diversity and community patterns of epibenthic- and benthic-boundary layer peracarid crustaceans at 75°N off East Greenland. *Polar Biol*. 17, 159–174. doi: 10.1007/s003000050118

Brandt, A. (2005). Diversity of peracarid crustaceans (Malacostraca) from the abyssal plain of the Angola Basin. *Org. Divers. Evol*. 5, 105–112. doi: 10.1016/j.ode.2004.10.007

Brandt, A., Błazewicz-Paszkowycz, M., Bamber, R. N., Mühlenhardt-Siegel, U., Malyutina, M. V., et al. (2012). Are there widespread peracarid species in the deep sea (Crustacea: Malacostraca)? *Pol. Polar Res*. 33. 139–162. doi: 10.2478/v10183-012-0012-5

Buchanan, J. B. (1957). The bottom fauna communities across the continental shelf off Accra, 571Ghana (Gold Coast). *P. Zool. Soc. Lon*. 130, 1–56. doi: 10.1111/j.1096-3642.1958.tb00562.x

Buchanan, J. B. (1984). "Sediment analysis," in *Methods for the Study of Marine Benthos*, eds N. A. Holme and A. D McIntyre (Oxford: Blackwell Scientific Publications), 41–65.

Cacabelos, E., Lourido, A., and Troncoso, J. S. (2010). Composition and distribution of subtidal and intertidal crustacean assemblages in soft-bottoms of the Ria de Vigo (NW Spain). *Sci. Mar*. 74, 455–464. doi: 10.3989/scimar.2010.74n3455

Cartes, J. E. (1993). Diets of two deep-sea decapods: nematocarcinusexilis (Caridea: Nematocarcinidae) and munidatenuimana (Anomura: Galatheidae) on the Western Mediterranean slope. *Ophelia* 37, 213–229. doi: 10.1080/00785326.1993.10429919

Cartes, J. E., Jaume, D., and Madurell, T. (2003). Local changes in the composition and community structure of suprabenthic peracarid crustaceans on the bathyal Mediterranean: influence of environmental factors. *Mar. Biol*. 143, 745–758. doi: 10.1007/s00227-003-1090-z

Cartes, J. E., and Sorbe, J. C. (1997). Bathyal cumaceans of the Catalan Sea (North-western Mediterranean): faunistic composition, diversity and near-bottom distribution along the slope (between 389 and 1,859 m). *J. Nat. Hist*. 31, 1041–1054. doi: 10.1080/00222939700770541

Carvalho, L. R. S., Loiola, M., and Barros, F. (2017). Manipulating habitat complexity to understand its influence on benthic macrofauna. *J. Exp. Mar. Biol. Ecol*. 489, 48–57. doi: 10.1016/j.jembe.2017.01.014

Clarke, K. R., and Warwick, R. M. (2001). *Change in Marine Communities: An Approach to Statistical Analysis and Interpretation*. Plymouth: PRIMER-E.

Coll, M., Piroddi, C., Steenbeek, J., Kaschner, K., Ben RaisLasram, F., Aguzzi, J., et al. (2010). The biodiversity of the Mediterranean Sea: estimates, patterns, and threats. *PLoS ONE* 5:e11842. doi: 10.1371/journal.pone.0011842

Corbera, J. (1995). Check-list of the Cumacea from the Iberian waters. *Arx. Misc. Zool*. 18, 57–75.

Corbera, J. (2000). Systematics and distribution of cumaceans collected during BENTAR-95 cruise around South Shetland Islands (Antarctica). *Sci. Mar*. 64, 9–28. doi: 10.3989/scimar.2000.64n19

Corbera, J., and Cardell, M. J. (1995). Cumaceans as indicators of eutrophication on soft bottoms. *Sci. Mar*. 59, 63–69.

Corbera, J., and Galil, S. J. (2016). Cumacean assemblages on the Levantine shelf (Mediterranean Sea) – spatiotemporal trends between 2005 and 2012. *Mar. Biol. Res*. 12, 663–672. doi: 10.1080/17451000.2016.1169297

Corbera, J., Martin, D., Pinedo, S., and Sarda, R. (2013). Cumacean density, biomass and productivity in the sandy bottoms of the Bay of Blanes (western Mediterranean). *Cah. Biol. Mar*. 54, 63–70. Available online at: http://hdl.handle.net/10261/63729

Corbera, J., San Vicente, C., and Sorbe, J. C. (2008). Cumaceans (Crustacea) from the Bellingshausen Sea and off the western Antarctic Peninsula: a deep-water link with fauna of the surrounding oceans. *Polar Biol*. 32, 611–622. doi: 10.1007/s00300-008-0561-6

Corbera, J., and Sorbe, J. C. (2020). Bathyal cumacean assemblages from the southern margin of the Cap Ferret Canyon (SE Bay of Biscay). *Sci. Mar*. 84:7. doi: 10.3989/scimar.05031.07A

Cristales, P. A., and Pires-Vanin, A. M. S. (2014). Structuring factors of the Cumacean communities of the continental shelf of Southeastern Brazil. *Braz. J. Oceanogr*. 62, 103–116. doi: 10.1590/S1679-87592014056206202

Cunha, M. R., Sorbe, J. C., and Bernardes, C. (1997). On the structure of the neritic suprabenthic communities from the Portuguese continental margin. *Mar. Ecol. Prog. Ser*. 157, 119–137. doi: 10.3354/meps157119

Danovaro, R., Canals, M., Gambi, C., Heussner, S., Lampadariou, N., and Vanreusel, A. (2009). Exploring benthic biodiversity patterns and hotspots on European margin slopes. *Oceanogr*. 22, 16–25. doi: 10.5670/oceanog.2009.02

Day, J. (1975). Southern African Cumacea. Part 1. families Bodotriidae, subfamily Vaunthompsoniinae. *Ann. S. Afr. Mus*. 66, 177–220.

Day, J. (1978). South African Cumacea, Part 3: families lampropidae and ceratocumatidae. *Ann. S. Afr. Mus*. 76, 137–189.

Day, J. (1980). Southern African Cumacea. Part 4. families gynodiastylidae and diastylidae. *Ann. S. Afr. Mus*. 82, 187–292.

De Broyer, C., and Danis, B. (2011). How many species in the Southern Ocean? Towards a dynamic inventory of the Antarctic marine species. *Deep Sea Res. Part II Top. Stud. Oceanogr*. 58, 5–17. doi: 10.1016/j.dsr2.2010.10.007

de-la-Ossa-Carretero, J. A., Del-Pilar-Ruso, Y., Gimenez-Casalduero, F., and Sanchez-Lizaso, J. L. (2012). Assessing reliable indicators to sewage pollution in coastal soft-bottom communities. *Environ. Monit. Assess*. 184, 2133–2149. doi: 10.1007/s10661-011-2105-8

Dixon, A. Y. (1944). Notes on certain aspects of the biology of Cumopsisgoodsiri (Van Beneden) and some other cumaceans in relation to their environment. *J. Mar. Biolog. Assoc*. 26, 61–71. doi: 10.1017/S0025315400014454

Djagoua, E. V., Kassi, J. B., Mobia, B., Kouadio, J. M., Dro, C., Affian, K., et al. (2011). Ivorian and Ghanaian upwelling comparison: intensity and impact on phytoplankton biomass. *AJSIR* 5, 740–747. doi: 10.5251/ajsir.2011.2.5.740.747

Donath-Hernández, F. E. (1987). Distribution of the Cumacea (Crustacea, Peracarida) of the Bahia De Todos Santos, Baja California, Mexico. *Cienc. Mar*. 13, 35–52. doi: 10.7773/cm.v13i4.555

Dos Santos, M. F., and Pires-Vanin, S. A. M. (1999). The Cumacea community of the southeastern Brazilian Continental Shelf: structure and dynamics. *Sci. Mar*. 63, 15–25. doi: 10.3989/scimar.1999.63n115

Doti, B. L., Chiesa, I. L., and Roccatagliata, D. (2020). Biodiversity of isopoda and Cumacea (Peracarida, Crustacea) from the Marine Protected Area Namuncurá-Burdwood Bank, South-West Atlantic. *Polar Biol*. 43, 1519–1534. doi: 10.1007/s00300-020-02725-z

Elezz, A. A., Mustafa Hassan, H., Abdulla Alsaadi, H., Easa, A., Al-Meer, S., Elsaid, K., et al. (2018). Validation of total mercury in marine sediment and biological samples, using cold vapour atomic absorption spectrometry. *Meth. Proth*. 1:31. doi: 10.3390/mps1030031

Folk, R. L., and Ward, W. C. (1957). Brazos River bar [Texas]; a study in the significance of grain size parameters. *J. Sediment. Res*. 27, 3–26. doi: 10.1306/74D70646-2B21-11D7-8648000102C1865D

Friedlander, A. M., Ballesteros, E., Fay, M., and Sala, E. (2014). Marine communities on oil platforms in Gabon, West Africa: high biodiversity oases in a low biodiversity environment. *PLoS One* 9:e103709. doi: 10.1371/journal.pone.0103709

Frutos, I., and Sorbe, J. C. (2014). Bathyal suprabenthic assemblages from the southern margin of the Capbreton Canyon ("Kostarrenkala" area), SE Bay of Biscay. *Deep Sea Res. II Top. Stud. Oceanogr*. 104, 291–309. doi: 10.1016/j.dsr2.2013.09.010

Frutos, I., and Sorbe, J. C. (2017). Suprabenthic assemblages from the Capbreton area (SE Bay of Biscay). Faunal recovery after a canyon turbidity disturbance.

Deep Sea Res. II Top. Stud. Oceanogr. 130, 36–46. doi: 10.1016/j.dsr.2017.10.007

Gaever, S., Olu, K., Derycke, S., and Vanreusel, A. (2009). Metazoan meiofaunal communities at cold 678 seeps along the Norwegian margin: influence of habitat heterogenity and evidence for connection with shallow-water habitats. *Deep Sea Res. I Oceanogr. Res. Pap*. 56, 772–785. doi: 10.1016/j.dsr.2008.12.015

Gage, J. D., Lambshead, P. J. D., Bishop, J. D. D., Stuart, C. T., and Jones, N. S. (2004). Large-scale biodiversity pattern of Cumacea (Peracarida: Crustacea) in the deep Atlantic. *Mar. Ecol. Prog. Ser*. 277, 181–196. doi: 10.3354/meps277181

Galéron, J., Menot, L., Renau, N., Crassous, P., Khripounoff, A., Treignier, C., et al. (2009). Spatial and temporal patterns of benthic macrofaunal communitites in the deep continental margin in the Gulf of Guinea. *Deep Sea Res. II Top. Stud. Oceanogr*. 56, 2299–2312. doi: 10.1016/j.dsr2.2009.04.011

Gerken, S. (2016). Leuconidae (Crustacea: Cumacea) from the collections of the Museum Victoria, Australia. *Zootaxa* 251, 251–292. doi: 10.11646/zootaxa.4067.3.1

Gerken, S. (2018). The Lampropidae (Crustacea: Cumacea) of the World. *Zootaxa* 4428, 1–192. doi: 10.11646/zootaxa.4428.1.1

Germain, J., and Armengol, C. (1999). Gulf of Guinea: a deep offshore oppotrunity. *ICEED*, 25, 87–95.

Giangrande, A., Licciano, M., and Musco, L. (2005). Polychaetes as environmental indicators revisited. *Mar. Poll. Bull*. 50, 1153–1162. doi: 10.1016/j.marpolbul.2005.08.003

Gladfelter, W. B. (1975). Quantitative distribution of shallow-water Cumacea from the vicinity of Dillon Beach, California, with descriptions of five new species. *Crustaceana* 29, 241–251. doi: 10.1163/156854075X00289

Gomez-Gesteira, J. L., Dauvin, J. C., and Salvande-Fraga, M. (2003). Taxonomic level for assessing oil spill effects on soft-bottom sublittoral benthic communities. *Mar. Pollut. Bull*. 46, 562–572. doi: 10.1016/S0025-326X(03)00034-1

Guerra-García, J., and García-Gómez, J. (2004). Crustacean assemblages and sediment pollution in an exceptional case study: a harbour with two opposing entrances. *Crustaceana* 77, 353–370. doi: 10.1163/1568540041181538

Hanson, R., and Kwarteng, T. (2019). Analysis of industrial effluent from some factories in Tema. *EJEE* 6, 19–29.

Honda, M., and Suzuki, N. (2020). Toxicities of polycyclic aromatic hydrocarbons for aquatic animals. *Int. J. Environ. Res. Public Health* 17:1363. doi: 10.3390/ijerph17041363

Jarquin-Gonzalez, J., and Garcia-Madrigal Mdel, S. (2013). Annotated checklist and keys for cumaceans (Crustacea: Peracarida) from the Tropical Eastern Pacific, with six new species from the Southern Mexican Pacific. *Zootaxa* 3721, 201–257. doi: 10.11646/zootaxa.3721.3.1

Jarvis, I., and Jarvis, K. E. (1992). Plasma spectrometry in the earth sciences: techniques, applications and future trends. *Chem. Geol*. 95, 1–33. doi: 10.1016/0009-2541(92)90041-3

Jones, N. S. (1956). Cumacea of the west coast of Africa. *Atlantide Rep*. 4, 195–197.

Jones, N. S. (1976). *British Cumaceans. Arthropoda: Crustacea. Keys and Notes for the Identification of the Species. Synopses of the British Fauna No. 7 by the Linnean Society of London*. London; New York, NY: Academic Press.

Jones, N. S., and Sanders, H. L. (1972). Distribution of Cumacea in the deep Atlantic. *Deep-Sea Res*. 19, 737–745. doi: 10.1016/0011-7471(72)90066-6

Józwiak, P., Pabis, K., Brandt, A., and Błazewicz, M. (2020). Epibenthic sled versus giant box corer – comparison of sampling gears for tanaidacean species richness assessment in the abyssal benthic ecosystem. *Prog. Oceanogr*. 181:102255. doi: 10.1016/j.pocean.2019.102255

Kuhn, M. (2020). *Caret: Classification and Regression Training. R PackageVersion 6.0–85*. Available online at: https://CRAN.R-project.org/package=caret

Le Loeuff, P., and Cosel, R. (1998). Biodiversity patterns of the marine benthic fauna on the Atlantic coast of tropical Africa in relation to hydroclimatic conditions and paleogeographic events. *ActaOecol*. 19, 309–321. doi: 10.1016/S1146-609X(98)80035-0

Le Loeuff, P., and Intés, A. (1999). Macrobenthic communities in the continental shelf of Côted'Ivoire. Seasonal and diel cycles in relation to hydroclimate. *ActaOecol* 22, 529–550. doi: 10.1016/S0399-1784(00)87685-9

Lenihan, H. S., Peterson, C. H., Miller, R. J., Kayal, M., and Potoski, M. (2018). Biotic disturbance mitigates effects of multiple stressors in a marine benthic community. *Ecosphere* 9:e02314. doi: 10.1002/ecs2.2314

Levin, L. A., and Sibuet, M. (2012). Understanding continental margin biodiversity: a new imperative. *Ann. Rev. Mar. Sci*. 4, 79–112. doi: 10.1146/annurev-marine-120709-142714

Lira, V. F., Santos, G. A. P., Derycke, S., Larrazabal, M. E. L., Fonsêca-Genevois, V. G., and andMoens, T. (2011). Effects of barium and cadmium on the population development of the marine nematode Rhabditis (Pellioditis) marina. *Mar. Environ. Res*. 72, 151–159. doi: 10.1016/j.marenvres.2011.07.003

Longhurst, A. R. (1958). *An Ecological Survey of the West African MarineBenthos*. London: Colonial Office Fisheries Publication, 1–102.

Longhurst, A. R. (1959). Benthos densities off tropical West Africa. Permanent International pour l'Exploration de la Mer. *J. deConseil/Coseil* 25, 21–28. doi: 10.1093/icesjms/25.1.21

Lourido, A., Sorbe, J. C., and Troncoso, J. S. (2008). Inventario de los crustáceosbentónicos de sedimentosinfralitorales de la Ría de Aldán (Galicia, NO PenínsulaIbérica). *Nova Acta Ci. Compostelana Biol*. 17, 149–168. Available online at: http://hdl.handle.net/10347/6557

Macdonald, J. M., Shields, J. D., and Zimmer-Faust, R. K. (1988). Acute toxicities of eleven metals to early life-history stages of the yellow crab Cancer anthonyi. *Mar. Biol*. 98, 201–207. doi: 10.1007/BF00391195

Magurran, A. E. (2012). "Biodiversity in the context of ecosystem function," in *Marine Biodiversity and Ecosystem Functioning: Frameworks, Methodologies, and Integration*, eds M. Solan, R. J. Aspden, and D. M. Paterson (Oxford: Oxford University Press), 16–23. doi: 10.1093/acprof:oso/9780199642250.003.0002

Main, C. E., Ruhl, H. A., Jones, D. O. B., Yool, A., Thornton, B., and Mayor, D. J. (2015). Hydrocarbon contamination affects deep-sea benthic oxygen uptake and microbial community composition. *Deep Sea Res. I Oceanogr. Res. Pap*. 100, 79–87. doi: 10.1016/j.dsr.2014.12.008

Marquiegui, M. A., and Sorbe, J. C. (1999). Influence of near-bottom environmental conditions on the structure of bathyal macrobenthic crustacean assemblages from the Capbreton canyon (Bay of Biscay, NE Atlantic). *ActaOecol* 20, 353–362. doi: 10.1016/S1146-609X(99)00131-9

Martin, D., Fernadez-Arcaya, U., Tirado, P., Dutrieux, É., and Corbera, J. (2010). Relationships between shallow-water cumacean assemblages and sediment characteristics facing the Iranian coast of the Persian Gulf. *J. Mar. Biolog. Assoc. U. K*. 90, 125–134. doi: 10.1017/S0025315409990695

McCallum, A. W., Woolley, S., Błazewicz-Paszkowycz, M., Browne, J., Gerken, S., Kloser, R., et al. (2015). Productivity enhances benthic species richness along an oligotrophic Indian Ocean continental margin. *Glob. Ecol. Biogeogr*. 24, 462–471 doi: 10.1111/geb.12255

Menegotto, A., and Rangel, T. F. (2018). Mapping knowledge gaps in marine diversity reveals a latitudinal gradient of missing species richness. *Nat. Commun*. 9:4713. doi: 10.1038/s41467-018-07217-7

Menot, L., Crassous, P., Desbruyeres, D., Galéron, J., Khriponoff, A., and Sibuet, M. (2009). Colonization patterns along the equatorial West African margin: implications for functioning and diversity maintenance of bathyal and abyssal communities. *Deep Sea Res. II Top. Stud. Oceanogr*. 82053, 2313–2325. doi: 10.1016/j.dsr2.2009.04.012

Menot, L., Sibuet, M., Carney, R. S., Levin, L. A., Rowe, G. T., Billett, D. S. M., et al. (2010). "New perceptions of continental margin biodiversity," in *Life in the World's Oceans*, ed A. D. McIntyre (Singapore: Wiley-Blackwell), 79–102. doi: 10.1002/9781444325508.ch5

Modlin, R. F., and Dardeau, M. (1987). Seasonal and spatial distribution of cumaceans in the Mobile Bay estuarine system, Alabama. *Estuaries* 10, 291–297. doi: 10.2307/1351886

Monroy-Velázquez, L. V., Rodríguez-Martínez, R. E., and Alvarez, F. (2017). Taxonomic richness and abundance of cryptic peracarid crustaceans in the Puerto Morelos Reef National Park, Mexico. *PeerJ* 5:e3411. doi: 10.7717/peerj.3411

Mühlenhardt-Siegel, U. (1996). Cumacea (Crustacea) from the Red Sea and the Maldives (Indian Ocean) in the collection of the Zoological Museum, Hamburg, with the description of seven new species and a new genus. *Beaufortia* 46, 105–134.

Mühlenhardt-Siegel, U. (1999). On the biogeography of Cumacea (Crustacea, Malacostraca). A comparison between South America, the Subantarctic Islands and Antarctica: present state of the art. *Sci. Mar*. 63, 295–302. doi: 10.3989/scimar.1999.63s1295

Mühlenhardt-Siegel, U. (2000). Cumacea (Crustacea) from the Seychelles, Maldives, Sri Lanka (western Indian Ocean), and the Red Sea, with the

description of six new species. *Beaufortia* 50, 197–222. Available online at: https://repository.naturalis.nl/pub/504899

Mühlenhardt-Siegel, U. (2005). Cumacea species (Crustacea: Peracarida) from the Deep-Sea Expedition DIVA-1 with RV "Meteor" to the Angola Basin in July 2000. Families Lampropidae, *Bodotriidae*. *Org. Divers. Evol*. 5, 113–130. doi: 10.1016/j.ode.2004.10.008

Mühlenhardt-Siegel, U. (2009). Cumacea (Crustacea, Peracarida) in the deep Mediterranean, with the description of one new species. *Zootaxa* 2096, 413–432. doi: 10.11646/zootaxa.2096.1.25

Mühlenhardt-Siegel, U. (2011). New and known species of the family Leuconidae (Cumacea, Peracarida) from Antarctic deep-sea basins. *Zootaxa* 3117, 1–68. doi: 10.11646/zootaxa.3117.1.1

Neff, J. M. (2002). *Bioaccumulation in Marine Organisms: Effect of Contaminants From Oil Well Produced Water*. Amsterdam: Elsevier. doi: 10.1016/B978-008043716-3/50002-6

Nieto, K., and Mélin, F. (2017). Variability of chlorophyll-a concentration in the Gulf of Guinea and its relation to physical oceanographic variables. *Prog. Oceanogr*. 151, 97–115. doi: 10.1016/j.pocean.2016.11.009

Oksanen, J., Blanchet, F. G., Friendly, M., Kindt, R., Legendre, P., McGlinn, D., et al. (2019). *Vegan: Community Ecology Package. R package version 2. 5-4*. Available online at: https://CRAN.R-project.org/package=vegan (accessed November 28, 2020).

Olsgard, F., Brattegard, T., and Holthe, T. (2003). Polychaetes as surrogates for marine biodiversity: 977 lower taxonomic resolution and indicator groups. *Biodiv. Conserv*. 12, 1033–1049. doi: 10.1023/A:1022800405253

Olsgard, F., and Gray, J. S. (1995). A comprehensive analysis of the effects of offshore oil and gas exploration and production on the benthic communities of the Norwegian continental shelf. *Mar. Ecol. Prog. Ser*. 122, 277–306. doi: 10.3354/meps122277

OSPAR (2017). *Guidelines for Monitoring the Environmental Impact of Offshore Oil 981and Gas Activities. Agreement 2017-02*. Cork: OSPAR Commission.

Owusu-Boadi, K., and Kuitunen, M. (2002). Urban waste pollution in the Korle Lagoon, Accra, Ghana. *Environmentalist* 22, 301–309. doi: 10.1023/A:1020706728569

Pabis, K., and Błazewicz-Paszkowycz, M. (2011). Distribution and diversity of cumacean assemblages in Admiralty Bay, King George Island. *Pol. Polar Res*. 32, 341–354. doi: 10.2478/v10183-011-0024-6

Pabis, K., Sobczyk, R., Siciński, J., Ensrud, T., and Serigstadt, B. (2020). Natural and anthropogenic factors nfluencing abundance of the benthic macrofauna along the shelf and slope of the Gulf of Guinea, a large marine ecosystem off West Africa. *Oceanologia* 62, 83–100. doi: 10.1016/j.oceano.2019.08.003

Petrescu, I. (1998). Cumaceans (Crustacea: Cumacea) collected by the expedition of "GrigoreAntipa" Museum of Natural History from the coasts of Tanzania (1973-1974). Part I. Family Bodotriidae. *Trav. Mus. Natl. Hist. Nat. GrigoreAntipa* 40, 227–310.

Petrescu, I. (2018). On the family Nannastacidae (Crustacea, Cumacea) from the Australian Museum collection. *Rec. Aust. Mus*. 70, 1–111. doi: 10.3853/j.2201-4349.70.2018.1645

Petrescu, I., and Sterrer, W. (2001). Cumacea (Crustacea) from shallow waters of Bermuda. *Ann. Naturhist. Mus. Wien B Bot. Zool*. 103, 89–128. Available online at: https://www.jstor.org/stable/41767206

Pilar-Cornejol, M., Calderon, J., and Vincx, M. (2004). Spatial patterns of the surf zone hyperbenthic fauna of Valdivia Bay (Ecuador). *Hydrobiologia* 529, 205–224. doi: 10.1007/s10750-004-6417-3

R Core Team (2020). *R: A Language and Environment for Statistical Computing*. Vienna: R Foundation for Statistical Computing.

Rehm, P., Thatje, S., Mühlenhardt-Siegel, U., and Brandt, A. (2007). Composition and distribution of the peracarid crustacean fauna along a latitudinal transect off Victoria Land (Ross Sea, Antarctica) with special emphasis on the Cumacea. *Polar Biol*. 30, 871–881. doi: 10.1007/s00300-006-0247-x

Rex, M. A., and Etter, R. J. (2010). *Deep-Sea Biodiversity; Patterns and Scale*. Cambridge, MA: Harvard University Press.

Reyss, D. (1973). Distribution of cumacea in the deep mediterranean. *Deep Sea Res. I Oceanogr. Res. Pap*. 20, 1119–1123. doi: 10.1016/0011-7471(73)90025-9

San Vicente, C., Munilla, T., Corbera, J., Sorbe, J. C., and Ramos, A. (2009). Suprabenthic fauna from the Bellingshausen Sea and western Antarctic Peninsula: spatial distribution and community structure. *Sci. Mar*. 73, 357–368. doi: 10.3989/scimar.2009.73n2357

San Vicente, C., and Sorbe, J. C. (1999). Spatio-temporal structure of the suprabenthic community from Creixell beach (western Mediterranean). *Acta Oecol*. 20, 377–389. doi: 10.1016/S1146-609X(99)00129-0

San Vicente, C., and Sorbe, J. C. (2001). Temporal changes in the structure of the suprabenthic community from Hendaya beach (southern Bay of Biscay): a comparison with a northwesternmediterranean beach community. *Bol. Inst. Esp. Oceanogr*. 17, 107–120. Available online at: https://citeseerx.ist.psu.edu/viewdoc/download?doi=10.1.1.537.6244&rep=rep1&type=pdf

Sarthou, C., Larpin, D., Fonty, É., Pavoine, S., and andPonge, J.-F. (2010). Stability of plant communities along a tropical inselberg ecotone in French Guiana (South America). *Flora* 205, 682–694. doi: 10.1016/j.flora.2010.04.005

Scheren, P. A., Ibe, A. C., Janssen, F. J., and Lemmens, A. M. (2002). Environmental pollution in the Gulf of Guinea – a regional approach. *Mar. Pollut. Bull*. 44, 633–641. doi: 10.1016/S0025-326X(01)00305-8

Sebens, K. P. (1991). "Habitat structure and community dynamics in marine benthic systems" in Habitat Structure: The physical arrangement of objects in space," eds S. S. Bell, E. D. McCoy, and H. R. Mushinsky (Dordrecht: Springer Netherlands), 211–234. doi: 10.1007/978-94-011-3076-9_11

Sobczyk, R., Czortek, P., Serigstad, B., and Pabis, K. (2021). Modelling of polychaete functional diversity: a Large Marine Ecosystem response tomultiple natural factors and human impacts on the West African continental margin. *Sci. Total Environ*. 792:148075. doi: 10.1016/j.scitotenv.2021.148075

Sorbe, J. C., and Elizalde, M. (2014). Temporal changes in the structure of a slope suprabenthic community from the Bay of Biscay (NE Atlantic Ocean). *Deep Sea Res. II Top. Stud. Oceanogr*. 106, 179–191. doi: 10.1016/j.dsr2.2013.09.041

Spalding, M. D., Fox, H. E., Allen, G. R., Davidson, N., Ferdaña, Z. A., Finlayson, M., et al. (2007). Marine ecoregions of the world: a bioregionalization of coastal and shelf areas. *BioScience* 57, 573–583. doi: 10.1641/B570707

Stark, J. S., Mohammad, M., McMinn, A., and Ingels, J. (2020). Diversity, abundance, spatial variation, and human impacts in marine meiobenthic Nematode and Copepod communities at Casey Station, East Antarctica. *Front. Mar. Sci*. 7:480. doi: 10.3389/fmars.2020.00480

StatSoft (2006). *Elektroniczny Podrecznik Statystyki PL. Krakow*. Available online at: http://www.statsoft.pl/textbook/stathome.html (accessed May 10, 2021).

Swaileh, K. M., and Adelung, D. (1995). Effect of body size and season on the concentrations of Cu, Cd, Pb and Zn in Diastylisrathkei (Kröyer) (Crustacea: Cumacea) from Kiel Bay, Western Baltic. *Mar. Pollut. Bull*. 31, 103–107. doi: 10.1016/0025-326X(94)00258-B

Thiel, M., González, E. R., Balanda, M. J., Haye, P., Heard, R., and Watling, L. (2003). "Diversity of Chilean peracarids (Crustacea: Malacostraca)," in *Contribuciones al Estudio de los Crustáceos del Pacífico Este*, ed M. E. Hendrickx (Mexico: Instituto de Ciencias del Mar y Limnología, UNAM), 177–189.

Ukwe, C. N., Ibe, C. A., Alo, B. I., and Yumkella, K. K. (2003). Achieving a paradigm shift in environmental and living resources management in the Gulf of Guinea: the large marine ecosystem approach. *Mar. Pollut. Bull*. 47, 219–225. doi: 10.1016/S0025-326X(02)00473-3

Ukwe, C. N., Ibe, C. A., and Sherman, K. (2006). A sixteen-country mobilization for sustainable fisheries in the Guinea Current Large Marine Ecosystem. *Ocean Coast. Manag*. 49, 385–412. doi: 10.1016/j.ocecoaman.2006.04.006

UNESCO Intergovernmental Oceanographic Commission (1982). *The Determination of Petroleum Hydrocarbons in Sediments (Manuals and Guides No. 11, Paris)*. Paris: UNESCO.

Wägele, J. W. (2005). *Foundations of Phylogenetic Systematics*. München: Verlag Dr. Friedrich Pfeil.

Walsh, C., and Mac Nally, R. (2013). *hier.part: Hierarchical Partitioning. R package version 1.0-4*. Available online at: https://CRAN.R-project.org/package=hier.part (accessed March 10, 2020).

Wang, Z., and Dauvin, J. C. (1994). The suprabenthic crustacean fauna of the infralittoral fine sand community from the Bay of Seine (Eastern English Channel): composition, swimming activity and diurnal variation. *Cah. Biol. Mar*. 35, 135–155.

Watling, L., and Gerken, S. (2021). *World Cumacea Database*. Available online at: http://www.marinespecies.org/cumaceaon~2021-04-27 (accessed July 7, 2020).

Wei, T., and Simko, V. (2017). *R Package "Corrplot": Visualization of a Correlation Matrix (Version 0.84)*. Available online at: https://guthub.com/taiyun/corrplot (accessed February 12, 2020).

Wieser, W. (1956). Factors influencing the choice of substratum in *Cumella vulgaris* Hart (Crustacea, Cumacea). *Limnol. Oceanogr*. 1, 274–285. doi: 10.4319/lo.1956.1.4.0274

Witman, J. D., Etter, R. J., and Smith, F. (2004). The relationship between regional and local species diversity in marine benthic communities: a global perspective. *Proc. Natl. Acad. Sci. U. S. A*. 101, 15664–15669. doi: 10.1073/pnas.0404300101

Conflict of Interest: The authors declare that the research was conducted in the absence of any commercial or financial relationships that could be construed as a potential conflict of interest.

Publisher's Note: All claims expressed in this article are solely those of the authors and do not necessarily represent those of their affiliated organizations, or those of the publisher, the editors and the reviewers. Any product that may be evaluated in this article, or claim that may be made by its manufacturer, is not guaranteed or endorsed by the publisher.

Copyright © 2021 Stępień, Pabis, Sobczyk and Serigstad. This is an open-access article distributed under the terms of the Creative Commons Attribution License (CC BY). The use, distribution or reproduction in other forums is permitted, provided the original author(s) and the copyright owner(s) are credited and that the original publication in this journal is cited, in accordance with accepted academic practice. No use, distribution or reproduction is permitted which does not comply with these terms.

frontiers in Marine Science

ORIGINAL RESEARCH
published: 11 August 2021
doi: 10.3389/fmars.2021.669478

Better Alone Than in Bad Company: New Species of Caudofoveate Limifossorid (Mollusca, Aplacophora) Unravels Patterns of Distribution Hidden in the Deep Atlantic

Flávio Dias Passos[1], Paulo Vinicius Ferraz Corrêa[2] and Marcel Sabino Miranda[1]*

[1] *Laboratory of Malacology, Department of Animal Biology, Institute of Biology, University of Campinas, Campinas, Brazil,*
[2] *Laboratory of Ecology and Evolution of Deep Sea, Department of Biological Oceanography, Oceanographic Institute, University of São Paulo, São Paulo, Brazil*

Aplacophorans are common inhabitants of the deep-sea, where many places remain unexplored regarding their biodiversity. Filling a gap in knowledge about these animals from the South Atlantic, *Scutopus variabilis* sp. nov. (Caudofoveata, Limifossoridae) is described; further, species distribution modelling (SDM) was performed to elucidate the distribution patterns of Atlantic species of *Scutopus*. The type materials of *S. megaradulatus* Salvini-Plawen (1972) and *S. chilensis* Salvini-Plawen (1972), were examined and a search was performed for specimens of *Scutopus* held in museum collections. *Scutopus variabilis* sp. nov. has a slender and highly variable body form and a very distinct suture line is present midventrally. Two dominant types of trunk sclerites were observed by Scanning Electron Microscopy (SEM): one elongated with lateral margins slightly concave in medial portion, and another longer, with narrower base; its radula bears up to eight rows of heavily sclerotized teeth bearing 12–16 small denticles. The species occurs in a wide bathymetric range (40–1300 m), being more abundant at the edge between the continental shelf and upper slope. Outside the areas from where these samples were obtained, suitable areas for *S. variabilis* sp. nov. were found in the Southern Caribbean Sea (from where *S. megaradulatus* is recorded) and in the Brazilian Northern coast; the Gulf of Mexico and the Brazilian Northeastern coasts were found as unsuitable. Species of *Scutopus* appear to exhibit different patterns of geographical distribution: the European *S. ventrolineatus* Salvini-Plawen (1968) and *S. robustus* Salvini-Plawen (1970) are known as widely distributed, while non-European representants, the American *S. megaradulatus*, *S. chilensis* and *S. variabilis* sp. nov., and the Japanese *S. schanderi* Saito and Salvini-Plawen (2014) and *S. hamatamii* Saito and Salvini-Plawen (2014) have more restricted distributions. However, clear and definite patterns of distribution of some of these species are probably blurred by sampling bias, for the European area is better studied. In the Atlantic, the SDM showed that species of *Scutopus* occur in a way that overlapping is minimized. Great sampling efforts combined with detailed descriptions based on SEM have revealed an interesting, abundant and up to now undescribed Brazilian deep-sea malacofauna.

Keywords: taxonomy, biogeography, species distribution modeling, Caudofoveata, Limifossoridae

OPEN ACCESS

Edited by:
Kevin Kocot,
University of Alabama, United States

Reviewed by:
Ekin Tilic,
University of Copenhagen, Denmark
Emanuel Redl,
University of Vienna, Austria
Nina Therese Mikkelsen,
University of Bergen, Norway

****Correspondence:***
Flávio Dias Passos
flaviodp@unicamp.br

Specialty section:
This article was submitted to Deep-Sea Environments and Ecology, a section of the journal Frontiers in Marine Science

Received: *18 February 2021*
Accepted: *20 July 2021*
Published: *11 August 2021*

Citation:
Passos FD, Corrêa PVF and Miranda MS (2021) Better Alone Than in Bad Company: New Species of Caudofoveate Limifossorid (Mollusca, Aplacophora) Unravels Patterns of Distribution Hidden in the Deep Atlantic. Front. Mar. Sci. 8:669478. doi: 10.3389/fmars.2021.669478

INTRODUCTION

Ubiquitous among the deep-sea organisms, aplacophorans form a molluscan group of particular phylogenetic interest (e.g., Kocot et al., 2011; Smith et al., 2011; Vinther et al., 2012, 2017; Mikkelsen et al., 2018, 2019), ecological importance (Scheltema, 1987, 1997; Scheltema and Ivanov, 2009), and biogeographical relevance (Scheltema, 1985; Ivanov and Scheltema, 2008; Corrêa et al., 2014, 2018; Bergmeier et al., 2017, 2019; Cobo and Kocot, 2020). They are generally characterized by their worm-like bodies covered by sclerites, and formed by two clades: Solenogastres, which are epifaunal and bear a ventral pedal furrow, and Caudofoveata, whose species are infaunal, without a ventral locomotory organ, and have an oral shield (that is absent in solenogasters). A total of 420 species of aplacophorans have been described so far, most of them occurring on the continental slope (Todt, 2013).

In the deep Atlantic Ocean, most reports on caudofoveates are for species from both European or North American waters, and fewer are based on specimens collected in the Southern Hemisphere. For the Brazilian coast (Southwestern Atlantic), in particular, eight species are known: *Chevroderma turnerae* Scheltema, 1985 recorded by Scheltema (1985) and Ivanov and Scheltema (2008), and *Spathoderma bulbosum* Ivanov and Scheltema, 2008 by Ivanov and Scheltema (2008); *Falcidens targatus* Salvini-Plawen, 1992 and *F. acutargatus* Salvini-Plawen, 1992 studied by Corrêa et al. (2014); *Claviderma amplum* Ivanov and Scheltema, 2008, *C. crassum* Ivanov and Scheltema, 2008 and *C. virium* Corrêa, Miranda and Passos, 2018 investigated by Corrêa et al. (2018); and *F. australocaudatus* Passos, Corrêa and Todt, 2016 described by Passos et al. (2018). Passos et al. (2019) have summarized all the records of aplacophorans from Brazilian waters up to that time, pointing out that most of them are from restricted oil-rich areas, there remaining large parts of its coast in which these molluscs were never reported (as its southernmost and northernmost portions), and that there are many other species to be investigated.

In the present contribution, a new species of the genus *Scutopus* Salvini-Plawen, 1968 is described, through the analysis of many specimens collected along the southeastern and southern coasts of Brazil, with some records for regions never explored before. This genus of Caudofoveata was created by Salvini-Plawen (1968), based on the description of *S. ventrolineatus* Salvini-Plawen, 1968, originally discovered near Bergen, Norway, Scandinavia. Afterward, a second European species was described by Salvini-Plawen (1970), *S. robustus* Salvini-Plawen, 1970, and two others by Salvini-Plawen (1972), *S. megaradulatus* Salvini-Plawen, 1972 and *S. chilensis* Salvini-Plawen, 1972, from the Caribbean Sea and Chile, respectively. More recently, Saito and Salvini-Plawen (2014) recorded *S. schanderi* Saito and Salvini-Plawen, 2014 and *S. hamatanii* Saito and Salvini-Plawen, 2014 from the Sea of Japan. The Brazilian new species is here described based on the general body morphology and on the details of its oral shield, sclerites, and radula, in comparison with those congeneric six species; further, their bathymetric and geographical distributions are modeled and discussed regarding how these can advance delineation and identification of deep-sea caudofoveate species. It is here emphasized that this new species has a highly variable body form, and only through the observation of the many available specimens it was possible to describe it in detail, complementing ongoing recent discoveries that have been performed on the malacofauna of the Brazilian deep-sea waters.

MATERIALS AND METHODS

Most specimens were collected off the coasts of the Espírito Santo (ES) and Rio de Janeiro (RJ) States, southeast Brazil, obtained from bottom sediment samples collected by box-corers and Van Veen grabs, through the activities of the Projects "Habitats" and "Ambes" [for details about these projects, see Passos and Machado (2014) and Machado and Passos (2016)]. These samples were initially fixed in 4% formaldehyde and after sieving the animals were sorted and transferred to a solution of 70% ethanol. Apart from the material of these projects, other samples were collected off the States of São Paulo (SP) (also in the southeast), and in the southern States of Paraná (PR) and Rio Grande do Sul (RS). These latter samples were obtained by three research projects: "Projeto Integrado," which occurred from 1985 to 1986 and collected in the shelf of Ubatuba (São Paulo) (Pires-Vanin and Matsuura, 1993), and by the Projects "MBT" and "Revizee," in which more scattered bottom samplings were performed along all this area, the former in 1970/1, the latter in 1998/9. These materials are deposited in the molluscan collections of the following institutions: Museum of Zoology of the State University of Campinas (ZUEC APL), Campinas (SP), Museum of Zoology of University of São Paulo (MZSP), SP, National Museum of Rio de Janeiro (MNRJ), RJ, and Museum of Zoology of Federal University of Sergipe (CZUFS APL), São Cristóvão (SE), all in Brazil.

The animals were initially observed under stereomicroscopes, and then some were sorted for more detailed analysis using Scanning Electron Microscopy (SEM). The methods employed were the same as the ones of Corrêa et al. (2014, 2018) and Passos et al. (2018). Because individuals (and specially the smaller ones) are hard to identify through only the general morphology, some of their sclerites were extracted from the trunk by using fine needles, and then placed on slides, air-dried and covered with Entellan and a cover slip for permanent preparations; these slides are also deposited in the respective collections.

Apart from the Brazilian specimens, samples of *S. megaradulatus* analyzed by Scheltema (1981) from North Carolina, United states, deposited in the Museum of Comparative Zoology (MCZ), Harvard University, Cambridge, MA, United states, as well as the samples of this species and of *S. chilensis* deposited in the American Museum of Natural History (AMNH), New York, United states, were observed. Further, while an analysis was performed in the MCZ and in the National Museum of Natural History, Smithsonian Institution (USNM) (Miranda et al., 2020), specimens identified as species of *Scutopus* were also searched in these molluscan collections.

To further investigate the potential distribution of the *Scutopus* species in the Atlantic, a species distribution model (SDM) was performed using MaxEnt 3.4.4.k (Phillips et al.,

2006), for the new species described herein, *S. robustus* and *S. ventrolineatus*. *Scutopus megaradulatus* was not included due to the few records available in literature (<10). For the new species, a total of 33 records were used, based on the samples observed in this study. For *S. robustus* (24 records) and *S. ventrolineatus* (15 records), datasets of records were produced based on the literature (see **Table 3**); those of *S. robustus* from Salvini-Plawen (1977) were not included as they are considered doubtful (Ivanov and Scheltema, 2001).

Environmental data were obtained from the Global Marine Environment Datasets (GMED) (Basher et al., 2018) with a resolution of 5′ (approx. 9.2 km near equator). As caudofoveates are benthic organisms, variables reflecting environment near the seabed were used, namely depth, slope, bottom temperature, primary productivity and bottom silicate. These variables had a weak to medium correlations ($r < 0.7$), calculated by the Pearson correlation in ENMTools 1.4.3 (Warren et al., 2010). To generate the model, 100,000 random background points were used, with a regularization multiplier of 1. 75% of presence records were randomly chosen and used in the model training while the remaining 25% were used in the model testing. Also, the "fade by clamping" option was set to reduce prediction into areas with environmental conditions that were not found during model training, and 10 replicates using Bootstrap as "Replicated run type" (Basher and Costello, 2016). All other parameters were used as default. To test model goodness of fitting, the area under the curve operating characteristics was used (AUC). The potential distribution was computed as Cloglog. Later, with this the output, to define the Minimum Presence Threshold (MPT), "10 percentile training presence" threshold was used (Morueta-Holme et al., 2010). The final output rasters were classified in not suitable (below the MPT) and suitable (above MPT) areas.

RESULTS

Family Limifossoridae Salvini-Plawen, 1969

Genus *Scutopus* Salvini-Plawen, 1968

Type species: *Scutopus ventrolineatus* Salvini-Plawen, 1968 by original designation.

Remarks: Salvini-Plawen (1968) characterized *S. ventrolineatus* by its long, undivided, cylindrical body which coils up spirally when it is disturbed, its radula composed by multiple rows of paired teeth, each tooth bearing median denticles, an undivided or homogeneous, post-oral shield, and the presence of a long midgut sac or digestive gland, and by its sclerites that ventrally are positioned in a divergent way forming a clear external ventral sutural line. Later, Salvini-Plawen (1975) and Ivanov (1981) highlighted that the characters of the oral shield and the radula are typical of *Scutopus* species. The new species described herein has these main characteristics, as shown below.

Scutopus variabilis sp. nov. Passos, Corrêa and Miranda (**Figures 1–6**, **8**)

LSID: urn:lsid:zoobank.org:act:A734DD68-A074-42FB-A9C4-A1DFAD68D4B9

Type Material

Holotype: ZUEC APL 277, sta HAB6-C7-R2(2-5) (22°59′52.609″S, 40° 47′ 45.008″W) (Brazil – off Rio de Janeiro State), "Habitats" Project coll., 30/vi/2008, 689.4 m; entire individual (**Figure 1A**) plus one slide with its sclerites. Total length: 11 mm; anterium plus neck: 2 mm; trunk: 8 mm; posterium: 1 mm.

Paratypes: All collected in the southeastern and southern Brazilian coasts, from off States of ES, RJ, SP, PR, and RS; 188 specimens in 71 samples (**Table 1**).

Type locality. Off Rio de Janeiro, 40°47′45.008″W, 22°59′52.609″S, 689.4 m.

Non-type material. All collected in the southeastern Brazilian coasts, from off States of ES and RJ; 153 specimens in 61 samples (**Supplementary Table 1**).

Diagnosis. Body long, slender, up to 14 mm in length, often contorted, almost uniform in diameter; in most specimens divided in three parts: an anterior part separated by a main collar from a median part, and a slightly tapered posterior part. Oral shield post-oral, ventral to the mouth. Midventral suture line present. Two main types of sclerites: one elongated, with lateral margins slightly concave in medial portion, with base wider and about a half of the blade length, and another shorter, triangular, base and blade with continuous straight lateral margins; in both, blade ornamented with a central keel and weak adjacent longitudinal grooves. Radula distichous, with up to eight transversal rows of heavily sclerotized teeth (except for the two most proximal pairs); each tooth inwardly curved, with 12–16 small median bent denticles present in all the extension of the concave, inner margin.

Etymology. The name *variabilis* refers to the variable form and color exhibited by the specimens of this species.

Description

External Appearance

Body whitish to brownish in color, opaque in most adult specimens; cylindrical in form, long, slender, up to 14 mm in length, often contorted; almost uniform in diameter, up to 0.9 mm in width (**Figures 1**, **2A–D,G**). Body almost homogeneous throughout its length, but in most specimens with three externally distinguishable parts: an anterior, separated by a main collar from a median part (**Figures 1B,F,I,K,M,O**, **2A–C,G**), and a slightly tapered posterior part (**Figures 1A,C,K**). Anterior part whitish to transparent, composed by a sometimes protruded peribuccal region (or anterium) (**Figures 1C,I**, **2A,B**) and a short foregut region (neck or prothorax) (**Figures 1A,H**, **2A,B**). Median part (trunk or metathorax) dark brown, reflecting the presence of the midgut internally; a secondary collar sometimes present separating this median part in two regions: an anterior short midgut region, and a long posterior midgut sac region (**Figure 1H**). Posterior part short, composed by a narrower, transparent prepallial region and a pallial region which is often slightly inflated; secretions of the animal occur over the sclerites, giving a reddish color to the entire posterior part, or more often around the pallial region or in the center of the posterior end (**Figures 1A,B,D–F,I,K**). When the peribuccal

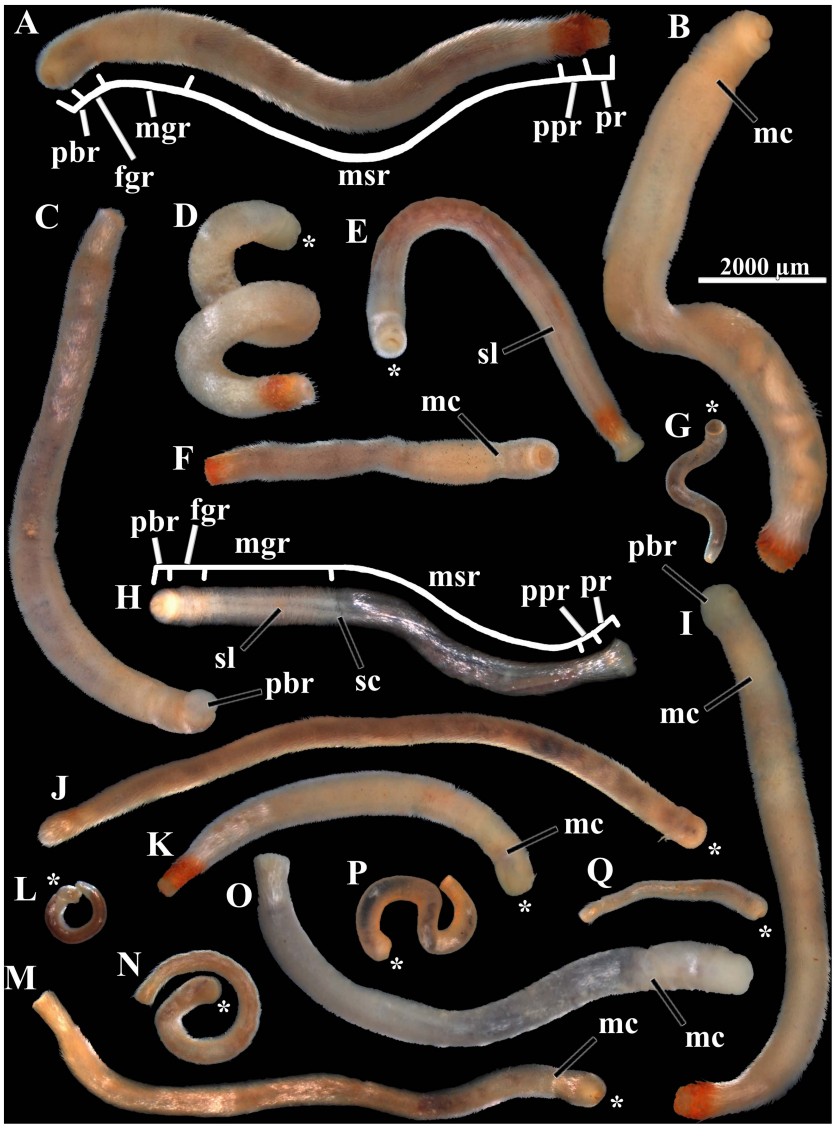

FIGURE 1 | *Scutopus variabilis* sp. nov. Photomicrographs under stereomicroscope of specimens of different sizes showing their variable body form and color (all in same scale). The body regions are shown in **(A)** (holotype) and **(H)**, **(B)** and **(D)** had their soft parts dissolved for the extraction of their radulas [which are shown in **Figures 4A,E**, respectively and of their sclerites from the different body regions. The peribuccal region is protruded in **(C)** and **(I)**. The midventral suture line is visible in **(E)** and **(H)**; the main collar in **(B)**, **(F)**, **(I)**, **(K)**, **(M)**, and **(O)**; and the secondary collar in **(H)**. The asterisks in **(D)**, **(E)**, **(G)**, **(J–N)**, **(P)**, and **(Q)** show the anterior end. fgr - foregut region; mc - main collar; mgr - midgut region; msr - midgut sac region; pbr - peribuccal region; ppr - prepallial region; pr - pallial region; sc - secondary collar; sl - midventral suture line. Voucher numbers: **(A)** – ZUEC APL 277, **(B)** – ZUEC APL 285, **(C)** – ZUEC APL 287, **(D)** – ZUEC APL 284, **(E)** – ZUEC APL 279, **(F)** – ZUEC APL 282, **(G)** – ZUEC APL 306, **(H)** – ZUEC APL 298, **(I)** – ZUEC APL 286, **(J)** – MZSP 154099, **(K)** – ZUEC APL 286, **(L)** – ZUEC APL 326, **(M)** – MNRJ 23638, **(N)** – ZUEC APL 331, **(O)** – ZUEC APL 291, **(P)** – ZUEC APL 311, **(Q)** – ZUEC APL 283.

region is swollen, the ventral oral shield is visible (**Figure 2E**); when contracted, the oral shield contracts in its midline, appearing divided in two lateral parts (bipartite) (**Figures 2F,H**). Sclerites uniformly cover all the surface of the body, except ventrally, where they are positioned in a divergent way, forming a midventral suture line along the foregut region and all the midgut and midgut sac regions (**Figures 1E**, **2A–C,G**). Variations in color and form occur among specimens of the same size, and among juveniles and adults; the main collar is not visible in many individuals and so they appear to have an undivided body (**Figure 1J**); smaller individuals tend to be slender, transparent, with the main collar and the ventral suture line quite indistinguishable (**Figures 1G,L,N,P,Q**).

Sclerites

Adpressed to the mantle, positioned parallel to the longitudinal body axis, except in the midgut region, where they are bristling in some specimens (**Figures 2C,G**). In the peribuccal region flat, small, 50 µm long × 25 µm wide, drop-shaped, without waist, pointed at the tip, smooth (**Figure 3A**); or triangular,

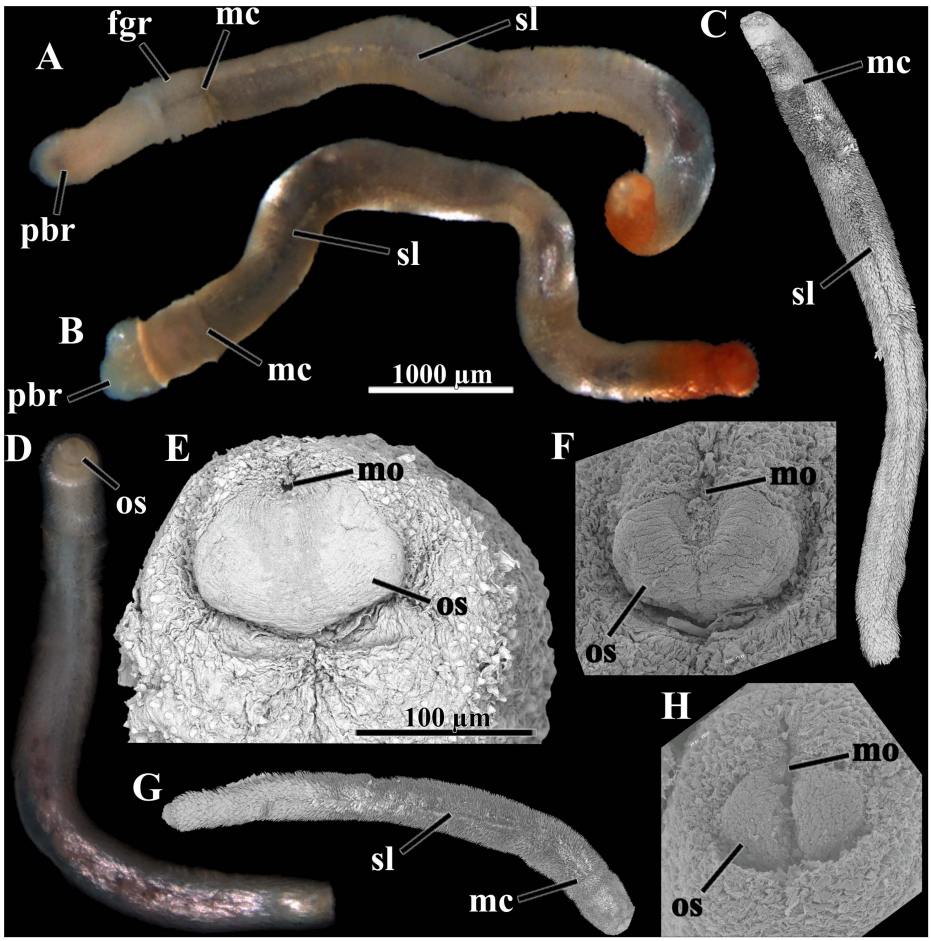

FIGURE 2 | *Scutopus variabilis* sp. nov. Photomicrographs under stereomicroscope [**(A)**, **(B),** and **(D)**] and SEM **(C,E–H)**; **(A–D)** and **(G)** are in same scale, as are **(E)**, **(F)** and **(H)**. **(E)**, **(F)**, and **(H)** are a detail of the anterior end, showing the oral shield in different degrees of contraction; **(E)** is the oral shield of **(D)**, which is in the most relaxed state; in **(F)** it is in an intermediary state and in **(H)** it is strongly contracted appearing bipartite. The peribuccal region is protruded in **(A)** and **(B)**. The midventral suture line and the main collar are visible in **(A–C)** and G. fgr – foregut region, mc – main collar, mo – mouth, os – oral shield, pbr – peribuccal region, sl – midventral suture line. Voucher numbers: **(A,B)** – MNRJ 23639, **(C)** – ZUEC APL 306, **(D)** – ZUEC APL 280, **(E)** – ZUEC APL 280, **(F)** – ZUEC APL 314, **(G)** – ZUEC APL 312, **(H)** – ZUEC APL 299.

longer, 86 µm long × 36 µm wide, with a distinct waist, base longer and wider than blade, blade ornamented with a central keel and pointed at the tip, basal margin almost straight (**Figure 3B**). In the foregut region 118 µm long × 28 µm wide, with a weak waist, base shorter but wider than blade, blade ornamented by a median keel sided by weak longitudinal grooves, basal margin almost straight (**Figure 3C**). In the midgut region, triangular, 95 µm long × 39 µm wide, without waist, base and blade with continuous straight lateral margins, blade ornamented by a central keel (**Figure 3D**); or elongated, 131 µm long × 56 µm wide, lateral margins slightly concave in medial portion, base wider and about a half of the blade length, blade ornamented with a keel and weak adjacent longitudinal grooves, basal margin slightly notched (**Figure 3E**). In midgut sac region, two dominants: one with the same shape as the latter, up to 162 µm long × 56 µm wide (**Figure 3F**), and another, longer, with narrower base, up to 194 µm long × 45 µm wide (**Figure 3G**); a third type, drop-shaped, less abundant, shorter, 86 µm long × 45 µm wide (**Figure 3H**). Midventral suture line with two types: one elongated, base wider, one third of the total length, blade with parallel lateral margins (**Figure 3I**), and other tapered in medial portion, with base weakly wider than blade (**Figure 3J**), both up to 193 µm long × 37 µm wide, with a keel and longitudinal grooves in blade, and a rounded basal margin. Prepallial region with two very elongated types: one lanceolate, with continuous base and blade lateral margins, 262 µm long × 62 µm wide (**Figure 3K**), and another narrower, with short base and long blade, parallel margins in most of its length, 287 µm long × 37 µm wide (**Figure 3L**); both with several grooves on blade and rounded basal margin. In pallial region: spatulate, narrow, short, 73 µm long × 11 µm wide, with a pointed smooth blade and wider base, present in the posterior margin of pallial region (**Figure 3M**); and large, 390 µm long × 48 µm wide, needle shaped or wider at base, with a

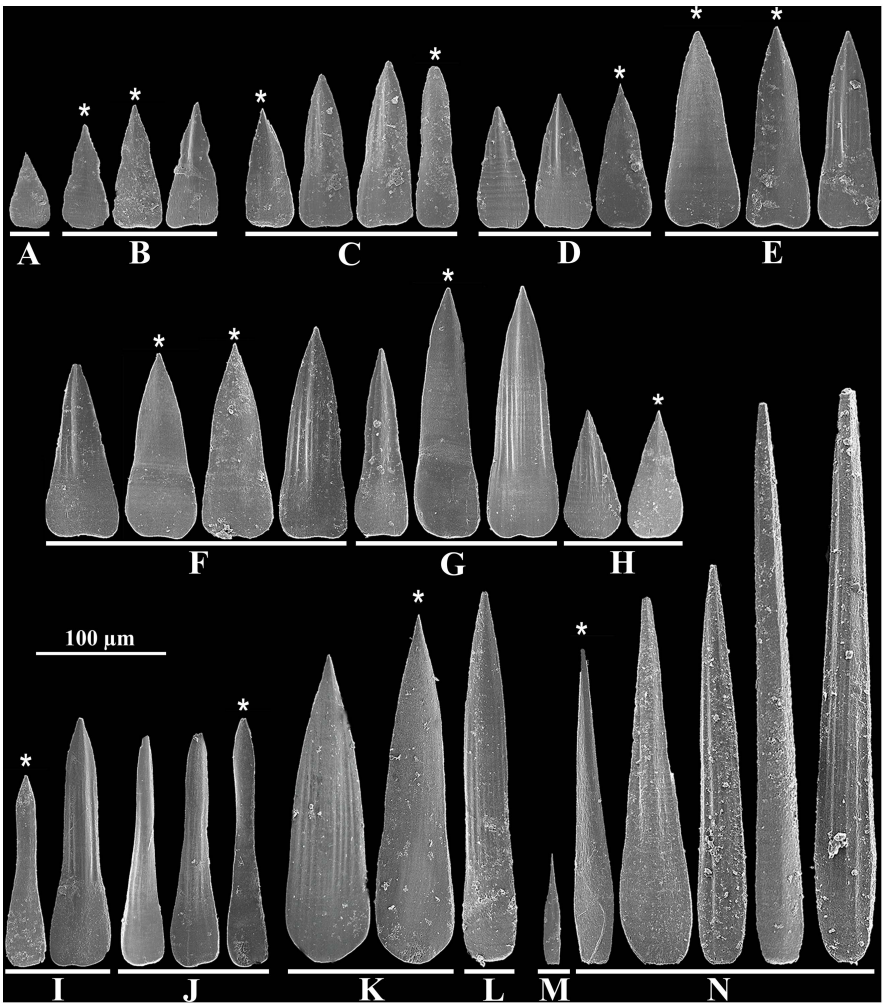

FIGURE 3 | *Scutopus variabilis* sp. nov. SEM photomicrographs of isolated sclerites from the different body regions: **(A)**, **(B)**, peribuccal region; **(C)**, foregut region; **(D)**, **(E)**, midgut region; **(F–H)**, midgut sac region; **(I)**, **(J)**, midventral suture line; **(K)**, **(L)**, prepallial region; **(M)**, **(N)**, pallial region. The asterisks point out the sclerites shown from the side facing the body. All in same scale.

keel and longitudinal grooves on all along the base and blade (**Figure 3N**). All the sclerites have a smooth surface facing the body (**Figure 3**, asterisks).

Radula

Large and elongated, up to 1.2 mm long, distichous, with up to eight transversal rows of paired teeth, which are heavily sclerotized, except the two most proximal pairs (**Figure 4A**). Each tooth is inwardly curved, up to 790 µm long × 385 µm wide, with 12–16 small median bent denticles that are present along the whole extension of the concave, inner margin of the tooth (**Figures 4B–E**).

Bathymetric and geographical distribution: A total of 342 specimens distributed in 133 samples were examined, most of them (123 samples) obtained from the States of Espírito Santo and Rio de Janeiro by the "Habitats" and "Ambes" Projects (**Figure 5**). In this area, samplings were more intensive and occurred in a wide bathymetric range, and so the specimens of *S. variabilis* sp. nov. were collected from 40 to 1300 m, with 62 samples coming from the shelf waters (less than 200 m). Ten samples were obtained from scattered points outside this area, proving that this species occurs all along the Brazilian southeastern and southern coasts; these samples were collected from only the continental shelf (less than 130 m depth) (**Figure 6**). The number of specimens per sample varies from 1 to 12, but in most (98 samples) there are up to 3 three individuals. This species can be characterized as occurring in a wide bathymetric range, with a great abundance at the edge (140–200 m) between the continental shelf and upper slope (**Figure 5**).

Species Distribution Modeling

For all the three analyzed species, the distribution model has a mean AUC > 0.996 for the training and test data, with a standard deviation of 0.001. The 10 percentile training presence threshold was 0.1167, 0.3075, and 0.4359, for *S. variabilis* sp. nov., *S. robustus*, and *S. ventrolineatus*, respectively. The

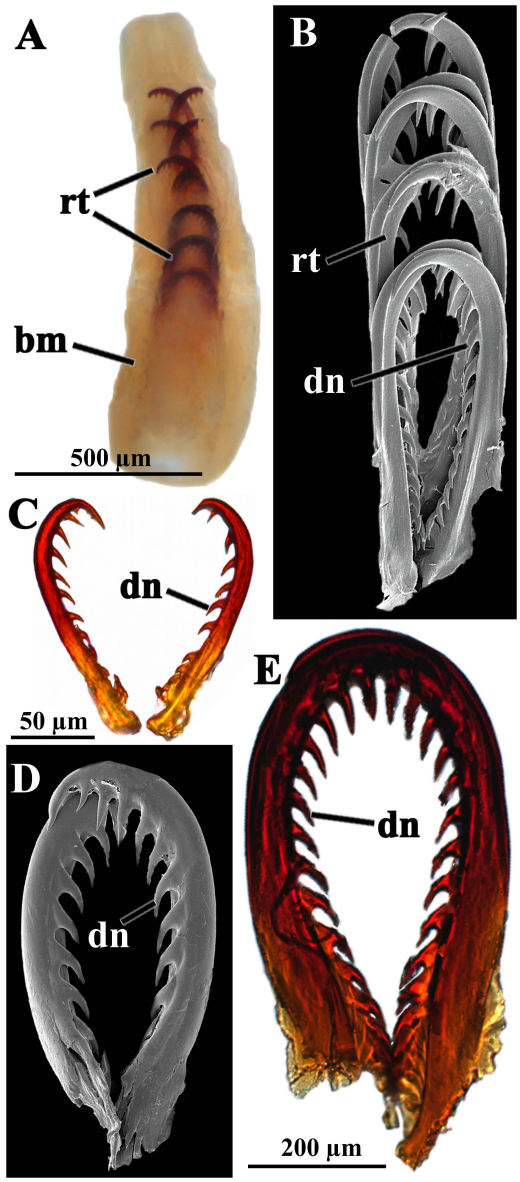

FIGURE 4 | *Scutopus variabilis* sp. nov. Photomicrographs under stereomicroscope **(A)**, SEM [**(B)** and **(D)**] and light microscopy [**(C)** and **(E)**] of the radula. In **(A)** (ZUEC APL 284) the entire radula of the individual shown in the **Figure 1D** is viewed immersed in the buccal mass. In **(B)** (ZUEC APL 319) four pairs of radular teeth are viewed in detail, and isolated pairs in **(C–E)**; in **(C)** (ZUEC APL 321) and **(D)** (ZUEC APL 319) the teeth were obtained from two small specimens (up to 4 mm in length), and in **(E)** (ZUEC APL 285) from the larger animal (about 11 mm) shown in **Figure 1 (B)**. **(B–D)** are in same scale. bm – buccal mass, dn – median denticles, rt – radular tooth.

environmental layer that most explained the potential habitat suitability of *S. variabilis* sp. nov. is depth, followed by bottom temperature (**Table 2**). Each of the other variables explained less than 10% of the habitat suitability. Depth and temperature had similar influences on the distribution of *S. robustus* (**Table 2**). Although depth had similar values of importance, for *S. ventrolineatus* silicates and primary productivity had relatively great importance in the final habitat suitability, with slope and temperature explaining less than 10% of habitat suitability (**Table 2**).

The generated maps show that main suitable areas of occurrence of *S. variabilis* sp. nov. are the Brazilian Southeastern and Southern coasts (Figure 7); the limits of distribution are the North of Espírito Santo in the north edge of this area, and the Chuí in the south. There were also some hotspots of suitability in Southern Caribbean Sea and a very narrow hotspot in the Brazilian Northern coast, east to the Amazon River mouth (States of Pará and Maranhão, Brazil). No suitability was found for *S. variabilis* sp. nov. in the Gulf of Mexico and in the Brazilian Northeastern coasts. In the Eastern Atlantic, points of suitability were found in Cape Verde and Angola Basins, in the Adriatic Sea (Albania) and in the area of the Suez Isthmus (Egypt).

Scutopus ventrolineatus was the species with the wider estimated distribution. The main suitable areas were between Southern Scandinavia and Britain, English Channel, Southwestern Ireland, Bay of Biscay, Iberian Peninsula, Strait of Gibraltar and Mediterranean of France (**Figure 7**). Wide suitable areas were found in Cape Verde, Guinea and Angola Basins in Africa. Outside the Eastern Atlantic, a continuous suitable area was found from Newfoundland to the North of Florida. Other areas were the Northern Gulf of Mexico, Tierra del Fuego, and Argentine Basin.

For *S. robustus*, the map shows that the main suitable areas are the Northwestern of Norway, Scotland, North of Ireland, South of Iceland, and Northern Lusitania, occurring in the outer part of West European Basin (**Figure 7**). In the Western Atlantic, suitable areas were found in Northeastern Falklands.

Through modeling, small areas of overlapping distribution of these species were detected (**Figure 7**). *Scutopus ventrolineatus* and *S. robustus* had the largest overlap in Southern Norway, and a small area occurred in the Iberian Basin. *Scutopus variabilis* sp. nov. had many islands of overlapping areas with *S. ventrolineatus* in Angola and Cape Verde Basins. No overlaps were found between *S. robustus* and *S. variabilis* sp. nov. or shared by all the three species.

Comments on Other Examined Species of *Scutopus*

Two lots of *S. megaradulatus* deposited in the AMNH collection were examined. One of them (AMNH 265347) was from the single sample listed by Salvini-Plawen (1972), which had two specimens when he originally described this species. Currently, this lot AMNH 265347 contains two small tubes: one bears the anteriormost body part of a specimen (the oral shield is visible) that lost some of its sclerites (**Figures 8A,B**); and the other has an incomplete animal (with its anterior body part missing, see detail in **Figure 8C**) which is the same illustrated in the original description of this species (compare **Figure 8C** with fig. 21 of Salvini-Plawen, 1972). The radula described by Salvini-Plawen (1972) was surely extracted from the latter individual, which was in turn designated as the lectotype by Boyko and Sage (1996). The other lot (AMNH 265348) contains a fragment of the trunk, presumably from the midgut region (the bristling

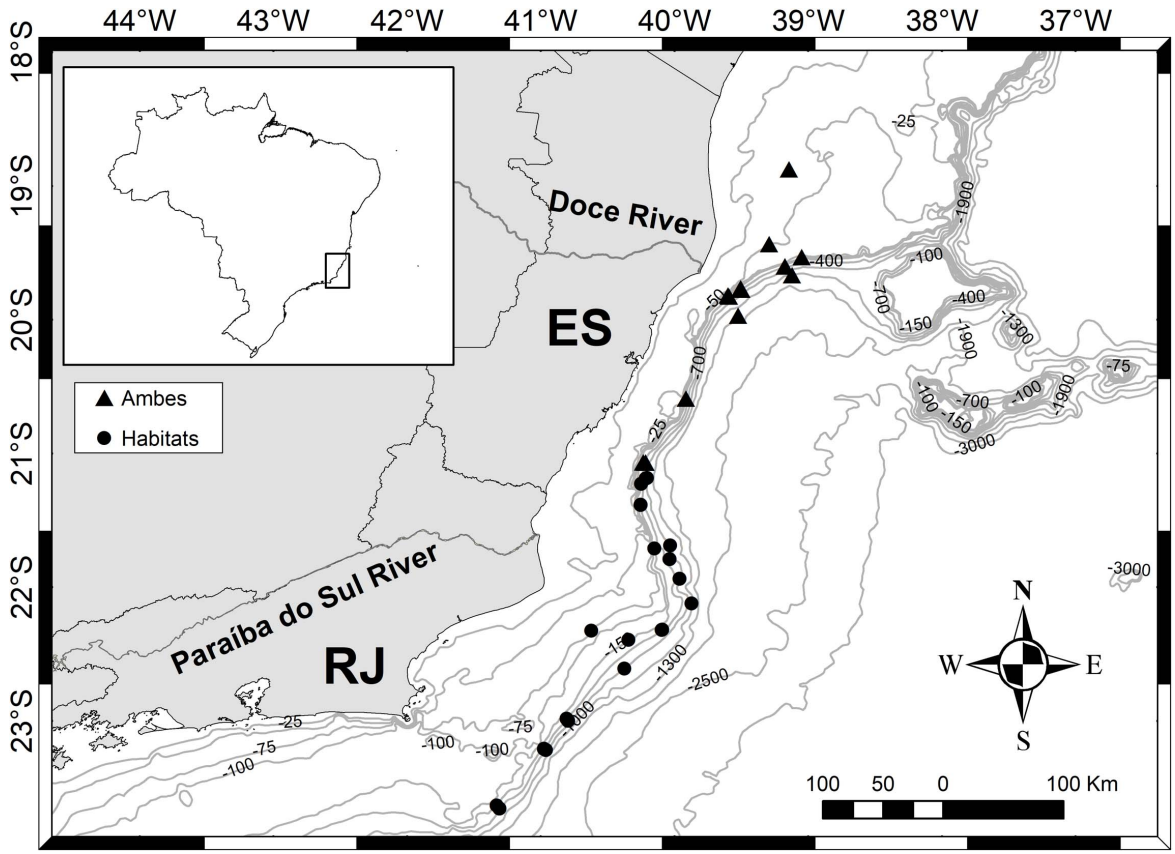

FIGURE 5 | *Scutopus variabilis* sp. nov. Sampling area of the "Habitats" (off Rio de Janeiro) and "Ambes" (off Espírito Santo) Projects showing the bathymetric distribution in the area of the Espírito Santo and Rio de Janeiro States.

sclerites are visible; **Figure 8D**) of one individual cited by Salvini-Plawen (1992) as a second examined sample collected in the same area of the Gulf of Darien, Caribbean Sea, at about 900 m depth, off Panama. Salvini-Plawen (1992) also referred to a third sample of *S. megaradulatus* which was obtained at 1861 meters depth off the western Cape coast, South Africa, but the place where it is deposited could not be tracked, and thus this single record of this species from the eastern Atlantic was not confirmed. Scheltema (1981) examined specimens of *S. megaradulatus* collected at 650 m depth off Cape Hatteras, and these compose the lot MCZ 396015.

Regarding *S. chilensis*, two lots deposited in the AMNH collection were examined, both with labels indicating that they were from the same sample collected in the Strait of Magellan, southern Chile, which was one of the three samples used by Salvini-Plawen (1972) for the description of this species; at that time, this sample contained two specimens and a type was not designated. Currently, the lot (AMNH 265349) has an individual which had its anterior and posterior parts dissected (**Figure 8E**), and it is not possible to affirm this is the same of the figure 26 of Salvini-Plawen (1972); the other (AMNH 265350) is a slide containing a hardly visible radula. They were designated by Boyko and Sage (1996) as the lectotype and paralectotype, respectively.

In the collection of the USNM, all the lots identified as *Scutopus* were analyzed, including the samples examined by Treece (1979) from the Gulf of Mexico, but they revealed to belong to species from other genera (*Psilodens*, for example). In South America, records of *Scutopus* spp. from Brazil were made by Rios (1994, as "*Scutopus* cf. *megaradulatus*"; and 2009, as "*Scutopus* sp. "), and from Uruguay by Forcelli and Narosky (2015, as "*Scutopus* sp."). However, the samples on which they were based could not be found, and so these records are doubtful.

DISCUSSION

Scutopus has been traditionally classified in the family Limifossoridae, along with other two genera, *Limifossor* Heath, 1904 and *Psilodens* Salvini-Plawen (1977), whose species have a characteristic multiseriate distichous radula; the inclusion of a fourth genus, *Metachaetoderma* Thiele, 1913, is debated and unsolved (Salvini-Plawen, 1969; Ivanov, 1981). In *Psilodens* and *Scutopus* the body is slender, sometimes bearing an annular constriction separating an anterior (formed by peribuccal plus foregut regions) from the median body part, while species of *Limifossor* have stouter bodies without externally visible divisions. Apart from this, the radula of *Psilodens* and *Scutopus*

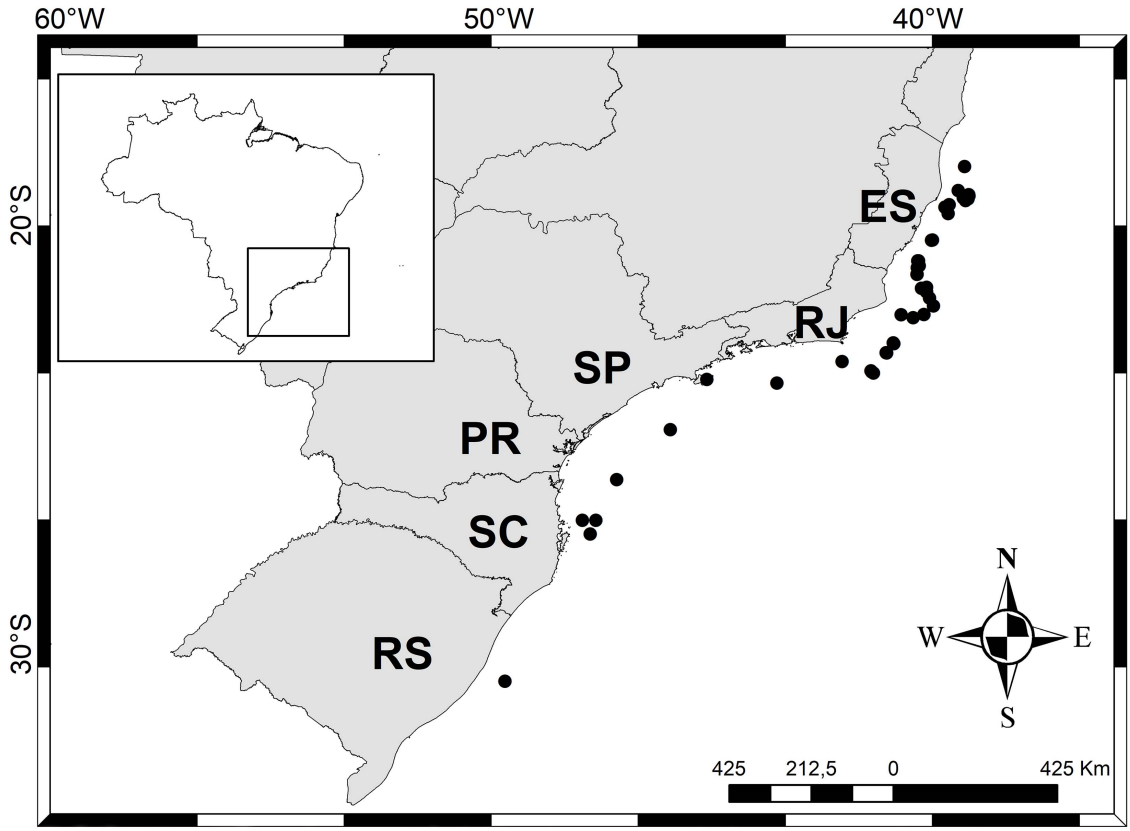

FIGURE 6 | *Scutopus variabilis* sp. nov. Distribution of this species along the States of the Southeastern and Southern Brazilian coasts.

is quite distinct from the one of *Limifossor*: in the former genera, each tooth is inwardly curved, like a sickle, the ones of *Scutopus* having a variable number of denticles distributed all along or in a part of the concave inner side of each tooth, while in *Psilodens* there are no denticles; in *Limifossor* each tooth consists of broad plates that bear a main lateral projection like a long hook-shaped stylet, and one or two small additional projections which form a jagged cutting inner edge (Salvini-Plawen, 1968, 1977, 1992; Ivanov, 1981; Scheltema, 1981). Differences among these genera also occur in the shape of the oral shield, that is undivided in species of *Scutopus* and bipartite in *Limifossor* and *Psilodens* (Salvini-Plawen, 1968, 1977, 1992; Ivanov, 1981; Scheltema, 1981). To date there are five species of *Limifossor* and three of *Psilodens*, and together with the seven species of *Scutopus* they characterize the Limifossoridae as the less diverse family among the caudofoveate aplacophorans; its other valid families, Chaetodermatidae Théel, 1875 and Prochaetodermatidae Salvini-Plawen (1972), have 85 and 39 described species, respectively.

As in other genera of Caudofoveata, the species of *Scutopus* are distinguished by external characters of the body morphology in conjunction with more detailed characteristics of the sclerites and radula (**Table 3**). Therefore, the presence of the midventral suture line, the size, shape, and sculpture of the sclerites from the different body regions, as well as the number and position of denticles in each radula tooth, have been the main characters for description of its species (**Table 3**). All of them have a long body shape, most presenting an anterior collar separating the anterior from the median body part. With many specimens available for the present study, it was possible to observe that the fixed specimens of *S. variabilis* sp. nov. exhibit a great variation in the form of the body caused by contractions of the musculature, being often contorted in different ways, narrowed and modified in its length:width proportions and in the relative sizes of the different body regions (specially the peribuccal, the foregut and the midgut regions). The anterior main collar is not visible in many specimens, this being particularly frequent in young individuals. For this reason, many animals can easily be confounded with other co-occurring caudofoveates, such as two undescribed species of *Psilodens* and *Falcidens*; in these cases, extraction of the sclerites is desirable for a more definite identification.

The midventral line is present in most species of *Scutopus* (Salvini-Plawen, 1968, 1972, 1975; Osorio, 1981; Saito and Salvini-Plawen, 2014), but was characterized as inconspicuous in *S. megaradulatus* (Salvini-Plawen, 1972), being absent only in *S. robustus* (Salvini-Plawen, 1970, 1972). Apart from this genus, the midventral line has been also recorded in *Falcidens sagittiferus* Salvini-Plawen (1968) (Ivanov et al., 2009) and in *Psilodens balduri* Mikkelsen and Todt (2014) (Mikkelsen and Todt, 2014),

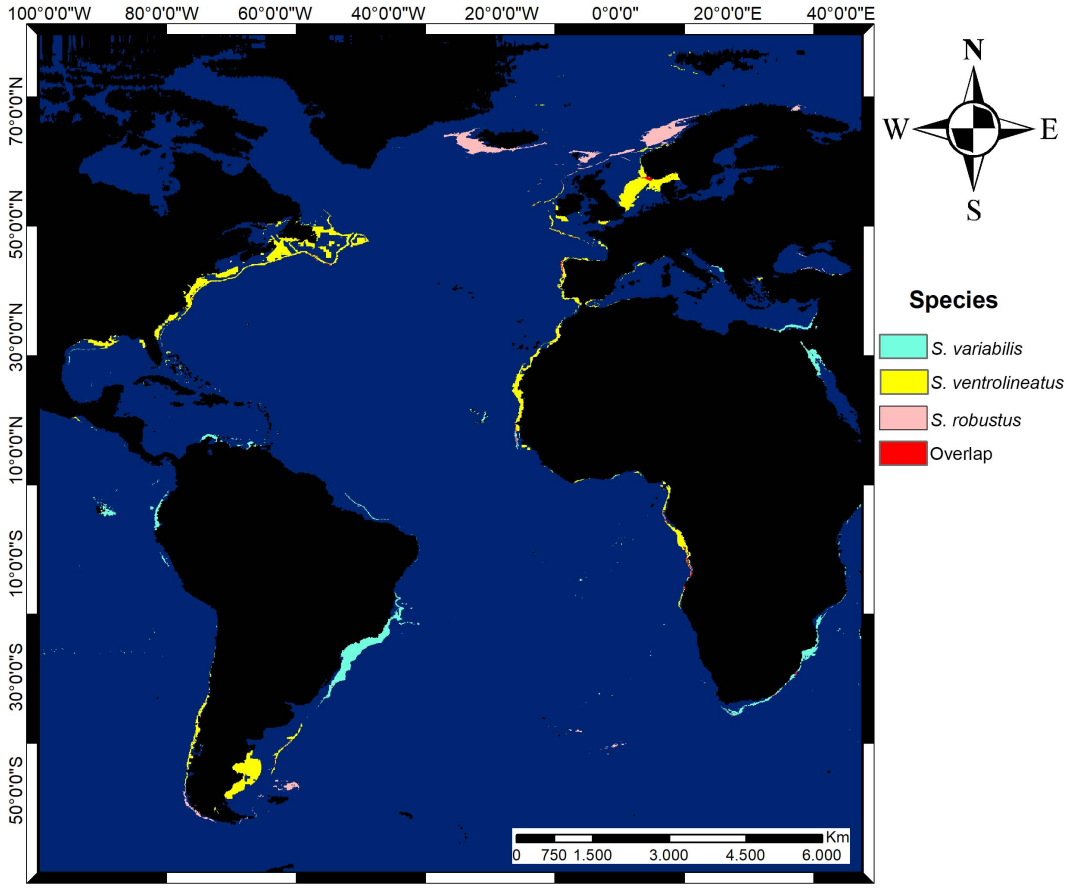

FIGURE 7 | Potential distribution map of suitable areas of *Scutopus* species in the Atlantic Ocean in thresholded format (10 percentile training presence). Overlapping areas of estimated species distribution are in red.

both on the anterior trunk, exhibiting characteristic adjacent sclerites, distinct in shape and size from the ones of the other body parts. In the Brazilian new species, the suture line is well visible in most specimens, especially by SEM, and has two types of adjacent sclerites, one with a wider base and longer blade that has almost parallel sides, and another which is narrower in the medial portion. This latter type was also observed in other species of *Scutopus*, such as *S. ventrolineatus*, *S. chilensis*, *S. schanderi,* and *S. hamatanii* (Salvini-Plawen, 1968, 1972; Saito and Salvini-Plawen, 2014), but not in *S. megaradulatus* (Salvini-Plawen, 1972).

In past times, SEM was a tool only for a general characterization in Caudofoveata (Scheltema, 1985, 1997; Scheltema et al., 1994), but more recently it has been used to furnish more complete descriptions (Schander et al., 2006; Ivanov et al., 2009; Mikkelsen and Todt, 2014; Saito, 2020), becoming a routine technique for the studies of the Brazilian species (Corrêa et al., 2014, 2018; Passos et al., 2018). In such way, apart from the general morphology of the animals, important characteristics of the oral shield, radula and sclerites can be observed. Regarding species of *Scutopus*, the sclerites are variable in form and size in the different body parts, there being dominant trunk sclerites which are important for the distinction of its species (**Figure 9**). Among them, *S. variabilis* sp. nov. is the first to have its sclerites described by SEM, with two dominant types observed in the median part: one elongated with lateral margins slightly concave in medial portion, and another longer, with narrower base. These are distinct from the ones of *S. megaradulatus*, in which they are slender and have parallel margins in the blade (Salvini-Plawen, 1972), and from the ones of *S. schanderi*, where they have an oar-blade shape (Saito and Salvini-Plawen, 2014). Some of the sclerites of *S. ventrolineatus*, *S. robustus*, *S. chilensis*, and *S. hamatanii* are like the ones of *S. variabilis* sp. nov., but in those species, there are dominant drop-shaped or lanceolate sclerites (Salvini-Plawen, 1968, 1972, 1975; Saito and Salvini-Plawen, 2014). The longitudinal sculpture of the sclerites appears to be also an important distinctive character: in *S. variabilis* sp. nov. the trunk sclerites have a main ridge and weak adjacent grooves in the blade, like in *S. megaradulatus* and *S. schanderi*, while in all other species there is only a main ridge, which appears to be more restricted to the distal end of the blade in *S. ventrolineatus*, *S. robustus*, and *S. chilensis*.

The present work also furnishes SEM images of the radula of a *Scutopus* species, a caudofoveate genus in which each species

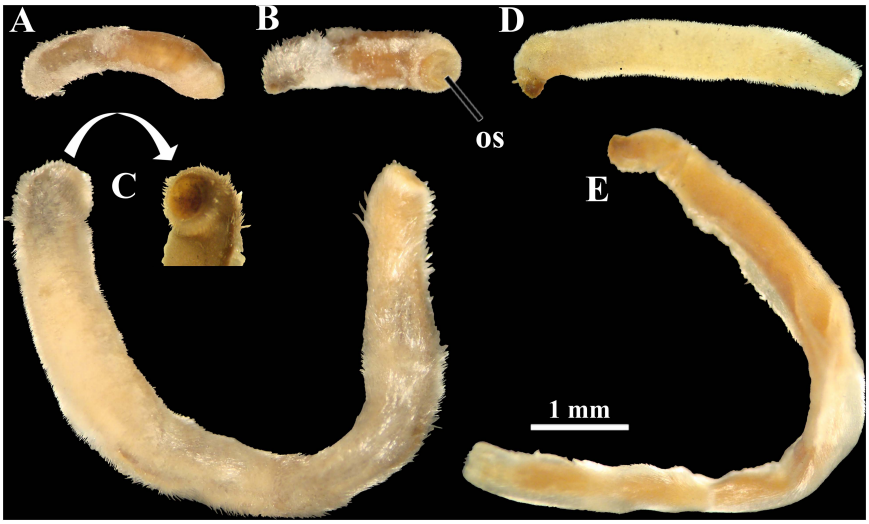

FIGURE 8 | Photomicrographs under stereomicroscope of examined lots of *Scutopus megaradulatus* **(A–D)** and *S. chilensis* (E). **(A–C)**, AMNH 265347: this lot contains two tubes, one with the anteriormost body part [**(A)**, **(B)**, in right lateral and ventral views, respectively; the oral shield is visible in **(B)**], and another with a dissected specimen **(C)** which has its anterior end missing (viewed in detail); note that this latter specimens is the same as the one illustrated by Salvini-Plawen (1972: fig. 21) (although he photographed it from the opposite left side). **(D)**, AMNH 265348, a fragment of the trunk (probably from the midgut region), shown from the left side. **(E)**, AMNH 265349, viewed from the left side. All in same scale. os - oral shield.

has a characteristic number of rows of radular teeth, which in turn are strengthened by different degrees of sclerotization and bear a number of median denticles (**Table 3**, **Figure 9**). In *S. variabilis* sp. nov., the radula is heavily sclerotized and has eight pairs of teeth, characters that are similar to *S. robustus*, *S. megaradulatus*, and *S. schanderi* (up to ten rows), and different from *S. ventrolineatus*, *S. chilensis*, and *S. hamatanii*, in which teeth are more numerous (more than 10 rows) and weakly sclerotized. The median denticles are more variable, but in those heavily sclerotized radulas they tend to occur in a higher number (12-22 denticles) and all along the inner margin of the teeth, while in the radulas with weak sclerotization the teeth bear a lower number of denticles (less than 11; except *S. chilensis*). In these latter cases, the denticles are proximally positioned, leaving a distal hook. Interestingly, these radular differences reflected in ecological characteristics found in species distribution modeling, as, excluding depth, *S. robustus* and *S. variabilis* sp. nov. were influenced by bottom temperature, while *S. ventrolineatus* were more influenced by silicate and primary productivity. These may reflect unknown interactions between the characteristics of the radula and the environment, like the advantage of one type of radula in one environment over another due to food availability, or perhaps one type of radula may be easier to produce in environments with higher concentration of silicate. Further studies are necessary to clarify if this radular and ecological variability may represent different genera.

Regarding the geographical and bathymetric distribution, patterns exhibited by the different species of *Scutopus* appear to be distinct among European and non-European representants, although clear and definite figures are probably blurred by sampling bias. *S. ventrolineatus* and *S. robustus* are well known from Scandinavia, Western Europe and the Mediterranean Sea (Salvini-Plawen, 1968, 1970, 1972, 1975, 1977; Ivanov and Scheltema, 2001, 2014; Mikkelsen and Todt, 2014; Señaris et al., 2017), and were also investigated in more detail in relation to aspects of their natural history (Salvini-Plawen, 1968), anatomy (Scheltema, 1981; Scheltema et al., 1994), larval morphology (Salvini-Plawen, 1990, 2003), and molecular biology (Osca et al., 2014; Mikkelsen et al., 2019). *Scutopus ventrolineatus* was recorded as abundant species in some places of the Nowergian Sea (Salvini-Plawen, 1975; Todt, 2013) and apart from European waters, it occurs in the Southwestern Indic Ocean (off Durban) (Salvini-Plawen, 1972), but its supposed distribution all along the eastern African coast has not been noticed. So, at least one of these European species (*S. ventrolineatus*) seems to be generally characterized as having wide geographical and bathymetric distributions.

The wide recorded distribution of *S. ventrolineatus* was reinforced by the species distribution modeling, through which suitable areas were found in the Western African coast, in Cape Verde, Guinea and Angola Basins. Although Prochaetodermatidae is well known from West Africa (Scheltema and Ivanov, 2000), records of limifossorids are still lacking for these areas and thus more surveys and studies are necessary to understand the real diversity of caudofoveates in this region. The suitability in North American coast and Gulf of Mexico for *S. ventrolineatus* deserves future investigations. These areas were extensively explored, *S. megaradulatus* was already recorded from North Carolina (Scheltema, 1981), but this species is morphologically related with other *Scutopus*, like *S. robustus* and *S. variabilis* sp. nov. In the Gulf of Mexico, the recorded limifossorids do not belong to *Scutopus*. The suitability found in Tierra del Fuego and Falklands for *S. ventrolineatus* and

TABLE 1 | *Scutopus variabilis* sp. nov. Paratype samples.

Catalog No.	State	Station	Collector	Coordinates	Depth (m)	Date	Content
ZUEC APL 278	RJ	HAB4-CANG7-R3(5-10)	Habitats	21°56′11.264″S, 39°57′43.702″W	712.6	28/v/08	1 spm
ZUEC APL 279	RJ	HAB6-A7-R1(2-5)	Habitats	23°39′20.061″S, 41°18′30.264″W	693.7	23/vi/08	4 spms + 1 slide with sclerites + 1 stub with 1 spm
ZUEC APL 280	RJ	HAB6-A7-R3(2-5)	Habitats	23°39′19.981″S, 41°18′30.534″W	732.9	25/vi/08	1 stub with 1 spm
ZUEC APL 281	RJ	HAB6-B7-R3(2-5)	Habitats	23°13′2.006″S, 40°57′36.765″W	724.6	28/vi/08	2 spms + 2 slides with sclerites
ZUEC APL 282	RJ	HAB6-B7-R3(5-10)	Habitats	23°13′2.006″S, 40°57′36.765″W	724.6	28/vi/08	1 spm + 1 slide with sclerites
ZUEC APL 283	RJ	HAB6-C7-R1(2-5)	Habitats	22°59′51.839″S, 40°47′42.838″W	710.1	29/vi/08	1 spm + 1 slide with sclerites
ZUEC APL 284	RJ	HAB6-C7-R1(5-10)	Habitats	2°59′51.839″S, 40°47′42.838″W	710.1	29/vi/08	1 stub with 6 radular teeth + 6 stubs with sclerites
ZUEC APL 285	RJ	HAB6-C7-R2(2-5)	Habitats	22°59′52.609″S, 40°47′45.008″W	689.4	30/vi/08	2 spms + 1 slide with sclerites + 1 slide with radula + 6 stubs with sclerites
ZUEC APL 286	RJ	HAB6-C7-R3(2-5)	Habitats	22°59′52.279″S, 40°47′45.398″W	686.1	01/vii/08	4 spms + 3 slides with sclerites
ZUEC APL 287	RJ	HAB6-CANAC7-R2(2-5)	Habitats	21°47′26.614″S, 40°2′13.765″W	752.5	06/vii/08	1 spm + 1 slide with sclerites
ZUEC APL 288	RJ	HAB6-D7-R2(2-5)	Habitats	22°36′27.325″S, 40°22′29.335″W	700	15/vii/08	1 spm
ZUEC APL 289	ES	HAB6-I7-R1(2-5)	Habitats	21°11′12.183″S, 40°12′52.020″W	693.9	17/vii/08	2 spms + 2 slides with sclerites
ZUEC APL 290	RJ	HAB7-C6-R1(5-10)	Habitats	22°59′1.179″S, 40°48′24.830″W	399.7	04/vii/08	1 spm
ZUEC APL 291	ES	HAB7-I7-R3(2-5)	Habitats	21°11′2.632″S, 40°12′18.218″W	792.4	05/vii/08	1 spm + 1 stub 1 pair and 8 radular teeth + 5 stubs with sclerites
ZUEC APL 292	RJ	HAB8-A7-R1(0-2)	Habitats	23°39′19.742″S, 41°18′28.369″W	699	28/i/09	2 spms
ZUEC APL 293	RJ	HAB8-A7-R2(2-5)	Habitats	23°39′20.559″S, 41°18′28.196″W	701	28/i/09	1 spm + 1 slide with sclerites
ZUEC APL 294	RJ	HAB8-B7-R2(2-5)	Habitats	23°13′2.799″S, 40°57′37.798″W	741.6	28/i/09	1 spm + 1 slide with sclerites
ZUEC APL 295	RJ	HAB8-C7-R2(0-2)	Habitats	22°59′53.839″S, 40°47′45.022″W	393.6	29/i/09	1 spm + 1 slide with sclerites
ZUEC APL 296	RJ	HAB9-CANG7-R3(2-5)	Habitats	21°56′12.105″S, 39°57′45.173″W	720	07/ii/09	1 spm + 1 slide with sclerites
ZUEC APL 297	RJ	HAB9-H7-R3(2-5)	Habitats	21°41′12.521″S, 40°1′56.515″W	702	06/ii/09	1 spm
ZUEC APL 298	ES	HAB9-I7-R3(0-2)	Habitats	21°11′12.228″S, 40°12′51.745″W	683	04/ii/09	1 stub with 1 spm
ZUEC APL 299	RJ	HAB13-I5-R3	Habitats	21°23′2.093″S, 40°15′9.173″W	145	06/iii/09	1 stub with 1 spm
ZUEC APL 300	RJ	HAB16-E5-R3	Habitats	22°23′39.088″S, 40°20′41.226″W	150	04/vii/09	1 spm + 1 slide with sclerites
ZUEC APL 301	RJ	HAB17-I5-R1	Habitats	21°23′3.544″S, 40°15′9.352″W	140	21/vii/09	1 stub with radula
ZUEC APL 302	ES	AMB3-CAND4-R3(0-10)	Ambes	19°31′51.66″S, 39°3′4.04″W	171	09/xii/11	1 spm + 1 slide with sclerites
ZUEC APL 303	ES	AMB5-A5-R1(2-5)	Ambes	21°4′9.61″S, 40°13′7.38″W	410	30/xii/11	4 spms + 4 slides with sclerites
ZUEC APL 304	ES	AMB6-CANWN4-R3(0-10)	Ambes	19°49′7.27″S, 39°36′8.52″W	158	14/i/12	3 spm + 3 slides with sclerites
ZUEC APL 305	ES	AMB6-CANWN5-R3(0-10/5-10)	Ambes	19°49′37.21″S, 39°35′41.25″W	410	14/i/12	1 spm + 1 slide with sclerites
ZUEC APL 306	ES	AMB6-D4-R1(0-10)	Ambes	19°45′55.39″S, 39°30′25.74″W	149	15/i/12	7 spms + 7 slides with sclerites + 1 stub with 1 spm
ZUEC APL 307	ES	AMB6-D4-R3(0-2)	Ambes	19°45′55.39″S, 39°30′25.74″W	149	15/i/12	12 spms + 12 slides with sclerites
ZUEC APL 308	ES	AMB6-D4-R3(2-5)	Ambes	19°45′55.39″S, 39°30′25.74″W	149	15/i/12	5 spms + 5 slides with sclerites
ZUEC APL 309	ES	AMB6-E4-R3(0-2)	Ambes	19°36′5.17″S, 39°10′32.93″W	153	24/i/12	1 spm
ZUEC APL 310	ES	AMB7-B4-R2	Ambes	20°35′25.16″S, 39°54′58.31″W	157	21/i/12	1 spm
ZUEC APL 311	ES	AMB7-D4-R2	Ambes	19°45′54.56″S, 39°30′25.23″W	144	15/i/12	5 spms + 5 slides with sclerites

(Continued)

TABLE 1 | Continued

Catalog No.	State	Station	Collector	Coordinates	Depth (m)	Date	Content
ZUEC APL 312	ES	AMB7-E4-R1	Ambes	19°36′4.32″S, 39°10′34.07″W	147	15/i/12	1 spm + 2 slides with with sclerites + 1 stub with 1 spm
ZUEC APL 313	ES	AMB7-E4-R2	Ambes	19°36′4.32″S, 39°10′34.07″W	147	15/i/12	1 spm + 2 slides with with sclerites + 1 stub with 1 spm
ZUEC APL 314	ES	AMB7-E4-R3	Ambes	19°36′4.32″S, 39°10′34.07″W	147	15/i/12	1 stub with 1 spm
ZUEC APL 315	ES	AMB7-F2-R3	Ambes	18°52′32.61″S, 39°8′42.82″W	40	18/i/12	1 spm
ZUEC APL 316	ES	AMB11-A5-R1(0-2/2-5)	Ambes	21°4′4.67″S, 40°13′6.06″W	415	08/vi/13	3 spm + 3 slides with sclerites + 1 stub with 1 spm
ZUEC APL 317	ES	AMB12-CAND4-R2(0-10)	Ambes	19°31′51.68″S, 39°3′4.79″W	171	29/vi/13	4 spms + 5 slides with sclerites
ZUEC APL 318	ES	AMB12-CANWN4-R2(0-2)	Ambes	19°49′6.26″S, 39°36′9.34″W	181	29/vi/13	11 spms + 11 slides with sclerites
ZUEC APL 319	ES	AMB12-D4-R1(5-10)	Ambes	19°45′53.43″S, 39°30′25.97″W	143	27/vi/13	1 spm + 2 slides with sclerites + 1 stub with radula
ZUEC APL 320	ES	AMB12-D4-R3(2-5)	Ambes	19°45′53.43″S, 39°30′25.97″W	143	27/vi/13	1 spm + 2 slides with sclerites
ZUEC APL 321	ES	AMB12-E4-R2	Ambes	19°36′3.57″S, 39°10′33.64″W	143	29/vi/13	1 slide with sclerites + 1 stub with 1 spm
ZUEC APL 322	ES	AMB14-A4-R3	Ambes	21°4′4.56″S, 40°14′14.08″W	141	11/vii/13	1 spm + 1 slide with sclerites + 1 slide with radula
MZSP 38414	SP	Sta. 6665	Revizee	25°26.88′S, 46°38.85′W	80	16/xii/97	1 spm + 1 slide with sclerites
MZSP 38416	SP	Sta. 6657	Revizee	25°17.30′S, 46°55.60′W	60	09/ii/98	3 spm
MZSP 38447	RJ	MBT 219	MBT	23°25′00′′ S, 42°00′00′′W	100	06/vi/71	2 spm + 1 slide with sclerites
MZSP 38451	RJ	MBT 204	MBT	23°55′00′′S, 43°31′00′′W	125	03/vi/71	4 spm + 1 slide with sclerites
MZSP 84438	SP	Sta. 344	Projeto Integrado	23°34′S, 44°43′W	No depth	No date	1 spm + 1 slide with sclerites
MZSP 137395	SP	Sta. 13 – PI	Projeto Integrado	23°50′00′′S, 45°09′00′′W	38	21/i/86	1 spm + 1 slide with sclerites
MZSP 137411	PR	Sta. 6789	Revizee	27°45′12.5′′S, 48°3′00′′W	95	15/iii/98	1 spm + 1 slide with sclerites
MZSP 137414	PR	Sta. 6780	Revizee	27°7′00′′S, 47°44′12.5′′W	102	13/iii/98	1 spm + 1 slide with sclerites
MZSP 137416	PR	Sta. 6788	Revizee	27°26′00′′S, 47°52′00′′W	110	15/iii/98	3 spm + 1 slide with sclerites
MZSP 143012	RS	MBT 139	MBT	30°52′00′′S, 49°51′00′′W	126	27/vi/70	1 spm + 1 slide with sclerites
MZSP 154097	RJ	HAB8-A8-R1(2-5)	Habitats	23°41′7.814″S, 41°16′4.710″W	1017.9	12/i/09	1 spm + 1 slide with sclerites
MZSP 154098	ES	HAB9-I7-R2(2-5)	Habitats	21°11′12,073″S, 40°12′52,126″W	680	04/ii/09	2 spm + 2 slides with sclerites
MZSP 154099	ES	HAB9 I7 R3 2-5	Habitats	21°11′12.228″S, 40°12′51.745″W	683	04/ii/09	4 spms + 4 slides with sclerites
MZSP 154100	ES	AMB7-A4-R1	Ambes	21°4′4.76″S, 40°14′14.14″W	153	23/i/12	7 spms + 7 slides with sclerites
MZSP 154101	ES	AMB7-A4-R2	Ambes	21°4′4.76″S, 40°14′14.14″W	153	23/i/12	8 spms + 8 slides with sclerites
MZSP 154102	ES	AMB7-D4-R3	Ambes	19°45′54.56″S, 39°30′25.23″W	144	15/i/12	3 spms + 3 slides with sclerites
MZSP 154103	ES	AMB11-B5-R1(0-10)	Ambes	20°35′15.33″S, 39°53′45.22″W	415	18/vi/13	3 spms + 3 slides with sclerites
MNRJ 23636	RJ	HAB4-CANG7-R2(0-2)	Habitats	21°56′10.244″S, 39°57′43.438″W	709.7	28/v/08	2 spms + 2 slides with sclerites
MNRJ 23637	RJ	HAB8-C6-R3(2-5)	Habitats	22°59′0.677″S, 40°48′28.837″W	376.6	31/i/09	2 spms + 2 slides with sclerites
MNRJ 23638	ES	HAB9-I7-R1(2-5)	Habitats	21°11′12.170″S, 40°12′51.838″W	682	04/ii/09	5 spms + 5 slides with sclerites
MNRJ 23639	RJ	HAB16-H4-R1	Habitats	21°42′53.895″S, 40°10′14.920″W	97	07/vii/09	3 spms + 3 slides with sclerites
MNRJ 23640	ES	AMB7-D4-R1	Ambes	19°45′54.56″S, 39°30′25.23″W	144	15/i/12	6 spms + 6 slides with sclerites
MNRJ 23641	ES	AMB12-CAND6-R2(0-10)	Ambes	19°37′45.14″S, 39°3′58.75″W	1050	25/vi/13	4 spms + 4 slides with sclerites
CZUFS APL 11	ES	AMB3-CAND4-R2(0-10)	Ambes	19°31′51.66″S, 39°3′4.04″W	171	09/xii/11	5 spms + 5 slides with sclerites
CZUFS APL 12	ES	AMB6-E4-R3(2-5)	Ambes	19°36′5.17″S, 39°10′32.93″W	153	24/i/12	2 spms + 2 slides with sclerites
CZUFS APL 13	ES	AMB12-E4-R1(2-5)	Ambes	19°36′3.57″S, 39°10′33.64″W	143	29/vi/13	2 spms + 2 slides with sclerites

TABLE 2 | Percentage of contribution of environmental layers in the species distribution modeling for each species.

Variable	*S. robustus*	*S. ventrolineatus*	*S. variabilis* sp. nov.
Depth	47.3	48.3	42.2
Bottom temperature	30.8	1.7	38.7
Silicates	11.1	23.9	8.6
Slope	4.1	6.4	6.8
Primary productivity	6.8	19.6	3.7

S. robustus sounds to be unlikely for both species, as it is a region very far from European waters, where these species are recorded. Besides this, these areas of the Southern Hemisphere are still unknown regarding their diversity of caudofoveates, and future exploration may clarify if a sister species is found there.

Outside European waters, all other species of *Scutopus* have been reported upon by only a few studies. In the Americas, *S. megaradulatus* is known from the Caribbean, where it was originally described (Salvini-Plawen, 1972), and from samples from North Carolina identified by Scheltema (1981). Its occurrence from off Cape coast, South Africa (Salvini-Plawen, 1992) is presumably doubtful, and the fact that this species has an amphiatlantic distribution must be confirmed. The record of *S. megaradulatus* from Brazil (Rios, 1994) should definitely be discharged. In the Pacific Ocean, *S. chilensis* appears to be restricted to Chile (Salvini-Plawen, 1972; Osorio, 1981), and *S. hamatanii* and *S. schanderi* were only recorded from the Sea of Japan (Saito and Salvini-Plawen, 2014). Accordingly, *S. variabilis* sp. nov. is probably a species of restricted distribution, occurring in the shelf and the upper continental slope of the Brazilian southeastern and southern coasts; the great effort of collection was, however, restricted to this area and so its occurrence further to the north, in the northeast and north of Brazil, and in the south (Uruguay and Argentina) deserves future investigations.

The potential distribution modeling showed that the main suitable areas of *S. variabilis* sp. nov. are the Brazilian Southeastern and Southern coasts, followed by some hotspots of suitability in the Southern Caribbean Sea and Brazilian Northern coast in the Western Atlantic, mainly explained by depth and temperature. Regarding the diversity of caudofoveates, the Caribbean Sea is only known by the few and punctual records of two species (Salvini-Plawen, 1972, 1992). Although it has a tropical climate and usually very narrow continental shelves, the Caribbean Sea has hundreds of islands that create suitable areas for species with the characteristics of *S. variabilis* sp. nov. Considering that *S, megaradulatus* is already recorded from this region, the hotpots in the Caribbean Sea for *S. variabilis* sp. nov. are expected and should indicate that these are sister species which live in similar environmental conditions. The suitable areas found in the Brazilian Northern coast can be explained by the enlargement of the shelf close to the Amazon River mouth, creating suitable conditions for stablishing a viable population of a species of *Scutopus*. This area is still almost unknown regarding to its deep-sea benthic fauna. Thus, more investigations are necessary to verify if there is an isolated population of *S. variabilis* sp. nov. or a new species in the area. Outside the Western Atlantic, the suitability found in the Mediterranean sounds an unlikely occurrence area, but more investigations are required to prospect possible occurrences of *S. variabilis* sp. nov. in the islands of Angola and Cape Verde basins, where no limifossorids were described so far.

The Gulf of Mexico and the Brazilian Northeastern coast were found as unsuitable areas for *S. variabilis* sp. nov. In the Gulf of Mexico, the unsuitability reinforced our results of not finding a *Scutopus* species in museum collections from this area. Although the Gulf has shelf areas similar to those of the Brazilian Southeastern and Southern coasts, the existence of warmer waters in the Gulf can prevents the occurrence of suitable areas for *S. variabilis* sp. nov. Ivanov and Scheltema (2008) characterized as similar the patterns of diversity of Prochaetodermatidae from the Gulf of Mexico (7 species, 2 endemic) and the Mediterranean Sea (4 species, 1 endemic). This similarity in Prochaetodermatidae contrasts with the different pattern of *Scutopus* for both regions. For the Brazilian Northeastern coast, through previous analysis of material from this region any *Scutopus* species were found (Miranda and Passos, pers. obs.), observation that was reinforced by modeling. This non-occurrence can be explained by the tropical climate and narrow shelf characteristic of this region, which acts like a barrier that create unsuitable areas for the occurrence of *S. variabilis* sp. nov.

By modeling, very few and small potential overlapping areas were found, even among the European species, which in some cases were already recorded from the same geographical areas (Salvini-Plawen, 1975). In the European Atlantic, *S. robustus* tends to occur in the Northern areas like Iceland, Scotland and Northern Norway, whereas *S. ventrolineatus* mainly occurs in southern areas, between southern Norway, south of England and Bay of Biscay, with few and small overlaps in Northern Iberian Peninsula and South of Norway, as an effect of differential influences of environmental variables in both species. In relation with *S. ventrolineatus* and *S. variabilis* sp. nov., exceedingly small potential overlaps were found in islands of Cape Verde and Angola Basins. This suggests that competition for space and resources are reduced by occurrences of different species of *Scutopus* in distinct regions.

Deep-sea organisms are hard to access, as their collections are less common, the environment is less accessible, the logistics is expensive, and in many cases, species are encountered in low specimen numbers. Moreover, many cruise collections protocols still use formalin to preserve specimens, making the use of molecular techniques problematic. However, these problems have been minimized, as the number of samples of deep-sea organisms are growing in museum collections due to increasing studies required for exploitation of fisheries, oil, gas and mining, although specialists for these groups are still scarce. This is the case of Brazil, in which a great amount of useful data for taxonomy and biogeography have been available through the analysis of extensive collections, as those

TABLE 3 | Summary data of main diagnostics characters, geographical and bathymetric distribution data of all *Scutopus* species described.

Species	Radula Sclerotization	Number of radular teeth rows	Number of median denticles of the radular teeth	Suture line	Bathymetry (m)	Distribution	References
S. chilensis	Weakly sclerotized	11 – 18	18 – 20	Present	263 – 642	Southeastern Pacific Ocean: Chile (from Valparaiso to Strait of Magellan)	Salvini-Plawen (1972, 1992); Osorio (1981); Linse (1999)
S. hamatanii	Sclerotized (except the 2 posteriormost pairs)	12	8 – 9	Present	51 – 105	Northwestern Pacific Ocean: Sea of Japan	Saito and Salvini-Plawen (2014)
S. megaradulatus	Heavily Sclerotized (except for the last posteriomost pair)	7	16 – 18	Inconspicuous	40 – 1300 (1861?)*	Northwestern Atlantic Ocean: North America, United States (North Carolina); Central America, Panama, Gulf of Darien	Salvini-Plawen (1972; 1992*); Scheltema (1981); Rios (1994**, 2009**); Forcelli and Narosky (2015***)
S. robustus	Heavily sclerotized (except the 1-3 posteriormost pairs)	6 – 10	20 – 22	Absent	50 – 800 (3542?) *	Northeastern Atlantic Ocean: Norway, England, Iceland, and Mediterranean	Salvini-Plawen (1970, 1972, 1975, 1977*, 1997); Salvini-Plawen and Warén (1972); Scheltema (1981); Ivanov and Scheltema (2001)****; Ivanov and Scheltema (2014); Mikkelsen and Todt (2014); Señaris et al. (2017)
S. schanderi	Heavily sclerotized (except the 2 posteriormost pairs)	8	16 – 18	Present	69 – 102	Northwestern Pacific Ocean: Sea of Japan	Saito and Salvini-Plawen (2014)
S. ventrolineatus	Weakly sclerotized (limited to the 2-4 anterior pairs)	10 – 16	9 – 11	Present	40 – 1248	Atlantic Ocean: Scandinavia (Western Sweden, Norway), Western Scotland, Irish Sea, Bay of Biscay and Mediterranean. Southwestern Indian Ocean: off Durban, South Africa,	Salvini-Plawen (1968, 1970, 1972, 1975, 1997), Osca et al. (2014)
Scutopus variabilis sp. nov.	Heavily sclerotized (except the 2 posteriormost pairs)	8	12 – 16	Present	40 – 1300	Southwestern Atlantic Ocean, Brazil, South and Southeastern coast	This study

** Salvini-Plawen (1992, tab. 1) cites the occurrence of S. megaradulatus in a coordinate of western Cape of Africa at 1861 m depth with 2 individuals of Falcidens non-targatus, but did not illustrate the material and said that its geographical distribution is complemented in his paper. This material was not deposited in any museum, thus we did not consider this record as valid.*

*** Rios (1994, 2009) cites the occurrence of Scutopus cf. megaradulatus and Scutopus sp. for Rios de Janeiro Coast in his Seashells catalogs, but did not furnish any bibliographical reference or material deposited in any museum, thus we did not consider this record as valid.*

**** Forcelli and Narosky (2015) cite the occurrence of Scutopus sp. deposited in the "Museo Argentino de Ciencias Naturales 'Bernardino Rivadavia" (Buenos Aires, Argentina), but this record was not confirmed in that institution (Alejandro Tablado, pers. commun.).*

***** Salvini-Plawen (1977) recorded S. robustus from the Mediterranen Sea at 2415, 2917, and 3540 m depth, but these were considered doubtful by Ivanov and Scheltema (2001).*

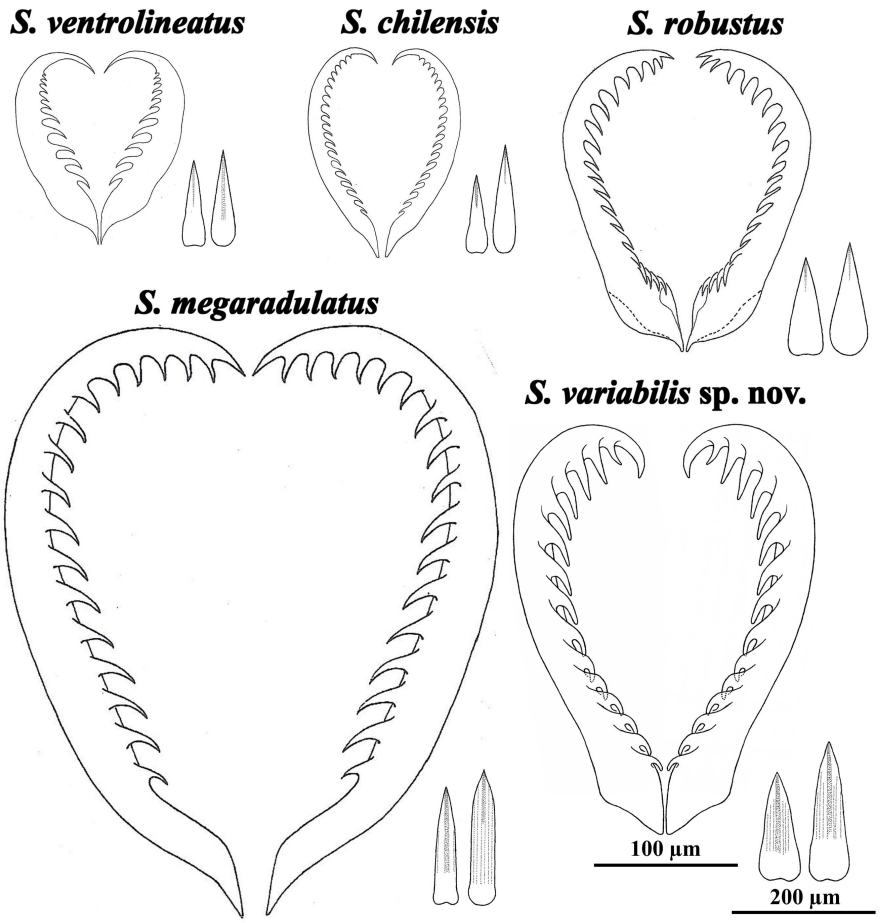

FIGURE 9 | Radula (in same scale) and trunk sclerites (idem) of *Scutopus* species, obtained from different sources: Salvini-Plawen (1970): figs. 1 (radula) and 3(i, l) (sclerites) of *S. ventrolineatus*, figs. 2 (radula) and 4(e, g) (sclerites) of *S. robustus*; Salvini-Plawen (1972): figs. 22 (radula) and 24(g, h) of *S. megaradulatus*, figs. 27 (radula) and 23(m, p) (sclerites) of *S. chilensis*. The radula of *S. variabilis* sp. nov. was drawn based on the **Figure 4**; its sclerites were based on the first illustrated in row (E) and the last of row (G) of **Figure 3**. The radula and sclerites of the Pacific *S. schanderi* and *S. hamatanii* were illustrated by Saito and Salvini-Plawen (2014).

made by the "Habitats" and "Ambes" projects. With these and in association with examination of other museums samples, a species distribution modeling was performed, this being a quantitative technique that started to be used only recently for deep-sea organisms (e.g., Basher and Costello, 2016; Schnurr et al., 2018; Bowden et al., 2021); it is used here for the first time for aplacophoran molluscs.

As it occurs with other deep-water animals, Aplacophora is a clear example of lesser-known group. However, especially in the last decade, this scenario is rapidly changing (Todt, 2013; Passos et al., 2019). Some techniques, like SEM and birefringence microscopy, particularly important for the study of these animals, are becoming more accessible (e.g., Corrêa et al., 2014, 2018; Mikkelsen and Todt, 2014; Passos et al., 2018; Saito, 2020), making the descriptions more detailed; moreover, previous molecular obstacles have been surpassed (e.g., Kocot et al., 2011; Mikkelsen et al., 2018, 2019; Bergmeier et al., 2021). Museum collections are increasingly with materials coming from new unexplored areas like the South Atlantic, allowing studies by recent biogeographical and ecological techniques, like species distribution modeling. In the specific literature on aplacophorans, there are some citations of undescribed species of *Scutopus*, for example, from off California and Oregon, United States (Barwick and Cadien, 2005; Mikkelsen et al., 2019), and Chile (Linse, 1999), and in fact there are large areas of the Pacific and Indian Oceans which are still very poorly sampled. As a part of a larger project that has been performed on the molluscan diversity of the Brazilian coast, in comparison with other Atlantic species (Corrêa et al., 2014, 2018; Passos et al., 2018, 2019; Miranda et al., 2020), this study gives a little step toward a better knowledge of these animals from the deep-sea of the Southern Hemisphere.

DATA AVAILABILITY STATEMENT

The original contributions presented in the study are included in the article/**Supplementary Material**, further inquiries can be directed to the corresponding author.

AUTHOR CONTRIBUTIONS

FP designed the study and prepared the text. PC conducted the morphological analysis, species distribution modeling, and made a critical review of the final version of the manuscript. MM designed the study, conducted the morphological analysis, species distribution modeling, and prepared the text. All authors contributed to the article and approved the submitted version.

FUNDING

This work was supported by the Centro de Pesquisas Leopoldo Américo Miguez de Mello (CENPES/Petrobras), Fundação de Amparo à Pesquisa do Estado de São Paulo (FAPESP) (grants numbers 2011/502917-4, 2018/06347-6, and 2018/10313-0), and Fundo de Apoio ao Ensino, à Pesquisa e à Extensão (FAEPEX) (grant number 362/2012) for FP. Scholarships were furnished for MM and PC by Capes and FAPESP (grants number 2017/01081-5 and 2018/17718-5).

ACKNOWLEDGMENTS

Thanks are due to AP Falcão, who invited FP to participate as a taxonomist of the "Habitats" and "Ambes" Project; ACS Sprogis and SMF Ferraz (Laboratório de Microscocopia Eletrônica – IB/UNICAMP), who helped in the techniques of microscopy; and LRL Simone, EE Strong, and AJ Baldinger for their kind reception of MM in the MZSP, USNM, and MCZ, respectively; NC Barrera (Texas A&M University) is also acknowledged for kindly commenting on the aplacophorans from the Gulf of Mexico. We also thank the editors Stephanie Kaiser and Kevin Kocot, and four reviewers for their useful comments that improved the final version of this manuscript.

SUPPLEMENTARY MATERIAL

The Supplementary Material for this article can be found online at: https://www.frontiersin.org/articles/10.3389/fmars.2021.669478/full#supplementary-material

REFERENCES

Barwick, K., and Cadien, D. (2005). Aplacophore Mollusks of the 2003 Regional Monitoring Survey of the Southern California Bight. *SCAMIT Suppl.* 23:66.

Basher, Z., Bowden, D. A., and Costello, M. J. (2018). *Global Marine Environment Datasets (GMED). World Wide Web electronic publication. Version 2.0 (Rev.02.2018)*. Available online at: http://gmed.auckland.ac.nz on (Accessed June 23, 2021)

Basher, Z., and Costello, M. J. (2016). The past, present and future distribution of a deep-sea shrimp in the Southern Ocean. *PeerJ.* 4:e1713. doi: 10.7717/peerj.1713

Bergmeier, F. S., Brandt, A., Schwabe, E., and Jörger, K. M. (2017). Abyssal Solenogastres (Mollusca, Aplacophora) from the Northwest Pacific: scratching the Surface of Deep-Sea Diversity Using Integrative Taxonomy. *Front. Mar. Sci.* 4:410. doi: 10.3389/fmars.2017.00410

Bergmeier, F. S., Haszprunar, G., Brandt, A., Saito, H., Kano, Y., and Jörger, K. M. (2019). Of basins, plains and trenches: systematics and distribution of Solenogastres (Mollusca, Aplacophora) in the Northwest Pacific. *Prog. Oceanogr.* 178:102187. doi: 10.1016/j.pocean.2019.102187

Bergmeier, F. S., Ostemair, L., and Jörger, K. M. (2021). Specialized predation by deepsea Solenogastres revealed by sequencing of gut contents. *Curr. Biol.* 31, R836–R837. doi: 10.1016/j.cub.2021.05.031

Bowden, D. A., Anderson, O. F., Rowden, A. A., Stephenson, F., and Cark, M. R. (2021). Assessing Habitat Suitability Models for the Deep Sea: is Our Ability to Predict the Distributions of Seafloor Fauna Improving? *Front. Mar. Sci.* 8:632389. doi: 10.3389/fmars.2021.632389

Boyko, C. B., and Sage, W. E. III (1996). Catalog of recent type specimens in the Department of Invertebrates, American Museum of Natural History. II. Mollusca Part 1 (Classes Aplacophora, Polyplacophora, Gastropoda [Subclass Opisthobranchia], Bivalvia, and Scaphopoda). *Am. Mus. Novit.* 3170, 1–50. doi: 10.1206/0003-0090(2001)262<0001:cortsi>2.0.co;2

Cobo, M. C., and Kocot, K. M. (2020). *Micromenia amphiatlantica* sp. nov.: first solenogaster (Mollusca, Aplacophora) with an amphi-Atlantic distribution and insight into abyssal solenogaster diversity. *Deep Sea Res. 1 Oceanogr. Res. Pap.* 157:103189. doi: 10.1016/j.dsr.2019.103189

Corrêa, P. V. F., Fassina, P. V., and Passos, F. D. (2014). *Falcidens targatus* and *F. acutargatus*: two species of Caudofoveata (Mollusca, Aplacophora) new for Brazil. *J. Nat. Hist.* 48, 2947–2963. doi: 10.1080/00222933.2014.959575

Corrêa, P. V. F., Miranda, M. S., and Passos, F. D. (2018). South America-Africa missing links revealed by the taxonomy of deep-sea molluscs: examples from prochaetodermatid aplacophorans. *Deep Sea Res. 1 Oceanogr. Res. Pap.* 132, 16–28. doi: 10.1016/j.dsr.2017.12.008

Forcelli, D. O., and Narosky, T. (2015). *Uruguayan Seashells – Moluscos Marinos – Argentina, Uruguay and Brazil*. Buenos Aires: Marquez Martini.

Ivanov, D. L. (1981). *Caudofoveatus tetradens* gen. *et* sp. n. and diagnosis of taxa in the subclass Caudofoveata (Mollusca, Aplacophora). *Zool. Zh.* 60, 18–28.

Ivanov, D. L., Mikkelsen, N. T., and Schander, C. (2009). *Falcidens sagittiferus* Salvini-Plawen, 1968: additional data on morphology and distribution (Mollusca. Aplacophora, Caudofoveata). *Fauna Norv.* 29, 3–9. doi: 10.5324/fn.v29i0.610

Ivanov, D. L., and Scheltema, A. H. (2001). Distribution of known caudofovetate species (Mollusca. Aplacophora) around Iceland. *Ruthenica.* 11, 1–6. doi: 10.1080/00364827.1989.10413419

Ivanov, D. L., and Scheltema, A. H. (2008). Western Atlantic Prochaetodermatidae from 35°N to the Argentine Basin including the Gulf of Mexico. *Zootaxa* 1885, 1–60. doi: 10.11646/zootaxa.1885.1.1

Ivanov, D. L., and Scheltema, A. H. (2014). Deep-sea fauna of European seas: an annotated species check-list of benthic invertebrates living deeper than 2000 m in the seas bordering Europe. *Aplacophora. Invert. Zool.* 11, 8–12.

Kocot, K. M., Cannon, J. T., Todt, C., Citarella, M. R., Koln, A. B., Meyer, A., et al. (2011). Phylogenomics reveals deep molluscan relationships. *Nature* 477, 452–456. doi: 10.1038/nature10382

Linse, K. (1999). Mollusca of the Magellan region. A checklist of the species and their distribution. *Sci. Mar.* 63, 399–407. doi: 10.3989/scimar.1999.63s1399

Machado, F. M., and Passos, F. D. (2016). Spheniopsidae Gardner, 1928 (Bivalvia): conchological characters of two new species from off Brazil, southwestern Atlantic. *Am. Malac. Bull.* 33, 212–220. doi: 10.4003/006.033.0207

Mikkelsen, N. T., Kocot, K. M., and Halanych, K. M. (2018). Mitogenomics reveals phylogenetic relationships of caudofoveate aplacophoran molluscs. *Mol. Phylogenet. Evol.* 127, 429–436. doi: 10.1016/j.ympev.2018.04.031

Mikkelsen, N. T., and Todt, C. (2014). Diversity of Caudofoveata (Mollusca) around Iceland and description of *Psilodens balduri* sp. n. Pol. *Polar Res.* 35, 279–290. doi: 10.2478/popore-2014-0014

Mikkelsen, N. T., Todt, C., Kocot, K. M., Halanych, K. M., and Willasen, E. (2019). Molecular phylogeny of Caudofoveata (Mollusca) challenges traditional views. *Mol. Phylogenet. Evol.* 132, 138–150. doi: 10.1016/j.ympev.2018.10.037

Miranda, M. S., Strong, E. E., and Passos, F. D. (2020). Type specimens of Caudofoveata (Mollusca, Aplacophora) in the molluscan collections of the National Museum of Natural History, Smithsonian Institution, and of the Museum of Comparative Zoology, Harvard University. *Zootaxa* 4895, 581–593. doi: 10.11646/zootaxa.4895.4.8

Morueta-Holme, N., Fløjgaard, C., and Svenning, J. C. (2010). Climate change risks and conservation implications for a threatened small-range mammal species. *PLoS One* 5:e10360. doi: 10.1371/journal.pone.0010360

Osca, D., Irisarri, I., Todt, C., Grande, C., and Zardoya, R. (2014). The complete mitochondrial genome of *Scutopus ventrolineatus* (Mollusca: Chaetodermomorpha) supports the Aculifera hypothesis. *BMC Evol. Biol.* 14:197. doi: 10.1186/s12862-014-0197-9

Osorio, C. (1981). Caudofoveata y Solenogastra de Chile. *Bol. Soc. Biol. Concepc.* 52, 115–128.

Passos, F. D., Corrêa, P. V. F., and Todt, C. (2018). A new species of *Falcidens* (Mollusca, Aplacophora, Caudofoveata) from the southeastern Brazilian coast: external anatomy, distribution, and comparison with *Falcidens caudatus* (Heath, 1918) from the USA. *Mar. Biodivers.* 48, 1135–1146. doi: 10.1007/s12526-016-0559-1

Passos, F. D., and Machado, F. M. (2014). A New Species of *Cyamiocardium* Soot-Ryen, 1951 from Shallow Waters off Brazil, with a Discussion on the Anatomical Characters of the Cyamiidae (Bivalvia: Cyamioidea). *Am. Malac. Bull.* 32, 122–131. doi: 10.4003/006.032.0110

Passos, F. D., Miranda, M. S., and Corrêa, P. V. F. (2019). Synopsis of the knowledge on the Brazilian aplacophorans (Mollusca: Caudofoveata and Solenogastres). *Biota Neotrop.* 19:e20180545. doi: 10.1590/1676-0611-BN-2018-0545

Phillips, S. J., Anderson, R. P., and Schapire, R. E. (2006). Maximum entropy modeling of species geographic distributions. *Ecol. Model.* 190, 231–259. doi: 10.1016/j.ecolmodel.2005.03.026

Pires-Vanin, A. M. S., and Matsuura, Y. (1993). Estrutura e função do ecossistema de plataforma continental da região de Ubatuba, Estado de São Paulo: uma introdução. *Publ. Esp. Inst. Oceanogr.* 10, 217-231.

Rios, E. C. (1994). *Seashells of Brazil 4th ed*. Rio Grande: Universidade do Rio Grande.

Rios, E. C. (2009). *Compendium of Brazilian Seashells*. Rio Grande: Evengraf.

Saito, H. (2020). A new species of *Falcidens* (Mollusca: Caudofoveata: Chaetodermatidae) from the Pacific Coast of Japan. *Bull. Natl. Mus. Nat. Sci.* 46, 79–87.

Saito, H., and Salvini-Plawen, L. V. (2014). Four new species of the aplacophoran class Caudofoveata (Mollusca) from the southern Sea of Japan. *J. Nat. Hist.* 48, 2965–2983. doi: 10.1080/00222933.2014.959577

Salvini-Plawen, L. V. (1968). Über Lebendbeobachtungen an Caudofoveata (Mollusca, Aculifera), nebst Bemerkungen zum System der Klasse. *Sarsia* 31, 105–126. doi: 10.1080/00364827.1968.10411115

Salvini-Plawen, L. V. (1969). Solenogastres und Caudofoveata (Mollusca, Aculifera): organisation und phylogenetische bedeutung. *Malacologia* 9, 191–216.

Salvini-Plawen, L. V. (1970). Die norwegischen Caudofoveata. *Sarsia* 45, 1–15. doi: 10.1080/00364827.1970.10411180

Salvini-Plawen, L. V. (1972). "Die Caudofoveata des Mittelmeeres und das Genus Scutopus (Mollusca, Aculifera)," in *Fifth European Marine Biology Symposium; 1970 ed*, ed. B. Battaglía (Padova: Piccin Editore), 27–51.

Salvini-Plawen, L. V. (1975). *Mollusca: Caudofoveata. Marine invertebrates of Scandinavia (4)*. Oslo: Scandinavian University Books.

Salvini-Plawen, L. V. (1977). Caudofoveata (Mollusca) des Forschungsprojektes Polymède. *Bull. Mus. Natl. Hist. Nat.* 3, 413–421.

Salvini-Plawen, L. V. (1990). Origin, phylogeny and classification of the phylum Mollusca. *Iberus* 9, 1–33.

Salvini-Plawen, L. V. (1992). "On certain Caudofoveata from the VEMA-Expedition," in *Proceedings of the 9th International Malacological Congress (Edinburgh 1986)*, eds E. Gittenberger and J. Gould (Leiden: Unitas Malacologica), 317–333.

Salvini-Plawen, L. V. (1997). Fragmented knowledge on West-European and Iberian Caudofoveata and Solenogastres. *Iberus* 15, 35–50.

Salvini-Plawen, L. V. (2003). On the phylogenetic significance of the aplacophoran Mollusca. *Iberus* 21, 67–97.

Salvini-Plawen, L. V., and Warén, A. (1972). Skandinasvische Caudofoveata (Mollusca): nachtrag. *Sarsia* 51, 3–6. doi: 10.1080/00364827.1972.10411220

Schander, C., Scheltema, A. H., and Ivanov, D. L. (2006). *Falcidens halanychi*, a new species of Chaetodermomorpha (=Caudofoveata) (Mollusca) from the northwest Atlantic Ocean. *Mar. Biol. Res.* 2, 303–315. doi: 10.1080/17451000600798795

Scheltema, A. H. (1981). Comparative morphology of the radula and alimentary tracts in the Aplacophora. *Malacologia* 20, 361–383.

Scheltema, A. H. (1985). The aplacophoran family Prochaetodermatidae in the North American Basin, including *Chevroderma* n.g. and *Spathoderma* n.g. (Mollusca; Chaetodermomorpha). *Biol. Bull.* 169, 484–529. doi: 10.2307/1541497

Scheltema, A. H. (1987). Reproduction and rapid growth in a deep-sea aplacophoran mollusc, *Prochaetoderma yongei*. *Mar. Ecol. Prog. Ser.* 37, 171–180. doi: 10.3354/meps037171

Scheltema, A. H. (1997). Aplacophoran molluscs: deep-sea analogs to polychaetes. *Bull. Mar. Sci.* 60, 575–583.

Scheltema, A. H., and Ivanov, D. L. (2000). Prochaetodermatidae of the Eastern Atlantic Ocean and Mediterranean Sea (Mollusca: Aplacophora). *J. Molluscan Stud.* 66, 313–362. doi: 10.1093/mollus/66.3.313

Scheltema, A. H., and Ivanov, D. L. (2009). A natural history of the deep-sea aplacophoran *Prochaetoderma yongei* and its relationship to confamilials (Mollusca, Prochaetodermatidae). *Deep Sea Res. II Top. Stud. Oceanogr.* 56, 1856–1864. doi: 10.1016/j.dsr2.2009.05.026

Scheltema, A. H., Tscherkassky, M., and Kuzirian, A. M. (1994). "Aplacophora," in *Microscopic Anatomy of Invertebrates. Volume 5: The Mollusca*, eds F. W. Harrison and A. J. Kohn (New York: Wiley – Liss, Inc), 13–54.

Schnurr, S., Osborn, K. J., Malyutina, M., Jennings, R., Brix, S., Driskell, A., et al. (2018). Hidden diversity in two species complexes of munnopsid isopods (Crustacea) at the transition between the northernmost North Atlantic and the Nordic Seas. *Mar. Biodivers.* 48, 813–843. doi: 10.1007/s12526-018-0877-6

Señaris, M. P., García-Álvarez, O., and Urgorri, V. (2017). The habitus of *Scutopus robustus* Salvini-Plawen, 1970 (Caudofoveata, Limifossoridae), a rare mollusc from the NW Iberian Peninsula. *Mar. Biodivers.* 47, 377–378. doi: 10.1007/s12526-016-0488-z

Smith, S. A., Wilson, N. G., Goetz, F. E., Feehery, C., Andrade, S. C. S., Rouse, G. W., et al. (2011). Resolving the evolutionary relationships of molluscs with phylogenomic tools. *Nature* 480, 364–367. doi: 10.1038/nature10526

Todt, C. (2013). Aplacophoran Mollusks—Still Obscure and Difficult?. *Am. Malacol. Bull.* 31, 181–187. doi: 10.4003/006.031.0110

Treece, G. D. (1979). Four new records of aplacophorous mollusks from the Gulf of Mexico. *Bull. Mar. Sci.* 29, 344–364.

Vinther, J., Parry, L., Briggs, D. E. G., and Roy, P. (2017). Ancestral morphology of crowngroup molluscs revealed by a new Ordovician stem aculiferan. *Nature* 542, 471–474. doi: 10.1038/nature21055

Vinther, J., Sperling, E. A., Briggs, D. E. G., and Peterson, K. J. (2012). A molecular palaeobiological hypothesis for the origin of aplacophoran molluscs and their derivation from chiton-like ancestors. *Proc. R. Soc. B.* 279, 1259–1268. doi: 10.1098/rspb.2011.1773

Warren, D. L., Glor, R. E., and Turelli, M. (2010). ENMTools: a toolbox for comparative studies of environmental niche models. *Ecography* 33, 607–611. doi: 10.1111/j.1600-0587.2009.06142.x

Conflict of Interest: The authors declare that the research was conducted in the absence of any commercial or financial relationships that could be construed as a potential conflict of interest.

Publisher's Note: All claims expressed in this article are solely those of the authors and do not necessarily represent those of their affiliated organizations, or those of the publisher, the editors and the reviewers. Any product that may be evaluated in this article, or claim that may be made by its manufacturer, is not guaranteed or endorsed by the publisher.

Copyright © 2021 Passos, Corrêa and Miranda. This is an open-access article distributed under the terms of the Creative Commons Attribution License (CC BY). The use, distribution or reproduction in other forums is permitted, provided the original author(s) and the copyright owner(s) are credited and that the original publication in this journal is cited, in accordance with accepted academic practice. No use, distribution or reproduction is permitted which does not comply with these terms.

frontiers in Marine Science

ORIGINAL RESEARCH
published: 29 November 2021
doi: 10.3389/fmars.2021.779001

Pseudotanais Sars, 1882 (Crustacea: Tanaidacea) From the SE Australian Slope: A Gap in Our Knowledge

Magdalena Błażewicz[1], Aleksandra Jakiel[2] and Graham J. Bird[3]*

[1] Department of Invertebrate Zoology and Hydrobiology, University of Łódź, Łódź, Poland, [2] Department of Genetics and Marine Biotechnology, Institute of Oceanology, Polish Academy of Sciences, Sopot, Poland, [3] Independent Researcher, Waikanae, New Zealand

In the current paper, we present the description of five new species of pseudotanaids sampled off the Bass Strait during two campaigns (SLOPE), which took place in 1986/8 and 1994 from the upper continental margin (slope) at depths 200–1550 m, hopefully starting to fill a gap in the knowledge of this major habitat. From five species, two occurred off eastern coast between Gippsland and Jervis Point and three others on the southern coast between Great Otway (Otway Point) and Kangaroo Island. These five species bring the total number of described pseudotanaid species 94 and to six in Australian waters.

Keywords: Peracarida, taxonomy, diversity, continental margin, Pseudotanaidae

OPEN ACCESS

Edited by:
Clara F. Rodrigues, University of Aveiro, Portugal

Reviewed by:
Juliana Lopes Segadilha, National Museum, Federal University of Rio de Janeiro, Brazil
Pedro L. Ardisson, Center for Research and Advanced Studies - Mérida Unit, Mexico

****Correspondence:***
Magdalena Błażewicz
magdalena.blazewicz@biol.uni.lodz.pl

Specialty section:
This article was submitted to Deep-Sea Environments and Ecology, a section of the journal Frontiers in Marine Science

Received: *17 September 2021*
Accepted: *11 October 2021*
Published: *29 November 2021*

Citation:
Błażewicz M, Jakiel A and Bird GJ (2021) Pseudotanais Sars, 1882 (Crustacea: Tanaidacea) From the SE Australian Slope: A Gap in Our Knowledge. Front. Mar. Sci. 8:779001. doi: 10.3389/fmars.2021.779001

INTRODUCTION

Pseudotanaidae Sieg, 1976 are small tanaidaceans from the superfamily Paratanaoidea Lang (1949), characterized by their compact (short) body, enlarged chelipeds and a brood pouch composed of one pair of oostegites (Lang, 1949; Sieg, 1977). Currently, the Pseudotanaidae is the third most species-rich family of Paratanaoidea after Leptocheliidae Lang, 1973 and Typhlotanaidae Sieg (1976) (with 132 and 116 nominal species, respectively)[1]. They are probably epifaunal or shallow sediment burrowers (infauna), and some are unselective predators and hosts for nematode parasites (Błażewicz et al., 2020).

Pseudotanaids are often numerous and a frequent element in macrobenthic communities, an example being the 36% contribution to the tanaid abundance (7% of macrofauna) on the bathyal Chatham Rise, SW Pacific (Bird and Holdich, 1984; Pabis et al., 2014, 2015; Kaiser et al., 2018). They are present in a variety of marine habitats (Bird and Holdich, 1989b; Bird, 1999; Bamber et al., 2009; Błażewicz-Paszkowycz and Bamber, 2011; Jakiel et al., 2015, 2019; Stępień et al., 2018) and are recorded over a wide bathymetric range. The shallowest record of the family belongs to *Akanthinotanais pedecerritulus* Tzeng and Hsueh, 2021 present in the intertidal of Taiwan, while the deepest record was recorded for *Pseudotanais longisetosus* Sieg (1977) and *P. nordenskioldi* Sieg (1977), which were recorded at 6050 m (Kudinova-Pasternak, 1993). Although a few large publications have focused specifically on the diversity of Pseudotanaidae (Sieg, 1977; Bird and Holdich, 1989b; Jakiel et al., 2018, 2019, 2020), knowledge about their diversity, community structure and spatial distribution is still severely limited.

Peracarid pseudotanaids, as with other brooders, are assumed to have limited dispersal ability and narrow zoographical ranges. This was tentatively confirmed with employment of

[1] http://www.marinespecies.org/index.php

morphometric and molecular methods (Jakiel et al., 2018, 2019, 2020) for investigation of their distribution in the deep North Atlantic and the abyssal of Central and NW Pacific (Bird and Holdich, 1989b; Jakiel et al., 2019, 2020). For this reason, pseudotanaids are possibly good indicators for effective environmental impact assessment, habitat resilience and its potential for reconstruction (Bird and Holdich, 1989b; O'Hara et al., 2020; Francesca et al., 2021).

In the Australian context, 162 tanaid species belonging to 66 genera have been described (e.g., Edgar, 1997, 2008, 2012; Bamber, 2005, 2008; Błażewicz-Paszkowycz and Bamber, 2007, 2009, 2012; Jóźwiak and Błażewicz, 2021). Most of the studies focused on the shelf tanaids and only nine species are formally described from below the shelf break: three from SE Australia (*Bathytanais fragilis* Larsen and Heard, 2001, *Pseudobathytanais gibberosus* Larsen and Heard, 2001, and *Acinoproskelos vermes* Bamber and Błażewicz-Paszkowycz, 2013) and six from W Australia (*Bunburia prima* Jóźwiak and Jakiel, 2012, *Abrotanais geniculum* Gellert and Błażewicz, 2018, *Macilenta ewae* Gellert and Błażewicz, 2018, *M. acetabula* Gellert and Błażewicz, 2018, *M. twor* Gellert and Błażewicz, 2018, *Waki australiensis* Gellert and Błażewicz, 2018) (Larsen and Heard, 2001; Jóźwiak and Jakiel, 2012; Gellert and Błażewicz, 2018). Only one pseudotanaid, *Akanthinotanais scrappi* Bamber, 2005, has been published, from a sandy bottom with rhodoliths in Esperance Bay at 38.4 m (Bamber, 2005). Two potentially new pseudotanaid species were recorded from two locations of the Great Barrier Reef (Stępień et al., 2018), although they stay undescribed.

The continental margins (continental slope) are a narrow oceanic zone covering 11% of the surface (Menot et al., 2010) and the huge extent of Australia's slopes are relatively understudied. Complicated geomorphology, chemistry and hydrodynamic processes augmented by the steep gradient of temperature, hydrostatic pressure, and oxygen levels make them the most complex and heterogenic zone of the oceanic floor. The steep slope, and often hard and unstable sediments are logistically demanding for sampling and hamper benthic faunal investigations. Analyzing the zoogeographical ranges, natural biodiversity, and factors determining their character makes a baseline for understanding the evolutionary processes and distribution patterns critical for management regimes and conservation reserves (Zardus et al., 2006; Jennings et al., 2013; Poore et al., 2015). In the current paper, we present the description of five new species of pseudotanaids sampled off the Bass Strait during two campaigns (SLOPE), which took place in 1986/8 and 1994 from the upper continental margin (slope) at depths 200–1550 m, hopefully starting to fill a gap in the knowledge of this major habitat.

MATERIALS AND METHODS

Stations and Collection

Pseudotanaids were recovered from a series of the samples collected at depths greater than 200 m, perpendicular to the East and South coasts of Australia during three campaigns of the O.R.V. *Franklin* 1986–1988 and 1994, respectively. Altogether, 213 samples were collected with different devices, e.g., Woods Hole Oceanographic Institute epibenthic sled, Reineck box-corer, Beam trawl (Poore et al., 1994; unpublished data). Pseudotanaids were recovered only at six stations (**Table 1**).

Morphological Analyses and Taxonomical Identification

Specimens were dissected with chemically sharpened tungsten needles and the dissected appendages mounted on slides with glycerine as a medium and sealed with paraffin-wax (Błażewicz et al., 2021). Drawings were prepared using a light microscope (Nikon Eclipse 50i) equipped with a *camera lucida*. Digital drawings were inked and arranged with Photoshop.

Morphological terminology is largely as in Jakiel et al. (2019, 2020);

- the unique blade-like spine, if present, located at the ventrodistal part of the pereopod carpus is characteristic of most pseudotanaids. It is categorized as "long" when is at least 0.6x propodus, "intermediate" when it is 0.5x propodus, and "short" when it is at most 0.3x the propodus;
- setal types are recognized as: (1) simple setae (= without ornamentation), (2) serrate – with serration or denticulation, (3) plumose – with any type of plumose or delicate setulae distributed along the main axis, (4) penicillate – with a tuft of setules located distally and with a small knob on which a seta is fixed to the tegument and (5) rod setae – slightly inflated distally and with a pore; and
- the dorsodistal seta occurring on the carpus of pereopods 4–6 has a chemosensory function – ("rod seta" Jakiel et al., 2019); it is categorized as "long" when it is at least 0.8x propodus, "intermediate" when it is 0.5x propodus, and "short" when it is at most 0.25x propodus.

The classification of the *Pseudotanais* into morpho-groups ("affinis + longisetosus," "denticulatus + abathagastor" and "forcipatus") follows Bird and Holdich (1989b) and Jakiel et al. (2019).

The type material was lodged at the Museums Victoria, Melbourne Museum (Australia).

Classification

In our study and analyses we have applied the system splitting *Pseudotanais* species into established four morphogroups, e.g., "affinis + longisetosus," "denticulatus + abathagastor," "forcipatus," and "spicatus" (Bird and Holdich, 1989b; Jakiel et al., 2019). The six species (*P. borceai* Băcescu, 1960; *P. lilljeborgi* Sars, 1882; *P. falcifer* Błażewicz-Paszkowycz and Bamber, 2011; *P. sigrunis* Jakiel et al., 2018; *P. colonus* Bird and Holdich, 1989a; *P. baresnauti* Bird, 1999) were gathered into working-group "colonus" characterized by robust chela, acuminate mandible, and relatively long pereonite-1. Three species: *P. intortus*, *P. oculatus* and *P. shirazi* sp. nov. are not classified to any group.

TABLE 1 | Stations where pseudotanaids were recovered off SE Australian collection made on O.R.V. *Franklin* 1986–1988 and 1994, respectively, Poore et al. (1994); unpublished data.

Station	Locality	Lat/Long	Date	Gear	Depth (m)
SLOPE 40	Victoria, S of Point Hicks	38°17.42′S, 149°11.18′E	24 Jul 1986	WHOI EBS	400
SLOPE 53	New South Wales, 54 km ESE of Nowra	34°52.43′S–34°54.18′S, 151°15.02′E–151°19.30′E	22 Oct 1988	WHOI EBS	996
SLOPE 67	Victoria, 67 km S of Point Hicks	38°23.57′S–38° 23.47′S, 149°17.01′E–149°15.14′E	25 Oct 1988	WHOI EBS	1277
SLOPE 118	Victoria, Off Portland	38°48.02′S–38° 48.07 S, 141° 47.14′E–141°47.14′E	12 May 1994	WHOI EBS	209
SLOPE 134	Victoria, Off Portland	38°51.02′S, 141°44.47 E	13 May 1994	Box Corer	1021
SLOPE 170	South Australia, Off Murray River Mouth Encounter Bay	37°05.53′S, 137°42.32′E	21 May 1994	Smith-McIntyre grab	1548

The zoogeographical classification of the marine zoogeographical regions of the oceans followed (Spalding et al., 2007; Watling et al., 2013).

Measurements, Developmental and Stage Identification

Total body length (BL) was measured along the main axis of symmetry from the rostrum to the end of the telson. Body width (BW) was measured at the widest point along the main axis of symmetry. The length was measured along the axis of symmetry, and the width perpendicular to the axis of symmetry at the widest spot. To simplify species descriptions, the expression "Nx" replaces "N times longer than/as long as" and "N L:W" replaces "N times longer than wide." The measurements were made with a camera connected to the microscope (Nikon Eclipse Ci-L) and NIS-Elements View software.[2] The body width and the length of the cephalothorax, pereonites, pleonites, and pleotelson were measured on whole specimens.

All individuals, developmental stages were identified. We refer to the following stages:

- two stages of manca, i.e., "manca-2" and "manca-3" which refer to specimens without or with buds of pereopod-6, respectively;
- preparatory female characterized by undeveloped oostegites ('buds') (Bird and Holdich, 1989b) and brooding female (with fully developed oostegites) were not recovered in the studied material;
- neuter – a stage that is morphologically like the juvenile female, but lacking oostegites buds; and
- 'juvenile male' that shows incompletely developed sexual dimorphic characters, i.e., resembling the neuter but has thicker antennules (equivalent to 'preparatory male' *sensu* Bird and Holdich, 1989b).

In our collection sexually mature males ("swimming" male) and brooding females were not recovered.

RESULTS

Nine individuals belonging to Pseudotanaidae were examined in the current paper. All of them were classified to the genus *Pseudotanais*: two of them represented "affinis + longisetosus" morphogroup (*Pseudotanais chardonnayi* n. sp. and *P. caberneti* n. sp.) and two "denticulatus + abathagastor" group: (*P. barossai* n. sp. and *P. coonawarrai* n. sp.). The fifth of described species *P. shirazi* is not assigned to any of the *Pseudotanais* groups.

[2]www.nikoninstruments.com

SYSTEMATICS

Order Tanaidacea Dana, 1849
Suborder Tanaidomorpha Sieg, 1980
Superfamily Paratanaoidea Lang, 1949
Family Pseudotanaidae Sieg, 1976

"affinis + longisetosus" group

Diagnosis. After Jakiel et al. (2019).

Species included. *Pseudotanais affinis* Hansen, 1887; *P. chanelae* Jakiel et al., 2020; *P. curieae* Jakiel et al., 2020; *P. gaiae* Jakiel et al., 2019; *P. geralti* Jakiel et al., 2019; *P. julietae* Jakiel et al., 2019; *P. longisetosus* Sieg, 1977; *P. longispinus* Bird and Holdich, 1989b; *P. macrocheles* Sars, 1882; *P. monroeae* Jakiel et al., 2020; *P. nipponicus* McLelland, 2007; *P. nordenskioldi* Sieg, 1977; *P. rapunzelae* Błażewicz et al., 2021; *P. romeo* Jakiel et al., 2019; *P. spatula* Bird and Holdich, 1989b; *P. scalpellum* Bird and Holdich, 1989b; *P. shackletoni* Błażewicz et al., 2021; *P. svavarssoni* Jakiel et al., 2018; *P. szymborskae* Jakiel et al., 2020; *P. uranos* Jakiel et al., 2019; *P. vitjazi* Kudinova-Pasternak, 1966; *P. yenneferae* Jakiel et al., 2019; *Pseudotanais* sp. O (*sensu* McLelland, 2008); *Pseudotanais* sp. P (*sensu* McLelland, 2008); *P. chardonnayi* sp. nov.; *P. caberneti* sp. nov.

***Pseudotanais chardonnayi* sp. nov.**

This species is registered in ZooBank number: LSIDurn:lsid:zoobank.org:act:420075F1-3622-4177-9BBC-4552CE1B3E07.

Diagnosis. Mandible molar subcoronal with distal spines. Pereopod-1 merus with seta. Pereopod-3 carpal blade-like spine long (0.7x propodus). Pereopods 4–6 merus with spine and seta; carpus with long rod seta; propodus with short and long ventral setae. Uropod exopod 0.7x endopod.

Material examined. Holotype, juvenile male 1.3 mm, SLOPE 40 (J61547). Paratypes: neuter 1.1 mm (J61515), dissected in slides, SLOPE 40.

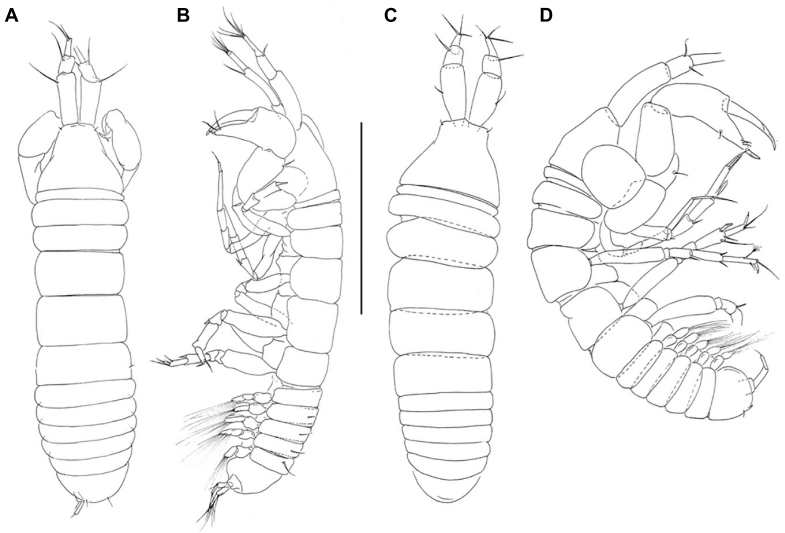

FIGURE 1 | *Pseudotanais chardonnayi* sp. nov; neuter (J61547), **(A)**, dorsal; **(B)**, lateral; juvenile male (J61515), **(C)**, dorsal, **(D)**, lateral. Scale line = 1 mm.

Etymology. The name is after a wine variety grown in the Gippsland area, close to the type locality, as genitive.

Description of neuter. BL = 1.4 mm. Body robust (**Figures 1A,B**) 3.8 L:W. Cephalothorax 0.7 L:W, 1.0x pereonites 1–3, 0.2 BL. Pereonites 0.5 BL, Pereonite-1 0.5x pereonite-2, pereonites-1–6: 0.1, 0.3, 0.3, 0.5 0.5 and 0.4 L:W, respectively. Pleon short, 0.4 BL. Pleonites 0.9 L:W, pleonites 2–5 with dorsolateral setae on each side of midline. Pleotelson 4.4x pleonite-5, with paired laterodistal setae.

Antennule (**Figure 2A**) article-1 6.0 L:W, 2.9x article-2, with long seta at mid-length, and one simple and three penicillate distal setae; article-2 2.9 L:W, 0.7x article-3, with two simple and one penicillate subdistal setae; article-3 5.8 L:W, with one simple, three bifurcated, one penicillate distal setae and one aesthetasc.

Antenna (**Figure 2B**) article-2 1.3 L:W; 1.0x article-3, with spine (0.3x article-2); article-3 1.3 L:W, 0.2x article-4, with spine (3.5x article-3); article-4 9.3 L:W, 2.2x article-5, with three simple (two broken) and three penicillate; article-5 5.0 L:W, 10.0x article-6, with simple distal seta; article-6 0.5 L:W, with six distal setae.

Labrum (**Figure 2C**) rounded, naked. Left mandible (**Figure 2D**) *lacinia mobilis* well developed, distally serrate, incisor distal margin beveled, serrate, molar subcoronal/acuminate with distal spines. Right mandible lost. Labium (**Figure 2E**) simple, rounded, glabrous. Maxillule (**Figure 2F**) endite with eight distal spines and outer two subdistal setae, palp (**Figure 2F'**) palp with two distal setae. Maxilla (**Figure 2G**) almost circular, naked. Maxilliped (**Figure 2H**) basis heart-shape, naked; palp article-1 1.8 L:W naked; article-2 1.1 L:W with one fine outer and three inner setae (two long and one short); article-3 1.4 L:W with one short and three long inner setae, article-4 3.3 L:W with six distal and subdistal setae; endites mostly fused but with central cleft (1/4 of endite total length), each with inner-distal gustatory cusp and short seta. Epignath (**Figure 2I**) linguiform, simple, naked.

Cheliped (**Figure 3A**) basis 1.8 L:W, dorsal seta not seen; merus with ventral seta; carpus 1.5 L:W, 0.8x palm, with two midventral setae and one dorsodistal simple seta; chela non-forcipate, palm 1.7 L:W with seta near dactylus insertion; fixed finger 3.0 L:W, cutting edge simple, poorly calcified, 0.8x palm with ventral seta, and with three setae on cutting edge; dactylus 5.9 L:W, cutting edge smooth, with dorsoproximal seta.

Pereopod-1 (**Figure 3B**) overall 14.9 L:W; coxa with small seta; basis 6.7 L:W, 4.2x merus, with one dorsoproximal and two ventral setae; ischium with ventral seta; merus 2.0 L:W and 0.7x carpus, with minute ventrodistal and one dorsodistal seta; carpus 3.0 L:W, 0.6x propodus, with two minute distal setae; propodus 8.4 L:W, 0.9x dactylus and unguis combined length, with short ventrodistal seta, dactylus 0.5x unguis.

Pereopod-2 (**Figure 3C**) overall 12.6 L:W; coxa not dissected; basis 6.5 L:W, 3.6x merus, with mid-dorsal penicillate seta; ischium with ventral seta; merus 2.3 L:W, 1.0x carpus, with seta and spine ventrodistally; carpus 2.0 L:W, 0.7x propodus, with dorsodistal seta, and long ventrodistal blade-like spine (0.6x propodus); propodus 6.3 L:W, 1.5x dactylus and unguis combined length, with long distal seta (0.7x dactylus and unguis combined length); dactylus 0.2x unguis.

Pereopod-3 (**Figure 3D**) overall 17.4 L:W; basis 3.7 L:W, 2.9x merus, with mid-ventral simple seta; ischium with ventral seta; merus 1.6 L:W, 0.9x carpus, with ventrodistal spine (seta not seen); carpus 2.0 L:W, 0.7x propodus, with dorsodistal robust seta, inner-distal minute seta, and long ventrodistal blade-like spine (0.7x propodus); propodus 5.4 L:W, 1.7x dactylus and unguis combined length, with distal seta (0.6x dactylus and unguis combined length); dactylus 0.5x unguis.

Pereopod-4 (**Figure 3E**) overall 9.2 L:W; basis 4.2 L:W, 4.2x merus, naked; ischium with two ventral setae; merus 1.4 L:W, 0.5x carpus, with one short seta and one spine; carpus 3.9 L:W, 0.9x propodus, with one short spine and one intermediate blade-like

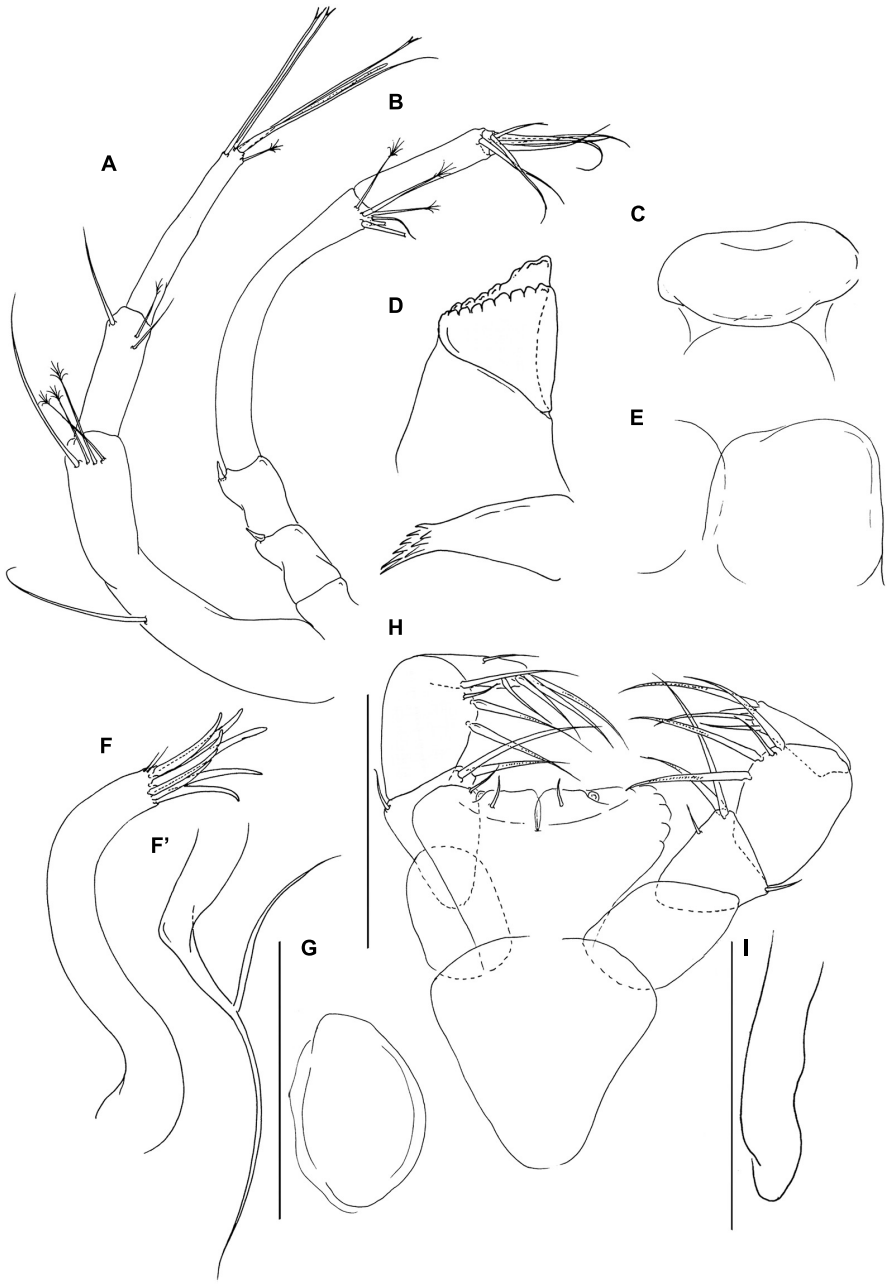

FIGURE 2 | *Pseudotanais chardonnayi* sp. nov; neuter (J61515), **(A)**, antennule; **(B)**, antenna; **(C)**, labrum; **(D)**, left mandible; **(E)**, labium; **(F)**, maxillule; **(F')** maxillule endite; **(G)**, maxilla; **(H)**, maxilliped; **(I)**, epignath. Scale lines = 0.1 mm.

spine (0.5x propodus); dorsal seta not seen; propodus 5.7 L:W, 2.4x dactylus and unguis combined length, with one subdorsal penicillate seta, two spines (short and long) ventrodistally, and long serrate dorsodistal seta (1.7x dactylus and unguis combined length); dactylus 1.8x unguis.

Pereopod-5 (**Figure 3F**) overall 10.0 L:W; basis 5.0 L:W, 5.9x merus, with long penicillate midlength seta; ischium with two ventral setae; merus 1.2 L:W, 0.4x carpus, with ventral spine (seta not seen); carpus 3.6 L:W, 1.2x propodus, with dorsodistal seta (1.3x propodus), one minute spine and one intermediate blade-like spine (0.5x propodus); propodus 5.0 L:W, 2.2x dactylus and unguis combined length, with one sub-dorsal penicillate seta, one serrate seta, one spine ventrally and one serrate dorsal seta (2.1 x dactylus and unguis combined length); dactylus 2.3x unguis.

Pereopod-6 (**Figure 3G**) basis 4.8 L:W, 4.5x merus, naked; ischium with two ventral setae; merus 1.5 L:W, 0.5x carpus, with spine (seta not seen); carpus 3.4 L:W, 1.1x propodus, with long dorsodistal seta (0.9x propodus), two spines (short and long) and one intermediate blade-like spine (0.5x propodus) ventrodistally;

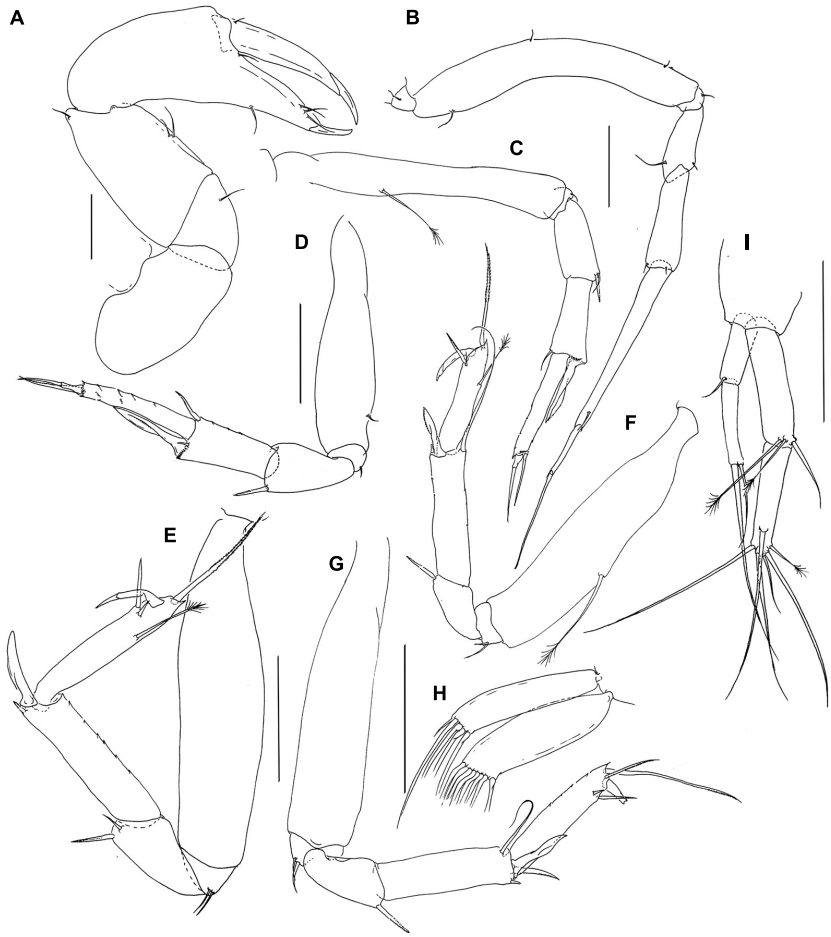

FIGURE 3 | *Pseudotanais chardonnayi* sp. nov.; neuter (J61515), **(A)**, cheliped; **(B)**, pereopod-1; **(C)**, pereopod-2, **(D)**, pereopod-3; **(E)**, pereopod-4; **(F)**, pereopod-5; **(G)**, pereopod-6; **(H)**, pleopod; **(I)**, uropod. Scale lines = 0.1 mm.

propodus 4.1 L:W, with two serrate ventral setae and two serrate dorsal setae; dactylus broken.

Pleopods (**Figure 3H**) rami narrow and elongate; exopod with five, endopod with seven distal setae.

Uropod (**Figure 3I**) peduncle 0.9 L:W; exopod with two articles; 6.0 L:W; article-1 2.7 L:W, with short distal seta; article-2 5.0 L:W, with two distal setae; endopod 7.9 L:W; article-1 4.3 L:W, with one simple and two penicillate distal setae; article-2 4.2 L:W, with one subdistal, four distal simple setae and one penicillate seta. Exopod 0.7x endopod.

Description of juvenile male. Similar to female, but antennule thicker (**Figures 1C,D**).

Distribution. The species is known only from the type locality: SE Australia (off Gippsland), at the depth 400 m.

Remarks. *Pseudotanais chardonnayi* sp. nov. has a dorsodistal spine on antenna articles 2–3, a relatively long propodal distal seta on pereopods 2–3, and a long dorsodistal seta on carpus of pereopods 5–6, that allow classification of the species to the "affinis + longisetosus" morpho-group (Bird and Holdich, 1989b; Jakiel et al., 2019), although the relatively short dorsodistal seta on the pereopod merus (rather long in "affinis + longisetosus" group) is anomalous we have decided to deposit *P. chardonnayi* in this group as this seta is still longer than in members of other groups where it is minute or absent.

The short dorsodistal seta on the pereopod-4 carpus distinguishes *P. chardonnayi* from *P. chanelae*, *P. curieae* and *P. longisetosus*, where this seta is long. The combination of a spine and seta on the pereopods 4–6 merus and carpal long rod seta of *P. chardonnayi* is similar to *P. romeo*, but it can be separated by the uropod exopod that is 0.7x endopod in *P. chardonnayi* and 0.9x in *P. romeo*. Additionally, the blade-like spine on the carpus of pereopod-3 is 0.7x propodus in *P. chardonnayi*, while *P. romeo* it is slightly longer (0.8x propodus). Finally, both species can be distinguished by the setation of ischium of pereopods 4–6, with two setae in *P. chardonnayi* and naked in *P. romeo*.

***Pseudotanais caberneti* sp. nov.**

This species is registered in ZooBank number: LSID urn:lsid: zoobank.org:act:FE1106E8-DBE6-4CB5-AD67-F631E08F9 A1C.

Diagnosis. Mandible molar subcoronal with distal spines. Pereopod-1 merus with seta. Pereopod-3 carpal blade-like spine long (0.7x propodus). Pereopods 4–6 merus with spine and seta; carpus with short dorsodistal seta; propodus with two ventral setae. Uropod exopod 0.7x endopod.

Material examined. Holotype, ovigerous female 1.8 mm, partly dissected (J62735) SLOPE 118.

Etymology. The species name is after one of most widely distributed and best-known wine grape varieties grown in SE Australia, as genitive.

Description of female. BL = 1.7 mm. Body robust (**Figures 4A,B**) 3.2 L:W. Cephalothorax 0.7 L:W, 1.4x pereonites 1–3 0.2x BL. Pereonites 0.6x BL; pereonite-1 0.4x pereonite-2, pereonites-1–6: 0.1, 0.2, 0.2, 0.5, 0.5, and 0.5 L:W, respectively; pereonites 1, 3–4 with small anterolateral setae. Pleon short, 0.4 BL. Pleonites 0.7 L:W, pleonites 1 and 4 with dorsolateral setae on each side of midline, and pleonite 5 with lateral seta. Pleotelson 5.4x pleonite-5, with pair of mid-distal setae.

Antennule (**Figure 4C**) article-1 3.9 L:W, 2.6x article-2, with two simple and three penicillate midlength setae, and one distal seta; article-2 3.9 L:W, 0.9x article-3, with one simple and one penicillate distal setae; article-3 7.5 L:W, with one subdistal seta and five simple setae and one aesthetasc distally.

Antenna (**Figure 4D**) article-2 1.6 L:W; 0.8x article-3, with spine (0.3x article-2); article-3 2.2 L:W, 0.4x article-4, with spine (0.2x article-3); article-4 10.0 L:W, 2.6x article-5, with two simple

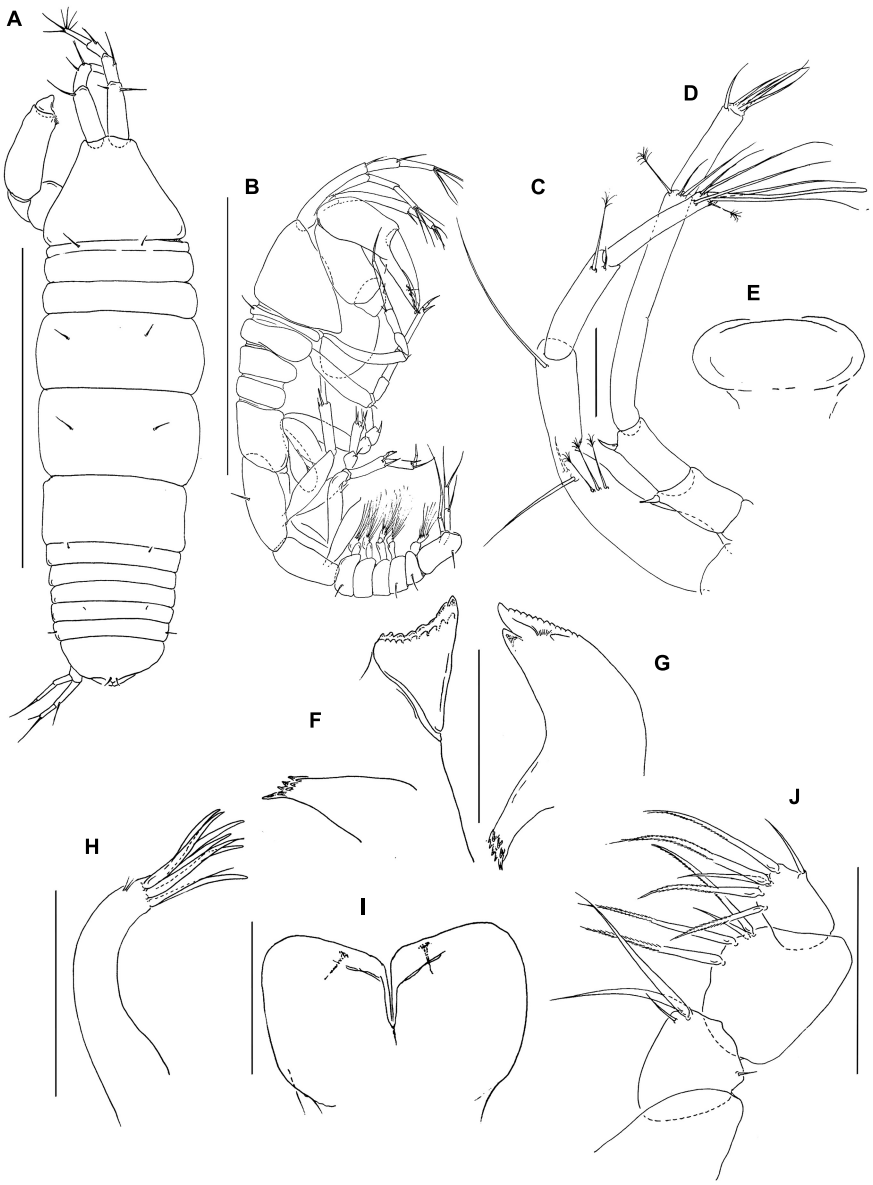

FIGURE 4 | *Pseudotanais caberneti* sp. nov; female, (J62735) **(A)**, dorsal; **(B)**, lateral; **(C)**, antennule; **(D)**, antenna; **(E)**, labrum; **(F)**, left mandible; **(G)**, right mandible; **(H)**, maxillule; **(I)**, labium; **(J)**, maxilliped palp. Scale lines **(A,B)** = 1 mm, **(C–J)** = 0.1 mm.

and one penicillate distal setae; article-5 3.8 L:W, 11.5x article-6, with distal seta; article-6 0.4 L:W, with four distal setae.

Labrum (**Figure 4E**) rounded, naked. Left mandible (**Figure 4F**) *lacinia mobilis* well developed, distally serrate, incisor distal margin beveled and serrate, molar subcoronal with distal spines. Right mandible (**Figure 4G**) incisor unequally bifid, distal margin serrate; molar as in left mandible. Labium simple, semi-rectangular (**Figure 4I**). Maxillule (**Figure 4H**) endite with seven distal spines and outer subdistal setae. Maxilla not observed.

Maxilliped (**Figure 4J**) palp article-1 naked, article-2 1.3 L:W, with fine outer and three inner setae (two long and one short); article-3 1.3 L:W with one shorter and three longer inner setae; article-4 1.4 L:W with six distal and subdistal setae. Maxilliped endite, basis not dissected.

Cheliped (**Figure 5A**) basis broken; merus ventral seta not seen; carpus 1.9 L:W, 1.2x palm, with two midventral setae and dorsodistal simple seta; chela non-forcipate, palm 1.4 L:W with comb of small setae on inner side, and one seta near dactylus insertion; fixed finger 4.0 L:W, 1.1x palm, with ventral seta,

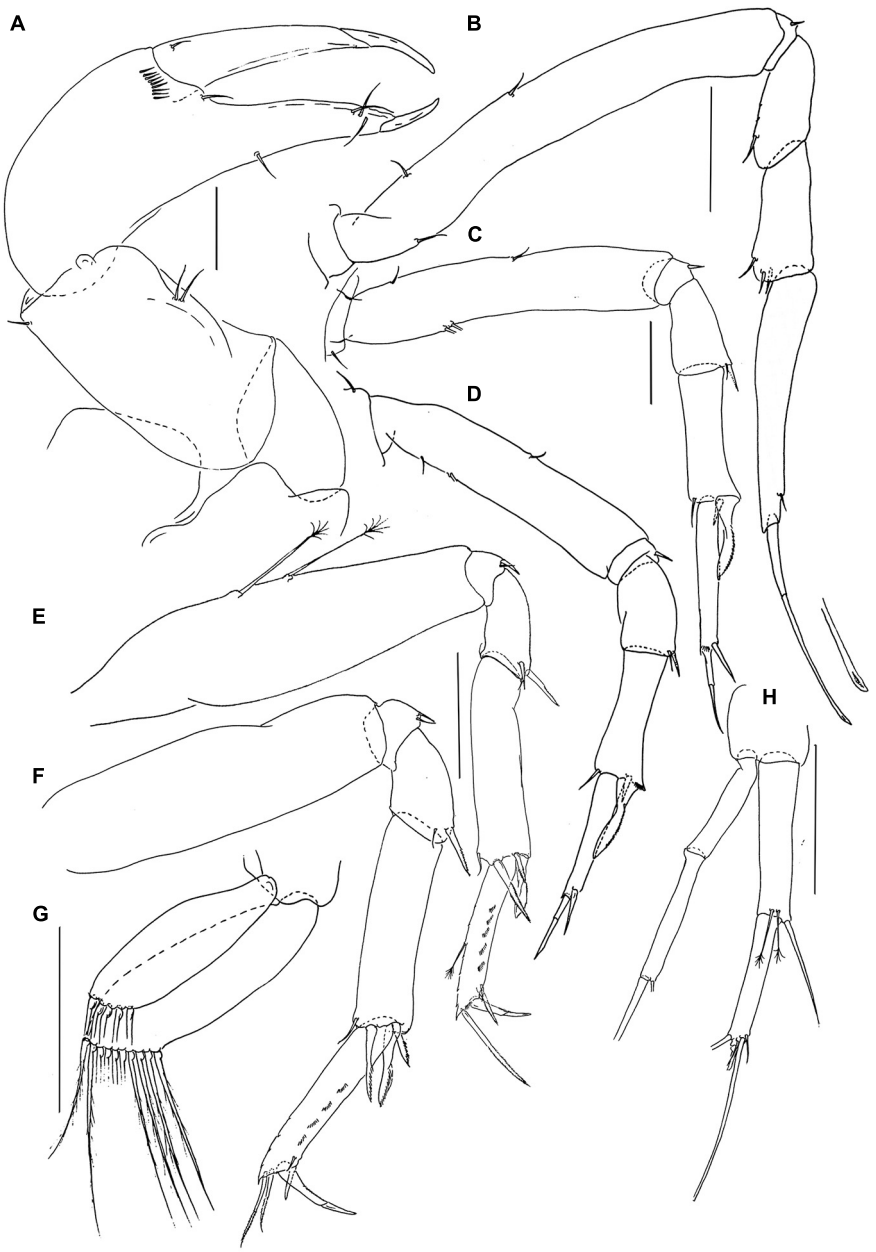

FIGURE 5 | *Pseudotanais caberneti* sp. nov.; female (J62735), **(A)**, cheliped; **(B)**, pereopod-1; **(C)**, pereopod-2, **(D)**, pereopod-3; **(E)**, pereopod-4; **(F)**, pereopod-6; **(G)**, pleopod; **(H)**, uropod. Scale lines = 0.1 mm.

cutting edge poorly calcified, almost simple, and with three setae; dactylus 5.6 L:W, cutting edge smooth, with dorsoproximal seta.

Pereopod-1 (**Figure 5B**) overall 16.8 L:W; basis 8.3 L:W, 4.6x merus, with one dorsoproximal and two ventral setae; ischium with ventral seta; merus 2.0 L:W and 0.8x carpus, with dorsodistal seta; carpus 2.2 L:W, 0.5x propodus, with three dorsodistal setae; propodus 6.4 L:W, 0.9x dactylus and unguis combined length, with one subdistal seta, dactylus 0.6x unguis.

Pereopod-2 (**Figure 5C**) overall 11.8 L:W; coxa with seta; basis 5.4 L:W, 3.6x merus, with two dorsoproximal (broken) and two ventral setae; ischium with ventral seta; merus 1.5 L:W, 0.7x carpus, with seta and spine ventrodistally; carpus 2.6 L:W, 0.9x propodus, with dorsodistal setae, simple ventrodistal spine and intermediate ventrodistal blade-like spine (0.5x propodus); propodus 6.5 L:W, 1.7x dactylus and unguis combined length, with ventrodistal robust seta (0.5x dactylus and unguis combined length); dactylus 0.7x unguis.

Pereopod-3 (**Figure 5D**) overall 22.8 L:W; coxa with seta; basis 4.8 L:W, 2.7x merus, with two dorsoproximal (one broken) and one ventral setae; ischium with ventral seta; merus 2.0 L:W, 0.8x carpus, with ventrodistal seta and spine; carpus 2.9 L:W, 1.1x propodus, with dorsodistal seta, simple ventrodistal spine and long ventrodistal blade-like spine (0.7x propodus); propodus 5.3 L:W, 1.6x dactylus and unguis combined length, with one distal seta (0.5x dactylus and unguis combined length); dactylus 0.6x unguis.

Pereopod-4 (**Figure 5E**) overall 8.1 L:W; basis 3.9 L:W, 5.0x merus, with two long penicillate ventral setae; ischium with two ventral setae; merus 1.6 L:W, 0.4x carpus, with one spine and one seta; carpus 4.3 L:W, 4.5x propodus, with small; dorsodistal seta, two distal spines and one short blade-like spine (0.4x propodus); propodus 6.8 L:W, 2.5x dactylus and unguis combined length, with two serrate ventral setae (short and long) and one serrate dorsal seta (1.5x dactylus and unguis combined length); dactylus 1.2x unguis.

Pereopod-5 similar to pereopod-4.

Pereopod-6 (**Figure 5F**) overall 8.1 L:W; basis 3.3 L:W, 3.3x merus, naked; ischium with two ventral setae; merus 1.6 L:W, 0.5x carpus, with one short seta and one robust spine; carpus 3.5 L:W, 1.1x propodus, with dorsodistal seta, two distal spines, and short blade-like spine (0.4x propodus); propodus 5.5 L:W, 2.2x dactylus and unguis combine length, with two serrate ventral setae (short and long) and two serrate dorsal setae (longer setae 0.9x dactylus and unguis combined length); dactylus 2.0x unguis.

Pleopods (**Figure 5G**) rami elongate, narrow; exopod with five, endopod with ten distal setae.

Uropod (**Figure 5H**) peduncle 1.0 L:W; exopod with two articles, 15.3 L:W; article-1 7.3 L:W, naked, article-2 8.0 L:W, with two setae; endopod 8.3 L:W; article-1 4.7 L:W, with one simple seta and two penicillate setae; article-2 7.3 L:W, with five distal setae. Exopod 0.9x endopod.

Distribution: Species known from SE Australia, off Cape Otway, from the depth 209 m.

Remarks. *Pseudotanais caberneti* sp. nov. with a relatively long seta on merus and carpus of pereopod-1 can be classified in the "affinis + longisetosus" morphogroup, although the short dorsodistal seta on the carpus of pereopods 5–6 differentiates it from fourteen species: *Pseudotanais chardonnayi, P. chanelae, P. curieae, P. gaiae, P. julietae, P. longisetosus, P. longispinus, P. monroeae, P. nipponicus, P. rapunzelae, P. romeo, P. spatula, P. uranos,* and *Pseudotanais* sp. O (*sensu* McLelland), which have a long seta. The combination of a spine and seta on the merus of pereopods 4–6 merus differentiates *P. caberneti* from *P. affinis, P. scalpellum, P. shackletoni, P. svavarssoni* and *Pseudotanais* sp. P. (*sensu* McLelland), which have either a spine or seta only (the latter *P. svavarssoni*). Furthermore, two setae on the ischium of pereopods 4–6 of P. caberneti is similar to *P. geratli* and *P. macrocheles*, although the uropodal exopod that is only slightly shorter than the endopod (0.9x) separates *P. caberneti* from both species, where this proportion is at most 0.6x.

Key for identification of *Pseudotanais* females of the "affinis + longisetosus" morpho-group.

1. Pereopods 5–6 carpus with:
   short seta.....2
   long seta.....3
2. Pereopod–4 ischium with:
   one seta.....4
   two setae.....5
3. Pereopod–4 carpus rod seta:
   short.....13
   long.....14
4. Uropod exopod to endopod ratio:
   < 0.8x.....06
   > 0.9x.....*P. vitjazi*
5. Uropod exopod to endopod ratio:
   0.6x.....7
   > 0.8x.....8
6. Pereopod–2 carpus blade-like spine to propodus ratio
   ≤ 0.6x.....11
   0.8x.....*P. scalpellum*
7. Cephalothorax to pereonites 1–3 ratio; pereopod–5 dactylus to unguis ratio:
   1.3x;1.6x..... *P. macrocheles*
   0.9x; 2.0x.....*P. geralti*
8. Cephalothorax to pereonites 1–3 ratio:
   < 1.2x.....9
   > 1.3x.....*P. caberneti* sp. nov.
9. Pereopods 4–6 merus spine, seta [0-absent, 1-present]:
   1.0..... 10
   0.1.....*P. svavarssoni*
10. Pereopod-5 dactylus to unguis ratio:
    1.0x.....*Pseudotanais* sp. P.
    2.3x.....*P. shackletoni*
    3.0x..... *P. affinis*
11. Cephalothorax to pereonites 1–3 ratio:
    < 1.2x.....12
    > 1.7x.....*P. yenneferae*
12. Pereonite-1 to pereonite-2 ratio; pereopods 4–6 merus spine, seta [0-absent, 1-present]:
    0.7x; 1,1..... *P. nordenskioldi*
    0.5x; 1,0.....*P. spatula*

13. Pereopod-3 carpus blade-like spine to propodus ratio
    0.5x..... 16
    ≥ 0.6x..... 17
14. Uropod exopod to endopod ratio:
    0.7x..... 15
    0.9x..... *P. curieae*
15. Cephalothorax to pereonites 1–3 ratio; pereonite-1 to pereonite-2 ratio:
    1.2x; 1,0x.....*P. longisetosus*
    0.9x; 0.5x..... *P. chanelae*
16. Pereopods 4–6 merus spine, seta [0-absent, 1-present]:
    0,2.....18
    1,0..... *P. gaiae*
17. Pereopod-2 carpus blade-like spine to propodus ratio
    ≥ 0.6x.....19
    0.5x..... *P. romeo*
18. Pereonite-1 to pereonite-2 ratio; pereopod-5 dactylus to unguis ratio:
    0.3x; 2.0x.....*P. uranos*
    0.6x; 1.4x.....*P. monroeae*
19. Pereopods 4–6 ischium with:
    One seta.....20
    Two setae.....21
20. Cephalothorax to pereonites 1–3 ratio; pereopod-5 dactylus to unguis ratio:
    1.0x; 2.0x..... *P. longispinus*
    1.3x; 2.5x.....*P. julietae*
21. Pereopods 4–6 merus spine, seta [0-absent, 1-present]:
    1,0..... 22
    0,2..... *P. nipponicus*
    1,1..... *P. chardonnayi* sp. nov.
22. Pereonite-1 to pereonite-2 length ratio; pereopod-2 blade-like spine to propodus ratio; pereopod-5 dactylus to unguis ratio:
    0.6x; 0.8x; 2.3x..... *P. rapunzelae*
    0.4x; 0.6x; 2.4x..... *P. szymborskae*
    0.4x; 0.7x; 1.5x..... *Pseudotanais* sp. O

"denticulatus + abathagastor" group

Diagnosis. After Błażewicz et al. (2021).

Species included. *Pseudotanais abathagastor* Bamber and Błażewicz-Paszkowycz, 2013; *P. amundseni* Błażewicz et al., 2021; *P. barnesi* Błażewicz et al., 2021; *P. biopearli* Błażewicz et al., 2021; *P. chaplini* Jakiel et al., 2019; *P. chopini* Jakiel et al., 2019; *P. corollatus* Bird and Holdich, 1989b; *P. denticulatus* Bird and Holdich, 1989b; *P. elephas* Błażewicz et al., 2021; *P. georgesandae* Jakiel et al., 2019; *P. kitsoni* Błażewicz et al., 2021; *P. mariae* Jakiel et al., 2019; *P. livingstoni* Błażewicz et al., 2021; *P. locueloae* Jakiel et al., 2019; *P. oloughlini* Jakiel et al., 2019; *P. palmeri* Błażewicz et al., 2021; *P. barossai* sp. nov.; *P. coonawarrai* sp. nov.

Pseudotanais barossai sp. nov.

This species is registered in ZooBank number: LSID urn:lsid: zoobank.org:act:F4C1D408-3731-449E-9F00-D18CBEF81 DB5.

Diagnosis. Antenna articles 2–3 with slender spine. Mandible molar coronal. Pereopod-2 carpus blade-like spine short (0.4x propodus). Pereopods 2–6 merus with single spine. Uropod exopod 0.8x endopod.

Material examined. Holotype, neuter 1.3 mm, partly dissected (J61545), SLOPE 170.

Etymology. From the Barossa Valley in South Australia, a premium wine-growing region, as genitive.

Description of female. BL = 1.6 mm. Body robust (**Figure 6A**) 3.0 L:W. Cephalothorax 1.0 L:W, 1.2x pereonites 1–3, 1.3x BL with pair of ocular setae. Pereonites 0.6x BL, pereonite-1 0.6x pereonite-2, pereonites-1–6: 0.2, 0.2, 0.4, 0.5, 0.6 and 0.4 L:W, respectively; pereonites 1, 4–6 with anterolateral setae. Pleon short, 0.5x BL. Pleonites 1.2 L:W. Pleotelson 1.9x pleonite-5, with laterodistal setae.

Antennule (**Figure 6B**) article-1 4.5 L:W, 2.2x article-2, with one simple and three penicillate midlength setae, and one distal seta; article-2 2.6 L:W, 1.3x article-3, with distal seta; article-3 4.0 L:W, with three simple and three bifurcated setae (aesthetasc not seen).

Antenna (**Figure 6C**) article-2 1.7 L:W; 1.1x article-3, with slender spine (0.3x article-2); article-3 1.6 L:W, 0.4x article-4, with slender spine (0.3x article-3); article-4 5.5 L:W, 1.7x article-5, with three simple and one penicillate distal setae; article-5 4.4 L:W, 11.7x article-6, with distal seta; article-6 0.4 L:W, with four distal setae.

Labrum (**Figure 6D**) rounded, naked. Left mandible (**Figure 6E**) *lacinia mobilis* well developed, distally serrate, incisor distal margin beveled slightly serrate, molar coronal. Right mandible (**Figure 6F**) incisor unequally bifid, distal margin serrate molar as left mandible. Labium (**Figure 6G**) simple, rounded, glabrous. Maxillule (**Figure 6H**) endite with nine distal spines and outer subdistal seta. Maxilla not recovered.

Maxilliped (**Figure 6I**) palp article-1 1.5 L:W, naked, article-2 1.0 L:W with fine outer seta and three inner setae; article-3 1.1 L:W with four inner setae, article-4 3.0 L:W with one sub-distal and five distal setae. Epignath not recovered.

Cheliped (**Figure 7A**) basis 1.9 L:W, with small seta near sclerite articulation; merus with ventral seta; carpus 1.8 L:W, 1.2x palm, with two midventral setae and mid-dorsal and dorsodistal simple setae; chela non-forcipate, palm 1.7 L:W; fixed finger 3.1 L:W, 0.9x palm with one ventral seta, and with three setae on cutting edge; dactylus 6.3 L:W, cutting edge smooth, proximal seta not seen.

Pereopod-1 (**Figure 7B**) overall 15.7 L:W; coxa with seta; basis 7.0 L:W, 3.7x merus, naked; ischium with ventral seta; merus 2.1 L:W and 0.8x carpus, naked; carpus 2.4 L:W, 0.5x propodus, with two short distal setae; propodus 5.6 L:W, 0.8x dactylus and unguis combined length, with ventrodistal seta; dactylus 0.6 x unguis.

Pereopod-2 (**Figure 7C**) overall 13.5 L:W; coxa with seta; basis 6.2 L:W, 3.2x merus, naked; ischium with ventral seta; merus 2.3 L:W, 0.8x carpus, with ventrodistal spine; carpus 2.5 L:W, 0.9x propodus, with dorsodistal spine, inner-distal seta, simple ventrodistal spine and short ventrodistal blade-like spine (0.4x propodus); propodus 6.3 L:W, 2.0x dactylus and unguis

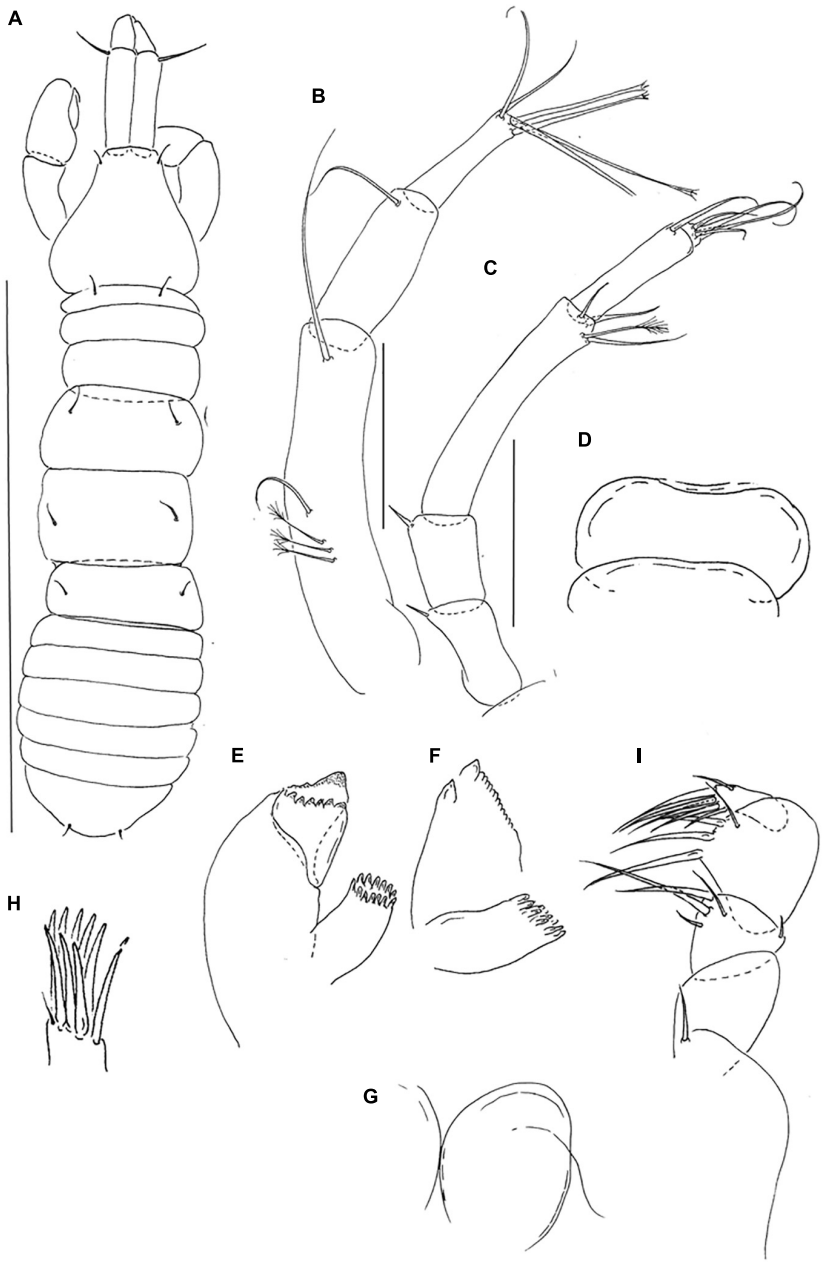

FIGURE 6 | *Pseudotanais barossai* sp. nov; neuter (J61545), **(A)**, dorsal; **(B)**, antennule; **(C)**, antenna; **(D)**, labrum; **(E)**, left mandible; **(F)**, right mandible; **(G)**, labium; **(H)**, maxillule; endite; **(I)**, maxilliped palp. Scale lines **(A)** = 1 mm, **(B–I)** = 0.1 mm.

combined length, with one distal seta (0.4x dactylus and unguis combined length); dactylus 0.5x unguis.

Pereopod-3 (**Figure 7D**) basis distally broken, naked; ischium with ventral seta; merus 4.6 L:W, 0.9x carpus, with ventrodistal spine; carpus 1.7 L:W, 1.0x propodus, with dorsodistal seta, simple ventrodistal small spine, and long ventrodistal blade-like spine (0.6x propodus); propodus 3.9 L:W, 3.9x dactylus and unguis combined length, with one ventrodistal robust seta (0.4x dactylus and unguis combined length); dactylus 0.9x unguis.

Pereopod-4 (**Figure 7E**) overall 8.4 L:W; basis 3.9 L:W, 3.5x merus, with penicillate ventral seta; ischium with ventral seta (second seta not seen); merus 1.8 L:W, 0.6x carpus, with spine; carpus 8.5 L:W, 1.1x propodus, with dorsodistal seta, and two spines (short and long) and one short blade-like spine (0.3x propodus) distally; propodus 4.3 L:W, 1.9x dactylus and unguis combined length, with two serrate ventral spines and one serrate dorsodistal seta (1.7x dactylus and unguis combined length), and one penicillate middorsal seta; dactylus 3.0x unguis.

Pereopod-5 (**Figure 7F**) overall 7.3 L:W; basis 3.3 L:W, 3.9x merus, with penicillate ventral seta; ischium with two ventral setae; merus 1.5 L:W, 0.6x carpus, with spine; carpus 2.6 L:W, 1.0x propodus, with dorsodistal seta, small spine and short blade-like spine (0.3x propodus) distally; propodus 5.0 L:W, 3.3x

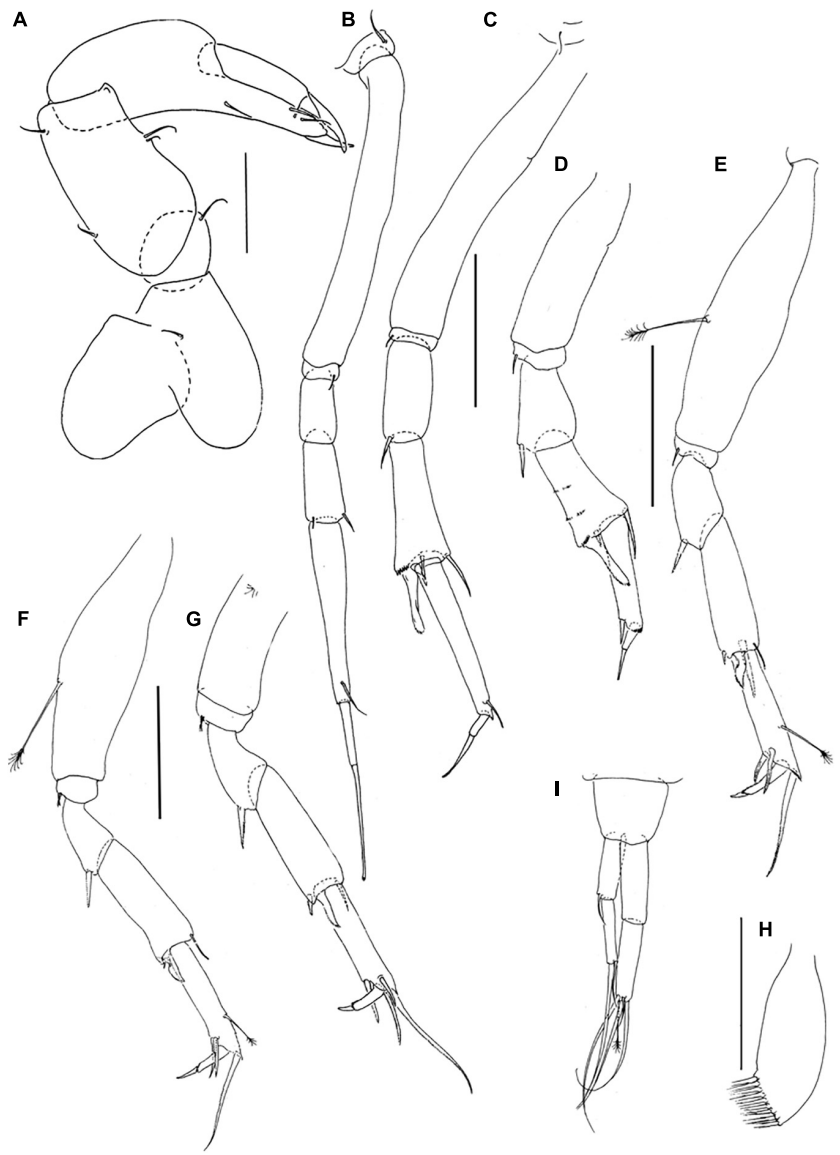

FIGURE 7 | *Pseudotanais barossai* sp. nov.; neuter (J61545), **(A)**, cheliped; **(B)**, pereopod-1; **(C)**, pereopod-2, **(D)**, pereopod-3; **(E)**, pereopod-4; **(F)**, pereopod-5; **(G)**, pereopod-6; **(H)**, pleopod; **(I)**, uropod. Scale lines = 0.1 mm.

dactylus and unguis combined length, with dorsal penicillate seta, two serrate ventrodistal spine, one serrate dorsodistal seta (1.7 dactylus and unguis combined length); dactylus 1.5x unguis.

Pereopod-6 (**Figure 7G**) basis broken; ischium with two ventral setae; merus 1.7 L:W, 0.6x carpus, with spine; carpus 3.1 L:W, 1.1x propodus, with dorsodistal seta, small spine and short blade-like spine (0.3x propodus) distally; propodus 5.0 L:W, 2.7x dactylus and unguis combine length, with two serrate ventrodistal setae and two serrate dorsodistal setae (longer setae 2.9x dactylus and unguis combined length); dactylus 2.7x unguis.

Pleopods (**Figure 7H**) poor condition, exopod not observed; endopod with nine setae.

Uropod (**Figure 7I**) peduncle 0.9 L:W; exopod with two articles; 6.6 L:W; article-1 3.2 L:W, with simple seta; article-2 5.7 L:W, with two distal setae (short and long); endopod 6.0 L:W; article-1 3.1 L:W, naked; article-2 4.0 L:W, with four simple setae and one penicillate distal seta. Exopod 0.8x endopod.

Distribution. Species known only from type locality, off Kangaroo Island (SE Australia) at depth 1548 m.

Remarks. *Pseudotanais barossai* sp. nov. has a thin spine on antenna article-2 and with this it can be separated from *P. abathagastor* and *P. mariae* which have a weaker seta at this position, and *P. barnesi* that lacks any seta. Furthermore, a thin spine on antennal article-3 also distinguishes *P. barossai* from *P. amundseni*, which has a weaker seta. In addition, a single spine on the pereopods 2–6 merus differentiates *P. barossai* from all other congeners that have a combination of spine and seta, two setae or being naked at this position.

***Pseudotanais coonawarrai* sp. nov.**

This species is registered in ZooBank number: LSID urn:lsid:zoobank.org:act:9C6979E0-B0A2-47FE-8C4B-54B5CA2CAC39.

Diagnosis. Antenna articles 2–3 with spine. Mandible molar coronal with two distal spines. Pereopod-2 carpus blade-like spine short (0.4x propodus). Pereopods 2–6 merus with spine and seta. Uropod exopod 0.8x endopod.

Material examined. Holotype, neuter 2.9 mm, partly dissected (J62734), SLOPE 134.

Etymology. In the Bindjali Aboriginal language, coonawarra is honeysuckle and a wine region from southern Australia, as genitive.

Description of female. BL = 2.9 mm. Body robust (**Figure 8A**) 4.1 L:W. Cephalothorax 0.9 L:W, 1.1x pereonites 1–3, 0.2x BL. Pereonites 0.6x BL, pereonite-1 0.5x pereonite-2, pereonites 1–6: 0.2, 0.2, 0.4, 0.6, 0.7, and 0.6 L:W, respectively; pereonites 1, 4–6 with small anterolateral setae. Pleon short, 0.4x BL. Pleonites 0.9 L:W, pleonites 1–2 and 4–5 with dorsolateral pair of setae. Pleotelson 5.3x pleonite-5, with pair of laterodistal setae.

Antennule (**Figure 8B**) article-1 3.9 L:W, 2.8x article-2, with one simple and two penicillate midlength setae, and one simple and three penicillate distal setae; article-2 2.5 L:W, 1.2x article-3, with two simple setae and one distal penicillate seta; article-3 3.7 L:W, with one simple, one penicillate, four bifurcated setae and one aesthetasc.

Antenna (**Figure 8C**) article-2 1.1 L:W; 0.9x article-3, with spine (0.3x article-2); article-3 1.4 L:W, 0.3x article-4, with spine (0.2x article-3); article-4 6.2 L:W, 2.7x article-5, with middorsal penicillate seta, three simple and three penicillate distal setae; article-5 3.3 L:W, 7.7x article-6, with distal seta; article-6 0.5 L:W, with four distal setae.

Labrum (**Figure 8D**) rounded, finely setulate. Left mandible (**Figure 8E**) *lacinia mobilis* well developed, distally serrate, incisor distal margin beveled and serrate, molar coronal with two longer distal spines. Right mandible not recovered. Labium (**Figure 8F**)

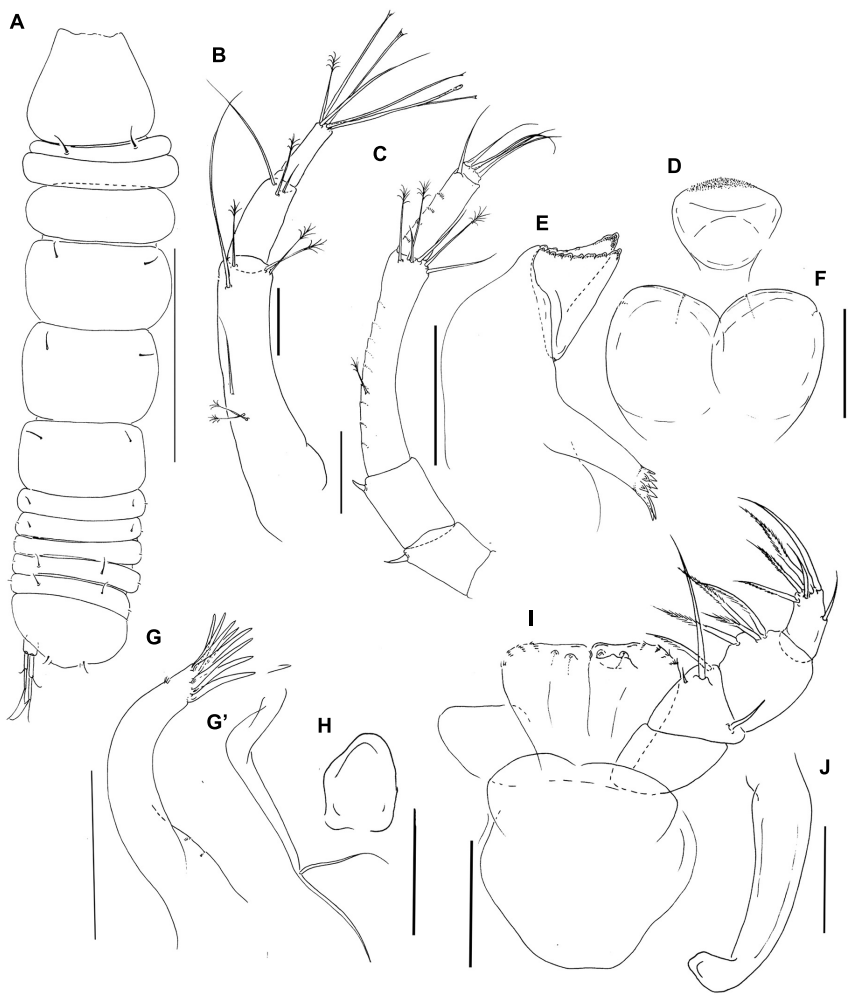

FIGURE 8 | *Pseudotanais coonawarrai* sp. nov; neuter (J62734), **(A)**, dorsal; **(B)**, antennule; **(C)**, antenna; **(D)**, labrum; **(E)**, left mandible; **(F)**, labium; **(G)**, maxillule; **(G')** maxillule endite; **(H)**, maxilla; **(I)**, maxilliped; **(J)**, epignath. Scale lines **(A)** = 1 mm, **(B–I)** = 0.1 mm.

simple, rounded, glabrous. Maxillule (**Figure 8G**) endite with eight distal spines and outer subdistal setae; palp (**Figure 8G'**) with two setae. Maxilla (**Figure 8H**) almost circular, naked.

Maxilliped (**Figure 8I**) palp article-1 1.2 L:W, naked, article-2 1.0 L:W, with fine outer and three inner setae (one minute, one very long); article-3 0.9 L:W, with one shorter and three longer inner setae, article-4 1.6 L:W, with one sub-distal and five distal setae. Maxilliped endites mostly fused but with distinct central cleft, each with two round gustatory cusps. Epignath (**Figure 8J**) linguiform, simple, naked.

Cheliped (**Figure 9A**) basis 1.5 L:W, naked; merus with ventral seta; carpus 1.6 L:W, 1.0x palm, with two midventral setae and middorsal seta; chela non-forcipate, palm 1.6 L:W with seta near the dactylus insertion; fixed finger 3.0 L:W, 0.7x palm, with three setae on cutting edge (ventral seta not seen); dactylus 4.7 L:W, cutting edge smooth, with dorsoproximal seta.

Pereopod-1 (**Figure 9B**) overall 14.3 L:W; basis 7.2 L:W, 4.0x merus, with one dorsoproximal and two (or three) ventral setae; ischium with ventral seta; merus 2.3 L:W and 0.8x carpus, with minute ventrodistal seta; carpus 2.4 L:W, 0.7x propodus, with one

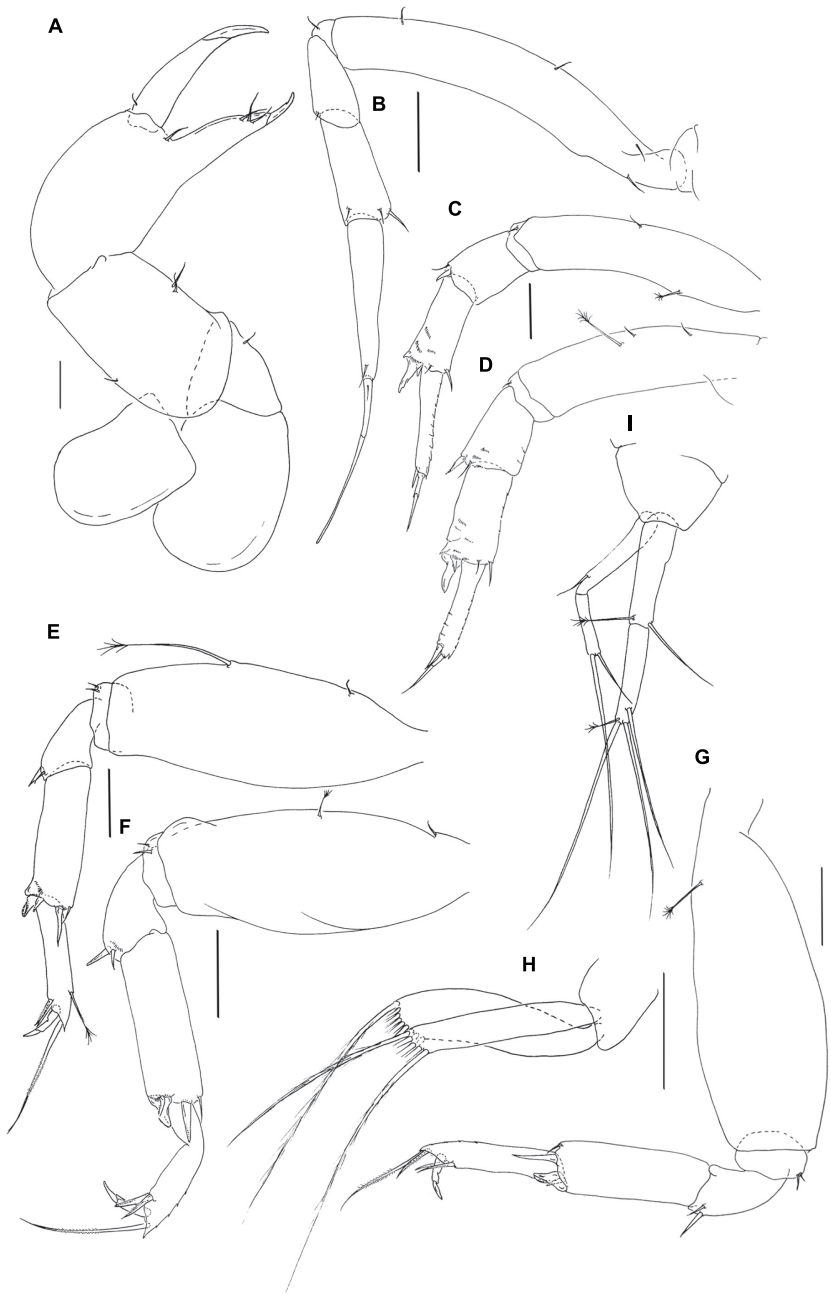

FIGURE 9 | *Pseudotanais coonawarrai* sp. nov.; neuter (J62734), **(A)**, cheliped; **(B)**, pereopod-1; **(C)**, pereopod-2, **(D)**, pereopod-3; **(E)**, pereopod-4; **(F)**, pereopod-5; **(G)**, pereopod-6; **(H)**, pleopod; **(I)**, uropod. Scale lines = 0.1 mm.

ventrodistal and two dorsodistal setae; propodus 4.4 L:W, 0.6x dactylus and unguis combined length, with one subdistal seta, dactylus 0.5x unguis, with proximal seta.

Pereopod-2 (**Figure 9C**) overall 9.6 L:W; basis 4.7 L:W, 4.3x merus, with mid-dorsal penicillate seta and mid-ventral simple seta; ischium with ventral seta; merus 1.1 L:W, 0.6x carpus, with seta and spine ventrodistally; carpus 2.3 L:W, 0.9x propodus, with dorsodistal seta, small distal seta, and short spine and blade-like spine (0.4x propodus) ventrodistally, several comb-like scales distally; propodus 5.0 L:W, 1.7x dactylus and unguis combined length, with one distal seta (0.3x dactylus and unguis combined length), with comb-like scales along dorsal margin; dactylus 0.5x unguis.

Pereopod-3 (**Figure 9D**) overall 15.9 L:W; basis 3.7 L:W, 2.9x merus, with two simple and one penicillate midventral setae; ischium with ventral seta; merus 1.4 L:W, 0.8x carpus, with seta and spine ventrodistally; carpus 2.0 L:W, 1.0x propodus, with dorsodistal seta, small seta, small spine and short ventrodistal blade-like spine (0.4x propodus) distally; propodus 4.5 L:W, 1.5x dactylus and unguis combined length, with one distal seta (0.4x dactylus and unguis combined length); dactylus 0.3x unguis.

Pereopod-4 (**Figure 9E**) overall 6.2 L:W; basis 2.5 L:W, 3.8x merus, with small simple ventroproximal seta and long penicillate midventral seta; ischium with two ventral setae; merus 1.3 L:W, 0.5x carpus, with seta and spine; carpus 3.3 L:W, 1.2x propodus, with one seta, two spines (short and longer) and short blade-like spine (0.2x propodus); propodus 4.7 L:W, 2.8x dactylus and unguis combined length, with two serrate ventrodistal setae and one serrate dorsal seta (2.3x dactylus and unguis combine length) and penicillate seta dorsally; dactylus 1.5x unguis.

Pereopod-5 (**Figure 9F**) overall 5.5 L:W; basis 2.7 L:W, 5.0x merus, with simple ventroproximal seta and short penicillate midventral seta; ischium with two ventral setae; merus 1.3 L:W, 0.4x carpus, with seta and spine; carpus 3.0 L:W, 1.2x propodus, with dorsodistal seta, two distal spines and short blade-like spine (0.2x propodus); propodus 4.6 L:W, 2.9x dactylus and unguis combined length, with two serrate ventrodistal setae and serrate dorsodistal seta (2.9x dactylus and unguis combined length); dactylus 1.7x unguis.

Pereopod-6 (**Figure 9G**) overall 5.4 L:W; basis 2.7 L:W, 4.6x merus, with proximal penicillate seta; ischium with two ventral setae; merus 1.6 L:W, 0.5x carpus, with seta and spine; carpus 2.7 L:W, 1.2x propodus, with one seta, two spines and short blade-like spine (0.3x propodus); propodus 4.6 L:W, 2.9x dactylus and unguis combined length, with two serrate ventral setae and two serrate dorsal setae (longer seta 2.5x dactylus and unguis combined length); dactylus 1.7x unguis.

Pleopods (**Figure 9H**) rami long and slender, exopod with five, endopod with nine setae.

Uropod (**Figure 9I**) peduncle 1.2 L:W; exopod with two articles; 9.5 L:W; article-1 6.0 L:W, with subdistal seta; article-2 4.7 L:W, with two setae distally; endopod 7.7 L:W; article-1 3.5 L:W, with one simple and one penicillate setae; article-2 4.5 L:W, with one subdistal and two simple setae, and one penicillate distal seta. Exopod 0.8x endopod.

Distribution. Species known only from the type locality off Cape Otway (SE Australia) at depth 1021 m.

Remarks. The combination of antenna articles 2–3 with spines, coronal mandible molar, short ventrodistal setae on the pereopod-1 merus and carpus, and slender uropods places *P. coonawarrai* sp. nov. in the "denticulatus + abathagastor" group. A spine on the antenna article-2 distinguishes the new species from *P. abathagastor* and *P. mariae*, which have a seta on this article, and from *P. barnesi*, which has this article naked. The uropod exopod, shorter than the endopod (0.8x), separates *P. coonawarrai* from *P. chaplini* and *P. oloughlini*, where exopod is 1.1x endopod, and from *P. palmeri* where the exopod and endopod are equal. The presence of a spine and seta on the merus of pereopods 4–6 separates *P. coonawarrai* from *P. biopearli*, *P. barossai*, *P. corollatus*, *P. georgesandae* and P. *locueloae,* which have a spine or two setae in this position. Finely, the absence of wide-based spines on pereopods 2–3 in *P. coonawarrai* is similar to *P. denticulatus* and *P. kitsoni* although it can be distinguished by a short pereopod-2 with an overall proportion of 9.6 L:W compared to > 13 L:W in *P. denticulatus* and *P. kitsoni*.

Key for the identification of *Pseudotanais* females of the "denticulatus + abathagastor" morpho-group.

1. Antenna article-3:
   with spine or seta.....2
   naked.....*P. barnesi*
2. Antenna article-3 with
   seta..... 3
   spine..... 4
3. Antenna article-2 with; pereopods 4–6 merus with:
   thin spine; spine and seta.....*P. amundseni*
   spine; two spines..... *P. elephas*
   seta; spine.....*P. mariae*
4. Pereopods 4–6 ischium with:
   one seta.....5
   two setae.....6
5. Antenna article-4 L:W ratio:
   < 7.0 L:W.....7
   > 9.2 L:W.....*P. locueloae*
6. Antenna article-4 L:W ratio
   < 8.2 L:W.....9
   > 8.3 L:W.....10
7. Antenna article-2 with:
   spine.....8
   seta..... *P. abathagastor*
8. Uropod exopod to endopod ratio:
   0.8x..... *P. livingstoni*
   1.1x. .....*P. oloughlini*
9. Antenna article-2 with:
   spine. 12
   seta..... *P. chopini*
10. Uropod exopod to endopod ratio:
    ≤ 0.9x0.....11
    ≥ 1.1x. .....*P. chaplini*
11. Uropod endopod L:W ratio; pereopod-3 carpus blade-like spine to propodus ratio; pereopod-6 carpus blade-like to propodus ratio:

9.0 L:W; 0.4x; 0.4x..... *P. biopearli*
9.6 L:W; 0.5x; 0.3x..... *P. denticulatus*
6.6 L:W; 0.3x; 0.2x..... *P. georgesandae*

12. Pereonite-1 to pereonite-2 length ratio:
≤ 0.6x.....13
0.9x.....*P. corollatus*
13. Uropod exopod L:W ratio:
≥ 8.2x.....14
6.6x.....*P. barossai* sp. nov.
14. Uropod endopod L:W ratio:
≤ 8.4 L:W.....15
10.0 L:W..... *P. kitsoni*
15. Antenna article-4 L:W; uropod exopod to endopod ratio:
6.7 L:W; 1.0x.....*P. palmeri*
6.2 L:W; 0.8x.....*P. coonawarrai* sp. nov.

***Pseudotanais shirazi* sp. nov.**

This species is registered in ZooBank number: LSID urn:lsid: zoobank.org:act:A52BE5EE-0195-4981-BBB2-7D9539660 95F.

Diagnosis. Antenna article 2–3 with seta. Mandible molar acuminate, with distal spines. Maxilliped endites fused with distinct central cleft, with one simple seta and two inner-distal tubercles. Chela non-forcipate, smooth on dorsal margin. Pereopods 4–6 unguis simple (not bifurcated).

Material examined. Holotype, neuter 1.8 mm (J59677), SLOPE 67. Paratype, female dissected 2.1mm (J61517), neuter 1.9 mm (J74952), SLOPE 40; neuter, broken (J62733), SLOPE 53.

Etymology. Shiraz is a grape varied, mostly used in Australia and South Africa, as genitive.

Description of female. BL = 2.1 mm. Body robust (**Figures 10A,B**) 3.3 L:W. Cephalothorax 0.8 L:W, 1.3x pereonites 1–3, 0.2x BL, with subocular pair of setae on. Pereonites 0.8x BL, pereonite-1 0.4x pereonit-2, pereonites-1–6: 0.1, 0.2, 0.3, 0.5, 0.6, and 0.3 L:W, respectively; pereonite 1 with midlateral seta; pereonites 3–5 each with a pair of small lateral setae. Pleon short, 0.2x BL. Pleonites 0.7 L:W, pleonite-4 with pair of dorsal setae, pereonite-5 with two pairs of setae on each side of midline. Pleotelson 1.2x pleonite-5, with pair of simple and penicillate laterodistal setae.

Antennule (**Figure 10C**) article-1 3.9 L:W, 2.5x article-2, with one simple and three penicillate midlength setae, and one simple subdistal and three penicillate distal setae; article-2 2.5 L:W, 1.3x article-3, with two simple and one penicillate distal setae; article-3 2.5 L:W, with five simple setae and one penicillate seta, aesthetasc not seen.

Antenna (**Figure 10D**) article-1 destroyed during dissection; article-2 1.3 L:W; 1.3x article-3, with seta (0.3x article-2); article-3 1.3 L:W, 0.3x article-4, with seta (0.5x article-3); article-4 6.3 L:W, 2.0x article-5, with three simple and three penicillate subdistal or distal setae; article-5 3.2 L:W, 9.5x article-6, with simple seta; article-6 0.5 L:W, with four simple setae.

Labrum (**Figure 10E**) rounded, naked. Left mandible (**Figure 10F**) lacinia mobilis well developed, distally serrate, incisor distal margin beveled, serrate. Right mandible (**Figure 10G**) incisor unequally bifid, distal margin serrate, molar acuminate with distal spines. Labium (**Figure 10I**) simple, slightly rectangular, glabrous. Maxillule (**Figure 10H**) endite with ten distal spines and several outer subdistal setae. Maxilla not recovered. Maxilliped (**Figure 10J**) basis with seta, little shorter than endites; palp article-1 naked, article-2 1.2 L:W with fine outer and three inner setae; article-3 1.4 L:W with one shorter and three longer inner setae; article-4 1.9 L:W with one subdistal and five distal setae.

Maxilliped endites mostly fused but with distinct central cleft, each with small middle seta and two gustatory cusps. Epignath (**Figure 10K**) linguiform, simple distally rounded.

Cheliped (**Figure 11A**) basis distally broken; merus with ventral seta; carpus 1.3 L:W, 1.0x palm, with two midventral setae, and one mid-dorsal and one dorsodistal small setae; chela non-forcipate, palm 1.3 L:W; fixed finger 3.0 L:W, 0.8x palm with one ventral seta, three setae on cutting edge, and one simple seta near dactylus insertion; dactylus 3.8 L:W, cutting edge smooth, without proximal seta.

Pereopod-1 (**Figure 11B**) overall 14.3 L:W; basis 7.5 L:W, 4.2x merus, with dorsoproximal seta; ischium with ventral seta; merus 2.0 L:W and 0.9x carpus, with two ventrodistal setae (short and long); carpus 2.5 L:W, 0.7x propodus, with two dorsodistal and one ventrodistal setae; propodus 4.3 L:W, 0.9x dactylus and unguis combined length, with one long ventrodistal seta; dactylus 0.4x unguis with proximal seta.

Pereopod-2 (**Figure 11C**) overall 13.4 L:W; coxa with seta; basis 7.0 L:W, 4.5x merus, with middorsal penicillate seta; ischium with ventral seta; merus 1.5 L:W, 0.6x carpus, with ventrodistal seta; carpus 2.5 L:W, 1.0x propodus, with dorsodistal spine, short ventrodistal spine and short blade-like spine (0.2x propodus); propodus 5.2 L:W, 1.5x dactylus and unguis combined length, with ventroproximal seta (0.2x dactylus and unguis combined length); dactylus 0.7x unguis.

Pereopod-3 (**Figure 11D**) overall 19.3 L:W; basis 2.6 L:W, 2.1x merus, with midventral penicillate seta; ischium with ventral seta; merus 1.3 L:W, 0.8x carpus, with two ventrodistal setae; carpus 2.0 L:W, 1.1x propodus, with dorsodistal spine, short ventrodistal spine and short blade-like spine (0.2x propodus); propodus 3.6 L:W, 1.6x dactylus and unguis combined length, with ventrodistal spine (0.3x dactylus); dactylus 0.8x unguis.

Pereopod-4 (**Figure 11E**) overall 5.0 L:W; basis 2.3 L:W, 3.7x merus, naked; ischium with ventral seta (second seta not seen); merus 1.5 L:W, 0.6x carpus, with two ventrodistal spines and several comb-like scales; carpus 3.3 L:W, 1.2x propodus, with two long spines and short blade-like spine (0.1x propodus); propodus 4.2 L:W, 3.6x dactylus and unguis combined length, with penicillate dorsal setae, two serrate ventrodistal spines and one serrate dorsodistal seta (1.5x dactylus and unguis combined length); dactylus 1.8x unguis.

Pereopod-5 (**Figure 11F**) overall 4.6 L:W; basis 2.3 L:W, 3.9x merus, with two midventral penicillate setae; ischium with two ventral setae; merus 1.6 L:W, 0.6x carpus, with two spines; carpus 2.8 L:W, 1.1x propodus, with dorsodistal seta and short blade-like spine (0.1x propodus) (spines not seen); propodus 4.0 L:W, 3.3x dactylus and unguis combined length, with penicillate dorsal seta, two serrate ventrodistal spines, and one

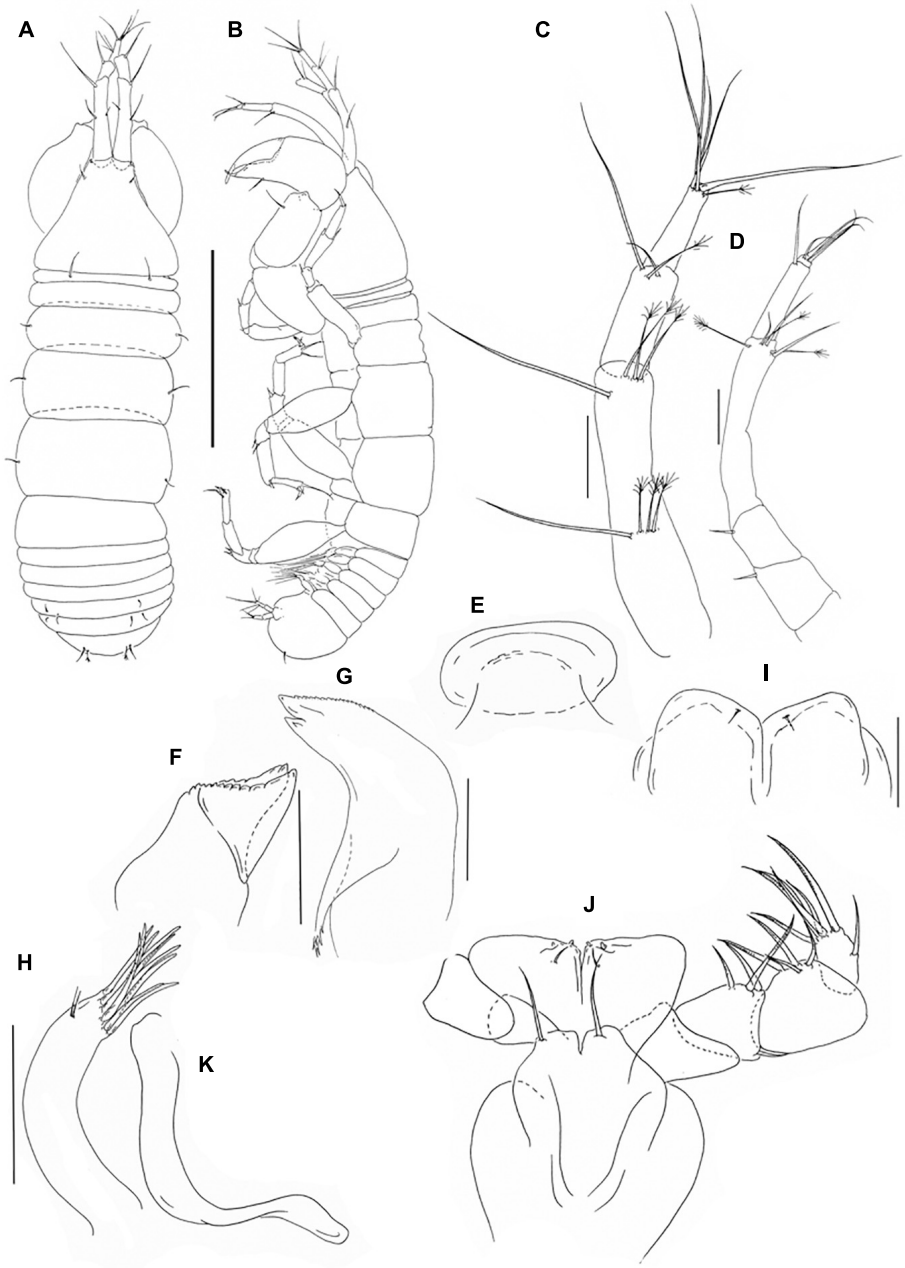

FIGURE 10 | *Pseudotanais shirazi* sp. nov; neuter (J59677), **(A)**, dorsal; **(B)**, lateral; **(C)**, antennule; **(D)**, antenna; **(E)**, labrum; **(F)**, left mandible; **(G)**, right mandible; **(H)**, maxillule; endite; **(I)**, labium; **(J)**, maxilliped; **(K)**, epignath. Scale lines **(A,B)** = 1 mm, **(C–J)** = 0.1 mm.

serrate dorsal seta (1.5x dactylus and unguis combined length); dactylus 3.0x unguis.

Pereopod-6 (**Figure 11G**) overall 5.4 L:W; basis 2.5 L:W, 3.3x merus, with minute ventroproximal seta; ischium with two ventral setae; merus 2.0 L:W, 0.8x carpus, with two spines; carpus 1.2 L:W, 0.9x propodus, with dorsodistal seta, two distal spines, and short blade-like spine (0.1x propodus); propodus 4.8 L:W, 6.0x dactylus and unguis combined length, with two serrate ventral setae and two serrate dorsal setae (longer setae 2.5x dactylus and unguis combined length); dactylus 2.0x unguis.

Pleopods (**Figure 11H**) rami long and slender, exopod with six, endopod with eight setae.

Uropod (**Figure 11I**) peduncle 1.3 L:W; exopod with two articles; 7.8 L:W; article-1 1.3 L:W, with distal seta; article-2 2.8 L:W, with two long setae; endopod 7.0 L:W; article-1 3.5 L:W, with one simple and two penicillate setae; article-2 4.2 L:W, with one subdistal and five distal setae. Exopod 0.7x endopod.

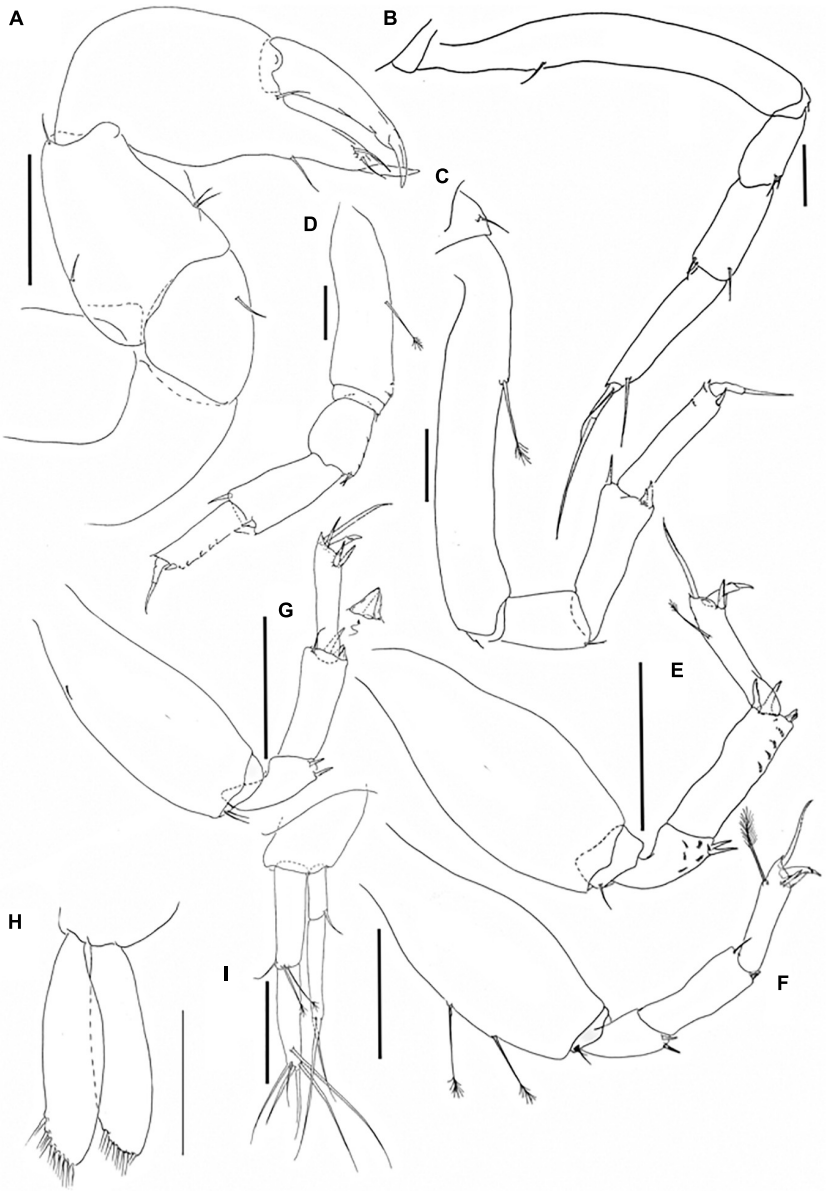

FIGURE 11 | *Pseudotanais shirazi* sp. nov.; neuter (J74952), **(A)**, cheliped; **(B)**, pereopod-1; **(C)**, pereopod-2, **(D)**, pereopod-3; **(E)**, pereopod-4; **(F)**, pereopod-5; **(G)**, pereopod-6; **(H)**, pleopod; **(I)**, uropod. Scale lines = 0.1 mm.

Distribution. The species is known from off Gippsland and Jervis Point SE Australia, at depths 400–1277 m.

Remarks. *Pseudotanais shirazi* sp. nov., with short conical blade like-spines on the carpus of pereopods 2–6, is the second species after *P. intortus* with this shape. Its maxilliped endites with a distinct medial cleft and each with one simple seta and two tubercles, distinguish it from *P. intortus* where the maxilliped endites are fused and each have only one tubercle. Additionally, the blade-like spine in pereopod-2 in *P. shirazi* is conical while, in *P. intortus* pereopod-2 is more flattened, with the cavity in the central part. A short propodal seta on pereopods 2–3 (0.2x dactylus and unguis combined length) in *P. shirazi* is different from *P. intortus*, where this spine is almost as long as dactylus and unguis combined length (0.8x). Finally, the pereopods 4–6 unguis is simple in contrast to *P. intortus* with a bifurcated unguis.

DISCUSSION

The present study provides for the first time information about Pseudotanaidae species from the continental margin of SE Australia near Bass Strait. From five species, two occurred off eastern coast between Gippsland and Jervis Point (*P. shirazi* and *P. chardonnayi*), and three on the southern coast between Great Otway (Otway Point) and Kangaroo Island (*P. caberneti*,

P. barossai and *P. coonawarrai*) (**Figure 12**). These five species bring the total number of described pseudotanaid species to 94. Until now the family was represented in Australian waters by only one species – the shallow-water *Akanthinotanais scrappi* (Bamber, 2005). Remarkably, the family is apparently absent in the well sampled Bass Strait (Błażewicz-Paszkowycz and Bamber, 2012; Bamber and Błażewicz-Paszkowycz, 2013), but they were recorded at the deeper shelf (around 100 m) and at the slope of West Australia (Bamber, 2005; McCallum et al., 2015; Poore et al., 2015); also, it was recorded in two locations of Great Barrier Reef *e.g.*, Lizard and Heron Is; (Stępień et al., 2018). Unfortunately, these collections were not identified to species level.

The Pseudotanaidae is cosmopolitan family that encompass all biogeographic zones (Watling et al., 2013). Collated literature date on the distribution of currently recognized pseudotanaid genera and the morpho-groups, allow to group pseudotanaids into few categories (**Table 2** and **Figure 13**):

- *Akanthinotanais* and "forcipatus" can be common on the shelf from the tropics to polar regions and have been only occasionally recorded below the continental margin (Sieg, 1977; Bird and Holdich, 1989a,b) or the abyssal (Jakiel et al., 2019). The former is still relatively understudied because of its relative scarcity, and exhibits a range of morphologies that may encompass several genera, even in a separate family;
- "denticulatus + abathagastor" and "affinis + longisetosus" represent deep-sea fauna, but several species have been recorded on the shelf of polar regions. This distribution supports a polar emergence phenomenon observed for several taxa (Wilson, 1998; Berkman et al., 2004; Błażewicz-Paszkowycz, 2005; Raupach et al., 2012). With some probability, this group could also be represented by *Beksitanais*, although this assumption could be revised when more records become available;
- "spicatus" is recorded on the upper, lower slope and in the abyss;
- *Parapseudotanais* is recorded only from the abyss;
- *Mystriocentrus* is known from lower slope and the abyss.

To confirm that *Parapseudotanais* and *Mystriocentrus* are deep-water genera requires more data. The species provisionally classified to the "colonus" group does not reveal a clear distribution pattern that suggest an artificial (non-monophyletic) character of the group.

Apart from the Pseudotanaidae, in general, the peracarid fauna of Australian coast is very diverse (Poore et al., 1994; Lowry and Stoddard, 2003; Poore and Bruce, 2012). With that background, tanaids are represented by 162 species in 66 genera (Edgar, 1997, 2008, 2012; Bamber, 2005, 2008; Błażewicz-Paszkowycz and Bamber, 2007, 2009, 2012; Jóźwiak and Błażewicz, 2021). This situation is apparently worse at the shelf break where only nine species from seven genera and

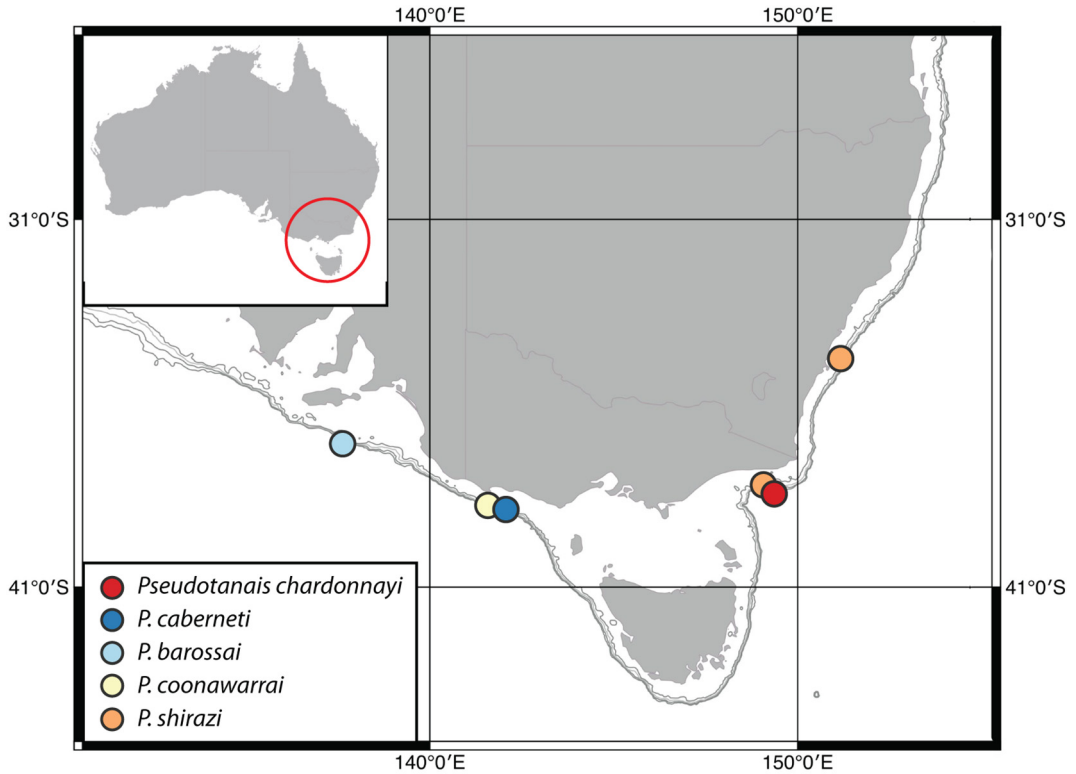

FIGURE 12 | Distribution of Pseudotanaidae (described in this study) on the coast of SE Australia.

TABLE 2 | Classification of Pseudotanaidae to genera and morpho-groups according to Bird and Holdich (1989b) and McLelland (2007).

Group	Species	Ocean	Depth zone	Province
"affinis + longisetosus"	*P. affinis*	Atlantic	shelf	Arctic
"affinis + longisetosus"	*P. macrocheles*	Atlantic	shelf	Northern European Seas
"affinis + longisetosus"	*P. rapunzelae*	Southern	shelf	Scotia Sea
"affinis + longisetosus"	*P. shackletoni*	Southern	shelf	Scotia Sea
"affinis + longisetosus"	*P. chardonnayi*	Pacific	upper slope	NZ-Kermadec
"affinis + longisetosus"	*P. caberneti*	Pacific	upper slope	Subantarctic
"affinis + longisetosus"	*P. longispinus*	Atlantic	lower slope	North Atlantic
"affinis + longisetosus"	*P. scalpellum*	Atlantic	lower slope	North Atlantic
"affinis + longisetosus"	*P. spatula*	Atlantic	lower slope	North Atlantic
"affinis + longisetosus"	*P. svavarssoni*	Atlantic	lower slope	North Atlantic
"affinis + longisetosus"	*P. nipponicus*	Pacific	lower slope	Northern Pacific Boreal
"affinis + longisetosus"	*P. longisetosus*	Southern	lower slope	Antarctic
"affinis + longisetosus"	*P. nordenskioldi*	Southern	lower slope	Antarctic
"affinis + longisetosus"	*P. gaiea*	Pacific	abyssal	Equatorial Pacific
"affinis + longisetosus"	*P. geralti*	Pacific	abyssal	Equatorial Pacific
"affinis + longisetosus"	*P. julietae*	Pacific	abyssal	Equatorial Pacific
"affinis + longisetosus"	*P. romeo*	Pacific	abyssal	Equatorial Pacific
"affinis + longisetosus"	*P. uranos*	Pacific	abyssal	Equatorial Pacific
"affinis + longisetosus"	*P. yenneferae*	Pacific	abyssal	Equatorial Pacific
"affinis + longisetosus"	*P. chanelae*	Pacific	abyssal	North Pacific
"affinis + longisetosus"	*P. curieae*	Pacific	abyssal	North Pacific
"affinis + longisetosus"	*P. monroeae*	Pacific	abyssal	North Pacific
"affinis + longisetosus"	*P. szymborskae*	Pacific	abyssal	North Pacific
"affinis + longisetosus"	*P. vitjazi*	Pacific	abyssal	North Pacific
Akanthinotanais	*A. breviaquas*	Atlantic	shelf	Lusitanian
Akanthinotanais	*A. siegi*	Atlantic	shelf	Lusitanian
Akanthinotanais	*A. similis*	Atlantic	shelf	Northern European Seas
Akanthinotanais	*A. mortenseni*	Atlantic	shelf	Warm Temperate Northwest Atlantic
Akanthinotanais	*A. scrappi*	Indian	shelf	Southwest Australian Shelf
Akanthinotanais	*A. gerlachi*	Indian	shelf	Central Indian Ocean Islands
Akanthinotanais	*A. malayensis*	Pacific	shelf	Marshall, Gilbert, and Ellis Islands
Akanthinotanais	*A. pedecerritulus*	Indian	shelf	South Kuroshio
Akanthinotanais	*A. gaussi*	Southern	shelf	Scotia Sea
Akanthinotanais	*A. guillei*	Southern	shelf	Scotia Sea
Akanthinotanais	*A. rossi*	Southern	shelf	Scotia Sea
Akanthinotanais	*A. kurchatovi*	Atlantic	upper slope	N Atlantic
Akanthinotanais	*A. makrothrix*	Pacific	upper slope	Cocos Plate
Akanthinotanais	*A. longipes*	Atlantic	lower slope	Northern Atlantic Boreal
Beksitanais	*B. vanhoeffeni*	Southern	shelf	Amundsen/Bellingshausen Sea
Beksitanais	*B. abyssi*	Atlantic	lower slope	Northern Atlantic Boreal
Beksitanais	*B. apocalyptica*	Pacific	abyssal	Equatorial Pacific
"colonus"	*P. borceai*	Atlantic	shelf	Black Sea
"colonus"	*P. lilljeborgi*	Atlantic	shelf	Northern European Seas
"colonus"	*P. falcifer*	Atlantic	upper slope	N Atlantic
"colonus"	*P. sigrunis*	Atlantic	upper slope	N Atlantic
"colonus"	*P. colonus*	Atlantic	lower slope	North Atlantic
"colonus"	*P. baresnauti*	Atlantic	abyssal	North Atlantic
"denticulatus + abathagastor"	*P. crassicornis*	Atlantic	shelf	Arctic
"denticulatus + abathagastor"	*P. amundseni*	Southern	shelf	Amundsen/Bellingshausen Sea
"denticulatus + abathagastor"	*P. barnesi*	Southern	shelf	Amundsen/Bellingshausen Sea
"denticulatus + abathagastor"	*P. biopearli*	Southern	shelf	Amundsen/Bellingshausen Sea
"denticulatus + abathagastor"	*P. kitsoni*	Southern	shelf	Amundsen/Bellingshausen Sea
"denticulatus + abathagastor"	*P. elephas*	Southern	shelf	Scotia Sea

(Continued)

TABLE 2 | (Continued)

Group	Species	Ocean	Depth zone	Province
"denticulatus + abathagastor"	*P. livingstoni*	Southern	shelf	Scotia Sea
"denticulatus + abathagastor"	*P. palmeri*	Southern	shelf	Scotia Sea
"denticulatus + abathagastor"	*P. abathagastor*	Pacific	upper slope	N Pacific Boreal
"denticulatus + abathagastor"	*P. denticulatus*	Atlantic	lower slope	North Atlantic
"denticulatus + abathagastor"	*P. corollatus*	Atlantic	lower slope	Northern Atlantic Boreal
"denticulatus + abathagastor"	*P. coonawarrai*	Pacific	lower slope	Subantarctic
"denticulatus + abathagastor"	*P. barrossai*	Pacific	lower slope	Subantarctic
"denticulatus + abathagastor"	*P. chaplini*	Pacific	abyssal	Equatorial Pacific
"denticulatus + abathagastor"	*P. chopini*	Pacific	abyssal	Equatorial Pacific
"denticulatus + abathagastor"	*P. georgesandae*	Pacific	abyssal	Equatorial Pacific
"denticulatus + abathagastor"	*P. mariae*	Pacific	abyssal	Equatorial Pacific
"denticulatus + abathagastor"	*P. oloughlini*	Pacific	abyssal	Equatorial Pacific
"denticulatus + abathagastor"	*P. locueolae*	Pacific	abyssal	North Pacific
"forcipatus"	*P. isabelae*	Atlantic	shelf	Mediterranean Sea
"forcipatus"	*P. mediterraneus*	Atlantic	shelf	Mediterranean Sea
"forcipatus"	*P. stiletto*	Atlantic	shelf	Mediterranean Sea
"forcipatus"	*P. unicus*	Atlantic	shelf	Mediterranean Sea
"forcipatus"	*P. forcipatus*	Atlantic	shelf	Northern European Seas
"forcipatus"	*P. jonesi*	Atlantic	shelf	Northern European Seas
"forcipatus"	*P. mexikolpos*	Atlantic	shelf	Warm Temperate Northwest Atlantic
"forcipatus"	*P. californensis*	Pacific	shelf	Tropical East Pacific
"forcipatus"	*P. enduranceae*	Southern	shelf	Amundsen/Bellingshausen Sea
"forcipatus"	*P. discoveryae*	Southern	shelf	Scotia Sea
"forcipatus"	*P. scotti*	Southern	shelf	Scotia Sea
"forcipatus"	*P. artoo*	Atlantic	upper slope	S Atlantic
"forcipatus"	*P. soja*	Pacific	upper slope	N Pacific Boreal
"forcipatus"	*P. falcicula*	Atlantic	lower slope	North Atlantic
"forcipatus"	*P. vulsella*	Atlantic	lower slope	North Atlantic
"forcipatus"	*P. misericorde*	Atlantic	lower slope	Northern Atlantic Boreal
"forcipatus"	*P. inflatus*	Pacific	abyssal	North Pacific
not classified	*P. intortus*	Pacific	upper slope	N Pacific Boreal
Mystriocentrus	*M. serratus*	Atlantic	lower slope	North Atlantic
Mystriocentrus	*M. biho*	Atlantic	lower slope	Northern Atlantic Boreal
Mystriocentrus	*M. hollandae*	Pacific	abyssal	North Pacific
not classified	*P. oculatus*	Atlantic	shelf	Arctic
Parapseudotanais	*P. abyssalis*	Atlantic	abyssal	Arctic Basin
not classified	*P. shirazi*	Pacific	upper slope	NZ-Kermadec
spicatus	*P. tympanobaculum*	Pacific	upper slope	N Pacific Boreal
spicatus	*P. spicatus*	Atlantic	lower slope	North Atlantic
spicatus	*P. kobro*	Pacific	abyssal	Equatorial Pacific

The zoogeographical and bathymetrical classification according to Spalding et al. (2007) and Watling et al. (2013).

four families (Apseudidae: one species; Agathotanaidae: two species, Anarthruridae six species, Paratanaidae: one species) are formally described (three species were described from SE Australia) (Larsen and Heard, 2001; Jóźwiak and Jakiel, 2012; Bamber and Błażewicz-Paszkowycz, 2013; Gellert and Błażewicz, 2018). For this reason tanaids are regarded as a comparatively non-diverse group, especially when compared to the other well studied taxa as Isopoda being represented in SE Australia by 51 families (Poore et al., 1994). However, exploration of the deeper shelf and slope of W Australia (McCallum et al., 2015; Poore et al., 2015) proves that tanaids below the continental break are diverse and the perceived lack of diversity mentioned above may be an illusion. The collection of Pseudotanaidae that we studied here is too limited to draw a conclusion about zoogeographical relationships and their link to the complex geological/tectonic history of SE Australia.

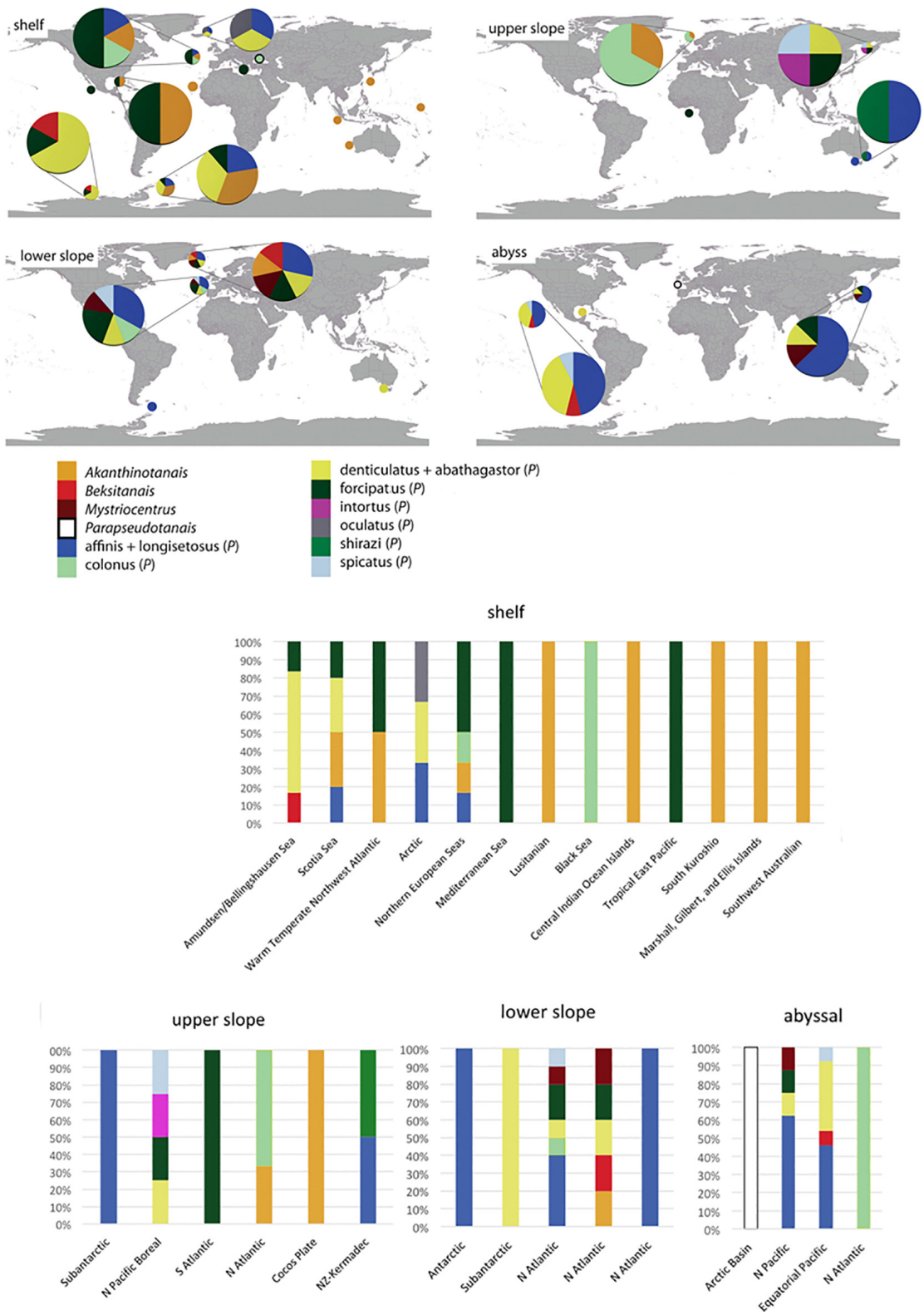

FIGURE 13 | Distribution of pseudotanaid genera and morpho-groups according to Bird and Holdich (1989b) and McLelland (2007) (for details see **Table 2**). The zoogeographical and bathymetrical classification according to Spalding et al. (2007) and Watling et al. (2013). The size of the pies corresponds to the number of species recorded.

DATA AVAILABILITY STATEMENT

This article is registered in ZooBank number: LSID urn:lsid:zoobank.org:pub:B15F3ACF-2FCC-4A3F-9EDC-0811EE99B9C6.

AUTHOR CONTRIBUTIONS

MB did the general concept and identification of the material. MB and AJ did the species, description, manuscript editing and figures editing. GB did the discussion and manuscript editing. All authors contributed to the article and approved the submitted version.

FUNDING

This work was supported by NCN Sonatina (2020/36/C/NZ8/00576) and NCN OPUS (2018/31/B/3115 NZ8/03198).

ACKNOWLEDGMENTS

We would like to thank to the staff from the Department Marine Invertebrate of Melbourne Museum (VIC, Australia), especially to Gary Poore for collecting the material, and to Mel McKenzie and Jo Taylor for careful curating that lovely and unique tanaid collection.

REFERENCES

Bamber, R. N. (2005). The tanaidaceans (Arthropoda: Crustacea: Peracarida: Tanaidacea) of Esperance, Western Australia, Australia. *Mar. Flora Fauna Esperance West. Aust. West. Aust. Museum Perth* 1963, 613–728.

Bamber, R. N. (2008). Tanaidaceans (Crustacea: Peracarida: Tanaidacea) from Moreton Bay, Queensland. *Mem. Queensl. Museum* 54, 143–218.

Bamber, R. N., and Błażewicz-Paszkowycz, M. (2013). Another inordinate fondness: diversity of the tanaidacean fauna of Australia, with description of three new taxa. *J. Nat. Hist.* 47, 25–28. doi: 10.1080/00222933.2012.742164

Bamber, R. N., Bird, G., Błażewicz-Paszkowycz, M., and Galil, B. (2009). Tanaidaceans (Crustacea: Malacostraca: Peracarida) from soft-sediment habitats off Israel, eastern Mediterranean. *Zootaxa* 2109, 1–44.

Berkman, P. A., Cattaneo-Vietti, R., Chiantore, M., and Howard-Williams, C. (2004). Polar emergence and the influence of increased sea-ice extent on the Cenozoic biogeography of pectinid molluscs in Antarctic coastal areas. *Deep. Res. Part II Top. Stud. Oceanogr.* 51, 1839–1855. doi: 10.1016/j.dsr2.2004.07.017

Bird, G. J. (1999). A new species of Pseudotanais (Crustacea, Tanaidacea) from cold seeps in the deep Caribbean, collected by the French submersible Nautile. *Zoosystema* 21, 445–451.

Bird, G. J., and Holdich, D. M. (1984). New deep-sea leptognathiid tanaids (Crustacea, Tanaidacea) from the north-east Atlantic. *Zool. Scr.* 13, 285–315. doi: 10.1111/j.1463-6409.1984.tb00044.x

Bird, G. J., and Holdich, D. M. (1989b). Tanaidacea (Crustacea) of the north−east Atlantic: the subfamily Pseudotanainae (Pseudotanaidae) and the family Nototanaidae. *Zool. J. Linn. Soc.* 97, 233–298. doi: 10.1111/j.1096-3642.1989.tb00548.x

Bird, G. J., and Holdich, D. M. (1989a). Recolonisation of artificial sediments in the deep Bay of Biscay by tanaidaceans (Crustacea: Peracarida), with a description of a new species of Pseudotanais. *J. Mar. Biol. Assoc. U K.* 69, 307–317. doi: 10.1017/S0025315400029428

Błażewicz, M., Jakiel, A., Bamber, R. N., and Bird, G. J. (2021). Pseudotanaidae Sieg, 1976 (Crustacea: Peracarida) from the Southern Ocean: diversity and bathymetric pattern. *Eur. Zool. J.* 2021, 1–76.

Błażewicz, M., Stępień, A., Jakiel, A., and Palero, F. (2020). "Biogeographic atlas of the deep NW Pacific fauna," in *Biogeographic Atlas of the Deep NW Pacific Fauna*, eds H. Saeedi and A. Brandt (Sofia: Pensoft), 462–500. doi: 10.3897/ab.e51315

Błażewicz-Paszkowycz, M. (2005). Revision of the genus *Peraeospinosus* Sieg, 1986 (Crustacea: Peracarida: Tanaidacea). *J. Nat. Hist.* 39, 3847–3901. doi: 10.1080/00222930500450879

Błażewicz-Paszkowycz, M., and Bamber, R. N. (2007). New apseudomorph tanaidaceans (Crustacea: Peracarida: Tanaidacea) from eastern Australia: Apseudidae, Whiteleggiidae, Metapseudidae and Pagurapseudidae. *Mem. Museum Victoria* 64, 107–148.

Błażewicz-Paszkowycz, M., and Bamber, R. N. (2009). A new genus of a new austral family of paratanaoid tanaidacean (Crustacea: Peracarida: Tanaidacea), with two new species. *Mem. Museum Victoria* 66, 5–15.

Błażewicz-Paszkowycz, M., and Bamber, R. N. (2011). Tanaidomorph tanaidacea (crustacea: Peracarida) from mud-volcano and seep sites on the Norwegian Margin. *Zootaxa* 3061, 1–35.

Błażewicz-Paszkowycz, M., and Bamber, R. N. (2012). The shallow-water Tanaidacea (Arthropoda: Malacostraca: Peracarida) of the Bass Strait, Victoria, Australia (other than the Tanaidae). *Mem. Museum Victoria* 69, 1–235. doi: 10.24199/j.mmv.2012.69.01

Edgar, G. J. (1997). A new genus and three new species of Apseudomorph Tanaidacean (Crustacea) From the Darwin region. *Proc. Sixth Int. Mar. Biol. Work. Mar. Flora Fauna Darwin Harbour North Territ. Aust.* 1997, 279–299.

Edgar, G. J. (2008). Shallow water Tanaidae (Crustacea: Tanaidacea) of Australia. *Zootaxa* 1836, 1–92.

Edgar, G. J. (2012). New Leptocheliidae (Crustacea: Tanaidacea: Tanaidomorpha) from Australian seagrass and macro-algal habitats, and a redescription of the poorly-known Leptochelia ignota from Sydney Harbour. *Zootaxa* 3276, 1–37. doi: 10.11646/zootaxa.3926.4.10

Francesca, P., Mevenkamp, L., Pape, E., Błażewicz, M., Bonifácio, P., Riehl, T., et al. (2021). A local scale analysis of manganese nodules influence on the Clarion-Clipperton Fracture Zone macrobenthos. *Deep Res. Part I Oceanogr. Res. Pap.* 168:103449. doi: 10.1016/j.dsr.2020.103449

Gellert, M., and Błażewicz, M. (2018). New species of Anarthruridae (Tanaidacea: Crustacea) of the western Australian slope. *Mar. Biodivers.* 49, 583–601. doi: 10.1007/s12526-017-0826-9

Jakiel, A., Palero, F., and Błażewicz, M. (2019). Deep ocean seascape and Pseudotanaidae (Crustacea: Tanaidacea) diversity at the Clarion-Clipperton Fracture Zone. *Sci. Rep.* 9:17305.

Jakiel, A., Palero, F., and Błażewicz, M. (2020). Secrets from the deep: Pseudotanaidae (Crustacea: Tanaidacea) diversity from the Kuril–Kamchatka Trench. *Prog. Oceanogr.* 183:102288. doi: 10.1016/j.pocean.2020.102288

Jakiel, A., Stępień, A., and Błażewicz, M. (2018). A tip of the iceberg — Pseudotanaidae (Tanaidacea) diversity in the North Atlantic. *Mar. Biodivers.* 48, 859–895. doi: 10.1007/s12526-018-0881-x

Jakiel, A., Stępień, A., Jóźwiak, P., Serigstad, B., and Błażewicz-Paszkowycz, M. (2015). First record of Tanaidacea (Crustacea) from a deep-sea coral reef in the Gulf of Guinea. *Zootaxa* 3991, 203–228. doi: 10.11646/zootaxa.3995.1.18

Jennings, R. M., Etter, R. J., and Ficarra, L. (2013). Population differentiation and species formation in the deep sea: the potential role of environmental gradients and depth. *PLoS One* 8:e77594. doi: 10.1371/journal.pone.0077594

Jóźwiak, P., and Błażewicz, M. (2021). *Muvi schmallenbergi* gen. nov., sp. nov. (Crustacea, Tanaidacea) from the southeast Australian coast, with comments on the distribution and habitat preferences of Chondropodinae. *PeerJ* 9:e11607. doi: 10.7717/peerj.11607

Jóźwiak, P., and Jakiel, A. (2012). A new genus and new species of Agathotanaidae (Crustacea, Tanaidacea) from West Australia. *Zookeys* 243, 15–26. doi: 10.3897/zookeys.243.3408

Kaiser, S., Lörz, A.-N., Bird, G., Malyutina, M., and Bowden, D. (2018). Benthic boundary layer macrofauna from the upper slope of the Chatham Rise (SW Pacific). *Mar. Ecol.* 2018:e12521. doi: 10.1111/maec.12521

Kudinova-Pasternak, R. (1993). Tanaidacea (Crustacea, Malacostraca) collected in the 43 cruize of the R/V "Dmitri Mendeleev" in the South-western Atlantic and the Weddell Sea.– Trudy Instituta okeanologii. *Akad. Nauk SSSR* 127, 134–145.

Lang, K. (1949). Contribution to the systematics and synonymics of the Tanaidacea. *Ark. För Zool.* 42, 1–14.

Larsen, K., and Heard, R. W. (2001). A new tanaidacean subfamily, Bathytanaidinae (Crustacea: Paratanaididae), from the Australian continental shelf and slope. *Zootaxa* 19, 1–22. doi: 10.11646/zootaxa.19.1.1

Lowry, J. K., and Stoddard, H. E. (2003). *Zoological catalogue of Australia, 19.2B. Crustacea: Malacostraca: Peracarida: Amphipoda, Cumacea, Mysidacea*. Canberra: CISRO Publishing.

McCallum, A. W., Woolley, S., Błażewicz-Paszkowycz, M., Browne, J., Gerken, S., Kloser, R., et al. (2015). Productivity enhances benthic species richness along an oligotrophic Indian Ocean continental margin. *Glob. Ecol. Biogeogr.* 24, 462–471. doi: 10.1111/geb.12255

McLelland, J. A. (2007). Family Pseudotanaidae Sieg, 1976. *Zootaxa* 1599, 87–99. doi: 10.11646/zootaxa.1599.1.5

McLelland, J. A. (2008). *A Systematic and Taxonomic Review of the Family Pseudotanaidae (Crustacea: Peracarida: Tanaidacea) Based Primarily on Morphometric Cladistic Analyses.* Ph. Dissetation, 298.

Menot, L., Sibuet, M., Carney, R. S., Levin, L. A., Rowe, G. T., David, S. M., et al. (2010). "New perceptions of continental margin biodiversity," in *Life in the World's Oceans: Diversity, Distribution, and Abundance*, ed. A. D. McIntyre (Hoboken, NJ: Blackwell Publishing Ltd), 79–101.

O'Hara, T. D., Williams, A., Althaus, F., Ross, A. S., and Bax, N. J. (2020). Regional-scale patterns of deep seafloor biodiversity for conservation assessment. *Divers. Distrib.* 26, 479–494. doi: 10.1111/ddi.13034

Pabis, K., Błażewicz-Paszkowycz, M., Jóźwiak, P., and Barnes, D. K. A. (2014). Tanaidacea of the Amundsen and Scotia seas: An unexplored diversity. *Antarct. Sci.* 27, 19–30. doi: 10.1017/S0954102014000303

Pabis, K., Jóźwiak, P., Lörz, A.-N. N., Schnabel, K., and Błażewicz-Paszkowycz, M. (2015). First insights into the deep-sea tanaidacean fauna of the Ross Sea: species richness and composition across the shelf break, slope and abyss. *Polar Biol.* 38, 1429–1437. doi: 10.1007/s00300-015-1706-z

Poore, G. C. B., and Bruce, N. L. (2012). Global diversity of marine isopods (except Asellota and crustacean symbionts). *PLoS One* 7:e43529. doi: 10.1371/journal.pone.0043529

Poore, G. C. B., Avery, L., Błażewicz-Paszkowycz, M., Browne, J., Bruce, N. L., Gerken, S., et al. (2015). Invertebrate diversity of the unexplored marine western margin of Australia: taxonomy and implications for global biodiversity. *Mar. Biodivers.* 45, 271–286. doi: 10.1007/s12526-014-0255-y

Poore, G. C. B., Just, J., and Cohen, B. F. (1994). Composition and diversity of Crustacea Isopoda of the southeastern Australian continental slope. *Deep Sea Res. Part I Oceanogr. Res. Pap.* 41, 677–693. doi: 10.1016/0967-0637(94)90049-3

Raupach, M. J., Mayer, C., Malyutina, M., Wägele, J. W., and Wagele, J.-W. (2012). Multiple origins of deep-sea Asellota (Crustacea: Isopoda) from shallow waters revealed by molecular data. *Proc. R. Soc. B Biol. Sci.* 276, 799–808. doi: 10.1098/rspb.2008.1063

Sieg, J. (1977). Taxonomische Monographie der Familie Pseudotanaidae (Crustacea, Tanaidacea). *Mitteilungen Museum Naturkd Berlin Zool. Museum Inst. Spez. Zool.* 53, 3–109. doi: 10.1002/mmnz.4830530102

Spalding, M. D., Fox, H. E., Allen, G. R., Davidson, N., Ferdaña, Z. A., Finlayson, M., et al. (2007). Marine Ecoregions of the World: A Bioregionalization of Coastal and Shelf Areas. *Bioscience* 57, 573–583. doi: 10.1641/B570707

Stępień, A., Pabis, K., and Błażewicz, M. (2018). Small-scale species richness of the Great Barrier Reef tanaidaceans — results of the CReefs compared with worldwide diversity of coral reef tanaidaceans. *Mar. Biodivers.* 49, 1169–1185. doi: 10.1007/s12526-018-0894-5

Watling, L., Guinotte, J., Clark, M. R., and Smith, C. R. (2013). A proposed biogeography of the deep ocean floor. *Prog. Oceanogr.* 111, 91–112. doi: 10.1016/j.pocean.2012.11.003

Wilson, G. D. F. (1998). *Historical Influences on Deep-sea Isopod Diversity in the Atlantic Ocean*. Oxford: Pergamon Press.

Zardus, J. D., Etter, R. J., Chase, M. R., Rex, M. A., and Boyle, E. E. (2006). Bathymetric and geographic population structure in the pan-Atlantic deep-sea bivalve Deminucula atacellana (Schenck, 1939). *Mol. Ecol.* 15, 639–651. doi: 10.1111/j.1365-294X.2005.02832.x

Conflict of Interest: The authors declare that the research was conducted in the absence of any commercial or financial relationships that could be construed as a potential conflict of interest.

Publisher's Note: All claims expressed in this article are solely those of the authors and do not necessarily represent those of their affiliated organizations, or those of the publisher, the editors and the reviewers. Any product that may be evaluated in this article, or claim that may be made by its manufacturer, is not guaranteed or endorsed by the publisher.

Copyright © 2021 Błażewicz, Jakiel and Bird. This is an open-access article distributed under the terms of the Creative Commons Attribution License (CC BY). The use, distribution or reproduction in other forums is permitted, provided the original author(s) and the copyright owner(s) are credited and that the original publication in this journal is cited, in accordance with accepted academic practice. No use, distribution or reproduction is permitted which does not comply with these terms.

frontiers in Marine Science

ORIGINAL RESEARCH
published: 07 December 2021
doi: 10.3389/fmars.2021.750180

Pandora's Box in the Deep Sea –Intraspecific Diversity Patterns and Distribution of Two Congeneric Scavenging Amphipods

Anna M. Jażdżewska[1†], Tammy Horton[2†], Ed Hendrycks[3], Tomasz Mamos[1†], Amy C. Driskell[4†], Saskia Brix[5†] and Pedro Martínez Arbizu[6†]*

[1] Department of Invertebrate Zoology and Hydrobiology, Faculty of Biology and Environmental Protection, University of Lodz, Lodz, Poland, [2] National Oceanography Centre, Southampton, United Kingdom, [3] Canadian Museum of Nature, Research and Collections, Ottawa, ON, Canada, [4] Laboratories of Analytical Biology, National Museum of Natural History, Smithsonian Institution, Washington, DC, United States, [5] Senckenberg am Meer, Department for Marine Biodiversity Research (DZMB), c/o Biocenter Grindel, CeNak: Zoological Museum, Hamburg, Germany, [6] German Center for Marine Biodiversity Research (DZMB), Senckenberg am Meer, Wilhelmshaven, Germany

Paralicella tenuipes Chevreux, 1908 and *Paralicella caperesca* Shulenberger and Barnard, 1976 are known as widely distributed deep-sea scavenging amphipods. Some recent studies based on genetic data indicated the presence of high intraspecific variation of *P. caperesca* suggesting it is a species complex. Based on published molecular data from the Pacific and Indian oceans and new material obtained from the North and South Atlantic, we integrated the knowledge on the intraspecific variation and species distribution of the two nominal taxa. The study included analysis of three genes (COI, 16S rRNA, 28S rRNA) and revealed the existence of a single Molecular Operational Taxonomic Unit (MOTU) within *P. tenuipes* and six different MOTUs forming *P. caperesca*. The distribution pattern of the recognized lineages varied with three (*P. tenuipes*, MOTU 1 and MOTU 5 of *P. caperesca*) being widely distributed. There was evidence of contemporary population connectivity expressed by the share of the same COI haplotypes by individuals from very distant localities. At the same time no signal of recent demographic changes was observed within the studied taxa. The time-calibrated phylogeny suggested the emergence of species to be at the time of Mesozoic/Cenozoic transition that may be associated with global changes of the ocean circulation and deep sea water cooling.

Keywords: biodiversity, biogeography, species connectivity, abyss, COI barcoding, 16S rRNA gene, 28S rRNA gene, species delimitation

OPEN ACCESS

Edited by:
Kevin M. Kocot,
University of Alabama, United States

Reviewed by:
Gustavo Fonseca,
Federal University of São Paulo, Brazil
Jon Thomassen Hestetun,
Norwegian Research Institute (NORCE), Norway

****Correspondence:***
Anna M. Jażdżewska
anna.jazdzewska@biol.uni.lodz.pl

†ORCID:
Anna M. Jażdżewska
orcid.org/0000-0003-2529-0641
Tammy Horton
orcid.org/0000-0003-4250-1068
Tomasz Mamos
orcid.org/0000-0002-0524-3015
Amy C. Driskell
orcid.org/0000-0001-8401-7923
Saskia Brix
orcid.org/0000-0002-3269-8904
Pedro Martínez Arbizu
orcid.org/0000-0002-0891-1154

Specialty section:
This article was submitted to Deep-Sea Environments and Ecology, a section of the journal Frontiers in Marine Science

Received: *30 July 2021*
Accepted: *20 October 2021*
Published: *07 December 2021*

Citation:
Jażdżewska AM, Horton T, Hendrycks E, Mamos T, Driskell AC, Brix S and Martínez Arbizu P (2021) Pandora's Box in the Deep Sea –Intraspecific Diversity Patterns and Distribution of Two Congeneric Scavenging Amphipods. Front. Mar. Sci. 8:750180. doi: 10.3389/fmars.2021.750180

INTRODUCTION

The deep sea, the largest ecosystem in the World, has received particular attention in recent decades. Apart from scientific curiosity, advances in technology allowing the collection of deep-sea mineral or biological resources (e.g., deep-sea mining or fisheries) have rendered this ecosystem of interest also for commerce (Victorero et al., 2018; Hein et al., 2020). At the same time, signs of human impact (both direct and indirect) and low recovery rate of the deep-sea communities have been

observed (Fischer et al., 2015; Gollner et al., 2017; Jones et al., 2017; Chiba et al., 2018). Despite the large efforts that scientists have put into the exploration and characterization of the deep-sea ecosystem, it is still insufficiently understood (Ramirez-Llodra et al., 2010). Central among the still poorly known factors are the identities, distributional ranges and population connectivity of the species that live there. Rex et al. (2005) concluded that the abyssal fauna is constituted by the populations of survivors from the bathyal and as such it is less diverse. Recent analyses of abyssal benthic communities have partly challenged the paradigm, reporting very high diversities of several invertebrate groups, especially when applying molecular studies (e.g., Brandt et al., 2007; Janssen et al., 2015; Jażdżewska and Mamos, 2019; Brix et al., 2020). It was also observed that underwater physiographic features, although not being surmountable barriers for species connectivity, may restrict dispersal, particularly for those taxa lacking a free-living larval stage (Bober et al., 2018; Riehl et al., 2018; Jakiel et al., 2019; Jażdżewska and Mamos, 2019; Brix et al., 2020). Comparison of the geographic range sizes of shallow-water and deep-sea fauna revealed that they are smaller in the former, however the differences are not that large and the results are significantly biased by the low availability of deep-sea data (Baco et al., 2016). Other studies have provided evidence for deep-sea species ranges that reach 500–2000 km, with several species having much more limited distributions (Taylor and Roterman, 2017; Brix et al., 2018; Janssen et al., 2019; Washburn et al., 2021). Moreover, application of molecular methods in studies of some presumed cosmopolitan deep-sea species revealed that they are complexes of taxa with more restricted ranges (Havermans, 2016; Verheye et al., 2016).

Marine scavengers play an important role in the deep-sea food web, recycling carbon reaching the seafloor as carrion and making it available for other fauna (Havermans and Smetacek, 2018). The macrobenthic deep-sea scavenger community is dominated by amphipod crustaceans (De Broyer et al., 2004; Jamieson et al., 2011; Havermans and Smetacek, 2018; Horton et al., 2020). Members of this specialist amphipod feeding guild are well adapted by the possession of chemosensory organs allowing for better localization of the carcass, and good swimming abilities (Premke et al., 2003; De Broyer et al., 2004). Amphipods are in the superorder Peracarida, a diverse group of small shrimp-like taxa that brood their young in a pouch, with no independent larval dispersal stage. Brandt et al. (2012) summarized the distribution ranges of deep-sea peracarids, and revealed that only 45 taxa were found in multiple regions, among them 11 species of Amphipoda. One of the species listed by these authors, *Eurythenes gryllus* (Mandt, 1822), appeared to be a species complex (Havermans, 2016) challenging former understanding of its cosmopolitan distribution. Of the amphipod species listed as widely distributed, half belong to the mobile deep-sea scavenger guild. Notable among these are *Paralicella caperesca* Shulenberger and Barnard, 1976 and *Paralicella tenuipes* Chevreux, 1908 that have been reported in large numbers from baited traps in all oceans except the Arctic and the Southern Ocean south of the Antarctic Polar Front (e.g., Chevreux, 1908; Shulenberger and Barnard, 1976; Ritchie et al., 2015; Duffy et al., 2016; Horton et al., 2020; Patel et al., 2020).

The genus *Paralicella* currently contains six accepted species (**Table 1**). The genus was created by Chevreux in 1908 for the species *Paralicella tenuipes*, which was collected in large numbers from baited traps in the North Atlantic (the lectotype was selected from a trap set in the region of the Canary Islands at 5285 m) (Chevreux, 1908).

A second species, *Paralicella fusiformis* (Birstein and Vinogradov, 1955), was described based on an ovigerous female of 17 mm length collected in a catch from 0 to 5500 m from the Kuril-Kamchatka Trench in the Pacific Ocean (Birstein and Vinogradov, 1955). The species was originally placed in the genus *Eurythenes*. A third species, *Paralicella microps* (Birstein and Vinogradov, 1958), was added, again in the genus *Eurythenes* (Birstein and Vinogradov, 1958). In 1960, a fourth species *Paralicella similis* Birstein and Vinogradov, 1960, was described, and the authors, recognizing Chevreux's earlier work, transferred their species to the genus *Paralicella*, and incorrectly synonymized the species *P. fusiformis* with *P. tenuipes* (Birstein and Vinogradov, 1960). The authors noted the lack of eyes in their specimens of *P. fusiformis* and the presence of them in Chevreux's *P. tenuipes* (but see note page 12 regarding presence/absence of eyes in preserved material). The authors also indicated the similarity between the beveled basis of the pereopod 7 of their species *P. microps*, and that of *P. tenuipes*.

In 1976, Shulenberger and Barnard described the new species *Paralicella caperesca*, from a collection of 220 specimens taken in a trap set north of Oahu, Hawaii, at 5720 m. Barnard and Shulenberger (1976) discussed the genus *Paralicella*, designating a lectotype specimen for the species *Paralicella tenuipes*, after noting that Chevreux's original material contained specimens of both *P. tenuipes* and *P. caperesca*. They also provide a key to the genus and discuss the validity of two of Birstein and Vinogradov's species (*P. fusiformis* and *P. microps*) indicating the possibility that these species are conspecific with *P. caperesca* and *P. tenuipes* respectively. Barnard and Ingram (1990) added the last species, *Paralicella vaporalis*, from the Pacific Ocean at the Hess Guyot and Jasper Seamount from 706 to 1040 m, and provided an updated key to the genus.

The separation of the six known species can be managed morphologically using a number of characters (**Table 1**). The presence of a small, red-brown eye and a strongly beveled basis on pereopod 7, separate *P. tenuipes* and *P. microps* from the remaining four species. These species can be separated by the arrangement of the nodular setae in the middle of the apical excavation of the inner plate of the maxilliped. This single, very minor difference was postulated to be a phenotypic anomaly by Barnard and Shulenberger (1976), and the species is in all probability a synonym of *P. tenuipes*. The remaining four species all lack a beveled basis on pereopod 7 and can be separated into two groups using coxa 1, which is reduced and tapering in *P. similis* and *P. vaporalis*, and expanded and adze-shaped in P. *fusiformis* and *P. caperesca*. *P. similis* can be separated from *P. vaporalis* on the shape of coxa 1 (rounded in *P. similis*, triangular in *P. vaporalis*), and the basal articles of pereopods 5–7 (narrow in *P. similis*). Separation of the two remaining species *P. fusiformis* and *P. caperesca* is more difficult and relies on a number of quantitative characters which may be the

TABLE 1 | The currently accepted *Paralicella* species with type localities and distinguishing morphological characters.

Species	***Paralicella tenuipes* (Chevreux, 1908)**	***Paralicella microps* (Birstein and Vinogradov, 1958)**	***Paralicella fusiformis* (Birstein and Vinogradov, 1955)**	***Paralicella caperesca* (Shulenberger and Barnard, 1976)**	***Paralicella similis* (Birstein and Vinogradov, 1960)**	***Paralicella vaporalis* (Barnard and Ingram, 1990)**
Type locality	Canary Islands, North Atlantic, 5285 m	Japan Trench, North West Pacific, 0–6580 m	Kuril-Kamchatka Trench, North West Pacific, 0–5500 m	North of Hawaii, Central Pacific, 5720 m	East of New Zealand, South-West Pacific, 0–3000 m	Hess Guyot and Jasper Seamount, Pacific Ocean, 706–1040 m
Eye	Small, non-ommatidial, red-brown pigment	Small, non-ommatidial, red-brown pigment	Apparently absent	Large, non-ommatidial, dispersed pigment, may disappear in preservatives	Apparently absent	Large, non-ommatidial, dispersed pigment, may disappear in preservatives
Coxa 1	Expanded and adze-shaped	Expanded and adze-shaped	Expanded and distally rounded	Expanded with anterodistal bevel	Reduced and tapering, rounded	Reduced and tapering, triangular
Apical excavation and nodular setae of the inner plate of the maxilliped	Weakly excavate. Left with one seta at distolateral corner and two closely appressed distomedially; right with three, closely appressed distomedially	Weakly excavate. Three equally spaced setae: one distolaterally corner one distomedially, and one in the center of the excavation	Not excavate. Nodular setae unclear.	Moderately excavate. Three unequally spaced setae: one at distolateral corner and two closely appressed distomedially	Weakly excavate. Three unequally spaced setae: one at distolateral corner and two closely appressed distomedially	Weakly excavate. Three unequally spaced setae: one at midpoint and two closely appressed distomedially
Basis of pereopods 5-7	P5 slightly broadened, P6-7 broadened with **strong bevel**	P5 slightly broadened, P6-7 broadened with **strong bevel**	P5 slightly broadened, P6 narrowing distally, P7 broadened and **unbevelled**	P5 slightly broadened, P6 narrowing distally, P7 broadened, with **slight bevel**	P5-6 narrow, with posteroventral lobe, P7 broadened, **unbevelled**, with posteroventral lobe	P5-6 broad, with small posteroventral lobe, P7 broadened, **unbevelled**, with posteroventral lobe
Main references	Chevreux, 1908; Barnard and Shulenberger, 1976; Shulenberger and Barnard, 1976	Birstein and Vinogradov, 1958; Barnard and Shulenberger, 1976; Shulenberger and Barnard, 1976	Birstein and Vinogradov, 1955; Barnard and Shulenberger, 1976; Shulenberger and Barnard, 1976	Barnard and Shulenberger, 1976; Shulenberger and Barnard, 1976	Birstein and Vinogradov, 1960; Barnard and Shulenberger, 1976; Shulenberger and Barnard, 1976	Barnard and Ingram, 1990
Notes		Probable synonym of *P. tenuipes*	Potential senior synonym of *P. caperesca*			

result of ontogenetic variation. If they are conspecific, the name *P. fusiformis* would take priority over the more recently described *P. caperesca*.

Barnard and Shulenberger (1976) studied both Pacific and Atlantic specimens of *P. caperesca* and noted that there were indeed some minor morphological differences, e.g., in the basal articles of the antenna 2 flagellum, the right lacinia mobilis, spination of the palp of maxilla 1, and cuticular spines and setules. Minor differences in the slope on the ventral margin of the basis of pereopod 7 were also noted, but these variations were common to specimens from both Atlantic and Pacific collections.

No further detailed morphological studies on the genus have been undertaken and there have been no further records of the any of the other four *Paralicella* species in literature since their original descriptions. It is now apparent from the recent molecular studies (Ritchie et al., 2015; Bribiesca-Contreras et al., 2021; Mohrbeck et al., 2021) that there are likely to be more species residing in the *P. caperesca* complex. Determining the true *P. caperesca* and *P. fusiformis* (if these do indeed represent valid separate species), and clarifying the morphological characters that separate the molecularly defined species will require very detailed study of specimens of a variety of sizes and sexes from each of the clearly defined MOTUs.

Owing to the availability of extensive published molecular data and new material of *Paralicella tenuipes* and *P. caperesca* from the Atlantic, Pacific and Indian Oceans we provide a synthesis of the knowledge of the two species. We investigate the hypothesis that these two apparently widely distributed deep-sea species are actually complexes of molecularly uniform and geographically and/or bathymetrically restricted taxa, and provide an analysis of the phylogenetic relationships and historical evolution of the genus.

MATERIALS AND METHODS

Data Assembly

In the present study, the datasets of two mitochondrial (cytochrome *c* oxidase subunit I [COI] and 16S rRNA) as well as one nuclear (28S rRNA) marker were analyzed. The material was obtained from published articles available by March 2021 (Ritchie et al., 2015; Jażdżewska and Mamos, 2019; Iguchi et al., 2020; Mohrbeck et al., 2021; Weston et al., 2021) supplemented by newly produced sequences. **Figure 1** summarizes all datasets that have been used in this study, and information on new material collection, DNA extraction, amplification and sequencing is presented below.

All chromatograms of the newly obtained sequences were visually inspected, edited when reading mistakes happened in Geneious 10.1.2, and primer sequences were trimmed. These sequences were uploaded to GenBank under accession numbers: COI: MZ655819–MZ655889, 16S: MZ655914–MZ655967, 28S: MZ655890–MZ655910. Relevant voucher information, taxonomic classifications, and sequences of all studied genes (except for already published 16S sequences) are deposited in the dataset "DS-PCAPTEN" in the Barcode of Life Data System (BOLD)[1] (Ratnasingham and Hebert, 2007)[2]. Additional summary that includes GenBank accession numbers for all sequences is available in the **Supplementary Material S1**.

New Material Collection and DNA Extraction

Thirty specimens of *Paralicella* (15 of each of *P. caperesca* and *P. tenuipes*) were analyzed from samples collected at the Porcupine Abyssal Plain Sustained Observatory (PAP-SO), situated in the subpolar North-East Atlantic, at 48°50′N 16°30′W and a water depth of 4850 m. Samples were collected by means of baited trap (for trap details see Horton et al., 2020, and sampling details in Hartman, 2019; Ruhl et al., 2019). In the South Atlantic, 41 individuals were collected at one station in the Brazilian Basin during the DIVA-3 expedition. These individuals were collected using a baited trap (its description and sampling procedure is described in Martínez Arbizu et al., 2015).

In the case of North Atlantic amphipods, the total genomic DNA was extracted from one-two pleopods using a mixture of 150 μl pure H_2O with 0.015 g Chelex® (SIGMA-ALDRICH Co.) and 10 μl proteinase K. The digestion at 55°C lasted for 6 h. The DNA of individuals from the Brazilian Basin were extracted using an AutoGenprep 965 extraction robot after overnight digestion at 55° in the AutoGen buffers with proteinase-K.

Cytochrome *c* Oxidase Subunit I Gene Amplification and Sequencing

For North Atlantic individuals, the barcoding fragment of the COI gene amplification was conducted with the degenerated LCO1490-JJ and HCO2198-JJ primer pair (**Table 2**) and the reaction conditions described in Hou et al. (2007). Sequences were obtained by Macrogen Inc., the Netherlands on the Applied Biosystems 3730xl capillary sequencer. One-way (forward) sequencing was the standard procedure for all samples, but in addition, at least one individual of each recognized MOTU was sequenced in both directions.

The barcode fragment of the COI gene for the South Atlantic specimens of the studied species was amplified and sequenced with degenerate primers (dgLCO-1490/dgHCO-2198, **Table 2**) according to the protocol described in Riehl et al. (2014).

Sequences were initially blasted using default parameters on NCBI BLASTn and translated into amino acid sequences to confirm that no stop codons were present.

16S rRNA Gene Amplification and Sequencing

The 16S marker of 24 individuals (18 from the Central Pacific and six from North Atlantic, preferably one-two per each recognized BIN) was amplified using the primer pair 16SFt_amp/16SRt_amp2 (**Table 2**) in the conditions presented by Lörz et al. (2018b). In the case of the Central Pacific specimens, polymerase chain reaction was performed with AccuStart II PCR SuperMix (Quantabio), while for North Atlantic ones DreamTaq

[1] www.boldsystems.org

[2] dx.doi.org/10.5883/DS-PCAPTEN

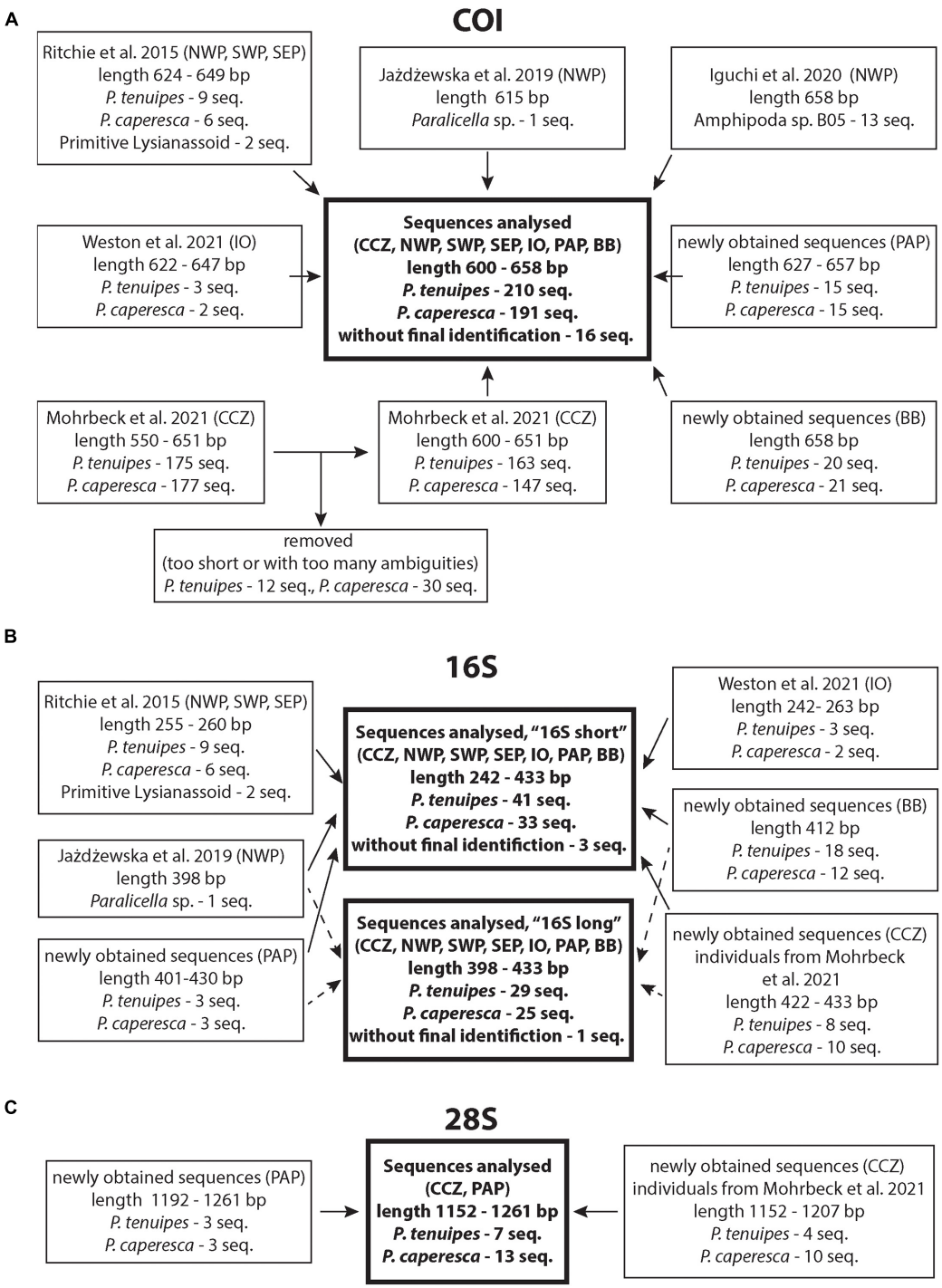

FIGURE 1 | Summary of data used in the study with indication of the literature source, number of sequences and their initial length, general locality and original identification. **(A)** COI gene dataset, **(B)** 16S rRNA gene dataset, **(C)** 28S rRNA gene dataset. Geographic codes: BB, Brazilian Basin; South Atlantic; CCZ, Clarion-Clipperton Zone, Central Pacific; IO, Indian Ocean; NWP, North-West Pacific; SEP, South-East Pacific; SWP, South-West Pacific; PAP, Porcupine Abyssal Plain, North Atlantic.

Green PCR Mastermix (Thermo Scientific) was used. Sequences were obtained from Macrogen Inc., the Netherlands, with the Applied Biosystems 3730xl capillary sequencer. Similarly to the COI gene, one-way (forward) sequencing was the standard procedure for all samples, but in addition, some individuals were sequenced in both directions. Additionally, 30 sequences of the

TABLE 2 | Summary of the primers used in the present study.

Gene	Name	Sequence 5′-3′	Direction	Reference
COI	LCO1490-JJ	CHACWAAYCATAAAGATATYGG	Forward	Astrin and Stüben, 2008
	HCO2198-JJ	AWACTTCVGGRTGVCCAAARAATCA	Reverse	Astrin and Stüben, 2008
	dgLCO-1490	GGTCAACAAATCATAAAGAYATYGG	Forward	Meyer, 2003
	dgHCO-2198	TAAACTTCAGGGTGACCAAARAAYCA	Reverse	Meyer, 2003
16S	16SFt_amp	GCRGTATIYTRACYGTGCTAAGG	Forward	Lörz et al., 2018b
	16SRt_amp2	CTGGCTTAAACCGRTYTGAACTC	Reverse	Lörz et al., 2018b
	16Sar	CGCCTGTTTATCAAAAACAT	Forward	Palumbi et al., 1991
	16Sbr	CCGGTCTGAACTCAGATCACG	Reverse	Palumbi et al., 1991
28S	28F	TTAGTAGGGGCGACCGAACAGGGAT	Forward	Hou et al., 2007
	28S-700F	AAGACGCGATAACCAGCCCACCA	Forward	Hou et al., 2007
	28R	GTCTTTCGCCCCTATGCCCAACTGA	Reverse	Hou et al., 2007
	28S-1000R	GACCGATGGGCTTGGACTTTACACC	Reverse	Hou et al., 2007

specimens from the South Atlantic were successfully amplified and sequenced using the primer pair 16Sar/16Sbr (**Table 2**) at the Smithsonian Institution's Laboratories of Analytical Biology. The protocol was as detailed in Riehl et al. (2014).

28S rRNA Gene Dataset

The analysis of the nuclear gene fragment was done on a restricted number of individuals from the central Pacific and North Atlantic. Twenty specimens representing 14 BINs (up to three individuals per BIN) were chosen, for which both COI and 16S sequences were already available. The fragment of 28S gene sequence amplification was conducted with the combination of two forward (28F, 28S-700F) and two reverse (28R, 28S-1000R) primers (**Table 2**) and reaction conditions published by Hou et al. (2007). Polymerase chain reaction was performed with AccuStart II PCR SuperMix (Quantabio) for central Pacific individuals, and DreamTaq Green PCR Mastermix (Thermo Scientific) for North Atlantic specimens. Sequencing in both directions was performed by Macrogen Inc., the Netherlands, while the editing of the sequences was similar to the procedure for COI and 16S genes, resulting in 20 sequences of 1152–1261 bp length.

Data Analysis

Separate alignments of the sequences of each gene were performed with MAFFT 7 (Katoh et al., 2002; Katoh and Standley, 2013) using the G-INS-i algorithm, the sequences were trimmed to have all of them of the same length. The RNA was homologous enough to use MAFFT software, the alignment was carefully inspected by eye and no ambiguous columns were found. Four alignments were produced: (1) full dataset of all COI sequences with the alignment length of 594 bp, (2) dataset of all available 16S sequences ("short": length 267 bp), (3) restricted dataset of 16S sequences ("long": length 398 bp), (4) dataset of all available 28S sequences (length: 1168 bp). Additionally, COI haplotypes were identified and a COI haplotype dataset generated using DNA SP v6 (Librado and Rozas, 2009).

Species Delimitation

Five molecular species delimitation methods were applied to reveal the Molecular Operational Taxonomic Units (MOTUs). Two methods were distance-based: Barcode Index Number (BIN) System (Ratnasingham and Hebert, 2013), and the Assemble Species by Automatic Partitioning (ASAP) (Puillandre et al., 2021). The following three were tree-based phylogenetic approaches using Generalized Mixed Yule Coalescent (GMYC) model-based method (Pons et al., 2006), according to Monaghan et al. (2009), the Bayesian implementation of the Poisson Tree Processes (bPTP) (Zhang et al., 2013) and multirate Poisson Tree Process (mPTP) (Kapli et al., 2017). The dataset of all COI sequences was used for BIN, ASAP and mPTP. Short 16S sequences were analyzed with ASAP and GMYC, while both the long ones and the 28S sequences were used for the above two methods and mPTP. The restricted datasets of haplotypes of all three markers were the basis for ASAP, bPTP, mPTP, and GMYC analyses.

The BIN method is implemented as part of the Barcode of Life Data system (BOLD; Ratnasingham and Hebert, 2007). It compares newly submitted sequences with the sequences already available. They are clustered according to their molecular divergence using distance-based algorithms (single linkage clustering followed by Markov clustering) that aim at finding discontinuities between Operational Taxonomic Units (OTUs). Each OTU receives a unique and specific code (aka Barcode Index Number or BIN), either already available or new if the submitted sequences do not cluster with already known BINs. Each BIN is registered in BOLD.

The Assemble Species by Automatic Partitioning (ASAP) (Puillandre et al., 2021) is a method that uses pairwise genetic distances to assemble individuals into groups and proposes species partitioning ranked according to a scoring system.

The GMYC method defines MOTUs through identification of the switch from intraspecific branching patterns (coalescent) to interspecific species branching patterns (Yule process) on a phylogenetic tree. Because for GMYC an ultrametric tree is required, as an input, a Bayesian tree was reconstructed in BEAST 2.6.3 (Bouckaert et al., 2019). The site model was set up with bModelTest (Bouckaert and Drummond, 2017). The tree prior

was set to Birth-Death following Bayes factors. Two runs of Markov chain Monte Carlo (MCMC) were performed each 20 M generations-long, sampled every 2,000 generations. Runs were examined for convergence in Tracer 1.7 (Rambaut et al., 2018). All runs reached the effective sample size (ESS) above 200 and were combined using LogCombiner 2.6.3. The final tree was summarized with TreeAnnotator 2.6.3, all being part of BEAST 2.6.3 package. The Bayesian tree was uploaded into the R 4.0.5 (R Core Team, 2021) software package 'SPLITS' (Species Limits by Threshold Statistics) (Ezard et al., 2009) and analyzed using the single threshold model.

For the following methods, a phylogenetic tree was reconstructed with Maximum Likelihood (ML) approach using RAxML 8.2.8 (Stamatakis, 2014) through raxmlGUI 2.0 (Edler et al., 2021). The best-scoring ML trees were produced using the GTRGAMMA substitution model. Bipartition information was drawn from the phylogenies obtained with the rapid hill climbing tree search algorithm. Statistical supports were estimated with thorough bootstrap tests set to 1000 repetitions.

The bPTP incorporates the number of substitutions in the model of speciation and assumes that the probability that a substitution gives rise to a speciation event follows a Poisson distribution (Zhang et al., 2013). The analysis was performed on the bPTP webserver[3] with 500,000 iterations of MCMC and 10% burn-in.

The mPTP method incorporates different levels of intraspecific genetic diversity deriving from differences in either the evolutionary history or sampling of each species. The method implements MCMC sampling that provides a fast and comprehensive evaluation of the inferred delimitation (Kapli et al., 2017). Five runs of 100 M MCMC generations long chain with a burn in of 10% were performed on a local server.

Pairwise p-distances between all recognized MOTUs and *P. tenuipes* were calculated on the complete COI dataset and on the restricted dataset of COI haplotypes. Within MOTUs, distances were also calculated using p-distance separately for six datasets (two for COI, three for 16S, and one for 28S). To visualize the MOTUs Neighbor-Joining (NJ) tree of all COI sequences was generated based on p-distances (transition and transversion substitution included and complete deletion) with 1000 bootstrap replicates (Felsenstein, 1985) in MEGA V7.0.18 (Kumar et al., 2016).

Molecular Operational Taxonomic Unit Distribution and Population Connectivity

The distribution of each recognized MOTU was plotted on the World map using QGIS 3.16 (QGIS.org, 2021). The distributions included all records of both nominal species extracted from the relevant literature (**Supplementary Material S2**). Furthermore, to present the molecular divergence of haplotypes and their geographical allocation, Median Joining Networks were generated in PopART 1.7 (Bandelt et al., 1999) separately for the two nominal species and independently for each recognized MOTU within *P. caperesca*.

Reconstruction of Phylogeny and Demography

Up to three individuals of each BIN were used to produce a time-calibrated phylogeny. It was based on the combined COI and 16S dataset, so only the individuals with sequences of both genes were included (except for the two BINs AEG2603 and ACZ4873, for which only COI sequence was available). The analysis was conducted in Beast 2.6.3 (Bouckaert et al., 2014). The molecular clock was set using a strict clock and general for gammarid amphipods the COI rate based on multiple calibration points (including fossils) of 0.01773 substitutions/site Ma-1 (Copilaş-Ciocianu et al., 2019). The value is in congruence with other works on Amphipoda (e.g. Mamos et al., 2016). The substitution model was selected via bModelTest (Bouckaert and Drummond, 2017). Birth-Death process was selected as a tree prior. Four runs of the MCMC, each 20 million generations long and sampled every 2,000 generations, were performed and examined for convergence in Tracer 1.7 (Rambaut et al., 2018). All runs reached the effective sample size (ESS) above 200 and were combined using LogCombiner2.6.3. The final tree was summarized with TreeAnnotator 2.6.3, all being part of BEAST 2.5.2 package.

Sampling of the studied taxa in different areas of the World Ocean differed, but it was possible to separate geographic populations for some of the MOTUs (MOTU 1, 4, and 5 of *P. caperesca* and *P. tenuipes*) and they were further studied for molecular diversity and demography. In this case, the minimum number of individuals of a particular population was seven. The COI molecular diversity of each population was calculated as the total number of haplotypes and haplotype diversity. Historical demographic patterns were explored using the COI data set employing two approaches. First, to test for a recent demographic expansion, Tajima's *D* (Tajima, 1989) and Fu's *Fs* (Fu, 1997), Fu and Li's *D* (Fu and Li, 1993), Fu and Li's *F* (Fu and Li, 1993; Achaz, 2009) Ramos-Onsins and Rozas's (Ramos-Onsins and Rozas, 2002) indices were calculated using DNASP 6. Their statistical significance was evaluated using 1000 simulated samples. Second, the extended Bayesian skyline plot (eBSP) (Drummond et al., 2005) in BEAST 2.5.2 was used to visualize the demographic changes through time. The clock model, as well as the rate and priors on the substitution models for each group, were determined in the same way as for the time-calibrated phylogeny population model was set to 0.5. The MCMC chain was run two times to ensure convergence for 20 million generations, sampled every 20,000 generations. One run for each data set was used to plot the eBSP in R script[4] after a 10% burn-in phase.

In order to assess putative relation between geographic and molecular distances we used linear regression model in R 4.0.5 (see footnote 4). The visualization was performed for *Paralicella tenuipes* and two MOTUs of *P. caperesca* (MOTU 1 and 5). Sampling locations were divided into the following groups (putative populations): CCZ (Clarion-Clipperton Zone, central Pacific), APEI 6 (North of CCZ, Central Pacific), NWP (North-West Pacific), BB (Brazilian Basin, South Atlantic), PAP (Porcupine Abyssal Plain, North Atlantic). Geographic distances

[3]https://species.h-its.org/ptp/

[4]http://www.r-project.org

were estimated using Google Earth Pro. Within an ocean they were measured by drawing straight line between central points of each station group. Considering that in the case of the distances between Pacific and Atlantic populations such method would draw the line across the continent, for calculating the distances between these groups of stations the line was drawn to surround South America through the Drake Passage. Because of the low number of groups to compare (max 10) we decided only to run a simple linear regression visualization instead of correlation and isolation by distance tests.

RESULTS

Species Delimitation

All species delimitation methods clearly separated the two main lineages leading to the nominal *Paralicella tenuipes* and *P. caperesca* (**Figure 2**). A few sequences identified as *P. tenuipes* that grouped with *P. caperesca* seem to be associated with identification mistakes and will be discussed later in the text. The interspecies distances of COI between the two species varied from 0.156 to 0.188 (**Table 3**).

Delimitation within *P. tenuipes* recognized from one (majority of methods) to four molecular units (**Figure 2**). The least conservative were BIN system and ASAP based on COI sequences that have recognized four units. GMYC recognized either three (16S short sequences, 28S sequences) or two (16S long sequences) MOTUs. The mean intraspecific p-distance of COI sequences was 0.018 (0.000-0.040), while for COI haplotypes – 0.021 (0.002–0.040) (**Table 4**). For the 16S dataset, in the case of short sequences the mean distance was 0.009, in the case of long sequences it was 0.005 (0.007 for haplotypes). All 28S sequences were identical.

Delimitation of MOTUs within *P. caperesca* varied strongly from the recognition of a single unit (ASAP on COI haplotypes and on all 16S combinations, mPTP on 16S haplotypes as well as on 28S sequences and haplotypes, bPTP on 16S and 28S haplotypes) to as many as 21 groups (bPTP on COI haplotypes) (**Figure 2**). It confirms the existence of separate lineages. After removing the extreme unifications and divisions, it may be observed that four lineages represented by the following BINs: BOLD:ADD2929 (MOTU 2), BOLD:AEH6662 (MOTU 3), BOLD:ACZ5628 (MOTU 4), BOLD:ADD2497 (MOTU 6) were most commonly separated from the rest of the groups. The lineages forming the remaining two groups did not present a stable pattern of unification/separation and for this study were treated as two separate MOTUs. MOTU 1 consisted of seven BINs (BOLD:AEG0263, BOLD:ACZ5625, BOD:ACZ5671, BOLD:ACZ5631, BOLD:ACZ4905, BOLD:ACZ4904, BOLD:ACZ5630), whereas MOTU 5 grouped six BINs (BOLD:ACZ5627, BOLD:ACZ5629, BOLD:ACZ4489, BOLD:ADP2618, BOLD:ACZ4873, BOLD:ACZ4903). The COI p-distances between discriminated MOTUs of *P. caperesca* ranged from 0.064 (between MOTU 1 and 2) to 0.128 (observed for the MOTU 2 and 4 pair) (**Table 3**). The intraspecific p-distances within nominal *P. caperesca* varied from 0.000 up to 0.133 of COI, from 0.000 to 0.094 of 16S and from 0.000 to 0.014 of 28S (**Table 4**). These values were clearly reduced when the species were divided into suggested MOTUs. Within MOTU 1 p-distance of COI reached up to 0.072 (mean 0.028 for sequences and 0.035 for haplotypes). Within 16S, the maximum p-distance was 0.027, when the dataset of short (ca. 250 bp) sequences was used, while it slightly raised up to 0.028 when the longer fragment (ca. 400 bp) was analyzed. The 28S sequences within MOTU 1 are identical. MOTUs 2, 3, 4, and 6 showed intraspecific p-distances not higher than 0.003 no matter the dataset explored. In the case of MOTU 5, the maximum p-distance of COI reached 0.059 (mean 0.029 for sequences, 0.031 for haplotypes). For the 16S gene, the dataset of short sequences showed lower values of p-distance (max – 0.019, mean – 0.009), while they reached up to 0.028 (mean 0.015 for sequences, 0.018 for haplotypes) in case of longer sequences. The nuclear gene was diverse with a mean p-distance of 0.011 (maximum – 0.014). MOTU 1 and 3 shared a 28S sequence, while MOTU 5 was represented by three clearly different sequences, additionally separated by the 28S sequence of MOTU 4 (**Supplementary Figure S1**).

Molecular Operational Taxonomic Unit Distribution and Populations Connectivity

The literature records of both nominal species come from all three oceans; the molecular study confirmed the pan-oceanic distribution of *P. tenuipes* (**Figure 3**) and MOTU 1 of *P. caperesca* (**Figure 4**). MOTU 5 was widely distributed in both Atlantic and Pacific oceans, whereas MOTUs 4 and 6 were observed at a few localities in the Pacific only. The most restricted geographically appeared to be MOTU 2 and MOTU 3, each recognized from a single station, the first in South-West Pacific and the second in the North Atlantic. Although in some localities only a single MOTU were observed, in the areas where more individuals of *P. caperesca* were collected and studied, different lineages co-occurred (**Figure 4**).

Out of the 19 haplotypes identified within *P. tenuipes,* seven were singletons, the remaining ones were often shared between the studied regions (**Figure 5**). As many as 171 individuals represented one of the five dominant haplotypes, 34 individuals characterized the remaining 14 haplotypes. The majority of haplotypes of *P. caperesca* (56 out of 80) were singletons. Within MOTU 1, there were four haplotypes shared between geographical regions, with one almost equally represented in Pacific and Atlantic oceans. One additional haplotype was shared between North and South Atlantic, while another one was found in South Atlantic and Indian Ocean (**Figure 6**). The structure of the haplotype network of MOTU 1 has a partially star-like topology with one central haplotype present in Central Pacific and several haplotypes, differing from it by a few mutations only, being widely distributed geographically. MOTU 2, MOTU 3, and MOTU 4 were each restricted to a single region, but all of them were represented by a few individuals only. Among the 22 haplotypes recognized within MOTU 5, only two were shared between regions, one identified in Central and South-East Pacific, while the second present in North-West and South-West Pacific. MOTU6 was represented

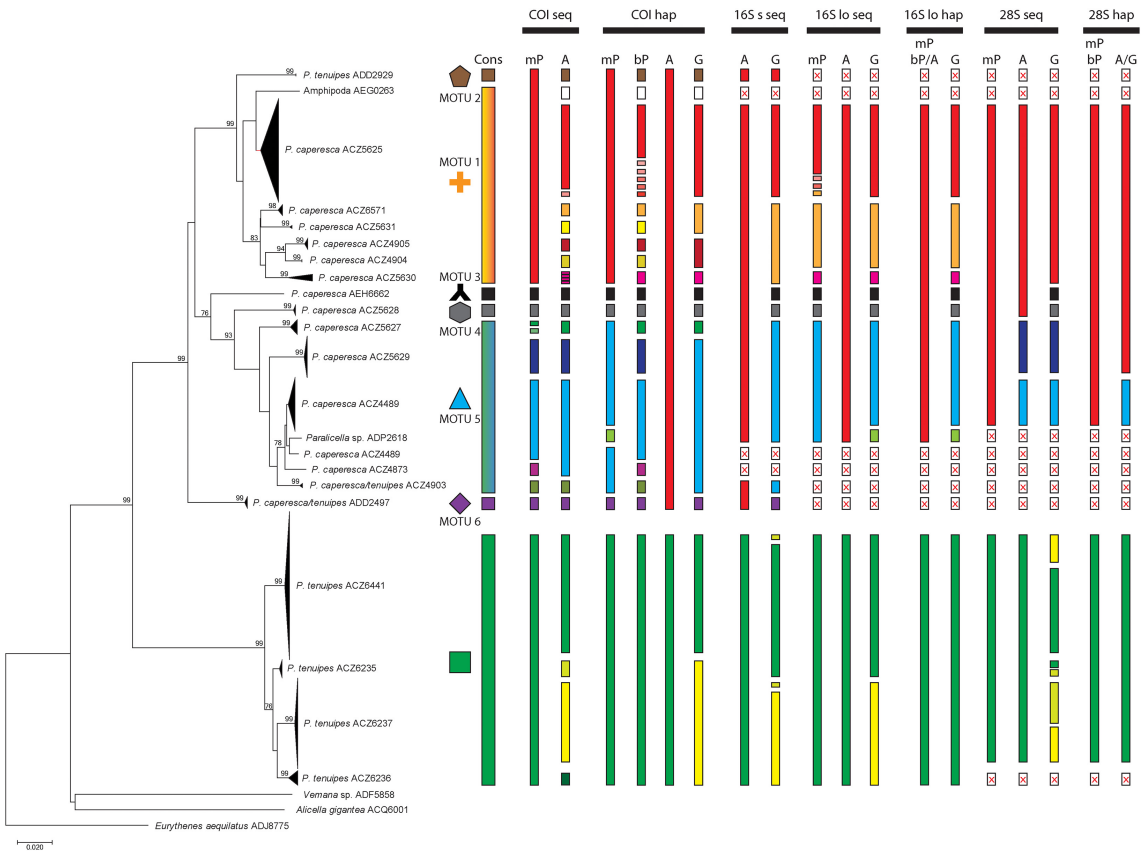

FIGURE 2 | Neighbor-Joining tree presenting the clustering of all studied sequences and indication of different species delimitation. The branches were collapsed according to the Barcode Index Numbers ascribed by BOLD. Cons, consensus MOTU delimitation. Data: COI seq, all COI sequences; COI hap, COI haplotypes; 16S s seq, 16S sequences (short ones); 16S lo seq, 16S sequences (long ones); 16S lo hap, 16S haplotypes (long sequences); 28S seq, 28S sequences; 28S hap, 28S haplotypes. Delimitation methods: mP, mPTP; bP, bPTP; A, ASAP; G, GMYC. Bootstrap support (1000 replicates), only values higher than 75 shown. Box with red X inside – missing data.

TABLE 3 | Inter-species COI p-distances between MOTUs identified within *P. caperesca*.

		Paralicella caperesca						***Paralicella tenuipes***
		MOTU 1	**MOTU 2**	**MOTU 3**	**MOTU 4**	**MOTU 5**	**MOTU 6**	
Paralicella caperesca	MOTU 1		*0.066*	0.093	0.113	0.108	0.096	0.186
	MOTU 2	*0.064*		0.118	**0.128**	0.125	0.112	0.181
	MOTU 3	0.092	0.118		0.087	0.094	0.085	0.176
	MOTU 4	0.111	**0.127**	0.087		0.071	0.085	0.185
	MOTU 5	0.109	0.124	0.098	0.076		0.094	0.188
	MOTU 6	0.095	0.111	0.086	0.085	0.089		0.156
Paralicella tenuipes		0.181	0.181	0.176	0.185	0.185	0.157	

Lower left – complete COI dataset, upper right – restricted dataset of COI haplotypes. In case of P. caperesca MOTUs highest values indicated in bold, the lowest – italicized.

by two haplotypes, one of them present in North-West and South-West Pacific.

Reconstruction of Phylogeny and Demography

The Bayesian phylogenetic reconstruction confirmed the existence of two main lineages leading to the nominal *Paralicella caperesca* and *P. tenuipes* (**Figure 7**). This separation can be estimated at ca. 37 Ma. The differentiation within *P. tenuipes* can be estimated as happening within the recent 1 Ma. The diversification within *P. caperesca* appeared between eight to two Ma. Around eight million years ago, the lineages were divided into two groups: combining MOTUs 1–3 and MOTUs 4–6. Soon after this, the MOTU 6 separated from the rest, and six million

TABLE 4 | Minimum, maximum, and mean p-distances calculated for the nominal species studied and the MOTUs identified within *P. caperesca*.

	COI seq		COI hap		16S s seq		16S lo seq		16S lo hap		28S seq	
	Minimum–maximum	Mean	Minimum–maximum	Mean	Minimum–maximum	Mean	Minimum–maximum	Mean	Minimum–maximum	Mean	Minimum–maximum	Mean
Paralicella caperesca	0.000–0.133	0.072	0.002–0.133	0.071	0.000–0.094	0.040	0.000–0.073	0.030	0.003–0.073	0.040	0.000–0.014	0.005
MOTU 1	0.000–0.072	0.028	0.002–0.072	0.035	0.000–0.027	0.009	0.000–0.028	0.010	0.003–0.028	0.016	0.000–0.000	0.000
MOTU 2	0.000–0.000	0.000	0.000–0.000	0.000	NA	NA	x	x	x	x	x	x
MOTU 3	NA	NA	NA	NA	NA	NA	NA	NA	NA	NA	NA	NA
MOTU 4	0.000–0.003	0.002	0.002–0.003	0.003	NA	NA	NA	NA	NA	NA	NA	NA
MOTU 5	0.000–0.059	0.029	0.002–0.059	0.031	0.000–0.019	0.009	0.000–0.028	0.015	0.008–0.028	0.018	0.000–0.014	0.011
MOTU 6	0.000–0.002	0.000	0.002–0.002	0.002	0.000–0.000	0.000	x	x	x	x	x	x
Paralicella tenuipes	0.000–0.040	0.018	0.002–0.040	0.021	0.000–0.039	0.009	0.000–0.010	0.005	0.003–0.010	0.007	0.000–0.000	0.000

COI seq, complete COI dataset; COI hap, dataset restricted to haplotypes; 16S s seq, all short (ca. 250 bp) sequences; 16S lo seq, restricted long (ca. 400 bp) sequences; 16S lo hap, haplotypes identified within 16S long sequences; 28S seq, all 28S sequences; NA, only one sequence available – no possibility to calculate the distance; x, no data.

years ago MOTU 3 diverged. Division between MOTU 4 and 5 happened ca. four Ma, while the most recent separation was of MOTU 2 and MOTU 1, estimated at ca. two million years ago.

All values of haplotype diversity of *P. tenuipes* were significant with the highest observed in the Central Pacific and the lowest in the North Atlantic (**Table 5**). Haplotype diversity of MOTU 1 of *P. caperesca* (represented by 104 individuals in our study) was highest in the North-West Pacific, but this value was not statistically significant (**Table 4**). In the Central Pacific population this measure was lower than in the North-West Pacific, but in contrast to this region it was significant. The Atlantic population was the least diverse of the three and the value was insignificant. Within MOTU 5, the haplotype diversity of the North Atlantic population was distinctly higher than that of the Central Pacific (both values significant), however, only nine individuals of MOTU 5 were collected in the whole Atlantic. From the results of neutrality tests, some recent population contraction of *Paralicella tenuipes* may be seen, particularly in South Atlantic. Whereas, in the case of MOTU 1 of *P. caperesca,* a slight population expansion in the Atlantic appeared. MOTU 5 seemed to have a stable population in the Central Pacific, while in the North Atlantic it was a sign of recent population contraction. The neutrality tests were significant only in a few cases of MOTU 1 of *P. caperesca*. The results of eBSP confirmed no significant drops or sudden expansion of populations of both species (**Supplementary Figures S2**, **S3**), whereas linear regression revealed no separation of the populations of *P. tenuipes* and MOTU 5 of *P. caperesca* and a weak signal of differentiation for MOTU 1 of the second species (**Supplementary Figure S4**).

DISCUSSION

Species Identification

Our study undoubtedly confirmed the separation of *P. tenuipes* and *P. caperesca*. All individuals identified morphologically by the taxonomists (TH, EH) as certain species were molecularly ascribed to the correct group. This confirms the former findings by Mohrbeck et al. (2021) and is in contrast with Ritchie et al. (2015), who indicated that the characters used for morphological species identification are not separating these two taxa correctly. Because the publication of wrongly identified sequences may have a large influence on future studies, it is important to clarify these issues which we have done here (**Table 6**). Using the sequence information of both COI and 16S, it can be seen that four individuals from Ritchie et al. (2015) identified as *P. tenuipes* and two presented as "unidentified primitive lysianassoid" appear to be representatives of different clades of *P. caperesca.* Moreover, one individual cited as *Valettietta anacantha* is represented by the COI sequence (GenBank accession number: KP713950) belonging to MOTU 1 (BOLD:ACZ5625) of *P. caperesca*. The 16S of the same individual does not show similarity to any *Paralicella* species but it groups with sequences of *V. anacantha* from the study of Ritchie et al. (2015). The relatively short fragment of the 18S gene (591 bp, GenBank accession number KT372893) is the only available sequence of 18S of the genus *Valettietta* and the whole family Valettiopsidae and presents 93-95% similarity

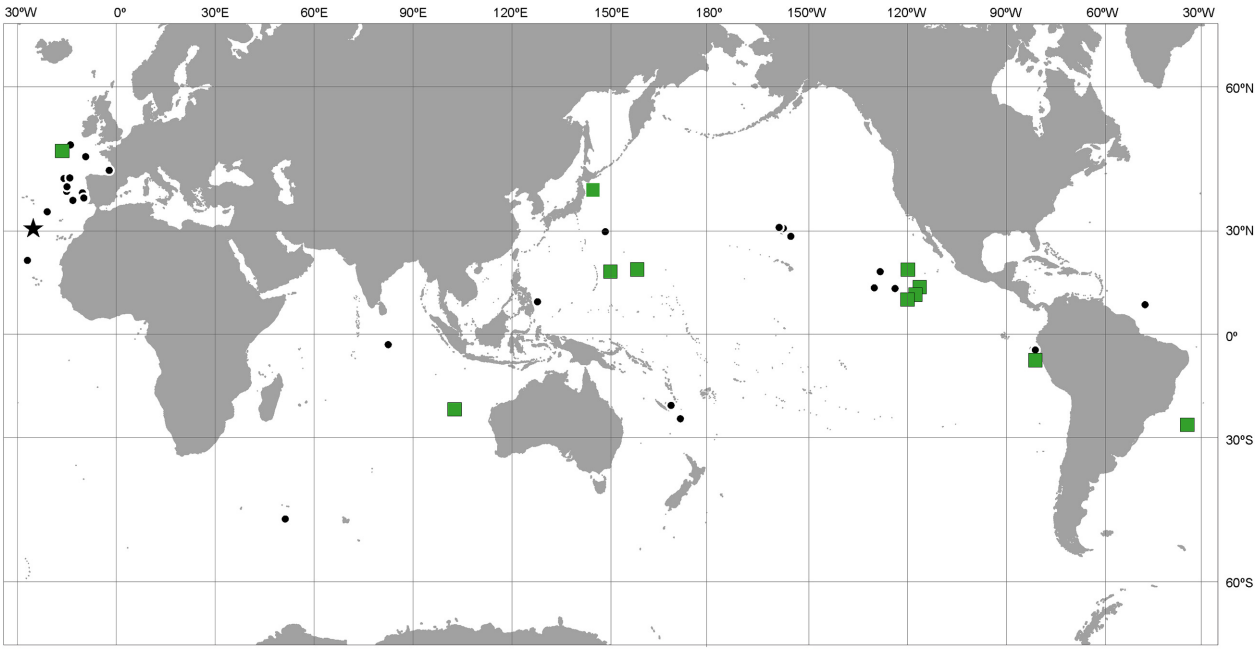

FIGURE 3 | Distribution map of *Paralicella tenuipes*. Black dots indicate literature records. Green squares show stations from where the individuals for molecular studies were obtained. Star – type locality of the species. Full list of references used to prepare the map in **Supplementary File S2**.

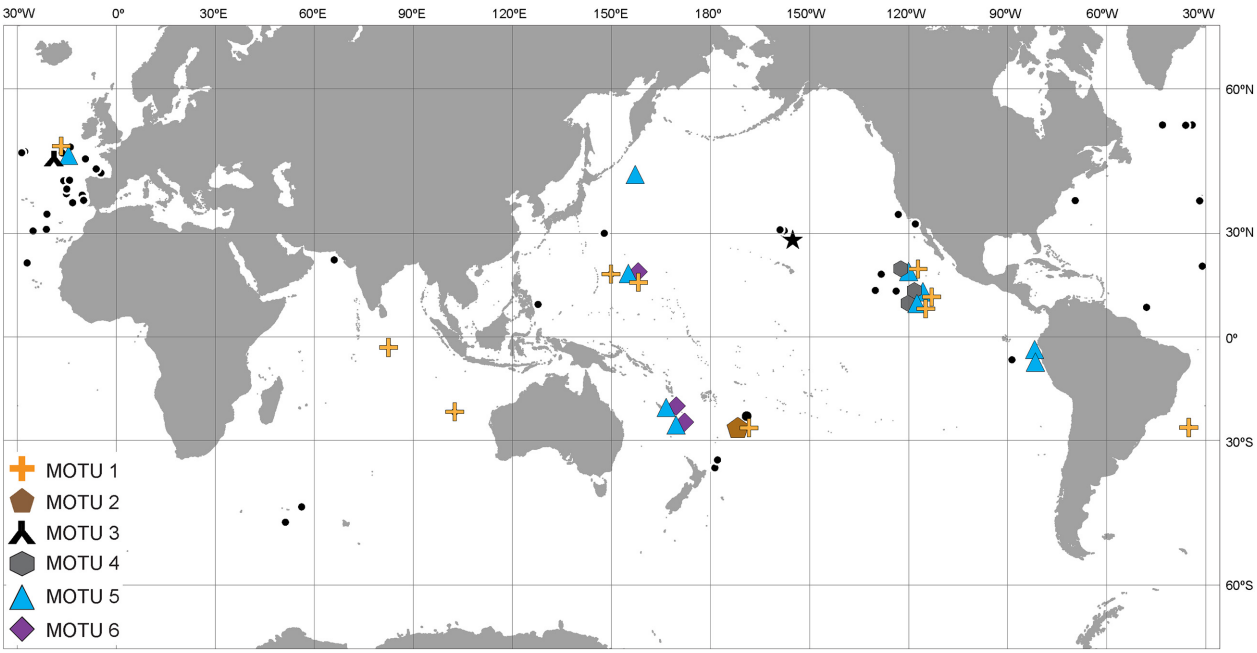

FIGURE 4 | Distribution map of *Paralicella caperesca*. Black dots indicate literature records. Color symbols (same as in **Figure 1**) show localities from where the individuals for molecular study were obtained. Star – type locality of the species. Full list of references used to prepare the map in **Supplementary File S2**.

to various species of Alicellidae from the same study. There are no sequences of this gene provided by other researchers to cross-validate the sequence identity. As a result, it is impossible to determine the reason why the COI sequence is almost identical to those of *P. caperesca* while the 16S resembles another taxon. As such, we recommend that this record be removed from GenBank, or updated with proper comment, to avoid further confusion. In a study by Iguchi et al. (2020), the identifications

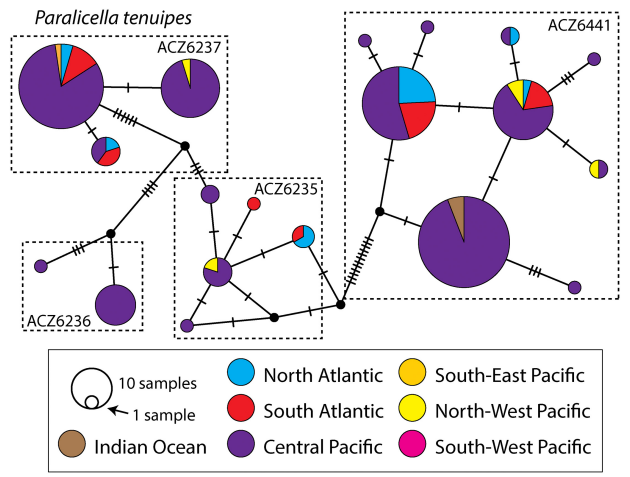

FIGURE 5 | Median Joining Network of all *Paralicella tenuipes* COI haplotypes with indication of the division of the taxon into BINs. Colors indicate geographic origin of haplotype.

were of Amphipoda at the order level. The comparison of COI sequences obtained by these researchers with our data revealed 12 individuals to be *P. caperesca* (three different MOTUs) and one individual of *P. tenuipes* (**Table 6**). There are also two sequences of *P. caperesca* from the region of the Crozet Islands, provided by Corrigan et al. (2014). They are both short (COI – 262 bp, 16S – 301 bp) and do not group with any available sequence of *Paralicella* stored either in GenBank or BOLD. These records should also be removed from public databases.

Cryptic Diversity

The diversity patterns of the two nominal species studied differ considerably. Recent work by Bribiesca-Contreras et al. (2021) and some species delimitation methods used by us (BINs, ASAP on sequences, and GMYC) suggested further division of *P. tenuipes,* but this is not supported by the majority of methods and should be treated as so-called oversplitting of taxa. The fact that mostly one unit was recognized and the observation of low intraspecific distances confirm that no further division of *P. tenuipes* is justified. Oversplitting has been reported for other deep-sea species of Amphipoda from the North-West Pacific (Lörz et al., 2018a; Jażdżewska and Mamos, 2019) and could partly be explained by unequal sampling of all populations of certain species. It is worth noting also that the length of the studied fragment of the gene may have an influence on the final delimitation results. In our study, it can be seen that in the case of 16S sequences, when the shorter fragment was considered (ca. 250 bp), both the mean and maximum uncorrected p-distance were higher than when the longer (ca. 400 bp) sequences were analyzed (**Table 4**). It derives from the higher concentration of variable sites (4.5%) in the shorter fragment of 16S amplified by former authors studying *P. tenuipes* (Ritchie et al., 2015; Weston et al., 2021).

The opposite situation can be seen within the nominal *P. caperesca* that was further divided into separate MOTUs by the majority of analytical methods (**Figure 2**) that suggests the existence of cryptic speciation. The least conservative methods suggested that *P. caperesca* consists of as many as 18-21 units (e.g., BINs in BOLD). In this case, it appears that the BIN system applied in BOLD may oversplit the taxa, which derives from the fact that the threshold used is set at ca. 2% of COI sequence similarity (Ratnasingham and Hebert, 2013). The threshold values for this gene more successfully separating amphipod species are set at 3–7% of molecular similarity and are suggested to be family specific (Costa et al., 2009; Knox et al., 2012; Lobo et al., 2017; Tempestini et al., 2018; Jażdżewska and Mamos, 2019). As a result, the best justified division suggests the existence of six separate MOTUs within *P. caperesca*. Apart from two dominant MOTUs (MOTU 1 and MOTU 5), the remaining ones are represented by one to eight individuals. Samples containing *Paralicella* generally contain very large numbers of individuals (hundreds to thousands of specimens in each sample) and the sorting and identification is therefore generally carried out by the use of rapidly assessed morphological characters, indicating initially that the specimen belongs to the genus *Paralicella*. This is followed by separation at the species level as either *P. tenuipes* (with a distinct small red/brown eye and a strong bevel on P7) or *P. caperesca* (lacking the distinct small red/brown eye and lacking a bevel on P7). It should be noted that *P. caperesca* specimens possess a white or orange pigmented diffuse non-ommatidial eye in fresh material, but this often fades after preservation, and therefore it cannot be relied on for species determination.

The fine characters which are needed to distinguish between the two nominal species in this study and the other members of the genus (*P. fusiformis*, *P. microps*, *P. similis*, and *P. vaporalis*) are not routinely checked during the sorting process. Now that there is a clear indication that the *P. caperesca* complex comprises more than a single entity, extra care will need to be taken when sorting and identifying *Paralicella* samples, including examination of coxa 1, uropods and possibly some mouthpart characters to determine the species of *Paralicella* that is being dealt with. Attention will need to be paid to the means by which it will be possible to clearly discriminate between the MOTUs, particularly considering the likelihood that they co-occur throughout their range. This will mean revisiting the already collected samples of many thousands of individuals, to first determine a means to distinguish between the MOTUs morphologically and to describe each in full (whilst in alignment with the known 6 species), only then will we be able to clarify their distribution and depth ranges. Presently, only a small group of specimens representing four of the MOTUs defined here was available for morphological study. Detailed description of the available molecularly defined specimens is now underway.

Until such work can be completed, where studies involve morphological species delimitation, *P. caperesca* should be treated as a species complex, and cited as such in all publications. It is also important to note that as for *P. tenuipes,* the length of the 16S sequence fragment influences the uncorrected p-distance results. In the case of MOTU 1, the use of a short fragment suggests only a slightly higher diversity of sequences in comparison to longer ones because the extension of the studied fragment does not change the proportion of the

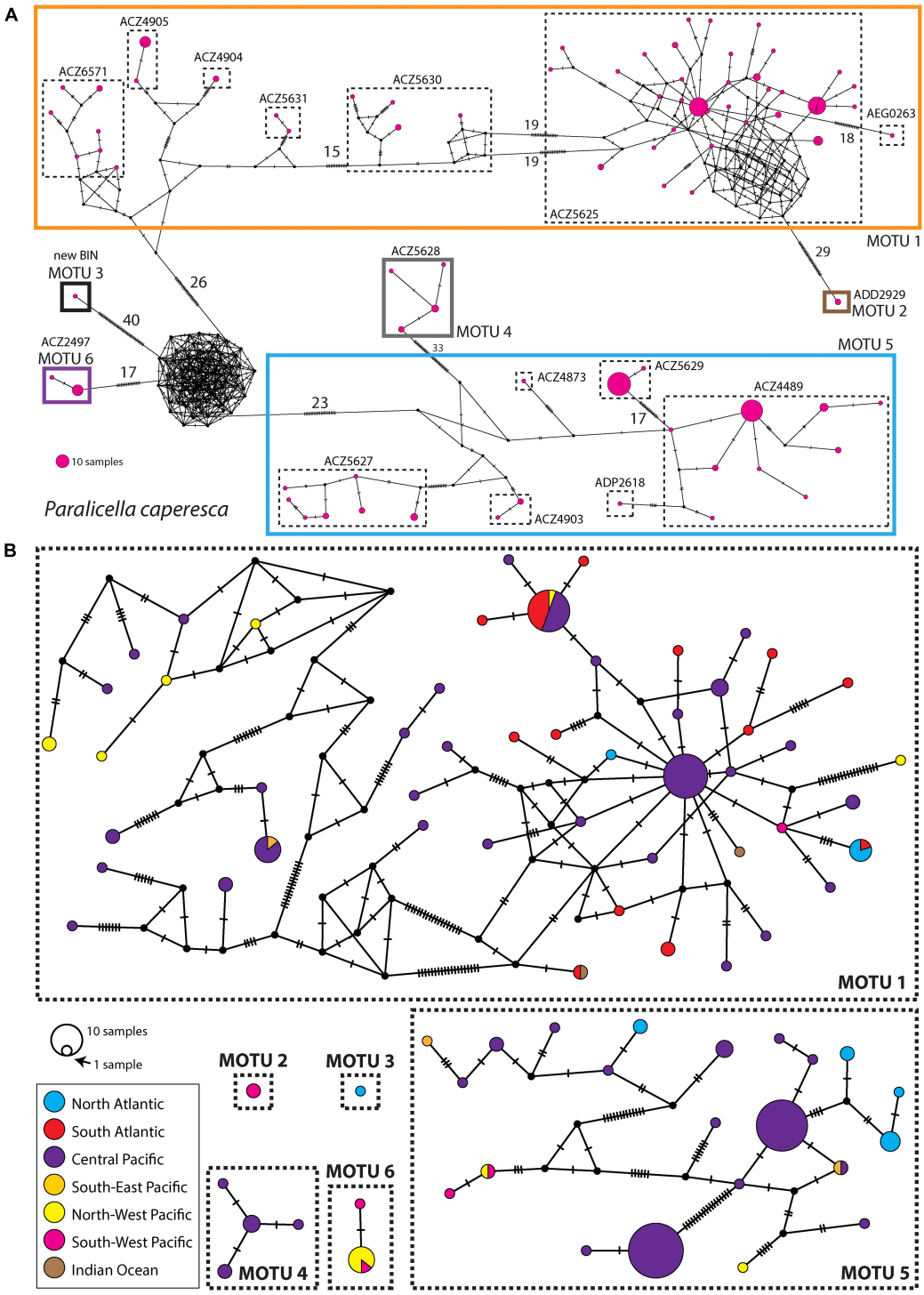

FIGURE 6 | (A) Median Joining Network of all *Paralicella caperesca* COI haplotypes with indication of the division of the taxon into BINs and final MOTUs studied. The numbers indicate mutation steps larger than 15. **(B)** Median Joining Networks of each studied MOTU of *P. caperesca*. Colors indicate geographic origin of haplotype.

variable sites reaching in both cases ca. 4.5%. For MOTU 5 the opposite pattern may be observed (**Table 4**) deriving from the considerable increase of variable sites (from two to six percent) in the longer sequence. The results derived from the longer fragment of 16S seem to be more congruent with the results from the other two genes studied, so it is highly

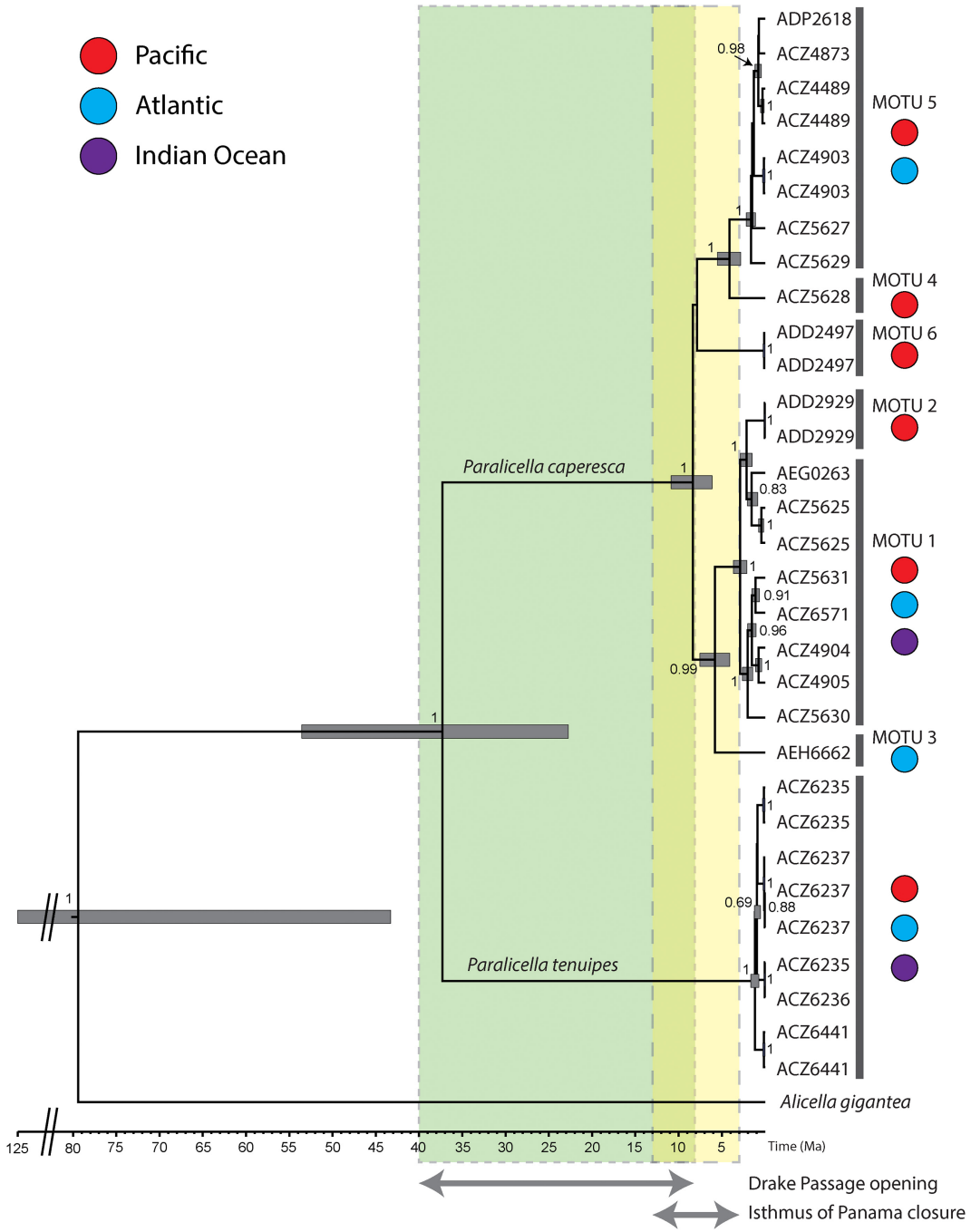

FIGURE 7 | Time-calibrated phylogeny of *Paralicella caperesca* and *P. tenuipes*. Maximum clade credibility chronogram was inferred from a strict molecular clock model based on the COI + 16S data set of studied taxa. The numbers given next to the respective main nodes indicate Bayesian posterior probabilities (>0.5). MOTUs 1–6 as separated by delimitation methods (in **Figure 2**). Colors indicate geographic distribution of given MOTU, while codes represent different BINs. Light green box indicate potential timeline of Drake Passage opening, light yellow box – the closure of the Isthmus of Panama, the overlap time marked in yellowish green.

recommended to use the longer fragment of 16S in future molecular studies.

Intraspecific diversification has already been observed by Ritchie et al. (2015) who distinguished four clades within the studied *Paralicella* specimens. 'Group 1' recognized in that study corresponds to *P. tenuipes*, 'Group 2' relates to our MOTU 6 of *P. caperesca*, 'Group 3' corresponds to our MOTU 5, whereas 'Group 4' combines individuals from our MOTU 1 and 2. In the subsequent paper, presenting the population structure of two *Paralicella* species collected in five distant Pacific trenches

TABLE 5 | Summary of genetic diversity and neutrality tests of three MOTUs within *P. caperesca* (MOTU1, MOTU4, and MOTU5) and *P. tenuipes* including separation of the geographic populations.

	N	h	Hd	FLD	FLF	Fu's Fs	R2	TD
P. caperesca MOTU1	104	50	0.93	– 0.58	– 0.69	– 9.37*	0.09	– 0.75
P. caperesca MOTU1 Central Pacific	67	30	0.89*	0.41	0.20	– 0.71	0.11	–0.33
P. caperesca MOTU1 Atlantic	26	14	0.88	– 2.17*	– 2.04*	– 2.67	0.08	– 1.33
P. caperesca MOTU1 North-West Pacific	7	6	0.95	0.17	0.12	1.51	0.17	– 0.27
P. caperesca MOTU4	7	4	0.81	– 0.52	– 0.55	– 1.39	0.17	– 0.65
P. caperesca MOTU5	88	22	0.78*	0.04	0.25	3.90	0.12	0.42
P. caperesca MOTU5 Central Pacific	73	14	0.69*	0.17	0.52	8.40	0.13	0.72
P. caperesca MOTU5 North Atlantic	9	4	0.78*	1.48	1.23	5.69	0.19	0.36
P. tenuipes	207	19	0.85*	– 0.78	0.28	7.49	0.13	1.60
P. tenuipes Central Pacific	163	17	0.83*	– 1.03	0.09	7.98	0.14	1.61
P. tenuipes Atlantic	35	7	0.76*	1.19	1.62	8.57	0.19	2.04
P. tenuipes North Atlantic	15	6	0.71*	1.21	1.16	4.10	0.18	0.84
P. tenuipes South Atlantic	20	6	0.80*	1.41	1.70	6.82	0.21	2.05

*N, number of individuals; h, number of haplotypes; Hd, haplotype diversity; FLD, Fu and Li's D; FLF, Fu and Li's F, Fu's Fs; R2, Ramos-Onsins and Rozas's; TD, Tajima's D. *Indicates statistically significant value ($p < 0.05$).*

(Ritchie et al., 2017) this division was only partly used – Group 1 (*P. tenuipes*) was named RFLP sp. 1, while groups 2–4 (*P. caperesca*) were combined into a single unit – RFLP sp. 2.

One of the important issues emerging from the use of molecular tools to identify species, particularly when cryptic diversity is noticed and the type collection used for species description is not available for genetic analysis, is to decide which of the molecularly recognized units represents the originally described taxon. For *P. tenuipes*, described from the region of Canary Islands (Chevreux, 1908), the closest area presently studied was the North Atlantic where representatives of three BINs were identified (**Figure 5**). Nevertheless, they all constitute a single species, and most probably they all inhabit the type locality of this taxon, which is further justified by the presence of the same BINs and haplotypes in the South Atlantic. Since cryptic diversity has been recognized within *P. caperesca*, deciding which of the lineages constitutes that originally described (Shulenberger and Barnard, 1976) is more difficult. This species was described from a large collection of amphipods from North of Hawaii; molecular analysis was not considered at that time. France and Kocher (1996) attempted to extract and study DNA of certain deep-sea scavenging species including *P. caperesca* and *P. tenuipes* collected in 1977 and 1978 in the Central North Pacific, most probably near the *locus typicus* of the first species. Their study resulted in four sequences of a short fragment of the 16S gene (ca. 160 bp) (GenBank accession numbers: U92692, U92693, U92694, U92695). The single sequence of *P. tenuipes* groups with sequences of individuals representing BOLD:ACZ6441 confirming its identity. Two sequences of *P. caperesca* have affinity to the 16S sequences of individuals ascribed to BOLD:ACZ5625, while the third is almost identical to the sequences of two individuals, one representing BOLD:ACZ6571, the second – BOLD:ACZ4905. All of these BINs belong to MOTU 1 of *P. caperesca*, which may suggest that the species description was based on individuals of this molecular unit. However, since the original collection studied by Shulenberger and Barnard (1976) consisted of several individuals and our study has already revealed that different MOTUs of *P. caperesca* co-exist in the Central Pacific, any decision on which MOTU can represent *P. caperesca sensu stricto* must be preceded by detailed morphological examination and, if possible, molecular study of the types.

Species Distribution and Population Genetics

Based on morphological studies, both studied species have been considered as widely spread or even cosmopolitan (**Table 7**; Shulenberger and Barnard, 1976; Brandt et al., 2012). Our study is the first that provides molecular evidence for the cosmopolitanism of *P. tenuipes*, as well as a very wide distribution of two of the MOTUs within *P. caperesca*. It confirms also the wide bathymetric ranges (2189–3673 vertical metres) of these species, mainly collected at abyssal depths (**Table 7**). It should be underlined that the restricted number of individuals (five in total) from the Indian Ocean for which the sequences were available might have an influence on our knowledge of these species' distributions. However, a recent molecular study of scavenging amphipods from hydrothermal vent fields in South-East and Central Indian Ridge did not reveal the presence of either *P. tenuipes* or any MOTU of *P. caperesca* there (Kniesz et al., in review[5]). The specific conditions of the areas adjacent to vent fields may influence the composition of the scavenging fauna and may be the reason for not recording the presently studied species. Additionally, the traps used in that study were placed relatively shallow (2500–2900 m) while *P. tenuipes* and *P. caperesca* seem to prefer greater depths. *P. tenuipes* was not recorded south of Antarctic Convergence, whereas individuals resembling *P. caperesca* have been recorded in the area of South Shetland and South Sandwich Islands as well as in the Lazarev Sea (De Broyer et al., 2004). Those animals however,

[5]Kniesz, K., Jażdżewska, A. M., Martinez Arbizu, P., and Kihara, T. C. (in review). DNA barcoding of scavenging amphipod community at active and inactive hydrothermal vents in the Indian Ocean. *Front. Mar. Sci.*

TABLE 6 | Molecular identification of sequences from Corrigan et al. (2014); Ritchie et al. (2015), and Iguchi et al. (2020).

	COI		16S		
Original ID	**GenBank acc. No**	**BIN**	**GenBank acc. No**	**Affinity to presently studied sequence**	**Final ID**
			Corrigan et al., 2014		
P. caperesca	**KF430243**	**No similarity to any *Paralicella* spp.**	**KF430270**	**No similarity to any *Paralicella* spp.**	**No identification possible to be made, records should be removed from public database**
			Ritchie et al., 2015		
P. tenuipes	KP713928	BOLD:ACZ6235	KP456110	*P. tenuipes*	*P. tenuipes*
P. tenuipes	KP713934	BOLD:ACZ6237	KP347450	*P. tenuipes*	*P. tenuipes*
P. tenuipes	KP713931	BOLD:ACZ6237	KP456113	*P. tenuipes*	*P. tenuipes*
P. tenuipes	KP713930	BOLD:ACZ6441	KP456112	*P. tenuipes*	*P. tenuipes*
P. tenuipes	KP713929	BOLD:ACZ6441	KP456111	*P. tenuipes*	*P. tenuipes*
P. caperesca	KP713925	BOLD:ACZ4905	KP456099	*P. caperesca*	*P. caperesca* MOTU 1
P. caperesca	KP713924	BOLD:ACZ5625	KP456101	*P. caperesca*	*P. caperesca* MOTU 1
Unidentified Primative Lysianassoid	**KP713917**	**BOLD:ACZ5625**	**KP456102**	***P. caperesca***	***P. caperesca* MOTU 1**
Unidentified Primative Lysianassoid	**KP713916**	**BOLD:ACZ6571**	**KP456100**	***P. caperesca***	***P. caperesca* MOTU 1**
P. tenuipes	**KP713932**	**BOLD:ADD2929**	**KP456104**	**Separate clade within *P. caperesca***	***P. caperesca* MOTU 2**
P. tenuipes	**KP713933**	**BOLD:ADD2929**	**KP456103**	**Separate clade within *P. caperesca***	***P. caperesca* MOTU 2**
P. caperesca	KP713923	BOLD:ACZ5627	KP456107	*P. caperesca*	*P. caperesca* MOTU 4
P. caperesca	KP713922	BOLD:ACZ4489	NA	NA	*P. caperesca* MOTU 5
P. caperesca	KP713921	BOLD:ACZ4903	KP456105	*P. caperesca*	*P. caperesca* MOTU 5
P. tenuipes	**KP713927**	**BOLD:ACZ4903**	**KP456106**	***P. caperesca***	***P. caperesca* MOTU 5**
P. tenuipes	**KP713926**	**BOLD:ADD2497**	**KP456098**	**Separate clade within *P. caperesca***	***P. caperesca* MOTU 6**
P. caperesca	**KP713920**	**BOLD:ADD2497**	**KP456097**	**Separate clade within *P. caperesca***	***P. caperesca* MOTU 6**
Valettietta anacantha	**KP713950**	**BOLD:ACZ5625**	**KP456094**	**No similarity to any *Paralicella* spp.**	**No identification possible to be made, records should be removed from public database**
			Iguchi et al., 2020		
Amphipoda sp. B05-5	LC484992	BOLD:ACZ6571	NA	NA	***P. caperesca* MOTU 1**
Amphipoda sp. B05-15	LC484983	BOLD:ACZ6571	NA	NA	***P. caperesca* MOTU 1**
Amphipoda sp. B05-16	LC484984	BOLD:ACZ6571	NA	NA	***P. caperesca* MOTU 1**
Amphipoda sp. B05-4	LC484991	BOLD:ACZ6571	NA	NA	***P. caperesca* MOTU 1**
Amphipoda sp. B05-7	LC484994	BOLD:AEG0263	NA	NA	***P. caperesca* MOTU 1**
Amphipoda sp. B05-10	LC484978	BOLD:ACZ4903	NA	NA	***P. caperesca* MOTU 5**
Amphipoda sp. B05-12	LC484980	BOLD:ADD2497	NA	NA	***P. caperesca* MOTU 6**
Amphipoda sp. B05-17	LC484985	BOLD:ADD2497	NA	NA	***P. caperesca* MOTU 6**
Amphipoda sp. B05-18	LC484986	BOLD:ADD2497	NA	NA	***P. caperesca* MOTU 6**
Amphipoda sp. B05-19	LC484987	BOLD:ADD2497	NA	NA	***P. caperesca* MOTU 6**
Amphipoda sp. B05-8	LC484995	BOLD:ADD2497	NA	NA	***P. caperesca* MOTU 6**
Amphipoda sp. B05-9	LC484996	BOLD:ADD2497	NA	NA	***P. caperesca* MOTU 6**
Amphipoda sp. B05-6	LC484993	BOLD:ACZ6441	NA	NA	***P. tenuipes***

In bold the cases where the incongruence between original and final identification occurred.

TABLE 7 | Summary of distribution of both species with respect to results based on morphology and molecular methods.

Northernmost station	Southernmost station	General distribution	Depth range [m]
	***Paralicella tenuipes* morphology**		
50°00.1′ N, 14°19.3′ W (Atlantic Ocean – PAP)	48°59′ S, 51°13′ E (Indian Ocean – Crozet Island)	Cosmopolitan	1414–6546
	***Paralicella tenuipes* genetics**		
49°00′18.0′′N, 16°28′15.6′′W (Atlantic Ocean – PAP)	26°33′10.8′′S 35°11′16.8′′W (Atlantic Ocean – Brazilian Basin)	Cosmopolitan	3818–6945
	***Paralicella caperesca* morphology**		
54°04.08′ N, 34°09.43′ W (Atlantic Ocean – PAP)	48°59′ S, 51°13′ E (Indian Ocean – Crozet Island)	Cosmopolitan	1740–6537
	***Paralicella caperesca* MOTU 1**		
49°00′18.0′′N 16°28′15.6′′W (Atlantic Ocean – PAP)	26°43′00.0′′S 175°11′00.0′′W (Pacific Ocean – Kermadec Trench)	Cosmopolitan	3818–6007
	***Paralicella caperesca* MOTU 2**		
26°43′00.0′′S 175°11′00.0′′W (Pacific Ocean – Kermadec Trench)	Known from one station only	Kermadec Trench	6007
	***Paralicella caperesca* MOTU 3**		
48°56′34.8′′N 16°29′06.0′′W (Atlantic Ocean – PAP)	Known from one station only	Porcupine Abyssal Plain	4846
	***Paralicella caperesca* MOTU 4**		
12°33′46.8′′N 116°43′01.2′′W (Pacific Ocean – CCZ)	19°27′03.6′′N 120°03′10.8′′W (Pacific Ocean – CCZ)	Clarion-Clipperton Zone	4057–4203
	***Paralicella caperesca* MOTU 5**		
49°00′18.0′′N 16°28′15.6′′W (Atlantic Ocean – PAP)	24°58′00.0′′S 171°03′00.0′′E (Pacific Ocean – SFB)	Atlantic & Pacific oceans	2500–6173
	***Paralicella caperesca* MOTU 6**		
19°22′31.8′′N 157°52′58.2′′E (Pacific Ocean – east of Mariana Trench)	24°58′00.0′′S 171°03′00.0′′E (Pacific Ocean – SFB)	West Pacific Ocean	2500–4100

PAP, Porcupine Abyssal Plain; CCZ, Clarion-Clipperton Zone; SFB, South Fidji Basin.

possessed certain characters that differed from the described species (De Broyer, personal communication), since they were not studied molecularly, we have not included these distribution records in our study.

Low genetic diversity and wide distribution of deep-sea species have been postulated by various authors (Zardus et al., 2006; McClain and Hardy, 2010; Etter et al., 2011) however, only a relatively low number of peracarid species are reported to present large horizontal ranges (Brandt et al., 2012). Recent studies of widely distributed species identified solely by morphology have revealed species complexes of multiple taxa with more restricted ranges when molecular methods are applied (Havermans et al., 2013; Verheye et al., 2016; Jakiel et al., 2019). Although cosmopolitanism of deep-sea species appears to be less common than previously thought, certain scavenging amphipod species have been confirmed by molecular studies as widely distributed. These include *Abyssorchomene distinctus* (Birstein and Vinogradov, 1960), *Eurythenes magellanicus* (Milne Edwards, 1848), *E. maldoror* (d'Udekem d'Acoz and Havermans, 2015), *Bathycallisoma schellenbergi* (Birstein and Vinogradov, 1958) and *Haptocallisoma abyssi* (Oldevig, 1959) (Havermans, 2016; Jażdżewska et al., 2020; Mohrbeck et al., 2021; Weston et al., 2021; Kniesz et al., in review[5]). Very few amphipod species have had a very wide (>2 km) vertical distribution molecularly confirmed, as has been observed here for *Paralicella*. Similar to the situation of wide geographic ranges inferred from morphological identification, several taxa previously listed as recorded from a wide bathymetric range appear to be more restricted when their genetic intraspecific structure is checked. Among amphipod species of confirmed wide bathymetric range

are *Abyssododecas styx* Takeuchi et al., 2016 and *Rhachotropis saskia* Lörz & Jażdżewska (Takeuchi et al., 2016; Lörz et al., 2018a). These two species inhabit abyssal and hadal depths of North-West Pacific, whereas the *Paralicella* species from our study are mainly abyssal taxa that are also collected in bathyal depths. There is a report of the collection of *P. caperesca* in the Indian Ocean that reached the research vessel deck still alive (Treude et al., 2002) suggesting high resistance of this species to decompression, however, this was an incidental case as the majority of collected individuals were dead on arrival at deck. However, other studies have confirmed the resistance of this species to decompression (Macdonald and Gilchrist, 1980; Yayanos, 1981). It is known that these species do cross the bathyal-abyssal border and have often been collected in the water column several metres above the seafloor (Ingram and Hessler, 1983; Thurston, 1990). Amphipods of the genus *Paralicella* are known to be obligate scavengers (Havermans and Smetacek, 2018; Horton et al., 2020). Carrion (particularly large carcasses of nekton), although providing nutrition for a long time and being more common in the deep sea than previously expected, is believed to be irregularly deposited and unevenly distributed over the seafloor (Smith and Baco, 2003; Havermans and Smetacek, 2018). Near feeding or spawning grounds as well as along species migration corridors, the availability of carrion is high (Smith, 2007) but in other open ocean areas this may not be the case. The irregularity of food availability implies their special adaptations including, their well-developed chemosensory system and good swimming abilities allowing quick access to available food sources (Hessler et al., 1978; Thurston, 1979; Ingram and Hessler, 1983; Klages et al., 2002; Premke et al., 2003). These adaptations may partly explain the wide horizontal ranges of the studied species, and to consider that resistance to changing pressure may also allow these amphipods to profit from food at different depths.

The separation of the two studied nominal *Paralicella* species from another species from the family Alicellidae (the supergiant amphipod, *Alicella gigantea* Chevreux, 1899) appeared to be ca. 80 Ma, which is earlier than recorded by Copilaş-Ciocianu et al. (2020). However, when considering the highest posterior density intervals in both cases the time of lineage separation overlap. The separation of the two nominal *Paralicella* species is reported here at ca. 35–37 Ma, which is similar to the divergence of *Paralicella caperesca* and *Valettietta anacantha* recorded by Copilaş-Ciocianu et al. (2020). However, in that study *P. tenuipes* was not considered. The time of diversification within Alicellidae, occurring from the Late Mesozoic to Middle Cenozoic (**Figure 7**), is congruent with the global climatic cooling during that period, and the transition from a halothermal ocean circulation into thermohaline one (McClain and Hardy, 2010; Copilaş-Ciocianu et al., 2020). The thermohaline ocean circulation is driven by high-latitude deep-water formation and results in cold, oxygenated waters at the bottom. Because amphipods are considered as well adapted to cold conditions with low tolerance to hypoxia (Copilaş-Ciocianu et al., 2020) the change of environmental conditions that has "opened" vast deep-sea bottom areas for colonization could have promoted the speciation of the studied species. The speciation of the two nominal species of *Paralicella* occurred at the time of serious reconfiguration of continents, when the Isthmus of Panama was still open, while the Drake Passage and the West Wind Drift was in the process of formation (Brandt et al., 2007; O'Dea et al., 2016; Straume et al., 2020). The fact that both species emerged already at that time may partly explain their present wide distribution – there was enough time to spread and different oceanic gateways were available. It should be considered that these species might have originated from shallow waters and only during the further stages of speciation submerged, so at the initial stage of expansion they might have been less dependent on the water depth both in the area of Isthmus of Panama and Drake Passage. The further speciation within *P. caperesca* is predicted as happening from ca. 7 Ma. At that time, only small and shallow water basins were present in the area of Isthmus of Panama, preventing the connection of the Central Pacific populations and may be responsible for the speciation of lineages geographically restricted to the Pacific (MOTUs 2, 4, 6) or to the Atlantic (MOTU 3). The full opening of the Drake Passage (reaching abyssal depths) and the formation of the West Wind Drift would have allowed maintenance of intraspecific connectivity. This contemporary Atlantic and Pacific population connectivity of *P. tenuipes*, as well as between MOTU 1 and MOTU 5 of *P. caperesca*, is confirmed by the distribution of haplotypes that are often shared between very distant regions (**Figures 5**, **6**) as well as by the lack, or very weak signal, of population separation within each of them (**Supplementary Figure S4**). On a more local scale, the constant gene flow within *P. tenuipes* and the two most widely distributed MOTUs of *P. caperesca* was recently observed by Bribiesca-Contreras et al. (2021) studying scavenging Amphipoda from three Areas of Particular Environmental Interest in the Clarion-Clipperton Zone. A similar pattern was recorded by Ritchie et al. (2017) for *Paralicella* RFLP sp. 1 that corresponds to *P. tenuipes.* In that case, although generally bidirectional, North-West direction of migration predominated. At the same time, a very weak signal of migration was observed for *Paralicella* RFLP sp. 2, but this may be explained by the fact that the taxon combined four different MOTUs of which two have a very restricted distribution. It should not be overlooked that the authors considered the studied species as the "trench" ones, not considering that from morphology-based literature both were reported from Central Pacific abyssal plain (Ritchie et al., 2017). It is also worth noting no evidence for recent population size changes of the *P. tenuipes* and the two MOTUs of *P. caperesca* that remains in contrast with other findings for deep-sea species. The significantly negative Tajima's *D* values observed for certain vent and non-vent taxa were interpreted as resulting from recent expansion of populations after disturbance events, suggestive of the instability of deep-sea habitats (Vrijenhoek, 2010; Taylor and Roterman, 2017). Although we are aware that some of the populations studied by us consist of a small number of individuals it appears that the populations of studied *Paralicella* species are stable over time, implying robustness and high plasticity of these taxa. It may be expected that they are less prone to unfavorable (human or non-human induced) events that occur in the abyss.

CONCLUSION

Our study has provided a detailed synthesis of the extensive published molecular data and incorporated new data on species in the genus *Paralicella*. We have shown that the two studied species have different intraspecific structures, with *Paralicella tenuipes* constituting a single molecular unit, while *P. caperesca* is a complex of potentially cryptic species. In terms of biogeography we have confirmed that *P. tenuipes* and two MOTUs of *P. caperesca* are widely distributed or even cosmopolitan taxa, while some of the lineages appear to have a more limited distribution. The two studied species' divergence occurred in the Eocene at the time of reconfiguration of the continents which might have allowed both species to colonize all oceans. The further speciation within *P. caperesca* is predicted as happening in the Miocene when the connection of the Atlantic and Pacific deep sea was already restricted, which may explain the recognition of some lineages with limited geographic ranges.

DATA AVAILABILITY STATEMENT

The datasets presented in this study can be found in online repositories. The names of the repository/repositories and accession number(s) can be found below: https://www.ncbi.nlm.nih.gov/genbank/, MZ655819–MZ655910, MZ655914–MZ655967, https://dx.doi.org/10.5883/DS-PCAPTEN, Barcode of Life Datasystems.

AUTHOR CONTRIBUTIONS

TH, EH, SB, and PMA collected and processed the samples. AJ and AD generated the genetic sequences. TH and EH carried out detailed morphological examination. AJ conceived the idea, with AJ and TM carrying out the analyses. All the authors contributed to drafting and reviewing the manuscript.

FUNDING

We thank the Masters and crew of the R/V *Meteor*, the R/V *Melville* and the R/V *Thomas G. Thompson*, and the RRS *James Cook* Cruise 165 and RRS *Discovery* Cruise 103 for their assistance during Meteor 79/1 DIVA-3, ABYSSLINE-1, ABYSSLINE-2, and expeditions to the Porcupine Abyssal Plain Sustained Observatory, respectively. The M79/1 DIVA-3 expedition was carried out with the support of German Science Foundation. The participation of EH in DIVA-3 was supported by the Canadian Museum of Nature funding numbers RS01, RS16 and RCZ09. Both ABYSSLINE cruises were funded by the UK Seabed Resources Ltd., while expeditions to the Porcupine Abyssal Plain Sustained Observatory were supported by the NERC National Capability funding to the National Oceanography Centre, as part of the Climate Linked Atlantic Section Science (CLASS) program (Grant Reference NE/R015953/1). The sorting of the material from DIVA-3 expedition took place at the DZMB Hamburg with help of Karen Jeskulke and Antje Fischer. The molecular work was conducted with the support of Smithsonian Institution and Canadian Centre for DNA Barcoding/Guelph, the CeDaMar "DNA barcoding deep-sea Peracarida" project and internal funds of the University of Lodz (B2011000000069). This is publication 82 of the Senckenberg am Meer Metabarcoding and DNA Laboratory.

SUPPLEMENTARY MATERIAL

The Supplementary Material for this article can be found online at: https://www.frontiersin.org/articles/10.3389/fmars.2021.750180/full#supplementary-material

Supplementary Material S1 | The summary of all sequences used in the study including identification (in case of published material presented as in the original papers), Barcode Index Numbers (BIN), station data and GenBank Accession Numbers.

Supplementary Material S2 | The full list of publications used to prepare the distribution maps of both *Paralicella* species.

Supplementary Figure S1 | Median Joining Network of 28S sequences. Colors of the circle according to the MOTU identified with delimitation methods. Codes indicate the BIN from which particular sequence type come from.

Supplementary Figure S2 | Extended Bayesian Skyline Plot of *Paralicella tenuipes*.

Supplementary Figure S3 | Extended Bayesian Skyline Plot of MOTUs 1, 4 and 5 of *Paralicella caperesca*.

Supplementary Figure S4 | Linear regression between geographic and molecular distances of *Paralicella tenuipes*, MOTU 1 and MOTU 5 of *Paralicella caperesca*. Below the graphs the summary of geographic distances between populations is presented (calculated with GoogleEarth Pro). Geographic codes: CCZ, Clarion-Clipperton Zone, Central Pacific; APEI 6, Area of Particular Environmental Interest 6, North of CCZ, Central Pacific; BB, Brazilian Basin, South Atlantic; NWP, North-West Pacific; PAP, Porcupine Abyssal Plain, North Atlantic. Genetic distances calculated with Kimura 2-parameter (K2P) for COI sequences.

REFERENCES

Achaz, G. (2009). Frequency spectrum neutrality tests: one for all and all for one. *Genetics* 183, 249–258. doi: 10.1534/genetics.109.104042

Astrin, J. J., and Stüben, P. E. (2008). Phylogeny in cryptic weevils: molecules, morphology and new genera of western Palaearctic Cryptorhynchinae (Coleoptera: Curculionidae). *Invertebr. Syst.* 22, 503–522. doi: 10.1071/is07057

Baco, A. R., Etter, R. J., Ribeiro, P. A., von der Heyden, S., Beerli, P., and Kinlan, B. P. (2016). A synthesis of genetic connectivity in deep-sea fauna and implications for marine reserve design. *Mol. Ecol.* 25, 3276–3298. doi: 10.1111/mec.13689

Bandelt, H. J., Forster, P., and Rohl, A. (1999). Median-joining networks for inferring intraspecific phylogenies. *Mol. Biol. Evol.* 16, 37–48. doi: 10.1093/oxfordjournals.molbev.a026036

Barnard, J. L., and Ingram, C. L. (1990). Lysianassoid Amphipoda (Crustacea) from deep-sea thermal vents. *Smithsonian Contrib. Zool.* 499, 1–80. doi: 10.5479/si.00810282.499

Barnard, J. L., and Shulenberger, E. (1976). Clarification of the abyssal amphipod *Paralicella tenuipes* Chevreux. *Crustaceana* 31, 267–274. doi: 10.1163/156854076X00053

Birstein, J. A., and Vinogradov, M. E. (1955). Pelagic gammarids (Amphipoda – Gammaridea) from Kuril-Kamchatka Trench. *Tr. Inst. Okeanologii* 12, 210–287. (in Russian)

Birstein, J. A., and Vinogradov, M. E. (1958). Pelagic gammarids (Amphipoda, Gammaridea) of NW Pacific. *Tr. Inst. Okeanologii* 27, 219–257. (in Russian)

Birstein, Y. A., and Vinogradov, M. E. (1960). Pelagic Gammaridea of the tropical part of the Pacific Ocean. *Tr. Inst. Okeanologii Akad. Nauk SSSR* 34, 165–241. [in Russian]

Bober, S., Brix, S., Riehl, T., Schwentner, M., and Brandt, A. (2018). Does the Mid-Atlantic Ridge affect the distribution of abyssal benthic crustaceans across the Atlantic Ocean? *Deep Sea Res. II Top. Stud. Oceanogr.* 148, 91–104. doi: 10.1016/j.dsr2.2018.02.007

Bouckaert, R. R., and Drummond, A. J. (2017). bModelTest: Bayesian phylogenetic site model averaging and model comparison. *BMC Evol. Biol.* 17:42. doi: 10.1186/s12862-017-0890-6

Bouckaert, R., Heled, J., Kühnert, D., Vaughan, T., Wu, C. H., Xie, D., et al. (2014). BEAST 2: a software platform for Bayesian evolutionary analysis. *PLoS Comput. Biol.* 10:e1003537. doi: 10.1371/journal.pcbi.1003537

Bouckaert, R., Vaughan, T. G., Barido-Sottani, J., Duchêne, S., Fourment, M., Gavryushkina, A., et al. (2019). BEAST 2.5: an advanced software platform for Bayesian evolutionary analysis. *PLoS Comput. Biol.* 15:e1006650. doi: 10.1371/journal.pcbi.1006650

Brandt, A., Błażewicz-Paszkowycz, M., Bamber, R., Mühlenhardt-Siegel, U., Malyutina, M., Kaiser, S., et al. (2012). Are there widespread peracarid species in the deep sea (Crustacea: Malacostraca)? *Pol. Polar Res.* 33, 139–162. doi: 10.2478/v10183-012-0012-5

Brandt, A., De Broyer, C., De Mesel, I., Ellingsen, K., Gooday, A., Hilbig, B., et al. (2007). The biodiversity of the deep Southern Ocean benthos. *Philos. Trans. R. Soc. B Biol. Sci.* 362, 39–66. doi: 10.1098/rstb.2006.1952

Bribiesca-Contreras, G., Dahlgren, T. G., Horton, T., Drazen, J. C., Drennan, R., Jones, D. O. B., et al. (2021). Biogeography and connectivity across habitat types and geographical scales in Pacific abyssal scavenging amphipods. *Front. Mar. Sci.* 8:705237. doi: 10.3389/fmars.2021.705237

Brix, S., Bober, S., Tschesche, C., Kihara, T. C., Driskell, A., and Jennings, R. M. (2018). Molecular species delimitation and its implications for species descriptions using desmosomatid and nannoniscid isopods from the VEMA fracture zone as example taxa. *Deep Sea Res. II Top. Stud. Oceanogr.* 148, 180–207. doi: 10.1016/j.dsr2.2018.02.004

Brix, S., Osborn, K. J., Kaiser, S., Truskey, S. B., Schnurr, S. M., Brenke, N., et al. (2020). Adult life strategy affects distribution patterns in abyssal isopods – implications for conservation in Pacific nodule areas. *Biogeosciences* 17, 6163–6184. doi: 10.5194/bg-17-6163-2020

Chevreux, E. (1899). Sur deux espèces géantes d'amphipodes provenant des campagnes du yacht princesse Alice. *Bull. Soc. Zool. Fr.* 24, 152–158.

Chevreux, E. (1908). Diagnoses d'amphipodes nouveaux provenant des campagnes de la „Princesse-Alice" dans l' Atlantique nord. *Bull. Inst. Océanogr. Monaco* 117, 1–13.

Chiba, S., Saito, H., Fletcher, R., Yogi, T., Kayo, M., Miyagi, S., et al. (2018). Human footprint in the abyss: 30 year records of deep-sea plastic debris. *Mar. Policy* 96, 204–212. doi: 10.1016/j.marpol.2018.03.022

Copilaş-Ciocianu, D., Borko, S., and Fiser, C. (2020). The late blooming amphipods: global change promoted post-Jurassic ecological radiation despite Palaeozoic origin. *Mol. Phylogenet. Evol.* 143:106664. doi: 10.1016/j.ympev.2019.106664

Copilaş-Ciocianu, D., Sidorov, D., and Gontcharov, A. (2019). Adrift across tectonic plates: molecular phylogenetics supports the ancient Laurasian origin of old limnic crangonyctid amphipods. *Org. Divers. Evol.* 19, 191–207. doi: 10.1007/s13127-019-00401-7

Corrigan, L. J., Horton, T., Fotherby, H., White, T. A., and Hoelzel, A. R. (2014). Adaptive evolution of deep-sea amphipods from the superfamily Lysianassoidea in the North Atlantic. *Evol. Biol.* 41, 154–165. doi: 10.1007/s11692-013-9255-2

Costa, F. O., Henzler, C. M., Lunt, D. H., Whiteley, N. M., and Rock, J. (2009). Probing marine *Gammarus* (Amphipoda) taxonomy with DNA barcodes. *Syst. Biodivers.* 7, 365–379. doi: 10.1017/S1477200009990120

De Broyer, C., Nyssen, F., and Dauby, P. (2004). The crustacean scavenger guild in Antarctic shelf, bathyal and abyssal communities. *Deep Sea Res. II Top. Stud. Oceanogr.* 51, 1733–1752. doi: 10.1016/j.dsr2.2004.06.032

Drummond, A. J., Rambaut, A., Shapiro, B. E. T. H., and Pybus, O. G. (2005). Bayesian coalescent inference of past population dynamics from molecular sequences. *Mol. Biol. Evol.* 22, 1185–1192. doi: 10.1093/molbev/msi103

d'Udekem d'Acoz, C., and Havermans, C. (2015). Contribution to the systematics of the genus *Eurythenes* S.I. Smith in Scudder, 1882 (Crustacea: Amphipoda: Lysianassoidea: Eurytheneidae). *Zootaxa* 3971, 1–80. doi: 10.11646/zootaxa.3971.1.1

Duffy, G. A., Gutteridge, Z. R., Thurston, M. H., and Horton, T. (2016). A comparative analysis of canyon and non-canyon populations of the deep-sea scavenging amphipod *Paralicella caperesca*. *J. Mar. Biol. Assoc. U. K.* 96, 1687–1699. doi: 10.1017/S0025315415002064

Edler, D., Klein, J., Antonelli, A., and Silvestro, D. (2021). raxmlGUI 2.0: a graphical interface and toolkit for phylogenetic analyses using RAxML. *Methods Ecol. Evol.* 12, 373–377. doi: 10.1111/2041-210X.13512

Etter, R. J., Boyle, E. E., Glazier, A., Jennings, R. M., Dutra, E., and Chase, M. R. (2011). Phylogeography of a pan-Atlantic abyssal protobranch bivalve: implications for evolution in the deep Atlantic. *Mol. Ecol.* 20, 829–843. doi: 10.1111/j.1365-294X.2010.04978.x

Ezard, T., Fujisawa, T., and Barraclough, T. G. (2009). *Splits: Species' Limits by Threshold Statistics. R Package Version 1.0-18/r45*.

Felsenstein, J. (1985). Phylogenies and the comparative method. *Am. Nat.* 125, 1–15. doi: 10.2307/2461605

Fischer, V., Elsner, N. O., Brenke, N., Schwabe, E., and Brandt, A. (2015). Plastic pollution of the Kuril–Kamchatka Trench area (NW pacific). *Deep Sea Res. II Top. Stud. Oceanogr.* 111, 399–405. doi: 10.1016/j.dsr2.2014.08.012

France, S. C., and Kocher, T. D. (1996). DNA sequencing of formalin-fixed crustaceans from archival research collections. *Mol. Mar. Biol. Biotechnol.* 5, 304–313.

Fu, Y.-X. (1997). Statistical tests of neutrality of mutations against population growth, hitchhiking and background selection. *Genetics* 147, 915–925. doi: 10.1093/genetics/147.2.915

Fu, Y.-X., and Li, W.-H. (1993). Statistical tests of neutrality of mutations. *Genetics* 133, 693–709. doi: 10.1093/genetics/133.3.693

Gollner, S., Kaiser, S., Menzel, L., Jones, D. O. B., Brown, A., Mestre, N. C., et al. (2017). Resilience of benthic deep-sea fauna to mining activities. *Mar. Environ. Res.* 129, 76–101. doi: 10.1016/j.marenvres.2017.04.010

Hartman, S. E., (2019). RRS Discovery Cruise 103 21 Jun- 10 Jul 2019. Water Column and Seafloor Time-Series Studies at the Porcupine Abyssal Plain Sustained Observatory. National Oceanography Centre Cruise Report, No. 61. Southampton: National Oceanography Centre, Southampton, 146.

Havermans, C. (2016). Have we so far only seen the tip of the iceberg? Exploring species diversity and distribution of the giant amphipod *Eurythenes*. *Biodiversity* 17, 12–25. doi: 10.1080/14888386.2016.1172257

Havermans, C., and Smetacek, V. (2018). Bottom-up and top-down triggers of diversification: a new look at the evolutionary ecology of scavenging amphipods in the deep sea. *Prog. Oceanogr.* 164, 37–51. doi: 10.1016/j.pocean.2018.04.008

Havermans, C., Sonet, G., d'Udekem d'Acoz, C., Nagy, Z. T., Martin, P., Brix, S., et al. (2013). Genetic and morphological divergences in the cosmopolitan deep-sea amphipod *Eurythenes gryllus* reveal a diverse abyss and a bipolar species. *PLoS One* 8:e74218. doi: 10.1371/journal.pone.0074218

Hein, J. R., Koschinsky, A., and Kuhn, T. (2020). Deep-ocean polymetallic nodules as a resource for critical materials. *Nat. Rev. Earth Environ.* 1, 158–169. doi: 10.1038/s43017-020-0027-0

Hessler, R. R., Ingram, C. L., Yayanos, A. A., and Burnett, B. R. (1978). Scavenging amphipods from the floor of the Philippine Trench. *Deep Sea Res.* 25, 1029–1047. doi: 10.1016/0146-6291(78)90585-4

Horton, T., Thurston, M. H., Vlierboom, R., Gutteridge, Z., Pebody, C. A., Gates, A. R., et al. (2020). Are abyssal scavenging amphipod assemblages linked to climate cycles? *Progr. Oceanogr.* 184:102318. doi: 10.1016/j.pocean.2020.102318

Hou, Z. G., Fu, J. H., and Li, S. Q. (2007). A molecular phylogeny of the genus *Gammarus* (Crustacea: Amphipoda) based on mitochondrial and nuclear gene sequences. *Mol. Phylogenet. Evol.* 45, 596–611. doi: 10.1016/j.ympev.2007.06.006

Iguchi, A., Nishijima, M., Yoshioka, Y., Miyagi, A., Miwa, R., Tanaka, Y., et al. (2020). Deep-sea amphipods around cobalt-rich ferromanganese crusts: taxonomic diversity and selection of candidate species for connectivity analysis. *PLoS One* 15:e0228483. doi: 10.1371/journal.pone.0228483

Ingram, C. L., and Hessler, R. R. (1983). Distribution and behavior of scavenging amphipods from the central North Pacific. *Deep Sea Res. A Oceanogr. Res. Pap.* 30, 683–706. doi: 10.1016/0198-0149(83)90017-1

Jakiel, A., Palero, F., and Błażewicz, M. (2019). Deep ocean seascape and Pseudotanaidae (Crustacea: Tanaidacea) diversity at the Clarion-Clipperton Fracture Zone. *Sci. Rep.* 9:17305. doi: 10.1038/s41598-019-51434-z

Jamieson, A. J., Kilgallen, N. M., Rowden, A. A., Fujii, T., Horton, T., Lörz, A. N., et al. (2011). Bait-attending fauna of the Kermadec Trench, SW Pacific Ocean: evidence for an ecotone across the abyssal–hadal transition zone. *Deep Sea Res. I Oceanogr. Res. Pap.* 58, 49–62. doi: 10.1016/j.dsr.2010.11.003

Janssen, A., Kaiser, S., Meißner, K., Brenke, N., Menot, L., and Martínez Arbizu, P. (2015). A reverse taxonomic approach to assess macrofaunal distribution patterns in abyssal pacific polymetallic nodule fields. *PLoS One* 10:e0117790. doi: 10.1371/journal.pone.0117790

Janssen, A., Stuckas, H., Vink, A., and Martínez Arbizu, P. (2019). Biogeography and population structure of predominant macrofaunal taxa (Annelida and Isopoda) in abyssal polymetallic nodule fields: implications for conservation and management. *Mar. Biodiver.* 49, 2641–2658. doi: 10.1007/s12526-019-00997-1

Jażdżewska, A. M., and Mamos, T. (2019). High species richness of Northwest Pacific deep-sea amphipods revealed through DNA barcoding. *Prog. Oceanogr.* 178:102184. doi: 10.1016/j.pocean.2019.102184

Jażdżewska, A. M., Thurston, M., and Ziemkiewicz, A. (2020). "Amphipoda. distribution of deep-sea benthic Amphipoda along the NW Pacific," in *Biogeographic Atlas of the Deep NW Pacific Fauna*, eds H. Saeedi, and A. Brandt (Sofia: Pensoft), 377–414. doi: 10.3897/ab.e51315

Jones, D. O., Kaiser, S., Sweetman, A. K., Smith, C. R., Menot, L., Vink, A., et al. (2017). Biological responses to disturbance from simulated deep-sea polymetallic nodule mining. *PLoS One* 12:e0171750. doi: 10.1371/journal.pone.0171750

Kapli, P., Lutteropp, S., Zhang, J., Kobert, K., Pavlidis, P., Stamatakis, A., et al. (2017). Multi-rate Poisson tree processes for single-locus species delimitation under maximum likelihood and Markov chain Monte Carlo. *Bioinformatics* 33, 1630–1638. doi: 10.1093/bioinformatics/btx025

Katoh, K., and Standley, D. M. (2013). MAFFT multiple sequence alignment software version 7: improvements in performance and usability. *Mol. Biol. Evol.* 30, 772–780. doi: 10.1093/molbev/mst010

Katoh, K., Misawa, K., Kuma, K., and Miyata, T. (2002). MAFFT: a novel method for rapid multiple sequence alignment based on fast Fourier transform. *Nucleic Acids Res.* 30, 3059–3066. doi: 10.1093/nar/gkf436

Klages, M., Muyakshin, S., Soltwedel, T., and Arntz, W. E. (2002). Mechanoreception, a possible mechanism for food fall detection in deep-sea scavengers. *Deep Sea Res. I Oceanogr. Res. Pap.* 49, 143–155. doi: 10.1016/S0967-0637(01)00047-4

Knox, M. A., Hogg, I. D., Pilditch, C. A., Lörz, A. N., Hebert, P. D. N., and Steinke, D. (2012). Mitochondrial DNA (COI) analyses reveal that amphipod diversity is associated with environmental heterogeneity in deep-sea habitats. *Mol. Ecol.* 21, 4885–4897. doi: 10.1111/j.1365-294X.2012.05729.x

Kumar, S., Stecher, G., and Tamura, K. (2016). MEGA7: molecular evolutionary genetics analysis version 7.0 for bigger datasets. *Mol. Biol. Evol.* 33, 1870–1874. doi: 10.1093/molbev/msw054

Librado, P., and Rozas, J. (2009). DnaSP v5: a software for comprehensive analysis of DNA polymorphism data. *Bioinformatics* 25, 1451–1452. doi: 10.1093/bioinformatics/btp187

Lobo, J., Ferreira, M. S., Antunes, I. C., Teixeira, M. A. L., Borges, L. M. S., Sousa, R., et al. (2017). Contrasting morphological and DNA barcode-suggested species boundaries among shallow-water amphipod fauna from the southern European Atlantic coast. *Genome* 60, 147–157. doi: 10.1139/gen-2016-0009

Lörz, A. N., Tandberg, A. H. S., Willassen, E., and Driskell, A. (2018b). *Rhachotropis* (Eusiroidea, Amphipoda) from the North East Atlantic. *Zookeys* 2018, 75–101. doi: 10.3897/zookeys.731.19814

Lörz, A.-N., Jażdżewska, A. M., and Brandt, A. (2018a). A new predator connecting the abyssal with the hadal in the Kuril-Kamchatka Trench, NW Pacific. *PeerJ* 6:e4887. doi: 10.7717/peerj.4887

Macdonald, A. G., and Gilchrist, I. (1980). Effects of hydraulic decompression and compression on deep-sea amphipods. *Comp. Biochem. Phys. A* 67, 149–153. doi: 10.1016/0300-9629(80)90420-X

Mamos, T., Wattier, R., Burzyński, A., and Grabowski, M. (2016). The legacy of a vanished sea: a high level of diversification within a European freshwater amphipod species complex driven by 15 My of Paratethys regression. *Mol. Ecol.* 3, 795–810. doi: 10.1111/mec.13499

Mandt, M. W. (1822). *Observationes in Historiam Naturalem et Anatomiam Comparatam in Itinere Groenlandico Factae. Dissertatio Inauguralis Quam Consensu et Auctoritate Gratiosi Micorum Ordinis in Universitate Literaria Berolinensi ut Summi in Medicina et Chirurgia Honores Rite.* 40.

Martínez Arbizu, P., Brix, S., Kaiser, S., Brandt, A., George, K., Arndt, H., et al. (2015). *Deep-Sea Biodiversity, Current Activity, and Seamounts in the Atlantic – Cruise No. M79/1 – June 10 – August 26, 2009 – Montevideo (Uruguay) – Ponta Delgada (Portugal). METEOR-Berichte, M79/1, 92 pp., DFG-Senatskommission für Ozeanographie*. doi: 10.2312/cr_m79_1

McClain, C. R., and Hardy, S. M. (2010). The dynamics of biogeographic ranges in the deep sea. *Proc. R. Soc. B Biol. Sci.* 277, 3533–3546. doi: 10.1098/rspb.2010.1057

Meyer, C. P. (2003). Molecular systematics of cowries (Gastropoda: Cypraeidae) and diversification patterns in the tropics. *Biol. J. Linn. Soc.* 79, 401–459. doi: 10.1046/j.1095-8312.2003.00197.x

Milne Edwards, H. (1848). Sur un crustacé amphipode, remarquable par sa grande taille. *Ann. Sci. Nat. Zool. Ser.* 3 9:398.

Mohrbeck, I., Horton, T., Jażdżewska, A. M., and Martínez Arbizu, P. (2021). DNA-barcoding and cryptic diversity of deep-sea acavenging amphipods in the Clarion-Clipperton Zone (Eastern Equatorial Pacific). *Mar. Biodiver.* 51:26. doi: 10.1007/s12526-021-01170-3

Monaghan, M. T., Wild, R., Elliot, M., Fujisawa, T., Balke, M., Inward, D. J., et al. (2009). Accelerated species inventory on Madagascar using coalescent-based models of species delineation. *Syst. Biol.* 58, 298–311. doi: 10.1093/sysbio/syp027

O'Dea, A., Lessios, H. A., Coates, A. G., Eytan, R. I., Restrepo-Moreno, S. A., Cione, A. L., et al. (2016). Formation of the Isthmus of Panama. *Sci. Adv.* 2:e1600883. doi: 10.1126/sciadv.1600883

Oldevig, H. (1959). *Arctic, Subarctic and Scandinavian Amphipods in the Collections of the Swedish Natural History Museum in Stockholm. Goteborgs Kungliga Vetenskaps- och Vitterhets-Samhalles Handlingar, Sjatte Foljden, (Ser B.),* Vol. 8. Göteborg: Elanders boktr, 1–132.

Palumbi, S. R., Martin, A., Romano, S., McMillan, W. O., Stice, L., and Grabowski, G. (1991). *The Simple Fool's Guide to PCR. Version 2*. Honolulu, HI: University of Hawaii Press, 45.

Patel, T., Robert, H., d'Udekem d'Acoz, C., Martens, K., De Mesel, I., Degraer, S., et al. (2020). Biogeography and community structure of abyssal scavenging Amphipoda (Crustacea) in the Pacific Ocean. *Biogeosciences* 17, 2731–2744. doi: 10.5194/bg-17-2731-2020

Pons, J., Barraclough, T. G., Gomez-Zurita, J., Cardoso, A., Duran, D. P., Hazell, S., et al. (2006). Sequence-based species delimitation for the DNA taxonomy of undescribed insects. *Syst. Biol.* 55, 595–609. doi: 10.1080/10635150600852011

Premke, K., Muyakshin, S., Klages, M., and Wegner, J. (2003). Evidence for long-range chemoreceptive tracking of food odour in deep-sea scavengers by scanning sonar data. *J. Exp. Mar. Biol. Ecol.* 285–286, 283–294. doi: 10.1016/S0022-0981(02)00533-6

Puillandre, N., Brouillet, S., and Achaz, G. (2021). ASAP: assemble species by automatic partitioning. *Mol. Ecol. Res.* 21, 609–620. doi: 10.1111/1755-0998.13281

QGIS.org (2021). *QGIS Geographic Information System. QGIS Association*. Available online at: http://www.qgis.org

R Core Team (2021). *R: A Language and Environment for Statistical Computing*. Vienna: R Foundation for Statistical Computing.

Rambaut, A., Drummond, A. J., Xie, D., Baele, G., and Suchard, M. A. (2018). Posterior summarization in Bayesian phylogenetics using Tracer 1.7. *Syst. Biol.* 67, 901–904. doi: 10.1093/sysbio/syy032

Ramirez-Llodra, E., Brandt, A., Danovaro, R., De Mol, B., Escobar, E., German, C. R., et al. (2010). Deep, diverse and definitely different: unique attributes of the world's largest ecosystem. *Biogeosciences* 7, 2851–2899. doi: 10.5194/bg-7-2851-2010

Ramos-Onsins, S. E., and Rozas, J. (2002). Statistical properties of new neutrality tests against population growth. *Mol. Biol. Evol.* 19, 2092–2100. doi: 10.1093/oxfordjournals.molbev.a004034

Ratnasingham, S., and Hebert, P. D. N. (2007). The barcode of life data system. (http://www.barcodinglife.org). *Mol. Ecol. Res.* 7, 355–364. doi: 10.1111/j.1471-8286.2007.01678.x

Ratnasingham, S., and Hebert, P. D. N. (2013). A DNA-based registry for all animal species: the barcode index number (BIN) system. *PLoS One* 8:e66213. doi: 10.1371/journal.pone.0066213

Rex, M. A., McClain, C. R., Johnson, N. A., Etter, R. J., Allen, J. A., Bouchet, P., et al. (2005). A source-sink hypothesis for abyssal biodiversity. *Am. Nat.* 165, 163–178. doi: 10.1086/427226

Riehl, T., Brenke, N., Brix, S., Driskell, A., Kaiser, S., and Brandt, A. (2014). Field and laboratory methods for DNA studies on deep-sea isopod crustaceans. *Pol. Polar Res.* 35, 203–224. doi: 10.2478/popore-2014-0018

Riehl, T., Lins, L., and Brandt, A. (2018). The effects of depth, distance, and the Mid-Atlantic Ridge on genetic differentiation of abyssal and hadal isopods (Macrostylidae). *Deep Sea Res. II Top. Stud. Oceanogr.* 148, 74–90. doi: 10.1016/j.dsr2.2017.10.005

Ritchie, H., Jamieson, A. J., and Piertney, S. B. (2015). Phylogenetic relationships among hadal amphipods of the superfamily Lysianassoidea: implications for taxonomy and biogeography. *Deep Sea Res. I Oceanogr. Res. Pap.* 105, 119–131. doi: 10.1016/j.dsr.2015.08.014

Ritchie, H., Jamieson, A. J., and Piertney, S. B. (2017). Population genetic structure of two congeneric deep-sea amphipod species from geographically isolated hadal trenches in the Pacific Ocean. *Deep Sea Res. I Oceanogr. Res. Pap.* 119, 50–57. doi: 10.1016/j.dsr.2016.11.006

Ruhl, H. A., Ballinger, T., Barone, G., Benoist, N., Bett, B., Biede, V., et al. (2019). *RRS James Cook Cruise 165 19 May - 12 Jun 2018. Water Column and Seafloor Time-Series Studies at the Porcupine Abyssal Plain Sustained Observatory. National Oceanography Centre Cruise Report, No. 57*. Southampton: National Oceanography Centre, Southampton, 15

Shulenberger, E., and Barnard, J. L. (1976). Amphipods from an abyssal trap set in the North Pacific Gyre. *Crustaceana* 31, 241–258. doi: 10.1163/156854076X00035

Smith, C. R. (2007). "Bigger is better: the role of whales as detritus in marine ecosystems," in *Whales, Whaling and Ocean Ecosystems*, eds P. D. Estes, D. P. De Master, R. L. Brownell, D. F. Doak, T. M. William, and D. Berkeley (Berkeley, CA: University of California Press), 286–301. doi: 10.1525/9780520933200-026

Smith, C. R., and Baco, A. R. (2003). Ecology of whale falls at the deep-sea floor. *Oceanogr. Mar. Biol. Ann. Rev.* 41, 311–354.

Stamatakis, A. (2014). RAxML version 8: a tool for phylogenetic analysis and post-analysis of large phylogenies. *Bioinformatics* 30, 1312–1313. doi: 10.1093/bioinformatics/btu033

Straume, E. O., Gaina, C., Medvedev, S., and Nisancioglu, K. H. (2020). Global cenozoic paleobathymetry with a focus on the northern hemisphere oceanic gateways. *Gondwana Res.* 86, 126–143. doi: 10.1016/j.gr.2020.05.011

Tajima, F. (1989). Statistical method for testing the neutral mutation hypothesis by DNA polymorphism. *Genetics* 123, 585–595. doi: 10.1093/genetics/123.3.585

Takeuchi, I., Tomikawa, K., and Lindsay, D. (2016). A new genus and species of Phtisicidae (Crustacea: Amphipoda) from abyssal depths in the Japan Trench, with special reference to similarities with Southern Ocean genera. *J. Crust. Biol.* 36, 469–506. doi: 10.1163/1937240X-00002457

Taylor, M. L., and Roterman, C. N. (2017). Invertebrate population genetics across Earth's largest habitat: the deep-sea floor. *Mol. Ecol.* 26, 4872–4896. doi: 10.1111/mec.14237

Tempestini, A., Rysgaard, S., and Dufresne, F. (2018). Species identification and connectivity of marine amphipods in Canada's three oceans. *PLoS One* 13:e0197174. doi: 10.1371/journal.pone.0197174

Thurston, M. H. (1979). Scavenging abyssal amphipods from the North-East Atlantic Ocean. *Mar. Biol.* 51, 55–68. doi: 10.1007/BF00389031

Thurston, M. H. (1990). Abyssal necrophagous amphipods (Crustacea: Amphipoda) in the northeast and tropical Atlantic Ocean. *Progr. Oceanogr.* 24, 257–274. doi: 10.1016/0079-6611(90)90036-2

Treude, T., Janßen, F., Queisser, W., and Witte, U. (2002). Metabolism and decompression tolerance of scavenging lysianassoid deep-sea amphipods. *Deep Sea Res. I Oceanogr. Res. Pap.* 49, 1281–1289. doi: 10.1016/S0967-0637(02)00023-7

Verheye, M. L., Backeljau, T., and d'Udekem d'Acoz, C. (2016). Looking beneath the tip of the iceberg: diversification of the genus *Epimeria* on the Antarctic shelf (Crustacea, Amphipoda). *Polar Biol.* 39, 925–945. doi: 10.1007/s00300-016-1910-5

Victorero, L., Watling, L., Deng Palomares, M. L., and Nouvian, C. (2018). Out of sight, but within reach: a global history of bottom-trawled deep-sea fisheries from >400m depth. *Front. Mar. Sci.* 5:98. doi: 10.3389/fmars.2018.00098

Vrijenhoek, R. C. (2010). Genetic diversity and connectivity of deep-sea hydrothermal vent metapopulations. *Mol. Ecol.* 19, 4391–4411. doi: 10.1111/j.1365-294X.2010.04789.x

Washburn, T. W., Menot, L., Bonifácio, P., Pape, E., Błażewicz, M., Bribiesca-Contreras, G., et al. (2021). Patterns of macrofaunal biodiversity across the Clarion-Clipperton Zone: an area targeted for seabed mining. *Front. Mar. Sci.* 8:626571. doi: 10.3389/fmars.2021.626571

Weston, J. N. J., Peart, R. A., Stewart, H. A., Ritchie, H., Piertney, S. B., Linley, T. D., et al. (2021). Scavenging amphipods from the Wallaby-Zenith Fracture Zone: extending the hadal paradigm beyond subduction trenches. *Mar. Biol.* 168:1. doi: 10.1007/s00227-020-03798-4

Yayanos, A. A. (1981). Reversible inactivation of deep-sea amphipods (*Paralicella capresca*) by a decompression from 601 bars to atmospheric pressure. *Comp. Biochem. Phys. A* 69, 563–565. doi: 10.1016/0300-9629(81)93020-6

Zardus, J. D., Etter, R. J., Chase, M. R., Rex, M. A., and Boyle, E. E. (2006). Bathymetric and geographic population structure in the pan-Atlantic deep-sea bivalve *Deminucula atacellana* (Schenck, 1939). *Mol. Ecol.* 15, 639–651. doi: 10.1111/j.1365-294X.2005.02832.x

Zhang, J., Kapli, P., Pavlidis, P., and Stamatakis, A. (2013). A general species delimitation method with applications to phylogenetic placements. *Bioinformatics* 29, 2869–2876. doi: 10.1093/bioinformatics/btt499

Conflict of Interest: The authors declare that the research was conducted in the absence of any commercial or financial relationships that could be construed as a potential conflict of interest.

Publisher's Note: All claims expressed in this article are solely those of the authors and do not necessarily represent those of their affiliated organizations, or those of the publisher, the editors and the reviewers. Any product that may be evaluated in this article, or claim that may be made by its manufacturer, is not guaranteed or endorsed by the publisher.

Copyright © 2021 Jażdżewska, Horton, Hendrycks, Mamos, Driskell, Brix and Martínez Arbizu. This is an open-access article distributed under the terms of the Creative Commons Attribution License (CC BY). The use, distribution or reproduction in other forums is permitted, provided the original author(s) and the copyright owner(s) are credited and that the original publication in this journal is cited, in accordance with accepted academic practice. No use, distribution or reproduction is permitted which does not comply with these terms.

frontiers in Marine Science

ORIGINAL RESEARCH
published: 09 December 2021
doi: 10.3389/fmars.2021.713022

A Global Red List for Hydrothermal Vent Molluscs

Elin A. Thomas[1], Aoife Molloy[1], Nova B. Hanson[2], Monika Böhm[3,4], Mary Seddon[5] and Julia D. Sigwart[1,6]*

[1] Queen's University Marine Laboratory, Queen's University Belfast, Belfast, United Kingdom, [2] Department of Ocean Sciences, Memorial University of Newfoundland, St John's, NL, Canada, [3] Global Center for Species Survival, Indianapolis Zoological Society, Indianapolis, IN, United States, [4] Institute of Zoology, Zoological Society of London, London, United Kingdom, [5] International Union for Conservation of Nature, Species Survival Commission (IUCN SSC) Mollusc Specialist Group, Devon, United Kingdom, [6] Senckenberg Research Institute and Museum, Frankfurt, Germany

With the accelerating development of direct and indirect anthropogenic threats, including climate change and pollution as well as extractive industries such as deep-sea mining, there is an urgent need for simple but effective solutions to identify conservation priorities for deep-sea species. The International Union for Conservation of Nature (IUCN) Red List of Threatened Species is an effective and well-recognized tool to promote the protection of species and presents an opportunity to communicate conservation threats to industry, policy makers, and the general public. Here, we present the Vent Red List for molluscs: a complete global assessment of the extinction risk of all described molluscs endemic to hydrothermal vents, a habitat under imminent threat from deep-sea mining. Of the 184 species assessed, 62% are listed as threatened: 39 are Critically Endangered, 32 are Endangered, and 43 are Vulnerable. In contrast, the 25 species that are fully protected from deep-sea mining by local conservation measures are assessed as Least Concern, and a further 45 species are listed as Near Threatened, where some subpopulations face mining threats while others lie within protected areas. We further examined the risk to faunas at specific vent sites and biogeographic regions using a relative threat index, which highlights the imperiled status of vent fields in the Indian Ocean while other vent sites within established marine protected areas have a high proportion of species assessed as Least Concern. The Vent Red List exemplifies how taxonomy-driven tools can be utilized to support deep-sea conservation and provides a precedent for the application of Red List assessment criteria to diverse taxa from deep-sea habitats.

Keywords: deep-sea mining, IUCN Red List, hydrothermal vents, conservation, molluscs

OPEN ACCESS

Edited by:
Greg W. Rouse,
University of California, San Diego,
United States

Reviewed by:
Damianos Chatzievangelou,
Jacobs University Bremen, Germany
Travis William Washburn,
University of Hawai'i at Mānoa,
United States

****Correspondence:***
Elin A. Thomas
ethomas07@qub.ac.uk

Specialty section:
This article was submitted to
Deep-Sea Environments and Ecology,
a section of the journal
Frontiers in Marine Science

Received: *21 May 2021*
Accepted: *30 September 2021*
Published: *09 December 2021*

Citation:
Thomas EA, Molloy A,
Hanson NB, Böhm M, Seddon M and
Sigwart JD (2021) A Global Red List
for Hydrothermal Vent Molluscs.
Front. Mar. Sci. 8:713022.
doi: 10.3389/fmars.2021.713022

INTRODUCTION

As a vast and relatively unexplored ecosystem, the deep sea presents unique conservation challenges. The heterogeneity of deep-sea habitats makes it difficult to identify representative systems for area-based conservation (Van Dover et al., 2018), variability in governance across Exclusive Economic Zones (EEZ) and Areas Beyond National Jurisdiction (ABNJ) engenders inconsistency in global deep-sea management (Gjerde et al., 2008), and restricted biological knowledge limits the capacity to understand the impact of threatening events to deep-sea taxa

(Danovaro et al., 2017). As industrial interest and commercial exploitation begins to accelerate faster than biological discovery, we face an increasingly urgent need for simple but effective tools to protect deep-sea species.

While the seafloor is home to incredible life, it is also characterized by large quantities of commercially valuable minerals including polymetallic sulfides at hydrothermal vents, manganese nodules on abyssal plains, and cobalt-rich ferromanganese crusts on seamounts (Hein et al., 2013; Petersen et al., 2016). The mining of these deep-sea environments and their resources is now being widely considered, and in some cases instigated (Okamoto et al., 2019), as demand for industrially important metals grows and technological capabilities improve (Sharma, 2011, 2015). Despite several studies concluding that mining will have an adverse and often irreversible impact on local deep-sea biodiversity (e.g., Gollner et al., 2017; Van Dover et al., 2017; Niner et al., 2018; Simon-Lledó et al., 2019), very few conservation measures have been implemented to date.

Of the deep-sea habitats threatened by mining, hydrothermal vents harbor the highest density of life (Van Dover et al., 2018). These are very small environments, occupying only ~ 50 km^2 of the seafloor, globally (Sigwart et al., 2017), yet each hydrothermal vent site is characterized by a multitude of unique species, hosting a relative biomass to that of coral reefs or tropical rainforests (Van Dover, 2000). As well as being highly insular and distinct in biodiversity from the surrounding benthos, hydrothermal vent communities also exhibit high levels of endemism and regional variation in species composition, with many endemics having only limited connectivity with other local vent sites (Rogers et al., 2012; Yahagi et al., 2019). Molluscs represent one of the dominant groups in vent habitats, with good global coverage and a large degree of vent-endemism (Wolff, 2005; Chapman et al., 2019). As important members of the vent community, they inhabit an array of niches including hosting endosymbiotic bacteria in specialized organs (Chen et al., 2018a), forming dense aggregations that provide substrate for other species (Laming et al., 2018; Sun et al., 2020), and exhibit unique ecological traits (e.g., Chen et al., 2018b).

Taxonomically driven solutions should be central to deep-sea conservation initiatives (Glover et al., 2018). A transparent and reliable evaluation of the conservation status of vent-endemic species would enable clear communication of threats to diverse stakeholders. The International Union for Conservation of Nature (IUCN) Red List of Threatened Species (hereafter, the Red List) is an internationally recognized taxon-based conservation tool that informs global policies by providing the most comprehensive and rigorous information available on species extinction risk (Rodrigues et al., 2006). The Red List allows for consistent assessment of extinction risk for any animal, plant, or fungal taxon through the use of standardized criteria, and its application has been widely successful in raising awareness of threats and ensuring the protection of species in other systems (Betts et al., 2020).

The Red List uses five categories with escalating risk that imply a higher expectation of extinction. Species with adequate data that are not threatened can fall into two categories: Least Concern, typically including widespread taxa or taxa not affected by threats, or Near Threatened, with taxa that are close to qualifying for a threatened category but do not meet all criteria (IUCN, 2012). Species that are threatened are subdivided into the following categories: Vulnerable, Endangered, and Critically Endangered, where taxa face a high, very high, or extremely high risk of extinction, respectively (IUCN, 2012). To be listed within a threatened category, species must meet the requirements and specific thresholds of at least one of the IUCN Red List Criteria: comprising criteria A and C which use data on population sizes and declines, criterion B which uses the geographic range of the species to estimate extinction risk, criterion D which is applicable to species with very restricted populations, and criterion E which uses quantitative analysis to assess probability of extinction (IUCN, 2012).

Deep-sea mining is already a recognized potential threat to vent ecosystems, as extensively discussed in recent literature (Van Dover et al., 2017; Miller et al., 2018; Niner et al., 2018), but it remains uncertain whether mining poses a sufficient threat to risk the total global extinction of vent species. The Red List presents an opportunity to assess the extent to which deep-sea mining would imperil individual vent-endemic species across different global sites (Sigwart et al., 2019). Furthermore, assessments of entire taxonomic groups are most effective as they allow for comprehensive comparison of threat (e.g., Carpenter et al., 2008). This study therefore aimed to assess the extinction risk of all molluscs endemic to hydrothermal vents using the Red List criteria. The resulting Vent Red List provides a universally recognized assessment of the threat of deep-sea mining for vent molluscs. All of these assessments have been reviewed and are published on the global IUCN Red List of species (IUCN, 2021). We further compare the distribution of species at risk to illustrate the relative threat levels to vent-endemic taxa across different biogeographic regions and regulatory areas.

MATERIALS AND METHODS

Taxon Selection

We used species records from existing studies (Wolff, 2005; Chapman et al., 2019) and expert knowledge to compile a complete list of all mollusc species described to date (up to 2021) endemic to active hydrothermal vent environments. As Red List assessments are taxon-specific, only named species were included in this study. Species were considered endemic where they had only been recorded at hydrothermal vents at time of assessment. Species that are also known from other deep-sea habitats, as well as vent-peripheral species (including all cephalopods), were excluded from this list, leaving a total of 184 vent-endemic molluscs (**Supplementary Material 1**). These species span five different mollusc classes: Gastropoda, Bivalvia, Monoplacophora, Polyplacophora, and Solenogastres.

Red List Assessments

We assessed the extinction risk of each species using the Red List criteria (IUCN, 2012), following IUCN guidelines and the method presented by Thomas et al. (2021). All assessments were made using Red List criteria B and/or D2 (**Table 1**), which use

TABLE 1 | Application of the IUCN Red List categories and criteria to hydrothermal vent-endemic molluscs, based on IUCN guidelines (IUCN, 2012) and definitions listed in Thomas et al. (2021).

Red List category	Category requirements
Critically Endangered (5)	Criterion B • EOO < 100 km^2 *and/or* AOO < 10 km^2 • 1 location* • Continuing decline† observed, estimated, inferred or projected in any of: EOO; AOO; area, extent and/or quality of habitat; number of locations or subpopulations; number of mature individuals
Endangered (4)	Criterion B • EOO < 5,000 km^2 *and/or* AOO < 500 km^2 • ≤ 5 locations* • Continuing decline† observed, estimated, inferred or projected in any of: EOO; AOO; area, extent and/or quality of habitat; number of locations or subpopulations; number of mature individuals
Vulnerable (3)	Criterion B • EOO < 20,000 km^2 *and/or* AOO < 2,000 km^2 • ≤ 10 locations* • Continuing decline† observed, estimated, inferred or projected in any of: EOO; AOO; area, extent and/or quality of habitat; number of locations or subpopulations; number of mature individuals **AND/OR** Criterion D2 • AOO < 20 km^2 *or* ≤ 5 locations • Plausible future threat° that could drive the species to Critically Endangered or Extinct in a very short time
Near Threatened (2)	Criterion B • EOO < 20,000 km^2 *and/or* AOO < 2,000 km^2, ≤ 10 locations, but no continuing decline† **AND/OR** Criterion D2 • AOO < 20 km^2 and ≤ 5 locations, but threat is not expected to drive species to Critically Endangered or Extinct in a very short time owing to the protection of some sites
Least Concern (1)	No continuing decline† or plausible future threat°

The assigned Risk Score of each category is indicated in brackets. EOO, Extent of Occurrence; AOO, Area of Occupancy.
**Location is a technical term in the context of Red List assessments, specifically, a distinct area where a threatening event can rapidly affect all individuals in the area (IUCN, 2012).*
†A continuing decline is inferred in areas of exploratory mining contracts signed by the International Seabed Authority or in the Exclusive Economic Zones of nations that have granted mining licenses (Thomas et al., 2021).
°A plausible future threat is considered where there are no regulations in place to protect from future deep-sea mining (Thomas et al., 2021).

geographic distribution data and information about continuing declines (criterion B) or plausible future threats causing extreme declines (criterion D2) to determine extinction risk. Nearly all vent species are lacking data to calculate population sizes and trends or run extinction risk models required for the other criteria (Thomas et al., 2021). Literature reviews were conducted for each species and data collected included the name, location, depth, biogeographic region, and local jurisdiction of the vent fields from which each species is known. Each assessment is therefore based on the best available published distribution data available at the time and may be subject to revisions as new data become available. Vent field names and coordinates listed in the literature were compared and aligned with the InterRidge Vents Database to ensure consistent nomenclature for sites (Beaulieu and Szafranski, 2020).

As the primary anthropogenic threat to vent-endemic species (Van Dover, 2014), deep-sea mining informed the criteria B and D2 requirements of continuing declines and plausible future threats for the Vent Red List assessments (**Table 1**). The local mining threat for each locality was determined based on regional seabed management objectives and the regulatory frameworks at sites within the range of each species (Thomas et al., 2021). Hydrothermal vents in EEZs are regulated by national governments and those in ABNJ are regulated by the International Seabed Authority (ISA) (Thompson et al., 2018). Key considerations for threat assessment included the implementation of deep-sea mining licenses, marine protected areas (MPAs), and mining moratoria. For example, continuing decline was inferred in areas of exploratory mining contracts signed by the ISA or in the EEZs of nations that have granted mining licenses (criterion B); plausible future threat was considered in areas where there are no regulations in place to protect from future deep-sea mining (criterion D2) (Thomas et al., 2021).

Threat Score

To illustrate the global distribution of extinction risk to vent species, all assessment data were amalgamated to produce a list of hydrothermal vent fields with the number of species assessed under each Red List category at each site (**Supplementary Material 2**). As with previous studies (e.g., Tingley et al., 2019), the five Red List categories were then assigned a sequential ranked risk score (Least Concern = 1, Near Threatened = 2, Vulnerable = 3, Endangered = 4, Critically Endangered = 5), and the number of species in each category were multiplied by its risk score and summed, to produce a total assessment of threat to all species at that vent field (Eq. 1).

$$Ranked\ Sum = \sum \left(Risk\ Score \times Number\ Spp.\right)_i \quad (1)$$

where i is each Red List category.

To reduce bias between sites with varying species richness, a standardized Threat Score was calculated by dividing the Ranked Sum by the total number of species across all categories at that site (Eq. 2).

$$Threat\ Score = \frac{Ranked\ Sum}{Species\ Richness} \quad (2)$$

For example, at the Menez Gwen vent field on the Mid-Atlantic Ridge, there are eight species, of which six species were assessed as Least Concern (risk score = 1) and two Near Threatened (risk score = 2). Thus, the Ranked Sum is (6*1)+(2*2) = 10, resulting in a Threat Score of 10/8 = 1.25 for that vent field.

RESULTS

Of the 184 vent-endemic mollusc species assessed for the Vent Red List, 114 (62%) are assessed as threatened (listed as Vulnerable, Endangered or Critically Endangered) by deep-sea mining, and a further 45 (24.4%) are listed as Near Threatened (**Table 2**, **Figure 1**, and **Supplementary Material 1**). Only 13.6% of species are listed as Least Concern, under the protection of MPAs. Sufficient data were available to complete assessments of extinction risk for all species and none are listed as Data Deficient. The majority of the molluscs assessed are highly restricted within their respective biogeographic regions (**Figure 1A**), with over 60% of species known only from one or two hydrothermal vent fields (**Figure 2**).

Generally, mollusc species richness is low at individual sites: of the 110 vent fields listed in this study, only 35 host five or more vent-endemic mollusc species, with over half hosting only one or two species (**Figure 1A**). Individual hydrothermal vent fields in the Northern East Pacific Rise have the greatest recorded species richness for vent-endemic molluscs, with the 13N, 21N and 9 50'N East Pacific Rise vent fields hosting 32, 28, and 28 species, respectively (**Supplementary Material 2**). The Mid-Atlantic Ridge has the greatest collective diversity, with an average species richness of 7.13 across its vent fields. The Northeast Pacific ridges and Southwest Pacific basins also have relatively high species richness, while the Indian Ocean and East Scotia Ridge vents have the lowest collective species richness across the nine biogeographic regions (**Figure 1A**).

The assignment of different Red List categories is dependent on local regulatory frameworks, with the threat level varying across different countries' EEZs, ISA mining license areas, and designated MPAs (**Figure 1B**; Thomas et al., 2021). The Threat Score illustrates the overall extinction risk for the endemic mollusc species at each vent field and is indicative of the threat posed by deep-sea mining to the area (**Figure 1C**). Globally, over half of vent fields have a Threat Score $\geq$ 3, signifying that hydrothermal vent species in those areas are at a high extinction risk. Individually, vent fields in the Indian Ocean and Northwest Pacific have the maximum Threat Score of 5, indicative of the Critically Endangered status assigned to species at these sites, whereas all vent fields on the East Scotia Ridge have the minimum Threat Score of 1, representative of assessments of Least Concern (**Figure 1C**).

Among the nine major biogeographical regions examined (**Figure 1A**), Indian Ocean vent molluscs are under the greatest extinction risk, with 100% of species listed in threatened categories, including 60% as Critically Endangered (**Table 2** and **Figure 1C**). This coincides with the distribution of ISA mining licenses across vent sites along the Central and Southwest Indian Ridges in the Indian Ocean (**Figure 1B**). Species at Northwest and Southwest Pacific vents, where there is a varying threat level across different countries' EEZs (**Figures 1B,C**), are also at high risk, with 77.8 and 95.7% listed in threatened categories, respectively (**Table 2**). The individual vent fields with the highest Threat Scores in these regions lie within the Japan and Papua New Guinea EEZs, where deep-sea mining licenses have been granted, whereas vent fields protected by the Marianas Trench Marine National Monument have a lower Threat Score (**Figure 1C**). Mid-Atlantic Ridge vent molluscs have the greatest spread of extinction risk, with 30% of species listed in threatened categories, 30% as Near Threatened, and 40% as Least Concern (**Table 2**). This corresponds with the incidence of both ISA mining licenses and the Azores' vent-specific MPAs along the Mid-Atlantic Ridge (**Figure 1B**).

The three East Pacific biogeographic regions have the greatest proportion of species assessed as Near Threatened, each with

TABLE 2 | Current IUCN Red List status for all 184 hydrothermal vent-endemic mollusc species described to date, by biogeographic region.

Biogeographic region	LC	NT	VU	EN	CR	Species richness	% Threatened	% Threatened + NT
Mid-Atlantic Ridge	8	6		4	1	19	26.3	57.9
Mid-Cayman Spreading Centre			1			1	100.0	100.0
East Scotia Ridge	4					4	0.0	0.0
Indian Ocean			1	3	6	10	100.0	100.0
Northeast Pacific	2	9	6			17	35.3	88.2
Northern East Pacific Rise	8	25	14			47	29.8	83.0
Southern East Pacific Rise		14	8			22	36.4	100.0
Northwest Pacific	3	5	3	15	10	36	77.8	91.7
Southwest Pacific		2	14	10	22	48	95.8	100.0
All	25	45	43	32	39	184	62.0	86.4

Note that some species are located at vent fields across multiple biogeographic regions. IUCN Red List Category abbreviations: CR, Critically Endangered; EN, Endangered; VU, Vulnerable; NT, Near Threatened; LC, Least Concern. Threatened categories include all species listed as VU, EN, or CR.

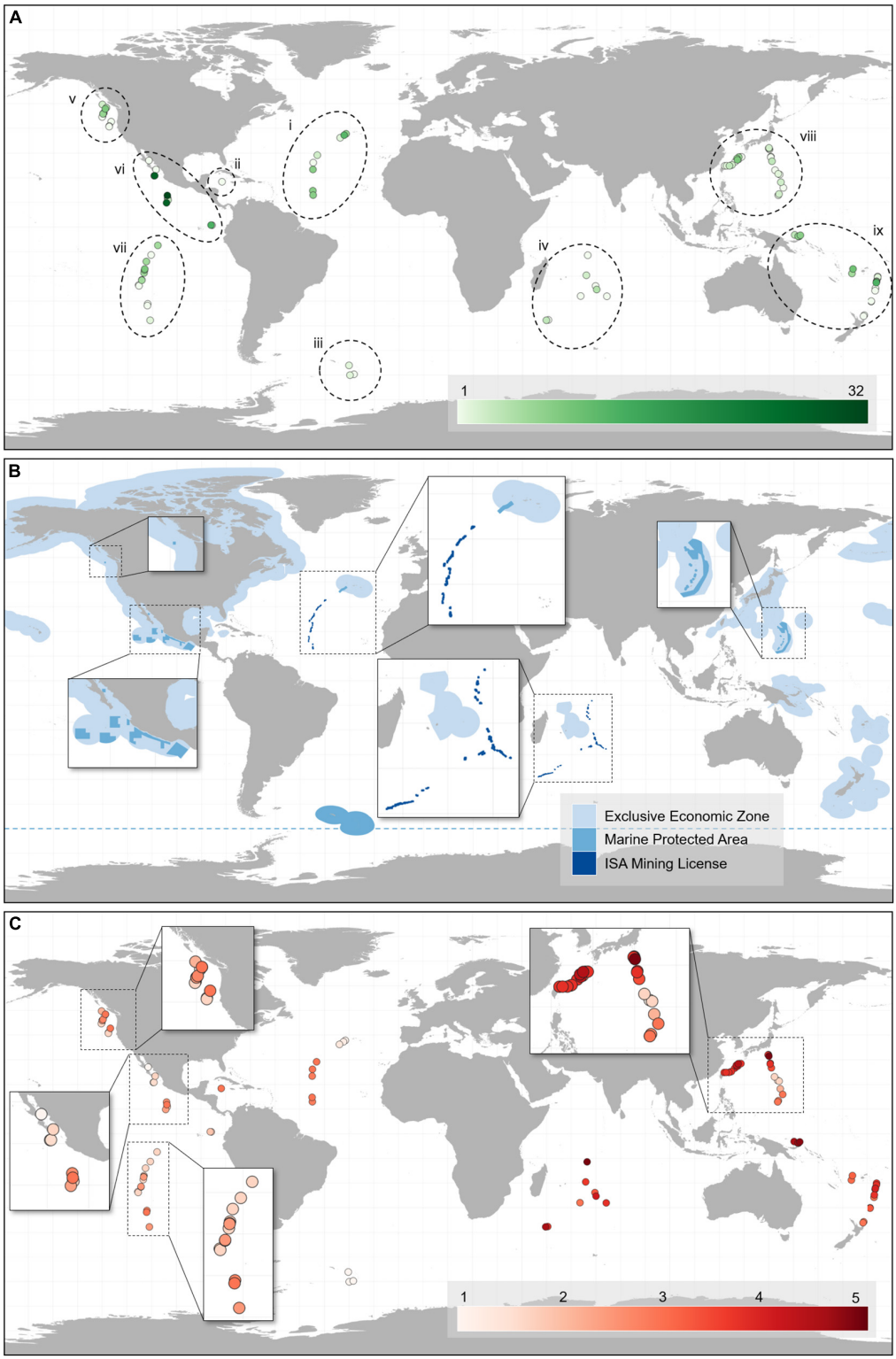

FIGURE 1 | Global distribution of threat to hydrothermal vent-endemic mollusc species from deep-sea mining, based on IUCN Red List assessments. **(A)** Map showing the species richness of vent-endemic molluscs described to date at the hydrothermal vent fields included in this study, where light green denotes low species richness and dark green denotes high species richness. Dashed shapes denote the different biogeographic regions for hydrothermal vents (Rogers et al., 2012): (i) Mid-Atlantic Ridge, (ii) Mid-Cayman Spreading Center, (iii) East Scotia Ridge, (iv) Indian Ocean, (v) Northeast Pacific, (vi) Northern East Pacific Rise, vii: Southern East Pacific Rise, (viii) Northwest Pacific, (ix) Southwest Pacific. **(B)** Map showing the locality and extent of different seabed regulatory areas relevant to the

(Continued)

FIGURE 1 | hydrothermal vent fields included within this study, including exploratory polymetallic sulfide mining licenses granted by the International Seabed Authority, Marine Protected Areas, and countries' Exclusive Economic Zones. Dashed mid blue line denotes the Antarctic Treaty boundary. Insets are included for areas with smaller details. **(C)** Map showing the scale of mining threat to each hydrothermal vent field included within this study, where 1 denotes a low Threat Score associated with Least Concern Red List assessments, and 5 denotes a high Threat Score associated with Critically Endangered assessments. Insets are included for areas with high density of vent fields.

over 50% of species located both within and outside MPAs implemented by Mexico and Canada (**Table 2** and **Figure 1**). There are no active mining licenses and as a consequence there are no species in the East Pacific assessed as Endangered or Critically Endangered (**Table 2**). Nonetheless, several vent fields in this region, especially along the Southern East Pacific Rise, lie in ABNJ without protection from deep-sea mining (**Figure 1B**). Species located in areas that have significant protection from deep-sea mining are consistently assessed at lowest risk; for example, all four East Scotia Ridge vent molluscs are assessed as Least Concern as a result of the Antarctic Treaty and the South Georgia and the South Sandwich Islands MPA (**Figure 1B**).

DISCUSSION

The Vent Red List is indicative of the unique biodiversity and threat profile of each hydrothermal vent field and biogeographic region, and can be used to effectively communicate and drive the conservation of these remarkable deep-sea habitats. The importance of mining licenses as a controlling factor in the determination of Red List status underlines the threat of potential mining to the conservation of vent-endemic species.

Biogeographic Distribution of Mining Threats

The distribution of threats to hydrothermal vents is closely tied to the regulation within each geographic area. In ABNJ, hydrothermal vents within ISA mining license areas along the Mid-Atlantic and Indian Ocean Ridges (Miller et al., 2018) have a higher Threat Score than those at the Northern and Southern East Pacific Rise, with Indian Ocean vent species exhibiting the greatest proportion of threatened Red List assessments. This is influenced by the overlap in species ranges with a variety of regulatory areas: species found at sites along the Mid-Atlantic Ridge have ranges across a mosaic of ABNJ and EEZs with differing protections. Threats to vent sites within individual EEZs are highly variable and dependent on current national regulation of the seabed. Vent fields that lie within the territorial waters of countries that have granted mining licenses, such as Japan (Okamoto et al., 2019) and Papua New Guinea (Hoagland et al., 2010), generally exhibit high Threat Scores. Conversely, vent species in countries and regions that have endeavored to preserve portions of the seabed with MPAs, such as the Azores (Calado et al., 2011; Abecasis et al., 2015) and Mexico (Menini and Van Dover, 2019), are at a much lower risk of extinction.

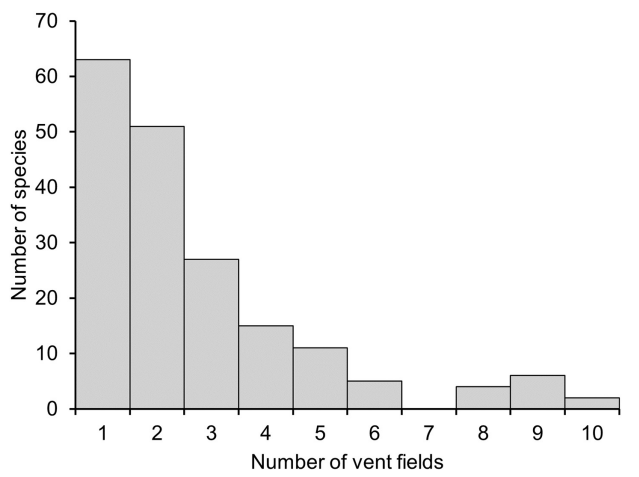

FIGURE 2 | Frequency distribution of the range of global vent-endemic mollusc species; histogram based on the numbers of hydrothermal vent sites in the range of species assessed in the Vent Red List.

While this study is focused on vent-endemic molluscs, our results are representative of the global distribution of mining threat for all vent-endemic taxa. Deep-sea species tend to be very data-limited, therefore future assessments of extinction risk for other vent taxa, including crustaceans and polychaetes, are expected to be reliant on the same Red List criteria as the Vent Red List (Thomas et al., 2021). Vent species exhibit high endemicity, and the primary anthropogenic threat is regionally controlled, thus the overall proportion of Red List categories for hydrothermal vent environments is unlikely to vary significantly with the addition of new taxa. The Red List is a species-based conservation tool, yet in this case it provides a comprehensive and reliable illustration of the geographic distribution of threats to a specific deep-sea habitat.

Red Listing the Deep Sea

Taxonomy-driven tools such as the Red List can cultivate deep-sea conservation; the application of Red List assessments to vent-endemic molluscs provides a precedent for other deep-sea taxa and habitats (Glover et al., 2018; Sigwart et al., 2019). Red List assessments are easily understood by a wide range of stakeholders (Rodrigues et al., 2006; Betts et al., 2020), and have the potential to provide an alternative perspective to ecosystem-based management approaches and enhance deep-sea conservation initiatives beyond hydrothermal vents.

The cobalt-rich ferromanganese crusts of seamounts, for example, are a target of five mining exploration licenses granted by the ISA to Brazil, China, Japan, Russia, and the South Korea (Miller et al., 2018; ISA, 2021). Seamounts are characterized by high productivity (Clark et al., 2010) and are rich in long-lived corals that likely take decades to millennia to recover from disturbance (Gollner et al., 2017; Watling and Auster, 2017). Likewise, gas hydrate deposits that occur in conjunction with cold

seeps, another important chemosynthetic habitat in the deep sea that hosts hundreds of similarly endemic species to vents (Wolff, 2005; Suess, 2018), are also under increasing consideration for commercial extraction (Chong et al., 2016; Miller et al., 2018). The insular nature, relatively well-documented global distribution, and imminent mining threat to both these habitats mean it is viable to apply a Red List approach to assess these hotspots of deep-sea biodiversity (Thomas et al., 2021).

Further Considerations

One potential limitation to our Red List approach, as with the majority of deep-sea research, is the underlying lack of observational data for different vent populations. None of the species included in this study were assessed as Data Deficient, yet it is recognized that the distribution and range of some mollusc species at hydrothermal vents is not fully known and requires further research. The global summary of endemic molluscs at hydrothermal vent sites illustrates overall low species richness across the majority of vent fields, compared to a few species-rich sites. This may be indicative of the paucity of baseline biodiversity knowledge for deep-sea habitats (Glover et al., 2018); however, this could also be a feature of the local and regional heterogeneity seen in vent communities arising from geographic variation in tectonic activity and vent geochemistry (Van Dover, 2000; Thaler and Amon, 2019). In the face of accelerating threats, assessments of extinction risk can only be based on the best available data at the time (IUCN, 2016), and although data are lacking for many groups (Glover et al., 2018), the Vent Red List demonstrates that there is sufficient information to assess even relatively data-poor species using Red List criteria (Thomas et al., 2021).

Specimen collection and taxonomic research are fundamental to deep-sea conservation, and present a bottleneck to the application of taxon-based conservation tools (Glover et al., 2018). This can be especially problematic where there is ongoing research that could result in taxonomic revisions, such as the study of species complexes. For example, among *Lepetodrilus* species on the East Pacific Rise, genetic evidence from multiple studies delineate separate lineages that are currently included within nominal species (Johnson et al., 2008; Matabos and Jollivet, 2019). Assessing a species complex as a single taxon could artificially lower the threat category in a Red List assessment because the taxon represents an over-estimation of combined abundance and range for several species. Taxonomic research and timely updates following reviews are, therefore, of the utmost importance to ensure accurate measures of extinction risk. Ongoing research can be integrated into Red List assessment text and taxa can be reassessed as frequently as required (IUCN, 2012). Furthermore, based on current findings, seabed management and mining regulation appears to have a greater impact on Red List assessment outcomes than the distribution data for individual species (Thomas et al., 2021).

A more concerning trend that has recently emerged is the potential North/South divide in the extent of biological research and deep-sea mining prospects (Thaler and Amon, 2019). We found a similar pattern in this study, with the Indian Ocean having the greatest proportion of threatened Red List assessments despite exhibiting one of the lowest collective species richness counts. The high proportion of Critically Endangered assessments at the Indian Ocean vent fields is indicative of their biodiversity uniqueness as species can only be assessed as Critically Endangered under Red List criterion B if they are known from a single location (Thomas et al., 2021). In fact, along with the Southwest Pacific, the Indian Ocean hosts the greatest proportion of locally endemic species known only from a single hydrothermal vent field. Further research is however required to determine whether this is simply a factor of low sampling effort in the Southern Hemisphere.

While entire vent biotas are threatened in biogeographic regions that have no protection from deep-sea mining, such as the Indian Ocean, the threat is significantly reduced in regions that straddle different regulatory areas, like the Mid-Atlantic Ridge. Despite several ISA mining licenses issued for the Mid-Atlantic Ridge, no vent fields in this region have a Threat Score greater than three as a result of the protection provided by the Azores MPA network (Abecasis et al., 2015). This highlights the importance of implementing conservation measures like MPAs to reduce extinction risk, yet at present, other than the South Georgia and South Sandwich Islands MPA, all other vent-related MPAs are located in the northern hemisphere. In an ecosystem that has well-documented, distinct faunal communities across different biogeographic regions, the preservation of areas representative of each region is essential.

Toward Protection for Hydrothermal Vents

The conservation of hydrothermal vent habitats and their unique fauna requires action to lower the extinction risk of vent species. While the incorporation of new data to the Vent Red List has potential to influence assessment outcome and lead to Red List category change, this would only constitute a non-genuine change under IUCN regulations (IUCN Standards and Petitions Committee, 2019); i.e., improved knowledge on the species rather than a true change in extinction risk. Furthermore, given the relatively broad category thresholds of the Red List criteria, the addition of new species distribution data does not always affect assessment result (Thomas et al., 2021). Consequently, to improve the extinction risk of vent species, real conservation measures would need to be implemented that mitigate the threat of deep-sea mining.

One conservation method that has potential to safeguard hydrothermal vents from deep-sea mining is the implementation of MPAs (Menini and Van Dover, 2019). Globally, 70 vent-endemic mollusc species were assessed as Least Concern or Near Threatened, based on the protection afforded by MPAs, either to the entire, or a proportion of the population. These assessment outcomes demonstrate the effectiveness of MPAs to protect individual species against the threat of extinction. However, the presence of an MPA alone does not always constitute protection and both assessment and real conservation outcomes are dependent on whether the threat is sufficiently mitigated by implementation of the MPA (Edgar et al., 2014). For example, while bottom fishing is prohibited within New Zealand's

Kermadec Benthic Protected Area, there is no active legislation against other commercial activities like seafloor mining, so vent sites are left unprotected (Van Dover et al., 2011). Furthermore, even MPAs that include specific regulation for the protection of hydrothermal vents are at times too small to afford protection from nearby threats. Research predicts that mining sediment plumes can spread up to 70 km (Luick, 2012; Miller et al., 2018), therefore hydrothermal vents within this proximity, protected or not, could possibly be impacted. For example, the Endeavor Hydrothermal Vents MPA in Canada encompasses five hydrothermal vents of interest, but is within 70 km of nearby unprotected vents. Likewise, proximity to inactive vent deposits that are also potential mining targets (Van Dover, 2019) should be considered. Therefore, it is imperative that MPAs are planned with reference to all vents in an area, including inactive deposits, and are established including a generous buffer zone, as a precautionary measure.

With increasing demand for metals to support renewable energy technologies, blanket MPAs may not be the most realistic approach for policy makers. A more measured approach may be to implement a moratorium on deep-sea mining to allow for further research into the biodiversity, ecology, connectivity, and resilience of vent communities (Glover et al., 2018; Van Dover et al., 2018). Several countries (Kakee, 2020) and, more recently, large corporations (No Deep Seabed Mining, 2021), have declared their support for a mining moratorium until sufficient advances have been made to inform environmentally sound mining legislation. The Red List assessments presented in this study provide a global overview of mining threat at hydrothermal vents and support a precautionary approach for deep-sea conservation, including the implementation of a deep-sea mining moratorium.

CONCLUSION

Whether in the form of MPAs or moratoria, we have an international obligation to protect hydrothermal vents from anthropogenic threats, and the Red List is a valuable conservation tool to help inform such policy decisions. In this case, the application of the Red List criteria to all known vent-endemic molluscs highlights the variation in mining threat across global biogeographic regions and the impact of jurisdiction status, with vent fields in mining license areas (e.g., Indian Ocean) exhibiting a greater threat level than those in protected areas (e.g., Azores MPA). The Vent Red List conveys the very real extinction risk that deep-sea mining poses to vent-endemic species to a wide audience and provides a new platform to ensure the conservation of this unique deep-sea habitat.

DATA AVAILABILITY STATEMENT

The original contributions presented in the study are included in the article/**Supplementary Material**, further inquiries can be directed to the corresponding author/s.

AUTHOR CONTRIBUTIONS

ET and JS conceived and designed the research. ET, AM, NH, and JS collected the data and completed IUCN Red List assessments. MB and MS facilitated and reviewed IUCN Red List assessments. ET analyzed the data and led the manuscript development. All authors contributed to writing and have approved the manuscript.

FUNDING

This work was partially supported by the Mohamed bin Zayed Species Conservation Fund grant (182518473). ET was supported by the studentship awarded by the Faculty of Medicine, Health and Life Sciences, Queen's University Belfast. NH was supported by the funding from the Canada Research Chairs Program. MB was supported by the grant from the Rufford Foundation. JS was supported by the Hong Kong Branch of Southern Marine Science and Engineering Guangdong Laboratory (Guangzhou). Publication of this study was supported by the Marine Institute under the Marine Research Programme with the support of the Irish Government.

ACKNOWLEDGMENTS

We thank the colleagues who have supported this study, especially Chong Chen, Caroline Pollock, Sarah Helyar, and Amanda Bates. We thank the two reviewers for providing valuable comments to improve this manuscript.

SUPPLEMENTARY MATERIAL

The Supplementary Material for this article can be found online at: https://www.frontiersin.org/articles/10.3389/fmars.2021.713022/full#supplementary-material

REFERENCES

Abecasis, R. C., Afonso, P., Colaço, A., Longnecker, N., Clifton, J., Schmidt, L., et al. (2015). Marine conservation in the azores: evaluating marine protected area development in a remote island context. *Front. Mar. Sci.* 2:104. doi: 10.3389/fmars.2015.00104

Beaulieu, S. E., and Szafranski, K. (2020). *InterRidge Global Database of Active Submarine Hydrothermal Vent Fields, Version 3.4*. Available online at: http://vents-data.interridge.org (accessed June 7, 2019).

Betts, J., Young, R. P., Hilton-Taylor, C., Hoffmann, M., Rodríguez, J. P., Stuart, S. N., et al. (2020). A framework for evaluating the impact of the IUCN red list of threatened species. *Conserv. Biol.* 34, 632–643. doi: 10.1111/cobi.13454

Calado, H., Ng, K., Lopes, C., and Paramio, L. (2011). Introducing a legal management instrument for offshore Marine protected areas in the Azores—the Azores Marine Park. *Environ. Sci. Policy* 14, 1175–1187. doi: 10.1016/j.envsci.2011.09.001

Carpenter, K. E., Abrar, M., Aeby, G., Aronson, R. B., Banks, S., Bruckner, A., et al. (2008). One-third of reef-building corals face elevated extinction risk from climate change and local impacts. *Science* 321, 560–563. doi: 10.1126/science.1159196

Chapman, A. S. A., Beaulieu, S. E., Colaço, A., Gebruk, A. V., Hilario, A., Kihara, T. C., et al. (2019). sFDvent: a global trait database for deep-sea hydrothermal-vent fauna. *Glob. Ecol. Biogeogr.* 28, 1538–1551. doi: 10.1111/geb.12975

Chen, C., Linse, K., Uematsu, K., and Sigwart, J. D. (2018a). Cryptic niche switching in a chemosymbiotic gastropod. *Proc. R. Soc. B* 285:20181099. doi: 10.1098/rspb.2018.1099

Chen, C., Marsh, L., and Copley, J. T. (2018b). Is it sex in chains? Potential mating stacks in deep-sea hydrothermal vent snails. *Plankton Benthos Res.* 13, 25–27. doi: 10.3800/pbr.13.25

Chong, Z. R., Yang, S. H. B., Babu, P., Linga, P., and Li, X.-S. (2016). Review of natural gas hydrates as an energy resource: prospects and challenges. *Appl. Energy* 162, 1633–1652. doi: 10.1016/j.apenergy.2014.12.061

Clark, M. R., Rowden, A. A., Schlacher, T., Williams, A., Consalvey, M., Stocks, K. I., et al. (2010). The ecology of seamounts: structure, function, and human impacts. *Annu. Rev. Mar. Sci.* 2, 253–278. doi: 10.1146/annurev-marine-120308-081109

Danovaro, R., Corinaldesi, C., Dell'Anno, A., and Snelgrove, P. V. R. (2017). The deep-sea under global change. *Curr. Biol.* 27, 461–465. doi: 10.1016/j.cub.2017.02.046

Edgar, G. J., Stuart-Smith, R. D., Willis, T. J., Kininmonth, S., Baker, S. C., Banks, S., et al. (2014). Global conservation outcomes depend on Marine protected areas with five key features. *Nature* 506, 216–220. doi: 10.1038/nature13022

Gjerde, K. M., Dotinga, H., Hart, S., Molenaar, E. J., Rayfuse, R., and Warner, R. (2008). *Regulatory and Governance Gaps in the International Regime for the Conservation and Sustainable Use of Marine Biodiversity in Areas beyond National Jurisdiction*. Gland: IUCN.

Glover, A. G., Wiklund, H., Chen, C., and Dahlgren, T. G. (2018). Managing a sustainable deep-sea 'blue economy' requires knowledge of what actually lives there. *eLife* 7:e41319.

Gollner, S., Kaiser, S., Menzel, L., Jones, D. O. B., Brown, A., Mestre, N. C., et al. (2017). Resilience of benthic deep-sea fauna to mining activities. *Mar. Environ. Res.* 129, 76–101. doi: 10.1016/j.marenvres.2017.04.010

Hein, J. R., Mizell, K., Koschinsky, A., and Conrad, T. A. (2013). Deep-ocean mineral deposits as a source of critical metals for high- and green-technology applications: comparison with land-based resources. *Ore Geol. Rev.* 51, 1–14. doi: 10.1016/j.oregeorev.2012.12.001

Hoagland, P., Beaulieu, S., Tivey, M. A., Eggert, R. G., German, C., Glowka, L., et al. (2010). Deep-sea mining of seafloor massive sulfides. *Mar. Policy* 34, 728–732. doi: 10.1016/j.marpol.2009.12.001

ISA (2021). *Minerals: Cobalt-Rich Ferromanganese Crusts, International Seabed Authority*. Available online at: https://www.isa.org.jm/exploration-contracts/cobalt-rich-ferromanganese (accessed July 14, 2021).

IUCN Standards and Petitions Committee (2019). *Guidelines for Using the IUCN Red List Categories and Criteria. Version 14*. Available online at: http://www.iucnredlist.org/documents/RedListGuidelines.pdf (accessed January 24, 2019).

IUCN (2012). *IUCN Red List Categories and Criteria. Version 3.1*, 2nd Edn. Gland: IUCN.

IUCN (2016). *Guidelines for Appropriate Uses of IUCN Red List Data. Version 3.0*. Available online at: https://www.iucnredlist.org/resources/guidelines-for-appropriate-uses-of-red-list-data (accessed May 18, 2021).

IUCN (2021). *The IUCN Red List of Threatened Species. Version 2021-3*. Available online at: https://www.iucnredlist.org

Johnson, S. B., Warén, A., and Vrijenhoek, C. (2008). DNA barcoding of *Lepetodrilus* limpets reveals cryptic species. *J. Shellfish Res.* 27, 43–51. doi: 10.2983/0730-8000(2008)27[43:dbollr]2.0.co;2

Kakee, T. (2020). Deep-sea mining legislation in Pacific Island countries: from the perspective of public participation in approval procedures. *Mar. Policy* 117:103881. doi: 10.1016/j.marpol.2020.103881

Laming, S. R., Gaudron, S. M., and Duperron, S. (2018). Lifecycle ecology of deep-sea chemosymbiotic mussels: a review. *Front. Mar. Sci.* 5:282. doi: 10.3389/fmars.2018.00282

Luick, J. L. (2012). *Physical Oceanographic Assessment of the Nautilus EIS for the Solwara 1 Project*. Available online at: http://www.deepseaminingoutofourdepth.org/wp-content/uploads/EIS-Review-FINAL-low-res.pdf (accessed January 10, 2013).

Matabos, M., and Jollivet, D. (2019). Revisiting the *Lepetodrilus elevatus* species complex (Vetigastropoda: Lepetodrilidae), using samples from the Galápagos and Guaymas hydrothermal vent systems. *J. Mollus. Stud.* 85, 154–165. doi: 10.1093/mollus/eyy061

Menini, E., and Van Dover, C. L. (2019). An atlas of protected hydrothermal vents. *Mar. Policy* 108:103654. doi: 10.1016/j.marpol.2019.103654

Miller, K. A., Thompson, K. F., Johnston, P., and Santillo, D. (2018). An overview of seabed mining including the current state of development, environmental impacts, and knowledge gaps. *Front. Mar. Sci.* 4:418. doi: 10.3389/fmars.2017.00418

Niner, H. J., Ardron, J. A., Escobar, E. G., Gianni, M., Jaeckel, A., Jones, D. O. B., et al. (2018). Deep-sea mining with no net loss of biodiversity—an impossible aim. *Front. Mar. Sci.* 5:53. doi: 10.3389/fmars.2018.00053

No Deep Seabed Mining (2021). *Business Statement Supporting a Moratorium on Deep Seabed Mining*. Available online at: https://www.noseabedmining.org/ (accessed April 19, 2021).

Okamoto, N., Shiokawa, S., Kawano, S., Yamaji, N., Sakurai, H., and Kurihara, M. (2019). "First lifting test for seafloor massive sulphides in the Okinawa Trough in the EEZ of Japan," in *Paper Presented at the 29th International Ocean and Polar Engineering Conference*, (Honolulu, HI).

Petersen, S., Krätschell, A., Augustin, N., Jamieson, J., Hein, J. R., and Hannington, M. D. (2016). News from the seabed – geological characteristics and resource potential of deep-sea mineral resources. *Mar. Policy* 70, 175–187. doi: 10.1016/j.marpol.2016.03.012

Rodrigues, A. S. L., Pilgrim, J. D., Lamoreux, J. F., Hoffmann, M., and Brooks, T. M. (2006). The value of the IUCN Red List for conservation. *Trends Ecol. Evol.* 21, 71–76. doi: 10.1016/j.tree.2005.10.010

Rogers, A. D., Tyler, P. A., Connelly, D. P., Copley, J. T., James, R., Larter, R. D., et al. (2012). The discovery of new deep-sea hydrothermal vent communities in the Southern Ocean and implications for biogeography. *PLoS Biol.* 10:e1001234. doi: 10.1371/journal.pbio.1001234

Sharma, R. (2011). Deep-sea mining: economic, technical, technological, and environmental considerations for sustainable development. *Mar. Technol. Soc. J.* 45, 28–41. doi: 10.4031/MTSJ.45.5.2

Sharma, R. (2015). Environmental issues of deep-sea mining. *Procedia Earth Planet. Sci.* 11, 204–211. doi: 10.1016/j.proeps.2015.06.026

Sigwart, J. D., Chen, C. and Marsh, L. (2017). Is mining the seabed bad for mollusks? *The Nautilus* 131, 43–50.

Sigwart, J. D., Chen, C., Thomas, E. A., Allcock, A. L., Böhm, M., and Seddon, M. (2019). Red listing can protect deep-sea biodiversity. *Nat. Ecol. Evol.* 3:1134. doi: 10.1038/s41559-019-0930-2

Simon-Lledó, E., Bett, B. J., Huvenne, V. A. I., Köser, K., Schoening, T., Greinert, J., et al. (2019). Biological effects 26 years after simulated deep-sea mining. *Sci. Rep.* 9:8040. doi: 10.1038/s41598-019-44492-w

Suess, E. (2018). "Marine cold seeps: background and recent advances," in *Hydrocarbons, Oils and Lipids: Diversity, Origin, Chemistry and Fate*, ed. H. Wilkes (Cham: Springer International Publishing), 1–21. doi: 10.1007/978-3-319-54529-5_27-1

Sun, J., Zhou, Y., Chen, C., Kwan, Y. H., Sun, Y., Wang, X., et al. (2020). Nearest vent, dearest friend: biodiversity of Tiancheng vent field reveals cross-ridge similarities in the Indian Ocean. *R. Soc. Open Sci.* 7:200110. doi: 10.1098/rsos.200110

Thaler, A. D., and Amon, D. (2019). 262 voyages beneath the sea: a global assessment of macro- and megafaunal biodiversity and research effort at deep-sea hydrothermal vents. *PeerJ* 7:e7397. doi: 10.7717/peerj.7397

Thomas, E. A., Böhm, M., Pollock, C., Chen, C., Seddon, M., and Sigwart, J. D. (2021). Assessing the extinction risk of insular, understudied marine species. *Conserv. Biol.* doi: 10.1111/cobi.13854

Thompson, K. F., Miller, K. A., Currie, D., Johnston, P., and Santillo, D. (2018). Seabed mining and approaches to governance of the deep seabed. *Front. Mar. Sci.* 5:480. doi: 10.3389/fmars.2018.00480

Tingley, R., Macdonald, S. L., Mitchell, N. J., Woinarski, J. C. Z., Meiri, S., Bowles, P., et al. (2019). Geographic and taxonomic patterns of extinction risk in Australian squamates. *Biol. Conserv.* 238:108203. doi: 10.1016/j.biocon.2019.108203

Van Dover, C. (2000). *The Ecology of Deep-Sea Hydrothermal Vents*. Princeton, NJ: Princeton University Press.

Van Dover, C. L. (2014). Impacts of anthropogenic disturbances at deep-sea hydrothermal vent ecosystems: a review. *Mar. Environ. Res.* 102, 59–72. doi: 10.1016/j.marenvres.2014.03.008

Van Dover, C. L. (2019). Inactive sulfide ecosystems in the deep sea: a review. *Front. Mar. Sci.* 6:461. doi: 10.3389/fmars.2019.00461

Van Dover, C. L., Ardron, J. A., Escobar, E., Gianni, M., Gjerde, K. M., Jaeckel, A., et al. (2017). Biodiversity loss from deep-sea mining. *Nat. Geosci.* 10, 464–465. doi: 10.1038/ngeo2983

Van Dover, C. L., Arnaud-Haond, S., Gianni, M., Helmreich, S., Huber, J. A., Jaeckel, A. L., et al. (2018). Scientific rationale and international obligations for protection of active hydrothermal vent ecosystems from deep-sea mining. *Mar. Policy* 90, 20–28. doi: 10.1016/j.marpol.2018.01.020

Van Dover, C., Smith, C. R., Ardron, J., Arnaud-Haond, S., Beaudoin, Y., Bezaury-Creel, J., et al. (2011). *Environmental Management of Deep-Sea Chemosynthetic Ecosystems: Justification of and Considerations for A Spatially Based Approach*. Technical Study No 9. Kingston: International Seabed Authority.

Watling, L., and Auster, P. J. (2017). Seamounts on the high seas should be managed as vulnerable marine ecosystems. *Front. Mar. Sci.* 4:14. doi: 10.3389/fmars.2017.00014

Wolff, T. (2005). Composition and endemism of the deep-sea hydrothermal vent fauna. *Cah. Biol. Mar.* 46, 97–104. doi: 10.1007/978-3-319-45340-8_4

Yahagi, T., Chen, C., and Kawagucci, S. (2019). What we know, what we can know, and what we will never know about the larval dispersal process at deep-sea chemosynthetic ecosystems. *Oceanogr. Japan* 28, 97–125. doi: 10.5928/kaiyou.28.4-5-6_97

Author Disclaimer: The views expressed in this paper do not necessarily reflect those of IUCN. Also, the designation of geographical entities, and the presentation of the material, do not imply the expression of any opinion whatsoever on the part of IUCN concerning the legal status of any country, territory, or area, or of its authorities, or concerning the delimitation of its frontiers or boundaries.

Conflict of Interest: The authors declare that the research was conducted in the absence of any commercial or financial relationships that could be construed as a potential conflict of interest.

Publisher's Note: All claims expressed in this article are solely those of the authors and do not necessarily represent those of their affiliated organizations, or those of the publisher, the editors and the reviewers. Any product that may be evaluated in this article, or claim that may be made by its manufacturer, is not guaranteed or endorsed by the publisher.

Copyright © 2021 Thomas, Molloy, Hanson, Böhm, Seddon and Sigwart. This is an open-access article distributed under the terms of the Creative Commons Attribution License (CC BY). The use, distribution or reproduction in other forums is permitted, provided the original author(s) and the copyright owner(s) are credited and that the original publication in this journal is cited, in accordance with accepted academic practice. No use, distribution or reproduction is permitted which does not comply with these terms.

frontiers in Marine Science

ORIGINAL RESEARCH
published: 06 January 2022
doi: 10.3389/fmars.2021.752360

DNA Barcoding of Scavenging Amphipod Communities at Active and Inactive Hydrothermal Vents in the Indian Ocean

Katharina Kniesz[1,2], Anna Maria Jażdżewska[3], Pedro Martínez Arbizu[1,2] and Terue Cristina Kihara[4]*

[1] Senckenberg am Meer, German Centre for Marine Biodiversity Research, Wilhelmshaven, Germany, [2] Carl von Ossietzky Universität Oldenburg, Oldenburg, Germany, [3] Department of Invertebrate Zoology and Hydrobiology, Faculty of Biology and Environmental Protection, University of Łódź, Łódź, Poland, [4] INES Integrated Environmental Solutions UG, Wilhelmshaven, Germany

OPEN ACCESS

Edited by:
Kevin M. Kocot,
University of Alabama, United States

Reviewed by:
Christopher Nicolai Roterman,
University of Oxford, United Kingdom
Jon Thomassen Hestetun,
Norwegian Research Institute
(NORCE), Norway

***Correspondence:**
Katharina Kniesz
katharina.kniesz@senckenberg.de

Specialty section:
This article was submitted to
Deep-Sea Environments and Ecology,
a section of the journal
Frontiers in Marine Science

Received: 02 August 2021
Accepted: 26 November 2021
Published: 06 January 2022

Citation:
Kniesz K, Jażdżewska AM,
Martínez Arbizu P and Kihara TC
(2022) DNA Barcoding of Scavenging
Amphipod Communities at Active
and Inactive Hydrothermal Vents
in the Indian Ocean.
Front. Mar. Sci. 8:752360.
doi: 10.3389/fmars.2021.752360

Hydrothermal vent areas have drawn increasing interest since they were discovered in 1977. Because of chemoautotrophic bacteria, they possess high abundances of vent endemic species as well as many non-vent species around the fields. During the survey conducted by the Bundesanstalt für Geowissenschaften und Rohstoffe (Federal Institute for Geosciences and Natural Resources, BGR) to identify inactive polymetallic sulfide deposits along Central and Southeast Indian Ridges, the INDEX project studied the scavenging amphipod community at three newly discovered hydrothermal fields. A sample consisting of 463 representatives of Amphipoda (Malacostraca: Crustacea) was collected by means of baited traps in active and inactive vents of three different sites and subsequently studied by both morphological and genetic methods. Molecular methods included the analysis of two mitochondrial (cytochrome *c* oxidase subunit I [COI] and 16S rRNA) and one nuclear (18S rRNA) genes. By six delimitation methods, 22 molecular operational taxonomic units (MOTUs) belonging to 12 genera and 10 families were defined. The existence of potential species complexes was noted for the representatives of the genus *Paralicella*. The inactive site, where 19 species were found, showed higher species richness than did the active one, where only 10 taxa were recorded. Seven genera, *Ambasiopsis*, *Cleonardo*, *Eurythenes*, *Parandania*, *Pseudonesimus*, *Tectovalopsis*, and *Valettiopsis*, were observed only at inactive sites, whereas *Haptocallisoma*, was collected exclusively at active ones. The species *Abyssorchomene distinctus* (Birstein and Vinogradov, 1960), *Hirondellea brevicaudata* Chevreux, 1910, and *Hirondellea guyoti* Barnard and Ingram, 1990, have been previously reported from vent sites in the Atlantic or Pacific oceans. The present study provides the first report of *Eurythenes magellanicus* (H. Milne Edwards, 1848) and five other already described species in the Indian Ocean. The addition of 356 sequences strongly increases the number of amphipod barcodes

in reference databases and provides for the first time COI barcodes for *Cleonardo neuvillei* Chevreux, 1908, *Haptocallisoma abyssi* (Oldevig, 1959), *Hirondellea guyoti*, *Tectovalopsis fusilus* Barnard and Ingram, 1990, and the genera *Haptocallisoma*, *Pseudonesimus*, and *Valettiopsis.*

Keywords: Indian Ocean, hydrothermal vent, barcoding, genetic diversity, Amphipoda, abyssal, deep sea, baited trap

INTRODUCTION

Much less is known about hydrothermal vents and the deep sea in general than about terrestrial and shallow-water ecosystems. The first hydrothermal vent was discovered in 1977 along the Galapagos Rift (Lonsdale, 1977). Over the past 50 years the study of hydrothermal vents has progressed, but most studied vents are located in the Pacific and Atlantic oceans (German and Von Damm, 2006). The first vent fields on the Central Indian Ridge were discovered in 2000 and 2001 (Gamo et al., 2001; Hashimoto et al., 2001; Van Dover et al., 2001). Compared to that of Atlantic and Pacific vents, the fauna of the Indian Ocean vents is underexplored (Ingole and Koslow, 2005; Nakamura et al., 2012).

Discovery of the first hydrothermal vent field changed the view of primary production in the world's oceans fundamentally (De Busserolles et al., 2009). At hydrothermal vent fields chemoautotrophic bacteria use inorganic substances such as ferrous iron, hydrogen sulfides, and methane for primary production (De Busserolles et al., 2009). They occur free living or in symbiosis with eukaryotic species. Because this food source is independent of primary production in the photic zone, many endemic species are found in these fields, but non-vent species also occur in higher abundance around the vents than in the rest of the deep sea (Podowski et al., 2009).

Kato et al. (2010) revealed that abundance, diversity, and activity of microbial communities within sulfide structures of inactive vents are higher than or comparable to those of active vents. Inactive vent fields consist of polymetallic sulfides, like active vents, but without any detectable emissions (Van Dover, 2011) and are located within or close to active vent fields. Inactive fields are often inhabited by a mix of general deep-sea species, inactive vent species, and a reduced number of vent species, which are found in low abundances (Erickson et al., 2009; Levin et al., 2009; Collins et al., 2012; Boschen et al., 2016).

The high food availability at active and inactive vent fields leads to the presence of specific scavenging megafaunal species (Gerdes et al., 2019a). In this benthic deep-sea environment food is a limiting factor, and scavengers play an important role in recycling the organic carbon reaching the ocean floor and providing it as food for higher trophic levels. Marine scavengers are found throughout all phyla and habitats (King et al., 2007). They include some fishes and many invertebrate taxa like ophiuroids, asteroids, holothurians, decapods, isopods, and amphipods. Scavenging amphipods have been collected in great numbers by means of baited traps (Perrone et al., 2002; Jamieson et al., 2009; Gallo et al., 2015) and include mainly the representatives of Lysianassoidea, from the genera *Abyssorchomene*, *Anonyx*, *Cyclocaris*, *Cyphocaris*, *Eurythenes*, *Hirondellea*, *Orchomene*, *Orchomenella*, and the alicelloid *Paralicella* (Shulenberger and Hessler, 1974; Sainte-Marie, 1986; Christiansen, 1996; Legeżyńska et al., 2000; Blankenship and Levin, 2007; Duffy et al., 2016).

Deep-sea scavenging amphipods are adapted to endure the extreme conditions and limitations, using chemosensory appendages to detect and take their bait (Tamburri and Barry, 1999). As one limiting factor in deep-sea environment is food, some scavenging amphipods complement their necrophagy with detritivory, carnivory, and even cannibalism (Blankenship and Levin, 2007; Jamieson et al., 2010; Havermans and Smetacek, 2018). Another recent finding of cellulase in one scavenging species, *Hirondellea gigas* (Birstein and Vinogradov, 1955), suggests that it may digest wood debris, although no wood particles were recorded in its digestive tract (Kobayashi et al., 2012). Other vent amphipod species, also well-adapted to their environment, feed on the microbes present there.

Ventiella sulfuris Barnard and Ingram, 1990, is the most abundant amphipod species at the Eastern Pacific Rise vent fields. It lives in symbiosis with microbial communities inhabiting its midgut and hindgut and is known to be vent endemic (Corbari et al., 2012). Another vent endemic amphipod species, *Dulichiopsis dianae* Corbari and Sorbe, 2017, was detected at hydrothermal vents along the Mid-Atlantic Ridge (Corbari and Sorbe, 2017), but several amphipods are reported to be caught at or near hydrothermal vent systems all over the world (Barnard and Ingram, 1990; Desbruyères et al., 2006; Bellan-Santini, 2007; Larsen, 2007) that are not necessarily vent endemic (*We use "endemic" to refer to species occurring within a biotope and not within a geographical region; as per Wolff, 2005).

Baited traps were deployed during INDEX 2018, providing the opportunity to examine scavenging amphipods at the vent fields in the Indian Ocean. The objectives of the present study were: (1) to identify scavenging amphipod species at the Southeast and Central Indian ridges and (2) to determine whether the distribution pattern of recorded species is associated with the hydrothermal activity.

MATERIALS AND METHODS

Sampling

Our study was part of the INDEX 2018 expedition on Dutch RV *Pelagia*. The Southeast and the Central Indian Ridges are located in the Indian Ocean about 1,400 km southeast of the island of Mauritius. At each of three newly discovered vent fields, an amphipod trap was placed by the Canadian Remotely

Operated Vehicle (ROV) *ROPOS*. It was deployed three times by the manipulators and placed traps at one inactive (AT1: on the Southeast Indian Ridge) and two active areas (AT2: on the Southeast Indian Ridge; AT3: on the Central Indian Ridge). The distance between AT1 and AT2 was approximately 342 km, that between AT2 and AT3, 210 km (**Table 1** and **Figure 1**).

To attract the scavenging fauna, fish and cat food were enclosed in a net (40 μm mesh size) inside each trap. After 7–29 h the trap was recovered by the ROV (**Table 1**). On shipboard, the larger individuals were hand-picked, and the smaller ones, including the sediment were, passed through a 40-μm sieve, and all samples preserved in 96% undenatured ethanol.

Morphological Analyses

All intact specimens were studied morphologically. Badly damaged specimens were not counted and processed. The material is stored at the German Centre for Marine Biodiversity Research (DZMB) in Wilhelmshaven.

In the first step all amphipods were identified by means of a Leica M 125 stereomicroscope and the relevant literature (Chevreux, 1889; Shulenberger and Barnard, 1976; Lincoln, 1979; Barnard and Ingram, 1990; Barnard and Karaman, 1991; Bousfield and Hendrycks, 1995; Berge and Vader, 2001; Hendrycks, 2007; Lowry and De Broyer, 2008; Lowry and Stoddart, 2010; Lowry and Kilgallen, 2014; d'Udekem d'Acoz and Havermans, 2015; Horton and Thurston, 2015; Kilgallen and Lowry, 2015). For purposes of the morphological work, one representative of each recognized morphospecies was dissected and all appendages were mounted on permanent slides with polyvinyl-lactophenol containing lignin pink.

Undescribed or unknown species were named according to the nomenclature rules of Sigovini et al. (2016). Because of taxonomic problems, specimens of the genus *Paralicella* were divided into two morphological groups, and "sp. group" identifier was added to the name. In addition, a unique species code was given to the species where the species-level identity was not known or the species was new to science (Horton et al., 2021). This species code is a standardized code in the INDEX project and combines storage, year of publication, and a serial number.

Photographing and Confocal Imaging

The 279 specimen used for molecular analysis were photographed with a Leica M 125 stereomicroscope equipped with a Leica MC 170 HD camera. In addition, one representative of each morphospecies [excluding the largest species, *Eurythenes magellanicus* (H. Milne Edwards, 1848)] was chosen for confocal laser scanning microscopy (**Supplementary Table 1**). The specimens were stained with a 1:1 solution of acid fuchsin and Congo red overnight according to procedures adapted from Michels and Büntzow (2010), then temporarily mounted on an objective slide with glycerine and self-adhesive reinforcement rings to support the coverslip (Michels and Büntzow, 2010). For larger specimens, double-sided tape pieces and some drops of Karo® light corn syrup were mounted between slide and coverslip (Brix et al., 2018).

The scanning was performed with a Leica TCS SP5 equipped with a Leica DM5000 B upright microscope and three visible-light lasers (DPSS 10 mW 561 nm; HeNe 10 mW 633 nm; Ar 100 mW 458 nm, 476 nm, 488 nm, and 514 nm), combined with the software LAS AF 2.2.1. Leica Application Suite Advanced Fluorescence (Kihara and Rocha, 2013) at the DZMB in Wilhelmshaven. To obtain the images, we used objective HCX PL APO CS 10.0 × 0.40 DRY UV and 561 nm excitation wavelength with 80% acousto-optic tuneable filter. Series of stacks were created with a resolution of 2,048 × 2,048 pixels. The final images were obtained by means of maximum projection. Finally, the individual images were merged in Adobe® Photoshop® 21.1.3 and edited for contrast and brightness.

Molecular Studies

For each recognized morphospecies a representation of one to ten individuals was chosen for DNA barcoding. In cases where taxa caused morphological identification problems the number of analyzed specimens was increased or all specimens were used. For 279 specimens genomic DNA was extracted from one pleopod or pereopod (for smaller specimens), which was removed and treated with 30 μl of CHELEX (BIO-RAD Insta Gene Matrix) for 20 min at 56°C and 10 min at 99°C. For some samples the additional purification of the chelex extract was performed with columns (E.Z.N.A.® Mollusc DNA Kit, NucleoSpin® Tissue) according to the manufacturer's protocol.

Polymerase chain reactions of the mitochondrial cytochrome *c* oxidase subunit I (COI) and mitochondrial ribosomal large subunit (16S) were performed with amphipod-specific primers (**Table 2**) and protocols provided by their authors (Costa et al., 2009; Lörz et al., 2018). The fragment of the COI gene was amplified for all chosen individuals, whereas 16S and the nuclear small ribosomal subunit (18S) was amplified on a subset of specimens. For 18S the universal primer set 18SE and 18SL (**Table 2**) was used, and the polymerase chain reaction conditions

TABLE 1 | Deployed amphipod traps with station ID, coordinates, ridge (Central Indian Ridge = CIR, Southeast Indian Ridge = SEIR), hydrothermal activity, collection depth, the deployment time of the trap on the seafloor and the measured environmental parameters (temperature, salinity, and pH-value).

Trap No.	Station ID	Coordinates	Ridge	Hydrothermal activity	Sampled depth (m)	Time on bottom (h)	Temperature (°C)	Salinity (psu)	pH
AT1	I18_067RO_AT1	27° 39′ S, 73° 53′ E	SEIR	inactive	2,508	29	1.79	34.72	3.10
AT2	I18_075RO_AT1	27° 15′ S, 72° 43′ E	SEIR	active	2,919	7	1.71	34.73	3.10
AT3	I18_099RO_AT1	25° 28′ S, 69° 56′ E	CIR	active	2,629	22	2.0	34.69	3.09

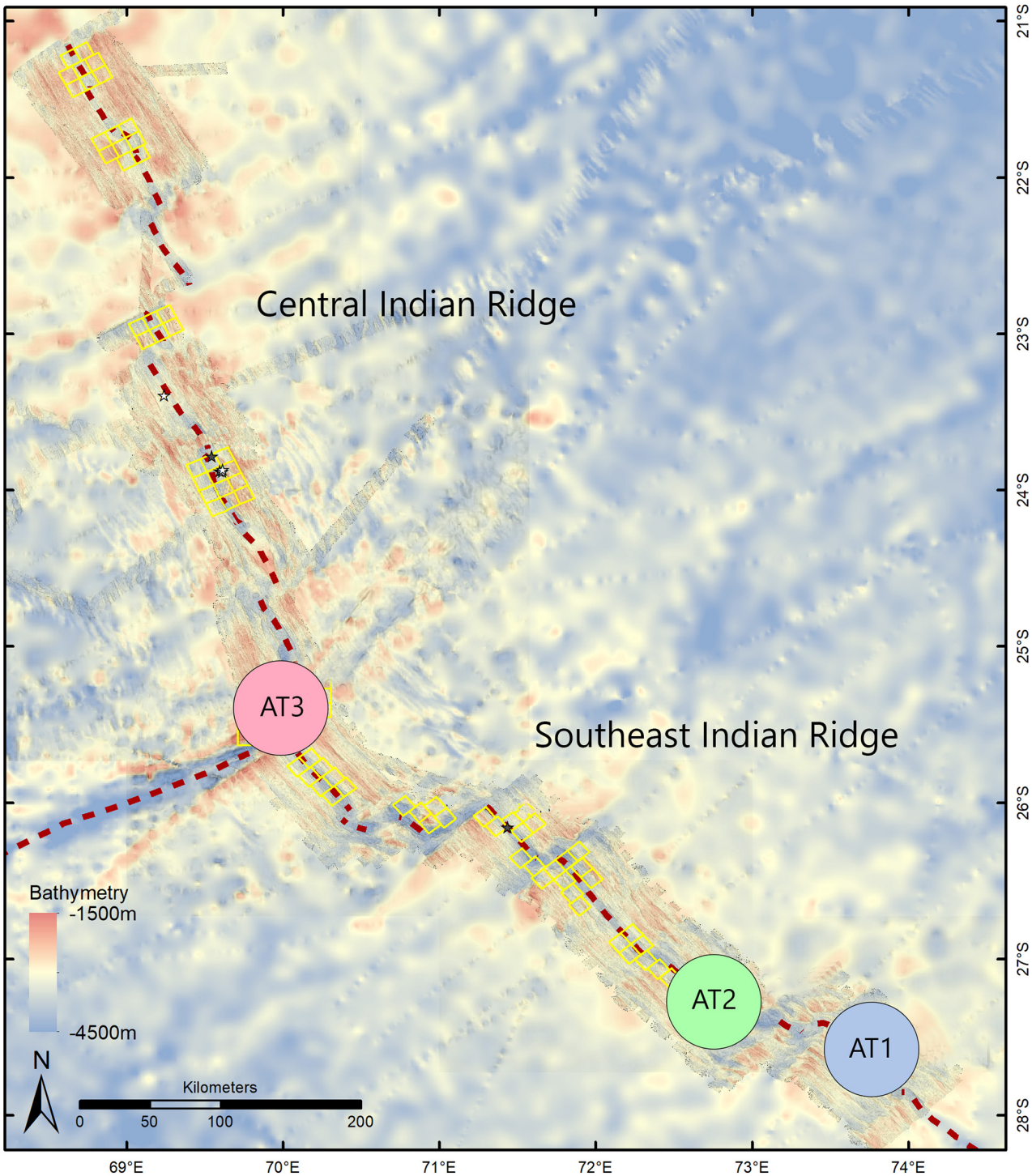

FIGURE 1 | Vent fields sampled on the Southeast Indian Ridge and Central Indian Ridge in the Indian Ocean: AT1 (inactive), AT2 (active), and AT3 (active).

were as follows: initial denaturation at 94°C for 3 min; 45 cycles of 30 s at 94°C, 45 s at an annealing temperature of 55°C, and 1 min at 72°C; final elongation for 3 min at 72°C. To all primers M13 tails were added to provide defined nucleotide sequences for sequencing (**Table 2**). All amplified products were purified with Exo-SAP-IT®. Afterwards they were sequenced by Macrogen Inc., The Netherlands. In order to assemble long DNA fragments of the 18S gene, we sequenced amplified fragments with intermediate primers synthetized by Macrogen Inc. (**Table 2**) in addition.

TABLE 2 | Primers used in the present study.

Gene	Name	Sequence 5′–3′	Direction	References
COI	UCOIR	ACWAAYCAYAAAGAYATYGG	Forward	Costa et al., 2009
	UCOIF	TAWACTTCDGGRTGRCCRAAAAAYCA	Reverse	Costa et al., 2009
16S	16SFt_amp	GCRGTATIYTRACYGTGCTAAGG	Forward	Lörz et al., 2018
	16SRt_amp2	CTGGCTTAAACCGRTYTGAACTC	Reverse	Lörz et al., 2018
18S	18SE	CTGGTTGATCCTGCCAGT	Forward	Hillis and Dixon, 1991
	18SL	CACCTACGGAAACCTTGTTACGACTT	Reverse	Hamby and Zimmer, 1988
	F-566	CAGCAGCCGCGGTAATTCC	Forward, intermediate	Hadziavdic et al., 2014
	R-1200	CCCGTGTTGAGTCAAATTAAGC	Reverse, intermediate	Hadziavdic et al., 2014
M13	M13-FP	TGTAAAACGACGGCCAGT	Forward	Schuelke, 2000
	M13R-pUC	CAGGAAACAGCTATGAC	Reverse	Messing, 1983

Each primer was added by the universal M13 tail (M13-FP, M13R-pUC).

The resulting sequences were edited with Geneious Prime® 2020.1.2 (Kearse et al., 2012) as a check for ambiguities and errors. All edited sequences were aligned and trimmed with MAFFT v7.450 (Katoh et al., 2002) alignment in Geneious by the automatic algorithm. Afterward, similarity analyses with Blastn (Altschul et al., 1990) search against GenBank and the Barcode of Life Data System (BOLD, Ratnasingham and Hebert, 2007) were performed. Short sequences and sequences with bad quality were not included in the analysis. All sequences were deposited in GenBank with the accession numbers COI, MZ197178–MZ197435; 16S, MZ197436–MZ197490; and 18S, MZ197491–MZ197533. Relevant voucher information, pictures, taxonomic classifications, and sequences were deposited in the dataset "DS-INMAC01" in BOLD (Ratnasingham and Hebert, 2007)[1] (doi: 10.5883/DS-INMAC01) (GenBank accession numbers: **Supplementary Table 1**).

Species Delimitation and Phylogenetic Analyses

To infer the number of species in the present study, we delimited them according to their morphology by grouping them to morphospecies and by analyzing genetic distances of molecular taxonomic units (MOTUs). The MOTUs were delimited on COI sequences by five methods–three distance-based and two tree-based.

Because, for some of the delimitation methods, a threshold is mandatory, intra- and interspecific distances for our dataset were first calculated by the Barcode Gap Analysis provided by BOLD (distance model: Kimura 2 Parameter; alignment options: BOLD aligner; ambiguous base/gap handling: pairwise deletion). As a result the threshold value for the species-delimitation methods was set at 0.976 or 97.6% (mean intraspecific divergence is 2.4 after exclusion of the species complex) (**Supplementary Figures 1, 2** and **Supplementary Table 2**), but note that the threshold for separating species within marine Amphipoda reported in the literature ranges from 93% to 97% and is suggested to be family specific (Knox et al., 2012; Tempestini et al., 2018; Mohrbeck et al., 2021).

Automatic Barcode Gap Discovery (ABGD) (Puillandre et al., 2012) is based on computing the threshold distance or "barcoding gap" between inter- and intraspecific variation that leads toward the number of groups. In the present case ABGD analyses were performed with the default settings (Pmin = 0.001, Pmax = 0.1, Steps = 10, X = 1.5, Nb bins = 20) on the ABGD website[2] with JC69 Jukes-Cantor parameter. This parameter reflects the assumption that base frequencies are equal with one substitution rate (Emerson et al., 2001) and gave the clearest barcoding gap within all tested parameters for our data.

Another distance-based method is CD-HIT (Li and Godzik, 2006), a heuristic clustering process that requires defined sequence similarity thresholds. The CD-HIT-EST method was used on the CD-HIT Suite web server at the University of California, San Diego,[3] and analyses were done with default settings and the predefined threshold of 97.6%.

The third method of delimitation that used calculated distances is the Barcode Index Numbers (BINs) system implemented in BOLD (Ratnasingham and Hebert, 2013). It registers each cluster of sequences and assigns a unique and specific code (BIN). An uploaded sequence goes through cluster analyses that try to find discontinuities between the clusters.

In contrast, general mixed Yule coalescence is a method that determines the point of transition from speciation to coalescent branching patterns on an ultrametric tree (Pons et al., 2006; Monaghan et al., 2009). When this method was performed, a Bayesian inference tree was built with BEAST v1.8.3 (Drummond et al., 2012). Yule-coalescent models as implemented in the R package "splits" (Suchard et al., 2018) were used.

Moreover, another method determining the transition from speciation to coalescent branching, the Bayesian Poisson tree process for larger datasets (Zhang et al., 2013) was tested on the web server.[4] As input file the Bayesian tree calculated by BEAST was used. The data were inserted as an unrooted tree, 100,000 MCMC generations, thinning of 100, and 0.1 burn-in.

For the graphic presentation of MOTUs and morphospecies, Bayesian tree analyses were conducted for the COI dataset. The

[1]http://www.boldsystems.org

[2]https://bioinfo.mnhn.fr/abi/public/abgd/abgdweb.html

[3]http://weizhong-lab.ucsd.edu/cdhit-web-server/cgi-bin/index.cgi

[4]http://species.h-its.org/ptp/

optimal model was identified by the modeltest carried out by MEGA X (Kumar et al., 2018) using both the Akaike Information Criterion (AIC) and the Bayesian Information Criterion (BIC). For the COI dataset the Tamura-Nei (TN93 + G + I) model was the best fitting model. For construction of the tree, the BEAST v1.8.3 package and Yule-coalescent model as implemented in the R package "splits" (Suchard et al., 2018) were applied. The tree was produced and annotated with Bayesian posterior probabilities (PP) with TreeAnnotator in the BEAST v1.8.3 package.

For inference of phylogenetic relationships among recorded species, 16S and 18S rDNA gene fragments from one to three representatives of recognized MOTUs were amplified and added to the COI dataset. The tree of concatenated sequences of all three markers studied (27 individuals) was generated by the software Mr. Bayes (Ronquist and Huelsenbeck, 2003) by means of 15,000,000 generations, 2 runs, 4 chains, and a burn-in of 4,000. Gaps in the alignment were treated as the nucleotide N. Individual models were calculated for each marker: COI, General Time Reversible (GTR + G); 16S, Hasegawa-Kishino-Yano (HKY + G + I); 18S, General Time Reversible (GTR + G). All trees were graphically adjusted with the software Adobe® Photoshop® 21.1.3.

Community Analyses and Population Connectivity

Rating the species richness was performed by generating the rarefaction curves (Hessler and Sanders, 1967). The individual rarefaction curve was processed by means of Past 4.05 (Hammer et al., 2001). In combination with the Venn diagram, it was adjusted in the software Adobe® Photoshop® 21.1.3.

For analysis of the population connectivity between the two locations, haplotype networks were generated by Population Analysis with Reticulate Trees (PopART).[5] Minimum spanning network (Bandelt et al., 1999) was applied for all MOTUs of the COI dataset. The haplotypes of all MOTUs of the genus *Paralicella* are presented together to demonstrate the differences and similarities between the recognized molecular units. Furthermore, for the COI dataset statistical tests were carried out by means of DnaSP6 (Librado and Rozas, 2009; Rozas et al., 2017) and Arlequin 3.5 (Excoffier and Lischer, 2010) for estimation of the gene diversity. For all populations with sample size $n \geq 4$, haplotype (h) and nucleotide (π) diversities (Tajima, 1983), Fu's Fs (Fu, 1996), and Tajima's D (Tajima, 1989) were calculated.

Additional diversity analyses on the COI dataset were performed in Arlequin 3.5 (Excoffier and Lischer, 2010). To detect species population differentiation within and among predefined groups, we performed an AMOVA with 1,000 permutations and pairwise differences. Two groups were selected–"active" and "inactive"–from analysis of the COI sequences obtained.

RESULTS

Species Delimitation and Identification

Baited traps AT1 and AT2 captured 463 scavenging amphipods, which could be identified morphologically as 18 different morphospecies (**Figures 2**, **3**) (AT1, 364 individuals; AT2, 99 individuals). Trap AT3 captured no amphipods. From 279 individuals used for molecular study, 258 high-quality sequences

[5]http://popart.otago.ac.nz

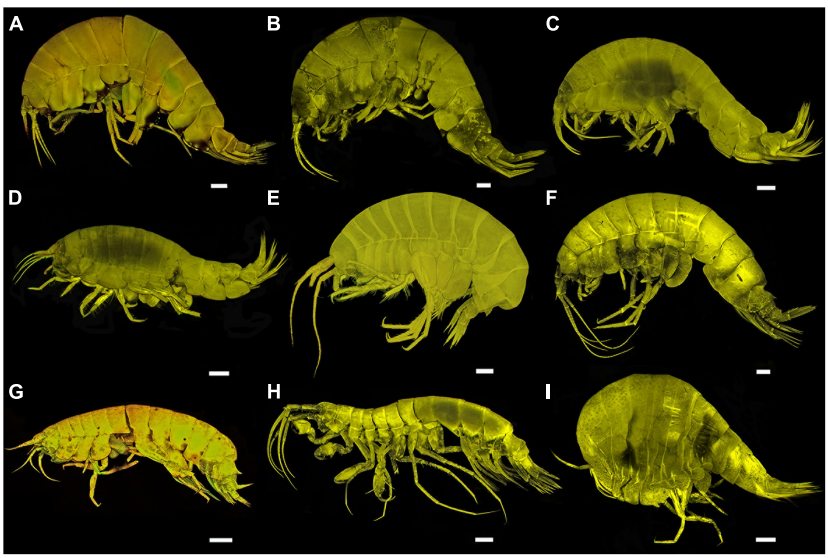

FIGURE 2 | Confocal images of all sampled taxa of Alicelloidea, Eusiroidea, and Stegocephaloidea. **(A)** *Paralicella* sp. group 1A DZMB_2021_0085. **(B)** *Paralicella* sp. group 1B DZMB_2021_0086. **(C)** *Paralicella* sp. group 2A DZMB_2021_0087. **(D)** *Paralicella* sp. group 2B DZMB_2021_0088. **(E)** *Tectovalopsis* aff. *diabolus*. **(F)** *Tectovalopsis fusilus*. **(G)** *Valettiopsis* sp. DZMB_2021_0091. **(H)** *Cleonardo neuvillei*. **(I)** *Parandania* sp. **(E,G)**: scale = 500 μm. **(A–D,F,H,I)**: scale = 1 mm.

of COI were obtained (PCR and sequencing success rate: 92.5%) (**Table 3**) (+21 individuals not sequenced +184 individuals checked only morphologically). Fragment lengths ranged from 527 to 658 bp; no indels or stop codons were found.

The molecular species delimitation methods revealed 20 to 29 MOTUs (**Table 3**, **Supplementary Figures 3–5**, and **Supplementary Tables 3–9**). From all the methods combined, consensus clusters were created for conform results of at least three of them. The result in all cases was a consensus cluster except for the genus *Paralicella*. Within this genus two entities were identified on the basis of morphology–*Paralicella* sp. group 1 (presenting morphological similarity to *Paralicella vaporalis* Barnard and Ingram, 1990) and group 2 (showing some similarities with *P. caperesca* Barnard and Shulenberger, 1976)–which were further divided by molecular study. Within the first all delimitation methods recognized two MOTUs, whereas in the second the number of molecular units ranged from three (ABGD, initial partition) to nine (general mixed Yule-coalescence and Bayesian Poisson tree process); in the second case four consensus MOTUs were defined. As a result, 24 MOTUs with 17 clusters and 7 singletons (**Figure 4**) were identified.

All recognized MOTUs were identified to genus level (from a combination of the morphological and molecular identification), and seven units were identified to species level (**Table 3**). For another three MOTUs, affinities with described species were found–*Tectovalopsis* aff. *diabolus* Barnard and Ingram, 1990, *Paracallisoma* aff. *alberti* Chevreux, 1903, and *Pseudonesimus* aff. *abyssi* Chevreux, 1926–whereas, four more recognized units are probably new to science–*Eurythenes* sp. DISCOLL PAP B, *Hirondellea* sp. nov. DZMB_2021_0092, *Ambasiopsis* sp. nov. DZMB_2021_0093, and *Paracallisoma* sp. nov. DZMB_2021_0094.

In addition to the COI dataset, 54 sequences of 16S (PCR and sequencing success rate: 81.8%) and 44 sequences of 18S (PCR and sequencing success rate: 66.7%) were obtained (**Table 3**). The phylogenetic tree containing 27 concatenated sequences represents 16 MOTUs within 4 superfamilies (**Figure 5**). The tree supports the separation of Lysianassoidea and Alicelloidea. Within Lysianassoidea, representatives of different families were grouped together. A different situation can be seen in the case of Alicelloidea, where representatives of two families (Valettiopsidae and Alicellidae) were mixed. The species *Tectovalopsis* aff. *diabolus* and *Paralicella* sp. group 1 formed one cluster with *Valettiopsis* sp. DZMB_2021_0091, whereas the *Paralicella* group 2 was clearly separated with high posterior probabilities.

Faunistic Composition and Population Connectivity

The 364 individuals collected by trap AT1 at the inactive field formed 19 MOTUs in 11 genera (**Figure 6A**). The 99 captured by trap AT2 at the active field, belonged to 10 MOTUs and five genera. Trap AT3, placed for 22 h close to an active field, captured no amphipods. Only seven MOTUs were captured at both AT1 and AT2. The calculations of the rarefaction curves indicated higher species richness at inactive fields; for active fields the curve approached asymptote and flattens out (**Figure 6B**).

The amphipod assemblage of the inactive site was dominated by *Tectovalopsis fusilus* and *Hirondellea guyoti*, which constituted 60.4% of all individuals collected (**Figure 7**). The remaining 17 MOTUs were represented by similar numbers of individuals. The dominating taxon at the active site was *Paralicella* sp. group 2B DZMB_2021_0088, which alone made up more than 50% of abundance. The other taxa contributing substantially to this assemblage were *Abyssorchomene distinctus*, *Hirondellea* sp. nov. DZMB_2021_0092, *Paracallisoma* sp. nov. DZMB_2021_0094, and *Paralicella* sp. group 1B DZMB_2021_0086. The genera *Eurythenes* and *Tectovalopsis* were collected exclusively at the inactive site.

In the whole area studied, three taxa (*Cleonardo neuvillei*, *Ambasiopsis* sp. nov. DZMB_2021_0093, and *Parandania* sp.) were each represented by a single individual (**Figure 8A**). Among the remaining species, haplotype numbers ranged from 1 to 30 (**Table 4**).

The haplotype diversity (h) was high for AT1 and for the combined data of AT1 and AT2 in *Paralicella* sp. group 2B DZMB_2021_0088 (h = 0.800–0.835), *Eurythenes* sp. DISCOLL PAP B (h = 0.857), *Hirondellea guyoti* (h = 0.709), and *Hirondellea* sp. nov DZMB_2021_0092 (h = 0.782, 0.833), whereas for *Paracallisoma* aff. *alberti* (h = 1.000) only AT1 and, for *Abyssorchomene distinctus* (h = 0.928–0.952), the whole set of data showed high haplotype diversity. Nucleotide diversity (π) was low for all populations, ranging between π = 0.00047 for *Paracallisoma* sp. nov. DZMB_2021_0094 (combined data) and π = 0.00674 for *Eurythenes* sp. DISCOLL PAP B (**Table 4**).

The haplotype network for the genus *Paralicella* (**Figure 8B**) indicated a clear separation between the six MOTUs, with a mutation rate of 29 to 103 substitutions. The three individuals constituting MOTU *Paralicella* sp. group 2A DZMB_2021_0087 showed 24 and 27 substitutions among its representatives.

The neutrality and population-expansion tests revealed that, for the populations of *Paralicella* sp. group 2B DZMB_2021_0088, *Tectovalopsis fusilus*, and *Abyssorchomene distinctus*, the Tajima's D values were negative and significant ($p < 0.05$), indicating an excess of rare nucleotides thus an expansion of the population or indicative of a selective sweep. Fu's Fs confirmed this theory with negative values and highly significant p-values ($p < 0.001$–0.0001). Similarly, evidence for expansion of populations was observed in *Hirondellea* sp. nov. DZMB_2021_0092, *Paracallisoma* aff. *alberti*, and *Paracallisoma* sp. nov. DZMB_2021_0094. The values for Tajima's D and Fu's Fs combined with mainly significant p-values (**Table 4**).

Within-population differences in the analysis of molecular variance (AMOVA) accounted for all the variation (100%) for most of the species, and no evidence supported separation into genetically distinct populations (**Table 5**). In addition, negative or near-zero Fst-values indicated that the studied populations were genetically homogeneous, but all p-values were not significant, indicating no population structure. The only exception was *Abyssochormene distinctus*, where the variation of the AMOVA within the population was 95.39% and the Fst was positive, but p-values were still not significant, indicating no population structure.

TABLE 3 | The list of taxa identified, with superfamily, family and genus information, number of sequences for COI, 16S, and 18S, morphological delimitation (M), number of MOTUs based on Automatic Barcode Gap Discovery (Ai, initial, and Ar, recursive, partition), CD-Hit (C), GMYC (G), bPTP (B), and BIN.

Superfamily	Family	Genus	Species	No. individuals		Marker			Species delimitation methods							BOLD BIN
				AT1	AT2	CO1	16S	18S	M	Ai	Ar	C	G	B	BIN	
Alicelloidea	Alicellidae	*Paralicella* Chevreux, 1908	*Paralicella* sp. group 1A DZMB_2021_0085	2	3	5	2	3	1	1	1	1	1	1	1	BOLD:AEF8804
			Paralicella sp. group 1B DZMB_2021_0086	0	6	6	1	2		1	1	1	1	1	1	BOLD:AEF6691
			Paralicella sp. group 2A DZMB_2021_0087	0	3	3	3	2		1	1	3	3	3	3	BOLD:AEF9380 BOLD:AEF9381 BOLD:AEF9383
			Paralicella sp. group 2B DZMB_2021_0088	16	54	63	10	6	1	1	1	1	3	4	1	BOLD:AEF6635
			Paralicella sp. group 2C DZMB_2021_0089	2	1	3	1	0		1	1	1	2	2	1	BOLD:AEF6636
			Paralicella sp. group 2D DZMB_2021_0090	1	0	1	1	1		1	1	1	1	1	1	BOLD:AEF9382
		Tectovalopsis Barnard and Ingram, 1990	*Tectovalopsis* aff. *diabolus* Barnard and Ingram, 1990	3	0	3	3	3	1	1	1	1	1	1	1	BOLD:AEF9480
			Tectovalopsis fusilus Barnard and Ingram, 1990	131	0	78	2	2	1	1	1	1	1	1	1	BOLD:AEF6344
	Valettiopsidae	*Valettiopsis* Holmes, 1908	*Valettiopsis* sp. DZMB_2021_0091	2	0	1	2	2	1	1	1	1	1	1	1	BOLD:AEF7847
Eusiroidea	Eusiridae	*Cleonardo* Stebbing, 1888	*Cleonardo neuvillei* Chevreux, 1908	1	0	1	1	1	1	1	1	1	1	1	1	BOLD:AEF6468
Lysianassoidea	Eurytheneidae	*Eurythenes* S. I. Smith in Scudder, 1882	*Eurythenes magellanicus* (H. Milne Edwards, 1848)	9	0	8	2	3	1	1	1	1	1	1	1	BOLD:ADD1766
			Eurythenes sp. DISCOLL PAP B	8	0	7	1	2	1	1	1	1	1	2	1	BOLD:AEF7086
	Hirondelleidae	*Hirondellea* Chevreux, 1889	*Hirondellea brevicaudata* Chevreux, 1910	6	0	5	3	2	1	1	1	1	1	1	1	BOLD:AEF6862
			Hirondellea guyoti Barnard and Ingram, 1990	89	0	11	1	2	1	1	1	1	1	1	1	BOLD:AEF7644
			Hirondellea sp. nov. DZMB_2021_0092	22	11	13	2	1	1	1	1	1	1	1	1	BOLD:AEF9394
	Lysianassoidea incertae sedis	*Ambasiopsis* K.H. Barnard, 1931	*Ambasiopsis* sp. nov. DZMB_2021_0093	1	0	0	1	1	1	–	–	–	–	–	–	–
	Scopelocheiridae	*Haptocallisoma* Horton and Thurston, 2015	*Haptocallisoma abyssi* (Oldevig, 1959)	0	3	3	3	0	1	1	1	1	1	1	1	BOLD:ADH7303
		Paracallisoma Chevreux, 1903	*Paracallisoma* aff. *alberti* Chevreux, 1903	10	2	9	4	3	1	1	1	1	2	2	2	BOLD:AEF7929 BOLD:AEF9456
			Paracallisoma sp. nov. DZMB_2021_0094	18	9	13	2	1	1	1	1	1	1	1	1	BOLD:AEF8324
	Tryphosidae	*Pseudonesimus* Chevreux, 1926	*Pseudonesimus* aff. *abyssi* Chevreux, 1926	23	0	6	3	3	1	1	1	1	1	1	1	BOLD:AEF6700
	Uristidae	*Abyssorchomene* De Broyer, 1984	*Abyssorchomene distinctus* (Birstein and Vinogradov, 1960)	19	7	18	5	4	1	1	1	1	1	1	1	BOLD:ACZ6415
Stegocephaloidea	Stegocephalidae	*Parandania* Stebbing, 1888	*Parandania* sp.	1	0	1	1	1	1	1	1	1	1	1	1	BOLD:AAF7953
Total numbers	**10**	**12**	**22**	**364**	**99**	**258**	**54**	**45**	**18**	**20**	**21**	**23**	**27**	**29**	**24**	

Last column provides the BIN code. Shading indicate cases where incongruence between different delimitation methods was noted.

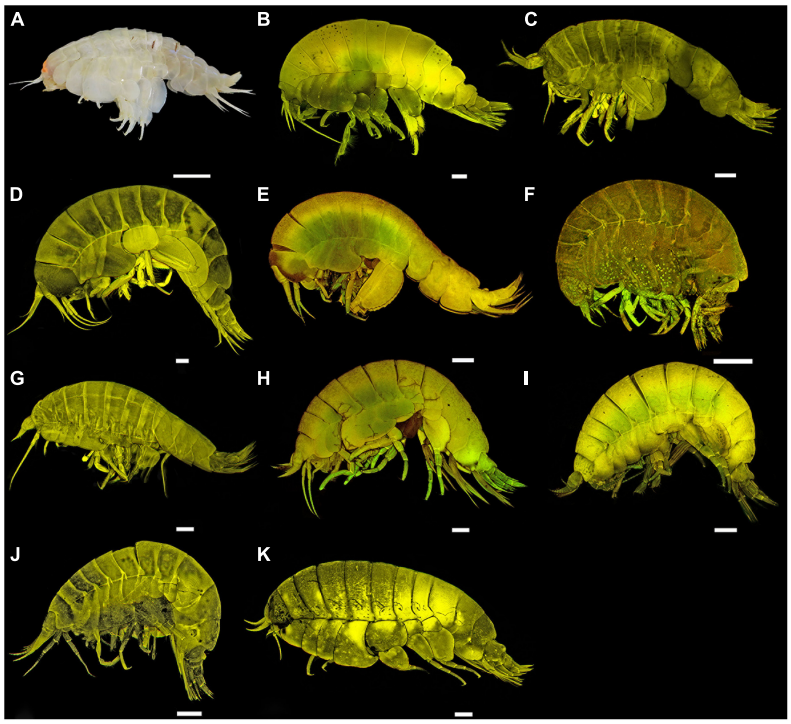

FIGURE 3 | Confocal images of all sampled taxa of Lysianassoidea (including one light microscopy image of a large species, **A**). **(A)** *Eurythenes magellanicus*. **(B)** *Eurythenes* sp. DISCOLL PAP B. **(C)** *Hirondellea brevicaudata*. **(D)** *Hirondellea guyoti*. **(E)** *Hirondellea* sp. nov. DZMB_2021_0092. **(F)** *Ambasiopsis* sp. nov DZMB_2021_0093. **(G)** *Haptocallisoma abyssi*. **(H)** *Paracallisoma* aff. *alberti*. **(I)** *Paracallisoma* sp. nov. DZMB_2021_0094. **(J)** *Pseudonesimus* aff. *abyssi*. **(K)** *Abyssorchomene distinctus*. **(A)**: scale = 2 cm. **(B,K)**: scale = 1 mm. **(C–J)**: scale = 500 μm.

DISCUSSION

Morphological vs. Molecular Identification of Amphipods

Studying baited-trap samples from hydrothermal vent areas by morphological methods supplemented by DNA barcoding led us to a total of 22 MOTUs belonging to 10 genera and four families. For the MOTUs collected, the morphology agreed with the molecular species delimitation, except for the genus *Paralicella.*

Paralicella includes six described species so far (WoRMS Editorial Board, 2021), but taxonomic issues have been mentioned for this genus. Ritchie et al. (2015) reported incongruence between the morphological and molecular identifications of two species within this genus but the discrepancies were not confirmed later (Mohrbeck et al., 2021). In contrast, high mean intraspecific divergences were reported for *Paralicella caperesca* (Jażdżewska et al., 2021; Mohrbeck et al., 2021). Our morphological study of the representatives of *Paralicella* separated them into two different groups, but they were further divided into molecular clades with non-distinct external appearance.

Additional morphological study is required to confirm that these taxa should be treated as cryptic species or to find the morphological characters that will allow separation of the MOTUs within these species complexes. Moreover, individuals within one MOTU of *Paralicella* sp. group 2 (group 2A DZMB_2021_0087) showed high COI sequence divergence (expressed among other evidence by ascription of three different BINs) that may reflect, for example, past population divergence and then subsequent introgression. Because only fragments of two mitochondrial and one nuclear gene loci were sequenced, definite delineation of species within these MOTUs is not possible–ideally data from more than one nuclear gene loci should be obtained.

Scavenging Community in the Studied Area

The known distribution of the taxa collected is shown in **Table 6**. *Abyssorchomene distinctus* is the only species in our collection that was previously detected in the Indian Ocean. Apart from *Cleonardo neuvillei*, all taxa recorded in the present study were previously caught with baited traps. *Cleonardo* species are considered bathypelagic and carnivorous (Bousfield and Hendrycks, 1995), so the presence of single individual in our samples can be regarded as a by-catch.

The genus *Eurythenes* is very commonly collected with baited traps (Jamieson et al., 2011; Havermans et al., 2013; Narahara-Nakano et al., 2018). Of *Eurythenes magellanicus*, we detected the largest individual (105 mm) reported so far that was still an immature female. The largest previously named representative for that species is a mature female 85 mm collected from the

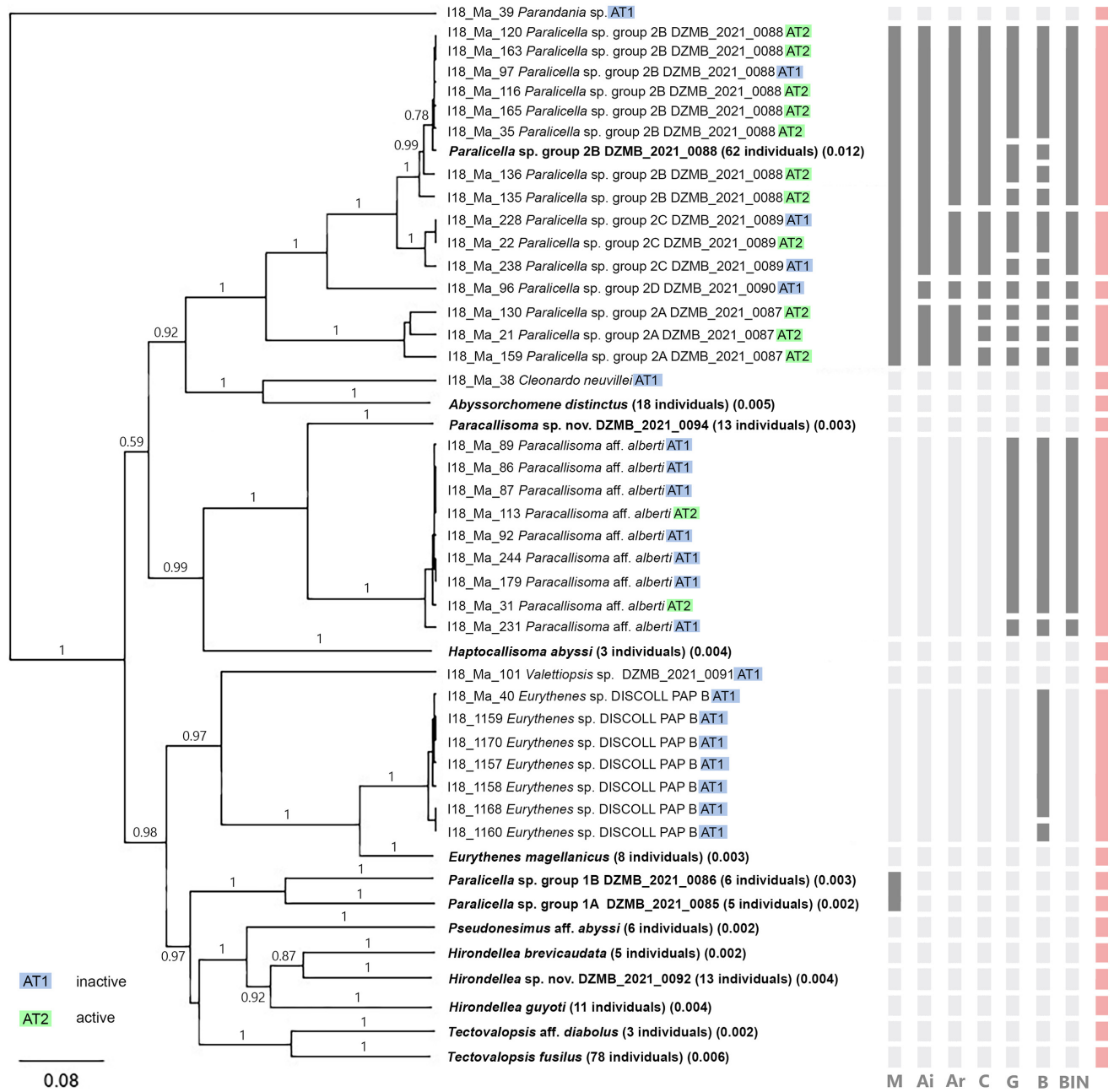

FIGURE 4 | Bayesian inference tree for CO1 data (258 individuals). Tree constructed by using Tamura-Nei substitution and Yule-coalescent model. Numbers represent posterior probabilities (only values higher than 40% are presented). Relevant species delimitation result is shown by vertical bars; disagreements are highlighted: M: morphology. Ai: Automatic Barcode Gap Discovery (initial partition). Ar: Automatic Barcode Gap Discovery (recursive partition). C: CD-Hit. G: general mixed Yule-coalescence GMYC. B: bPTP and BIN. The red bar presents the consensus of all delimitation methods. Samples from AT1 (inactive) and AT2 (active) are color-coded; individuals of one MOTU with matching delimitation results are summarized and highlighted in bold.

stomach of a fish off Cape Horn (Stoddart and Lowry, 2004). The deep-sea species belonging to the genus *Hirondellea* are commonly found in baited traps (Jamieson et al., 2011; Ritchie et al., 2015; Duffy et al., 2016) as well as at hydrothermal vent fields (Barnard and Ingram, 1990). *Ambasiopsis*, another genus belonging to Lysianassoidea, has been recorded from the Indian Ocean before, and it was represented by *Ambasiopsis brevipes* Ledoyer, 1986 collected at Banc du Geyser (Ledoyer, 1986). A detailed check of our *Ambasiopsis* material revealed, however, that it is a different species.

Some species from the superfamily Alicelloidea were collected as well. The genus *Paralicella* is known from all three oceans, including Antarctic waters (Chevreux, 1908; Shulenberger and Barnard, 1976; De Broyer et al., 2004; Horton and Thurston,

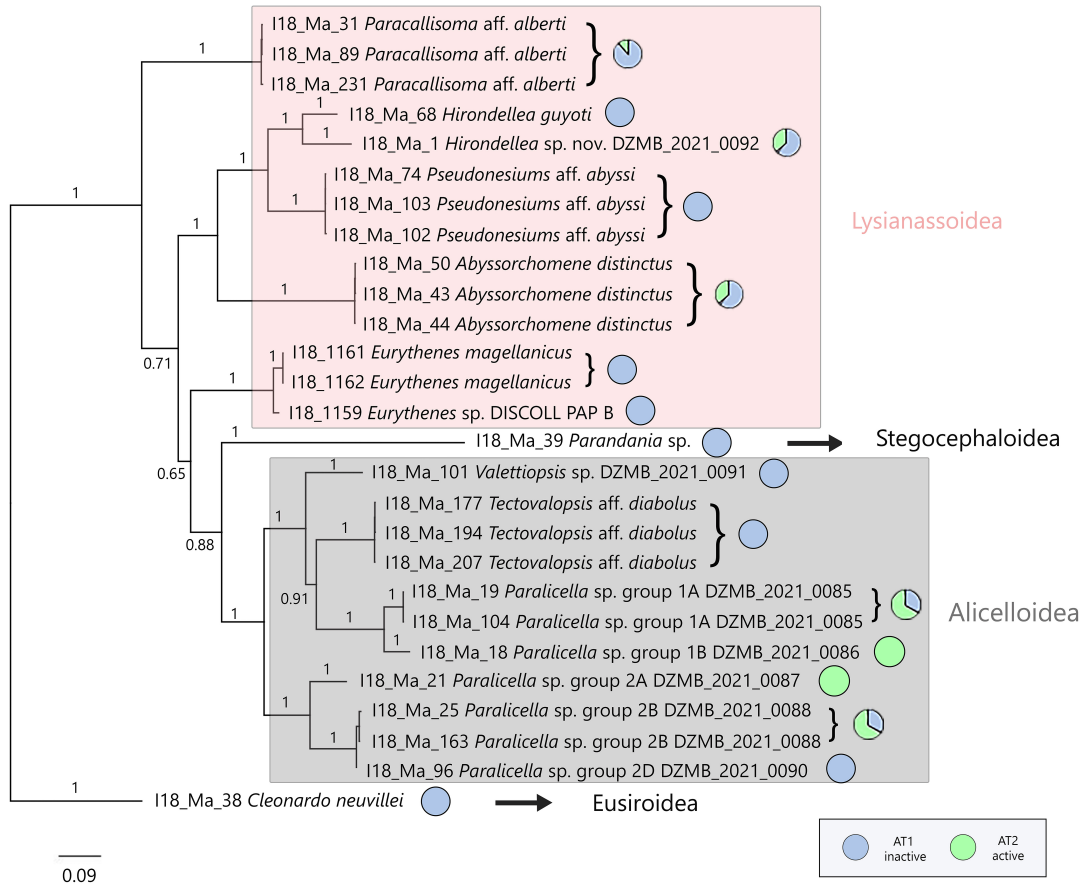

FIGURE 5 | Bayesian inference tree construction on the concatenate three-gene dataset (COI, 16S rDNA, 18S rDNA). The distances were calculated with the General Time Reversible model (COI, 18S) and the Hasegawa-Kishino-Yano model (16S). Numbers represent posterior probabilities. Next to the tree information about the relative abundances for the two locations are given. The superfamilies are indicated on the right.

2009; Horton et al., 2020b; Weston et al., 2021; Jażdżewska et al., 2021) and has been collected at hydrothermal vent fields before (Barnard and Ingram, 1990), as has *Valettiopsis* (Juan de Fuca Ridge in the Pacific Ocean) (Tsurumi, 2001). The genus *Parandania* is not only a worldwide distributed genus, but was also sampled at hydrothermal vents (Wang et al., 2019). One species within this genus, *Parandania boecki* is panoceanic and reported from Indian Ocean (De Broyer et al., 2007).

Population Connectivity and Community Analyses

Our study provides the first known records for scavenging amphipods caught with the help of baited traps at hydrothermal vent fields in the Indian Ocean. Nevertheless, sampling in the deep sea is sometimes challenging, and certain limitations to the study must be mentioned. The first is lack of replicates, second that the active and inactive sites are some distance apart and without adjacent non-vent abyssal controls, and third that the traps were left on the sea floor for different periods of time (**Table 1**). These factors might produce differences within the species composition and abundance. Similarly, differences in abiotic factors at the three traps locations might influence the fauna that approached them.

The distribution of organic matter and the hydrostatic pressure are important in defining the composition of hadal scavenging communities (Wolff, 1959; Beliaev and Brueggeman, 1989). Experimental study has revealed that some amphipod species are not flexible enough to colonize highly disturbed zones, for example glacier melting areas or bottom sections opened after ice shelf collapse because of changes in salinity and intensive sedimentation (Seefeldt et al., 2017). Hydrothermally active areas can also be considered disturbed areas, with irregular abiotic factors like bursting chimneys, hypoxia (Hourdez and Lallier, 2007), high temperatures (Chevaldonné et al., 1991, 1992), and high levels of hydrogen sulfide, methane, ammonia, and heavy metals (Campbell et al., 1988a,b). In comparison, inactive areas offer stable environmental conditions that are more attractive to general deep-sea organisms (Erickson et al., 2009; Levin et al., 2009; Boschen et al., 2016). Similar values of temperature, salinity and pH were observed at all three locations, so these factors cannot explain the complete failure of trap AT3 even though it spent similar time on the bottom as the very successful AT1 trap. Of the three sites AT3

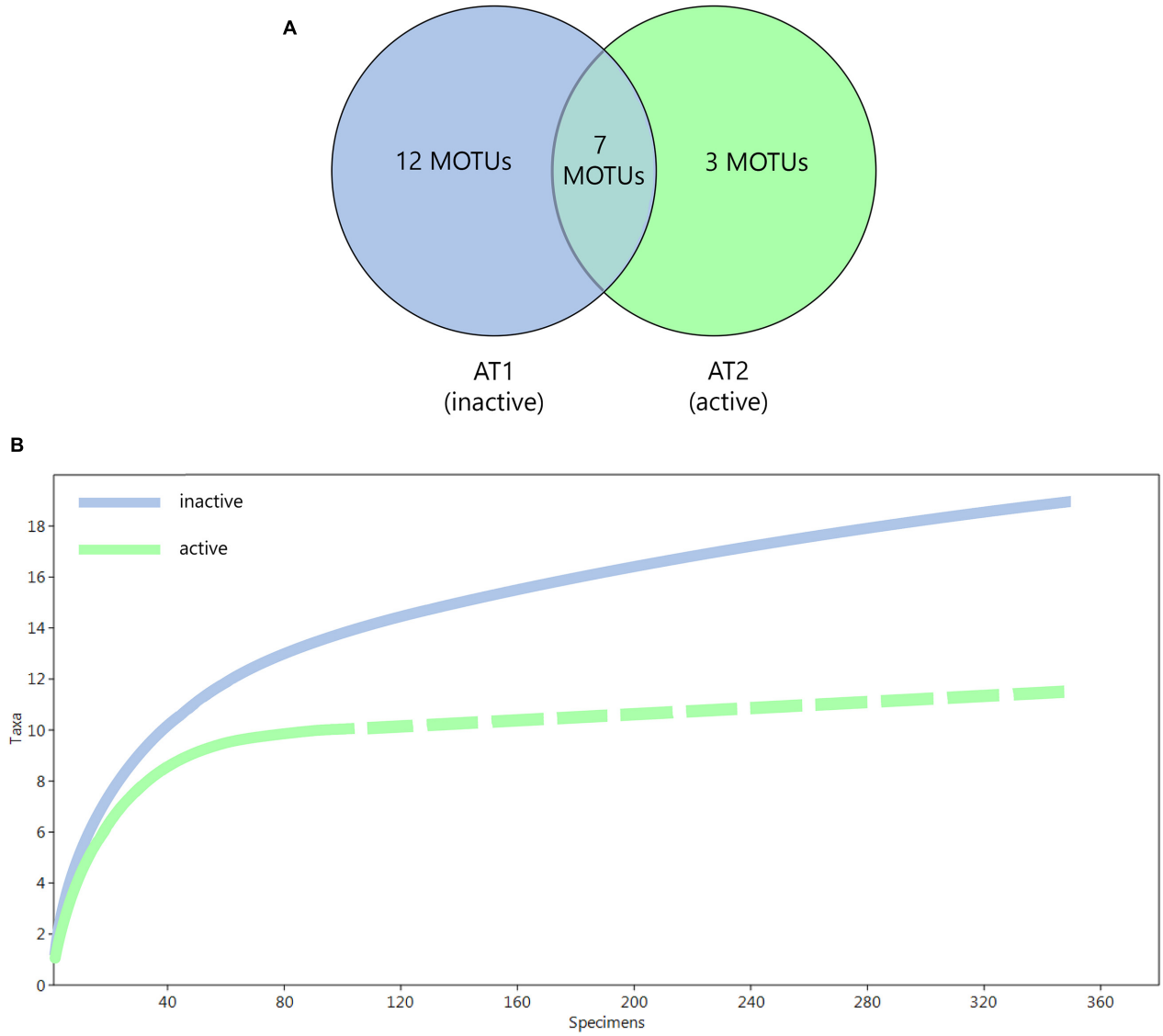

FIGURE 6 | Comparison of active and inactive sites. **(A)** Venn-diagram presenting the different MOTUs and their collection locations. **(B)** Assessment of the species richness by individual-based rarefaction curve.

was situated in the closest vicinity of the active vent. The emissions from vents are associated with oxygen depletion in the surrounding waters (Hourdez and Lallier, 2007) while amphipods are regarded as having low tolerance to hypoxia (Modig and Ólafsson, 1998; Wu and Or, 2005; Copilaş-Ciocianu et al., 2020) that may caused their absence there. Unfortunately, the oxygen concentration data are not available for the studied sites, so this issue must remain open question. At the other two traps 463 amphipods were captured, but are these amphipods only occasional visitors to the fields or might they be vent endemic?

At hydrothermal vent fields life depends on the presence of chemoautotrophic microbes. In the Indian Ocean, the microbes support the high abundance of the shrimp *Rimicaris kairei* Watabe and Hashimoto, 2002, which in turn sustains a variety of other vent endemic taxa, including fish species (Gerdes et al., 2021; Thiel et al., 2021). Generally, vent endemic species occur in high abundance around the active fields (Ingole and Koslow, 2005; Thornton et al., 2016), but despite the special food source, typical vent-endemic amphipods have not previously been reported from the Indian Ocean, even though knowledge about the vent fields along the Central and Southeast Indian Ridges has increased during the last decade as a result of the massive sulfide exploration program in the German license area (Gerdes et al., 2019a,b, 2021). The absence up to now of any amphipod records and abundance that is on average lower than those reported in the literature for baited traps (Duffy et al., 2012; Horton et al., 2020b; Patel et al., 2020), we conclude that the presently

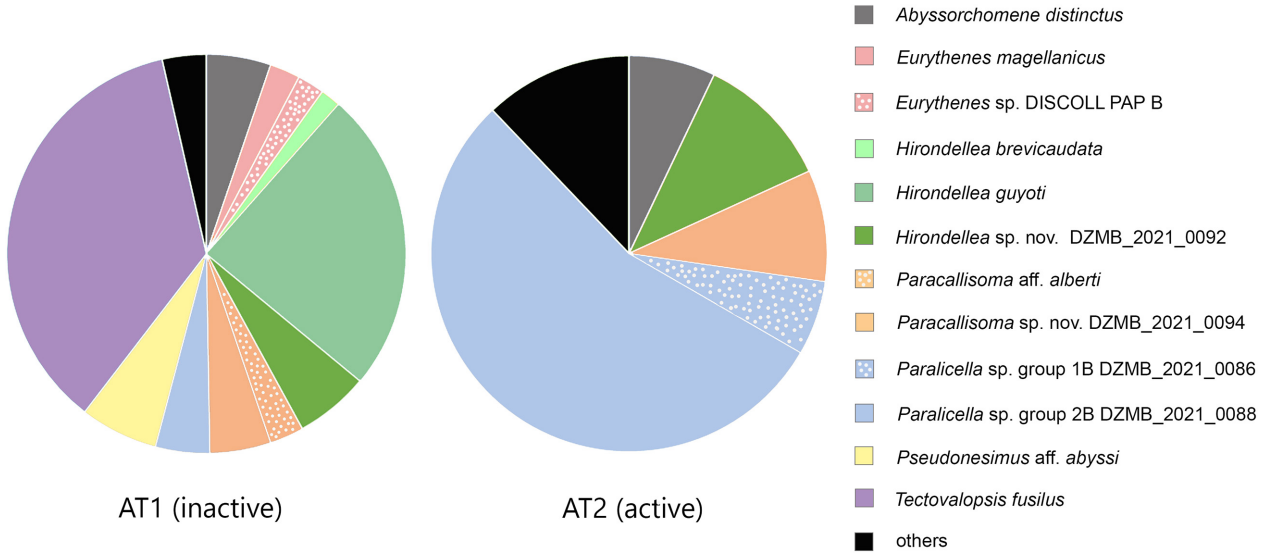

FIGURE 7 | Relative abundance of MOTUs at the active and inactive areas. Unnamed MOTUs with $n \leq 3$ are grouped together as "others." More details about numbers of each MOTU can be found in **Table 3**.

studied scavenging amphipod assemblage is probably not vent endemic. The three previously described species (*Hirondellea guyoti*, *Tectovalopsis fusilus*, and *T.* aff. *diabolus*) have so far been recorded exclusively from hydrothermal vent fields (Barnard and Ingram, 1990; Desbruyères et al., 2006), however, and we report four species new to science that have not yet been collected elsewhere. These species do not depend directly on the chemoautotrophic bacteria and primary production in the vent fields, but they may be more resistant to hypoxic conditions than other deep-sea amphipod species and may profit from the primary production that is offered by the vent fields. They may therefore be treated as vent related, but because no baited traps were set in the abyssal plain adjacent to the presently studied area, the presence of these species also outside the hydrothermal vent fields cannot be excluded.

Differences in amphipod assemblages between hydrothermally active and inactive regions can be observed. The inactive site was characterized by higher abundance and species richness (**Table 3** and **Figures 6**, **7**) than the active area. Rarefaction results indicated that the higher diversity at the inactive site would still be the expected result. In addition, the population analyses indicate a significant population expansion of the *Paralicella* sp. group 2B DZMB_2021_0088, *Tectovalopsis fusilus*, and *Abyssorchomene distinctus* (**Table 5**); the other species studied also tended to expand. Expanding populations are a general deep-sea phenomenon particularly in vent-endemic species (Vrijenhoek, 2010; Taylor and Roterman, 2017). Furthermore, the analyses of Tajima's D and Fu's Fs did not reveal clear differences within genetic diversity between populations at active and inactive sites. In addition, AMOVA reinforced this statement by comparing the mitochondrial COI sequences of active and inactive populations for six species from the Southeast Indian Ridge, resulting in a lack of genetic structure, as suggested by negative or non-significant values for Fst. On this basis, we speculate that no "active" or "inactive" vent communities are present. Instead, just one population probably approaches the different fields. The expansion of the populations in the deep sea may be associated with recent bottlenecks, dispersal of random individuals between patchy habitats, or positive selection (Taylor and Roterman, 2017) and, however, signify a large population size.

Different feeding strategies might explain the difference between the traps from active and inactive vents. These differences are not only quantitative (although the quantitative difference should be viewed with caution) but also qualitative, because the active area was dominated by *Paralicella* sp. group 2B DZMB_2021_0088. This genus is known to consist of obligate scavengers (Horton et al., 2020b) that are very successful in locating baits in the deep sea and depend only on this specific kind of food. Horton et al. (2020b) revealed that temporal changes in environmental conditions in the ocean may influence the scavenger community. These changes are reflected in the switch from obligate necrophagous amphipod dominance (*Paralicella*) to a more diverse assemblage with larger numbers of facultative scavengers (*Abyssorchomene* sp., *Eurythenes* spp.). In the present case, the differences in environmental conditions between the active and inactive sites may reflect the temporal changes observed by Horton et al. (2020b). These authors have also observed that the scavenger community changes with the time the bait spends on the bottom, from the dominance of obligate scavengers, to a more diverse assemblage with a higher share of facultative scavengers (Janßen et al., 2000). In our study the trap at the active site spend a shorter amount of time on the bottom, a difference that might have prevented less specialized amphipod species from reaching it, but the rarefaction curve for the active site sample

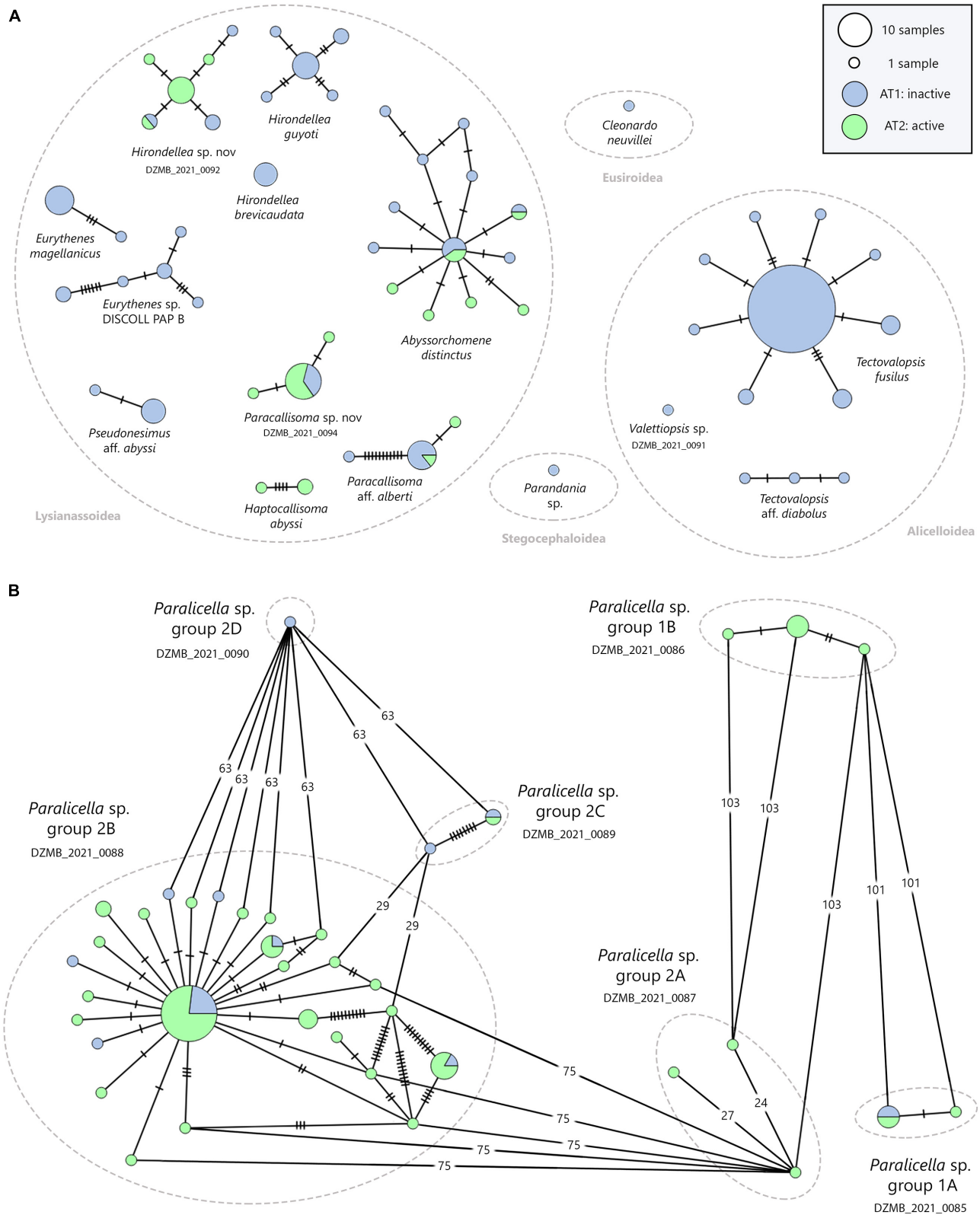

FIGURE 8 | Results of the statistical haplotype network analysis based on the COI data-set (258 individuals). Colors refer to the different sampling localities and the size of each circle is proportional to the number of individuals (see legends). Hatch marks show single substitutions. Minimum spanning networks for **(A)** Alicelloidea, Eusiroidea, Lysianassoidea and Stegocephaloidea. **(B)** *Paralicella*; differentiated into six groups. Mutations ($n > 10$) are presented as numbers.

TABLE 4 | Genetic diversity indices, parameters of demographic history and neutrality and population expansion tests calculated for the COI dataset.

Species		n	No. haplotypes	Haplotype diversity (h)	Nucleotide diversity (π)	Tajima's D	Fu's *Fs*
Paralicella sp. group 1A DZMB_2021_0085	AT1	2	1	–	–	–	–
	AT2	3	2	0.667	0.00101	–	0.20067
	com	5	2	0.400	0.00061	–0.81650	0.09021
Paralicella sp. group 1B DZMB_2021_0086	AT2	6	3	0.600	0.00203	–1.29503	0.29690
Paralicella sp. group 2B DZMB_2021_0088	AT1	15	9	0.800	0.00377	–1.95478*	–2.10318
	AT2	53	23	0.835	0.00560	–1.95004*	–16.22493***
	com	68	30	0.823	0.00510	–2.05811*	–22.31432***
Tectovalopsis fusilus	AT1	78	9	0.305	0.00077	–2.09503*	–7.04595***
Eurythenes magellanicus	AT1	9	2	0.222	0.00122	–1.44751	1.41490
Eurythenes sp. DISCOLL PAP B	AT1	8	5	0.857	0.00674	0.09834	0.12110
Hirondellea brevicaudata	AT1	5	1	–	–	–	–
Hirondellea guyoti	AT1	11	5	0.709	0.00238	-1.40298	-0.97174
Hirondellea sp. nov. DZMB_2021_0092	AT1	4	3	0.833	0.00329	-0.06501	0.25081
	AT2	9	4	0.583	0.00101	–1.51297	–1.89165*
	com	13	6	0.782	0.00175	–1.01207	–2.69176*
Paracallisoma aff. *alberti*	AT1	7	2	0.286	0.00478	–1.62257*	4.56086
	AT2	2	2	1.000	0.00152	–	–
	com	9	3	0.417	0.00405	–1.87639*	2.51104
Paracallisoma sp. nov.	AT1	4	1	–	–	–	–
	AT2	9	3	0.417	0.00068	–1.36240	–1.08110*
	com	13	3	0.295	0.00047	–1.46801*	–1.40150*
Pseudonesimus aff. *abyssi*	AT1	6	2	0.333	0.00051	–0.93302	–0.00275
Abyssorchomene distinctus	AT1	11	9	0.945	0.00254	–1.21775	–7.38058***
	AT2	7	6	0.952	0.00261	–1.52412*	–3.70942**
	com	18	13	0.928	0.00260	–1.88027*	–11.98916***

Significant P-values are marked with asterisks. < 0.05, < 0.001**, < 0.0001 ***. Only MOTUs represented by a total n ≥ 4 shown. Combined populations from AT1 and AT2 are presented as "com."*

approached the asymptote, so no addition of new species in this assemblage was predicted.

Nevertheless, in another study the species *Eurythenes gryllus* (Lichtenstein in Mandt, 1822) is reported to be rather an obligate scavenger (Dauby et al., 2001), but as the genus *Eurythenes* has never been collected at hydrothermal vent areas, it seems to avoid areas with active hydrothermal activity. Dauby et al. (2001) also reported one species of *Abyssorchomene* [*A. nodimanus* (Walker, 1903)] as an obligate scavenger, in contrast with Horton et al. (2020b). For *A. distinctus*, which we captured on both active and inactive site in more or less equal numbers, we might conclude it is resistant enough to environmental conditions to feed at the active site and has no preference for habitat. The genus *Hirondellea* has been reported to be either an obligate scavenger (Blankenship and Levin, 2007) or a micropredatory browsing type, so scavenging is just an alternative feeding mode for the species (Dauby et al., 2001). In the stomach of *Hirondellea antarctica* (Schellenberg, 1926) hydrozoans and sea anemones were detected (Dauby et al., 2001). The two described species of *Hirondellea* presently we captured may be assumed to be facultative scavengers avoiding the active vent sites, whereas *Hirondellea* sp. nov. DZMB_2021_0092, collected in both locations, may be an obligate scavenger or may also feed on the vent fauna. Little is known about the dominant species in the inactive site–*Tectovalopsis fusilus*. Similarly to *Paralicella* this genus is regarded as grouping obligate scavengers (Lowry and De Broyer, 2008), but *T. fusilus* has so far been collected only once and is known from single individual, so a final decision cannot be drawn about how variable its food composition is.

Our study leads to the conclusions that the scavenging amphipods at the vent fields are not restricted to the locations studied and that only some of the most resistant species may be able to deal with the difficult conditions at the active area.

TABLE 5 | Analysis of molecular variance (AMOVA) based on pairwise difference among haplotypes; significance calculated by 1,000 permutations of the COI dataset.

Source of variation	Sampling site (active/inactive) = population		
		Percentage of variation	FST (*p*-value)
Paralicella sp. group 1A DZMB_2021_0085	Among populations	–20.00	–0.20000 (1.00000)
	Within populations	120.00	
Paralicella sp. group 2B DZMB_2021_0088	Among populations	–3.20	–0.03200 (1.00000)
	Within populations	103.20	
Hirondellea sp. nov. DZMB_2021_0092	Among populations	–12.78195	–0.12782 (1.00000)
	Within populations	112.78195	
Paracallisoma aff. *alberti*	Among populations	–18.23	–0.18226 (0.43109)
	Within populations	118.23	
Paracallisoma sp. nov.	Among populations	–11.62791	–0.11628 (1.00000)
	Within populations	111.62791	
Abyssorchomene distinctus	Among populations	4.61522	0.04615 (0.11926)
	Within populations	95.38478	

The populations were arranged in active and inactive groups. All p-values are non-significant.

TABLE 6 | Summary of known distribution of presently sampled species indicating the presence at hydrothermal vent areas.

	Atlantic ocean	Pacific ocean	Hydrothermal vents	References
Tectovalopsis aff. *diabolus*	Not recorded	East Pacific Rise: 13°N vent site (type locality; only record so far)		Barnard and Ingram, 1990; Desbruyères et al., 2006
Tectovalopsis fusilus	Not recorded	Guerrero, off Punta San Telmo, North East Pacific (type locality)		Barnard and Ingram, 1990
Cleonardo neuvillei	Canary Islands (type locality), only record so far	Not recorded	Not recorded	Chevreux, 1910
Eurythenes magellanicus	North and South Atlantic	Cape Horn (type locality), Taiwan, Okinawa Island	Not recorded	Stoddart and Lowry, 2004; Havermans et al., 2013; Havermans, 2016; Narahara-Nakano et al., 2018; Horton et al., 2020a
Eurythenes sp. DISCOLL PAP B	Porcupine Abyssal Plain, Northeast and Northwest Atlantic	Peru-Chile Trench, South East Pacific	Not recorded	France and Kocher, 1996 (identified as *Eurythenes gryllus* ICE-1); Ritchie et al., 2015 (identified as *Eurythenes* sp. 2 HR-2015); Horton et al., 2020a
Hirondellea brevicaudata	North Atlantic (type locality)	North of Hawaii, central Pacific		Chevreux, 1910; Barnard and Ingram, 1990; France, 1993
Hirondellea guyoti	Not recorded	Hess Guyot in the North Pacific (type locality), only record so far		Barnard and Ingram, 1990
Haptocallisoma abyssi	Greenland Sea (type locality), North Atlantic	Not recorded	Not recorded	Oldevig, 1959; Horton and Thurston, 2015; Jażdżewska et al., 2018 (erroneously identified as *Scopelocheirus* sp.)
Paracallisoma aff. *alberti*	Azores (type locality), North Atlantic	Not recorded	Not recorded	Horton and Thurston, 2015
Pseudonesimus aff. *abyssi*	Bay of Biscay (type locality), North Atlantic	Cedros Trench, North East Pacific	Not recorded	Chevreux, 1926; Barnard, 1967
Abyssorchomene distinctus	South of Palau (type locality), worldwide distributed in the abyss, the only species previously recorded in the Indian Ocean		Guaymas Basin, East Pacific Rise 13°N	Vinogradov, 1993; Bellan-Santini, 1998; Desbruyères et al., 2006; Jamieson et al., 2011; Ritchie et al., 2015; Duffy et al., 2016; Patel et al., 2020; Weston et al., 2021

Reinforcing the patterns observed in our study, we intend to improve our results by increasing the sample size, placing the traps at different distances from the field and setting a standard for the distance between trap and vent field, and the deployment time. Finally, our results show that the amphipod fauna of the ecosystems of the Central and Southeast Indian Ridges are still widely unexplored and that further studies, particularly of environments such as the inactive and active hydrothermal areas, have great potential for the discovery of more scavenging amphipods.

DATA AVAILABILITY STATEMENT

The datasets generated for this study can be found in the Barcode of Life Data System (BOLD) as "DS-INMAC01." All sequences were in addition deposited in GenBank with the accession numbers: COI (MZ197178–MZ197435), 16S (MZ197436–MZ197490), and 18S (MZ197491–MZ197533). Additional information about the analyses presented here is included in the **Supplementary Material**.

AUTHOR CONTRIBUTIONS

TCK was the head of the project. TCK and PMA contributed to the conception and design of the study. AMJ performed the morphological studies and identification of the amphipods. KK did the molecular work, constructed the database, and wrote the first draft of the manuscript. All authors contributed to manuscript revision, read, and approved the submitted version.

FUNDING

AMJ received support in 2019 from the internal funds of the University of Łódź (1.01.01.00.000) to visit DZMB in Wilhelmshaven and verify the identification of the studied collection. KK received a grant from Senckenberg Gesellschaft für Naturforschung (SGN) to work on the Ph.D. (4.02.00065).

ACKNOWLEDGMENTS

We would like to thank Thomas Kuhn, current Chief-Scientist of the INDEX exploration program; Ulrich Schwarz-Schampera, Chief-Scientist of the INDEX exploration program during the INDEX2018 cruise; and the captain and crew of the RV *Pelagia* and the ROV team of *ROPOS* for their help during sampling. Maps and samples presented in this study originate from the INDEX exploration project for marine polymetallic sulfides by the Federal Institute for Geosciences and Natural Resources (BGR) on behalf of the German Federal Ministry for Economic Affairs and Energy. Exploration activities are carried out in the framework and under the regulations of an exploration license with the International Seabed Authority. Thanks to our colleagues at DZMB Wilhelmshaven for their help with the molecular work and data analysis. In this regard special thanks to Sahar Khodami. This publication is number 84 from the Senckenberg am Meer Metabarcoding and Molecular Laboratory and number 61 based on data from the Senckenberg am Meer Confocal Laser scanning Microscope Facility: (SGN-SaM-cLSM).

SUPPLEMENTARY MATERIAL

The Supplementary Material for this article can be found online at: https://www.frontiersin.org/articles/10.3389/fmars.2021.752360/full#supplementary-material

REFERENCES

Altschul, S. F., Gish, W., Miller, W., Myers, E. W., and Lipman, D. J. (1990). Basic local alignment search tool. *J. Mol. Biol.* 215, 403–410. doi: 10.1016/S0022-2836(05)80360-2

Bandelt, H. J., Forster, P., and Röhl, A. (1999). Median-joining networks for inferring intraspecific phylogenies. *Mol. Biol. Evol.* 16, 37–48. doi: 10.1093/oxfordjournals.molbev.a026036

Barnard, J. L. (1967). Bathyal and abyssal gammaridean Amphipoda of Cedros Trench, Baja California. *U. S. Natl. Museum Bull.* 260, 1–205; 92 figs.

Barnard, J. L., and Ingram, C. L. (1990). Lysianassoid Amphipoda (Crustacea) from deep-sea thermal vents. *Smithson. Contrib. Zool.* 449, 1–80. doi: 10.5479/si.00810282.499

Barnard, J. L., and Karaman, G. S. (1991). The families and genera of marine gammaridean Amphipoda (except marine gammaroids). Part 2. *Rec. Aust. Mus. Suppl.* 13, 419–866. doi: 10.3853/j.0812-7387.13.1991.367

Beliaev, G. M., and Brueggeman, P. L. (1989). *Deep Sea Ocean Trenches and their Fauna*. Moscow: Nauka Publishing House.

Bellan-Santini, D. (1998). Crustacés amphipodes des sources hydrothermales: bilan des connaissances. *Cah. Biol. Mar.* 39, 143–152.

Bellan-Santini, D. (2007). New amphipods of hydrothermal vent environments on the Mid-Atlantic Ridge, Azores Triple junction zone. *J. Nat. Hist.* 41, 567–596. doi: 10.1080/00222930701262537

Berge, J., and Vader, W. (2001). Revision of the amphipod (Crustacea) family Stegocephalidae. *Zool. J. Linn. Soc.* 133, 531–592. doi: 10.1111/j.1096-3642.2001.tb00638.x

Blankenship, L. E., and Levin, L. A. (2007). Extreme food webs: foraging strategies and diets of scavenging amphipods from the ocean's deepest 5 kilometers. *Limnol. Oceanogr.* 52, 1685–1697. doi: 10.4319/lo.2007.52.4.1685

Boschen, R., Rowden, A., Clark, M., Pallentin, A., and Gardner, J. (2016). Seafloor massive sulfide deposits support unique megafaunal assemblages: implications for seabed mining and conservation. *Mar. Environ. Res.* 115, 78–88. doi: 10.1016/j.marenvres.2016.02.005

Bousfield, E. L., and Hendrycks, E. A. (1995). The amphipod superfamily Eusiroidea in the North American Pacific region. I. Family Eusiridae: systematics and distributional ecology. *Amphipacifica* 1, 3–59.

Brix, S., Bober, S., Tschesche, C., Kihara, T. C., Driskell, A., and Jennings, R. (2018). Molecular species delimitation and its implications for species descriptions using desmosomatid and nannoniscid isopods from the VEMA fracture zone as example taxa. *Deep Sea Res. Part II Top. Stud. Oceanogr.* 148, 180–207. doi: 10.1016/j.dsr2.2018.02.004

Campbell, A. C., Bowers, T. S., Measures, C. I., Falkner, K. K., Khadem, M., and Edmond, J. M. (1988a). A time series of vent fluid compositions from 21°N, East Pacific Rise (1979, 1981, 1985), and the Guaymas Basin, Gulf of California (1982, 1985). *J. Geophys. Res. Solid Earth* 93, 4537–4549. doi: 10.1029/JB093iB05p04537

Campbell, A. C., Palmer, M. R., Klinkhammer, G. P., Bowers, T. S., Edmond, J. M., Lawrence, J. R., et al. (1988b). Chemistry of hot springs on the Mid-Atlantic Ridge. *Nature* 335, 514–519. doi: 10.1038/335514a0

Chevaldonné, P., Desbruyères, D., and Childress, J. J. (1992). Some like it hot ... and some even hotter. *Nature* 359, 593–594.

Chevaldonné, P., Desbruyères, D., and Haître, M. L. (1991). Time-series of temperature from three deep-sea hydrothermal vent sites. *Deep Sea Res. Part I Oceanogr. Res. Pap.* 38, 1417–1430. doi: 10.1016/0198-0149(91)90014-7

Chevreux, E. (1889). Amphipodes nouveaux provenant des campagnes de "l'Hirondelle" 1887–1888. *Bull. Soc. Zool. Fr.* 14, 283–289.

Chevreux, E. (1908). Diagnoses d'amphipodes nouveaux provenant des campagnes de la "Princesse-Alice" dans l'Atlantique nord. *Bull. Inst. Oceanogr. Monaco* 117, 1–13.

Chevreux, E. (1910). Diagnoses d'amphipodes nouveaux provenant des campagnes de la "Princesse-Alice" dans l'Atlantique nord. *Bull. Inst. Oceanogr. Monaco* 117, 1–113.

Chevreux, E. (1926). Diagnoses d'amphipodes nouveaux provenant des campagnes de la "Princesse-Alice," dans l'Atlantique et dans l'Océan Arctique. Lysianassidae. *Bull. Inst. Océanogr. Monaco* 475, 1–12.

Christiansen, B. (1996). Bait-attending amphipods in the deep sea: a comparison of three localities in the north-eastern Atlantic. *J. Mar. Biol. Assoc. U.K.* 76, 345–360. doi: 10.1017/S0025315400030599

Collins, P., Kennedy, R., and Van Dover, C. (2012). A biological survey method applied to seafloor massive sulphides (SMS) with contagiously distributed hydrothermal-vent fauna. *Mar. Ecol. Prog. Ser.* 452, 89–107.

Copilaş-Ciocianu, D., Borko, Š, and Fišer, C. (2020). The late blooming amphipods: global change promoted post-Jurassic ecological radiation despite Palaeozoic origin. *Mol. Phylogenet. Evol.* 143:106664. doi: 10.1016/j.ympev.2019.106664

Corbari, L., and Sorbe, J.-C. (2017). First observations of the behaviour of the deep-sea amphipod *Dulichiopsis dianae* sp. nov. (Senticaudata, Dulichiidae) in the TAG hydrothermal vent field (Mid-Atlantic Ridge). *Mar. Biodivers.* 48, 631–645. doi: 10.1007/s12526-017-0788-y

Corbari, L., Durand, L., Cambon-Bonavita, M.-A., Gaill, F., and Compère, P. (2012). New digestive symbiosis in the hydrothermal vent Amphipoda *Ventiella sulfuris*. *C. R. Biol.* 335, 142–154. doi: 10.1016/j.crvi.2011.12.005

Costa, F. O., Henzler, C. M., Lunt, D. H., Whiteley, N. M., and Rock, J. (2009). Probing marine *Gammarus* (Amphipoda) taxonomy with DNA barcodes. *Syst. Biodivers.* 7, 365–379. doi: 10.1017/S1477200009990120

d'Udekem d'Acoz, C., and Havermans, C. (2015). Contribution to the systematics of the genus *Eurythenes* S.I. Smith in Scudder, 1882 (Crustacea: Amphipoda: Lysianassoidea: Eurytheneidae). *Zootaxa* 3971, 1–80. doi: 10.11646/zootaxa.3971.1.1

Dauby, P., Scailteur, Y., and De Broyer, C. (2001). Trophic diversity within the Eastern Weddell Sea amphipod community. *Hydrobiologia* 443, 69–86. doi: 10.1023/A:1017596120422

De Broyer, C., Lowry, J., Jażdżewski, K., and Robert, H. (2007). Census of Antarctic Marine Life. Synopsis of the Amphipoda of the Southern Ocean. Part. 1. Catalogue of the Gammaridean and Corophiidean Amphipoda (Crustacea) of the Southern Ocean with distribution and ecological data. *Bull. Inst. R. Sci. Nat. Belgique* 77, 1–325.

De Broyer, C., Nyssen, F., and Dauby, P. (2004). The crustacean scavenger guild in Antarctic shelf, bathyal and abyssal communities. *Deep Sea Res. Part II Top. Stud. Oceanogr.* 51, 1733–1752. doi: 10.1016/j.dsr2.2004.06.032

De Busserolles, F., Sarrazin, J., Gauthier, O., Gélinas, Y., Fabri, M. C., Sarradin, P. M., et al. (2009). Are spatial variations in the diets of hydrothermal fauna linked to local environmental conditions? *Deep Sea Res. Part II Top. Stud. Oceanogr.* 56, 1649–1664. doi: 10.1016/j.dsr2.2009.05.011

Desbruyères, D., Segonzac, M., and Bright, M. (2006). Handbook of deep-sea hydrothermal vent fauna. *Denisia* 18, 1–544. Linz, Austria.

Drummond, A. J., Suchard, M. A., Xie, D., and Rambaut, A. (2012). Bayesian phylogenetics with BEAUti and the BEAST 1.7. *Mol. Biol. Evol.* 29, 1969–1973. doi: 10.1093/molbev/mss075

Duffy, G., Horton, T., and Billett, D. S. M. (2012). Deep-sea scavenging amphipod assemblages from the submarine canyons of the Western Iberian Peninsula. *Biogeosciences* 9, 4861–4869. doi: 10.5194/bg-9-4861-2012

Duffy, G., Lawler, S. F., and Horton, T. (2016). Scavenging amphipods of the Angolan deep-sea habitat, with a focus on *Abyssorchomene distinctus* (Birstein and Vinogradov, 1960) (Amphipoda: Lysianassoidea). *J. Crustac. Biol.* 36, 417–426. doi: 10.1163/1937240X-00002448

Emerson, B. C., Ibrahim, K. M., and Hewitt, G. M. (2001). Selection of evolutionary models for phylogenetic hypothesis testing using parametric methods. *J. Evol. Biol.* 14, 620–631. doi: 10.1046/j.1420-9101.2001.00306.x

Erickson, K. L., Macko, S. A., and Van Dover, C. L. (2009). Evidence for a chemoautotrophically based food web at inactive hydrothermal vents (Manus Basin). *Deep Sea Res. II Top. Stud. Oceanogr.* 56, 1577–1585. doi: 10.1016/j.dsr2.2009.05.002

Excoffier, L., and Lischer, H. E. L. (2010). Arlequin suite ver 3.5: a new series of programs to perform population genetics analyses under Linux and Windows. *Mol. Ecol. Resour.* 10, 564–567. doi: 10.1111/j.1755-0998.2010.02847.x

France, S. C. (1993). Geographic variation among three isolated populations of the hadal amphipod *Hirondellea gigas* (Crustacea: Amphipoda: Lysianassoidea). *Mar. Ecol. Prog. Ser.* 92, 277–287.

France, S. C., and Kocher, T. D. (1996). DNA sequencing of formalin-fixed crustaceans from archival research collections. *Mol. Mar. Biol. Biotechnol.* 5, 304–313.

Fu, Y. X. (1996). New statistical tests of neutrality for DNA samples from a population. *Genetics* 143, 557–570.

Gallo, N., Cameron, J., Hardy, K., Fryer, P., Bartlett, D., and Levin, A. L. (2015). Submersible- and lander-observed community patterns in the Mariana and New Britain trenches: influence of productivity and depth on epibenthic and scavenging communities. *Deep Sea Res. Part I Oceanogr. Res. Pap.* 99, 119–133. doi: 10.1016/j.dsr.2014.12.012

Gamo, T., Chiba, H., Yamanaka, T., Okudaira, T., Hashimoto, J., Tsuchida, S., et al. (2001). Chemical characteristics of newly discovered black smoker fluids and associated hydrothermal plumes at the Rodriguez Triple Junction, Central Indian Ridge. *Earth Planet. Sci. Lett.* 193, 371–379. doi: 10.1016/S0012-821X(01)00511-8

Gerdes, K. H., Kihara, T. C., Martínez Arbizu, P., Kuhn, T., Schwarz-Schampera, U., and Mah, C. L. (2021). Megafauna of the German exploration license area for seafloor massive sulphides along the Central and South East Indian Ridge (Indian Ocean). *Biodivers. Data J.* 9, e69955.

Gerdes, K. H., Martínez Arbizu, P., Schwarz-Schampera, U., Schwentner, M., and Kihara, T. C. (2019a). Detailed mapping of hydrothermal vent fauna: a 3D reconstruction approach based on video imagery. *Front. Mar. Sci.* 6:96. doi: 10.3389/fmars.2019.00096

Gerdes, K. H., Martínez Arbizu, P., Schwentner, M., Freitag, R., Schwarz-Schampera, U., Brandt, A., et al. (2019b). Megabenthic assemblages at the southern Central Indian Ridge—spatial segregation of inactive hydrothermal vents from active-, periphery- and non-vent sites. *Mar. Environ. Res.* 151:104776. doi: 10.1016/j.marenvres.2019.104776

German, C. R., and Von Damm, K. L. (2006). "Hydrothermal processes," in *The Oceans and Marine Geochemistry*, eds H. D. Holland and K. K. Turekian (Amsterdam: Elsevier), 181–222.

Hadziavdic, K., Lekang, K., Lanzen, A., Jonassen, I., Thompson, E. M., and Troedsson, C. (2014). Characterization of the 18S rRNA gene for designing universal eukaryote specific primers. *PLoS One* 9:e87624. doi: 10.1371/journal.pone.0087624

Hamby, R. K., and Zimmer, E. A. (1988). Ribosomal RNA sequences for inferring phylogeny within the grass family (Poaceae). *Plant Syst. Evol.* 160, 29–37. doi: 10.1007/BF00936707

Hammer, O., Harper, D., and Ryan, P. (2001). PAST: paleontological statistics software package for education and data analysis. *Palaeontol. Electron.* 4, 1–9.

Hashimoto, J., Ohta, S., Gamo, T., Chiba, H., Yamaguchi, T., Tsuchida, S., et al. (2001). First hydrothermal vent communities from the Indian Ocean discovered. *Zool. Sci.* 18, 717–721. doi: 10.2108/zsj.18.717

Havermans, C. (2016). Have we so far only seen the tip of the iceberg? Exploring species diversity and distribution of the giant amphipod *Eurythenes*. *Biodiversity* 17, 12–25. doi: 10.1080/14888386.2016.1172257

Havermans, C., and Smetacek, V. (2018). Bottom-up and top-down triggers of diversification: a new look at the evolutionary ecology of scavenging amphipods in the deep sea. *Prog. Oceanogr.* 164, 37–51. doi: 10.1016/j.pocean.2018.04.008

Havermans, C., Sonet, G., d'Udekem d'Acoz, C., Nagy, Z. T., Martin, P., Brix, S., et al. (2013). Genetic and morphological divergences in the cosmopolitan deep-sea amphipod *Eurythenes gryllus* reveal a diverse abyss and a bipolar species. *PLoS One* 8:e74218. doi: 10.1371/journal.pone.0074218

Hendrycks, E. A. (2007). A new species of *Valettiopsis* Holmes, 1908 (Crustacea: Gammaridea: Lysianassoidea) from abyssal waters off California. *Zootaxa* 1501, 45–56. doi: 10.11646/zootaxa.1501.1.3

Hessler, R. R., and Sanders, H. L. (1967). Faunal diversity in the deep-sea. *Deep Sea Res. Oceanogr. Abstr.* 14, 65–70. doi: 10.1016/0011-7471(67)90029-0

Hillis, D. M., and Dixon, M. T. (1991). Ribosomal DNA: molecular evolution and phylogenetic inference. *Q. Rev. Biol.* 66, 411–453. doi: 10.1086/417338

Horton, T., and Thurston, M. (2009). *Hirondellea sindhusagar* (Crustacea: Amphipoda: Lysianassoidea), a new deepwater scavenger species from the Indian Ocean, with a key to the genus *Hirondellea*. *Zootaxa* 2096, 433–441. doi: 10.11646/zootaxa.2096.1.26

Horton, T., and Thurston, M. (2015). A revision of the genus *Paracallisoma* Chevreux, 1903 (Crustacea: Amphipoda: Scopelocheiridae: Paracallisominae) with a redescription of the type species of the genus *Paracallisoma*, the

description of two new genera and two new species from the Atlantic Ocean. *Zootaxa* 3995, 91–132.

Horton, T., Thurston, M., Vlierboom, R., Gutteridge, Z., Pebody, C., Gates, A., et al. (2020b). Are abyssal scavenging amphipod assemblages linked to climate cycles? *Prog. Oceanogr.* 184:102318. doi: 10.1016/j.pocean.2020.102318

Horton, T., Cooper, H., Vlierboom, R., Thurston, M., Hauton, C., and Young, C. R. (2020a). Molecular phylogenetics of deep-sea amphipods (*Eurythenes*) reveal a new undescribed species at the Porcupine Abyssal Plain, north east Atlantic Ocean. *Prog. Oceanogr.* 183:102292. doi: 10.1016/j.pocean.2020.102292

Horton, T., Marsh, L., Bett, B., Gates, A., Jones, D., Benoist, N., et al. (2021). Recommendations for the standardisation of open taxonomic nomenclature for image-based identifications. *Front. Mar. Sci.* 8:620702. doi: 10.3389/fmars.2021.620702

Hourdez, S., and Lallier, F. H. (2007). Adaptations to hypoxia in hydrothermal-vent and cold-seep invertebrates. *Rev. Environ. Sci. Biotechnol.* 6, 143–159. doi: 10.1007/s11157-006-9110-3

Ingole, B., and Koslow, J. A. (2005). Deep-sea ecosystems of the Indian Ocean. *Indian J. Mar. Sci.* 34, 27–34.

Jamieson, A. J., Fujii, T., Mayor, D. J., Solan, M., and Priede, I. G. (2010). Hadal trenches: the ecology of the deepest places on Earth. *Trends Ecol. Evol.* 25, 190–197. doi: 10.1016/j.tree.2009.09.009

Jamieson, A. J., Kilgallen, N. M., Rowden, A. A., Fujii, T., Horton, T., Lörz, A.-N., et al. (2011). Bait-attending fauna of the Kermadec Trench, SW Pacific Ocean: evidence for an ecotone across the abyssal–hadal transition zone. *Deep Sea Res. Part I Oceanogr. Res. Pap.* 1, 49–62. doi: 10.1016/j.dsr.2010.11.003

Jamieson, A. J., Solan, M., and Fujii, T. (2009). Imaging deep-sea life beyond the abyssal zone. *Sea Technol.* 50, 41–46.

Janßen, F., Treude, T., and Witte, U. (2000). Scavenger assemblages under differing trophic conditions: a case study in the deep Arabian Sea. *Deep Sea Res. Part II Top. Stud. Oceanogr.* 47, 2999–3026. doi: 10.1016/S0967-0645(00)00056-4

Jażdżewska, A. M., Corbari, L., Driskell, A., Frutos, I., Havermans, C., Hendrycks, E., et al. (2018). A genetic fingerprint of Amphipoda from Icelandic waters—the baseline for further biodiversity and biogeography studies. *ZooKeys* 731, 55–73. doi: 10.3897/zookeys.731.19931

Jażdżewska, A. M., Horton, T., Hendrycks, E., Mamos, T., Driskell, A., Brix, S., et al. (2021). Pandora's box in the deep sea –intraspecific diversity patterns and distribution of two congeneric scavenging amphipods. *Front. Mar. Sci.* 8:750180. doi: 10.3389/fmars.2021.750180

Kato, S., Takano, Y., Kakegawa, T., Oba, H., Inoue, K., Kobayashi, C., et al. (2010). Biogeography and biodiversity in sulfide structures of active and inactive vents at deep-sea hydrothermal fields of the southern Mariana Trough. *Appl. Environ. Microbiol.* 76, 2968–2979. doi: 10.1128/AEM.00478-10

Katoh, K., Misawa, K., Kuma, K., and Miyata, T. (2002). MAFFT: a novel method for rapid multiple sequence alignment based on fast Fourier transform. *Nucleic Acids Res.* 30, 3059–3066. doi: 10.1093/nar/gkf436

Kearse, M., Moir, R., Wilson, A., Stones-Havas, S., Cheung, M., Sturrock, S., et al. (2012). Geneious Basic: an integrated and extendable desktop software platform for the organization and analysis of sequence data. *Bioinformatics* 28, 1647–1649. doi: 10.1093/bioinformatics/bts199

Kihara, T. C., and Rocha, C. E. F. (2013). First record of *Clausidium* (Copepoda, Clausidiidae) from Brazil: a new species associated with ghost shrimps *Neocallichirus grandimana* (Gibbes, 1850) (Decapoda, Callianassidae). *ZooKeys* 335, 47–67. doi: 10.3897/zookeys.335.5490

Kilgallen, N. M., and Lowry, J. K. (2015). A review of the scopelocheirid amphipods (Crustacea, Amphipoda, Lysianassoidea), with the description of new taxa from Australian waters. *Zoosystematics Evol.* 91, 1–43. doi: 10.3897/zse.91.8440

King, N. J., Bailey, D., and Priede, I. (2007). Role of scavengers in marine ecosystems—introduction. *Mar. Ecol. Prog. Ser.* 350, 175–178. doi: 10.3354/meps07186

Knox, M. A., Hogg, I. D., Pilditch, C. A., Lörz, A.-N., Hebert, P. D. N., and Steinke, D. (2012). Mitochondrial DNA (COI) analyses reveal that amphipod diversity is associated with environmental heterogeneity in deep-sea habitats. *Mol. Ecol.* 21, 4885–4897. doi: 10.1111/j.1365-294X.2012.05729.x

Kobayashi, H., Hatada, Y., Tsubouchi, T., Nagahama, T., and Takami, H. (2012). The hadal amphipod *Hirondellea gigas* possessing a unique cellulase for digesting wooden debris buried in the deepest seafloor. *PLoS One* 7:e42727. doi: 10.1371/journal.pone.0042727

Kumar, S., Stecher, G., Li, M., Knyaz, C., and Tamura, K. (2018). MEGA X: molecular evolutionary genetics analysis across computing platforms. *Mol. Biol. Evol.* 35, 1547–1549. doi: 10.1093/molbev/msy096

Larsen, K. (2007). Amphipoda (Crustacea; Peracarida) from the hydrothermal vent system of the Juan De Fuca Ridge, Escabana trough and Gorda ridge, northeast Pacific. Part I. Lysianassidae and Sebidae. *Zootaxa* 1445, 1–26. doi: 10.11646/zootaxa.1445.1.1

Ledoyer, M. (1986). Crustacés amphipodes gammariens. familles des haustoriidae à vitjazianidae. *Faune Madagascar* 59, 599–1112.

Legeżyńska, J., Węsławski, J. M., and Presler, P. (2000). Benthic scavengers collected by baited traps in the high Arctic. *Polar Biol.* 23, 539–544. doi: 10.1007/s003000000118

Levin, L. A., Mendoza, G. F., Konotchick, T., and Lee, R. (2009). Macrobenthos community structure and trophic relationships within active and inactive Pacific hydrothermal sediments. *Deep Sea Res. Part II Top. Stud. Oceanogr.* 56, 1632–1648. doi: 10.1016/j.dsr2.2009.05.010

Li, W., and Godzik, A. (2006). Cd-hit: a fast program for clustering and comparing large sets of protein or nucleotide sequences. *Bioinformatics* 22, 1658–1659. doi: 10.1093/bioinformatics/btl158

Librado, P., and Rozas, J. (2009). DnaSP v5: a software for comprehensive analysis of DNA polymorphism data. *Bioinformatics* 25, 1451–1452. doi: 10.1093/bioinformatics/btp187

Lincoln, R. J. (1979). *British marine Amphipoda: Gammaridea*. London: British Museum (Natural History). Natural History Museum Publications.

Lonsdale, P. (1977). Clustering of suspension-feeding macrobenthos near abyssal hydrothermal vents at oceanic spreading centers. *Deep Sea Res.* 24, 857–863. doi: 10.1016/0146-6291(77)90478-7

Lörz, A.-N., Tandberg, A. H. S., Willassen, E., and Driskell, A. (2018). *Rhachotropis* (Eusiroidea, Amphipoda) from the north east Atlantic. *ZooKeys* 731, 75–101. doi: 10.3897/zookeys.731.19814

Lowry, J. K., and De Broyer, C. (2008). Alicellidae and Valettiopsidae, two new callynophorate families (Crustacea: Amphipoda). *Zootaxa* 1843, 57–66. doi: 10.11646/zootaxa.1843.1.5

Lowry, J. K., and Kilgallen, N. M. (2014). A generic review of the lysianassoid family Uristidae and descriptions of new taxa from Australian waters (Crustacea, Amphipoda, Uristidae). *Zootaxa* 3867, 1–92. doi: 10.11646/zootaxa.3867.1.1

Lowry, J. K., and Stoddart, H. E. (2010). The deep-sea scavenging genus *Hirondellea* (Crustacea: Amphipoda: Lysianassoidea: Hirondelleidae fam. nov.) in Australian waters. *Zootaxa* 2329, 37–55. doi: 10.11646/zootaxa.2329.1.3

Messing, J. (1983). New M13 vectors for cloning. *Methods Enzymol.* 101, 20–78. doi: 10.1016/0076-6879(83)01005-8

Michels, J., and Büntzow, M. (2010). Assessment of Congo red as a fluorescence marker for the exoskeleton of small crustaceans and the cuticle of polychaetes. *J. Microsc.* 238, 95–101. doi: 10.1111/j.1365-2818.2009.03360.x

Modig, H., and Ólafsson, E. (1998). Responses of Baltic benthic invertebrates to hypoxic events. *J. Exp. Mar. Biol. Ecol.* 229, 133–148. doi: 10.1016/S0022-0981(98)00043-4

Mohrbeck, I., Horton, T., Jażdżewska, A., and Martínez Arbizu, P. (2021). DNA barcoding and cryptic diversity of deep-sea scavenging amphipods in the Clarion-Clipperton Zone (Eastern Equatorial Pacific). *Mar. Biodivers.* 51:26. doi: 10.1007/s12526-021-01170-3

Monaghan, M. T., Wild, R., Elliot, M., Fujisawa, T., Balke, M., Inward, D. J. G., et al. (2009). Accelerated species inventory on Madagascar using coalescent-based models of species delineation. *Syst. Biol.* 58, 298–311. doi: 10.1093/sysbio/syp027

Nakamura, K., Watanabe, H., Miyazaki, J., Takai, K., Kawagucci, S., Noguchi, T., et al. (2012). Discovery of new hydrothermal activity and chemosynthetic fauna on the Central Indian Ridge at 18°–20°S. *PLoS One* 7:e32965. doi: 10.1371/journal.pone.0032965

Narahara-Nakano, Y., Nakano, T., and Tomikawa, K. (2018). Deep-sea amphipod genus *Eurythenes* from Japan, with a description of a new *Eurythenes* species from off Hokkaido (Crustacea: Amphipoda: Lysianassoidea). *Mar. Biodivers.* 48, 603–620. doi: 10.1007/s12526-017-0758-4

Oldevig, H. (1959). Arctic, subarctic and Scandinavian amphipods in the collections of the Swedish Natural History Museum in Stockholm. *Goteb. K.*

Vetenskaps Vitterhets Samhalles Handlingar Sjatte Foljden (Ser. B.) 8, 1–132; 4 pls.

Patel, T., Robert, H., d'Udekem d'Acoz, C., Martens, K., De Mesel, I., Degraer, S., et al. (2020). Biogeography and community structure of abyssal scavenging Amphipoda (Crustacea) in the Pacific Ocean. *Biogeosciences* 17, 2731–2744. doi: 10.5194/bg-17-2731-2020

Perrone, F. M., Dell'Anno, A., Danovaro, R., Della Croce, N., and Thurston, M. H. (2002). Population biology of *Hirondellea* sp. nov. (Amphipoda: Gammaridea: Lysianassoidea) from the Atacama Trench (south-east Pacific Ocean). *J. Mar. Biol. Assoc. UK* 82, 419–425. doi: 10.1017/S0025315402005672

Podowski, E. L., Moore, T. S., Zelnio, K. A., Luther, G. W. III, and Fisher, C. R. (2009). Distribution of diffuse flow megafauna in two sites on the Eastern Lau Spreading Center, Tonga. *Deep Sea Res. Part I Oceanogr. Res. Pap.* 56, 2041–2056. doi: 10.1016/j.dsr.2009.07.002

Pons, J., Barraclough, T. G., Gomez-Zurita, J., Cardoso, A., Duran, D. P., Hazell, S., et al. (2006). Sequence-based species delimitation for the DNA taxonomy of undescribed insects. *Syst. Biol.* 55, 595–609. doi: 10.1080/10635150600852011

Puillandre, N., Lambert, A., Brouillet, S., and Achaz, G. (2012). ABGD, automatic barcode gap discovery for primary species delimitation. *Mol. Ecol.* 21, 1864–1877. doi: 10.1111/j.1365-294X.2011.05239.x

Ratnasingham, S., and Hebert, P. D. N. (2007). BOLD: the Barcode of Life Data System (http://www.barcodinglife.org). *Mol. Ecol. Notes* 7, 355–364. doi: 10.1111/j.1471-8286.2007.01678.x

Ratnasingham, S., and Hebert, P. D. N. (2013). A DNA-based registry for all animal species: the Barcode Index Number (BIN) system. *PLoS One* 8:e66213. doi: 10.1371/journal.pone.0066213

Ritchie, H., Jamieson, A. J., and Piertney, S. B. (2015). Phylogenetic relationships among hadal amphipods of the superfamily Lysianassoidea: implications for taxonomy and biogeography. *Deep Sea Res. Part I Oceanogr. Res. Pap.* 105, 119–131. doi: 10.1016/j.dsr.2015.08.014

Ronquist, F., and Huelsenbeck, J. (2003). MRBAYES 3: Bayesian phylogenetic inference under mixed models. *Bioinformatics* 19, 1572–1574. doi: 10.1093/bioinformatics/btg180

Rozas, J., Ferrer-Mata, A., Sánchez-DelBarrio, J. C., Guirao-Rico, S., Librado, P., Ramos-Onsins, S. E., et al. (2017). DnaSP 6: DNA sequence polymorphism analysis of large data sets. *Mol. Biol. Evol.* 34, 3299–3302. doi: 10.1093/molbev/msx248

Sainte-Marie, B. (1986). Effect of bait size and sampling time on the attraction of the lysianassid amphipods *Anonyx sarsi* Steele & Brunel and *Orchomenella pinguis* (Boeck). *J. Exp. Mar. Biol. Ecol.* 99, 63–77. doi: 10.1016/0022-0981(86)90021-3

Schuelke, M. (2000). An economic method for the fluorescent labeling of PCR fragments. *Nat. Biotechnol.* 18, 233–234. doi: 10.1038/72708

Seefeldt, M., Weigand, A., Havermans, C., Moreira, E., and Held, C. (2017). Fishing for scavengers: an integrated study to amphipod (Crustacea: Lysianassoidea) diversity of Potter Cove (South Shetland Islands, Antarctica). *Mar. Biodivers.* 48, 2081–2104. doi: 10.1007/s12526-017-0737-9

Shulenberger, E., and Barnard, J. L. (1976). Amphipods from an abyssal trap set in the North Pacific Gyre. *Crustaceana* 31, 241–258. doi: 10.1163/156854076X00035

Shulenberger, E., and Hessler, R. R. (1974). Scavenging abyssal benthic amphipods trapped under oligotrophic central North Pacific Gyre waters. *Mar. Biol.* 28, 185–187. doi: 10.1007/BF00387296

Sigovini, M., Keppel, E., and Tagliapietra, D. (2016). Open nomenclature in the biodiversity era. *Methods Ecol. Evol.* 7, 1217–1225.

Stoddart, H., and Lowry, J. (2004). The deep-sea lysianassoid genus *Eurythenes* (Crustacea, Amphipoda, Eurytheneidae n. fam.). *Zoosystema* 26, 425–468.

Suchard, M. A., Lemey, P., Baele, G., Ayres, D. L., Drummond, A. J., and Rambaut, A. (2018). Bayesian phylogenetic and phylodynamic data integration using BEAST 1.10. *Virus Evol.* 4:vey016. doi: 10.1093/ve/vey016

Tajima, F. (1983). Evolutionary relationship of DNA sequences in finite populations. *Genetics* 105, 437–460.

Tajima, F. (1989). Statistical method for testing the neutral mutation hypothesis by DNA polymorphism. *Genetics* 123, 585–595.

Tamburri, M. N., and Barry, J. P. (1999). Adaptations for scavenging by three diverse bathyal species, *Eptatretus stouti*, *Neptunea amianta* and *Orchomene obtusus*. *Deep Sea Res. Part I Oceanogr. Res. Pap.* 46, 2079–2093. doi: 10.1016/S0967-0637(99)00044-8

Taylor, M. L., and Roterman, C. N. (2017). Invertebrate population genetics across Earth's largest habitat: the deep-sea floor. *Mol. Ecol.* 26, 4872–4896. doi: 10.1111/mec.14237

Tempestini, A., Rysgaard, S., and Dufresne, F. (2018). Species identification and connectivity of marine amphipods in Canada's three oceans. *PLoS One* 13:e0197174. doi: 10.1371/journal.pone.0197174

Thiel, R., Knebelsberger, T., Kihara, T. C., and Gerdes, K. H. (2021). Description of a new eelpout *Pachycara angeloi* sp. nov. (Perciformes: Zoarcidae) from deep-sea hydrothermal vent fields in the Indian Ocean. *Zootaxa* 4980, 99–112. doi: 10.11646/zootaxa.4980.1.6

Thornton, B., Bodenmann, A., Pizarro, O., Williams, S., Friedman, A., Nakajima, R., et al. (2016). Biometric assessment of deep-sea vent megabenthic communities using multi-resolution 3D image reconstructions. *Deep Sea Res. Part I Oceanogr. Res. Pap.* 116, 200–219. doi: 10.1016/j.dsr.2016.08.009

Tsurumi, M. (2001). *Ecology of Hydrothermal Vents on Three Segments of the Juan de Fuca Ridge, Northeast Pacific.* Doctoral dissertation. Victoria, BC: University of Victoria, 325.

Van Dover, C. L. (2011). Mining seafloor massive sulphides and biodiversity: what is at risk? *ICES J. Mar. Sci.* 68, 341–348. doi: 10.1093/icesjms/fsq086

Van Dover, C. L., Humphris, S. E., Fornari, D., Cavanaugh, C. M., Collier, R., Goffredi, S. K., et al. (2001). Biogeography and ecological setting of Indian Ocean hydrothermal vents. *Science* 294, 818–823. doi: 10.1126/science.1064574

Vinogradov, G. M. (1993). Amphipoda (Crustacea) from thermal vents in the Eastern Pacific. *Hydrobiol. J.* 26, 77–92.

Vrijenhoek, R. C. (2010). Genetic diversity and connectivity of deep-sea hydrothermal vent metapopulations. *Mol. Ecol.* 19, 4391–4411. doi: 10.1111/j.1365-294X.2010.04789.x

Wang, Y., Zhu, C., Sha, Z., and Ren, X. (2019). A new species of *Parandania* (Amphipoda, Stegocephalidae, Parandaniinae) from the Okinawa Trough. *Crustaceana* 92, 1427–1434. doi: 10.1163/15685403-00003944

Weston, J. N. J., Peart, R. A., Stewart, H. A., Ritchie, H., Piertney, S. B., Linley, T. D., et al. (2021). Scavenging amphipods from the Wallaby-Zenith Fracture Zone: extending the hadal paradigm beyond subduction trenches. *Mar. Biol.* 168:1. doi: 10.1007/s00227-020-03798-4

Wolff, T. (1959). The hadal community, an introduction. *Deep Sea Res.* 6, 95–124. doi: 10.1016/0146-6313(59)90063-2

Wolff, T. (2005). Composition and endemism of the deep-sea hydrothermal vent fauna. *Biol. Mar.* 46, 97–104. doi: 10.1007/978-3-319-45340-8_4

WoRMS Editorial Board (2021). *World Register of Marine Species*. Available online at: http://www.marinespecies.org at VLIZ (accessed August 2, 2021).

Wu, R., and Or, Y. Y. (2005). Bioenergetics, growth and reproduction of amphipods are affected by moderately low oxygen regimes. *Mar. Ecol. Prog. Ser.* 297, 215–223. doi: 10.3354/meps297215

Zhang, J., Kapli, P., Pavlidis, P., and Stamatakis, A. (2013). A general species delimitation method with applications to phylogenetic placements. *Bioinformatics* 29, 2869–2876. doi: 10.1093/bioinformatics/btt499

Conflict of Interest: The authors declare that the research was conducted in the absence of any commercial or financial relationships that could be construed as a potential conflict of interest.

Publisher's Note: All claims expressed in this article are solely those of the authors and do not necessarily represent those of their affiliated organizations, or those of the publisher, the editors and the reviewers. Any product that may be evaluated in this article, or claim that may be made by its manufacturer, is not guaranteed or endorsed by the publisher.

Copyright © 2022 Kniesz, Jażdżewska, Martínez Arbizu and Kihara. This is an open-access article distributed under the terms of the Creative Commons Attribution License (CC BY). The use, distribution or reproduction in other forums is permitted, provided the original author(s) and the copyright owner(s) are credited and that the original publication in this journal is cited, in accordance with accepted academic practice. No use, distribution or reproduction is permitted which does not comply with these terms.

frontiers in Marine Science

ORIGINAL RESEARCH
published: 12 January 2022
doi: 10.3389/fmars.2021.760194

Computed Microtomography (Micro-CT) in the Anatomical Study and Identification of Solenogastres (Mollusca)

Jesús Martínez-Sanjuán[1†], Kevin Kocot[2†], Óscar García-Álvarez[1†], María Candás[1†] and Guillermo Díaz-Agras[1†]*

[1] REBUSC, Rede de Estacións Biolóxicas da Universidade de Santiago de Compostela, Estación de Bioloxía Mariña da Graña, Universidade de Santiago de Compostela, Santiago de Compostela, Spain, [2] Department of Biological Sciences and Alabama Museum of National History, University of Alabama, Tuscaloosa, AL, United States

OPEN ACCESS

Edited by:
Clara F. Rodrigues,
University of Aveiro, Portugal

Reviewed by:
Ekin Tilic,
University of Copenhagen, Denmark
Nina Therese Mikkelsen,
University of Bergen, Norway

***Correspondence:**
Jesús Martínez-Sanjuán
jesmarsan14@gmail.com

[†] These authors have contributed equally to this work

Specialty section:
This article was submitted to Deep-Sea Environments and Ecology, a section of the journal Frontiers in Marine Science

Received: 17 August 2021
Accepted: 13 December 2021
Published: 12 January 2022

Citation:
Martínez-Sanjuán J, Kocot K, García-Álvarez Ó, Candás M and Díaz-Agras G (2022) Computed Microtomography (Micro-CT) in the Anatomical Study and Identification of Solenogastres (Mollusca). Front. Mar. Sci. 8:760194. doi: 10.3389/fmars.2021.760194

Solenogastres are vermiform marine molluscs characterised by an aculiferous mantle, a longitudinal ventral pedal groove and a terminal or subterminal pallial cavity. Their classification is based in part on the type of mantle sclerites, but identification to even the family level generally requires the study of internal anatomical characters. Taxonomically important internal characters include those related to radular structure, the type of ventrolateral glandular organs of the pharynx and the reproductive system, among others. In order to study their internal anatomical organisation, according to the classical reconstruction method, serial histological sections of specimens are made, from which the 2D internal anatomy of the specimen can be reconstructed manually. However, this is a time-consuming technique that results in destruction of the specimen. Computed microtomography or micro-CT is a non-destructive technique based on the measurement of the attenuation of X-rays as they pass through a specimen. Micro-CT is faster than histology for studying internal anatomy and it is non-destructive, meaning that specimens may be used for e.g., DNA extraction or retained as intact vouchers. In this paper, the utility of micro-CT for studying taxonomically important internal anatomical structures was assessed. Results of the 3D anatomical study of the soft parts of four specimens of three species using micro-CT are presented: *Proneomenia sluiteri* Hubrecht, 1880, *Dorymenia menchuescribanae* García-Álvarez et al., 2000 and *Anamenia gorgonophila* Kowalevsky, 1880. Micro-CT enabled detailed study of most taxonomically important anatomical characters, precise measurements of structures, and observation of the relative position of organs from a variety of angles. However, it was not possible to observe the radula and some details of the ventral foregut organs could not be discerned. Despite these limitations, results of this study highlight micro-CT as a valuable tool to compliment histology in the study of solenogaster anatomy and in non-destructively identifying animals to the family and even genus-level.

Keywords: Solenogastres, micro-CT, anatomy, *Proneomenia sluiteri, Dorymenia menchuescribanae, Anamenia gorgonophila*

INTRODUCTION

Solenogastres are vermiform marine molluscs with no distinct head or other regionalisation. They are characterised by a mantle bearing calcareous scales or spines called sclerites, a longitudinal ventral pedal groove and a terminally or subterminally positioned pallial (= mantle) cavity. Knowledge about their biology is scarce and data on their diversity and geographic distribution are limited and uneven due to the fact that their study has been focused on restricted geographic areas, the difficulties of sampling and that many of the species have only been described from very few specimens. However, it cannot be said that they are rare animals as their presence extends from the coast to the deep sea (García-Álvarez et al., 2014).

To date, 293 species of Solenogastres have been described. They are grouped into four orders, whose classification is based primarily on the type of mantle sclerites. However, the order-level taxonomy of the group has been called into question (Kocot et al., 2019) and, for the classification of families, genera and species, it is essential to study their internal organisation in order to get to know the radular structure, the type of ventrolateral glandular organs of the pharynx and the other internal organs, especially the reproductive system (García-Álvarez and Salvini-Plawen, 2007).

In order to study the internal anatomical organisation, according to the classical reconstruction method, serial histological sections of specimens are made. From these, the internal anatomy may be reconstructed in a sagittal representation, obtaining a 2D anatomical view of the specimen. In addition, 3D computerised anatomical reconstruction can be performed by means of reconstruction software that stacks and aligns photographs of all the serial histological sections (Pedrouzo et al., 2019). Notably, this approach only works well for specimens embedded in resin, as paraffin sections tend to vary in their degree of compression, which makes image stacking and alignment challenging to impossible. Such 3D visualisation software offers the possibility of rotating, zooming in and out, and isolating different parts to observe different characters. Also, by not using fixed reference points, the distortion of the final image is reduced. However, histological sectioning and both manual and computerised anatomical reconstruction are highly labor-intensive and destructive approaches.

Computed microtomography or micro-CT is a non-destructive technique based on the measurement of the attenuation of X-rays when they pass through a sample while it rotates on itself (180° or 360°), resulting in a large number of radiographs (called X-ray projection images). From these projections, virtual 2D sections are obtained in the three planes (transverse, frontal and sagittal) comparable to histological ones, as well as 3D models that allow the external and internal structure of the scanned sample to be visualised. The advantage of this technique is that, as the sample is not destroyed, it is possible to carry out complementary studies at a later date. This is of paramount importance in Solenogastres where many species are rare and often only one specimen of a new species may be available. Whereas histology destroys the specimen and precludes other types of analysis, it is now possible to employ a workflow that collects data using light microscopy, micro-CT, scanning electron microscopy (SEM), and DNA barcoding all from the same specimen (Faulwetter et al., 2013b; Gignac et al., 2016). In addition, micro-CT eliminates possible image distortions, which are common in classical reconstruction methods.

The main aim of this work is to test the potential of micro-CT to describe the anatomy of the soft parts of Solenogastres. A description of the soft parts of each of the specimens is given based on the images obtained by micro-CT and some anatomical details are given in relation to the descriptions already published for each of the species and based on the data obtained by means of classical histological studies. The iconography of the anterior and posterior parts of *Proneomenia sluiteri* is completed in 3D micro-CT. In addition, the possibilities offered by this methodology for the study and identification of Solenogastres species are discussed. Regarding the sclerites of the mantle of Solenogastres, they are not discussed here, since their observation and study does not require the destruction of the specimens (García-Álvarez et al., 2014) and their calcareous nature is similar to the calcareous spicules of other marine molluscs already studied by this technique (Alba-Tercedor and Sánchez-Tocino, 2011; Paz-Sedano et al., 2021; Urgorri et al., 2021).

This paper presents the results of 3D anatomical study of the soft parts of one specimen of *Proneomenia sluiteri* Hubrecht, 1880, one specimen of *Dorymenia menchuescribanae* García-Álvarez et al., 2000 and two specimens of *Anamenia gorgonophila* Kowalevsky, 1880 using computed microtomography or micro-CT. Several studies have demonstrated the efficiency of this technique in the study of small marine molluscs (Golding and Jones, 2007; Alba-Tercedor and Sánchez-Tocino, 2011; Candás et al., 2016, 2017). Regarding Aplacophora, some experiments have been conducted with some species of Solenogastres (Candás et al., 2018; Pedrouzo et al., 2019) and Caudofoveata (Metscher, 2009).

MATERIALS AND METHODS

Four specimens representing three described species of a size suitable for this first comparative study were studied: one specimen of *Proneomenia sluiteri* Hubrecht, 1880 from East Iceland, one specimen of *Dorymenia menchuescribanae* García-Álvarez et al., 2000 from South Shetland Islands, Antarctica and two specimens of *Anamenia gorgonophila* Kowalevsky, 1880 one from Reykjanes Ridge, Iceland and one from Alborán Sea, South Iberian Peninsula.

The four specimens, which were fixed and preserved in 70% ethanol, were subjected to alcoholic dehydration by ethanol baths (80, 90, and 96%) for 24 h each. The two *A. gorgonophila* specimens were then stained with iodine in 96% ethanol for 3 days and dehydrated with Hexamethyldisilazane (HMDS) and air dried overnight. The specimens of *P. sluiteri* and *D. menchuescribanae* were stained with iodine in 96% ethanol for 1 week, dehydrated with HMDS and left to dry overnight. Prior to dehydration with HDMS, specimens were rinsed with 96° ethanol to remove excess iodine. Hexamethyldisilizane (HDMS) removes water from tissues effectively increasing the clarity of boundaries between air and tissue which in turn enhances the

contrast when scanning with X-rays (Paterson et al., 2014). The use of HDMS improves image quality by avoiding artifacts caused during scanning of samples in liquid (Faulwetter et al., 2013a; Keklikoglou et al., 2019).

The four specimens studied were previously scanned without any staining. The images obtained are not presented in this article because they are not of sufficient quality to be able to study the internal anatomy.

The specimens were scanned on a Skyscan 1172 microtomograph (Bruker, Belgium) applying the parameters: 55 kv, 165 μA and 360° sample rotation. Pixel sizes were 6.78 μm for the *P. sluiteri* specimen, 5.97 μm for the *D. menchuescribanae* specimen and between 2.98 and 4.95 μm for the *A. gorgonophila* specimens.

NRecon software (Bruker, Belgium) was used to reconstruct the X-ray projection images obtained during scanning, resulting in 2D sections. Subsequently, CTAn and DataViewer software (Bruker, Belgium) were used to obtain cross-sectional, frontal and sagittal sections, as well as to clean the images. Finally, three-dimensional models of each of the scanned specimens were made using CTVox software (Bruker, Belgium).

Datasets of transverse 2D images of studied specimens were uploaded to Morphosource[1].

RESULTS

(Classification following: García-Álvarez and Salvini-Plawen, 2007)

Order **CAVIBELONIA** Salvini-Plawen (1978)

Family **PRONEOMENIIDAE** Simroth and Bronn (1893)

Genus *Proneomenia* Hubrecht, 1880

Proneomenia sluiteri Hubrecht, 1880

Material examined: 1 specimen. East Iceland, Norwegian Sea. ICEAGE (66°17′43″N, 12°21′45″W—66°18′06″N, 12°22′37″W), Meteor M85/3, Area 30. 662–729 m deep (**Figures 1–6**).

Habitus: Body elongated, circular in section (36 mm long, 5 mm in average diameter), with a slight narrowing in its anterior and posterior regions, being more pronounced in the latter (**Figure 1A**). No keels or papillae on the mantle surface. The openings of the atriobuccal cavity (Abc, **Figure 1B**) (1 mm long) at the anterior end of the body and of the pallial cavity (Pc, **Figure 1D**) (3 mm long) at the posterior end are well visible. The pedal groove (Pg, **Figures 1A,B,D**, **3D,F**, **6D,F**) is well visible externally (24 mm long), running ventrally from the pedal pit (Pp, **Figures 1B**, **3B,C**), located posterior to the atriobuccal opening, up to the opening of the pallial cavity. No sclerites attached to the pedal groove are visible.

Mantle: Cuticle 250 μm thick (Cu, **Figures 2A**, **3A,C,E**). No tegumentary excrescences or sclerite formations toward the outside of the mantle.

Pallial cavity: The cavity (4 mm long, 2 mm high and 2 mm wide) opens to the outside through a long and wide opening (3 mm long and 700 μm wide) in the ventroposterior area of the body (Pc, **Figures 4**, **5**, **6A**). The pallial cavity bears two groups of abdominal spicules (Ab, **Figures 4B**, **5C,E,F**, **6B,C**), located on either side of the opening of the pallial cavity, extending 2 mm in length and running laterally to the pallial cavity itself. The rectum (Re, **Figures 4B**, **5A,E,F**, **6B–D**) opens into the anus (1 mm in diameter) located on the dorsorrostral wall of the cavity. Ventrally to the rectum, the unpaired opening of the spawning ducts (1 mm in diameter) is located (Sd, **Figures 4A**, **5**, **6C,D**). Diverticula (Di, **Figures 5A,B,D**, **6A**), nor respiratory folds, are observed in the dorsoposterior region of the pallial cavity.

Digestive system: The atriobuccal cavity (Abc, **Figures 2A,C**) (3 mm long, 1.5 mm wide and 2 mm high), opens to the outside through an opening in the ventroanterior region of the body (1 mm long and 300 μm wide). The posterior wall of the atriobuccal cavity contains the mouth, which is oval (1.5 mm high and 2 mm wide). The pharynx (Ph, **Figures 2**, **3A**) is short, wide and circular in section (4 mm long and 1 mm in diameter), covered internally by a thick cuticle (150 μm thick) and bears glands on the dorsal wall. The ventral glandular organs of the pharynx (Vfg, **Figures 2**, **3B–D,E**) lead to the ventroposterior pharyngeal area, anterior to the radular sac (Rs, **Figures 2**, **3B,C**). These glandular organs are of type C (García-Álvarez and Salvini-Plawen, 2007), consisting of two ducts (11 mm long and 0.6 mm in diameter) whose lumen is not delimited by a muscular wall and run ventrally to the intestine (Vfg, **Figures 3D,E**). The oesophagus (Oe, **Figures 2**, **3B–D**) is 3 mm long and of the same diameter as the pharynx. The oesophagus leads dorsorostrally and slightly ventrally into the intestine (Oe, **Figures 2A**, **3D**). From the dorsoanterior region of the intestine, a long, dorsoventrally flattened dorsal caecum (Dc, **Figures 2A,B**, **3A–C**) (6 mm long, 1 mm wide and 0.5 mm high) projects anteriorly, reaching into the area of the atriobuccal cavity. The intestine (Mg, **Figures 2A,B**, **3D,E**) occupies most of the interior of the animal (22 mm long and 2.5 mm in average diameter), its inner walls show folds and remains of Alcyonacea (Al, **Figures 2C**, **3F**). The folds formed by the dorsoventral musculature (Dvm, **Figures 2B,C**, **3D,E**, **4**, **5A**) along the length of the intestine can be seen. The intestine continues into the rectum (Re, **Figures 4B**, **5A,D–F**, **6B–D**), 1 mm in diameter, and opens into an anus, circular (1 mm in diameter) located dorsorrostrally in the pallial cavity.

Sense organs: The atrial region (At, **Figures 2A,B**) (1 mm long, 1.5 mm wide and 2 mm high) is located in the dorsoanterior area of the atriobuccal cavity and bears narrow-necked sensory papillary protrusions attached directly to the anterior, dorsal and lateral walls of the atrium. The specimen bears a dorsoterminal sense organ (Dso, **Figures 1C**, **4B**, **5E**, **6B**), located in the midline of the body, at the level of the pallial cavity.

Gonopericardial system: The pair of gonads (Go, **Figures 2**, **3F**, **4A**) (18 mm long and 1 mm in diameter) are filled with oocytes, situated on both sides of the thin central septum separating the two gonads. The gonads are attached to the pericardium (Pr, **Figure 4**) through two gonopericardioducts (Gd, **Figures 4**, **6F**) (1 mm long and 100 μm in diameter). The pericardium (Pr, **Figures 4**, **5F**, **6D,E**) is wide and slightly narrowed dorsoventrally (4 mm long, 2.5 mm at its maximum

[1]https://www.morphosource.org/projects/000384772

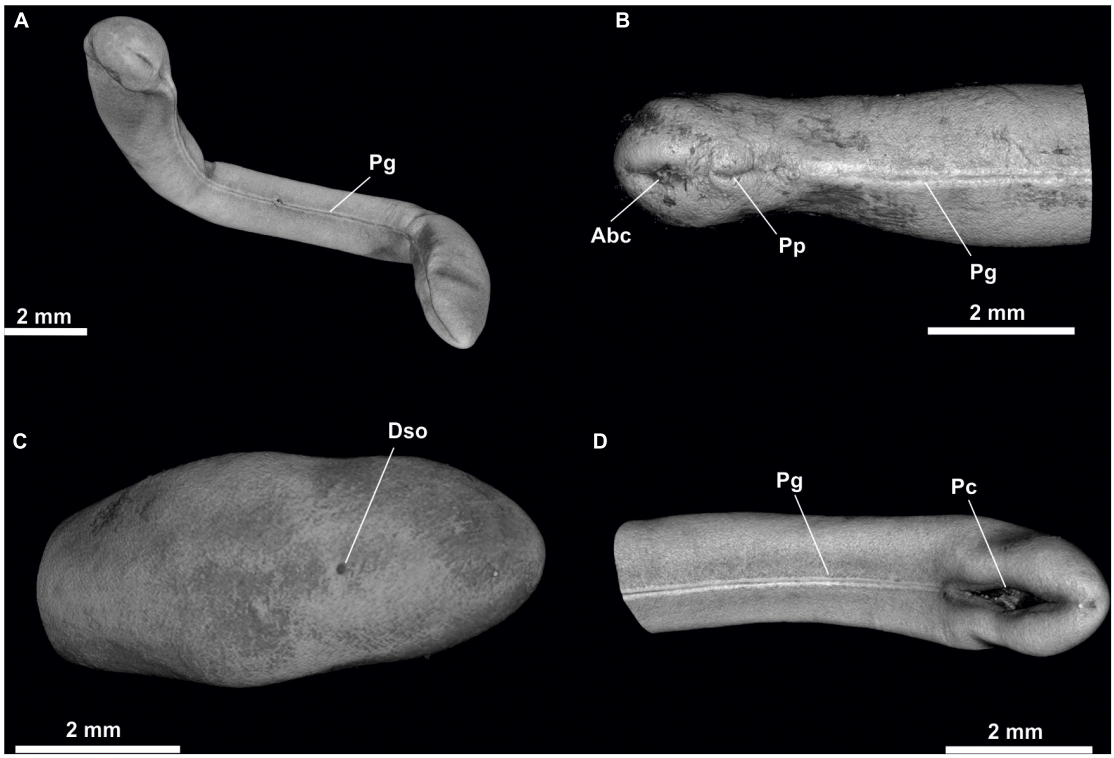

FIGURE 1 | *Proneomenia sluiteri*. **(A)** Habitus. **(B)** Anterior body. **(C)** Posterior body from dorsal view. **(D)** Posterior body from ventral view. Abc, Atriobuccal cavity; Dso, Dorsoterminal sense organ; Pc, Pallial cavity; Pg, Pedal groove; Pp, Pedal pit.

width and 2 mm high); oocytes are visible inside (**Figures 4**, **6D,E**). The heart (Ht, **Figures 4**, **6D,E**), located in the dorsal wall of the pericardium, is an elongated and narrow chamber (3 mm long and 100 μm in diameter). The two pericardioducts (Pd, **Figures 4A**, **5A,B**, **6C–F**) (5 mm long and 100 μm in diameter) originate from the posterior region of the pericardium, which first run briefly toward the posterior region of the body and then turn and run anteriorly, until they lead to the anterior region of the spawning ducts (Pd, Sd, **Figures 5E**, **6F**). There is a pair of elongated, undulating seminal receptacles (Sr, **Figures 5A,B,D,F**; **6E**) (3 mm long, 200 μm in diameter), attached to the pericardioducts through a short tube (150 μm long, 50 μm in diameter) located at the junction of the pericardioducts with the spawning ducts. The pair of spawning ducts (Sd, **Figures 4**, **5A,B,D–F**, **6C–F**) (4.5 mm long, 900 μm in diameter) merge posteriorly into a short, wide duct (600 μm long, 1 mm in diameter) that leads onto the rostral wall of the pallial cavity, ventrally to the rectum (Sdo, **Figure 6B**).

Genus Dorymenia Heath, 1911

Dorymenia menchuescribanae García-Álvarez et al., 2000

Material examined: 1 specimen of the type material (paratype 1. Collection of Estación de Bioloxía Mariña da Graña. Ferrol. Spain). South of Livingston Island, South Shetland Islands, Antarctica. BENTART-94 (62°43′24″S, 60°26′34″W), Station 71-R. 50 m deep (García-Álvarez et al., 2000) (**Figures 7–11**).

Habitus: Elongated body, circular in section (45 mm long and 4.5 mm in diameter), tapering at the anterior and posterior ends (**Figure 8**). No keels or papillae protruding from the mantle surface. The openings of the atriobuccal cavity (1 mm long) (Abc, **Figure 7B**) and of the pallial cavity (1.5 mm long) are well visible (Pc, **Figure 7D**). The pedal groove (**Figure 7D**) is visible externally (40 mm long), and runs along the ventral region of the animal from the pedal pit (Pp, **Figure 8A**), situated posterior to the atriobuccal cavity, until it enters the pallial cavity.

Mantle: Cuticle 200–300 μm thick. No outward projections of sclerites or other structure protruding from the mantle.

Pallial cavity: The cavity (2 mm long, 1.5 mm wide and 1 mm high) (**Figures 9**, **10A**, **11A,B,D**) opens to the outside through an elongated and wide opening (1.5 mm long and 100 μm wide) located in the ventroposterior area of the body (**Figure 7D**). The pallial cavity has abdominal sclerites located along almost the entire length of the opening of the pallial cavity (1 mm in extent). The pallial cavity has, in its dorsoanterior part, two sacs or compartments (**Figure 9B**); the dorsal sac is wider (700 μm long, 1.5 mm high and 1.5 mm wide) than the ventral one (400 μm long, 800 μm and 800 μm high). In the dorsal sac, the rectum (Re, **Figures 9B**, **10B**) opens into the anus (1.5 mm in diameter) located dorsorrostrally; and on the rostral wall of the ventral sac is the unpaired opening of the spawning ducts (700 μm in diameter) (Sd, **Figures 9B**, **10B**). The pallial cavity also bears a pair of 1 mm long copulatory stylets (Co, **Figures 9A**, **10A**, **11A,E**), with strong musculature surrounding them; the

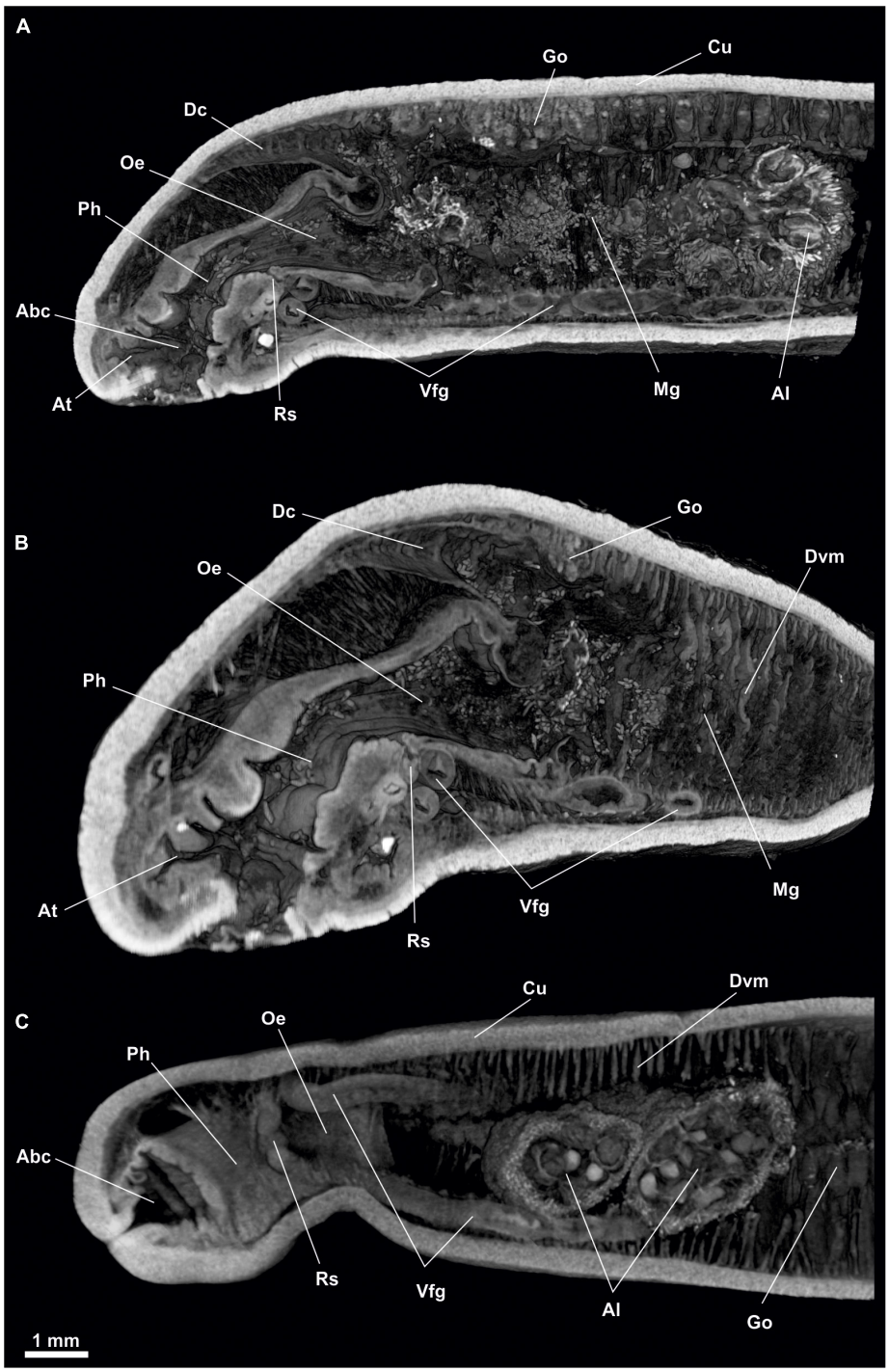

FIGURE 2 | *Proneomenia sluiteri*. Anterior body. **(A)** Sagittal view. **(B)** Frontal-sagittal view. **(C)** Ventral view. Abc, Atriobuccal cavity; Al, Alcyonacea; At, Atrium; Cu, Cuticle; Dc, Dorsal caecum; Dvm, Dorsoventral musculature; Go, Gonad; Mg, Midgut; Oe, Oesophagus; Ph, Pharynx; Rs, Radular sac; Vfg, Ventral foregut glands.

stylets are situated ventrolaterally to the pallial cavity and run slightly diagonally from the anterior region of the cavity to its central region. The pallial cavity has diverticula in its dorsal wall (Di, **Figures 9**, **10A**, **11B,D**). The pallial cavity bears no respiratory folds.

Digestive system: The atriobuccal cavity (2 mm long, 1 mm wide and 1 mm high) (Abc, **Figure 8A**) opens to the outside through an opening 1 mm long, located in the ventroanterior region of the body (Abc, **Figure 7B**). On the posterior wall of the atriobuccal cavity is the circular mouth (1 mm in diameter). The

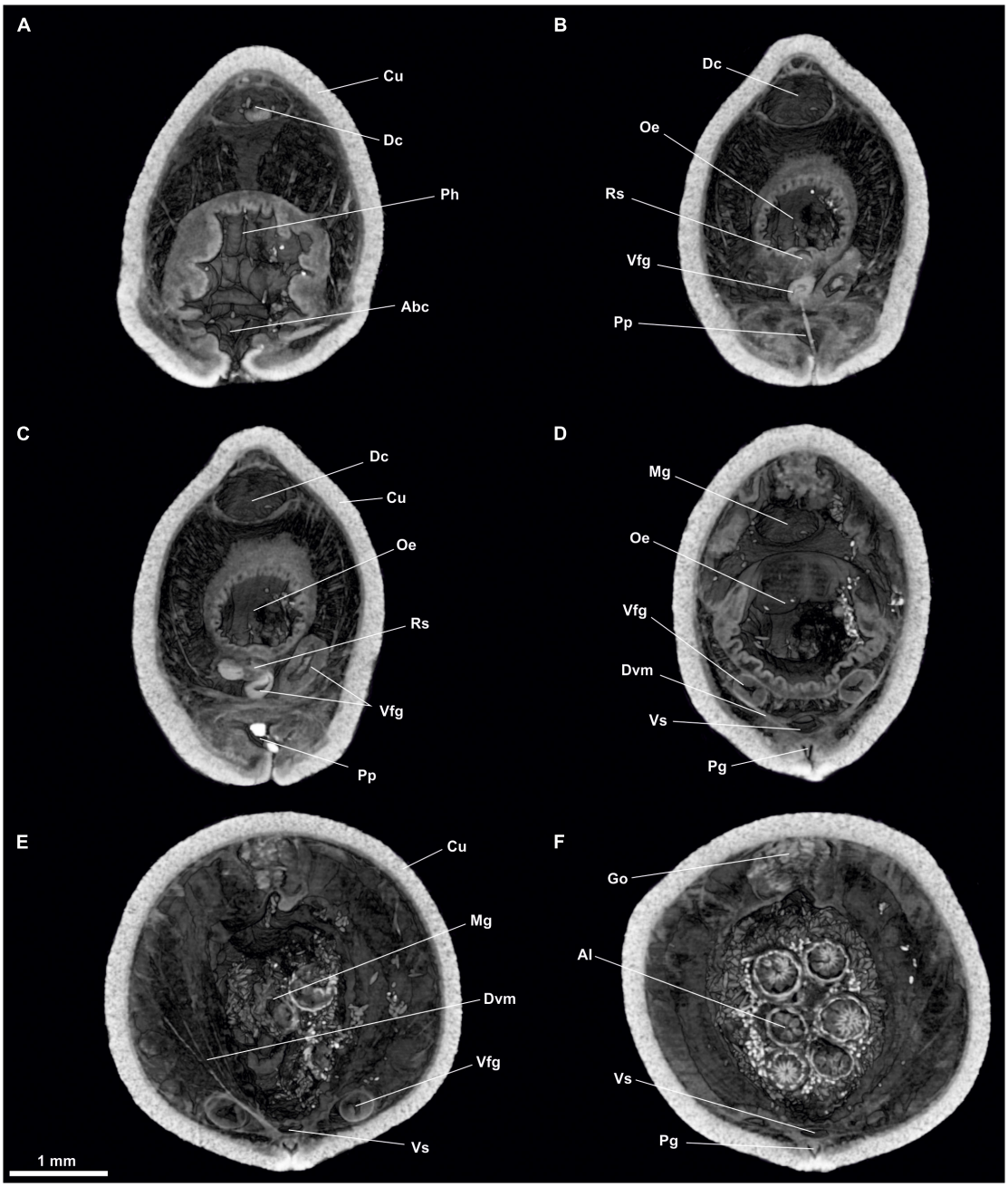

FIGURE 3 | *Proneomenia sluiteri*. Anterior body. **(A)** Cross-section through the atriobuccal cavity. **(B–D)** Cross-section through the oesophagus. **(E,F)** Cross-section through the midgut. Abc, Atriobuccal cavity; Al, Alcyonacea; Cu, Cuticle; Dc, Dorsal caecum; Dvm, Dorsoventral musculature; Go, Gonad; Mg, Midgut; Oe, Oesophagus; Pg, Pedal groove; Ph, Pharynx; Pp, Pedal pit; Rs, Radular sac; Vfg, Ventral foregut glands; Vs, Ventral senus.

pharynx (Ph, **Figure 8**) is 4 mm long and 0.8 mm in diameter, has a thick cuticle (100 μm thick) accompanied by glands. In the ventroposterior region of the pharynx, the ventral glandular organs of the pharynx (Vfg, **Figure 8**) end, slightly anterior to the radular sac (Rs, **Figure 8**). These organs are of type C (García-Álvarez and Salvini-Plawen, 2007), consisting of a pair of ducts 30 mm long and 0.5 mm in diameter, whose lumen is not delimited by a muscular wall, and run ventrally to the intestine. The pharynx joins ventrally to the intestine, it lacks an oesophagus. From the anterodorsal region of the intestine, the dorsoanterior caecum (Dc, **Figure 8A**) projects, slightly flattened dorsoventrally (2 mm long, 600 μm wide and 200 μm high) and reaches the height of the atriobuccal cavity. The intestine (Mg, **Figures 8**, **9**, **11A,D**) continues along the body (30 mm long and 2 mm in diameter); rest of Octocorallia (Oc **Figures 9B**, **10B**, **11D**) are observed up to the rectum (2 mm long and 1.5 mm in

FIGURE 4 | *Proneomenia sluiteri*. Posterior body. **(A)** Sagittal view through the spawining duct. **(B)** Sagittal view through the rectum. Ab, Abdominal spicules; Al, Alcyonacea; Dso, Dorsoterminal sense organ; Dvm, Dorsoventral musculature; Gd, Gonopericardioduct; Go, Gonad; Ht, Heart; Mg, Midgut; Ov, Oocyte; Pc, Pallial cavity; Pd, Pericardioduct; Pr, Pericardium; Re, Rectum; Sd, Spawning duct.

diameter) which runs into the anus (1.5 mm in diameter), located in the dorsorrostral wall of the pallial cavity.

Sense organs: Atrium (At, **Figure 8**) of small size (1 mm long, 1 mm wide and 1 mm high), located in the anterior part of the atriobuccal cavity, has a preatrial sense organ (Po, **Figure 8A**) located on the anterior wall of the atrium and sensory papillae on the anterior and lateral walls. The specimen bears a dorsoterminal sense organ (Dso, **Figures 7A,C**, **11B**) located in the dorsal midline of the body, at the end of the pallial cavity, visible externally.

Gonopericardial system: The pair of gonads (Go, **Figures 8B**, **9B**) (28 mm long and 1.5 mm in diameter) have oocytes on the thin septum that separates them. The gonads are attached to the pericardium by a pair of gonopericardioducts (Gd, **Figure 9B**) (1.5 mm long and 200 μm in diameter). The pericardium (Pr, **Figures 9B**, **10**, **11E**) is broad (2 mm long, 1 mm wide and 0.5 mm high); the elongated and narrow heart (2 mm long and 100 μm in diameter) lies on its dorsal wall. The pericardium extends posteriorly into two compartments, from which the two pericardioducts originate (Pd, **Figure 11C**), which first run toward the posterior region of the body and then turn and run anteriorly along the lateral regions of the body (3 mm long and 100 μm in diameter) until they lead to their respective spawning ducts (**Figures 9A**, **11B,D,E**). The specimen has a pair of spherical seminal receptacles (Sr, **Figures 9A**, **10A**, **11D**) (400 μm in diameter) located anterior to each spawning

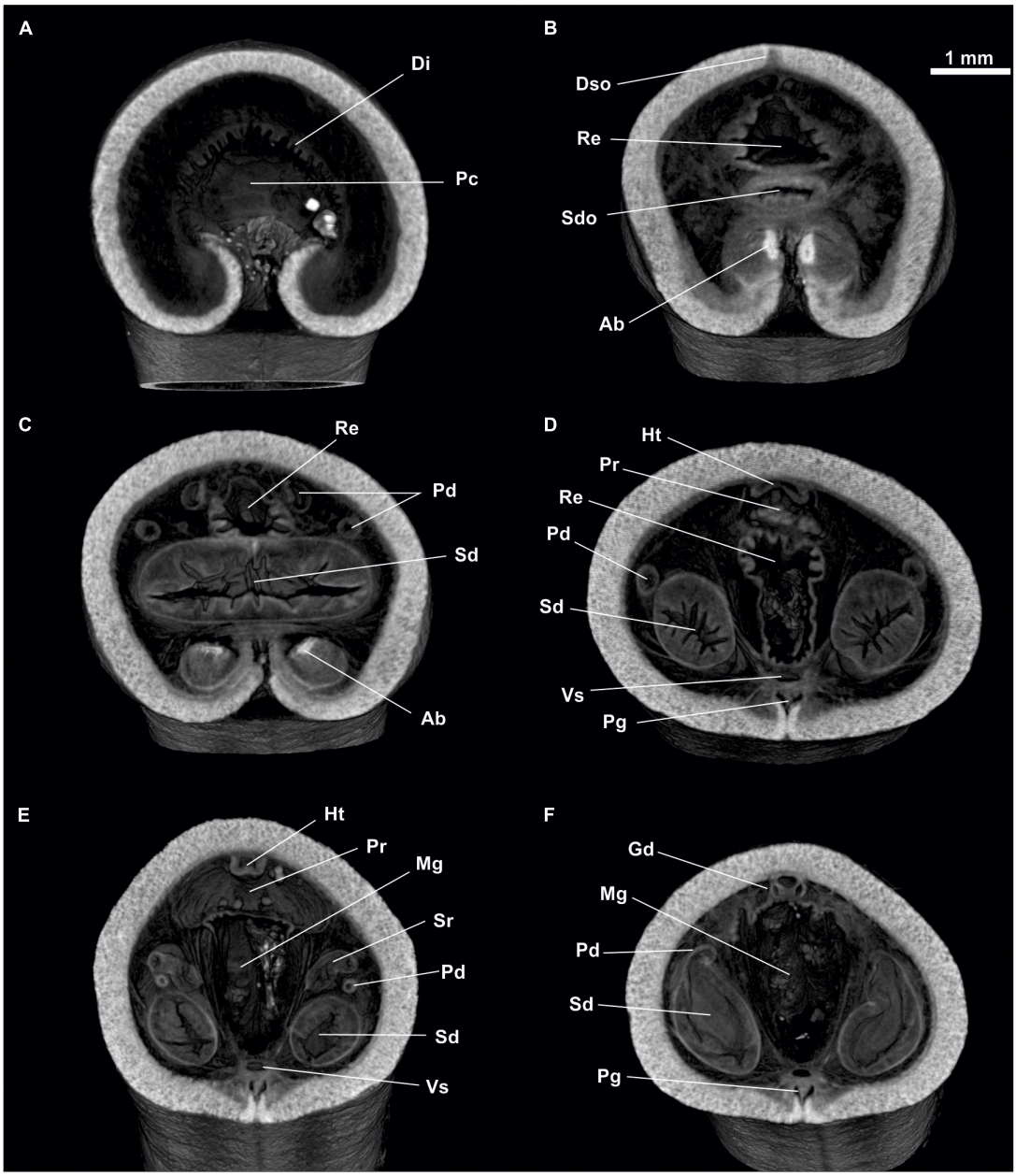

FIGURE 5 | *Proneomenia sluiteri*. Posterior body. **(A)** Cross-section through the pallial cavity. **(B)** Cross-section through the spawining duct opening. **(C–F)** Cross-section through the spawining duct. Ab, Abdominal spicules; Di, Diverticles; Dso, Dorsoterminal sense organ; Gd, Gonopericardioduct; Ht, Heart; Mg, Midgut; Pc, Pallial cavity; Pd, Pericardioduct; Pg, Pedal groove; Pr, Pericardium; Re, Rectum; Sd, Spawning duct; Sdo, Spawning duct opening; Sr, Seminal receptacles; Vs, Ventral sinus.

duct and attached to them through a narrow duct (300 μm long and 50 μm in diameter) in the area where the spawning ducts join the pericardioducts. The spawning ducts (**Figures 9**, **10**, **11A,C,D,E**), 2 mm long and 600 μm in diameter, continue toward the posterior region until they merge into a single duct 300 μm long and 700 μm in diameter, which leads to the rostral wall of the ventral sac of the pallial cavity (**Figures 9B**, **10B**, **11**).

Family STROPHOMENIIDAE Salvini-Plawen, 1978

Genus *Anamenia* Nierstrasz, 1908

Anamenia gorgonophila Kowalevsky, 1880

Material examined: 1 specimen. Reykjanes Ridge, Iceland. ICEAGE (60°16′55″N, 29°19′08″W), MSM 75, DZMB-HH 61716, station 188. 646 m deep (**Figure 12**).

Habitus: Body elongate, slightly narrowed laterally (30 mm long, 1.5 mm wide and 2 mm high), flattened ventrally and with narrower anterior and posterior ends. Surface irregular,

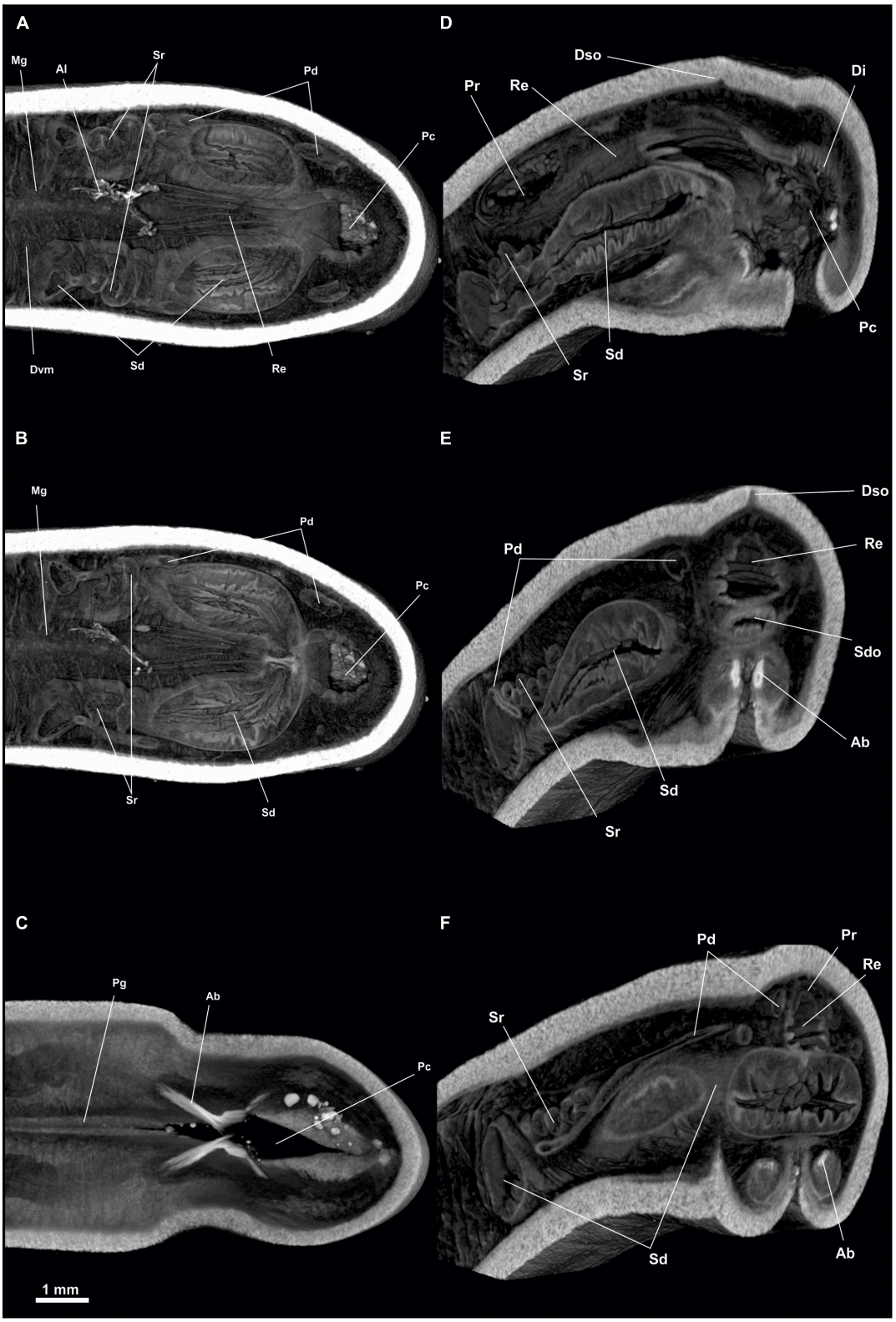

FIGURE 6 | *Proneomenia sluiteri*. Posterior body. **(A)** Dorsal view through the rectum. **(B)** Dorsal view through the spawning duct. **(C)** Dorsal view through the abdominal spicules. **(D–F)** Frontal-sagittal view Ab, Abdominal spicules; Al, Alcyonacea; Di, Diverticles; Dso, Dorsoterminal sense organ; Dvm, Dorsoventral musculature; Mg, Midgut; Pc, Pallial cavity; Pd, Pericardioduct; Pg, Pedal groove; Re, Rectum; Sd, Spawning duct; Sdo, Spawning duct opening; Sr, Seminal receptacles.

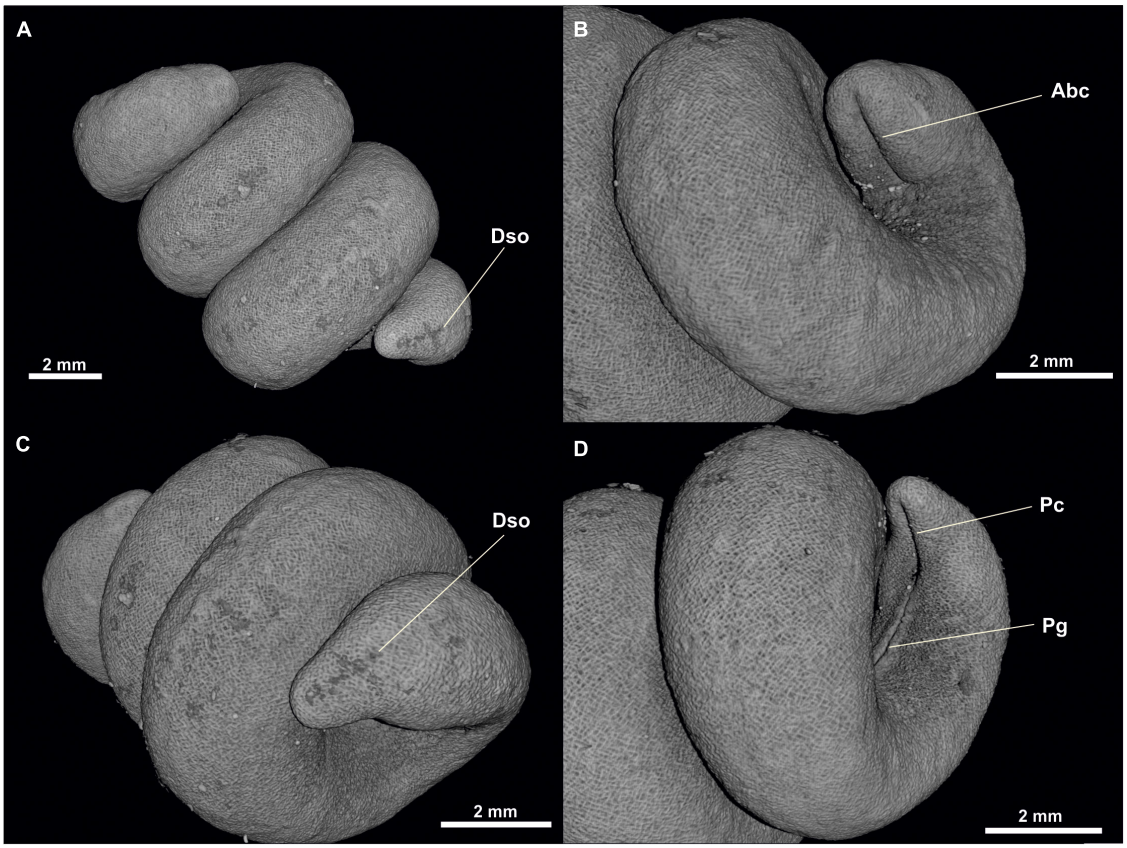

FIGURE 7 | *Dorymenia menchuescribanae*. **(A)** Habitus. **(B)** Anterior body from ventral view. **(C)** Posterior body from dorsal view. **(D)** Posterior body from ventral view. Abc, Atriobuccal cavity; Dso, Dorsoterminal sensitive organ; Pc, Pallial cavity; Pg, Pedal groove.

with acicular sclerites protruding from the mantle surface (**Figure 12A**), giving the animal a hirsute appearance. Pedal groove (Pg, **Figure 12A**) visible (20 mm long), with spicules on both sides, running along the ventral region of the animal from the pedal pit, situated posterior to the atriobuccal cavity, up to the pallial cavity without entering it.

Mantle: Cuticle 100–150 μm thick. With criss-crossed acicular sclerites and some protruding from the mantle surface. No integumentary structures such as keels or papillae. Long scales on both sides of the peduncle furrow along its entire length.

Pallial cavity.- The cavity (1 mm long and 700 μm in diameter) opens to the exterior through a 1 mm long opening in the ventroposterior region of the body (Pc, **Figure 12C**). The pallial cavity bears diverticula on the dorsal and lateral walls of the pallial cavity. The anus (400 μm in diameter) opens dorsorostrally and the spawning ducts (Sd, **Figure 12C**) (200 μm in diameter each) open paired and ventrally to it. The pallial cavity has a small ventrorrostral sac (200 μm long, 100 μm wide and 50 μm high) ventrally to the openings of the spawning ducts.

Digestive system.- The atriobuccal cavity (500 μm long and 250 μm in diameter) opens to the exterior through a 400 μm long opening and is located in the ventroanterior region of the body. The mouth occupies the posterior wall of the atriobuccal cavity and is circular (250 μm in diameter). The pharynx (Ph, **Figure 12B**) is long, circular in section (2.5 mm long and 200 μm in diameter) and covered by a thin cuticle (25 μm thick). The ventral glandular organs of the pharynx lead into the ventroposterior region of the pharynx, anterior to the radular sac. These organs are of type B (García-Álvarez and Salvini-Plawen, 2007) and are formed by a pair of serpentine ducts 8 mm long and 100 μm in diameter, whose lumen is delimited by a muscular wall, and run ventrally to the intestine. The pharynx joins ventrally the intestine (Mg, **Figure 12B**) and bears no oesophagus. From the anterodorsal region of the intestine, the caecum (Dc, **Figure 12B**) projects dorsoanteriorly (2 mm long, 200 μm wide and 100 μm high) reaching the height of the atriobuccal cavity. The intestine continues along the body (22 mm long and 1 mm in diameter), with remains of gorgonians inside. The folds formed by the dorsoventral musculature (Dvm, **Figure 12B**) along the intestine are clearly visible. The intestine is followed by the rectum (1 mm long and 400 μm in diameter), which leads to the anus (400 μm in diameter), located in the dorsorrostral wall of the pallial cavity.

Sense organs.- Atrium 200 μm long, 250 μm wide and 250 μm high (At, **Figure 12B**), occupying the anterior region of the atriobuccal cavity, with sensory papillary projections on its anterior, dorsal and lateral walls. The specimen bears a dorsoterminal sense organ (Dso, **Figure 12C**) in the dorsal midline of the body, at the level of the end of the pallial cavity, not visible externally.

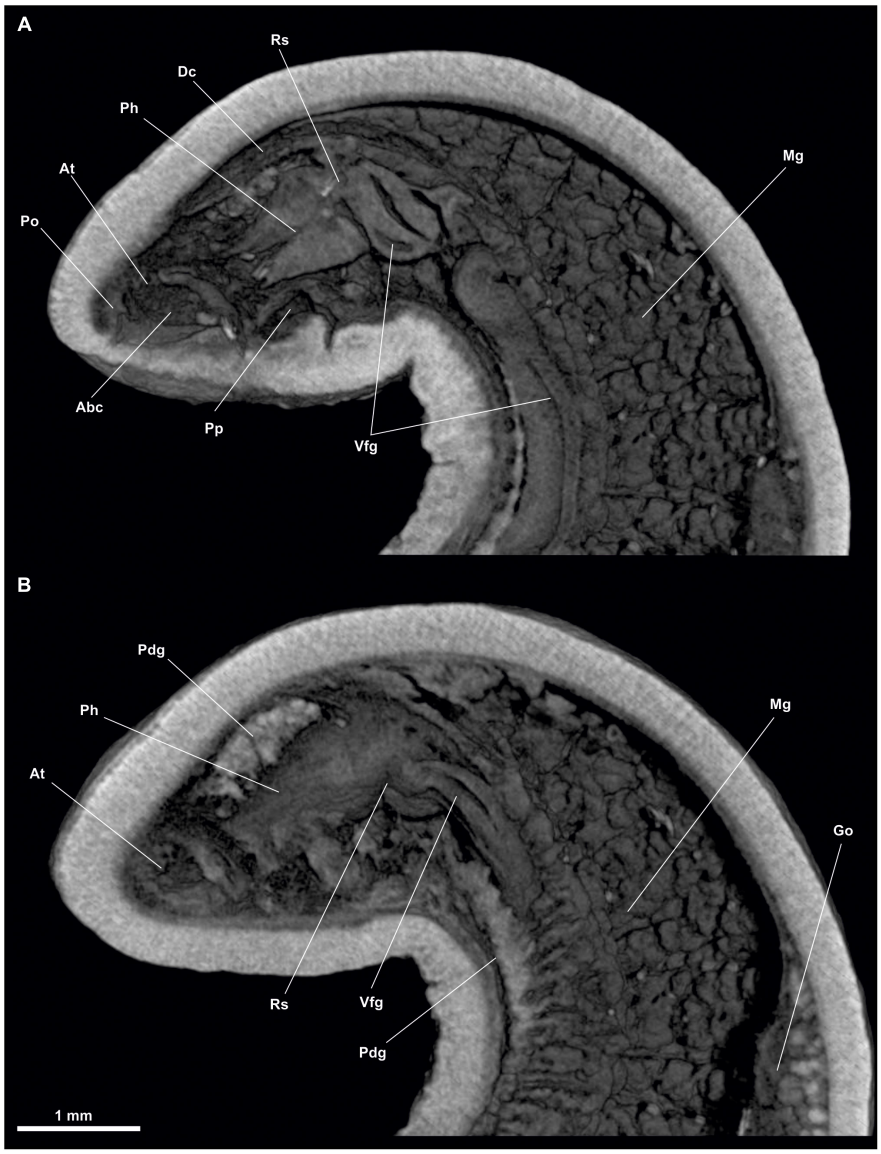

FIGURE 8 | *Dorymenia menchuescribanae*. **(A,B)** Sagittal views of the anterior body. Abc, Atriobuccal cavity; At, Atrium; Dc, Dorsal caecum; Go, Gonad; Mg, Midgut; Pdg, Pedal gland, Ph, Pharynx; Po, Preatrial organ; Pp, Pedal pit; Rs, Radular sac; Vfg, Ventral foregut glands.

Gonopericardial system.- The pair of gonads (Go, **Figure 12B**) (20 mm long and 400 μm in diameter) have oocytes on the septum separating them. A pair of gonopericardioducts (200 μm long and 100 μm in diameter) join the gonads to the pericardium. The pericardium is broad (1.5 mm long and 1 mm in diameter) with oocytes inside; on its dorsal wall, the heart is elongated and narrow (1 mm long and 80 μm in diameter). The posterior region of the pericardium extends into two compartments, from which the two pericardioducts emerge from a terminal lateral position, run toward the posterior region of the body, turn and run anteriorly along the lateral regions of the body (1.5 mm long and 60 μm in diameter), until they lead (Sd, **Figure 12C**) to each spawning duct. The seminal receptacles (Sr, **Figure 12C**) (together measuring 400 μm long and 300 μm in diameter) lead in bundles into the anterior region of each spawning duct. The two spawning ducts (Sd, **Figure 12C**) are slightly flattened (1 mm long, 200 μm wide and 100 μm high) and extend posteriorly until they each end individually (Sdo, **Figure 12C**) at the rostral wall of the pallial cavity, ventral to the rectum and dorsal to the ventrorrostral sac of the cavity.

Anamenia gorgonophila Kowalevsky, 1880

Material examined: 1 specimen. Alboran Sea (South Iberian Peninsula). FAUNA IBÉRICA IV (35°50′01″N, 03°15′13″E–35°49′46″N, 03°14′27″E), Station 316. 90–240 m depth (**Figures 13–15**).

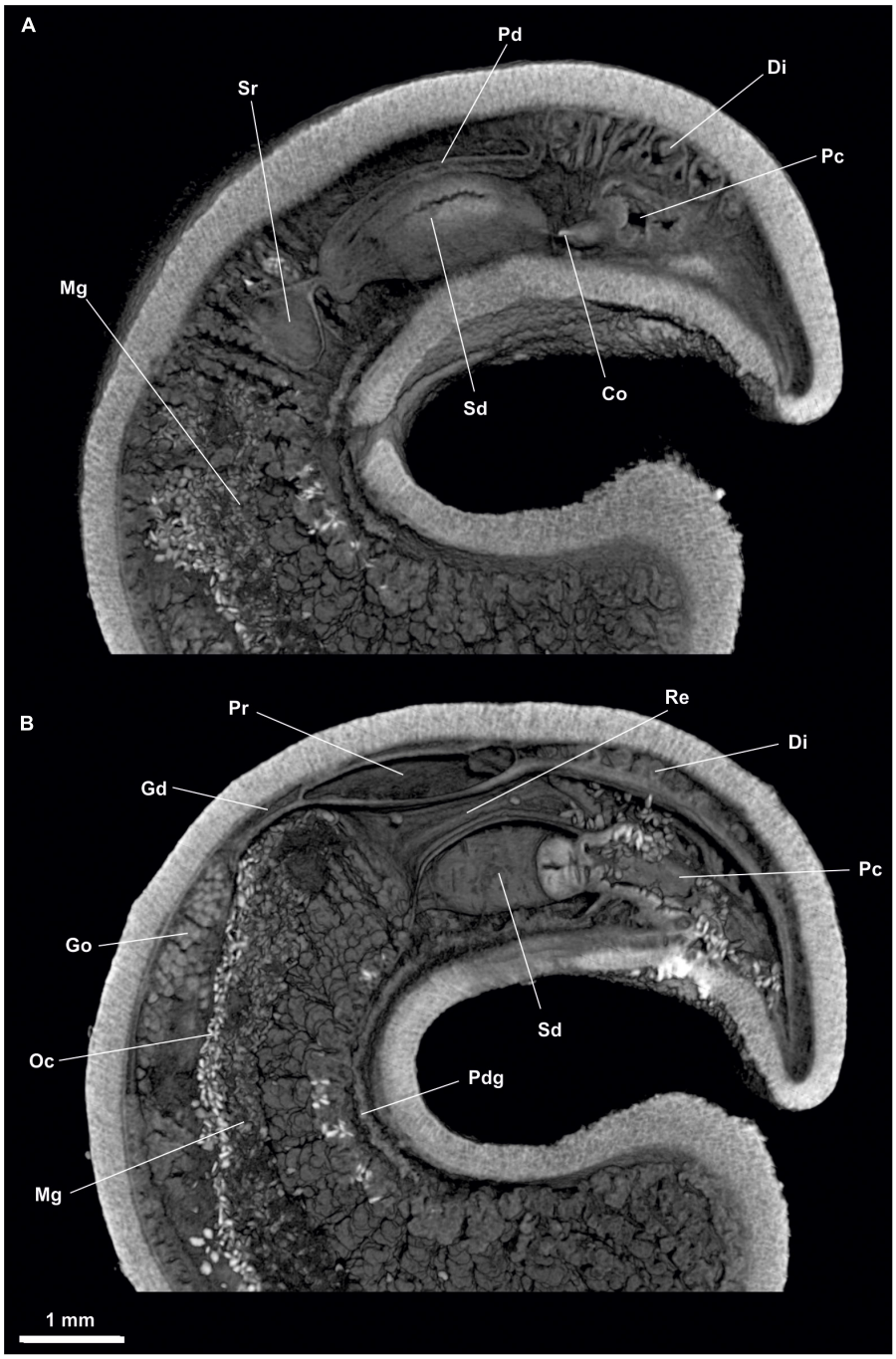

FIGURE 9 | *Dorymenia menchuescribanae*. **(A)** Sagittal view of the posterior body through spawning duct. **(B)** Sagittal view of the posterior body through rectum. Co, Copulatory stylets; Di, Diverticles; Gd, Gonopericardioduct; Go, Gonad; Mg, Midgut; Oc, Octocorallia; Pc, Pallial cavity; Pd, Pericardioduct; Pdg, Pedal gland; Pr, Pericardium; Re, Rectum; Sd, Spawning duct; Sr, Seminal receptacles.

Habitus.- Elongated body (**Figure 13A**), circular in section (30 mm long and 1 mm in diameter) with flattened ventral surface. Surface irregular, with interwoven acicular sclerites; some protruding from the mantle, giving the animal a hirsute appearance. Pedal groove (Pg, **Figures 13B,C**, **14E**, **15C,E**) visible from the outside (27 mm long), running ventrally from the pedal pit (Pp, **Figures 14A,D**), located posteriorly to the atriobuccal cavity, up to the pallial cavity without entering it. With scales on both sides of the pedal groove (**Figures 13B,C**).

Mantle.- Cuticle 80 μm thick. Acicular, interwoven sclerites (**Figure 13A**), some protruding from the mantle and projecting outwards. Elongated scales accompanying the pedal groove

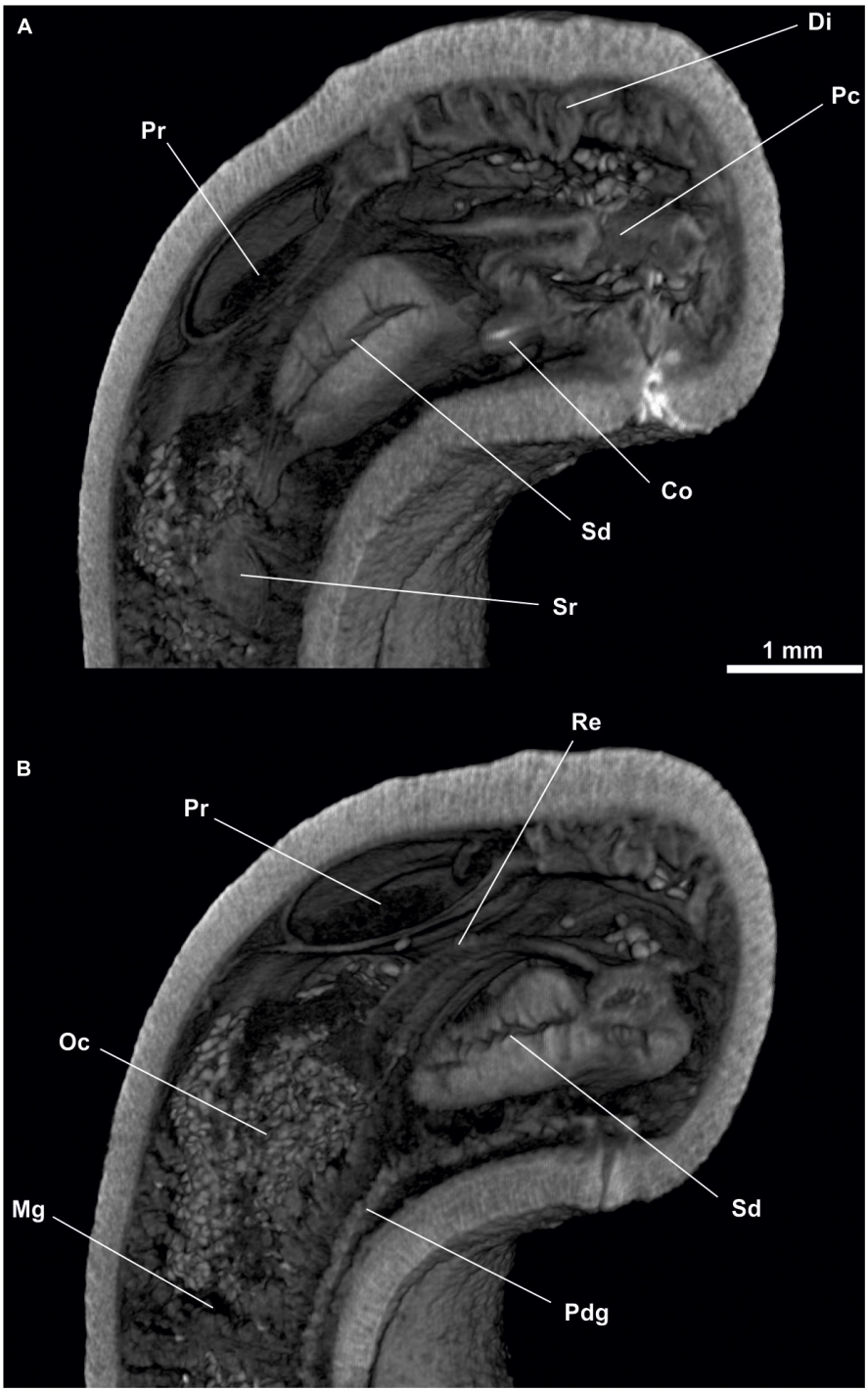

FIGURE 10 | *Dorymenia menchuescribanae*. **(A)** Cross-sagittal view through spawning duct. **(B)** Cross-sagittal view through rectum. Co, Copulatory stylets; Di, Diverticles; Mg, Midgut; Oc, Octocorallia; Pc, Pallial cavity; Pdg, Pedal gland; Pr, Pericardium; Re, Rectum; Sd, Spawning duct; Sr, Seminal receptacles.

along its entire length. No integumentary structures such as keels.

Pallial cavity.- The cavity (700 μm long and 400 μm in diameter) (Pc, **Figures 15A,B**) opens to the outside through a small opening, slightly wider than the pedal groove (700 μm long and 100 μm wide), in the ventroposterior region of the body. The pallial cavity bears marked diverticula (Di, **Figures 15B,C**) on the dorsal and lateral walls. The rostral region of the pallial cavity narrows slightly. The anus (150 μm in diameter) is located dorsorrostrally; the paired opening of the spawning ducts (Sdo,

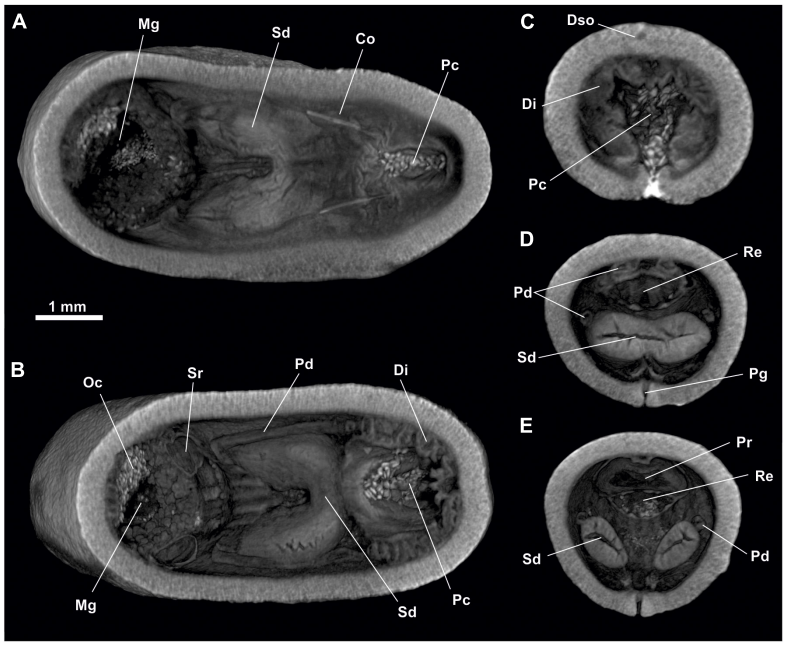

FIGURE 11 | *Dorymenia menchuescribanae*. **(A,B)** Dorsal view of the posterior body. **(C)** Cross-section of the posterior body through pallial cavity. **(D)** Cross-section of the posterior body through spawning duct opening and rectum. **(E)** Cross-section of the posterior body through pericardium. Co, Copulatory stylets; Di, Diverticles; Dso, Dorsoterminal sense organ; Mg, Midgut; Oc, Octocorallia; Pc, Pallial cavity; Pd, Pericardioduct; Pg, Pedal groove; Pr, Pericardium; Re, Rectum; Sd, Spawning duct; Sr, Seminal receptacles.

Figures 15A–C) (100 μm in diameter each) are located ventrally to the anus. The pallial cavity bears a ventrorrostral sac (Pvs, **Figure 15C**) projecting anteriorly (80 μm long and 100 μm in diameter) and abdominal spicules (Ab, **Figure 15A**).

Digestive system.- The atriobuccal cavity (500 μm long and 200 μm in diameter) opens to the outside through an opening 300 μm long, located in the ventroanterior region of the body. The mouth (Mo, **Figure 14B**) is located on the posterior wall of the atriobuccal cavity and is slightly flattened dorsoventrally (200 μm wide and 100 μm high). The pharynx (Ph, **Figures 14A,B,D**) is long and circular (1.3 mm long and 200 μm in diameter), has numerous glands on its dorsal wall, and a cuticle 25 μm thick. The ventral glandular organs of the pharynx (Vfg, **Figures 14A,E**) open onto the ventroposterior region of the pharynx and a little anterior to the radular sac (Rs, **Figure 14A**). These organs are of type B (García-Álvarez and Salvini-Plawen, 2007) and are formed by a pair of ducts 10 mm long and 80 μm in diameter, whose lumen is delimited by a muscular wall, and run ventrally to the intestine, intertwining on occasion. The pharynx (**Figures 14A,B,D**) enters ventrally into the intestine, it lacks an oesophagus. From the anterodorsal region of the intestine (Mg, **Figures 14A,B,E**), the dorsoanterior caecum (**Figures 14A,C,D**) projects, slightly flattened dorsoventrally (1.5 mm long, 150 μm wide and 100 μm high) reaching the height of the atriobuccal cavity. The dorsoventral musculature is visible (Dvm, **Figure 14E**). The intestine (Mg, **Figures 15B,E**) continues along the body (25 mm long and 500 μm in diameter) and ends in the rectum (Re, **Figures 15B,C**) (500 μm long and 150 μm in diameter), whose anus (150 μm in diameter) opens in the dorsorrostral wall of the pallial cavity.

Sense organs.- Small atrium (At, **Figures 14A,B**) (250 μm long, 200 μm wide and 200 μm high) occupying the anterior wall of the atriobuccal cavity (Abc, **Figure 14C**). The atrium bears thin, narrow-necked sensory papillary projections on the anterior, dorsal and lateral walls. The specimen has a dorsoterminal sense organ (Dso, **Figure 13C**) in the dorsal midline of the body, at the end of the pallial cavity, barely visible externally.

Gonopericardial system.- The pair of gonads (Go, **Figure 14B**) (24 mm long and 400 μm in diameter), have oocytes (Ov, **Figures 15D,E**) in the thin septum separating them. The gonopericardioducts (Gd, **Figure 15B**) (500 μm long and 300 μm in diameter) connect them to the rostral region of the pericardium (**Figure 15E**). The pericardium (Pr, **Figures 15D,E**) is wide (1 mm long and 600 μm in diameter) and has oocytes inside. The elongated and narrow heart (Ht, **Figure 15D**) is situated on its dorsal wall (1 mm long and 60 μm in diameter). The pericardium extends into two compartments posteriorly, from which both pericardioducts (Pd, **Figure 15D**) emerge from a laterotermial position; they run posteriorly, rotate, and run anteriorly along the sides of the body (1 mm long and 70 μm in diameter) and end in the anterior region of the spawning ducts (Sd, **Figures 15A,B,D**). The seminal receptacles (Sr, **Figures 15A,B,E**) form bundles (300 μm long and 150 μm in diameter as a whole), which end at the rostral wall of the spawning ducts, near the union with the pericardioducts. The two spawning ducts (1 mm long and 200 μm in diameter)

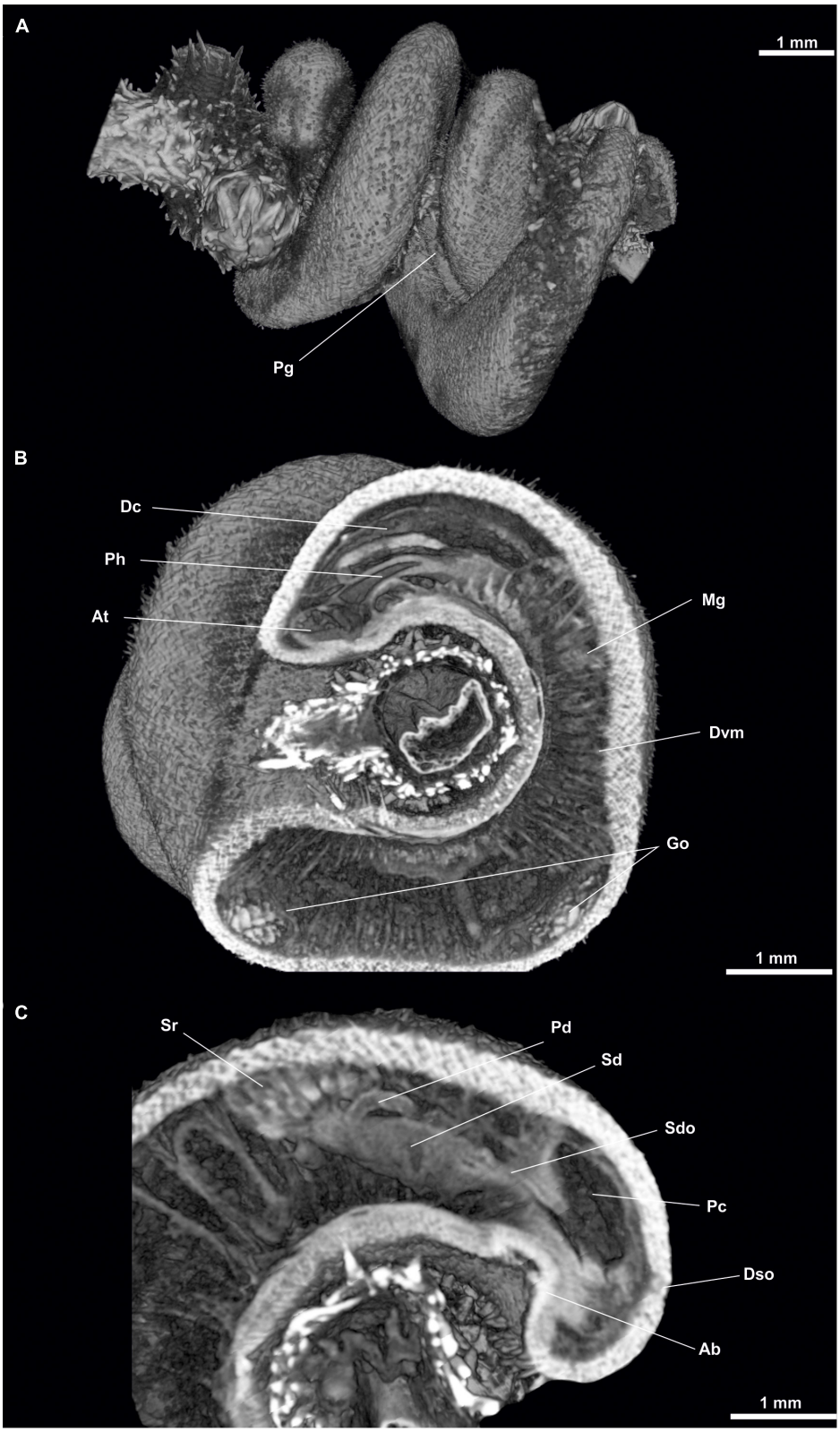

FIGURE 12 | *Anamenia gorgonophila* (Iceland). **(A)** Habitus. **(B)** Sagittal sections of the anterior body. **(C)** Sagittal view of posterior body through spawning duct. Ab, Abdominal spicules; At, Atrium; Dc, Dorsal caecum; Dvm, Dorsoventral musculature; Dso, Dorsoterminal sense organ; Go, Gonad; Mg, Midgut; Pc, Pallial cavity; Pg, Pedal groove; Ph, Pharynx; Sd, Spawning duct; Sdo, Spawning duct opening; Sr, Seminal receptacles.

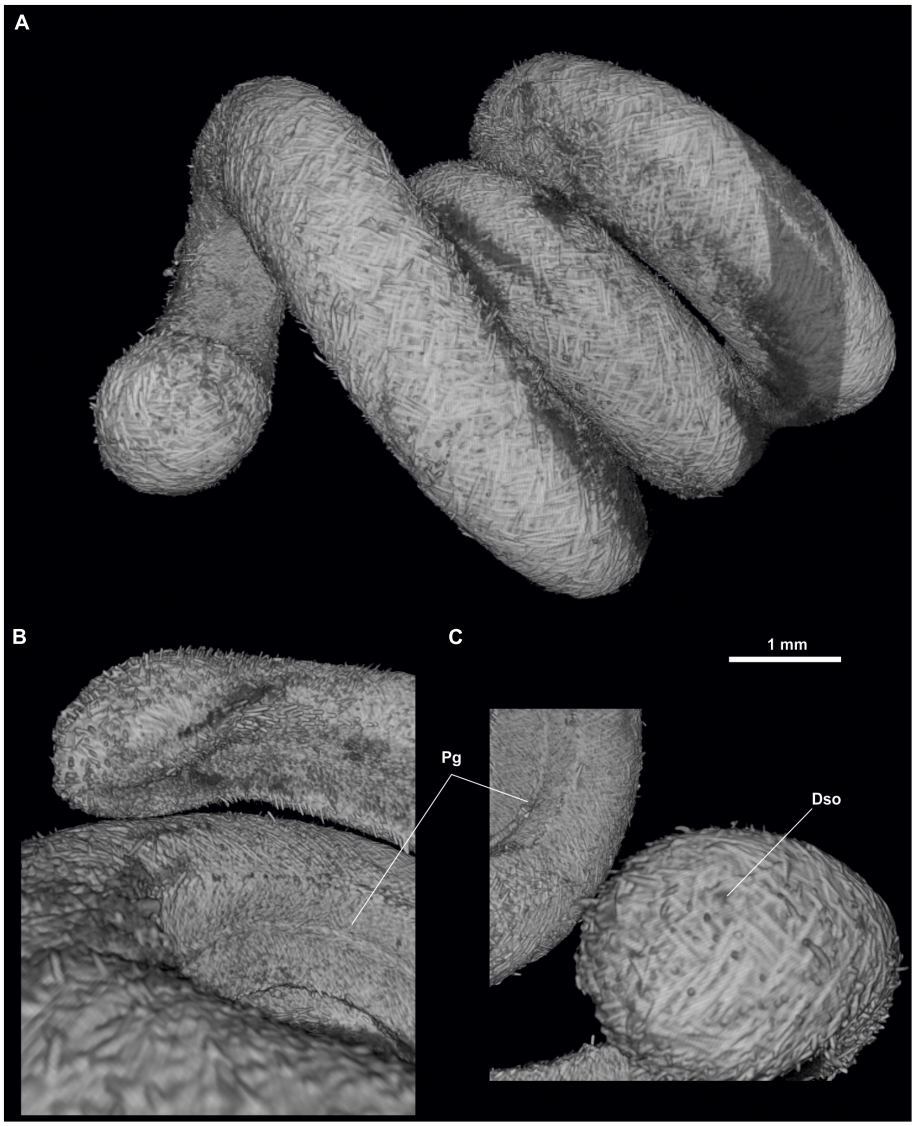

FIGURE 13 | *Anamenia gorgonophila* (Alborán). **(A)** Habitus. **(B)** Ventral view of the anterior body. **(C)** Dorsal view of the posterior body. Dso, Dorsoterminal sense organ; Mo, Mouth; Pc, Pallial cavity; Pg, Pedal groove.

run in a posterior direction, until they each lead individually (Sdo, **Figures 15A–C**) (100 μm in diameter) into the rostral wall of the pallial cavity, ventral to the anus and dorsal to the ventrorrostral sac.

DISCUSSION

Here, we assessed the utility of micro-CT for the study of solenogaster internal anatomy and present the 3D internal anatomy the most taxonomically informative body regions of the four specimens studied. There are very few precedents in the use of this technique in the study of Solenogastres (Candás et al., 2018; Pedrouzo et al., 2019). Descriptions based on micro-CT images have not been performed in other Solenogastres species and are a good complementary tool to anatomical studies based on classical histological sections.

The specimen of *Proneomenia sluiteri* studied here comes from eastern Iceland (IceAGE Expedition), from a collection of 5 specimens presented at the 7th Congress of the European Malacological Societies. In the book of abstracts of the Congress they appear as *Dorymenia* sp., although in the posters that were presented, they were already correctly listed as *Proneomenia* sp. (Cobo et al., 2014; Pedrouzo et al., 2014a). These specimens were collected at the same IceAGE Expedition station as those studied and published by Todt and Kocot (2014). The description of the soft parts matches previously published descriptions (Hubrecht, 1880, 1881; Heuscher, 1892; Thiele, 1913; Todt and Kocot, 2014). The specimen studied measures 36 mm in length, within the range of 2–12 cm reported by Todt and Kocot (2014),

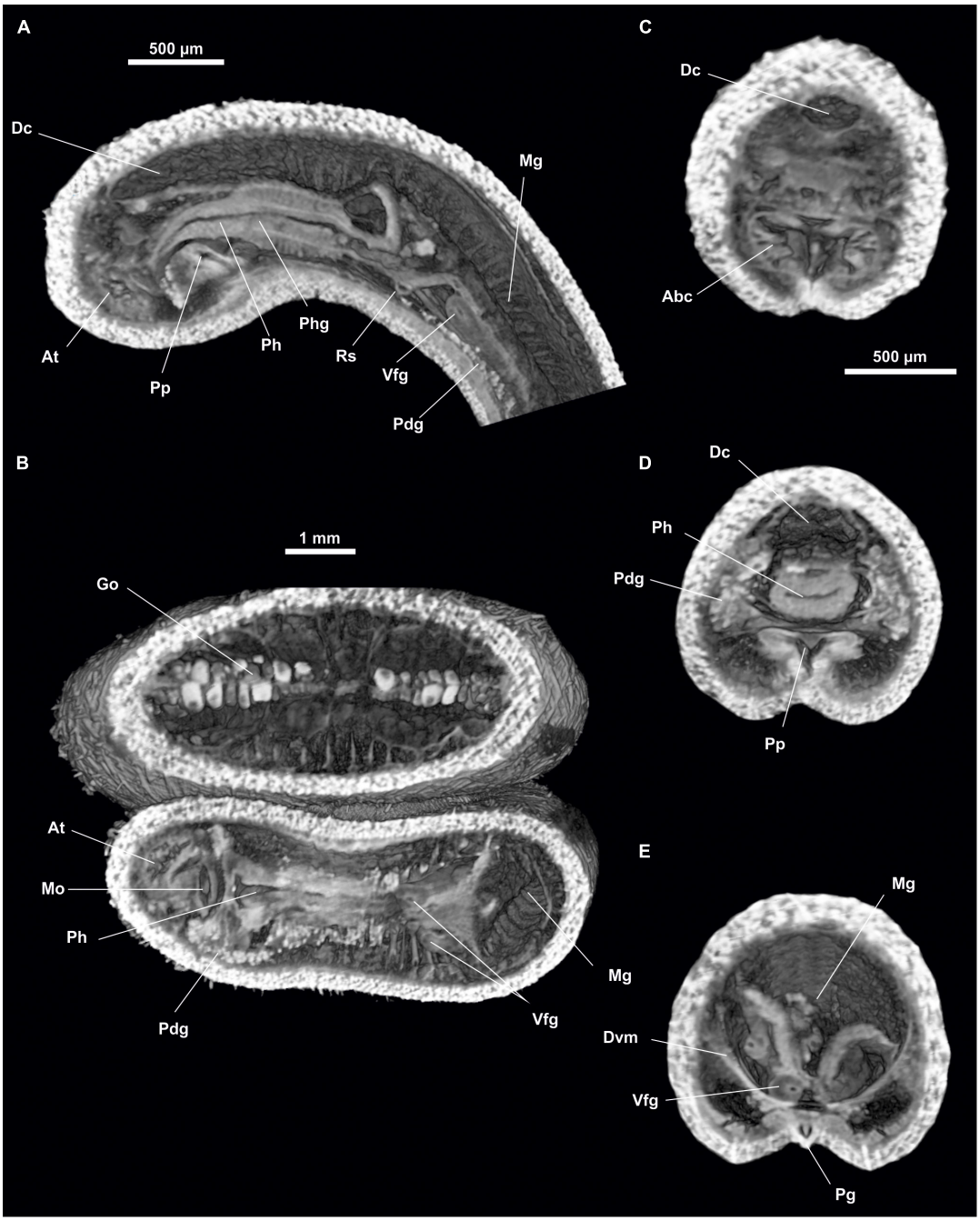

FIGURE 14 | *Anamenia gorgonophila* (Alborán). **(A)** Sagittal view of the anterior body through pharynx. **(B)** Dorsal view of the anterior body through atrium. **(C)** Cross section of the anterior body through atrium. **(D)** Cross section of the anterior body through pharynx. **(E)** Cross section of the anterior body through the midgut. Abc, Atriobucal cavity; At, Atrium; Dc, Dorsal caecum; Dvm, Dorsoventral musculature; Go, Gonad; Mg, Midgut; Mo, Mouth; Pdg, Pedal glands; Pg, Pedal groove; Ph, Pharynx; Phg, Pharynx glands; Pp, Pedal pit; Rs, Radular sack; Vfg, Ventral foregut glands.

or the 13 cm maximum length reported by Thiele (1913); it has an average diameter of 5 mm, also within the proportions stated by Thiele (1913), which indicates a diameter/length ratio of approximately 1:11. The cuticle is 250 µm thick, slightly thinner than other observations, which indicated 0.4 mm thickness (Thiele, 1913). The ventral glandular organs of the pharynx are 11 mm long and occupy 1/3 of the body length. It has an oesophagus, in agreement with other descriptions (Hubrecht, 1880, 1881). Intestinal contents have been observed, corresponding to Alcyonacea on which it feeds (Salvini-Plawen, 1972a). The seminal receptacles are elongated and undulating, and their attachment to the pericardioducts is observed very close

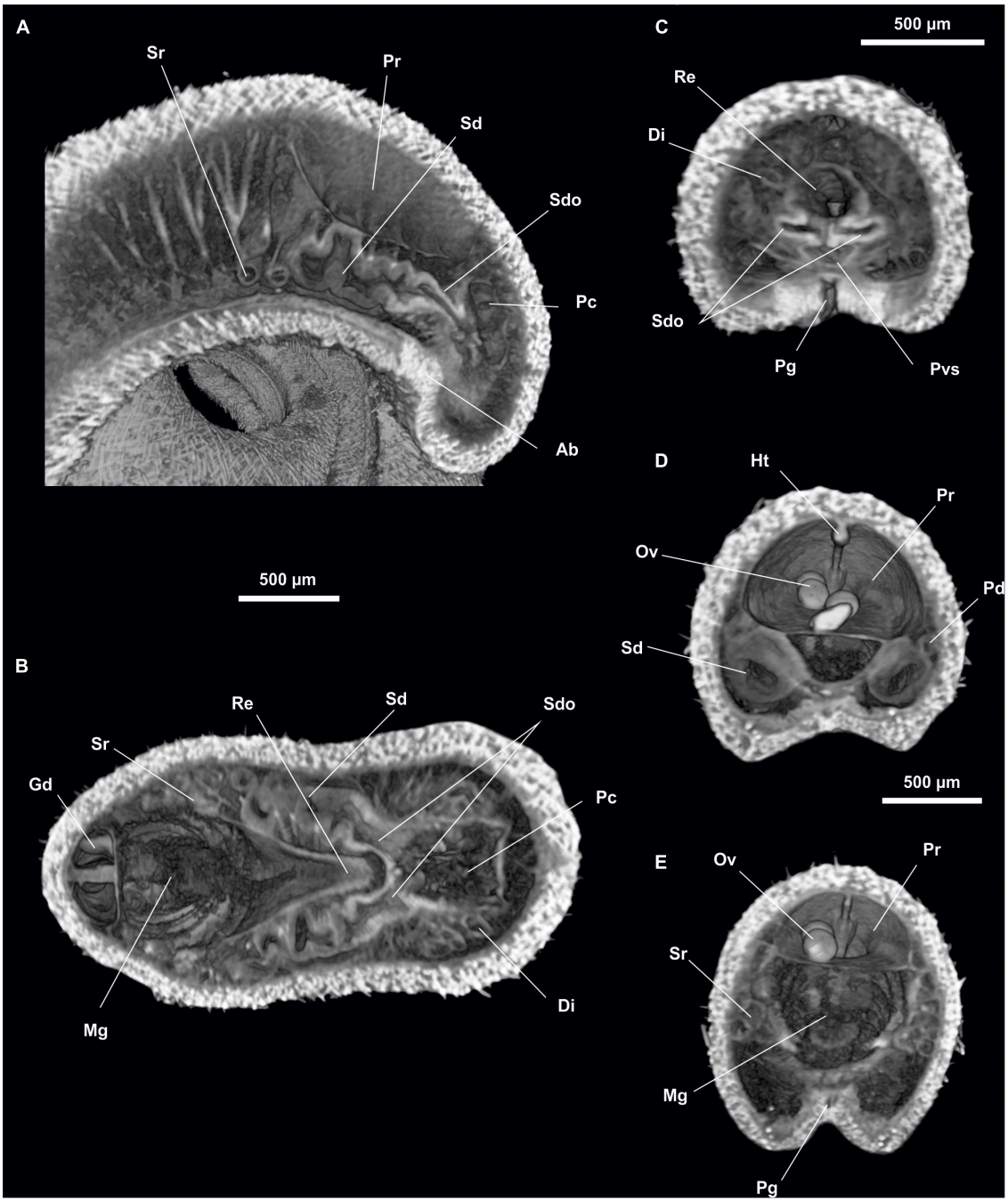

FIGURE 15 | *Anamenia gorgonophila* (Alborán). **(A)** Sagittal view of the posterior body through spawning duct. **(B)** Dorsal view of the posterior body through spawning ducts. **(C)** Cross section of the posterior body through spawning duct opening. **(D)** Cross section of the posterior body through spawning ducts. **(E)** Cross section of the posterior body through seminal receptacles. Ab, Abdominal spicules; Di, Diverticles; Gd, Gonopericardioduct; Ht, Heart; Mg, Midgut; Ov, Oocyte; Pc, Pallial cavity; Pd, Pericardioducts; Pg, Pedal groove; Pr, Pericardium; Pvs, Pallial cavity ventral sac; Re, Rectum; Sd, Spawning duct; Sdo, Spawning duct opening; Sr, Seminal receptacles.

to their point of attachment to the spawning ducts, although in other descriptions they have been observed just at the point of attachment (Todt and Kocot, 2014). The spawning ducts end oddly at the rostral wall of the pallial cavity. A dorso-terminal sensory organ is present.

The specimen studied here of *Dorymenia menchuescribanae*, paratype 1 of the type material and not cut in serial sections (García-Álvarez et al., 2000), matches the original description. The specimen measures 45 mm long, slightly less than in the original description, which states a range of 50–58 mm, but

within the range of 34–51 mm reported later for specimens from the same geographical area (García-Álvarez et al., 2009). The cuticle of 200–300 μm is within the range observed in García-Álvarez et al. (2009) (see **Figure 8**) although less thick than the original description where a thickness of 500 μm is indicated. Only 1 dorsoterminal sense organ was observed here, whereas previous descriptions indicated 2–4 organs (García-Álvarez et al., 2000, 2009). It has a preatrial sense organ located in the anterior wall of the atrium as noted by García-Álvarez et al. (2009). The ventral glandular organs of the pharynx are longer (30 mm in a 45 mm animal) than indicated, first third of the body, in the original description and their mouth is slightly anterior to the radular sac. The pericardium extends posteriorly into two compartments, not described above, from which each of the pericardioducts originates. The spawning duct leads unpaired onto the rostral wall of the ventral sac of the pallial cavity, as indicated in the original description, whereas in García-Álvarez et al. (2009) (see **Figure 11D**) it did so in a ventral position.

The description of the specimen of *Anamenia gorgonophila* collected in Iceland matches the original description. The specimen measures 30 mm long, 2 mm high and 1.5 mm wide and is slightly narrowed laterally. These measurements are in line with what has already been observed (Salvini-Plawen, 1972b; García-Álvarez et al., 1998; Pedrouzo et al., 2014b; Zamarro et al., 2015), although the lateral narrowing had not been noted. The cuticle measures 100–150 μm, thinner than reported by Pedrouzo et al. (2014b) and Zamarro et al. (2015) (200–220 μm), but slightly thicker than observed in García-Álvarez et al. (1998) (85–125 μm). It has 1 dorsoterminal sense organ, which is consistent with what had been previously described, 1–2 organs (Salvini-Plawen, 1972b; García-Álvarez et al., 1998; Zamarro et al., 2015). The seminal receptacles have been observed with difficulty to form bundles of 8, within the range of 6–15 already known (García-Álvarez et al., 1998; Zamarro et al., 2015). The two spawning ducts individually lead to the rostral wall of the pallial cavity, which is characteristic of this species (García-Álvarez et al., 1998; Zamarro et al., 2015).

The description of the specimen of *Anamenia gorgonophila* collected in Alboran Sea matches the original description. The specimen measures 30 mm long and 1 mm in diameter, with its ventral surface flattened; the measurements are within the range of other descriptions (Salvini-Plawen, 1972b; García-Álvarez et al., 1998; Pedrouzo et al., 2014b; Zamarro et al., 2015). The cuticle of this specimen is 80 μm thick, thinner than that indicated by García-Álvarez et al. (1998), 85–125 μm thick, and by Pedrouzo et al. (2014b) and Zamarro et al. (2015), which indicate a cuticle of 200–220 μm thick. Seminal receptacles are in bundles, 7 have been observed here with difficulty, similar to most descriptions indicating 6–15 per bundle (García-Álvarez et al., 1998; Zamarro et al., 2015).

The specimens were fixed in 70% ethanol as the mantle sclerites (which are calcium carbonate in composition) have to be preserved in good condition, as it is necessary to study the type of sclerites in the identification of Solenogastres. Furthermore, ethanol does not interfere with DNA sequencing and allows future molecular research on the same specimen that has been previously scanned.

Because the aim of this work was to study internal anatomy using three-dimensional models, these specimens were stained with iodine, which substantially increases the sharpness of the soft tissues in both 2D sections and 3D models. Iodine has been previously tested on other Solenogastres species (Pedrouzo et al., 2019). This compound stains virtually all tissue types, although it seems to have a preference for calcified structures and polysaccharides (Metscher, 2009; Faulwetter et al., 2013a). In images obtained in animals without iodine staining, it is not possible to visualise the internal anatomy. However, once stained, soft tissues are clearly visible (Candás et al., 2018). On the other hand, the sclerites are much clearer in the unstained specimens. In the iodine-treated specimens, the sclerites are covered by an excess of stain that was not removed by the ethanol rinse prior to dehydration with HMDS, which makes them appear too bright in the images and their arrangement is not clearly visible. This is clearly related to the preference of iodine for calcified structures.

The use of other stains such as phosphotungstic acid (PTA), phosphomolybdic acid (PMA) or osmium tetroxide have shown excellent results in other groups of Molluscs such as Bivalvia, Gastropoda, Scaphopoda and even Caudofoveata (Golding and Jones, 2007; Metscher, 2009; Faulwetter et al., 2013a; Candás et al., 2016, 2017; Marcondes Machado et al., 2018; Ziegler et al., 2018). Osmium tetroxide is a very toxic compound, so its use in this study was discarded. As for PTA, we have performed different tests with Solenogastres whose results show that it is not a good stain in the study of these animals as it seems to destroy the sclerites, possibly due to its acidic nature (Candás et al., 2018; Kocot, unpublished data). Another advantage of iodine staining is that it is possible to extract nucleic acids from specimens after scanning (Green et al., 2017).

Computed microtomography or micro-CT made it possible to study most of the anatomical structures of the specimens under study, which have a relatively large size in relation to the small average size of Solenogastres. With this technique it was possible to obtain 2D images that adequately complement those obtained by means of serial histological sections, and also a very relevant 3D view of the internal anatomical structure, which allowed both precise measurements and observation of the relative position of the organs with different focus and angles. However, it was not possible to observe the radula, possibly due to its small size. The observation of ventral foregut organs by micro-CT is not easy. In the specimens studied here, which are relatively large, it was possible to observe them and determine their type. However, in other small-sized specimens, the observation of these organs is difficult, even impossible in some cases, especially if the organs are small like clustered-type, type A or *Simrothiella*-like (Pedrouzo et al., 2019). Neither was it possible to visualise the nervous system, nor to clearly define the glandular structures. In other larger marine molluscs (Cephalopoda) it has been possible to see the nervous structures using PTA as a contrast agent (Ziegler et al., 2018). Despite some limitations, results of this study highlight micro-CT as a valuable

tool for the non-destructive study of solenogaster morphology. In particular, it is very useful for identifying animals to the family and even genus level, which allows us to start identification or classification work by means of classical histological techniques without destroying the specimens.

Hence, Micro-CT is proved to be a very useful tool for an initial, quick, non-destructive approximation for most of the internal structures of Solenogastres, making it possible to reach family or even genus taxonomic level. Nonetheless, histology is still required for the description of small or glandular parts, which are important for species-level identification in many cases. Therefore, these techniques remain complementary.

DATA AVAILABILITY STATEMENT

Data are available through the following link in morphosource: https://www.morphosource.org/projects/000384772.

AUTHOR CONTRIBUTIONS

JM-S, KK, ÓG-Á, MC, and GD-A: anatomical study, figure production, article redaction, and images production with micro-CT. All authors contributed to the article and approved the submitted version.

FUNDING

KK received funding from the United States National Science Foundation (NSF DEB 1846174).

ACKNOWLEDGMENTS

We would like to thank the scientists and crew of the Me-85/IceAGE cruise, the DZMB, and Senckenberg. We would also like to acknowledge the University of Alabama Water Institute for their contribution to the fee for publishing this article.

REFERENCES

Alba-Tercedor, J., and Sánchez-Tocino, L. (2011). The use of the SkyScan 1172 high resolution micro-CT to elucidate if the spicules of the sea slugs (Mollusca: Nudibranchia, Opisthobranchia) have a structural or a defensive function. *Skyscan Users Meet* 2011, 113–121.

Candás, M., Díaz-Agras, G., Abad, M., Barrio, L., Cunha-Veira, X., Pedrouzo, L., et al. (2016). Application of micro-CT in the study of the anatomy of small marine molluscs. *Microsc. Anal.* 30, S8–S11.

Candás, M., Díaz-Agras, G., García-Álvarez, O., and Urgorri, V. (2018). "Study of the applicability of micro-CT for identification of *Mollusca Solenogastres*," in *Proceedings of the Bruker Micro-CT User Meeting Abstract Book*, Ghent, 32–40.

Candás, M., Díaz-Agras, G., and Urgorri, V. (2017). "First steps in morphological analysis of the of the reproductive system of *Doto pinnatifida* (Montagu,1804)," in *Proceedings of the Bruker Micro-CT User Meeting Abstract Book*, Brussels, 112–116.

Cobo, M. C., Pedrouzo, L., Candás, M., García-Álvarez, O., and Urgorri, V. (2014). "The use of Micro-CT vs classical histological techniques in the study of the internal anatomy of Solenogastres," in *Proceedings of the 7th Congress of the European Malacological Societies, Conference Programme* & *Book of Abstracts*, ed. T. S. White (Bruges: Cambridge).

Faulwetter, S., Vasileiadou, A., Kouratoras, M., Dailianis, T., and Arvanitidis, C. (2013b). Micro-computed tomography: introducing new dimensions to taxonomy. *Zookeys* 263, 1–45. doi: 10.3897/zookeys.263.4261

Faulwetter, S., Dailianis, T., Vasileiadou, A., and Arvanitidis, C. (2013a). Contrast enhancing techniques for the application of micro-CT in marine biodiversity studies. *Microsc. Anal.* 27, S4–S7. doi: 10.1007/978-3-319-17001-5_53-1

García-Álvarez, O., and Salvini-Plawen, L. (2007). Species and diagnosis of the families and genera of *Solenogastres* (Mollusca). *Iberus* 25, 73–143.

García-Álvarez, O., Salvini-Plawen, L., and Urgorri, V. (2014). "Solenogastres," in *Mollusca, Solenogastres, Caudofoveata, Monoplacophora*, Vol. 38, eds O. García-Álvarez, L. Salvini-Plawen, V. Urgorri, J. S. Troncoso, F. Ibérica, and M. Ramos (Madrid: Museo Nacional de Ciencias Naturales), 31–163.

García-Álvarez, O., Urgorri, V., and Cristobo, F. J. (1998). Sobre la presencia de Anamenia gorgonophila (Kowalevsky, 1880) (Mollusca, Solenogastres: Cavibelonia) en las costas de la Península Ibérica. *Nova Acta Científ. Compost.* 9, 249–258.

García-Álvarez, O., Urgorri, V., and Salvini-Plawen, L. (2000). Two new species of *Dorymenia* (Mollusca: Solenogastres: Proneomeniidae) from the South Shetland Islansds (Antarctica). *J. Mar. Biol. Assoc. U. K.* 80, 835–842. doi: 10.1017/S0025315400002812

García-Álvarez, O., Zamarro, M., and Urgorri, V. (2009). Proneomeniidae (Solenogastres, Cavibelonia) from the Bentart-2006 Expedition, with description of a new species. *Iberus* 27, 67–78.

Gignac, P. M., Kley, N. J., Clarke, J. A., Colbert, M. W., Morhardt, A. C., Cerio, D., et al. (2016). Diffusible iodine-based contrast-enhanced computed tomography (diceCT): an emerging tool for rapid, high-resolution, 3-D imaging of metazoan soft tissues. *J. Anat.*. 228, 889–909. doi: 10.1111/joa.12449

Golding, R. E., and Jones, A. S. (2007). Micro-CT as a novel technique for 3D reconstruction of molluscan anatomy. *Mollusc. Res.* 27, 123–128.

Green, R. M., Leach, C. L., Hoehn, N., Marcucio, R. S., and Hallgrímsson, B. (2017). Quantifying three-dimensional morphology and RNA from individual embryos. *Dev. Dyn.* 246, 431–436. doi: 10.1002/dvdy.24490

Heuscher, J. (1892). Zur anatomie und histologie der proneomenia sluiteri hubrecht. *Jenaische Zeitschr. Nat.* 27, 477–512.

Hubrecht, A. A. W. (1880). Proneomenia sluiteri, gen. et sp. n. eine neue archaische Molluskenform aus dem Eismeere. *Zool. Anzeig.* 3, 589–590.

Hubrecht, A. A. W. (1881). Proneomenia sluiteri, gen. et sp. n. with remarks upon the anatomy and histology of the Amphineura. *Niederl. Arch. Zool.* 2, 1–75.

Keklikoglou, K., Faulwetter, S., Chatzinikolaou, E., Wils, P., Brecko, J., Kvaček, J., et al. (2019). Micro-computed tomography for natural history specimens: a handbook of best practice protocols. *Eur. J. Tax.* 522, 1–55. doi: 10.5852/ejt.2019.522

Kocot, K. M., Todt, C., Mikkelsen, N. T., and Halanych, K. M. (2019). Phylogenomics of Aplacophora (Mollusca, Aculifera) and a solenogaster without a foot. *Proc. R. Soc. B* 286:20190115. doi: 10.1098/rspb.2019.0115

Kowalevsky, A. (1880). Ueber die bau und die lebensersegeinungen von *Neomenia gorgonophilus*. *Zool. Anz.* 3, 190–191.

Marcondes Machado, F., Dias Passos, F., and Giribet, G. (2018). The use of micro-computed tomography as a minimally invasive tool for anatomical study of bivalves (*Mollusca: Bivalvia*). *Zool. J. Linn. Soc.* 186, 46–75. doi: 10.1093/zoolinnean/zly054

Metscher, B. D. (2009). MicroCT for comparative morphology: simple staining methods allow high-contrast 3D imaging of diverse non-mineralized animal tissues. *BMC Physiol.* 9:11. doi: 10.1186/1472-6793-9-11

Nierstrasz, H. (1908). The Solenogastres of the discovery-expedition. *Nat. Antarct. Exp. 1901–1904 Nat. Hist.* 4, 38–46.

Paterson, G. L., Sykes, D., Faulwetter, S., Merk, R., Ahmed, F., Hawkins, L. E., et al. (2014). The pros and cons of using micro-computed tomography in gross and

micro-anatomical assessments of polychaetous annelids. *Mem. Mus. Victor.* 71, 237–246. doi: 10.24199/j.mmv.2014.71.18

Paz-Sedano, S., Candás, M., Gosliner, T. M., and Pola, M. (2021). Undressing *Lophodoris danielsseni* (Friele & Hansen, 1878) (Nudibranchia: Goniodorididae). *Organ. Divers. Evol.* 21, 107–117. doi: 10.1007/s13127-020-00470-z

Pedrouzo, L., Cobo, M. C., García-Álvarez, O., Rueda, J. L., Gofas, S., and Urgorri, V. (2014a). Solenogastres (*Mollusca*) from expeditions off the South Iberian Peninsula, with the description of a new species. *J. Nat. Hist.* 48, 2985–3006. doi: 10.1080/00222933.2014.959576

Pedrouzo, L., Cobo, M. C., Señarís, M. P., García-Álvarez, O., and Urgorri, V. (2014b). "A deep-sea Dorymenia sp. (*Mollusca, Solenogastres*) from East Iceland, Norwegian Sea (lceAGE-project)," in *Proceedings of the 7th Congress of the European Malacological Societies, Conference Programme* & *Book of Abstracts*, ed. T. S. White (Cambridge: The Malacological Society of London).

Pedrouzo, L., García-Álvarez, O., Urgorri, V., and Pérez-Señarís, M. (2019). New data and 3D reconstruction of four species of *Pruvotinidae* (Mollusca: Solenogastres) from the NW Iberian Peninsula. *Mar. Biodivers.* 49, 277–287. doi: 10.1007/s12526-017-0793-1

Salvini-Plawen, L. (1972b). Revision der monegassischen solenogastres (Mollusca, Aculifera). *J. Zool. Syst. Evol. Res.* 10, 215–240. doi: 10.1111/j.1439-0469.1972.tb00799.x

Salvini-Plawen, L. (1972a). Cnidaria as food-sources for marine invertebrates. *Cah. Biol. Mar.* 13, 385–400.

Salvini-Plawen, L. V. (1978). Antarktische und subantarktische Solenogastres. *Zoologica* 128, 1–305.

Simroth, H., and Bronn, H. G. (1893). *Klassen und Ordnungen des Tierreichs*.

Thiele, J. (1913). "Solenogastres," in *Friedländer und Sohn*, ed. D. Tierreich (Berlin: Verlag von R), 1–57. doi: 10.5962/bhl.title.51964

Todt, C., and Kocot, K. M. (2014). New records for the solenogaster *Proneomenia sluiteri* (Mollusca) from Icelandic waters and description of Proneomenia custodiens sp. n. *Pol. Polar Res.* 35, 291–310. doi: 0.2478/popore-2014-0012

Urgorri, V., Señarís, M. P., Díaz-Agras, G., Candás, M., and Gómez-Rodríguez, C. (2021). Doris adrianae sp. nov. (Heterobranchia; Nudibranchia; Doridina) from the Galician coasts (NW Iberian Peninsula). *Nova Acta Científ. Compost.* 28, 1–33.

Zamarro, M., García-Álvarez, O., and Urgorri, V. (2015). New anatomical and biogeographical data on solenogastres cavibelonia from the Galician Continental margin (NW Spain). *Iberus* 33, 1–26.

Ziegler, A., Bock, C., Ketten, D. R., Mair, R. W., Mueller, S., Nagelmann, N., et al. (2018). Digital three-dimensional im-aging techniques provide new analytical pathways for malacological research. *Am. Malacol. Bull.* 36, 248–273. doi: 10.4003/006.036.0205

Conflict of Interest: The authors declare that the research was conducted in the absence of any commercial or financial relationships that could be construed as a potential conflict of interest.

Publisher's Note: All claims expressed in this article are solely those of the authors and do not necessarily represent those of their affiliated organizations, or those of the publisher, the editors and the reviewers. Any product that may be evaluated in this article, or claim that may be made by its manufacturer, is not guaranteed or endorsed by the publisher.

Copyright © 2022 Martínez-Sanjuán, Kocot, García-Álvarez, Candás and Díaz-Agras. This is an open-access article distributed under the terms of the Creative Commons Attribution License (CC BY). The use, distribution or reproduction in other forums is permitted, provided the original author(s) and the copyright owner(s) are credited and that the original publication in this journal is cited, in accordance with accepted academic practice. No use, distribution or reproduction is permitted which does not comply with these terms.

frontiers in Marine Science

PERSPECTIVE
published: 12 January 2022
doi: 10.3389/fmars.2021.797140

Framing Cutting-Edge Integrative Deep-Sea Biodiversity Monitoring via Environmental DNA and Optoacoustic Augmented Infrastructures

Sergio Stefanni[1], Luca Mirimin[2], David Stanković[3,4], Damianos Chatzievangelou[5], Lucia Bongiorni[6], Simone Marini[1,7], Maria Vittoria Modica[1], Elisabetta Manea[6], Federico Bonofiglio[7], Joaquin del Rio Fernandez[8], Neven Cukrov[9], Ana Gavrilović[10], Fabio C. De Leo[11,12] and Jacopo Aguzzi[1,5]**

[1] Stazione Zoologica Anton Dohrn, Villa Comunale, Naples, Italy, [2] Department of Natural Resources and the Environment, Marine and Freshwater Research Centre, School of Science and Computing, Galway-Mayo Institute of Technology, Galway, Ireland, [3] Department of Organisms and Ecosystems Research, National Institute of Biology, Ljubljana, Slovenia, [4] Marine Biology Station Piran, National Institute of Biology, Piran, Slovenia, [5] Marine Science Institute, ICM-CSIC, Barcelona, Spain, [6] Institute of Marine Sciences, CNR-ISMAR, Venice, Italy, [7] Institute of Marine Sciences, CNR-ISMAR, La Spezia, Italy, [8] SARTI-MAR Research Group, Universitat Politècnica de Catalunya, Vilanova i la Geltrú, Spain, [9] Ruđer Bošković Institute, Zagreb, Croatia, [10] Department of Fisheries, Apiculture, Wildlife Management and Special Zoology, Faculty of Agriculture, University of Zagreb, Zagreb, Croatia, [11] Ocean Networks Canada (ONC), University of Victoria, Victoria, BC, Canada, [12] Department of Biology, University of Victoria, Victoria, BC, Canada

OPEN ACCESS

Edited by:
Kevin M. Kocot,
University of Alabama, United States

Reviewed by:
Miriam Isabelle Brandt,
Norwegian Research Institute (NORCE), Norway
Xavier Turon,
Spanish National Research Council (CSIC), Spain

***Correspondence:**
Sergio Stefanni
sergio.stefanni@szn.it
Jacopo Aguzzi
jaguzzi@icm.csic.es

Specialty section:
This article was submitted to Deep-Sea Environments and Ecology, a section of the journal Frontiers in Marine Science

Received: 18 October 2021
Accepted: 29 November 2021
Published: 12 January 2022

Citation:
Stefanni S, Mirimin L, Stanković D, Chatzievangelou D, Bongiorni L, Marini S, Modica MV, Manea E, Bonofiglio F, del Rio Fernandez J, Cukrov N, Gavrilović A, De Leo FC and Aguzzi J (2022) Framing Cutting-Edge Integrative Deep-Sea Biodiversity Monitoring via Environmental DNA and Optoacoustic Augmented Infrastructures. Front. Mar. Sci. 8:797140. doi: 10.3389/fmars.2021.797140

Deep-sea ecosystems are reservoirs of biodiversity that are largely unexplored, but their exploration and biodiscovery are becoming a reality thanks to biotechnological advances (e.g., omics technologies) and their integration in an expanding network of marine infrastructures for the exploration of the seas, such as cabled observatories. While still in its infancy, the application of environmental DNA (eDNA) metabarcoding approaches is revolutionizing marine biodiversity monitoring capability. Indeed, the analysis of eDNA in conjunction with the collection of multidisciplinary optoacoustic and environmental data, can provide a more comprehensive monitoring of deep-sea biodiversity. Here, we describe the potential for acquiring eDNA as a core component for the expanding ecological monitoring capabilities through cabled observatories and their docked Internet Operated Vehicles (IOVs), such as crawlers. Furthermore, we provide a critical overview of four areas of development: (i) Integrating eDNA with optoacoustic imaging; (ii) Development of eDNA repositories and cross-linking with other biodiversity databases; (iii) Artificial Intelligence for eDNA analyses and integration with imaging data; and (iv) Benefits of eDNA augmented observatories for the conservation and sustainable management of deep-sea biodiversity. Finally, we discuss the technical limitations and recommendations for future eDNA monitoring of the deep-sea. It is hoped that this review will frame the future direction of an exciting journey of biodiscovery in remote and yet vulnerable areas of our planet, with the overall aim to understand deep-sea biodiversity and hence manage and protect vital marine resources.

Keywords: omics sensors, eDNA metabarcoding, genetic markers, imaging, artificial intelligence, data repositories, deep sea conservation

INTRODUCTION

The deep sea (generally below the 200 m limit of the euphotic zone) accounts for the majority of the world's ocean (>95%; Costello et al., 2010; Wedding et al., 2013). This vast environment hosts a wealth of hydrocarbon and mineral resources and provides a series of ecosystem services associated with its functioning (e.g., nutrients regeneration and global biogeochemical cycles), resulting in a vast repository of complex organic molecules and unexplored biodiversity (Pikitch et al., 2014; Thurber et al., 2014; Kroodsma et al., 2018).

The biodiversity of deep-sea ecosystems is increasingly threatened by anthropogenic impacts resulting from pollutants and other activities such as the extraction of geochemical resources and minerals (Levin and Le Bris, 2015). Marine biodiversity conservation is in growing conflict with resource exploitation, especially when it comes to key deep-sea habitats such as abyssal plains (associated to manganese nodule mining), hydrothermal vents fields (associated to sulfide deposits) or submarine canyons (associated to oil and gas drilling) (Danovaro et al., 2017a). In the context of increasing climatic and human disturbances, deep-sea ecosystems, and biodiversity found in areas beyond national jurisdiction are prime conservation targets (as identified by the United Nations Convention on the Law of the Sea (UNCLOS) and the International Union for Conservation of Nature (IUCN), where the preservation of marine ecosystem functions should be balanced with sustainable use of resources (Danovaro et al., 2008, 2020; McIntyre, 2010; Morato et al., 2010; Pusceddu et al., 2014; Ramírez et al., 2017).

Scientific research must thoroughly investigate all ecosystems' life components prior to onset of mass industrial activities, among which impending deep-sea mining raises particular concerns (e.g., Koschinsky et al., 2018; Washburn et al., 2019). This demand has resulted in the development of management guidelines for sustainable use of the sea, as reflected in the Aichi Target 11 (Convention on Biological Diversity, CBD) and by the Sustainable Development Goal 14 "Life below water" and the post-2020 Zero draft CBD proposal (UN 2030 Agenda for Sustainable Development; UNEP, 2020; UNESCO, 2020). A more comprehensive and multidimensional understanding of marine biodiversity in all its facets, including how it is shaped by the environment, human impacts, and climate, represents a critical knowledge framework that is needed to inform resource management operators (Howell et al., 2020). To gain this comprehensive knowledge, deep-sea research is merging the information on the number of species (or taxonomic units) with data on their ecological relationships and information on their spatiotemporal distribution (Berry et al., 2019; Costa et al., 2020).

Need for Filling Knowledge Gaps of the Deep-Sea

Biodiversity knowledge relies on access to adequate taxonomic information with emphasis on *in situ* sample collection, observation, and monitoring strategies (Glover et al., 2018). Nonetheless, the deep sea is still virtually unknown to science as <0.0001% of its surface area has been explored in detail (Ramirez-Llodra et al., 2011). Although it has been argued that richness of marine pelagic species decreases sharply with depth (Colloca et al., 2003; Costello and Chaudhary, 2017), major knowledge gaps still exist with current data likely to be biased by uneven and scattered sampling (Higgs and Attrill, 2015). In particular, less than 1% of the deep pelagic realm has been sampled to date due to its vastness and remoteness (Higgs and Attrill, 2015 and references therein). Overall, it is estimated that about 1.5 million deep-sea species have yet to be discovered (Costello and Chaudhary, 2017; Danovaro et al., 2017b).

Despite growing efforts to collect, store and publicly share biological and ecological data on the deep-sea through international programs such as the Census of Marine Life (CoML), the Ocean Biodiversity Information System (OBIS) and the Deep Ocean Observation System (DOOS), the baseline knowledge in biodiversity is still inadequate, and data on the distribution of deep-sea species over extended spatial and temporal scales are almost entirely lacking (Glover et al., 2010; Wedding et al., 2013). Reports of species occurrence in a given area depend on direct sampling for final taxonomic assignment (Glover et al., 2018; Danovaro et al., 2020). This is typically carried out by vessel-assisted methods and technologies [e.g., remotely operated vehicles (ROVs) and autonomous underwater vehicles (AUVs)], with considerable practical and logistic limitations still affecting sample collection and spatiotemporal replication (Aguzzi et al., 2019). Indeed, the capability of vessel-based research expeditions has advanced significantly in the past decades, however the data gathered provide a snapshot of the local biological complexity but are restricted to the relatively narrow timeframe of the cruise period (Ruth, 2006). This limitation is further emphasized in the deep-sea, where tidal and inertial currents can result in massive benthic and pelagic populations displacements (Gage and Tyler, 1992; Aguzzi and Company, 2010; Aguzzi et al., 2011a, 2015). In addition to the many technical constraints of deep-sea surveys, sampling is often targeting specific taxonomic groups, habitats, ecological traits, sizes or behaviors, limiting the taxonomic resolution of species inventories (Hatch et al., 2020; McCowin et al., 2020; Weston et al., 2020). The most notorious example of such limitations is found in deep-sea fishery surveys, where data is collected either by trawl nets of a certain mesh size or using ROVs for habitat characterization, both of which target only benthic megafauna and also have known biases due to selective captures/sampling (e.g., Common Fishery Policy Data Collection Multiannual Program; Aymà et al., 2016; Jac et al., 2021).

Emerging Technological Advances in Deep-Sea Monitoring

Cabled observatories (seabed oceanographic research platforms connected to network systems to provide a continuous monitoring, observing, and recording of various seafloor activities) are constantly transforming ocean research, by establishing networks of interactive, globally distributed sensors for real-time data collection (Danovaro et al., 2017a; Aguzzi et al., 2019; Jahanbakht et al., 2021). These platforms enable the combination of data collection by optoacoustic (HD

video and multi-beam rotary or dual-frequency sonar imaging devices), oceanographic and geochemical sensor technologies, in a continuous, high-frequency and long-lasting fashion (e.g., Thomsen et al., 2012, 2017; Howe et al., 2019; **Table 1**). Coupling the presence of species to the environmental conditions surrounding them makes these platforms the core of emerging *in situ* marine ecosystem-level laboratories (Rountree et al., 2020). These platforms can provide long-term imagery data sets (e.g., decades), hence enabling the compilation of comprehensive multiannual species richness lists (Juniper et al., 2013; Doya et al., 2017; Chauvet et al., 2018; del Rio et al., 2020). Taxonomic characterization of monitored communities by visual means is also complemented by Passive Acoustic Monitoring (PAM) systems with the use of specific acoustic markers for species identification (e.g., Juanes, 2018).

To overcome the spatial constraints imposed by limited fixed-point observation nodes, mobile platforms are being developed to monitor both the seafloor and the water column (Aguzzi et al., 2019). Internet Operated Vehicles (IOVs), such as crawlers and rovers, are benthic mobile platforms that are either tethered to cabled observatories (Purser et al., 2013) or completely free of direct physical connection (Brandt et al., 2016), and can operate with preloaded navigation plans to autonomously return to their docking station (i.e., the cabled observatory) to recharge and offload data (Thomsen et al., 2012, 2017; Aguzzi et al., 2020a). A recent addition to cabled observatories allows the study of subatomic particles such as neutrinos (Agostini et al., 2020). Using a suite of photomultipliers and other light-sensitive sensors, these neutrino telescopes are also capable of continuously monitoring bioluminescence from migrating deep-scattering layers and bacterioplankton (Martini et al., 2013, 2014; Tamburini et al., 2013; Bailly et al., 2021). These cross-disciplinary infrastructures will provide key complementary data for long-term monitoring of bentho-pelagic coupling in a rapidly changing ocean (Chatzievangelou et al., 2021).

Most observatories rely on information acquired by imaging to provide both qualitative and quantitative data on local biodiversity (Bicknell et al., 2016). Thus, the quality of biodiversity information relies upon the ability to classify organisms to the species level, that in turn can be used to compile local inventories (i.e., richness) and relative abundance estimates (Aguzzi et al., 2020a). Unfortunately, imaging does not always allow sufficiently high taxonomical precision, and generally requires the physical collection of samples to validate species identification. Furthermore, organisms' attraction to or avoidance of submerged infrastructures is likely to cause some degree of bias toward the local communities (Widder et al., 2005; Aguzzi et al., 2019; Rountree et al., 2020; Garcia-Vazquez et al., 2021).

Significant advances in molecular methodology and bioinformatics, accompanied by a steady increase in computational power, have made "omics" technologies and data increasingly accessible, with great potential to fill gaps in biodiversity monitoring capabilities of deep-sea cabled observatories (Heidelberg et al., 2010; Garcia-Vazquez et al., 2021). One of the more recent contributions of "omics" to biodiversity monitoring is linked to the collection and analysis of genetic material extracted directly from environmental samples (sediment, water, ice, and air, etc.; Taberlet et al., 2012; Barnes and Tuner, 2016; Cristescu and Hebert, 2018), which can include a mixture of whole organisms and/or environmental DNA (eDNA) (*sensu* Rodriguez-Ezpeleta et al., 2021). Sequencing of eDNA by means of High Throughput Sequencing (HTS) technology has enabled the development of eDNA metabarcoding. Here, amplicon sequencing with universal primers is used to generate a extremely large (hundreds of thousands to millions) of DNA (mini)barcode reads (Meusnier et al., 2008; Hajibabaei and McKenna, 2012). These are preprocessed and curated using dedicated bioinformatic pipelines. This includes trimming the reads so that only marker sequences remain and quality filtering (e.g., DADA2 – Callahan et al., 2016; Cutadapt – Martin, 2011; Vsearch – Rognes et al., 2016). The quality filtered reads are then clustered into OTUs based on similarity (e.g., 99%, 97%) or taxonomically assigned directly using DNA reference databases (e.g., BOLD – Ratnasingham and Hebert, 2007; GenBank – Benson et al., 2013; PR2 – Guillou et al., 2013; SILVA – Quast et al., 2013; PLANiTS – Banchi et al., 2020; MZG-db – Bucklin et al., 2021). Reads that cannot be assigned to the desired taxonomic level (e.g., species, genus, and family) can still be used to assess alpha and beta diversity evaluation (e.g., Stefanni et al., 2018). eDNA metabarcoding approaches are revolutionizing marine biodiversity assessment and monitoring because they can be used to simultaneously determine entire species communities, even when the exact composition of these assemblages is unknown (e.g., Deiner et al., 2017; Djurhuus et al., 2017; Stefanni et al., 2018; Eble et al., 2020; Kolda et al., 2020; McClenaghan et al., 2020; Seymour et al., 2020; Kawato et al., 2021). eDNA metabarcoding is becoming a particularly valuable tool for deep-sea biodiversity research and monitoring given high species diversity, low animal numbers, difficulties in taxonomic identification due to limited taxonomic expertise, large and remote location, and associated logistical constraints for sample/specimen acquisition (Thomsen et al., 2016; Kersten et al., 2019; Atienza et al., 2020; Canals et al., 2021; Kawato et al., 2021; Merten et al., 2021).

Much of the eDNA work on deep-sea communities has focused on sediment samples to study benthic communities (e.g., Guardiola et al., 2016a; Atienza et al., 2020; Lins et al., 2021) as opposed to fish and pelagic communities. While fish taxa detected by eDNA metabarcoding are generally comparable to those identified by conventional fish survey methods, eDNA captures greater fish diversity than conventional methods when considering a single conventional approach. For example, eDNA metabarcoding in the deep sea generally outperforms trawling because of the presence of species that are typically elusive, small, rare or located on rocky surfaces or steep slopes (Thomsen et al., 2016; Closek et al., 2019; Afzali et al., 2020; Fraija-Fernández et al., 2020; McClenaghan et al., 2020). The advantage of deep ocean water eDNA metabarcoding has also been demonstrated for the study of other communities, including cephalopods (Merten et al., 2021; Visser et al., 2021) and zooplankton (Kersten et al., 2019; Laroche et al., 2020b; Govindarajan et al., 2021). In addition, eDNA extracted from water has also been used to study deep-sea benthic communities (Everett and Park, 2018;

TABLE 1 | List of some of the best known coastal and deep marine cabled observatories that are presently engaged in the recompilation of large image data sets with the implementation of eDNA prospection.

Site	Web	Geographic area	Depth (m)	Oceanographic regime/Environmental control	Key species	Reference publications
OBSEA	www.obsea.es	NW Mediterranean	20	Day-night variations	Abundant fauna (e.g., sparids, cephalopods) imaged since more than a decade	Marini et al. (2018); del Rio et al. (2020)
SmartBay	www.smartBay.ie	Western Atlantic	20	Day-night variations plus strong tides	Abundant fauna (e.g., Norway lobster, Cod, *Trisopterus*, cetacean) imaged and cross-checked *via* eDNA	Aguzzi et al. (2020e,c); Mirimin et al. (2021)
Acqua Alta	www.ismar.cnr.it/infrastrutture/piattaforma-acqua-alta	Northern Adriatic (Eastern Mediterranean)	15	Day-night variations plus weak tides	Abundant fauna (sparids, cephalopods and potentially invasive species)	Alberotanza et al. (2004)
*Shibenik	https://www.sibenik-meteo.com/podvodna-kamera	Central Adriatic (Eastern Mediterranean)	5	Day-night variations plus weak tides	Abundant fauna (sparids, cephalopods, tuna and marine turtles and potentially invasive species)	Aguzzi et al. (2020d)
*NEREA	–	Tyrrhenian Sea	650	Aphotic plus inertial currents	Abundant deep-sea fauna studied with different sampling methods in the past three decades	Fanelli et al. (2020)
*ANTARES	https://twitter.com/hashtag/BathyBot?src=hash	NW Mediterranean	3200	Aphotic plus inertial currents	Elusive deep-sea fauna in oligotrophic areas plus taxonomic composition of deep scattering layers	Chatzievangelou et al. (2021)
*NEMO	https://www.km3net.org/research/research-infrastructure/km3net-it-site/	Central Mediterranean	2300	Aphotic plus inertial currents	Elusive deep-sea fauna (e.g., sharks) in oligotrophic areas plus taxonomic composition of deep scattering layers	Aguzzi et al. (2017, 2019)
*Lovoten Vesterålen (LoVe) Ocean Observatory	https://love.statoil.com/	North Atlantic	100–2500	Disphotic and aphotic plus strong tides	Deep-sea abundant fauna (e.g., rockfish, crabs, shrimps, cold water corals, and cetaceans) imaged and since more than a decade	Osterloff et al. (2016); Nattkemper et al. (2019); Aguzzi et al. (2020a); Lopez-Vasquez et al. (2020); Zuazo et al. (2020)
*Mohn's Ridge, Fåvne vent field (EMSO-Mohn)	https://www.uib.no/en/noremso/140162/infrastructure#emso-mohn	North Atlantic, Greenland and Norwegian Seas	3050	Aphotic plus inertial currents	Deep-sea macro and mega fauna, small invertebrates and bacterial mat associated to hydrothermal vent field	
DELOS	https://www.delos-project.org/	Eastern Atlantic (off Angola)	1400	Oil field	Deep-sea macro and mega fauna	Bagley et al. (2007); Milligan et al. (2020)
VENUS (Strait of Georgia); Ocean Network Canada (ONC)	www.oceannetworks.ca	Northeast Pacific, Salish Sea	100–300	Inlet area with strong seasonal cycles in anoxia	Deep-water fauna (e.g., galatheids squat lobsters and flat fishes), other sessile species (e.g., anemone), zooplankton scattering layers and bacterial mat	Dewey et al. (2007); Ross and Lawson (2009); Aguzzi et al. (2011b); Matabos et al. (2011, 2015); Doya et al. (2015)
NEPTUNE (Barkley Canyon); Ocean Network Canada (ONC)	www.oceannetworks.ca	Northeast Pacific	420–990	Aphotic plus strong tides	Deep-sea abundant fauna (e.g., sablefish, rockfish, hagfish, tanner crab and cetaceans) imaged and since more than a decade	Best et al. (2007); Aguzzi et al. (2012; 2019; 2021a); Juniper et al. (2013); Doya et al. (2014, 2017); Matabos et al. (2014); Chatzievangelou et al. (2016, 2020); Seabrook et al. (2018, 2019)
MARS	https://www.mbari.org/at-sea/cabled-observatory/	North Pacific	891	Aphotic plus inertial currents	Deep-sea abundant fauna (e.g., fishes as sablefish and cephalopods), images and sounds	Yeh and Drazen (2011); Dunlop et al. (2018)
ALOHA	https://aco-ssds.soest.hawaii.edu/	North Pacific (Hawaii)	4800	Aphotic plus inertial currents	Deep-sea abundant fauna, images and sounds	Howe et al. (2011); Favali et al. (2015)

**Indicates those observatories that should be deployed and engaged in the near future.*

Laroche et al., 2020a). However, some studies have shown that samples from the water column are not a viable alternative to sediment samples for benthic diversity inventories (Brandt et al., 2021). Due to the patchiness of benthic fauna (Rosli et al., 2017), eDNA analysis of deep-sea sediment requires sampling of multiple biological replicates and larger samples sizes (Guardiola et al., 2016a,b; Atienza et al., 2020; Brandt et al., 2020). eDNA analysis of sediments may describe past rather than present communities, as sediments contain ancient DNA (aDNA) in addition to contemporary DNA, thus sediment eDNA analysis often targets the very top layer of sediment (Atienza et al., 2020; Brandt et al., 2020) and/or longer amplicons (e.g., COI – Leray et al., 2013).

In the present manuscript, we identify and discuss potential developments in the use of eDNA metabarcoding for deep-sea biodiversity assessment at cabled observatories and associated mobile platforms. Methodological developments are discussed in relation to: (i) Integrating eDNA with optoacoustic imaging; (ii) Development of eDNA repositories and cross-linking with other biodiversity databases; (iii) Artificial Intelligence (AI) for eDNA analyses and integration with imaging data; and (iv) Benefits of eDNA augmented observatories for the conservation and sustainable management of deep-sea biodiversity. We conclude by discussing the technical limitations and recommendations for future eDNA monitoring of the deep-sea.

Integrating Environmental DNA With Optoacoustic Imaging

Among the main benefits of using eDNA as a monitoring tool are the fact that it is an indirect non-invasive technique (i.e., no need to capture the target organism) and it does not require specialist taxonomic expertise to detect taxa across the tree of life (Goricki et al., 2017; Stefanni et al., 2018), though the latter strongly depends on availability of comprehensive reference DNA databases (as further discussed below). Once an environmental sample such as water, biofilm or sediment is acquired (Brandt et al., 2021), the collected eDNA can be queried either by using "universal" markers targeting whole communities by means of HTS (Jerde et al., 2019), or by targeted species-specific assays usually performed by real-time quantitative PCR (qPCR) or digital PCR (dPCR) (Goldberg et al., 2016). The effectiveness of both approaches depends on the availability of reference data, for taxonomy identification of sequenced reads with eDNA metabarcoding and for the development of species-specific assays with the targeted approach. These DNA-based tools offer several advantages over traditional techniques. They improve the ability to unravel the "hidden" biodiversity (e.g., detect rare, cryptic, elusive, and non-native species in the early stage of invasion), which is particularly relevant in the case of remote environments such as the deep-sea, and enable near real-time global census of species (Stat et al., 2017; LeBlanc et al., 2020).

Such features may enable the full integration of eDNA analysis into ecological monitoring procedures when its measurement is coupled with other non-molecular data as optoacoustic imaging (e.g., Stat et al., 2019; Easson et al., 2020; Mirimin et al., 2021). For this purpose, eDNA water sampling should also be provided in real-time by autonomous and independent samplers (e.g., Yamahara et al., 2019; Hansen et al., 2020; Jacobsen, 2021; Moore et al., 2021), with prototypes presently under construction (e.g., the Adjustable Volume eDNA Sampler[1], and the Robotic Cartridge Sampling Instrument-RoCSI[2]) or that can be adjusted for this purpose, as the SALSA system (Kersten et al., 2019; Brandt et al., 2021)[3]. An alternative to water samplers, would be an opportunistic use of filter feeding organisms such as sponges or bivalves, that act as natural "DNA traps," concentrating eDNA from water that can be retrieved at different time points (Mariani et al., 2019; Turon et al., 2020; Weber et al., 2021). The advantage of adding eDNA to ecological monitoring protocols is its ability to cross-validate data from other methodologies (e.g., imaging) (e.g., Aguzzi et al., 2019). On the other hand, it is reported that samples from the water column do not provide a good characterization of the underlying benthic taxa suggesting that benthic biodiversity surveys should be also performed (Antich et al., 2021b; Brandt et al., 2021). Seabed sediment acquisition technologies are continuously improved and optimized, so as to obtain more authentic and reliable samples to meet the ever-increasing demands on sampling capabilities (He et al., 2020) and adaptation to cabled observatory infrastructures.

Recent eDNA advancements allow us to study a wide range of taxa (including vertebrates) that are otherwise inaccessible by direct capture or optoacoustic technologies (e.g., Lacoursière-Roussel et al., 2018; Cowart et al., 2020; Laroche et al., 2020b; Canals et al., 2021). Though still limited to the near surface waters, the combined use of video-monitoring and eDNA metabarcoding has also been successfully applied using Baited Remote Underwater Video Systems (BRUVs) to monitor Marine Protected Areas (MPAs) (Stat et al., 2019) or integrated in cabled observatories (Mirimin et al., 2021). In these cases, taxa analyses were represented by visually conspicuous biota (mainly fish) and all post-sample collection steps were carried out off site in dedicated molecular laboratories. The way forward involves the integration and development of sampling methodology and sensing protocols adapted to operate on ROVs, AUVs and even biomimetic platforms (e.g., Aguzzi et al., 2021a), hence further expanding the sampling capability to most remote habitats while minimizing sampling disturbance (e.g., Trenkel et al., 2019).

Development of Environmental DNA Repositories and Cross-Linking With Other Biodiversity Databases

When identifying organisms, scientists can narrow down taxonomic possibilities thanks to the use of a single approach or, preferably, by combining and integrating multiple approaches, although a degree of uncertainty in taxa identification will always remain (Danovaro et al., 2020). In recent years, molecular tools have been integrated into classical morphology-based taxonomic approaches (e.g., Stefanni et al., 2021),

[1]https://twilightzone.whoi.edu/work-impact/technology/high-volume-edna-sampler/

[2]https://www.iatlantic.eu/imirabilis2-expedition/science/edna_sampling/

[3]https://wwz.ifremer.fr/gm_eng/Cruises-and-data/Years/Cruises-sheets/Welcome-to-the-blog-of-the-HERMINE-Cruise/Exploration-tools/SALSA

which has proven extremely useful in resolving the taxonomic status of cryptic species (e.g., Carreiro-Silva et al., 2017). However, in an ideal integrative taxonomy framework, different lines of evidence obtained at the genetic, physiological, morphological, behavioral, and habitat level should be considered and all combined within Hutchinson's (1957) multimodal niche (Schlick-Steiner et al., 2010).

Nowadays, most biodiversity data are recompiled into open-access online databases (Gemeinholzer et al., 2020). In the case of marine life, the most comprehensive database – the World Register of Marine Species (WoRMS) – is regularly updated by active communities of marine taxonomists (Costello et al., 2013). Building on this foundation, the World Register of Deep-Sea Species (WoRDSS; Glover et al., 2021), a taxonomic database of deep-sea species, was launched in 2012 by the International Network for Scientific Investigation of Deep-sea Ecosystems (INDEEP). This database also includes the global-scale trait database for the fauna of deep-sea hydrothermal-vents, the sDiv-funded trait database for the Functional Diversity of vents (sFDvent; Chapman et al., 2019). These inventories are exclusively based on records of collected organisms. In parallel, genetic and genomic databases have been implemented, that are either inclusive as in the case of GenBank (Clark et al., 2016) or BOLD (Ratnasingham and Hebert, 2013), or restricted to selected groups of organisms, such as MZGdb (Bucklin et al., 2021), PR2 (Guillou et al., 2013) and PLANiTS (Banchi et al., 2020).

As in conventional DNA barcoding, eDNA sequences are usually compared with a reference database of the expected species community to translate the obtained molecular operational taxonomic units into biological species for the final data interpretation. These matching processes are reliable when based on a comprehensive reference library supported by morphological description of the reference taxon. However, such reference databases are still far from complete, especially for deep-sea communities (Weigand et al., 2019). Additionally, misidentifications of reference sequences have been frequently reported, highlighting the need of refinement and curation of these databases to reduce false negatives, and conflicts in taxonomic assignment (Stefanni et al., 2018; Schroeder et al., 2020; Bucklin et al., 2021).

The performance of eDNA in providing accurate estimates of species' diversity by matching different genetic repositories, has also been tested. For example, fishes are both a frequent target in eDNA studies and widely represented in genetic repositories by multi-marker sequences. Recently, the performance of eDNA from surface water samples in determining fish diversity, was evaluated by a comparing it to bottom trawl catches (Stoeckle et al., 2021). Fish diversity estimation obtained by eDNA was equal to, or greater than, that obtained from a single 66 million liters trawl. Most (70–87%) species detected by trawl in a given month were also detected by eDNA, and *vice versa*, including nearly all (92–100%) abundant species (Stoeckle et al., 2021). For a more comprehensive assessment of the local biodiversity including benthic taxa (from metazoans to protist and prokaryotic communities), eDNA from sediment should also be analyzed as only a fraction of total molecular clusters is shared between the eDNA of these two environmental matrices (Atienza et al., 2020; Zhao et al., 2020; Brandt et al., 2021). Furthermore, meiofauna, micro-eukaryotes, and bacteria constitute a large portion of deep-sea abundance and biomass and should not be neglected (Rex et al., 2006; Ingels et al., 2021). Even if these small-size organisms cannot be taxonomically identified due to lack of appropriate reference databases, their contribution to biodiversity can still be evaluated with taxonomy-free approaches (Cordier et al., 2019b).

The improvement of existing marine genetic databases and the development of portals exclusively dedicated to eDNA sequences are considered priorities for global biodiversity assessment and for filling taxonomic and spatial gaps in bio-surveys (Berry et al., 2021). Early initiatives have already been undertaken worldwide to integrate eDNA into biodiversity databases that provide accurate spatial information on aquatic species occurrence based solely on eDNA records collected according to standardized protocols (e.g., United States, New Zealand, and Sweden) (Young et al., 2018; DFO, 2020; Sundberg et al., 2020; Abbott et al., 2021). Integrating dedicated eDNA sequence repositories with high-resolution imaging or other attributes collected *in situ* (e.g., sound generated by animals; Mooney et al., 2020) can maximize the identification of species together with spatial and temporal resolution (e.g., Bicknell et al., 2016; Howell et al., 2019; Horton et al., 2021; Mirimin et al., 2021). Such integrated open-access online biodiversity databases can further enable a putative taxonomic identification of species detected (as particular OTUs), but not identified by eDNA. If the closest taxonomic match for eDNA sequences is below the percentage that would allow species-level identification, a putative identification of the sequence in question could be made using image or sound identifications taken along, at least until a specimen is collected and properly examined and a reference sequence record deposited for future use. This would provide information on what to expect in future biodiversity inventories in a given remote area.

A further step toward integration of marine biodiversity data repositories has been provided by BOLD, which contains open access records of organisms (including imaging) tagged with one or more standardized short DNA genetic markers (Ratnasingham and Hebert, 2007, 2013). A further step toward integrating marine biodiversity data repositories could be the creation of a single open access platform where data of different origins and typologies (including eDNA markers) are freely searchable (as in the case of the Global Biodiversity Information Facility, GBIF) (Andersson et al., 2020; Heberling et al., 2021). These database platforms have begun to include eDNA records as a new type of biological observation that can be accessed alongside millions of conventional biodiversity records (Berry et al., 2021). The development of AI algorithms (as indicated in the previous section) can facilitate better operational cross-linking between *in situ* eDNA data and other complementary data (e.g., temperature, pH, current, and etc.). These "Big Data" analyses could be fully embedded into cabled observatories protocols for autonomous data processing to

provide reliable spatiotemporal assessment of biodiversity in almost near real time.

Artificial Intelligence for Environmental DNA Analyses and Integration With Imaging Data

The step forward to efficiently augment the *in situ* deep-sea ecological monitoring capability of cabled observatories and their docked platforms envisions the ability to collect genetic and imaging data *in situ* and process the information in real time using automated pipelines (e.g., Osterloff et al., 2016, 2019; Lopez-Vasquez et al., 2020; Zuazo et al., 2020). These developments rely on the establishment of AI algorithms for taxonomic assignment as well as dedicated reference DNA sequence databases.

The fully automated integration of eDNA and imaging data represents one of the core development aspects to augment the monitoring capability of deep-sea biodiversity at cabled observatories, enabling the detection of organisms over a wide range of taxa and different body sizes when it comes to fishes. Currently, there are several initiatives to automate *in situ* eDNA analyses in near real time (Scholin et al., 2017; Ribeiro et al., 2019; Yamahara et al., 2019). Integration of eDNA and imaging data involves the development of appropriate pipelines for: (i) automatic taxonomic identification of eDNA sequences to the highest level (e.g., species); and (ii) cross-check of eDNA taxonomic identification with large image repositories, accounting for a multi-annual status of local richness and biodiversity (i.e., based on species tracking and classification, resulting in time series of data on community structure as well as relative abundance). Both steps can be implemented by applying AI algorithms using Machine Learning (ML) methods.

Analysis of eDNA metabarcoding data using ML methods is a new and developing field. There are two main approaches in the use of ML methods for biodiversity monitoring, and while one operates on taxonomically assigned OTUs, the other is taxonomy-free, where there is no longer the need of a reference database, thus overcoming the limits of taxonomy-based eDNA bioassessment (Cordier et al., 2018). Such taxonomy-free approach still requires "training" data sets in order to feed into predictive models that can be used to make inference on previously unexplored taxa (Cordier et al., 2018).

Cordier et al. (2017) focused on the problem of lacking inventories for eDNA data from benthic foraminifera and showed that supervised ML approaches (i.e., random-forests and self-organizing-maps) can classify unknown sequences and infer biotic indices of macro-invertebrates reasonably well. They argued that ML makes good predictions and outperforms analyses based only on known sequences (Cordier et al., 2018).

Machine learning tools are currently part of many pipelines for eDNA data analysis. Dully et al. (2021a; 2021b) showed that ML-based pipelines are sufficiently robust even for rarefied samples. Other authors reached similar conclusions (Cordier et al., 2019a; Apothéloz-Perret-Gentil et al., 2021; Frühe et al., 2021; He et al., 2021) and Mathon et al. (2021) reviewed literature on "eDNA and Machine Learning." In ML analysis, data is first pre-processed with common bioinformatic pipelines as for general metabarcoding analysis (Mathon et al., 2021) and subsequently processed through an automated DNA-Barcode Classifier (taxonomy assignment). ML supports this classification task with a consolidated pipeline. Sequences contained in DNA-barcode repositories (e.g., GenBank, GB; Barcoding of Life Database, BOLD) are first used to train a ML-based classifier (e.g., Cordier et al., 2017, 2019a; Frühe et al., 2021). The trained classifier is then ready to identify the taxa contained in the sample. We prospect, that in the framework of cabled observatories further assessment of the identification results could be obtained by cross-checking the eDNA taxonomy classification with organism identified through video/image data analysis. In this case, images have to be acquired contextually to eDNA sampling and a content-based image classification have to be performed in order to classify the framed organisms (e.g., fishes).

Applied underwater image classification based on ML demonstrated to provide high quality results (Langenkämper et al., 2020; Lopez-Vasquez et al., 2020; Malde et al., 2020; Mathur et al., 2020). The ML-based image classifier needs to be trained from an image ground-truth dataset. Then, the taxa of the classified specimens can be compared with those returned by the eDNA classifier. The diagram in **Figure 1** shows a conceptual pipeline for handling the eDNA data and image cross-check.

Benefits of Using Environmental DNA-Augmented Observatories for the Conservation and Sustainable Management of Deep-Sea Biodiversity

Achieving conservation and sustainability goals through ecosystem-based management is challenging, particularly for deep-sea ecosystems, as lack of knowledge hinders science-based prioritization of appropriate management and conservation strategies (Glover et al., 2018; Howell et al., 2020; Manea et al., 2020). Cabled observatories have already been recognized as key tools capable of filling knowledge gaps through systematic monitoring (Danovaro et al., 2017a; Aguzzi et al., 2020a,b, 2021b). Integration eDNA surveillance within the monitoring capabilities offered by cabled observatories makes them even more promising (Mirimin et al., 2021). Indeed, eDNA has been highlighted as a key approach that will enable conservation managers and marine spatial planners to detect target species for conservation, provide biotic indexes for impact assessment, increase the spatio-temporal capability of biodiversity surveys, and map vulnerable deep-sea species or ecosystems (Aylagas et al., 2014; Pawlowski et al., 2018; Bani et al., 2020; Kutti et al., 2020). Another value of eDNA augmented cable observatories is their potential contribution to two synergistic global initiatives addressing monitoring of the marine environment: The Essential Ocean Variables (EOVs), supported by the Global Ocean Observing System (GOOS); the Essential Biodiversity Variables (EBVs), developed by the Group on Earth

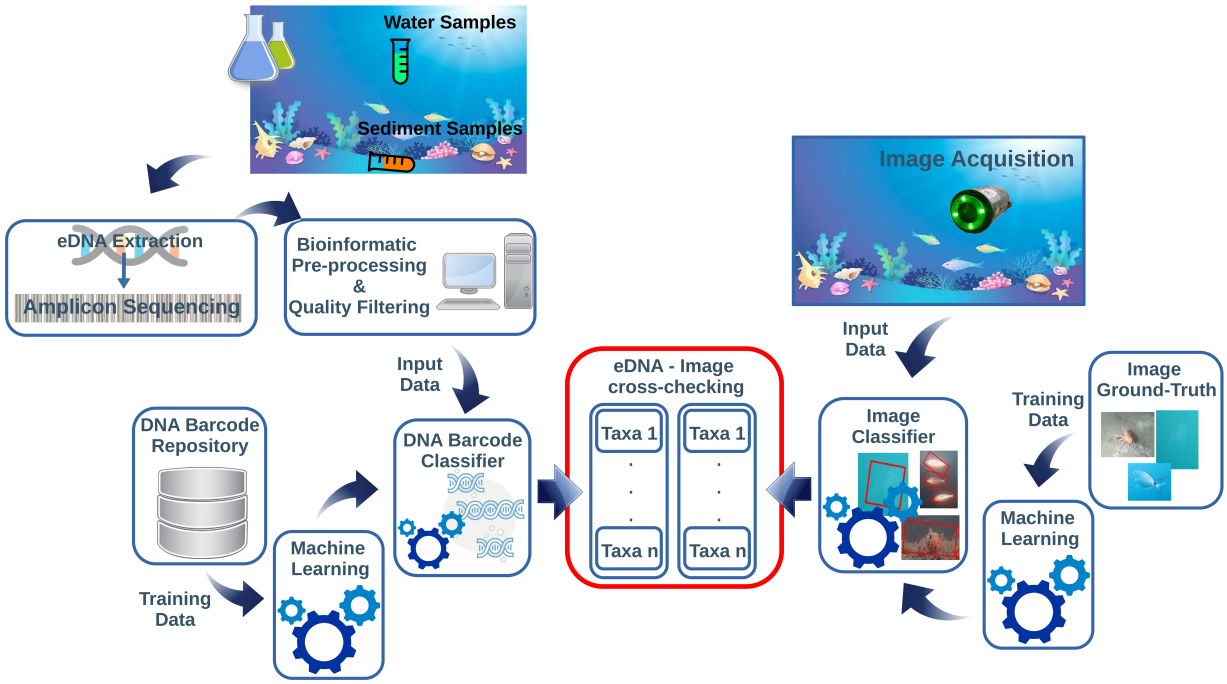

FIGURE 1 | This diagram is summarizing the main steps of the pipeline for eDNA and imaging data integration. The eDNA is collected from the water or sediment and processed through metabarcoding protocols. This step includes several bioinformatics pre-processing actions before going through an automated DNA-barcode classifier pipeline. The images acquired on cameras contextually to eDNA sampling are post-processed through an image classifier routine. Both protocols need independent reference repositories to train the ML classifiers before the cross-checking of the taxonomic assignments derived from eDNA and images.

Observations Biodiversity Observation Network (GEOBON) (Pereira et al., 2013; Bax et al., 2018). These two frameworks are being developed to inform global policies and sustainability strategies, and produce comparable and integrated data through harmonization of monitoring (Canonico et al., 2019; Jetz et al., 2019).

Addressing conservation priorities in the deep sea, and monitoring the level of effectiveness of conservation measures are critical steps. The use of eDNA analyses has been recently extended to biodiversity assessment in the context of deep-seabed mining of polymetallic nodules to guide management of this deep-sea resource exploitation that is foreseen to have one of the highest environmental impacts in the near future (Wedding et al., 2015; Laroche et al., 2020a; Leray and Machida, 2020), being also suggested as a cost-effective method (Le et al., 2021). The performance of this high throughput approach has also been tested in impact assessment of offshore oil and gas drilling and extraction (Laroche et al., 2018), and in fish stock assessment to inform fishery management (Salter et al., 2019).

DNA-based tools coupled with cabled observatories and supported by visual and acoustic census can enhance monitoring capability within MPAs, as it has been tested in recent biodiversity assessments (Stat et al., 2019; Gold et al., 2021). Such an approach would be greatly beneficial to the monitoring of Large Scale Marine Protected Areas (LSMPAs). LSMPAs are greater than 150,000 km^2 and may encompass critical habitats for migratory species (Lewis et al., 2017), but monitoring such areas is challenging if not impractical (O'Leary et al., 2018).

Furthermore, boosting knowledge of deep-sea biodiversity would help in the prioritization of deep-sea areas of conservation. The Ecologically and Biologically Significant Marine Areas (EBSAs) have been previously proposed to focus attention on where and what type of conservation measures could be established in offshore and deep-sea areas, including the designation of new MPAs (Ardron et al., 2009; Portman et al., 2013; Johnson et al., 2018). However, many potential EBSAs have been removed from the original list due to insufficient knowledge needed to inform the selection criteria, and a call has been made to strengthen scientific research in these areas (Johnson et al., 2019). Both LSMPAs and EBSAs initiatives are hindered by the absence of concrete knowledge of connectivity within and between regions (Cannizzo et al., 2021), as well as by the challenge of describing the links between ocean depths and the fundamental bentho-pelagic coupling (Johnson et al., 2018; O'Leary and Roberts, 2018) – these issues might be resolved by eDNA augmented observatories applying metaphylogeography tools for the analysis within OTUs connectives (Turon et al., 2019; Antich et al., 2021a).

Finally, in response to the urgency to increase knowledge of deep-sea ecosystems and manage deep-sea resources in a scientifically sound manner, the Deep Ocean Observing Strategy

(DOOS) has been established to coordinate monitoring and observing efforts. As part of this strategy, genetic studies have been identified as key knowledge sources for biodiversity and connectivity assessment (Baco et al., 2016; Levin et al., 2019), as well as prioritizing the need of defining deep-sea ecological variables to feed global monitoring frameworks (Danovaro et al., 2020).

Technical Limitations and Steps Forward for Environmental DNA Monitoring in the Deep-Sea

While underwater imaging in deep-sea cabled observatories is usually used to detect and identify big to medium sized animals, advantages in image processing and pattern recognition have also made it possible to automatically or semi-automatically identify zooplankton (Gorsky et al., 2010). Zooplankton imaging instruments have gone beyond just laboratory bench-top application (e.g., ZooScan) and now allow in-flow onboard counting and classification (e.g., ZooCAM; Colas et al., 2018) or are mounted on AUVs (Ohman et al., 2018) or even integrated into shallow water cabled observatories (the COSYNA-AWIPEV observatory in the Kongsfjorden Arctic fjord system and the COSYNA-Helgoland observstory; Fischer et al., 2020). It is prospected that similar imaging systems could be integrated into deep-sea cabled observatories for imaging of mero-planktonik larvae. Future modification of such systems could be used to analyse meiobenthos (e.g., FlowCAM; Kitahashia et al., 2018) or benthos could also be studied with the assistance of Sediment Profiling Imaging (SPI) systems.

Despite the rapid and widespread adoption of eDNA metabarcoding analysis for species identification, limitations still exist, and are the subject of much active research. Sequence length constrains imposed by HTS technology may contribute to the detection of false positives, when the target species is absent but its DNA, or rather the DNA of a close match, is recovered. Moreover, primer biases may generate false negatives, i.e., species that are not detected even though they are present. These limitations have been carefully evaluated but only partially overcome (Taberlet et al., 2012; Cristescu and Hebert, 2018 and references therein). Strategies to address such limitations can be intrinsic to the eDNA approach, e.g., the use of multiple markers, (Stefanni et al., 2018; Liu and Zhang, 2021), capture by hybridization approach (Günther et al., 2021), or long reads sequencing (Davidov et al., 2020) but it is also expected that this will improve with the integration of multidisciplinary survey approaches (e.g., combining imaging with eDNA).

Although ML methods (see previous section) could provide valuable tools to reduce errors, their application presents some difficulties. ML methods require *ad hoc* training sets of sequences and images, that are used as benchmark data repositories to reduce problems with taxonomy assignments of sequences, such as in the cases of: (i) false positives, when incorrect species are assigned to certain sequences based on sequence similarity with a close match; and (ii) rarity or endemism, when eDNA sequences match species that are not detected by video or in the historical records of the area. The above-mentioned data gaps and erroneous entries in genetic repositories are another source of uncertainty for classifier algorithms. ML methods are capable to solve these issues by using existing datasets and generating multiple species trees based on a percentage of similarities. Moreover, by applying the Lowest Common Ancestor (LCA) algorithm, ML can still identify unassigned sequences whose taxonomy is deficient due to the lack of reference sequences deposited in publicly accessible repositories. A different ML based methodology involves the taxonomy-free approach, where bio-monitoring information is obtained through the treatment of data obtained from DNA sequencing without taxonomic assignment (Apothéloz-Perret-Gentil et al., 2017; Feio et al., 2020). The main limits of this approach are the possibility to the under-sampling the input data and the need to calibrate the used bio-index (Apothéloz-Perret-Gentil et al., 2017).

The discovery and implementation of new barcoding markers will be necessary to address low resolution power of existing markers in taxa characterized by exceptionally low rates of mitochondrial evolution (e.g., anthozoans; Hebert et al., 2003) or recently diverged species (e.g., cypraeid marine gastropods; Meyer and Paulay, 2005). A solution may be found in complementing short read amplicon sequencing with sequencing technologies (ONT, PacBio) capable of longer read lengths (e.g., full genes or even mitogenomes). The development of such approaches could indeed be facilitated by integration with video/image data analysis and reference sequence repositories to further enhance species level identification capabilities.

Further technological limitations for eDNA methodology derive from knowledge gaps regarding the persistence and transport of eDNA (Collins et al., 2018; Murakami et al., 2019), which are largely unexplored in deep-sea environments. Persistence of eDNA in the marine environment can be assessed according to specific seascape properties of the sampled water mass, which can be easily measured by cabled observatories multiparametric habitat sensors assets (Aguzzi et al., 2010). eDNA decay involves multiple processes, including cellular, microbial degradation, and also spontaneous degradation of DNA caused and/or accelerated by UV, temperature, and pH (Collins et al., 2018; Harrison et al., 2019; Hunter et al., 2019). Furthermore, the spatial coverage of species detection by eDNA depends on local hydrodynamics (i.e., strength and direction of currents), which affects the dispersal and transport of molecules from neighboring areas (Harrison et al., 2019). The combined action of oceanographic and biogeochemical variables should be carefully considered when inferring the temporal and spatial coverage of the information provided by eDNA markers (Harrison et al., 2019), and taken into account in sampling design and collection.

Spatiotemporal coverage of environmental data collected by networks of observatories provides a unique opportunity to define optimized eDNA sampling strategies, in terms of the best timing for seawater collection based on eDNA persistence

and passive dispersion in the local marine environment (i.e., as a "molecular connectivity"). This may be even further aided by continuous multiparametric data collection and increasing knowledge of environmental conditions favoring eDNA detection. Data integration, performed for example with Lagrangian models of eDNA dispersal (Andruszkiewicz et al., 2019), can form the basis for innovative sampling scenarios (e.g., timing and repetition of sampling depending un current status). In this way, the spatial and temporal distribution of a species across a given area could be predicted even before planning the eDNA sampling, based on the status of a combined set of local environmental factors (e.g., currents, temperature, and nutrients), complemented by video-counts of target species (see previous section).

Some examples of time-strategies for eDNA sampling that would benefit from this approach include: (i) pre-programming continuous or time-lapse sampling based on modeled, forecasted environmental conditions; (ii) pre-programming surveillance approaches based on real-time remote sampling that is activated only when a predefined set of conditions is met (e.g., within a range of current intensity, pH, temperature, or while the camera is activated); and (iii) synchronous sampling over large areas (by multiple samplers) thanks to the network of IOVs operating away from the cabled observatories.

Final Remarks

There is an impending need for the laying out of a roadmap for the effective collection and synthesis of high-quality deep-sea biodiversity data to fill knowledge gaps required for policy decisions and environmental management (Levin et al., 2020). This requires the identification of (i) consensus biodiversity variables to be monitored, and (ii) adequate and harmonized methods for their monitoring and assessment.

While optoacoustics can help generate baseline data on some taxa and their size and relative abundance, integration of DNA-based approaches (Scholin, 2010) can provide precise taxonomic information on species richness, including their response to shifts in local environmental conditions. In particular, eDNA metabarcoding allows augmented monitoring of biodiversity because it has the potential to detect organisms across the tree of life. It can be used for a variety of studies, from detecting invasive species to measuring the impact of human activities on ecosystems.

Integration of datasets obtained from eDNA, images, and other sources such as sound, can now be almost completely automated thanks to ML algorithms. Several existing coastal and deep-sea cabled observatories can host pilot studies. For those that have been in operation for many years, long-term time series of biological, and environmental data in different ecological contexts are already available hence providing solid baseline datasets (**Table 1**). Some of these observatories have already started to experiment with inclusion of long-term images acquisition and eDNA analyses, while others are planning to include eDNA surveys in the future. Cabled observatories and the network of IOVs operating from these platforms augmented by eDNA sensors could not only provide a framework to evaluate the effectiveness of eDNA protocols *in situ*, but could more importantly improve our knowledge on deep-sea biodiversity at an unprecedented spatial and temporal dimension. Under this vision, eDNA augmented observatories provide unprecedented opportunities to fill knowledge gaps on deep-sea biodiversity and ecosystem functioning, thus supporting monitoring and conservation strategies and contributing to the decade of deep-sea exploration that is now upon us.

AUTHOR CONTRIBUTIONS

SS, LM, JA, and SM conceptualized and proposed the idea. SS and LM provided background knowledge to molecular technology and sequencing. LB, EM, and AG provided background knowledge to international conservation and management initiatives. DS and MM provided background knowledge to genetic databanks and bioinformatics. SM and FB provided background knowledge to imaging data analysis and machine learning methods. JA, FD, NC, JR, DC, and SS provided background knowledge to technology development. All authors contributed to the writing and finalization of the manuscript.

FUNDING

This research has been funded within the framework of the following project activities: ARIM (Autonomous Robotic Sea-Floor Infrastructure for Benthopelagic Monitoring; MarTERA ERA-Net Cofound); RESBIO (TEC2017-87861-R; Ministerio de Ciencia, Innovación y Universidades); JERICO-S3: (Horizon 2020; Grant Agreement no. 871153); ENDURUNS (Research Grant Agreement H2020-MG-2018-2019-2020 n.824348); Slovenian Research Agency (Research Core Funding Nos. P1-0237 and P1-0255 and project ARRS-RPROJ-JR-J1-3015). We also profited of the funding from the Spanish Government through the "Severo Ochoa Centre of Excellence" accreditation (CEX2019-000928-S) and Italian Ministry of Education (MIUR) under the "Bando premiale FOE 2015" (nota prot. N. 850, dd. 27 ottobre 2017) with the project EarthCruisers "EARTH's CRUst Imagery for Investigating Seismicity, Volcanism, and Marine Natural Resources in the Sicilian Offshore". Ocean Networks Canada was funded through Canada Foundation for Innovation-Major Science Initiative (CFI-MSI) fund 30199.

ACKNOWLEDGMENTS

JA, JR, and DC are members of the Research Unit Tecnoterra (ICM-CSIC/UPC), providing the conceptual framework for technological development applied to ecosystem remote, autonomous, and long-lasting multidisciplinary monitoring. The authors wish to thank the two reviewers whose work has greatly improved the manuscript.

REFERENCES

Abbott, C., Coulson, M., Gagné, N., Lacoursière-Roussel, A., Parent, G. J., Bajno, R., et al. (2021). *Guidance on the Use of Targeted Environmental DNA (eDNA) Analysis for the Management of Aquatic Invasive Species and Species at Risk*. Available online at: https://www.dfo-mpo.gc.ca/csas-sccs/Publications/ResDocs-DocRech/2021/2021_019-eng.html

Afzali, S.F., Bourdages, H., Laporte, M., Mérot, C., Normandeau, E., Audet, C., Bernatchez, L. (2020). Comparing environmental metabarcoding and trawling survey of demersal fish communities in the Gulf of St. Lawrence, Canada. *Environmental DNA* 3, 22-42.

Agostini, M., Böemer, M., Bosma, J., Clark, K., and Danninger, M. (2020). The pacific neutrino experiment. *Nat. Astron.* 4, 913–915. doi: 10.1038/s41550-020-1182-4

Aguzzi, J., Albiez, J., Flögel, S., Rune, Godø, O., Grimsbø, E., et al. (2020a). A flexible autonomous robotic observatory infrastructure for bentho-pelagic monitoring. *Sensors* 20:1614. doi: 10.3390/s20061614

Aguzzi, J., Chatzievangelou, D., Francescangeli, M., Marini, S., Bonofiglio, F., del Rio, J., et al. (2020b). The hierarchic treatment of marine ecological information from spatial networks of benthic platforms. *Sensors* 20:1751. doi: 10.3390/s20061751

Aguzzi, J., Chatzievangelou, D., Company, J. B., Thomsen, L., Marini, S., Bonofiglio, F., et al. (2020c). Fish-stock assessment using video imagery from worldwide cabled observatory networks. *ICES J. Mar. Sci.* 77, 2396–2410. doi: 10.1093/icesjms/fsaa169

Aguzzi, J., López-Romero, D., Marini, S., Costa, C., Berry, A., Chumbinho, R., et al. (2020e). Multiparametric monitoring of fish activity rhythms in an Atlantic coastal cabled observatory. *J. Mar. Syst.* 212:103424. doi: 10.1016/j.jmarsys.2020.103424

Aguzzi, J., Iveša, N., Gelli, M., Costa, C., Gavrilovic, A., Cukrov, N., et al. (2020d). Ecological video monitoring of marine protected areas by underwater cabled surveillance cameras. *Mar. Policy* 119:104052. doi: 10.1016/j.marpol.2020.104052

Aguzzi, J., and Company, J. B. (2010). Chronobiology of deep-water decapod crustaceans on continental margins. *Adv. Mar. Biol.* 58, 155–225. doi: 10.1016/B978-0-12-381015-1.00003-4

Aguzzi, J., Chatzievangelou, D., Marini, S., Fanelli, E., Danovaro, R., Flögel, S., et al. (2019). New high-tech interactive and flexible networks for the future monitoring of deep-sea ecosystems. *Environ. Sci. Technol.* 53, 6616–6631. doi: 10.1021/acs.est.9b00409

Aguzzi, J., Company, J. B., Costa, C., Matabos, M., Azzurro, E., Mànuel, A., et al. (2012). Challenges to assessment of benthic populations and biodiversity as a result of rhythmic behaviour: video solutions from cabled observatories. *Oceanogr. Mar. Biol. Annu. Rev.* 50, 235–286.

Aguzzi, J., Company, J. B., Costa, C., Menesatti, P., Garcia, J. A., Bahamon, N., et al. (2011a). Activity rhythms in the deep-sea: a chronobiological approach. *Front. Biosci.* 16, 131–150. doi: 10.2741/3680

Aguzzi, J., Costa, C., Robert, K., Matabos, M., Antonucci, F., Juniper, K., et al. (2011b). Automated image analysis for the detection of benthic crustaceans and bacterial mat coverage using the VENUS undersea cabled network. *Sensors* 11, 10534–10556. doi: 10.3390/s111110534

Aguzzi, J., Costa, C., Furushima, Y., Chiesa, J. J., Company, J. B., Menesatti, P., et al. (2010). Behavioral rhythms of hydrocarbon seep fauna in relation to internal tides. *Mar. Ecol. Prog. Ser.* 418, 47–56. doi: 10.3354/meps08835

Aguzzi, J., Fanelli, E., Ciuffardi, T., Schirone, A., Craig, G., The, N. E. M. O., et al. (2017). Inertial bioluminescence rhythms at the central mediterranean KM3NeT deep-sea neutrino telescope. *Sci. Rep.* 7:44938. doi: 10.1038/srep44938

Aguzzi, J., Flögel, S., Marini, S., Thomsen, L., Lbiez, J., Weiss, P., et al. (2021a). Developing technological synergies between deep-sea and space research. *Elementa*. (in press).

Aguzzi, J., Nixon, B., O'Malley, C., Berry, A., Gaughan, P., Doyle, J., et al. (2021b). Burrow emergence rhythms of Nephrops norvegicus: UWTV, surveying biases and novel technological scenarios. *ICES Sci. Rep.* 3, 15–17. doi: 10.1038/s41598-021-85240-3

Aguzzi, J., Sbragaglia, V., Tecchio, S., Navarro, J., and Company, J. B. (2015). Rhythmic behaviour of marine benthopelagic species and the synchronous dynamics of benthic communities. *Deep Sea Res. I* 95, 1–11. doi: 10.1016/j.dsr.2014.10.003

Alberotanza, L., Chiggiato, J., and Profeti, G. (2004). Analysis of the seasonal stratification at the Acqua Alta Oceanographic Tower, northern Adriatic Sea. *Int. J. Remote Sens.* 25, 1473–1480. doi: 10.1080/01431160310001592472

Andersson, A. F., Bissett, A., Finstad, A., Fossøy, F., Grosjean, M., Hope, M., et al. (2020). *Publishing DNA-Derived Data Through Biodiversity data Platforms [Community Review Draft]*. Copenhagen: GBIF Secretariat.

Andruszkiewicz, E. A., Koseff, J. R., Fringer, O. B., Ouellette, N. T., Lowe, A. B., Edwards, C. A., et al. (2019). Modeling environmental DNA transport in the coastal ocean using Lagrangian particle tracking. *Front. Mar. Sci.* 6:477. doi: 10.3389/fmars.2019.00477

Antich, A., Palacín, C., Cebrian, E., Golo, R., Wangensteen, O. S., and Turon, X. (2021a). Marine biomonitoring with eDNA: can metabarcoding of water samples cut it as a tool for surveying benthic communities? *Mol. Ecol.* 30, 175–3188. doi: 10.1111/mec.15641

Antich, A., Palacin, C., Wangensteen, O. S., and Turon, X. (2021b). To denoise or to cluster, that is not the question: optimizing pipelines for COI metabarcoding and metaphylogeography. *BMC Bioinformatics* 22:177. doi: 10.1186/s12859-021-04115-6

Apothéloz-Perret-Gentil, L., Bouchez, A., Cordier, T., Cordonier, A., Guéguen, J., Rimet, F., et al. (2021). Monitoring the ecological status of rivers with diatom eDNA metabarcoding: a comparison of taxonomic markers and analytical approaches for the inference of a molecular diatom index. *Mol. Ecol.* 30, 2959–2968. doi: 10.1111/mec.15646

Apothéloz-Perret-Gentil, L., Cordonier, A., Straub, F., Iseli, J., Esling, P., and Pawlowski, J. (2017). Taxonomy-free molecular diatom index for high-throughput eDNA biomonitoring. *Mol. Ecol. Resour.* 17, 1231–1242. doi: 10.1111/1755-0998.12668

Ardron, G., Dunn, D., Corrigan, C., Gjerde, K., Halpin, P., Rice, J., et al. (2009). "Defining ecologically or biologically significant areas in the open oceans and deep seas: Analysis, tools, resources and illustrations," in *Proceedings of the Convention on Biological Diversity Expert Workshop on Scientific and Technical Guidance on the Use of Biogeographic Classification Systems and Identification of Marine Areas Beyond National Jurisdiction in Need of Protection*, Ottowa, CA.

Atienza, S., Guardiola, M., Præbel, K., Antich, A., Turon, X., and Wangensteen, O. S. (2020). DNA metabarcoding of deep-sea sediment communities using COI: community assessment, spatio-temporal patterns and comparison with 18S rDNA. *Diversity* 12:123. doi: 10.3390/d12040123

Aylagas, E., Borja, Á, and Rodríguez-Ezpeleta, N. (2014). Environmental status assessment using DNA metabarcoding: towards a genetics based marine biotic index (gAMBI). *PLoS One* 9:e90529. doi: 10.1371/journal.pone.0090529

Aymà, A., Aguzzi, J., Canals, M., Lastras, G., Bahamòn, N., Mecho, A., et al. (2016). Behavioural observations of deep-water fauna in submarine canyons of the Northwestern Mediterranean Sea. *Deep Sea Res. I* 114, 149–159. doi: 10.1016/j.dsr.2016.05.013

Baco, A. R., Etter, R. J., Ribeiro, P. A., von, der Heyden, S., Beerli, P., et al. (2016). A synthesis of genetic connectivity in deep-sea fauna and implications for marine reserve design. *Mol. Ecol.* 25, 3276–3298. doi: 10.1111/mec.13689

Bagley, P. M., Smith, K., Bett, B., Priede, I. G., Rowe, G., Clarke, J., et al. (2007). "Deep-ocean Environmental Long-term Observatory System (DELOS): long-term (25 year) monitoring of the deep-ocean animal community in the vicinity of offshore hydrocarbon operations," in *Proceedings of the OCEANS 2007 - Europe, VOLS 1-3*, (Piscataway, NJ: IEEE Press). doi: 10.1109/OCEANSE.2007.4302250

Bailly, N., Beddard, J., Bömer, M., Bosma, J., and Brussow, D. (2021). Two-year optical site characterization for the Pacific Ocean Neutrino Experiment (P-ONE) in the Cascadia Basin. *Eur. Phys. J. C.* 81:1071. doi: 10.1140/epjc/s10052-021-09872-5

Banchi, E., Ametrano, C. G., Greco, S., Stanković, D., Muggia, L., and Pallavicini, A. (2020). PLANiTS: a curated sequence reference dataset for plant ITS DNA metabarcoding. *Database* 2020:baz155. doi: 10.1093/database/baz155

Bani, A., De Brauwer, M., Creer, S., Dumbrell, A. J., Limmon, G., Jompa, J., et al. (2020). Informing marine spatial planning decisions with environmental DNA. *Adv. Ecol. Res.* 62, 375–407. doi: 10.1016/bs.aecr.2020.01.011

Barnes, M. A., and Tuner, C. R. (2016). The ecology of environmental DNA and implications for conservation genetics. *Conserv. Genet.* 17, 1–17. doi: 10.1007/s10592-015-0775-4

Bax, N. J., Appeltans, W., Brainard, R., Duffy, J. E., Dunstan, P., Hanich, Q., et al. (2018). Linking capacity development to GOOS monitoring networks to achieve sustained ocean observation. *Front. Mar. Sci.* 5:346. doi: 10.3389/fmars.2018.00346

Benson, D. A., Cavanaugh, M., Clark, K., Karsch-Mizrachi, I., Lipman, D. J., Ostell, J., et al. (2013). GenBank. *Nucleic Acids Res.* 41, D36–D42. doi: 10.1093/nar/gks1195

Berry, O., Jarman, S., Bissett, A., Hope, M., Paeper, C., Bessey, C., et al. (2021). Making environmental DNA (eDNA) biodiversity records globally accessible. *Environ. DNA* 3, 699–705. doi: 10.1002/edn3.173

Berry, T. E., Saunders, B. J., Coghlan, M. L., Stat, M., Jarman, S., and Richardson, A. J. (2019). Marine environmental DNA biomonitoring reveals seasonal patterns in biodiversity and identifies ecosystem responses to anomalous climatic events. *PLoS Genet*. 2019:e1007943. doi: 10.1371/journal.pgen.1007943

Best, M. M., Bornhold, B. D., Juniper, S. K., and Barnes, C. R. (2007). NEPTUNE Canada regional cabled observatory: science plan. *Sea Technol.* 49, 10–14. doi: 10.1109/OCEANS.2007.4449316

Bicknell, A. W., Godley, B. J., Sheehan, E. V., Votier, S. C., and Witt, M. J. (2016). Camera technology for monitoring marine biodiversity and human impact. *Front. Ecol. Environ.* 14:424–432. doi: 10.1002/fee.1322

Brandt, A., Gutt, J., Hildebrandt, M., Pawlowski, J., Schwendner, J., Soltwedel, T., et al. (2016). Cutting the umbilical: new technological perspectives in benthic deep-sea research. *J. Mar. Sci. Eng.* 4:36. doi: 10.3390/jmse4020036

Brandt, M. I., Pradillon, F., Trouche, B., Henry, N., Liautard-Haag, C., Cambon-Bonavita, M.-A., et al. (2021). Evaluating sediment and water sampling methods for the estimation of deep-sea biodiversity using environmental DNA. *Sci. Rep.* 11:7856. doi: 10.1038/s41598-021-86396-8

Brandt, M. I., Trouche, B., Henry, N., Liautard-Haag, C., Maignien, L., de Vargas, C., et al. (2020). An assessment of environmental metabarcoding protocols aiming at favoring contemporary biodiversity in inventories of deep-sea communities. *Front. Mar. Sci.* 7:234. doi: 10.3389/fmars.2020.00234

Bucklin, A., Peijnenburg, K. T. C. A., Kosobokova, K. N., O'Brien, T. D., Blanco-Bercial, L., Cornils, A., et al. (2021). Toward a global reference database of COI barcodes for marine zooplankton. *Mar. Biol.* 168:78. doi: 10.1007/s00227-021-03887-y

Callahan, B. J., McMurdie, P. J., Rosen, M. J., Han, A. W., Johnson, A. J. A., and Holmes, S. P. (2016). DADA2: high-resolution sample inference from Illumina amplicon data. *Nat. Methods* 13, 581–583. doi: 10.1038/nmeth.3869

Canals, O., Mendibil, I., Santos, M., Irigoien, X., and Rodríguez-Ezpeleta, N. (2021). Vertical stratification of environmental DNA in the open ocean captures ecological patterns and behavior of deep-sea fishes. *Limnol. Oceangr.* 6, 339–347. doi: 10.1002/lol2.10213

Cannizzo, Z. J., Lausche, B., and Wenzel, L. (2021). *Advancing Marine Conservation Through Ecological Connectivity: Building Better Connections for Better Protection*. Berkeley: Parks Stewardship Forum. doi: 10.5070/P537354731

Canonico, G., Buttigieg, P. L., Montes, E., Muller-Karger, F. E., Stepien, C., Wright, D., et al. (2019). Global observational needs and resources for marine biodiversity. *Front. Mar. Sci.* 6:367. doi: 10.3389/fmars.2019.00367

Carreiro-Silva, M., Ocaña, O., Braga Henriques, A., Matos, V., Sampaio, I., Porteiro, F. M., et al. (2017). Zoantharians (Hexacorallia: Zoantharia) associated with cold-water corals in the azores region: new species and associations in the deep sea. *Front. Mar. Sci.* 4:88. doi: 10.3389/fmars.2017.00088

Chapman, A. S. A., Beaulieu, S. E., Colaço, A., Gebruk, A. V., Hilario, A., Kihara, T. C., et al. (2019). sFDvent: a global trait database for deep-sea hydrothermal-vent fauna. *Glob. Ecol. Biogeogr.* 28, 1538–1551. doi: 10.1111/geb.12975

Chatzievangelou, D., Aguzzi, J., Ogston, A., Suárez, A., and Thomsen, L. (2020). Spatio-temporal monitoring of key deep-sea megafauna with Internet Operated crawlers as a tool for ecological status assessment. *Prog. Oceanogr.* 184:102321. doi: 10.1016/j.pocean.2020.102321

Chatzievangelou, D., Bahamon, N., Martini, S., del Rio, J., Riccobene, G., Tangherlini, M., et al. (2021). Integrating diel vertical migrations of bioluminescent deep scattering layers into monitoring programs. *Front. Mar. Sci.* 8:661809.

Chatzievangelou, D., Doya, C., Mihály, S., Sastri, A. R., Thomsen, L., and Aguzzi, J. (2016). High-frequency patterns in the abundance of benthic species near a cold-seep: an internet operated vehicle application. *PLoS One* 11:e0163808. doi: 10.1371/journal.pone.0163808

Chauvet, P., Metaxas, A., Hay, A. E., and Matabos, M. (2018). Annual and seasonal dynamics of deep-sea megafaunal epibenthic communities in Barkley Canyon (British Columbia, Canada): a response to climatology, surface productivity and benthic boundary layer variation. *Prog. Oceanogr.* 169, 89–105. doi: 10.1016/j.pocean.2018.04.002

Clark, K., Karsch-Mizrachi, I., Lipman, D. J., Ostell, J., and Sayers, E. W. (2016). GenBank. *Nucleic Acids Res.* 44, D67–D72. doi: 10.1093/nar/gkv1276

Closek, C. J., Santora, J. A., Starks, H. A., Schroeder, I. D., Andruszkiewicz, E. A., Sakuma, K. M., et al. (2019). Marine vertebrate biodiversity and distribution within the central california current using environmental DNA (eDNA) metabarcoding and ecosystem surveys. *Front. Mar. Sci.* 6:732. doi: 10.3389/fmars.2019.00732

Colas, F., Tardivel, M., Perchoc, M., Lunven, M., Forest, B., and Guyader, G. (2018). The ZooCAM, a new in-flow imaging system for fast onboard counting, sizing and classification of fish eggs and metazooplankton. *Prog. Oceanogr.* 166, 54–65. doi: 10.1016/j.pocean.2017.10.014

Collins, R. A., Wangensteen, O. S., O'Gorman, E. J., Mariani, S., Sims, D. W., and Genner, M. J. (2018). Persistence of environmental DNA in marine systems. *Commun. Biol.* 1:185. doi: 10.1038/s42003-018-0192-6

Colloca, F., Cardinale, M., Belluscio, A., and Ardizzone, G. (2003). Pattern of distribution and diversity of demersal assemblages in the central Mediterranean Sea. *Estuarine Coast. Shelf. Sci.* 56, 469–480. doi: 10.1016/S0272-7714(02)00196-8

Cordier, T., Esling, P., Lejzerowicz, F., Visco, J., Ouadahi, A., Martins, C., et al. (2017). Predicting the ecological quality status of marine environments from eDNA metabarcoding data using supervised machine learning. *Environ. Sci. Technol.* 51, 9118–9126. doi: 10.1021/acs.est.7b01518

Cordier, T., Forster, D., Dufresne, Y., Martins, C. I. M., Stoeck, T., and Pawlowski, J. (2018). Supervised machine learning outperforms taxonomy-based environmental DNA metabarcoding applied to biomonitoring. *Mol. Ecol. Resour.* 18, 1381–1391. doi: 10.1111/1755-0998.12926

Cordier, T., Frontalini, F., Cermakova, K., Apothéloz-Perret-Gentil, L., Treglia, M., Scantaburlo, E., et al. (2019a). Multi-marker eDNA metabarcoding survey to assess the environmental impact of three offshore gas platforms in the North Adriatic Sea (Italy). *Mar. Environ. Res.* 146, 24–34. doi: 10.1016/j.marenvres.2018.12.009

Cordier, T., Lanzén, A., Apothéloz-Perret-Gentil, L., Stoeck, T., and Pawlowski, J. (2019b). Embracing environmental genomics and machine learning for routine biomonitoring. *Trends Microbiol.* 27, 387–397. doi: 10.1016/j.tim.2018.10.012

Costa, C., Fanelli, E., Marini, S., Danovaro, R., and Aguzzi, J. (2020). Global deep-sea biodiversity research trends highlighted by science mapping approach. *Front. Mar. Sci.* 7:384. doi: 10.3389/fmars.2020.00384

Costello, M. J., and Chaudhary, C. (2017). Marine biodiversity, biogeography, deep-sea gradients, and conservation. *Curr. Biol.* 27, R511–R527. doi: 10.1016/j.cub.2017.06.015

Costello, M. J., Bouchet, P., Boxshall, G., Fauchald, K., Gordon, D., Hoeksema, B. W., et al. (2013). Global coordination and standardisation in marine biodiversity through the world register of marine species (WoRMS) and related databases. *PLoS One* 8:e51629. doi: 10.1371/journal.pone.0051629

Costello, M. J., Cheung, A., and De Hauwere, N. (2010). Surface area and the seabed area, volume, depth, slope, and topographic variation for the world's seas, oceans, and countries. *Environ. Sci. Technol.* 44, 8821–8828. doi: 10.1021/es1012752

Cowart, D. A., Matabos, M., Brandt, M. I., Marticorena, J., and Sarrazin, J. (2020). Exploring environmental DNA (eDNA) to assess biodiversity of hard substratum faunal communities on the lucky strike vent field (Mid-Atlantic Ridge) and investigate recolonization dynamics after an induced disturbance. *Front. Mar. Sci.* 6:783.

Cristescu, M. E., and Hebert, P. D. N. (2018). Uses and misuses of environmental DNA in biodiversity science and conservation. *Ann. Rev. Ecol. Evol. Syst.* 49, 209–230. doi: 10.1146/annurev-ecolsys-110617-062306

Danovaro, R., Aguzzi, J., Fanelli, E., Billet, D., Gjerde, K., Jamieson, A., et al. (2017a). A new international ecosystem-based strategy for the global deep ocean. *Science* 355, 452–454. doi: 10.1126/science.aah7178

Danovaro, R., Corinaldesi, C., Dell'Anno, A., and Snelgrove, P. V. R. (2017b). The deep-sea under global change. *Curr. Biol.* 27, R461–R465. doi: 10.1016/j.cub.2017.02.046

Danovaro, R., Fanelli, E., Aguzzi, J., Billett, D., Carugati, L., Corinaldesi, C., et al. (2020). Ecological variables for developing a global deep-ocean monitoring and conservation strategy. *Nat. Ecol. Evol.* 4, 181–192. doi: 10.1038/s41559-019-1091-z

Danovaro, R., Gambi, C., Dell'Anno, A., Corinaldesi, C., Fraschetti, S., Vanreusel, A., et al. (2008). Exponential decline of deep-sea ecosystem functioning linked to benthic biodiversity loss. *Curr. Biol.* 18, 1–8. doi: 10.1016/j.cub.2007.11.056

Davidov, K., Iankelevich-Kounio, E., Yakovenko, I., Koucherov, Y., Rubin-Blum, M., and Oren, M. (2020). Identification of plastic-associated species in the Mediterranean Sea using DNA metabarcoding with Nanopore MinION. *Sci. Rep.* 10:17533. doi: 10.1038/s41598-020-74180-z

Deiner, K., Bik, H. M., Mächler, E., Seymour, M., Lacoursière-Roussel, A., Altermatt, F., et al. (2017). Environmental DNA metabarcoding: transforming how we survey animal and plant communities. *Mol. Ecol.* 26, 5872–5895. doi: 10.1111/mec.14350

del Rio, J., Nogueras, M., Aguzzi, J., Toma, D., Masmitja, I., Carandell, M., et al. (2020). A decadal balance for a cabled observatory deployment. *IEEE Access* 8, 33163–33177. doi: 10.1109/access.2020.2973771

Dewey, R., Round, A., Macoun, P., Vervynck, J., and Tunnicliffe, V. (2007). "The VENUS cabled observatory: engineering meets science on the seafloor," in *Proceedings of the OCEANS 2007*, (Vancouver, BC).

DFO (2020). *Advice on the Use of Targeted Environmental DNA (eDNA) Analysis for the Management of Aquatic Invasive Species and Species at Risk*. Available Online at: https://publications.gc.ca/collections/collection_2021/mpo-dfo/fs70-6/Fs70-6-2020-058-eng.pdf

Djurhuus, A., Port, J., Closek, C. J., Yamahara, K. M., Romero-Maraccini, O., Walz, K. R., et al. (2017). Evaluation of filtration and DNA extraction methods for environmental DNA biodiversity assessments across multiple trophic levels. *Front. Mar. Sci.* 4:314.

Doya, C., Aguzzi, J., Chatzievangelou, D., Costa, C., Company, J. B., and Tunnicliffe, V. (2015). The seasonal use of small-scale space by benthic species in a transiently hypoxic area. *J. Mar. Syst.* 154, 280–290.

Doya, C., Aguzzi, J., Pardo, M., Matabos, M., Company, J. B., Costa, C., et al. (2014). Diel behavioral rhythms in the sablefish (Anoplopoma fimbria) and other benthic species, as recorded by deep-sea cabled observatories in Barkley canyon (NEPTUNE-Canada). *J. Mar. Syst.* 130, 69–78. doi: 10.1016/j.jmarsys.2013.04.003

Doya, C., Chatzievangelou, D., Bahamon, N., Purser, A., De Leo, F., Juniper, K., et al. (2017). Seasonal monitoring of deep-sea cold-seep benthic communities using an Internet Operated Vehicle (IOV). *PLoS One* 12:e0176917. doi: 10.1371/journal.pone.0176917

Dully, V., Balliet, H., Frühe, L., Däumer, M., Thielen, A., Gallie, S., et al. (2021a). Robustness, sensitivity and reproducibility of eDNA metabarcoding as an environmental biomonitoring tool in coastal salmon aquaculture–an inter-laboratory study. *Ecol. Indic.* 121:107049. doi: 10.1016/j.ecolind.2020.107049

Dully, V., Wilding, T. A., Mühlhaus, T., and Stoeck, T. (2021b). Identifying the minimum amplicon sequence depth to adequately predict classes in eDNA-based marine biomonitoring using supervised machine learning. *Comput. Struct. Biotechnol. J.* 19, 2256–2268. doi: 10.1016/j.csbj.2021.04.005

Dunlop, K. M., Jarvis, T., Benoit-Bird, K. J., Waluk, C. M., Caress, D. W., Thomas, H., et al. (2018). Detection and characterisation of deep-sea benthopelagic animals from an autonomous underwater vehicle with a multibeam echosounder: a proof of concept and description of data-processing methods. *Deep Sea Res. Part I: Oceanogr. Res. Papers* 134, 64–79. doi: 10.1016/j.dsr.2018.01.006

Easson, C. G., Boswell, K. M., Tucker, N., Warren, J. D., and Lopez, J. V. (2020). Combined eDNA and acoustic analysis diel vertical migration of mixed consortia in the gulf of Mexico. *Front. Mar. Sci.* 7:552.

Eble, J. A., Daly-Engel, T. S., DiBattista, J. D., Koziol, A., and Gaither, M. R. (2020). "Chapter two - marine environmental DNA: approaches, applications, and opportunities," in *Advances in Marine Biology*, ed. C. Sheppard (Cambridge, MA: Academic Press). doi: 10.1016/bs.amb.2020.01.001

Everett, M. V., and Park, L. K. (2018). Exploring deep-water coral communities using environmental DNA. *Deep Sea Res. Part II Top. Stud. Oceanogr.* 150, 229–241. doi: 10.11646/zootaxa.4878.3.2

Fanelli, E., Aguzzi, J., Marini, S., del Rio, J., Nogueras, M., Canese, S., et al. (2020). Towards Naples Ecological REsearch for Augmented observatories (NEREA): the NEREA-fix module, a stand-alone platform for long-term deep-sea ecosystem monitoring. *Sensors* 20:2911. doi: 10.3390/s20102911

Favali, P., Laura, B., and Angelo, D. S. (2015). *Seafloor Observatories: a New Vision of the Earth From the Abyss*. Berlin: Springer.

Feio, M. J., Serra, S. R. Q., Mortágua, A., Bouchez, A., Rimet, F., Vasselon, V., et al. (2020). A taxonomy-free approach based on machine learning to assess the quality of rivers with diatoms. *Sci. Total Environ.* 722:137900. doi: 10.1016/j.scitotenv.2020.137900

Fischer, P., Brix, H., Baschek, B., Kraberg, A., Brand, M., Cisewski, B., et al. (2020). Operating cabled underwater observatories in rough shelf-sea environments: a technological challenge. *Front. Mar. Sci.* 7:551.

Fraija-Fernández, N., Bouquieaux, M.-C., Rey, A., Mendibil, I., Cotano, U., and Irigoien, I. (2020). Marine water environmental DNA metabarcoding provides a comprehensive fish diversity assessment and reveals spatial patterns in a large oceanic area. *Ecol. Evol.* 10, 7560–7584. doi: 10.1002/ece3.6482

Frühe, L., Cordier, T., Dully, V., Breiner, H.-W., Lentendu, G., Pawloski, J., et al. (2021). Supervised machine learning is superior to indicator value inference in monitoring the environmental impacts of salmon aquaculture using eDNA metabarcodes. *Mol. Ecol.* 30, 2988–3006. doi: 10.1111/mec.15434

Gage, J. D., and Tyler, P. A. (1992). *Deep-Sea Biology. a Natural History of Organisms at the Deep-Sea Floor*. Cambridge, UK: Cambridge University Press.

Garcia-Vazquez, E., Georges, O., Fernandez, S., and Ardura, A. (2021). eDNA metabarcoding of small plankton samples to detect fish larvae and their preys from Atlantic and Pacific waters. *Sci. Rep.* 11:7224. doi: 10.1038/s41598-021-86731-z

Gemeinholzer, B., Vences, M., Beszteri, B., Bruy, T., Felden, J., Kostadinov, I., et al. (2020). Data storage and data re-use in taxonomy—the need for improved storage and accessibility of heterogeneous data. *Org. Divers. Evol.* 20, 1–8. doi: 10.1007/s13127-019-00428-w

Glover, A. G., Gooday, A. J., Bailey, D. M., Billett, D. S. M., Chevaldonné, P., Colaço, A., et al. (2010). Temporal change in deep-sea benthic ecosystems: a review of the evidence from recent time-series studies. *Adv. Mar. Biol.* 58, 1–95. doi: 10.1016/B978-0-12-381015-1.00001-0

Glover, A. G., Higgs, N., and Horton, T. (2021). *World Register of Deep-Sea species (WoRDSS)*. Available Online at http://www.marinespecies.org/deepsea (accessed July 15, 2021).

Glover, A. G., Wiklund, H., Chen, C., and Dahlgren, T. G. (2018). Managing a sustainable deep-sea 'blue economy' requires knowledge of what actually lives there. *eLife* 7:e41319. doi: 10.7554/eLife.41319

Gold, Z., Sprague, J., Kushner, D. J., Zerecero Marin, E., and Barber, P. H. (2021). eDNA metabarcoding as a biomonitoring tool for marine protected areas. *PLoS One* 16:e0238557. doi: 10.1371/journal.pone.0238557

Goldberg, C. S., Turner, C. R., Deiner, K., Klymus, K. E., Thomsen, P. F., Murphy, M. A., et al. (2016). Critical considerations for the application ofenvironmental DNA methods to detect aquatic species. *Methods Ecol. Evol.* 7, 1299–1307. doi: 10.1111/2041-210x.12595

Goricki, Š, Stanković, D., Snoj, A., Kuntner, M., Jeffery, W. R., Trontelj, P., et al. (2017). Environmental DNA in subterranean biology: range extension and taxonomic implications for Proteus. *Sci. Rep.* 7:45054. doi: 10.1038/srep45054

Gorsky, G., Ohman, M. D., Picheral, M., Gasparini, S., Stemmann, L., Romagnan, J.-B., et al. (2010). Digital zooplankton image analysis using the ZooScan integrated system. *J. Plankton Res.* 32, 285–303. doi: 10.1093/plankt/fbp124

Govindarajan, A. F., Francolini, R. D., Jech, J. M., Lavery, A. C., Llopiz, J. K., Wiebe, P. H., et al. (2021). Exploring the use of environmental DNA (eDNA) to detect animal taxa in the mesopelagic zone. *Front. Ecol. Evol.* 9:574877.

Guardiola, M., Uriz, M. J., Taberlet, P., Coissac, E., Wangensteen, O. S., and Turon, X. (2016a). Deep-sea, deep-sequencing: metabarcoding extracellular DNA from sediments of marine canyons. *PLOS one* 11:e0153836.

Guardiola, M., Wangensteen, O. S., Taberlet, P., Coissac, E., Uriz, M. J., and Turon, X. (2016b). Spatiotemporal monitoring of deep-sea communities using metabarcoding of sediment DNA and RNA. *PeerJ* 4:e2807.

Guillou, L., Bachar, D., Audic, S., Bass, D., Berney, C., Bittner, L., et al. (2013). The Protist Ribosomal Reference database (PR2): a catalog of unicellular eukaryote small sub-unit rRNA sequences with curated taxonomy. *Nucleic Acids Res.* 41, D597–D604. doi: 10.1093/nar/gks1160

Günther, B., Marre, S., Defois, C., Merzi, T., Blanc, P., Peyret, P., et al. (2021). Capture by hybridization for full-length barcode-based eukaryotic and prokaryotic biodiversity inventories of deep sea ecosystems. *Mol. Ecol. Resour.* Online ahead of print. doi: 10.1111/1755-0998.13500

Hajibabaei, M., and McKenna, C. (2012). DNA mini-barcodes. *Methods Mol. Biol.* 858, 339–353. doi: 10.1007/978-1-61779-591-6_15

Hansen, B. K., Jacobsen, M. W., Middelboe, A. L., Preston, C. L., Marin, R., Bekkevold, D., et al. (2020). Remote, autonomous real-time monitoring of environmental DNA from commercial fish. *Sci. Rep.* 10:13272. doi: 10.1038/s41598-020-70206-8

Harrison, J. B., Sunday, J. M., and Rogers, S. M. (2019). Predicting the fate of eDNA in the environment and implications for studying biodiversity. *Proc. R. Soc. B* 286:20191409. doi: 10.1098/rspb.2019.1409

Hatch, A., Liew, H., Hourdez, S., and Rouse, G. (2020). Hungry scale worms: phylogenics of peinaleopolynoe (Polynoidae, Annelida), with four new species. *Zookeys* 932, 27–74. doi: 10.3897/zookeys.932.48532

Heidelberg, K. B., Gilbert, J., and Joint, I. (2010). Marine genomics: at the interface of marine microbial ecology and biodiscovery. *Microb. Biotechnol.* 3, 531–543.

He, S., Peng, Y., Jin, Y., Wan, B., and Liu, G. (2020). Review and analysis of key techniques in marine sediment sampling. *Chin. J. Mech. Eng.* 33:66.

He, X., Gilmore, S. R., Sutherland, T. F., Hajibabaei, M., Miller, K. M., Westfall, K. M., et al. (2021). Biotic signals associated with benthic impacts of salmon farms from eDNA metabarcoding of sediments. *Mol. Ecol.* 30, 3158–3174. doi: 10.1111/mec.15814

Heberling, J. M., Miller, J. T., Noesgaard, D., Weingart, S. B., and Schigel, D. (2021). Data integration enables global biodiversity synthesis. *Proc. Natl. Acad. Sci. USA* 118:e2018093118. doi: 10.1073/pnas.2018093118

Hebert, P. D. N., Ratnasingham, S., and deWaard, J. R. (2003). Barcoding animal life: cytochrome oxidase subunit 1 divergences among closely related species. *Proc. R. Soc. London B* 270(Suppl.), S96–S99.

Higgs, N. D., and Attrill, M. J. (2015). Biases in biodiversity: wide-ranging species are discovered first in the deep sea. *Front. Mar. Sci.* 2:61.

Horton, T., Marsh, L., Bett, B. J., Gates, A. R., Jones, D. O. B., Benoist, N. M. A., et al. (2021). Recommendations for the standardisation of open taxonomic nomenclature for image-based identifications. *Front. Mar. Sci.* 8:620702.

Howe, B. M., Arbic, B. K., Aucan, J., Barnes, C. R., Bayliff, N., Becker, N., et al. (2019). SMART cables for observing the global ocean: science and implementation. *Front. Mar. Sci.* 6:424.

Howe, B. M., Roger, L., Fred, D., and David, K. (2011). "ALOHA cabled observatory installation," in *Proceedings of the OCEANS'11 MTS/IEEE KONA*, (Waikoloa, HI).

Howell, K. L., Davies, J. S., Allcock, A. L., Braga-Henriques, A., Buhl-Mortensen, P., Carreiro-Silva, M., et al. (2019). A framework for the development of a global standardised marine taxon reference image database (SMarTaR-ID) to support image-based analyses. *PLoS One* 14:e0218904. doi: 10.1371/journal.pone.0218904

Howell, K. L., Hilário, A., Allcock, A. L., Bailey, D. M., Baker, M., Clark, M. R., et al. (2020). A blueprint for an inclusive, global deep-sea ocean decade field program. *Front. Mar. Sci.* 7:999.

Hunter, M. E., Ferrante, J. A., Meigs-Friend, G., and Ulmer, A. (2019). Improving eDNA yield and inhibitor reduction through increased water volumes and multi-filter isolation techniques. *Sci. Rep.* 9:5259. doi: 10.1038/s41598-019-40977-w

Hutchinson, G. E. (1957). Concluding remarks. *Cold Spring Harbor Symp. Quant. Biol.* 22, 415–427.

Ingels, J., Vanreusel, A., Pape, E., Pasotti, F., Macheriotou, L., Arbizu, P. M., et al. (2021). Ecological variables for deep-ocean monitoring must include microbiota and meiofauna for effective conservation. *Nat. Ecol. Evol.* 5, 27–29.

Jac, C., Desroy, N., Duchêne, J.-C., Foveau, A., Labrune, C., Lescure, L., et al. (2021). Assessing the impact of trawling on benthic megafauna: comparative study of video surveys vs. Scientific Trawling. *ICES J. Mar. Sci.* 78, 1636–1649. doi: 10.1093/icesjms/fsab033

Jacobsen, M. W. (2021). Autonomous in situ sampling and analysis of eDNA using an Environmental Sample Processor (ESP). *ARPHA Conference Abstracts* 4:e65171.

Jahanbakht, M., Xiang, W., Hanzo, L., and Azghadi, M. R. (2021). Internet of underwater things and big marine data analytics—a comprehensive survey. *IEEE Commun. Surveys Tutorials* 23, 904–956. doi: 10.1109/comst.2021.3053118

Jerde, C. L., Wilson, E. A., and Dressler, T. L. (2019). Measuring global fish species richness with eDNA metabarcoding. *Mol. Ecol. Resour.* 19, 19–22. doi: 10.1111/1755-0998.12929

Jetz, W., McGeoch, M. A., Guralnick, R., Ferrier, S., Beck, J., Costello, M. J., et al. (2019). Essential biodiversity variables for mapping and monitoring species populations. *Nat. Ecol. Evol.* 3, 539–551. doi: 10.1038/s41559-019-0826-1

Johnson, D. E., Barrio Froján, C., Bax, N., Dunstan, P., Woolley, S., Halpin, P., et al. (2019). The global ocean biodiversity initiative: promoting scientific support for global ocean governance. *Aquatic Conserv. Mar. Freshw. Ecosyst.* 29, 162–169. doi: 10.1007/s00267-017-0993-2

Johnson, D. E., Froján, C. B., Turner, P. J., Weaver, P., Gunn, V., Dunn, D. C., et al. (2018). Reviewing the EBSA process: improving on success. *Mar. Policy* 88, 75–85.

Juanes, F. (2018). Visual and acoustic sensor for early detection of biological invasions: current uses and future potential. *J. Nat. Conserv.* 42, 7–11. doi: 10.1016/j.jnc.2018.01.003

Juniper, S. K., Matabos, M., Mihaìly, S., Ajayamohan, R. S., Gervais, F., and Bui, A. O. V. (2013). A year in barkley canyon: a time-series observatory study of mid-slope benthos and habitat dynamics using the NEPTUNE Canada network. *Deep Sea Res. II* 92, 114–123.

Kawato, M., Yoshida, T., Miya, M., Tsuchida, S., Nagano, Y., Nomura, M., et al. (2021). Optimization of environmental DNA extraction and ampli?cation methods for metabarcoding of deep-sea ?sh. *MethodsX* 8:101238. doi: 10.1016/j.mex.2021.101238

Kersten, O., Vetter, E. W., Jungbluth, M. J., Smith, C. R., and Goetze, E. (2019). Larval assemblages over the abyssal plain in the Pacific are highly diverse and spatially patchy. *PeerJ* 7:e7691. doi: 10.7717/peerj.7691

Kitahashia, T., Watanabea, H. K., Tsuchiyaa, M., Yamamotob, H., and Yamamoto, H. (2018). A new method for acquiring images of meiobenthic images using the FlowCAM. *MethodsX* 5, 1330–1335. doi: 10.1016/j.mex.2018.10.012

Kolda, A., Gavrilović, A., Jug-Dujaković, J., Ljubešić, Z., El-Matboulie, M., Lillehaugf, A., et al. (2020). Profiling of bacterial assemblages in the marine cage farm environment, with implications on fish, human and ecosystem health. *Ecol. Indic.* 118:106785. doi: 10.1016/j.ecolind.2020.106785

Koschinsky, A., Heinrich, L., Boehnke, K., Cohrs, J. C., Markus, T., Shani, M., et al. (2018). Deep-sea mining: interdisciplinary research on potential environmental, legal, economic, and societal implications. *Integr. Environ. Assess. Manag.* 14, 672–691. doi: 10.1002/ieam.4071

Kroodsma, D. A., Mayorga, J., Hochberg, T., Miller, N. A., Boerder, K., Ferretti, F., et al. (2018). Tracking the global footprint of fisheries. *Science* 359, 904–908. doi: 10.1126/science.aao5646

Kutti, T., Johnsen, I. A., Skaar, K. S., Ray, J. L., Husa, V., and Dahlgren, T. G. (2020). Quantification of eDNA to map the distribution of cold-water coral reefs. *Front. Mar. Sci.* 7:446.

Lacoursière-Roussel, A., Howland, K., Normandeau, E., Grey, E. K., Archambault, P., Deiner, K., et al. (2018). eDNA metabarcoding as a new surveillance approach for coastal Arctic biodiversity. *Ecol. Evol.* 8, 7763–7777. doi: 10.1002/ece3.4213

Langenkämper, D., van Kevelaer, R., Purser, A., and Nattkemper, T. W. (2020). Gear-induced concept drift in marine images and its effect on deep learning classification. *Front. Mar. Sci.* 7:506.

Laroche, O., Kersten, O., Smith, C. R., and Goetze, E. (2020a). Environmental DNA surveys detect distinct metazoan communities across abyssal plains and seamounts in the western clarion clipperton zone. *Mol. Ecol.* 29, 4588–4604. doi: 10.1111/mec.15484

Laroche, O., Kersten, O., Smith, C. R., and Goetze, E. (2020b). From sea surface to seafloor: a benthic allochthonous eDNA survey for the abyssal ocean. *Front. Mar. Sci.* 7:682.

Laroche, O., Wood, S. A., Tremblay, L. A., Ellis, J. I., Lear, G., and Pochon, X. (2018). A cross-taxa study using environmental DNA/RNA metabarcoding to measure biological impacts of offshore oil and gas drilling and production operations. *Mar. Pollut. Bull.* 127, 97–107. doi: 10.1016/j.marpolbul.2017.11.042

Le, J. T., Levin, L. A., Lejzerowicz, F., Cordier, T., Gooday, A. J., and Pawlowski, J. (2021). Scientific and budgetary tradeoffs between morphological and

molecular methods for deep-sea biodiversity assessment. *Integr. Environ. Assess. Manag.* Online ahead of print. doi: 10.1002/ieam.4466

LeBlanc, F., Belliveau, V., Watson, E., Coomber, C., Simard, N., DiBacco, C., et al. (2020). Environmental DNA (eDNA) detection of marine aquatic invasive species (AIS) in Eastern Canada using a targeted species-specific qPCR approach. *Manag. Biol. Invasions* 11, 201–217. doi: 10.3391/mbi.2020.11.2.03

Leray, M., and Machida, R. J. (2020). Seabed mining could come at a high price for a unique fauna. *Mol. Ecol.* 29, 506–4509. doi: 10.1111/mec.15678

Leray, M., Yang, J. Y., Meyer, C. P., Mills, S. C., Agudelo, N., and Ranwez, V. (2013). A new versatile primer set targeting a short fragment of the mitochondrial COI Region for metabarcoding metazoan diversity: application for characterizing coral reef fish gut contents. *Front. Zool.* 10:34. doi: 10.1186/1742-9994-10-34

Levin, L. A., Amon, D. J., and Lily, H. (2020). Nature challenges to the sustainability of deep-seabed mining. *Nat. Sustain.* 3, 784–794. doi: 10.1038/s41893-020-0558-x

Levin, L. A., and Le Bris, N. (2015). The deep ocean under climate change. *Science* 350, 766–768. doi: 10.1126/science.aad0126

Levin, L. A., Bett, B. J., Gates, A. R., Heimbach, P., Howe, B. M., Janssen, F., et al. (2019). Global observing needs in the deep ocean. *Front. Mar. Sci.* 6:241.

Lewis, N., Day, J. C., Wilhelm, A., Wagner, D., Gaymer, C., Parks, J., et al. (2017). *Large-Scale Marine Protected Areas: Guidelines for design and Management. Best Practice Protected Area Guidelines Series, No. 26*. Switzerland: IUCN.

Lins, L., Zeppilli, D., Menot, L., Michel, L. N., Bonifácio, P., Brandt, M., et al. (2021). Toward a reliable assessment of potential ecological impacts of deep-sea polymetallic nodule mining on abyssal infauna. *Limnol. Oceanogr. Methods* 19, 626–650.

Liu, J., and Zhang, H. (2021). Combining multiple markers in environmental DNA metabarcoding to assess deep-sea benthic biodiversity. *Front. Mar. Sci.* 8:684955.

Lopez-Vasquez, V., Lopez-Guede, J.-M., Marini, S., Fanelli, E., Johnsen, E., and Aguzzi, J. (2020). Video-imaging enhancement and machine learning pipeline for animal tracking and classification at cabled observatories. *Sensors* 20:726. doi: 10.3390/s20030726

Malde, K., Handegard, N. O., Eikvil, L., and Salberg, A.-B. (2020). Machine intelligence and the data-driven future of marine science. *ICES J. Mar. Sci.* 77, 1274–1285. doi: 10.1093/icesjms/fsz057

Manea, E., Bianchelli, S., Fanelli, E., Danovaro, R., and Gissi, E. (2020). Towards an ecosystem-based marine spatial planning in the deep Mediterranean Sea. *Sci. Total Environ.* 715:136884. doi: 10.1016/j.scitotenv.2020.136884

Mariani, S., Baillie, C., Colosimo, G., and Riesgo, A. (2019). Sponges as natural environmental DNA samplers. *Curr. Biol.* 29, R401–R402. doi: 10.1016/j.cub.2019.04.031

Marini, S., Fanelli, E., Sbragaglia, V., Azzurro, E., del Rio, J., and Aguzzi, J. (2018). Tracking fish abundance by underwater image recognition. *Sci. Rep.* 8:13748. doi: 10.1038/s41598-018-32089-8

Martin, M. (2011). Cutadapt removes adapter sequences from high-throughput sequencing reads. *EMBnet J.* 17, 10–12. doi: 10.1089/cmb.2017.0096

Martini, S., Guasco, S., Michotey, V., Casalot, L., Garel, M., Lefevre, D., et al. (2013). Temporal survey, presence and activity of bioluminescent bacteria at the deep ANTARES station (Mediterranean Sea, 2200 m depth). *Rapp. Comm. Int. Mer Médit.* 40:422.

Martini, S., Nerini, D., and Tamburini, C. (2014). Relation between deep bioluminescence and oceanographic variables: a statistical analysis using time–frequency decompositions. *Prog. Oceanogr.* 127, 117–128. doi: 10.1016/j.pocean.2014.07.003

Matabos, M., Aguzzi, J., Robert, K., Costa, C., Menesatti, P., Company, J. B., et al. (2011). Multi-parametric study of behavioural modulation in demersal decapods at the VENUS cabled observatory in Saanich Inlet, British Columbia, Canada. *J. Exp. Mar. Biol. Ecol.* 401, 89–96.

Matabos, M., Bui, A. O., Mihály, S., Aguzzi, J., Juniper, D. S. K., and Ajayamohan, R. S. (2014). High-frequency study of benthic megafaunal community dynamics in Barkley canyon: a multidisciplinary approach using the NEPTUNE Canada network. *J. Mar. Syst.* 130, 56–68. doi: 10.1016/j.jmarsys.2013.05.002

Matabos, M., Piechaud, N., De Montigny, F., Sarradin, P. M., and Sarrazin, J. (2015). The VENUS cabled observatory as a method to observe fish behaviour and species assemblages in a hypoxic fjord, Saanich Inlet (British Columbia, Canada). *Can. J. Fish. Aquat. Sci.* 72, 24–36. doi: 10.1139/cjfas-2013-0611

Mathon, L., Valentini, A., Guérin, P. E., Normandeau, E., Noel, C., Lionnet, C., et al. (2021). Benchmarking bioinformatic tools for fast and accurate eDNA metabarcoding species identification. *Mol. Ecol. Resour.* 21, 2565–2579. doi: 10.1111/1755-0998.13430

Mathur, M., Vasudev, D., Sahoo, S., Jain, D., and Goel, N. (2020). Crosspooled FishNet: transfer learning based fish species classification model. *Multimed. Tools Appl.* 79, 31625–31643. doi: 10.1007/s11042-020-09371-x

McClenaghan, B., Fahner, N., Cote, D., Chawarski, J., McCarthy, A., Rajabi, H., et al. (2020). Harnessing the power of eDNA metabarcoding for the detection of deep-sea fishes. *PLoS One* 15:e0236540. doi: 10.1371/journal.pone.0236540

McCowin, M., Feehery, C., and Rouse, G. (2020). Spanning the depths or depth-restricted: three new species of Bathymodiolus (Bivalvia, Mytilidae) and a new record for the hydrothermal vent Bathymodiolus thermophilus at methane seeps along the Costa Rica margin. *Deep Sea Res. Part I: Oceanogr. Res. Papers* 164:103322. doi: 10.1016/j.dsr.2020.103322

McIntyre, A. (2010). *Life in the World's Oceans: Diversity, Distribution, and Abundance*. Chichester: Wiley-Blackwell.

Merten, V., Bayer, T., Reusch, T. B. H., Puebla, O., Fuss, J., Stefanschitz, J., et al. (2021). An integrative assessment combining deep-sea net sampling, in situ observations and eDNA analysis identifies Cabo Verde as a cephalopod biodiversity hotspot in the Atlantic Ocean. *Front. Mar. Sci.* 8:760108.

Meusnier, I., Singer, G. A., Landry, J. F., Hickey, J.-F., Hebert, P. D. N., and Hajibabaei, M. (2008). A universal DNA mini-barcode for biodiversity analysis. *BMC Genomics* 9:214. doi: 10.1186/1471-2164-9-214

Meyer, C. P., and Paulay, G. (2005). DNA barcoding: error rates based on comprehensive sampling. *PLoS Biol.* 3:e422. doi: 10.1371/journal.pbio.0030422

Milligan, R. J., Scott, E. M., Jones, D. O. B., Bett, J. B., Jemieson, A. J., and O'Brien, R. (2020). Evidence for seasonal cycles in deep-sea fish abundances: a great migration in the deep SE Atlantic? *J. Anim. Ecol.* 89, 1593–1603. doi: 10.1111/1365-2656.13215

Mirimin, L., Desmet, S., López Romero, D., Fernandez Fernandez, S., Miller, D., Mynott, S., et al. (2021). Don't catch me if you can – Using cabled observatories as multidisciplinary platforms for marine fish community monitoring: a case study combining underwater video and environmental DNA (eDNA) data. *Sci. Total Environ.* 773:145351. doi: 10.1016/j.scitotenv.2021.145351

Mooney, T. A., Iorio, L. D., Lammers, M., Lin, T.-H., Nedelec, S. L., Parsons, M., et al. (2020). Listening forward: approaching marine biodiversity assessments using acoustic methods. *R. Soc. Open Sci.* 7:201287. doi: 10.1098/rsos.201287

Moore, S. K., Mickett, J. B., Doucette, G. J., Adams, N. G., Mikulski, C. M., Birch, J. M., et al. (2021). An autonomous platform for near real-time surveillance of harmful algae and their toxins in dynamic coastal shelf environments. *J. Mar. Sci. Eng.* 9:336. doi: 10.3390/jmse9030336

Morato, T., Hoyle, S. D., Allain, V., and Nicol, S. J. (2010). Seamounts are hotspots of pelagic biodiversity in the open ocean. *Proc. Nat. Acad. Sci.* 107, 9707–9711. doi: 10.1073/pnas.0910290107

Murakami, H., Yoon, S., Kasai, A., Minamoto, T., Yamamoto, S., Sakata, M. K., et al. (2019). Dispersion and degradation of environmental DNA from caged fish in a marine environment. *Fish Sci.* 85, 327–337. doi: 10.1007/s12562-018-1282-6

Nattkemper, T., Osterloff, J., Nilssen, I., Van Engeland, T., Buhl-Mortensen, P., and Järnegren, J. (2019). Computer vision enables short- and long-term analysis of *Lophelia pertusa* polyp behaviour and colour from an underwater observatory. *Sci. Rep.* 9:6578. doi: 10.1038/s41598-019-41275-1

O'Leary, B. C., Ban, N. C., Fernandez, M., Friedlander, A. M., García-Borboroglu, P., Golbuu, Y., et al. (2018). Addressing criticisms of large-scale marine protected areas. *Bioscience* 68, 359–370. doi: 10.1093/biosci/biy021

Ohman, M. D., Davis, R. E., Sherman, J. T., Grindley, K. R., Whitmore, B. M., Nickels, C. F., et al. (2018). Zooglider: an autonomous vehicle for optical and acoustic sensing of zooplankton. *Limnol. Oceanogr. Methods* 17, 69–86. doi: 10.1002/lom3.10301

O'Leary, B. C., and Roberts, C. M. (2018). Ecological connectivity across ocean depths: implications for protected area design. *Glob. Ecol. Conserv.* 15:e00431.

Osterloff, J., Nilssen, I., and Nattkemper, T. W. (2016). A computer vision approach for monitoring the spatial and temporal shrimp distribution at the LoVe observatory. *Methods Oceanog.* 15, 114–128.

Osterloff, J., Nilssen, I., Järnegren, J., Van Engeland, T., Buhl-Mortensen, P., and Nattkemper, T. W. (2019). Computer vision enables short-and long-term analysis of *Lophelia pertusa* polyp behaviour and colour from an underwater observatory. *Sci. Rep.* 9:6578.

Pawlowski, J., Levin, L., Recio-Blanco, X., Le, J., Lejzerowicz, F., Cordier, T., et al. (2018). *Enabling the use of Environmental DNA for Regulatory Policymaking in the Marine Industrial Revolution. SNIS Project Working Paper*. Available online at: https://snis.ch/wp-content/uploads/2020/01/2015_Pawlowski_Working-Paper.pdf

Pereira, H. M., Ferrier, S., Walters, M., Geller, G. N., Jongman, R. H. G., Scholes, R. J., et al. (2013). Essential biodiversity variables. *Science* 339, 277–278.

Pikitch, E. K., Rountos, K. J., Essington, T. E., Santora, C., Pauly, D., Watson, R., et al. (2014). The global contribution of forage fish to marine fisheries and ecosystems. *Fish Fish.* 15, 43–64. doi: 10.1111/faf.12004

Portman, M. E., Notarbartolo-di-Sciara, G., Agardy, T., Katsanevakis, S., Possingham, H. P., and Di-Carlo, G. (2013). He who hesitates is lost: why conservation in the Mediterranean Sea is necessary and possible now. *Mar. Policy* 42, 270–279.

Purser, A., Thomsen, L., Hofbauer, M., Menzel, M., Wagner, H., Chapman, R., et al. (2013). Temporal and spatial benthic data collection via internet operated deep sea crawler. *Methods Oceanogr.* 5, 1–18. doi: 10.1016/j.mio.2013.07.001

Pusceddu, A., Bianchelli, S., Martín, J., Puig, P., Palanques, A., Masqué, P., et al. (2014). Chronic and intensive bottom trawling impairs deep-sea biodiversity and ecosystem functioning. *Proc. Nat. Acad. Sci.* 111, 8861–8866. doi: 10.1073/pnas.1405454111

Quast, C., Pruesse, E., Yilmaz, P., Gerken, J., Schweer, T., Yarzaet, P., et al. (2013). The SILVA ribosomal RNA gene database project: improved data processing and web-based tools. *Nucleic Acids Res.* 41, D590–D596. doi: 10.1093/nar/gks1219

Ramírez, F., Afán, I., Davis, L. S., and Chiaradia, A. (2017). Biodiversity losses and conservation responses in the Anthropocene. *Sci. Adv.* 3:e1601198. doi: 10.1126/science.aam9317

Ramirez-Llodra, E., Tyler, P. A., Baker, M. C., Bergstad, O. A., Clark, M. R., Escobar, E., et al. (2011). Man and the last great wilderness: human impact on the deep sea. *PLoS One* 6:e22588. doi: 10.1371/journal.pone.0022588

Ratnasingham, S., and Hebert, P. D. (2013). A DNA-based registry for all animal species: the barcode index number (BIN) system. *PLoS One* 8:e66213. doi: 10.1371/journal.pone.0066213

Ratnasingham, S., and Hebert, P. D. N. (2007). BOLD: the barcode of life data system (http://www.barcodinglife.org). *Mol. Ecol. Notes* 7, 355–364. doi: 10.1111/j.1471-8286.2007.01678.x

Rex, M., Etter, R., Morris, J., Crouse, J., McClain, C., Johnson, N., et al. (2006). Global bathymetric patterns of standing stock and body size in the deep-sea benthos. *Mar. Ecol. Progr. Ser.* 317, 1–8. doi: 10.3354/meps317001

Ribeiro, H., Martins, A., Gonçalves, M., Guedes, M., Tomasino, M. P., Dias, N., et al. (2019). Development of an autonomous biosampler to capture in situ aquatic microbiomes. *PLoS One* 14:e0216882. doi: 10.1371/journal.pone.0216882

Rodriguez-Ezpeleta, N., Morissette, O., Bean, C. W., Manu, S., Banerjee, P., Lacoursière-Roussel, A., et al. (2021). Trade-offs between reducing complex terminology and producing accurate interpretations from environmental DNA: comment on "environmental DNA: what's behind the term?" by Pawlowski et al., (2020). *Mol. Ecol.* 30, 4601–4605. doi: 10.1111/mec.15942

Rognes, T., Flouri, T., Nichols, B., Quince, C., and Mahé, F. (2016). VSEARCH: a versatile open source tool for metagenomics. *PeerJ* 4:e2584. doi: 10.7717/peerj.2584

Rosli, N., Leduc, D., Rowden, A. A., and Probert, K. (2017). Review of recent trends in ecological studies of deep-sea meiofauna, with focus on patterns and processes at small to regional spatial scales. *Mar. Biodivers.* 48, 13–34. doi: 10.1007/s12526-017-0801-5

Ross, T., and Lawson, G. (2009). Long-term broadband acoustic observations of zooplankton scattering layers in Saanich Inlet, British Columbia. *J. Acoust. Soc. Am.* 125, 2551–2551. doi: 10.1121/1.4783649

Rountree, R., Aguzzi, J., Marini, S., Fanelli, E., De Leo, F., Del Rio, J., et al. (2020). Towards an optimal design for ecosystem-level ocean observatories. *Oceanogr. Mar. Biol. Annu. Rev.* 58, 79–106. doi: 10.1201/9780429351495-2

Ruth, L. (2006). Gambling in the deep sea. *EMBO Rep.* 7, 17–21. doi: 10.1038/sj.embor.7400609

Salter, I., Joensen, M., Kristiansen, R., Steingrund, P., and Vestergaard, P. (2019). Environmental DNA concentrations are correlated with regional biomass of Atlantic cod in oceanic waters. *Commun. Biol.* 2:461. doi: 10.1038/s42003-019-0696-8

Schlick-Steiner, B. C., Steiner, F. M., Seifert, B., Stauffer, C., Christian, E., and Crozier, R. H. (2010). Integrative taxonomy: a multisource approach to exploring biodiversity. *Annu. Rev. Entomol.* 55, 421–438. doi: 10.1146/annurev-ento-112408-085432

Scholin, C. A. (2010). What are "ecogenomic sensors?" a review and thoughts for the future. *Ocean Sci.* 6, 51–60. doi: 10.5194/os-6-51-2010

Scholin, C. A., Birch, J., Jensen, S., Marin, R., Massion, E., and Pargett, D. (2017). The quest to develop ecogenomic sensors: a 25-Year history of the Environmental Sample Processor (ESP) as a case study. *Oceanography* 30, 100–113. doi: 10.5670/oceanog.2017.427

Schroeder, A., Stanković, D., Pallavicini, A., Gionechetti, F., Pansera, M., and Camatti, E. (2020). DNA metabarcoding and morphological analysis - assessment of zooplankton biodiversity in transitional waters. *Mar. Environ. Res.* 160:104946. doi: 10.1016/j.marenvres.2020.104946

Seabrook, S., De Leo, F. C., and Thurber, A. R. (2019). Flipping for food: the use of a methane seep by tanner Crabs (Chionoecetes tanneri). *Front. Mar. Sci.* 6:43.

Seabrook, S., De Leo, F. C., Baumberger, T., Raineault, N., and Thurber, A. R. (2018). Heterogeneity of methane seep biomes in the Northeast Pacific. *Deep Sea Res. Part II Top. Stud. Oceanogr.* 150, 195–209. doi: 10.1016/j.dsr2.2017.10.016

Seymour, M., Edwards, F. K., Cosby, B. J., Kelly, M. G., Gary, de Bruyn, M., et al. (2020). Executing multi-taxa eDNA ecological assessment via traditional metrics and interactive networks. *Sci. Total Environ.* 729:138801. doi: 10.1016/j.scitotenv.2020.138801

Stat, M., Huggett, M. J., Bernasconi, R., DiBattista, J. B., Berry, T. E., Newman, S. J., et al. (2017). Ecosystem biomonitoring with eDNA: metabarcoding across the tree of life in a tropical marine environment. *Sci. Rep.* 7:12240. doi: 10.1038/s41598-017-12501-5

Stat, M., John, J., DiBattista, J. D., Newman, S. J., Bunce, M., and Harvey, E. S. (2019). Combined use of eDNA metabarcoding and video surveillance for the assessment of fish biodiversity. *Conserv Biol.* 33, 196–205. doi: 10.1111/cobi.13183

Stefanni, S., Catarino, D., Ribeiro, P., Freitas, M., Menezes, G., Neat, F., et al. (2021). Molecular systematics of the long-snouted deepwater dogfish (Centrophoridae, Deania) with implication to taxonomy and conservation. *Front. Mar. Sci.* 7:588192. doi: 10.3389/fmars.2020.588192

Stefanni, S., Stanković, D., Borme, D., de Olazabal, A., Juretić, T., Pallavicini, A., et al. (2018). Multi-marker metabarcoding approach to study mesozooplankton at basin scale. *Sci. Rep.* 8:12085. doi: 10.1038/s41598-018-30157-7

Stoeckle, M. Y., Adolf, J., Charlop-Powers, Z., Dunton, K. J., Hinks, G., and VanMorter, S. M. (2021). Trawl and eDNA assessment of marine fish diversity, seasonality, and relative abundance in coastal New Jersey, USA. *ICES J. Mar. Sci.* 78, 293–304. doi: 10.1093/icesjms/fsaa225

Sundberg, P., Obst, M., Dahlgren, T., Panova, M., and Axberg, A. (2020). *Swedish eDNA*. Gotherburg: University of Gotherburg.

Taberlet, P., Coissac, E., Hajibabaei, M., and Rieseberg, L. H. (2012). Environmental DNA. *Mol. Ecol.* 21, 1789–1793. doi: 10.1111/j.1365-294X.2012.05542.x

Tamburini, C., Canals, M., Durrieu, de Madron, X., Houpert, L., Lefèvre, D., et al. (2013). Deep-sea bioluminescence blooms after dense water formation at the ocean surface. *PLoS One* 8:e67523. doi: 10.1371/journal.pone.0067523

Thomsen, L., Aguzzi, J., Costa, F. C., De Leo, F. C., Ogston, A., and Purser, A. (2017). The oceanic biological pump: rapid carbon transfer to depth at continental margins during winter. *Sci. Rep.* 7:10763. doi: 10.1038/s41598-017-11075-6

Thomsen, L., Barnes, C., Best, M., Chapman, R., Pirenne, B., Thomson, R., et al. (2012). Ocean circulation promotes methane release from gas hydrate outcrops at the NEPTUNE Canada Barkley Canyon node. *Geophys. Res. Lett.* 39, n/a–n/a. doi: 10.1029/2012GL052462

Thomsen, P. F., Møller, P. R., Sigsgaard, E. E., Knudsen, S. W., Jørgensen, O. A., and Willerslev, E. (2016). Environmental DNA from seawater samples correlate with trawl catches of subarctic, deepwater fishes. *PLoS One* 11:e0165252. doi: 10.1371/journal.pone.0165252

Thurber, A. R., Sweetman, A. K., Narayanaswamy, B. E., Jone, D. O. B., Ingels, J., and Hansman, R. L. (2014). Ecosystem function and services provided by the deep sea. *Biogeosciences* 11, 3941–3963. doi: 10.5194/bg-11-3941-2014

Trenkel, V. M., Vaz, S., Albouy, C., Brind'Amour, A., Laffargue, P., Romagnan, J. B., et al. (2019). We can reduce the impact of monitoring on marine living resources. *Mar. Ecol. Prog. Ser.* 609, 277–282. doi: 10.3354/meps12834

Turon, M., Angulo-Preckler, C., Antich, A., Præbel, K., and Wangensteen, O. S. (2020). More than expected from old sponge samples: a natural sampler dna metabarcoding assessment of marine fish diversity in Nha Trang Bay (Vietnam). *Front. Mar. Sci.* 7:605148. doi: 10.3389/fmars.2020.605148

Turon, X., Antich, A., Palacin, C., Præbel, K., and Wangensteen, O. S. (2019). From metabarcoding to metaphylogeography: separating the wheat from the chaff. *Ecol. Appl.* 30:e02036. doi: 10.1002/eap.2036

UNEP (2020). *Zero Draft of the Post-2020 Global Biodiversity Framework*. Kunming: Convention of Biological Diversity.

UNESCO (2020). *Progress Towards the Sustainable Development Goals Report of the Secretary-General, High-level Political Forum on Sustainable Development, Convened Under the Auspices of the Economic and Social Council (E/2020/57)*. Paris: UNESCO.

Visser, F., Merten, V. J., Bayer, T., Oudejans, M. G., de Jonge, D. S. W., Puebla, O., et al. (2021). Deep-sea predator niche segregation revealed by combined cetacean biologging and eDNA analysis of cephalopod prey. *Sci. Adv.* 7:eabf5908. doi: 10.1126/sciadv.abf5908

Washburn, T. W., Turner, P. J., Durden, J. M., Jones, D. O. B., Weaver, P., and Van Dover, C. L. (2019). Ecological risk assessment for deep-sea mining. *Ocean Coast. Manag.* 176, 24–39. doi: 10.1016/j.ocecoaman.2019.04.014

Weber, S., Brink, L., Wörner, M., Künzel, S., Veith, M., Teubner, D., et al. (2021). Molecular diet analysis in zebra and quagga mussels (Dreissena spp.) and an assessment of the utility of aquatic filter feeders as biological eDNA filters. *BioRxiv* doi: 10.1101/2021.03.01.432951

Wedding, L. M., Friedlander, A. M., Kittinger, J. N., Watling, L., Gaines, S. D., Bennett, M., et al. (2013). From principles to practice: a spatial approach to systematic conservation planning in the deep sea. *Proc. R. Soc. Lond. B* 280:20131684. doi: 10.1098/rspb.2013.1684

Wedding, L. M., Reiter, S. M., Smith, C. R., Gjerde, K. M., Kittinger, J., Friedlander, A. M., et al. (2015). Managing exploitation of the deep seabed. *Science* 349, 144–145. doi: 10.1126/science.aac6647

Weigand, H., Beermann, A. I., Čiampor, F., Costa, F. O., Csabai, Z., et al. (2019). DNA barcode reference libraries for the monitoring of aquatic biota in Europe: gap-analysis and recommendations for future work. *Sci. Total Environ.* 678, 499–524. doi: 10.1016/j.scitotenv.2019.04.247

Weston, J., Carrillo-Barragan, P., Linley, T., Reid, W., and Jamieson, A. (2020). New species of Eurythenes from hadal depths of the mariana Trench, Pacific Ocean (Crustacea: Amphipoda). *ZooTaxa* 4748:zootaxa. doi: 10.11646/zootaxa.4748.1.9

Widder, E. A., Robison, B. H., Reisenbichler, K. R., and Haddock, S. H. D. (2005). Using red light for in situ observations of deep-sea fishes. *Deep Sea Res. Part I* 52, 2077–2085. doi: 10.1016/j.dsr.2005.06.007

Yamahara, K. M., Preston, C. M., Birch, J., Walz, K., Marin, R., Jensen, S., et al. (2019). In situ autonomous acquisition and preservation of marine environmental DNA using an autonomous underwater vehicle. *Front. Mar. Sci.* 6:373. doi: 10.3389/fmars.2019.00373

Yeh, J., and Drazen, J. C. (2011). Baited-camera observations of deep-sea megafaunal scavenger ecology on the California slope. *Mar. Ecol. Prog. Ser.* 424, 145–156.

Young, M. K., Isaak, D. J., Schwartz, M. K., McKelvey, K. S., Nagel, D. E., Franklin, T. W., et al. (2018). *Species Occurrence data from the Aquatic eDNAtlas Database: Forest Service Research Data Archive*. Madison: US Department of Agriculture.

Zhao, F., Filker, S., Xu, K., Huang, P., and Zheng, S. (2020). Microeukaryote communities exhibit phyla-specific distance-decay patterns and an intimate link between seawater and sediment habitats in the Western Pacific Ocean. *Deep Res. Part I Oceanogr. Res. Pap.* 160:103279. doi: 10.1016/j.dsr.2020.103279

Zuazo, A., Grinyó, J., López-Vázquez, V., Rodríguez, E., Costa, C., Ortenzi, L., et al. (2020). An automated pipeline for image processing and data treatment to track activity rhythms of *Paragorgia arborea* in relation to hydrographic conditions. *Sensors* 20:6281. doi: 10.3390/s20216281

Conflict of Interest: The authors declare that the research was conducted in the absence of any commercial or financial relationships that could be construed as a potential conflict of interest.

The reviewer XT declared a shared affiliation, though no other collaboration, with several of the authors DC and JA to the handling editor.

Publisher's Note: All claims expressed in this article are solely those of the authors and do not necessarily represent those of their affiliated organizations, or those of the publisher, the editors and the reviewers. Any product that may be evaluated in this article, or claim that may be made by its manufacturer, is not guaranteed or endorsed by the publisher.

Copyright © 2022 Stefanni, Mirimin, Stanković, Chatzievangelou, Bongiorni, Marini, Modica, Manea, Bonofiglio, del Rio Fernandez, Cukrov, Gavrilović, De Leo and Aguzzi. This is an open-access article distributed under the terms of the Creative Commons Attribution License (CC BY). The use, distribution or reproduction in other forums is permitted, provided the original author(s) and the copyright owner(s) are credited and that the original publication in this journal is cited, in accordance with accepted academic practice. No use, distribution or reproduction is permitted which does not comply with these terms.

frontiers in Marine Science

ORIGINAL RESEARCH
published: 27 January 2022
doi: 10.3389/fmars.2021.795196

Correct Species Identification and Its Implications for Conservation Using Haploniscidae (Crustacea, Isopoda) in Icelandic Waters as a Proxy

Karlotta Kürzel[1], Stefanie Kaiser[2], Anne-Nina Lörz[3], Sven Rossel[4], Eva Paulus[5,6], Janna Peters[5], Martin Schwentner[6], Pedro Martinez Arbizu[4], Charles Oliver Coleman[7], Jörundur Svavarsson[8] and Saskia Brix[5]*

[1] Department of Biology, University of Hamburg, Hamburg, Germany, [2] Department of Invertebrate Zoology and Hydrobiology, Faculty of Biology and Environmental Protection, University of Łódź, Łódź, Poland, [3] Institute for Hydrobiology and Fisheries Science, Center for Earth System Research and Sustainability (CEN), University of Hamburg, Hamburg, Germany, [4] German Centre for Marine Biodiversity Research (DZMB), Senckenberg am Meer, Wilhelmshaven, Germany, [5] German Centre for Marine Biodiversity Research (DZMB), Senckenberg am Meer, Biocenter Grindel, Hamburg, Germany, [6] Naturhistorisches Museum Wien, Vienna, Austria, [7] Museum für Naturkunde, Leibniz Institute for Evolution and Biodiversity Science, Berlin, Germany, [8] Department of Life and Environmental Sciences, University of Iceland, Reykjavík, Iceland

OPEN ACCESS

Edited by:
Elva G. Escobar-Briones, National Autonomous University of Mexico, Mexico

Reviewed by:
Gary C. B. Poore, Museum Victoria, Australia
Hiroshi Yamasaki, Kyushu University, Japan

***Correspondence:**
Karlotta Kürzel
Lotta.kuerzel@gmx.de

Specialty section:
This article was submitted to Deep-Sea Environments and Ecology, a section of the journal Frontiers in Marine Science

Received: *14 October 2021*
Accepted: *29 November 2021*
Published: *27 January 2022*

Citation:
Kürzel K, Kaiser S, Lörz A-N, Rossel S, Paulus E, Peters J, Schwentner M, Martinez Arbizu P, Coleman CO, Svavarsson J and Brix S (2022) Correct Species Identification and Its Implications for Conservation Using Haploniscidae (Crustacea, Isopoda) in Icelandic Waters as a Proxy. Front. Mar. Sci. 8:795196. doi: 10.3389/fmars.2021.795196

Correct identification of species is required to assess and understand the biodiversity of an ecosystem. In the deep sea, however, this is only possible to a limited extent, as a large part of the fauna is undescribed and the identification keys for most taxa are inadequate or missing. With the progressive impact of climate change and anthropogenic activities on deep-sea ecosystems, it is imperative to define reliable methods for robust species identification. In this study, different techniques for the identification of deep-sea species are tested, including a combination of morphological, molecular (DNA barcoding, and proteomic fingerprinting), biogeographical and ecological modeling approaches. These are applied to a family of isopods, the Haploniscidae, from deep waters around Iceland. The construction of interactive identification keys based on the DELTA format (DEscription Language for TAxonomy) were a major pillar of this study, the evaluation of which was underpinned by the application of the supplementary methods. Overall, interactive keys have been very reliable in identifying species within the Haploniscidae. Especially in a deep-sea context, these types of keys could become established because they are easy to adapt and flexible enough to accommodate newly described species. Remarkably, in this study, the interactive key enabled identification of a supposedly new species within the Haploniscidae that was later verified using both molecular genetic – and proteomic methods. However, these keys are limited given that they are based on purely morphological characteristics, including where species with strong ontogenetic or sexual dimorphism occur as both genders are not always described. In this case, integrative taxonomy is the method of choice and the combination presented here has been shown to be very promising for correct identification of deep-sea isopods.

Keywords: Peracarida, deep-sea, taxonomy, interactive keys, COI barcoding, MALDI-TOF MS, depth distribution, geographical distribution

INTRODUCTION

Species determination is the first step in conducting almost any kind of biological research. Without identifying known and scientifically describing newly discovered species, drawing conclusions about species diversity, their distribution and their ecology is impossible. Species delimitation describes the process by which species boundaries are identified and defined involving the identification of (known) species as well as of species new to science (e.g., Wiens et al., 2007). The question of how one species can be differentiated from another is irrevocably linked to the question of "what is called a species?"

Just like in other habitats in the deep sea, defined as depth >200 m (Gage and Tyler, 1991), species are often identified based on their morphological appearance. However, deep-sea sampling is known to be challenging; long hauls over several hours and subsequent sampling and sorting processes can damage specimens and thus conceal important morphological characters. In addition, morphological identifications are limited by the high rate of new species discoveries (Brandt et al., 2007), combined with a high diversity and typically low densities of deep-sea communities. The latter in turn imposes restrictions on the evaluation of intra- and interspecific variations (e.g., Brandt et al., 2007; Lim et al., 2012). Since the deep-sea environment also has a high proportion of morphologically similar but genetically different species, so-called cryptic species (Raupach and Wägele, 2006; Vrijenhoek, 2009; Brasier et al., 2016), the morpho-species approach tends to underestimate true biodiversity and, conversely, to overestimate the range of species and their population size. In addition, intraspecific morphological variability, including ontogenetic variation, polymorphism, or sexual dimorphism, poses a challenge to species assignment based on morphological characters alone (Raupach and Wägele, 2006; Riehl et al., 2012; Zaharias et al., 2020; Paulus et al., 2021).

In the last two decades, major leaps have been made in the development of taxonomic approaches and methodologies, including DNA-based taxonomy and (meta-) barcoding, "-omic" techniques, imaging tools, and integrative approaches linking different types of taxonomic information (Dayrat, 2005; Boistel et al., 2011; Raupach et al., 2016; Paulus et al., 2021). Many of these methods, despite their apparent advantage in facilitating and accelerating species delimitation, have been slow to find their way into deep-sea taxonomy. However, with increasing human impacts on deep-sea ecosystems, new methods and ideas for identifying and delimiting species are urgently needed (Brix et al., 2020).

In this study, we use a relatively well known deep-sea benthic group, isopod crustaceans (Brix and Svavarsson, 2010; Brix et al., 2018), from a relatively well known region, waters around Iceland (Brökeland and Svavarsson, 2017), to apply a range of (morphological and molecular) methods and procedures for the identification of deep-sea species. Situated right at the border between the Northern North Atlantic and the Nordic seas and separated by the Greenland-Iceland-Faroe (GIF) ridge, Icelandic waters provide a very heterogeneous marine environment linked to complex water masses and diverse submarine topography that strongly influence faunal distributions. Additionally, the fauna is threatened by climate change, including warming, acidification, freshening and productivity changes (Hanna et al., 2006; Arnason, 2007; D'alba et al., 2010; Pecl et al., 2017) which in turn could lead to changes in species diversity and geographic ranges (e.g., D'alba et al., 2010; Pecl et al., 2017). To properly assess these future impacts, understanding where species occur and how they are distributed is imperative, and thus they must be properly identified.

Isopod crustaceans are commonly found in deep-sea benthic communities, and they are also widespread in Icelandic waters (Svavarsson et al., 1993; Brix and Svavarsson, 2010; Brökeland and Svavarsson, 2017; Schnurr et al., 2018). The isopod family Haploniscidae Hansen, 1916 is considered a typical deep-sea family, although members are also found at shelf depth (Brökeland and Svavarsson, 2017; Johannsen et al., 2020). Due to their ubiquity and widespread occurrence in Icelandic waters, Haploniscidae, and the genus *Haploniscus* Richardson, 1908 in particular, are well suited as proxies for assessing species distributions around Iceland.

The basis for the current study is provided by sampling carried out in the course of the BIOICE (Benthic Invertebrates of Icelandic Waters) and the IceAGE (Icelandic marine Animals:

Genetics and Ecology) projects leading to a very comprehensive data set that is also suitable for genetic and "omic" studies (Brix et al., 2014; Riehl et al., 2014; Meißner et al., 2018). Morphology-based approaches (interactive identification keys) were used to separate haploniscid genera occurring around Iceland (*Antennuloniscus* Menzies, 1962, *Chauliodoniscus* Lincoln, 1985b and *Haploniscus*) and to identify species within the genus *Haploniscus*. In addition, bathymetric and geographic information for species in the family Haploniscidae around Iceland are compiled as part of an integrative taxonomic framework. These data are complemented by genetic [using Cytrocrome oxidase I (COI) as barcoding marker] and proteomic fingerprinting tools to foster species identification. The assumption was that many of the Icelandic haploniscid species are described and can therefore be reliably recognized as such with the interactive key as not many cryptic species are to be expected. That is, we sought to test whether the species identified by the key are "valid," and what were the limiting factors for correct species identification? This combined approach has the power to overcome problems of taxonomic standardization with data being made publicly available (e.g., via BOLD, OBIS) and enhancing species identification, for instance by fellow taxonomists, para-taxonomists and students, through online-identification keys (Balke et al., 2013).

MATERIALS AND METHODS

Study Area, Sampling and Data Collection

Specimens of the isopod family Haploniscidae were collected around Iceland during BIOICE (Benthic Invertebrates of Icelandic waters) with yearly expeditions between 1992 and 2004 and IceAGE with four expeditions: IceAGE (2011), IceAGE2 (2013), IceAGE_RR (2018) and IceAGE3 in 2020 (**Figure 1**).

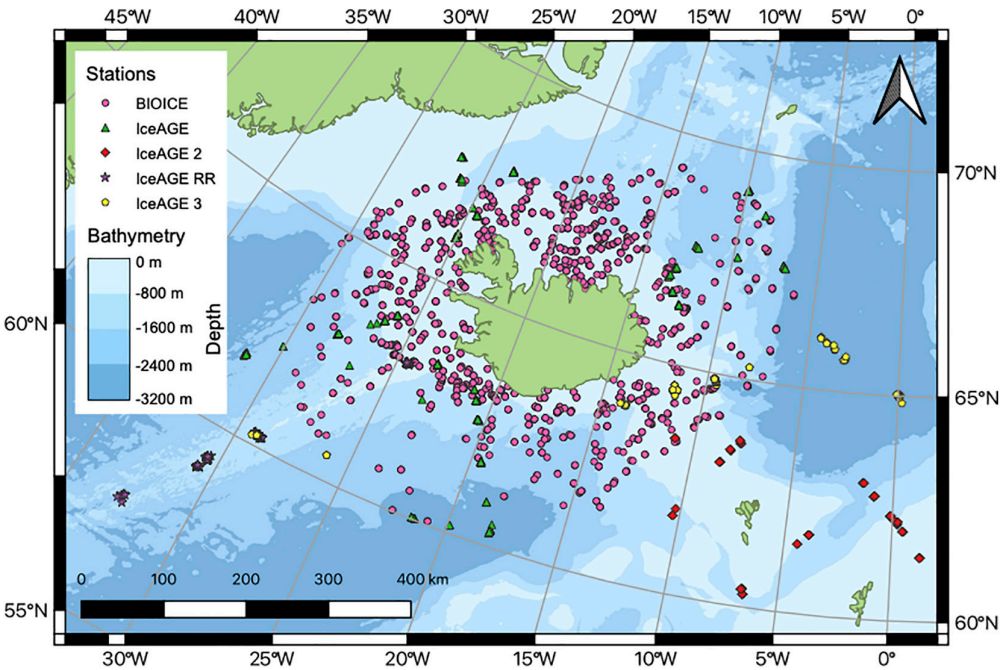

FIGURE 1 | Stations sampled during the BIOICE and IceAGE projects with the latter including the following four expeditions: IceAGE (M85/3), IceAGE 2 (POS456), IceAGE RR (MSM75), IceAGE 3 (SO276).

For the molecular analyses, only specimens were taken that were collected during the IceAGE, IceAGE2 and IceAGE_RR cruises respectively using an epibenthic sledge (EBS) or a van Veen grab (Brix and Devey, 2019). These samples were fixed in cooled high-grade ethanol to ensure genetic analysis. The material was first examined morphologically and given a unique database number at the DZMB (German Centre for Marine Biodiversity Research, Hamburg). For the species distribution models as well as bathymetry and geological distribution analyses, specimens from BIOICE and IceAGE (IceAGE, IceAGE2, IceAGE_RR, IceAGE3) were utilized.

During the BIOICE project, specimens were collected using a detritus sledge (Sneli sled; Sneli, 1998), a RP sledge (Rothlisberg and Pearcy sledge; Rothlisberg and Pearcy, 1976), a triangle dredge and an Agassiz trawl. The RP samples were elutriated through a 0.5 mm sieve, and the remaining sediment and animals were processed through a series of sieves (4, 2, 1, and 0.5 mm). The detritus sledge samples were then processed through two vertically stacked (1 and 0.5 mm) sieves. The Agassiz and triangle dredge samples were hand-picked on board. After the sorting process the BIOICE samples were stored in 5% buffered formalin (Brökeland and Svavarsson, 2017). Samples that were collected during the four different IceAGE expeditions and included in the analyses come from the EBS (EBS, Brenke, 2005) and triangle dredge.

Interactive Identification Keys

Interactive keys were developed for identifying genera of the family Haploniscidae as well as for identifying species of the genus *Haploniscus* distributed around Iceland by examining the relevant literature of species and genera descriptions to derive distinguishing morphological characters (Lincoln, 1985a,b; Sars, 1896-1899; Richardson, 1908; Hansen, 1916; Menzies, 1962; Hessler, 1970; Chardy, 1974; Brökeland and Wägele, 2004; Brökeland, 2005; Brökeland and Svavarsson, 2017). The genus *Haploniscus* was present with nine species: *H. aduncus* Lincoln, 1985a, *H. ampliatus* Lincoln, 1985a, *H. angustus* Lincoln, 1985a, *H. astraphes* Brökeland and Svavarsson, 2017, *H. bicuspis* (Sars, 1877), *H. borealis* Lincoln, 1985a, *H. foresti* Chardy, 1974, *H. hamatus* Lincoln, 1985a and *H. spinifer* Hansen, 1916. The genera *Antennuloniscus* and *Chauliodoniscus* were only represented by one species each with *Antennuloniscus simplex* Lincoln, 1985a and *Chauliodoniscus armadilloides* (Hansen, 1916).

Length-width ratios of body segments and appendages were measured according to Hessler (1970); total width refers to the widest part of the habitus, while total length was measured from the anterior beginning of the head (excluding the rostrum if present) to the exterior medial end of the pleotelson. Length and width measurements for the appendage ratios always describe the greatest length of the articles. Arabic numerals were used to refer to body segments (Wolff, 1962; Hessler, 1970).

For distinguishing characters as well as digital habitus drawings were created. To illustrate these, literature drawings were modified, first by scanning the image and then tracing them manually using a Wacom Intuos M Drawing Pad, while using the vector-based software Adobe Illustrator CC (Lincoln, 1985a,b; Sars, 1896-1899; Hessler, 1970; Coleman, 2003; Brökeland and Wägele, 2004; Brökeland, 2005; Coleman, 2009; Brökeland and Svavarsson, 2017; Adobe Inc, 2019).

To create the interactive keys, the software package DELTA (DEscription Language for TAxonomy) (Dallwitz, 1980; Dallwitz et al., 2006; Coleman et al., 2010) was utilized, running in a virtual machine (Oracle, 2021) with Microsoft Windows XP as operating system. Characters, character states, species-specific links to worms.org and obis.org as well as taxa were added and put into the DELTA editor together with previously created character and taxon illustrations. Afterward this was exported into natural language descriptions and a multi-access key (INTKEY) using the actions set's directive files tonatr and toint. Finally, the interactive keys were published online.[1]

Molecular Analysis

Cytrocrome Oxidase I Barcoding

The focus of the molecular analysis was on the genus *Haploniscus*. Five individuals of each species were studied, where available. *Haploniscus bicuspis* has been previously shown to represent a species complex (see Paulus et al., 2021) and thus representative sequences of all three cryptic species identified by Paulus et al. (2021) were included.

DNA extraction was performed using the Marine Animal Tissue Genomic DNA Extraction Kit (Neo Biotech) or the Genomic DNA from tissue kit with NucleoSpin technology (Macherey-Nagel) following the manufacturer's recommendations. The gut was removed prior to DNA extraction and only the midsection of the specimens was utilized. A 70 μL elution buffer was added to elute the DNA. For PCR amplification of COI, 1 μL of the DNA extract was utilized together with PuReTaq Ready-To-Go PCR Beads (GE Healthcare) and 1 μL of either dgLCO (GGT CAA CAA ATC ATA AAG AYA TYG G; Meyer, 2003)/dgHCO (TAA ACT TCA GGG TGA CCA AAR AAY CA; Meyer, 2003) or LCOJJ(CHACWAAYCATAAAGATATYGG; Astrin and Stüben, 2008)/HCOJJ (AWACTTCVGGRTGVCCAAARAATCA; Astrin and Stüben, 2008) primers as well as 22 μL nuclease-free water. The PCR program comprised of an initial denaturation step at 95°C for 5 min, followed by 38 cycles of 95°C for 45 s, 45°C for 50 s and 72°C for 1 min as well as a final elongation at 72°C for 5 min. Successful amplification was assessed via gel electrophoresis (1% TAE gels). Excess primers were removed with ExoSAP and the final PCR products were bidirectionally sequenced by Macrogen using the PCR primers. Forward and reverse sequences were assembled and quality checked in GENEIOUS Prime version 2019.2.3. Sequences were aligned with MUSCLE (v 3.8.425, Edgar, 2004) including *Chauliodoniscus* sp. (GenBank accession: JF283447) as an outgroup.

To identify genetic lineages that may correspond to species, two different computational approaches were employed: general mixed Yule coalescent (GMYC; Pons et al., 2006) and assembling species by automatic partitioning (ASAP; Puillandre et al., 2021). ASAP partitions species by ranked genetic distances. Pairwise uncorrected *p*-distances were pre-computed with MEGA-X 10.0.5 (Kumar et al., 2018). The online version of ASAP was run using standard settings, except for increasing the maximum considered distance to 15%. GMYC delimits species based on branching patterns in an ultrametric tree. The ultrametric tree was computed with BEAST2 2.63 (Bouckaert et al., 2019), employing a Yule prior and enforcing the monophyly of the ingroup. Each haplotype was included only once. BEAST2 was run for 10^6 generations, sampling every 1000th tree. Convergence was assessed with Tracer and the final tree annotated with TreeAnnotator (BEAST2 package), removing the first 25% of retained trees as burn-in. GMYC was run in R (R Core Team, 2020) using the once the single and once the multiple threshold method.

Phylogenetic analysis was performed with MrBayes (v 3.2.7a, Ronquist et al., 2012) using the best-fitting model (GTR + G + I) with four runs and six chains for 10^7 generations. Every 5000th tree was retained and the first 25% were removed as burn-in. The best-fitting model was determined with MEGA-X following the AIC, and the analysis was performed on the CIPRES Science Gateway (Miller et al., 2010). The resulting tree was visualized with FigTree (Version 1.4.4).

Character	Drawing	Character states	
Articles 5 and 6 of antenna 2	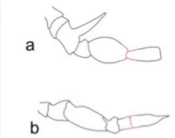	**Not fused (a)** *Haploniscus* *Chauliodoniscus*	**Fused (diffuse suture still visible) (b)** *Antennuloniscus*
Anterior angles of pereonite 2-4 not prolonged	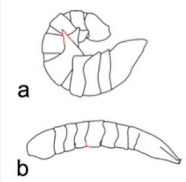	**At least one pereonite prolonged (a)** *Chauliodoniscus*	**Not prolonged (b)** *Haploniscus* *Antennuloniscus*

FIGURE 2 | Summary of morphological characters and character states used to create the interactive identification key for genera within Haploniscidae.

Matrix-Assisted Laser Desorption/Ionization Time-of-Flight Mass Spectrometry

From the same specimens used for COI barcoding, a single pereopod with the attached muscles was used for matrix-assisted laser desorption/ionization time-of-flight mass spectrometry (MALDI-TOF MS) measurements. The tissue was incubated in 5 μl of a matrix solution containing α-Cyano-4-hydroxycinnamic acid (HCCA) as a saturated solution in 50% acetonitrile, 47.5% molecular grade water and 2.5% trifluoroacetic acid. After 5 min of incubation, 1.5 μl of the extract solution was applied to one spot for crystallization on a target plate. Measurements were carried out on a Microflex LT/SH System (Bruker Daltonics), employing the flexControl 3.4 (Bruker Daltonics) software. Masses were measured in a range from 2,000 to 20,000 Dalton (Da). During measurements, peaks were evaluated using a centroid peak detection algorithm, a signal-to-noise threshold of 2, and a minimum intensity threshold of 600, with a peak resolution higher than 400 in a range from 2,000 to 10,000 Da.

[1]https://www.researchgate.net/project/Use-of-computers-for-taxonomy/update/5d78f8333843b0b98263acf3

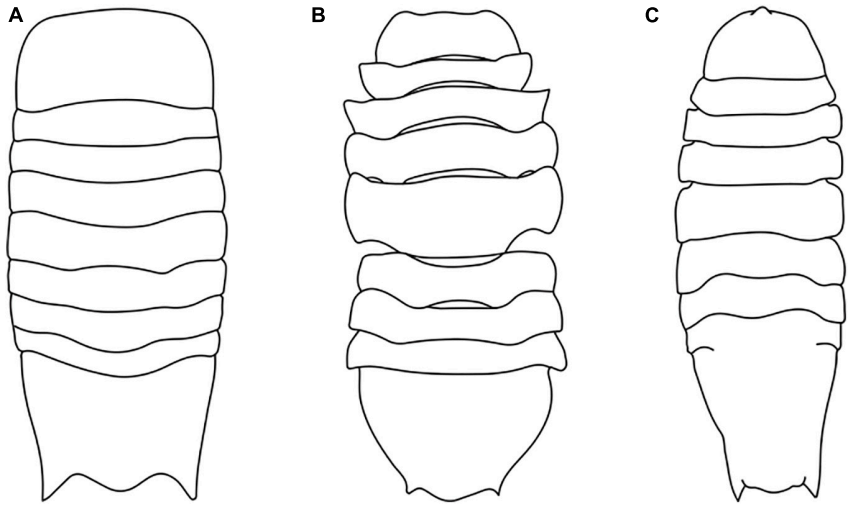

FIGURE 3 | Habitus drawing of *Antennuloniscus* **(A)**, *Chauliodoniscus* **(B)**, and *Haploniscus* **(C)** (Modified after Lincoln, 1985a,b; Brökeland and Wägele, 2004).

For fuzzy control the Proteins/Oligonucleotide method was employed with a maximal resolution ten times above the threshold. Analyses included mass spectra from *H. bicuspis* (I-III = 6, IV = 5, V = 5), *H. foresti* A (n = 3), *H. foresti* B (n = 1), *H. angustus* (n = 3), *H. hamatus* (n = 4) and *H.* n. sp. A (n = 4).

Data were processed in R (R Core Team, 2020) using R packages MALDIquant and MALDIquantForeign (Gibb and Strimmer, 2012; Gibb, 2015), trimming mass spectra to an identical range from 2,000 to 20,000 Da. Data were smoothed with the Savitzky-Golay method (Savitzky and Golay, 1964) and the baseline was removed using the SNIP baseline estimation method (Ryan et al., 1988) using 15 iterations. After normalization was done using the TIC method, a noise reduction using a signal to noise ratio (SNR) of 3 was applied. For peak picking, a half window size of 14 was used, applying the MAD method implemented in MALDIquant. Repeated peak binning was carried out with a tolerance of 0.002 in a strict approach. Missing values were interpolated from the corresponding mass spectra and all signals below a SNR of 1.75 were assumed to be below the detection limit and set to zero. The resulting data matrix was Hellinger transformed (Legendre and Gallagher, 2001).

To test group differentiation for classification approaches, a Random Forest (RF) (Breiman, 2001) analysis was carried out using R package Random Forest (Liaw and Wiener, 2002) (ntree = 2000, mtry = 35). Only species with at least three specimens were used for RF models. Significant deviation from random of the observed model errors was calculated with the function MVSF.test from package RFtools[2] (Rossel and Martínez Arbizu, 2018). Classification success was tested by creating RF models whereby one sample was omitted in each case and this was then classified using the model. Classification was tested using the *post hoc* test described by Rossel and Martínez Arbizu (2018) from the R package Rftools using a 1% alpha value for false positive recognition. Data were visualized in R using a Barnes-Hut implementation of t-Distributed Stochastic Neighbor Embedding (Krijthe and Van der Maaten, 2015) (perplexity = 5, max.iter = 4,000).

Biogeography

Geographical and Depth Distribution of Haploniscidae Species Distributed Around Iceland

To analyze the geographical species distribution, one map for each haploniscid species distributed around Iceland was created as well as one projection encompassing all species together. Data were visualized using QGIS 3.4.7-Madeira (QGIS Development Team, 2020) with the WGS 84 (ESPG: 32631) coordinate reference system. Individuals of *Halploniscus bicuspis* were assigned to the three species found within the species complex in Paulus et al. (2021) based on their distribution. To analyze the species' depth distribution, a box and whisker plots was created with Excel 16.53 (Microsoft Corporation, 2021). The whiskers boxplot is based on the same data as utilized in the geographical distribution maps although each station finding was only included once per species.

Species Distribution Models

Species distribution models (SDM) were calculated using the random forest approach (Breiman, 2001). Random Forest is a non-parametric and non-linear modeling approach based on decision trees (Hastie et al., 2009), which has been successfully applied to the modeling of species distributions around Iceland in both classification (Meißner et al., 2014; Paulus et al., 2021) and regression problems (Ostmann and Arbizu, 2018).

Predictive variables include particulate organic carbon (POC) flux, bottom water temperature, salinity, oxygen, and depth. The georeferenced predictive layers with a pixel resolution of 5-arc minute were retrieved from Global

[2]https://github.com/pmartinezarbizu/RFtools

Character	Drawing	Character state			
Rostrum presence	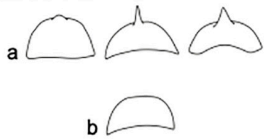	**Present (a)**	**Absent (b)**		
		H. ampliatus *H. aduncus* *H. bicuspis* *H. borealis* *H. hamatus*	*H. angustus* *H. foresti* *H. spinifer* *H. astraphes*		
Rostrum length-width ratio	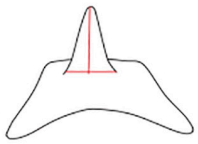	**Longer than wide**	**About as wide as long or wider than long**		
		H. aduncus *H. hamatus*	*H. ampliatus* *H. bicuspis* *H. borealis*		
Pleotelson fusion	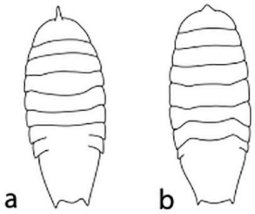	**Fused with pereonite 6 and 7 (a)**	**Fused with pereonite 7 (b)**		
		H. foresti *H. aduncus*	*H. ampliatus* *H. angustus* *H. astraphes* *H. bicuspis* *H. borealis* *H. hamatus* *H. spinifer*		
Head length compared to first segment length	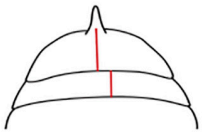	**Length of first segment fits over 1.5 times into head length**	**Length of first segment fits under 1.5 times into head length**		
		H. aduncus *H. angustus* *H. astraphes* *H. bicuspis*	*H. ampliatus* *H. borealis* *H. foresti* *H. hamatus* *H. spinifer*		
Head shape		**Half circular (a)**	**Trapezoid (b)**	**Slightly concave (c)**	**Rectangular (d)**
		H. aduncus *H. ampliatus* *H. angustus* *H. bicuspis* *H. borealis* *H. spinifer*	*H. hamatus*	*H. foresti*	*H. astraphes*
Body shape	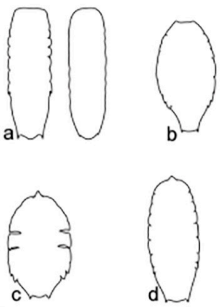	**Straight (a)**	**Fish- like (b)**	**Plate-shaped (c)**	**Slightly convex (d)**
		H. angustus *H. astraphes*	*H. foresti*	*H. ampliatus*	*H. aduncus* *H. bicuspis* *H. borealis* *H. hamatus* *H. spinifer*

FIGURE 4 | Summary of characters and character states used to create the interactive identification key for species within *Haploniscus* occurring around Iceland (Modified after Lincoln, 1985a; Brökeland and Wägele, 2004; Brökeland and Svavarsson, 2017).

Marine Environment Dataset (Basher et al., 2014). The training dataset consists of 1,511 sampling events with information on presence or absence of the isopod species under consideration. A separate model was calculated for each of the 14 taxa. Haploniscidae was found in 189 samples, while 1,322 samples had no Haploniscidae. Because of the great unbalanced distribution of classes presence and absences, for training the models, the sample size argument was adjusted, so that the number of absence samples in each of the 5,000 random trees was set to half of the number of

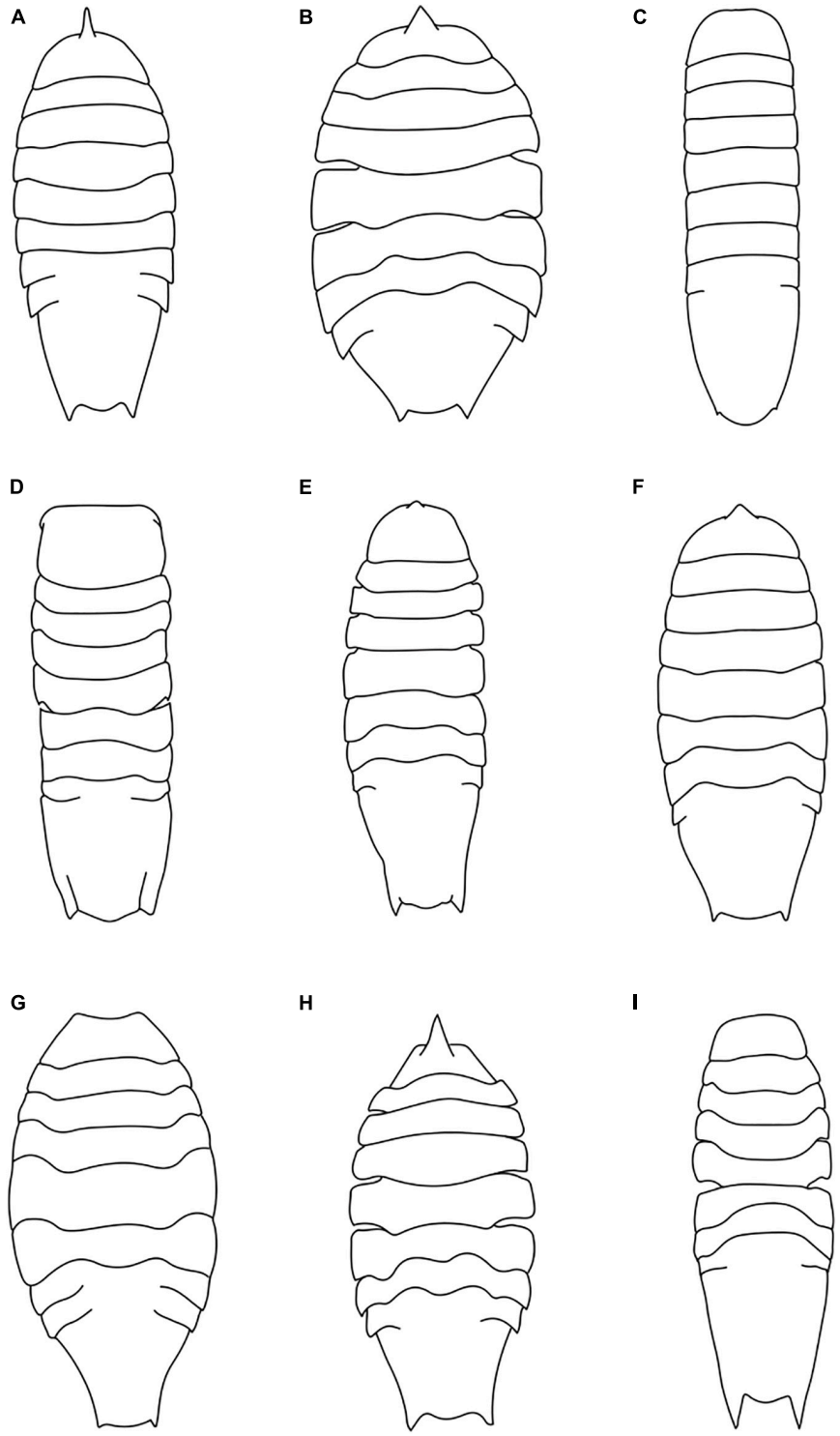

FIGURE 5 | Habitus drawings of Haploniscus aduncus **(A)** *H. ampliatus* **(B)** *H. angustus* **(C)** *H. astraphes* **(D)** *H. bicuspis* **(E)** *H. borealis* **(F)** *H. foresti* **(G)** *H. hamatus* **(H)** *H. spinifer* **(I)** (Modified after Brökeland and Wägele, 2004; Brökeland and Svavarsson, 2017).

presences. The probability of occurrence of the haploniscid species was predicted on 88,785 locations around Iceland. Computations were carried out in the statistical environment of R using the package randomForest (Liaw and Wiener, 2002). The spatial distribution was visualized in QGIS (QGIS Development Team, 2020).

RESULTS

Interactive Determination Keys

Generic Level – Haploniscidae

To distinguish between the three haploniscid genera that are distributed around Iceland, two determination characters were utilized in the Interactive key (**Figure 2**) the articles five and six of the second antenna show a visible suture only in the genus *Antennuloniscus*. The remaining two genera are distinguishable from each other as at least one of the anterior angles of the pereonites two to four, which are prolonged in *Chauliodoniscus* but not in *Haploniscus*. For the interactive key, each character as well as habitus are illustrated (**Figures 2**, **3**). The key was published online: https://doi.org/10.5281/zenodo.5682763.

Species Level – *Haploniscus*

To distinguish between the nine described *Haploniscus* species that are distributed around Iceland, six identification characters were utilized. Each distinguishing character as well as habitus are illustrated in the interactive key (**Figures 4**, **5**). The species can be categorized into four different body shapes: (1) a slightly convex body shape (*H. aduncus, H. bicuspis, H. borealis, H. hamatus* and *H. spinifer*); (2) a rather straight body shape (*H. angustus* and *H. astraphes* B); (3) a plate-shaped body (*H. ampliatus*); and lastly (4) a fish-like body shape (*H. foresti).*

Furthermore, four head shapes are found in the species: (1) half circular (*H. aduncus, H. ampliatus, H. bicuspis and H. borealis*) (2) trapezoid (*H. hamatus*) (3) slightly concave (*H. foresti*) and (4) rectangular (*H. astraphes*). Furthermore, the absence (*H. angustus, H. foresti, H. spinifer* and *H. astraphes*) or presence (*H. ampliatus, H. aduncus, H. bicuspis, H. borealis, H. hamatus*) of the rostrum was used as another distinguishing character. In addition, of the species with a rostrum, its length- and width ratio differs between species. In some species (*H. aduncus* and *H. hamatus*), the rostrum is longer than wide, while in others (*H. ampliatus, H. bicuspis*, *H. borealis*), the rostrum is at least as wide as long or even wider than long. The species can also be categorized into two different types of pleotelson fusion: (1) the pleotelson is fused with sixth and seventh pereonite (*H. aduncus*, *H. foresti*); or (2) the pleotelson is only fused with the seventh pereonite (*H. ampliatus, H. angustus, H. astraphes*, *H. aduncus, H. borealis, H. bicuspis, H. hamatus*, *H. spinifer*). Finally, comparing the ratio of the head length (without rostrum if present) relative to the first segment length can be used to differentiate between the nine different *Haploniscus* species. The length of the first segment either fits over 1.5 times (*H. aduncus H. angustus*, *H. astraphes*, *H. bicuspis*) or under 1.5 times into the head length (*H. ampliatus H. borealis, H. foresti, H. hamatus* and *H. spinifer*). The key was published online: https://doi.org/10.5281/zenodo.5701346.

During the testing of the interactive key for *Haploniscus*, a new species has been discovered, which was not identifiable with the produced key. In addition, we consulted species descriptions of all other described species in the genus, which confirmed that it is new to science. This species is most similar to *Haploniscus aduncus*, *Haploniscus astraphes* and *Haploniscus hamatus.* It differs from the other *Haploniscus* species around Iceland in possessing the unique character combination of: The pleotelson is only fused with pereonite 7, no rostrum is present, and the species has a different head shape. In the following, we provisionally name this undescribed species "*Haploniscus* sp. A" and include it into all molecular, proteomic and biogeographical analyses, while it does not occur in the interactive key.

Molecular Analyses

Cytochrome Oxidase I

The COI alignment included sequences of 37 *Haploniscus* specimens with a length of 652 bp. No indels or stop codons were present. ASAP (Threshold 11%, *p*-value $1.22e^{-02}$) and the single threshold analysis of GMYC suggested the presence of seven putative species: *H. angustus*, *H. hamatus*, *H. bicuspis* (all three cryptic species identified by Paulus et al. (2021) grouped together), *H.* sp. A and three putative species identified as *H. foresti* (*H. foresti* A–C) (**Figure 6**). These putative species are all separated by > 17% interspecific *p*-distances (**Table 1**). Two of the putative *H. foresti* species are potential sister species (*H. foresti* A and B, ∼17% genetic distance), while *H. foresti* C is more divergent from the other two with ∼24% genetic distance. The GMYC multiple threshold resulted in ten putative species by additionally delimiting the three cryptic species of *H. bicuspis* (following Paulus et al., 2021) and by further splitting *H.* sp. A into two putative species (**Figure 6**). While the three cryptic species of *H. bicuspis* are separated by ∼ 4–6% genetic distance from each other (**Table 1**), the two putative species are separated by only 2.4%. The 2nd and 3rd highest scoring ASAP partitions resulted in either six (grouping *H. foresti* A and B together; threshold 18.2%, *p*-value $2.97e^{-01}$) or 12 (splitting *H. angustus* and *H.* sp. A into two and *H. bicuspis* into four putative species; threshold 1.7%, *p*-value $3.67e^{-01}$) putative species.

Haploniscus foresti A and C occurred sympatrically at station 983 (South of Iceland), *H. foresti* B was recorded from station 106 (Reykjanes Ridge). The relatively large intraspecific distances of up to 2.3% within *H. angustus* were observed among specimens collected at the same station (Station 1148). The two most divergent putative species within *H.* sp. A did not occur sympatrically, but one occurred along the Reykjanes Ridge (Stations 106 and 137) and the other from the Irminger Sea (Station 1054; Close to the Reykjanes Ridge) to eastern Iceland (Station 1219).

Matrix-Assisted Laser Desorption/Ionization Time-of-Flight Mass Spectrometry

In total, mass spectra from 31 specimens of eight species were assessed (**Figure 7A**). The PCA of the raw data (**Figure 7B**) depicts clear differences between the different species, except for the highly similar *H. bicuspis* complex. Significant differences were found between all groups using a pairwise Wilcoxon test. Constraining the data toward the respective species in a RF model (OOB error = 0.03), results in a clear distinction of the different species, even for the specimens belonging to the *H. bicuspis* complex of which only a single specimen was misclassified within the RF model (**Figure 7C**). Creating RF models, leaving out one specimen for each species respectively and subsequently using this model to classify the left-out specimen resulted in 100%

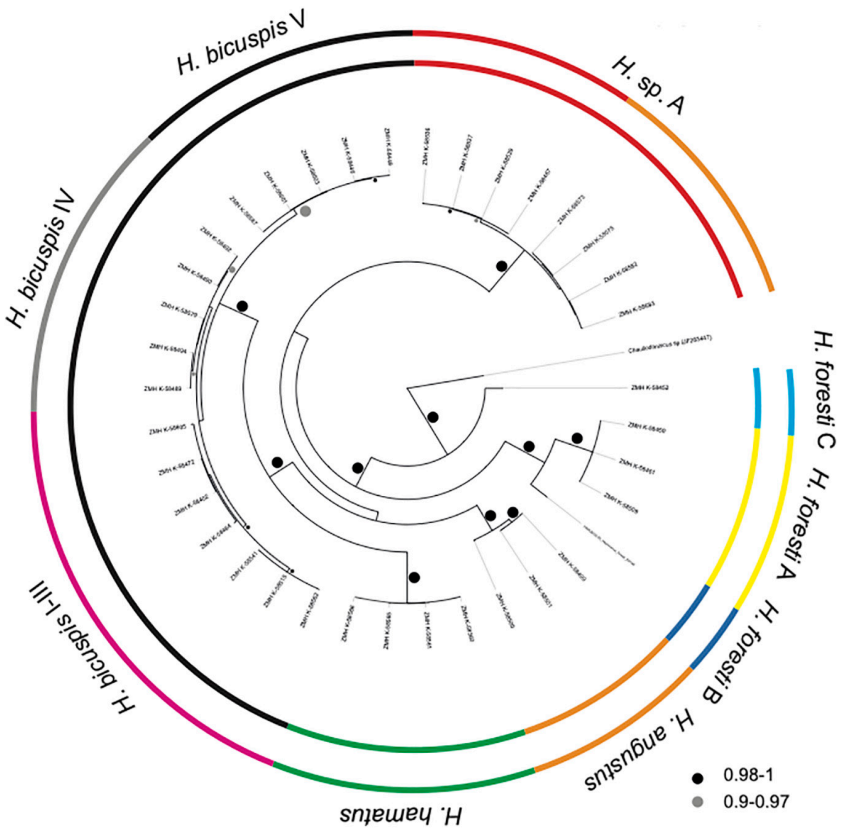

FIGURE 6 | Bayesian phylogenetic tree of COI. Posterior probabilities are shown on branches. The colored circles show delimited putative species. The inner circle corresponds to ASAP and single threshold GMYC, the outer to multiple threshold GMYC.

TABLE 1 | Uncorrected COI *p*-distances among putative Haploniscus species.

	***H. foresti* A (EP72)**	***H. foresti* B (EP199)**	***H. foresti* C (EP74)**	***H. angustus***	***H. hamatus***	***H.* sp. A**	***H. bicuspis* I-III**	***H. bicuspis* IV**	***H. bicuspis* V**
H. foresti A (EP72)	0.0–0.3								
H. foresti B (EP199)	17.3–17.6	–							
H. foresti C (EP74)	24.4–24.7	23.8	–						
H. angustus	23.2–23.5	21.9–22.4	20.1–20.4	0.0–2.3					
H. hamatus	23.2–23.5	23.3–23.5	23.6	21.8–22.4	0.0–0.2				
H. sp. A	25.2–26.2	23.3–23.9	20.4–21.3	19.9–20.4	24.1–25.8	0.0–2.4			
H. bicuspis I-III	25.6–26.4	23.9–25.9	23.6–23.9	20.6–21.0	20.4–20.9	22.4–23.7	0.0–3.5		
H. bicuspis IV	22.9–24.8	22.2–23.8	23.1–23.5	20.2–21.0	20.2–20.7	20.9–22.7	4.1–5.2	0.0–1.5	
H. bicuspis V	25.5–25.8	24.4–24.7	23.5–23.8	19.2–20.6	20.4	22.0–22.9	5.5–6.4	4.8–5.4	0.0–0.5

Intraspecific distances are along the diagonal, interspecific distances below the diagonal.

identification success supported by the *post hoc* test in all cases. None of the specimens were misclassified and no classification was recognized as a false positive by the *post hoc* test.

Biogeography

Geographical Distribution

Distribution maps for thirteen haploniscid species identified from the BIOICE and IceAGE samples were created in QGIS (**Figure 8**). Except for *Haploniscus borealis* Lincoln, 1985a, our data included all species previously recorded from Icelandic waters as well as *Haploniscus* sp. A. Where possible records of *Haploniscus bicuspis* were assigned to the respective cryptic species (Paulus et al., 2021), whose distribution was shown separately (**Figure 9**). The distribution of the three potentially cryptic species suggested for *H. foresti* by the genetic data was not analyzed separately as we cannot assign the various distribution records accordingly.

Only one species each of the genera *Antennuloniscus* and *Chauliodoniscus* were present, both species occurring only to

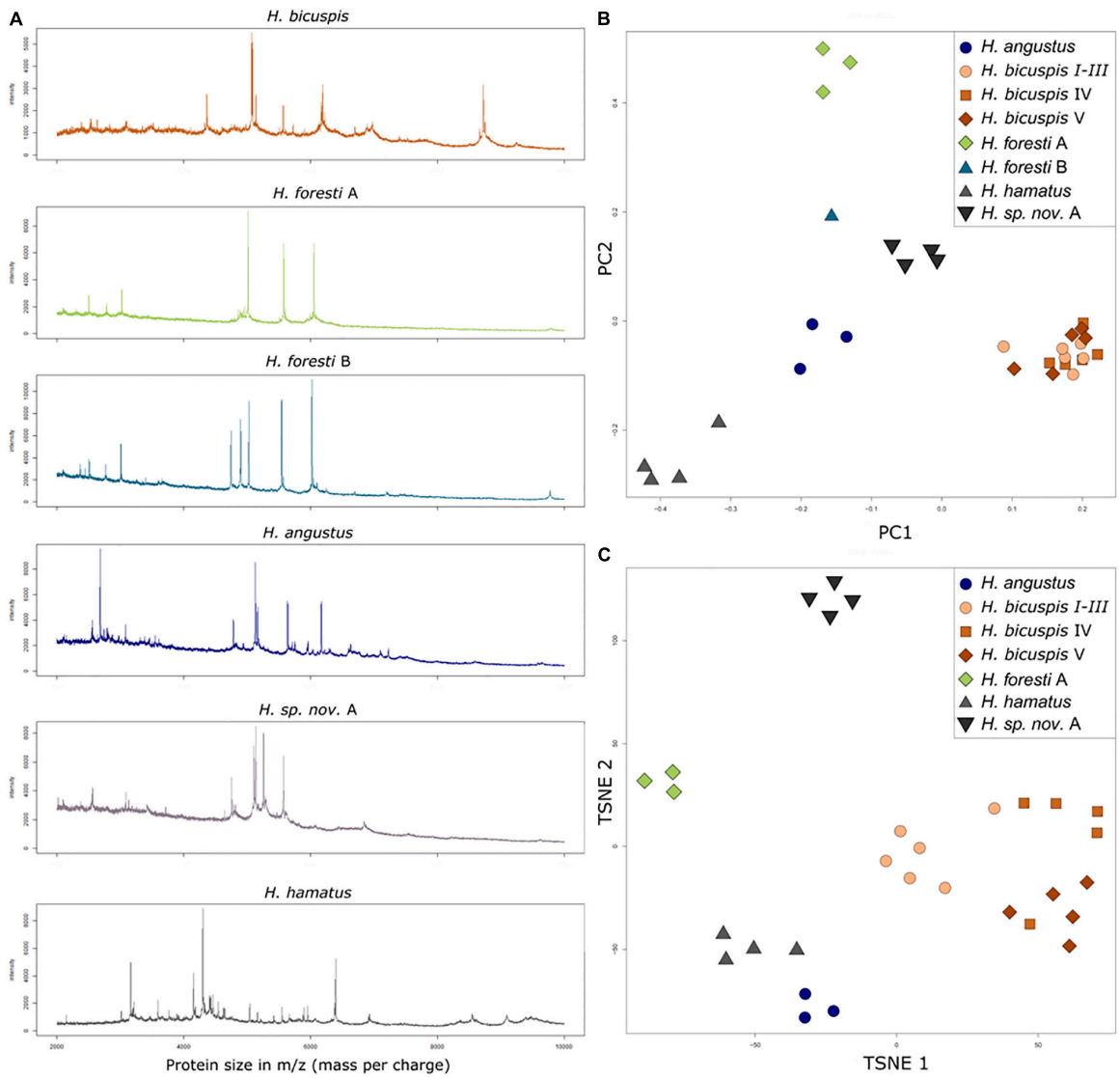

FIGURE 7 | Results of the MALDI-TOF MS measurements. **(A)** Mass spectra of different species colored according to the species colors in the TSNE plots. Because of the high similarity between the three *H. bicuspis* lineages, only a single spectrum is shown for this morphotype. **(B)** PCA of the hellinger transformed raw data. **(C)** Rf model.

the south of the GIF ridge. Within the genus *Haploniscus*, the distribution of seven species was restricted to either the north or south of the GIF ridge. *H. aduncus*, *H. ampliatus*, *H. bicuspis* IV (compare Paulus et al., 2021), *H. bicuspis* V (compare Paulus et al., 2021), *H. foresti* and *H. hamatus* occurred solely south of the ridge, while *H. bicuspis* I–III (compare Paulus et al., 2021) was restricted to the north of the ridge.

Four species showed a near-circum-Iceland distribution. *Haploniscus angustus* Lincoln, 1985a was present at four stations in the south as well as at five stations north of the GIF ridge and *Haploniscus spinifer* occurred at two stations south as well as at three stations north of the ridge. *Haploniscus astraphes* and *H.* sp. A were both found at three stations south and only at one station north of the ridge.

Bathymetric Distribution

Haploniscid species are primarily distributed at bathyal depths (**Figure 10**), with only one species, *Haploniscus bicuspis* I–III (compare Paulus et al., 2021), recorded at shelf depth (minimum depth: 64 m). Most species occur across a relatively large depth range (>1000 m), with *Haploniscus bicuspis* I-III exhibiting the widest depth range (64–2613 m [median: 1108 m]). In contrast, *H. hamatus* was bathymetrically the most restricted species, having been found between 2568 and 2670 m (median: 2619 m). Notably, species within the *H. bicuspis* species complex (compare Paulus et al., 2021) all show fairly broad, overlapping depth distributions (**Figure 10**).

Species found only in the south of the GIF ridge and those found north of the ridge showed some differences in

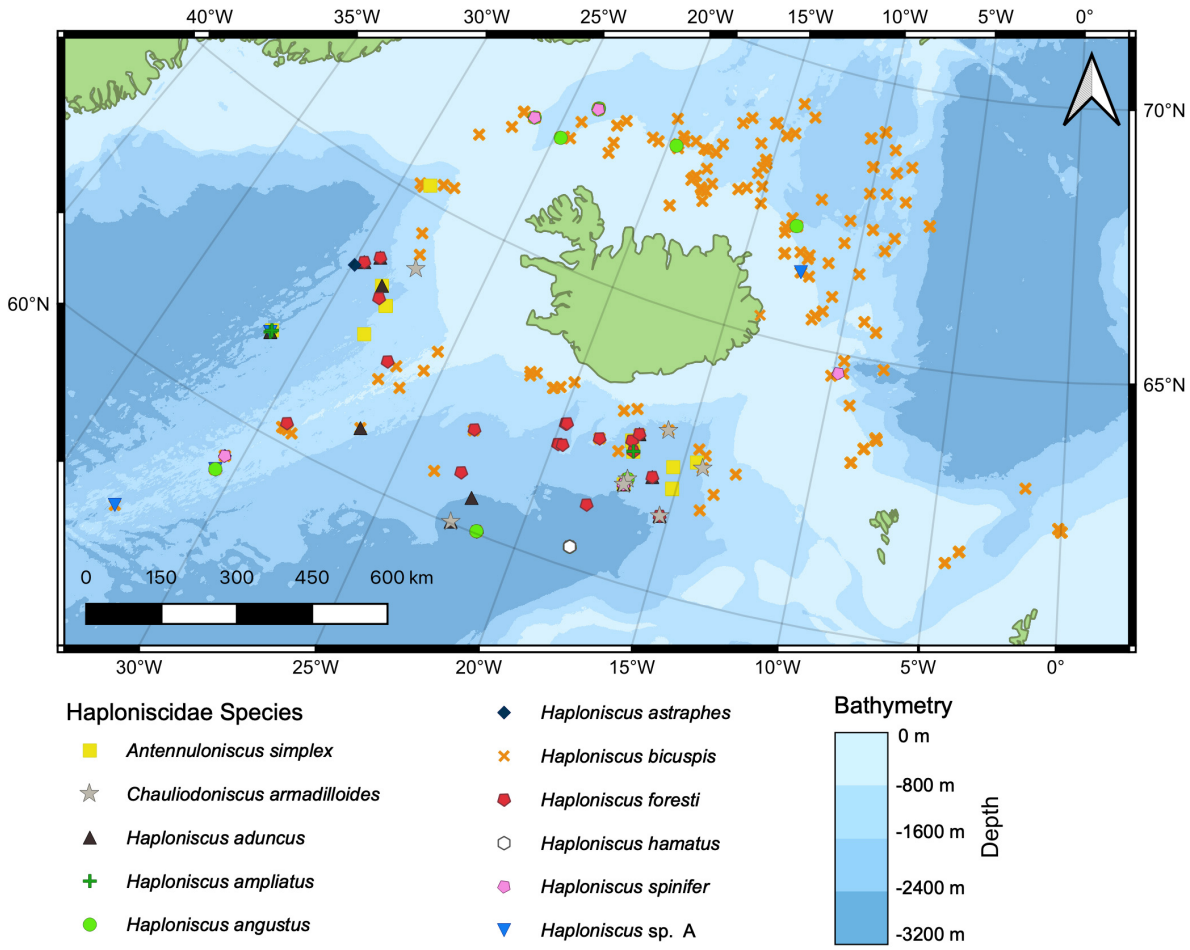

FIGURE 8 | Distribution of all Haploniscidae species found around Iceland collected during the BIOICE and IceAGE projects (Source for bathymetry: GEBCO Bathymetric Compilation Group, 2020).

bathymetric distribution; most southern species (*A. simplex, C. armadilloides, H. aduncus, H. ampliatus*, *H. bicuspis* V, *H. foresti* and *H. hamatus*) were only found in a depth deeper than 800 m, except *H. bicuspis* IV which is present between 778 and 2850 m (median: 1412 m). In contrast, *H. angustus*, *H. astraphes*, *H. bicuspis* V, *H. spinifer* and *H.* sp. A, whose distribution is either limited to the north or that occur on both sides of the ridge, can also be found above 800 m.

Species Distribution Models

The prediction of the probability of occurrence of the species in geographic space is shown in **Figure 11**. Probabilities below 0.5 are considered "absence" and are not shown. The models show that four of the species, viz. *A. simplex, H. aduncus*, *H. foresti* (here the three potential cryptic species were not treated separately) and *H. bicuspis* IV, are sympatric having their main distribution in deep waters in the Icelandic basin, but they slightly differ in the probability of occurrence in the Irminger Sea. Only *H. bicuspis* I-III shows a clear preference for areas influenced by the colder deep-waters in the Iceland and Norwegian Seas.

Model accuracy is shown in **Table 2**. The prediction error is larger for the class "n" (absent) and is relatively low for class "y" (presence). This results in a relatively high combined error for the model, which is however, not compromising accuracy for presence. In other words, the models are failing to predict where the species is truly absent.

DISCUSSION

Progressive destruction and/or transformation of deep-sea ecosystems and associated loss of biological diversity has raised concerns about the consequences for overall ecosystem functioning (Danovaro et al., 2008). Concomitantly a call for sustainable use of the services provided by the deep sea (Armstrong et al., 2012; Thurber et al., 2014; Glover et al., 2018). Deep-sea ecosystems and fauna found around Iceland could be significantly impaired primarily by climate-related changes (Arnason, 2007; Astthorsson et al., 2007). Mitigating and managing the impacts of such changes on the marine environment, however, requires broadening of taxonomic

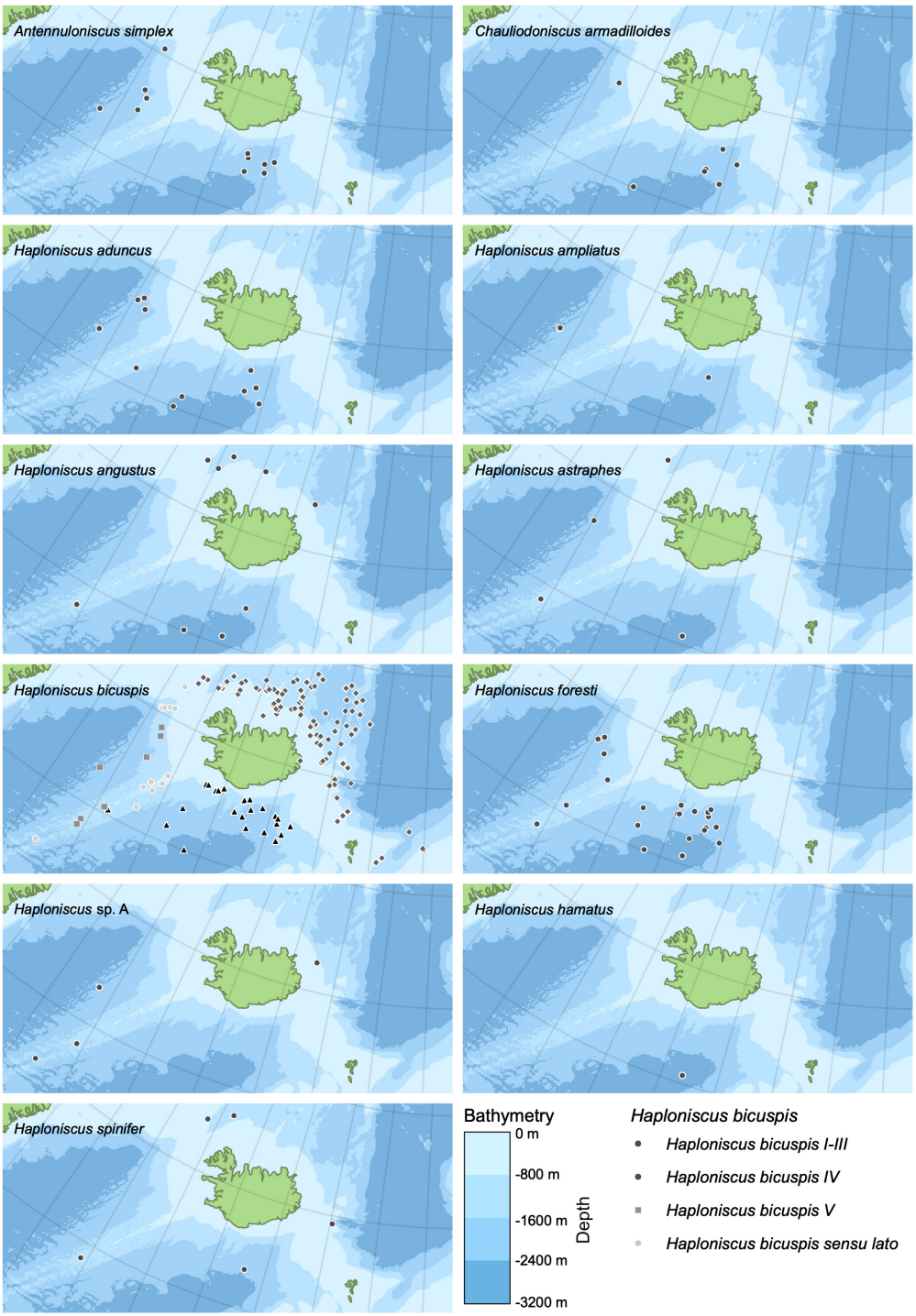

FIGURE 9 | Distribution maps of individual Haploniscidae species found around Iceland (Source for bathymetry: GEBCO Bathymetric Compilation Group, 2020).

knowledge in order to identify patterns and drivers of diversity, forecast potential alterations of the deep-sea environment, and ultimately inform marine spatial planning (Howell et al., 2020). Correct identification of the species is central to achieving this, but often poses a challenge when dealing with deep-sea samples.

Interactive keys have proven to be a valuable tool to aid species identification of Icelandic haploniscids. Originating in the 1970s, interactive keys using Descriptive Language for Taxonomy (DELTA) methodologies as an instrument for identifying species are not new (Dallwitz, 1974), but their use in deep-sea taxonomy

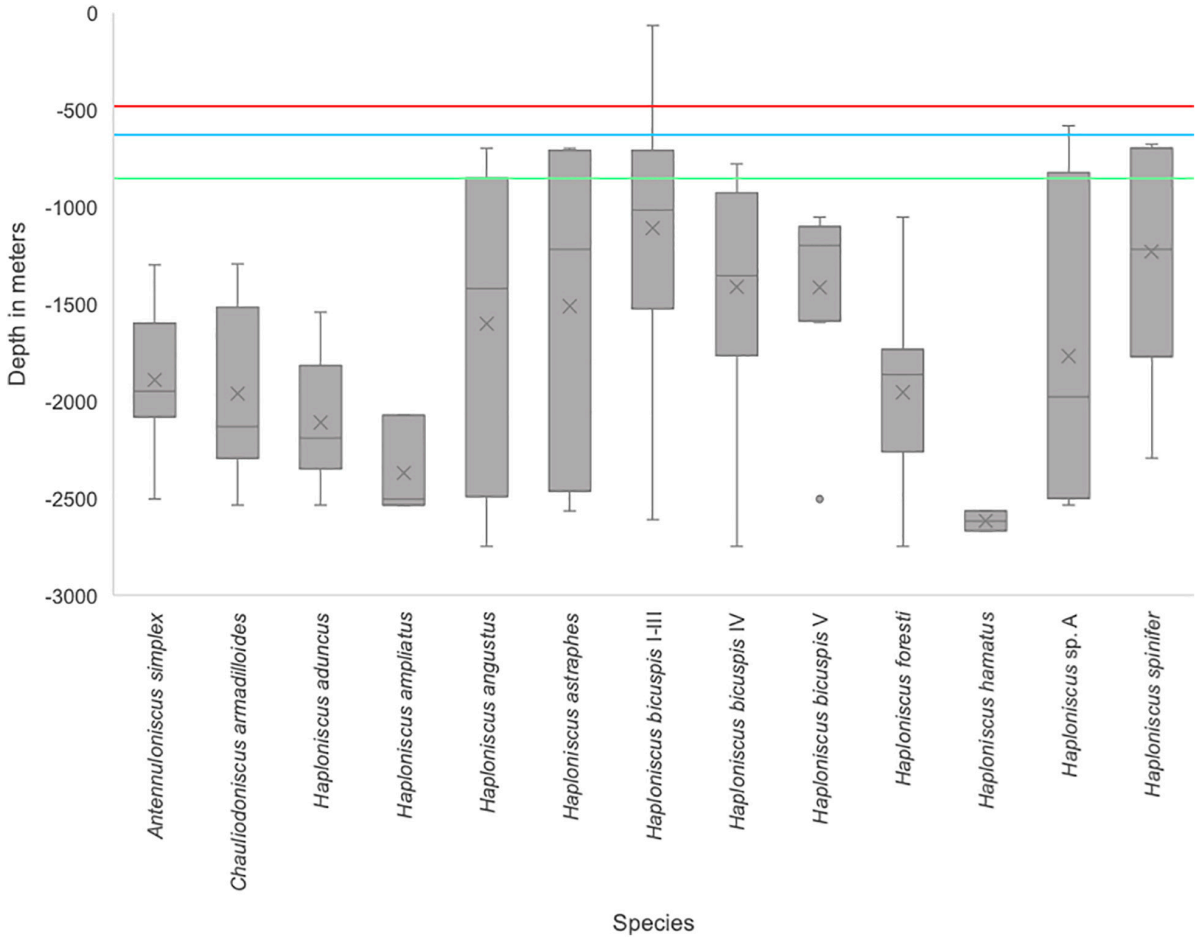

FIGURE 10 | Depth distribution of Haploniscidae species around Iceland. The colored lines mark the deepest saddle depths: 1) in the Faroe Channel at 840 m (green line), 2) between Greenland and Iceland at 620 m (blue line), and 3) between the Faroe Islands and Iceland (red line). Depth lines are implemented following the information Hansen and Østerhus (2000) and Brix and Svavarsson (2010).

has thus far been rudimentary (Saucède et al., 2021). Overall, there is a paucity of any type (paper or digital) of identification key and guide in general[3] and for deep-sea taxa in particular (Miljutin et al., 2010; Gollner et al., 2014; Bergmeier et al., 2017); instead, identifications are mostly based on descriptive works that are distributed throughout the literature (cf. Glover et al., 2021). This makes the identification process on the one hand arduous and lengthy, and on the other hand exclusive, since non-experts are not familiar with or have no access to often historical monographs. In addition, these historical monographs are often inadequately illustrated, further hindering easy species identification. Yet, given the increasing human pressures on the deep sea, the need to generate important biodiversity information is currently enormous. At the same time, the number of professional taxonomists performing this vital task is declining. As an antidote, non-experts could increasingly be called upon to identify species (Langenkämper et al., 2019; Saucède et al., 2021). To this end, it is also critical that increased efforts are made to develop keys, particularly those that are easy to use and access, such as interactive keys deposited in open repositories. Accompanying this, taxonomic efforts to describe species from the deep sea should be intensified by trained taxonomists, since only what we know can be preserved (Glover et al., 2018).

Both traditional and interactive keys, including those created in this paper, are based on formal species descriptions (e.g., Drinkwater, 2009). The applicability of these keys therefore strongly depends on the level of known and described biodiversity in the area for which they were created. Around Iceland, the deep-sea isopod fauna is considered to be relatively well known (Brix et al., 2018) and the assumption was that most species should therefore be easily identifiable with the generated key. When creating keys for taxa in other deep-sea areas, the situation is different. In these areas, typically a high percentage of undescribed crustacean species is expected (e.g., Poore, 2008; Poore et al., 2015). Here, created keys would be less applicable, as these undescribed species would not be contained in the key and thus naturally not be identifiable. However, this would also be the case with conventional dichotomous keys. In fact, where a major

[3]https://www.cbd.int/gti/problem.shtml

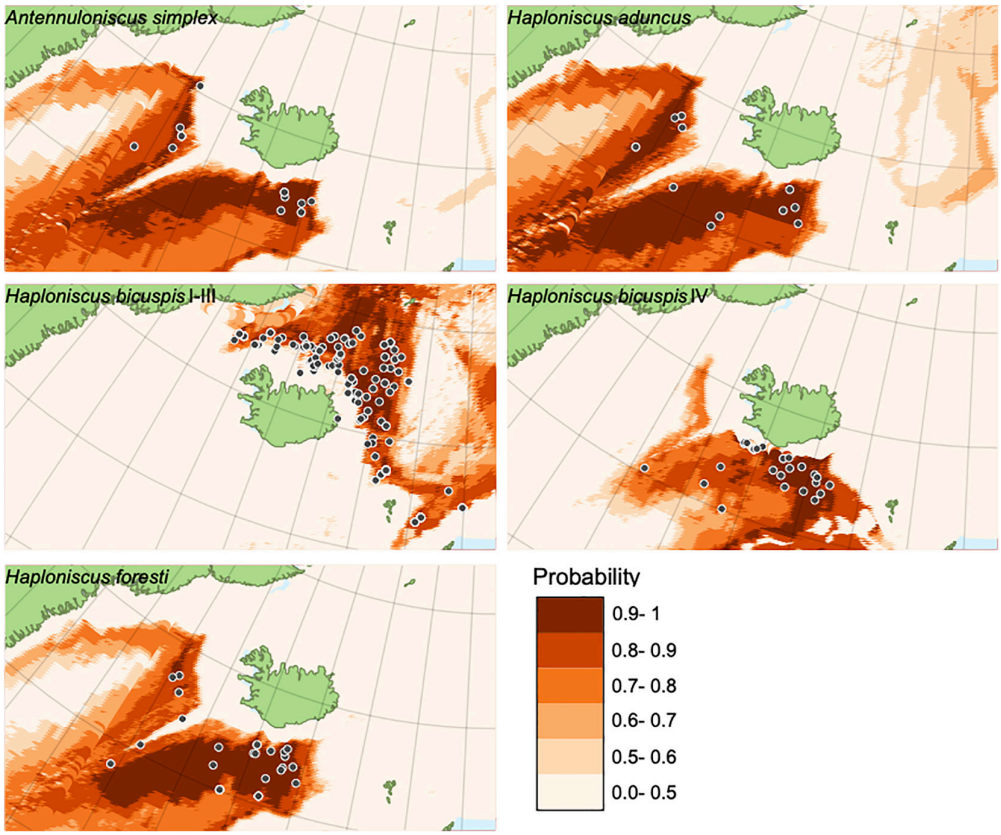

FIGURE 11 | Statistically significant species distribution models of Haploniscidae species around Iceland.

advantage of interactive keys over conventional keys comes into effect as these keys have been proven to be highly customizable. This is particularly important for deep-sea crustaceans, where much of the fauna is unknown (Appeltans et al., 2012). Indeed, interactive keys can keep pace with the dynamics of continuous new species discoveries (and descriptions) as well as a changing taxonomy (through revisions), as these can be expanded and added to rather swiftly (Coleman et al., 2010). However, this presupposes that the keys are publicly accessible (e.g., on a website provided for this purpose), easy to find (e.g., advertised on commonly used taxonomic websites) and that the necessary capacities are available to maintain them over the long term (Coleman and Radulovici, 2020).

Lately there have been numerous initiatives to bring taxonomy to the web and thus make it accessible to a wider public. Among these efforts, EDIT (European Distributed Institute of Taxonomy[4]), CATE (Creating a taxonomic e-science, Godfray et al., 2007) and Scratchpad[5] deserve special mention. The advantage of these services is that they are backed by institutes that guarantee that the infrastructure remains in place for the long term and can be brought up to date. Web-based services that are provided by individuals often lack the manpower to consistently renew their content and make it sustainable (Coleman and Radulovici, 2020). An example of this is crustacea-net[6] of the Australian Museum, Sydney, which has provided interactive keys for numerous crustacean taxa, yet its owner is now retired and the project is currently not being continued (Coleman and Radulovici, 2020). For deep-sea taxa, the World Register of Deep-Sea Species (WoRDSS) collects (traditional and interactive) keys and relevant literature that help in species identification, which now contains records from more than 600 publications – yet with a notably very low representation of sources for isopods (Glover et al., 2021). There are also individual researchers behind WoRDSS, but it is linked to the World Register of Marine Species (WoRMS, WoRMS Editorial Board, 2021), providing a catalog of all marine species names. As it is supported by the mass of deep-sea taxonomists, it is likely to be carried forward. Through this type of web-based taxonomic projects, a variety of other meta information could be added to complement species identification, including biogeographical, ecological, and collection data, as well as images and sketches (Farr, 2006). The latter would facilitate the exchange of data between researchers on undescribed species, as this is the case in many deep-sea regions, and

[4]https://cybertaxonomy.eu/
[5]http://scratchpads.org/about/concept
[6]https://australian.museum/learn/collections/natural-science/marine-invertebrates/crustacea/

TABLE 2 | Model accuracy.

	Species	*n*	y	n error	*n*	y	y error	Model error
1	*Antennuloniscus simplex*	1,296	214	0.142	0	14	0	14.042
2	*Haploniscus aduncus*	1,265	248	0.164	1	10	0.091	16.339
3	*Haploniscus bicuspis* I-III	1,081	326	0.232	9	108	0.077	21.982
4	*Haploniscus bicuspis* IV	1,209	289	0.193	0	26	0	18.963
5	*Haploniscus foresti*	1,267	232	0.155	2	23	0.080	15.354

thus facilitating taxonomic intercalibration (International Seabed Authority [ISA], 2020; Lins et al., 2021). In practice, one could imagine integrating undescribed species based on preliminary identifications into interactive keys (cf. Yamasaki et al., 2020), whereby the identifications are certainly not robust, but would help immensely in solving problems of species identification in highly diverse deep-sea areas. Since many interactive keys not only offer a web-based user interface, but also an offline version for download (such as Intkey), they are flexible enough to be used in the field or on a research vessel, regardless of internet access.

Interactive keys have a number of further assets compared to conventional dichotomous keys, which can also be advantageous in a deep-sea context. For example, the identification process does not require a strict order of the identification features. Instead, the user can freely choose the sequence of the determination characters and avoid those which are either unclear to the identifier or that are simply not present because specimens are damaged (Dallwitz, 2018). This is especially important when recruiting non-experts for species identification as they tend to have difficulties in recognizing described identification features. In addition, the use of interactive keys can be more efficient compared to dichotomous keys, as programs, such as DELTA, can autonomously specify the most suitable identification features (Dallwitz, 2018), and thus the user is able to choose the identification character that will identify individuals most quickly. In some cases, this can be tied to just one diagnostic character, for example in *Haploniscus hamatus* the unique, trapezoid head shape.

In general, a sensible selection of the identification features influences the applicability of interactive and binary keys equally. It is desirable to utilize conspicuous determination features that are retained even after rough sampling of the animals; fragile crustacean specimens in particular can lose appendages when retrieving samples from greater depth and subsequent sample processing. Therefore, determination features that can break off easily, such as antennae or legs, are often unsuitable, since damaged or missing determination features can lead to the identification in traditional keys being aborted. On the other hand, some flashy characters harbor the risk that crucial but less conspicuous features for species identification could be overlooked. Within Desmosomatidae, *Eugerdella serrata* Brix, 2006, for example, a pronounced jagged rostrum is present, with this feature enabling identification from several oceans (Brix, 2006; Lörz et al., 2013; Kaiser et al., 2021). But it is now clear that it represents a complex of species, containing at least two (Brix et al., 2018), but probably even more species. The Haploniscidae family is morphologically very conservative, and often only subtle differences are decisive in distinguishing between species and genera (Park, 2000; Brökeland, 2005). Here, in particular, the overall body form and the shape of the rostrum were emphasized as valuable diagnostic features for intraspecific delimitation and identification (Brökeland and Raupach, 2008). Further characters, such as setation patterns of pereopods or uropods have been also studied to deduce intraspecific differences, but these are often not useful as segregating characters in identification keys, as they are not visible at first glance and setae are often broken off (Brökeland, 2005). We have therefore tried to strike a balance between the practicality of the keys in the sense of easily recognizable features and those that are robust and constant within a species. Therefore, for haploniscid taxa in this study, preferably habitus characteristics and the shape of the rostrum were used to distinguish genera and species within Haploniscidae.

Interactive keys reach their limits in similar places as conventional keys but can partially counteract them. For example, many traditional keys only focus on female characters, which is largely due to the fact that female isopods are more prevalent in the deep sea, and male descriptions are often lacking (Riehl et al., 2012; Kaiser, 2015). In addition, there is a strong sexual dimorphism encountered in many isopod families (incl. Haploniscidae), with males and females differing greatly in certain features (Riehl et al., 2012); in Haploniscidae this is, for example, expressed in the form that in males the second antenna is more robust and setose, and pleotelson processes are more distinct (Park, 2000; Brökeland, 2010; Paulus et al., 2021). As a result, many of the original species' descriptions only describe the female, since the male, if any, was difficult to assign and, therefore many identification keys are ultimately better suited to identify female individuals.

The identification keys produced here were based on gender-neutral characters, where a description for both sexes was available. With the help of this, however, it was not possible to identify males and females in the same way if they exhibit strong sexual dimorphism or even different male stages (such as within *Haploniscus bicuspis*, cf. Paulus et al., 2021). So, it becomes clear that using interactive keys, despite its flexible nature, would not solve the problem of identifying highly sexually dimorphic species. The same applies to ontogenetic dimorphism and the identification and differentiation of potentially cryptic species or severely damaged specimens. Many interactive keys for Crustacea, including the ones presented in this paper, are only able to identify adult individuals (e.g., Dallwitz, 2021). This is because of differing determination features depending on the developmental stage of the animals (e.g., Hessler, 1970; Wilson et al., 2011). The result could be misidentification or termination of the identification process. While there have been few studies on selected species on how the various ontogenetic stages differ (e.g., Hessler, 1970; Brökeland, 2010; Riehl and Kühn, 2020), and these characteristics could easily be fitted into an interactive key, ultimately there is often not enough material from deep-sea samples to investigate this in greater detail.

Molecular approaches, such as DNA barcoding, are a great tool to identify individuals which cannot be easily determined with morphological characters, for example in juveniles, species

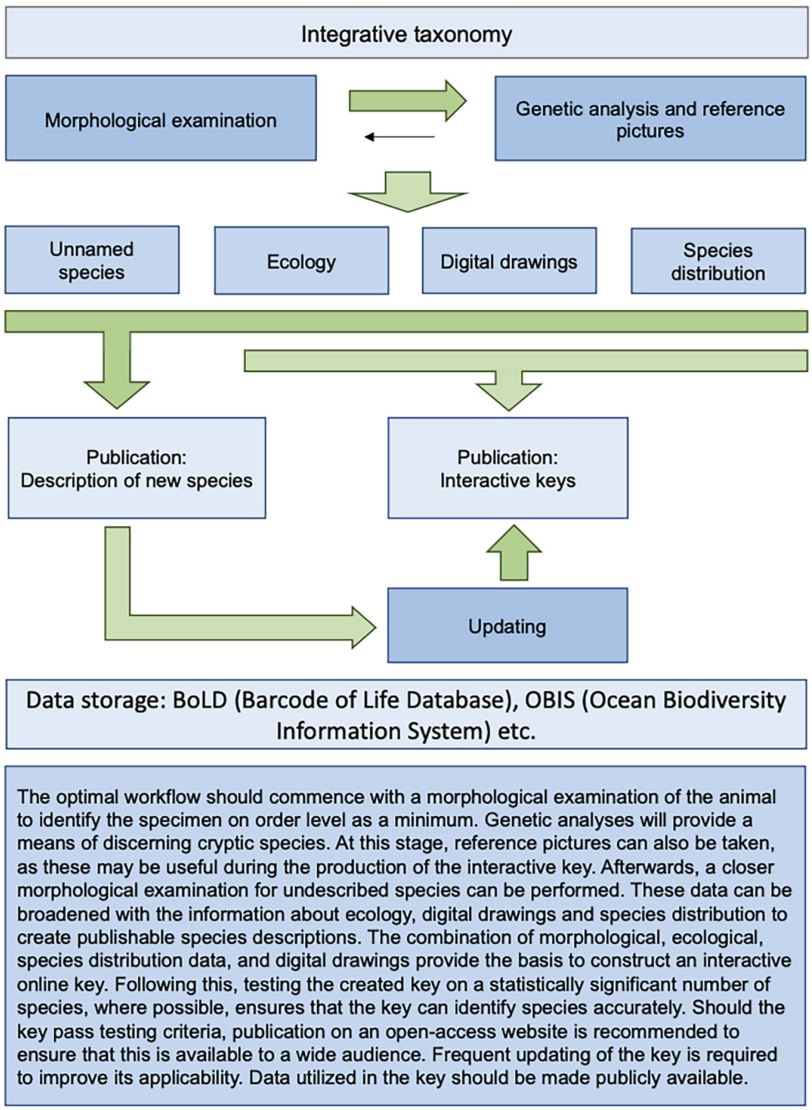

FIGURE 12 | Ideal workflow for interactive keys and integrated taxonomy.

with strong sexual dimorphism or damaged individuals. The identification of known species requires that DNA sequences of the respective species are available. DNA barcoding can further assist in the delimitation of hitherto unknown species by revealing genetically highly divergent lineages, which might correspond to (cryptic) species new to science.

Our molecular-genetic analysis of the haploniscids consistently separated all of the morphologically identified species from each other, and further uncovered a number of cryptic species, notably within *H. foresti* and *H. bicuspis* (see also Paulus et al., 2021), as well as to delimit the newly discovered species within *Haploniscus* (sp. A).

Similar to COI barcoding, MALDI-TOF MS can help in the identification of those animals which are difficult to determine with interactive keys alone. In our data proteomic fingerprinting further supported the distinctiveness of *H. bicuspis* (see also Paulus et al., 2021). Nearly all of the genetically suggested species, including the cryptic species of *H. foresti,* differed distinctly in their proteomic spectrum as well. However, differences between the putative species of *H. bicuspis* were very small and referred to a recent speciation process of this complex (Paulus et al., 2021). In a classification test, all specimens were classified correctly, showing the use of mass spectra for specimen identification. These results are in concordance with previous studies showing the high success of proteome fingerprinting in metazoan specimen identification on taxa such as fish (Mazzeo and Siciliano, 2016; Rossel et al., 2021), insects (Dieme et al., 2014; Raharimalala et al., 2017) or other crustaceans (Bode et al., 2017; Rossel et al., 2019; Renz et al., 2021). Overall, MALDI-TOF MS seems to be a promising fast and low-cost tool for the identification of deep-sea isopods. However, reference spectra need to be available to facilitate good identification

success especially for highly similar groups such as the different *H. bicuspis* lineages. It can be worthwhile to create internal databases with mass spectra for species from a defined area, especially for ongoing projects such as IceAGE.

In addition to the morphological and molecular approaches, analyzing geographical and depth distribution may provide further indications for correct species identification. This is because the distribution of benthic species around Iceland is strongly influenced by water mass properties, depth and topography, and here in particular by the GIF ridge. The latter is a major obstacle for marine invertebrates due to topographic constraints and confluence of different water masses (e.g., Svavarsson et al., 1993; Weisshappel and Svavarsson, 1998; Jöst et al., 2017; Lörz et al., 2021). This probably applies in particular to brooding taxa such as isopods, which do not have a swimming larval stage and are therefore likely to have limited dispersal capacity (Pearse et al., 2009; Brix et al., 2020). Although we recognize that this could be a circular argument, since the true geographic distribution of many deep-sea species is unknown, we have derived the assumption from the foregoing that the isopod species would be confined to a certain depth or geographic area. Hence, we could, for example, deduce a possible identification error from an unusually large geographic or depth distribution, which will need to be further assessed using an integrative taxonomy. Overall, distribution patterns helped to predict species entities to some extent, including the example of *H. bicuspis* I–III occurring north of the GIF ridge from the remaining putative species occurring only south of the ridge. However, there were many overlapping distributions both geographically and bathymetrically (**Figures 8–10**), which therefore did not aid species identification. Furthermore, distribution patterns of some species raise the question of whether they are not actually two species; for example, *Haploniscus angustus* and *H. spinifer* both have records north and south of the GIF ridge. Unfortunately, no species records of any of these two species from the north and south of the ridge are included in our molecular data to refute or confirm this hypothesis. In view of their depth distribution, there would be at least the possibility for both species to cross the GIF ridge at its deepest point (i.e., the Faroe channel at 840 m, **Figure 10**).

Finally, it was investigated whether species can be better differentiated from one another and thus identified using species distribution models. The underlying assumption here was that each species occupies its own niche space, which is defined by a certain set of environmental variables. The models presented here suffer from the fact that the number of sampling events with presence of the species is remarkably low compared to the number of sampling events where the species were not found. Yet, not finding a species in a sample does not mean that the species is not living in this location, it just means that the species was eventually not found at this sampling event. Because of the "pseudoabsence" nature of our class "n", it is not dramatic that the prediction accuracy in the training dataset for class "n" is relatively high (14–23% error). In contrast the prediction accuracy for presence (class "y") was low 0–9%, indicating that the models provide a good estimate of the potential distribution of the species. Using the distribution of *Haploniscus bicuspis* species as an example where an adequate number of data points were available, it was, however, possible to demonstrate the potential of this method; it could be shown that the predicted occurrences diverge in at least two species or groups of species (*H. bicuspis* sp. I–III restricted to the north of the GIF and *H. bicuspis* IV to the south). The addition of more environmental layers and biogeographic data will likely contribute to a better prediction of species distributions.

In summary, biogeographic and ecological species demarcation and identification is only helpful in areas in which biodiversity and distribution have been well studied and sampled. But even in one of the better-known areas like Iceland, our results have shown that knowledge gaps still exist, as demonstrated by a number of cryptic and supposedly new species. This can only be remedied through ongoing morphological examination, together with molecular methods and additional sampling. Certainly, the creation of interactive keys when combined with molecular, bathymetric and environmental datasets can increase their effectiveness as a tool for robust species identification (**Figure 12**).

CONCLUSION

In our analysis of Haploniscidae around Iceland, the use of interactive keys was proven to be a powerful tool to identify described, but also to recognize potentially new species. In particular, the easier involvement of non-experts in the identification process is highlighted, especially when additional information, such as images or biogeographical data, is included. Since interactive keys are based solely on morphology, they are subject to some restrictions due to "phenomena" such as cryptic species, sexual and ontogenetic dimorphism, or when species are severely damaged. Therefore, genetic or -omic techniques such as COI barcoding, metabarcoding, and proteomics amongst others, are essential to complement the morphological assessment.

We deliberately examined specimens from a comparatively well-known group from a comparatively well-known area, but nonetheless discovered some supposedly new isopod species. Our intention was not to evaluate various morphological and genetic methods for species identification, but to test how robustly species can be identified. Nevertheless, we found molecular tools very helpful to support the morphological identification of species, in particular proteomics as a novel tool for identifying isopod species. Despite some limitations (e.g., issues of intercalibration of mass spectra between different data sets), the latter could become a valuable alternative to the more expensive and time-consuming DNA barcoding approach.

In the longer term, all newly discovered species in this study – be it part of a species complex *(H. bicuspis*) or entirely new (*H.* sp. A) – should be included in the key. Ultimately, interactive keys for other Icelandic crustacean taxa are to be developed and made publicly available in order to build a framework of taxonomic information that will help professionals and non-experts to identify the marine fauna of Iceland and thus to gain a more complete picture of the local biodiversity. The interactive key

presented in this paper is the first for isopods, and the first step toward completing an atlas of the Icelandic marine isopod fauna. At present, even dichotomous keys on paper do not exist although the BIOICE inventory of the Icelandic fauna is used as baseline knowledge for species distributions. As mentioned in the beginning, we rely on original species descriptions and their comparison for most taxa. These missing keys highlight the need for taxonomic expertise in times of the "taxonomic impediment" (Coleman, 2015). While part of this is due to the lack of skilled taxonomists, there is an argument that taxonomists could improve accessibility of species descriptions through online databases and syntheses of taxonomic information to create identification keys. Through summarizing published species description and allowing easy adaptation, interactive online keys can help achieve this goal.

This study shows that interactive keys are an important, but hitherto underutilized tool, for obtaining an understanding of species within a given ecosystem. Within the context of the UN's Ocean Decade (2021 to 2030), interactive keys may provide the solution toward the objective of re-establishing taxonomic knowledge in the young generation of scientists, which is imperative for assessing ecosystem function and future change within the Anthropocene.

DATA AVAILABILITY STATEMENT

The datasets presented in this study can be found in online repositories. The names of the repository/repositories and accession number(s) can be found below: http://www.boldsystems.org/index.php/Public_SearchTerms?query=DS-HAPLB, accession number(s) can be found in the additional information for this paper: https://doi.org/10.5061/dryad.r2280gbcd; https://zenodo.org/record/5710070#.YZqyzC2l2u4; https://zenodo.org/record/5701346#.YZqy873P3eo; https://zenodo.org/record/5682763#.YZqzAi2l2u4.

AUTHOR CONTRIBUTIONS

JS was one of the organizers of the BIOICE expeditions and sampling. SB organized the IceAGE expeditions and sampling. JS and SB conducted the species identification. A-NL supervised the theses of KK. EP sequenced the COI data. MS performed the genetic distance and phylogenetic analyses. SR, JP, EP, and SB created the MALDI-TOF MS data and discussed with PM. PM created the species distribution models and KK visualized them. KK, CC, A-NL, and SB constructed the interactive keys. KK performed geological mapping and species bathymetry distribution analyses. KK, SK, MS, SR, JP, PM, CC, and SB drafted the first version of the manuscript. All authors contributed to the final version of the manuscript.

FUNDING

The expeditions in the frame of the IceAGE project were supported by the German Science Foundation (DFG) under contract nos BR3843/3-1,4-1, MerMet17-15 and MerMet17-06 to SB and the German Ministry for Education (BMBF). SK acknowledges a grant by the Narodowa Agencja Wymiany Akademickiej (NAWA, Poland) under the ULAM program. This work was also supported by the DFG initiative 1991 "Taxonomics" (Grant number RE2808/3-1 and RE2808/3-2).

ACKNOWLEDGMENTS

We are thankful for the sampling efforts of the scientific and ship's crew of the BIOICE (Håkon Mosby, Bjarni Saemundsson, and Magnus Heinason) and IceAGE expeditions on board of all vessels (RVs Meteor, Poseidon, Maria S. Merian, and Sonne). We are grateful for Karen Jeskulke and Nicole Gatzemeier for the technical support during sampling, data management, and laboratory assistance. We highly appreciate Jenny Neuhaus' help testing the interactive keys. Many thanks to Craig Hammock for proof-reading before submission. This is publication 15 of the Senckenberg am Meer Proteomics Laboratory.

SUPPLEMENTARY MATERIAL

The Supplementary Material for this article can be found online at: https://www.frontiersin.org/articles/10.3389/fmars.2021.795196/full#supplementary-material

REFERENCES

Adobe Inc (2019). *Adobe Illustrator CC (Version 23.0.2)*. Available online at: https://adobe.com/products/illustrator (accessed February 01, 2021).

Appeltans, W., Ahyong, S. T., Anderson, G., Angel, M. V., Artois, T., Bailly, N., et al. (2012). The magnitude of global marine species diversity. *Curr. Biol.* 22, 2189–2202. doi: 10.1016/j.cub.2012.09.036

Armstrong, C. W., Foley, N. S., Tinch, R., and van den Hove, S. (2012). Services from the deep: steps towards valuation of deep sea goods and services. *Ecosyst. Servic.* 2, 2–13. doi: 10.1016/j.ecoser.2012.07.001

Arnason, R. (2007). Climate change and fisheries: assessing the economic impact in Iceland and Greenland. *Nat. Resour. Model.* 20, 163–197. doi: 10.1111/j.1939-7445.2007.tb00205.x

Astrin, J. J., and Stüben, P. E. (2008). Phylogeny in cryptic weevils: molecules, morphology and new genera of western Palaearctic Cryptorhynchinae (Coleoptera: Curculionidae). *Inverteb. Syst.* 22, 503–522. doi: 10.1071/IS07057

Astthorsson, O. S., Gislason, A., and Jonsson, S. (2007). Climate variability and the Icelandic marine ecosystem. *Deep Sea Res. Part II Top. Stud. Oceanogr.* 54, 2456–2477. doi: 10.1016/j.dsr2.2007.07.030

Balke, M., Schmidt, S., Hausmann, A., Toussaint, E. F., Bergsten, J., Buffington, M., et al. (2013). Biodiversity into your hands–a call for a virtual global natural history 'metacollection'. *Front. Zool.* 10:55. doi: 10.1186/1742-9994-10-55

Basher, Z., Bowden, D., and Costello, M. (2014). *Global Marine Environment Dataset (GMED). Version 1.0 (Rev.01.2014)*. Available online at: http://gmed.auckland.ac.nz (accessed August 01, 2021)

Bergmeier, F. S., Brandt, A., Schwabe, E., and Jörger, K. M. (2017). Abyssal *Solenogastres* (Mollusca, Aplacophora) from the Northwest Pacific: scratching the surface of deep-sea diversity using integrative taxonomy. *Front. Mar. Sci.* 4:410. doi: 10.3389/fmars.2017.00410

Bode, M., Laakmann, S., Kaiser, P., Hagen, W., Auel, H., and Cornils, A. (2017). Unravelling diversity of deep-sea copepods using integrated morphological and molecular techniques. *J. Plankton Res.* 39, 600–617. doi: 10.1093/plankt/fbx031

Boistel, R., Swoger, J., Kržič, U., Fernandez, V., Gillet, B., and Reynaud, E. G. (2011). The future of three-dimensional microscopic imaging in marine biology. *Mar. Ecol.* 32, 438–452. doi: 10.1111/j.1439-0485.2011.00442.x

Bouckaert, R., Vaughan, T. G., Barido-Sottani, J., Duchêne, S., Fourment, M., Gavryushkina, A., et al. (2019). BEAST 2.5: an advanced software platform for Bayesian evolutionary analysis. *PLoS Comput. Biol.* 15:e1006650. doi: 10.1371/journal.pcbi.1006650

Brandt, A., De Broyer, C., De Mesel, I., Ellingsen, K., Gooday, A., Hilbig, B., et al. (2007). The biodiversity of the deep Southern Ocean benthos. *Philos. Trans. R. Soc. B Biol. Sci.* 362, 39–66. doi: 10.1098/rstb.2006.1952

Brasier, M. J., Wiklund, H., Neal, L., Jeffreys, R., Linse, K., Ruhl, H., et al. (2016). DNA barcoding uncovers cryptic diversity in 50% of deep-sea Antarctic polychaetes. *R. Soc. Open Sci.* 3:160432. doi: 10.1098/rsos.160432

Breiman, L. (2001). Random forests. *Mach. Learn.* 45, 5–32. doi: 10.1023/A:1010933404324

Brenke, N. (2005). An epibenthic sledge for operations on marine soft bottom and bedrock. *Mar. Technol. Soc. J.* 39, 10–21. doi: 10.4031/002533205787444015

Brix, S. (2006). *A New Species of Desmosomatidae (Isopoda: Crustacea) From the Deep Southern Ocean: Eugerdella Serrata sp. nov. Including Remarks to the Morphological Variability Within Eugerdella Hessler, 1970*. Hamburg: Mitteilungen aus dem hamburger zoologischen Museum und Institut, 69–84.

Brix, S., and Devey, C. (2019). Stationlist of the IceAGE project (Icelandic marine Animals: genetics and ecology) expeditions. *Mar. Data Arch.*. doi: 10.14284/349

Brix, S., Meissner, K., Stansky, B., Halanych, K. M., Jennings, R. M., Kocot, K. M., et al. (2014). The IceAGE project–a follow up of BIOICE. *Polish Polar Res.* 35, 141–150. doi: 10.2478/popore-2014-0010

Brix, S., Osborn, K. J., Kaiser, S., Truskey, S. B., Schnurr, S. M., Brenke, N., et al. (2020). Adult life strategy affects distribution patterns in abyssal isopods–implications for conservation in Pacific nodule areas. *Biogeosciences* 17, 6163–6184. doi: 10.5194/bg-17-6163-2020

Brix, S., Stransky, B., Malyutina, M., Pabis, K., Svavarsson, J., and Riehl, T. (2018). Distributional patterns of isopods (*Crustacea*) in Icelandic and adjacent waters. *Mar. Biodivers.* 48, 783–811. doi: 10.1007/s12526-018-0871-z

Brix, S., and Svavarsson, J. (2010). Distribution and diversity of desmosomatid and nannoniscid isopods (*Crustacea*) on the Greenland–Iceland–Faeroe Ridge. *Polar Biol.* 33, 515–530. doi: 10.1007/s12526-018-0871-z

Brökeland, W. (2005). *Systematics, Zoogeography, Evolution and Biodiversity of Antarctic Deep-Sea Isopoda (Crustacea: Malacostraca)*. Hamburg: Staats-und Universitätsbibliothek Hamburg Carl von Ossietzky.

Brökeland, W. (2010). Redescription of *Haploniscus rostratus* (Menzies, 1962)(Crustacea: Peracarida: Isopoda) with observations on the postmarsupial development, size ranges and distribution. *Zootaxa* 2521, 1–25. doi: 10.11646/zootaxa.2521.1.1

Brökeland, W., and Raupach, M. J. (2008). A species complex within the isopod genus *Haploniscus* (Crustacea: Malacostraca: Peracarida) from the Southern Ocean deep sea: a morphological and molecular approach. *Zool. J. Linn. Soc.* 152, 655–706. doi: 10.1111/j.1096-3642.2008.00362.x

Brökeland, W., and Svavarsson, J. (2017). Distribution of haploniscids (Isopoda, Asellota, Haploniscidae) in Icelandic waters, with description of *Haploniscus astraphes* n. sp. from the Iceland basin and the Southeast Atlantic Ocean. *Zootaxa* 4231, 301–326. doi: 10.11646/zootaxa.4231.3.1

Brökeland, W., and Wägele, J.-W. (2004). Redescription of three species of *Haploniscus* Richardson, 1908 (Isopoda, Asellota, Haploniscidae) from the Angola Basin. *Organ. Divers. Evol.* 4:237. doi: 10.1016/j.ode.2004.02.004

Chardy, P. (1974). Les Haploniscidae (Crustacés Isopodes Asellotes) de l'Atlantique. Description de huit espèces nouvelles. *Bull. Mus. Natl. Hist. Nat.* 3, 1137–1166.

Coleman, C. O. (2003). "Digital inking": how to make perfect line drawings on computers. *Organ. Divers. Evol.* 3:303. doi: 10.1078/1439-6092-00081

Coleman, C. O. (2009). Drawing setae the digital way. *Zoosyst. Evol.* 85, 305–310. doi: 10.1002/zoos.200900008

Coleman, C. O. (2015). Taxonomy in times of the taxonomic impediment–examples from the community of experts on amphipod crustaceans. *J. Crustac. Biol.* 35, 729–740. doi: 10.1163/1937240X-00002381

Coleman, C. O., Lowry, J. K., and Macfarlane, T. (2010). *DELTA for Beginners: An Introduction Into the Taxonomy Software Package DELTA*, Vol. 45. Sofia: PenSoft Publishers LTD.

Coleman, C. O., and Radulovici, A. E. (2020). Challenges for the future of taxonomy: talents, databases and knowledge growth. *Megataxa* 1, 28–34. doi: 10.11646/megataxa.1.1.5

D'alba, l, Monaghan, P., and Nager, R. G. (2010). Advances in laying date and increasing population size suggest positive responses to climate change in common eiders *Somateria mollissima* in Iceland. *Ibis* 152, 19–28.

Dallwitz, M., Paine, T., and Zurcher, E. (2006). *User's Guide to the DELTA System: A General System for Processing Taxonomic Descriptions*. Canberra, ACT: CSIRO Division of Entomology.

Dallwitz, M. J. (1974). A flexible computer program for generating identification keys. *Syst. Biol.* 23, 50–57. doi: 10.1093/sysbio/23.1.50

Dallwitz, M. J. (1980). A general system for coding taxonomic descriptions. *Taxon* 29, 41–46. doi: 10.2307/1219595

Dallwitz, M. J. (2018). *Overview of the DELTA System*. Available online at: https://www.delta-intkey.com/www/overview.htm (accessed August 6, 2021)

Dallwitz, M. J. (2021). *Descriptions, Illustrations, Interactive Identification, And Information Retrieval From DELTA Databases*. Available online at: https://www.delta-intkey.com/www/data.htm (accessed October 6, 2021)

Danovaro, R., Gambi, C., Lampadariou, N., and Tselepides, A. (2008). Deep-sea nematode biodiversity in the Mediterranean basin: testing for longitudinal, bathymetric and energetic gradients. *Ecography* 31, 231–244. doi: 10.1111/j.2007.0906-7590.05484.x

Dayrat, B. (2005). Towards integrative taxonomy. *Biol. J. Linn. Soc.* 85, 407–417. doi: 10.1111/j.1095-8312.2005.00503.x

Dieme, C., Yssouf, A., Vega-Rúa, A., Berenger, J.-M., Failloux, A.-B., Raoult, D., et al. (2014). Accurate identification of Culicidae at aquatic developmental stages by MALDI-TOF MS profiling. *Parasit. Vectors* 7, 1–14. doi: 10.1186/s13071-014-0544-0

Drinkwater, R. E. (2009). Insights into the development of online plant identification keys based on literature review: an exemplar electronic key to Australian Drosera. *Biosci. Horiz.* 2, 90–96. doi: 10.1093/biohorizons/hzp007

Edgar, R. C. (2004). MUSCLE: multiple sequence alignment with high accuracy and high throughput. *Nucleic Acids Res.* 32, 1792–1797. doi: 10.1093/nar/gkh340

Farr, D. F. (2006). On-line keys: more than just paper on the web. *Taxon* 55, 589–596. doi: 10.2307/25065636

Gage, J. D., and Tyler, P. A. (1991). *Deep-Sea Biology: A Natural History of Organisms at the Deep-Sea Floor*. Cambridge: Cambridge University Press.

GEBCO Bathymetric Compilation Group (2020). *The GEBCO_2020 Grid - A Continuous Terrain Model of the Global Oceans and Land*. Liverpool: British Oceanographic Data Centre, National Oceanography Centre, NERC.

Gibb, S. (2015). MALDIquantForeign: Import/Export Routines for MALDIquant. A package for R. Available online at: https://cran.r-project.org/package=MALDIquantForeign (accessed July 5, 2021).

Gibb, S., and Strimmer, K. (2012). MALDIquant: a versatile R package for the analysis of mass spectrometry data. *Bioinformatics* 28, 2270–2271. doi: 10.1093/bioinformatics/bts447

Glover, A. G., Higgs, N., and Horton, T. (2021). *World Register of Deep-Sea species (WoRDSS)*. Available online at: http://www.marinespecies.org/deepsea (accessed October 6, 2021)

Glover, A. G., Wiklund, H., Chen, C., and Dahlgren, T. G. (2018). Point of view: managing a sustainable deep-sea 'blue economy'requires knowledge of what actually lives there. *Elife* 7:e41319. doi: 10.7554/eLife.41319

Godfray, H. C. J., Clark, B., Kitching, I., Mayo, S., and Scoble, M. (2007). The web and the structure of taxonomy. *Syst. Biol.* 56, 943–955. doi: 10.1080/10635150701777521

Gollner, S., Ivanenko, V. N., Arbizu, P. M., and Bright, M. (2014). Correction: advances in taxonomy, ecology, and biogeography of dirivultidae (Copepoda) associated with chemosynthetic environments in the deep sea. *PLoS One* 9:e9801. doi: 10.1371/journal.pone.0009801

Hanna, E., Jónsson, T., and Box, J. E. (2006). Recent changes in Icelandic climate. *Weather* 61, 3–9. doi: 10.1256/wea.80.04

Hansen, B., and Østerhus, S. (2000). North Atlantic–Nordic Seas exchanges. *Prog. Oceanogr.* 45, 109–208. doi: 10.1016/S0079-6611(99)00052-X

Hansen, H. J. (1916). Crustacea Malacostraca. III. V. The order Isopoda. *Dan. Ingolf–Exp.* 3:262.

Hastie, T., Tibshirani, R., and Friedman, J. (2009). *The Elements of Statistical Learning; Data Mining, Inference and Prediction*, Vol. 2nd. New York, NY: Springer Science & Business Media.

Hessler, R. R. (1970). *The Desmosomatidae (Isopoda, Asellota) of the Gay Head-Bermuda Transect*. London: University of California press.

Howell, K. L., Hilário, A., Allcock, A. L., Bailey, D. M., Baker, M., Clark, M. R., et al. (2020). A Blueprint for an inclusive, global deep-sea ocean decade field program. *Front. Mar. Sci.* 7:999. doi: 10.3389/fmars.2020.584861

International Seabed Authority [ISA] (2020). *Workshop On the Deep-Sea Taxonomic Standardization: Strategic Approaches For Collaboration*. Available online at: https://isa.org.jm/files/files/documents/AnnAgd-Taxonomic.pdf (accessed February 2, 2021).

Johannsen, N., Lins, L., Riehl, T., and Brandt, A. (2020). Changes in species composition of Haploniscidae (Crustacea: Isopoda) across potential barriers to dispersal in the Northwest Pacific. *Prog. Oceanogr.* 180:102233. doi: 10.1016/j.pocean.2019.102233

Jöst, A. B., Yasuhara, M., Okahashi, H., Ostmann, A., Arbizu, P. M., and Brix, S. (2017). Vertical distribution of living ostracods in deep-sea sediments, North Atlantic Ocean. *Deep Sea Res. Part I Oceanogr. Res. Pap.* 122, 113–121. doi: 10.1016/j.dsr.2017.01.012

Kaiser, S. (2015). A new species of *Regabellator* Siebenaller & Hessler, 1981 (Isopoda, Asellota, Nannoniscidae) from the Amundsen sea shelf (Southern Ocean). *Crustaceana* 88, 405–421. doi: 10.1163/15685403-00003417

Kaiser, S., Kihara, T. C., Brix, S., Mohrbeck, I., Janssen, A., and Jennings, R. M. (2021). Species boundaries and phylogeographic patterns in new species of *Nannoniscus* (Janiroidea: Nannoniscidae) from the equatorial Pacific nodule province inferred from mtDNA and morphology. *Zool. J. Linn. Soc.* 193, 1020–1071. doi: 10.1093/zoolinnean/zlaa174

Krijthe, J. H., and Van der Maaten, L. (2015). *Rtsne: T-Distributed Stochastic Neighbor Embedding Using Barnes-Hut Implementation. R package version 0.13*. Available online at: https://github.com/jkrijthe/Rtsne (accessed July 5, 2021).

Kumar, S., Stecher, G., Li, M., Knyaz, C., and Tamura, K. (2018). MEGA X: molecular evolutionary genetics analysis across computing platforms. *Mol. Biol. Evol.* 35:1547. doi: 10.1093/molbev/msy096

Langenkämper, D., Simon-Lledó, E., Hosking, B., Jones, D. O., and Nattkemper, T. W. (2019). On the impact of citizen science-derived data quality on deep learning based classification in marine images. *PLoS One* 14:e0218086. doi: 10.1371/journal.pone.0218086

Legendre, P., and Gallagher, E. D. (2001). Ecologically meaningful transformations for ordination of species data. *Oecologia* 129, 271–280. doi: 10.1007/s004420100716

Liaw, A., and Wiener, M. (2002). Classification and regression by randomForest. *R News* 2, 18–22.

Lim, G. S., Balke, M., and Meier, R. (2012). Determining species boundaries in a world full of rarity: singletons, species delimitation methods. *Syst. Biol.* 61, 165–169. doi: 10.1093/sysbio/syr030

Lincoln, R. (1985b). *The Marine Fauna of New Zealand: Deep-Sea Isopoda Asellota, Family Haploniscidae*, Vol. 94. Wellington: New Zealand Oceanographic Institute.

Lincoln, R. (1985a). Deep-sea asellote isopods of the north-east Atlantic: the family Haploniscidae. *J. Nat. Hist.* 19, 655–695. doi: 10.1080/00222938500770411

Lins, L., Zeppilli, D., Menot, L., Michel, L. N., Bonifácio, P., Brandt, M., et al. (2021). Toward a reliable assessment of potential ecological impacts of deep-sea polymetallic nodule mining on abyssal infauna. *Limnol. Oceanogr. Methods* 19, 626–650. doi: 10.1002/lom3.10448

Lörz, A.-N., Kaiser, S., and Bowden, D. (2013). Macrofaunal crustaceans in the benthic boundary layer from the shelf break to abyssal depths in the Ross Sea (Antarctica). *Polar Biol.* 36, 445–451. doi: 10.1007/s00300-012-1269-1

Lörz, A.-N., Kaiser, S., Oldeland, J., Stolter, C., Kürzel, K., and Brix, S. (2021). Biogeography, diversity and environmental relationships of shelf and deep-sea benthic Amphipoda around Iceland. *PeerJ* 9:e11898. doi: 10.7717/peerj.11898

Mazzeo, M. F., and Siciliano, R. A. (2016). Proteomics for the authentication of fish species. *J. Proteomics* 147, 119–124. doi: 10.1016/j.jprot.2016.03.007

Meißner, K., Brix, S., Halanych, K. M., and Jażdżewska, A. M. (2018). Preface—biodiversity of Icelandic waters. *Mar. Biodivers.* 48, 715–718. doi: 10.1007/s12526-018-0884-7

Meißner, K., Fiorentino, D., Schnurr, S., Arbizu, P. M., Huettmann, F., Holst, S., et al. (2014). Distribution of benthic marine invertebrates at northern latitudes—an evaluation applying multi-algorithm species distribution models. *J. Sea Res.* 85, 241–254. doi: 10.1016/j.seares.2013.05.007

Menzies, R. J. (1962). *The Isopods of Abyssal Depths in the Atlantic Ocean*. New York, NY: Columbia University Press.

Meyer, C. P. (2003). Molecular systematics of cowries (Gastropoda: Cypraeidae) and diversification patterns in the tropics. *Biol. J. Linn. Soc.* 79, 401–459. doi: 10.1046/j.1095-8312.2003.00197.x

Microsoft Corporation (2021). *Microsoft Excel*. Available online at: https://office.microsoft.com/excel (accessed August 3, 2021).

Miljutin, D. M., Gad, G., Miljutina, M. M., Mokievsky, V. O., Fonseca-Genevois, V., and Esteves, A. M. (2010). The state of knowledge on deep-sea nematode taxonomy: how many valid species are known down there? *Mar. Biodivers.* 40, 143–159. doi: 10.1007/s12526-010-0041-4

Miller, M. A., Pfeiffer, W., and Schwartz, T. (2010). "Creating the CIPRES science gateway for inference of large phylogenetic trees," in *Proceedings of the 2010 Gateway Computing Environments Workshop (GCE)*, (New Orleans, LA: IEEE), 1–8. doi: 10.1109/GCE.2010.5676129

Oracle, V. M. (2021). *VirtualBox (Version 6.1)*. Available online at: https://www.virtualbox.org (accessed May 3, 2021).

Ostmann, A., and Arbizu, P. M. (2018). Predictive models using randomForest regression for distribution patterns of meiofauna in Icelandic waters. *Mar. Biodivers.* 48, 719–735. doi: 10.1007/s12526-018-0882-9

Park, J. Y. (2000). A revision of the isopod genus *Mastigoniscus* (Asellota, Haploniscidae) with descriptions of three new species. *Zoosyst. Evol.* 76, 195–229. doi: 10.1002/mmnz.20000760204

Paulus, E., Brix, S., Siebert, A., Arbizu, P. M., Rossel, S., Peters, J., et al. (2021). Recent speciation and hybridization in Icelandic deep-sea isopods: an integrative approach using genomics and proteomics. *Mol. Ecol.* 1–18. doi: 10.1111/mec.16234

Pearse, J. S., Mooi, R., Lockhart, S. J., and Brandt, A. (2009). "Brooding and species diversity in the Southern Ocean: selection for brooders or speciation within brooding clades?," in *Smithsonian at the Poles: Contributions to International Polar Year Science*, eds I. Krupnik, M. A. Lang, and S. E. Miller (Washington, DC: IPY), doi: 10.5479/si.097884601X.13

Pecl, G. T., Araújo, M. B., Bell, J. D., Blanchard, J., Bonebrake, T. C., Chen, I.-C., et al. (2017). Biodiversity redistribution under climate change: impacts on ecosystems and human well-being. *Science* 355:eaai9214. doi: 10.1126/science.aai921

Pons, J., Barraclough, T. G., Gomez-Zurita, J., Cardoso, A., Duran, D. P., Hazell, S., et al. (2006). Sequence-based species delimitation for the DNA taxonomy of undescribed insects. *Syst.Biol.* 55, 595–609. doi: 10.1080/10635150600852011

Poore, G. (2008). Decapod Crustacea of the continental margin of southwestern and central Western Australia: preliminary identifications of 524 species from FRV Southern Surveyor voyage SS10-2005. *Mus. Vict. Sci. Rep.* 11, 1–106.

Poore, G. C., Avery, L., Błażewicz-Paszkowycz, M., Browne, J., Bruce, N. L., Gerken, S., et al. (2015). Invertebrate diversity of the unexplored marine western margin of Australia: taxonomy and implications for global biodiversity. *Mar. Biodivers.* 45, 271–286.

Puillandre, N., Brouillet, S., and Achaz, G. (2021). ASAP: assemble species by automatic partitioning. *Mol. Ecol. Resour.* 21, 609–620. doi: 10.1111/1755-0998.13281

QGIS Development Team (2020). *QGIS Geographic Information System (Version 3.4.7-Madeira): Open Source Geospatial Foundation Project*. Available online at: http://qgis.osgeo.org

R Core Team (2020). *R: A Language and Environment for Statistical Computing*. Vienna: R Foundation for Statistical Computing.

Raharimalala, F., Andrianinarivomanana, T., Rakotondrasoa, A., Collard, J., and Boyer, S. (2017). Usefulness and accuracy of MALDI-TOF mass spectrometry as a supplementary tool to identify mosquito vector species and to invest in development of international database. *Med. Vet. Entomol.* 31, 289–298. doi: 10.1111/mve.12230

Raupach, M. J., Amann, R., Wheeler, Q. D., and Roos, C. (2016). The application of "-omics" technologies for the classification and identification of animals. *Organ. Divers. Evol.* 16, 1–12. doi: 10.1007/s13127-015-0234-6

Raupach, M. J., and Wägele, J.-W. (2006). Distinguishing cryptic species in Antarctic Asellota (Crustacea: Isopoda)-a preliminary study of mitochondrial DNA in *Acanthaspidia drygalskii*. *Antarct. Sci.* 18, 191–198. doi: 10.1017/S0954102006000228

Renz, J., Markhaseva, E. L., Laakmann, S., Rossel, S., Martinez Arbizu, P., and Peters, J. (2021). Proteomic fingerprinting facilitates biodiversity assessments in understudied ecosystems: a case study on integrated taxonomy of deep sea copepods. *Mol. Ecol. Resour.* 21, 1936–1951. doi: 10.1111/1755-0998.13405

Richardson, H. (1908). Some new Isopoda of the superfamily Aselloidea from the Atlantic coast of North America. *Proc. U.S. Natl. Mus.* 35, 71–86. doi: 10.5479/si.00963801.35-1633.71

Riehl, T., Brenke, N., Brix, S., Driskell, A., Kaiser, S., and Brandt, A. (2014). Field and laboratory methods for DNA studies on deep-sea isopod crustaceans. *Polish Polar Res.* 35, 203–224. doi: 10.2478/popore-2014-0018

Riehl, T., and Kühn, M. A. (2020). Uniting what belongs together—reevaluation of the isopod species *Macrostylis grandis* and *M. ovata* using ontogenetic, morphological and genetic evidence. *Prog. Oceanogr.* 181:102238.

Riehl, T., Wilson, G. D., and Hessler, R. R. (2012). New Macrostylidae Hansen, 1916 (Crustacea: Isopoda) from the Gay Head-Bermuda transect with special consideration of sexual dimorphism. *Zootaxa* 3277, 1–26. doi: 10.11646/zootaxa.3277.1.1

Ronquist, F., Teslenko, M., Van Der Mark, P., Ayres, D. L., Darling, A., Höhna, S., et al. (2012). MrBayes 3.2: efficient Bayesian phylogenetic inference and model choice across a large model space. *Syst. Biol.* 61, 539–542. doi: 10.1093/sysbio/sys029

Rossel, S., Barco, A., Kloppmann, M., Arbizu, P. M., Huwer, B., and Knebelsberger, T. (2021). Rapid species level identification of fish eggs by proteome fingerprinting using MALDI-TOF MS. *J. Proteomics* 231, 103993. doi: 10.1016/j.jprot.2020.103993

Rossel, S., Khodami, S., and Martínez Arbizu, P. (2019). Comparison of rapid biodiversity assessment of meiobenthos using MALDI-TOF MS and metabarcoding. *Front. Mar. Sci.* 6:659. doi: 10.3389/fmars.2019.00659

Rossel, S., and Martínez Arbizu, P. (2018). Automatic specimen identification of Harpacticoids (Crustacea: Copepoda) using random forest and MALDI-TOF mass spectra, including a post hoc test for false positive discovery. *Methods Ecol. Evol.* 9, 1421–1434. doi: 10.1111/2041-210X.13000

Rothlisberg, P., and Pearcy, W. G. (1976). An epibenthic sampler used to study the ontogeny of vertical migration of *Pandalus dordani* (Decapoda caridea). *Fish. Bull.* 74, 994–997.

Ryan, C., Clayton, E., Griffin, W., Sie, S., and Cousens, D. (1988). SNIP, a statistics-sensitive background treatment for the quantitative analysis of PIXE spectra in geoscience applications. *Nucl. Instrum. Methods Phys. Res. B* 34, 396–402. doi: 10.1016/0168-583X(88)90063-8

Sars, G. (1877). Prodromus descriptionis Crustaceorum et Pycnogonidarum, quae in expeditione norvegica anno 1876 observavit. *Archiv. Math. Naturvid. Krist.* 2, 237–271.

Sars, G. O. (1896-1899). *An Account of the Crustacea of Norway with Short Descriptions and Figures of All the Species. Isopoda*, Vol. II. Bergen: Bergen Museum.

Saucède, T., Eléaume, M., Jossart, Q., Moreau, C., Downey, R., Bax, N., et al. (2021). Taxonomy 2.0: computer-aided identification tools to assist Antarctic biologists in the field and in the laboratory. *Antarct. Sci.* 33, 39–51. doi: 10.1017/S0954102020000462

Savitzky, A., and Golay, M. J. (1964). Smoothing and differentiation of data by simplified least squares procedures. *Anal. Chem.* 36, 1627–1639. doi: 10.1021/ac60214a047

Schnurr, S., Osborn, K. J., Malyutina, M., Jennings, R., Brix, S., Driskell, A., et al. (2018). Hidden diversity in two species complexes of munnopsid isopods (Crustacea) at the transition between the northernmost North Atlantic and the Nordic Seas. *Mar. Biodivers.* 48, 813–843. doi: 10.1007/s12526-018-0877-6

Sneli, J.-A. (1998). A simple benthic sledge for shallow and deep-sea sampling. *Sarsia* 83, 69–72. doi: 10.1080/00364827.1998.10413670

Svavarsson, J., Stromberg, J.-O., and Brattegard, T. (1993). The deep-sea asellote (Isopoda, Crustacea) fauna of the Northern Seas: species composition, distributional patterns and origin. *J. Biogeogr.* 20, 537–555. doi: 10.2307/2845725

Thurber, A. R., Sweetman, A. K., Narayanaswamy, B. E., Jones, D. O., Ingels, J., and Hansman, R. (2014). Ecosystem function and services provided by the deep sea. *Biogeosciences* 11, 3941–3963. doi: 10.5194/bg-11-3941-2014

Vrijenhoek, R. C. (2009). Cryptic species, phenotypic plasticity, and complex life histories: assessing deep-sea faunal diversity with molecular markers. *Deep Sea Res. II Top. Stud. Oceanogr.* 56, 1713–1723. doi: 10.1016/j.dsr2.2009.05.016

Weisshappel, J., and Svavarsson, J. (1998). Benthic amphipods (Crustacea: Malacostraca) in Icelandic waters: diversity in relation to faunal patterns from shallow to intermediate deep Arctic and North Atlantic Oceans. *Mar. Biol.* 131, 133–143. doi: 10.1007/s002270050304

Wiens, J., Parra-Olea, G., García-París, M., and Wake, D. (2007). Phylogenetic history explains elevational biodiversity patterns in tropical salamanders. *Proc. R. Soc. Lond. B* 274, 919–928. doi: 10.1098/rspb.2006.0301

Wilson, G. D., Sims, C. A., and Grutter, A. S. (2011). Toward a taxonomy of the Gnathiidae (Isopoda) using juveniles: the external anatomy of *Gnathia aureamaculosa* zuphea stages using scanning electron microscopy. *J. Crustac. Biol.* 31, 509–522. doi: 10.1651/10-3432.1

Wolff, T. (1962). *The Systematics and Biology of Bathyal and Abyssal Isopoda Asellota (Galathea Report)*. Copenhagen: Danish Science Press.

WoRMS Editorial Board (2021). *World Register of Marine Species*. Available online at: https://www.marinespecies.org (accessed October 6, 2021)

Yamasaki, H., Herranz, M., and Sørensen, M. V. (2020). An interactive identification key to species of *Echinoderidae* (Kinorhyncha). *Zool. Anz.* 287, 14–16. doi: 10.1016/j.jcz.2020.05.002

Zaharias, P., Kantor, Y. I., Fedosov, A. E., Criscione, F., Hallan, A., Kano, Y., et al. (2020). Just the once will not hurt: DNA suggests species lumping over two oceans in deep-sea snails (*Cryptogemma*). *Zool. J. Linn. Soc.* 190, 532–557. doi: 10.1093/zoolinnean/zlaa010

Conflict of Interest: The authors declare that the research was conducted in the absence of any commercial or financial relationships that could be construed as a potential conflict of interest.

Publisher's Note: All claims expressed in this article are solely those of the authors and do not necessarily represent those of their affiliated organizations, or those of the publisher, the editors and the reviewers. Any product that may be evaluated in this article, or claim that may be made by its manufacturer, is not guaranteed or endorsed by the publisher.

Copyright © 2022 Kürzel, Kaiser, Lörz, Rossel, Paulus, Peters, Schwentner, Martinez Arbizu, Coleman, Svavarsson and Brix. This is an open-access article distributed under the terms of the Creative Commons Attribution License (CC BY). The use, distribution or reproduction in other forums is permitted, provided the original author(s) and the copyright owner(s) are credited and that the original publication in this journal is cited, in accordance with accepted academic practice. No use, distribution or reproduction is permitted which does not comply with these terms.

frontiers in Marine Science

ORIGINAL RESEARCH
published: 18 February 2022
doi: 10.3389/fmars.2022.779134

A Paradise for Rare Species: Tanaidacean Fauna of the West African Continental Margin

Piotr Jóźwiak[1], Krzysztof Pabis[1], Robert Sobczyk[1] and Bjorn Serigstad[2]*

[1] Department of Invertebrate Zoology and Hydrobiology, Faculty of Biology and Environmental Protection, University of Łódź, Łódź, Poland, [2] Center for Development Cooperation in Fisheries, Institute of Marine Research, Bergen, Norway

The benthic ecology of the Gulf of Guinea is critically understudied, and knowledge about the composition and biodiversity of the tanaidacean communities remains lacking. Our analysis of tanaidacean collection from 270 quantitative samples collected using 0.1 m^2 van Veen grab along the Ghanaian coast (nine transects, six stations at each transect, 25–1,000 m depth range) reveals a high species richness and very low abundance. The mean density of Tanaidacea across all the samples equals only 0.03 ± 0.55 ind./0.1 m^2. A total of 87 tanaidacean species were recorded, of which only three were known for science (3.4%), emphasizing the need for intensified taxonomic effort in this region. *Circa* 40% of the species were singletons, 98% of the species had a total abundance lower than 10 individuals, and approximately half of the species were found only in one sample. The highest species richness was recorded in the slope (500–1,000 m), despite the elevated levels of barium and hydrocarbons at those depths. This area was also characterized by the most unique species composition. Species accumulation curves did not reach an asymptote, suggesting an undersampling of the area and a great rarity of the species. Results of the canonical correspondence analysis (CCA) and cluster analysis demonstrated a positive influence of oxygen concentration and fluorescence, particularly in the shallow shelf sites (25–50 m), which were characterized by a higher abundance of Tanaidacea. Depth zonation of tanaidacean communities with a division between shallow-water taxa (Leptocheliidae Lang, 1973 and Kalliapseudidae Lang, 1956) through families with wide bathymetric range (Pseudotanaidae Sieg, 1976, Apseudidae Leach, 1814) to the true deep-sea forms (Paranarthrurellidae Błażewicz, Jóźwiak and Frutos, 2019) is also evident. We further discuss the problems associated with multivariate analysis of highly speciose but less abundant taxa.

Keywords: Gulf of Guinea, West Africa, continental margin, depth gradient, singletons, rare species, Tanaidacea

OPEN ACCESS

Edited by:
Torben Riehl,
Senckenberg Museum, Germany

Reviewed by:
Helena Passeri Lavrado,
Federal University of Rio de Janeiro, Brazil
Saskia Brix,
Senckenberg Museum, Germany

****Correspondence:***
Piotr Jóźwiak
piotr.jozwiak@biol.uni.lodz.pl

Specialty section:
This article was submitted to Deep-Sea Environments and Ecology, a section of the journal Frontiers in Marine Science

Received: *18 September 2021*
Accepted: *07 January 2022*
Published: *18 February 2022*

Citation:
Jóźwiak P, Pabis K, Sobczyk R and Serigstad B (2022) A Paradise for Rare Species: Tanaidacean Fauna of the West African Continental Margin. Front. Mar. Sci. 9:779134. doi: 10.3389/fmars.2022.779134

INTRODUCTION

The importance of the rare species in the functioning of marine benthic ecosystems and their ecological significance is the topic of renewed debate (Lyons et al., 2005; Ellingsen et al., 2007; Włodarska-Kowalczuk et al., 2012; Mouillot et al., 2013; Leroy et al., 2017; Chapman et al., 2018; Säterberg et al., 2019). The role of species with restricted ranges and/or a very small population size has often been neglected in the terrestrial and marine studies alike, while greater attention is directed to dominant species or the so-called foundation taxa (Grime, 1998; Ellison et al., 2005; Angelini et al., 2011). However, recent analysis has demonstrated that even a small size and a less

abundant species may be very important for the stability of the whole ecosystem. Such species that may increase functional redundancy are an important element of trophic webs and might be crucial for ecosystem services (Ellingsen et al., 2007; Dee et al., 2019; Säterberg et al., 2019). Moreover, dominant species may only provide a short-term resistance to ecosystem changes, whereas the loss of rare species may lead to the erosion of an ecosystem functioning over longer time periods (Smith and Knapp, 2003). Leitão et al. (2016) showed that rare species disproportionately contribute to the functional structure of species assemblages. The majority of these hypotheses have as yet only been tested for specific ecosystems and for a small number of taxonomic groups. Therefore, it remains difficult to draw broader conclusions that can be applied to various terrestrial, freshwater, and marine ecosystems across spatial and temporal scales.

Studies of potentially rare and ecologically important taxa are crucial for future conservation planning and studies of ecosystem response to changes (Costello and Chaudary, 2017). Rare taxa are often difficult to study due to undersampling and the lack of taxonomic experts (Guisan et al., 2006; Jóźwiak et al., 2020). Results of the analysis on the role of rare species are often difficult to interpret and could be biased due to their extremely low abundance. Therefore, the application of modern modeling techniques and attempts to link the data on species distribution and abundance with environmental variables often does not allow for straightforward conclusions (Reiss et al., 2015).

Rare species are also considered more vulnerable to both natural and anthropogenic changes associated with climate warming, pollution events, or dynamics in natural geochemical processes (Leitão et al., 2016; Obst et al., 2018). The loss of rare species might cause a significant decline in the abundance of other trophic levels (Bracken and Low, 2012). This disparity between their potential importance and difficulties in data analysis may preclude meaningful assessments of their functional ecology.

Tanaidacean diversity is significantly understudied, with the estimated number of species an order of magnitude higher than the currently described forms (Appeltans et al., 2012). Our knowledge of this group of crustaceans is centered in taxonomy (Błażewicz-Paszkowycz et al., 2012). Few deep-sea biodiversity assessments of tanaidacean communities exist, but all demonstrate a large number of singletons and a high percentage of species new to science (Pabis et al., 2014, 2015; Błażewicz-Paszkowycz et al., 2015; Stępień et al., 2018, 2019; Błażewicz et al., 2019a; Jóźwiak et al., 2020). Even fewer studies were based on quantitative samples (Błażewicz-Paszkowycz et al., 2015; Błażewicz et al., 2019a; Jóźwiak et al., 2020), though general information like the total number of species or the total number of individuals can be also found in less targeted studies of deep-sea macrofauna (e.g., Grassle and Maciolek, 1992; Cosson et al., 1997; McCallum et al., 2015; Wilson, 2017). It is therefore possible that many rare tanaidaceans may become extinct even before they are described (Costello et al., 2013) and their functional ecology deduced.

The collective knowledge of the biology of particular tanaidacean species remains in its infancy. A majority of the species are suggested to be free-living epibenthic crustaceans feeding on detritus, though some taxa construct sediment tubes for protection (Hassack and Holdich, 1987; Błażewicz-Paszkowycz and Ligowski, 2002; Larsen, 2005). However, a variety of life strategies have been recorded within Tanaidacea. For example, representatives of Metapseudidae Lang, 1970 and Tanzanapseudidae Băcescu, 1975 inhabit coral reefs or hydroid colonies (Błażewicz-Paszkowycz et al., 2012; Jóźwiak and Błażewicz, 2021), whereas some Kalliapseudidae are associated with seagrasses (Leite, 1995). Some tanaidaceans are also trophically specialized, for example, Kalliapseudinae species are suspension-feeders, filtering food particles from the water column (Drumm and Heard, 2011), where *Exspina typica* is considered a parasite that digs cavities in the bodies of holothurians (Alvaro et al., 2011). Locally, tanaidacean densities as high as 53,000 ind./m^2 were recorded (Dayton and Oliver, 1977), and their abundance might be a significant element of the whole community (Sokolova, 1972; McCallum et al., 2015; Golovan et al., 2019). Combined with their role as the prey of various benthic invertebrates such as polychaetes (Oliver and Slattery, 1985), decapods (Balasubramanian et al., 1979), isopods (Kneib, 1985), amphipods (Guţu and Sieg, 1999), as well as numerous species of fishes (Larsen, 2005) and even wading birds (Băcescu and Guţu, 1975), tanaidaceans may represent a group of high ecological importance.

Studies of benthic diversity of the Gulf of Guinea and the whole West African coast are still scarce and mostly focus on shallow water sites (e.g., Buchanan, 1957; Longhurst, 1958, 1959; Bassindale, 1961; Le Loeuff and Intès, 1999; Pabis et al., 2020). Recent analysis has revealed exceptionally high species richness of some benthic invertebrates, like cumaceans (Stępień et al., 2021) and polychaetes (Sobczyk et al., 2021). Just 10 species of Tanaidacea have previously been described in the Gulf of Guinea, whereas the number of species known from the whole west coast of Africa totals 80 (Jóźwiak et al., 2017). The Gulf of Guinea is a large marine ecosystem influenced by multiple natural factors, such as ocean currents (including Guinea Current, Benguela Current, and South Equatorial Counter Current), upwelling events, and nutrient input from land drainage. This basin is also characterized by a high diversity of habitats (Scheren et al., 2002; Ukwe et al., 2003; Ayamdoo, 2016).

The Gulf of Guinea is host to a very high diversity of benthic fauna. Yet, this ecosystem is threatened by human activities including oil excavation and the dyeing industry (Scheren et al., 2002; Ayamdoo, 2016; Sobczyk et al., 2021). In this study, we provide the first biodiversity assessment of tanaidacean communities from the West African coast based on a large set of 270 quantitative samples collected in the Gulf of Guinea. We identified the most important natural and anthropogenic factors that may shape tanaidacean communities along a depth gradient from 25 to 1,000 m along the coast of Ghana.

MATERIALS AND METHODS

Study Area

The Gulf of Guinea is a large open bay on the Atlantic coast of West Africa between latitudes 58°N and 58°S and longitudes

88°W and 128°E (Ukwe et al., 2003). The main currents of this basin are the Guinea Current, by the Benguela Current, and the South Equatorial Counter Current (Schneider, 1990; Ukwe et al., 2006). The Gulf of Guinea is characterized by the occurrence of oxygen minimum zones (Levin, 2003; Levin et al., 2009) and by dynamic sedimentation phenomena associated with coastal erosion (Ukwe et al., 2003). The coastal areas of Ghana, stretched across a distance of 565 km, are located in the atypical tropical climate region (Le Loeuff and Cosel, 1998), and are characterized by high dynamics of water masses and upwellings (Djagoua et al., 2011). This part of the coastline contains no large river systems, except for the Volta River estuary, which is located in the eastern part of the coast.

Sampling

Samples were collected in October and November of 2012 in the Gulf of Guinea off Ghana from onboard the RV *Dr. Fridtjof Nansen* at nine transects (**Figure 1** and **Supplementary Appendix 1**). A total of 270 samples were gathered using 0.1 m^2 van Veen grab supported with the video-assisted monitoring system (VAMS) allowing for appropriate sediment penetration and avoiding any underestimations associated with sampling. For each transect, seven stations were designated from the littoral to bathyal depths (0, 25, 50, 100, 250, 500, 1,000 m). Five samples were collected at each station. The material was sieved through 0.3-mm sieves, preserved primarily in 4% formaldehyde solution, sorted, and finally transferred to 70% ethanol.

The material will be deposited at the University Museum of Bergen (Norway).

Physical and chemical properties, including temperature, conductivity, and oxygen level (Seabird 911 CTD Plus and SBE 21 Seacat thermosalinographs were used) were measured at each station. Additionally, sediment samples were collected for further laboratory analysis of sediment structure, total organic matter (TOM) content, fluorescence, level of hydrocarbons, and toxic metals. Sediment grain size was determined by mixing the sediment with water and sieving it through a 0.063-mm sieve. Larger particles were then sieved through Endecott sieves. For calculations, we used the equations of Folk and Ward (1957) and Buchanan (1984). TOM was determined as the weight loss in a 2–3 g dried sample (1,058°C for 20 h) after 2 h of combustion at 4,808°C. Petroleum hydrocarbon content was determined using a gas chromatograph with a flame ionization detector (GC/FID) according to the Intergovernmental Oceanographic Commission, Manuals and Guides No. 11, UNESCO Intergovernmental Oceanographic Commission (1982). Metals (Ba, Cd, Cr, Cu, Pb, Zn) were analyzed *via* inductively coupled plasma-atomic emission spectrometry (ICP-AES), whereas mercury (Hg) was determined *via* cold vapor atomic emission spectrometry (CVAAS) after drying, sieving, and digestion (Jarvis and Jarvis, 1992; Elezz et al., 2018).

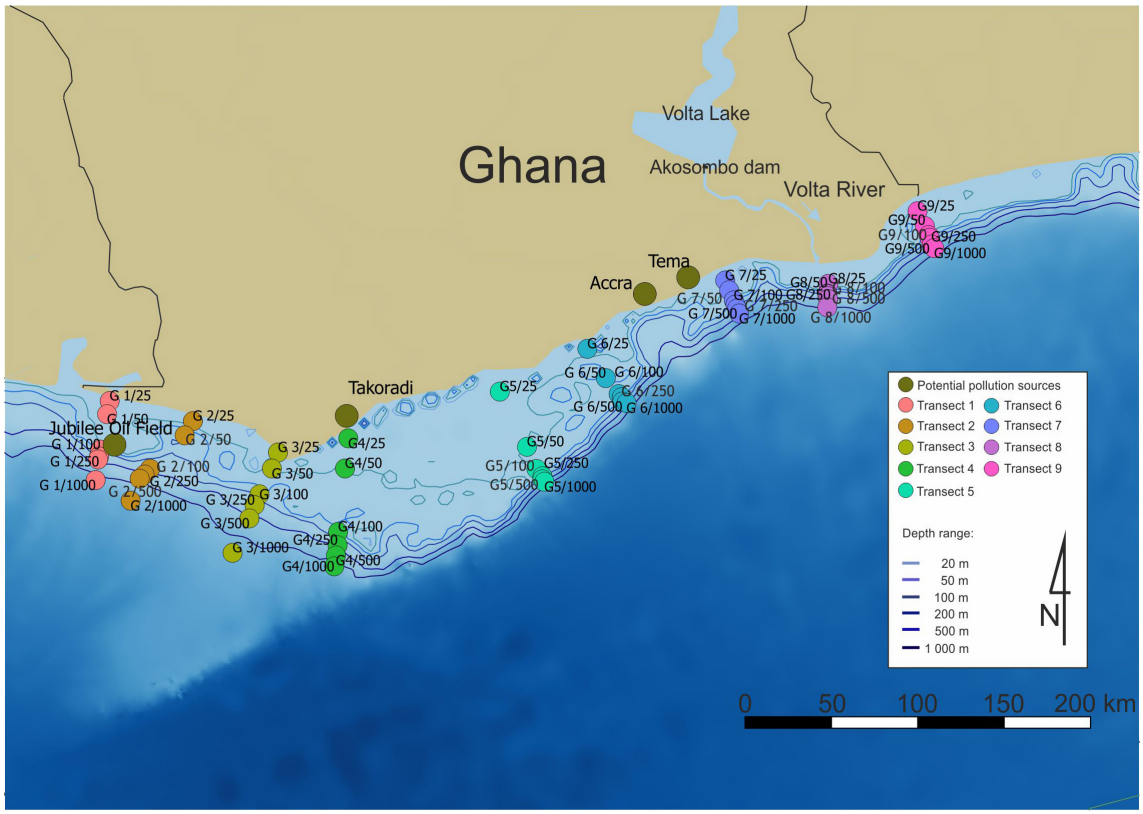

FIGURE 1 | Distribution of sampling stations along the Ghanaian coast.

Data Analysis

Specimens were identified to the morphospecies level (Wägele, 2005). Mean values of abundance (± 1 SD) and mean values of species richness per sample were calculated for each station (25, 50, 100, 250, 500, and 1,000 m) to investigate trends in abundance and species richness along a depth gradient of the Ghanaian shelf and slope. The Kruskal–Wallis test was used to assess statistically significant differences in tanaidacean abundance and species richness between depths. *Post hoc* testing was performed using Dunn's test with the software package Statistica 13. Species Chao 1 accumulation curve averaging over 999 permutations was created using the vegan package (*vegan:specaccum*; Oksanen et al., 2020) in R software (R Core Team, 2019).

The number of rare species recorded in the material was assessed. Singletons were defined as species represented by only one individual in the whole material. We have also calculated the number of unique species (species found in one sample only). Additionally, we have calculated the number of species common to a given depth zone and common to different transects. In addition, bathymetric distribution of each species and family was described.

Hierarchical agglomerative clustering based on Bray–Curtis formula was used to analyze the similarity between the samples *via* the group average method on transformed data (presence–absence). Similarity profile routine tests (SIMPROF) with a 1% significance were also applied (*clustig:simprof*, *clustig:simprof.plot*; Clarke et al., 2008; Whitaker and Christman, 2014).

The association between tanaidacean communities and all the collected environmental factors was done in R software (R Core Team, 2019). To transform environmental data for reducing biases associated with unequal ranges of some variables (for example barium and gravel), we used Yeo-Johnson power transformation from "caret" package (*caret:preProcess()* function; Kuhn, 2020). Further, canonical correspondence analysis (CCA) was performed using the *cca* function from the *vegan* package (Oksanen et al., 2020) with initial 21 variables (for the full list of variables see **Supplementary Appendix 2**). The *anova.cca* function from the *vegan* package (Oksanen et al., 2020) was used to determine the statistically significant factors in shaping diversity on each station. By using *vif* function from the *car* package (Fox and Weisberg, 2019), we assessed the degree of multicollinearity between analyzed variables. We compared the results with Pearson correlation matrix (*corrplot:corrplot*; Wei and Simko, 2017; **Figure 2**) to exclude strongly correlated variables ($r > 0.68$). Variables with the highest correlation and vif value, as well as those statistically insignificant, were excluded before another ordination analysis. Four variables were included in the final version of CCA.

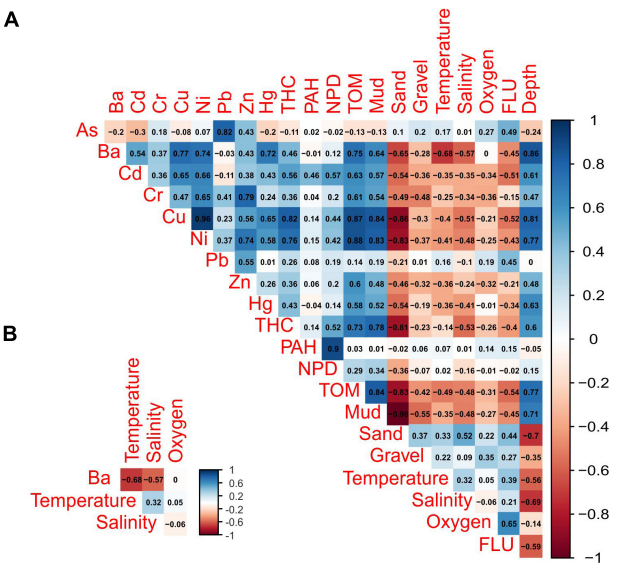

FIGURE 2 | Pearson's correlation matrix of environmental variables **(A)**. Only four of the least correlated ($r < 0.70$) variables were used in the CCA analysis **(B)**.

RESULTS

Eighty-seven species (646 individuals) representing 19 families were found in the analyzed material (**Table 1**). Four families (Akanthophoreidae Sieg, 1986; Anarthruridae Lang, 1971; Pseudotanaidae and Typhlotanaidae Sieg, 1984) were the most speciose with 10 or more species recorded. Apseudidae (209 individuals), Leptocheliidae (95 individuals), and Parapseudidae Guțu, 1981 (90 individuals) accounted for more than 60% of tanaidacean material.

The mean abundance of tanaidaceans from all collected samples was 0.03 ± 0.55 ind./0.1 m^2. The frequency of occurrence in samples was also very low. Tanaidaceans were recorded in 113 out of 270 samples (42% of samples). Mean abundance decreased along the depth gradient up to 250 m stations (**Figure 3**). Then, abundance increased at 500 and 1,000 m (**Figure 3**), although there were no statistically significant differences between each depth zone (Kruskal–Wallis test, Dunn's test). The material revealed large numbers of singletons and uniques, with 35 singletons (40% of all species) and 53 uniques found. Eighty-five species (98% of all species) had a total abundance lower than 10 individuals.

Mean species richness per sample (S) was greatest in the shallows (25–50 m) and on the slope (500–1,000 m). However, significant differences were only found between 50 and 250 m depth zones (**Figure 4**). The highest numbers of species were recorded at 500 and 1,000 m (33 and 34 species, respectively), and this area was also characterized by the highest number of species unique to those depth zones (**Figure 5**). Species accumulation curves did not reach the asymptotic level, which may suggest undersampling of the studied area (**Figure 6**). Low numbers of species were recorded despite a collection of five replicate samples at each station (**Supplementary Appendix 3**). The rarity and restricted distribution of taxa was also visible in the low number of species common to different depth zones (**Table 2**). Commonality of species between transects was

TABLE 1 | Total abundance and maximum abundance recorded in a single sample of each species, together with depth range in the studied material.

	Max	Total	Depth range [m]
Akanthophoreidae			
Chauliopleona sp. 1	1	1	500
Chauliopleona sp. 2	1	2	1000
Chauliopleona sp. 3	1	1	1000
Parakanthophoreus sp. 1	1	1	250
Parakanthophoreus sp. 2	3	5	100–500
Parakanthophoreus sp. 3	1	2	250–500
Parakanthophoreus guineus	1	3	500–1000
Parakanthophoreus sp. 4	3	6	1000
Parakanthophoreus sp. 5	2	2	500
Parakanthophoreus sp. 6	1	1	1000
Anarthruridae			
Anarthruridae sp.1	1	2	250–500
Anarthruridae sp. 2	1	2	1000
Anarthruridae sp. 4	1	1	1000
Anarthruridae sp.5	1	1	1000
Anarthruridae sp. 6	2	3	500
Anarthruridae sp. 7	1	1	500
Anarthruridae sp. 8	1	1	1000
Anarthruridae sp. 9	1	1	500
Anarthruridae sp. 10	1	2	500–1000
Olokun puellamaritima	2	4	500–1000
Pseudotanaidae			
Pseudotanais sp. 1	2	6	250–500
Pseudotanais sp. 2	3	7	50–100
Pseudotanais sp. 3	2	3	500
Pseudotanais sp. 4	2	3	500
Pseudotanais sp. 5	8	11	500
Pseudotanais sp. 6	2	7	1000
Pseudotanais sp. 7	1	3	500
Pseudotanais sp. 8	3	5	25
Pseudotanais sp. 9	1	1	50
Pseudotanais sp. 10	1	1	500
Agathotanaidae			
Agathotanais sp. 1	1	1	500
Paragathotanais sp. 1	2	6	500–1000
Paranarthrura sp. 1	4	18	500–1000
Paranarthrura sp. 2	1	1	1000
Paranarthrura sp. 3	2	2	1000
Typhlotanaidae			
Meromonakantha sp. 1	1	2	500
Meromonakantha sp. 2	1	1	1000
Paratyphlotanais sp.1	1	2	250–500
Torquella sp. 1	1	1	1000
Typhlotanais sp. 1	1	1	500
Typhlotanais sp. 2	2	6	500–1000
Typhlotanais sp. 3	1	1	1000
Typhlotanais sp. 4	5	8	250–500
Typhlotanais sp. 5	2	2	100
Typhlotanais sp. 6	1	1	500
Typhlotanais sp. 7	2	2	500
Typhlotanais sp. 8	4	7	1000

(Continued)

TABLE 1 | (Continued)

	Max	Total	Depth range [m]
Nototanaidae			
Nototanaidae sp.1	4	4	50
Nototanaidae sp. 2	4	5	50
Nototanaidae sp. 3	1	1	50
Paranathurellidae			
Paranarthrurella sp. 1	1	2	1000
Leptocheliidae			
Leptocheliidae sp. 1	7	11	50
Leptocheliidae sp. 2	17	60	25–50
Leptocheliidae sp. 3	5	10	25
Leptocheliidae sp. 4	9	11	25–50
Mesotanais sp. 1	1	3	100–250
Colletteidae			
Cetiopyge/Collettea sp. 1	1	1	1000
Collettea sp. 1	1	3	500
Collettea sp. 2	3	7	1000
Collettea agnesi	2	5	1000
Leptognathiella sp. 1	3	5	500–1000
Nematotanais sp. 1	1	2	1000
Leptognathiidae			
Leptognathia sp. 1	1	1	1000
Leptognathia sp. 2	1	1	250
Leptognathia sp. 3	1	3	500
Tanaellidae			
Araphura sp. 1	1	1	250
Arhaphuroides sp. 1	1	1	1000
Tanaopsidae			
Tanaopsis sp. 1	1	1	250
Tanaissuidae			
Tanaissuidae sp. 1	4	7	100
Tanaissuidae sp. 2	1	4	50–100
Paratanaidae			
Paratanaidae sp. 1	1	1	50
Incertae sedis			
Insociabilitanais sp. 1	3	6	1000
Parafilitanais sp. 1	1	1	500
Apseudidae			
Apseudes sp. 1	1	1	500
Apseudes sp. 2	8	10	500–1000
Apseudes sp. 3	18	83	25–100
Apseudes sp. 4	44	111	25
Apseudes sp. 5	1	1	1000
Carpoapseudes sp. 1	1	3	500–1000
Kalliapseudidae			
Paraleiopus sp. 1	2	5	25
Paraleiopus sp. 2	7	23	50
Kalliapseudes sp. 1	2	2	25
Kalliapseudes sp. 2	2	10	25–50
Metapseudidae			
Calozodion sp. 1	4	11	100
Hoplopolemius sp. 1	24	71	25–50
Parapseudidae			
Parapseudidae sp.1	3	6	25–50
Parapseudidae sp. 2	1	2	25–50

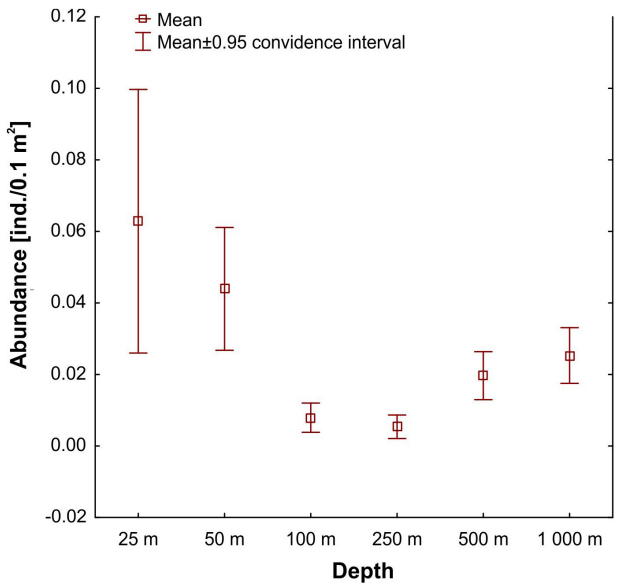

FIGURE 3 | Mean abundance at each sampled depth.

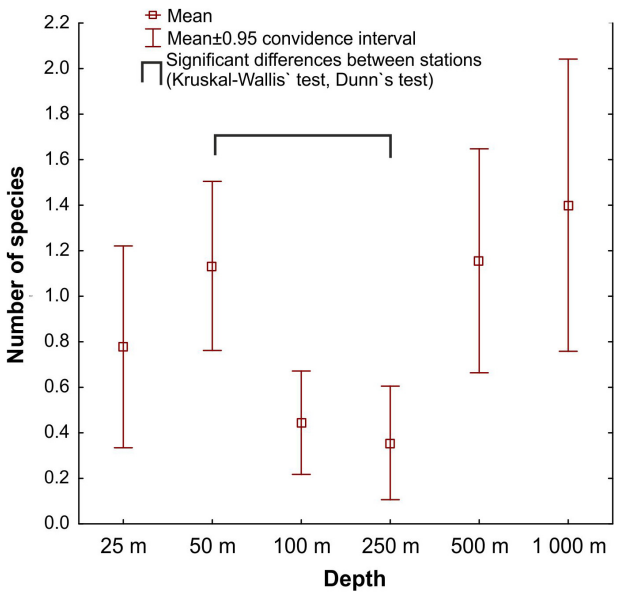

FIGURE 4 | Mean species richness per sample (S) at each sampled depth.

also low, demonstrating a restricted spatial distribution of the majority of the species (**Table 3**).

Only one family of tanaidaceans (Pseudotanaidae) was distributed along a whole depth gradient. We have recorded two main groups of families, one associated with shallow shelf areas (Kalliapseudidae, Parapseudidae, Metapseudidae, Leptocheliidae, Nototanaidae Sieg, 1976, and Paratanaidae Lang, 1949) and the second associated with slope depths (Agathotanaidae Lang, 1971, Colletteidae Larsen and Wilson, 2002, and Paranarthurellidae) (**Table 1** and **Figure 7**).

Clustering analysis revealed five distinct groups supported by 1% SIMPROF (**Figure 8**) with a low similarity between each group (3–22%). The first group contained three stations from 250 m in which seven species were grouped within six families. This cluster was characterized by low oxygen concentration (1.4 ± 0.2). Group 2 comprised 6 stations, mostly from 500 m, and grouped 28 species within 9 families. High concentration of heavy metals such as barium (152.3 ± 115.6), chromium (60.2 ± 7.6), total hydrocarbons (13.3 ± 6.6), and organic matter (11.2 ± 3.7), as well as the domination of silty sediment were characteristic of these stations. Nine stations from the deepest sections (500–1,000 m) were grouped in cluster 3 which, in general, was characterized by a similar set of variables as cluster 2 with 31 species within 12 families. Stations from the shallowest sites were grouped as cluster 4. Twelve stations were characterized by the highest oxygen concentration (4.2 ± 0.2), temperature (24.7 ± 1.7), and the highest gravel content in the sediments (4.3 ± 6.4). Heavy metals reached the lowest concentration (e.g., barium 16.6 ± 8.3, nickel 13.3 ± 7.4), but elevated arsenic concentration (39.7 ± 55.0) at stations located at transect 4 (25 m: 106.84) and 8 (50 m: 186.78) were recorded. Despite this fact, tanaidaceans reached the highest abundance at stations located at 25 and 50 m depth. The last cluster grouped nine stations, mostly from 100 m. The group is characterized by the highest salinity (35.7 ± 0.1) and the lowest abundance of tanaidaceans.

Canonical correspondence analysis with four environmental variables: barium, oxygen concentration, salinity, and temperature revealed that species composition of tanaidaceans along the Ghanaian coast is depth-related rather than transect-specific or sediment particle size-specific (**Figure 9** and **Supplementary Appendix 4**). All the four factors were statistically significant (**Table 4**). The ordination analysis clearly showed separation of each depth zone, except of 25–50 m stations which were grouped together. CCA axis 1 distinguishes the stations into two groups: the first is characterized by higher oxygen concentration at shallowest (25–50 m; mean: 4.21 ± 0.31) and the deepest stations (1,000 m; mean: 3.55 ± 0.29); and the second by a decreased oxygen level at stations at 250 m (mean: 1.53 ± 0.17) and 500 m (mean: 1.81 ± 0.30). CCA axis 2 divided stations based on a salinity, temperature, and barium gradient. Sites located at bathyal zone (500 m; mean: 87.92 ± 48.92 and 1,000 m; mean: 216.83 ± 78.56) were characterized by a higher barium concentration than those from the continental shelf (25–50 m; mean: 15.58 ± 9.44). Salinity was highest at 100 m stations and lowest at 1,000 m. Temperature decreased with depth reaching 27.49 ± 1.48 at 25 m and 14.19 ± 11.90 at 1,000 m.

DISCUSSION

Diversity Patterns Along a Depth Gradient

Our study of tanaidacean diversity in the Gulf of Guinea revealed very high species richness. With a total of 87 species of which 84 appeared to be new for science, the number of species across the whole west coast of Africa now reached totals 164

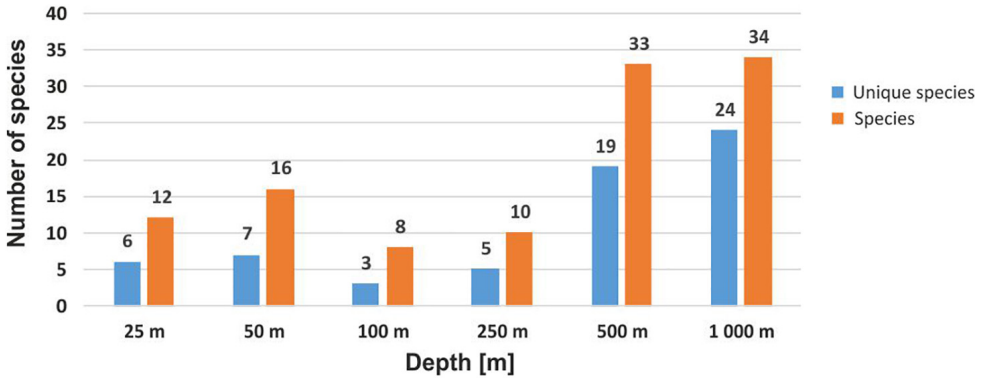

FIGURE 5 | Total number of species recorded at each depth, together with the number of species unique to a given depth.

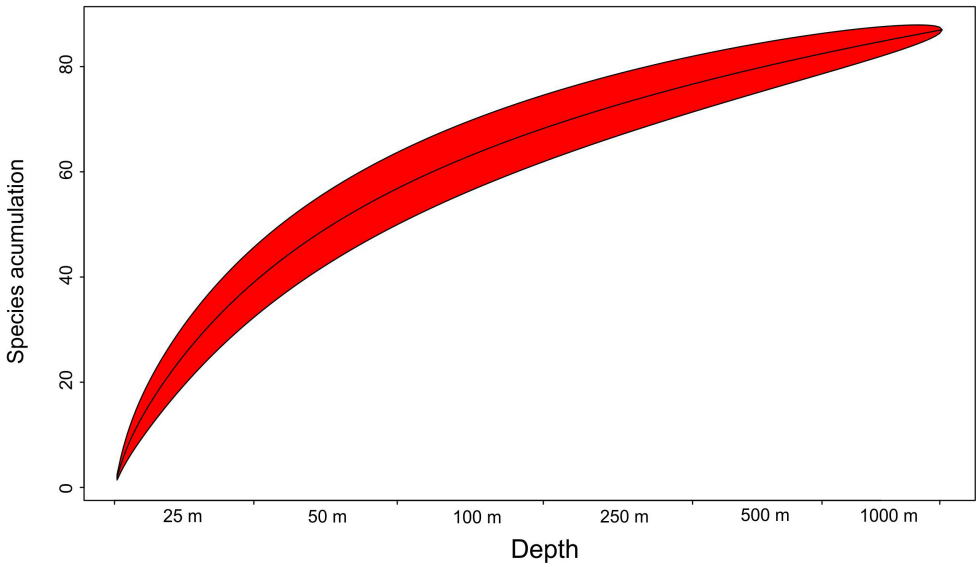

FIGURE 6 | Species accumulation curve with Chao 1.

TABLE 2 | Number of species common to particular depths.

	25 m					
25 m	**12**	50 m				
50 m	7	**16**	100 m			
100 m	1	3	**8**	250 m		
250 m	0	0	1	**10**	500 m	
500 m	0	0	1	4	**33**	1000 m
1000 m	0	0	0	0	8	**34**

***Bolded** values showed total number of species at each analyzed depth.*

TABLE 3 | Number of species common to transects.

	G1								
G1	**13**	G2							
G2	3	**17**	G3						
G3	2	2	**10**	G4					
G4	5	6	4	**22**	G5				
G5	4	11	3	8	**24**	G6			
G6	3	7	2	7	10	**24**	G7		
G7	2	5	1	5	5	6	**28**	G8	
G8	4	6	1	3	5	4	6	**23**	G9
G9	1	0	1	1	0	1	1	0	**4**

***Bolded** values showed total numer of species on each analyzed transect.*

(Jóźwiak et al., 2017). Our results may be attributed to the high sampling efforts across both the continental shelf and slope depths, as each was characterized by a distinct set of species.

Despite our quantitative sampling methodology collecting the fauna at localized scales, our results are similar to the results of earlier studies based on less precise epibenthic sledge (EBS) and other trawling devices that are indiscriminately designed to collect large number of taxa from large bottom areas. Cumulatively, we have sampled 27 m^2 of seabed. Comparison of this sampling area with studies based on qualitative samplers,

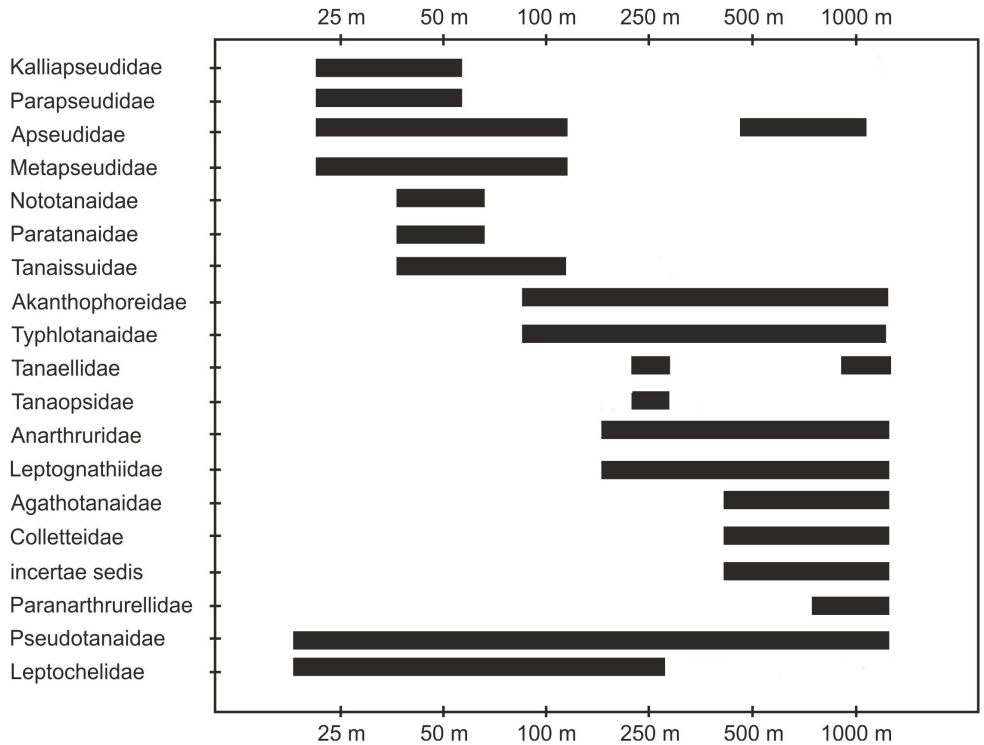

FIGURE 7 | Depth range of tanaidacean families recorded in the Gulf of Guinea.

such as the KuramBio cruise where total area sampled using EBS equaled 53,709 m^2 (Jóźwiak et al., 2020) or benthic sampling in the Ross Sea, where the area of only single EBS sample varied between 247 and 1,493 m^2 (Pabis et al., 2015), shows the unique character of our results. Earlier studies, based mostly on a relatively small set of several EBS samples, also demonstrated high species richness of tanaidacea, for example, Ross Sea (72 species) (Pabis et al., 2015), Amundsen Sea (37 species), Scotia Sea (51 species) (Pabis et al., 2014), and region of the Kuril-Kamchatka Trench (48 species; Błażewicz-Paszkowycz et al., 2015), at significantly lesser spatial resolutions. The scale of the sampled area is crucial for all species richness assessments because it allows for the penetration of a larger number of habitats (Błażewicz et al., 2019a). Nevertheless, a large number of species new to science and a large number of singletons were visible in all earlier tanaidacean studies (Pabis et al., 2014, 2015; Błażewicz-Paszkowycz et al., 2015; Stępień et al., 2018, 2019; Błażewicz et al., 2019a; Jóźwiak et al., 2020), although not at the scale recorded in the Gulf of Guinea.

We have recorded a striking rarity of tanaidacean species along the coast of Ghana. Despite the high sampling effort and the replicated sampling scheme, which allows for penetration of larger areas of the bottom and minimizes undersampling of species (Somerfield and Clarke, 1997; Eleftheriou and McIntyre, 2005), 40% of the species were singletons, 98% of the species had total abundance lower than 10 individuals, and approximately half of the species were unique to specific samples. Similar results were observed in deep-sea tanaidacean assemblages from other basins, for example, from the Amundsen and Scotia Seas 85 species were recorded, with about 90% species new for science, and most of the species were found only in a single sample (uniques) (Pabis et al., 2015). Similarly, studies in CCFZ area revealed 98 tanaidacean species, out of which 47 of them were singletons while 57 were uniques (Błażewicz et al., 2019a). Recorded in our studies, values of singletons and rare species are much higher than the average values recorded for various macrofaunal taxa that are most often characterized by 30–35% share of singletons (Ellingsen et al., 2007). Moreover, an earlier analysis of sampling replicability at the same station in the studies of tanaidacean fauna did not show such a strong level of rarity on a small scale (Jóźwiak et al., 2020). Some species may, however, display locally higher abundances. Such patchy distribution was recorded for *Apseudes* sp. 4, where 44 of the 111 individuals of this species were found in one sample (**Table 1**).

Very steep species accumulation curves were also present for tanaidaceans in the classic deep-sea study of Grassle and Maciolek (1992). This study was based on 233 boxcorer samples (1,500–2,500-m depth range), collected off of the North American coast. Really high abundances of tanaidaceans were rarely recorded, with the majority found in the very shallow areas, and mostly comprised a single species (Bailey-Brock, 1984; Sheridan, 1997). In the deep-sea, relatively high abundances of these crustaceans have only been recorded in some more productive sites in the northeast Atlantic (Cosson et al., 1997).

A high number of singletons is not atypical for the deep-sea, although it is often difficult to assess if the large number of

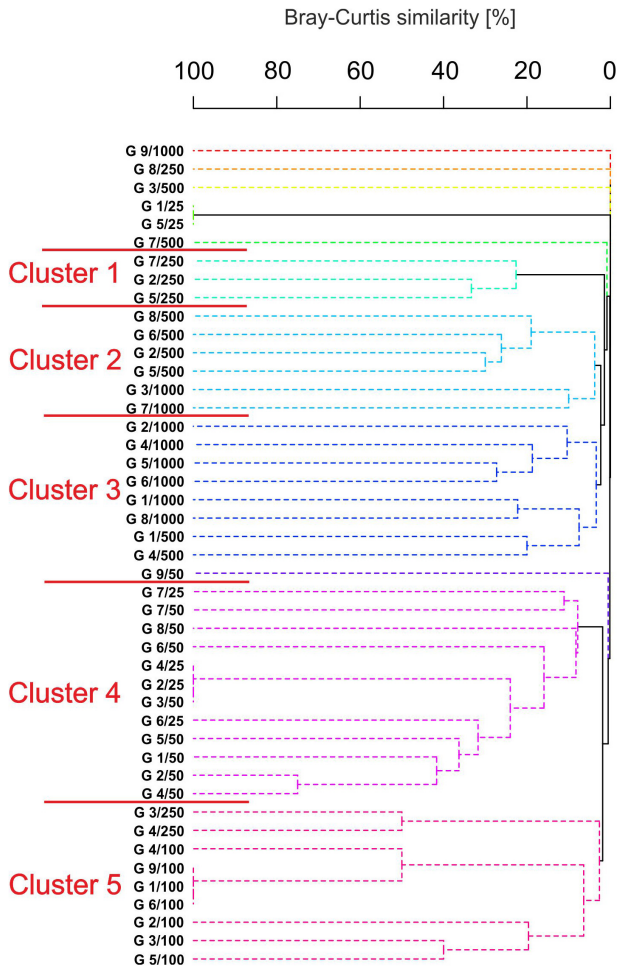

FIGURE 8 | Dendrogram of samples for Bray Curtis similarity, square root transformed data, and group average grouping method with 1,000 iterations. (Spotted lines indicate the samples that cannot be significantly differentiated by SIMPROF).

singletons is due to sampling effort and methodology, or if it reflects environmentally driven patterns (Rex and Etter, 2010). The deep-sea studies generally suffer from undersampling and are subject to huge bias in biodiversity inventories, assessments of rarity, and description of distribution patterns (Jóźwiak et al., 2020; Rex and Etter, 2010). A very high number of singletons accompanied by a high share of species new to science was also recorded for other groups of peracarid crustacean, namely cumaceans and isopods (e.g., Brandt et al., 2007; Stępień et al., 2021). Peracarid diversity from the Southern Ocean demonstrated another interesting pattern. The majority of species were recorded in a low number of samples, but the authors suggested that they are not rare, but instead, their distribution is highly patchy (Kaiser et al., 2007). The study, however, was based on only 19 EBS samples, and this problem requires further investigation. The patterns we observed in Ghana appear different due to the large number of samples collected and high degree of replication, yet they still yielded a very high number of singletons accompanied by a large number of samples without tanaidaceans.

Unfortunately, we cannot analyze functional diversity of tanaiadaceans due to the lack of comprehensive data about their biology. It has been suggested that the majority of taxa are likely detritus feeders and that their ecological diversity seems to be low (Błażewicz-Paszkowycz et al., 2012). Conversely, a taxonomic group characterized by such exceptionally high species richness must be an important element of ecosystem functioning, suggesting a complicated set of mutual interactions between various species and their habitats (Buhl-Mortensen et al., 2010). This is poignant in a marine ecosystem like the Ghanaian coast, where even core benthic taxa like polychaetes have a relatively low abundance (Sobczyk et al., 2021). A total of 87 species of tanaiadacea is a very high number, even compared to the 251 species of polychaetes recorded in the same material (Sobczyk et al., 2021), especially given that polychaetes belong to the most dominant benthic taxa, both in terms of abundance and diversity (Rouse and Pleijel, 2001). We might speculate that even if tanaidaceans are not the most important consumers, they may comprise a major component of trophic webs as prey for predatory polychaetes, decapods, or fishes (Balasubramanian et al., 1979; Nagelkerken and van der Velde, 2004; Larsen, 2005; Jumars et al., 2015). At the same time, predatory polychaetes like Goniadidae Kinberg, 1866; Glyceridae Grube, 1850 and Polynoidae Kinberg, 1856 are among the most important groups of benthic fauna on the coast of Ghana, especially in the shallower shelf sites (Sobczyk et al., 2021) along with a high diversity of decapods (Podwysocki et al., unpublished results).

Despite their small size, tanaidaceans may be important for bioturbation of the bottom sediments, especially in the surface layers, like in the case of shallow water Apseudomorpha (Larsen, 2005), which was the dominant element of fauna in our material. Rare and small organisms are typically a minor element of the sediment reworking processes. However, in the coast of Ghana, burrowing polychaetes, the most important biotubators, were highly diverse (71 species), yet their abundance and size were low (Sobczyk et al., 2021), potentially elevating the functional importance of other taxa. The mean total abundance of macrofauna in the same set of samples was relatively low, particularly on the lower shelf and slope (Pabis et al., 2020), making tanaidaceans a proportionally important element of those communities. Polychaete functional diversity also decreased from shelf to slope (Sobczyk et al., 2021), suggesting that the role of tanaidaceans in the benthic ecosystem may increase proportionally with depth. Our results are verified by studies from the Australian continental slope, where tanaidaceans were the second most abundant group of benthic macrofauna, after polychaetes, although their abundance remained relatively low with 561 individuals collected in *c.* 1000.1 m^2 Smith–McIntyre grab samples (McCallum et al., 2015).

Our earlier results suggested that the Gulf of Guinea may have a high ecosystem resilience due to exceptionally high diversity (Sobczyk et al., 2021; Stępień et al., 2021). High diversity may allow for functional redundancy within the ecosystem where multiple species play the same role (Biggs et al., 2020). This observation might be crucial in the context of strong

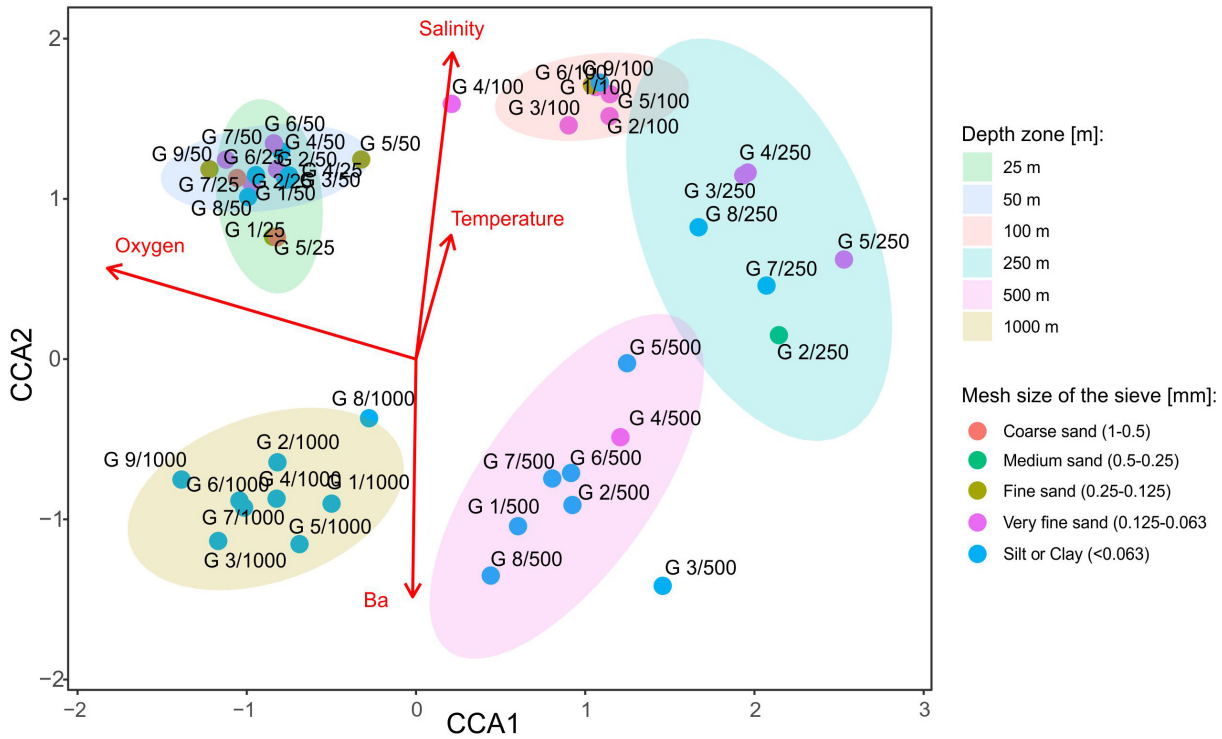

FIGURE 9 | Canonical correspondence analysis (CCA) showing species composition differences on each sampling site with selected environmental factors as red arrows (barium, temperature, salinity, and oxygen). Sediment size is differentiated by the color of the points. In addition, to describe species composition along the depth gradient, depth zones were distinguished as ellipses with 0.95 confidence intervals. Only statistically significant variables were included into ordination analysis. See **Supplementary Appendix 1** for a full list of factors.

TABLE 4 | Value of variance influence factor and statistical significance of selected variables used in final version of canonical correspondence analysis.

	VIF	Sig
Ba	2.56	0.002
Temperature	1.78	0.012
Salinity	1.51	0.045
Oxygen	1.30	0.001

anthropopressure recorded in the Gulf of Guinea (Scheren et al., 2002), especially with ongoing industrialization and oil excavation (Scheren et al., 2002; Ukwe et al., 2003; Ayamdoo, 2016; Sobczyk et al., 2021). Our results revealed links between tanaidacean communities and changes in environmental factors, although multivariate analysis bias on a count of low abundances cannot be discounted (Reiss et al., 2015). The similarity level recorded in the cluster analysis was very low, and results of the CCA did not demonstrate a very strong pattern. Taking into account the above mentioned problems, these results have to be treated cautiously. Therefore, the possible use of tanaidacean communities as indicators of changes in benthic ecosystem in the Gulf of Guinea is doubtful despite their importance for overall biodiversity.

Depth was an important factor in structuring tanaidacean communities along the coast of Ghana. The clear separation of the slope samples, bottom area affected by larger concentrations of barium and hydrocarbons in the sediments, was not accompanied by a decrease in abundance or species richness, unlike Cumacea and Polychaeta (Sobczyk et al., 2021; Stępień et al., 2021). This is somewhat surprising since barium is known for its toxic influence on benthic fauna (Olsgard and Gray, 1995; Gomez-Gesteira et al., 2003; Stark et al., 2020), However, barium and other toxic metal concentrations were similar to the background levels according to the OSPAR and KLIF (Norwegian Pollution Authority) guidelines, and the general environmental status of investigated sites was good, with only some local pollution (Iversen et al., 2011; Pabis et al., 2020; Sobczyk et al., 2021). In the case of the Ghanaian coast, toxic metals originated from oil excavation and the dyeing industry (Scheren et al., 2002; Ayamdoo, 2016; Sobczyk et al., 2021). As such, we suggest that the higher diversity recorded on the slope (**Figure 3**) could be explained by the fact that bathyal is a major hot spot of benthic diversity in the Worlds Ocean (Danovaro et al., 2009). This pattern is supported by earlier studies of tanaidacean communities at slope depths (Pabis et al., 2014, 2015; Błażewicz-Paszkowycz et al., 2015). This may prove important for the stability of slope ecosystems in the Gulf of Guinea, where even an elevated level of pollutants might be compensated by the presence of a large number of species. Abundant and speciose communities were also recorded at shallow shelf sites characterized by higher oxygen contents and higher fluorescence. Both factors are very

important for various benthic invertebrates (Levin and Sibuet, 2012), and thus it is not surprising that they exerted a positive influence on the tanaidacean communities.

Our results demonstrate that the analysis of rare and less abundant but highly speciose taxa, such as small peracarid crustaceans, should become an important element of future studies of marine benthic ecosystems. Some studies of particular species suggest that tanaidaceans may constitute good indicators of changes in environmental conditions (Ambrosio et al., 2014). However, the analysis of their communities might prove difficult as changes in community structure are hard to detect due to a high degree of rarity and their low abundance. Therefore, studies of such small size and rare taxonomic groups might require different sampling strategies and/or the use of more specialized sampling equipment.

It is important to consider that though we sampled *c*. 500 km of coastline during our study, we only recorded a very low number of tanaidacean species common to different transects. Deciphering range descriptions in the case of species that likely have a small population size, patchy distribution, and low abundance is difficult. Our results strongly suggest that the majority of tanaidaceans have very restricted spatial distribution, even at a moderate scale. The restricted vertical range of many species (**Table 1** and **Figure 4**) is not surprising and is due mostly to affinities of tanaidacean families to given depth zones that are associated with their phylogeny, for example, phylogenetically young families have colonized the deep-sea relatively recently (Błażewicz-Paszkowycz et al., 2012).

High total species richness might be also a consequence of microhabitat diversity. Previous studies demonstrate strong affinities between bottom type or complexity of habitats and composition of tanaidacean fauna (Holdich and Bird, 1985; Siciński et al., 2012). Sediment grain size was not a significant factor in the CCA analysis, although grain size is likely an important factor for small crustaceans that are associated with soft bottom ecosystems (Błażewicz-Paszkowycz et al., 2012). Significant knowledge gaps remain as surrounding links between sediment character and composition of tanaidacean fauna, whereas interpretation of our results is difficult due to the low abundances encountered.

Life history characteristics of a given species may differ strongly with environmental conditions and habitat characteristics (Rumbold et al., 2015). Ellingsen et al. (2007) postulated links between habitat diversity and degree of rarity. This may hold for the Gulf of Guinea, an area characterized by highly dynamic environmental factors and diverse habitats (Brind'Amour et al., 2009; Buhl-Mortensen et al., 2017; Pabis et al., 2020). The small size and low dispersal potential of Tanaidacea (Larsen, 2005; Błażewicz-Paszkowycz et al., 2012) strongly influence their distribution patterns. Though we do not know the habitat requirements and environmental tolerance of the particular tanaiadacean species recorded in our study, habitat-specific species are considered to be rare (Ellingsen et al., 2007). In the case of organisms with a size that often does not exceed 2 or 3 mm, the scale of the potential microhabitat diversity might be significantly reduced compared with larger taxa characterized by higher mobility and the presence of planktonic larval stages.

Families Distribution Along a Depth Gradient

Material collected along the coast of Ghana has provided a unique opportunity to analyze changes in Tanaidacea composition along a depth gradient (25–1,000 m). This is the first study of this nature since Jakiel et al. (2018) exacted tanaidacean collection from Icelandic waters, and since Pabis et al. (2015) analysed material from the Ross Sea. The former study was, however, limited only to representatives of the family Pseudotanaidae, whereas the latter analyzed samples from completely different depths (365–3,490 m). The sampling effort in both of those studies was very low. The Tanaidacea recorded in the Gulf of Guinea showed a clear transition from taxa known as typically shallow-water (Leptocheliidae and Kalliapseudidae), through families with a wide bathymetric range (Pseudotanaidae and Apseudidae) to the true deep-sea forms (Paranarthrurellidae) (Błażewicz-Paszkowycz et al., 2012).

Fourteen out of the 22 known families of suborder Tanaidomorpha were found in the Gulf of Guinea. Leptocheliidae are generally described as tanaidaceans with well-developed functional eyes and inhabiting the shelf, although the genera *Bathyleptochelia* and *Mesotanais* have been previously recorded below shelf depths (Błażewicz-Paszkowycz et al., 2012). Earlier observations fully correspond with our results: *Mesotanais* sp. 1 was only found at stations from 100 to 250 m depth; non-*Mesotanais* Leptocheliidae were collected only at 25 and 50 m. Other tanaidomorphan families found on the shelf (50 m depth) in the Gulf of Guinea include Nototanaidae and Paratanaidae, which similar to Leptocheliidae, are considered shallow-water taxa, with some deep-sea exceptions. Leptocheliidae may be a polyphyletic group, which makes comparisons of their bathymetric range with wider studies doubtful and uncertain (Błażewicz-Paszkowycz et al., 2012). In contrast, the monophyly of Tanaissuidae Bird and Larsen, 2009 is well-supported (Bird and Larsen, 2009), but the family is mostly represented by shelf taxa and some single deep-water forms, like *Bathytanaissus* (Bird and Holdich, 1989). In our material, this family was recorded in a depth range between 50 and 100 m.

Members of the family Tanaopsidae Błażewicz-Paszkowycz and Bamber, 2012 were recorded in the Gulf of Guinea only from one sample taken at 250 m. This family is known to have a worldwide distribution and wide bathymetric range, from intertidal to over 3,000 m, which is likely explained by its polyphyletic nature (Błażewicz-Paszkowycz and Bamber, 2012).

We also found a group of tanaidomorphan families characterized by exceptionally wide depth ranges. For example, Akanthophoreidae (100–1,000 m in Gulf of Guinea) are generally well represented in the deep-sea worldwide, but found also on the shelf (Larsen and Araújo-Silva, 2014). Anarthruridae (250–1,000 m in the Gulf of Guinea) are a well-defined, cosmopolitan family recorded primarily in the deep-sea (Larsen, 2013), albeit with some shallow water representatives (Dojiri and Sieg, 1997). In our material, this family was only present at depths below the shelf, supporting the suggested deep-water origins of this group (Błażewicz-Paszkowycz et al., 2012). Pseudotanaidae is another family with worldwide distribution and with the highest diversity

recorded in the deep sea, as well as enormous depth range, from intertidal to over 7,000 m (Jakiel et al., 2018). Intriguingly, this family can be morphologically and bathymetrically divided into shallow-water forms with functional eyes and blind, deep-sea forms (Błażewicz-Paszkowycz and Bamber, 2012). Our results support those observations, as Pseudotanaidae were recorded along a full depth range (25–1,000 m), with only two species characterized by the presence of eyes found at shallowest stations, and remaining eight blind species were collected in the deep water (**Table 1**). Typhlotanaidae is a family of possible deep-sea origin (Błażewicz-Paszkowycz et al., 2012), that also has representatives on the shelf depths (Błażewicz-Paszkowycz, 2007; Segadilha and Lavrado, 2018). In the Gulf of Guinea typhlotanaids were primarily recorded from deeper parts of the basin (250–1,000 m), but a single species—*Typhlotanais* sp. 5—was found also on the shelf (100 m). Tanaellidae Larsen and Wilson, 2002 likely have a deep-sea origin, but Blażewicz-Paszkowycz and Bamber (2012) found representatives of this family in the shallow waters of Bass Strait. This family was represented exclusively by deep-sea forms in our data, namely *Araphura* sp. 1 recorded at 250 m and *Arhaphuroides* sp. 1 found at 1,000 m.

Two other families representing the suborder Tanaidomorpha (Colletteidae and Leptognathiidae Sieg, 1976) have a relatively wide depth range in the Gulf of Guinea, but representatives of both families were recorded on the slope (from 500 to 1,000 m and from 250 to 10,000 m, respectively). Those two taxa comprised very important elements of deep-sea Tanaidacea communities analyzed in earlier studies (Pabis et al., 2014, 2015; Błażewicz-Paszkowycz et al., 2015). Though wider literature indicates shallow-water records of those families, they need to be treated cautiously because both groups are clearly polyphyletic (Bird and Larsen, 2009; Błażewicz-Paszkowycz et al., 2013). The problem is even more pronounced in Leptognathiidae because the family itself, as well as the type genus *Leptognathia,* were treated as a repository group for decades (Bird, 2007).

The family Agathotanaidae is almost exclusively a deep-sea group, with the majority of the records from below 1,000 m depth. Only single species were found at shallower sites, e.g., *Agathotanais misakiensis* and *A. toyoshioae* from 211 to 493 and 95 m depth, respectively (Kakui and Kohtsuka, 2015). In the Gulf of Guinea, five agathotanaid species were recorded, all of which were present at the deepest stations (500 and 1,000 m). Finally, the family Paranarhrurellidae, a group that was recorded twice in our material but only at the deepest stations (1,000 m), confirms the true deep-sea origin of this family. This matches the described range of this group, starting from the bathyal and ending at hadal depths (Błażewicz et al., 2019b).

Apseudomorpha were represented in the Gulf of Guinea by only four families and most of their records are from the shelf. This observation is in accordance with the general distributional patterns of this suborder, as only one from 12 known families of Apseudomorpha (family Gigantapseudidae Kudinova-Pasternak, 1978) is considered an exclusively deep-sea taxon. The family Kalliapseudidae was found in the Gulf of Guinea at the shallowest stations (25 and 50 m), aligning our results with other studies of this group. Kalliapseudids are generally characterized as shallow marine and estuarine tanaidaceans, mainly occurring at depths higher than 200 m (Drumm and Heard, 2011). At the same depths (25–50 m), we found representatives of another typically shallow-water tropical family, the Parapseudidae Guţu, 2008. The third apseudomorphan family, the Metapseudidae, were recorded slightly deeper, from 25 to 100 m, also in accordance with previous findings (Stępień and Blażewicz-Paszkowycz, 2013; Jóźwiak and Błażewicz, 2021). The last family recorded on the coast of Ghana are the Apseudidae and they have a very wide and disjunct bathymetrical range. These can be differentiated into two subfamilies: firstly the Apseudinae, that group primarily shallow-water taxa and some deep-sea exceptions; and secondly, the Leviapseudinae that are composed of exclusively deep-water forms (Błażewicz-Paszkowycz et al., 2012).

CONCLUDING REMARKS

The great diversity of Tanaidacea, Cumacea (Stępień et al., 2021), and Polychaeta (Sobczyk et al., 2021), encountered in benthic communities to date, make the Gulf of Guinea an area of particular interest for conservation strategies in the Atlantic. The Gulf of Guinea seems to be a great natural laboratory for studies of ecosystem resilience to changes associated with pollution and climate warming. Our study establishes the region as a good model for studies of Large Marine Ecosystem response to human pressure. As a region characterized by high benthic diversity, it provides an opportunity to study links between species richness, habitat diversity, and ecosystem stability. The high number of species new to science uncovered in our materials reveal a great potential for studies related to interactions between local and regional species pools. Our results from a relatively small part of the Ghanaian coast have increased the number of Tanaidacea known from the whole west coast of Africa by over 100%, from 80 to 164 species (Jóźwiak et al., 2017), demonstrating a great need of further taxonomic studies. It emphasizes the role of taxonomic expertise as a foundation for biodiversity inventories and ecological analysis, especially in the regions that were previously neglected in studies of benthic fauna. Currently, only four species from this collection were officially described (Jóźwiak et al., 2017), but next descriptions will follow this general inventory.

Rare or narrow range species belong to the most underestimated marine invertebrates (Higgs and Attrill, 2015), and studies of their diversity should be amongst the priorities of marine science. The steep species accumulation curve encountered despite the high sampling effort further necessitates a more comprehensive evaluation of the most appropriate sampling strategies in the future monitoring of this region. To facilitate a more comprehensive taxonomic analysis, we need not only a larger number of replicated samples (Hughes et al., 2021), but also the simultaneous use of various sampling methodologies (Jóźwiak et al., 2020). The analysis of sampling

efficiency and replication schemes should be prioritized in future studies to better record novel species.

Tanaidaceans belong to the most underestimated groups of benthic organisms (Appeltans et al., 2012). Despite the increased taxonomic effort in recent years (Błażewicz-Paszkowycz et al., 2012), the number of recorded new species remains much higher than the number currently described. This problem is widespread in studies of other groups of peracarid crustaceans. Kaiser et al. (2009) found that in the Amundsen Sea, 96% of collected isopods were new to science, and a large majority of those taxa are yet to be described, as in tanaidacean studies (Pabis et al., 2014, 2015; Błażewicz-Paszkowycz et al., 2015; Stępień et al., 2018, 2019; Błażewicz et al., 2019a; Jóźwiak et al., 2020). These problems must be addressed with studies of both particular taxonomic groups and particular regions of the world. Without a comprehensive taxonomic analysis, it is impossible to deduce meaningful estimates of marine benthic diversity on a global scale or to analyze the problems associated with ecosystem functioning, conservation priorities, and management strategies (Costello et al., 2012; Higgs and Attrill, 2015; Costa et al., 2020).

DATA AVAILABILITY STATEMENT

The original contributions presented in the study are included in the article/**Supplementary Material**, further inquiries can be directed to the corresponding author/s.

AUTHOR CONTRIBUTIONS

PJ: concept of the manuscript, taxonomic identification, statistical analysis, sampling design, and manuscript writing. KP: concept of the manuscript, statistical analysis, writing of the manuscript, sampling design, and coordination of benthic ecology in the project. RS: statistical analysis and manuscript writing. BS: sampling design, proofreading, and head of the FAO project. All authors contributed to the article and approved the submitted version.

FUNDING

The sampling cruise and the environmental data analysis within this program were funded by the Norwegian Agency for Development Cooperation (NORAD) (Oil for Development Program—OfD) and by the Food and Agriculture Organization of the United Nations (FAO). PJ and KP were also supported by University of Łódź.

ACKNOWLEDGMENTS

We would like to thank the crew of RV *Fridtjof Nansen* and the scientists from Ghana for their assistance in the collecting and processing of the samples. We thank to both reviewers of the manuscript, their valuable comments substantially improved the article.

SUPPLEMENTARY MATERIAL

The Supplementary Material for this article can be found online at: https://www.frontiersin.org/articles/10.3389/fmars.2022.779134/full#supplementary-material

REFERENCES

Alvaro, M. C., Błażewicz-Paszkowycz, M., Davey, N., and Schiaparelli, S. (2011). Skin digging tanaids: the unusual parasitic behaviour of *Exspina typica* in Antarctic waters and worldwide deep basins. *Antarct. Sci.* 23, 343–348. doi: 10.1017/s0954102011000186

Ambrosio, E. S., Ferreira, A. C., and Rodrigues-Capitulo, A. (2014). The potential use of *Sinelobus stanfordi* (Richardson, 1901) (*Crustacea*, *Tanaidacea*) as a biological indicator of water quality in a temperate estuary of South America. *Limnetica* 33, 139–152.

Angelini, C., Altieri, A. H., Silliman, B. R., and Bertness, M. D. (2011). Interactions among Foundation Species and Their Consequences for Community Organization, Biodiversity, and Conservation. *BioScience* 61, 782–789. doi: 10.1525/bio.2011.61.10.8

Appeltans, W., Ahyong, S. T., Anderson, G., Angel, M. V., Artois, T., Bailly, N., et al. (2012). The magnitude of global marine species diversity. *Cur. Biol.* 22, 2189–2202. doi: 10.1016/j.cub.2012.09.036

Ayamdoo, N. A. (2016). Protecting the Gulf of Guinea in an oil boom: regulating offshore petroleum pollution in a divided world. *J. World Energ. Law Bus.* 619, 219–232. doi: 10.1093/jwelb/jww007

Băcescu, M., and Guţu, M. (1975). A new genus (*Discapseudes* n. g.) and three new species of Apseudidae (Crustacea. Tanaidacea) from the northeastern coast of South America. *Zool. Meded.* 49, 95–113.

Bailey-Brock, J. H. (1984). Ecology of the tube-building polychaete *Diopatra leuckarti* Kinberg, 1865 (Onuphidae) in Hawaii: community structure, and sediment stabilizing properties. *Zool. J. Linn. Soc.* 80, 191–199. , doi: 10.1111/j.1096-3642.1984.tb01972.x

Balasubramanian, N. C., Lalithambika-Devi, B., and Krishnankutty, M. J. (1979). Feeding behaviour and preying efficiency of *Metapenaeus dobsoni*. *Indian J. Mar. Sci.* 8, 197–200.

Bassindale, R. (1961). On the marine fauna of Ghana. *Proc. Zool. Soc. Lond.* 137, 481–510. doi: 10.1111/j.1469-7998.1961.tb06086.x

Biggs, C. R., Yeager, L. A., Bolser, D. G., Bonsell, C., Dichiera, A. M., Hou, Z., et al. (2020). Does functional redundancy affect ecological stability and resilience? A review and meta-analysis. *Ecosphere* 11:e03184. doi: 10.1002/ecs2.3184

Bird, G. J. (2007). Families Anarthruridae Lang, 1971, Colletteidae Larsen & Wilson, 2002, and Leptognathiidae Sieg, 1976. In: Larsen, K., and M. Shimomura (eds.), *Tanaidacea* (*Crustacea*: *peracarida*) From Japan III. The Deep Trenches: the Kurile-Kamchatka Trench and Japan Trench. *Zootaxa* 1599, 61–85.

Bird, G. J., and Holdich, D. M. (1989). Tanaidacea (Crustacea) of the north-east Atlantic: the subfamily Pseudotanainae (Pseudotanaidae) and the family Nototanaidae. *Zool. J. Linn. Soc.* 97, 233–298.

Bird, G. J., and Larsen, K. (2009). Tanaidacean phylogeny – the second step: the basal paratanaoidean families (Crustacea: Malacostraca). *Arthropod Syst. Phylogeny* 67, 137–158.

Błażewicz, M., Jóźwiak, P., Jennings, R. M., Studzian, M., and Frutos, I. (2019a). Integrative systematics and ecology of a new deep-sea family of tanaidacean crustaceans. *Sci. Rep.* 9:18720. doi: 10.1038/s41598-019-53446-1

Błażewicz, M., Jóźwiak, P., Menot, L., and Pabis, K. (2019b). High species richness and unique composition of the tanaidacean communities associated with five areas in the Pacific polymetallic nodule fields. *Prog. Oceanogr.* 176:102141. doi: 10.1016/j.pocean.2019.102141

Błażewicz-Paszkowycz, M. (2007). A revision of the family Typhlotanaidae Sieg, 1984 (Crustacea: Tanaidacea) with the remarks on the Nototanaidae Sieg, 1976. *Zootaxa* 1598, 1–141. doi: 10.11646/zootaxa.1598.1.1

Błażewicz-Paszkowycz, M., and Ligowski, R. (2002). Diatoms as food source indicator for some Antarctic Cumacea and Tanaidacea (Crustacea). *Antarct. Sci.* 14, 11–15. doi: 10.1017/s0954102002000524

Błażewicz-Paszkowycz, M., Bamber, R. N., and Jóźwiak, P. (2013). Tanaidaceans (Crustacea: Peracarida) from the SoJaBio joint expedition in slope and deeper waters in the Sea of Japan. *Deep Sea Res. II Top. Stud. Oceanogr.* 86–87, 181–213.

Błażewicz-Paszkowycz, M., Bamber, R., and Anderson, G. (2012). Diversity of Tanaidacea (Crustacea: Peracarida) in the World's Oceans – How Far Have We Come? *PLoS One* 7:e33068. doi: 10.1371/journal.pone.0033068

Błażewicz-Paszkowycz, M., Pabis, K., and Jóźwiak, P. (2015). Tanaidacean fauna of the Kuril-Kamchatka Trench and adjacent abyssal plain—abundance, diversity and rare species. *Deep-Sea Res. Part II Top. Stud. Oceanogr.* 86, 181–213.

Bracken, M. E., and Low, N. H. (2012). Realistic losses of rare species disproportionately impact higher trophic levels. *Ecol. Lett.* 15, 461–467. doi: 10.1111/j.1461-0248.2012.01758.x

Brandt, A., Brix, S., Brökeland, W., Choudhury, M., Kaiser, S., and Malyutina, M. (2007). Deep-sea isopod biodiversity, abundance, and endemism in the Atlantic sector of the Southern Ocean—Results from the ANDEEP I-III expeditions. *Deep-Sea Res. Part II Top. Stud. Oceanogr.* 54, 1760–1775. doi: 10.1016/j.dsr2.2007.07.015

Brind'Amour, A., Menot, L., Galeron, J., and Crassous, P. (2009). Spatial organization of a sedimentary macrobenthic community located on the West African Equatorial margin. *Deep Sea Res. II Top. Stud. Oceanogr.* 56, 2292–2298. doi: 10.1016/j.dsr2.2009.04.010

Buchanan, J. B. (1957). The bottom fauna communities across the continental shelf off Accra, Ghana (Gold Coast). *Proc. Zool. Soc. Lond.* 130, 1–56. doi: 10.1111/j.1096-3642.1958.tb00562.x

Buchanan, J. B. (1984). "Sediment analysis," in *McIntyre Methods for the Study of Marine Benthos*, eds N. A. Holme and A. D. McIntyre (Oxford: Blackwell Scientific Publications), 41–65.

Buhl-Mortensen, L., Serigstad, B., Buhl-Mortensen, P., Olsen, M. N., Ostrowski, M., Błażewicz-Paszkowycz, M., et al. (2017). First observations of the structure and megafaunal community of a large *Lophelia* reef on the Ivorian-Ghanaian margin (the Gulf of Guinea). *Deep-Sea Res. Part II Top. Stud. Oceanogr.* 137, 148–156. doi: 10.1016/j.dsr2.2016.06.007

Buhl-Mortensen, L., Vanreusel, A., Gooday, A. J., Levin, L. A., Priede, I. G., Buhl-Mortensen, P., et al. (2010). Biological structures as a source of habitat heterogeneity and biodiversity on the deep ocean margins. *Mar. Ecol.* 31, 21–50.

Chapman, A. S. A., Tunnicliffe, V., and Bates, A. E. (2018). Both rare and common species make unique contributions to functional diversity in an ecosystem unaffected by human activities. *Divers. Distrib.* 24, 568–578. doi: 10.1111/ddi.12712

Clarke, K. R., Sommerfield, P. J., and Gorley, R. N. (2008). Testing of null hypotheses in explanatory community analyzes: similarity profiles and biota-environment linkage. *J. Exp. Mar. Biol. Ecol.* 366, 56–69. doi: 10.1016/j.jembe.2008.07.009

Cosson, N., Sibuet, M., and Galeron, J. (1997). Community structure and spatial heterogeneity of the deep-sea macrofauna at three contrasting stations in the tropical northeast Atlantic. *Deep Sea Res. Part I Oceanogr. Res. Pap.* 44, 247–269. doi: 10.1016/S0967-0637(96)00110-0

Costa, C., Fanelli, E., Marini, S., Danovaro, R., and Aguzzi, J. (2020). Global Deep-Sea Biodiversity Research Trends Highlighted by Science Mapping Approach. *Front. Mar. Sci.* 7:384. doi: 10.3389/fmars.2020.00384

Costello, M. J., and Chaudary, C. (2017). Marine biodiversity, biogeography, deep-sea gradients, and conservation. *Curr. Biol.* 27, 511–527. doi: 10.1016/j.cub.2017.04.060

Costello, M. J., May, R. M., and Stork, N. E. (2013). Can we name Earth's species before they go extinct? *Science* 339, 413–416. doi: 10.1126/science.1230318

Costello, M. J., Wilson, S., and Houlding, B. (2012). Predicting total global species richness using rates of species description and estimates of taxonomic effort. *Syst. Biol.* 61:871–883. doi: 10.1093/sysbio/syr080

Danovaro, R., Canals, M., Gambi, C., Heussner, S., Lampadariou, N., and Vanreusel, A. (2009). Exploring benthic biodiversity patterns and hotspots on European margin slopes. *Oceanography* 22, 16–25. doi: 10.5670/oceanog.2009.02

Dayton, P. K., and Oliver, J. S. (1977). Antarctic soft bottom benthos in oligotrophic and eurythropic environments. *Science* 197, 55–58. doi: 10.1126/science.197.4298.55

Dee, L. E., Cowles, J., Isbell, F., Pau, S., Gaines, S. D., and Reich, P. B. (2019). When do ecosystem services depend on rare species? *Trends Ecol. Evol.* 34, 746–758. doi: 10.1016/j.tree.2019.03.010

Djagoua, E. V., Kassi, J. B., Mobia, B., Kouadio, J. M., Dro, C., Affian, K., et al. (2011). Ivorian and Ghanaian upwelling comparison: intensity and impact on phytoplankton biomass. *Am. J. Sci. Ind. Res.* 2, 740–747. doi: 10.5251/ajsir.2011.2.5.740.747

Dojiri, M., and Sieg, J. (1997). "The *Tanaidacea*," in *Taxonomic Atlas of the Benthic Fauna of the Santa Maria Basin and Western Santa Barbara Channel. Volume 11. The Crustacea Part 2. The Isopoda, Cumacea and Tanaidacea*, eds J. A. Blake and P. H. Scott (Santa Barbara, CA: Santa Barbara Museum of Natural History), 181–278.

Drumm, D. T., and Heard, R. W. (2011). Systematic revision of the family Kalliapseudidae (Crustacea: Tanaidacea). *Zootaxa* 3142, 1–172. doi: 10.11646/zootaxa.3142.1.1

Eleftheriou, A., and McIntyre, A. D. (eds) (2005). *Methods For The Study Of Marine Benthos*, 3rd Edn. Oxford: Blackwell Science.

Elezz, A. A., Mustafa Hassan, H., Abdulla Alsaadi, H., Easa, A., Al-Meer, S., Elsaid, K., et al. (2018). Validation of total mercury in marine sediment and biological samples, using cold vapour atomic absorption spectrometry. *Methods Protoc.* 1:31. doi: 10.3390/mps1030031

Ellingsen, K. E., Hewitt, J. E., and Thrush, S. F. (2007). Rare species, habitat diversity and functional redundancy in marine benthos. *J. Sea Res.* 58, 291–301. doi: 10.1016/j.seares.2007.10.001

Ellison, A. M., Bank, M. S., Clinton, B. D., Colburn, E. A., Elliott, K., Ford, C. R., et al. (2005). Loss of foundation species: consequences for the structure and dynamics of forested ecosystems. *Front. Ecol. Environ.* 3, 479–486. doi: 10.2307/3868635

Folk, R. L., and Ward, W. C. (1957). Brazos River bar [Texas]; a study in the significance of grain size parameters. *J. Sediment. Res.* 27, 3–26. doi: 10.1306/74D70646-2B21-11D7-8648000102C1865D

Fox, J., and Weisberg, S. (2019). *An {R} Companion to Applied Regression, Third edition*. Thousand Oaks CA: Sage.

Golovan, O. A., Błażewicz, M., Brandt, A., Jażdżewska, A., Jóźwiak, P., Lavrenteva, A. V., et al. (2019). Diversity and distribution of peracarid crustaceans (Malacostraca) from the abyss adjacent to the Kuril-Kamchatka Trench. *Mar. Biodivers.* 49, 1343–1360. doi: 10.1007/s12526-018-0908-3

Gomez-Gesteira, J. L., Dauvin, J. C., and Salvande-Fraga, M. (2003). Taxonomic level for assessing oil spill effects on soft-bottom sublittoral benthic communities. *Mar. Pollut. Bull.* 46, 562–572. doi: 10.1016/S0025-326X(03)00034-1

Grassle, J. F., and Maciolek, N. J. (1992). Deep-sea richness, regional and local diversity estimates from quantitative bottom samples. *Am. Nat.* 139, 313–341. doi: 10.1086/285329

Grime, J. P. (1998). Benefits of Plant Diversity to Ecosystems: immediate, Filter and Founder Effects. *J. Ecol.* 86, 902–910. doi: 10.1046/j.1365-2745.1998.00306.x

Guisan, A., Broennimann, O., Engler, R., Vust, M., Yoccoz, N. G., Lehmann, A., et al. (2006). Using niche-based models to improve the sampling of rare species. *Conserv. Biol.* 20, 501–511. doi: 10.1111/j.1523-1739.2006.00354.x

Guțu, M., and Sieg, J. (1999). "Ordre des Tanaidaces," in *Traite de Zoologie 7(3)(A), Crustaces Pericarides*, ed. J. Forest (Monaco: Mermoires de I'Institut Oceanographique), 353–389.

Hassack, E., and Holdich, D. M. (1987). The tubulicous habit amongst the Tanaidacea (Crustacea, Peracarida) with particular reference to deep-sed speckles. *Zool. Sci.* 16, 223–233. doi: 10.1111/j.1463-6409.1987.tb00069.x

Higgs, N. D., and Attrill, M. J. (2015). Biases in biodiversity: wide-ranging species are discovered first in the deep sea. *Front. Mar. Sci.* 2:61. doi: 10.3389/fmars.2015.00061

Holdich, D. M., and Bird, G. J. (1985). Tanaidacea (Crustacea) from sublittoral waters off West Scotland, including the description of two new genera. *J. Nat. Hist.* 20, 79–100. doi: 10.1080/00222938600770081

Hughes, A. C., Orr, M. C., Ma, K., Costello, M. J., Waller, J., Provoost, P., et al. (2021). Sampling biases shape our view of the natural world. *Ecography* 44, 1259–1269. doi: 10.1111/ecog.05926

Iversen, P. E., Green, A. M. V., Lind, M. J., Petersen, M. R. H. P., Bakke, T., Lichtenthaler, R., et al. (2011). *Guidelines for Offshore Environmental Monitoring on the Norwegian Continental Shelf. Klif Report*. Oslo: Climate and Pollution Agency.

Jakiel, A., Stępień, A., and Błażewicz, M. (2018). A tip of the iceberg—Pseudotanaidae (Tanaidacea) diversity in the North Atlantic. *Mar. Biodivers.* 48, 859–895. doi: 10.1007/s12526-018-0881-x

Jarvis, I., and Jarvis, K. E. (1992). Plasma spectrometry in the earth sciences: techniques, applications and future trends. *Chem. Geol.* 95, 1–33. doi: 10.1016/0009-2541(92)90041-3

Jóźwiak, P., and Błażewicz, M. (2021). *Muvi schmallenbergi* gen. nov., sp. nov. (Crustacea, Tanaidacea) from the southeast Australian coast, with comments on the distribution and habitat preferences of Chondropodinae. *PeerJ* 9:e11607. doi: 10.7717/peerj.11607

Jóźwiak, P., Janicka, M., Dębiec, P., Stępiński, A., Mielczarz, K., Serigstad, B., et al. (2017). New Tanaidacea (Crustacea: Peracarida) from the Gulf of Guinea. *Mar. Biodivers.* 48, 1715–1730. doi: 10.1007/s12526-017-0646-y

Jóźwiak, P., Pabis, K., Brandt, A., and Błażewicz, M. (2020). Epibenthic sled versus giant box corer – comparison of sampling gears for tanaidacean species richness assessment in the abyssal benthic ecosystem. *Prog. Oceanogr.* 181:102255. doi: 10.1016/j.pocean.2019.102255

Jumars, P. A., Dorgan, K. M., and Lindsay, S. M. (2015). Diet of worms emended: an update for polychaete feeding guilds. *Ann. Rev. Mar. Sci.* 7, 497–520. doi: 10.1146/annurev-marine-010814-020007

Kaiser, K., Barnes, D. K. A., and Brandt, A. (2007). Slope and deep-sea abundance across scales: Southern Ocean isopods show how complex the deep sea can be. *Deep-Sea Res. Part II Top. Stud. Oceanogr.* 54, 1776–1789. doi: 10.1016/j.dsr2.2007.07.006

Kaiser, S., Barnes, D. K., Sands, C. J., and Brandt, A. (2009). Biodiversity of an unknown Antarctic Sea: assessing isopod richness and abundance in the first benthic survey of the Amundsen continental shelf. *Mar. Biodivers.* 39:27. doi: 10.1007/s12526-009-0004-9

Kakui, K., and Kohtsuka, H. (2015). Two New Shallow-water Species of *Agathotanais* (Crustacea: Tanaidacea) from Japan. *Species Divers.* 20, 45–58. doi: 10.12782/sd.20.1.045

Kneib, T. (1985). Patterns in the utilisation of the intertidal salt marsh by larvae and juveniles of *Fundulus heteroclits* (Linneaus) and *Fundulus luciae* (Baird). *J. Exp. Mar. Biol. Ecol.* 83, 41–51. doi: 10.1016/0022-0981(84)90116-3

Kuhn, M. (2020). *Caret: classification and Regression Training. R package version 6.0-85*.

Larsen, K. (2005). *Deep-Sea Tanaidacea (Peracarida) from the Gulf of Mexico*. Leiden: Brill.

Larsen, K. (2013). The ANDEEP Tanaidacea (Crustacea: Peracarida) revisited II: the family Anarthruridae and family incertae sedis, with descriptions of three new species and the erection of a new genus. *Zootaxa* 3694, 367–380. doi: 10.11646/zootaxa.3694.4.5

Larsen, K., and Araújo-Silva, C. L. (2014). The ANDEEP Tanaidacea (Crustacea: Peracarida) revisited III: the family Akanthophoreidae. *Zootaxa* 3796, 237–264. doi: 10.11646/zootaxa.3796.2.2

Le Loeuff, P., and Cosel, R. (1998). Biodiversity patterns of the marine benthic fauna on the Atlantic coast of tropical Africa in relation to hydroclimatic conditions and paleogeographic events. *Acta Oecol.* 19, 309–321. doi: 10.1016/S1146-609X(98)80035-0

Le Loeuff, P., and Intès, A. (1999). Macrobenthic communities in the continental shelf of Côte-d'Ivoire. Seasonal and diel cycles in relation to hydroclimate. *Acta Oceanol.* 22, 529–550. doi: 10.1016/S0399-1784(00)87685-9

Leitão, R. P., Zuanon, J., Villéger, S., Williams, S. E., Baraloto, C., Fortunel, C., et al. (2016). Rare species contribute disproportionately to the functional structure of species assemblages. *Proc. R. Soc. B* 283, 494–499. doi: 10.1098/rspb.2016.0084

Leite, P. P. (1995). Seasonal and spatial distribution of *Kalliapseudes schubarti* Mane-Garzon (Tanaidacea, Crustacea), in the Araca region, Sao Sebastiao. *Arq. Biol. Tecnol.* 38, 605–618.

Leroy, B., Gallon, R., Feunteun, E., Robuchon, M., and Frédéric, Y. (2017). Cross-taxon congruence in the rarity of subtidal rocky marine assemblages: no taxonomic shortcut for conservation monitoring. *Ecol. Indic.* 77, 239–249. doi: 10.1016/j.ecolind.2017.02.012

Levin, L. A. (2003). Oxygen minimum zone benthos: adaptation and community response to hypoxia. *Oceanogr. Mar. Biol.* 41, 1–45.

Levin, L. A., and Sibuet, M. (2012). Understanding continental margin biodiversity: a new imperative. *Ann. Rev. Mar. Sci.* 4, 79–112. doi: 10.1146/annurev-marine-120709-142714

Levin, L., Whitcraft, C. R., Mendoza, G. F., Gonzalez, J. P., and Cowie, G. (2009). Oxygen and organic matter thresholds for benthic faunal activity on the Pakistan margin oxygen minimum zone (700—1100 m). *Deep Sea Res. II Top. Stud. Oceanogr.* 56, 449–471. doi: 10.1016/j.dsr2.2008.05.032

Longhurst, A. R. (1958). *An Ecological Survey of the West African MarineBenthos*. London: Colonial Office Fisheries Publication, 1–102.

Longhurst, A. R. (1959). Benthos densities off tropical West Africa. *ICES Mar. Sci. Symp.* 25, 21–28. doi: 10.1093/icesjms/25.1.21

Lyons, K. G., Brigham, C. A., Traut, B. H., and Schwartz, M. W. (2005). Rare species and ecosystem functioning. *Conserv. Biol.* 19, 1019–1024. doi: 10.1111/j.1523-1739.2005.00106.x

McCallum, A. W., Woolley, S., Błażewicz-Paszkowycz, M., Browne, J., Gerken, S., Kloser, R., et al. (2015). Productivity enhances benthic species richness along an oligotrophic Indian Ocean continental margin. *Glob. Ecol. Biogeogr.* 24, 462–471. doi: 10.1111/geb.12255

Mouillot, D., Bellwood, D. R., Baraloto, C., Chave, J., Galzin, R., Harmelin-Vivien, M., et al. (2013). Rare species support vulnerable functions in high-diversity ecosystems. *PLoS Biol.* 11:e1001569. doi: 10.1371/journal.pbio.1001569

Nagelkerken, I., and van der Velde, G. (2004). Relative importance of interlinked mangroves and seagrass beds as feeding habitats for juvenile reef fish on a Caribbean island. *Mar. Ecol. Prog. Ser.* 274, 153–159. doi: 10.3354/meps274153

Obst, M., Vicario, S., Lundin, K., Berggren, M., Karlsson, A., Haines, R., et al. (2018). Marine long-term biodiversity assessment suggests loss of rare species in the Skagerrak and Kattegat region. *Mar. Biodivers.* 48, 2165–2176. doi: 10.1007/s12526-017-0749-5

Oksanen, J., Blanchet, F. G., Friendly, M., Kindt, R., Legendre, P., McGlinn, D., et al. (2020). *Vegan: community Ecology Package. R package version 2. 5-7*. Available Online at: https://CRAN.R-project.org/package=vegan.

Oliver, J. S., and Slattery, P. N. (1985). Effects of crustacean predators on species composition and population structure of soft bodied infauna from McMurdo Sound, Antarctica. *Ophelia* 24, 155–175. doi: 10.1080/00785326.1985.10429725

Olsgard, F., and Gray, J. S. (1995). A comprehensive analysis of effects of offshore oil and gas exploration and production on the benthic communities of the Norwegian continental shelf. *Mar. Ecol. Prog. Ser.* 122, 277–306. doi: 10.3354/meps122277

Pabis, K., Błażewicz-Paszkowycz, M., Jóźwiak, P., and Barnes, D. K. A. (2014). Tanaidacea of the Amundsen and Scotia seas: unexplored diversity. *Antarct. Sci.* 27, 19–30. doi: 10.1017/S0954102014000303

Pabis, K., Jóźwiak, P., Lörz, A. N., Schnabel, K., and Błażewicz-Paszkowycz, M. (2015). First insights into the deep-sea tanaidacean fauna of the Ross Sea – species richness and composition across the shelf break, slope and abyss. *Polar Biol.* 38, 1429–1437. doi: 10.1007/s00300-015-1706-z

Pabis, K., Sobczyk, R., Siciński, J., Ensrud, T., and Serigstadt, B. (2020). Natural and anthropogenic factors influencing abundance of the benthic macrofauna along the shelf and slope of the Gulf of Guinea, a large marine ecosystem off West Africa. *Oceanologia* 62, 83–100. doi: 10.1016/j.oceano.2019.08.003

R Core Team (2019). *R: a Language And Environment For Statistical Computing*. Vienna, Austria: R Foundation for Statistical Computing.

Reiss, H., Birchenough, S., Borja, A., Buhl-Mortensen, L., Craeymeersch, J., Dannheim, J., et al. (2015). Benthos distribution modelling and its relevance for marine ecosystem management. *ICES J. Mar. Sci.* 72, 297–315. doi: 10.1093/icesjms/fsu107

Rex, M. A., and Etter, R. J. (2010). *Deep-Sea Biodiversity; Patterns and Scale*. Cambridge, MA: Harvard University Press.

Rouse, G. W., and Pleijel, F. (2001). *Polychaetes*. Oxford, UK: Oxford University Press.

Rumbold, C. E., Obenat, S. M., and Spivak, E. D. (2015). Comparison of life history traits of *Tanais dulongii* (Tanaidacea: Tanaididae) in natural and artificial marine environments of the south-western Atlantic. *Helgol. Mar. Res.* 69, 231–242. doi: 10.1007/s10152-015-0432-9

Säterberg, T., Jonsson, T., Yearsley, J., Berg, S., and Ebenman, B. (2019). A potential role for rare species in ecosystem dynamics. *Sci. Rep.* 9:11107. doi: 10.1038/s41598-019-47541-6

Scheren, P. A., Ibe, A. C., Janssen, F. J., and Lemmens, A. M. (2002). Environmental pollution in the Gulf of Guinea – a regional approach. *Mar. Pollut. Bull.* 44, 633–641. doi: 10.1016/S0025-326X(01)00305-8

Schneider, W. (1990). *Field Guide to the Commercial Marine Resources of the Gulf of Guinea*. Rome: Food and Agriculture Organization of the United Nations.

Segadilha, J. L., and Lavrado, H. P. (2018). Tanaidacea fauna (Peracarida, Crustacea) from the shallow sublittoral zone of Admiralty Bay, King George Island, Antarctica, with new records. *Polar Biol.* 41, 589–597. doi: 10.1007/s00300-017-2220-2

Sheridan, P. (1997). Benthos of adjacent mangrove, seagrass and non-vegetated habitats in Rookery Bay, Florida, USA. *Estuar. Coast. Shelf Sci.* 44, 455–469. doi: 10.1006/ecss.1996.0125

Siciński, J., Pabis, K., Jażdżewski, K., Konopacka, A., and Błażewicz-Paszkowycz, M. (2012). Macrozoobenthos of two Antarctic glacial coves: a comparison with non-disturbed bottom areas. *Polar Biol.* 35, 355–367. doi: 10.1007/s00300-011-1081-3

Smith, M. D., and Knapp, A. K. (2003). Dominant species maintain ecosystem function with non-random species loss. *Ecol. Lett.* 6, 509–517. doi: 10.1046/j.1461-0248.2003.00454.x

Sobczyk, R., Czortek, P., Serigstad, B., and Pabis, K. (2021). Modelling of polychaete functional diversity: a Large marine ecosystem response tomultiple natural factors and human impacts on the West African continental margin. *Sci. Total Environ.* 792:148075. doi: 10.1016/j.scitotenv.2021.148075

Sokolova, M. N. (1972). Trophic structure of deep-sea macrobenthos. *Mar. Biol.*16, 1–12. doi: 10.1007/bf00347841

Somerfield, P. J., and Clarke, K. R. (1997). A comparison of some methods commonly used for the collection of sublittoral sediments and their associated fauna. *Mar. Environ. Res.* 43, 145–156.

Stark, J. S., Mohammad, M., McMinn, A., and Ingels, J. (2020). Diversity, abundance, spatial variation, and human impacts in marine meiobenthic Nematode and Copepod communities at Casey Station, East Antarctica. *Front. Mar. Sci.* 7:480. doi: 10.3389/fmars.2020.00480

Stępień, A., and Blażewicz-Paszkowycz, M. (2013). Four new species and two new genera of Metapseudidae (Crustacea: Tanaidacea: Apseudomorpha) from Australian coral reefs. *Zootaxa* 3717, 559–592. doi: 10.11646/zootaxa.3717.4.7

Stępień, A., Pabis, K., and Błażewicz, M. (2018). Small-scale species richness of the Great Barrier Reef tanaidaceans—results of the CReefs compared with worldwide diversity of coral reef tanaidaceans. *Mar. Biodivers.* 49, 1169–1185. doi: 10.1007/s12526-018-0894-5

Stępień, A., Pabis, K., and Błażewicz, M. (2019). Tanaidacean faunas of the Sea of Okhotsk and northern slope of the Kuril-Kamchatka Trench. *Prog. Oceanogr.* 178:102196. doi: 10.1016/j.pocean.2019.102196

Stępień, A., Pabis, K., Sobczyk, R., and Serigstad, B. (2021). High Species Richness and Extremely Low Abundance of Cumacean Communities Along the Shelf and Slope of the Gulf of Guinea (West Africa). *Front. Mar. Sci.* 8:703547. doi: 10.3389/fmars.2021.703547

Ukwe, C. N., Ibe, C. A., Alo, B. I., and Yumkella, K. K. (2003). Achieving a paradigm shift in environmental and living resources management in the Gulf of Guinea: the large marine ecosystemapproach. *Mar. Pollut. Bull.* 47, 219–225. doi: 10.1016/S0025-326X(02)00473-3

Ukwe, C. N., Ibe, C. A., and Sherman, K. (2006). A sixteen-country mobilization for sustainable fisheries in the Guinea Current Large Marine Ecosystem. *Ocean Coast. Manag.* 49, 385–412. doi: 10.1016/j.ocecoaman.2006.04.006

UNESCO Intergovernmental Oceanographic Commission (1982). *The Determination of Petroleum Hydrocarbons in Sediments (Manuals and Guides No. 11, Paris)*. Paris: UNESCO.

Wägele, J. W. (2005). *Foundations of Phylogenetic Systematics*. München: Verlag Dr. Friedrich Pfeil.

Wei, T., and Simko, V. (2017). *R Package "corrplot": visualization of a Correlation Matrix (Version 0.84)*. Available Online at: https://guthub.com/taiyun/corrplot.

Whitaker, D., and Christman, M. (2014). *Clustig: significant cluster analysis. R package version 1.1*. Available Online at: https://CRAN.R-project.org/package=clustsig.

Wilson, G. D. F. (2017). Macrofauna abundance, species diversity and turnover at three sites in Clipperton-Clarion Fracture Zone. *Mar. Biodivers.* 47, 323–347.

Włodarska-Kowalczuk, M., Renaud, P. E., Węsławski, J. M., Cochrane, S. K. J., and Denisenko, S. G. (2012). Species diversity, functional complexity and rarity in arctic fjordic versus open shelf benthic system. *Mar. Ecol. Prog. Ser.* 463, 73–87.

Conflict of Interest: The authors declare that the research was conducted in the absence of any commercial or financial relationships that could be construed as a potential conflict of interest.

Publisher's Note: All claims expressed in this article are solely those of the authors and do not necessarily represent those of their affiliated organizations, or those of the publisher, the editors and the reviewers. Any product that may be evaluated in this article, or claim that may be made by its manufacturer, is not guaranteed or endorsed by the publisher.

Copyright © 2022 Jóźwiak, Pabis, Sobczyk and Serigstad. This is an open-access article distributed under the terms of the Creative Commons Attribution License (CC BY). The use, distribution or reproduction in other forums is permitted, provided the original author(s) and the copyright owner(s) are credited and that the original publication in this journal is cited, in accordance with accepted academic practice. No use, distribution or reproduction is permitted which does not comply with these terms.

frontiers in Marine Science

ORIGINAL RESEARCH
published: 16 March 2022
doi: 10.3389/fmars.2021.741536

Diversity of Pacific *Agathotanais* (Peracarida: Tanaidacea)

Anna Stępień[1], Piotr Jóźwiak[1], Aleksandra Jakiel[2], Alicja Pełczyńska[1] and Magdalena Błażewicz[1]*

[1] Department of Invertebrate Zoology and Hydrobiology, University of Łódź, Łódź, Poland, [2] Department of Genetics and Marine Biotechnology, Institute of Oceanology, Polish Academy of Sciences, Sopot, Poland

Agathotanais is one of the seven genera classified into the family Agathotanaidae. So far, 12 species have been described for the genus, seven of which are known from the Pacific. However, considering the present poor state of knowledge on deep-sea environments, a much higher number of *Agathotanais* species than currently known can be suspected. Among the studied material, collected from below 1,000 m during five deep-sea expeditions in different parts of the Pacific Ocean, we identified eight species: two of them were already known to the science and five species were identified as new to knowledge and their formal description is presented in the paper: two from the North West Pacific (the Sea of Okhotsk and Kuril-Kamchatka Trench), two from the Central Pacific (Clarion-Clipperton Fracture Zone), and one from the Australian slope. The eighth *Agathotanais* species in our material was determined using a molecular approach, but it was represented by only one partially destroyed individual and could therefore not be formally described. The proportion of *Agathotanais* collected at the Sea of Okhotsk was the highest (22%), whereas the numbers were substantially lower for the Kuril-Kamchatka Trench, and the Central and the Southern Pacific. Molecular analyses confirmed the monophyly of *Agathotanais* and *Paragathotanais* and a close relationship between both genera. Moreover, a close relationship between the two Australian species was revealed. As a result of our findings, the number of species known from the Pacific increased from 5 to 11, with the total number of species in this genus increasing from 12 to 17. An updated identification key for *Agathotanais* species is given.

Keywords: Sea of Okhotsk, Kuril-Kamchatka Trench, Clarion-Clipperton Fracture Zone, Australia, biodiversity of West and Central Pacific

OPEN ACCESS

Edited by:
Clara F. Rodrigues, University of Aveiro, Portugal

Reviewed by:
David Drumm, EcoAnalysts, Inc., United States
Andres G. Morales-Nunez, University of Maryland Eastern Shore, United States

****Correspondence:***
Anna Stępień
anna.stepien@biol.uni.lodz.pl

Specialty section:
This article was submitted to Deep-Sea Environments and Ecology, a section of the journal Frontiers in Marine Science

Received: *14 July 2021*
Accepted: *19 November 2021*
Published: *16 March 2022*

Citation:
Stępień A, Jóźwiak P, Jakiel A, Pełczyńska A and Błażewicz M (2022) Diversity of Pacific Agathotanais (Peracarida: Tanaidacea). Front. Mar. Sci. 8:741536. doi: 10.3389/fmars.2021.741536

INTRODUCTION

Genus *Agathotanais* was established to allocate *Agathotanais ingolfi* Hansen, 1913, discovered off Iceland during the *Danish Ingolf Expedition* (Hansen, 1913). It was described and marked as the most aberrant among all tanaids due to its rudimentary antenna, cheliped attached directly to the cephalothorax, the appearance of the pleopods in juvenile males (Hansen, 1913), and the setulose surface of its body (Larsen, 2005; Jóźwiak and Jakiel, 2012; Kakui and Kohtsuka, 2015). Hansen (1913) placed *Agathotanais* within the family Tanaidae Dana (1849), the only existing tanaidacean family at that time, but few decades later the *Agathotanais*, together with *Paragathotanais*, was transferred to the newly erected family Agathotanaidae Lang, 1971. The family was successively supplemented by newly erected genera and new species

(Sieg, 1986; Bird and Holdich, 1988; Błażewicz-Paszkowycz and Bamber, 2012; Jóźwiak and Jakiel, 2012). Currently, Agathotanaidae includes 54 species in seven genera, and *Agathotanais*, with 12 species, is the third genus in terms of species number after *Paranarthrura* (21 species) and *Paragathotanais* (16 species) (Hansen, 1913; Kudinova-Pasternak, 1970, 1989, 1990; Lang, 1971; Larsen, 1999, 2007; Kakui and Kohtsuka, 2015; Chim and Tong, 2021).

The history of the exploration of Pacific deep-sea regions started in the XIX century with the HMS *Challenger* expedition (1872–1876), during which the polymetallic nodules and the Mariana Trench were discovered (Schofield, 2018). Those explorations were continued for the next century aboard the RV *Vitjaz* (1949–1966), the RV *Galathea* (1951–1952), the RV *Dmitry Mendeleev* (1975–1976), or the RV *Tangaroa* (1982) (O'Hara, 2019). The regions previously considered as monotonous deserts were revealed as having a diverse topography, high nutrient densities, and a rich local diversity (Frutos et al., 2016; Golovan et al., 2018; Błażewicz et al., 2019; Washburn et al., 2021). The firsts Pacific agathotanaids described during that time (*Agathotanais splendidus* Kudinova-Pasternak, 1970, *Paranarthrura vitjazi* Kudinova-Pasternak, 1970 and *Paragathotanais zevinae* Kudinova-Pasternak, 1970) appeared as an unabundant component of macrobenthic communities, represented by several individuals only (Kudinova-Pasternak, 1970, 1983). More recently, the intensive investigation of the Pacific has applied advanced methodologies to explore the Pacific floor and trenches (Brandt and Barthel, 1995; Larsen and Shimomura, 2007; Riehl et al., 2014; Frutos et al., 2016; O'Hara et al., 2020a,b; Saeedi and Brandt, 2020; Washburn et al., 2021). As a result, six new species belonging to genus *Agathotanais* were added to the list of Pacific agathotanaids, namely: *Agathotanais hadalis* Larsen, 2007 from the North West Pacific abyssal, *Agathotanais misakiensis* Kakui and Kohtsuka, 2015 and *Agathotanais toyoshioae* Kakui and Kohtsuka, 2015 from the coast of Japan, *Agathotanais spinipoda* Larsen, 1999 from the slope of Bass Strait, and *Agathotanais manganicus* Larsen, 1999 and *Agathot*anais ahyongi Larsen, 1999 from the Central Pacific abyssal (Larsen, 1999, 2007; Kakui and Kohtsuka, 2015).

In this article, we have analyzed the new collections of the *Agathotanais* obtained from several most recent deep-sea expeditions, which explored the abyssal of the Pacific and represent the next step for discovering the variability of deep-sea tanaid diversity. Using morphological and genetic tools, we present the description of five new species of *Agathotanais* collected from four areas of the Pacific: Clarion-Clipperton Fracture Zone (two species), off East Australia (one species), the Sea of Okhotsk (one species), and the Kuril-Kamchatka Trench (KKT) (one species). We discuss their bathymetric and zoogeographical distributions. Additionally, with genetic tools, we have detected one more new species off SE Australia, that was represented by only one speciemen in poor condition. This speciem was dissected and prepared into slides. It would provide a holotype of substandard quality and therefore it is not be formally described as a named species in this article.

MATERIALS AND METHODS

Sampling

A total of 738 specimens of the genus *Agathotanais* were collected from from five deep-sea projects (**Supplementary Table 1**).

1. A total of 634 specimens were collected in the Sea of Okhotsk during the German-Russian expedition SokhoBio (Sea of Okhotsk Biodiversity Studies) aboard the RV *Academic M.A. Lavrentyev* between July and August of 2015 (Malyutina et al., 2015). Specimens of *Agathotanais* were found in twelve epibenthic sledge (EBS) samples.
2. A total of 70 specimens were collected in the KKT and the adjacent abyssal zone during two expeditions: KuramBio (Kuril-Kamchatka Biodiversity Study, NW Pacific abyssal, and western KKT slope) and KuramBio II (KKT slope) in 2012 and 2016, respectively aboard the RV *Sonne*. *Agathotanais* was present in 12 EBS samples taken during KuramBio and KuramBio II.
3. A total of 21 specimens were collected in 2015 in the Central Pacific (Clarion-Clipperton Fracture Zone, CCZ) during the EcoResponse (SO-239) cruise, one of the Joint Project Initiative Oceans (JPIO) expeditions. From a total of eleven EBS deployments, *Agathotanais* was found in the following License Areas: Bundesanstalt fur Geowissenschalfen und Rofstoffe (BGR, Germany); Interoceanometal Joint Organisation (IOM); Global Sea Mineral Resources NV, Belgium (GSR); Areas of Particular Environmental Interest 3 (APEI3).
4. Five specimens were collected off the SE Australian coast during the ABYSS (Sampling the Abyss) expedition in 2017 from aboard the RV *Investigator*. *Agathotanais* were found in three EBS samples.
5. Two specimens collected in the continental slope off SE Australia, during the SLOPE campaign in 1988 and 1994. *Agathotanais* was found in two samples collected by dredging.

Except for the SLOPE collection that was preserved in formalin, all specimens were fixed in 96% ethanol. Specimens from the Sea of Okhotsk, the KKT, and Central Pacific have been loaned from the Zoological Museum Hamburg (ZMH), Natural History Museum in Frankfurt (NHM) and A.V. Zhirmunsky National Scientific Center of Marine Biology in Vladivostok (MIMB). Material from the Australian and Tasmanian coast has been loaned from the Museum Victoria in Melbourne (catalog numbers start with J and NMV).

Phylogenetic and Genetic Distance Analyses

The analyses included 16 specimens from the Sea of Okhotsk (SokhoBio collection), 16 from the KKT (KuramBio collection), 21 from the Central Pacific (JPIO collection), and two specimens from Australia (ABYSS collection). For the DNA extraction, the whole specimen was taken as starting material using sterile needles and following the Chelex (InstaGene Matrix, Bio-Rad) method as in Palero et al. (2010). The ribosomal RNA18S and

the histone H3 genes were amplified using a 25 μl-volume reaction containing 13 μl AccuStart II GelTrack PCR SuperMix, 10 μl H_2O, 0.5 μl of each primer (10 pmol/μl) and 2 μL DNA template. The 18S fragments were amplified using the universal primers SSU_F04 and SSU_R22 (Blaxter et al., 1998) following the protocol: 95°C for 2 min, 95°C for 1 min, 57°C for 45 s, 72°C for 3 min, for 35 cycles, and a final elongation of 10 min at 72°C. The H3AF and H3AR fragments (Colgan et al., 1998) were obtained according to the protocol: 95°C for 3 min, 95°C for 30 s, 50°C for 30 s, 72°C for 1 min, for 35 cycles, and a final elongation of 15 min at 72°C. A 2 μl-aliquot of the PCR product was visualized in a Midori Green-stained (Nippon Genetics) 1.5% agarose gel to verify its quality and length. PCR purification and sequencing using forward and reverse primers were carried out by MACROGEN (Amsterdam, Netherlands). Consensus sequences were built using Geneious version 9.1.3[1] and compared with the GenBank database with BLAST (basic local alignment search tool, NCBI) (Altschul et al., 1990) to discard contamination from non-arthropod sources. Sequences were aligned using the option L-INSi of MAFFT (multiple alignment using fast Fourier transform) (Katoh and Standley, 2013), as implemented in Geneious. Genetic distances were calculated using pairwise distances and run-on *p*-distance model using MEGA 7 (Molecular Evolutionary Genetics Analysis, Pennsylvania State University) (Kumar et al., 2018). Before running molecular phylogenetic analyses, the most suitable nucleotide substitution model was selected according to the AICc (The Akaike information criterion) and BIC (the Bayesian information criterion) criteria as implemented in MEGA 7 (Kumar et al., 2018). The aligned sequences and selected evolutionary model were then used to obtain a Maximum Likelihood phylogenetic tree in BEAST (BEAST Developers) (Drummond et al., 2012). Node support was evaluated with, bootstrap replicates. MCMC (Markov chain Monte Carlo) analyses were set for 10 million generations whereas all Effective Sample Size (ESS) values were calculated with Trace Analysis Tool (Tracer v1.5.0) software (Rambaut et al., 2018). To analyze the MCMC outputs Tree Annotator v1.7.5 (Drummond and Rambaut, 2007) was used with the default parameters.

Species Description

Chemically sharpened tungsten needles were used for the dissection of the individuals selected for detailed morphological analyses. The dissected appendages were placed on a microscope slide on a drop of glycerine, protected with a cover glass, and sealed with a ring of melted paraffin (Błażewicz et al., 2021). Drawings were prepared using a light microscope (Nikon Eclipse 50*i*, Japan) equipped with a *camera lucida*. Publication-quality illustrations were prepared using a digital tablet and Adobe Illustrator (Adobe inc.) (Coleman, 2003). Total body length (BL) was measured along the main axis of symmetry from the frontal margin to the end of the telson. Body width (BW) was measured at the widest point along the main axis of symmetry. The measurements of specimens were made with the help of a camera connected to the microscope (Nikon Eclipse Ci-L) using NIS-Elements View software[2]. The morphological description follows Jakiel et al. (2019), where the expression '*N*x' replaces '*N* times as long as' and '*N* L:W' replaces '*N* times as long as wide.'

For appendage ornamentation, we have followed the classification according to Garm and Watling (2013). Following types were used: (1) simple setae; (2) plumose setae; (3) serrated setae; (4) setules; (5) spines. For more specific ornamentation we used the following definition: (6) penicillate seta – with a tuft of setules located distally and with a small knob on which a seta is fixed to the tegument; and (7) spinule – short, tiny spine.

The stages recognized among the studied individuals were: manca (II and III), neuter, and a juvenile male. Specifically, the term 'manca' describes juveniles with (manca III) or without (manca II) buds on pereopod-6. 'Neuter' is retained for the development stage after manca that cannot be classified as either female or juvenile male. Juvenile male refers to individuals with initially developed pleopods.

Confocal Laser Scanning Microscopy

Two individuals from the SokhoBio collection (neuter: ZMH K-61187, juvenile male: ZMH K-61184) and two individuals from the KuramBio collection (neuter: ZMH K-61178) were used for imaging. Pictures were obtained with a confocal laser scanning microscope CLSM 780 (Zeiss) equipped with a Plan-Apochromat 10x/0.47 M27 objective and the InTune tunable excitation laser system (set to excitation at wavelength 555 nm).

Ethanol-preserved specimens were stained for 48 h with a mixture of equal volumes of saturated aqueous solutions of Congo red and acid fuchsin. Animals were sequentially washed in 80% glycerol and 100% glycerol and kept in 100% glycerol. Fluorescence was registered in the emission range 560–696 nm. Scan images were collected for further editing. Images were pseudo-colored in gold and reconstructed into a 2D stack image with maximum intensity projection using ZEN 2012 (Zeiss).

Scanning Electron Microscopy

One individual from the SokhoBio material (neuter: ZMH K-61187) and two individuals from the Clarion-Clipperton Fracture Zone material (neuter: ZMH-K-61146, neuter: ZMH-K-61156) were used for imaging with a Phenom ProX microscope. Specimens for the scanning electron microscopy analysis were initially rinsed with distilled water to remove the ethanol from their surface and tissues and then transferred to the SEM stub mounted in a temperature-controlled sample holder and frozen at –10°C.

RESULTS

Diversity, Abundance, and Distribution

A total of 736 specimens of *Agathotanais* were classified into eight species, five of which were new to science: *A. beatae* n. sp., *A. frutosae* n. sp. *A. jani* n. sp., *A. oharai* n. sp., *A. paleroi* n. sp. One of the species was represented by only one individual as was

[1]www.geneious.com

[2]www.nikoninstruments.com

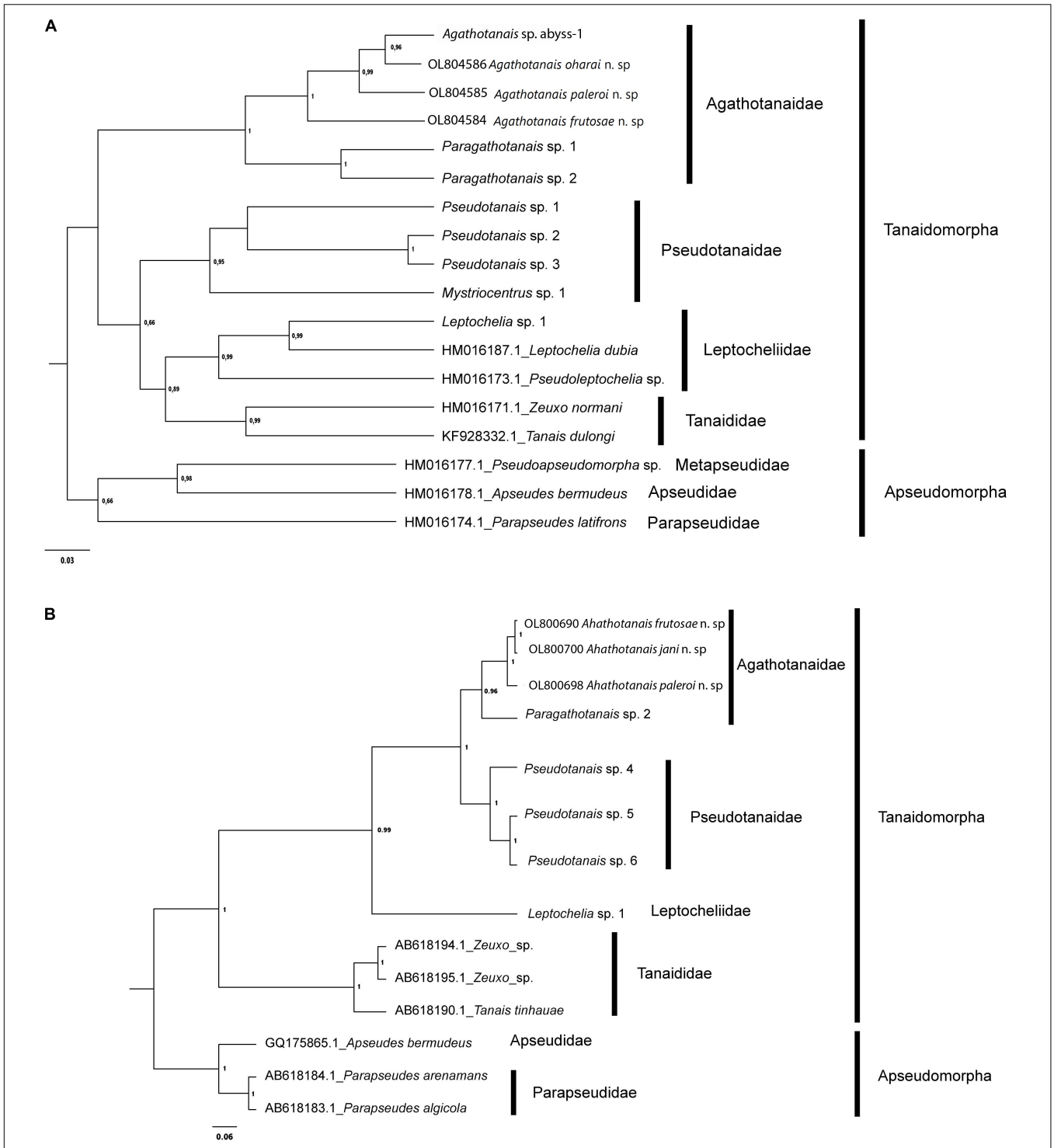

FIGURE 1 | Evolutionary relationships of Agathotanaidae species inferred by using the Histone H3 **(A)** and 18S **(B)** sequences and the Maximum Likelihood method. The percentage of trees in which the associated taxa clustered together (bootstrap support) is shown next to the branches. Only values above 0.6 are shown.

not formally described (*Agathotanais* sp. abyss-1). Only two of the sampled species: *A. hadalis* and *A. spinipoda*, from the Japan Trench (NW Pacific) and the SE Australian Slope, respectively, were already known (Larsen, 1999, 2007).

Most of the species studied here were represented by several specimens. However, *A. frutosae* was extremely abundant in the Sea of Okhotsk, represented by 634 specimens. The majority of them were found in the Kuril Basin, the deepest part of the Sea,

and only ten specimens were collected on the outer slope of Kuril Island (st. 9-7). In the KKT and the adjacent abyssal, we have recorded two species. One of them, *A. hadalis*, was identified on the basis of only three specimens, but *A. paleroi*, was relatively abundant and represented by 67 specimens that were all collected from the western side of the KKT, except for one specimen, found on the eastern side (st. 3-9). In the Central Pacific (CCZ), *Agathotanais* was represented by 21 specimens: four of them were identified as *A. beatae* and 17 as *A. jani*. Finally, six individuals were found off the Australian coast: two specimens were assigned to the species *A. spinipoda*, three to *A. oharai,* and one was classified as *Agathotanais* sp. abyss-1.

Phylogenetic and Genetic Distance Analysis

A total of four H3 and three 18S different haplotypes were obtained (**Figure 1**), representing *Agathotanais* species. The sequence alignments spanned 298 bp for H3 and 550 bp for 18S. For H3 the Kimura 2-parameter (K2+G+I) model showed the lowest AICc (AICc = 3614.52) and BIC (BIC = 3837.83) scores. The non-uniformity of evolutionary rates among sites was modeled using a Gamma distribution (+G = 1.39). The rate variation model revealed that some positions were evolutionarily invariable (+I = 44% sites). The Maximum Likelihood tree with the highest log-likelihood value (lnL = –1,770.90) was obtained.

For 18S the Kimura 2-parameter (K2+G) model showed the lowest AICc (AICc = 1313.07) and BIC (BIC = 1475.82) scores, which is considered to describe the best substitution pattern. Non-uniformity of evolutionary rates among sites was modeled using a Gamma distribution (+G = 0.32). The Maximum Likelihood tree with the highest log-likelihood value (lnL = –624.84) is shown in **Figure 1**.

All *Agathotanais* species included in the analyses were grouped into a well-supported clade. Additionally, the genetic clustering in the ML trees of the obtained haplotypes agrees with the morphological identification of taxa (see below).

The pairwise genetic p-distances between all the agathotanaid specimens ranged between 5.4 and 17.4% for H3, while for 18S sequences they ranged between 1 and 4% (**Supplementary Table 2**). The intraspecific genetic variation was very low, as expected given the limited sample size per species, represented in all cases by one haplotype for both markers. The evolutionary divergences for sequence pairs for H3 were largest between *A. frutosae* and both Australian species (*A. frutosae* – *Agathotanais* sp. abyss-1 1.174 ± 0.023 and *A. frutosae* – *A. oharai* 0.161 ± 0.022), while the lowest divergences were observed between *Agathotanais* sp. abyss and *A. oharai* (0.054 ± 0.012). Divergences between 18S sequences are shown in **Supplementary Table 2**.

Taxonomic Description

Genus: *Agathotanais* Lang, 1971

Diagnosis (amended after Larsen, 2005). Body strongly calcified, with a pitted surface. Pleon narrower or similar in width to pereon or pleotelson. Antennule with three articles. The antenna is usually one-articled (except *A. manganicus* antenna two-articled). The mandible molar process conical, left mandible *lacinia mobilis* is absent or reduced. Labium with the spiniform distal process and lateral process. Maxilliped bases partially fused. Cheliped slender, attached ventrally to cephalotorax, carpal sclerite absent (basal lobe truncated). Marsupium (where known) with four pairs of oostegistes. Pereopod coxa present. Uropods short, exopod reduced and fused with the basal article, endopod one- or two-articled. All appendages are covered with dense setules apart from the distal part of cheliped and pereopod dactyli.

Species included: *Agathotanais ahyongi* Larsen, 1999, *A. beatae* **n. sp.**, *A. brevis* Kudinova-Pasternak, 1990, *A. cilacapicus* Chim and Tong, 2021, *A. frutosae* **n. sp.**, *A. ghilarovi* Kudinova-Pasternak, 1989, *A. hadalis* Larsen, 2007, *A.* hanseni Lang, 1971, *A. ingolfi* Hansen, 1913, *A. jani* **n. sp.**, *A. manganicus* Larsen, 1999, *A. misakiensis* Kakui and Kohtsuka, 2015, *A. oharai* **n. sp.**, *A. paleroi* **n. sp.**, *A. spinipoda* Larsen, 1999, *A. splendidus* Kudinova-Pasternak, 1970, *A. toyoshioae* Kakui and Kohtsuka, 2015.

***Agathotanais hadalis* Larsen, 2007**

Material examined: Juvenile male, broken, KuramBio st. 2-10, (NHM 58020); neuter, broken, KuramBio st. 8-1, (NHM 58021).

Distribution: Kuril-Kamchatka Trench (**Figure 2**); depth range 4700–5700 m.

***Agathotanais spinipoda* Larsen, 1999**

Material examined: Neuter, broken, SLOPE st. 134, (NMV J61570); neuter, broken, SLOPE st. 62 (NMV J68224).

Distribution: Bass Strait Slope (SE Australia) (**Figure 2**); depth range 400–1840 m.

***Agathotanais beatae* n. sp. Jóźwiak and Pełczyńska**.
This species is register under the zoobank number:
urn:lsid:zoobank.org:act:26601B4E-AEBA-4C15-9EFC-35A664309F8F

(**Figures 3**, **4**)

Material examined: Holotype: neuter, 3.3 mm, JPIO st. 96, (ZMH-K-61146).

Paratypes: neuter, 3.1 mm, dissected on slides, JPIO st. 158, (ZMH-K-61147); neuter, damaged, JPIO st. 24, (ZMH-K-61148).

Diagnosis of neuter: Body narrow (about 11 L:W). Carapace without lateral setae in posterior margin. Pereonite-1 without pair of dorsal setae. Pereonites 4–6 longer than wide. Pereonite-6 1.5× pleonites 1–5 combined. The pleonites 1–5 width subequal to pereonite-6. Antennule article-1 longer than the remaining articles combined, about 2.0× article-3. Antenna one-articled. Cheliped palm 1.3 L:W. Pereopods 2–3 carpus dorsodistal seta 0.4× propodus. Pereopods 4–6 unguis serrated, but without distinct, pointed teeth ventrally. Uropod endopod one-articled.

Etymology: Species is named after Mrs. Beata Pełczyńska, mother of AP.

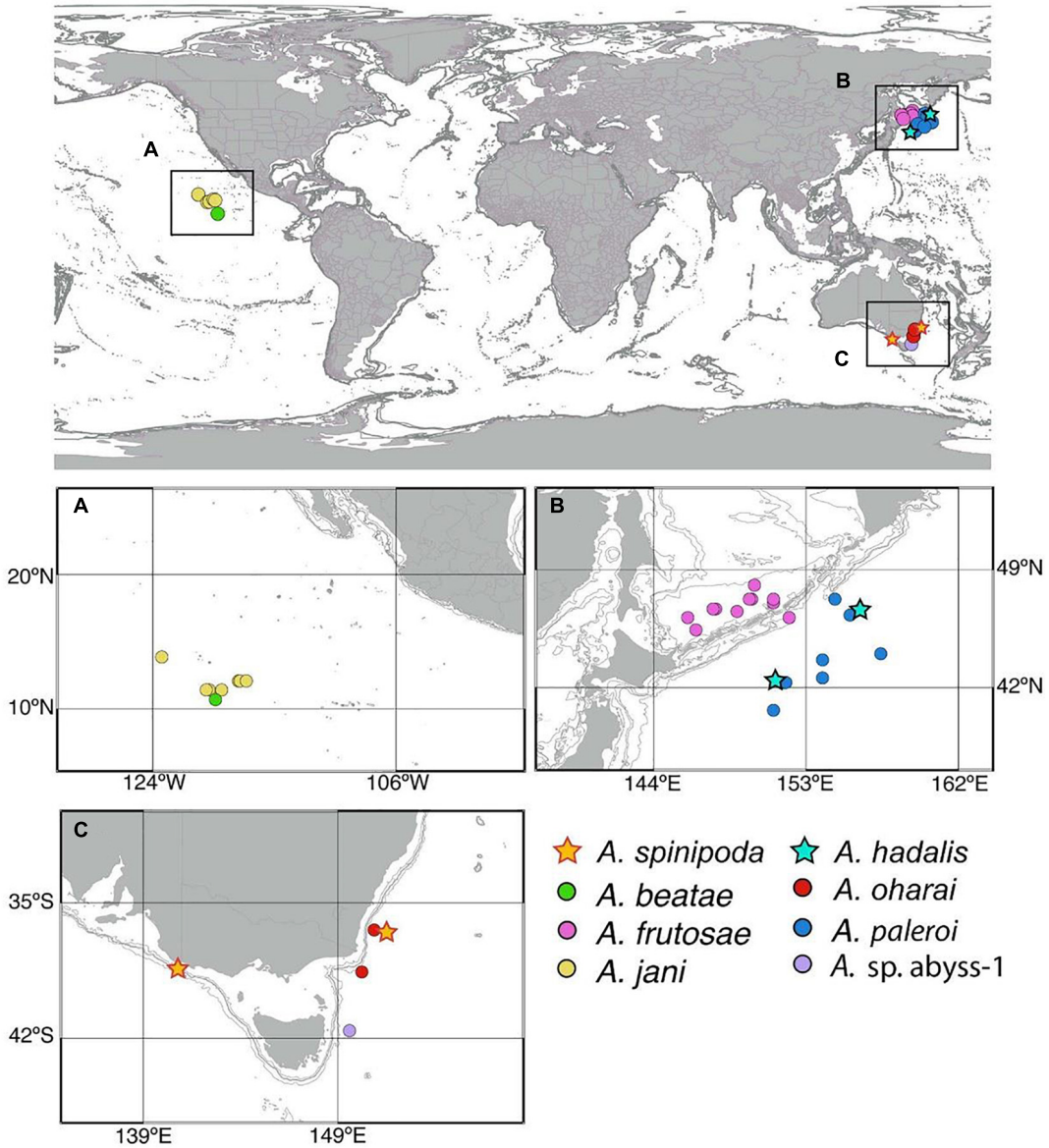

FIGURE 2 | Distribution of new species of *Agathotanais* collected from central Pacific **(A)**, Sea of Okhotsk, Kuril-Kamchatka Trench (KKT) **(B)**, and along Australian coast **(C)**.

Description of neuter: Body from the holotype (ICUL1786), appendages from the paratype (ICUL10315). BL = 3.4 mm. Body (**Figures 3A,B**) 10.5 L:W, cylindrical and elongated. Carapace 1.2 L:W, 0.2× BL. Pereon 0.8× BL. Pereonites 1–6: 0.7, 1.0, 1.0, 1.3, 1.6, and 1.3 L:W, respectively. Pleon with pleotelson 0.1× BL. Pleonites 1–5 0.2 L:W each. Pleotelson dorsally almost as long as pleonites 2–5 combined, acorn-shaped in the dorsal view, apex blunt, pointed, directed backward.

Antennule (**Figure 3C**) article-1 3.7 L:W, 4.2× article-2, with five penicillate midinner setae, three penicillate subdistal setae and two short and one penicillate distal setae; article-2 1.3 L:W, 0.5× article-3, with two subdistal setae: one inner and one outer; article-3 3.4 L:W, with six simple setae, one penicillate seta, and one aesthetasc.

Antenna (**Figure 3D**) one-articled, 3.0 L:W, tipped with a short distal seta.

Mouthparts: Right mandible (**Figures 3E,E'**) incisor broad and smooth.

Left mandible (**Figure 3F**) incisor with three teeth; *lacinia mobilis* narrow, rounded.

Maxillule endite (**Figure 3G**) with eight distal spines.

Labrum (**Figure 3H**) rounded, densely covered with setae of different lengths.

Maxilliped (**Figure 3I**) palp article-1 1.4 L:W, naked; article-2 1.3 L:W, with two inner plumose setae; article-3 2.4 L:W, with

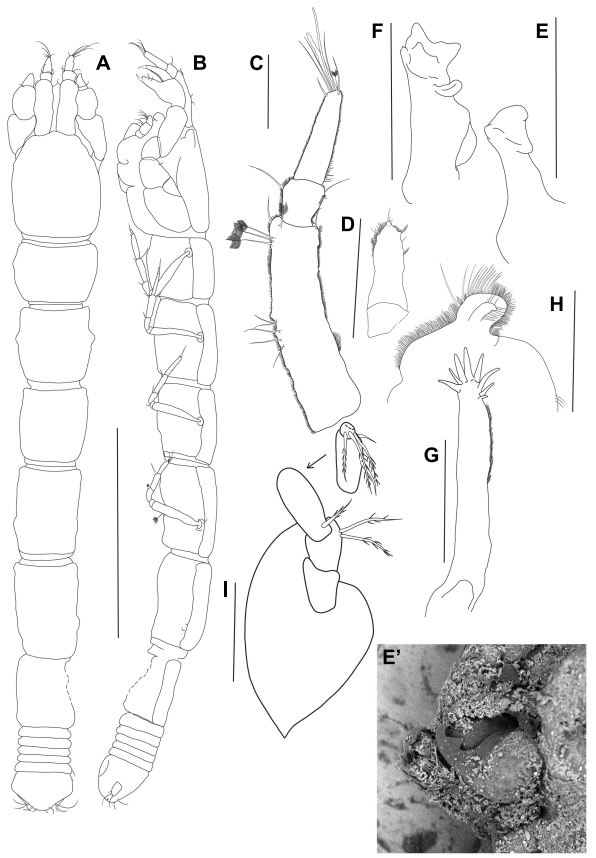

FIGURE 3 | *Agathotanais beatae* n. sp., neuter, holotype (**A,B**: ZMH-K-61146; **C–I** ZMH-K-61147). **(A)** dorsal view; **(B)** lateral view; **(C)** antennule; **(D)** antenna; **(E)** right mandible; **(E')** details of right mandible (SEM image); **(F)** left mandible; **(G)** maxillule; **(H)** labrum; **(I)** maxilliped. Scale bars: **(A,B)** = 1 mm, **(C–I)** = 10 μm.

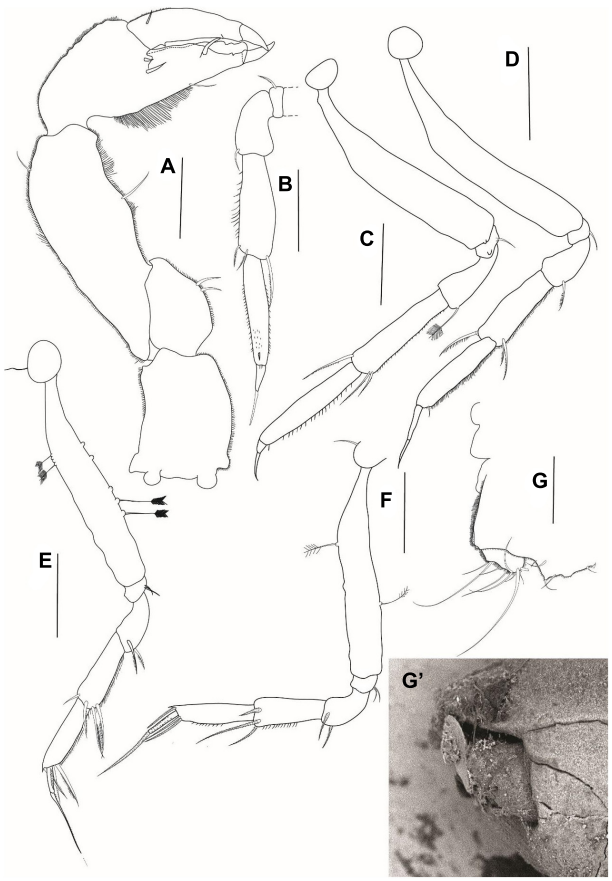

FIGURE 4 | *Agathotanais beatae* n. sp., neuter, holotype (ZMH-K-61146). **(A)** cheliped; **(B)** pereopod-1; **(C)** pereopod-2; **(D)** pereopod-3; **(E)** peropod-5; **(F)** peropod-6; **(G)** uropod; **(G')** detail of uropod (SEM image). Scale bar: **(A–G)** = 100 μm.

plumose proximal seta and two inner setae; article-4 2.2 L:W, with three plumose distal setae. Basis margins rounded.

Cheliped (**Figure 4A**) basis 1.5 L:W, naked; merus with two midventral setae; carpus 2.6 L:W, slightly shorter than propodus and fixed finger combined, with one midventral and one dorsodistal setae; palm 1.3 L:W, with two short spines near dactylus insertion, fixed finger subequal palm, with ventral seta and numerous long setules, cutting margin irregular, with one seta visible, terminal spine large and sharp; dactylus as long as fixed finger, with short dorsoproximal seta, cutting margin with two teeth; unguis robust and sharp.

Pereopod-1 (**Figure 4B**) basis damaged; ischium with ventrodistal seta; merus 2.0 L:W, 0.6× carpus, with ventrodistal seta; carpus 3.0 L:W, 0.9× propodus, with two serrated ventrodistal and one serrated dorsodistal (0.4× propodus) setae; propodus 5.0 L:W, 4.1× dactylus and unguis combined, with ventrodistal minute spine; dactylus 3.4 L:W, 0.8× unguis; dactylus and unguis unarmed, unguis with a tip pointed.

Pereopod-2 (**Figure 4C**) coxa naked; basis 5.7 L:W, naked; ischium with ventrodistal seta; merus 2.4 L:W, 0.6× carpus, with penicillate ventrodistal seta; carpus 4.5 L:W, 0.9× propodus, with three serrated setae: two ventrodistal and one dorsodistal (0.4× propodus); propodus 5.4 L:W and 4.5× dactylus and unguis combined, with small ventrodistal seta; dactylus 3.4 L:W, 0.8× unguis, unarmed; unguis unarmed with a pointed tip.

Pereopod-3 (**Figure 4D**) coxa naked; basis 8.0 L:W, naked; ischium with ventrodistal seta; merus 1.9 L:W, 0.6× carpus, with serrated ventrodistal seta; carpus 3.0 L:W, 0.8× propodus, with three serrated setae: two ventrodistal and one dorsodistal (0.4× propodus); propodus 4.6 L:W and 3.2× dactylus and unguis combined, with short ventrodistal seta; dactylus 5.0 L:W, 0.5× unguis, unarmed; unguis unarmed with a pointed tip.

Pereopod-4 (**Figure 4E**) coxa with seta; basis 6.0 L:W, with two penicillate dorsal setae, and five penicillate ventral setae (some setae broken); ischium with two ventrodistal setae; merus 1.4 L:W, 0.5× carpus, with two serrated ventrodistal setae; carpus 2.9 L:W, 1.1× propodus, with two serrated ventrodistal setae, one serrated subdistal seta, and one dorsodistal seta; propodus 4.2 L:W, 2.9× dactylus and unguis combined, with two serrated ventrodistal setae and one serrated dorsodistal seta; dactylus 4.2 L:W, 0.4× unguis, ventrally serrated; unguis ventrally serrated, with a pointed tip.

Pereopod-5 was damaged in the dissected specimen, but in other individuals like pereopod-4.

Pereopod-6 (**Figure 4F**) coxa with seta; basis 6.6 L:W, with one middorsal and one midventral penicillate setae; ischium with two ventrodistal setae; merus 1.7 L:W, 0.6× carpus, with two serrated ventrodistal setae; carpus 2.6 L:W, 0.9× propodus, with two serrated ventrodistal setae and one serrated dorsodistal seta; propodus 3.7 L:W and 2.2× dactylus and unguis combined, with three serrated distal setae; dactylus 6.0 L:W, 0.5× unguis; unguis ventrally serrated, with a pointed tip.

Uropod (**Figures 4G,G'**) exopod reduced and fused with the basal article; endopod one-articled, with two lateral setae and five distal setae on terminal segment.

Distribution: Central Pacific, Clarion-Clipperton Fracture Zone, IOM (**Figure 2**); depth: 4418 m.

Remarks. One-articled antenna distinguishes *A. beatae* n. sp. from *A. ahyongi* and *A. manganicus*, which have a fully reduced or two-articled antenna, respectively (Larsen, 1999). Pereonites 4–5 longer than wide allow to separate *A. beatae* from *A. brevis* having those pereonites wider than long (Kudinova-Pasternak, 1990), and *A. ingolfi* that has these pereonites subequal in length (Hansen, 1913). A longer than wide pereonite-6 differentiates *A. beatae* from *A. hadalis*, *A. frutosae*, *A. paleroi*, and *A. spinipoda*, which have the pereonite-6 as long as wide (*A. frutosae*, *A. paleroi*, and *A. spinipoda*) or clearly wider than long (*A. hadalis*).

A relatively long article-3 in antennule (about 0.5× article-1) distinguishes *A. beatae* from *A. splendidus*, and *A. toyoshiae*. In these two species the length of article-3 is about 0.3× article-1 (Kudinova-Pasternak, 1970; Kakui and Kohtsuka, 2015). A serrated ventral margin of the unguis in pereopods 4–6 separates *A. beatae* from *A. ghilarovi*, *A. hanseni*, *A. oharai*, and *Agathotanais* sp. abyss-1, for which the unguis is unarmed (Lang, 1971; Kudinova-Pasternak, 1989), and from *A. jani* which has two or three distinct teeth on the unguis. Furthermore, the new species differs from *A. misakiensis* by having a carapace shorter than the combined length of the two succeeding pereonites (for *A. misakensis* the carapace is subequal to pereonites 1–2). A two-articled uropodal endopod observed in *A. cilacapicus* separates this species from *A. beatae* that has a one-articled uropod (**Table 1**).

***Agathotanais frutosae* n. sp. Stępień, Jakiel, and Błażewicz**.

This species is register under the zoobank number: LSIDurn:lsid:zoobank.org:act:E07E39AE-D3ED-4128-B8F9-CA4194A05496

(**Figures 5–7**)

Material examined: Holotype: neuter, 3 mm, SokhoBio st. 7-4, (NHM 58033).

Paratypes: neuter, dissected on slides, 2.9 mm, SokhoBio st. 7-4, (NHM 58034); neuter, 3.1 mm, dissected on slide, SokhoBio st. 11-6, (NHM 58035); juvenile male, 3 mm, SokhoBio st. 2-7, (ZMH K-61184) juvenile male, dissected on slides, 2.6 mm, SokhoBio st. 11-6, (ZMH K-61183); seven juvenile males, 2.1–2.6 mm, SokhoBio st. 7-4, (ZMH K-61185); four neuters, 2.7–3.3 mm, SokhoBio st. 9-7, (ZMH K-61186); two neuters, 2.8–3.2 mm, SokhoBio st. 9-7, (NHM 58036); manca III, 1.8 mm,

TABLE 1 | Diagnostic features distinguishing the species of *Agathotanais*: (1) Pereonites 4–5 L:W; (2) Pereonite-6 L:W; (3) Pleon: pereonite-6; (4) Antennule article-3:article-1; (5) Antenna numbers of articles; (6) Maxilliped endites distal denticles; (7) Cheliped palm L:W; (8) Fixed finger number of setae; (9) Pereopod-2 dorsodistal carpal seta: propodus length; (10) Pereopod-3 dorsodistal carpal seta length: propodus; (11) Pereopod-4 propodus row of small spines; (12) Pereopods 4–6 dactylus small accessory spine; (13) Pereopods 4–6 unguis ventral ornamentation; (14) Uropod endopod number of articles.

Species/features	1	2	3	4	5	6	7	8	9	10	11	12	13	14
A. ahyongi	Longer	Longer	Narrower	0.6	0	Absent	1.6	1?	0.1	0.1	Absent	Absent	Unarmed	One
***A. beatae* n. sp.**	Longer	Longer	As wide	0.5	1	ND	1.3	1	0.4	0.4	Absent	Absent	Serrated	One
A. brevis	Wider	Wider	Narrower	0.5	1	Absent	1.6	1	ND	ND	Absent	Absent	Unarmed	One
A. cilacapicus	Longer	As long as wide	As wide	0.4	1	Absent	1.7	1	0.2	0.2	Absent	Absent	Setulated	Two
***A. frutosae* n. sp.**	Longer	As long as wide	Narrower	0.6	1	ND	1.6	1	0.6	0.4	Absent	Absent	Unarmed	One
A. ghilarovi	Longer	Wider	As wide	0.6	1	Present	1	1	ND	ND	Present	Absent	Unarmed	Two
A. hadalis	Longer	Wider	Narrower	0.5	1	Absent	1.7	1	0.5	0.7	Absent	Absent	Serrated (P4)	One
A. hanseni	Longer	Wider	Narrower	0.5	1	Absent	2	1	0.8	1	Absent	Absent	Unarmed	One
*A. ingolfi**	Subequal	Wider	Narrower	0.5	1	Absent	1.7	ND	0.7	0.5	Absent	Present	Unarmed	One
***A. jani* n. sp.**	Longer	Longer	Narrower	0.6	1	Present	1.6	1	0.9	0.7	?	Absent	Distinct teeth	One
A. manganicus	Longer	Longer	Narrower	0.3	2	Absent	1.3	1	0.6	ND	Absent	Absent	Unarmed	One
A. misakiensis	Longer	Wider	Narrower	0.4	1	Absent	1.8	1	0.5	0.4	Absent	Absent	Serration	Two
***A. oharai* n. sp.**	Longer	Longer	Narrower	0.4	1	ND	1.2	1	0.8	0.8	Absent	Absent	Unarmed	One
***A. paleroi* n. sp.**	Longer	As long as wide	Narrower	0.5	1	Absent	1	1	0.7	0.7	Absent	Absent	Serrated (P5, P6)	One
***Agathotanais* sp. abyss-1**	Longer	Longer	Narrower	0.5	1	Absent	1.4	1	0.7	ND	Absent	Absent	Unarmed	One
A. spinipoda	Longer/wider	As long as wide	Narrower	0.3	1	Absent	1.4	1	ND	ND	Present	Absent	Unarmed	One
A. splendidus	Longer	As long as wide	As wide	0.3	0?	Absent	1.1	0	ND	ND	Absent?	Absent	Unarmed	One
A. toyoshioae	Longer	As long as wide	Narrower	0.3	1	Absent	1.6	1	0.4	0.4	Absent	Absent	Serrated	One

**According to Bird and Holdich (1988). Bold – new species described in the paper. ND – no data.*

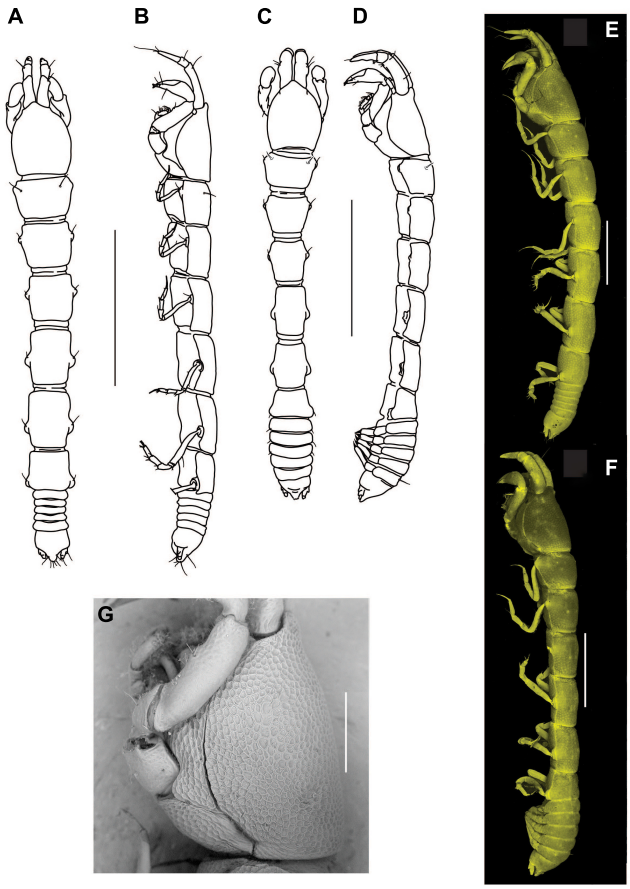

FIGURE 5 | *Agathotanais frutosae* n. sp., neuter, holotype (**A,B**: NHM 58033), juvenile male, paratype (**C,D**: ZMH K-61184), neuter, paratype (**E,G**: ZMH K-61187), juvenile male, paratype (**F**: ZMH K-61184). **(A)** dorsal view; **(B)** lateral view; **(C)** dorsal view; **(D)** lateral view; **(E)** lateral view (confocal picture); **(F)** lateral view (confocal picture); **(G)** pitted surface of body (SEM picture). Scale bars: **(A–D)** = 1 mm, **(E–F)** = 500 μm, **(G)** = 200 μm.

five neuters, 2.9–3.3 mm, SokhoBio st. 11-6, (NHM 58037); two juvenile males, 2.3–2.7 mm, three neuters, 2.9–3.1 mm, SokhoBio st. 11-6, (NHM 58038); manca II, 1.3 mm, manca III, 1.8 mm, three neuters, 2.3–3.4 mm, SokhoBio st. 11-6, (ZMH K-61187); juvenile male, 2.7 mm, SokhoBio st. 11-6, (ZMH K-61188); juvenile male, 2.3 mm, SokhoBio st. 11-6, (ZMH K-61189); neuter, 2.3 mm, SokhoBio st. 7-4, (ZMH K-61189); manca II, 1.6 mm, two mancas III, 1.6 mm, two juvenile males, 2.3–2.4 mm, five neuters, 2.3–3.2 mm, SokhoBio st. 7-4, (NHM 58039); neuter, 3.1 mm, SokhoBio st. 7-3, (NHM 58040); four mancas II, 1.3–1.7 mm, juvenile male, 2.3 mm, two neuters, 2.3–2.5 mm, SokhoBio st. 7-3, (NHM 58041); five mancas II, 1.3–1.8 mm, two mancas III, 2.1 mm, eleven neuters, 2.2–3.5 mm, SokhoBio st. 7-3, (ZMH K-61191); six mancas II, 1.3–1.5 mm, two mancas III, 1.8 mm, two juvenile males, 2.1 mm, nine neuters, 2.1–3.1 mm, SokhoBio st. 7-3, (ZMH K-61192); five juvenile males, 2.3–2.8 mm, SokhoBio st. 7-3, (ZMH K-61193); juvenile male, 2.5 mm, SokhoBio st. 2-7, (NHM 58042); juvenile male, 2.6 mm, SokhoBio st. 7-3, (NHM 58043); three juvenile males, 2.4–2.7 mm, SokhoBio st. 7-3, (NHM 58044); neuter, broken, SokhoBio st. 4-10, (NHM 58045); neuter, broken, SokhoBio st. 4-9, (ZMH K-61194); two mancas II, 1.6–1.7 mm, two juvenile males, 2.0–2.4 mm, neuter, 2.1 mm, SokhoBio st. 4-9, (ZMH K-61195); neuter, 2.9 mm, ICUL5167, SokhoBio st. 6-6, (ZMH K-61196); two juvenile males, 2.3–2.3 mm, neuter, 3.3 mm, SokhoBio st. 7-3, (ZMH K-61197); two mancas III, 1.8–1.9 mm, five neuters, 2.3–3.4 mm, SokhoBio st. 7-3, (ZMH K-61198); two neuters, 2.7–3.2 mm, SokhoBio st. 7-3, (NHM 58046); juvenile male, broken, SokhoBio st. 2–7, (NHM 58047); neuter, 3.2 mm, SokhoBio st. 3-9, (NHM 58048); juvenile male, 2.7 mm, SokhoBio st. 3-9, (NHM 58049); three mancas II, 1.4 mm, two mancas III, 1.4–1.7 mm, two juvenile males, 2.2–2.3 mm, seven neuters, 2.8–3.2 mm, SokhoBio st. 4-9, (ZMH K-61199); eight juvenile males, 2.1–3.4 mm, neuter, 3.3 mm, SokhoBio st. 2-8, (ZMH K-61200); three juvenile males, 2.6–2.7 mm, SokhoBio st. 2-7, (ZMH K-61201); three juvenile males, 2.3–2.6 mm, SokhoBio st. 2-8, (ZMH K-61202); juvenile male, 2.7 mm, SokhoBio st. 2-7, (ZMH K-61203); two mancas II, 1.4 mm, SokhoBio st. 2-7, (ZMH K-61204); three mancas III, 1.7 mm, six juvenile males, 2.1–2.6 mm, SokhoBio st. 2-7, (ZMH K-61204); fifty one neuters, 2.1–3.8 mm, SokhoBio st. 2-7, (ZMH K-61204); two juvenile males, 2.2–2.7 mm, three mancas

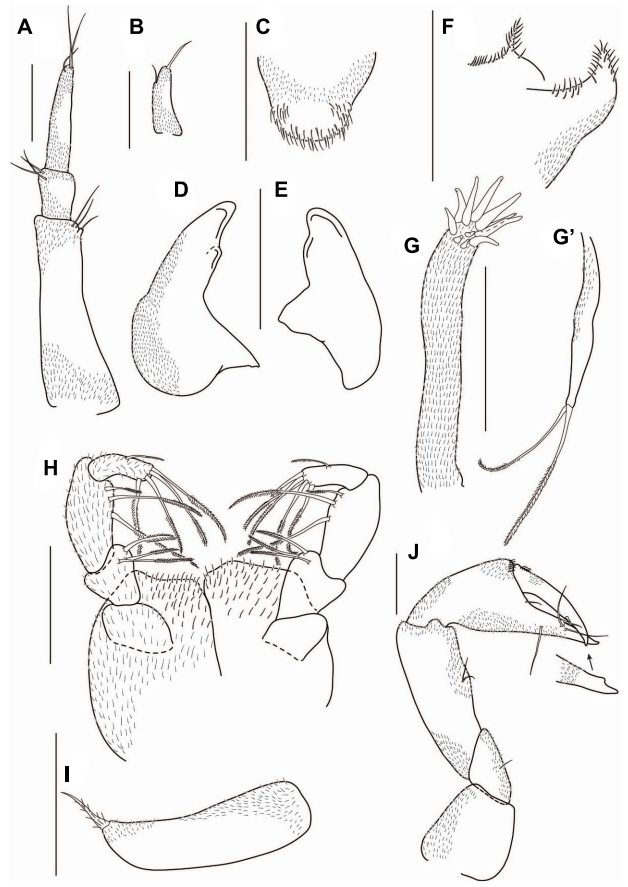

FIGURE 6 | *Agathotanais frutosae* n. sp., neuter, paratype (**A,F,J**: NHM 58034; **B–E**, **G–I**: NHM 58035). **(A)** antennule; **(B)** antenna; **(C)** labrum; **(D)** left mandible; **(E)** right mandible; **(F)** labium; **(G)** maxillule; **(G')** palp of maxillule; **(H)** maxilliped; **(I)** epignath; **(J)** cheliped. Scale bars: **(C–I)** = 10 μm, **(A,B,J)** = 100 μm.

II, 1.3–1.6 mm, SokhoBio st. 2-8, (MIMB 42497); sixteen mancas III, 1.6–2.0 mm, SokhoBio st. 2-8, (MIMB 42497); eighteen neuters, 2.2–3.7 mm, SokhoBio st. 2-8, (MIMB 42497); two mancas II, 1.3–1.4 mm, two mancas III, 1.5 mm, juvenile male, 2.4 mm, 5 neuters, 2.9–3.2 mm, SokhoBio st. 2-7, (MIMB 42498); neuter, broken, SokhoBio st. 2-7, (MIMB 42499); neuter, broken, SokhoBio st. 2-7, (MIMB 42500); four mancas III, 1.6–1.8 mm, two neuters, 2.9 mm, SokhoBio st. 2-7, (MIMB 42501); manca III, 1.9 mm, juvenile male, 3.2 mm, neuter, broken, SokhoBio st. 2-7, (MIMB 42502); six juvenile males, 2.5–3.3 mm, SokhoBio st. 2-7, (MIMB 42503); six juvenile males, 2.0–2.7 mm, SokhoBio st. 2-7, (MIMB 42504); manca II, 1.5 mm, manca III, 1.9 mm, neuter, 2.3 mm, SokhoBio st. 2-7, (MIMB 42505); manca II, 1.5 mm, SokhoBio st. 2-8, (MIMB 42506); two mancas III, 1.5–2.5 mm, two neuters, 3.0–2.4 mm, SokhoBio st. 2-7, (MIMB 42507); manca II, 1.4 mm, two mancas III, 1.6–1.8 mm, juvenile male, 2.3 mm, four neuters, 2.2–3.3 mm, SokhoBio st. 2-7, (MIMB 42508); two mancas III, 1.6–1.8 mm, five neuters, 2.2–3.3 mm, SokhoBio st. 2-8, (MIMB 42509); two juvenile males, 2.6 mm, SokhoBio st. 1-8, (MIMB 42510); two neuters, 3.2 mm, SokhoBio st. 1-9, (MIMB 42511); four neuters, 2.7–3.1 mm, SokhoBio st. 1-9, (MIMB 42512); neuter, broken, SokhoBio st. 1-8, (MIMB 42512); brooding female, 3.0 mm, 3 juvenile males, 1.8–3.3 mm, four neuters, 2.0–2.9 mm, SokhoBio st. 1-8, (MIMB 42514); juvenile male, 2.8 mm, SokhoBio st. 1-9, (MIMB 42515); juvenile male, broken, SokhoBio st. 1-9, (MIMB 42516); manca III, 1.8 mm, juvenile male, 2.3 mm, SokhoBio st. 2-7, (MIMB 42517); juvenile male, 2.3 mm, SokhoBio st. 4-9, (MIMB 42518); six juvenile males, 2.1–2.7 mm, SokhoBio st. 4-10, (MIMB 42519); manca, broken, SokhoBio st. 4-9, (MIMB 42520); juvenile male, 2.9 mm, neuter, 3.0 mm, SokhoBio st. 4-9, (MIMB 42521); juvenile male, 2.2 mm, SokhoBio st. 4-9, (MIMB 42522); juvenile male, 2.5 mm, SokhoBio st. 4-9, (MIMB 42523); juvenile male, 2.7 mm, SokhoBio st. 4-9, (MIMB 42524); five juvenile males, 2.3–2.7 mm, SokhoBio st. 4-10, (MIMB 42525); manca, broken, SokhoBio st. 11-6, (MIMB 42527); eight mancas II, 1.4–1.7 mm, two mancas III, 1.7–1.8 mm, four neuters, 2.2–3.5 mm, SokhoBio st. 11-6, (MIMB 42526).

Diagnosis of neuter: Body narrow (7.7 L:W). Carapace without pair of lateral setae in posterior margin. Pereonite-1 with pair of dorsal setae. Pereonites 4–6 longer than wide. Pereonite-6 0.9× pleonites 1–5 combined. Pleonites 1–5 narrower than pereonite-6. Antennule article-1 longer than other articles combined, about 1.6× article-3. Antenna one-articled. Cheliped palm 1.6 L:W. Pereopods 2–3 carpus with dorsodistal seta, 0.6× and 0.4× propodus, respectively. Pereopods 4–6 unguis unarmed. Uropod endopod one-articled.

Etymology: Species is dedicated to Dr. Inmaculada Frutos (University of Łódź), our colleague and peracarid specialist, who collected tanaids during the SokhoBio expedition to the Sea of Okhotsk.

Description of neuter: Body from the holotype (NHM 58033), appendages from paratypes (NHM 58034 and 58035). BL = 3.0 mm. Body (**Figures 5A,B,E,G**) 7.7 L:W, cylindrical. Carapace 1.1 L:W, 0.1× BL. Pereon 0.6× BL. Pereonites 1–6: 0.7, 0.8, 1.0, 1.3, 1.3, and 0.8 L:W, respectively. Pereonite-1 with pair of setae in the proximal half of the dorsal surface. Pleon with pleotelson 0.1× BL. Pleonites 1–5 0.4 L:W each. Pleotelson dorsally 0.7× pleonites 1–5.

Antennule (**Figure 6A**) article-1 3.5 L:W, 3.7× article-2, with three distal setae; article-2 1.2 L:W, 0.4× article-3, with three distal setae; article-3 4.5 L:W, with two distal and one subdistal setae.

Antenna (**Figure 6B**) one-articled, 2.8 L:W, with one subdistal and one distal seta.

Mouthparts: Labrum (**Figure 6C**) hood-shaped, covered by numerous setae of different lengths.

Left mandible (**Figure 6D**) incisor with a blunt tooth, *lacinia mobilis* short and rounded.

Right mandible (**Figure 6E**) incisor with rounded tooth.

Labium (**Figure 6F**) with the spiniform distal process and lateral process, covered by numerous setae.

Maxillule endite (**Figure 6G**) with eleven distal spines. Palp (**Figure 6G'**) with two plumose terminal setae.

Maxilliped (**Figure 6H**) palp article-1 rectangular, naked; article-2 0.8 L:W, with three inner plumose setae; article-3 2.2 L:W, with three inner plumose setae; left palp article-4 with

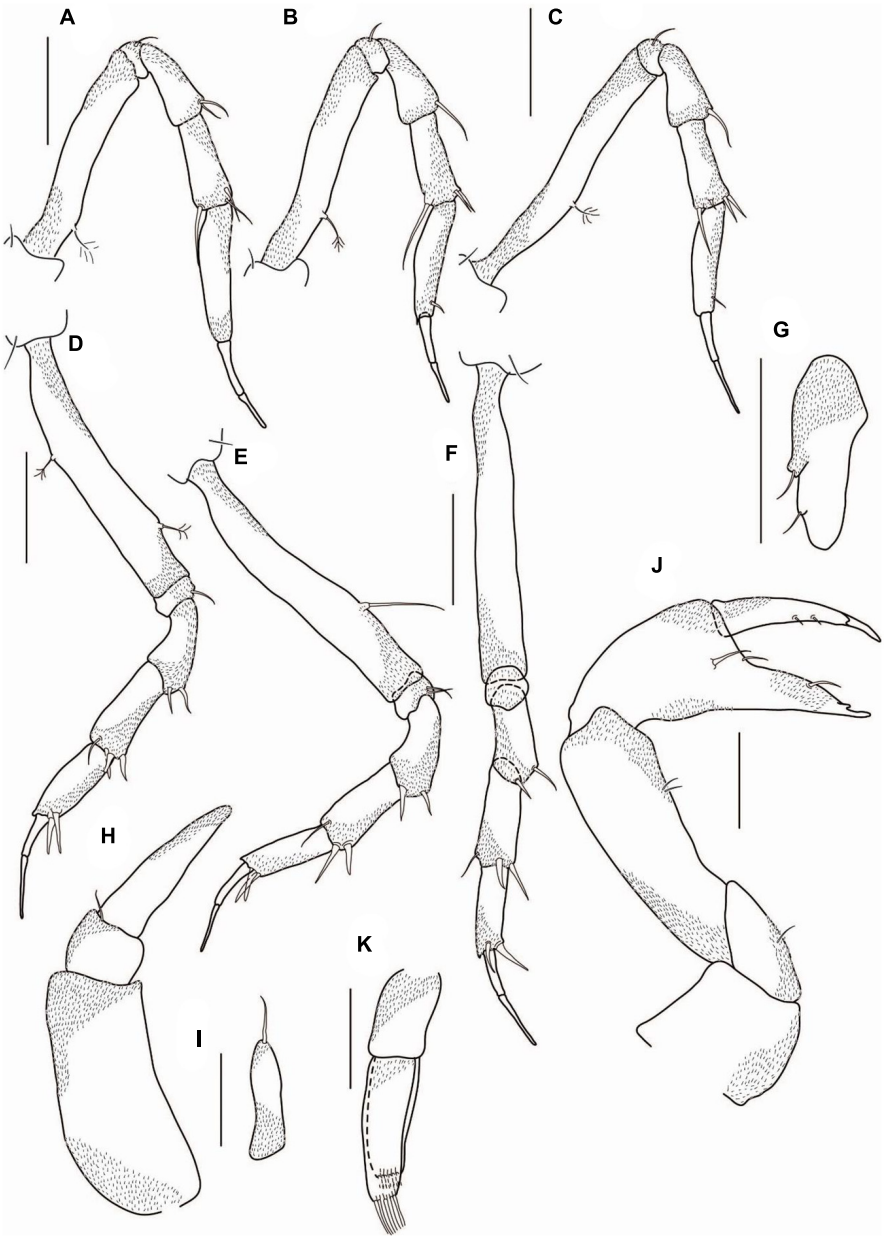

FIGURE 7 | *Agathotanais frutosae* n. sp., neuter, paratypes (**A–G**: NHM 58034); juvenile male, paratype (**H–K**: ZMH K-61184). **(A)** peropod-1; **(B)** pereopod-2; **(C)** pereopod-3; **(D)** pereopod-4; **(E)** pereopod-5; **(F)** pereopod-6; **(G)** uropod; **(H)** antennule; **(I)** antenna; **(J)** cheliped; **(K)** pleopod. Scale bar: **(A–K)** = 100 μm.

four plumose distal and plumose outer setae; right palp article-4 with five plumose distal setae and with plumose outer seta. Basis covered with dense, numerous setae of different lengths.

Epignath (**Figure 6I**) elongated, with plumose, robust terminal seta.

Cheliped (**Figure 6J**) basis 1.0 L:W, naked; merus with midventral seta; carpus 2.5 L:W, slightly shorter than propodus and fixed finger combined, with two midventral setae; palm 1.6 L:W, with a row of short setae near dactylus insertion; fixed finger 0.6× palm, cutting edge with distal protrusion and three setae, one ventral seta, distal spine small; dactylus 1.1× fixed finger, cutting edge with midlength spine; unguis sharp.

Pereopod-1 (**Figure 7A**) coxa with seta; basis 6.2 L:W, 2.4× merus, with penicillate dorsoproximal seta; ischium with ventrodistal seta; merus 2.5 L:W and 0.9× carpus, with two ventrodistal setae; carpus 2.5 L:W, 0.6× propodus, with two ventrodistal setae, and with long (0.4× propodus) dorsodistal seta; propodus 4.6 L:W, 1.3× dactylus and unguis combined, naked; dactylus 1.4× unguis, unarmed; unguis unarmed, with rounded tip.

Pereopod-2 (**Figure 7B**) coxa with seta; basis 6.0 L:W, 2.8× merus, with penicillate, dorsoproximal seta; ischium with ventrodistal seta; merus 2.3 L:W, 0.8× carpus, with ventrodistal seta; carpus 2.7 L:W, 0.7× propodus, with two short ventrodistal setae, and long (0.6× propodus) dorsodistal seta; propodus 4.0 L:W, with ventrosubdistal short seta, and with spinules near dactylus insertion; dactylus 0.8× unguis, unarmed; unguis unarmed, with rounded tip.

Pereopod-3 (**Figure 7C**) coxa with seta; basis 8.0 L:W, 3.6× merus, with penicillate dorsoproximal seta; ischium with ventrodistal seta; merus 2.0 L:W, 0.8× carpus, with ventrodistal seta; carpus 2.7 L:W, 0.8× propodus, with two ventrodistal, one short middistal, and one long (0.4× propodus) dorsodistal setae; propodus 3.7 L:W, 1.0× dactylus and unguis combined, with ventrosubdistal seta; dactylus 0.8× unguis, unarmed; unguis unarmed, with rounded tip.

Pereopod-4 (**Figure 7D**) coxa with seta; basis 6.3 L:W, 3.3× merus, with two penicillate setae: one dorsal and one ventral; ischium with ventrodistal seta; merus 2.0 L:W, 0.8× carpus, with two ventrodistal setae; carpus 2.3 L:W, 1.0× propodus, with three robust ventrodistal and one simple dorsodistal setae; propodus 2.4 L:W, 0.8× dactylus and unguis combined, with two robust ventrodistal setae; dactylus 0.7× unguis, unarmed; unguis unarmed, with rounded tip.

Pereopod-5 (**Figure 7E**) coxa with seta; basis 7.0 L:W, 3.0× merus, with middorsal seta; ischium with two ventrodistal setae; merus 2.4 L:W, 1.0× carpus, with two robust ventrodistal setae; carpus 2.2 L:W, 1.0× propodus, with two robust ventrodistal setae and simple dorsodistal seta; propodus 3.0 L:W, with two strong ventrodistal setae; dactylus 0.7× unguis, unarmed; unguis unarmed, with rounded tip.

Pereopod-6 (**Figure 7F**) coxa with seta; basis 7.2 L:W, 3.0× merus; ischium naked; merus 2.5 L:W, 0.9× carpus, with two ventrodistal setae; carpus 2.7 L:W, 1.2× propodus, with two robust ventrodistal and simple dorsodistal setae; propodus 3.4 L:W, 0.8× dactylus and unguis combined, with two robust (ventrodistal and middistal) setae; dactylus 0.7× unguis, unarmed; unguis unarmed, with rounded tip.

Pleopods absent.

Uropod (**Figure 7G**) exopod reduced and fused with basal article, tipped with seta; endopod one-articled, 3.0 L:W, with lateral seta.

Description of juvenile male: Body from paratype (ZMH K-61184), appendages from paratype (ZMH K-61183). BL = 3.0 mm. Body 7.6 L:W (**Figures 5C,D,F**). Carapace 1.1 L:W, 0.1× BL. Pereon 0.6× BL, pereonites 1–6: 0.5, 0.8, 1.0, 1.5, 1.3, and 0.6 L:W, respectively. Pleon combined with pleotelson 0.2× BL. Pleonites 1–5 0.3 L:W each. Pleotelson directed backward.

Antennule (**Figure 7H**) article-1 2.4 L:W, 1.4× article-3, naked; article-2 0.8 L:W, 0.3× article-3, with distal seta; article-3 2.5 L:W, naked.

Antenna (**Figure 7I**) one-articled, 3.7 L:W, tipped with seta.

Cheliped (**Figure 7J**) basis 0.9 L:W; merus with midventral seta; carpus 3.0 L:W, 1.7× palm; palm 1.3 L:W, with two setae near dactylus insertion; fixed finger 3.4 L:W, 1.0× palm, cutting edge with a proximal protrusion, with seta and small distal spine; dactylus 6.0 L:W, cutting edge with two spines on inner margin, unguis slender.

Pleopods (**Figure 7K**) endopod with eight setae along distal margin; exopod 0.8× endopod, with eight setae along the distal margin.

Intraspecific variation: Manca II: length 1.3–1.8 mm.

Manca III: length 1.5–2.1 mm.

Neuter: length 2.0–3.8 mm; maxilliped palp article-4 with four/five distal seta on left and right palp, respectively; cheliped carpus with one/two midventral seta; pereopod-5 ischium with one/two ventrodistal setae; pereopod-6 ischium with zero/one ventrodistal seta.

Juvenile male: length 1.8–3.4 mm; antenna article-2 with zero/two distal setae; article-3 with one/three simple setae distally; cheliped fixed finger with one/three ventral setae.

Distribution: NW Pacific, Sea of Okhotsk, Kuril Basin (**Figure 2**); depth range: 3206–3374 m.

Remarks. A pair of dorsal setae on pereonite-1 is a unique feature of *A. frutosae* n. sp. Moreover *A. frutosae* belongs to the species of *Agathotanais* with an elongated cheliped palm (L:W >1.6), together with *A. ahyongi*, *A. cilacapicus*, *A. brevis*, *A. hadalis*, *A. hanseni*, *A. ingolfi*, *A. misakiensis*, *A. toyoshioae,* and *A. jani.* All the other species have a chelipedal palm clearly shorter (*A. ghilarovi*, *A. splendidus,* and *A. oharai*, is 1.0–1.2 L:W), or slightly shorter (*A. beatae, A. manganicus*, *A. spinipoda,* and *Agathotanais* sp. abyss-1 it is 1.3–1.4 L:W) (**Table 1**).

From the *Agathotanais* with elongated palm, *A. frutosae* can be distinguished by unarmed dactylus and unguis of pereopods 4–6. Unguis is serrated in *A. hadalis*, *A. misakiensis*, and *A. toyoshioae*; *A. cilacapicus* has a setulose unguis; *A. jani* has distinct teeth on unguis, and *A. ingolfi* has a small accessory spine on its dactylus, near the unguis. An unarmed dactylus and unguis are also present in *A. hanseni*, *A. ahyongi* and *A. brevis*. However, *A. frutosae* differs from *A. hanseni* and *A. ahyongi* in the length of the dorsodistal carpal seta of pereopods 2 and 3. It is 0.6 in relation to propodus in *A. frutosae,* and 0.8 and 1.0 in *A. hanseni*; *A. ahyongi* has only two short carpal setae in pereopods 2 and 3 (about 0.1 of propodus length) (**Table 1**).

***Agathotanais jani* n. sp. Jóźwiak and Pełczyńska**.

This species is register under the zoobank number:
LSIDurn:lsid:zoobank.org:act:375FCFD9-C32B-4248-9F52-583A6037179F

(**Figures 8–10**)

Material examined: Holotype: neuter, 3.8 mm, JPIO SO239 st. 118, (ZMH-K-61149).

Paratype: neuter, dissected on slides, JPIO st. 99, (ZMH-K-61150); neuter, 2.5 mm, JPIO st. 99, (ZMH-K-61151); juvenile male damaged, JPIO st. 99, (ZMH-K-61152); specimen damaged, JPIO st. 81, (ZMH-K-61153); specimen damaged, JPIO st. 81, (ZMH-K-61154); juvenile male, 2.4 mm, JPIO st. 118, (ZMH-K-61155); neuter, 2.8 mm, JPIO st. 59, (ZMH-K-61156); neuter, broken, JPIO st. 59, (ZMH-K-61157); neuter, damaged, JPIO st.

24, (ZMH-K-61158); juvenile male, damaged, JPIO st. 24, (ZMH-K-61159); neuter, broken, JPIO st. 50, (ZMH-K-61160); juvenile male, broken, JPIO st. 99, (ZMH-K-61161); neuter, 2.9 mm, JPIO st. 20, (ZMH-K-61162); neuter, damaged, JPIO st. 20, (ZMH-K-61163); juvenile male, 3.0 mm, JPIO st. 57, (ZMH-K-61164); juvenile male, 3.2 mm, JPIO st. 57, (ZMH-K-61165); juvenile male, broken, JPIOst. 12, (ZMH-K-61166); specimen damaged, JPIO st. 12, (ZMH-K-61167); neuter, 2.9 mm, JPIO st.12, (ZMH-K-61168); neuter, broken, JPIO st. 12, (ZMH-K-61169).

Diagnosis of neuter: Body narrow (about 12.8 L:W). Carapace without pair of lateral setae in posterior margin. Pereonite-1 without pair of dorsal setae. Pereonites 4–6 longer than wide. Pereonite-6 as long as pleonites 1–5 combined. Pleonites 1–5 as wide as pereonite-6. Antennule article-1 longer than remaining articles combined, less than 2.0× article-3. Antenna one-articled. Cheliped palm 1.6 L:W. Pereopods 2–3 carpus with dorsodistal seta 0.9× and 0.7× propodus, respectively. Pereopods 4–6 unguis with distinct, pointed ventral teeth – two in pereopod-4 and three in pereopods 5–6. Uropod endopod one-articled.

Etymology: The species is dedicated to Jan Jóźwiak, beloved son of PJ.

Description of neuter: Body from the holotype (ZMH-K-61149), appendages from paratype (ZMH-K-61150). BL = 3.6 mm. Body (**Figures 8A,B**) 12.8 L:W, elongated. Carapace 1.3 L:W, 0.2× BL. Pereon 0.8× BL. Pereonites 1–6: 0.6, 1.1, 1.4, 1.5, 1.9, and 1.2 L:W, respectively. Pleon with pleotelson 0.1× BL. Pleonites 1–5 0.3 L:W each. Pleotelson in dorsal view 0.7× pleonites 1–5, almost square, apex pointed, directed backward.

Antennule (**Figure 9A**) article-1 4.9 L:W, 4.3× article-2, with three subdistal setae; article-2 1.5 L:W, 0.4× article-3, with outer subdistal seta; article-3 4.6 L:W, with seven distal setae.

Antenna (**Figure 9A**) one-articled, 2.5 L:W, with long distal seta (one distal seta broken).

Mouthparts: Labrum (**Figure 9B**) hood-shaped, covered with numerous setae of different lengths.

Left mandible (**Figure 9C**) incisor with three small rounded teeth; *lacinia mobilis* rounded and short.

Right mandible (**Figure 9D**) incisor with three rounded teeth.

Maxillule endite (**Figures 9E,E'**) with eleven robust distal spines of various lengths and numerous setules along outer and inner margin; palp not observed.

Maxilla (**Figure 9F**) elongated and simple.

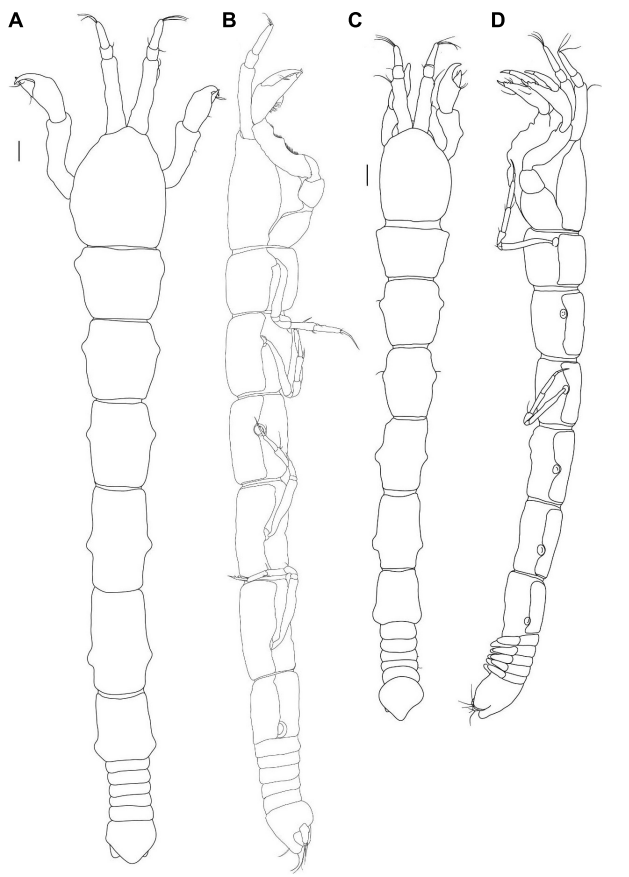

FIGURE 8 | *Agathotanais jani* n. sp., neuter, holotype (**A,B**: ZMH-K-61149), juvenile male, paratype (**C,D**: ZMH-K-61159). **(A)** Dorsal view; **(B)** lateral view; **(C)** dorsal view; **(D)** lateral view. Scale bar: **(A–D)** = 100 μm.

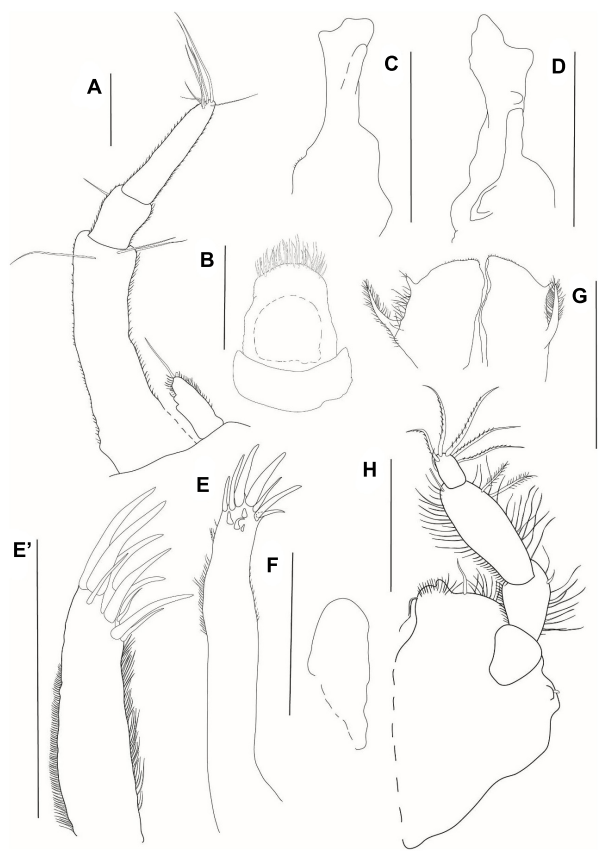

FIGURE 9 | *Agathotanais jani* n. sp., neuter, paratype (ZMH-K-61150). **(A)** antennule and antenna; **(B)** labrum; **(C)** left mandible; **(D)** right mandible; **(E)** maxillule; **(E')** details of maxillule; **(F)** maxilla; **(G)** labium; **(H)** maxilliped. Scale bar: **(A–H)** = 10 μm.

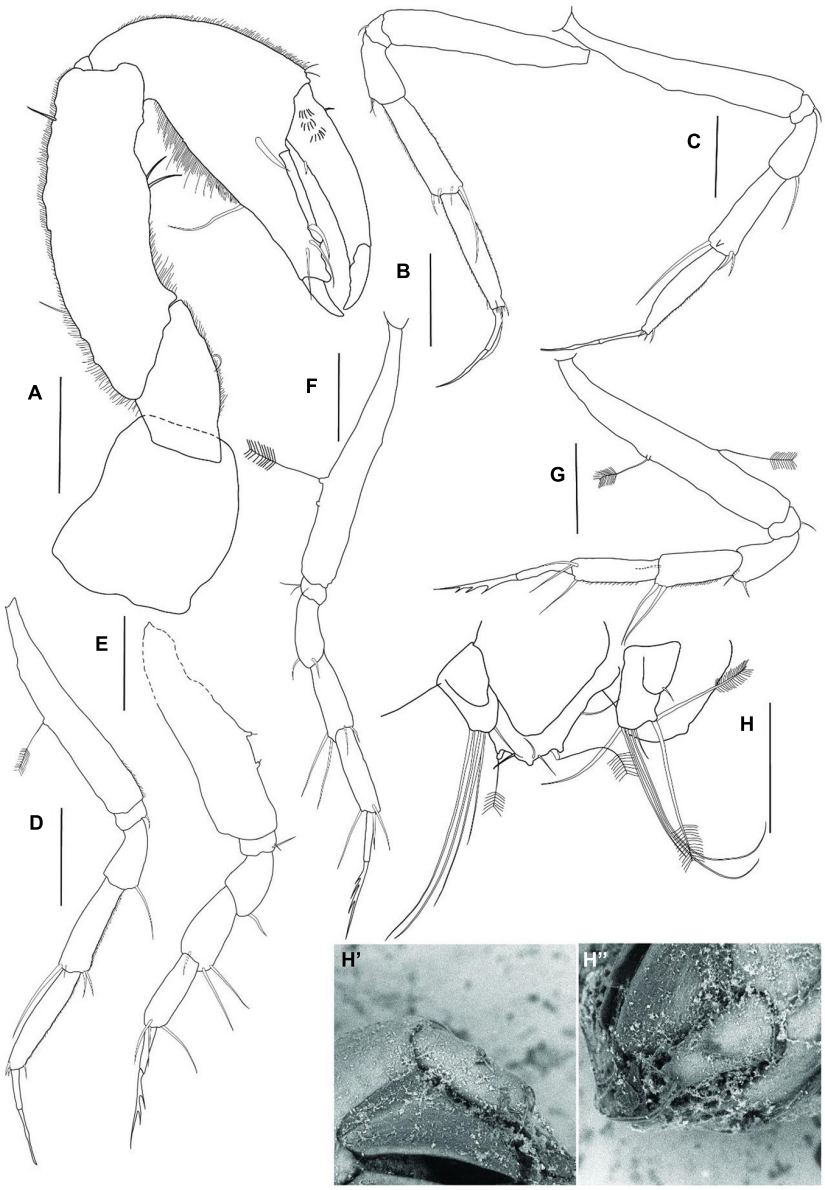

FIGURE 10 | *Agathotanais jani* n. sp., neuter, paratype (ZMH-K-61150). **(A)** cheliped; **(B)** pereopod-1; **(C)** pereopod-2; **(D)** pereopod-3; **(E)** pereopod-4; **(F)** pereopod-5; **(G)** pereopod-6; **(H)** uropod; **(H')** detail of uropod – ventral view (SEM picture); **(H")** detail of uropod – lateral view (SEM picture). Scale bar: **(A–D)** = 100 μm.

Labium (**Figure 9G**) with the spiniform distal process and long lateral process, covered by numerous setae.

Maxilliped (**Figure 9H**) endite with gustatory cups seta and numerous fine setae on distal margin; palp article-1 1.3 L:W, naked; article-2 1.4 L:W, with inner seta and numerous fine setae of various lengths on inner and outer margins; article-3 2.4 L:W, with two inner subdistal plumose setae, margins with numerous fine setae; article-4 1.7 L:W, with one subdistal and five serrated distal setae. Endites short with one midlength seta and numerous fine setae distally.

Cheliped (**Figure 10A**) basis 0.9 L:W, naked; merus with midventral seta; carpus 3.0 L:W, marginally shorter than propodal palm and fixed finger combined, with two midventral setae and two dorsal (one proximal and one subdistal) setae; palm 2.5 L:W, with robust seta at dactylus insertion; fixed finger subequal to palm, with long ventral seta, cutting edge gently undulated with three setae, distal spine robust; dactylus as long as a fixed finger, with dorsoproximal short seta, cutting edge with proximal seta; unguis robust.

Pereopod-1 (**Figure 10B**) basis 6.2 L:W, naked; ischium with ventrodistal seta; merus 2.0 L:W, 0.5× carpus, with two ventrodistal setae; carpus 3.6 L:W, 0.9× propodus, with three short distal setae and long (0.6× propodus) dorsodistal seta;

propodus 5.5 L:W, 2.7× dactylus and unguis combined, with short ventrodistal seta and some spinules near dactylus insertion; dactylus 8.0 L:W, 0.7× unguis, with proximal seta; unguis unarmed, with a pointed tip.

Pereopod-2 (**Figure 10C**) basis 8.1 L:W, naked; ischium with ventrodistal seta; merus 2.1 L:W, 0.7× carpus, with long ventrodistal seta; carpus 3.5 L:W, 0.9× propodus, with two ventrodistal setae, and long (0.9× propodus) dorsodistal seta; propodus 4.6 L:W and 2.5× dactylus and unguis combined, distally damaged, with short ventrodistal seta and some spinules near dactylus insertion; dactylus 13.0 L:W, 1.0× unguis, unarmed; unguis unarmed, with a pointed tip.

Pereopod-3 (**Figure 10D**) basis 6.8 L:W, with penicillate dorsal seta; ischium with ventrodistal seta; merus 2.0 L:W, 0.7× carpus, with long ventrodistal seta; carpus 3.4 L:W, 0.8× propodus, with two ventrodistal setae, short and long (0.7× propodus) dorsodistal setae; propodus 5.1 L:W and 2.8× dactylus and unguis combined, with short ventrodistal seta and spinules near dactylus insertion; dactylus 6.7 L:W, 0.7× unguis, unarmed; unguis unarmed, with a pointed tip.

Pereopod-4 (**Figure 10E**) basis partly broken, with two penicillate ventral setae; ischium with two ventrodistal setae; merus 1.3 L:W, 0.7× carpus, with ventrodistal seta; carpus 1.9 L:W, 0.9× propodus, with two long ventrodistal and one dorsodistal setae; propodus 3.0 L:W, with two dorsodistal and ventrodistal setae; dactylus 5.7 L:W, 0.5× unguis; unguis with two pointed ventral teeth.

Pereopod-5 (**Figure 10F**) basis 7.4 L:W, with two penicillate midventral setae; ischium with two short ventrodistal setae; merus 2.6 L:W, 0.9× carpus, with two short ventrodistal setae; carpus 2.9 L:W, 0.8× propodus, with two long ventrodistal and two short dorsodistal setae; propodus 4.1 L:W and 2.7× dactylus and unguis combined, with two dorsodistal and one ventrodistal setae; dactylus 4.5 L:W, 0.4× unguis; unguis with three pointed ventral teeth.

Pereopod-6 (**Figure 10G**) basis 7.4 L:W, with one middorsal and one midventral penicillate setae; ischium with ventrodistal seta; merus 1.6 L:W, 0.6× carpus, with two ventrodistal setae; carpus 2.7 L:W, 1.0× propodus, with two long ventrodistal and one distal setae; propodus 3.8 L:W and 1.5× dactylus and unguis combined, with ventrodistal seta and two dorsodistal setae; dactylus 7.5 L:W, 0.7× unguis; unguis with three pointed ventral teeth.

Pleopods absent.

Left uropod (**Figures 10H,H',H"**) exopod reduced and fused with basal article, tipped with seta; endopod one-articled, with four distal and two plumose subdistal setae.

Description of juvenile male: Body and appendages from paratype (ZMH-K-61159). BL = 2.8 mm. Body (**Figures 8C,D**) elongated, 13.1 L:W; carapace 1.8 L:W. Pereonites 1–6: 0.8, 1.2, 1.5, 1.7, 1.7, and 1.2 L:W, respectively. Pleon combined with pleotelson 0.1× total body length. Pleonites 1–5 equal, 0.2 L:W each. Pleotelson 0.8× pleonites 1–6 combined, almost square in the dorsal view, apex pointed, directed backward. Appendages similar to those observed in neuters, but in juvenile males, pleopods are present although not fully developed.

Intraspecific variation: Manca III: length 1.3–1.8 mm.

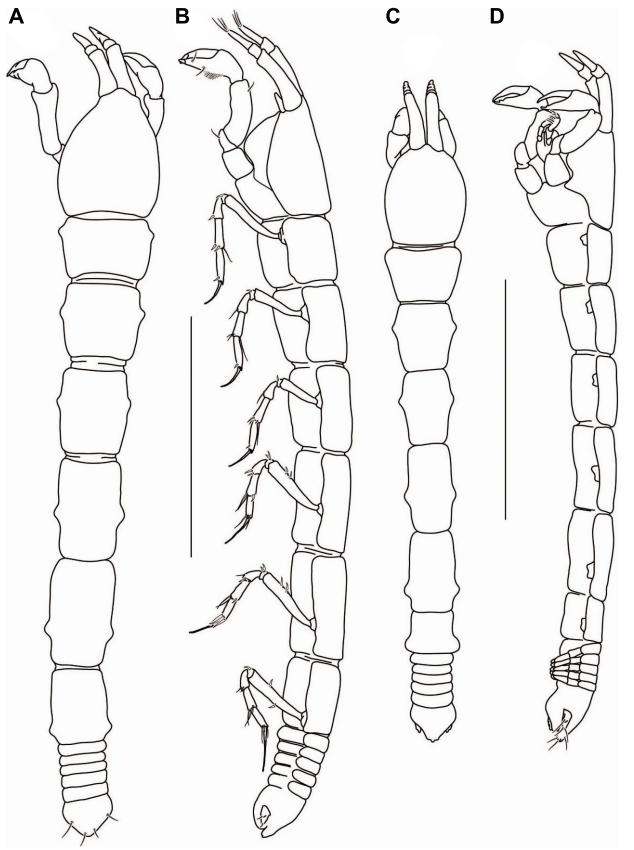

FIGURE 11 | *Agathotanais oharai* n. sp., neuter, holotype (**A,B**: NMV J 74742), juvenile male, paratype (**C,D**: NMV J 74725). **(A)** dorsal view; **(B)** lateral view; **(C)** dorsal view; **(D)** lateral view. Scale bar: **(A–D)** = 1 mm.

Neuter: length: 2.5–3.8 mm; uropod endopod with zero/two plumose setae distally (might be differences between right and left uropod).

Juvenile male: length 2.4–3. 2 mm.

Distribution: Central Pacific, Clarion-Clipperton Fracture Zone (IOM, BGR, GSR, APEI-3) (**Figure 2**); depth range: 4093–4511 m.

Remarks. The presence of distinct pointed ventral teeth on the unguis in pereopods 4–6 is a unique character that allows distinguishing *A. jani* from congeners. In *A. hadalis*, *A. misakiensis*, *A. toyoshioae, A. paleroi,* and *A. beatae* only a weak serration is present (Larsen, 2007; Kakui and Kohtsuka, 2015), while in other *Agathotanais* species the unguis in those pereopods is unarmed (**Table 1**).

***Agathotanais oharai* n. sp. Stępień, Jakiel and Błażewicz**.
This species is register under the zoobank number:
LSIDurn:lsid:zoobank.org:act:C3E44847-F819-4CCE-A2AF-687C060321D9

(**Figures 11–13**)

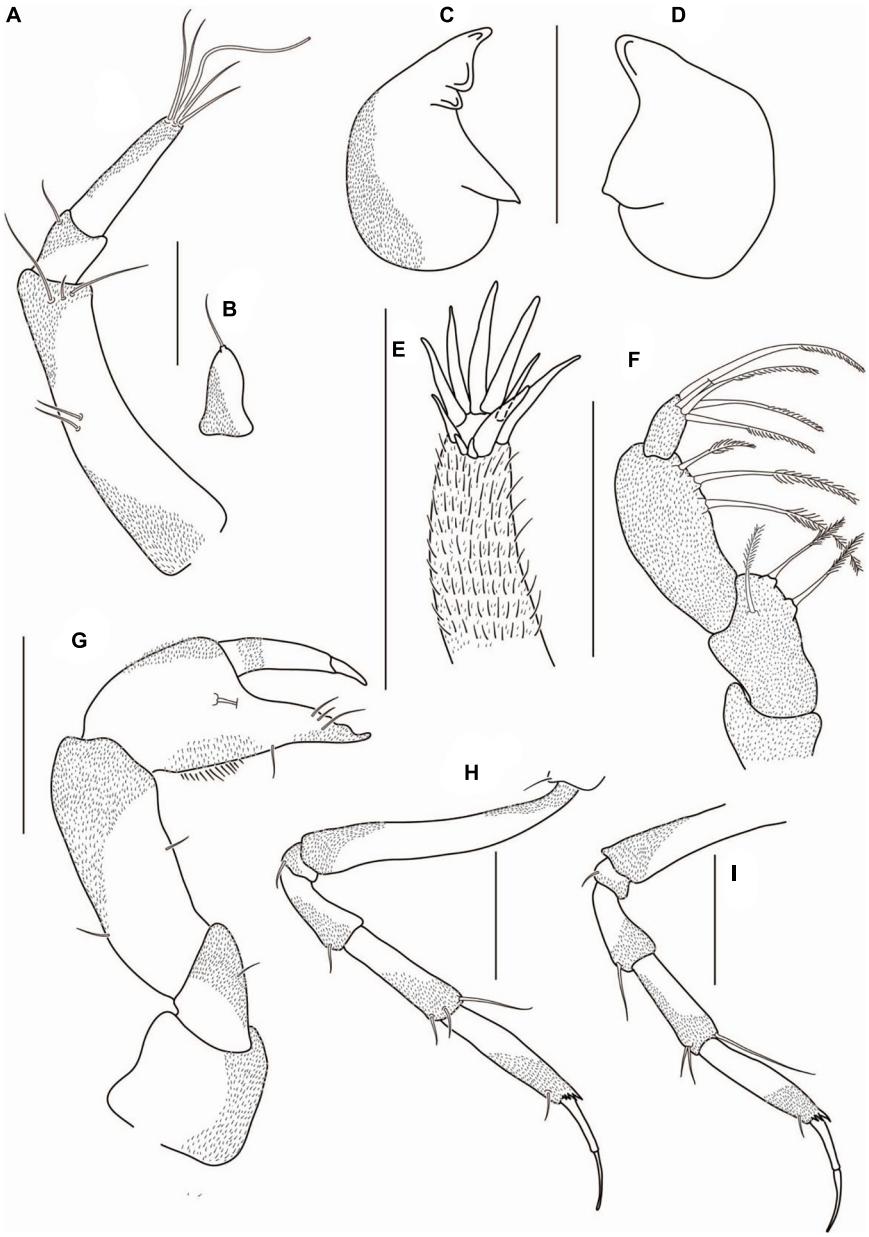

FIGURE 12 | *Agathotanais oharai* n. sp., neuter, paratype (NMV J 74742); **(A)** antennule; **(B)** antenna; **(C)** left mandible; **(D)** right mandible; **(E)** maxillule; **(F)** maxilliped; **(G)** cheliped; **(H)** pereopod-1; **(I)** pereopod-2. Scale bars: **(A–F)** = 10 μm, **(G–I)** = 100 μm.

Material examined: Holotype: neuter, 3 mm, ABYSS st. 42, (NMV J 74742).

Paratype: juvenile male, 2.5 mm, partly dissected on slides, ABYSS st. 33, (NMV J 74725); neuter, broken, dissected on slides ABYSS st. 42, (NMV J 74742).

Diagnosis of neuter: Body narrow (about 7.3 L:W). Carapace without pair of lateral setae on posterior margin. Pereonite-1 without pair of dorsal setae. Pereonites 4–6 longer than wide. Pereonite-6 1.3× pleonites 1–5 combined. Pleonites 1–5 little narrower than pereonite-6. Antennule article-1 longer than the remaining articles combined, about 2.0× article-3. Antenna one-articled. Cheliped palm 1.1 L:W. Pereopods 2–3 carpus with dorsodistal seta 0.8× propodus. Pereopods 4–6 unguis unarmed. Uropod endopod one-articled.

Etymology: The species is named in honor of Tim O'Hara, senior curator of the Marine Invertebrates Section in Museums Victoria (Melbourne) and specialist in biogeography.

Description of neuter: Body from the holotype (NMV J 74742), appendages from paratype (NMV J 74725). BL = 3 mm. Body (**Figures 11A,B**) 7.3 L:W. Carapace 1.0 L:W, 0.2× BL. Pereon 0.7× BL, pereonites 1–6: 0.6, 0.9, 1.2, 1.4, 1.7, and 1.3 L:W, respectively, rectangular in dorsal view. Pleon with

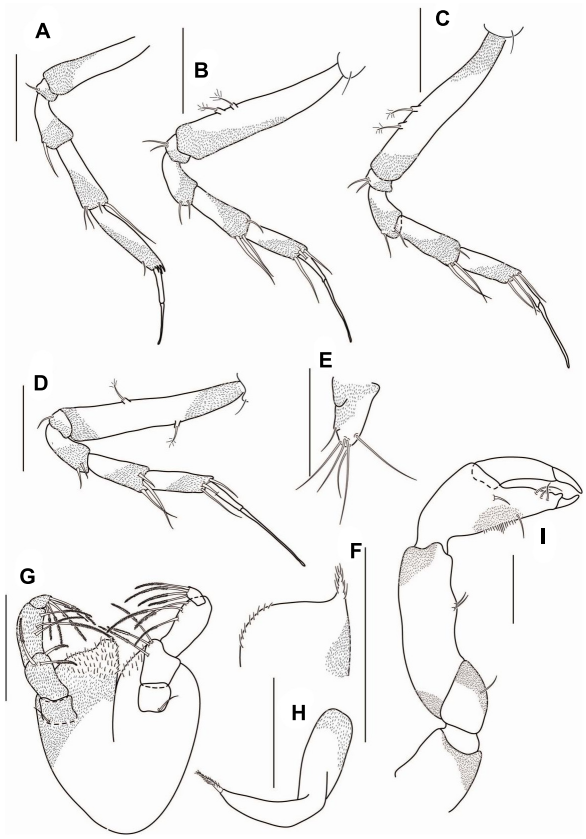

FIGURE 13 | *Agathotanais oharai* n. sp., neuter, paratype (**A–E**: NMV J 74742), juvenile male (**F–I**: NMV J 74725). **(A)** pereopod-3; **(B)** pereopod-4; **(C)** pereopod-5; **(D)** pereopod-6; **(E)** uropod; **(F)** labium; **(G)** maxilliped; **(H)** epignath; **(I)** cheliped. Scale bars: **(A–E,I)** = 100 μm; **(F–H)** = 10 μm.

pleotelson 0.1× BL. Pleonites 1–6 0.1 L:W each. Pleotelson in dorsal view 1.3× pleonites 5–6, with two pairs of lateral setae.

Antennule (**Figure 12A**) article-1 4.5 L:W, 4.3× article-2, with two midlength setae, and with three subdistal setae; article-2 1.7 L:W, 0.5× article-3, with outer distal seta; article-3 3.7 L:W, with four setae and aesthetasc distally.

Antenna (**Figure 12B**) one-articled, 1.8 L:W, tipped with seta.

Mouthparts: Left mandible (**Figure 12C**) incisor with two blunt teeth, *lacinia mobilis* short and rounded.

Right mandible (**Figure 12D**) incisor with a broad triangular tooth.

Maxillule endite (**Figure 12E**) with ten distal spines.

Maxiliped (**Figure 12F**) palp article-1 broken, naked distally; article-2 1.8 L:W, with three inner plumose setae; article-3 2.2 L:W, with three inner plumose setae; article-4 left palp 1.3 L:W, with five inner plumose distal setae.

Cheliped (**Figure 12G**) basis 0.8 L:W, with small subventral seta; merus with midventral seta; carpus 2.5 L:W, marginally shorter than propodus and fixed finger combined, with one middorsal and one midventral setae; palm 1.2 L:W, with seta near dactylus insertion and a row of ventral setae; fixed finger 0.8× palm, with one ventral seta, cutting edge with three tubercles and three setae, terminal spine small; dactylus as long as a fixed finger, curved, naked; unguis moderate size.

Pereopod-1 (**Figure 12H**) coxa with seta; basis 7.0 L:W, 3.0× merus, naked; ischium with ventrodistal seta; merus 2.0 L:W and 0.7× carpus, with ventrodistal seta; carpus 3.2 L:W, 0.9× propodus, with two ventrodistal setae and long (0.5× propodus) dorsodistal seta; propodus 3.8 L:W, 1.0× dactylus and unguis combined, with projections near dactylus insertion and ventrosubdistal seta; dactylus 1.1× unguis, unarmed; unguis unarmed, with rounded tip.

Pereopod-2 (**Figure 12I**) basis broken; ischium with ventrodistal seta; merus 1.8 L:W, 0.7× carpus, with ventrodistal seta; carpus 2.7 L:W, 0.8× propodus, with two short ventrodistal and one long (0.8× propodus) dorsodistal setae; propodus 4.7 L:W, 1.0× dactylus and unguis combined, with spinules near dactylus insertion and ventrosubdistal seta; dactylus 0.7× unguis, unarmed; unguis unarmed, with rounded tip.

Pereopod-3 (**Figure 13A**) basis broken; ischium with ventrodistal seta; merus 1.8 L:W, 0.7× carpus, with ventrodistal seta; carpus 2.7 L:W, 0.8× propodus, with two ventrodistal, short middistal, and long (0.8× propodus) dorsodistal setae; propodus 4.5 L:W, 1.0× dactylus and unguis combined, with spinules near dactylus insertion and ventrosubdistal seta; dactylus 0.8× unguis, unarmed; unguis unarmed, with rounded tip.

Pereopod-4 (**Figure 13B**) coxa with seta; basis 5.3 L:W, 3.6× merus, with two penicillate ventral setae; ischium with two ventrodistal setae; merus 2.0 L:W, 0.8× carpus, with two ventrodistal setae; carpus 2.4 L:W, 1.0× propodus, with one short dorsodistal and two long ventrodistal setae; propodus 3.4 L:W, 0.6× dactylus and unguis combined, with two ventrodistal, one dorsodistal setae; dactylus 0.4× unguis, unarmed; unguis unarmed, with rounded tip.

Pereopod-5 (**Figure 13C**) similar to pereopod-4.

Pereopod-6 (**Figure 13D**) similar to pereopod-4, but basis with one midventral and one middorsal penicillate setae, and ischium with ventrodistal seta.

Pleopods absent

Uropod (**Figure 13E**) exopod reduced and fused with the basal article, endopod one-articled, 1.2 L:W, with two subdistal and four distal setae.

Description of juvenile male: Body and appendages from paratype (NMV J 74725). BL = 2.5 mm. Body (**Figures 11C,D**) 7.5 L:W. Carapace 1.2 L:W, 0.2× BL. Pereonites 0.6× BL, pereonites 1-6: 0.6, 1.0, 1.3, 1.8, 1.5, and 0.8 L:W, respectively. Pleon combined with pleotelson 0.2× BL. Pleonites 0.2 L:W each. Pleotelson 1.4× pleonites 5–6.

Labium (**Figure 13F**) with the spiniform distal process (broken, not figured) and lateral process, covered by numerous setae.

Maxilliped (**Figure 13G**) palp article-1 rectangular, with proximal seta; article-2 1.8 L:W, with three inner plumose setae; article-3 2.2 L:W, with three inner plumose setae; article-4 left palp 1.3 L:W, with five inner plumose distal setae; article-4 right palp 1.4 L:W, with four inner plumose setae distally. Basis covered with numerous setae of different lengths, with rounded distal projection, minute seta near palp insertion.

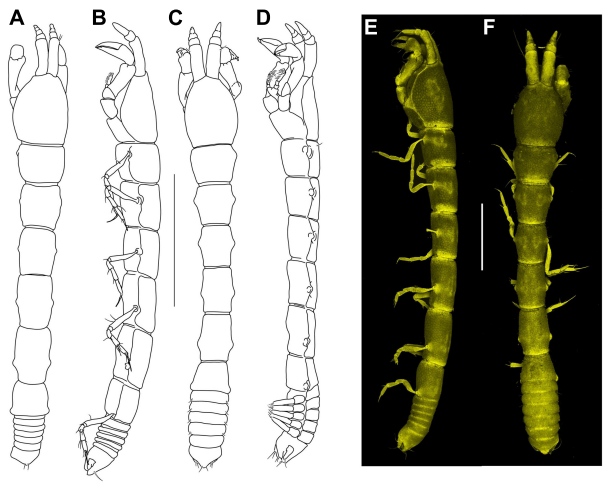

FIGURE 14 | *Agathotanais paleroi* n. sp., neuter, holotype (**A,B**: ZMH K-61175), juvenile male, paratype (**C,D**: NHM 58023), neuter, paratype (**E,F**: ZMH K-61178). **(A)** Dorsal view; **(B)** lateral view; **(C)** dorsal view; **(D)** lateral view; **(E)** lateral view (confocal picture); **(F)** dorsal view (confocal picture). Scale bars: **(A–D)** = 1 mm, **(E,F)** = 500 μm.

Epignath (**Figure 13H**) narrow, curved, with terminal robust plumose seta.

Cheliped (**Figure 13I**) basis 1.2 L:W, naked; merus with midventral seta; carpus 2.8 L:W, marginally shorter than propodus and fixed finger combined, with two midventral setae; palm 1.2 L:W, with seta near dactylus insertion and a row of ventral setae; fixed finger as long as palm, with one ventral seta, cutting edge with two tubercles and three setae; dactylus as long as a fixed finger, curved, naked; unguis moderate size.

Intraspecific variation: Juvenile male: maxilliped palp article-4 with four-five distal setae on the left and right palp, respectively.

Distribution: SE Australian coast, off Bermagui, East Gippsland (**Figure 2**); depth range: 4064–4744 m.

Remarks. *Agathotanais oharai* belongs to the group of *Agathotanais* with a short cheliped palm (L:W 1.0–1.2), together with *A. ghilarovi*, *A. splendidus*, and *A. paleroi* (**Table 1**). It differs from *A. paleroi* in the unguis of pereopod-6, which is unarmed in *A. oharai* and serrated in *A. paleroi.* Additionally *A. oharai* has a pleon narrower than pereonite-6, what distinguishes it from *A. splendidus* and *A. ghilarhovi*, which have the pleon as wide as peronite-6 (**Table 1**).

***Agathotanais paleroi* n. sp. Stępień, Jakiel and Błażewicz**.
This species is register under the zoobank number:
LSIDurn:lsid:zoobank.org:act:05C2DC1B-33B8-492F-B319-FA70B2FE0C22

(**Figures 14–16**)

Material examined: Holotype: neuter, 3.0 mm, KuramBio st. 2-9, (ZMH K-61175).

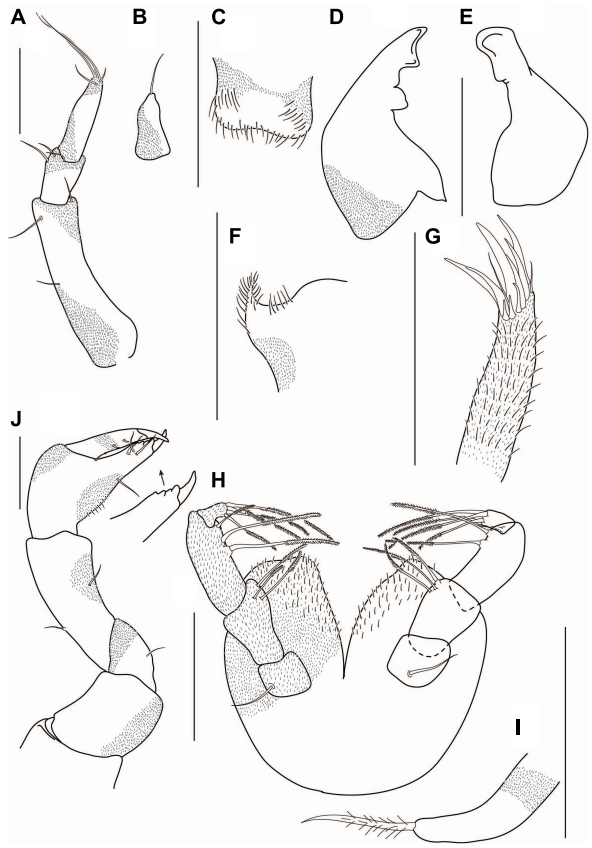

FIGURE 15 | *Agathotanais paleroi* n. sp., neuter, paratype (**A,C,F,J**: NHM 58022; **B,D,E,G–I**: ZMH K-61177). **(A)** antennule; **(B)** antenna; **(C)** labrum; **(D)** left mandible; **(E)** right mandible; **(F)** labium; **(G)** maxillule; **(H)** maxilliped; **(I)** epignath; **(J)** cheliped. Scale bars: **(A–I)** = 10 μm, **(J)** = 100 μm.

Paratypes: juvenile male, 3.5 mm, KuramBio st. 2-10, (NHM 58023); neuter, dissected on slides, 3.0 mm, KuramBio st. 5-10, (NHM 58022); juvenile male dissected on slides, 2.9 mm, KuramBio st. 2-9, (ZMH K-61176); juvenile male, 2.4 mm, KuramBio st. 2-10, (NHM 58024); neuter, 3.1 mm, KuramBio st. 2-9, (NHM 58025); neuter, 2.6 mm, KuramBio st. 5-9, (NHM 58026); neuter, 2.9 mm, KuramBio st. 6-11, (ZMH K-61178); manca II, 1.4 mm, KuramBio st. 8-12, (ZMH K-61179); manca III, 1.8 mm, KuramBio st. 8-12, (ZMH K-61179); neuter, 2.8 mm, KuramBio st. 8-12, (ZMH K-61179); neuter, 2.8 mm, KuramBio st. 8-9, (NHM 58027); neuter, 3.1 mm, partly dissected on slide, KuramBio st. 1-11, (ZMH K-61177); neuter, 2.3 mm, KuramBio st. 8-1, (NHM 58028); manca III, 1.9 mm, KuramBio st. 8-1, (NHM 58029); neuter, 3.2 mm, KuramBio st. 6-12, (NHM 58030); neuter, broken, KuramBio st. 5-9, (NHM 58031); neuter, 3.2 mm, KuramBio st. 3-9, (NHM 58032); two neuters, broken, KuramBio st. 2-9, (ZMH K-61180); manca, broken, KuramBio st. 5-10, (ZMH K-61181); neuter, broken, KuramBio st. 5-9, (ZMH K-61182).

Diagnosis of neuter: Body narrow (7.0 L:W). Carapace without pair of lateral setae in posterior margin. Pereonite-1 without pair of dorsal setae. Pereonites 4–6 longer than

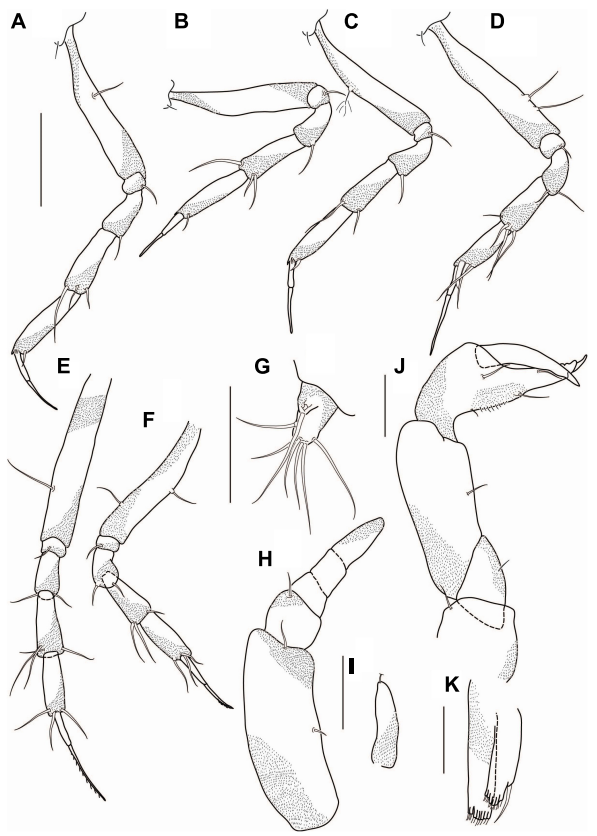

FIGURE 16 | *Agathotanais paleroi* n. sp., neuter, paratype (**A–G**: NHM 58022), juvenile male, paratype (**H–K**: ZMH K-61176). **(A)** Pereopod-1; **(B)** pereopod-2; **(C)** pereopod-3; **(D)** pereopod-4; **(E)** pereopod-5; **(F)** pereopod-6; **(G)** uropod; **(H)** antennule; **(I)** antenna; **(J)** cheliped; **(K)** pleopod. Scale bar: **(A–G)** = 100 μm.

wide. Pereonite-6 similar in length to pleonites 1–5 combined. Pleonites 1–5 narrower than pereonite-6. Antennule article-1 longer than the remaining articles combined, about 2.0× article-3. Antenna one-articled. Cheliped palm as long as wide. Pereopods 2–3 carpus with dorsodistal seta 0.7× propodus. Pereopod 4 unguis unarmed, pereopods 5–6 unguis with serration. Uropod endopod one-articled.

Etymology: Species is dedicated to Dr. Ferran Palero (University of Valencia), a great colleague, fellow, and peracarid specialist.

Description of neuter: Body from the holotype (ZMH K-61175), appendages from paratypes (NHM 58022 and ZMH K-61177). BL = 3 mm. Body (**Figures 14 A,B,E,F**) 7.0 L:W, elongated. Carapace 1.2 L:W, 0.1× BL, with rounded lateral margins. Pereon 0.7× BL, pereonites 1–6: 0.7, 1.0, 1.2, 1.5, 1.6, and 0.9 L:W, respectively, all pereonites rectangular. Pleon with pleotelson 0.1× BL. Pleonites 1–5 0.1 L:W each.

Antennule (**Figure 15A**) article-1 4.5 L:W, 3.0× article-2, with one midlength, one subdistal and one distal seta; article-2 1.5 L:W, 0.6× article-3, with three outer subdistal setae; article-3 3.5 L:W, with two short subdistal and two long distal setae.

Antenna (**Figure 15B**) one-articled, 2.0 L:W, subtriangular, tipped with seta.

Mouthparts: Labrum (**Figure 15C**) hood-shaped, covered with numerous setae of different lengths.

Left mandible (**Figure 15D**) incisor with two blunt teeth, *lacinia mobilis* rounded and short-fused with incisor.

Right mandible (**Figure 15E**) incisor with blunt tooth distally.

Labium (**Figure 15F**) with a spiniform distal process (broken, not pictured) and lateral process, covered by numerous setae.

Maxillule endite (**Figure 15G**) with ten distal spines and distal fine setae of different lengths.

Maxilliped (**Figure 15H**) palp article-1 rectangular, with proximal seta; article-2 1.8 L:W, with three inner plumose setae; article-3 2.3 L:W, with three inner plumose setae (one hidden under the article-4); article-4 1.8 L:W, with four distal plumose setae. Basis rounded, covered by numerous setae of different lengths.

Epignath (**Figure 15I**) elongated, tipped with plumose setae.

Cheliped (**Figure 15J**) basis 1.0 L:W, naked; merus with midventral seta; carpus 2.6 L:W, marginally shorter than propodus and fixed finger combined, with one middorsal and one midventral setae; palm 1.0 L:W, with seta near dactylus insertion and with a row of setae ventrally; fixed finger similar in length to palm, with midventral seta, cutting edge with tubercles and three setae, terminal spine sharp; dactylus as long as a fixed finger, cutting edge with two spines; unguis slender.

Pereopod-1 (**Figure 16A**) coxa with seta, basis 5.5 L:W, 4.5× merus, with midventral seta; ischium with ventrodistal seta; merus 1.3 L:W and 0.4× carpus, with ventrodistal seta; carpus 2.7 L:W, 0.8× propodus, with two short ventrodistal and long (0.7× propodus) dorsodistal setae; propodus 1.7 L:W, 1.0× dactylus and unguis combined, with spinules near dactylus insertion and ventrodistal seta; dactylus 0.7× unguis, unarmed; unguis unarmed, with rounded tip.

Pereopod-2 (**Figure 16B**) coxa with seta; basis 5.0 L:W, 3× merus, naked; ischium with ventrodistal seta; merus 2.0 L:W, 0.5× carpus, with ventrodistal seta; carpus 2.8 L:W, 0.8× propodus, with two ventrodistal and long (0.7× propodus) dorsodistal setae; propodus 3.8 L:W, 1.2× dactylus and unguis combined, with spinules near dactylus insertion and ventrodistal seta; dactylus 0.8× unguis, unarmed; unguis unarmed, with rounded tip.

Pereopod-3 (**Figure 16C**) coxa with seta; basis 5.8 L:W, 3.3× merus, with penicillate middorsal seta; ischium with ventrodistal seta; merus 2.0 L:W, 0.5× carpus, with ventrodistal seta; carpus 2.8 L:W, 0.8× propodus, with ventrodistal seta and long (0.7× propodus) dorsodistal seta; propodus 5.0 L:W, 1.0× dactylus and unguis combined, with spinules near dactylus insertion and ventrodistal seta; dactylus 0.5× unguis, unarmed; unguis unarmed, with rounded tip.

Pereopod-4 (**Figure 16D**) coxa with seta; basis 5.0 L:W, 3.8× merus, with two midventral seta; ischium with ventrodistal seta; merus 1.6 L:W, 0.7× carpus, with two ventrodistal setae; carpus 2.3 L:W, 1.0× propodus, with three long dorsodistal and one short ventrodistal setae; propodus 2.7 L:W, 0.6×

dactylus and unguis combined, with two simple and one robust dorsodistal setae; dactylus 0.4× unguis, unarmed; unguis unarmed, with rounded tip.

Pereopod-5 (**Figure 16E**) basis 5.1 L:W, 3.4× merus, with midventral seta; ischium with middistal seta; merus 2.2 L:W, 0.7× carpus, with two distal setae; carpus 2.6 L:W, 1.0× propodus, with four distal setae; propodus 3.2 L:W, 0.6× dactylus and unguis combined, with two ventrodistal, one dorsodistal setae; dactylus 0.5× unguis, unarmed; unguis serrated ventrally.

Pereopod-6 (**Figure 16F**) basis 5.2 L:W, 3.4× merus, with one ventral and one dorsal setae; ischium with middistal seta; merus 1.6 L:W, 0.6× carpus, with two ventrodistal setae; carpus 2.2 L:W, 1.0× propodus, with two ventrodistal and one dorsodistal setae; propodus 2.4 L:W, 0.7× dactylus and unguis combined length, with two ventrodistal one dorsodistal setae; dactylus 0.8× unguis, dactylus unarmed; unguis serrated ventrally.

Pleopods absent.

Uropod (**Figure 16G**) exopod reduced and fused with the basal article, tipped with two setae (one broken); endopod one-articled, with four distal and two subdistal setae.

Description of the juvenile male: Body from paratype (NHM 58023), appendages from paratype (ZMH K-61176). BL = 3.5 mm. Body elongated (**Figures 15 C,D**) 7.4 L:W. Carapace 1.3 L:W, 0.9× pereonites 1–2, 0.1× BL. Pereonites 0.7× BL, pereonites 1–6: 0.7, 1, 1.1, 1.4, 1.3, and 0.7 L:W, respectively, last pereonite trapezoidal in dorsal view. Pleon combined with pleotelson 0.1× BL. Pleonites 0.2 L:W. Pleotelson 0.7× pleonites 4–5.

Antennule (**Figure 16H**) with five articles; article-1 2.7 L:W, 1.6× article-2, with one midlength and one distal seta; article-2 0.8 L:W, 0.3× article-3, with distal seta; article-3 0.5 L:W, naked, article-4 0.7 L:W, naked, article-5 2.3 L:W, naked.

Antenna (**Figure 16I**) one-articled, 3.4 L:W, tipped with a seta.

Cheliped (**Figure 16J**) basis 1.0 L:W, with the dorsodistal seta; merus with midventral seta; carpus 2.5 L:W, 1.6× palm, with midventral seta; chela palm 1.5 L:W, with seta near dactylus insertion and with row of ventral setae; fixed finger with ventral seta, cutting edge with two inner setae, and with three tubercles distally, distal spine sharp; dactylus as long as a fixed finger; unguis slender.

Pleopod (**Figure 16K**) exopod with six distal and one subdistal setae; endopod with eight setae.

Intraspecific variation: Manca III: length 1.8–1.9 mm.

Neuter: length 2.3–3.2 mm; antenna article-1 with zero/one midlength seta; cheliped carpus with one/two midventral setae.

Juvenile male: length 2.4–2.9 mm; cheliped fixed finger cutting edge with one/three inner setae.

Distribution: NW Pacific, Kuril-Kamchatka Trench (**Figure 2**); depth range: 4976–5388 m.

Remarks. *Agathotanais paleroi* n. sp., collected from the KKT, belongs to the species of *Agathotanais* with a short cheliped palm (L:W 1.0–1.2). It differs from other short-palm species by the appearance of the unguis of pereopod-6: serrated in *A. paleroi* but unarmed in *A. ghilarovi*, *A. splendidus*, and *A. oharai*. Furthermore, *A. paleroi* has a pleon narrower than pereonite-6, distinguishing it from *A. splendidus* and *A. ghilarhovi* with a pereonite-6 that is as wide as pleon (**Table 1**).

***Agathotanais* sp. abyss-1**.

(**Supplementary Figures 1, 2**)

Material examined: Neuter, 3.3 mm, dissected on the slides, ABYSS st. 9, (NMV J 74664).

Description of neuter: BL = 3.3 mm. Body (**Supplementary Figures 1A,B**) 7.7 L:W. Carapace 1.2 L:W, 0.1× BL, with pair of lateral posterior setae. Pereon 0.7× BL, pereonites 1–6: 0.8, 1.0, 1.3, 1.6, 2.0, and 1.4 L:W, respectively, all pereonites rectangular in dorsal view. Pleon with pleotelson 0.1× BL. Pleonites 1–5 0.3 L:W each. Pleotelson in dorsal view 0.8× pleonites 1–5.

Antennule (**Supplementary Figure 1C**) article-1 3.8 L:W, 4.7× article-2, with three inner setae: one midlength and three subdistal setae; article-2 1.2 L:W, 0.5× article-3, with two subdistal setae; article-3 3.3 L:W, with three long and one short distal setae.

Antenna (**Supplementary Figure 1D**) one-articled, 2.0 L:W, tipped with a seta.

Mouthparts: Labrum (**Supplementary Figure 1E**) rounded, with numerous setae of different lengths.

Left mandible (**Supplementary Figure 1F**) incisor with two blunt teeth, *lacinia mobilis* small and fused with incisor.

Right mandible (**Supplementary Figure 1G**) incisor with a blunt tooth.

Labium (**Supplementary Figure 1H**) with a spiniform distal process (broken, not pictured) and lateral process, covered by numerous setae.

Maxillule endite (**Supplementary Figure 1I**) with eleven distal spines of different lengths.

Maxilliped (**Supplementary Figure 1J**) palp article-1 broken; article-2 2.2 L:W, with three inner plumose setae, article-3 2.6 L:W, with three inner plumose setae, article-4 1.6 L:W, with five subdistal and distal setae, and one short outer seta.

Epignath (**Supplementary Figure 1K**) elongated, tipped with a plumose seta.

Cheliped (**Supplementary Figure 2A**) basis 1.0 L:W, naked, rectangular; merus with midventral seta; carpus 2.2 L:W, marginally shorter than propodus and fixed finger combined, with two midventral, one dorsoproximal, and one dorsosubdistal setae; chela palm 1.4 L:W, with seta near dactylus insertion and with row of ventral setae; fixed finger 0.8× palm, cutting edge with three setae; dactylus as long as a fixed finger, cutting edge with short proximal seta.

Pereopod-1 (**Supplementary Figure 2B**) coxa with seta; basis 6.0 L:W, 3.7× merus, naked; ischium with ventrodistal seta; merus 1.6 L:W and 0.5× carpus, with two ventrodistal seate; carpus 3.3 L:W, 0.7× propodus, with two ventrodistal and long (0.5× propodus) dorsodistal setae; propodus 6.6 L:W, with projection near dactylus insertion, and with ventrodistal seta; dactylus unarmed; unguis is broken.

Pereopod-2 (**Supplementary Figure 2C**) coxa with seta; basis 7.5 L:W, 4.0× merus, with penicillate middorsal seta; ischium with ventrodistal seta; merus 1.7 L:W, 0.8× carpus, with ventrodistal seta; carpus 2.2 L:W, 0.6× propodus, with

two ventrodistal and long (0.7× propodus) dorsodistal setae; propodus 4.8 L:W, 1.0× dactylus and unguis combined, with projection near dactylus insertion, and with ventrodistal seta; dactylus 0.7× unguis, unarmed; unguis unarmed, with rounded tip.

Pereopod-3 (**Supplementary Figure 2D**) coxa with seta; basis 6.0 L:W, 3.4× merus, naked; ischium naked; merus 1.7 L:W, 0.6× carpus, with ventrodistal seta; carpus 3.3 L:W, 0.8× propodus, with ventrodistal and dorsodistal setae; propodus 4.8 L:W, 1.0× dactylus and unguis combined length, with subdistal seta; dactylus 0.6× unguis, unarmed; unguis unarmed, with rounded tip.

Pereopod-4 missing.

Pereopod-5 (**Supplementary Figure 2E**) coxa with seta; basis 5.6 L:W, 5.0× merus, with penicillate middorsal seta; ischium with two ventrodistal setae; merus 1.3 L:W, 1.0× carpus, with ventrodistal seta; carpus 2.6 L:W, 1.0× propodus, with two ventrodistal and one dorsodistal setae; propodus 3.5 L:W, 0.7× dactylus and unguis combined, with two ventrodistal and one dorsodistal setae; dactylus 0.4× unguis, unarmed; unguis unarmed, with rounded tip.

Pereopod-6 (**Supplementary Figure 2F**) coxa with seta; basis 6.0 L:W, 4.8× merus, with penicillate midventral seta; ischium with ventrodistal seta; merus 1.6 L:W, 0.7× carpus, with ventrodistal seta, dorsodistal seta not seen; carpus 2.3 L:W, 1.0× propodus, with two ventrodistal setae; propodus 3.0 L:W, 0.7× dactylus and unguis combined, with two ventrodistal and one dorsodistal setae; dactylus 0.4× unguis, unarmed; unguis unarmed, with rounded tip.

Pleopods absent.

Uropod (**Supplementary Figure 2G**) exopod reduced and fused with basal article, tipped with seta; endopod one-articled, 2.2 L:W, with two distal setae.

Distribution: SE Australia, off the Tasmanian coast, Freycinet Marine Park (**Figure 2**); depth range: 4021–4035 m.

Remarks: *Agathotanais* sp. abbys-1 belongs to the species of *Agathotanais* with a moderate elongated cheliped palm (L:W 1.3–1.4) (**Table 1**). It differs from *A. beatae* by an unarmed pereopod-4 unguis (serrated in *A. beatae*). Moreover, in *Agathotanais* sp. abbys-1 the pleonites are narrower than pereonite-6, whereas in *A. beatae* they are similar in width. On the other hand, it can be distinguished from *A. manganicus* by a one-articled antenna (two-articled in *A. manganicus*). Finally, *Agathotanais* sp. abbys-1 differs from *A. spinipoda* by the propodus of pereopod-6. It is smooth in *Agathotanais* sp. abyss-1 but has a row of spines in *A. spinipoda* (**Table 1**).

Agathotanais indet.

Additional material: *Agathotanais* indet: poor condition, st. 9, NMV74664. SE Pacific, Tasmania coast, Freycinet Marine Park; depth range: 4021–4035 m.

DISCUSSION

The Pacific is a vast ocean with a high variety of benthic environments and ecosystems (Gage and Tyler, 1991). Many of its regions have never been explored, and its fauna and diversity remain simply unknown. This deficient biological recognition is particularly evident when it comes to the identification of a group of organisms that is particularly poorly understood (Błażewicz-Paszkowycz and Bamber, 2012) and it is seen in the proportion of the new taxa discovered (e.g., Larsen and Shimomura, 2007; Błażewicz-Paszkowycz et al., 2013; Bird, 2015; Jakiel et al., 2019, 2020). This work presented findings on just one genus of small macrobenthic peracarids, which was collected from several locations of the North Pacific. Only two of eight identified species were previously described, regardless of the fact that some areas had been previously investigated, e.g., the KKT (Larsen, 2007; Larsen and Shimomura, 2007) or the Clarion Clipperton Fracture Zone (Larsen, 1999). As a result of our study, the number of species known from the Pacific has raised from five to ten, and the total number of species classified into this genus increases from 12 to 17.

Phylogenetic and Genetic Analyses

The current research presents the first results from studies on the extensive collections of *Agathotanais* performed in the frame of an integrative taxonomy approach, combining molecular and morphological techniques. So far, only five agathotanaid sequences were deposited at GenBank and only two of them were identified down to species level — *A. ingolfi* (Błażewicz-Paszkowycz et al., 2014). In the present study, we upgrade the number of sequences to 12, adding three fragments of 18S from species: *A. frutosae*, *A. jani,* and *A. paleroi*, and four H3 sequences from *A. frutosae*, *A. oharai, A. paleroi,* and *Agathotanais* sp. abyss-1. These results, based on two markers, should be considered merely as the first step into more complex phylogenetic studies in the future. Nevertheless, the results allow us to confirm the monophyletic character of *Agathotanais*, as well as of another agathotanaid genus — *Paragathotanais.* Moreover, both genera grouped within the same clade in both obtained phylogenetic trees, confirming their close relationship, although for full phylogenetic resolution and testing of the monophyletic character of Agathotanaidae more genetic data including also other genera are needed.

Within the *Agathotanais*, *A. oharai* from the Australian slope and *Agathotanais* sp. abbys-1 from the Tasmanian slope showed a close relationship (**Figure 1**). Both species present similar body appearance, with similar sizes, a gently rounded lateral margin of the carapace, pereonites rectangular in dorsal view. They both reveal similar proportions of the antennule articles and ratios of length to width in antenna and uropod. The next similarities are the appearance of the pereopods, with elongated carpus and propodus in pereopods 1–3 and unarmed unguis in pereopods 4–6. The molecular and morphological similarities of both species are

supported by a relatively small geographic distance between their known distributions.

Agathotanais oharai and *Agathotanais* sp. abbys-1 were located on the tree close to *A. paleroi*. *Agathotanais paleroi* is separated by several thousands of kilometers from the two species *A. oharai* and *Agathotanais* sp. abbys-1. The taxonomical characters that support genetic similarities are the appearance of the cheliped and the length of the distroventral setae on pereopods 2–3. All three species are characterized by a short or moderately short cheliped palm (L:W less than 1.4) and long dorsodistal setae on the carpus of pereopods 2 and 3 (0.7–0.8× propodus). These features distinguish these species from *A. frutosae*, with a long cheliped palm (1.6 L:W) and short setae on the carpus (0.4–0.6× propodus). Moreover, *A. frutosae* bears a pair of setae on the dorsal surface of the first pereonite, a character that is unique among *Agathotanais* species. The pereopods of *A. frutosae* are thicker and armed with strong setae (e.g., carpus and propodus of pereopods 1–3). The place of occurrence of *A. frutosae* – a semi-enclosed sea – may influence the isolation of the species and the evolution of characters different from other *Agathotanais* species.

Distribution

The genus *Agathotanais* is a cosmopolitan taxon. It was recorded in temperate and tropical zones of the Atlantic, Indian, and Pacific Oceans (Kakui and Kohtsuka, 2015; Chim and Tong, 2021). So far, the genus is absent only from the south of the Antarctic Polar Front (Błażewicz-Paszkowycz and Siciński, 2014; Pabis et al., 2014), although one undescribed species of *Agathotanais* was registered for the slope of the Scotia Sea (Pabis et al., 2015). Since the slope and the abyssal zone of the Southern Ocean are vast and still unexplored areas (Brandt et al., 2007) it can be assumed that the distribution of *Agathotanais* in the Antarctic may be wider, although yet to be discovered.

Regardless of the wide zoogeographical distribution of the genus, each species of *Agathotanais* usually has a narrow zoogeographical range (with the exception of *A. hanseni* and *A. ingolfi*; see Kakui and Kohtsuka, 2015; Chim and Tong, 2021). They are often limited to a defined basin (e.g., sea or trench), although in the case of *A. jani* the boundary is not physically obvious. That species was, however, present only at the closest stations of the Central Pacific (CCZ), separated by a maximal distance of less than 1,000 km (**Figure 2**). The mechanisms which support the connectivity in deep-sea populations are not fully understood yet. The data on population genetics combined with biophysical transport models and trace-element signatures that scrutinized the dispersal potential of deep-sea fauna is just one order of magnitude larger than for shallow water fauna (Baco et al., 2016). Those findings question the paradigm of unlimited distribution of deep-sea species. It is not clear how tube-building small tanaids can sustain genetic connectivity for their low numbers and sparsely distributed populations. The presence in the deep-sea population of mobile males "swimming" (Błażewicz-Paszkowycz et al., 2014) along with favorable hydrological regimes and near-bottom currents adds to the rationale of this phenomenon, although it does not explore the problem. Moreover, neither physical nor hydrological connections warrant an unlimited distribution. *A. frutosae* is known from the Sea of Okhotsk, isolated from the open Pacific by the Kuril Islands. Although hydrological contact between the sea and the Pacific is sustained by numerous straits (Bussol Strait is 2,300 m deep), they do not perform as a zoogeographical passage that would allow the species to disperse.

Depth Ranges

Agathotanais is considered a deep-water genus (Kudinova-Pasternak, 1970, 1989, 1990; Larsen, 2007), which mainly occurs below continental shelf depths; hence their lack of eyes supports a deep-sea origin. In the North West and Central Pacific, they occur between 3,400 and 5,500 m (e.g., Larsen, 1999; Kakui and Kohtsuka, 2015; Chim and Tong, 2021), but three species, two off Japan (*A. toyoshioae*; *A. misakiensis*) and one-off SE Australia (*A. spinipoda* Larsen, 1999), were found on the shelf (95 m; 200–493 m) and the slope 400–1,840 m, respectively (Larsen, 1999; Kakui and Kohtsuka, 2015).

Abundances

Food availability is an essential factor that shapes the diversity in the oceans. The heterotrophic deep-sea fully depends on the external source of the energy that is produced on land or in the photic zone of the ocean. The flux of particulate organic matter (POM) to the seafloor declines in the bathyal and abyssal zones; hence, the coastal oceanic regions are more productive and sustain higher diversity than the open ocean (Woolley et al., 2016; Sweetman et al., 2017). A high primary productivity driven by complex hydrological conditions (Nürnberg and Tiedemann, 2004) justifies the high abundances of *A. frutosae* in the western and deeper part of the Sea of Okhotsk (22% of all collected tanaids; Stępień et al., 2019), observed also for other groups of the benthos, e.g., polychaetes, isopods, amphipods, diatoms (Artemova et al., 2018; Brandt et al., 2018a,b; Frutos and Jażdżewska, 2019). Despite *A. frutosae* being recorded on both sides of Kuril Island, its distribution range was limited to stations of similar depth (about 3000 m), physical parameters (salinity, temperature), and relatively high amounts of carbon in the sediment (Stępień et al., 2019).

Agathotanais frutosae has been collected only inside the Sea of Okhotsk, although the hydrological connectivity between the sea and adjacent basins is sustained. It absent from the neighboring Sea of Japan (Błażewicz-Paszkowycz et al., 2013) as well as from deeper (4,000–5,000 m) abyssal zones surrounding the Kuril-Kamchatka Trench (Kudinova-Pasternak, 1970; Larsen, 2007; Błażewicz et al., 2019). In the open oceanic waters of the North West Pacific, *Agathotanais* was represented by *A. paleroi* and *A. hadalis*. *Agathotanais paleroi* was identified in our studies through integrative methods. It was located on both sides of the

trench, similar to other tanaids and isopods (Lörz et al., 2018; Bober et al., 2019; Jakiel et al., 2019).

DATA AVAILABILITY STATEMENT

This article is registered in ZooBank number: urn:lsid:zoobank.org :pub:F17F01E3-5FF7-41A6-A7A7-6DA8277AA417.

AUTHOR CONTRIBUTIONS

AS: general concept, identification of the material (SokhoBio, KuramBio, ABYSS collection), description and figures of new species, and writing the manuscript. PJ: identification of the material (SO-239 collection), description and figures of new species, SEM images, and editing the manuscript. AJ: DNA and lab work, analysis of the molecular data, light microscope images, editing the figures, and editing the manuscript. AP: description and figures of new species. MB: general concept, identification of the material (SO-239, ABYSS collection), and editing the manuscript. All authors contributed to the article and approved the submitted version.

FUNDING

The material was collected and sorted within the framework of several large international projects. The KuramBio I and II projects and the SokhoBio project were financially supported by the German Ministry for Science and Education, grant 03G0857A, KuramBio I BMBF grant 03G0223A, as well as KuramBio II BMBF grant 03G0250A thanks to Angelika Brandt, Senckenberg Museum, Frankfurt, Germany. The projects were supported by the Russian Foundation of Basis Research (projects 13-04-02144, 16-04-01431), the Council of the President of the Russian Federation (project МК-2599.2013.4), Russian Federation Government Grant No. 11.G34.31.0010, grant of Presidium of the Far East Branch of RAS (12–I–P30–07), and Otto Schmidt Laboratory grant (OSL-14-15). Project ABYSS funding was provided by the Marine Biodiversity Hub, supported through the Australian Government's National Environmental Science Program (NESP). This work was also supported by NCN OPUS 2018/31/B/NZ8/03198.

ACKNOWLEDGMENTS

The materials from Central Pacific was collected in the framework of the Joint Programming Initiative Healthy and Productive Seas and Oceans (JPIOceans) project "Ecological Aspects of Deep-sea Mining" (project EcoResponse Assessing the Ecology, Connectivity, and Resilience of Polymetallic Nodule Field Systems–Chief scientist: Pedro Martínez Arbizu). The authors thank the crews of the RV *Sonne* and *Akademik M.A. Lavrentyev* for their help onboard and all student helpers and technicians for support and help with sorting of the extensive expedition material. The authors wish to thank the CSIRO Marine National Facility (MNF) for its support in the form of sea time on RV *Investigator,* including personnel, scientific equipment, and data management. The authors also thank all the scientific staff and crew who participated in voyage IN2017_V03. All data and samples acquired on the voyage are made publicly available in accordance with the MNF Policy. Special thanks to Emma Palacios Theil for linguistic corrections and Maciej Studzian for confocal images.

SUPPLEMENTARY MATERIAL

The Supplementary Material for this article can be found online at: https://www.frontiersin.org/articles/10.3389/fmars.2021.741536/full#supplementary-material

Supplementary Figure 1 | *Agathotanais* sp. abyss-1, neuter, (NMV J 74664). **(A)** Dorsal view; **(B)** lateral view; **(C)** antennule; **(D)** antenna; **(E)** labrum; **(F)** right mandible; **(G)** left mandible; **(H)** labium; **(I)** maxillule; **(J)** maxilliped; **(K)** epignath. Scale bar: **(A,B)** = 1 mm, **(C–K)** = 10 μm.

Supplementary Figure 2 | *Agathotanais* sp. abyss-1, neuter, (NMV J 74664). **(A)** cheliped; **(B)** pereopod-1; **(C)** pereopod-2; **(D)** pereopod-3; **(E)** pereopod-5; **(F)** pereopod-6; **(G)** uropod. Scale bar: **(A–G)** = 100 μm.

Supplementary Table 1 | Detailed information about deep-sea expeditions during which *Agathotanais* specimens were collected; Expeditions: SokhoBio, Sea of Okhotsk Biodiversity Studies; KuramBio, Kuril-Kamchatka Biodiversity Study; JPIO, European Joint Project Initiative Oceans; ABYSS, Sampling the abyss; SLOPE, campaign to continental slope of Bass Strait; MANGAN, expedition to CCZ under the framework of Ecological Aspects of Deep Sea Mining; License Areas: BGR, Bundesanstalt fur Geowissenschaften und Rofstoffe, Germany; IOM, Interoceanometal Joint Organisation; GSR, Global Sea Mineral Resources NV, Belgium; APEI3, Areas of Particular Environmental Interest 3; Gear: EBS, epibenthic sledge; S, supranet; E, epinet; BC, box corer.

Supplementary Table 2 | Pairwise genetic distances between agathotanaids species for H3 and 18S sequences.

Supplementary Material | Key for *Agathotanais* species.

REFERENCES

Altschul, S. F., Gish, W., Miller, W., Myers, E. W., and Lipman, D. J. (1990). Basic local alignment search tool. *J. Mol. Biol.* 215, 403–410. doi: 10.1016/S0022-2836(05)80360-2

Artemova, A. V., Sattarova, V. V., and Vasilenko, Y. P. (2018). Distribution of diatoms and geochemical features of holocene sediments from the Kuril Basin (Sea of Okhotsk). *Deep Sea Res. Part II Top. Stud. Oceanogr.* 154, 10–23.

Baco, A. R., Etter, R. J., Ribeiro, P. A., der Heyden, S., Beerli, P., and Kinlan, B. P. (2016). A synthesis of genetic connectivity in deep-sea fauna and implications for marine reserve design. *Mol. Ecol.* 25, 3276–3298. doi: 10.1111/mec.13689

Bird, G. J. (2015). Tanaidacea (Crustacea) of the kermadec discovery expedition 2011, with a new sub-family of paratanaidae: metatanainae. *Bull. Auckland Mus.* 20, 369–404.

Bird, G. J., and Holdich, D. M. (1988). Deep-sea Tanaidacea (Crustacea) of the North-East Atlantic: the tribe Agathotanaini. *J. Nat. Hist.* 22, 1591–1621. doi: 10.1080/00222938800771001

Blaxter, M. L., De Ley, P., Garey, J. R., Llu, L. X., Scheldeman, P., Vierstraete, A., et al. (1998). A molecular evolutionary framework

for the phylum Nematoda. *Nature* 392, 71–75. doi: 10.1038/32160

Błażewicz, M., Jakiel, A., Bamber, R. N., and Bird, G. J. (2021). Pseudotanaidae Sieg, 1976 (Crustacea: Peracarida) from the Southern Ocean: diversity and bathymetric pattern. *Eur. Zool. J.* 88, 1–76.

Błażewicz, M., Jóźwiak, P., Menot, L., and Pabis, K. (2019). High species richness and unique composition of the tanaidacean communities associated with five areas in the Pacific polymetallic nodule fields. *Prog. Oceanogr.* 176:102141. doi: 10.1016/j.pocean.2019.102141

Błażewicz-Paszkowycz, M., and Bamber, R. N. (2012). The shallow-water Tanaidacea (Arthropoda: Malacostraca: Peracarida) of the Bass Strait, Victoria, Australia (other than the Tanaidae). *Mem. Mus. Vic.* 69, 1–235. doi: 10.24199/j.mmv.2012.69.01

Błażewicz-Paszkowycz, M., Bamber, R. N., and Jóźwiak, P. (2013). Tanaidaceans (Crustacea: Peracarida) from the SoJaBio joint expedition in slope and deeper waters in the Sea of Japan. *Deep Sea Res. Part II Top. Stud. Oceanogr.* 8, 181–213. doi: 10.1016/j.dsr2.2012.08.006

Błażewicz-Paszkowycz, M., Jennings, R. M., Jeskulke, K., and Brix, S. (2014). Discovery of swimming males of Paratanaoidea (Tanaidacea). *Pol. Polar Res.* 35, 415–453. doi: 10.2478/popore-2014-0022

Błażewicz-Paszkowycz, M., and Siciński, J. (2014). Diversity and distribution of Tanaidacea (Crustacea) along the Victoria Land Transect (Ross Sea. Southern Ocean). *Pol. Biol.* 37, 519–529. doi: 10.1007/s00300-014-1452-7

Bober, J., Brandt, A., Frutos, I., and Schwentner, M. (2019). Diversity and distribution of Ischnomesidae (Crustacea: Isopoda: Asellota) along the Kuril-Kamchatka Trench – A genetic perspective. *Prog. Oceanog.* 178:102174. doi: 10.1016/j.pocean.2019.102174

Brandt, A., Alalykina, I., Fukumori, H., Golovan, O., Kniesz, K., Lavrenteva, A., et al. (2018a). First insights into macrofaunal composition from the SokhoBio expedition (Sea of Okhotsk, Bussol Strait and northern slope of the Kuril-Kamchatka Trench). *Deep Sea Res. Part II Top. Stud. Oceanogr.* 154, 106–120. doi: 10.1016/j.dsr2.2018.05.022

Brandt, A., and Barthel, D. (1995). An improved supra- and epibenthic sledge for catching Peracarida (Crustacea, Malacostraca). *Ophelia* 43, 15–23. doi: 10.1080/00785326.1995.10430574

Brandt, A., Frutos, I., Bober, S., Brix, S., Brenke, N., Guggolz, T., et al. (2018b). Composition of abyssal macrofauna along the Vema Fracture Zone and the hadal Puerto Rico Trench, northern tropical Atlantic. *Deep Sea Res. Part II Top. Stud. Oceanogr.* 148, 35–44. doi: 10.1016/j.dsr2.2017.07.014

Brandt, A., Gooday, A. J., Brandão, S. N., Brix, S., Brökeland, W., Cedhagen, T., et al. (2007). First insights into the biodiversity and biogeography of the Southern Ocean deep sea. *Nature* 447, 307–311. doi: 10.1038/nature05827

Chim, C. K., and Tong, S. J. W. (2021). Three new species of agathotanaids (Tanaidacea: Paratanaoidea: Tanaidomorpha) from the lower bathyal zone off southwestern Java, Indonesia, Indian Ocean with notes on the global distribution and diversity of Agathotanaidae. *Zootaxa* 5004, 067–106. doi: 10.11646/zootaxa.5004.1.3

Coleman, C. O. (2003). Digital inking: how to make perfect line drawings on computers. *Org. Divers. Evol.* 3, 303–304. doi: 10.1078/1439-6092-00081

Colgan, D., McLauchlan, A., Wilson, G. D., Livingston, S., Edgecombe, G., Macaranas, J., et al. (1998). Molecular phylogenetics of the Arthropoda: relationships based on histone H3 and U2 snRNA DNA sequences. *Aust. J. Zool.* 46, 419–437.

Dana, J. D. (1849). Conspectus crustaceorum. conspectus of the crustacea of the exploring expedition. *Am. J. Sci.* 8, 424–428.

Drummond, A. J., and Rambaut, A. (2007). BEAST: bayesian evolutionary analysis by sampling trees. *BMC Evol. Biol.* 7:214. doi: 10.1186/1471-2148-7-214

Drummond, A. J., Suchard, M. A., Xie, D., and Rambaut, A. (2012). Bayesian phylogenetics with BEAUti and the BEAST 1.7. *Mol. Biol. Evol.* 29, 1969–1973. doi: 10.1093/molbev/mss075

Frutos, I., Brandt, A., and Sorbe, J. C. (2016). "Deep-sea suprabenthic communities: the forgotten biodiversity," in *Marine Animal Forests*, eds S. Rossi, L. Bramanti, A. Gori, and C. Orejas Saco del Valle (Cham: Springer International Publishing), 1–29.

Frutos, I., and Jażdżewska, A. M. (2019). Deep-sea amphipod fauna of the Sea of Okhotsk. *Prog. Oceanogr.* 178, 102147. doi: 10.1016/j.pocean.2019.102147

Gage, J. D., and Tyler, P. A. (1991). *Deep-Sea Biology: A Natural History of Organisms at the Deep-Sea Floor*. Cambridge: Cambridge University Press.

Garm, A., and Watling, L. (2013). "The crustacean integument: Setae, setules, and other ornamentation," in *The Natural History of the Crustacea. Volume 1 Functional Morphology and Diversity*, eds L. Watling and M. Thiel (Oxford: Oxford University Press), 167–198.

Golovan, O. A., Błażewicz, M., Brandt, A., Jażdżewska, A. M, Jóźwiak, P., Lavrenteva, A. V., et al. (2018). Diversity and distribution of peracarid crustaceans (Malacostraca) from the abyss adjacent to the Kuril-Kamchatka Trench. *Mar. Biodiver.* 49, 1343–1360. doi: 10.1007/s12526-018-0908-3

Hansen, H. J. (1913). Crustacea Malacostraca. *Danish Ingolf Expedition* 3, 1–145.

Jakiel, A., Palero, F., and Błażewicz, M. (2019). Deep ocean seascape and *Pseudotanaidae* (Crustacea: Tanaidacea) diversity at the Clarion-Clipperton Fracture Zone. *Sci. Rep.* 9:17305. doi: 10.1038/s41598-019-51434-z

Jakiel, A., Palero, F., and Błażewicz, M. (2020). Secrets from the deep: pseudotanaidae (Crustacea: Tanaidacea) diversity from the Kuril–Kamchatka Trench. *Prog. Oceanogr.* 183:102288. doi: 10.1016/j.pocean.2020.102288

Jóźwiak, P., and Jakiel, A. (2012). A new genus and new species of Agathotanaidae (Crustacea. Tanaidacea) from West Australia. *ZooKeys* 243, 15–26. doi: 10.3897/zookeys.243.3408

Kakui, K., and Kohtsuka, H. (2015). Two new shallow-water species of *Agathotanais* (Crustacea : Tanaidacea) from Japan. *Species Divers.* 20, 45–58. doi: 10.12782/sd.20.1.045

Katoh, K., and Standley, D. M. (2013). MAFFT multiple sequence alignment software version 7: improvements in performance and usability. *Mol. Biol. Evol.* 30, 772–780. doi: 10.1093/molbev/mst010

Kudinova-Pasternak, R. K. (1970). Tanaidacea of the Kurile-Kamchatka Trench. *Akademiya Nauk SSSR* 86, 341–380.

Kudinova-Pasternak, R. K. (1983). The abyssal Tanaidacea (Crustacea) of the Iberian and west-european hollows of the Atlantic Ocean. *Zool. Zhurnal.* 62, 1170–1176.

Kudinova-Pasternak, R. K. (1989). Tanaidacees abyssales (Crustacea, Tanaidacea) des parties nord-est et centrale de l'ocean Indien (d'apres des materiaux de l'expedition francaise "Safari-II"). 2. Sous-order Tanaidomorpha. *Zool. Zhurnal* 68, 27–40.

Kudinova-Pasternak, R. K. (1990). Tanaidacea from southeastern Atlantic Ocean and north of Elephant I. Trudy Instituta Okeanologii. *Akademiya Nauk SSSR* 126, 90–107.

Kumar, S., Stecher, G., Li, M., Knyaz, C., and Tamura, K. (2018). MEGA X: molecular evolutionary genetics analysis across computing platforms. *Battistuzzi FU (Ed). Mol. Biol. Evol.* 35, 1547–1549. doi: 10.1093/molbev/msy096

Lang, K. (1971). Die Gattungen *Agathotanais* Hansen Und *Paragathotanais* n. gen. (Tanaidacea). *Crustaceana* 21, 57–71. doi: 10.1163/156854071x00229

Larsen, K. (1999). Pacific Tanaidacea (Crustacea): revision of the genus *Agathotanais* with Description of Three New Species. *Rec. Aust. Mus.* 51, 99–112.

Larsen, K. (2005). *Deep-Sea Tanaidacea (Peracarida) From the Gulf of Mexico*. Leiden: Brill, doi: 10.1163/9789047416883

Larsen, K. (2007). Family Agathotanaidae Lang, 1971. *Zootaxa* 1599, 41–60.

Larsen, K., and Shimomura, M. (2007). Tanaidacea (Crustacea: Peracarida) from Japan III. The deep trenches: the Kurile-Kamchatka Trench and Japan Trench. *Zootaxa* 1599, 1–149.

Lörz, A. N., Jażdżewska, A. M., and Brandt, A. (2018). A new predator connecting the abyssal with the hadal in the Kuril-Kamchatka Trench. *NW Pacific. PeerJ* 6, e4887. doi: 10.7717/peerj.4887

Malyutina, M. V., Brandt, A., and Ivin, V. V. (2015). *The Russian-German Deep-Sea Expedition SokhoBio (Sea of Okhotsk Biodiversity Studies) to the Kurile Basin of the Sea of Okhotsk on Board of the R/V Akademik MA Lavrentyev. 71st Cruise, July 6th-August 6th, 2015. The Cruise Report. 1–103 (Report submitted to: Ministry of Education and Science (Russia) and Federal Ministry of Education and Research (Germany)*. Sofia: Ministry of Education and Science.

Nürnberg, D., and Tiedemann, R. (2004). Environmental change in the Sea of Okhotsk during the last 1.1 million year. *Paleoceanography* 19, A4011. doi: 10.1029/2004PA001023

O'Hara, T. D. (2019). The Eastern Australian Marine Parks: Biodiversity, Assemblage Structure, Diversity and Origin. Report to Parks Australia from

the National Environmental Science Program Marine Biodiversity Hub. Melbourne: Museum Victoria.

O'Hara, T. D., Williams, A., Althaus, F., Ross, A. S., and Bax, N. J. (2020a). Regional-scale patterns of deep seafloor biodiversity for conservation assessment. *Divers Distrib.* 26, 479–494. doi: 10.1111/ddi.13034

O'Hara, T. D., Williams, A., Ahyong, S. T., Alderslade, P., Alvestad, T., Bray, D., et al. (2020b). The lower bathyal and abyssal seafloor fauna of eastern Australia. *Mar. Biodivers. Rec.* 13:11. doi: 10.1186/s41200-020-00194-1

Pabis, K., Błażewicz-Paszkowycz, M., Jóźwiak, P., and Barnes, D. K. A. (2014). Tanaidacea of the Amundsen and Scotia seas: an unexplored diversity. *Antarct. Sci.* 27, 19–30. doi: 10.1017/s0954102014000303

Pabis, K., Jóźwiak, P., Lörz, A.-N. N., Schnabel, K. E., and Błażewicz-Paszkowycz, M. (2015). First insights into the deep-sea tanaidacean fauna of the Ross Sea: species richness and composition across the shelf break, slope and abyss. *Polar Biol.* 38, 1429–1437. doi: 10.1007/s00300-015-1706-z

Palero, F., Hall, S., Clark, P. F., Johnston, D., MacKenzie-Dodds, J., and Thatje, S. (2010). DNA extraction from formalin-fixed tissue: new light from the deep sea. *Sci. Mar.* 74, 465–470. doi: 10.3989/scimar.2010.74n3465

Rambaut, A., Drummond, A. J., Xie, D., Baele, G., and Suchard, M. A. (2018). Posterior summarization in Bayesian phylogenetics using Tracer 1.7. *Syst. Biol.* 67, 901–904. doi: 10.1093/sysbio/syy032

Riehl, T., Brenken, N., Brix, S., Driskell, A., Kaiser, S., and Brandt, A. (2014). Field and laboratory methods for DNA studies on deep-sea isopod crustaceans. *Pol. Polar Res.* 35, 203–224.

Saeedi, H., and Brandt, A. (2020). *Biogeographic Atlas of the Deep NW Pacific Fauna*. Electronic publication: Pensoft. doi: 10.3897/ab.e51315.

Schofield, C. (2018). "Exploring the deep frontier," in *Global Commons and the Law of the Sea*, ed. K. Zou (Leiden: Brill), 151–167. doi: 10.1163/9789004373334_010

Sieg, J. (1986). *Tanaidacea (Crustacea) von der Antartiks und Subantarktis. II. Tanaidacea gesammelt von Dr. J. W. Wägele während der Deutschen Antarktis Expedition 1983*. Kiel: Mitteilungen aus dem Zoologischen Museum der Universität Kiel, 1–80.

Stępień, A., Pabis, P., and Błażewicz, M. (2019). Tanaidacean faunas of the sea of okhotsk and northern slope of the Kuril-Kamchatka Trench. *Prog. Oceanogr.* 178:102196. doi: 10.1016/j.pocean.2019.102196

Sweetman, A. K., Thurber, A. R., Smith, C. R., Levin, L. A., Mora, C., Wei, C., et al. (2017). Major impacts of climate change on deep-sea benthic ecosystems. *Elementa Sci. Anthrop.* 5, 4. doi: 10.1525/elementa.203

Washburn, T. W., Menot, L., Bonifácio, P., Pape, E., Błażewicz, M., Bribiesca-Contreras, G., et al. (2021). Patterns of macrofaunal biodiversity across the clarion-clipperton zone: an area targeted for seabed mining. *Front. Mar. Sci.* 8:626571. doi: 10.3389/fmars.2021.626571

Woolley, S. N. C., Tittensor, D. P., Dunstan, P. K., Guillera-Arroita, G., Lahoz-Monfort, J. J., Wintle, B. A., et al. (2016). Deep-sea diversity patterns are shaped by energy availability. *Nature* 533, 393–396. doi: 10.1038/nature 17937

Conflict of Interest: The authors declare that the research was conducted in the absence of any commercial or financial relationships that could be construed as a potential conflict of interest.

Publisher's Note: All claims expressed in this article are solely those of the authors and do not necessarily represent those of their affiliated organizations, or those of the publisher, the editors and the reviewers. Any product that may be evaluated in this article, or claim that may be made by its manufacturer, is not guaranteed or endorsed by the publisher.

Copyright © 2022 Stępień, Jóźwiak, Jakiel, Pełczyńska and Błażewicz. This is an open-access article distributed under the terms of the Creative Commons Attribution License (CC BY). The use, distribution or reproduction in other forums is permitted, provided the original author(s) and the copyright owner(s) are credited and that the original publication in this journal is cited, in accordance with accepted academic practice. No use, distribution or reproduction is permitted which does not comply with these terms.

frontiers | Frontiers in Marine Science

REVIEW
published: 30 June 2022
doi: 10.3389/fmars.2022.799191

Challenges and Advances in the Taxonomy of Deep-Sea Peracarida: From Traditional to Modern Methods

Inmaculada Frutos[1], Stefanie Kaiser[1†], Łukasz Pułaski[2,3], Maciej Studzian[2,3] and Magdalena Błażewicz[1]*

[1] Department of Invertebrate Zoology and Hydrobiology, Faculty of Biology and Environmental Protection, University of Lodz, Łódź, Poland, [2] Department of Molecular Biophysics, Faculty of Biology and Environmental Protection, University of Lodz, Łódź, Poland, [3] Laboratory of Transcriptional Regulation, Institute of Medical Biology, Polish Academy of Sciences, Łódź, Poland

OPEN ACCESS

Edited by:
Ana Colaço,
Marine Research Institute (IMAR),
Portugal

Reviewed by:
Oliver Simon Ashford,
OceanMind, United Kingdom
Andres G. Morales-Nunez,
University of Maryland Eastern Shore,
United States

***Correspondence:**
Inmaculada Frutos
inmaculada.frutos@biol.uni.lodz.pl

†Present address:
Stefanie Kaiser,
INES Integrated Environmental
Solutions UG, c/o DZMB,
Wilhelmshaven, Germany

Specialty section:
This article was submitted to
Deep-Sea Environments and Ecology,
a section of the journal
Frontiers in Marine Science

Received: 21 October 2021
Accepted: 05 May 2022
Published: 30 June 2022

Citation:
Frutos I, Kaiser S, Pułaski Ł,
Studzian M and Błażewicz M (2022)
Challenges and Advances in the
Taxonomy of Deep-Sea Peracarida:
From Traditional to Modern Methods.
Front. Mar. Sci. 9:799191.
doi: 10.3389/fmars.2022.799191

As one of the oldest branches of biology, taxonomy deals with the identification, classification and naming of living organisms, using a variety of tools to explore traits at the morphological and molecular level. In the deep sea, particular challenges are posed to the taxonomic differentiation of species. Relatively limited sampling effort coupled with apparent high diversity, compared to many other marine environments, means that many species sampled are undescribed, and few specimens are available for each putative species. The resulting scarce knowledge of intraspecific variation makes it difficult to recognize species boundaries and thus to assess the actual diversity and distribution of species. In this review article, we highlight some of these challenges in deep-sea taxonomy using the example of peracarid crustaceans. Specifically, we offer a detailed overview of traditional as well as modern methods that are used in the taxonomic analysis of deep-sea Peracarida. Furthermore, methods are presented that have not yet been used in peracarid taxonomy, but have potential for the analysis of internal and external structures in the future. The focus of this compilation is on morphological methods for the identification, delimitation and description of species, with references to molecular analysis included where relevant, as these methods are an indispensable part of an integrative taxonomic approach. The taxonomic impediment, i.e. the shortage of taxonomists in view of a high undescribed biodiversity, is discussed in the context of the existing large taxonomic knowledge gaps in connection with the increasing threat to deep-sea ecosystems. Whilst peracarid crustaceans are used here as an exemplary taxon, the methodology described has broad relevance to many other deep-sea taxa, and thus will support broader research into deep-sea biodiversity and ecology more widely.

Keywords: integrative taxonomy, morphology, microscopy, imaging, suprabenthos, Isopoda, Tanaidacea, Amphipoda

1 INTRODUCTION

The dichotomy in deep-sea biodiversity research consisting of a gap between the sheer scale of the deep sea and our incomplete knowledge of what actually lives there, is immense; areas away from the shelf edge making up the deep sea cover more than two-thirds of the Earth's global surface, but only a tiny portion of this has been examined by scientists (Ramirez-Llodra et al., 2010; Costello and Chaudhary, 2017). It is in part because of this limited knowledge that estimates of how many metazoan species to expect in the deep sea vary widely, ranging between 0.5 to more than 10 Mio. species (May, 1992; Grassle and Maciolek, 1992; Poore and Wilson, 1993; Lambshead and Boucher, 2003; Appeltans et al., 2012). There are currently > 26,000 named species catalogued in the World Register of Deep-Sea Species (WoRDSS; Glover et al., 2021), but certainly many more are to be discovered, especially among the inconspicuous, small-size and short-ranged fractions (Mora et al., 2011).

The discovery and description of the first species from the deep sea, the sea pen *Umbellula encrinus* (Linnaeus, 1758), heralded the beginning of the taxonomic study of deep-sea organisms. Remarkably, this coincided with the revision of the previous classification system and the birth of modern taxonomy as introduced by Linnaeus (1735) *Systema Naturae*. Our knowledge of deep-sea species has been thereby closely linked, on the one hand, with the ever-improving technology and logistics for taking samples from the deep sea and, on the other hand, with methodological advances to make external and internal parts of organisms visible. Here, the invention of the first compound microscopes towards the end of the 16th century had pushed taxonomic work forward considerably since it allowed to study the smaller size fractions and thus greatly increased the number of known species (Rosenthal, 2009; Manktelow, 2010). Regarded today as art, the detailed scientific illustrations of taxonomists at the earliest time such as Carl Linnaeus (1707–1778), Alexander von Humboldt (1769–1859), Ernst Haeckel (1834–1919), or Georg Ossian Sars (1837–1927) were indispensable in the absence of the photographic imaging techniques available today (**Figures 1A–G**). Isolated deep-sea samples had already been collected prior, but it was only 150 years ago that a global collection as part of the HMS *Challenge*r Expedition (1872–1876) could refute the thesis that the deep sea is devoid of life (Murray and Renard, 1891). Research into deep-sea biodiversity has gradually shifted from a more exploratory focus that involved a mere inventory of species to a more systematic approach that addresses issues such as how deep-sea diversity is structured. Likewise, taxonomy, as a legacy of Charles Darwin (1809–1882), Ernst Haeckel and more recently the German systematist Willi Hennig (1913–1976), has made a transition from classifying taxa based on their morphological appearance (phenetics) to using homologous characters to illuminate phylogenetic relationships (cladistics).

To date, referring to morphological features is still the means of choice when delimiting, identifying and describing deep-sea species. This is likely because it seems easy to apply, and others, such as the biological species concept *sensu* Mayr (1942; "Species are groups of interbred natural populations reproductively isolated from other such groups") cannot readily be applied due to the difficulty to obtain data on reproduction of deep-sea species (see also Brandt et al., 2012). With the advent of molecular approaches in taxonomy in general and deep-sea taxonomy in particular, however, many complications are associated with the phenotypic data, including evidence of sexually dimorphic or polymorphic species, convergence, and phenotypic plasticity (Raupach and Wägele, 2006; Vrijenhoek, 2009; Błażewicz-Paszkowycz et al., 2012; Brandt et al., 2012; Riehl et al., 2012; Błażewicz-Paszkowycz et al., 2014; Brandt et al., 2014; Mohrbeck et al., 2021). While molecular techniques have certainly helped expedite species identification and delimitation, phylogenetic relationships and biodiversity assessment, also on the background of intensifying anthropogenic impacts on deep-sea ecosystems, the description and naming of species remains pivotal to understanding their ecological function and evolution. Traditional taxonomy, however, in general cannot keep up with automated, high-throughput molecular methods that generate large amounts of data at a rapid pace, resulting in a large number of unnamed species on taxonomists' shelves, which remain unavailable for conservation purposes (Pante et al., 2015; Gellert et al., 2022). Moreover, for many (and not only) biologists, species identification also reduced to the pragmatic ability to distinguish between species remains far from a satisfactory solution. The simple curiosity to know and understand biodiversity in every detail at different levels of life organization, as well as the search for answers to *how* and *why*, goes beyond rapid and precise species identification (Will et al., 2005; Wheeler, 2018; Dupérré, 2020).

In that regard, morphological techniques used in deep-sea taxonomy did not stand still, but are constantly being further developed or have been introduced as new applications. For example, Confocal Laser Scanning Microscopy (CLSM) was originally developed in the 1950s to map the anatomy of the human nervous system and is now increasingly being used for the taxonomic analysis of microscopic invertebrates in the deep sea (Michels and Büntzow, 2010; Brandt et al., 2014; Meißner et al., 2017; Martínez Arbizu and Petrunina, 2018; Jennings et al., 2018; Kaiser et al., 2018; Błażewicz et al., 2019; Chim and Tong, 2020; Kaiser et al., 2021; Demidov et al., 2021). 3-D visualizations of internal structures are reconstructed from histological sections (Neusser et al., 2016; Bober et al., 2018; Gooday et al., 2018). Underwater Hyperspectral Imagery has been employed to aid identification of deep-sea megafaunal species owing to their specific spectral profiles alongside automated tools for the annotation of benthic fauna from video or still imagery (Langenkämper et al., 2017; Dumke et al., 2018; Kakui and Fujiwara, 2020; Singh and Mumbarekar, 2021).

The remit of this review article is to compile and evaluate available traditional and modern tools and techniques in morphology-based taxonomy with a focus on peracarid crustaceans. With more than 21,000 described species, the malacostracan superorder Peracarida is a highly diverse group containing about a third of the total richness of crustaceans (Appeltans et al., 2012; Wilson and Ahyong, 2015). Common to

FIGURE 1 | Scientific illustrations of peracarids as complement of taxa description from past to present. **(A)** Isopod genus *Astacilla* Cordiner, 1793 illustrated by Cordiner (1793). **(B)** *Mesopodopsis slabberi* (van Beneden, 1861), the earliest illustrated mysid by Slabber (1778). **(C)** *Diastylis scorpioides* (Lepechin, 1780), the earliest published illustration of a cumacean as *Oniscus scorpioides* Lepechin, 1780 (see Holthuis, 1964). **(D)** *Diastylis scorpioides* (Lepechin, 1780), illustrated by G.O. Sars more than one century later (G.O. Sars, 1900). **(E)** The amphipod *Pardalisca abyssi* Boeck, 1871 illustrated after the voyage of H.M.S. *Challenger* during the years 1873–76 (Stebbing, 1888). **(F)** Original hand inked drawing made by Roger Bamber for the description of the tanaid *Zeuxo holdichi* Bamber, 1990. **(G)** Original plate outline with the drawings made by Édouard Chevreux for the amphipod description *Pontogeneia minuta* Chevreux, 1908 (Crustacean collection MNHN). **(H)** Compound microscope equipped with *camera lucida* to draw specimens for taxonomical purposes (photo I Frutos). **(I)** Preparing a plate by hand inking from previously made pencil drawings (photo I Frutos). **(J)** Electronical inking of drawings using a drawing tablet and computer (photo I Frutos).

all peracarids is brood care, whereby embryos are carried around in a ventral brood pouch formed by coxal oostegites until juveniles are released. Peracarids occur in all aquatic habitats, including caves, freshwater, stygobiont and marine environments, but only the oniscidean isopods contain truly terrestrial species. Besides extant species, they have occurrences in the fossil record, including deep-sea areas (Secrétan and Riou, 1986; Selden et al., 2016; San Vicente and Cartanyà, 2017; Luque and Gerken, 2019). Spanning different size classes, from meio- to megafauna, the highest diversity of peracarids is likely to be found within the macrofauna, where they represent one of the most diverse groups in the deep sea (Hessler and Jumars, 1974; Sanders et al., 1985; Frutos et al., 2017a; Brandt et al., 2019; Washburn et al., 2021). Peracarids are the main component of suprabenthos, which includes all swimming bottom-dependent animals performing, with varying amplitude, intensity, and regularity, seasonal or daily vertical migrations above the seafloor (Brunel et al., 1978; Frutos et al., 2017a; Ashford et al., 2018). Most species of deep-sea peracarids are benthic, with tanaidaceans and some isopod taxa living mostly infaunally, whilst many amphipods, isopods and cumaceans are known as good swimmers (Błażewicz-Paszkowycz et al., 2012; Poore and Bruce, 2012). Shrimp-like mysids and lophogastrids similarly have good swimming capacities, representing members of suprabenthic (mysids) and pelagic (lophogastrids) communities (San Vicente et al., 2014a). Although the variety of lifestyles, morphologies and functions of deep-sea peracarids is large, with some exceptions, a general suite of taxonomic working methods can be applied to their study (including the study of some fossil specimens).

This review is intended to describe the entire process required for the morphological examination of deep-sea peracarids, from deep-sea sampling to long-term storage in historical collections. The focus is on fixation and conservation for microscopy as well as the selection and application of imaging techniques. Although this compilation is dedicated to the morphological analysis, recommendations for sample preparation are also given with regard to genetic/omic studies as part of an integrative workflow. Given the great diversity of peracarids in the deep sea, we hope that this overview will find broad application and importance in exploring the cornerstone of any biological research there, the species.

2 METHODS FOR SAMPLE PREPARATION

Deep-sea science is indisputably expensive and logistically difficult. Study areas are usually far away from the coast, sampling itself takes long hours, and apart from vents or seeps, faunal densities are typically low. Moreover, the ship-time costs, the effort and number of people involved to get a sample, with all the physical difficulties to successfully work at great ocean depth, make deep-sea material very precious. While this is common sense, prior to sampling consideration should therefore be given to how best to sample, process and fix samples simultaneously for various purposes (e.g., morphological, molecular, ecological and biochemical) in order to get the most out of the material. At the same time, media and methods for long-term storage need to be evaluated so that the vouchers and slides are retained for future work. A full representation of the described workflow of sample collection and processing is shown in **Figure 2**.

2.1 Sampling and Sample Processing

Basically, two ways of collecting data are common: 1) still or video imagery *in situ,* and 2) direct sampling (Schiaparelli et al., 2016). Identification to the species level using images is difficult or even impossible for the megafauna (Hanafi-Portier et al., 2021; Horton et al., 2021), so that *ex-situ* examinations are required or even mandatory for the mostly much smaller Peracarida. The majority of deep-sea peracarids are sediment-bound, i.e. living in, on or just above the seabed (suprabenthic lifestyle). Depending on lifestyle and mobility of the target organisms, a variety of benthic sampling devices are used in deep-sea research. On soft bottoms, in general, coring devices, including box corer, multi- and megacorer, collect epi- and infaunal species; towed apparatus (trawls, sledges and dredges) is used for the epi- and supra-fauna; as well as baited and sediment traps, for the collections of more mobile and/or pelagic species. Manned submersibles or remotely operated vehicles (ROV) can help in the sample collection by means of push-corer, suction pump, small nets or picking up larger structures on hard substrata (for sampling specificities see Jamieson, 2016; Kaiser and Brenke, 2016; Kelley et al., 2016; Narayanaswamy et al., 2016; Frutos et al., 2017a). In water column studies, pelagic peracarid species are collected by means of mid-water trawls or plankton nets (Kürten et al., 2013; MacIsaac et al., 2014; Papiol et al., 2019); the latter are also suitable as collector of benthic peracarids if they are used as additional sampler attached to trawling devices such as otter or beam trawls (Nouvel and Lagardère, 1976; Lagardère, 1977). In addition, peracarids can also be sampled indirectly by examining the gut content of decapod or the fish stomach content, because they are their food source (Sorbe, 1981; Carrasón and Matallanas, 2001; Preciado et al., 2017). The advantages or disadvantages for the use of the aforementioned types of sampling devices are summarized in **Table 1**; however, an optimal choice is the combination of different equipment types to sample (Taylor et al., 2021; Ríos et al., 2022), which also provides complementary information on species behavior (Frutos and Sorbe, 2010; San Vicente et al., 2014b).

The choice of sampling devices depends on the target taxon (with regard to size class and lifestyle), seafloor topography, substrate type and depth, as well as data requirements (qualitative *vs*. quantitative). Benthic sledges are useful, for instance, to collect specimens with high swimming capacities (i.e. mysids and lophogastrids; Frutos, 2006), as well as relatively high specimen numbers, and thereby enable more coherent morphological and genetic assessment. Although sledges provide large numbers of peracarid fauna, additional equipment (such as opening/closing system of nets, flowmeters or pingers in the sledge frame) is required to better express abundances as densities (Brunel et al., 1978; Sorbe, 1983; Cartes et al., 1994; Dauvin et al, 1995; Frutos, 2006; Frutos et al., 2017a). Corers, by contrast, only provide low faunal densities, but offer

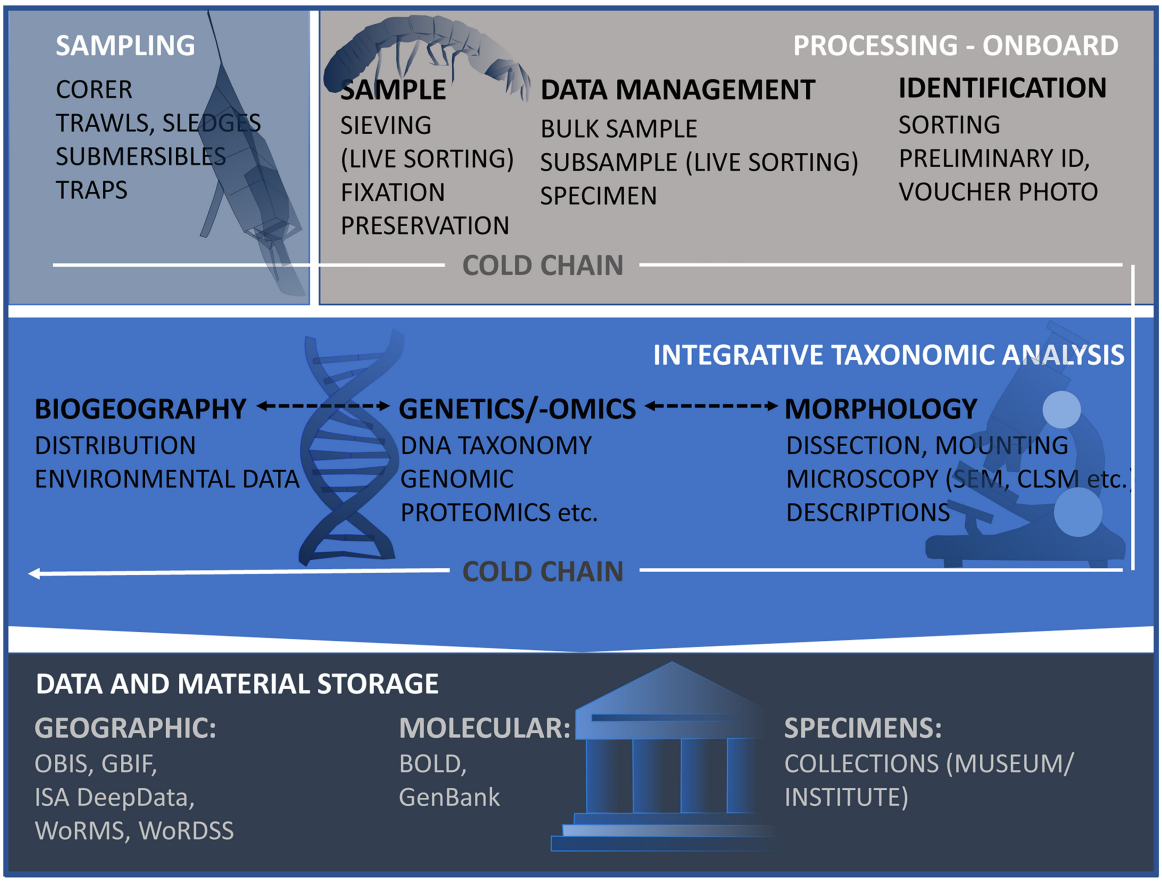

FIGURE 2 | Workflow to illustrate all steps that are required for the taxonomic investigation of the deep-sea peracarid fauna under the cold chain regime (Riehl et al., 2014) - from sampling, morphological taxonomic investigation, molecular and biogeographic analysis to the final storage of samples and data. Links to: OBIS, Ocean Biogeographic Information System[1]; GBIF, Global Biodiversity Information Facility[2]; DeepData, Deep Seabed and Ocean Database of the International Seabed Authority[3]; WoRMS, World Register of Marine Species[4]; WoRDSS, World Register of Deep-Sea Species[5]; BoLD, Barcode of Life Data System[6]; and Genbank[7]. ([1]https://obis.org/; [2]https://www.gbif.org/; [3]https://data.isa.org.jm/isa/map/; [4]http://www.marinespecies.org/; [5]http://www.marinespecies.org/deepsea/; [6]https://www.boldsystems.org/; [7]https://www.ncbi.nlm.nih.gov/genbank/).

quantitative insights when collecting undisturbed sediment surfaces (Jóźwiak et al., 2020; Lins and Brandt, 2020).

In all cases, minimizing mechanical damage to the specimens during sampling and processing to avoid loss of taxonomic information, and considering different preservation options for the same sample are important considerations. On the one hand, this includes careful handling during sampling and sample processing (washing and sieving), but also swift storage of the samples, especially if genetic or biochemical analyses are to be carried out. For example, precautions should be taken for trawled devices prior to sampling to avoid hard substrate entering the nets and grinding individuals (Kaiser and Brenke, 2016). Since sediment is part of the sample, it is important to remove it by sieving to maximize fixative concentration and thus improve sample preservation. As crustaceans can easily lose their legs and antennae, which is often essential for taxonomic identification, sediment samples should therefore be carefully sieved, if necessary with prior elutriation of the sediment samples in seawater.

Processing the samples for different purposes needs specimens to be removed from the sediment as soon as possible after the arrival of the sample on deck. Here, the maintenance in high ethanol content may arguably be even more crucial for genetic analysis (see *3.2.1 Light Microscopy*) than to maintain a cold chain protocol. The latter has been thought to be essential for molecular work on deep-sea isopods (Riehl et al., 2014). For sampling under tropical climatic conditions, however, it is strongly recommended that the samples are transferred to a cold environment as soon as possible. A disadvantage of fixing the entire sample in ethanol, however, is that the tegument/cuticle of the peracarids becomes hard and stiff and could impede further morphological examination (e.g. of subcuticular elements), while the setae required for morphological determination, become brittle and can break off. Furthermore, some morphological features can only be observed in live (unfixed) specimens. For example, in deep-sea amphipods, optical structures often can only be visualized in live animals: *Leucothoe cathalaa* is showing the

TABLE 1 | The most common types of sampling devices used for collecting peracarids.

Type of sampling	Type of sampler	Sampling Equipment	Advantages	Disadvantages	References
Direct (Biological)	Coring devices	Grab	Mainly infaunal species Quantitative samples	Small number of individuals Optimal at shallower depths	Esquete et al., 2014 Jakiel et al., 2018 Rodríguez et al., 2021
		Box-corer	Mainly infaunal species Does not disturb sediments Quantitative samples	Small number of individuals High-mobility species not represented	Chardy, 1979 Błażewicz-Paszkowycz et al., 2011 Wilson, 2017 Ashford et al., 2018
		Multi-corer	Meiobenthic species Undisturbed sediments Quantitative samples	Small-sized specimens small number of individuals	Schmidt and Martínez Arbizu, 2015; Rosli et al., 2016 Schmidt et al., 2018
	Towed devices	Dredge	Epibenthic species Hard-bottom sampling	only large specimens small number of individuals	Kensley, 1989 Bamber, 2007 Frutos et al., 2017b
		Beam trawl	Epibenthic species Large specimens	small number of individuals Accidental pelagic species	Moreira, 1973 Bruce, 2005 Serrano et al., 2017
		Sledge	High number of individuals Epi- and suprabenthic species	High-tech models are heavy and expensive	Hessler and Sanders, 1967 Buhl-Jensen, 1986 Almeida et al., 2017 Frutos et al., 2017a
		Otter trawl	Epi- and suprabenthic species Big-sized specimens Peracarids can be recovered from decapod/fish stomach contents	Small number of individuals From stomach contents, peracarids are partially digested	Sánchez et al., 2008 Serrano et al., 2011 Preciado et al., 2017
		Plankton net	Pelagic species Attached to trawls provides high numbers of benthic peracarids	Net can be damaged on rough bottoms	Nouvel and Lagardère, 1976 Zeidler, 1990; Shimomura and Ohtsuka, 2005 Kürten et al., 2013 Papiol et al., 2019
	Traps	Baited	Huge number of individuals	Only scavengers	Barnard and Ingram, 1990 Frutos and Sorbe, 2010 Horton et al., 2020
		Sediment	Specimens perfectly preserved Good-swimming peracarids	Accidental catches Unusable for genetics (formalin fixation)	Corbera, 2006 Guidi-Guilvard et al., 2007 Kraft et al., 2013
In situ observation	Underwater vehicles	ROV	Imaging species in their habitat Collecting peracarids from hard bottoms Species from vulnerable and extreme habitats Most of taxa are new to science	Species identification requires the specimen Small number of individuals	Tandberg et al., 2012 Corbari and Sorbe, 2018 Lörz and Horton, 2021
		Manned submersibles	Scientist is onboard to sample Collecting peracarids by means of push-corer & nets Species from vulnerable and extreme habitats Most of taxa are new to science	Species identification requires the specimen Small number of individuals	Shaw, 1989 Martin et al., 1993 Bellan-Santini and Thurston, 1996 Corbera et al., 2008

Sampling equipment is classified in general terms. Advantages/disadvantages are specified with regard to abundance or body size of collected individuals. For additional sampling equipment specificities see Jamieson, 2016; Kaiser and Brenke, 2016; Kelley et al., 2016; Narayanaswamy et al., 2016; Frutos et al., 2017a.

whitish pigmentation of the rounded eye before storage in preservative medium (**Figure 3E**, while its eyes are hardly visible in preserved specimens, even under light microscope (Frutos and Sorbe, 2013). Equally, samples that are to be frozen, e.g. for biochemistry studies, should be identified as accurate as possible and pictured before being preserved. Thus, live sorting should be considered, whenever possible, whereby the respective individuals are selected directly from the sample and individually identified, photographed and fixed (Brix et al., 2020; Ahyong et al., 2022).

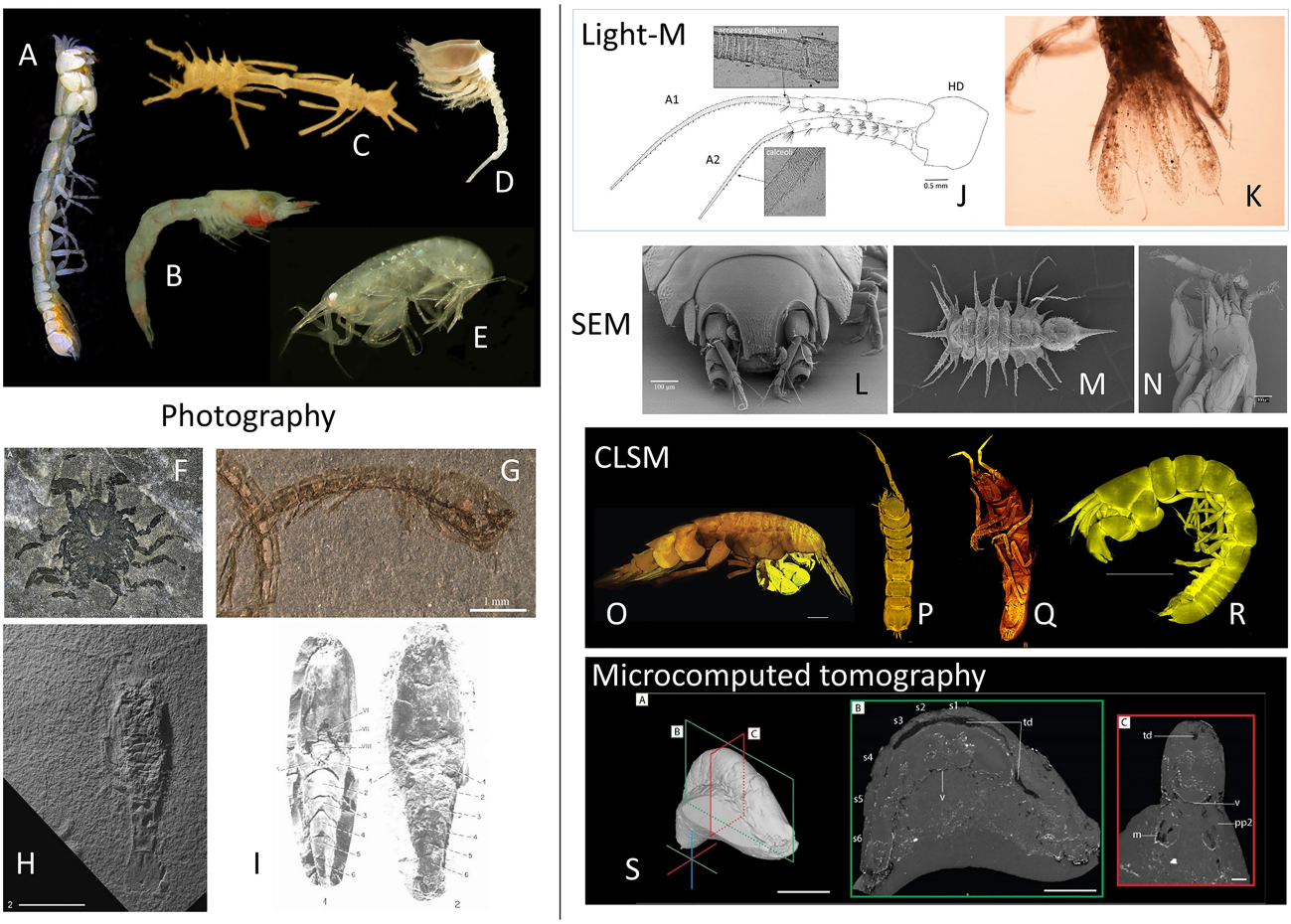

FIGURE 3 | Peracarida specimens visualized applying different modern imaging techniques to complement the taxonomical description of species. **(A–G)** Digital still camera on stereomicroscope. **(H, I)** Still camera. **(J, K)** dissected specimen under Light microscope. **(L–N)** Scanning Electron Microscope. **(O–R)** Confocal Laser Scanning Microscope. **(S)** Microcomputed tomograph. **(A)** The paranarthrurellid tanaidacean *Armatognathia swing* Błażewicz and Jóźwiak, 2019 from Błażewicz et al. (2019) under Creative Commons license. **(B)** The mysid *Paramblyops rostratus* (Holt and Tattersall, 1905) from Frutos (2017). **(C)** The ischnomesid isopod *Cornuamesus longiramus* (Kavanagh and Sorbe, 2006), and **(D)** the diastylid cumacean *Campylaspis vitrea* Calman, 1906 from Frutos et al. (2017a). **(E)** The leucothoid amphipod *Leucothoe cathalaa* Frutos and Sorbe, 2013 from Frutos and Sorbe (2013). **(F)** The first asellote isopod from the fossil record *Fornicaris calligarisi* Wilson and Selden, 2016 from Selden et al. (2016),© The Crustacean Society, reprinted with permission of Oxford University Press on benhalf of The Crustacean Society. **(G)** The oldest crown cumacean *Eobodotria muisca* Luque and Gerken, 2019 from Luque and Gerken (2019), reprinted with permission of Royal Society Publishing. **(H)** The oldest known fossil mysid *Aviamysis pinetellensis* San Vicente and Cartanyà, 2017 from San Vicente and Cartanyà (2017), reprinted with permission of Cambridge University Press. **(I)** Two fossil lophogastrids of family Lophogastridae from Secrétan and Riou (1986), reprinted with permission of Annales of Paléontologie. **(J)** The eusirid amphipod *Dorotea papuana* Corbari, Frutos and Sorbe, 2019 from Corbari et al. (2019). **(K)** The paranthurid isopod *Paranthura santiparrai* Frutos, Sorbe and Junoy, 2011 from Frutos et al. (2011). **(L)** The nannoniscid isopod *Austroniscus obscurus* Kaiser and Brandt, 2007 from Kaiser and Brandt (2007). **(M)** The paramunnid isopod *Pentaceration bifficlyro* Kaiser and Marner, 2012 from Kaiser and Marner (2012). **(N)** The paranthurid isopod *Paranthura santiparrai* Frutos, Sorbe and Junoy, 2011 from Frutos et al. (2010). **(O)** The oedicerotid amphipod *Oedicerina teresae* Jażdżewska, 2021 from Jażdżewska et al. (2022) under Creative Commons license. **(P)** The nannoniscid isopod *Thaumastosoma platycarpus* Hessler, 1970 from Kaiser et al. (2018). **(Q)** The nannoniscid isopod *Nannoniscus magdae* Kaiser, Brix and Jennings, 2021 from Kaiser et al. (2021). **(R)** The paranthrurellid tanaidacean *Paranarthrurella arctophylax* (Norman and Stebbing, 1886), from Błażewicz et al. (2019) under Creative Commons license. **(S)** Fossil lophogastrid specimen showing internal anatomy after microcomputed tomography, from Jauvion (2020).

2.2 Fixation

Fixation of specimens in taxonomic studies aims to prevent the spontaneous deterioration of taxonomically important features of the collected animals and thus its methods should be selected and applied with a thorough regard for the subsequently planned discovery pipeline of methods. The two main threats to morphological and genetic features of marine crustaceans that have to be prevented by fixation are dead cell/tissue autolysis by endogenous enzymes and destruction of biological material by microbial (bacterial/fungal) contaminants. An optimal fixative should aim to prevent both threats at the same time. Specimen fixation is of paramount importance if a significant time lapse occurs between collection and analysis, which is usually the case for marine samples, especially deep-sea ones, collected on board of research vessels and later analyzed in research institutions on dry land. In fact, the current average shelf life of new species

between discovery and description is about 21 years (Fontaine et al., 2012). Furthermore, good preservation is also extremely important for material of taxonomic significance, especially type material that has to be available for subsequent re-analysis in museum collections. While the term "preservation" is usually used for application of fixatives for prolonged storage of museum specimens, both underlying principles and specific compounds used are analogous to fixation for general purposes and will be discussed together here.

Fixation inevitably changes the physico-chemical properties of the specimen, so it has to be performed in a way that is compatible with downstream taxonomic techniques, both with regard to imaging morphology for identification purposes and to analyzing genetic and biochemical make-up of the specimen. Thus, selection of proper fixative is always a trade-off between efficiency and durability of preservation on one hand and lack of significant interference with taxonomically important features of the specimen (Eltoum et al., 2001). Among the properties that need to be considered are i.e.: crude shape changes which may result from physico-chemical processes (drying, osmotic swelling); delicate morphological elements that may be damaged during the fixation process itself; physical features that may deteriorate upon chemical reactions with the fixative, especially upon prolonged exposure (color, transparency, flexibility, malleability etc.); biochemical composition (e.g. lipid or carbohydrate content of specific tissues); integrity of nucleic acids and their accessibility to isolation; antigenic properties and/or enzymatic activity of proteins (Barbosa et al., 2014). With regard to deep-sea biological investigations, another consideration that has to be taken into account is the availability of fixative at the collection site: this includes questions of logistics (ease of transport, security), legal issues, shelf life of the fixative itself etc. Sometimes, a two-tier fixation protocol may be adopted, with simpler fixative applied on board the collection vessel for short-term preservation and subsequent exchange for museum-grade fixative during preparation for long-term storage in a biological collection. Of course, taxonomists are often confronted by the fact that the specimens to be examined have not been collected and preserved by themselves, so they no longer have a choice of fixation method, but some fixatives can be exchanged for others (e.g. ethanol can be replaced with formaldehyde and *vice versa*) prior to analysis if interference is expected (Pereira et al., 2019). As the published literature is contradictory about the compatibility of some fixation protocols with subsequent taxonomic analysis (especially by nucleic acid isolation, PCR and/or next generation sequencing) and anecdotal evidence for the suitability of individual protocols prevails, taxonomists are recommended to understand the physico-chemical principles of fixation and of genetic methods, so that an informed decision may be made. A classification of the fixatives most commonly used in the Peracarida taxonomic community and short description of their main advantages and disadvantages is included in **Table 2**.

In some cases, taxonomic studies are performed not on specimens from extant taxa collected while still alive, but on subfossil or fossil material which is already naturally "fixed" or transformed into a relatively permanent, physico-chemically stable form. Morphology of preserved tissues may be studied in such samples using the same imaging techniques as described below for extant material – optical microscopy, electron microscopy or microcomputed tomography (Sánchez-García et al., 2016; Nagler et al., 2017; Jauvion, 2020; Luque et al., 2021; Robin et al., 2021), but the physical preparation of the sample lacks the fixation step, instead involving mechanical preparation (slicing, milling, polishing). For some taxa of deep-sea Peracarida, morphological studies of fossils using recently available imaging techniques led to taxonomic corrections and reclassification of whole groups of specimens: a decapod tail described as amphipod (McMenamin et al., 2013; Starr et al., 2016); samples that upon close investigation contained not amphipods but previously unknown genera and species of tanaids (Vonk and Schram, 2007); a new mysid genus (Cartanyà, 1991; San Vicente and Cartanyà, 2017) or a new lophogastrid taxon (Secrétan and Riou, 1986; Jauvion, 2020).

2.2.1 Common Fixatives

The most common fixative types in aquatic zoology can be classified into two groups: those relying on quick dehydration and those relying on molecular cross-linking of biochemical components. Both aim to quickly and efficiently inhibit the activity of enzymes (endogenous or microbial ones) which could destroy the biological macromolecules that the specimen consists of: proteases for proteins, nucleases for nucleic acids or glycosidases for carbohydrates. Dehydration withdraws the main reaction substrate for hydrolytic reactions and inactivates enzymes by coagulation-mediated denaturation. Cross-linking prevents enzyme-substrate interactions by stopping diffusion as well as by preventing conformational changes of the enzyme molecule that are crucial for its activity. Some fixation methods aim also to inhibit major lytic enzyme groups by specific biochemical interactions with their co-substrates or active sites, or to target microbial life with antibiotic toxins (**Table 2**).

The most universal and frequently used fixatives based on the dehydration principle are aliphatic alcohols, especially ethanol. Ethanol works by quickly mixing with water, penetrating the specimen, and removing the solvation shells from proteins and other molecules. The most efficient and rapid-acting concentration of 95–96% is considered the optimal fixative both for field fixation and long-term storage when preservation of tissue structure, biochemical composition and DNA for genetic analysis are important (Palero et al., 2010; Wetzer, 2015; Martin, 2016; Beninde et al., 2020).

While 70% ethanol is also historically used for long-term storage in museum collections due to its superior anti-microbial activity, numerous studies have shown that the increased water content and insufficient lytic enzyme inhibition leads to detectable levels of DNA degradation, correlating with storage time and therefore making subsequent genetic studies on material stored in the manner more difficult – especially for taxonomically valuable material (e.g. type specimens) (Marquina et al., 2021); moreover, the high-water content and lowered pH of 70% ethanol may lead to cuticle decalcification upon long-term storage, which is important especially for those peracarids

TABLE 2 | The most common types of fixatives used by peracarid taxonomists with their advantages and disadvantages summarized.

Type of fixative	Active agent	Advantages	Disadvantages	References
Dehydrating	Ethanol	Efficient fixation, relatively non-toxic, allows posterior genetic studies	Tissue shrinkage and brittleness, fast evaporation, legal issues	Wetzer, 2015; Martin, 2016;
	Isopropanol	Stronger fixation than ethanol	Slower action than ethanol	Hughes and Kaji, 2016
	Hydrophobic solvent (Carnoy's)	Preservation of hard tissues	Damage to cellular components of the specimen, removal of pigments	Presnell and Schreibman, 1997
Cross-linking	Formaldehyde	Efficient fixation, low evaporation and shrinkage, high flexibility of exoskeleton	Damages nucleic acids and hampers their isolation, relatively toxic, needs buffering	Palero et al., 2010; Wetzer, 2015;
	Glutaraldehyde	More durable fixation and less toxic than formaldehyde	Difficult sample manipulation after fixation, irreversible damage to nucleic acids	Brooker et al., 2012b
Freezing	Phase transition	Cheap and easy, allows biochemical analysis	Effective in very short term, disrupts micromorphology	Martin, 2016; Turner et al., 2016;
Coagulant	Organic acids (Bouin's)	Quick fixation and good preservation of overall morphology	Dissolves calcium carbonate in exoskeleton, may disrupt delicate morphological features	Göpel and Wirkner, 2018
	Mercuric salts (Zenker's)	Fixative and anti-microbial action at the same time	Highly toxic, not efficient in preserving hard tissues	Fryer, 1968
	Osmium tetroxide	Good fixation for fat-rich tissues, serves as fixative and electron microscopy stain at the same time	Expensive, damages nucleic acids	Kaji et al., 2014
Anti-microbial	Antibiotic/antifungal agents	Long-term protection against microbial contamination	Must be combined with an actual fixative for preservation of specimen morphology	Stegner et al., 2015
Stabilising nucleic acids	Quaternary ammonium/ caesium ions (RNAlater)	Good DNA and RNA preservation	Very expensive, does not preserve morphology well	Wetzer, 2015; Porter, 2016
	Propylene glycol	Cheap, good DNA preservation	Distortion of some morphological features	Robinson et al., 2021
	EDTA/DMSO (DESS)	Good DNA preservation	Short-term storage	Boxshall et al., 2016; Lins et al., 2021;
	EDTA/SDS	Good DNA preservation	Destruction of protein-based morphological features	Pokluda et al., 2014

that have taxonomically important calcium carbonate deposits in different forms (amorphous, calcite, aragonite) in the exoskeleton, e.g. isopods. On the other hand, rapid and complete dehydration by concentrated ethanol has the disadvantage of making arthropod exoskeletons stiff and brittle, as their natural elasticity depends to a large extent on extracellular matrix proteins which lose their properties when denatured/coagulated by water loss, leading to mechanical damage in transport or during dissection (Costa et al., 2021). The fragility of tegument is especially problematic in the case of some deep-sea Peracarida where delicate appendages and armament are often essential for taxonomic identification – therefore, an addition of up to 5% glycerol (by volume) during fixation and preservation would be strongly recommended as it softens the exoskeleton and makes it less fragile. In some cases, the tegument may also become opaque due to coagulated protein precipitation, hampering internal observation (e.g., of musculature or gut content), and taxonomically important pigmentation may be partially or totally dissolved, e.g. making eyes difficult to notice visually (Frutos and Sorbe, 2013; Campean and Coleman, 2018). Therefore, while 95% ethanol remains the optimal concentration for on-site fixation and long-term storage, it may be preferably exchanged for 70% ethanol in sample transit and before laboratory manipulations. Absolute (~100%) ethanol is much more expensive than 95% ethanol and may sometimes introduce microscopic morphological artefacts due to its extreme hygroscopy.

Methanol, while used in histological fixation, is ineffective for long-term storage of specimens for taxonomic purposes and should be avoided since its dehydration power is relatively weak, leading to insufficient protein coagulation and residual lytic activities. Isopropanol is as efficient in protein coagulation as ethanol and does not stiffen carbohydrate structures (carapaces) as much, but this advantage is offset by its relatively high price and slow diffusion into larger biological structures, leading to potential loss of fine details or DNA contained in internal structures (King and Porter, 2004).

Despite prevailing misconceptions in literature about ethanol with additives that make it unsuitable for human consumption (so-called denatured alcohol), these additives (e.g. methanol, ether or acetone) have no discernible effect on the fixation process, long-term preservation and downstream applications (when nucleic acids are isolated for genetic analysis, these additives are removed together with ethanol itself, and they are present in far too low concentrations to impact downstream processes anyway). The same is true for traces of benzene or its derivatives present in absolute ethanol. The misplaced recommendations against using denatured alcohol for

specimen preservation for genetic analysis stem from faulty interpretation of several studies where "pure ethanol" at 95% was compared to "denatured alcohol" at 70% (as this is the concentration readily available commercially in many countries), and the above-mentioned inferior performance of the latter in DNA preservation was mistakenly ascribed to the denaturing additives (Wall et al., 2014). If denatured 95% ethanol is available, it may be used for fixing deep-sea Peracarida equally to pure 95% ethanol. The main advantages of ethanol as a fixative for taxonomy of deep-sea Peracarida include: low cost, fast action, potential for long-term storage, good preservation of DNA and proteins (including linear antigenic determinants). The main disadvantages include: high volatility (and therefore potential for evaporation from non-hermetic storage containers), flammability, legal issues (especially with transport to the collection site), need for time-consuming removal for some downstream applications (especially involving nucleic acid isolation), potential for morphological distortion by rapid water removal from small specimens with delicate exoskeletons, as well as fragility of dehydrated specimens.

The most frequently used cross-linking fixative is formaldehyde which reacts with proteins, nucleic acids as well as some lipids and carbohydrates to form a durable network of covalently linked macromolecules. For long-term storage, formaldehyde is usually used at concentration of 4% (or sometimes higher). The working solution is obtained by diluting so-called formalin (stabilized concentrated solution of ca. 36%) or by de-polymerizing the solid polymer paraformaldehyde. Formaldehyde penetrates tissues quickly and preserves structures efficiently, while not dehydrating the specimen at the molecular level, leading to full preservation of flexibility of appendages and tegument, making dissection easy. Since aquatic solutions of formaldehyde are acidic (due to hydrolysis and forming of geminal methanediol), it is crucial that this fixative is buffered to neutral or slightly basic pH (7.5–8.5) when used on marine crustaceans if biochemical integrity of the tegument is to be preserved, to prevent dissolution of calcium carbonate in their exoskeleton. The most frequently used buffering agents for this task are sodium borate (borax), sodium phosphate, sodium bicarbonate and hexamethylenetetramine (urotropin) (Presnell and Schreibman, 1997; Martin, 2016). On the other hand, decalcification in acidic formaldehyde solutions makes some tegument more transparent, allowing for easier microscopic observation of internal structures. For small aquatic animals with shells or carapaces, formaldehyde is sometimes combined with compounds that accelerate protein coagulation during the initial specimen soaking (picric and acetic acids) - this fixative is called Bouin's solution and may be recommended where careful preservation of deep tissue morphology is of importance. An alternative for formaldehyde is the higher molecular weight bifunctional molecule, glutaraldehyde, which forms more stable and durable crosslinks, but is much more expensive, makes tissues hard and difficult to dissect and prevents any subsequent molecular analysis. The advantages of formaldehyde for peracarid taxonomy, especially used in commercial and monitoring studies, include: low cost, fast action, capacity for long-term storage (low volatility). The main disadvantages are: high toxicity (which necessitates careful handling, especially during transport), strong biochemical changes which are sometimes irreversible (DNA and RNA may be isolated from formaldehyde-fixed specimens after de-crosslinking, but it is of significantly lower quality; while some proteins retain antigenic properties, some do not), deterioration of some physical features of the specimen (tissue hardening, "tanning" - generation of secondary pigments), deformation of microscopic features by spontaneously precipitating paraformaldehyde crystals. It has been demonstrated that formaldehyde-crosslinked nucleic acids are more labile to hydrolysis, which is why they yield worse quality sequencing data; de-crosslinking is most efficient at 70°C in dilute buffer at pH=8.0 (Evers et al., 2011).

2.2.2 Less Common Fixatives

A historically common preservation technique for short-term maintenance of collected specimens until the availability of more efficient fixative is refrigeration or freezing of sample in the seawater in which it was collected. Refrigeration does not stop degradation processes, it only slows them down, while freezing (e.g., flash-freezing in liquid nitrogen) strongly disrupts microscopic morphology owing to generation of ice crystals within tissues, so these methods are recommended only when the main purpose of material collection is biochemical analysis in the near future.

While ethanol works by dehydration at the molecular level, water may be removed from the specimen also physically by drying (spontaneous, heat-induced or using hygroscopic materials such as silica gel). While common as a preservation procedure in terrestrial arthropods, this method is of highly limited applicability for marine peracarids: morphology is strongly disturbed by the drying process itself and by marine water salts, dry specimens are extremely delicate with regard to mechanical damage, inhibition of lytic enzymes and microbial growth is inefficient, nucleic acid chains tend to break. The only exception is preparation of specimens for SEM where liquid needs to be removed while preserving micromorphology – freeze-drying (lyophilisation) or critical point drying in liquid carbon dioxide are the fixation methods of choice here.

Organic solvent-based dehydrating fixatives, which are commonly used in histology, are also sometimes applied for preservation of marine crustaceans, although this is mainly of historical significance and should be discouraged for modern taxonomic analysis. Specifically, acetone or Carnoy's solution (ethanol with chloroform and acetic acid) dissolve and wash out hydrophobic components of the specimen, including biological membranes and lipid pigments, much more strongly than ethanol, preserving only the crude external structures (e.g. the exoskeleton), which is not acceptable for museum-quality preservation.

A group of less frequently used fixatives are inorganic salt coagulants involving heavy metals that act on negatively charged groups in proteins and lipids. Osmium tetroxide is an efficient fixative for lipid-rich tissues, but its application for crustaceans is mostly limited to concurrent fixation and staining for electron microscopy (see below). Similarly, in some histological work on marine crustaceans, Zenker's fixative is used. This solution contains highly toxic mercuric chloride acting as coagulant and providing excellent tissue fixation for detailed histological

analysis. Its usage nowadays is limited, since it has to be handled with extreme care and produces hazardous waste that requires costly disposal.

Sometimes, antimicrobial additives (amphothericin, thimerosal, azide etc.) are used to prevent microbial contamination and degradation of the sample, but as they usually have a relatively narrow spectrum of action and do not influence the spontaneous degradation of dead tissue by endogenous enzymes, they can have an auxiliary function at best.

Several specialized fixatives have been developed for specimens destined for subsequent nucleic acid isolation and genetic analysis. While RNA is both inherently unstable and subject to degradation by ubiquitous and abundant RNAses, DNA (a more common object of genetic analysis for taxonomic purposes) is chemically very stable, degrading only under specific conditions, and its deterioration in unfixed specimens is mostly due to action of microbial digestive enzymes because tissues of marine invertebrates are very poor in endogenous nucleases. Thus, while commercial fixatives like RNAlater™ and other chaotropic salt-based protein denaturants aimed at rapid and efficient elimination of RNAse activity are crucial to any transcriptomic (RNA-based) analysis, they are very expensive and simpler fixatives (like ethanol) are just as efficient in DNAse inhibition if only DNA-based analysis is foreseen. Alternatives to ethanol as a fixative for DNA-based studies have been proposed (e.g. propylene glycol-containing antifreeze solution (Robinson et al., 2021) or solutions containing metal chelators that deprive DNAses of cofactors mixed with detergents (Pokluda et al., 2014) or polar solvents (Lins et al., 2021) and they facilitate subsequent DNA isolation, but they are not efficient in preserving morphology or in long-term prevention of microbial contamination, so they should be used only in targeted taxonomic studies (e.g. barcoding or metabarcoding). When selecting the fixative for a specimen that will (or may) be subjected to genetic analysis by DNA sequencing, it is important to take into account the specific technique to be used: some techniques (e.g. Illumina) sequence short fragments and thus may be efficiently used even on DNA of low quality, e.g. isolated from formaldehyde-fixed specimens; some techniques (e.g. nanopore) need long DNA molecules and thus should be applied only for material fixed with ethanol or DNA-specific fixatives. Importantly, both freeze-thaw cycles and drying-rehydration cycles contribute to DNA strand breakage and should be avoided if longer DNA is required.

2.3 Dissection for Morphological Examination

Body length of peracarids rarely exceeds several millimeters. For this reason, the morphological identification of the peracarids involves observation of the details of head/cephalothorax, thorax, and abdomen appendages as well as additional components such as labrum, labium or epignath. The dissection of microscopic size requires experience, "surgical" dexterity, and precise tools. The needles used for the preparation of larger crustaceans are much too large for working with small crustaceans, while thin entomological needles are too flexible for dissection of the crustaceans. Tungsten needles, with tips although extremely fine, remain rigid and inelastic, are an ideal solution for peracarid dissection. Nowadays there are many companies on the market that offer tungsten needles, but sharpening can also be done in the lab, using solution of KOH, as copper as cathode and a low electric voltage.

3. METHODS FOR MORPHOLOGICAL STUDIES

3.1 Preparing Drawings

Scientific drawings are the pillar of taxonomic research. Drawing practiced with the support of a *camera lucida* microscope enable future researchers to recognize named species (**Figure 1H**). In the early Linnean days of taxonomy, it was essential to prepare drawings to visualize features, but recently they are increasingly being replaced by other (e.g., photographic) techniques (Wilson, 2003; Anderson, 2014; d'Udekem d'Acoz and Verheye, 2017; Lörz and Horton, 2021), that are also being applied to fossilised specimens (Selden et al., 2016; Jauvion, 2020). There have been fierce debates over photographs or microscopic images to become substitutes for drawings or even types (cf. Zhang et al., 2017). Although changes to the International Code for Zoological Nomenclature now have a certain consistency with regard to the type problem (Zhang et al., 2017), the idea of describing species purely based on imagery or molecular taxonomic units (MOTUs) (Jörger and Schrödl, 2013; Sharkey et al., 2021) still remains the exception for peracarids.

Drawings provide an interpretation often in a rather schematic way. The traditional scientific drawing workflow is clearly a lengthy one, starting with pencil drawings, followed by inking, scanning, as well as editing and arranging plates (**Figures 1G–J**). Yet, pencil and ink drawings, on the one hand, aid in-depth examination of the morphology and, on the other hand, distracting details may be omitted if they are systematically uninformative. Besides, drawing habitus of poorly calcified specimens enables us to visualize the morphological characters which cannot be well pictured by camera because of low contrast. Images, on the other hand, ideally give a precise representation of the morphological structures (also with regard to coloration and patterns, see amphipod example above), even more so with the development of high-resolution imaging techniques (Kaiser et al., 2018; Błażewicz et al., 2019; Jażdżewska et al., 2022). In addition, photography is far less subjective than creating drawings, but despite these advantages has so far rarely found its way into peracarid taxonomy.

The preparation of drawings presenting details of morphological structure has been historically/traditionally carried out by means of a *camera lucida* attached to the microscope. This device is a simple system of mirrors (Wollaston, 1807) which makes it possible to reproduce an object (body habitus or appendages) on a sheet of paper placed next to the microscope (**Figure 1H**). Despite the simplicity of its design, the *camera* is a relatively expensive piece of optical microscope equipment: only few optical companies

manufacture them, and they are not usually exchangeable between different models of microscopes. In addition to the traditional use of *camera lucida*, focus-stacked microphotographs can be the baseline for drawings (Coleman, 2006) or even substitute for pencil drawings (d'Udeckem d'Acoz and Verheye, 2017; Wilson and Humphrey, 2020). Nevertheless, both *camera lucida* and stacked microphotographs techniques can also be applied together for producing drawings of fossils (Selden et al., 2016). The appropriate camera and acquisition software to equip the microscope are also expensive.

Microscopic images are useful to complement scientific drawings when studying rare (singleton or unique) species. While this is a general phenomenon in the description of species (Lim et al., 2012; Wells et al., 2019), it becomes particularly evident in the morphological analyses of deep-sea species including peracarids (Brandt et al., 2012; Higgs and Attrill, 2015). Drawings without dissecting parts of the specimen are often sought not to sacrifice the holotype, but it is thanks to the use of imaging techniques, chiefly non-destructive methods (such as CLSM, see below), it is possible to fill in missing gaps of morphological information. However, it is clear that not always taxonomist have access to all facilities to use such as useful techniques and methods.

So far, however, no efforts to refrain from drawings in peracarid taxonomy have been taken but, on the contrary to bring together as much information as possible (including molecular, ecological, and biogeographic) as part of an integrative process (Brix et al., 2015; Malyutina et al., 2018; Kaiser et al., 2018; Schnurr et al., 2018; Błażewicz et al., 2019; Jakiel et al., 2019; Riehl and De Smet, 2020; Kaiser et al., 2021). Above all, the use of digital drawing techniques and the corresponding software (something expensive as well) has made a significant contribution to reducing the time required for, and improving the quality of species illustrations (Coleman, 2003; Coleman, 2009; Bober and Riehl, 2014; Montesanto, 2015). However, much greater advances appear to have been achieved in the development of 3D reconstruction and imaging techniques.

3.2 Specialized Techniques of Specimen Imaging

Morphology (i.e., shape of the organisms and its parts) is still the most important taxonomic characteristic and thus methods of its recording and analysis – imaging methods – are crucial tools in the armory of a taxonomist of deep-sea Peracarida (**Figure 3**). Concentrating on imaging for taxonomic purposes, we need to differentiate the imaging of overall morphology (habitus) which may be performed without any previous zoological knowledge (**Figures 3A–I**), and imaging of specialized, taxonomically important features, the choice of which must be informed by accumulated knowledge and expertise. For deep-sea peracarids, where specimens are difficult to obtain (complicated logistics), available in limited numbers and thus are highly valuable, an important consideration is the distinction between imaging taxonomically important morphological features *in situ* (in intact specimens) *versus* imaging of prepared or isolated body parts (*ex situ*, after dissection and/or sectioning, **Figures 3J, K**), which may be sometimes necessary even for type specimens. When selecting imaging techniques, some thought must be also paid to the location of taxonomically distinctive features within the body of the crustacean – some techniques are exclusively suited to imaging external morphology (e.g. SEM, **Figures 3L–N**, or CLSM, **Figures 3O–R**), while others were developed specifically for imaging internal organs and hidden features (e.g. microCT, **Figure 3S**). Finally, a modern taxonomist must bear in mind that imaging can be used not only for purely morphological (shape-related) analysis, but specific contrast techniques are available to draw conclusions about biochemical composition of tissue elements as well as course of physiological processes which may be helpful as additional taxonomic characteristics and form an additional level of analysis (apart from morphological and genetic ones). **Table 3** includes recent examples of application of specific imaging techniques which will be reviewed below to Peracarida and other crustaceans.

3.2.1 Light Microscopy

3.2.1.1 Bright Field and Optical Contrast Microscopy

While bright field light microscopy is the original method in taxonomy of any small organisms, its applicability to deep-sea Peracarida is limited by the relative lack of inherent contrast in their bodies. Light microscopy relies mainly on absorption, refraction, and dispersion of incident rays in the specimen, and marine crustaceans tend to be colorless (low absorption) and with optical refringence that is uniform and similar to surrounding seawater. While habitus imaging may be performed on whole specimens by reflected light stereomicroscopy in air (Hegna, 2010), the resulting images are poor in details and thus of low usefulness in taxonomy.

Most commonly, zoological specimens are prepared in a procedure called mounting, where the animal is placed on a glass slide in a drop of liquid and covered with another flat piece of glass (the thickness of this cover glass is adapted to the working distance of the microscope objective to be applied). Mounting has two main purposes: to prevent the desiccation-related destruction of specimen, and to provide an environment with uniform refraction properties in order to minimize image blurring due to photon scattering on phase borders. Therefore, the mounting medium for marine crustaceans must mix well and rapidly with seawater, and its refractive index should be as close as possible to that of glass (1.52). While animals can be mounted in water itself for short-term observation (e.g. on board), it evaporates quickly and a different mounting medium is needed if the specimen is to be stored as microscope slide. The most important decision in the choice of mounting medium is related to the desired permanence of the slide: specimens in non-permanent (liquid- or gel-based) media may be manipulated, moved around, remounted, or even removed from the slide for other type of analysis; permanent (solidifying) medium preserves the slide permanently in the same attitude of the specimen. Sometimes, the mounting medium includes components that have additional functions with regard to the specimen itself: clearing (optical homogenization by removal of light-scattering inclusions) and/or maceration (chemical removal of unwanted tissue, e.g. muscles inside the tegument). These components are

TABLE 3 | Selected examples of literature references where different imaging techniques were used to study the taxonomy of peracarids and other crustaceans or were applied to visualize peracarids for non-taxonomic purposes.

Imaging method	Special technique	Staining/preparation for visualization	PERACARIDA		CRUSTACEA
			Taxonomy	Other purpose	taxonomy
Optical contrast light microscopy	Bright field	Alcian blue		Žnidaršič et al., 2018	
		Alizarin red	Haug et al., 2011a	Žnidaršič et al., 2018	
		Azure II		Wirkner and Richter, 2004; Mrak et al., 2012 Žnidaršič et al., 2018	
		Chlorazol black	Corbera and Martín, 2002		
		Hematoxylin	Hegna, 2010		
		Hematoxylin/eosin		Žnidaršič et al., 2018	
		Ink	Hegna, 2010		
		Lignin pink	Hadjab et al., 2020; Jażdżewska et al., 2022		
		Toluidine blue	Bober et al., 2018		
		None	Curatolo et al., 2013		
	Dark field	None			Haug et al., 2011b
Fluorescence microscopy	Widefield	Autofluorescence	Haug et al., 2011b Haug et al., 2011a	Giurginca et al., 2015 Glenn et al., 2013 Nagler and Haug, 2016	Eiler et al., 2016 Marek, 2017
		Alizarin red		Mrak et al., 2013	Haug et al., 2011b
		Hoechst		Kreissl et al., 2008	
		Chitin-binding probe		Žnidaršič et al., 2018	
		Immunofluorescence		Kenning and Harzsch, 2013 Kreissl et al., 2008	
	Laser scanning confocal	Autofluorescence	Hughes and Kaji, 2016 Riehl and De Smet, 2020	Bruce and Patel, 2020 Kakui, 2014 Kenning and Harzsch, 2013 Stegner et al., 2015	Galassi et al., 1998 Michels, 2007 Lee et al., 2009 Valdecasas and Abad, 2011
		Acid fuchsin	Riehl and De Smet, 2020		Kottmann et al., 2013
		Congo red	Brökeland et al., 2010 Michels and Büntzow, 2010 Riehl and De Smet, 2020		Kihara and Martinez Arbizu, 2012 Menzel, 2011 Michels and Büntzow, 2010
		Congo red/acid fuchsin	Brandt et al., 2014		Kamanli et al., 2017
		Blankophor			Brooker et al., 2012a; Brooker et al., 2012b
		DiI		Stemme et al., 2014	
		Eosin Y			Lee et al., 2009
		Gomori			Brooker et al., 2012a; Brooker et al., 2012b
		Mercurochrome			Lee et al., 2009
		Phalloidin		Jirikowski et al., 2013 Jirikowski et al., 2015 Göpel and Wirkner, 2018	
		Rose bengal	Chim and Tong, 2020		
		Safranin			Lee et al., 2009
		Shirlastain A	Riehl and De Smet, 2020		
		Sytox Green		Wolff, 2009	
		Immunofluorescence		Kenning and Harzsch, 2013 Stegner et al., 2015 Stemme et al., 2014	

(Continued)

TABLE 3 | Continued

Imaging method	Special technique	Staining/preparation for visualization	PERACARIDA		CRUSTACEA
			Taxonomy	Other purpose	taxonomy
	Spinning disk confocal	Autofluorescence	Haug et al., 2011b		
Electron microscopy	TEM	Uranium/immunogold Uranium/lead Lectin-gold		Štrus et al., 2019 Geiselbrecht and Melzer, 2013a Žnidaršič et al., 2018	
	SEM	Gold		Geiselbrecht and Melzer, 2014 Kaji et al., 2016 Wirkner and Richter, 2004 Wolff, 2009	
		Gold/palladium	Haug et al., 2011a		
		Osmium		Kaji et al., 2014	
		Carbon	Bober et al., 2018 Brandt et al., 2014		
		Other	Hughes and Ahyong, 2016 Riehl and De Smet, 2020	Štrus et al., 2019	Kamanli et al., 2017 Haug et al., 2011b
	FIB-SEM	Gold/palladium	Haug et al., 2011a		
	SBF-SEM	Osmium/lead/gold		Kaji et al., 2016	
MicroCT	X-ray	Iodine None	Haug et al., 2011a	Štrus et al., 2019 Nagler and Haug, 2016 Wirkner and Richter, 2004 Göpel and Wirkner, 2018	Maeno et al., 2019 Landschoff et al., 2018 Haug et al., 2011b
	Synchrotron	None			Betz et al., 2007

usually acids (e.g. lactic acid) or bases (e.g. potassium hydroxide), and care must be taken not to exceed the necessary dosage and, if possible, to remove the agent before final mounting, as they may progressively destroy taxonomically important features or even the whole specimen during prolonged storage. **Table 4** lists the commonly used mounting media for microscopic imaging of Peracarida with their main advantages and disadvantages.

The most common components of non-permanent mounting media used for taxonomic imaging of small marine arthropods include: glycerol (higher refractive index than water and negligible evaporation; sometimes mixed with 10% saline to facilitate mixing during slide preparation), gelatin (less recommendable as it is prone to desiccation and cracking), polyvinyl alcohol (included in the popular commercial mounting medium Mowiol and in the complex self-made medium polyvinyl lactophenol), and chloral hydrate (included together with glycerol in popularly used Hoyer's medium, where it contributes to its high refractive index). They are often used in personally formulated mixtures based on experience and anecdotal evidence on performance – it is possible that some are more suitable for certain systematic groups of Peracarida than others, but systematic studies are lacking and it seems that subjective personal preference remains the main argument for mounting medium choice. Oil-based mounting media are also available, but rarely used for invertebrate taxonomy as they do not perform well with carbohydrate exoskeletons. Permanent (solidifying/hardening, either by physical curing or by chemical polymerisation) mounting media are also often used for museum specimen storage, but this practice prevents any further manipulation of the specimen (including potential new molecular discrimination techniques) and should be discouraged for rare type material where methodological developments in molecular studies may warrant the need for access to relatively unchanged biological material in distant future. However, permanent mounting may be recommended for long-term storage of dissected parts (e.g. appendages) which are of purely morphological value. While some resin-based solidifying media are marketed as reversible (they may be liquefied by heating with an excess of solvent), both morphological structure and biochemical composition is usually compromised by such treatment and all solidifying mounting media should be treated as permanent. The most common base ingredients of solidifying mounting media used in taxonomy of Peracarida include natural resins (Canada balsam, Euparal and others that solidify by gradual solvent evaporation and vitrification), synthetic resins (included in such preparations as DPX or Permount) and formaldehyde-based polymers (mainly dimethylhydantoin formaldehyde – DMHF – which is recognized as superior to resins due to much less cracking and bubbling artefacts; Bameul, 1990).

If the entire or dissected specimen is to be preserved in long-term storage in the form of microscope slide mounted in liquid medium, this slide must be also sealed using impermeant sealants that isolate the specimen from external moisture and oxygen (numerous commercial products are available, e.g. based on linseed oil, plant resins, paraffin or acrylic glue; even simple nail

TABLE 4 | Advantages and disadvantages of mounting media commonly used for light-microscopy studies of peracarids.

Type of mounting medium	Components/ media	Advantages	Disadvantages	References
Non-permanent liquid	Water	Easy application	Weak optical properties, strong evaporation, very low durability	Wittmann et al., 2016
	Glycerol	Good optical properties, easy application and removal for other techniques, very low evaporation	Need for complex sealing methods,	Maybury et al., 1991; Neuhaus et al., 2017
	Chloral hydrate (Hoyer's)	High refractive index, strong clearing action	Short-term storage, easy evaporation, difficult sealing	Kodama and Kawamura, 2019
Semi-permanent solidifying	Gelatin	Easy application	Easy cracking and microbial contamination in long-term storage	Jersabek, 2005; Neuhaus et al., 2017
	Polyvinyl alcohol (PVA)	May include clearing and macerating agents (lactic acid, phenol)	Possibility of microbial contamination, difficult remounting	Koomen and von Vaupel Klein, 1995; Neuhaus et al., 2017
Permanent resin-based	Euparal	Long-term preservation without dehydration	Time-consuming preparation, some dehydration	Coleman, 2006
	Canada balsam	Very durable (hundred-year permanence)	Impossible to remount, specimen no longer accessible for other methods, complex specimen preparation (dehydration)	Koomen and von Vaupel Klein, 1995; Neuhaus et al., 2017
	Dibuthyl phthalate (DPX)	Easy to apply, relatively durable	Toxic, generates some morphological distortion of delicate features	Geiselbrecht and Melzer, 2013b; Nagler and Haug, 2016;
Permanent polymer-based	Dimethylhydantoin formaldehyde (DMHF)	Easy to apply, concomitant maceration	Crystal formation during long-term storage, damage to nucleic acids	Steedman, 1958; Bameul, 1990; Bourque et al., 2020

varnish may be used for this purpose, but care must be taken that its components do not interfere with any staining that was applied) (Allington-Jones and Sherlock, 2007). When considering long-term storage in non-permanent mounting media, the question of microbial contamination potential must be also taken into account: glycerol-based media are most resistant to contamination, while microbes grow most easily in those containing gelatin. Since the function of the mounting medium requires the compounds involved to thoroughly permeate the specimen, it needs to be extensively washed if it is required at some later point to release it from the slide after microscopy for some other (e.g. genetic) analysis. Common liquid mounting media (e.g. glycerol-based) do not damage nucleic acids and can be removed by washing, but polymerizing permanent mounting makes isolating DNA from the sample impossible.

For transmitted light imaging, the standard procedure is to stain the specimen with light-absorbing dyes to create contrast. In current practice for taxonomic purposes, researchers aim to use non-selective stains to visualize most tissue types and structures (in crustaceans, the most important element being usually the exoskeleton and its outgrowths, especially on the appendages). The most commonly used dyes are hematoxylin (which stains nucleic acids – and thus living tissue – dark blue) (Hegna, 2010) and eosin (which stains most biological macromolecules, including those in the extracellular matrix and exoskeleton, pink), most often combining these two as counterstains (Žnidaršič et al., 2018). Other, more selective dyes can also be used to stain crustaceans, including azure II (stains polysaccharides, including cuticle components), alizarin red (stains calcium deposits in calcified carapace), chlorazol black (basic dye that stains anionic macromolecules, mainly nucleic acids), alcian blue (basic dye for acidic glycans in connective tissue), toluidine blue, lignin pink (both glycan-selective stains with differing affinity) or even the non-selective India ink that stains by physical interactions. Specimens stained using these techniques are usually mounted by immobilization on standard microscope slides, but sectioned or dissected samples may be also prepared after staining. Image is recorded by photographic cameras attached to standard light microscopes or even simply by drawing (see *Preparing Drawings*). If a specimen stained with a cationic dye is to be subsequently used for DNA isolation, an additional washing step may be included to remove the bound dye which might impact downstream reaction efficiency. Some fluorescent DNA-binding (intercalating) dyes (see below) are virtually impossible to remove from DNA during isolation, but there are few reports (from experiments on tissues of vertebrates) finding them interfering even in complex genetic procedures (e.g. next generation sequencing), so this should not be a critical issue in invertebrate taxonomy.

The indisputable advantage of bright field light microscopy imaging is the common availability of cheap instrumentation which requires little specialist training on the part of the researcher. Light microscopes are usually available, even on board research vessels, and can be used for imaging of freshly collected specimens before fixation. When combined with staining, this technique can provide convincing basis for quantitative measurements and rudimentary conclusions with regard to biochemical composition of some structures (e.g. carapace calcification). The central disadvantage is the

relatively poor contrast, both against the background and internally within the imaged specimen, leading to potential obfuscation of taxonomically important morphological differences and features. Standard light microscopy (both in reflected and transmitted light) is poor in rendering internal structures of the body and requires extensive dissection to image complex elements (like appendages). Efficiently imaging three-dimensional structures is not possible, even though they may be observed by stereomicroscopy (attempts have been made to construct and publish 3D images of Amphipoda to be viewed through red-cyan glasses, with limited success (Haug et al., 2011a). Nevertheless, taxonomical descriptions relying on bright field images of unstained or stained Peracarida continue to be routinely published, e.g. new amphipod species imaged after lignin pink staining (Hadjab et al., 2020) or new isopod species stained with chlorazol black (Pereira et al., 2019).

The contrast problem has led to the application of some specialized variants of optical contrast light microscopy (which all require technical add-on enhancements to the microscope itself which are relatively rare in zoological laboratories). One technique which has found use in taxonomically useful imaging of arthropods is dark field microscopy, where incident light is directed at the specimen in such a way that it does not pass into the objective unless deflected (reflected, refracted or scattered) by the specimen, leading to improved contrast against background and higher salience of delicate surface structures (Haug et al., 2011b). Another applicable method is polarization contrast that can underline differences in thickness and density of thicker homogenous structures formed by the cuticle (Fernández del Río et al., 2016; Melzer et al., 2021). Finally, interference contrast (also known as Nomarski contrast) is a powerful technique enabling the visualization of fine ultrastructural details. It has hitherto found application in deep-sea isopod and amphipod species taxonomy (Bruce, 1995; Bruce, 1997; Just, 2001; Tomikawa and Mawatari, 2006; Storey and Poore, 2009) but also in coastal and freshwater species (Shimomura and Mawatari, 1999; Shimomura and Mawatari, 2000; Tanaka, 2004; Jaume and Queinneck, 2007), demonstrating its power in imaging fine morphological structure of appendages (Maruzzo et al., 2007).

3.2.1.2 Fluorescence Microscopy

The most common solution to the contrast problem in biological microscopy is to make use of fluorescence, the physical phenomenon where some compounds (called fluorophores) absorb light of higher energy (lower wavelength) and subsequently emit light of lower energy (higher wavelength). This difference in wavelength, called Stokes shift, makes it possible to design microscopes which separate the incident (illumination) light from the light emanating from the sample, and thus obtain an image exclusively of the fluorescent elements within the sample. For most biological specimens, fluorescence microscopy requires staining with fluorescent dyes (fluorophore-containing compounds which bind to specific structures in the sample). Crustaceans (and arthropods in general), however, usually display relatively strong fluorescence of endogenous compounds (so-called autofluorescence) in intact specimens, allowing for easy fluorescence microscopy imaging and accounting for the widespread use of this technique in taxonomy. While biochemical studies of compounds responsible for autofluorescence in crustaceans are still too few and this field needs further intensive research, most parts of crustacean exoskeleton exhibit a broad-spectrum, near UV-excited autofluorescence that is a consequence of its highly cross-linked structure with glycan and protein components both contributing to the resulting fluorophores. Serendipitously, formaldehyde fixation tends to strengthen this broad-spectrum fluorescence component, making it even easier to image specimens fixed in this way (Hughes and Ahyong, 2016). Another source of autofluorescence is the elastomeric protein resilin, abundant in sites that are under strong mechanical stress such as tegument joints or mouthpart appendages, which contains dityrosine crosslinks that generate autofluorescence. Finally, some metabolic compounds (flavins, pterins, porphyrins, etc.) present in tissues also have fluorescent properties, enhancing the potential for fluorescent imaging of unstained specimens (Riehl and De Smet, 2020). Some arthropods have evolved dedicated autofluorescent compounds, probably important for ecological interactions, such as in some hoplocarid mantis shrimps with markings containing a yellow fluorescent fluorophore that are important in visual recognition or in shallow water copepods which contain dedicated fluorescent proteins similar to the more well-known ones from cnidarians. This ecologically motivated autofluorescence is even more common in terrestrial arthropods such as scorpions (which produce coumarin pigments) or millipedes (which rely on pterins). However, in crustaceans from the aphotic zone these dedicated fluorophores have not been detected yet and the observed autofluorescence seems to be a side effect of the biochemical structure of tissues and tegument (Glenn et al., 2013). Fluorescent properties may be used to enhance the visual signal generated by bioluminescence in deep-sea Peracarida that display this property, thus being ecologically important for visual communication within the species or between different species. Examples include, the lanceolid amphipod *Megalanceola stephenseni* (Chevreux, 1920) and amphipods from the families Pronoidae, Scinidae and Lysianassidae (Herring, 1981; Zeidler, 2009), mysids from family Mysidae (Herring, 1981) and the lophogastrid *Neognathophausia ingens* (Dohrn, 1870) (Frank et al., 1984), the fluorescence of which seems not to originate from the species itself, but rather to be dependent upon components of its food (Wittmann et al., 2014). This topic needs further studies on living specimens, preferably *in situ* (Macel et al., 2020). In any case, the presence of autofluorescence does not preclude the use of additional staining of specific structures in the crustacean body with fluorescent dyes for taxonomic purposes, but its continued presence needs to be taken into account for potential spectral overlap when selecting imaging channels.

When using fluorescence microscopy for taxonomic purposes, specimens are often stained with fluorescent dyes to further enhance contrast and facilitate the imaging of structures with defined biochemical composition. With regard to their mode of action, these dyes can be divided into four groups:

1) Broad specificity acidic dyes, which bind mainly to carbohydrates in the tegument. They are useful in detailed

imaging of appendages, exoskeleton protrusions etc., while staining virtually the whole body of the animal to a different extent. The most commonly used dyes from this group are acid fuchsin (Riehl and De Smet, 2020; Kaiser et al., 2021) and Congo red (Michels and Büntzow, 2010; Kihara and Martinez Arbizu, 2012). An interesting example is rose bengal, a halogenated fluorescein derivative which has the capacity to bind cellular components as well, but in the presence of abundant extracellular carbohydrate material binds mostly to it. In the taxonomy of deep-sea Peracarida, its main use is for transient staining of (usually formaldehyde-fixed) mixed material to aid in visual sorting (due to its strong color) (Hegna, 2010), but its fluorescent properties allow it also to be used in whole-body fluorescence microscopy (Chim and Tong, 2020).

2) Carbohydrate-specific dyes, mostly taken over from the textile industry. They are i.a. Blankophor/Calcofluor (Brooker et al., 2012b), Shirlastain or aniline blue, which bind mainly to chitin in the exoskeleton (Riehl and De Smet, 2020).
3) Calcium binding stains, that are useful to identify calcified parts of the skeleton, such as calcein or alizarin red (Haug et al., 2011a).
4) Cationic dyes, which mainly bind to nucleic acids and stain living tissues more or less uniformly. They are safranin, eosin, DAPI or Hoechst family dyes (Kakui and Hiruta, 2017).

More specialized fluorescent probes binding to cellular or subcellular elements with restricted distribution may also be used, e.g. cytoskeleton-specific binders such as phalloidin or fluorescent antibodies (this technique is called immunofluorescence), but this is of limited usefulness in taxonomy and more commonly found in physiological or embryological studies. Both autofluorescence and probe/dye fluorescence is subject to a phenomenon called photobleaching, where long-term illumination causes a chemical reaction that destroys fluorophore molecules, leading to decreased image brightness. This can be slowed down by including so-called anti-fade components in the mounting medium, but this is rarely necessary with the bright and stable fluorophores used for taxonomically relevant imaging of crustaceans.

With regard to instrumentation, the simplest application of the fluorescence microscopy principle is the widefield fluorescence microscope which uses the same optical principle as a bright field microscope, but separates optical paths of excitation and emission light using filters and dichroic mirrors. Images generated in a widefield microscope can be viewed directly through the eyepiece or recorded using photographic or motion cameras. They can also be overlaid in-microscope with bright field images, pinpointing the location of fluorescent structures within the whole body of the animal. Widefield image quality is restricted by the so-called out-of-focus blur, i.e. light emitted from above and below the focal plane which enters the objective and decreases the image sharpness. This can be strongly limiting in the imaging of small taxonomically important elements within a larger structure. Therefore, an increasing number of taxonomic studies make use of another fluorescence imaging modality, so-called confocal microscopy. A confocal microscope retains only the objective lens from a standard optical microscope setup and images only a single point within the sample (so-called confocal volume), using regulated apertures (here called pinholes) to cut off out-of-focus illumination from both excitation and emission light paths. Therefore, a confocal microscope does not generate an image, but measures the fluorescence intensity in a spatially defined point within the sample. An image is subsequently reconstructed digitally by dedicated computer software from data collected from various confocal volumes, as the illumination is scanned across the sample. The scan may be effected in two ways: either by using optically deflected laser beams (laser-scanning confocal microscopy, in zoology usually known under the less logical name confocal laser scanning microscopy or CLSM) or by using spinning discs (Nipkow discs) with multiple pinholes (spinning disc confocal microscopy). While spinning disc confocal microscopy generates images much faster and with higher inherent brightness, these advantages are mostly important in imaging live specimens, which is rare for deep-sea taxonomical purposes. The relative rarity and costliness of spinning disc microscopes combined with their lack of versatility make them a niche tool for crustacean taxonomy when compared to laser-scanning microscopes (Haug et al., 2011b).

A confocal image is not "recorded" in a way that a camera records a widefield image, but is reconstructed from individual pixels in silico, so the native form of this image is already digital and with no loss of quality upon digitization. Since the confocal volume can be moved across the sample in all directions, a confocal microscope can be used to record three-dimensional images of specimens, making it especially useful in crustacean taxonomy where many important features such as appendage structure are inherently three-dimensional (**Figures 3O–R**). Properties of light, however, restrict the image resolution in the Z axis (parallel to the long axis of the objective) to ca. 2–3 times less than lateral resolution, so confocal images are never truly 3D-isomorphic. If isomorphism is absolutely necessary for taxonomic purposes, several images with different specimen orientation must be recorded. Since laser scanning confocal microscopy involves moving a small confocal volume around a large specimen, it is notoriously slow, with a good resolution image of an average-sized deep-sea crustacean taking more than 10 hours to record. Moreover, because for good resolution it is necessary to use medium-magnification objectives which usually do not allow the whole animal to fit in a single field of view, sophisticated software must be used to reconstruct the whole image from several adjacent scans in a procedure called tiling – its success (the lack of visible artifacts on scan joints) depends largely on the quality of the objective (spherical aberration correction). When recording 3D confocal images and using them for taxonomy, the way that they will be presented and disseminated in the literature must be considered, because the original files are usually too large to include even as supplementary information in published articles. A number of 2D projections (most common being maximum intensity

projection and surface projection) have been developed to help present 3D data.

3.2.2 Electron Microscopy

Electron microscopy is a group of imaging techniques which use physical effects which happen when the sample is illuminated with a stream of high-energy electrons: usually, transmitted, scattered or secondary electrons are detected. The main advantage of electron microscopy in biological imaging is the potential to generate images of much higher inherent resolution than light microscopy, since the electron beam is equivalent to radiation with a very short wavelength compared to visible light. However, for purposes of taxonomy of macroscopic invertebrates, this aspect rarely comes into play, since subcellular features (and generally features of submicrometric size) are not often used as taxonomically defining. The variant of this technique that is most often used by taxonomists is scanning electron microscopy (SEM), where the sample is illuminated by a narrow electron beam which moves across its surface and secondary electrons emitted from every spot on the way (only from the surface since they have too low energies to escape from lower layers of material) are measured using an array of detectors, recreating in real time a spatial map of the surface relief. The main advantages of this method which make it so attractive for imaging for taxonomic purposes are: high sensitivity to small changes in surface geometry which makes it possible to efficiently image surface texture and generate high-resolution images of delicate and complex structures such as those abounding on crustacean exoskeletons and appendages; high depth of field which retains in focus structures that are far away from each other along the z axis, generating a realistic and sharp image of the whole macroscopic specimen while retaining sub-microscopic resolution; the ability to modify magnification in a wide range (from several-fold to tens of thousands-fold) in a contiguous, real-time manner while conducting observations; and the possibility to easily reconstruct three-dimensional measurements from images or generate true 3D images of the specimen by recording images from two different angles. However, the method has also significant disadvantages, mostly related to the onerous and highly invasive sample preparation required for imaging in a typical SEM instrument: since both the high-energy illumination electrons and the low-energy secondary electrons that are being imaged can be deflected by interactions with air molecules, low-pressure vacuum environment is needed around the sample, which means it cannot contain water (so, biological samples must be dehydrated before imaging); since atoms contained in organic compounds do not interact with high-energy electrons efficiently and do not generate many secondary electrons, it is often necessary to coat the specimen surface with a layer of higher atomic number atoms which will produce a brighter image; the absorption of electrons by the specimen generates a high static electrical charge which would quickly lead to scanning artifacts, discharges and specimen destruction if not removed, thus the specimen must be electrically conductive or coated with a material which conducts electricity. For these reasons, SEM is a destructive technique and specimens of Peracarida prepared for SEM imaging cannot usually be used subsequently for any further preparation or analysis using other methods. The sample preparation process for deep-sea crustaceans for SEM imaging has several important steps at which different approaches may be taken depending on specific needs of the researcher. Due to the high energies and harsh treatment involved, the specimen needs to be fixed in a strong fixating agent, usually glutaraldehyde or a mixture of glutaraldehyde and formaldehyde. Dehydration cannot be achieved by air drying as this would destroy delicate surface structures, so water is first replaced by an organic solvent (e.g. ethanol or acetone), and this solvent with higher vapor pressure may be either evaporated directly with less damage to the specimen or it may be replaced with liquid carbon dioxide which then evaporates in conditions around its phase transition critical point (where gas and liquid densities are equal, removing the damaging surface tension - so-called critical point drying). For imaging, the specimen may then be coated with a thin layer of metal (such as gold, platinum, palladium or their mixtures) which provides both better secondary electron emission and electrical conductance, or with a layer of powdered carbon (graphite) which only increases conductance. Another useful metal with unique properties is osmium – its tetroxide is an efficient fixative due to the ability to bind lipids (see the chapter on fixation), coating with osmium itself provides conductivity, and both treatments strongly increase contrast due to efficient secondary electron generation.

Apart from standard SEM, other electron microscopy techniques have been used to image aquatic crustaceans, including deep-sea Peracarida. Environmental SEM (ESEM) is a variation of SEM where differential pumping and pressure-limiting apertures allow the placement of the specimen in a gaseous environment. While this still requires a low-pressure environment, water vapor pressure may be kept at saturation levels, allowing the imaging of water-containing (non-dehydrated) specimens (Drumm, 2005). This is of high importance for potential taxonomic usage as imaging is thus non-destructive and the specimen may be re-used in studies using other methods (however, the pressures used in ESEM are usually low enough to cause the sample to freeze, and the freeze-thaw cycle may break up longer DNA molecules, so the sample may be no longer ideal for e.g. nanopore sequencing). The gaseous environment requires low electron beam energies and specialized detectors, which has both practical advantages (most importantly there is no need to coat the sample in conductive material as there is no static electricity build-up, confirming the non-destructive characteristics of this methodology) and disadvantages (the depth of field is severely limited, making low magnification imaging of large specimens difficult). While for terrestrial arthropods, this has allowed the imaging of even live individuals, the applicability of ESEM for aquatic animals is less apparent due to imaging artifacts from liquid droplets at fine structures, but the technological advances in recent years will probably remove this impediment. While SEM is usually used to image the specimen surface, it can be modified for three-dimensional imaging of deeper tissue layers, which is of special interest for crustacean taxonomists as it allows to recreate high-

resolution images of small appendages with complex structure (e.g. mouthparts). One such modification is serial block-face SEM (SBF-SEM) where the animal is stained with heavy metals (osmium, gold, uranium or lead), embedded in a block of epoxy resin and placed in the imaging chamber of a SEM microscope. The top layers of the block are subsequently serially removed with an ultramicrotome which is contained within the imaging chamber itself, and SEM images of the surface at each cutting depth are combined into a 3D image (Kaji et al., 2016). Alternatively, top layers of biological material (e.g. exoskeleton) may be removed by so-called ion beam milling (abrasion by bombardment with a focused stream of high-energy ions) in a technique called focused ion beam SEM (FIB-SEM) (Haug et al., 2011a). The advantage of FIB-SEM in comparison to SBF-SEM is that location of in-depth imaging is determined by the researcher, the 3D image resolution is uniform in all dimensions and the sample does not require embedding, while SBF-SEM is significantly faster (and having the resolution in the vertical dimension limited by the thickness of ultramicrotome slice is usually not a problem for taxonomically relevant features of crustacean bodies). Finally, traditional transmission electron microscopy (TEM), which involves preparing ultra-thin slices of the sample and treating them with heavy metal stains or probes, has also been applied in proof-of-concept studies to image the fine structure of tissue of some peracarids, but its applicability in taxonomy is not related to morphological studies, but limited to determination of differences in molecular composition of proteins, e.g. by immunogold staining, or carbohydrates, e.g. by lectin-gold staining (this potential has not yet been practically applied for taxonomic purposes in Peracarida).

3.2.3 X-Ray Microtomography

Computed tomography refers to any technique that allows three-dimensional imaging of internal structure by techniques that do not require physical dissection/slicing of the specimen (such as magnetic resonance imaging or positron emission tomography). However, in practical usage in zoology, this term (and the subordinate term microcomputed tomography, or μCT, when applied to microscopic objects) is understood exclusively as applying to imaging *via* X-ray illumination and multi-point detection of transmitted and scattered X-rays (more properly known as X-ray tomography). The principle is the three-dimensional analogue of standard medical X-ray imaging of tissue, with pixel size in the micrometric range. This allows the non-destructive imaging of internal structure of zoological specimens and has become one of mainstays of morphology studies of deep-sea crustaceans for taxonomic purposes (Gutiérrez et al., 2018) and specially for treatment of fossil records (Jauvion et al, 2016; Jauvion, 2020; see Figure 3S). Specimen preparation is simple: while the samples may be unfixed (e.g. flash-frozen), it is usual to use specimens fixed in the standard manner (since μCT allows for subsequent use of the same specimen in any other analysis or imaging protocol). Both ethanol and formaldehyde fixatives work fine, with some studies recommending the use of acidic coagulants (in the form of Bouin's fixative) to yield higher image contrast (this is, however, not necessary for crustacean taxonomy in most cases, as the inherent contrast between soft and hard tissue is sufficient anyway) (Wirkner and Richter, 2004). Image quality may be enhanced by stains (in this technique idiosyncratically called "contrast agents"), with the most common ones (providing superior X-ray scattering capabilities) containing atoms of iodine (e.g. Lugol's solution) or osmium (e.g. osmium tetroxide) (Grams and Richter, 2021). This staining helps especially to differentiate between soft tissues with different fat content, but it has not hitherto been shown to be important for crustacean taxonomy, with enough endogenous contrast present in virtually all cases. While the specimens do not need to be dry for imaging itself to be successful, the lengthy scanning process often leads to spontaneous evaporation (air-drying) and consequential morphological artifacts, which makes many researchers opt for specimen dehydration (usually by critical point drying) before μCT imaging. It must be reminded that this makes the sample unsuitable for some potential downstream analysis, including some optical microscopy methods (e.g. immunofluorescence) or nucleic acid isolation for long-chain sequencing. In some studies where precise discrimination between small internal features was necessary (e.g. in neuroanatomy of arthropods), higher energies of X-ray illumination (derived from a large device known as a synchrotron) have been used (Betz et al., 2007). However, for taxonomically important morphological features laboratory-scale μCT (which uses fully shielded bench-size X-ray sources) is fully sufficient. The main advantages of μCT for imaging morphological features of deep-sea Peracarida is the non-destructive character of imaging (thus, it can be used even for the most valuable type samples), the ease of sample preparation and the isomorphic resolution of three-dimensional images (allowing reliable measurement of spatial features). Disadvantages are limited to low access to relevant equipment in some academic centers (although this is currently changing with increasing affordability of μCT equipment) and lack of obvious links between physico-chemical composition of biological tissues and structures and contrast features of the image (which is, however, usually not important for taxonomists).

3.3 Species Descriptions

The naming of species according to defined standards serves to link new information with existing knowledge. The purpose of formal species descriptions is therefore to show how a species is characterized, how it differs from other known species, and ultimately to make the name available for biogeographical, conservational, or phylogenetic studies amongst others. In the past, species descriptions consisted only of the name and diagnosis of the most important segregating features, later detailed descriptions followed, which are extensive, time consuming and (arguably) not necessary (Riedel et al., 2013; Renner, 2016).

A detailed morphological description clearly contradicts ongoing efforts to accelerate taxonomic work. New methodologies and integrative approaches also do not contribute much to the goal of making taxonomy faster, on the contrary, they tend to increase complexity. This is also due to the

fact that with increasing use of molecular tools in taxonomy, often more (new) species are discovered than being described (Pante et al., 2015), a condition that is also observed in studies of deep-sea peracarids (Jennings et al., 2018; Brix et al., 2020; Kaiser et al., 2021; Mohrbeck et al., 2021). Reasons for this gap are manifold: for instance, definitive (morphological and molecular) evidence of a new species is absent, the authors lack taxonomic expertise or there is not enough time to describe all the species in the duration of a (post doc) project (Pante et al., 2015; Brix et al., 2020; Malyutina et al., 2020; Kaiser et al., 2021).

From a peracarid study point of view, there arguably has hardly been any progress in deviating from the so-called taxonomic impediment, i.e. the description of the many, especially small-sized taxa by declining number of taxonomists (Convention on Biological Diversity [CBD], 2010; Mora et al., 2011; Coleman, 2015; Engel et al., 2021). Over the past decades, novel tools have been introduced to put taxonomy into the fast lane, from automated species descriptions (e.g., using DELTA - DEscriptive Language for TAxonomy, Dallwitz et al., 2000), turbo- (Riedel et al., 2013) and cybertaxonomy (Zhang, 2008), to descriptions based exclusively on DNA sequences as diagnostic characters (Jörger and Schrödl, 2013). Turbotaxonomy, for example, describes the approach of linking molecular sequences, morphological descriptions, and high-resolution digital imaging to enable the rapid formal description of a relatively large number of new species (Riedel et al., 2013). While the appropriateness of some new approaches is certainly controversial (e.g., DNA sequences as diagnostic characters, Meier et al., 2022), so far only a few of the modern endeavors mentioned above have been translated into the description of new deep-sea peracarid species (e.g., Lowry and Myers, 2012; Sittrop et al., 2015).

The task of describing all peracarid species from the deep sea is enormous. Hundreds of species are already known within the Peracarida from there, especially within the Isopoda and Tanaidacea (Brandt et al., 2012; Błażewicz-Paszkowycz et al., 2012). Yet, the number of undescribed species is probably much larger, although robust estimates are scarce (Wilson, 2017). From the central abyssal Pacific, for example, 187 and 98 supposedly new species within Isopoda and Tanaidacea, respectively, could be identified from a single sample campaign (Błażewicz et al., 2019; Brix et al., 2020). Add to this, the need of taxonomic revisions and redescriptions of earlier works, which is crucial, but also leads to a step backwards in the description and assessment of deep-sea peracarid biodiversity (Brandt et al., 2012).

For the hypothetical case that around 10,000 deep-sea species within the Isopoda and Tanaidacea still have to be described, existing taxonomists would need around 1,000-2,500 years with a current average rate of 4–9 descriptions per year (**Figure 4**). However, this also requires that sufficient taxonomic expertise remains available and that its number do not decrease any further. Therefore, taxonomic intercalibration exercises in the form of the exchange of sketches and informal taxonomic information were encouraged in order to compare undescribed biodiversity between different regions (International Seabed Authority ISA, 2020; Lins et al., 2021; Washburn et al., 2021). Furthermore, lengthy morphometric investigations and descriptions of new species have already been replaced by proteomic profiles (Yeom et al., 2021). In addition, molecular methods such as e-DNA metabarcoding approaches are propagated, which record biodiversity in a certain area by circumventing formal species descriptions (Dell'Anno et al., 2015; Pawlowski et al., 2018).

Despite the urgency to describe deep-sea fauna in the wake of augmented human impacts, we believe that species should still be formally named and described. Furthermore, descriptions should adhere to common standards, such as according to the International Code of Zoological Nomenclature (ICZN). Species descriptions take time to be accurate and robust, but they could become standardized and more automated (e.g., using programs such as DELTA or MANTIS; Dallwitz et al., 2000; Naskrecki, 2008; Brown, 2013). In addition, experts for a specific group could agree on the lowest common denominator of diagnostic features necessary for the delineation and identification of species, while supplementary microscopic images (such as CLSM see above) provide further taxonomically important information, as well as biogeography, environmental parameters, or DNA barcoding. Overall, we agree with Glover et al. (2018) that only through a comprehensive study of deep-sea species can we gain a better understanding of their function and value for the for deep-sea ecosystems.

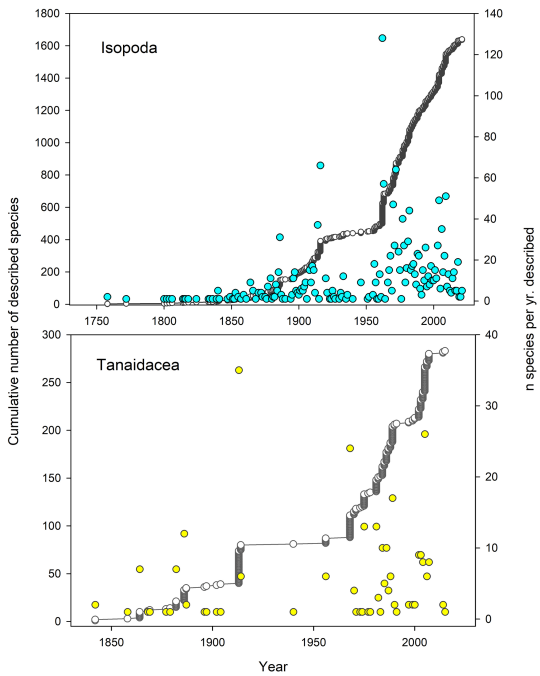

FIGURE 4 | Rate of deep-sea species descriptions within Isopoda (top) and Tanaidacea (below); the line indicates the cumulative number of species (corresponding left y-axis), and the scatter plot indicates the actual number of species described (right y-axis) per year. The average description rate in the last ten years was ~4 and 9 species for tanaidaceans and isopods respectively. Data retrieved from WoRDSS (Glover et al., 2021) and updated through WoRMS (WoRMS Editorial Board, 2021). According to WoRDSS (Glover et al., 2021) only species described from below 500 m are included.

4 DISCUSSION

Undoubtedly, peracarids are an integral part of deep-sea benthic ecosystems (Hessler and Wilson, 1983; Błażewicz-Paszkowycz et al., 2012; Frutos et al., 2017a). Within the particularly species-rich groups, isopods and tanaidaceans, so far around 2,000 species have been described (**Figure 4**), and that should be only a fraction of what is actually present. While well-established traditional methods are often still in use to describe and classify deep-sea Peracarida, new methodologies, notably molecular and microscopic imaging tools, have taken their taxonomic analysis to a new (integrative) level. Specifically, these methods have helped solve some common issues in peracarid taxonomy, including, but not limited to, the delineation of morphologically the same or similar species (Havermans et al., 2013; Brandt et al., 2014; Brix et al., 2015; Jakiel et al., 2020; Kaiser et al., 2021), those with strong sexual or ontogenetic dimorphism (Riehl et al., 2012; Błażewicz-Paszkowycz et al., 2014; Riehl and Kühn, 2020), polymorphism (Larsen, 2001) or incomplete, damaged specimens (Kaiser et al., 2018). The latter is more the rule than the exception. In particular, fragile peracarid crustaceans are damaged when taking samples from greater depths or during sample processing. In addition, fixatives, especially ethanol, although the latter being still first choice, also make the specimens brittle, so they tend to lose their legs or antennae (even if the latter may be mitigated by using small amounts of glycerol (Wilson and Humphrey, 2020). The ability to identify damaged specimens is therefore certainly an advantage of molecular methods over traditional morphological identification (Mohrbeck et al., 2015).

While the methodologies considered here are focused on deep-sea peracarids, they can be applied, in the same way, to the study of other benthic small-sized crustaceans, i.e. ostracods and copepods. With special requirements for efficient sampling (<300 μm mesh-size nets or multi-corer; see Narayanaswamy et al., 2016), the identification of specimens of meiofaunal harpacticoid copepods often demands the dissection of their smallest appendages (Kihara and Martinez Arbizu, 2012; Rossel and Martínez Arbizu, 2018). They are studied in a similar workflow using modern imaging tools under an integrative approach for species identification (Easton and Thistle, 2016; Khodami et al., 2020), however, special techniques adapted to their tiny size (i.e. mass spectrometry) are also suitable for their identification (Rossel and Martínez Arbizu, 2018; Rossel and Martinez Arbizu, 2019).

Overall, the introduction of new taxonomic methods for application to deep-sea specimens seems to be delayed compared to those in shallow waters or on land. 'Omic' approaches, for instance, are increasingly being utilized for classification and identification of species (Bourlat et al., 2013; Raupach et al., 2016; Rossel and Martinez Arbizu, 2019). Whole-genome data, that are already used to separate prokaryote strains, may also be applied to eukaryote taxonomy in the future (Raupach et al., 2016). Yet, in the marine realm and even more so in the deep sea, the application of genomics is still in its infancy. In recent years, genomes have been published for a number of marine species (Wilson et al., 2005; Ritchie et al., 2017; Li et al., 2019), here in particular for amphipods, but also genomes from a number of tanaidacean species have been now analyzed (Kakui and Kano, 2021). For deep-sea isopods and tanaidaceans this is still pending though. Another promising approach is proteomic fingerprinting, which has already been used successfully in the identification of deep-sea isopods (Paulus et al., 2021; Kürzel et al., 2022). The advantages are the faster and cheaper application of proteomics, for example compared to the molecular genetic approach. Yet, it requires a library of protein mass spectra and, overall, the technology is not yet mature enough to reliably delineate species from an unknown deep-sea sample from one another and thus needs further evaluation (Kürzel et al., 2022).

The 'hesitation' in testing new methods is probably partly due to the challenges of deep-sea sampling itself, as fauna densities are typically low especially at greater depths (Frutos and Sorbe, 2014; Wilson, 2017; Malyutina et al., 2018) and therefore the number of organisms usually needed for any kind of molecular analysis may not be achieved. In addition, most deep-sea peracarids, with the exception of a few giant isopods and amphipods, are small, and often only a few millimetres in size, which makes it difficult to extract DNA from these specimens while keeping a whole animal as a voucher. Finally, many of these methods come at a price, require special facilities and equipment as well as expertise (e.g. Pinu et al., 2019, but see Le et al., 2021). Yet, there is no question that now is the time to look more closely than ever before into describing deep-sea biodiversity, which also means to delve deeper into these new approaches, but also to critically evaluate those that have been applied so far (e.g. with respect to long-term preservation of samples and slides, **Table 4**). The deep-sea environment could be used to a greater extent for its resources in the future and is already affected by deep-sea fisheries (e.g. Clark et al., 2016), environmental pollution (Chiba et al., 2018) and climate change (Sweetman et al., 2017). So, time is of the essence to describe more species rather quickly in order to better understand these impacts and their consequences for deep-sea ecosystems.

Despite all the advances, taxonomy has probably never been as challenging as it is today. It starts with the fact that the importance of taxonomic research is not recognized and in turn not well promoted or funded (e.g. Wägele et al., 2011; Saunders, 2020; Britz et al., 2020). In part, this is because the quality of scientific progress is measured by the Impact Factor of journals, with taxonomic journals often falling behind (Wägele et al., 2011). Chairs with a purely taxonomic focus have become a rarity, and taxonomy has become often only a sub-area of otherwise molecular or ecological subjects (e.g., Lester et al., 2014). Since taxonomic research appears to have no future, only a few young scientists can get enthusiastic about the topic, and there is already a shortage of well-trained taxonomists evident today. This taxonomic impediment mentioned above, in which a decreasing number of taxonomists are faced with a high undescribed diversity, is also noticeable among (deep-sea) peracarid taxonomists (Błażewicz-Paszkowycz et al., 2012). Within the last ten years there have been seven and 16 active

taxonomists (only first authors counted), who have described deep-sea species within the Tanaidacea and Isopoda, respectively, but only few of them holding a permanent position (Glover et al., 2021). For amphipods, Coleman (2015) counted nine active taxonomists, although these include the entire diversity of this speciose group - from freshwater to marine. Yet, with regard to the methods and techniques presented in this review, we show how diverse and demanding the taxonomic work is, which not only includes the time-consuming work of describing new species, but often also dealing with unsolved phylogenetic histories including species' redescription and assessment of museum's type material. Among other things, this not only requires a taxonomist to have profound theoretical knowledge of species concepts and phylogenetic analytical methods but also methodical skills, for example in the application of various microscopy techniques or imaging processes as well as relevant molecular methods, while at the same time having to keep up with the pace of how the latter are developing.

It is not a new topic that taxonomic work is highly underrated, and at the same time it is not an individual problem that taxonomists do not get recognition for their work, but that is placed in a broader context and ultimately linked to how society values biodiversity and nature. In our opinion, this is exactly where we have to start, namely to convey taxonomic research and thus the diversity of life to other scientists, but also the wider public. New methods can play a special role here, because the application of the new imaging processes opens up a new world not only to taxonomists, but also to other scientists. SEM let us recognize surfaces that were previously invisible and provides information about the hardness of the tegument; CLSM or computed tomography help to recognize internal structures and thus contribute to the understanding of the functional morphology, embryology or even to the recognition of the material quality that defines the respective structures. All of this not only gives us the opportunity to learn what type of animal we are seeing, but also how it is constructed and how it functions. Thus, these new techniques (including imaging), which are primarily geared towards taxonomy, are an important link to other sciences thus making taxonomy a highly integrative field of science. For laypeople, of course, this only plays a subordinate role; instead, ethical and aesthetic reasons to value or reject something are often in the foreground (cf. Jamieson et al., 2021). Analogous to Haeckel's drawings, the art factor (microscopic images) could be used to reach the public and convince them of the beauty of deep-sea life, and thus also to raise their awareness of how biodiverse the deep sea is and that this diversity is threatened.

5 CONCLUSIONS

Learning more about the deep sea and its inhabitants is an urgent need, and taxonomy will play an important role in this endeavor. Therefore, changes must be addressed here too, in order to describe deep-sea species and thus biodiversity more quickly and at the same time to ensure high-quality taxonomic work. Although great advances have been made in microscopy and imaging tools, it has been shown that relying on morphology alone to describe species poses a number of pitfalls. Therefore, integrative taxonomy in describing deep-sea species is the way forward, as it provides multiple lines of evidence to reliably differentiate species from one another. So, whenever possible, both morphological and molecular (if fixation allows), as well as possibly a description of the environment among others should be sought when describing species. In this paper we have also discussed a number of methods that have not yet or only rarely been so far used in peracarid taxonomy, but that may become more important in the future. Here, particular mention should be made of (non-destructive) microscopic techniques such as CLSM, ESEM or μCT or 'omic' approaches including genomics and proteomics. Above all, however, taxonomic work is to be recognized as what it is, i.e. a multidisciplinary science that makes an essential part of research into deep-sea biodiversity and thus a significant contribution to its conservation.

AUTHOR CONTRIBUTIONS

IF and MB developed the idea; IF and SK produced the figures. All authors contributed to drafting and editing the text, read and approved the submitted version.

FUNDING

SK acknowledges a grant by the Polish National Agency for Academic Exchange (NAWA) under the ULAM program (PPN/ULM/2019/1/00169); IF acknowledges PPN/BFR/2019/1/00031/U/00001 PHC-Polonium; MB and IF acknowledge – NCN OPUS 2018/31/B/NZ8/03198 and NCN OPUS 2016/13/B/NZ8/02495.

ACKNOWLEDGMENTS

Preparation of this manuscript began during the Covid-19 pandemic, which did not allow co-authors to meet in person until restrictions were relaxed. The authors are therefore indebted to the online technology that made the advancement of this article possible. We would like to thank Laure Corbari and Paula Martín-Lefevre, Musée national d'Histoire Naturelle in Paris, who kindly provided the scan of the original plate outline of Chevreux; and two reviewers for their comments that substantially improved this manuscript.

REFERENCES

Ahyong, S. T., Chan, B. K. K., Chan, T.-Y., Corbari, L., Ďuriš, Z., Frutos, I, et al. (2022). "Crustacean Diversity and Discovery," in *The Marine Fauna and Flora of the Bismarck Sea. Patrimoines Naturels*. Eds. P. Bouchet, C. Payri, R. Sabroux and S Samadi. Paris:Muséum national d'Histoire Naturelle

Allington-Jones, L., and Sherlock, E. (2007). Choosing a Microscope Slide Sealant: A Review of Aging Characteristics and the Development of a New Test, Using Low Oxygen Environments. *NatSCA News* 12, 4–14.

Almeida, M., Frutos, I., Company, J. B., Martin, D., Romano, C., and Cunha, M. R. (2017). Biodiversity of Suprabenthic Peracarid Assemblages From the Blanes Canyon Region (NW Mediterranean Sea) in Relation to Natural Disturbance and Trawling Pressure. *Deep Sea Res. Pt. II Top. Stud. Oceanogr.* 137, 390–403. doi: 10.1016/j.dsr2.2016.06.019

Anderson, G. (2014). Endangered: A Study of Morphological Drawing in Zoological Taxonomy. *Leonardo* 47 (3), 232–240. doi: 10.1162/LEON_a_00675

Appeltans, W., Ahyong, S. T., Anderson, G., Angel, M. V., Artois, T., Bailly, N., et al. (2012). The Magnitude of Global Marine Species Diversity. *Curr. Biol.* 22 (23), 2189–2202. doi: 10.1016/j.cub.2012.09.036

Ashford, O. S., Kenny, A. J., Barrio Frojan, C. R. S., Bonsall, M. B., Horton, T., Brandt, A., et al. (2018). Phylogenetic and Functional Evidence Suggests That Deep-Ocean Ecosystems are Highly Sensitive to Environmental Change and Direct Human Disturbance. *Proc. R. Soc B.* 285, 20180923. doi: 10.1098/rspb.2018.0923

Bamber, R. N. (2007). New Apseudomorph Tanaidaceans (Crustacea, Peracarida, Tanaidacea) From the Bathyal Slope Off New Caledonia. *Zoosystema* 29 (1), 51–81.

Bameul, F. (1990). Le DMHF: Un Excellent Milieu De Montage En Entomologie. *L'Entomologiste* 46 (5), 233–239.

Barbosa, P., Berry, D. L., and Kary, C. S. (2014). *Insect Histology: Practical Laboratory Techniques* (John Wiley and Sons, Ltd). doi: 10.1002/9781118876114

Barnard, J. L., and Ingram, C. L. (1990). Lysianassoid Amphipoda (Crustacea) From Deep-Sea Thermal Vents. *Smithson Contrib. Zool.* 449, 1–80. doi: 10.5479/si.00810282.499

Bellan-Santini, D., and Thurston, M. H. (1996). Amphipoda of the Hydrothermal Vents Along the Mid-Atlantic Ridge. *J. Nat. Hist.* 30, 685–702. doi: 10.1080/00222939600770381

Beninde, J., Möst, M., and Meyer, A. (2020). Optimized and Affordable High-Throughput Sequencing Workflow for Preserved and Nonpreserved Small Zooplankton Specimens. *Mol. Ecol. Resour.* 20, 1632–1646. doi: 10.1111/1755-0998.13228

Betz, O., Wegst, U., Weide, D., Heethoff, M., Helfen, L., Lee, W.-K., et al. (2007). Imaging Applications of Synchrotron X-Ray Phase-Contrast Microtomography in Biological Morphology and Biomaterials Science. I. General Aspects of the Technique and Its Advantages in the Analysis of Millimetre-Sized Arthropod Structure. *J. Microsc.* 227, 51–71. doi: 10.1111/j.1365-2818.2007.01785.x

Błażewicz, M., Jóźwiak, P., Jennings, R. M., Studzian, M., and Frutos, I. (2019). Integrative Systematics and Ecology of a New Deep-Sea Family of Tanaidacean Crustaceans. *Sci. Rep.* 9 (1), 1–70. doi: 10.1038/s41598-019-53446-1

Błażewicz-Paszkowycz, M., Bamber, R., and Anderson, G. (2012). Diversity of Tanaidacea (Crustacea: Peracarida) in the World's Oceans–How Far Have We Come? *PloS One* 7 (4), e33068. doi: 10.1371/journal.pone.0033068

Błażewicz-Paszkowycz, M., Bamber, R. N., and Cunha, M. R. (2011). New Tanaidomorph Tanaidacea (Crustacea: Peracarida) From Submarine Mud-Volcanoes in the Gulf of Cadiz (North-East Atlantic). *Zootaxa* 2769 (1), 1–53. doi: 10.11646/zootaxa.2769.1.1

Błażewicz-Paszkowycz, M., Jennings, R. M., Jeskulke, K., and Brix, S. (2014). Discovery of Swimming Males of Paratanaoidea (Tanaidacea). *Pol. Polar. Res.* 35 (2), 415–453. doi: 10.2478/popore-2014-0022

Bober, S., and Riehl, T. (2014). Adding Depth to Line Artwork by Digital Stippling – A Step-by-Step Guide to the Method. *Org. Divers. Evol.* 14 (3), 327–337. doi: 10.1007/s13127-014-0173-7

Bober, S., Riehl, T., and Brandt, A. (2018). An Organ of Equilibrium in Deep-Sea Isopods Revealed: The Statocyst of Macrostylidae (Crustacea, Peracarida, Janiroidea). *Zoomorph* 137 (1), 71–82. doi: 10.1007/s00435-017-0376-5

Bourlat, S. J., Borja, A., Gilbert, J., Taylor, M. I., Davies, N., Weisberg, S. B., et al. (2013). Genomics in Marine Monitoring: New Opportunities for Assessing Marine Health Status. *Mar. Poll. Bull.* 74 (1), 19–31. doi: 10.1016/j.marpolbul.2013.05.042

Bourque, D. A., Morey, K. C., Bradley, D. L., Fost, B., Daley, J. M., Jacobson, N., et al. (2020). Dimethyldimethyl Hydantoin: An Alternative Fluid for Morphological and Genetic Preservation. *Biopreserv. Biobank.* 18, 283–289. doi: 10.1089/bio.2020.0001

Boxshall, G. A., Kihara, T. C., and Huys, R. (2016). Collecting and Processing Non-Planktonic Copepods. *J. Crust. Biol.* 36, 576–583. doi: 10.1163/1937240X-00002438

Brandt, A., Alalykina, I., Brix, S., Brenke, N., Błażewicz, M., Golovan, O. A., et al. (2019). Depth Zonation of Northwest Pacific Deep-Sea Macrofauna. *Prog. Oceanogr.* 176, 102131. doi: 10.1016/j.pocean.2019.102131

Brandt, A., Błażewicz-Paszkowycz, M., Bamber, R. N., Mühlenhardt-Siegel, U., Malyutina, M. V., Kaiser, S., et al. (2012). Are There Widespread Peracarid Species in the Deep Sea (Crustacea: Malacostraca)? *Pol. Polar. Res.* 33 (2), 139–162. doi: 10.2478/v10183-012-0012-5

Brandt, A., Brix, S., Held, C., and Kihara, T. C. (2014). Molecular Differentiation in Sympatry Despite Morphological Stasis: Deep-Sea *Atlantoserolis* Wägele 1994 and Glabroserolis Menzies 1962 From the South-West Atlantic (Crustacea: Isopoda: Serolidae). *Zool. J. Linn. Soc* 172 (2), 318–359. doi: 10.1111/zoj.12178

Britz, R., Hundsdörfer, A., and Fritz, U. (2020). Funding, Training, Permits—the Three Big Challenges of Taxonomy. *Megataxa* 1 (1), 49–52. doi: 10.11646/megataxa.1.1.10

Brix, S., Leese, F., Riehl, T., and Kihara, T. C. (2015). A New Genus and New Species of Desmosomatidae Sars 1897 (Isopoda) From the Eastern South Atlantic Abyss Described by Means of Integrative Taxonomy. *Mar. Biodiv.* 45, 7–61. doi: 10.1007/s12526-014-0218-3

Brix, S., Osborn, K. J., Kaiser, S., Truskey, S. B., Schnurr, S. M., Brenke, N., et al. (2020). Adult Life Strategy Affects Distribution Patterns in Abyssal Isopods – Implications for Conservation in Pacific Nodule Areas. *Biogeosciences* 17, 6163–6184. doi: 10.5194/bg-17-6163-2020

Brökeland, W., Guðmundsson, G., and Svavarsson, J. (2010). Diet of Four Species of Deep-Sea Isopods (Crustacea: Malacostraca: Peracarida) in the South Atlantic and the Southern Ocean. *Mar. Biol.* 157, 177–187. doi: 10.1007/s00227-009-1308-9

Brooker, A., Bron, J., and Shinn, A. (2012a). Description of the Free-Swimming Juvenile Stages of *Lernaeocera Branchialis* (Pennellidae), Using Traditional Light and Confocal Microscopy Methods. *Aquat. Biol.* 14, 153–163. doi: 10.3354/ab00388

Brooker, A., Shinn, A., and Bron, J. (2012b). Use of Laser Scanning Confocal Microscopy for Morphological Taxonomy and the Potential for Digital Type Specimens (E-Types). *Aquat. Biol.* 14, 165–173. doi: 10.3354/ab00389

Brown, B. V. (2013). Automating the" Material Examined" Section of Taxonomic Papers to Speed Up Species Descriptions. *Zootaxa* 3683 (3), 297–299. doi: 10.11646/zootaxa.3683.3.8

Bruce, N. L. (1995). The Taxonomy and Phylogeny of Tube-Tailed Sphaeromatid Isopods (Crustacea) With Descriptions of New Species and a New Genus From Southern Australia. *Ophelia* 43 (2), 127–180. doi: 10.1080/00785326.1995.10429829

Bruce, N. L. (1997). A New Genus of Marine Isopod (Crustacea: Flabellifera: Sphaeromatidae) From Australia and the Indo- Pacific Region. *Mem. Mus. Vic.* 56, 145–234. doi: 10.24199/j.mmv.1997.56.08

Bruce, N. L. (2005). Two New Species of the Mesopelagic Isopod Genus *Syscenus* Harger 1880 (Crustacea: Isopoda: Aegidae) From the Southwestern Pacific. *Zootaxa* 1070, 31–42. doi: 10.11646/zootaxa.1070.1.2

Bruce, H. S., and Patel, N. H. (2020). Knockout of Crustacean Leg Patterning Genes Suggests That Insect Wings and Body Walls Evolved From Ancient Leg Segments. *Nat. Ecol. Evol.* 4, 1703–1712. doi: 10.1038/s41559-020-01349-0

Brunel, P., Besner, M., Messier, D., Poirier, L., Granger, D., and Weinstein, M. (1978). Le Traîneau Macer-GIROQ: Appareil Amélioré Pour L'échantillonnage Quantitatif De La Petite Faune Nageuse Au Voisinage Du Fond. *Int. Rev. Ges Hydrobiol.* 63 (6), 815–829. doi: 10.1002/iroh.19780630612

Buhl-Jensen, L. (1986). The Benthic Amphipod Fauna of the West-Norwegian Continental Shelf Compared With the Fauna of Five Adjacent Fjords. *Sarsia* 71, 193–208. doi: 10.1080/00364827.1986.10419690

Campean, A. J., and Coleman, C. O. (2018). A New Species of Sicafodia Just 2004 (Crustacea, Amphipoda, Sicafodiidae) From the North Atlantic. *Mar. Biodiver.* 48, 939–948. doi: 10.1007/s12526-017-0635-1

Carrasón, M., and Matallanas, J. (2001). Feeding Ecology of the Mediterranean Spiderfish, *Bathypterois Mediterraneus* (Pisces: Chlorophthalmidae), on the Western Mediterranean Slope. *Fish. Bull.* 99 (2), 266–274.

Cartanyà, J. (1991). Nous Crustacis Al Registre Fossil De La Conca De Barberà. *Reboll* 2, 27–30.

Cartes, J. E., Sorbe, J. C., and Sardà, F. (1994). Spatial Distribution of Deep-Sea Decapods and Euphausiids Near the Bottom in the Northwestern Mediterranean. *J. Exp. Mar. Biol. Ecol.* 179, 131–144. doi: 10.1016/0022-0981(94)90021-3

CBD, Secretariat of the Convention on Biological Diversity (2010). Guide to the Global Taxonomy Initiative. *CBD Tech. Ser.* 30 (1–195), i–viii.

Chardy, P. (1979). Structure of Deep Sea Asellota Assemblages in the Bay of Biscay; Relationships With the Abyssal Environment. *Ambio Special Rep.* 6, 79–82.

Chiba, S., Saito, H., Fletcher, R., Yogi, T., Kayo, M., Miyagi, S., et al. (2018). Human Footprint in the Abyss: 30 Year Records of Deep-Sea Plastic Debris. *Mar. Pol.* 96, 204–212. doi: 10.1016/j.marpol.2018.03.022

Chim, C. K., and Tong, S. J. (2020). Two New Species of Paratanaoid Tanaidaceans of the Family Incertae Sedis (Crustacea: Peracarida) From Polymetallic Nodule Fields in the Eastern Clarion-Clipperton Fracture Zone. *Zootaxa* 4758 (3), 461–485.

Clark, M. R., Althaus, F., Schlacher, T. A., Williams, A., Bowden, D. A., and Rowden, A. A. (2016). The Impacts of Deep-Sea Fisheries on Benthic Communities: A Review. *ICES J. Mar. Sci.* 73 (1), i51–i69. doi: 10.1093/icesjms/fsv123

Coleman, C. O. (2003). "Digital Inking": How to Make Perfect Line Drawings on Computers. *Org. Divers. Evol.* 14, 1–14. doi: 10.1078/1439-6092-00081

Coleman, C. O. (2006). Substituting Time-Consuming Pencil Drawings in Arthropod Taxonomy Using Stacks of Digital Photographs. *Zootaxa* 1360, 61–68. doi: 10.11646/zootaxa.1360.1.4

Coleman, C. O. (2009). Drawing Setae the Digital Way. *Zoosyst. Evol.* 85 (2), 305–310. doi: 10.1002/zoos.200900008

Coleman, C. O. (2015). Taxonomy in Times of the Taxonomic Impediment–Examples From the Community of Experts on Amphipod Crustaceans. *J. Crust. Biol.* 35 (6), 729–740. doi: 10.1163/1937240X-00002381

Corbari, L., Frutos, I., and Sorbe, J. C. (2019). *Dorotea* Gen. Nov., a New Bathyal Genus (Amphipoda, Eusiridae) From the Solomon Sea (Papua New Guinea). *Zootaxa* 4568, 69–80. doi: 10.11646/zootaxa.4568.1.4

Corbera, J. (2006). "Arthropoda Cumacea," in *Handbook of Deep-Sea Hydrothermal Vent Fauna. Denisia*, vol. 18. Eds. D. I. Desbruyères, M. Segonzac and M. Bright, 370–371.

Corbera, J., and Martín, D. (2002). Two New Cumacean Species (Crustacea: Peracarida) From Shallow Waters Off Thailand. *Sci. Mar.* 66, 407–415. doi: 10.3989/scimar.2002.66n4407

Corbera, J., Segonzac, M., and Cunha, M. R. (2008). A New Deep-Sea Genus of Nannastacidae (Crustacea, Cumacea) From the Lucky Strike Hydrothermal Vent Field (Azores Triple Junction, Mid-Atlantic Ridge). *Mar. Biol. Res.* 4 (3), 180–192. doi: 10.1080/17451000801898576

Cordiner, C. (1793). Remarkable ruins, and romantic prospects, of North Britain. With ancient monuments, and singular subjects of natural history. Peter Mazell, London. 96 plates with letterpress.

Costa, A. B., Silva, M.B.da, Fraga, R. E., Rocha, A.A.da, Nishiyama, P. B., Anjos, M.S.d., et al. (2021). Evaluation of an Alternative Technique for Preserving Crustaceans in Dry Conditions With Joint Mobility: A Proposal for Didactic Purposes. *Acta Sci. Biol. Sci.* 43, e53450. doi: 10.4025/actascibiolsci.v43i1.53450

Costello, M. J., and Chaudhary, C. (2017). Marine Biodiversity, Biogeography, Deep-Sea Gradients, and Conservation. *Curr. Biol.* 27 (11), R511–R527. doi: 10.1016/j.cub.2017.06.015

Curatolo, T., Calvaruso, C., Galil, B. S., and Lo Brutto, S. (2013). Geometric Morphometry Supports a Taxonomic Revision of the Mediterranean *Bathyporeia Guilliamsoniana* (Spence Bate 1857) (Amphipoda, Bathyporeiidae). *Crustaceana* 86, 820–828. doi: 10.1163/15685403-00003217

Dallwitz, M. J., Paine, T. A., and Zurcher, E. J. (2000) *Principles of Interactive Keys*. Available at: http://delta-intkey.com (Accessed 5 July 2012).

Dauvin, J. C., Sorbe, J. C., and Lorgeré, J. C. (1995). The Benthic Boundary Layer Macrofauna From the Upper Continental Slope and the Cap-Ferret Canyon (Bay of Biscay). *Oceanol. Acta* 18, 113–122.

Dell'Anno, A., Carugati, L., Corinaldesi, C., Riccioni, G., and Danovaro, R. (2015). Unveiling the Biodiversity of Deep-Sea Nematodes Through Metabarcoding: Are We Ready to Bypass the Classical Taxonomy? *PloS One* 10 (12), e0144928. doi: 10.1371/journal.pone.0144928

Demidov, O., Kihara, T. C., Martinez Arbizu, P., and Clark, P. F. (2021). The Megalopal Stage of the Hydrothermal Vent Crab *Austinograea Rodriguezensis* Tsuchida and Hashimoto 2002 (Decapoda: Bythograeidae): A Morphological Description Based on CLSM Images. *Zootaxa* 5040 (3), 365–387. doi: 10.11646/zootaxa.5040.3.3

Drumm, D. T. (2005). Comparative Morphology of the Mouthparts, Chelipeds and Foregut of Two Kalliapseudid Apseudomorphans (Crustacea: Tanaidacea). *P. Acad. Nat. Sci. Phil.* 154, 137–147. doi: 10.1635/0097-3157(2004)154[0137:CMOTMC]2.0.CO;2

d'Udekem d'Acoz, C., and Verheye, M. H. (2017). *Epimeria* of the Southern Ocean With Notes on Their Relatives (Crustacea, Amphipoda, Eusiroidea). *Eur. J. Taxon.* 359, 1–553. doi: 10.5852/ejt.2017.359

Dumke, I., Purser, A., Marcon, Y., Nornes, S. M., Johnsen, G., Ludvigsen, M., et al. (2018). Underwater Hyperspectral Imaging as an *in Situ* Taxonomic Tool for Deep-Sea Megafauna. *Sci. Rep.* 8 (1), 1–11. doi: 10.1038/s41598-018-31261-4

Dupérré, N. (2020). Old and New Challenges in Taxonomy: What Are Taxonomists Up Against? *Megataxa* 1, 59–62. doi: 10.11646/megataxa.1.1.12

Easton, E. E., and Thiestle, D. (2016). Do Some Deep-Sea, Sediment-Dwelling Species of Harpacicoid Copepods Have 1000-km-Scale Range Sizes? *Mol. Ecol.* 25, 4301–4318. doi: 10.1111/mec.13744

Eiler, S. M., Haug, C., and Haug, J. T. (2016). Detailed Description of a Giant Polychelidan Eryoneicus-Type Larva With Modern Imaging Techniques. *Spixiana* 39, 22–60.

Eltoum, I., Fredenburgh, J., Myers, R. B., and Grizzle, W. E. (2001). Introduction to the Theory and Practice of Fixation of Tissues. *J. Histotechnol.* 24, 173–190. doi: 10.1179/his.2001.24.3.173

Engel, M. S., Ceríaco, L. M. P., Daniel, G. M., Dellapé, P. M., Löbl, I., Marinov, M., et al. (2021). The Taxonomic Impediment: A Shortage of Taxonomists, Not the Lack of Technical Approaches. *Zool. J. Linn. Soc* 193, 381–387. doi: 10.1093/zoolinnean/zlab072

Esquete, P., Wilson, G. D. F., and Troncoso, J. S. (2014). Ecology and Systematics of a New Species of *Uromunna* (Crustacea: Isopoda) From Spanish Eelgrass Beds. *Helgol. Mar. Res.* 68 (2), 329–339. doi: 10.1007/s10152-014-0393-4

Evers, D. L., Fowler, C. B., Cunningham, B. R., Mason, J. T., and O'Leary, T. J. (2011). The Effect of Formaldehyde Fixation on RNA: Optimization of Formaldehyde Adduct Removal. *J. Mol. Diagn.* 13 (3), 282–288. doi: 10.1016/j.jmoldx.2011.01.010

Fernández del Río, L., Arwin, H., and Järrendahl, K. (2016). Polarizing Properties and Structure of the Cuticle of Scarab Beetles From the *Chrysina* Genus. *Phys. Rev. E* 94, 12409. doi: 10.1103/PhysRevE.94.012409

Fontaine, B., Perrard, A., and Bouchet, P. (2012). Twenty-One Years of Shelf Life Between Discovery and Description of New Species. *Curr. Biol.* 22, 943–944. doi: 10.1016/j.cub.2012.10.029

Frank, T. M., Widder, E. A., Latz, M. I., and Case, J. F. (1984). Dietary Maintenance of Bioluminescence in a Deep-Sea Mysid. *J. Exp. Biol.* 109, 385–389. doi: 10.1242/jeb.109.1.385

Frutos, I. (2006). *Estudio De Las Comunidades Suprabentónicas Submareales De La Ría De La Coruña Y Plataforma Continental Adyacente* (NW Península Ibérica: Universidad de Alcalá).

Frutos, I. (2017). "Mysida," in *Inventario De La Biodiversidad Marina De Galicia: Proyecto LEMGAL*(Santiago de Compostela:Consellería do Mar, Xunta de Galicia), 443–448 pp.

Frutos, I., Brandt, A., Sorbe, J. C., and Orejas Saco del Valle, C. (2017a). "Deep-Sea Suprabenthic Communities: The Forgotten Biodiversity," in *Marine Animal Forests. The Ecology of Benthos Biodiversity Hotspots*. Eds. S. Rossi, L. Bramanti and A. Gori (Springer), 475–503 pp. doi: 10.1007/978-3-319-21012-4_21

Frutos, I., Corbari, L., and Sorbe, J. C. (2017b). Diversity of Deep-Sea Amphipoda From Papua New Guinea (SW Pacific Ocean). *Biodivers. J.* 8 (2), 505–506.

Frutos, I., and Sorbe, J. C. (2010). *Politolana Sanchezi* Sp. Nov. (Crustacea: Isopoda: Cirolanidae), a New Benthic Bioturbating Scavenger From Bathyal Soft-Bottoms of the Southern Bay of Biscay Northeastern Atlantic Ocean.

Zootaxa (Alicante, Spain:XVI SIEBM Abstract book) 2640, 20–34. doi: 10.11646/zootaxa.2640.1.2

Frutos, I., and Sorbe, J. C. (2013). *Leucothoe Cathalaa* Sp. Nov. (Crustacea: Amphipoda: Leucothoidae) a New Bathyal Benthic Species From the Le Danois Bank ("El Cachucho" Spanish MPA), Southern Bay of Biscay. *J. Mar. Biol. Assoc. UK* 93 (3), 659–666.

Frutos, I., and Sorbe, J. C. (2014). Bathyal Suprabenthic Assemblages From the Southern Margin of the Capbreton Canyon ("Kostarrenkala" Area), SE Bay of Biscay. *Deep Sea Res. Pt. II Top. Stud. Oceanogr.* 104, 291–309. doi: 10.1016/j.dsr2.2013.09.010

Frutos, I., Sorbe, J. C., and Junoy, J. (2010). "La Primera Especie Ciega Del Género *Paranthura* (Crustacea: Isopoda: Anthuridea) Habita En El Mar Cantábrico (N España)," in *XVI Simposio Ibérico de Estudios de Biología Marina*, Alicante (España, Septiembre 2010, Vol. 6–10.

Frutos, I., Sorbe, J. C., and Junoy, J. (2011). The First Blind *Paranthura* Species (Crustacea, Isopoda, Paranthuridae) From the "El Cachucho" Marine Protected Area (Le Danois Bank, Southern Bay of Biscay). *Zootaxa* 2971, 17–32. doi: 10.11646/zootaxa.2971.1.2

Fryer, G. (1968). Evolution and Adaptive Radiation in the Chydoridae (Crustacea: Cladocera): A Study in Comparative Functional Morphology and Ecology. *Phil. T. R. Soc London Ser. B.* 254, 221–382+384. doi: 10.1098/rstb.1968.0017

Galassi, D. M. P., De Laurentiis, P., and Giammatteo, M. (1998). Integumental Morphology in Copepods: Assessment by Confocal Laser Scanning Microscopy (CLSM). *Frag. Entomol.* 30, 79–92.

Geiselbrecht, H., and Melzer, R. R. (2013a). How do Mandibles Sense? – The Sensory Apparatus of Larval Mandibles in *Palaemon Elegans* Rathke 1837 (Decapoda, Palaemonidae). *Arthropod. Struct. Dev.* 42, 1–16. doi: 10.1016/j.asd.2012.09.001

Geiselbrecht, H., and Melzer, R. R. (2013b). Nervous Systems in 3D: A Comparison of Caridean, Anomuran, and Brachyuran Zoea-I (Decapoda). *J. Exp. Zool. B.: Mol. Dev. Evol.* 320, 511–524. doi: 10.1002/jez.b.22528

Geiselbrecht, H., and Melzer, R. R. (2014). Fine Structure and Ecdysis of Mandibular Sensilla Associated With the Lacinia Mobilis in *Neomysis Integer* (Leach 1814) (Crustacea, Malacostraca, Peracarida). *Arthropod. Struct. Dev.* 43, 221–230. doi: 10.1016/j.asd.2014.01.002

Gellert, M., Bird, G. J., Stępień, A., Studzian, M., and Błażewicz, M. (2022). A Hidden Diversity in the Atlantic and the SE Pacific: Hamatipedidae N. Fam. *Front. Mar. Sci.* 8, 773437. doi: 10.3389/fmars.2021.773437

Giurginca, A., Šustr, V., Tajovsky, K., Giurginca, M., and Matei, I. (2015). Spectroscopic Parameters of the Cuticle and Ethanol Extracts of the Fluorescent Cave Isopod *Mesoniscus Graniger* (Isopoda, Oniscidea). *ZooKeys* 515, 111–125. doi: 10.3897/zookeys.515.9395

Glenn, D., Caldwell, R. L., and Pakes, M. J. (2013). Fluorescence in Arthropoda Informs Ecological Studies in Anchialine Crustaceans, Remipedia, and Atyidae. *J. Crust. Biol.* 33, 620–626. doi: 10.1163/1937240X-00002170

Glover, A. G., Higgs, N., and Horton, T. (2021). World Register of Deep-Sea Species (WoRDSS). doi: 10.14284/352

Glover, A. G., Wiklund, H., Chen, C., and Dahlgren, T. G. (2018). Point of View: Managing a Sustainable Deep-Sea 'Blue Economy'requires Knowledge of What Actually Lives There. *Elife* 7, e41319. doi: 10.7554/eLife.41319.005

Gooday, A. J., Sykes, D., Góral, T., Zubkov, M. V., and Glover, A. G. (2018). Micro-CT 3D Imaging Reveals the Internal Structure of Three Abyssal Xenophyophore Species (Protista, Foraminifera) From the Eastern Equatorial Pacific Ocean. *Sci. Rep.* 8 (1), 1–12. doi: 10.1038/s41598-018-30186-2

Göpel, T., and Wirkner, C. S. (2018). Morphological Description, Character Conceptualization and the Reconstruction of Ancestral States Exemplified by the Evolution of Arthropod Hearts. *PloS One* 13, e0201702. doi: 10.1371/journal.pone.0201702

Grams, M., and Richter, S. (2021). Locomotion in *Anaspides* (Anaspidacea, Malacostraca) – Insights From a Morpho-Functional Study of Thoracopods With Some Observations on Swimming and Walking. *Zoology* 144, 125883. doi: 10.1016/j.zool.2020.125883

Grassle, J. F., and Maciolek, N. J. (1992). Deep-Sea Species Richness: Regional and Local Diversity Estimates From Quantitative Bottom Samples. *Am. Nat.* 139 (2), 313–341. doi: 10.1086/285329

Guidi-Guilvard, L. D., Thistle, D., and Khripounoff, A. (2007). Two-Year Temporal Variability of Small Hyperbenthos Collected 4 M Above the Bottom in the Deep, (2347 M) NW Mediterranean. *ICES* 05, 5.

Gutiérrez, Y., Ott, D., Töpperwien, M., Salditt, T., and Scherber, C. (2018). X-Ray Computed Tomography and its Potential in Ecological Research: A Review of Studies and Optimization of Specimen Preparation. *Ecol. Evol.* 8, 7717–7732. doi: 10.1002/ece3.4149

Hadjab, R., Ayati, K., and Piscart, C. (2020). A New Species of Freshwater Amphipods *Echinogammarus* (Amphipoda, Gammaridae) From Algeria. *Taxonomy* 1, 36–47. doi: 10.3390/taxonomy1010005

Hanafi-Portier, M., Corbari, L., Chan, T.-Y., Chen, W.-J., Chen, J.-N., Lee, M.-Y., et al. (2021). When Imagery and Physical Sampling Work Together: Towards an Integrative Methodology of Image-Based Megafauna Identification. *Front. Mar. Sci.* 8, 749078. doi: 10.3389/fmars.2021.749078

Haug, J. T., Haug, C., Kutschera, V., Mayer, G., Maas, A., Liebau, S., et al. (2011b). Autofluorescence Imaging, an Excellent Tool for Comparative Morphology: Autofluorescence Imaging. *J. Microsc. Oxford* 244, 259–272. doi: 10.1111/j.1365-2818.2011.03534.x

Haug, C., Mayer, G., Kutschera, V., Waloszek, D., Maas, A., and Haug, J. T. (2011a). Imaging and Documenting Gammarideans. *Int. J. Zool.* doi: 10.1155/2011/380829

Havermans, C., Sonet, G., d'Udekem d'Acoz, C., Nagy, Z. T., Martin, P., Brix, S., et al. (2013). Genetic and Morphological Divergences in the Cosmopolitan Deep-Sea Amphipod *Eurythenes Gryllus* Reveal a Diverse Abyss and a Bipolar Species. *PloS One* 8, e74218. doi: 10.1371/journal.pone.0074218

Hegna, T. A. (2010). Photography of Soft-Bodied Crustaceans *via* Drying, Whitening, and Splicing. *J. Crust. Biol.* 30, 351–356. doi: 10.1651/09-3253.1

Herring, P. J. (1981). Studies on Bioluminescent Marine Amphipods. *J. Mar. Biol. Assoc. U.K.* 61 (1), 161–176. doi: 10.1017/S0025315400045999

Hessler, R. R., and Jumars, P. A. (1974). Abyssal Community Analysis From Replicate Cores in the Central North Pacific. *Deep Sea Res. Oceanogr. Abstr.* 21 (3), 185–209. doi: 10.1016/0011-7471(74)90058-8

Hessler, R. R. , and Sanders, H. L. (1967). Faunal Diversity in the Deep-Sea. *Deep Sea Res. Part I Oceanogr. Res.* 14(1), 65–78. doi: 10.1016/0011-7471(67)90029

Hessler, R. R., and Wilson, G. D. F. (1983). "The Origin and Biogeography of Malacostracan Crustaceans in the Deep Sea," in *Evolution, Time, and Space: The Emergence of the Biosphere*, vol. 23 . Eds. R. W. Sims, J. H. Price and P. E. S. Whalley (Whalley: Systematics Association, Special Publication), 227–254.

Higgs, N. D., and Attrill, M. (2015). Biases in Biodiversity: Wide-Ranging Species Are Discovered First in the Deep Sea. *Front. Mar. Sci.* 2. doi: 10.3389/fmars.2015.00061

Holthuis, L. B. (1964). The Earliest Published Record of a Cumacean. *Crustaceana* 7, 317–318. doi: 10.1163/156854064X00533

Horton, T., Marsh, L., Bett, B. J., Gates, A. R., Jones, D. O. B., Benoist, N. M. A., et al. (2021). Recommendations for the Standardisation of Open Taxonomic Nomenclature for Image-Based Identifications. *Front. Mar. Sci.* 8. doi: 10.3389/fmars.2021.620702

Horton, T., Thurston, M. H., Vlierboom, R., Gutteridge, Z., Pebody, C. A., Gates, A. R., et al. (2020). Are Abyssal Scavenging Amphipod Assemblages Linked to Climate Cycles? *Prog. Oceanogr.* 184, 102318. doi: 10.1016/j.pocean.2020.102318

Hughes, L. E., and Ahyong, S. T. (2016). Collecting and Processing Amphipods. *J. Crust. Biol.* 36, 584–588. doi: 10.1163/1937240X-00002450

Hughes, L. E., and Kaji, T. (2016). Description of a New Species of Quadrivisio Stebbing 1907, From Songkhla Lake, Thailand (Crustacea: Peracarida: Amphipoda: Maeridae). *Raffles B. Zool.* 9 (64), 351–359.

ISA (2020). Workshop on Deep-Sea Taxonomic Standardization: Strategic Approaches for Collaboration. *ISA Workshop*, 15–16.

Jażdżewska, A. M., Brandt, A., Arbizu, P. M., and Vink, A. (2021). Exploring the Diversity of the Deep Sea — Four New Species of the Amphipod Genus *Oedicerina* Described Using Morphological and Molecular Methods. *Zool. J. Linn. Soc* 194(1), 181–225. doi: 10.1093/zoolinnean/zlab032 .

Jakiel, A., Palero, F., and Błażewicz, M. (2019). Deep Ocean Seascape and Pseudotanaidae (Crustacea: Tanaidacea) Diversity at the Clarion-Clipperton Fracture Zone. *Sci. Rep.* 9, 17305. doi: 10.1038/s41598-019-51434-z

Jakiel, A., Palero, F., and Błażewicz, M. (2020). Secrets From the Deep: Pseudotanaidae (Crustacea: Tanaidacea) Diversity From the Kuril-

Kamchatka Trench. *Prog. Oceanogr.* 183, 102288. doi: 10.1016/j.pocean.2020.102288

Jakiel, A., Stępień, A., and Błażewicz, M. (2018). A Tip of the Iceberg – Pseudotanaidae (Tanaidacea) Diversity in the North Atlantic. *Mar. Biodiv.* 48, 859–895. doi: 10.1007/s12526-018-0881-x

Jamieson, A. J. (2016). "Landers: Baited Cameras and Traps," in *Biological Sampling in the Deep Sea*. Eds. M. R. Clark, M. Consalvey and A. A. Rowden (John Wiley and Sons Ltd), 228–259 pp.

Jamieson, A. J., Singleman, G., Linley, T. D., and Casey, S. (2021). Fear and Loathing of the Deep Ocean: Why Don't People Care About the Deep Sea? *ICES J. Mar. Sci.* 78 (3), 797–809. doi: 10.1093/icesjms/fsaa234

Jaume, D., and Queinneck, E. (2007). A New Species of Freshwater Isopod (Sphaeromatidea: Sphaeromatidae) From an Inland Karstic Stream on Espíritu Santo Island, Vanuatu, Southwestern Pacific. *Zootaxa* 1653, 41–55. doi: 10.11646/zootaxa.1653.1.3

Jauvion, C. (2020). *De La Vie a La Pierre: Préservation Exceptionnelle D'arthropodes Marins Fossils* (MNHN Paris: Museum national d'histoire naturelle), 429 pp.

Jauvion, C., Audo, D., Charbonnier, S., and Vannier, J. (2016). Virtual Dissection and Lifestyle of a 165 - Million-Year-Old Female Polychelidan Lobster. *Arthropod. Struct. Dev.* 45, 122–132. doi: 10.1016/j.asd.2015.10.004

Jennings, R. M., Brix, S., Bober, S., Svavarsson, J., and Driskell, A. (2018). More Diverse Than Expected: Distributional Patterns of *Oecidiobranchus* Hessler 1970 (Isopoda, Asellota) on the Greenland-Iceland-Faeroe Ridge Based on Molecular Markers. *Mar. Biodiv.* 48 (2), 845–857. doi: 10.1007/s12526-018-0857-x

Jersabek, C. D. (2005). The 'Frank J. Myers Rotifera Collection' at the Academy of Natural Sciences of Philadelphia. *Hydrobiol* 546, 137–140. doi: 10.1007/s10750-005-4110-9

Jirikowski, G., Richter, S., and Wolff, C. (2013). Myogenesis of Malacostraca — the "Egg-Nauplius" Conceptrevisited. *Front. Zool.* 10, 76. doi: 10.1186/1742-9994-10-76

Jirikowski, G., Wolff, C., and Richter, S. (2015). Evolution of Eumalacostracan Development — New Insights Into Loss and Reacquisition of Larval Stages Revealed by Heterochrony Analysis. *Evo. Devo* 6, 4. doi: 10.1186/2041-9139-6-4

Jörger, K. M., and Schrödl, M. (2013). How to Describe a Cryptic Species? Practical Challenges of Molecular Taxonomy. *Front. Zool.* 10 (1), 1–27. doi: 10.1186/1742-9994-10-59

Jóźwiak, P., Pabis, K., Brandt, A., and Błażewicz, M. (2020). Epibenthic Sled Versus Giant Box Corer – Comparison of Sampling Gears for Tanaidacean Species Richness Assessment in the Abyssal Benthic Ecosystem. *Prog. Oceanogr.* 181. doi: 10.1016/j.pocean.2019.102255

Just, J. (2001). Bathyal Joeropsididae (Isopoda: Asellota) From South-Eastern Australia, With Description of Two New Genera. *Mem. Mus. Vic.* 58 (2), 297–333. doi: 10.24199/j.mmv.2001.58.16

Kaiser, S., and Brandt, A. (2007). Two New Species of the Genus *Austroniscus* Vanhoeffen 1914 (Isopoda: Asellota: Nannoniscidae) From the Antarctic Shelf. *Zootaxa* 1394, 47–68. doi: 10.11646/zootaxa.1394.1.3

Kaiser, S., and Brenke, N. (2016). "Epibenthic Sledges," in *Biological Sampling in the Deep Sea*. Eds. M. R. Clark, M. Consalvey and A. A. Rowden (John Wiley and Sons Ltd), 184–206 pp.

Kaiser, S., Brix, S., Kihara, T. C., Janssen, A., and Jennings, R. M. (2018). Integrative Species Delimitation in the Deep-Sea Genus *Thaumastosoma* Hessler 1970 (Isopoda, Asellota, Nannoniscidae) Reveals a New Genus and Species From the Atlantic and Central Pacific Abyss. *Deep Sea Res. Pt. II Top. Stud. Oceanogr.* 148, 151–179. doi: 10.1016/j.dsr2.2017.05.006

Kaiser, S., Kihara, T. C., Brix, S., Mohrbeck, I., Janssen, A., and Jennings, R. M. (2021). Species Boundaries and Phylogeographic Patterns in New Species of *Nannoniscus* (Janiroidea: Nannoniscidae) From the Equatorial Pacific Nodule Province Inferred From mtDNA and Morphology. *Zool. J. Linn. Soc*, 193(3), 1020–1071. doi: 10.1093/zoolinnean/zlaa174

Kaiser, S., and Marner, M. (2012). A New Species of Pentaceration Just 2009 (Isopoda, Asellota, Paramunnidae) From the Challenger Plateau, New Zealand (Tasman Sea). *Zoosystem Evol.* 88, 171–184. doi: 10.1002/zoos.201200015

Kaji, T., Fritsch, M., Schwentner, M., Olesen, J., and Richter, S. (2014). Male Claspers in Clam Shrimps (Crustacea, Branchiopoda) in the Light of Evolution: A Case Study on Homology Versus Analogy: Male Claspers in Clam Shrimps. *J. Exp. Zool. (Mol. Dev. Evol.)* 322, 269–280. doi: 10.1002/jez.b.22574

Kaji, T., Kakui, K., Miyazaki, N., Murata, K., and Palmer, A. R. (2016). Mesoscale Morphology at Nanoscale Resolution: Serial Block-Face Scanning Electron Microscopy Reveals Fine 3D Detail of a Novel Silk Spinneret System in a Tube-Building Tanaid Crustacean. *Front. Zool.* 13, 14. doi: 10.1186/s12983-016-0146-0

Kakui, K. (2014). A Novel Transmission Pathway: First Report of a Larval Trematode in a Tanaidacean Crustacean. *Fauna Ryukyuana* 17, 13–22.

Kakui, K., and Fujiwara, Y. (2020). First *In Situ* Observations of Behavior in Deep-Sea Tanaidacean Crustaceans. *Zool. Sci.* 37, 1–4. doi: 10.2108/zs200028

Kakui, K., and Hiruta, C. (2017). Tube Construction by a Tanaidacean Crustacean Using a Novel Mucus Secretion System Involving the Anal Opening. *Zool. Lett.* 3, 20. doi: 10.1186/s40851-017-0082-7

Kakui, K., and Kano, Y. (2021). First Complete Mitochondrial Genome of a Tanaidacean Crustacean (*Arctotanais Alascensis*). *Zool. Sci.* 38 (3), 267–272. doi: 10.2108/zs200167

Kamanli, S. A., Kihara, T. C., Ball, A. D., Morritt, D., and Clark, P. F. (2017). A 3D Imaging and Visualization Workflow, Using Confocal Microscopy and Advanced Image Processing for Brachyuran Crab Larvae: 3D Imaging of Crab Larvae Using CLSM. *J. Microsc. Oxford* 266, 307–323. doi: 10.1111/jmi.12540

Kelley, C., Kerby, T., Sarradin, P.-M., Sarrazin, J., and Lindsay, D. J. (2016). "Submersibles and Remotely Operated Vehicles," in *Biological Sampling in the Deep Sea*. Eds. M. R. Clark, M. Consalvey and A. A. Rowden (John Wiley and Sons Ltd), 285–305 pp.

Kenning, M., and Harzsch, S. (2013). Brain Anatomy of the Marine Isopod *Saduria Entomon* Linnaeus 1758 (Valvifera, Isopoda) With Special Emphasis on the Olfactory Pathway. *Front. Neuroanat.* 7. doi: 10.3389/fnana.2013.00032

Kensley, B. (1989). Marine Isopod Crustaceans From the St. Paul and Amsterdam Islands, Southern Indian Océan. *Bull. Mus. Natn. Hist. Nat. 4° Sér.* 11 (1), 147–164.

Khodami, S., Mercado-Salas, N. F., and Martinez Arbizu, P. (2020). Genus Level Molecular Phylogeny of Aegisthidae Gisbrecht 1893 (Copepoda: Harpacticoida) Reveals Morphological Adaptations to Deep-Sea and Plagic Habitats. *BMC Evol. Biol.* 20, 36. doi: 10.1186/s12862-020-1594-x

Kihara, T. C., and Martinez Arbizu, P. (2012). Three New Species of Cerviniella Smirnov 1946 (Copepoda: Harpacticoida) From the Arctic. *Zootaxa* 3345, 1–33. doi: 10.11646/zootaxa.3345.1.1

King, J. R., and Porter, S. D. (2004). Recommendations on the Use of Alcohols for Preservation of Ant Specimens (Hymenoptera, Formicidae). *Insect. Soc.* 51, 197–202. doi: 10.1007/s00040-003-0709-x

Kodama, M., and Kawamura, T. (2019). A New Species of Bemlos Shoemaker 1925 (Amphipoda: Aoridae) From Deep Water Off Tanabe Bay, Japan, With a Review of the Deep-Sea Aorids and Their Adaptations to the Deep Sea. *J. Crust. Biol.* 39, 54–61. doi: 10.1093/jcbiol/ruy098

Koomen, P., and von Vaupel Klein, J. C. (1995). The Suitability of Various Mounting Media for Permanent Mounts of Small Chitinous Crustaceans, With Special Reference to the Observation of Integumental Organs. *Crustaceana* 68, 428–437. doi: 10.1163/156854095X01583

Kottmann, J., Kihara, T. C., Glatzel, T., and Veit-Köhler, G. (2013). A New Species of *Wellsopsyllus* (Copepoda, Harpacticoida, Paramesochridae) From the Deep Southern Ocean and Remarks on its Biogeography. *Helgol. Mar. Res.* 67, 33–48. doi: 10.1007/s10152-012-0302-7

Kraft, A., Bauerfeind, E., Nöthig, E.-M., Klages, M., Beszczynska-Möller, A., and Bathmann, U. V. (2013). Amphipods in Sediment Traps of the Eastern Fram Strait With Focus on the Life-History of the Lysianassoid Cyclocaris Guilelmi. *Deep Sea Res. Part I. Oceanogr. Res.* 73, 62–72. doi: 10.1016/j.dsr.2012.11.012

Kreissl, S., Uber, A., and Harzsch, S. (2008). Muscle Precursor Cells in the Developing Limbs of Two Isopods (Crustacea, Peracarida): An Immunohistochemical Study Using a Novel Monoclonal Antibody Against Myosin Heavy Chain. *Dev. Genes. Evol.* 218, 253–265. doi: 10.1007/s00427-008-0216-1

Kürten, B., Frutos, I., Struck, U., Painting, S. J., Polunin, N. V. C., and Middelburg, J. J. (2013). Trophodynamics and Functional Feeding Groups of North Sea Fauna: A Combined Stable Isotope and Fatty Acid Approach. *Biogeochemistry* 113, 189–212. doi: 10.1007/s10533-012-9701-8

Kürzel, K., Kaiser, S., Lörz, A. N., Rossel, S., Paulus, E., Peters, J., et al. (2022). Correct Species Identification and Its Implications for Conservation Using

Haploniscidae (Crustacea, Isopoda) in Icelandic Waters as a Surrogate. *Front. Mar. Sci.* 8, 795196. doi: 10.3389/fmars.2021.795196

Lagardère, J. P. (1977). Recherches Sur La Distribution Vertical Et Sur L'alimentation Des Crustacés Décapodes Benthiques De La Pente Continentale Du Golfe De Gascogne. *Bull. Cent. Etud. Rech. Sci. Biarritz* 11 (4), 367–440.

Lambshead, P. J. D., and Boucher, G. (2003). Marine Nematode Deep-Sea Biodiversity–Hyperdiverse or Hype? *J. Biogeogr.* 30 (4), 475–485. doi: 10.1046/j.1365-2699.2003.00843.x

Landschoff, J., Komai, T., du Plessis, A., Gouws, G., and Griffiths, C. L. (2018). MicroCT Imaging Applied to Description of a New Species of Pagurus Fabricius 1775 (Crustacea: Decapoda: Anomura: Paguridae), With Selection of Three-Dimensional Type Data. *PloS One* 13, e0203107. doi: 10.1371/journal.pone.0203107

Langenkämper, D., Zurowietz, M., Schoening, T., and Nattkemper, T. W. (2017). Biigle 2.0-Browsing and Annotating Large Marine Image Collections. *Front. Mar. Sci.* 4, 83. doi: 10.3389/fmars.2017.00083

Larsen, K. (2001). Morphological and Molecular Investigation of Polymorphism and Cryptic Species in Tanaid Crustaceans: Implications for Tanaid Systematics and Biodiversity Estimates. *Zool. J. Linn. Soc* 131, 353–379. doi: 10.1111/j.1096-3642.2001.tb02241.x

Lee, S., Brown, R. L., and Monroe, W. (2009). Use of Confocal Laser Scanning Microscopy in Systematics of Insects With a Comparison of Fluorescence From Different Stains. *Syst. Entomol.* 34, 10–14. doi: 10.1111/j.1365-3113.2008.00451.x

Le, J. T., Levin, L. A., Lejzerowicz, F., Cordier, T., Gooday, A. J., and Pawlowski, J. (2021). Scientific and Budgetary Tradeoffs Between Morphological and Molecular Methods for Deep-Sea Biodiversity Assessment. *Integr. Environ. Assess. Manage* 18(3), 665–663. doi: 10.1002/ieam.4466

Lepechin, I. (1780). Tres *Oniscorum* Species Descriptae. *Acta Acad. Sci. Imperialis Petropolitanae* 1778, 248–249.

Lester, P. J., Brown, S. D. J., Edwards, E. D., Holwell, G. I., Pawson, S. M., Ward, D. F., et al. (2014). Critical Issues Facing New Zealand Entomology. *N. Z. Entomol.* 37 (1), 1–13. doi: 10.1080/00779962.2014.861789

Lim, G. S., Balke, M., and Meier, R. (2012). Determining Species Boundaries in a World Full of Rarity: Singletons, Species Delimitation Methods. *Syst. Biol.* 61 (1), 165–169. doi: 10.1093/sysbio/syr030

Linnaeus, C. (1735). Systema Naturae; Sive, Regna Tria Naturae: Systematice Proposita Per Classes, Ordines, Genera and Species. *Haak*.

Lins, L., and Brandt, A. (2020). Comparability Between Box-Corer and Epibenthic-Sledge Data on Higher Taxon Level: A Case Study Based on Deep-Sea Samples From the NW Pacific. *Prog. Oceanogr.* 182, 102273. doi: 10.1016/j.pocean.2020.102273

Lins, L., Zeppilli, D., Menot, L., Michel, L. N., Bonifácio, P., Brandt, M., et al. (2021). Toward a Reliable Assessment of Potential Ecological Impacts of Deep-Sea Polymetallic Nodule Mining on Abyssal Infauna. *Limnol. Oceanogr. Meth.* 19, 626–650. doi: 10.1002/lom3.10448

Li, J. Y., Song, Z. L., Yan, G. Y., and He, L. S. (2019). The Complete Mitochondrial Genome of the Largest Amphipod, *Alicella Gigantea*: Insight Into Its Phylogenetic Relationships and Deep Sea Adaptive Characters. *Int. J. Biol. Macromol.* 141, 570–577. doi: 10.1016/j.ijbiomac.2019.09.050

Lörz, A.-N., and Horton, T. (2021). Investigation of the Amathillopsidae (Amphipoda, Crustacea), Including the Description of a New Species, Reveals a Clinging Lifestyle in the Deep Sea Worldwide. *ZooKeys* 1031, 19–39. doi: 10.3897/zookeys.1031.62391

Lowry, J. K., and Myers, A. A. (2012). Podosiridae, a New Family of North Atlantic Deep Sea Amphipod (Crustacea, Amphipoda). *Zootaxa* 3546 (1), 81–84. doi: 10.11646/zootaxa.3546.1.6

Luque, J., and Gerken, S. (2019). Exceptional Preservation of Comma Shrimp From a Mid-Cretaceous Lagerstätte of Colombia, and the Origins of Crown Cumacea. *Proc. R. Soc. B.* 286, 20191863. doi: 10.1098/rspb.2019.1863

Luque, J., Xing, L., Briggs, D. E. G., Clark, E. G., Duque, A., Hui, J., et al. (2021). Crab in Amber Reveals an Early Colonization of Nonmarine Environments During the Cretaceous. *Sci. Adv.* 7 (43), eabj5689. doi: 10.1126/sciadv.abj5689

Macel, M.-L., Ristoratore, F., Locascio, A., Spagnuolo, A., Sordino, P., and D'Aniello, S. (2020). Sea as a Color Palette: The Ecology and Evolution of Fluorescence. *Zool. Lett.* 6, 9. doi: 10.1186/s40851-020-00161-9

MacIsaac, K. G., Kenchington, T. J., Kenchington, E. L. R., and Best, M. (2014). The Summer Assemblage of Large Pelagic Crustacea in the Gully Submarine Canyon: Major Patterns. *Deep Sea Res. Pt. II Top. Stud. Oceanogr.* 104, 51–66. doi: 10.1016/j.dsr2.2013.08.017

Maeno, A., Kohtsuka, H., Takatani, K., and Nakano, H. (2019). Microfocus X-Ray CT (microCT) Imaging of *Actinia Equina* (Cnidaria), *Harmothoe* Sp. (Annelida), and *Xenoturbella Japonica* (Xenacoelomorpha). *J. Vis. Exp.*, 150 e59161. doi: 10.3791/59161

Malyutina, M., Frutos, I., and Brandt, A. (2018). Diversity and Distribution of the Deep-Sea Atlantic *Acanthocope* (Crustacea, Isopoda, Munnopsidae), With Description of Two New Species. *Deep Sea Res. Pt. II Top. Stud. Oceanogr.* 148, 130–150. doi: 10.1016/j.dsr2.2017.11.003

Malyutina, M. V., Kihara, T. C., and Brix, S. (2020). A New Genus of Munnopsidae Lilljeborg 1864 (Crustacea, Isopoda), With Descriptions of Two Abyssal New Species From the Clarion Clipperton Fracture Zone, North-Eastern Tropical Pacific. *Mar. Biodiv.* 50, 42. doi: 10.1007/s12526-020-01061-z

Manktelow, M. (2010). "History of Taxonomy," in *Lecture From Dept. Of Systematic Biology* (Uppsala University).

Marek, P. (2017). Ultraviolet-Induced Fluorescent Imaging for Millipede Taxonomy. *Res. Ideas Outcomes* 3, e14850. doi: 10.3897/rio.3.e14850

Marquina, D., Buczek, M., Ronquist, F., and Łukasik, P. (2021). The Effect of Ethanol Concentration on the Morphological and Molecular Preservation of Insects for Biodiversity Studies. *Peer J* 9, e10799 2020. doi: 10.7717/peerj.10799

Martin, J. W. (2016). Collecting and Processing Crustaceans: An Introduction. *J. Crust. Biol.* 36, 393–395. doi: 10.1163/1937240X-00002436

Martínez Arbizu, P., and Petrunina, (2018). Two New Species of Tantulocarida From the Atlantic Deep Sea With First CLSM Pictures of Tantulus Larva. *Mar. Biodiv.* 48 (1), 231–237. doi: 10.1007/s12526-016-0627-6

Martin, J. W., France, S. C., and Van Dover, C. L. (1993). *Halice Hesmonectes*, a New Species of Pardaliscid Amphipod (Crustacea, Peracarida) From Hydrothermal Vents in the Eastern Pacific. *Can. J. Zool.* 71, 1724–1732. doi: 10.1139/z93-244

Maruzzo, D., Minelli, A., Ronco, M., and Fusco, G. (2007). Growth and Regeneration of the Second Antennae of Asellus Aquaticus (Isopoda) in the Context of Arthropod Antennal Segmentation. *J. Crust. Biol.* 27, 184–196. doi: 10.1651/S-2756.1

May, R. (1992). Bottoms Up for the Oceans. *Nature* 357, 278–279. doi: 10.1038/357278a0

Maybury, C., Morrison, L., and Stewart, V. (1991). The Search for a Reliable Mounting Medium for Recent 'Live' Foraminifera. *J. Micropalaeontol.* 9, 172–172. doi: 10.1144/jm.9.2.172

Mayr, E. (1942). *Systematics and the Origin of Species* (New York: Columbia University Press), 315 pp.

McMenamin, M. A. S., Zapata, L. P., and Hussey, M. C. (2013). A Triassic Giant Amphipod From Nevada, USA. *J. Crust. Biol.* 33 (6), 751–759. doi: 10.1163/1937240X-00002192

Meißner, K., Bick, A., and Götting, M. (2017). Arctic *Pholoe* (Polychaeta: Pholoidae): When Integrative Taxonomy Helps to Sort Out Barcodes. *Zool. J. Linn. Soc* 179 (2), 237–262. doi: 10.1111/zoj.12468

Meier, R., Blaimerb, B. B., Buenaventura, E., Hartopb, E., vonRintelen, T., Srivathsana, A., et al. (2022). A Re-Analysis of the Data in Sharkey Et Al.'s, (2021) Minimalist Revision Reveals That BINs do Not Deserve Names, But BOLD Systems Needs a Stronger Commitment to Open Science. *Cladistics*, 38, 264–275. doi: 10.1111/cla.12489

Melzer, R. R., Spitzner, F., Šargač, Z., Hörnig, M. K., Krieger, J., Haug, C., et al. (2021). Methods to Study Organogenesis in Decapod Crustacean Larvae II: Analysing Cells and Tissues. *Helgol. Mar. Res.* 75, 2. doi: 10.1186/s10152-021-00547-y

Menzel, L. (2011). First Descriptions of Copepodid Stages, Sexual Dimorphism and Intraspecific Variability of Mesocletodes Sars 1909 (Copepoda, Harpacticoida, Argestidae), Including the Description of a New Species With Broad Abyssal Distribution. *ZooKeys* 96, 39–80. doi: 10.3897/zookeys.96.1496

Michels, J. (2007). Confocal Laser Scanning Microscopy: Using Cuticular Autofluorescence for High Resolution Morphological Imaging in Small Crustaceans. *J. Microsc. Oxford* 227, 1–7. doi: 10.1111/j.1365-2818.2007.01787.x

Michels, J., and Büntzow, M. (2010). Assessment of Congo Red as a Fluorescence Marker for the Exoskeleton of Small Crustaceans and the Cuticle of Polychaetes. *J. Microsc.* 238 (2), 95–101. doi: 10.1111/j.1365-2818.2009.03360.x

Mohrbeck, I., Horton, T., Jażdżewska, A. M., and Arbizu, P. M. (2021). DNA Barcoding and Cryptic Diversity of Deep-Sea Scavenging Amphipods in the Clarion-Clipperton Zone (Eastern Equatorial Pacific). *Mar. Biodiv.* 51 (2), 1–15. doi: 10.1007/s12526-021-01170-3

Mohrbeck, I., Raupach, M. J., Martínez Arbizu, P., Knebelsberger, T., and Laakmann, S. (2015). High-Throughput Sequencing—The Key to Rapid Biodiversity Assessment of Marine Metazoa? *PloS One* 10 (10), e0140342. doi: 10.1371/journal.pone.0140342

Montesanto, G. (2015). A Fast GNU Method to Draw Accurate Scientific Illustrations for Taxonomy. *ZooKeys* 515, 191–206. doi: 10.3897/zookeys.515.9459

Mora, C., Tittensor, D. P., Adl, S., Simpson, A. G., and Worm, B. (2011). How Many Species Are There on Earth and in the Ocean? *PloS Biol.* 9 (8), e1001127.

Moreira, P. S. (1973). Especies De Isopoda (Crustacea, Peracarida). *Programa Rio Grande Do Sul II*. Parte I, Publicaçao Especial do Instituto Oceanografico. 3(2), 213–229.

Mrak, P., Žnidaršič, N., and Štrus, J. (2013). Alizarin Red S Staining of the Crustacean Cuticle: Implementation in the Study of Porcellio Scaber Larvae. *ABS* 56, 51–62.

Mrak, P., Žnidaršič, N., Tušek-Žnidarič, M., Klepal, W., Gruber, D., and Strus, J. (2012). Egg Envelopes and Cuticle Renewal in *Porcellio* Embryos and Marsupial Mancas. *ZooKeys* 176, 55–72. doi: 10.3897/zookeys.176.2418

Murray, J., and Renard, A. F. (1891). *Report on Deep-Sea Deposits Based on the Specimens Collected During the Voyage of HMS Challenger in the Years 1872 to 1876* (HM Stationery Office).

Nagler, C., and Haug, J. T. (2016). Functional Morphology of Parasitic Isopods: Understanding Morphological Adaptations of Attachment and Feeding Structures in *Nerocila* as a Pre-Requisite for Reconstructing the Evolution of Cymothoidae. *PeerJ* 4, e2188. doi: 10.7717/peerj.2188

Nagler, C., Hyžný, M., and Haug, J. T. (2017). 168 Million Years Old "Marine Lice" and the Evolution of Parasitism Within Isopods. *BMC Evol. Biol.* 17, 76. doi: 10.1186/s12862-017-0915-1

Narayanaswamy, B. E., Bett, B. J., Lamont, P. A., Rowden, A. A., Bell, E. M., and Menot, L. (2016). "Corers and Grabs," in *Biological Sampling in the Deep Sea*. Eds. M. R. Clark, M. Consalvey and A. A. Rowden (John Wiley and Sons Ltd), 207–227 pp.

Naskrecki, P. (2008) *Mantis V. 2.0 - A Manager of Taxonomic Information and Specimens*. Available at: http://insects.oeb.harvard.edu/mantis (Accessed 30 July 2012).

Neuhaus, B., Schmid, T., and Riedel, J. (2017). Collection Management and Study of Microscope Slides: Storage, Profiling, Deterioration, Restoration Procedures, and General Recommendations. *Zootaxa* 4322, 1–173. doi: 10.11646/zootaxa.4322.1.1

Neusser, T. P., Jörger, K. M., Lodde-Bensch, E., Strong, E. E., and Schrödl, M. (2016). The Unique Deep Sea—Land Connection: Interactive 3D Visualization and Molecular Phylogeny of *Bathyhedyle Boucheti* N. Sp. (Bathyhedylidae N. Fam.)—The First Panpulmonate Slug From Bathyal Zones. *PeerJ* 4, e2738. doi: 10.7717/peerj.2738

Nouvel, H., and Lagardère, J. P. (1976). Les Mysidacés Du Talus Continental Du Golfe De Gascogne I. Tribu Des Erythropini (Genre *Erythrops* Excepté). *Bull. Mus. Natn. Hist. Nat.* 414 (291), 1243–1324.

Palero, F., Hall, S., Clark, P. F., Johnston, D., Mackenzie-Dodds, J., and Thatje, S. (2010). DNA Extraction From Formalin-Fixed Tissue: New Light From the Deep Sea. *Sci. Mar.* 74, 465–470. doi: 10.3989/scimar.2010.74n3465

Pante, E., Schoelinck, C., and Puillandre, N. (2015). From Integrative Taxonomy to Species Description: One Step Beyond. *Syst. Biol.* 64, 152–160. doi: 10.1093/sysbio/syu083

Papiol, V., Cartes, J. E., Vélez-Belchí, P., and Martín-Sosa, P. (2019). Near-Bottom Zooplankton Over Three Seamounts in the East Canary Islands: Influence of Environmental Variables on Distribution and Composition. *Deep Sea Res. Part I. Oceanogr. Res.* 149, 1030025. doi: 10.1016/j.dsr.2019.04.003

Paulus, E., Brix, S., Siebert, A., Arbizu, P. M., Rossel, S., Peters, J., et al. (2021). Recent Speciation and Hybridization In Icelandic Deep-Sea Isopods: An Integrative Approach Using Genomics and Proteomics. Authorea Preprints.

Pawlowski, J., Kelly-Quinn, M., Altermatt, F., Apothéloz-Perret-Gentil, L., Beja, P., Boggero, A., et al. (2018). The Future of Biotic Indices in the Ecogenomic Era: Integrating (E) DNA Metabarcoding in Biological Assessment of Aquatic Ecosystems. *Sci. Tot. Environ.* 637, 1295–1310. doi: 10.1016/j.scitotenv.2018.05.002

Pereira, E., Roccatagliata, D., and Doti, B. L. (2019). *Xiphoarcturus* – a New Genus and Two New Species of the Family Antarcturidae (Isopoda: Valvifera) From the Mar Del Plata Submarine Canyon and its Phylogenetic Relationships. *Arthropod. Syst. Phyl.* 77, 303–323. doi: 10.26049/ASP77-2-2019-07

Pinu, F. R., Beale, D. J., Paten, A. M., Kouremenos, K., Swarup, S., Schirra, H. J., et al. (2019). Systems Biology and Multi-Omics Integration: Viewpoints From the Metabolomics Research Community. *Metabolites* 9 (4), 76. doi: 10.3390/metabo9040076

Pokluda, P., Čížek, L., Stříbrná, E., Drag, L., Lukeš, J., and Novotný, V. (2014). A Goodbye Letter to Alcohol: An Alternative Method for Field Preservation of Arthropod Specimens and DNA Suitable for Mass Collecting Methods. *Eur. J. Entomol.* 111, 175–179. doi: 10.14411/eje.2014.024

Poore, G. C. B., and Bruce, N. L. (2012). Global Diversity of Marine Isopods (Except Asellota and Crustacean Symbionts). *PloS One* 7, e43529. doi: 10.1371/journal.pone.0043529

Poore, G. C. B., and Wilson, G. D. (1993). Marine Species Richness. *Nature* 361 (6413), 597–598.

Porter, M. L. (2016). Collecting and Processing Mysids, Stygiomysids, and Lophogastrids. *J. Crust. Biol.* 36, 592–595. doi: 10.1163/1937240X-00002443

Preciado, I., Cartes, J. E., Punzón, A., Frutos, I., López-López, L., and Serrano, A. (2017). Food Web Functioning of the Benthopelagic Community in a Deep-Sea Seamount Based on Diet and Stable Isotope Analyses. *Deep Sea Res. Pt. II Top. Stud. Oceanogr.* 137, 56–68. doi: 10.1016/j.dsr2.2016.07.013

Presnell, J. K., and Schreibman, M. P. (1997). *Humason's Animal Tissue Techniques. 5th ed* (Baltimore (Md: Johns Hopkins University press).

Ramirez-Llodra, E., Brandt, A., Danovaro, R., Mol, B. D., Escobar, E., German, C. R., et al. (2010). Deep, Diverse and Definitely Different: Unique Attributes of the World's Largest Ecosystem. *Biogeosciences* 7 (9), 2851–2899. doi: 10.5194/bg-7-2851-2010

Raupach, M. J., Amann, R., Wheeler, Q. R., and Roos, R. (2016). The Application of "–Omics" Technologies for the Classificationand Identification of Animals. *Org. Divers. Evol.* 16, 1–12. doi: 10.1007/s13127-015-0234-6

Raupach, M. J., and Wägele, J. W. (2006). Distinguishing Cryptic Species in Antarctic Asellota (Crustacea: Isopoda)-A Preliminary Study of Mitochondrial DNA in *Acanthaspidia Drygalskii*. *Antarc. Sci.* 18 (2), 191. doi: 10.1017/S0954102006000228

Renner, S. S. (2016). A Return to Linnaeus's Focus on Diagnosis, Not Description: The Use of DNA Characters in the Formal Naming of Species. *Syst. Biol.* 65 (6), 1085–1095. doi: 10.1093/sysbio/syw032

Riedel, A., Sagata, K., Suhardjono, Y. R., Tänzler, R., and Balke, M. (2013). Integrative Taxonomy on the Fast Track-Towards More Sustainability in Biodiversity Research. *Front. Zool.* 10 (1), 1–9. doi: 10.1186/1742-9994-10-15

Riehl, T., Brenke, N., Brix, S., Driskell, A., Kaiser, S., and Brandt, A. (2014). Field and Laboratory Methods for DNA Studies on Deep-Sea Isopod Crustaceans. *Pol. Polar. Res.*, 35(2) 203–224. doi: 10.2478/popore-2014-0018

Riehl, T., and De Smet, B. (2020). *Macrostylis Metallicola* Spec. Nov. — An Isopod With Geographically Clustered Genetic Variability From a Polymetallic-Nodule Area in the Clarion-Clipperton Fracture Zone. *PeerJ* 8, e8621. doi: 10.7717/peerj.8621

Riehl, T., and Kühn, M. A. L. (2020). Uniting What Belongs Together—Reevaluation of the Isopod Species *Macrostylis Grandis* and *M. Ovata* Using Ontogenetic, Morphological and Genetic Evidence. *Prog. Oceanogr.* 181, 102238. doi: 10.1016/j.pocean.2019.102238

Riehl, T., Wilson, G. D., and Hessler, R. R. (2012). New Macrostylidae Hansen 1916 (Crustacea: Isopoda) From the Gay Head-Bermuda Transect With Special Consideration of Sexual Dimorphism. *Zootaxa* 3277 (1), 1–26. doi: 10.11646/zootaxa.3277.1.1

Ríos, P., Cristobo, J., Altuna, A., Frutos, I., Manjón-Cabeza, E., García, Guillén, et al. (2022). Avilés Canyon System: Increasing the Benthic Biodiversity Knowledge. *Estuar. Coast. Shelf Sci.* 274, 107924. doi: 10.1016/j.ecss.2022.107924

Ritchie, H., Jamieson, A. J., and Piertney, S. B. (2017). Genome Size Variation in Deep-Sea Amphipods. *R. Soc Open Sci.* 4 (9), 170862. doi: 10.1098/rsos.170862

Robin, N., Gueriau, P., Luque, J., Jarvis, D., Daley, A. C., and Vonk, R. (2021). The Oldest Peracarid Crustacean Reveals a Late Devonian Freshwater Colonization by Isopod Relatives. *Biol. Lett.* 17, 20210226. doi: 10.1098/rsbl.2021.0226

Robinson, C. V., Porter, T. M., Wright, M. T. G., and Hajibabaei, M. (2021). Propylene Glycol-Based Antifreeze Is an Effective Preservative for DNA Metabarcoding of Benthic Arthropods. *Freshw. Sci.* 40, 77–87. doi: 10.1086/712232

Rodríguez, J. G., Garmendia, J. M., Muxika, I., Gómez-Ballesteros, M., Quincoces, I., Díez, I., et al. (2021). Macrofaunal Variability in the Continental Shelf and Canyons in the Southeastern Bay of Biscay. *Reg. Stud. Mar. Sci.* 48, 102012. doi: 10.1016/j.rsma.2021.102012

Rosenthal, C. K. (2009). The Beginning. *Nat. Cell Biol.* 11 (1), S6–S6. doi: 10.1038/ncb1938

Rosli, N., Leduc, D., Rowden, A. A., Clark, M. R., Probert, P. K., Berkenbusch, K., et al. (2016). Differences in Meiofauna Communities With Sediment Depth Are Greater Than Habitat Effects on the New Zealand Continental Margin: Implications for Vulnerability to Anthropogenic Disturbance. *PeerJ* 4, e2154. doi: 10.7717/peerj.2154

Rossel, S., and Martínez Arbizu, P. (2018). Automatic Specimen Identification of Harpacticoids (Crustacea : Copepoda) Using Random Forest and MALDI-TOF Mass Spectra, Including a *Post Hoc* Test for False Positive Discovery. *Methods Ecol. Evol.* 9, 1421–1434. doi: 10.1111/2041-210X.13000

Rossel, S., and Martinez Arbizu, P. (2019). Revealing Higher Than Expected Diversity of Harpacticoida (Crustacea: Copepoda) in the North Sea Using MALDI-TOF MS and Molecular Barcoding. *Sci. Rep.* 9 (1), 1–14. doi: 10.1038/s41598-019-45718-7

Sánchez-García, A., Peálver, E., Bird, G. J., Perrichot, V., and Delclòs, X. (2016). Palaeobiology of Tanaidaceans (Crustacea: Peracarida) From Cretaceous Ambers: Extending the Scarce Fossil Record of a Diverse Peracarid Group. *Zool. J. Linn. Soc.* 178, 492–522. doi: 10.1111/zoj.12427

Sánchez, F., Serrano, A., Parra, S., and Cartes, J. E. (2008). Habitat Characteristics as Determinant of the Structure and Spatial Distribution of Epibenthic and Demersal Communities of Le Danois Bank (Cantabrian Sea, N Spain). *J. Mar. Syst.* 72, 64–86. doi: 10.1016/j.jmarsys.2007.04.008

Sanders, H. L., Hessler, R. R., and Garner, S. P. (1985). *Hirsutia Bathyalis*, a New Unusual Deep-Sea Benthic Peracaridan Crustacean From the Tropical Atlantic. *J. Crust. Biol.* 5 (1), 30–57. doi: 10.2307/1548219

San Vicente, C., and Cartanyà, J. (2017). A New Mysid (Crustacea, Mysida) From the Ladinian Stage (Middle Triassic) of Conca De Barberà (Catalonia, NE Iberian Peninsula). *J. Paleontol.* 91 (5), 968–980. doi: 10.1017/jpa.2017.24

San Vicente, C., Frutos, I., and Cartes, J. E. (2014b). *Petalophthalmus Papilloculatus* Sp. Nov. (Crustacea: Mysida: Petalophthalmidae), A New Bathyal Suprabenthic Mysid From the Galicia Bank (NE Atlantic Ocean). *Zootaxa* 3765 (1), 77–91. doi: 10.11646/zootaxa.3765.1.5

San Vicente, C., Guerao, G., and Olensen, J. (2014a). "Lophogastrida and Mysida," in *Atlas of Crustacean Larvae*. Eds. J. W. Martin, J. Olensen and J. T. Høeg (Baltimore: Johns Hopkins University Press), 199–205.

Sars, G. O. (1900). An account of the Crustacea of Norway. Vol III. Cumacea. Part V and VI Diastylidae. Bergen. pp. 41–68, plates XXXIII–XLVIII.

Saunders, T. E. (2020). Taxonomy at a Crossroads: Communicating Value, Building Capability, and Seizing Opportunities for the Future. *Megataxa* 1 (1), 63–66. doi: 10.11646/megataxa.1.1.13

Schiaparelli, S., Schnabel, K. E., Richer de Forges, B., and Chan, T.-Y. (2016). "Sorting, Recording, Preservation and Storage of Biological Samples," in *Biological Sampling in the Deep Sea*. Eds. M. R. Clark, M. Consalvey and A. A. Rowden (John Wiley and Sons).

Schmidt, C., Escobar Wolf, K., Lins, L., Martínez Arbizu, P., and Brandt, A. (2018). Meiofauna Abundance and Community Patterns Along a Transatlantic Transect in the Vema Fracture Zone and in the Hadal Zone of the Puerto Rico Trench. *Deep Sea Res. Pt. II Top. Stud. Oceanogr.* 148, 223–235. doi: 10.1016/j.dsr2.2017.12.021

Schmidt, C., and Martínez Arbizu, P. (2015). Unexpectedly Higher Metazoan Meiofauna Abundances in the Kuril-Kamchatka Trench Compared to the Adjacent Abyssal Plains. *Deep Sea Res. Pt. II Top. Stud. Oceanogr.* 111, 60–75. doi: 10.1016/j.dsr2.2014.08.019

Schnurr, S., Osborn, K. J., Malyutina, M., Jennings, R., Brix, S., Driskell, A., et al. (2018). Hidden Diversity in Two Species Complexes of Munnopsid Isopods (Crustacea) at the Transition Between the Northernmost North Atlantic and the Nordic Seas. *Mar. Biodiv.* 48, 813–843. doi: 10.1007/s12526-018-0877-6

Secrétan, S., and Riou, B. (1986). Les Mysidacés (Crustacea, Peracarida) Du Callovien De La Voulte-Sur-Rhône. *Ann. Paleontol.* 72 (4), 295–323.

Selden, P., Wilson, G. D. F., Simonetto, L., and Dalla Vecchia, F. (2016). First Fossil Asellote (Isopoda: Asellota), From the Upper Triassic (Norian) of the Carnic Prealps (Friuli, Northeastern Italy). *J. Crust. Biol.* 36 (1), 68–86. doi: 10.1163/1937240X-00002387

Serrano, A., Cartes, J. E., Papiol, V., Punzón, A., García-Alegre, A., Arronte, J. C., et al. (2017). Epibenthic Communities of Sedimentary Habitats in a NE Atlantic Deep Seamount (Galicia Bank). *J. Sea Res.* 130, 154–165. doi: 10.1016/j.seares.2017.03.004

Serrano, A., Sánchez, F., Punzón, A., Velasco, F., and Olaso, I. (2011). Deep Sea Megafaunal Assemblages Off the Northern Iberian Slope Related to Environmental Factors. *Sci. Mar.* 75 (3), 425–437. doi: 10.3989/scimar.2011.75n3425

Sharkey, M. J., Janzen, D. H., Hallwachs, W., Chapman, E. G., Smith, M. A., Dapkey, T., et al. (2021). Minimalist Revision and Description of 403 New Species in 11 Subfamilies of Costa Rican Braconid Parasitoid Wasps, Including Host Records for 219 Species. *ZooKeys* 1013, 1–665. doi: 10.3897/zookeys.1013.55600

Shaw, P. (1989). New Amphipods From Geothermal Vent Sites Off the West Coast of Vancouver Island, British Columbia, With a Reappraisal of the Amphipod Family Sebidae. *Can. J. Zool.* 67 (8), 1882–1890. doi: 10.1139/z89-269

Shimomura, M., and Mawatari, S. F. (1999). *Paramunna Rhipis*, a New Species of Asellote Isopod (Paramunnidae) From Japan. *Crust. Res.* 28, 153–159. doi: 10.18353/crustacea.28.0_153

Shimomura, M., and Mawatari, S. F. (2000). *Santia Katoi* Sp. Nov., a New Isopod Crustacean From Shirahama, Japan. *Publ. Seto Mar. Bioi. Lab.* 39 (1), 29–34. doi: 10.5134/176292

Shimomura, M., and Ohtsuka, S. (2005). "Deep-Sea Asellote Isopods (Crustacea Peracarida) of Nansei Islands, Southwestern Japan," in *Deep-Sea Fauna and Pollutans in Nansei Islands*, vol. 29 . Eds. K. Hasegawa, G. Shinohara and M. Takeda (National Science Museum Monographs), 249–259.

Singh, R., and Mumbarekar, V. (2021). *Neural Network Model Approach for Automated Benthic Animal Identification* (ICT Express).

Sittrop, D. J., Serejo, C. S., Souza-Filho, J. F., and Senna, A. R. (2015). New Genera and Species of Urothoidae (Amphipoda) From the Brazilian Deep Sea, With the Re-Assignment of *Pseudurothoe* and *Urothopsis* to Phoxocephalopsidae. *J. Nat. Hist.* 49 (9–10), 527–552. doi: 10.1080/00222933.2014.953227

Slabber, M. (1769–1778a). Natuurkundige Verlustigingen 15, Tweede Waarneeming van een Steur-garnael met trompetswyze oogen, pp. 136–139, pls. 15, figs 3–4. Haarlem.

Sorbe, J. C. (1981). Rôle Du Benthos Dans Le Régime Alimentaire Des Poissons Démersaux Du Secteur Sud Gascogne. *Kieler Meeresforsch. Sonderh.* 5, 479–489.

Sorbe, J. C. (1983). Description D'un Traîneau Destiné a L'échantillonnage Quantitatif Etagé De La Faune Suprabenthique Néritique. *Ann. Inst. Océanogr.* 59 (2), 117–126.

Starr, H. W., Hegna, T. A., and McMenamin, M. A. S. (2016).). Epilogue to the Tale of the Triassic Amphipod: *Rosagammarus* McMenamin, Zapata and Hussey 2013 is a Decapod Tail (Luning Formation, Nevada, USA). *J. Crust. Biol.* 36 (4), 525–529. doi: 10.1163/1937240X-00002444

Stebbing, T. R. R. (1888). Report on the Amphipoda Collected by H.M.S. Challenger During the Years 1873–76. Report on the Scientific Results of the Voyage of H.M.S. Challenger During the Years 1873–1876. *Zoology* 29, xxiv + 1737.

Steedman, H. F. (1958). Dimethyl Hydantoin Formaldehyde: A New Water-Soluble Resin for Use as a Mounting Medium. *J. Cell Sci.* s3–99, 451–452. doi: 10.1242/jcs.s3-99.48.451

Stegner, M. E., Stemme, T., Iliffe, T. M., Richter, S., and Wirkner, C. S. (2015). The Brain in Three Crustaceans From Cavernous Darkness. *BMC Neurosci.* 16, 19. doi: 10.1186/s12868-015-0138-6

Stemme, T., Eickhoff, R., and Bicker, G. (2014). Olfactory Projection Neuron Pathways in Two Species of Marine Isopoda (Peracarida, Malacostraca, Crustacea). *Tissue Cell* 46, 260–263. doi: 10.1016/j.tice.2014.05.010

Storey, M., and Poore, G. C. B. (2009). New Species of *Brucerolis* (Crustacea: Isopoda: Serolidae) From Seas Around New Zealand and Australia. *Mem. Mus. Vic.* 66, 147–173. doi: 10.24199/j.mmv.2009.66.15

Štrus, J., Tušek-Žnidarič, M., Repnik, U., Blejec, A., and Summers, A. (2019). Microscopy of Crustacean Cuticle: Formation of a Flexible Extracellular Matrix in Moulting Sea Slaters *Ligia Pallasii*. *J. Mar. Biol. Ass.* 99, 857–865. doi: 10.1017/S0025315418001017

Sweetman, A. K., Thurber, A. R., Smith, C. R., Levin, L. A., Mora, C., Wei, C. L., et al. (2017). Major Impacts of Climate Change on Deep-Sea Benthic Ecosystems. *Elem. Sci. Anth.* 5(4).

Tanaka, K. (2004). A New Species of *Gnathia* (Isopoda: Cymothoida: Gnathiidae) From Ishigaki Island, the Ryukyus, Southwestern Japan. *Crustacean Res.* 33, 51–60. doi: 10.18353/crustacea.33.0_51

Tandberg, A. H., Tore Rapp, H., Schander, C., Vader, W., Sweetman, A. K., and Berge, J. (2012). *Exitomelita Sigynae* Gen. Et Sp. Nov.: A New Amphipod From the Arctic Loki Castle Vent Field With Potential Gill Ectosymbionts. *Polar. Biol.* 35, 705–716. doi: 10.1007/s00300-011-1115-x

Taylor, J., Devey, C., Le Saout, M., Petersen, S., Frutos, I., Linse, K., et al. (2021). The Discovery and Preliminary Geological and Faunal Descriptions of Three New Steinahóll Vent Sites, Reykjanes Ridge, Iceland. *Front. Mar. Sci.* 8. doi: 10.3389/fmars.2021.520713

Tomikawa, K., and Mawatari, S. F. (2006). A New Species of the Genus *Amathillopsis* (Crustacea: Amphipoda: Amathillopsidae) From Japan. *Species Div.* 11 (3), 199–207. doi: 10.12782/specdiv.11.199

Turner, L. M., Ricevuto, E., Massa Gallucci, A., Lorenti, M., Gambi, M.-C., and Calosi, P. (2016). Metabolic Responses to High Pco2 Conditions at a CO2 Vent Site in Juveniles of a Marine Isopod Species Assemblage. *Mar. Biol.* 163, 211. doi: 10.1007/s00227-016-2984-x

Valdecasas, A. G., and Abad, A. (2011). Morphological Confocal Microscopy in Arthropods and the Enhancement of Autofluorescence After Proteinase K Extraction. *Microsc. Microanal.* 17, 109–113. doi: 10.1017/S1431927610094213

Vonk, R., and Schram, F. (2007). Three New Tanaid Species (Crustacea, Peracarida, Tanaidacea) From the Lower Cretaceous Álava Amber in Northern Spain. *J. Paleont.* 81 (6), 1502–1509. doi: 10.1666/05-020.1

Vrijenhoek, R. C. (2009). Cryptic Species, Phenotypic Plasticity, and Complex Life Histories: Assessing Deep-Sea Faunal Diversity With Molecular Markers. *Deep Sea Res. Pt. II Top. Stud. Oceanogr.* 56 (19–20), 1713–1723. doi: 10.1016/j.dsr2.2009.05.016

Wägele, H., Klussmann-Kolb, A., Kuhlmann, M., Haszprunar, G., Lindberg, D., Koch, A., et al. (2011). The Taxonomist-an Endangered Race. A Practical Proposal for its Survival. *Front. Zool.* 8 (1), 1–7. doi: 10.1186/1742-9994-8-25

Wall, A., Campo, D., and Wetzer, R. (2014). Genetic Utility of Natural History Museum Specimens: Endangered Fairy Shrimp (Branchiopoda, Anostraca). *ZooKeys* 457, 1–14. doi: 10.3897/zookeys.457.6822

Washburn, T. W., Menot, L., Bonifácio, P., Pape, E., Błażewicz, M., Bribiesca-Contreras, G., et al. (2021). Patterns of Macrofaunal Biodiversity Across the Clarion-Clipperton Zone: An Area Targeted for Seabed Mining. *Front. Mar. Sci.* 8. doi: 10.3389/fmars.2021.626571

Wells, A., Johanson, K. A., and Dostine, P. (2019). Why are So Many Species Based on a Single Specimen? *Zoosymposia* 14 (1), 32–38. doi: 10.11646/zoosymposia.14.1.5

Wetzer, R. (2015). Collecting and Preserving Marine and Freshwater Isopoda (Crustacea: Peracarida). *Biodivers. Data J.* 3, e4912. doi: 10.3897/BDJ.3.e4912

Wheeler, Q. (2018). Blank Canvas: The Case for Descriptive Taxonomy. *Integr. Comp. Biol.* 58, 1118–1121. doi: 10.1093/icb/icy067

Will, K. W., Mishler, B. D., and Wheeler, Q. D. (2005). The Perils of DNA Barcoding and the Need for Integrative Taxonomy. *Syst. Biol.* 54, 844–851. doi: 10.1080/10635150500354878

Wilson, G. D. F. (2003). A New Genus of Tainisopidae Fam. Nov. (Crustacea: Isopoda) From the Pilbara, Western Australia. *Zootaxa* 245, 1–20. doi: 10.11646/zootaxa.245.1.1

Wilson, G. D. F. (2017). Macrofauna Abundance, Species Diversity and Turnover at Three Sites in the Clipperton-Clarion Fracture Zone. *Mar. Biodivers.* 47, 323–347. doi: 10.1007/s12526-016-0609-8

Wilson, G. D. F., and Ahyong, S. T. (2015). Lifestyles of the Species-Rich and Fabulous: The Deep-Sea Crustaceans. in *The Natural History of the Crustacea: Lifestyles and feeding Biology*. Eds.M. F. Thiel and L. Watling (Oxforf University Press), 279–298.

Wilson, G. D. F., and Humphrey, C. L. (2020). The Eophreatoicus Nicholls 1926 Species Flock From Kakadu and Arnhem Land, With a Description of a New Genus of Amphisopidae (Crustacea: Isopoda: Phreatoicidea). *Zootaxa* 4854, 1–303. doi: 10.11646/zootaxa.4854

Wilson, K., Thorndyke, M., Nilsen, F., Rogers, A., and Martinez, P. (2005). Marine Systems: Moving Into the Genomics Era. *Mar. Ecol.* 26 (1), 3–16. doi: 10.1111/j.1439-0485.2005.00041.x

Wirkner, C. S., and Richter, S. (2004). Improvement of Microanatomical Research by Combining Corrosion Casts With MicroCT and 3D Reconstruction, Exemplified in the Circulatory Organs of the Woodlouse. *Microsc. Res. Tech.* 64, 250–254. doi: 10.1002/jemt.20076

Wittmann, K. J., Ariani, A. P., and Lagardère, J. P. (2014). "Orders Lophogastrida Boas 1883, Stygiomysida Tchindonova 1981, and Mysida Boas 1883 (Also Known Collectively as Mysidacea)," in *Treatise on Zoology – Anatomy, Taxonomy, Biology. The Crustacea*, vol. vol 4 Part B . Eds. J. C. von Vaupel Klein, M. Charmantier-Daures and F. R. Schram (Leiden: Koninklijke Brill NV), pp 189–pp 396.

Wittmann, K. J., Ariani, A. P., and Daneliya, M. (2016). The Mysidae (Crustacea: Peracarida: Mysida) in Fresh and Oligohaline Waters of the Mediterranean. Taxonomy, Biogeography, and Bioinvasion. *Zootaxa* 4142, 1–70. doi: 10.11646/zootaxa.4142.1.1

Wolff, C. (2009). The Embryonic Development of the Malacostracan Crustacean *Porcellio Scaber* (Isopoda, Oniscidea). *Dev. Genes Evol.* 219, 545–564. doi: 10.1007/s00427-010-0316-6

Wollaston, W. H. (1807). Description of the Camera Lucida. *J. Nat. Phil. Chem. Arts.* 17, 1–5.

WoRMS Editorial Board (2021) *World Register of Marine Species*. Available at: https://www.marinespecies.org.

Yeom, J., Park, N., Jeong, R., and Lee, W. (2021). Integrative Description of Cryptic *Tigriopus* Species From Korea Using MALDI-TOF MS and DNA Barcoding. *Front. Mar. Sci.* 8, 495. doi: 10.3389/fmars.2021.648197

Zeidler, W. (1990). Pelagic Amphipods, Infraorder Physosomata (Crustacea: Amphipoda. Hyperiidea) From the CSK International Zooplankton Collection (Western North Pacific) With the Description of Four New Species of *Scina*. *Publ. Seto Mar. Biol.* 34 (4/6), 167–200.

Zeidler, W. (2009). A Review of the Hyperiidean Amphipod Superfamily Lanceoloidea Bowman and Gruner 1973 (Crustacea: Amphipoda: Hyperiidea). *Zootaxa* 2000, 1–117. doi: 10.11646/zootaxa.2000.1.1

Zhang, Z. Q. (2008). Zoological Taxonomy at 250: Showcasing Species Descriptions in the Cyber Era. *Zootaxa* 1671 (1), 1–2. doi: 10.11646/zootaxa.1671.1.1

Zhang, R., Zhou, Y., Lu, B., and Wang, C. (2017). A New Species in the Genus *Styracaster* (Echinodermata: Asteroidea: Porcellanasteridae) From Hadal Depth of the Yap Trench in the Western Pacific. *Zootaxa* 4338, 153–162. doi: 10.11646/zootaxa.4338.1.8

Žnidaršič, N., Mrak, P., Rajh, E., Soderžnik, K.Ž., Čeh, M., and Štrus, J. (2018). Cuticle Matrix Imaging by Histochemistry, Fluorescence, and Electron Microscopy. *Resol. Discovery* 3, 5–12. doi: 10.1556/2051.2018.00052

Conflict of Interest: The authors declare that the research was conducted in the absence of any commercial or financial relationships that could be construed as a potential conflict of interest.

Publisher's Note: All claims expressed in this article are solely those of the authors and do not necessarily represent those of their affiliated organizations, or those of the publisher, the editors and the reviewers. Any product that may be evaluated in this article, or claim that may be made by its manufacturer, is not guaranteed or endorsed by the publisher.

Copyright © 2022 Frutos, Kaiser, Pułaski, Studzian and Błażewicz. This is an open-access article distributed under the terms of the Creative Commons Attribution License (CC BY). The use, distribution or reproduction in other forums is permitted, provided the original author(s) and the copyright owner(s) are credited and that the original publication in this journal is cited, in accordance with accepted academic practice. No use, distribution or reproduction is permitted which does not comply with these terms.

Advantages of publishing in Frontiers

OPEN ACCESS
Articles are free to read for greatest visibility and readership

FAST PUBLICATION
Around 90 days from submission to decision

HIGH QUALITY PEER-REVIEW
Rigorous, collaborative, and constructive peer-review

TRANSPARENT PEER-REVIEW
Editors and reviewers acknowledged by name on published articles

Frontiers
Avenue du Tribunal-Fédéral 34
1005 Lausanne | Switzerland

Visit us: www.frontiersin.org
Contact us: frontiersin.org/about/contact

REPRODUCIBILITY OF RESEARCH
Support open data and methods to enhance research reproducibility

DIGITAL PUBLISHING
Articles designed for optimal readership across devices

FOLLOW US
@frontiersin

IMPACT METRICS
Advanced article metrics track visibility across digital media

EXTENSIVE PROMOTION
Marketing and promotion of impactful research

LOOP RESEARCH NETWORK
Our network increases your article's readership